USGS
science for a changing world

Prepared in cooperation with the
USDA Forest Service and
U.S. Environmental Protection Agency

Integrated Investigations of Environmental Effects of Historical Mining in the Basin and Boulder Mining Districts, Boulder River Watershed, Jefferson County, Montana

Professional Paper 1652

U.S. Department of the Interior
U.S. Geological Survey

Cover. View from Eva May mine looking across Cataract Creek valley at Hoodoo Creek drainage. Photograph by D.A. Nimick.

Integrated Investigations of Environmental Effects of Historical Mining in the Basin and Boulder Mining Districts, Boulder River Watershed, Jefferson County, Montana

Edited by David A. Nimick, Stanley E. Church, and Susan E. Finger

Prepared in cooperation with the
USDA Forest Service and
U.S. Environmental Protection Agency

Volume comprises Chapters A, B, C, D1–D10, E1–E3, F, and G,
and an accompanying CD-ROM

Professional Paper 1652

U.S. Department of the Interior
U.S. Geological Survey

U.S. Department of the Interior
Gale A. Norton, Secretary

U.S. Geological Survey
Charles G. Groat, Director

U.S. Geological Survey, Reston, Virginia: 2004
First printing: 2004

For sale by U.S. Geological Survey, Information Services
Box 25286, Denver Federal Center
Denver, CO 80225

For more information about the USGS and its products:
Telephone: 1-888-ASK-USGS
World Wide Web: http://www.usgs.gov/

ISBN = 0-607-94344-0

Volume Contents

Summary and Conclusions from Investigation of the Effects of Historical Mining in the Boulder River Watershed, Jefferson County, Montana

By U.S. Geological Survey

Chapter A of

Integrated Investigations of Environmental Effects of Historical Mining in the Basin and Boulder Mining Districts, Boulder River Watershed, Jefferson County, Montana

Edited by David A. Nimick, Stanley E. Church, and Susan E. Finger

Professional Paper 1652–A

U.S. Department of the Interior
U.S. Geological Survey

Contents

Figures

Chapter A
Summary and Conclusions from Investigation of the Effects of Historical Mining in the Boulder River Watershed, Jefferson County, Montana

By U.S. Geological Survey

Introduction

The Boulder River watershed is one of many watersheds in the western United States where historical mining has left a legacy of acid mine drainage and elevated concentrations of potentially toxic trace elements. Abandoned mine lands commonly are located on or affect Federal land. Cleaning up these Federal lands will require substantial investment of resources. As part of a cooperative effort with Federal land-management agencies, the U.S. Geological Survey implemented an Abandoned Mine Lands Initiative in 1997. The goal of the initiative was to use the watershed approach to develop a strategy for gathering and communicating the scientific information needed to formulate effective and cost-efficient remediation of affected lands in a watershed. The watershed approach is based on the premise that contaminated sites that have the most profound effect on water and ecosystem quality within an entire watershed should be identified, characterized, and ranked for remediation.

The watershed approach provides an effective means to evaluate the overall status of affected resources and helps to focus remediation at sites where the most benefit will be gained in the watershed. Such a large-scale approach can result in the collection of extensive information on the geology and geochemistry of rocks and sediment, the hydrology and water chemistry of streams and ground water, and the diversity and health of aquatic and terrestrial organisms. During the assessment of the Boulder River watershed, we inventoried historical mines, defined geological conditions, assessed fish habitat, collected and chemically analyzed hundreds of water and sediment samples, conducted toxicity tests, analyzed fish tissue and indicators of physiological malfunction, examined invertebrates and biofilm, and defined hydrological regimes. Land- and resource-management agencies are faced with evaluating risks associated with thousands of potentially harmful mine sites, and this level of effort is not always feasible for every affected watershed. The detailed work described in this report can help Federal land-management agencies decide which characterization efforts would be most useful in characterization of other affected watersheds.

Study Area

The Boulder River watershed is located near the town of Basin in southwestern Montana (fig. 1). Our study area includes Basin, Cataract, and High Ore Creeks and the short reach of the Boulder River into which these tributaries flow. The watershed study area does not include the large upstream drainage of the Boulder River or the downstream reach of the Boulder River between Little Galena Gulch and the Jefferson River, even though the effects of historical mining are apparent through this reach. Many of the areas affected by historical mining in the Boulder River watershed are within the Beaverhead-Deerlodge National Forest or on land managed by the Bureau of Land Management (Church, Nimick, and others, this volume, Chapter B).

The Boulder River watershed study area encompasses the Boulder and Basin mining districts. Mining of ore deposits containing base metals (copper, lead, and zinc) and precious metals (primarily silver and some gold) started in the early 1860s. The main period of mining was from about 1880 to 1907, and peak production occurred during 1895–1903. Mining had generally ceased by the 1940s. Ore deposits were found primarily in polymetallic quartz-vein deposits, which are thin (less than 50 feet wide) and occur within granitic host rocks, which are widespread in the watershed (O'Neill and others, this volume, Chapter D1). More than 140 inactive mines, such as the Eva May mine (fig. 2), and mining-related sites lie in the Boulder River watershed study area (Martin, this volume, Chapter D3). These sites include mines, where ore was recovered; prospects, where rock was removed in search of ore deposits; and mills, where ore was crushed and processed to concentrate the valuable metals.

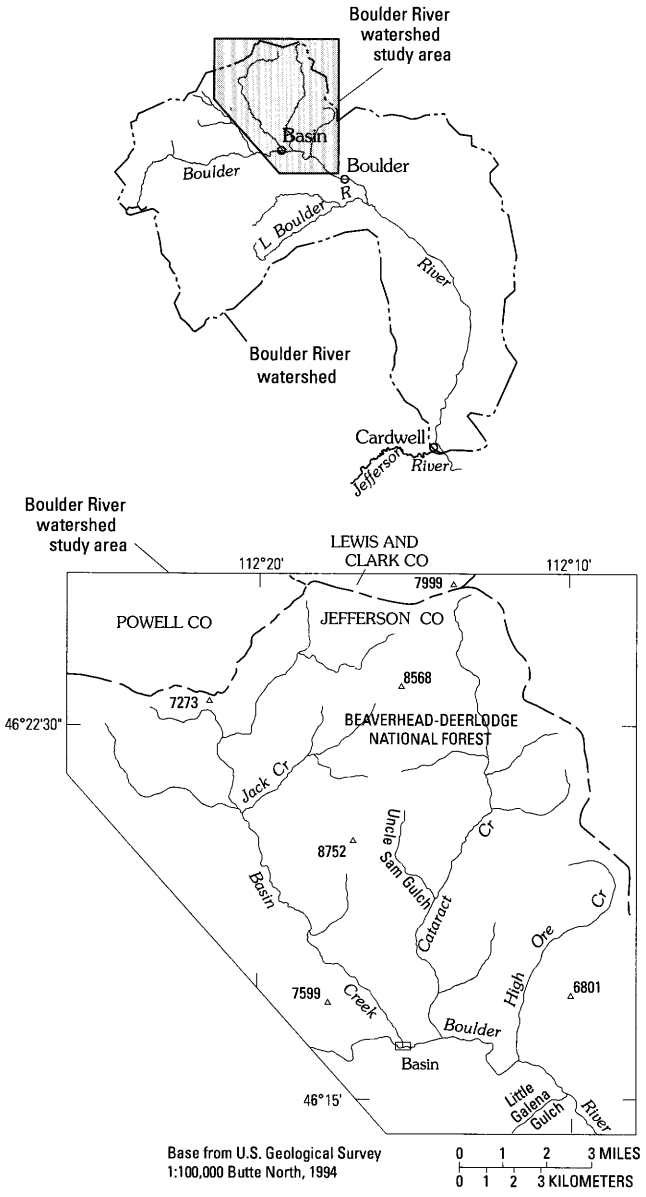

Figure 1. Location of Boulder River watershed and watershed study area, Montana. Elevations are in feet.

Environmental Effects

During historical mining, mine waste and mill tailings were discharged with little regard for any potential effect on the landscape or streams (fig. 3). Although most mining in the Boulder River watershed occurred nearly a century or more ago, effects on the environment are still present today. Physical manifestations of these effects were evident locally as land disturbances, unvegetated areas, and colorful mine drainage near mine and mill sites. At a watershed scale, these effects occurred primarily in streams, where aquatic organisms are affected downstream from the historical mine and mill sites.

In some mining districts, trace-element concentrations in soil, streambed sediment, stream water, and aquatic organisms were elevated long before any mining occurred because mineralized rocks were weathering and contributing acid and trace elements to streams. However, in the Boulder River watershed, this was not the case (Nimick and Cleasby, this volume, Chapter D5; Church, Unruh, and others, this volume, Chapter D8). At present, acidic and trace-element-rich water within the study area is associated with

- mine adits that opened and exposed the quartz-vein deposits and channeled subsurface water to the surface, or
- dumps containing mineralized mine waste or mill tailings.

Prior to mine development, the quartz-vein deposits likely produced small amounts of acid, which were neutralized by the moderate acid-neutralizing potential contained in many of the rocks in the watershed (McCafferty and others, this volume, Chapter D2).

The most important environmental effect of historical mining in the watershed was impairment of aquatic life in streams. All species of fish were absent in stream reaches downstream from a few large mines because of the high trace-element concentrations caused by acid mine drainage (fig. 4). Farther downstream, trout were found in these highly contaminated reaches, but exposure to high trace-element concentrations affected the health of these fish. The presence of dissolved trace elements in the water column was shown to directly affect fish. Similarly, the presence of toxic trace elements in streambed sediment was shown to affect the aquatic food chain of fish and cause health effects through dietary exposure in trout (Farag and others, this volume, Chapter D10).

Ongoing drainage from historical mine sites has degraded the quality of water in some stream reaches. In most streams, pH values were near-neutral to slightly alkaline, but a few small streams were acidic because of drainage from mine adits. Concentrations of cadmium, copper, lead, and zinc, which are the trace elements that most strongly affect aquatic organisms in watershed streams, commonly exceeded chronic aquatic-life standards established by the U.S. Environmental Protection Agency. The highest concentrations (fig. 5, zinc as example) were in streams downstream from three large inactive mines: Crystal mine in a tributary to Cataract Creek, Comet mine in High Ore Creek, and Bullion mine in a tributary to Jack Creek (Nimick and Cleasby, this volume).

Trace elements derived from mine waste and acidic drainage typically accumulate in streambed sediment. Similar to the pattern found for water, the highest concentrations of trace elements in streambed sediment occurred immediately downstream from the Comet, Crystal, and Bullion mines. For example, figure 6 shows the pattern of concentrations of zinc, which is one of the trace elements that strongly affect aquatic organisms. All major tributary basins (Basin, Jack, Cataract, and High Ore Creeks and Uncle Sam Gulch) and the Boulder River downstream from Basin Creek had concentrations of arsenic, copper, and lead that exceeded the apparent effects threshold for aquatic organisms. These effects were traced in the Boulder River for a distance of 55 miles downstream to the confluence with the Jefferson River (Church, Unruh, and others, this volume).

Figure 2. Eva May mine in Cataract Creek valley, September 1998. Photograph by D.A. Nimick.

Figure 3. Mill tailings in High Ore Creek valley at Comet mine site, October 1996. Photograph by D.A. Nimick.

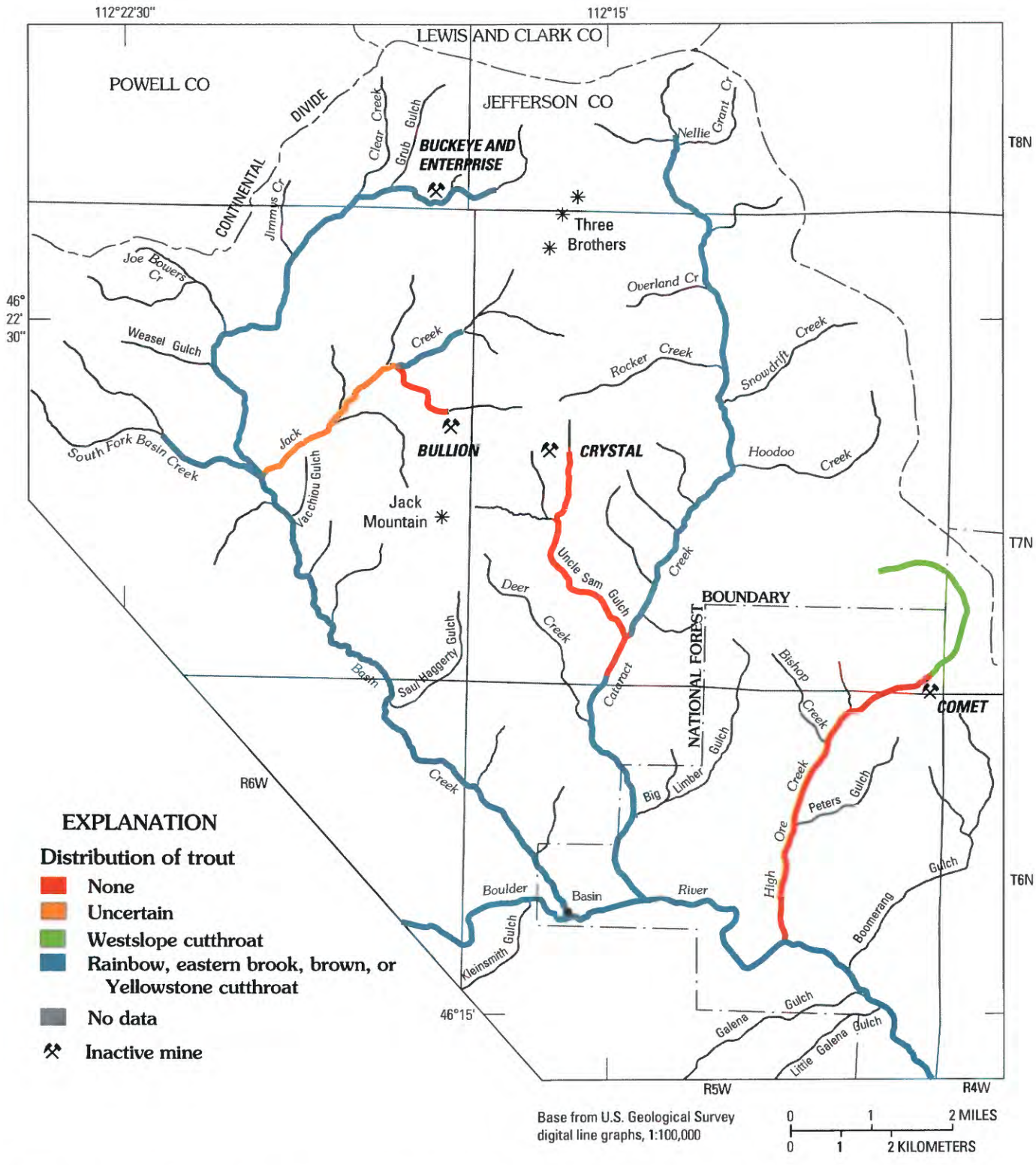

Figure 4. Estimated distribution of trout in study area prior to start of large-scale remediation activities.

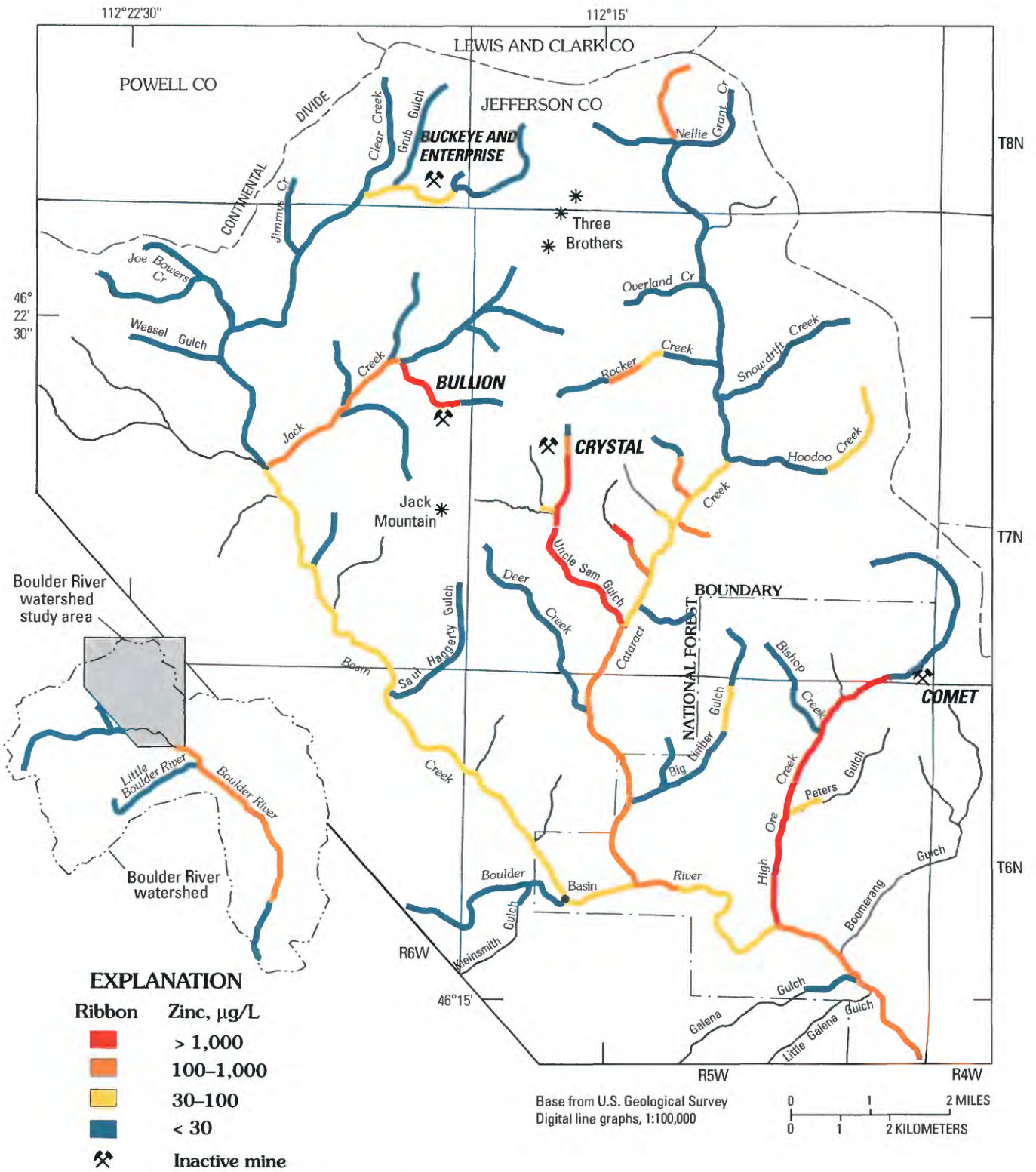

Figure 5. Approximate concentrations of dissolved zinc during low streamflow conditions, 1991–2000.

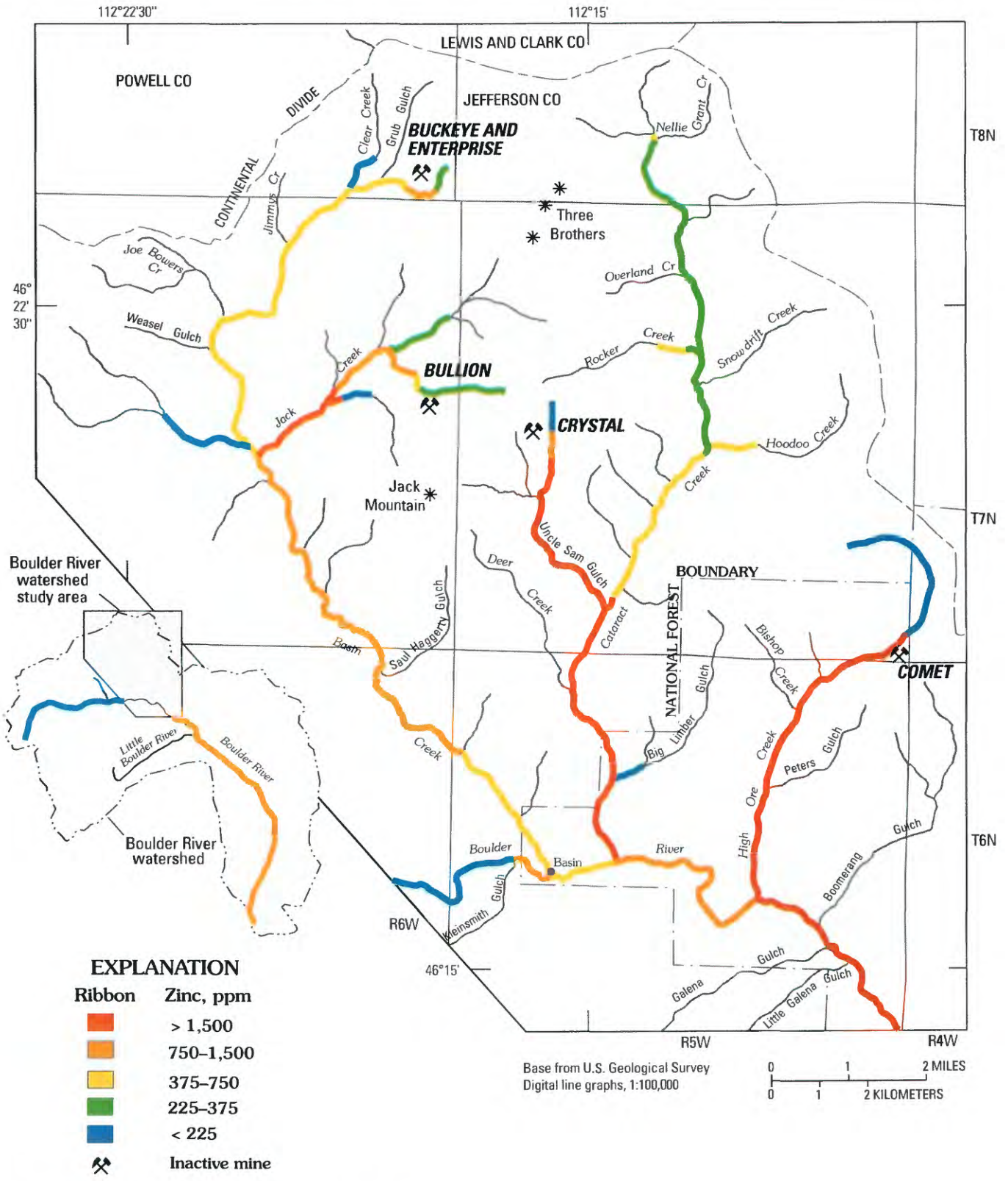

Figure 6. Concentrations of zinc in streambed sediment.

Sources of Trace Elements

Land-management agencies are charged with the task of remediating inactive mines in the Boulder River watershed. Numerous inactive mine sites contribute trace elements to streams in the study area. Therefore, the challenge facing the agencies is one of source determination. The highest concentrations of cadmium, copper, lead, and zinc in water, streambed sediment, and aquatic organisms occur just downstream from the Crystal, Bullion, and Comet mines. Because the concentrations below these mine sites are so high, the three sites clearly are the major sources of trace elements in the watershed. However, the main delivery mechanism for trace elements is not the same at each mine site. Study of streambed sediment demonstrated that much of the contaminated sediment in the Boulder River came from High Ore Creek (Church, Unruh, and others, this volume). The dam holding the mill tailings deposited in the High Ore Creek valley from the Comet mill (fig. 3) has been breached and the tailings extensively eroded and transported downstream into the Boulder River (Gelinas and Tupling, this volume, Chapter E2). Study of water quality demonstrated that Cataract and Basin Creeks contributed more than 80 percent of the dissolved cadmium and more than 50 percent of the dissolved copper and zinc to the Boulder River (Nimick and Cleasby, this volume). These and other data indicated that the Crystal mine (fig. 7) in Uncle Sam Gulch and Bullion mine (fig. 8) in a tributary to Jack Creek were the largest contributors of dissolved trace elements in the watershed (Kimball and others, this volume, Chapter D6). Based on detailed metal-loading studies, discharge from one or two adits was by far the most significant source of trace elements at each of these mine sites.

The overall conclusion from our analysis of trace-element sources is that three large mines appear to be the most important sources of trace elements in the Boulder River watershed (Finger, Farag, and others, this volume, Chapter C). Smaller loadings occur from some other sites, such as the Buckeye mine and mill and Enterprise mine in upper Basin Creek and the Hattie Ferguson, Boulder Chief, Ida M., and Eva May mine sites along Cataract Creek.

Potential for Restoration

Many of the mine sites identified as contributors of trace elements have been targeted for remediation by Federal land-management agencies. Large-scale remediation efforts began in 1997 at the Comet mine in High Ore Creek. The Montana Department of Environmental Quality removed the large quantity of mill tailings (about 500,000 yd^3 or about 750,000 tons) that had been impounded in the valley (fig. 3). In 1999, the Bureau of Land Management began removal and in-place treatment of tailings that had been washed downstream by floods and deposited on the High Ore Creek flood plain. The United States Department of Agriculture (USDA) Forest Service began remediation efforts at the Buckeye and Enterprise mine site in 2000 (fig. 9) and at the Bullion mine in 2002. Part of the earlier planning efforts by USDA Forest Service had been location of suitable repository sites for safe storage of mine waste and mill tailings removed from historical mine sites. The U.S. Environmental Protection Agency (USEPA) has recently taken over the open pit at the recently closed Basin Creek mine and converted it to a regional repository (Smith and others, this volume, Chapter E3) for mine wastes in the Boulder River and other neighboring watersheds. Basin and Cataract Creeks were added to the National Priority List (Superfund) in 1999. Soon afterwards, USEPA began removing mine and mill waste within the town of Basin, and in 2002, began cleanup work at the Crystal mine. However, to date (2003), no work has been initiated to remediate acid drainage coming from mine adits such as those at the Crystal, Bullion, or Enterprise mines.

Monitoring is an important tool for evaluating the effectiveness of remediation efforts and assessing the extent of ecological restoration. Without collecting and analyzing comprehensive monitoring data, land managers cannot objectively evaluate how successfully a remedial action performs and whether remediation goals have been met. In the Boulder basin, the primary focus of the watershed approach has been on the identification of factors affecting the health and potential for recovery of the aquatic community and its supporting habitat. Ongoing monitoring of High Ore Creek has shown that remediation has substantially reduced dissolved zinc concentrations, but that dissolved arsenic concentrations have increased slightly, probably because the imported material used to amend mine wastes increases the solubility of arsenic (fig. 10). Monitoring has also recorded improvements in High Ore Creek after remediation (Gelinas and Tupling, this volume). Continued improvements in water quality and reduced sediment loading should result in improved survival, growth, and reproduction in the fish community. Future monitoring that incorporates biological and chemical measurements will be able to demonstrate the degree of success of all cleanup projects in the watershed. However, the success of ecological restoration will be determined not only by the degree of improvement achieved in the aquatic environment, but also by the recovery of associated flood-plain and riparian habitat within the watershed. Although not specifically addressed in this volume, the issues of revegetation of the riparian area and stabilization of the flood plain are important to land managers in the overall environmental restoration of an area. Monitoring the improvement of flood-plain and riparian soils after the physical removal of tailings can be accomplished by use of both geochemical characterization and soil toxicity assessments. Such monitoring can determine the potential for successful revegetation of an area. In addition, monitoring the health and recovery of wildlife communities dependent on this terrestrial habitat can provide valuable information on ecological restoration. Although economic limitations often result in the reduction or elimination of a monitoring program following cleanup, only through a well-designed and rigorously implemented monitoring program can the success of a remedial effort be validated (Finger, Church, and Nimick, this volume, Chapter F).

Figure 7. Crystal mine, June 1997. Acidic discharge drains from adit (out of view near lower right of photograph) to Uncle Sam Gulch on far left. Photograph by D.A. Nimick.

Figure 8. Bullion mine, August 1998. Acidic drainage flows downhill from mine adit behind mine-waste piles in top center of photograph. Photograph by D.A. Nimick.

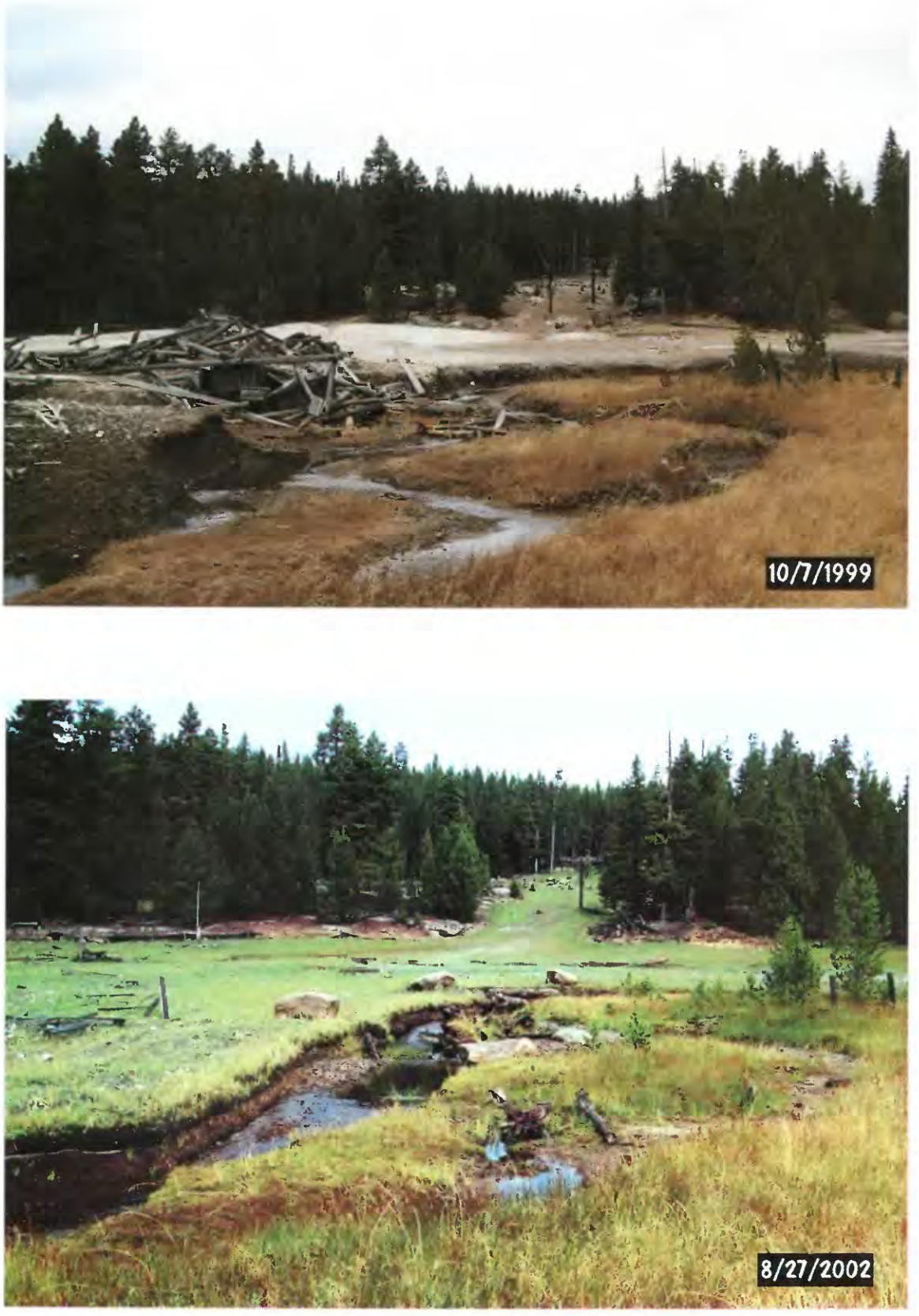

Figure 9. Buckeye flotation mill site, upper Basin Creek, before (top) and after (bottom) remediation. Photographs by Ray TeSoro.

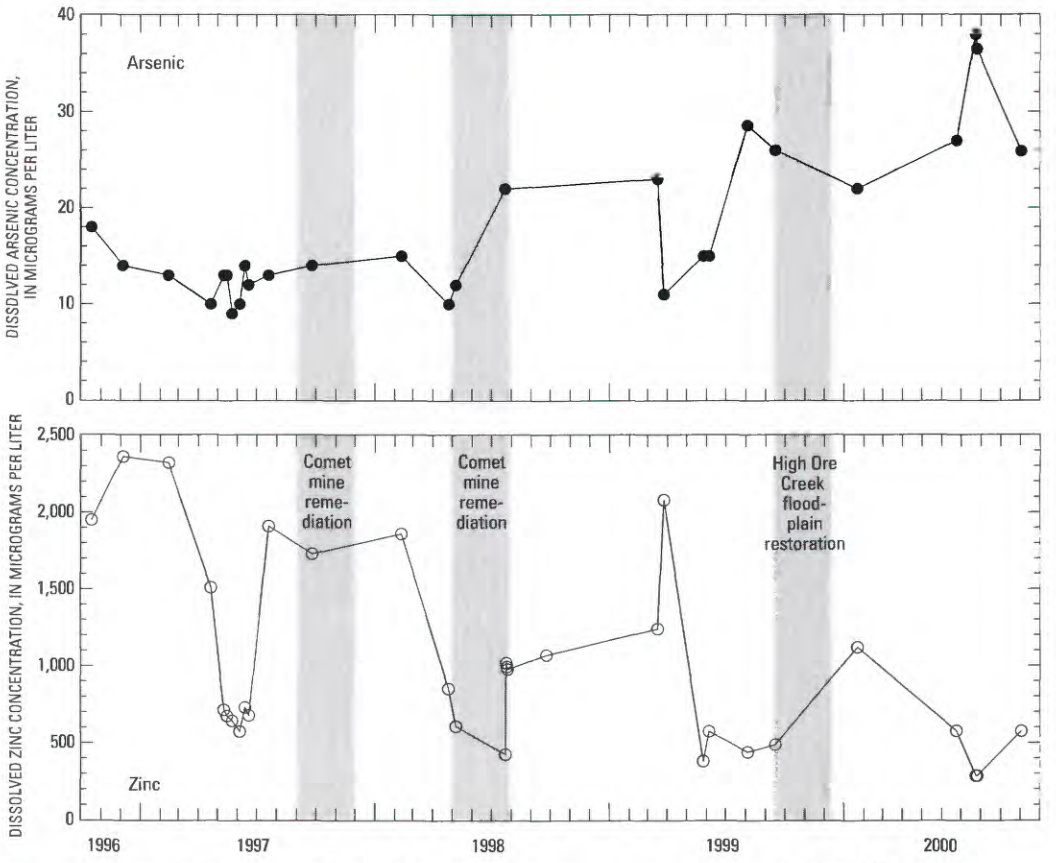

Figure 10. Dissolved arsenic (top) and zinc (bottom) concentrations at mouth of High Ore Creek, 1996–2000.

The Boulder River Watershed Study, Jefferson County, Montana

By Stanley E. Church, David A. Nimick, Susan E. Finger, and J. Michael O'Neill

Chapter B of

Integrated Investigations of Environmental Effects of Historical Mining in the Basin and Boulder Mining Districts, Boulder River Watershed, Jefferson County, Montana

Edited by David A. Nimick, Stanley E. Church, and Susan E. Finger

Professional Paper 1652–B

U.S. Department of the Interior
U.S. Geological Survey

Contents

Figures

Chapter B
The Boulder River Watershed Study, Jefferson County, Montana

By Stanley E. Church, David A. Nimick, Susan E. Finger, and J. Michael O'Neill

Introduction

Thousands of inactive hard-rock mines have left a legacy of acid drainage and toxic metals across mountain watersheds in the western United States. More than 40 percent of the watersheds in or west of the Rocky Mountains have headwater streams in which the effects of historical hard-rock mining are thought to represent a potential threat to human and ecosystem health. In many areas, unmined mineral deposits, waste rock, and mill tailings in abandoned mine lands (AML) may increase metal concentrations and lower pH, thereby contaminating the surrounding watershed and ecosystem. Streams near abandoned, inactive mines can be so acidic or metal laden that fish and aquatic insects cannot survive and terrestrial bird species are negatively affected by uptake of metals through the food chain. Although estimates of the number of abandoned, inactive mine sites vary, observers agree that the scope of this problem is huge, particularly in the western United States where public lands contain thousands of inactive mines. Clearly, remediation of Federal lands affected by inactive historical mines will require substantial investment of resources.

Numerous AML sites are located on or adjacent to public lands, or affect aquatic or wildlife habitat on public lands. In 1995, personnel from a U.S. Department of the Interior and U.S. Department of Agriculture (USDA) interagency task force, including the Bureau of Land Management, National Park Service, USDA Forest Service, and U.S. Geological Survey (USGS), developed a coordinated strategy for the cleanup of environmental contamination from inactive historical mines associated with Federal lands. As part of the interagency effort, the USGS implemented an Abandoned Mine Lands Initiative to develop a strategy for gathering and communicating the scientific information needed to formulate effective and cost-efficient remediation of inactive historical mines on Federal land. Objectives of the AML Initiative included watershed-scale and site characterization, understanding of the effect and extent of natural sources, and communication of these results to stakeholders, land managers, and the general public. Additional objectives included transfer of technologies developed within the AML Initiative into practical methods at the field scale and demonstration of their applicability to solve this national environmental problem in a timely manner within the framework of the watershed approach. Finally, developing working relationships with the private sector, local citizens, and State and Federal land-management and regulatory agencies will establish a scientific basis for consensus and an example for future investigations of watersheds affected by inactive historical mines.

The combined interagency effort has been conducted in two pilot watersheds (fig. 1), the upper Animas River watershed in Colorado (U.S. Geological Survey, 2000) and the Boulder River watershed in Montana. In selection of a pilot watershed in Montana for the AML Initiative, five candidate watersheds were considered. These watersheds were ranked on the basis of geologic factors, metal loading, the status of ongoing remediation activities, general knowledge of the candidate watersheds, and extent of Federal lands within the watershed. The Boulder River watershed was selected from these five candidate watersheds in May 1996.

Land-management and regulatory agencies face two fundamental questions when they approach a region or watershed affected by abandoned mines. First, with potentially hundreds of dispersed contaminated inactive historical mine sites, how should resources for prioritizing, characterizing, and restoring the watershed be invested to achieve cost-effective and efficient cleanup? Second, how can realistic remediation targets be identified, considering

- The potential for adverse effects from unmined mineralized deposits (including any effects that may have been present even under premining conditions or still may persist from unmined deposits adjacent to existing abandoned or inactive mines)

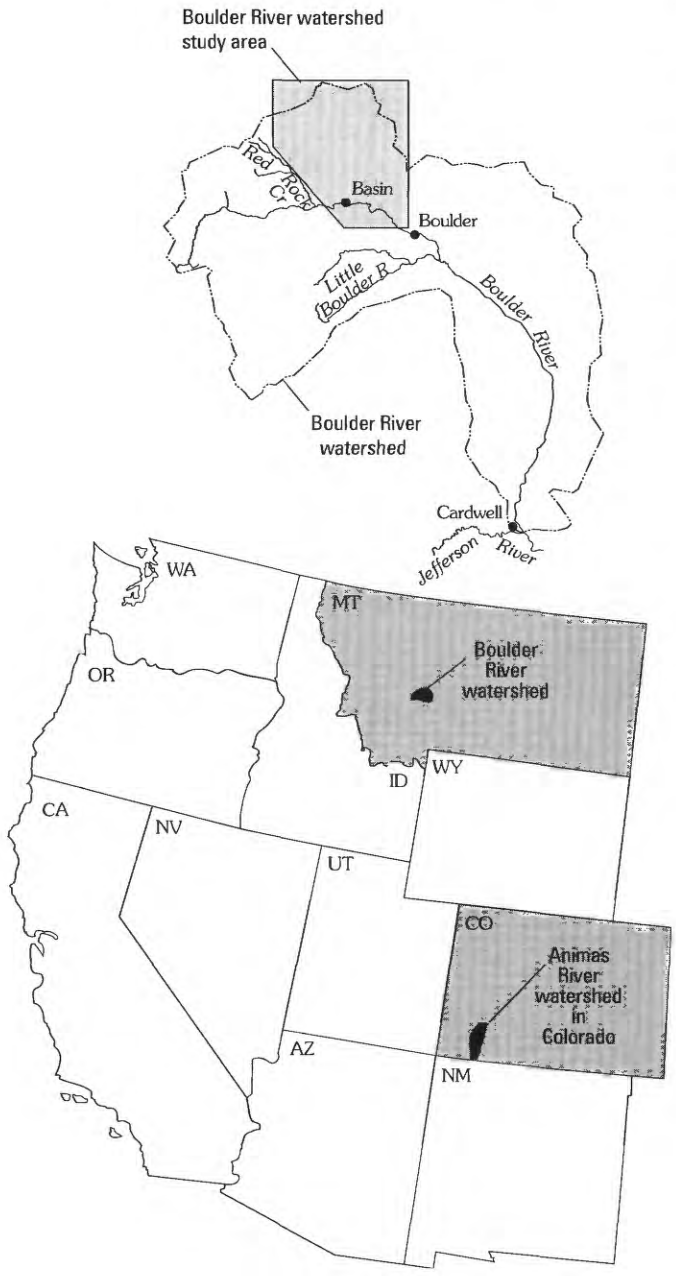

Figure 1. Location of the Boulder and Animas River watershed study areas in the western United States. Watershed boundaries are based on the 8-digit hydrologic units as defined by U.S. Geological Survey (1982).

- The possible impact of incomplete cleanup of specific inactive historical mine sites
- Other factors that may limit sustainable development of desired ecosystems?

To answer these questions, the Abandoned Mine Lands Initiative adopted a watershed approach rather than a site-by-site approach to characterize and remediate abandoned mines (Buxton and others, 1997). This approach is based on the premise that watersheds affected by acid mine drainage in a State or region should be prioritized on the basis of its effect on the biologic resources of the watershed so that the resources spent on remediation will have the greatest benefit on affected streams. Within these watersheds, contaminated sites that have the greatest impact on water quality and ecosystem health within the watershed would then be identified, characterized, and ranked for remediation. The watershed approach establishes a framework in which interdisciplinary scientific knowledge and methods can be employed at similar inactive historical mine sites throughout the Nation. The watershed approach

- Gives high priority to actions most likely to significantly improve water quality and ecosystem health
- Enables assessment of the cumulative effect of multiple and (or) nonpoint sources of contamination
- Encourages collaboration among Federal, State, and local levels of government and stakeholders
- Provides information that will assist disposal-siting decisions
- Accelerates remediation and reduces total cost compared to remediating on a site-by-site basis
- Enables consideration of revenue generation from selected sites to supplement overall watershed remediation costs.

This report provides a detailed review of work conducted in the Boulder River watershed during 1996–2000. The objectives of this work were to

- Estimate premining geochemical baseline (background) conditions
- Define current geochemical baseline conditions
- Characterize processes affecting contaminant dispersal and effects on ecosystem health
- Develop remediation goals on the basis of scientific study of watershed conditions
- Transfer data and information to users in a timely and effective manner.

Expertise in water quality, hydrology, geology, geochemistry, geophysics, biology, mapping, and digital-data collection and management was applied during these investigations. Investigations were coordinated with stakeholders, the Montana Department of Environmental Quality, Montana Fish, Wildlife and Parks, Montana Bureau of Mines and Geology, U.S. Environmental Protection Agency, USDA Forest Service, and Bureau of Land Management, all of which are coordinating the design and implementation of remediation activities within the watershed.

Acknowledgments

Our work would not have been possible without the assistance of individuals in several State and Federal agencies. We thank personnel in the following agencies:

Montana Fish, Wildlife and Parks, particularly Don Skaar, Ron Spoon, and Kurt Hill, for their assistance with collection and analysis of fisheries data.

U.S. Fish and Wildlife Service, particularly Elizabeth MacConnell, for assistance with analysis of fisheries data.

Montana Department of Environmental Quality, particularly Vic Anderson and Ben Quinones, for providing data on their agency's efforts to evaluate mine sites.

Montana Bureau of Mines and Geology, particularly John Metesh for data and discussions on particular mines and their impact on the environment, and Joel Hall for his assistance with merging of the two geologic maps.

U.S. Environmental Protection Agency, particularly Mike Bishop for his efforts to coordinate subsequent Superfund work in the Boulder River and Tenmile Creek watersheds, and Steve Way for providing U.S. EPA and unpublished contractor reports related to the Luttrell pit.

USDA Forest Service, particularly Robert Wintergerst, Ray TeSoro, David Ruppert, Grant Godbolt, and Pat Barringer, for GIS data sets and general information about the study area, and for arranging access to some private lands.

Bureau of Land Management, particularly Tim Bozorth and Mike Browne, for their support and information on environmental issues in the High Ore Creek basin.

We also thank Dan Adams, Basin Creek mine geologist, formerly of Pegasus Gold Corp., for his assistance with the report on the Luttrell pit (Smith and others, this volume, Chapter E3). Finally, we thank the land owners in the Boulder River watershed who allowed us access to their property during this study. We also thank the residents of the towns of Basin and Boulder, Mont., for their hospitality while we were conducting fieldwork in the area.

Funding for some of the site-characterization work in the study area was provided by the USDA Forest Service and U.S. Environmental Protection Agency.

Description of Study Area

The Boulder River watershed is located in southwestern Montana (fig. 1). The Boulder River watershed study area, as defined in this study, is the drainage area of three large tributaries (Basin, Cataract, and High Ore Creeks) and the approximately 9 mi reach of the Boulder River that extends from just upstream to just downstream of these tributaries. The watershed study area does not include the large upstream drainage of the Boulder River or the reach downstream to the Jefferson River, even though effects of historical mining are apparent through these reaches. Studies focused on the watershed; however, some added sampling and regional investigations were conducted outside this study area to document the extent of enriched trace-element concentrations in adjacent areas and to provide reference localities unaffected by historical mining. The Basin and Cataract Creek basins are within the Beaverhead-Deerlodge National Forest, while much of the land in the High Ore Creek basin is managed by the Bureau of Land Management.

The watershed area is mountainous (fig. 2): elevations range from about 4,900 to 8,800 feet above sea level. Mean annual precipitation ranges from about 18 to 26 in./yr (Parrett, 1997). Although the population varies seasonally as temporary residents move into the area during the summer, about 200 people live year-around in the Boulder River watershed study area. Residents are engaged primarily in mining, logging, or tourism.

For ease of discussion, figure 2 includes various basin and subbasin boundaries where work in the study area was concentrated. In the Basin Creek basin, the upper Basin Creek subbasin and the Jack Creek subbasin contain the Buckeye and Bullion mine sites, respectively. The Cataract Creek basin is subdivided into the upper, middle, and lower Cataract Creek subbasins and the Uncle Sam Gulch subbasin, which contains the Crystal mine. The High Ore Creek basin has not been subdivided.

The trace elements in which we were particularly interested for this investigation were those related to the mineral deposits in the watershed and that occur in concentrations sufficiently high to cause concern about their potential effect on aquatic organisms. These trace elements include arsenic, cadmium, copper, lead, silver, and zinc. In contrast, other trace elements such as chromium, cobalt, strontium, titanium, and many others occur in rocks throughout the watershed but are not concentrated in the mineral deposits.

Hydrologic Setting

Streamflow in the Boulder River watershed study area is typical of mountain streams throughout the northern Rocky Mountains. Streamflow is dominated by snowmelt runoff, which typically occurs between April and June; this snowmelt runoff often is augmented by rain. Streamflow typically peaks in May or June and decreases as the shallow ground-water system drains. Spring runoff conditions extend into July. Low streamflow conditions are typical from August to March (fig. 3). The nearest streamflow gauging station is 5 mi downstream of the study area on the Boulder River near Boulder, Mont. Although the magnitude of streamflow is less than at this gauging station, streamflow in study area streams is proportional (based on drainage area) to that at the gauge and has similar seasonality.

Water quality in many study area streams is good; however, water quality is degraded by high trace-element concentrations in reaches downstream from some of the inactive mines. The major-ion chemistry of stream water varies depending on geology and the relative amount of mine drainage. Calcium or calcium-sodium bicarbonate water is the

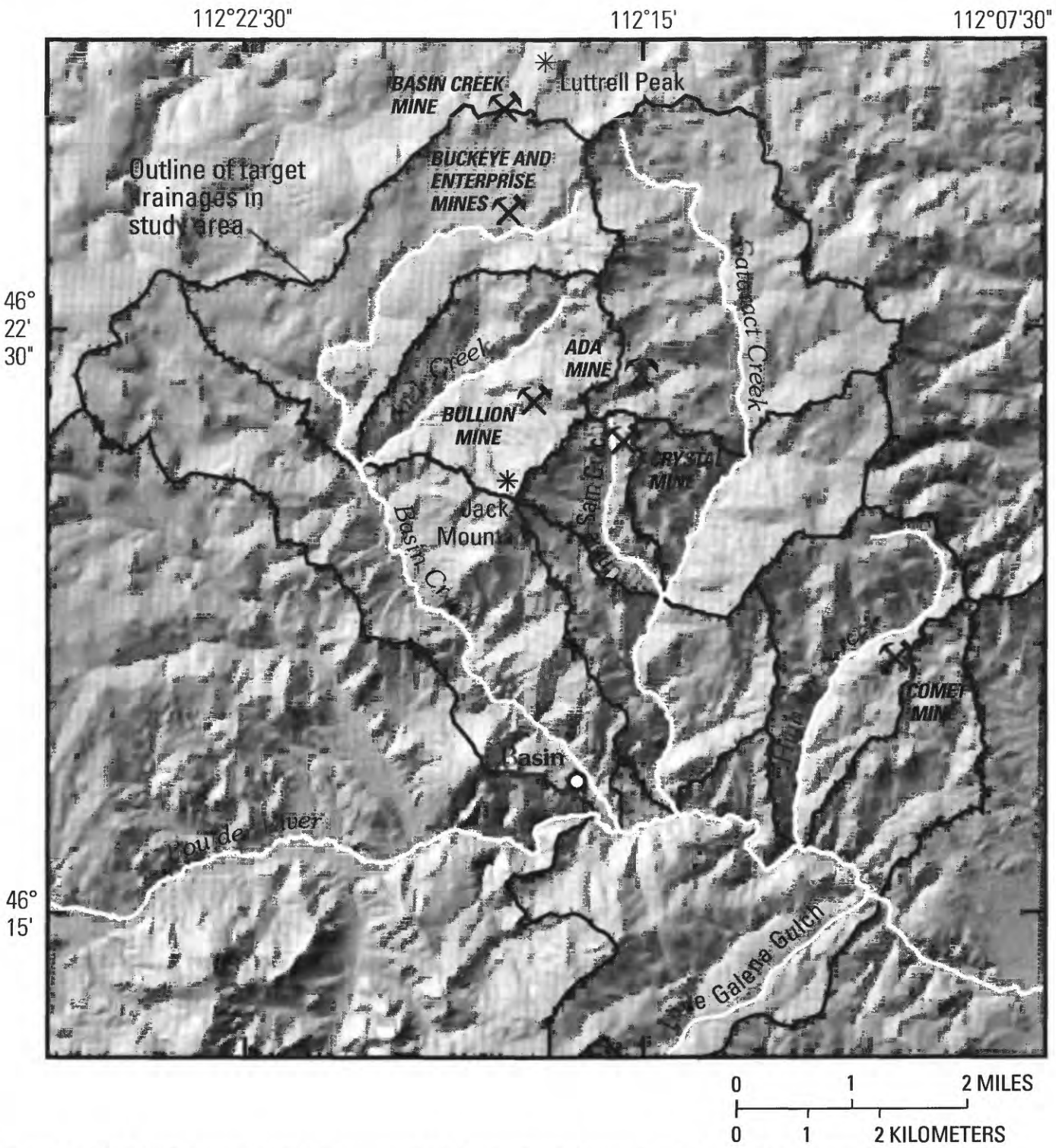

Figure 2. Shaded relief map of Boulder River watershed showing the study area; Boulder River; the three main tributaries—Basin, Cataract, and High Ore Creeks, impacted by past mining in the study area; and selected subbasins. Basin Creek basin was subdivided into three subbasins: upper Basin Creek, which contains the Buckeye mine and the Basin Creek mine; Jack Creek subbasin, which contains the Bullion mine; and lower Basin Creek subbasin. Cataract Creek basin is subdivided into four subbasins: lower, middle, and upper Cataract Creek, and Uncle Sam Gulch subbasins. Drainage from the Crystal mine affects both the Uncle Sam Gulch and the lower Cataract Creek subbasins. High Ore Creek basin, which contains the Comet mine, was not subdivided. The generalized Boulder River watershed study area boundary is the area of these three targeted tributary drainages (outlined in black). Area south of Boulder River, containing Galena and Little Galena Gulches, is not included in this study. Luttrell pit at Basin Creek mine site southwest of Luttrell Peak is the U.S. EPA repository site for mine wastes from both Boulder River watershed and Tenmile Creek watershed to north.

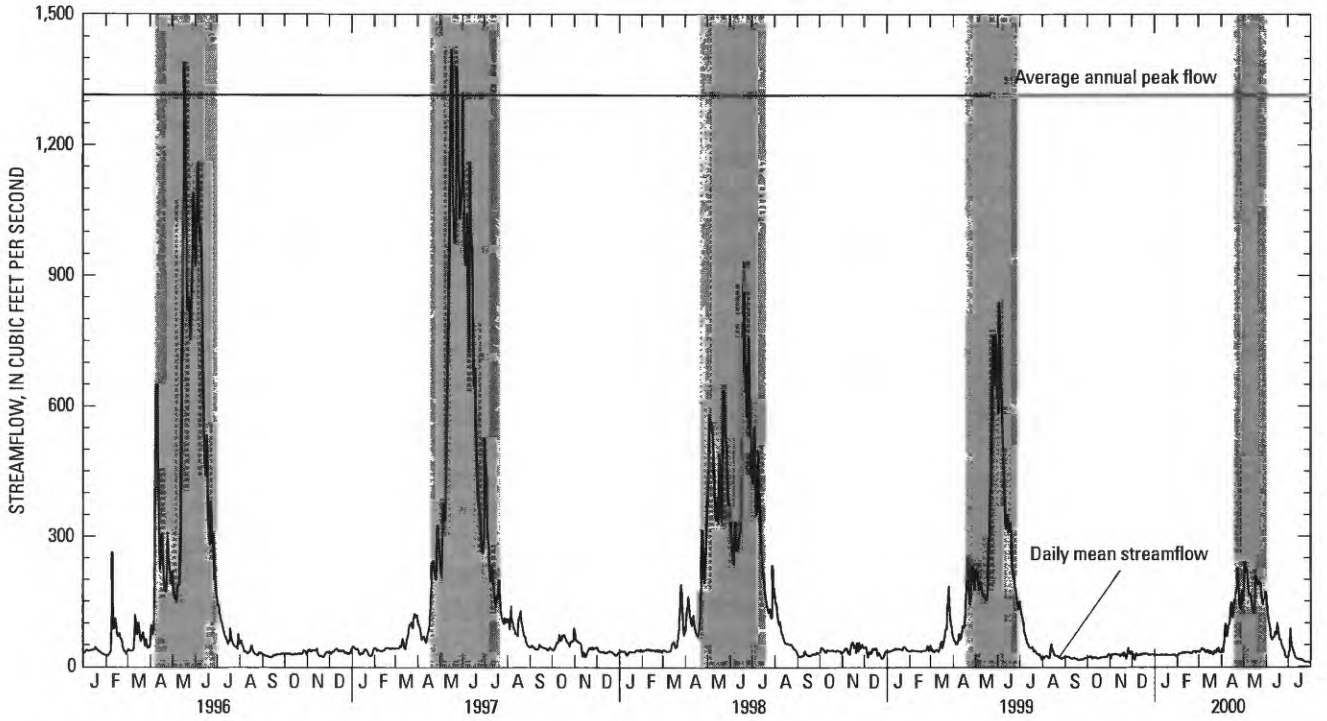

Figure 3. Daily mean streamflow during 1996–2000 at the Boulder River at Boulder, Mont. (USGS gauging station 06033000). Average annual peak flow is for water years 1929–72, 1975, 1981, and 1985–2000. Shaded areas indicate periods of spring runoff, which was arbitrarily defined as streamflow greater than 150 cubic feet per second.

norm. Streams affected by inactive mines have larger proportions of sulfate. All but a few small streams receiving adit discharge have alkaline pH (Nimick and Cleasby, this volume, Chapter D5).

Near-surface ground-water flow is largely controlled by topography, by the distribution of unconsolidated Tertiary and Quaternary deposits that overlie the Boulder batholith (fig. 4), and by the decrease in hydraulic conductivity of geologic units with depth (McDougal and others, this volume, Chapter D9). Topography strongly controls the direction of ground-water flow and the location of discharge areas. Recharge primarily occurs on topographic highs, and greater amounts of recharge occur in areas with the greatest precipitation and hydraulic conductivity. Discharge, in the form of numerous seeps and small springs, occurs in topographic lows and at breaks in slope. The upper, thin unit of unconsolidated deposits has the largest hydraulic conductivity. Flow paths in this near-surface aquifer, from recharge to discharge areas, are short, commonly less than a few thousand feet. Regional ground-water flow is limited by the low permeability of the underlying bedrock, except in areas of high fracture intensity. The uppermost, fractured and weathered zone in the igneous bedrock has a smaller hydraulic conductivity than the overlying unconsolidated deposits but has a much greater hydraulic conductivity than the underlying unweathered granitic to granodioritic Butte pluton. Fractures are the major conduit for ground-water flow in bedrock, with more flow in the uppermost zone (about 50 ft) where the fractures are weathered and fairly open.

Biologic Setting

Little historical information is available on biological communities in the Boulder River watershed (fig. 1), making it difficult to determine biological conditions in this watershed prior to mining. In recent years, however, a complete biological characterization of the watershed was done by the Montana Department of Fish, Wildlife and Parks (1989). Mule deer, elk, moose, and antelope are year-round residents in the Boulder River watershed, and black bear are present seasonally. Mink and beaver also are found in the river and riparian zone.

The Boulder River upstream from the town of Boulder (fig. 1) has a narrow flood plain, and the riparian vegetation is dominated by willow, alder, conifer, and, to a lesser extent, cottonwood and aspen. At the lower elevations, downstream from the town of Boulder, the river meanders with a gradual gradient; as a result, riparian vegetation consists of cottonwood, aspen, and willow. The river supports brook trout, brown trout, rainbow trout, and mountain whitefish; some tributaries of the Boulder River provide habitat for native westslope cutthroat trout. Other species, such as mottled sculpin, longnose dace, longnose sucker, and white sucker, also reside in the Boulder River.

Past mining activity has affected aquatic communities in this watershed. Gardner (1977) found that elevated concentrations of metals and sedimentation affected the distribution and abundance of aquatic invertebrates. Vincent (1975) and Nelson (1976) attributed reduced populations of trout in the lower Boulder River to elevated concentrations of metals in the water and streambed sediment.

Geologic Setting

The geologic setting of a watershed provides a framework for understanding the scope and cause of environmental effects of historical mining. The geologic setting includes the main types of rock and their spatial distribution in the watershed, the degree of faulting and fractures in these rocks, and finally the type and location of the mineralized areas, ore deposits, and associated mines. These factors play an important role in determining the way the watershed responds to mine discharge and waste and in controlling the flow of ground water to and from these sites. In addition, understanding the rock composition and geologic architecture can help identify suitable mine-waste repository sites that have more abundant acid-neutralizing capacity but yet have limited geologic- or fracture-controlled ground-water flow.

The Boulder River watershed is largely underlain by the Cretaceous Boulder batholith, which is a large mass of granitic rock that cooled and crystallized at depth, and the overlying Elkhorn Mountains Volcanics, which formed as the molten granitic magma erupted (fig. 4). This entire assemblage of granitic and volcanic rocks was later eroded so that lower elevation areas of the watershed, such as valley bottoms, generally are carved through granitic rocks while higher elevation areas, such as ridges and mountain tops, are formed in the overlying volcanic rocks.

The bulk of the Boulder batholith within the study area is the granitic to granodioritic Butte pluton (Becraft and others, 1963; Ruppel, 1963; O'Neill and others, this volume, Chapter D1). Most of the intrusive rocks are porphyritic and contain variable amounts of mafic minerals (5–15 percent biotite and hornblende; Ruppel, 1963) and vein calcite, all of which contribute to the acid-neutralization capacity of rocks in the watershed (Desborough, Briggs, and Mazza, 1998; O'Neill and others, this volume). The presence of these minerals may help explain why, in general, few streams in the study area are acidic even though acidic conditions existed at many mine sites. The Elkhorn Mountains Volcanics include welded tuff, tuff and flow breccia, and volcanic sandstone and conglomerate. The volcanic rocks are predominantly quartz latite to andesite and also include varying amounts of mafic minerals. Andesite intrusions within the Elkhorn Mountains Volcanics occur near the confluence of Basin and Jack Creeks (Ruppel, 1963).

Small outcrops of the Lowland Creek Volcanics of Eocene age (Smedes and Thomas, 1965) and of quartz latite composition also are present but are restricted to the southern and eastern parts of the study area. In addition to volcanic rocks, the Lowland Creek Volcanics include tuffaceous sandstone and siltstone as well as structurally controlled northeast-trending dike swarms.

Unconformably overlying the older Elkhorn Mountains and Lowland Creek Volcanics are lower Oligocene rhyolitic flows (younger volcanic rocks in fig. 4), part of the nearby Avon volcanic field. Tertiary rhyolitic flows occur extensively in the western and northern parts of the study area (Becraft and others, 1963; Ruppel, 1963). These rhyolitic rocks host the disseminated gold-pyrite ore deposit in the northern part of the study area near Luttrell Peak (location, fig. 2).

The Butte pluton is extensively jointed; the joints consist of three prominent sets that trend north or east or are subhorizontal (Ruppel, 1963; Becraft and others, 1963). Because the sets of joints in the Butte pluton commonly are filled with leucocratic veins that most likely represent late-stage magmatic fluids, Ruppel (1963) interpreted them to be related to batholithic cooling phenomena. This interpretation has been confirmed on the basis of new $^{40}Ar/^{39}Ar$ ages determined in this study (O'Neill and others, this volume; Lund and others, 2002). Associated with the intrusion of these late-stage aplites is an altered leucocratic granite that is exposed in rubble in Uncle Sam Gulch upstream from the Crystal mine.

The batholithic rocks are cut by numerous faults and lineaments of uncertain age. Some of the faults are mineralized and host the largest ore deposits in the study area. Most of the faults trend east or northeast; a minor but important subset of faults and lineaments trends northwest (fig. 4). The northeast- and northwest-trending faults appear to be recurrently active, related to tectonic activity restricted to the northeast-trending Great Falls tectonic zone (O'Neill and Lopez, 1985) or to southwest-northeast-directed basin and range extension (Reynolds, 1979). The east-trending, strongly mineralized faults or shear zones appear to be related to emplacement of the Boulder batholith (Schmidt and others, 1990; O'Neill and others, this volume).

Acid-neutralizing potential of bedrock is an important control on water quality in mined areas. The granitic rocks that underlie much of the study area contain minerals that provide a moderate amount of acid-neutralizing potential. These minerals include iron and magnesium minerals (for example, biotite and hornblende) that formed when the magma was cooling, and calcite (calcium carbonate) that formed later after the magma cooled. These minerals are widely disseminated and provide significant and widespread acid-neutralizing capacity. The presence of these minerals may help explain why, in general, few streams in the study area are acidic even though acidic conditions existed at many mine sites.

Pleistocene glacial till is present on some of the upland surfaces in the study area. Till is present in many of the flat areas in the valleys, and lateral moraines are present along some of the valleys, such as along Jack Creek. Outwash deposits are present in a few of the larger valleys. Tertiary unconsolidated sand and gravel locally mantle upland surfaces in areas previously mapped as glacial deposits (Ruppel, 1963; J.M. O'Neill, written commun., 1999). Holocene fluvial-alluvial and minor pond and bog deposits have accumulated in the study area along valley floors.

Mining History

The mineral deposits of the Boulder River watershed include disseminated deposits of auriferous pyrite, placer deposits of gold and tin, and a large number of base- and

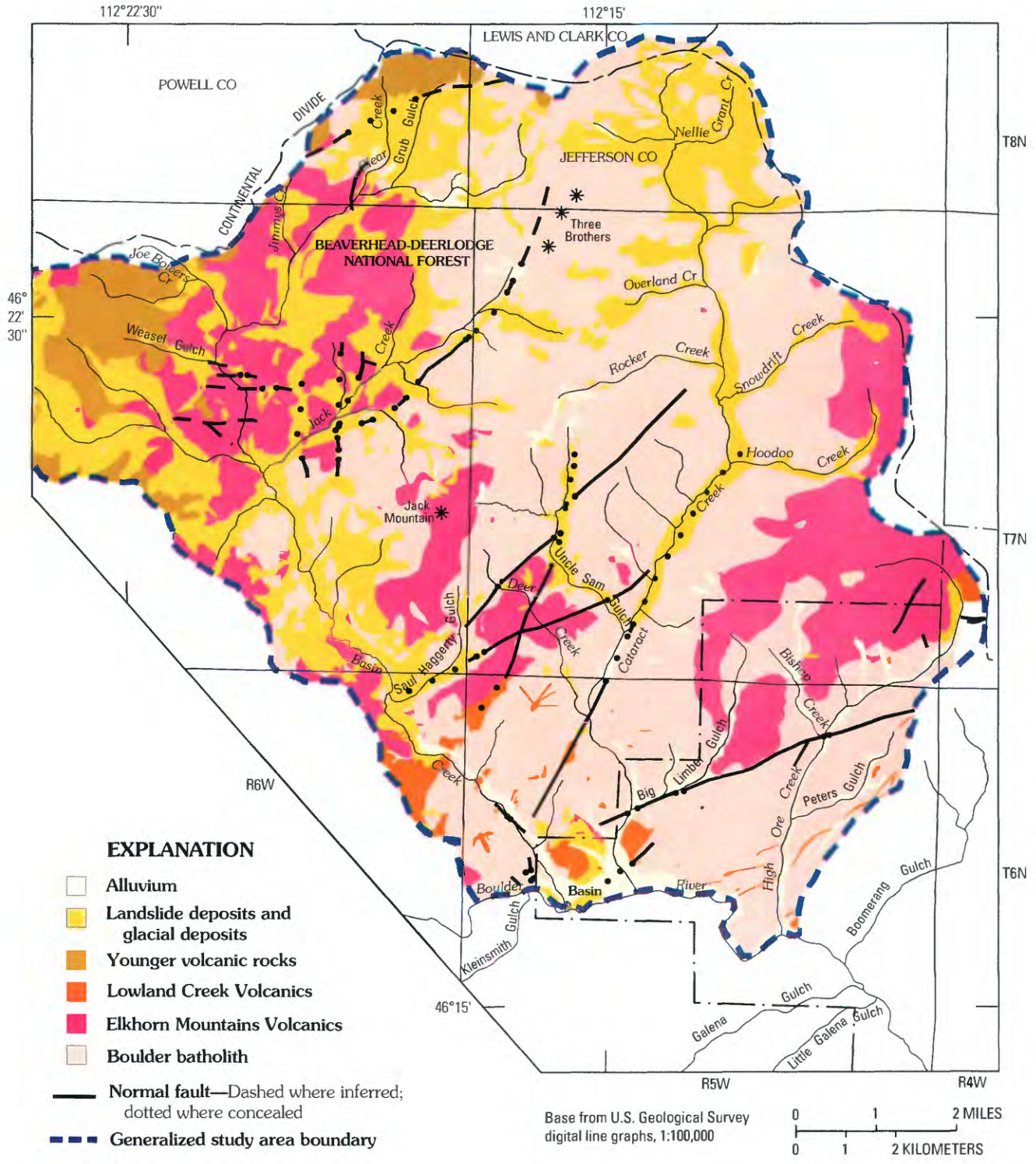

Figure 4. Generalized geology of Boulder River watershed study area (modified from O'Neill and others, this volume, Chapter D1, pl. 1). Dashed outline shows the area of the target drainages in the study area.

precious-metal-bearing quartz veins. Auriferous pyrite occurs in rhyolite on the divide between Tenmile and Basin Creeks at the Basin Creek mine (fig. 2). Most placer deposits are in coarse gravel deposits along upper Basin Creek downstream of the area of rhyolite outcrop (younger volcanic rocks, fig. 4; Becraft and others, 1963; Ruppel, 1963).

The ore deposits in the watershed occur primarily in thin veins, which formed as the last vestiges of molten rock from the cooling granitic body filled thin fractures and small faults in the solidified magma rock and overlying volcanic rocks. These ore deposits are called polymetallic quartz-vein deposits and were mined primarily for silver and for base metals (copper, lead, and zinc), although some contained economic quantities of gold. The inactive mines in the study area are located mostly along these veins. The polymetallic quartz veins typically are short, but some extend for as much as several miles. Most of the largest ore-bearing veins occupy east-trending Late Cretaceous extensional structures. The hydrothermal alteration common in and adjacent to all veins generally is confined to thin zones, typically about 1 ft thick and rarely more than a few feet thick. The veins contain abundant base-metal sulfides with high silver:gold ratios. Pyrite is the most abundant sulfide mineral but had no economic value to miners. Other sulfide minerals, such as arsenopyrite, chalcopyrite, tetrahedrite, galena, and sphalerite, contained the metals that miners targeted.

The Boulder River watershed study area encompasses the Boulder and Basin mining districts. Mining in these districts started in the mid-1860s with the discovery of gold placer deposits. Production of placer gold reached a maximum between 1868 and 1872, although placer operations continued intermittently through about 1940. Roby and others (1960) reported that an estimated 845 fine ounces of placer gold were recovered between 1933 and 1938 from lower Basin Creek. A small amount of placer gold was also recovered from the Boulder River during this time period. Auriferous pyrite deposits that had been mined previously in small underground mines were mined briefly by open-pit and cyanide extraction at the Basin Creek mine in the early 1990s.

The first discoveries of base-metal vein deposits were made at about the same time as the first placer discoveries. Lead-silver ore was discovered at the Ada mine in the early 1860s and gold was discovered at the Buckeye mine in 1868. After 1872, lode mining completely overshadowed placer mining. The main period of lode mining began about 1880, reached a peak between 1895 and 1903, and ended about 1907. Production prior to 1902 is largely undocumented because records were not kept prior to Montana statehood. After 1907, mining was intermittent and largely restricted to a few mines, especially the Comet, Gray Eagle, Crystal, and Bullion mines, which yielded most of the ore mined in the study area (Martin, this volume, Chapter D3). Mining generally had ceased by the 1940s at these mines, but some production continued into the 1960s and 1970s. Figure 5 shows the recorded production from Jefferson County from approximately 1900 through 1958 from the Basin-Cataract mining district (Roby and others, 1960). Many of the smaller mines and prospects were reopened from time to time after 1903 for further exploration and for speculation, but none yielded appreciable quantities of ore (Becraft and others, 1963; Ruppel, 1963). Much of the mining occurred on privately owned (patented) mining claims. However, some mine, mill, and smelter sites, and some mill-tailings deposits, along with eroded tailings distributed along various reaches of stream channels and flood plains, are located on Federal land.

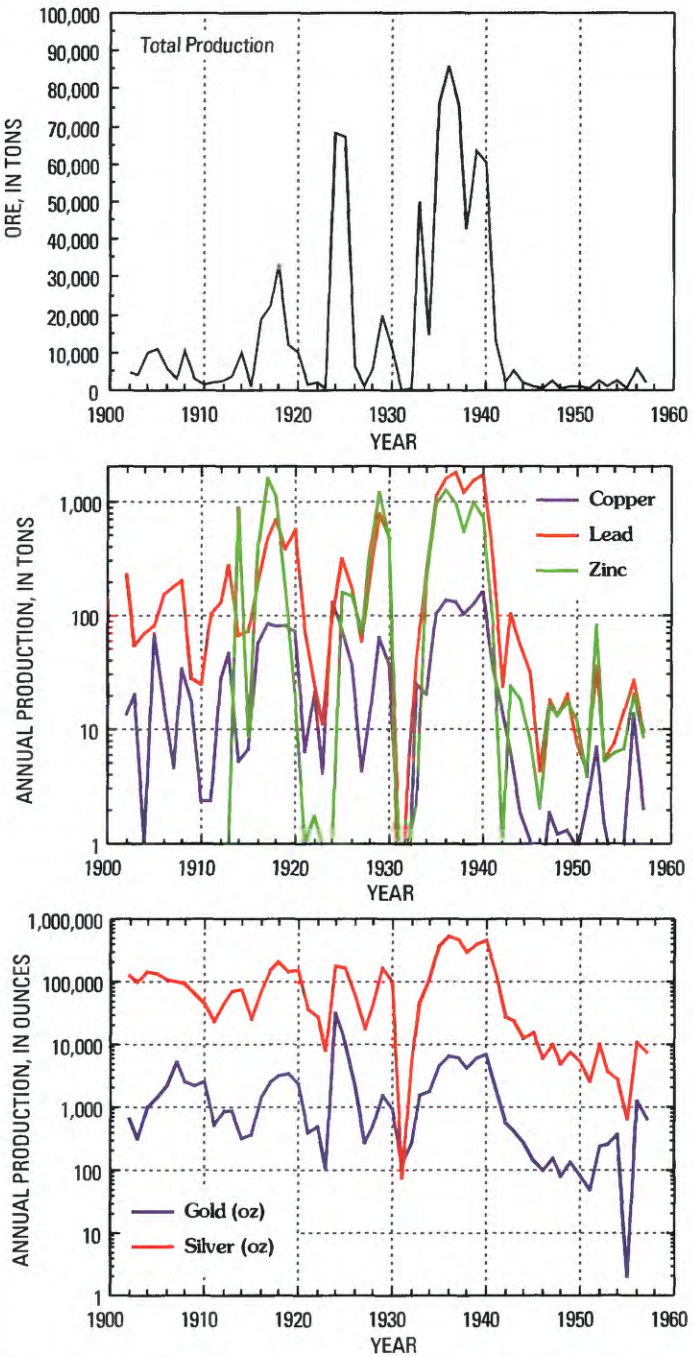

Figure 5. Produced tonnage of copper, lead, and zinc; annual production, expressed as tons (2,000 lb) of ore; and production of gold and silver, in troy ounces, from the Basin-Cataract mining district from 1902 to 1958 (Roby and others, 1960).

In the 1800s and early 1900s, mills treated ores by crushing and grinding and then concentration by gravity separation, or, after about 1914, by flotation methods. Some of the larger mines had small stamp mills at the mine site. Ore from smaller mines was transported to off-site mills. Concentrates from these mills generally were transported to smelters in Basin or outside the Boulder River watershed (Metesh and others, 1994).

More than 140 inactive mine-related sites lie in the Boulder River watershed study area (Martin, this volume). These sites include mines, where ore was recovered, and prospects, where rock was removed in search of ore deposits. Rock that was mined but that had insufficient economic value typically was left near the mine in waste-rock piles. Ore was stockpiled at mine sites for later transport to a mill, and some stockpiles remain in the watershed. Ore was crushed and processed at a mill to concentrate the valuable metals. Wastes from mills, called tailings, typically were discharged to areas, including valley bottoms, downhill from the mill. Many of the mine and mine-related sites in the study area had been inventoried for State and Federal agencies to help target likely mine and mill sites for remediation. Inactive mine-related sites affect streams through direct discharge of acid drainage from adits, seepage from waste-rock and tailings piles, and erosion of tailings piles and fluvial tailings deposits by storm runoff or streambank erosion.

Remediation Activities

Interest in reducing the environmental effects of the many inactive mines and prospects in the Boulder River watershed increased in the 1980s as the studies of the effects of historical mining on water quality increased. One of the first actions taken was the construction of a diversion channel in the 1980s to route High Ore Creek (fig. 2) around the large quantity of tailings deposited in the valley bottom at the Comet mine site. The State of Montana inventoried and ranked inactive mines in the study area (Montana Department of State Lands, 1995) and conducted a preliminary watershed analysis (Montana Department of Environmental Quality, 1997). Federal land-management agencies began planning for cleanup activities in the mid-1990s after the completion of inventories of inactive mines (Metesh and others, 1994, 1995, 1996; Marvin and others, 1997). Studies were conducted to locate suitable sites for small, local mine-waste repositories (Desborough and Fey, 1997; Desborough and Driscoll, 1998; Desborough, Briggs, and Mazza, 1998; Desborough and others, 1998) as well as to site a larger regional repository at the Luttrell pit at the Basin Creek mine (fig. 2; Smith and others, this volume, Chapter E3). In 1997, the State of Montana began cleanup activities at the Comet mine, and large quantities of mill tailings in the High Ore Creek valley bottom were removed to the former open pit at the Comet mine site. In 1999, the BLM removed flood-plain tailings from the valley floor along the 4-mi reach between the Comet mine and the Boulder River (Gelinas and Tupling, this volume, Chapter E2) to a new repository near the Comet mine. In 1999, the U.S. Environmental Protection Agency listed the Basin and Cataract Creek drainages and the adjacent Tenmile Creek drainage immediately to the north as Superfund sites on the National Priorities List. Also in 1999, the U.S. EPA and USDA Forest Service cooperatively developed the Luttrell pit as a repository for mine wastes that would be removed from sites in the Boulder River and Tenmile Creek watersheds. In 2000, the U.S. EPA continued moving mine wastes from the Tenmile Creek area to the Luttrell pit. The USDA Forest Service removed mine wastes and flood-plain tailings from the Buckeye and Enterprise mine area to the Luttrell pit in 2000.

Overview of this Volume

Chapters in this volume are arranged from general conclusions to more specific detailed and technical studies. The following summaries provide an overview and summary of the chapters contained in this report for those who have limited time or are unaware of which subjects presented in the volume would be most applicable to their interests. Chapter A, "Summary and Conclusions from Investigation of the Effects of Historical Mining in the Boulder River Watershed, Jefferson County, Montana," provides a brief summary of our major findings. Historical mining has elevated the concentrations of cadmium, copper, and zinc in surface water of the Boulder River watershed study area. Weathering of mine wastes, and particularly of mill tailings in the study area, has also resulted in elevated concentrations of arsenic, cadmium, copper, lead, and zinc in streambed sediment in Basin Creek downstream from the Buckeye and Enterprise mines, in Jack Creek downstream from the Bullion mine, in Uncle Sam Gulch downstream from the Crystal mine, in High Ore Creek downstream from the Comet mine, and in the Boulder River downstream from the Jib Mill site. Studies of fish in the stream reaches downstream of these sites indicate that fish cannot survive in the most severely affected reaches; chronic effects were documented where trace-element concentrations were significantly elevated. The Montana Department of Environmental Quality, Bureau of Land Management, USDA Forest Service, and U.S. Environmental Protection Agency initiated remediation planning of these sites following our initial characterization studies summarized in this volume.

Chapter C, "Synthesis of Water, Sediment, and Biological Data Using Hazard Quotients to Assess Ecosystem Health," by Susan E. Finger, Aïda M. Farag, David A. Nimick, Stanley E. Church, and Tracy C. Sole, is a multidisciplinary synthesis of the studies conducted in the watershed, using what is called an ecological risk assessment approach. This approach explains the relevance of the combined studies, hydrologic, geologic, and biologic, in terms of remediation and recovery at the watershed level. This chapter evaluates the physical and chemical characteristics of the watershed that may limit the

recovery of those species that are negatively affected by historical mining. Specifically, it evaluates effects of trace-element exposure on fish communities. Such exposure can be from the water in which these organisms live and (or) through the food chain. The potential for adverse biological effects associated with elevated concentrations of cadmium, copper, and zinc in water and streambed sediment is assessed by comparison with aquatic regulatory standards for water and consensus-based sediment-quality guidelines. Ribbon maps showing the distribution of trace elements in stream water and streambed sediment demonstrate the severity of contamination in specific stream reaches within the study area. Chronic effects are documented in trout in some Boulder River tributaries.

Chapter D, consisting of "subchapters" D1–D10, provides the scientific basis for the conclusions and recommendations made in this volume. The subchapters describe detailed scientific studies focused on particular aspects of the Boulder River watershed study.

Chapter D1, "Geologic Framework," by J. Michael O'Neill, Karen Lund, Bradley S. Van Gosen, George A. Desborough, Tracy C. Sole, and Ed H. DeWitt, summarizes the geology of the study area. Polymetallic quartz-vein deposits, which were emplaced along tensional structures in the Butte pluton, formed the sulfide ore veins that were exploited in the Basin and Boulder mining districts between 1868 and about 1970. Premining water and streambed-sediment geochemistry was controlled by the composition of the granitic Butte pluton, which underlies most of the Boulder River watershed study area. In contrast, the water and streambed-sediment geochemistry today is significantly affected by the accelerated weathering of disturbed waste rock and mill tailings produced by historical mining. Studies of the chemistry of the rocks indicate that unaltered Butte pluton probably contained sufficient calcite to neutralize much of the acid generated by sulfides exposed prior to mining.

Chapter D2, "Geophysical Characterization of Geologic Features with Environmental Implications from Airborne Magnetic and Apparent Resistivity Data," by Anne E. McCafferty, Bradley S. Van Gosen, Bruce D. Smith, and Tracy C. Sole, summarizes aeromagnetic and resistivity geophysical data that were collected using airborne data sensors flown over the study area with a helicopter. The airborne geophysical data primarily reflect the mineralogy of the bedrock to depths of several hundred feet and are able to see through shallow ground cover. These data provide a more complete coverage of the bedrock features than can be mapped by standard geologic field methods. The airborne geophysical data were used to show where hydrothermal alteration events caused subtle changes in the mineralogy and chemistry of the Butte pluton. About 20 percent of the Butte pluton has been altered by hydrothermal activity, and these areas of altered rock would not constitute suitable sites for repositories for mine waste, because they have been leached of their acid-neutralizing potential by the hydrothermal alteration processes. The data provide one basis for the interpretation of the environmental geology of the watershed study area.

Chapter D3, "Mine Inventory," by E. Paul Martin, is an inventory of significant mines, mill sites, and prospects in the watershed study area. One hundred forty-three sites were identified from literature searches and then accurately located from digital orthophoto quadrangles (DOQs). Detailed site characteristics, including flow rates and pH of acid mine drainage, numbers of mine features, and size estimates of mill tailings and mine wastes, were compiled into a single database.

Chapter D4, "Metal Leaching in Mine-Waste Materials and Two Schemes for Classification of Potential Environmental Effects of Mine-Waste Piles," by David L. Fey and George A. Desborough, provides data on mine wastes from 10 mine sites in the study area. Mine-waste piles are of particular environmental concern because large quantities of acid and trace elements commonly leach from the rock material in these piles. These factors are key in determining how large an effect an individual mine-waste pile might have on the environment. A new surface-sampling procedure was developed that provided a statistically representative sample of an individual waste pile. These samples were analyzed for total and water-soluble trace-element content of each sample, the amount of specific minerals likely to release acid or trace elements, and the potential to produce or neutralize acid. Two water-leach methods for evaluating metal mobility were compared. The standard EPA 1312 protocol was compared with a less labor-intensive static leach method. Both methods gave similar results. Mineralogical studies of the samples indicated that the secondary sulfates anglesite and jarosite were present in about 80 percent of the mine wastes, indicating active weathering in the mine waste. Results from these chemical analyses suggest that the mine-waste dumps represent an essentially infinite source of water-soluble trace elements and acid.

To help land managers prioritize these piles for remediation, the authors developed a ranking system based on the size of the pile and used results of the chemical analyses in developing the rankings. The ranking system was used to classify 19 waste piles that they had permission to sample. For the sampled mine sites, the ranking system showed that waste piles at the Buckeye, Bullion, Daily West, Cracker, and Boulder Chief mine sites had a high potential for environmental degradation, whereas piles at the Crystal and Sirius mine sites had intermediate potential, and piles at the Morning Marie and Waldy mine sites had low potential.

Chapter D5, "Trace Elements in Water in Streams Affected by Historical Mining," by David A. Nimick and Thomas E. Cleasby, describes surface-water chemistry in the watershed, focusing on variation in major-element chemistry and concentrations, loads, and sources of trace elements. Few stream reaches have pH less than 6.5 in contrast to what is typical of many other historical mining districts. Dissolved concentrations (0.45-micrometer filtered water) of cadmium, copper, lead, and zinc commonly exceeded aquatic-life standards downstream from inactive historical mine sites. Ribbon maps show the distribution of pH and metal concentrations in stream reaches in the watershed. The Bullion, Comet, and Crystal mine sites produced most of the dissolved

trace-element load in the study area. Cataract Creek contributed larger dissolved loads than either Basin or High Ore Creeks.

Chapter D6, "Quantification of Metal Loading by Tracer Injection and Synoptic Sampling, 1997–98," by Briant A. Kimball, Robert L. Runkel, Thomas E. Cleasby, and David A. Nimick, describes the results from detailed metal-loading studies conducted in Cataract Creek, Uncle Sam Gulch, and the Bullion Mine tributary on Jack Creek. Individual sources of metals were identified and quantified from the downstream changes in metal loads in each study reach. Metal loads were calculated using data from the dilution of a tracer (sodium chloride) that was injected at the upstream end of each study reach and from metal concentration data determined in synoptic water-quality samples. The major sources of metal loadings for dissolved metals in these creeks were shown to be the Crystal mine adit flow on Uncle Sam Gulch and the Bullion mine adit flow on the Bullion Mine tributary. The Crystal mine adit flow provided a daily load of about 35 lb of zinc to Cataract Creek whereas the zinc load from the Bullion mine adit was about 7 lb per day. About one-third of the calculated zinc load in Cataract Creek came from unsampled inflows, possibly ground water, and about one-third was lost to colloidal deposition on the streambed.

Chapter D7, "Short-Term Variation of Trace-Element Concentrations during Base Flow and Rainfall Runoff in Small Basins, August 1999," by John H. Lambing, David A. Nimick, and Thomas E. Cleasby, details the short-term variation of arsenic, copper, manganese, and zinc concentrations in High Ore, Jack, and Cataract Creeks. Dissolved zinc concentrations varied by a factor of three in High Ore Creek over the 24-hour observation period. Maximum dissolved zinc concentrations occurred in early morning hours, whereas minimum concentrations occurred in the late afternoon. Interpretation of these data suggests that the cause of this variation may be the sorption of dissolved zinc onto particulate material in the stream as temperature and pH of the water change throughout the day.

Concentrations of these trace elements were also shown to increase in response to runoff during rainfall. The lag time following onset of rainfall before the arrival of the peak concentration of dissolved metals was short, on the order of 3 hours, whereas the decay curve following the rainstorm lasted 8–10 hours. Both phenomena, the changes in trace-element concentrations caused by daily fluctuations in temperature and the changes caused by a rainfall event, may have substantive effects on the toxicity of dissolved trace elements on aquatic life. At sites where the dissolved metal concentrations were measured late in the day, the daily variation would result in a calculated toxicity for aquatic life that would be underestimated. During periods following runoff from a summer thunderstorm, the calculated toxicity would be dependent on the time lag associated with runoff for each mine waste site.

Chapter D8, "Trace Elements and Lead Isotopes in Streambed Sediment in Streams Affected by Historical Mining," by Stanley E. Church, Daniel M. Unruh, David L. Fey, and Tracy C. Sole, is a study of the present streambed-sediment geochemistry of the watershed. Concentrations of arsenic, cadmium, copper, lead, and zinc exceed published sediment-quality guidelines in many of the streams downstream from historical mine sites. The effect of historical mining on trace-element concentrations in streambed sediment in the Boulder River can be followed all the way to the confluence with the Jefferson River 55 mi downstream from the Basin and Boulder mining districts. Studies of the concentrations of these trace elements in premining streambed sediment preserved in terrace deposits in the watershed show that these trace elements are concentrated in streambed sediments today by factors of 50 to 100 times more than were present in the streambed sediment prior to historical mining.

Lead isotopes provide a "fingerprint" that can be used to tie sources of metals to groups of mineral deposits. The signature from the polymetallic veins exploited in the Basin and Cataract Creek basins is different from that in the High Ore Creek basin at the Comet mine. The lead isotope data have been used to quantify the contributions of the inactive historical mines to Boulder River streambed sediment. These calculations indicate that (1) about 35 percent of the lead in streambed sediment of the Boulder River was derived from Basin Creek and the Jib Mill site located on the Boulder River immediately above the confluence of Basin Creek, (2) 13 percent of the lead in streambed sediment was derived from Cataract Creek, and (3) about 50 percent of the lead in streambed sediment was derived from High Ore Creek. Data from streambed sediment in a terrace immediately downstream from the Jib Mill indicate that ores from outside the district were milled at this site and contributed elevated trace-element concentrations to Boulder River streambed sediment.

Chapter D9, "Hydrogeology of the Boulder River Watershed Study Area and Examination of the Regional Ground-Water Flow System Using Interpreted Fracture Mapping from Remote Sensing Data," by Robert R. McDougal, M.R. Cannon, Bruce D. Smith, and David A. Ruppert, describes a reconnaissance level study of ground-water flow in the study area. Ground water can play an important role in determining the extent of contamination in historically mined areas. If ground water moves freely, dispersal of trace elements can be large, whereas if ground-water movement is restricted, effects of historical mining can be more localized. A conceptual model of how ground water flows in the study area was developed based on observations made in the field near the Buckeye, Bullion, and Crystal mines. The model then was used to help interpret the metal-loading studies and field observations made by other scientists. Ground water occurs primarily in the surficial unconsolidated deposits that blanket much of the study area and in the upper 50 ft of the bedrock, where the fractures are open and allow flow. At depth, fractures in the bedrock are tight and restrict ground-water flow. Flow paths for ground water from areas of recharge to areas of discharge are generally short (less than 1,000 ft) because

of the shallow nature of the permeable rocks. Ground-water flow from adits appears to be the major contribution from the ground-water system; ground-water flow through major geologic structures does not appear to contribute significantly to water-quality degradation in the study area. This conceptual idea of ground-water flow was expanded by mapping of linear features visible on images of the watershed taken from satellites and aircraft. These linear features were assumed to represent the expression at the land surface of faults, joints, fractures, and mineralized veins that cut the bedrock. Quantification of the primary orientations, the average lengths, and the relative spatial frequency of the features allowed areas where recharge and discharge might be more likely to be identified.

Chapter D10, "Aquatic Health and Exposure Pathways of Trace Elements," by Aïda M. Farag, David A. Nimick, Briant A. Kimball, Stanley E. Church, Don Skaar, William G. Brumbaugh, Christer Hogstrand, and Elizabeth MacConnell, assesses aquatic community health, food supply, and pathways of exposure for toxic trace elements in the aquatic ecosystem. Laboratory and field methods were applied to evaluate the effects of metals released by past mining activity on fish at the individual organism and the population levels. Population surveys confirmed the absence of fish in some reaches of the watershed near mine sites, but trout populations were documented downstream of these source areas. Instream experiments using caged trout showed that elevated concentrations of cadmium, copper, and zinc in the water column were associated with increased trout mortality at sites near mine-waste sources. Physiological changes in the gill tissue from these fish indicated that the cause of death was related to elevated trace-element concentrations in the water column. Assessment of resident trout revealed impaired health at a downstream site in lower Cataract Creek, where reduced fish population densities also occurred. Exposure pathways and partitioning of metals in the aquatic environment were determined by measurement of trace-element concentrations in water, colloids, streambed sediment, biofilm (that is, algae and bacteria that grow on rocks in the stream), invertebrates, and fish at many sites throughout the watershed. The interrelationship of the trace elements accumulating in these biotic and abiotic components suggests that copper, cadmium, and zinc concentrations increased in fish tissues as a result of direct exposure from water and sediment and from indirect exposure through the food chain. Through contact by these two pathways, the health of aquatic biota in the watershed has been compromised.

Chapter E, consisting of three "subchapters," describes site-specific studies that focused on important aspects of abandoned mine land remediation. The three subchapters describe site characterization of the Buckeye and Enterprise mine sites on upper Basin Creek, water-quality monitoring of the Comet mine on High Ore Creek, and geologic evaluation of the Luttrell pit mine-waste repository site at the Basin Creek mine.

Chapter E1, "Understanding Trace-Element Sources and Transport to Upper Basin Creek in the Vicinity of the Buckeye and Enterprise Mines," by M.R. Cannon, Stanley E. Church, David L. Fey, Robert R. McDougal, Bruce D. Smith, and David A. Nimick, describes detailed studies of the mine wastes and mill tailings at the Buckeye and Enterprise mines, in particular, their effect on water quality in upper Basin Creek. Geochemical studies of a mill-tailings site at the Buckeye mine indicated that weathering of processed sulfide wastes had resulted in widespread dispersion of oxidized materials containing high concentrations of arsenic, cadmium, copper, lead, and zinc on the Basin Creek flood plain. Trenching at the site showed that unoxidized sulfides existed at depth. Data for chemistry, water levels, and hydraulic characteristics from 10 shallow ground-water wells showed that although concentrations of trace elements were high in ground water near the mill and Enterprise mine sites, ground-water discharge contributed only a small part of the trace-element load to upper Basin Creek. Ground geophysical studies helped define the extent of the inferred plume of contaminated ground water. Observations of the local hydrology indicated that saturation of the mill-tailings pile on the flood plain occurred in the spring during snowmelt, and as a result, trace elements were transported both in solution and as suspended sediment into upper Basin Creek during high flow. Mill tailings and waste rock were removed to the Luttrell pit repository during summer 2000.

Chapter E2, "Monitoring Remediation—Have Mine-Waste and Mill-Tailings Removal and Flood-Plain Restoration Been Successful in the High Ore Creek Valley?" by Sharon L. Gelinas and Robert Tupling, describes the cleanup actions taken by the Montana Department of Environmental Quality and the Bureau of Land Management in the High Ore Creek valley. The Comet mine operated as a small open-pit mine briefly during the early 1970s. Mill tailings were impounded in High Ore Creek. The tailings impoundment was breached, and eroded tailings contaminated High Ore Creek and the Boulder River. Water quality and streambed-sediment quality in High Ore Creek and the Boulder River are affected by trace elements leached from these dispersed mill tailings. The tailings impoundment and the High Ore Creek flood plain were reclaimed during the course of this study. Preliminary evaluation of water-quality data collected before and after cleanup indicates that dissolved zinc concentrations have decreased, whereas dissolved arsenic concentrations have increased. Variations of the concentrations of these trace elements indicate a significant change in dissolved trace-element concentrations downstream of High Ore Creek in the Boulder River, but the dissolved trace-element concentrations have not stabilized.

Chapter E3, "Geologic, Geophysical, and Seismic Characterization of the Luttrell Pit as a Mine-Waste Repository," by Bruce D. Smith, Robert R. McDougal, and Karen Lund, provides an evaluation of the geologic suitability of the Luttrell pit site as a mine-waste repository. The Basin Creek mine went into Chapter 11 Bankruptcy by Pegasus Gold Corp. in 1999. The U.S. EPA eventually acquired the site and requested an evaluation of the geologic suitability of the site as a mine-waste repository. Detailed drilling data, mine-site geology, and fracture density at the Basin Creek mine site were provided by

Pegasus Gold for USGS evaluation of the site to determine the local geologic characteristics and suitability as a mine-waste repository. No evidence of recent faulting in the vicinity of the Luttrell pit was found. Historical seismic data were evaluated to determine that the risk of earthquakes at the proposed repository site was acceptable. Fracture analysis indicated areas where ground-water flow paths from the repository may intersect local structures; these areas were suggested as sites for monitoring wells for the repository. A brief summary of the liner and drain system engineered by independent contractors documents the level of protection provided to prevent escape of any potentially toxic wastes from the Luttrell mine-waste repository site.

Chapter F, "Evaluating the Success of Remediation in the Boulder River Watershed," by Susan E. Finger, Stanley E. Church, and David A. Nimick, describes the potential for successful ecological restoration and recovery of the aquatic community in the study area. Successful restoration is influenced by both the removal of the residual levels of contamination and the establishment of physical or chemical conditions that will support desired or realistic biological communities. Any restoration action involves a certain amount of risk of failure, including the realities of natural environmental variability, the scale of the restoration effort, and external catastrophic influences such as flood or drought. Although the desire of land-management agencies may be for ecological recovery to a preexisting baseline condition, this is often not feasible. Numerous factors must be considered before identifying the restoration alternative that has the highest probability of success. The success of any restoration effort can be best documented via a well-designed monitoring program that collects physical, chemical, and biological information to provide a comparison with conditions prior to cleanup activities. Necessary monitoring activities are recommended to chart the progress of aquatic recovery following these remediation efforts.

Chapter G, "Digital Databases and CD-ROM for the Boulder River Watershed," by Carl L. Rich, David W. Litke, Matthew Granitto, Richard T. Pelltier, and Tracy C. Sole, describes the content and format of the data and information contained on the accompanying CD-ROM. Included are a relational database, a GIS database, and various map, image, and graphic products created during the study. The relational database contains sample site data collected and produced for the study, and an inventory and description of mine-related sites located and compiled for the study. The GIS database contains the sample site data and the information for mine-related sites stored as data layers and associated tables. In addition, the GIS database contains base cartographic data and other thematic data layers collected or produced during this study, as well as data layers and information that resulted from use of a GIS to analyze the sample site, mine-related site, base cartographic, and thematic data.

References Cited

Becraft, G.E., Pinckney, D.M., and Rosenblum, Sam, 1963, Geology and mineral deposits of the Jefferson City quadrangle, Jefferson and Lewis and Clark Counties, Montana: U.S. Geological Survey Professional Paper 428, 101 p., 4 plates.

Buxton, H.T., Nimick, D.A., von Guerard, Paul, Church, S.E., Frazier, Ann, Gray, J.R., Lipin, B.R., Marsh, S.P., Woodward, Daniel, Kimball, Briant, Finger, Susan, Ischinger, Lee, Fordham, J.C., Power, M.S., Bunck, Christine, and Jones, J.W., 1997, A science-based, watershed strategy to support effective remediation of abandoned mine lands: Proceedings of the Fourth International Conference on Acid Rock Drainage, Vancouver, B.C., May 31–June 6, 1997, p. 1869–1880.

Desborough, G.A., Briggs, P.H., and Mazza, Nilah, 1998, Chemical and mineralogical characteristics and acid-neutralizing potential of fresh and altered rocks and soils of the Boulder River headwaters in basin and Cataract Creeks of northern Jefferson County, Montana: U.S. Geological Survey Open-File Report 98–40, 21 p.

Desborough, G.A., Briggs, P.H., Mazza, Nilah, and Driscoll, Rhonda, 1998, Acid-neutralizing potential of minerals in intrusive rocks of the Boulder batholith in northern Jefferson County, Montana: U.S. Geological Survey Open-File Report 98–364, 21 p.

Desborough, G.A., and Driscoll, Rhonda, 1998, Mineralogical characteristics and acid-neutralizing potential of drill core samples from eight sites considered for metal-mine related waste repositories in northern Jefferson County, Montana: U.S. Geological Survey Open-File Report 98–790, 6 p.

Desborough, G.A., and Fey, D.L., 1997, Preliminary characterization of acid-generating potential and toxic metal solubility of some abandoned metal-mining related wastes in the Boulder River headwaters, northern Jefferson County, Montana: U.S. Geological Survey Open-File Report 97–478, 21 p.

Gardner, W.M., 1977, The effects of heavy metals on the distribution and abundance of aquatic insects in the Boulder River, Montana: Bozeman, Mont., Montana State University M.S. thesis, 84 p.

Lund, Karen, Aleinikoff, J.N., Kunk, M.J., Unruh, D.M., Zeihen, G.D., Hodges, W.C., duBray, E.A., and O'Neill, J.M., 2002, SHRIMP U-Pb and $^{40}Ar/^{39}Ar$ age constraints for relating plutonism and mineralization in the Boulder batholith region, Montana: Economic Geology, v. 97, p. 241–267.

Marvin, R.K., Metesh, J.J., Bowler, T.P., Lonn, J.D., Watson, J.E., Madison, J.P., and Hargrave, P.A., 1997, Abandoned-inactive mines program, U.S. Bureau of Land Management: Montana Bureau of Mines and Geology Open-File Report 348, 506 p.

Metesh, J.J., Lonn, J.D., Duaime, T.E., and Wintergerst, Robert, 1994, Abandoned-inactive mines program, Deerlodge National Forest—Volume I, Basin Creek drainage: Montana Bureau of Mines and Geology Open-File Report 321, 131 p.

Metesh, J.J., Lonn, J.D., Duaime, T.E., Marvin, R.K., and Wintergerst, Robert, 1995, Abandoned-inactive mines program, Deerlodge National Forest—Volume II, Cataract Creek drainage: Montana Bureau of Mines and Geology Open-File Report 344, 201 p.

Metesh, J.J., Lonn, J.D., Marvin, R.K., Madison, J.P., and Wintergerst, Robert, 1996, Abandoned-inactive mines program, Deerlodge National Forest—Volume V, Jefferson River drainage: Montana Bureau of Mines and Geology Open-File Report 347, 179 p.

Montana Department of Environmental Quality, 1997, Watershed analysis of abandoned hardrock mine priority sites 1997: Prepared by Pioneer Technical Services, Inc., Butte, Mont., and Integrated Geoscience, Inc., Helena, Mont., for the Mine Waste Cleanup Bureau, variously paginated.

Montana Department of Fish, Wildlife and Parks, 1989, Application for reservations of water in the Missouri River Basin above Fort Peck Dam—Volume 2, Reservations requests for waters above Canyon Ferry Dam: 620 p.

Montana Department of State Lands, 1995, Abandoned hardrock mine priority sites, 1995 summary report: Prepared by Pioneer Technical Services, Inc., Butte, Mont., for the Abandoned Mine Reclamation Bureau, variously paginated.

Nelson, F.A, 1976, The effects of metals on trout populations in the upper Boulder River, Montana: Bozeman, Mont., Montana State University M.S. thesis, 60 p.

O'Neill, J.M., and Lopez, D.A., 1985, Character and regional significance of the Great Falls tectonic zone, east-central Idaho and west-central Montana: American Association of Petroleum Geologists Bulletin, v. 69, p. 437–447.

Parrett, Charles, 1997, Regional analysis of annual precipitation maxima in Montana: U.S. Geological Survey Water-Resources Investigations Report 97–4004, 51 p.

Reynolds, M.W., 1979, Character and extent of basin-range faulting, western Montana and east-central Idaho, *in* Newman, G.W., and Goode, H.D., eds., Basin and Range symposium and Great Basin field conference: Rocky Mountain Association of Geologists, p. 185–193.

Roby, R.N., Ackerman, W.C., Fulkerson, F.B., and Crowley, F.A., 1960, Mines and mineral deposits (except fuels), Jefferson County, Montana: Montana Bureau of Mines and Geology Bulletin 16, 120 p.

Ruppel, E.T., 1963, Geology of the Basin quadrangle, Jefferson, Lewis and Clark, and Powell Counties, Montana: U.S. Geological Survey Bulletin 1151, 121 p., 7 plates.

Schmidt, C.J., Smedes, H.W., and O'Neill, J.M., 1990, Syncompressional emplacement of the Boulder and Tobacco Root batholith (Montana-U.S.A.) by pull-apart along old fault zones: Geological Journal, v. 25, p. 305–318.

Smedes, H.W., and Thomas, H.H., 1965, Reassignment of the Lowland Creek Volcanics to Eocene age: Journal of Geology, v. 73, p. 508–510.

U.S. Geological Survey, 1982, A U.S. Geological Survey data standard, Codes for the identification of hydrologic units in the United States and the Caribbean outlying areas: U.S. Geological Survey Circular 878–A, 115 p.

U.S. Geological Survey, 2000, Interim report on the scientific investigations in the Animas River watershed, Colorado to facilitate remediation decisions by the U.S. Bureau of Land Management and the U.S. Forest Service, March 29, 2000, meeting, Denver, Colo.: U.S. Geological Survey Open-File Report 00–245, 34 p.

Vincent, E.R., 1975, Southwestern Montana fishery investigation, Inventory of waters of the project area: Bozeman, Montana Department of Fish and Game, Project F–9–R–23, Job I–a, 12 p.

Synthesis of Water, Sediment, and Biological Data Using Hazard Quotients to Assess Ecosystem Health

By Susan E. Finger, Aïda M. Farag, David A. Nimick, Stanley E. Church, and Tracy C. Sole

Chapter C of

Integrated Investigations of Environmental Effects of Historical Mining in the Basin and Boulder Mining Districts, Boulder River Watershed, Jefferson County, Montana

Edited by David A. Nimick, Stanley E. Church, and Susan E. Finger

Professional Paper 1652–C

U.S. Department of the Interior
U.S. Geological Survey

Contents

Figures

Tables

Chapter C
Synthesis of Water, Sediment, and Biological Data Using Hazard Quotients to Assess Ecosystem Health

By Susan E. Finger, Aïda M. Farag, David A. Nimick, Stanley E. Church, and Tracy C. Sole

Abstract

The level of effort expended in the Boulder River watershed to assess the effects of trace elements on aquatic life is not feasible for land- and resource-management agencies when faced with evaluating risks associated with thousands of potential inactive historical mine sites. However, the comprehensive data set for the Boulder River watershed offered the opportunity to estimate potential ecological effects from measured geologic, geochemical, and hydrological conditions and to validate these estimates by comparing them with measured biological responses. Hazard quotients calculated with chronic water-quality criteria and with sediment probable-effects concentrations generally agreed with measurements of biology to designate the primary areas of potential hazard in the Boulder River watershed. Sampling sites that potentially represent high hazards to aquatic life included the Bullion Mine tributary, Jack Creek, Uncle Sam Gulch, Cataract Creek downstream from Uncle Sam Gulch, lower Cataract Creek (upstream from the Boulder River), High Ore Creek downstream from the Comet mine, and lower High Ore Creek (upstream from the Boulder River). Fish were absent from all of these sites except lower Cataract Creek, and poor survival during 96-hour survival experiments suggested that trout would be unable to survive in these stream reaches. Adult fish were present in lower Cataract Creek, but the biomass, density, and individual health of trout were adversely affected, suggesting that chronic effects on the fishery in Cataract Creek existed. The only exceptions to the agreement between hazard quotients for water and sediment were in the Bullion Mine tributary and Jack Creek, where the lower pH of the water reduced the ability of trace elements to sorb to colloids and streambed sediment. Therefore, consideration of pH is critical for the interpretation of water and sediment chemistry from regions of historical mining activity. Remediation of the major inactive mine sites in the basins upstream from the primary areas of potential hazard could include removal of mine wastes located on valley floors and reduction of trace-element loading from draining adits. Our hazard-quotient analyses suggest that such remediation could result in substantial improvement of ecological health in the watershed.

Introduction

The watershed approach provides an effective means to evaluate the overall status of ecological resources in an area affected by historical mining and helps focus remediation and restoration strategies on regions that will most benefit from recovery of the watershed. Such a large-scale approach can entail the collection of extensive information on geology and geochemistry, hydrology and water chemistry, and ecological structure, health, and organization within the watershed of concern. During the assessment of the Boulder River watershed, mines were inventoried, geologic conditions were defined, aquatic habitat was assessed, hundreds of water and sediment samples were chemically analyzed, toxicity tests were conducted, fish tissues and indicators of physiological malfunction were analyzed and assessed, invertebrates and biofilm were examined, and hydrological regimes were defined. This level of effort is not feasible for land- and resource-management agencies to undertake routinely when faced with evaluating risks associated with thousands of potential inactive historical mine sites. However, this comprehensive data set offers the opportunity to use geologic, geochemical, and hydrological conditions measured throughout the watershed to estimate potential ecological effects on the aquatic communities and to validate these estimates by comparing them with measured biological responses. Although the focus of this volume is on the health of the aquatic community, a similar watershed-level approach could be used to evaluate the potential health of the terrestrial flora and fauna, or to evaluate the potential problems that might be encountered in attempts to revegetate the riparian corridor. Standard methods are available for measuring effects on the survival, growth, and reproductive health of terrestrial organisms (USEPA, 1992). Similarly, standard procedures to evaluate toxicity of soils to plants could be combined with information on sediment geochemistry to establish conditions in the flood-plain and riparian corridor (Linder and others, 1993).

Ecological risk assessments evaluate the potential that adverse effects may occur as the result of exposure to one or more stressors. These assessments provide a framework for organizing and evaluating data and offer an approach

for environmental managers to consider available scientific information in determining a course of action. The ecological risk assessment approach was developed to address anthropogenic changes that have potentially undesirable outcomes such as adverse effects on an ecosystem. Therefore, this general approach is appropriate and useful in evaluation of the effects of inactive mine sites on ecological health. The level of complexity of a risk assessment may vary from highly quantitative to a qualitative process depending on the objectives of the project. The end result should provide a relative means to rank the potential for adverse effects in the environment at the individual, population, or community level.

Purpose and Scope

The purpose of this chapter is to present an integrated assessment of environmental conditions in the Boulder River watershed and rank those conditions based on their potential to influence the health and recovery of the aquatic community. Information from a range of geologic, geochemical, hydrological, and biological studies is evaluated within an ecological risk assessment framework.

Scientific information collected during our studies in the Boulder River watershed, standard U.S. Environmental Protection Agency assessment methods, and information from the scientific literature are combined to

- Identify stressors that influence ecosystem health
- Identify pathways of exposure
- Calculate hazard quotients for ranking severity of effects
- Compare the ranking to measured biological responses.

Ecosystem Stressors

Historical mining activity in the Boulder River watershed significantly affected the physical and biological nature of the region. Fish were absent from some areas in the watershed directly downstream of draining mine adits, but populations of brook trout (*Salvelinus fontinalis*), rainbow trout (*Oncorhynchus mykiss*), and cutthroat trout (*Oncorhynchus clarki*) occurred further downstream in tributaries and in the Boulder River (fig. 1). In addition, native populations of westslope cutthroat trout (*Oncorhynchus clarkii lewisi*) existed upstream of the Comet mine in the High Ore Creek basin (Farag and others, this volume, Chapter D10). Although current information suggests that both fish and invertebrate populations are adversely affected in the Boulder River watershed, absence of physical habitat does not appear to be a major limiting factor. The persistence of an aquatic community in some parts of the watershed provides a basis for future ecosystem restoration.

Contaminants in surface water and streambed sediment are major stressors on the aquatic ecosystem in the Boulder River watershed. Specifically, copper, lead, zinc, arsenic, cadmium, silver, and antimony are the major contaminants in the watershed. Elevated concentrations of these trace elements can be linked directly to historical mining at the Buckeye and Enterprise mines in upper Basin Creek, the Bullion mine on a tributary of Jack Creek, the area of Cataract Creek upstream from Uncle Sam Gulch, the Crystal mine in upper Uncle Sam Gulch, and the Comet mine in upper High Ore Creek (Martin, this volume, Chapter D3). Although some trace elements, such as copper and zinc, are essential to normal growth and development of aquatic life, excess concentrations of trace elements are associated with abnormal reproduction, growth, and development (Rand and Petrocelli, 1985). Our characterization of the Boulder River watershed documented concentrations of a range of trace elements in water, sediment, colloids, biofilm, benthic macroinvertebrates, and trout. This approach provided the information necessary to characterize exposure pathways and to document the extent and severity of contamination in the watershed as a result of the exposure of aquatic life to their environment.

In streambed sediment from the sites just described, concentrations of trace elements associated with ore deposits were substantially higher than concentrations in premining streambed sediment (Church, Unruh, and others, this volume, Chapter D8). Similarly, the Bullion, Crystal, and Comet mines also produced most of the dissolved trace-element load to the watershed. Cadmium, copper, and zinc concentrations were most commonly elevated in stream water downstream from these sites (Nimick and Cleasby, this volume, Chapter D5). However, pH of most streams was near neutral. In contrast to many regions where inactive mines occur, the mineralogical and textural character of the bedrock in the Boulder River watershed exhibits a widespread acid-neutralizing capacity, thus minimizing the presence of acid water drainage in the basin (O'Neill and others, this volume, Chapter D1).

The contributions of streambed sediment from Basin and Cataract Creeks to the Boulder River were similar, but the impact of the contamination in streambed sediment from High Ore Creek dominated the concentrations of trace elements in streambed sediment of the Boulder River from High Ore Creek downstream to the Jefferson River (Church, Unruh, and others, this volume). In contrast, surface water from Cataract Creek contributed larger trace element loads to the Boulder River than either Basin Creek or High Ore Creek (Nimick and Cleasby, this volume). The major source of metal loading to Cataract Creek was the discharge to Uncle Sam Gulch from the Crystal mine adit. For example, about 75 percent of the zinc load to Cataract Creek came from Uncle Sam Gulch (Kimball and others, this volume, Chapter D6). The relative importance of streambed sediment from High Ore Creek contrasted with the importance of surface-water loading from Cataract Creek highlights the fact that both water and sediment quality must be considered when the potential for biological effects in an ecosystem is evaluated.

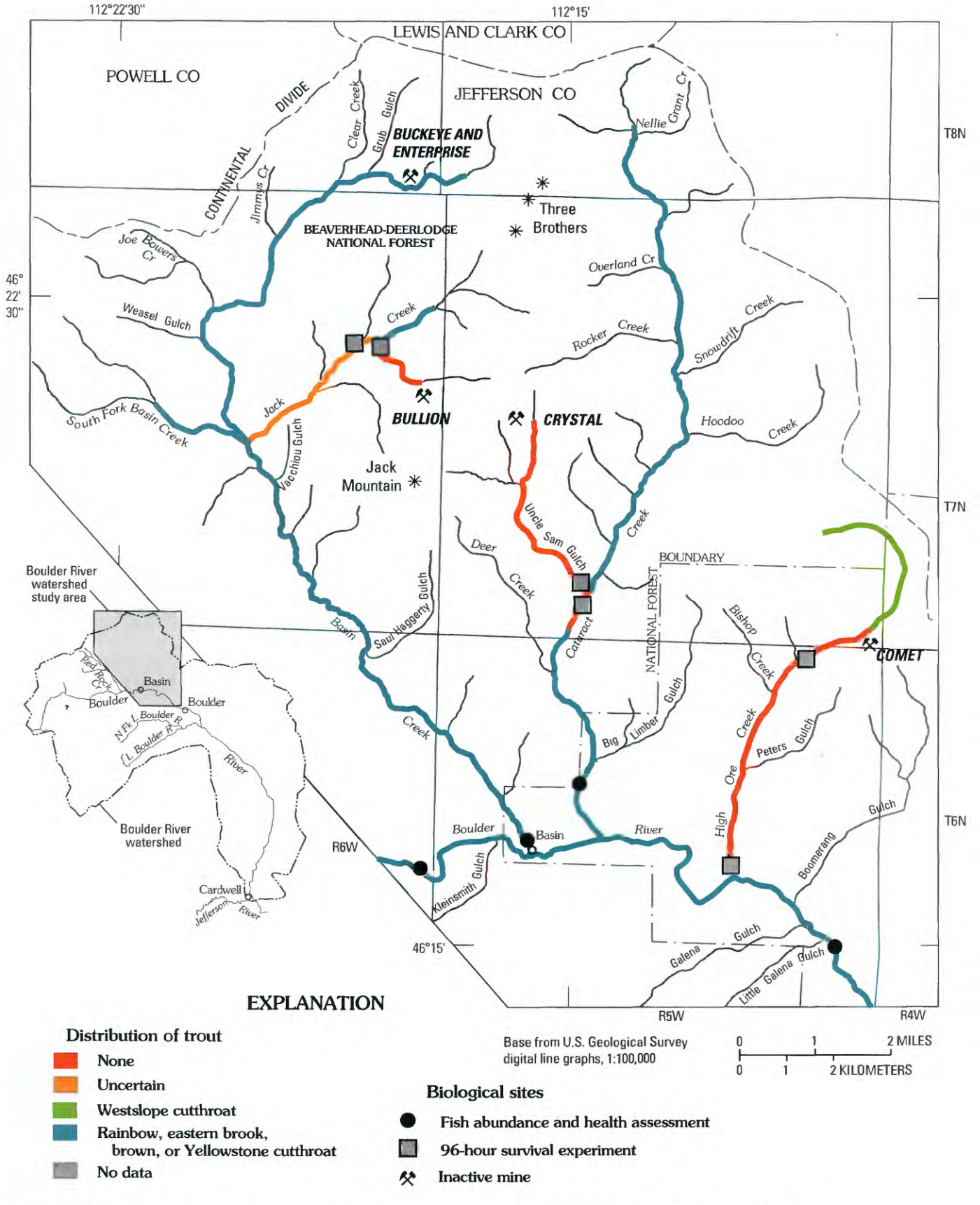

Figure 1. Estimated distribution of trout prior to large-scale remediation work in Boulder River watershed study area.

Exposure Pathways

In biological studies, Farag and others (this volume) suggest that the accumulation of trace elements in tissues of benthic macroinvertebrates and fish in the Boulder River watershed occurs through two pathways and is associated with adverse effects on the overall health of the watershed. Accumulation of trace elements in fish tissue results from direct exposure through water and sediment and indirect exposure through dietary pathways. Thus, the exposure pathways to trout include biofilm, benthic macroinvertebrates, water, colloids, and sediment.

Streambed sediment and surface water provide major pathways for transport and distribution of contaminants through the watershed and for direct exposure of the biological community. Exposure of an organism is dependent on the concentration of the trace elements in both the water and sediment pathways. Accumulation of trace elements and resulting toxicological responses are determined by both concentration and duration of exposure. Chemical data for individual water-quality samples reflect an instantaneous measure of conditions at a single point in time. Trace-element concentrations in streams may vary widely depending on time of day, streamflow, ground-water inflow, and season. Trace-element concentrations in streambed sediment have less temporal variability than concentrations in water because streambed sediment integrates contaminant conditions over an extended period of time. This integration occurs because coatings on sediment grains, particles, and colloidal material sorb trace elements from the water column. This geochemical reaction reduces the dissolved trace-element concentrations in water and increases concentrations in streambed material.

Iron and aluminum colloids, defined as particles between 0.001 and 0.45 µm (micrometers) in size, are transported downstream suspended in the water column. Because the association of colloids and trace elements is dynamic, trace elements may sorb and desorb frequently during downstream transport. These colloids may be trapped by biofilm on rock surfaces and may accumulate trace elements when they become available. Both colloids and biofilm (also referred to as *aufwuchs*) appear to play an important role in the movement of trace elements through the food chain. Farag and others (this volume) observed significant correlation between concentrations of arsenic, copper, lead, and zinc in colloids and biofilm, which indicates a possible relation between trace elements in the two components.

These exposure pathways are important in the Boulder River watershed because they provide multiple encounters between aquatic life and elevated concentrations of trace elements. As a result of these exposures, survival of trout may be limited in parts of the Basin and Cataract Creek basins and in High Ore Creek downstream from the Comet mine. Furthermore, the number of trout present and the health of individual fish are also affected in lower Cataract Creek.

Ranking Stream Reaches Using Hazard Quotients

Assessment of environmental hazards from trace-element exposure can be definitively accomplished by direct measurement of biological effects. To measure biological effects at all points in a stream system is usually impractical; therefore, ecological risk assessment methods have been developed to estimate environmental hazards associated with contaminant exposure. One of the basic strategies used to perform these types of assessments is to compare the environmental concentration of trace elements with a measured biological effect or no-effect level. Thus, estimates of trace-element concentrations in water or sediment may be compared to results from toxicological criteria, regulatory standards and guidelines, or individual threshold values that encompass the concentration-response relationship between a trace element and an organism. This is known as the quotient approach to hazard assessment (Urban and Cook, 1986). If the environmental concentration of a contaminant in an aquatic ecosystem exceeds an effect concentration, then a hazard exists. Similarly, if the environmental concentration is far below the no-effect level, then one may assume the hazard is minimal or not a threat.

Potential hazards in the Boulder River watershed were determined by use of hazard quotients to compare relative risks among reaches. For the assessment, we calculated hazard quotients (HQ) for individual trace elements in water or sediment by dividing the trace-element concentration for an environmental sample either by the U.S. Environmental Protection Agency (USEPA) chronic water quality criteria or by the sediment guideline for probable-effects concentration. If the $HQ < 0.1$, no adverse effect is expected. If $0.1 < HQ < 1$, the hazard is low, but potential for adverse effects should be considered; and if $1.0 > HQ < 10$, some adverse effect or moderate hazard is probable. If $HQ > 10$, high hazard is anticipated.

Hazard quotients were developed for water and streambed sediment from the Boulder River watershed study area. Based on the analysis of exposure pathways presented by Farag and others (this volume) and summarized in the preceding section, cadmium, copper, and zinc were the key metals that appear to cause toxicity in the watershed. In addition, arsenic and lead were measured in fish tissues and may contribute to hazards present in the watershed. For example, arsenic may contribute to morphological changes observed in skin of fish held in High Ore Creek (Farag and others, this volume).

Because water and streambed sediment were collected over a multi-year period during various hydrologic and geochemical conditions in the study area, we chose a subset of the data representing conditions most toxic to aquatic life for calculation of hazard quotients. These conditions coincide with low flow, which occurs from late summer through early spring (Church, Nimick, and others, this volume, Chapter B). In addition, only data collected prior to large-scale remediation efforts (which began in 1997 in the watershed) were selected.

We constructed ribbon maps to depict individual hazard quotients for cadmium, copper, and zinc in water (figs. 2–4) and for cadmium, copper, lead, and zinc streambed sediment (figs. 6–9). Streams were color-coded upstream and downstream from the sample sites with calculated hazard quotients. The color codes were based on our knowledge of metal sources, metal attenuation, and expected dilution effects of tributaries. Because so many hazard quotients exceeded a value of 1 for the Boulder River watershed, the HQ interval between 1 and 10 was divided into three categories to facilitate ranking of reaches. Note that the multiple colors, and hence, multiple intervals, were not chosen for biological relevance (that is, hazard quotients greater than 1 generally indicate that hazards may exist for biota), but were chosen to delineate reaches where restoration might provide the most significant benefits.

Hazard quotients are most useful in determination of either high or low risks and for relative comparisons of the potential for adverse effects among stream reaches. Hazard quotients estimate the hazard associated with individual rather than multiple trace elements and therefore do not account for additive, antagonistic, or synergistic interactions commonly associated with chemical mixtures. Hazard quotients based on measurements of environmental concentrations and measured biological effect or no-effect levels should not be used to evaluate hazards associated with elements that biomagnify such as selenium and mercury.

To address the issue of interactions of multiple contaminants in an aquatic system, Sprague and Ramsey (1965) suggested that the strength of a contaminant could be expressed as a fraction of its lethal concentration using a ratio identical to that now used in calculating hazard quotients. They referred to these values as toxic units. Sprague (1970) further suggested that the toxic unit for each element in a mixture could be calculated and these values summed to estimate the overall toxicity of the mixture. This approach assumes that elements exhibit the same modes of action and that the toxicity of mixtures is strictly additive. Nonetheless, it provides a reasonable and now commonly used approach for evaluating mixture toxicity. Furthermore, a compilation of results for 76 studies that assessed the toxicity of mixtures including elements such as copper, zinc, cadmium, mercury, nickel, and chromium demonstrated that the toxic unit approach closely approximated the toxicity of the mixture in 87 percent of the cases. Lloyd (1982) concluded that although antagonistic and synergistic interactions definitely occur, the joint action of toxic mixtures of common trace elements is likely to be additive.

We constructed maps that show the summation of hazard quotients by site in an effort to exhibit the potential hazard from a combination of trace elements in water or sediment. These maps summed the individual hazard quotients for cadmium, copper, and zinc in water (fig. 5) and in sediment (fig. 10). It should be noted that the sum of the hazard quotients in many places was greater than 30 in water (fig. 5). Therefore, the color designations in the mixture hazard quotient maps reflect greater hazard quotients than those depicted in the maps for individual trace elements.

Water

For water, aquatic-life water-quality criteria established by the USEPA (1999, 2001) are suitable criteria for the "no adverse effect" concentration used in the denominator of the hazard quotient formula. These criteria are an estimate of the concentration of a trace element in surface water to which an aquatic community can be exposed briefly (acute criteria) or indefinitely (chronic criteria) without experiencing an adverse effect. Chronic criteria, which are determined from controlled laboratory experiments with a number of freshwater species, were used to calculate hazard quotients. Thus, a hazard quotient calculated using the chronic criteria (HQ_C) provides an assessment of potential chronic toxicity incorporating effects such as impairment of growth and reproductive success. These are the types of effects that likely occurred at sites such as lower Cataract Creek (Farag and others, this volume). Hazard quotients calculated with acute criteria revealed a pattern of degraded reaches similar to those identified by the HQ_C values. As a result, the hazard quotients computed using acute criteria are not presented.

We calculated the HQ_C for waterborne elemental concentrations using the ratio of the environmental concentration in a filtered (0.45-µm) water sample to the USEPA chronic water-quality criterion.

$$HQ_C = \text{Elemental Concentration / USEPA Chronic Water-Quality Criterion} \quad (1)$$

Chronic aquatic-life water-quality criteria (table 1) were calculated as defined by U.S. Environmental Protection Agency (USEPA, 1999, 2001). The criteria are dependent on hardness (as mg/L $CaCO_3$), which was calculated from measured concentrations of dissolved calcium and magnesium (in mg/L) using the following equation:

$$\text{Hardness} = ((Ca/40.08)+(Mg/24.31))*100 \quad (2)$$

A single sample collected during low flow, which would represent the most toxic conditions to aquatic life, was selected for each water-quality sampling site. Approximately 50 percent of the sites in the watershed were sampled in September 1997, and these data were used in the HQ_C calculations. For the sites not sampled during September 1997, data from a sample collected during September or October in 1996, 1998, or 2000 were used, because streamflow conditions were similar to the September 1997 flows. However, only October 1996 data were used for High Ore Creek and the Boulder River downstream of High Ore Creek, because remediation had started in the High Ore Creek basin in September 1997. Maps showing hazard quotients for cadmium, copper, and zinc in water are in figures 2–4, and the sum of the three calculated hazard quotient values is in figure 5.

Table 1. Chronic aquatic-life water-quality criteria for cadmium, copper, and zinc.[1]

Cadmium:

$Cd_{chronic} = (e^{(0.7852[\ln(hardness)] - 2.715)}) * [(1.101672 - \ln(hardness) * (0.041833)]$

Copper:

$Cu_{chronic} = (e^{(0.8545[\ln(hardness)] - 1.702)}) * 0.960$

Zinc:

$Zn_{chronic} = (e^{(0.8473[\ln(hardness)] = 0.884)}) * 0.986$

[1]U.S. Environmental Protection Agency (USEPA, 1999, 2001).

Streambed Sediment

For streambed sediment, the probable-effect concentration was used in the denominator of the hazard quotient formula. The probable-effect concentration is the concentration of a trace element above which harmful effects on sediment-dwelling organisms are expected to occur frequently (MacDonald and others, 2000). These consensus-based concentrations are reliable and predictive of sediment toxicity based on evaluation of samples on both a national and a regional basis.

We calculated the HQ_S for sediment elemental concentrations using the ratio of the environmental concentration in a total digest of a sediment sample to the probable-effect concentration.

$$HQ_S = \text{Total Elemental Concentration / Probable Effects Concentration} \quad (3)$$

The consensus-based probable-effect concentrations used in calculating these quotients were 4.98 µg/g cadmium, 149 µg/g copper, 128 µg/g lead, and 459 µg/g zinc (MacDonald and others, 2000). Maps showing the hazard quotients for cadmium, copper, lead, and zinc in sediment are in figures 6–9, and the sum of the calculated hazard-quotient values for cadmium, copper, and zinc in sediment is in figure 10.

As was observed for water, the concentrations of trace elements in sediment were generally higher during low-flow than during high-flow conditions. These higher concentrations likely occur during the fall each year, so the 1996 data were used for environmental concentrations. Some sites were not sampled in 1996, and for these sites, 1997 or 1998 data were used. Streambed-sediment samples were analyzed for leachable and total trace-element concentrations; the total concentrations were used to calculate hazard quotients.

Comparisons of Hazard Quotients and Biological Effects

The hazard-quotient maps indicate that areas of potential hazard to biota exist in Basin Creek, Cataract Creek, and High Ore Creek, the three main tributaries in the Boulder River watershed. Both chronic water and sediment hazard quotients show that the hazard potential is most widespread and extreme in Uncle Sam Gulch, lower Cataract Creek, and High Ore Creek.

The combined hazard quotients for chronic effects of surface water indicate highest concern for adverse effects on the biological community to be in Uncle Sam Gulch, Cataract Creek downstream from Uncle Sam Gulch, the Bullion Mine tributary, Jack Creek downstream from the Bullion Mine tributary, High Ore Creek downstream from the Comet mine, and, to a slightly lesser extent, lower High Ore Creek. The individual chronic hazard quotients are greater than 10 for cadmium, copper, and zinc in water in sections of Jack Creek, the Bullion Mine tributary, and Uncle Sam Gulch, and for cadmium and zinc in High Ore Creek downstream of the Comet mine (figs. 2–4). Therefore, high hazard is anticipated in these reaches based on the concentrations of just one of these trace elements. As a result, these areas have combined chronic hazard quotients greater than 30, except lower High Ore Creek, which is 21–30 (fig. 5).

Chronic effects encompass nonlethal biological responses including reduced growth, reproductive impairment or failure, behavioral changes, or physiological malfunction. Any of these would result in reduced health at the individual or population level. In fact, fish health and biomass/density estimates (Farag and others, this volume) confirm that individual fish health and biomass/density were compromised at lower Cataract Creek. This is the same area that hazard quotients calculated with chronic water-quality criteria define as a potential high hazard for aquatic biota.

Comparisons of acute water-quality criteria to environmental concentrations in water demonstrate the same pattern of potential hazards as the chronic water-quality criteria (maps of hazard quotients calculated using acute criteria not presented). Acute criteria (and hazard quotients based on them) imply that significant mortality will result if aquatic life is exposed to water at sites in the Boulder River watershed just listed. These findings of potential hazard related to mortality agree with survival experiments performed by Farag and others (this volume). Westslope cutthroat trout held in Uncle Sam Gulch, Cataract Creek downstream from Uncle Sam

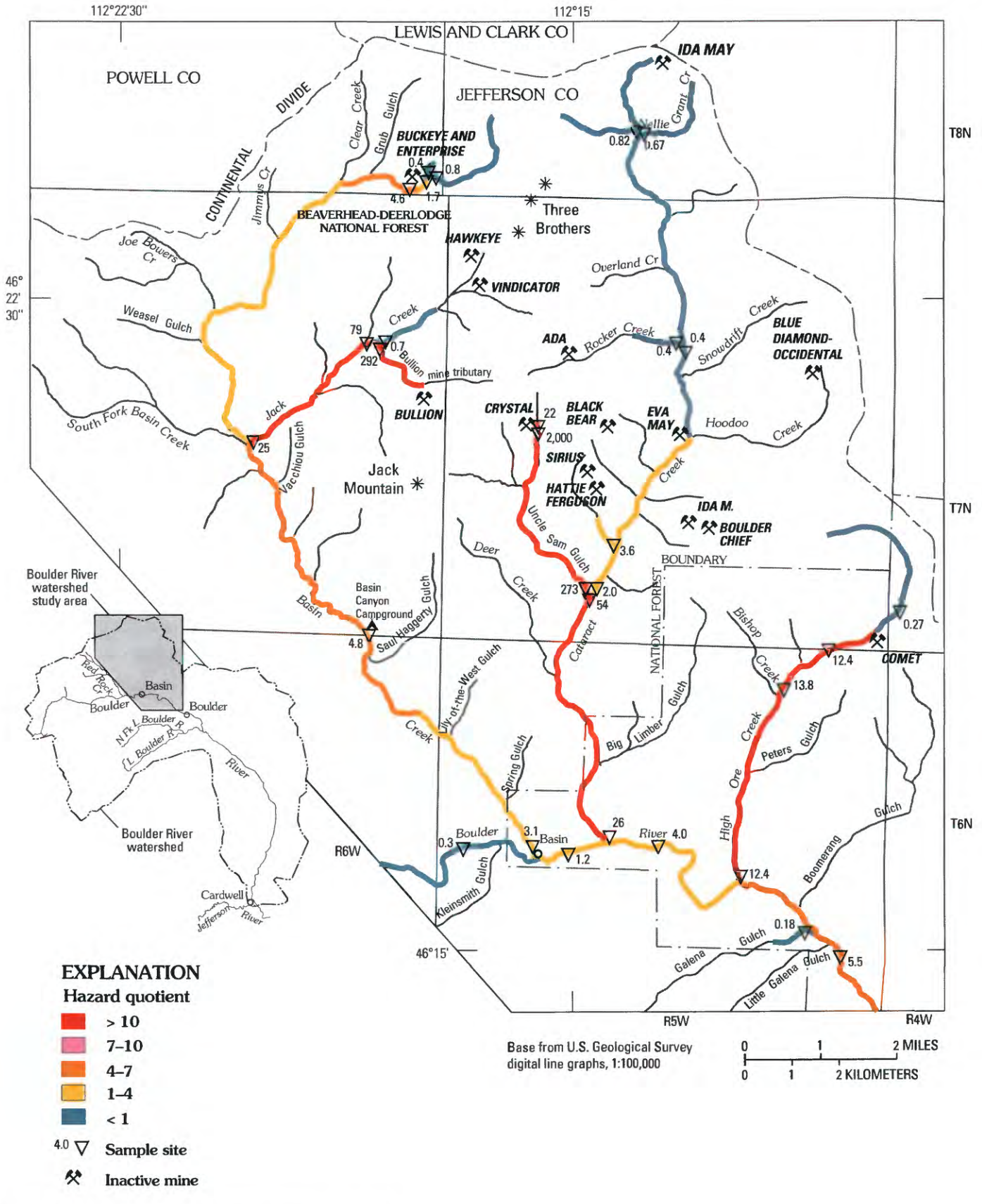

Figure 2. Cadmium chronic hazard quotients for water.

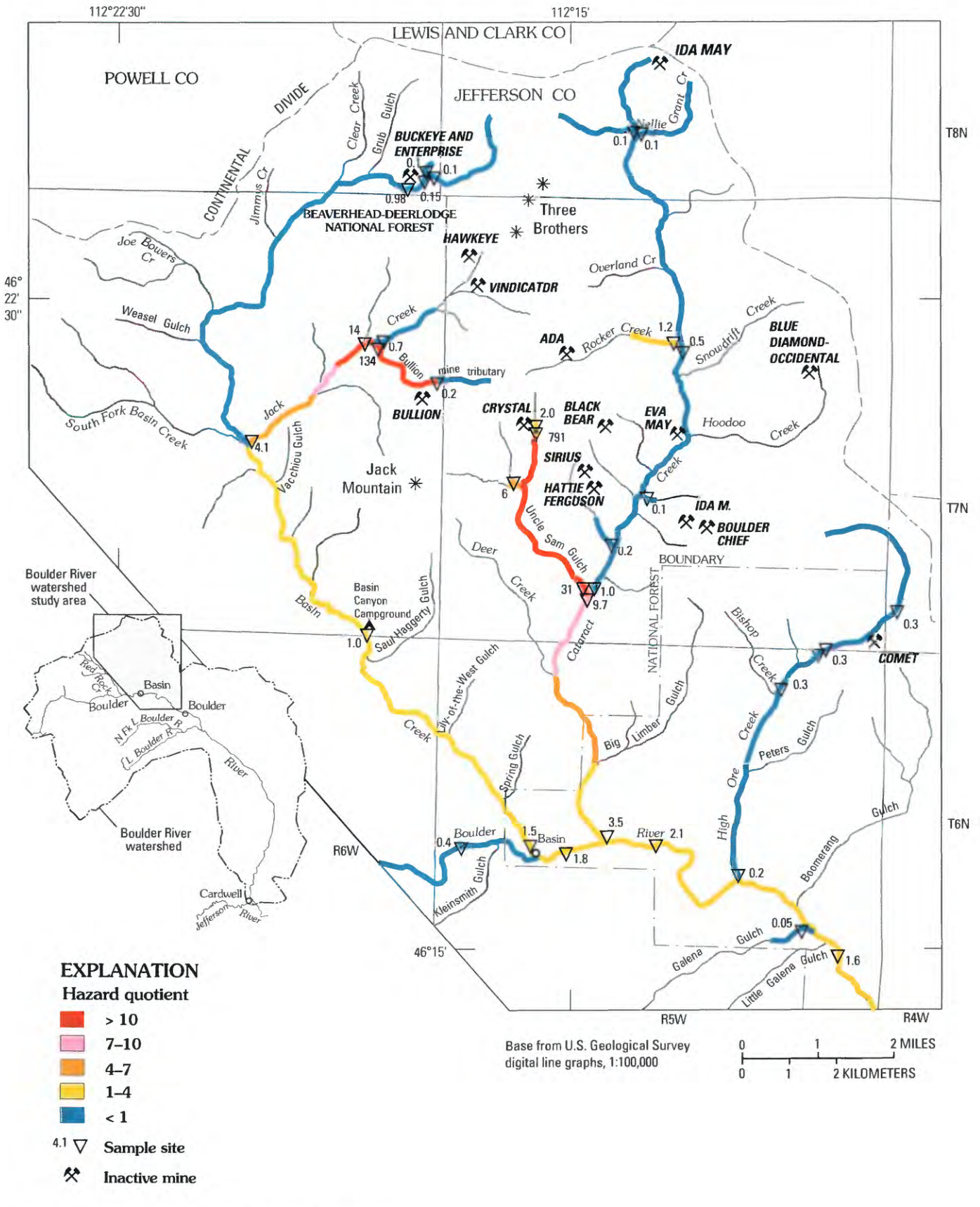

Figure 3. Copper chronic hazard quotients for water.

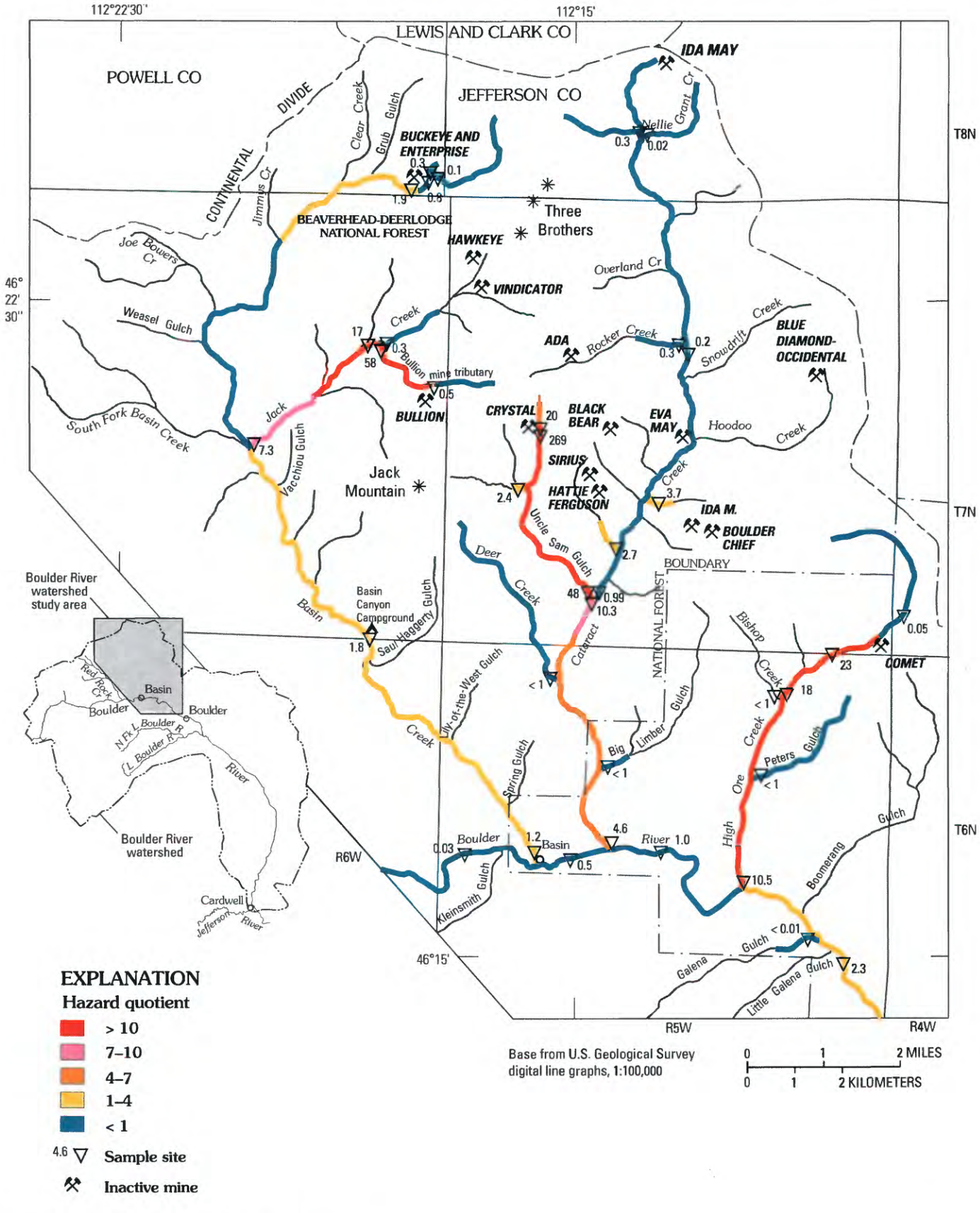

Figure 4. Zinc chronic hazard quotients for water.

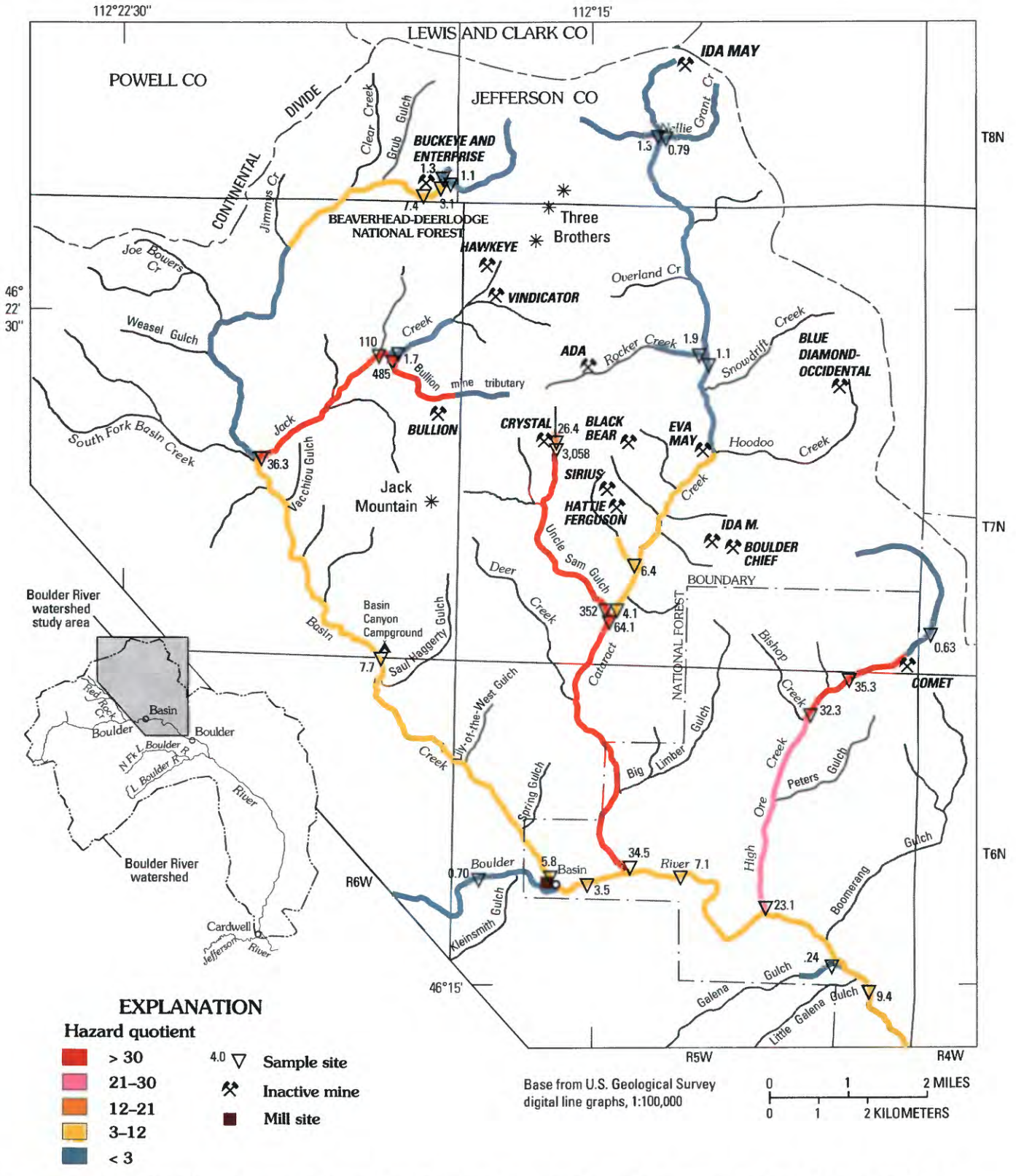

Figure 5. Estimated risk based on sum of chronic hazard quotients for water for cadmium, copper, and zinc. Mill site immediately upstream from confluence of Basin Creek with Boulder River shown for reference.

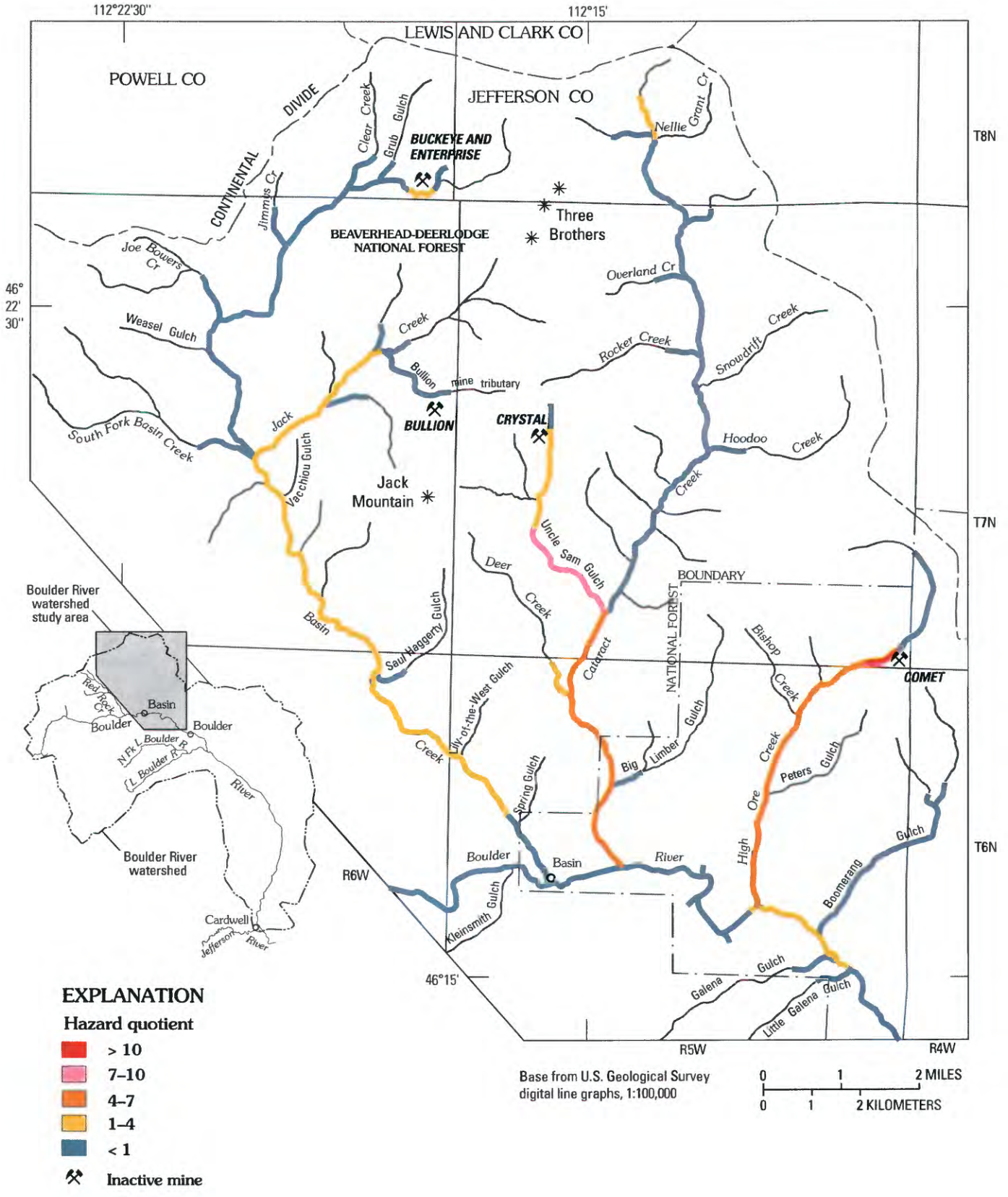

Figure 6. Cadmium hazard quotients for streambed sediment.

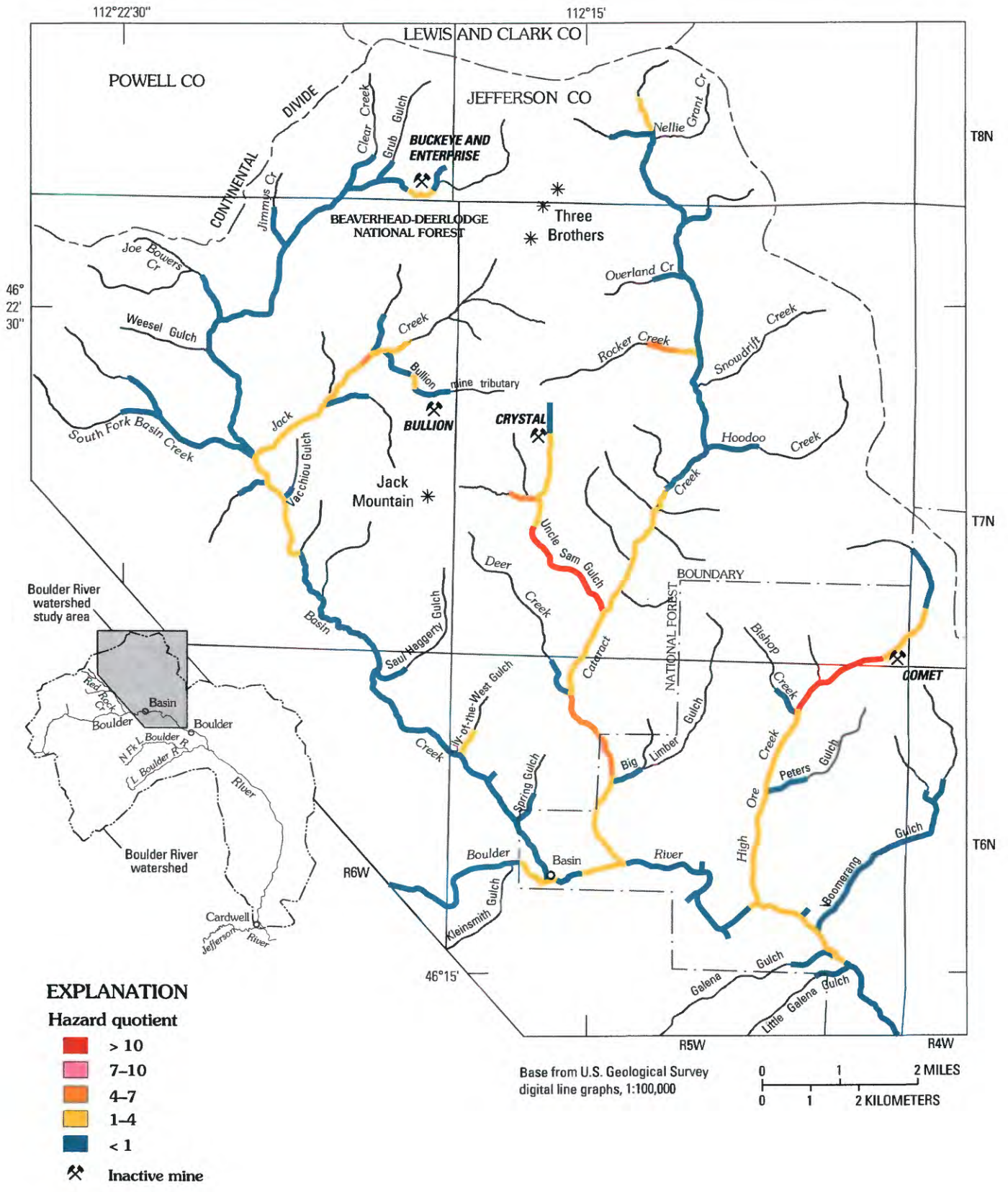

Figure 7. Copper hazard quotients for streambed sediment.

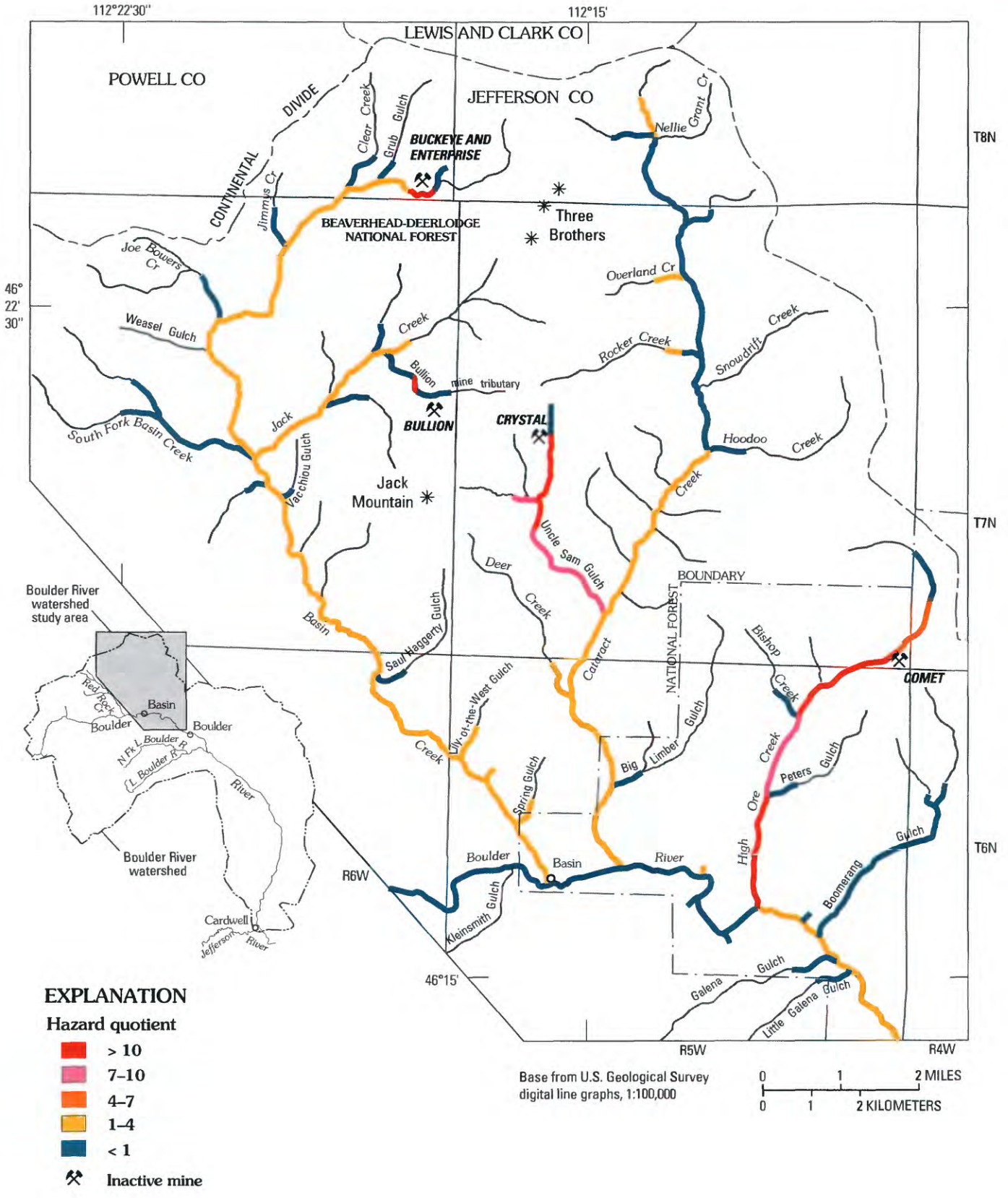

Figure 8. Lead hazard quotients for streambed sediment.

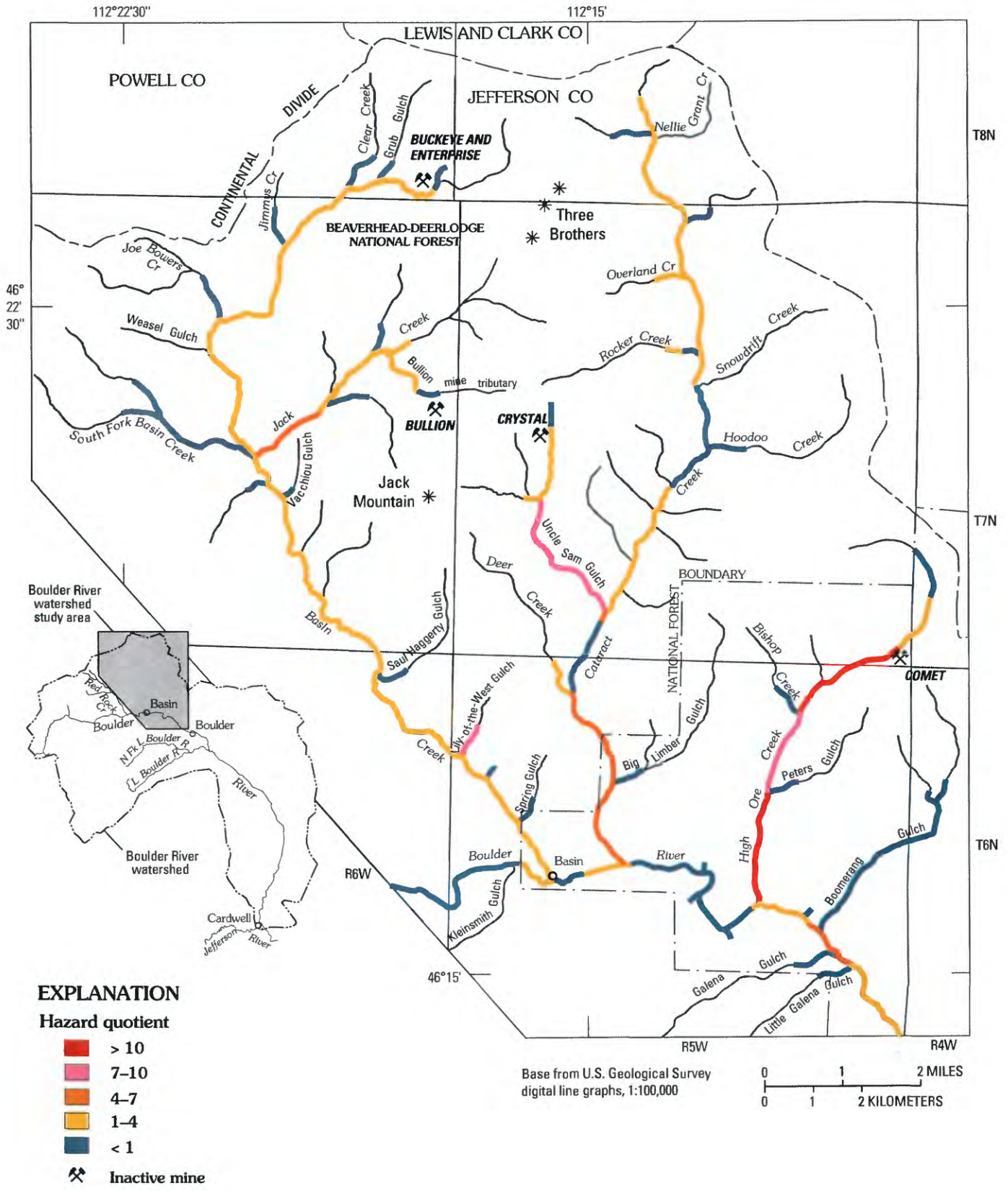

Figure 9. Zinc hazard quotients for streambed sediment.

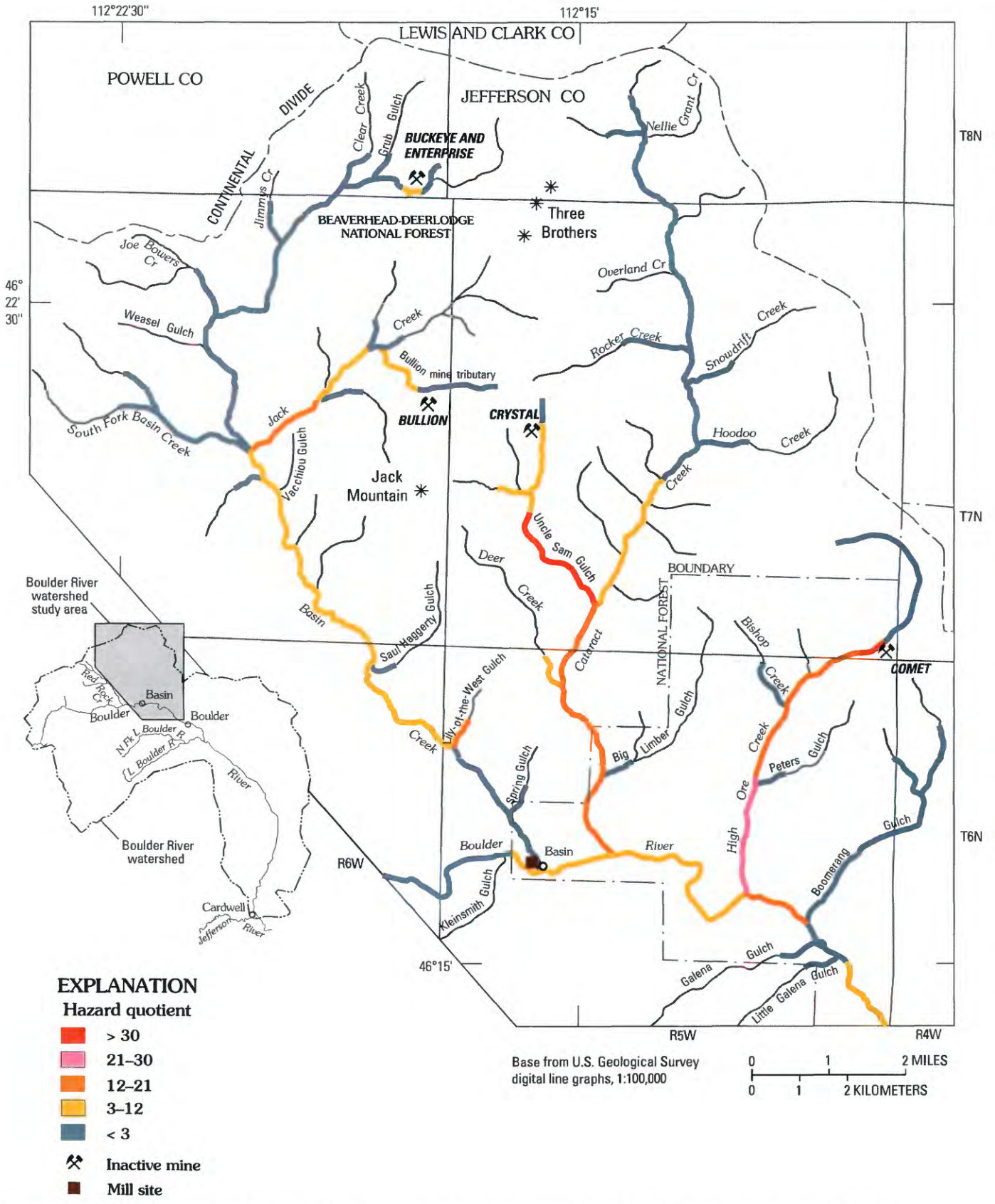

Figure 10. Estimated risk based on sum of hazard quotients for streambed sediment for cadmium, copper, and zinc. Mill site immediately upstream from confluence of Basin Creek with Boulder River shown for reference.

Gulch (but not as far downstream as lower Cataract Creek), the Bullion Mine tributary, Jack Creek downstream from the Bullion Mine tributary, High Ore Creek downstream from the Comet mine, and lower High Ore Creek experienced extensive mortality in the 96-hr survival experiments (Farag and others, this volume).

If the chronic and acute water-quality standards provide the same pattern of potential hazard in the Boulder River watershed, then why do we see any fish in lower Cataract Creek? If trace-element concentrations at this site exceed the acute water-quality criteria, would it not be rendered completely uninhabitable by fish? Two explanations exist for this contradiction. First, the acute criteria were established for multiple species of aquatic life and focus on the survival of larval and swim-up stages that are generally believed to be the most sensitive to contaminant exposure. Adult fish were observed and collected in lower Cataract Creek. It is possible that early life-stage fish would not survive at this site.

Second, acclimation and avoidance behavior may explain the presence of fish in lower Cataract Creek whereas they were not observed immediately downstream from Uncle Sam Gulch. Farag and others (this volume) discuss the likelihood that fish collected in lower Cataract Creek have acclimated to metals in the water at that site. Additionally, the authors document that the cost of this acclimation may be exhibited by reduced biomass/density and physiological changes interpreted in a decline in overall fish health.

Furthermore, anecdotal observations during the in-place 96-hr survival experiments provide evidence that an avoidance response occurs in sections of Cataract Creek. During the experiments, trout were observed in Cataract Creek upstream from Uncle Sam Gulch. These trout fed in a riffle located near the confluence and moved quickly back upstream if they were carried below the confluence. Several dead trout were also found downstream from the confluence with Uncle Sam Gulch. These observations are anecdotal and do not prove behavioral avoidance in this section of the stream, but they suggest the relevance of avoidance behavior in this area. It is possible that some fish in lower Cataract Creek overcame the avoidance response to respond to more immediate stressors such as the need for food (though amounts available may be less than at other sites with lesser concentrations of metals) and a lack of competition from other fish at that site.

Hazard-quotient maps for sediment (figs. 6–9) point to the same general areas of potential hazard as do the maps for water. Combined hazard quotients for sediment (fig. 10) indicate that the areas of highest concern for adverse effects on the biological community were in Uncle Sam Gulch and High Ore Creek downstream from the Comet mine, and to a lesser extent, High Ore Creek downstream from Peters Gulch. Additional areas of concern were Jack Creek downstream from an unnamed tributary draining the Jack Mountain area (figs. 9 and 10), Cataract Creek downstream from Uncle Sam Gulch, and High Ore Creek between Bishop Creek and Peters Gulch. For each of these reaches, one or more of the hazard quotients for cadmium, copper, lead, or zinc exceeded 10. In the case of High Ore Creek downstream from the Comet mine, the hazard quotient exceeded 10 for all four of these trace elements.

Although the hazard quotients calculated from the sediment data point to the same general areas of concern as those calculated from the water, the hazard quotients calculated from the sediment data for Jack Creek and the Bullion Mine tributary (hazard quotients are 3–21 with sediment data, fig. 10) were not as large as those calculated from water-quality data (hazard quotients > 30 with water data, fig. 5). Such differences may be attributed to the lower pH of surface water in the Bullion Mine tributary. If the pH of the water is slightly acidic, cadmium, copper, and zinc, but not lead and arsenic, remain in the water column rather than sorb onto colloidal particles. The pH of water in the Bullion Mine tributary was measured as low as 5.2 in August 1999 (Nimick and Cleasby, 2000). Therefore, the low pH of water at a site lowers the hazard quotients slightly in sediment versus water.

Evaluation of the ecological health of a stream is commonly based on the condition of its fisheries resources because fish represent the top of the food chain in streams and are considered an important resource to land managers and the public. Ecological health of a system is dependent on the chemical and physical conditions in the habitat. If hazard quotients are good estimators of ecological health, then biological conditions of individuals, populations, and communities should reflect interpretations similar to those derived from these simple ratio estimators.

The impaired health of the fish community in lower Cataract Creek corresponded to adverse effects suggested by the hazard quotient method of ranking. The HQ_C values for water suggested extreme hazard for aquatic life in Jack Creek, Bullion Mine tributary, Uncle Sam Gulch, and High Ore Creek downstream from the Comet mine. Fish survival was poor during 96-hr survival in-place experiments performed at these sites (Farag and others, this volume). These reaches should pose the most immediate concern for land managers. Also, the hazard quotients and the survival data may provide explanations about the presence or absence of fish species throughout the Boulder River watershed (fig. 1). Fish were not present in the Bullion Mine tributary, Uncle Sam Gulch, Cataract Creek downstream from Uncle Sam Gulch, and High Ore Creek downstream from the Comet mine. The combined hazard quotients for water agree with the 96-hr survival experiments and point to these reaches as areas of potential high hazard. Except for the Bullion Mine tributary and Jack Creek (as discussed previously), the sediment hazard quotients also indicate these as areas of potential high hazard. Therefore, biology measurements and hazard quotients calculated with water-quality criteria and sediment probable-effects concentrations provide a complete picture of the probable hazards that exist in the Boulder River watershed.

Furthermore, biomass of all species of trout was the smallest at the lower Cataract Creek site. The reduced fish population biomass and density cannot be explained by habitat differences alone (Farag and others, this volume). In addition, concentrations of most trace elements in the livers, gills, and

whole-fish tissue of resident rainbow trout were the greatest in fish from the lower Cataract Creek site. The impairment of physiological function was also most pronounced in the rainbow trout from lower Cataract Creek. Similar effects on population biomass and density, tissue contamination, and physiological impairment were not detected at the lower Basin Creek site, nor did the quotient ranking indicate that they would occur. In addition, using total Ephemeroptera (mayflies), Plecoptera (stoneflies), and Tricoptera (caddis flies) taxa as indicators of macroinvertebrate health, Boyle and Gustina (2000) showed that macroinvertebrate communities in High Ore Creek, Jack Creek downstream from the Bullion Mine tributary, and Cataract Creek were the three sites most affected by historical mining in the Boulder River watershed.

Elevated trace-element concentrations were also measured in fish from lower Basin Creek and the Boulder River downstream from Galena Gulch (Farag and others, this volume). However, physiological changes and changes in biomass and density were not significant at those two sites. Therefore, the biological data suggest that these may be areas land-use managers should continue to monitor, but as shown by the hazard quotient for water and sediment, trace-element concentrations in these two areas do not represent the level of hazard noted in lower Cataract Creek. Some sections of the Boulder River have combined hazard quotients from 3 to 12 for water and sediment (figs. 5 and 10), which suggests that some moderate hazard is possible in both lower Basin Creek and the Boulder River downstream from the mill site immediately upstream from Basin Creek. The combined ranking of information for both chronic water-quality criteria and sediment probable-effects concentrations identified the six most biologically impaired sites: Bullion Mine tributary, Jack Creek, Uncle Sam Gulch, Cataract Creek downstream from Uncle Sam Gulch, High Ore Creek downstream from the Comet mine, and lower High Ore Creek (table 2). These sites, where acute effects on organism survival are anticipated, overlapped with sites where a high potential for chronic effects was estimated. We surmise that remediation efforts, including removal of mine wastes located on valley floors and reduction of trace-element loading from draining adits, of inactive mine sites in the basins draining to these six reaches will result in substantial improvement of ecological conditions in the watershed. Additionally, restoration efforts in the Cataract Creek basin are most likely to positively affect fish biomass, density, and individual health in lower Cataract Creek.

Summary

Hazard quotients calculated with chronic water-quality criteria and with sediment probable-effects concentrations generally agreed with measurements of biology to designate the primary areas of potential hazard in the Boulder River watershed (table 2). The sites where potential for high hazards to aquatic life exists included the Bullion Mine tributary, Jack Creek, Uncle Sam Gulch, Cataract Creek downstream from Uncle Sam Gulch, lower Cataract Creek (upstream from the Boulder River), High Ore Creek downstream from the Comet mine, and lower High Ore Creek (upstream from the Boulder River). Fish were absent from all of these sites except lower Cataract Creek, and poor survival during 96-hr survival experiments suggested that trout would be unable to survive in these locations. Adult fish were present in lower Cataract Creek, but the biomass, density, and individual health of trout were affected, which suggests that chronic effects on the fishery in Cataract Creek exist.

The only exception to the agreement between hazard quotients for water and sediment was in the Bullion Mine tributary and Jack Creek, where the lower pH of the water in the Bullion Mine tributary reduced the ability of trace elements to sorb to colloidal material in the sediment. Therefore, it is

Table 2. Comparisons of biological assessment endpoints with estimated risk based on hazard quotients.

[Hazard quotients calculated using chronic water-quality criteria (HQ_C) and sediment probable-effects concentrations (HQ_S). Endpoints not assessed are labeled N/A]

Site	HQ_C	HQ_S	Resident fish	Resident biomass/density effects	Resident fish health effects	Individual survival effects (96-hr tests)
Uncle Sam Gulch	High	High	Absent	N/A	N/A	Yes
Cataract Creek downstream from Uncle Sam Gulch.	High	High	Absent	N/A	N/A	Yes
High Ore Creek downstream from Comet mine.	High	High	Absent	N/A	N/A	Yes
Lower High Ore Creek	High	High	Absent	N/A	N/A	Yes
Lower Cataract Creek	High	High	Present	Yes	Yes	N/A
Bullion Mine tributary	High	Low	Absent	Yes	N/A	Yes
Jack Creek	High	Low	Absent	N/A	N/A	Yes
Upper Basin Creek	Low	Low	Present	N/A	N/A	N/A
Lower Basin Creek	Low	Low	Present	No	No	N/A
Boulder River	Low	Low	Present	No	No	N/A

critical that pH be monitored to interpret water and sediment chemistry.

As a result of hazard-quotient analyses, we estimate that remediation could result in substantial improvement of ecological conditions in the Boulder River watershed study area. These efforts could include removal of mine wastes located on the valley floors of these basins and reduction of trace-element loading from draining adits of the major inactive mine sites in the basins upstream from the primary areas of potential hazard. With remediation, the likelihood that aquatic life will survive at sites where survival was minimal during 96-hr survival experiments will be improved. Additionally, remediation efforts in the Cataract Creek basin are most likely to positively affect fish biomass/density and individual health in lower Cataract Creek.

References Cited

Boyle, T.P., and Gustina, G.W., 2000, A strategy for use of multivariate methods of analysis of benthic macroinvertebrate communities to assess mine-related ecological stress, *in* ICARD 2000; Proceedings of the Fifth International Conference on Acid Rock Drainage, Volume 2: Society for Mining, Metallurgy, and Exploration, Inc., p. 1425–1431.

Linder, Greg, Callahan, Clarence, and Pascoe, Gary, 1993, A strategy for ecological risk assessments for Superfund: Biological methods for evaluating soil contamination, *in* Hoddinott, K.B., ed., Superfund risk assessment in soil contamination studies: Philadelphia, Pa., American Society for Testing and Materials, ASTM STP 1158, p. 288–308.

Lloyd, R., 1982, The toxicity of mixtures of chemical to fish—An overview of European laboratory and field experience, *in* Bergman, H.L., Kimerle, R.A., and Maki, A.W., eds., Environmental hazard assessment of effluents: New York, John Wiley, 265 p.

MacDonald, D.D., Ingersoll, C.G., and Berger, T.A., 2000, Development and evaluation of consensus-based sediment quality guidelines for freshwater ecosystems: Archives of Environmental Contamination and Toxicology, v. 39, p. 20–31.

Nimick, D.A., and Cleasby, T.E., 2000, Water-quality data for streams in the Boulder River watershed, Jefferson County, Montana: U.S. Geological Survey Open-File Report 00–99, 70 p.

Rand, G.M., and Petrocelli, S.R., 1985, Fundamentals of aquatic toxicology: New York, Hemisphere Publishing Corporation, 666 p.

Sprague, J.B., 1970. Measurement of pollutant toxicity to fish—II, Utilizing and applying bioassay results: Water Research, v. 4, p. 3–32.

Sprague, J.B., and Ramsey, B.A., 1965, Lethal levels of mixed copper-zinc solutions for juvenile salmon: Journal of Fisheries Research Board of Canada, v. 22, p. 425–432.

Urban, D.L., and Cook, N.J., 1986, Hazard evaluation, Standard evaluation procedure, Ecological risk assessment: Washington, D.C., U.S. Environmental Protection Agency, EPA540–9–85–001.

U.S. Environmental Protection Agency (USEPA), 1992, Evaluation of terrestrial indicators for use in ecological assessments at hazardous waste sites. Corvallis, Oregon, U.S. Environmental Protection Agency, 600/R–92/183.

U.S. Environmental Protection Agency (USEPA), 1999, National recommended water quality criteria—Correction: Washington, D.C., Office of Water, EPA 822–R–01–001, 35 p.

U.S. Environmental Protection Agency (USEPA), 2001, Update of ambient water quality criteria for cadmium: Washington, D.C., Office of Water, EPA 822–R–01–001, 35 p.

Geologic Framework

By J. Michael O'Neill, Karen Lund, Bradley S. Van Gosen, George A. Desborough, Tracy C. Sole, and Ed H. DeWitt

Chapter D1 of
Integrated Investigations of Environmental Effects of Historical Mining in the Basin and Boulder Mining Districts, Boulder River Watershed, Jefferson County, Montana
Edited by David A. Nimick, Stanley E. Church, and Susan E. Finger

Professional Paper 1652–D1

U.S. Department of the Interior
U.S. Geological Survey

Contents

Plates

[Plates in this report are on accompanying CD-ROM]

Figures

Tables

Chapter D1
Geologic Framework

By J. Michael O'Neill, Karen Lund, Bradley S. Van Gosen, George A. Desborough, Tracy C. Sole, and Ed H. DeWitt

Abstract

The Boulder River watershed study area is underlain by the Late Cretaceous Butte pluton of the Boulder batholith. The elongate, northeast-trending batholith is interpreted to have been emplaced in a slowly opening pull-apart along strike-slip faults that were active during tectonic development of the Cordilleran overthrust belt. Batholithic emplacement was accompanied by voluminous cogenetic volcanism; these volcanic rocks formed the roof of the intrusive complex and are now preserved as roof pendants within the study area. Subsequent erosion has exposed only the upper few thousand feet of the batholith, which is interpreted to be as much as 10 miles thick. The exposed, upper part of the batholith is cut by two well-developed fracture systems. Fractures that developed during emplacement of the batholith are widely spaced and through-going; they are related to the dynamics of the pull-apart mechanism of pluton emplacement. These syn-emplacement fractures were commonly filled with late-stage magmatic fluids that crystallized to form aplitic to pegmatitic dikes commonly associated with thin polymetallic quartz veins. The second set of fractures appear to be related to cooling of the batholithic mass; they are unmineralized, closely spaced, and restricted to the outer margins of the batholith. The cooling fractures greatly influence near-surface groundwater flow in the study area.

The Butte pluton in the study area contains numerous polymetallic quartz-vein deposits as well as well-developed cooling fracture systems. Inactive mines and prospects in the watershed are located along widely spaced polymetallic quartz veins. Geochemical studies of plutonic rocks that host the polymetallic quartz-vein deposits have shown that iron- or magnesium-bearing minerals, an integral part of the mineralogic composition of the Butte pluton, are capable of neutralizing acidic waters. Prior to mine development, the polymetallic quartz-vein deposits were likely minor point-source acid-producing sites surrounded by rocks with high acid-neutralizing potential. Closely spaced cooling fractures that control the current hydrologic character of the area greatly assist the effectiveness of neutralizing potential of the bedrock. At present, acidic water within the study area is associated with (1) inactive mine adits that have opened and exposed the quartz-vein deposits and channeled the flow of ground water, or (2) mine dumps and mill tailings that have concentrated mineralized rock waste.

Introduction

The Boulder River watershed study area is located in southwestern Montana approximately midway between Butte and Helena (fig. 1). The study area is in the north-central part of the large Late Cretaceous Boulder batholith and is centered on the Basin and Boulder mining districts north and northeast of the town of Basin. The mining districts comprise numerous base- and precious-metal mines that explored thin polymetallic quartz veins filling fractures and small faults in the basins of Basin, Cataract, and High Ore Creeks, tributaries to the Boulder River (pl. 1). The aim of this report is to characterize the geologic framework and associated mineral deposits in the watershed, to identify and prioritize the major contributors of acid mine drainage and deposit-related trace elements to primary streams and tributaries, and to assess the natural acid-neutralizing capacity of the bedrock that hosts the polymetallic vein deposits.

The Boulder River study area is located in an area that was the focus of an earlier, comprehensive study undertaken by the U.S. Geological Survey in the 1950s and 1960s. The result of that original undertaking was the publication of numerous maps and reports on the geology of the central part of the Boulder batholith (fig. 1). The Boulder River study area was mapped and described in the maps and reports of Ruppel (1963) for the Basin 15-minute quadrangle and Becraft and others (1963) for the adjacent Jefferson City 15-minute quadrangle. This report is in many ways a summary of the previous work as it pertains to the Boulder River watershed study area. The reader is encouraged to refer to the previous reports for amplification of details of the geologic investigations.

Previous Work

Lindgren (1886) made the first study of the igneous rocks in this area. These igneous rocks were soon thereafter named

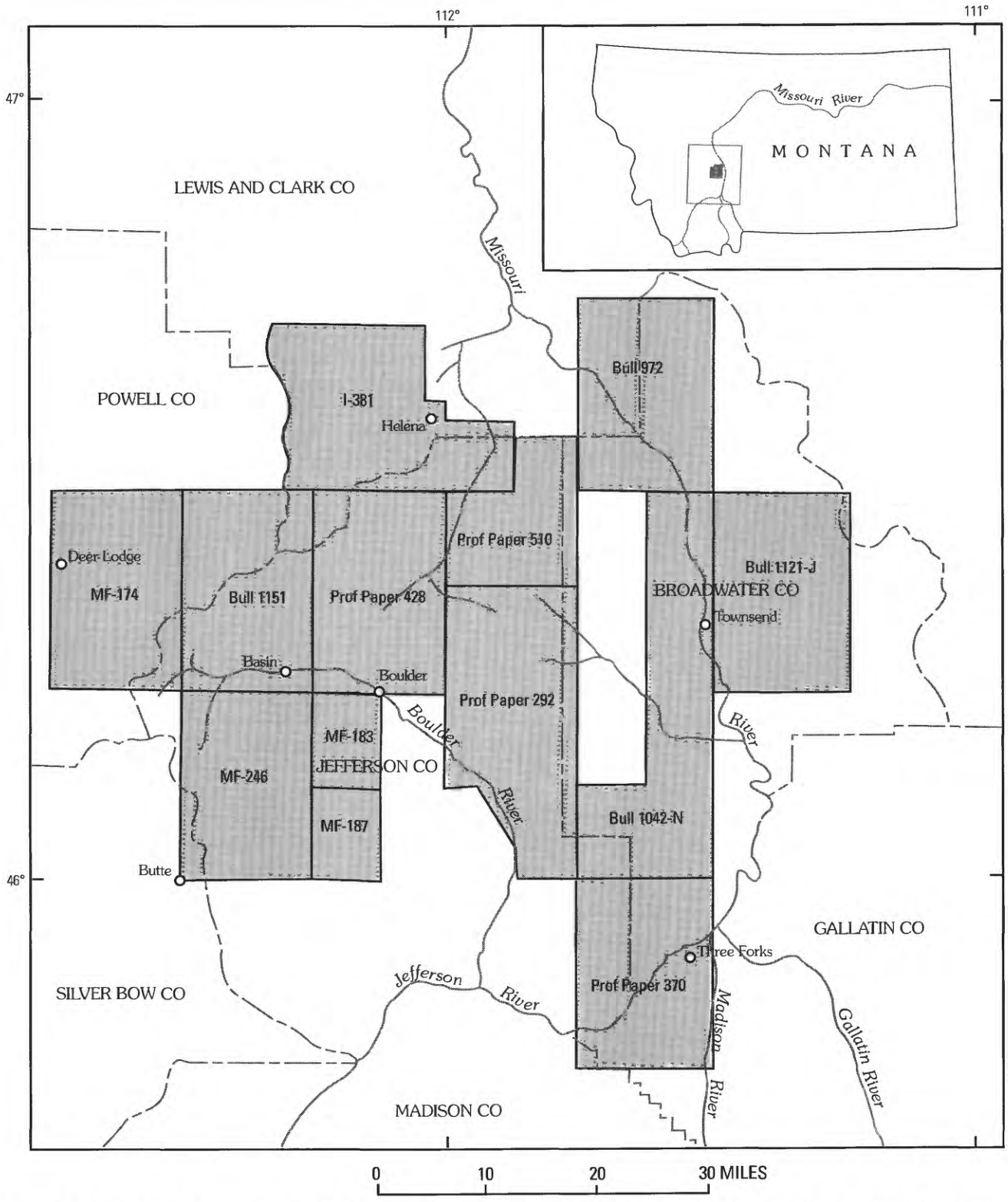

Figure 1. Index map to area described in this report. Labels refer to publications of the U.S. Geological Survey (from Smedes, 1966, fig. 1). Plate 1 covers the area of USGS publications Professional Paper 428 (Becraft and others, 1963) and Bulletin 1151 (Ruppel, 1963).

the Boulder batholith by Weed (1887) in a study of the area around Butte. The Boulder River study area is included in a report by Knopf (1913) on the northern part of the Boulder batholith. During the 1950s and 1960s, the U.S. Geological Survey conducted geologic investigations of 13 quadrangles covering the north-central part of the Boulder batholith (fig. 1). The careful descriptive manner in which the plutonic rocks were described and depicted on these maps allowed us to compile consistent units across the batholith and provided a remarkable view of the geometry of the entire intrusive complex. The closely coordinated individual studies formed the basis for several batholith-wide topical studies, including chemistry (Tilling, 1968, 1973, 1974), timing (Tilling and others, 1968), magmatic evolution (Robinson and others, 1968; Rutland and others, 1989), emplacement models (Hamilton and Myers, 1967; Klepper and others, 1971), and regional tectonic syntheses (Robinson and others, 1968; Schmidt and others, 1990) that have been influential in the studies of magmatic systems and their settings. Mapping studies by Ruppel (1963) and Becraft and others (1963) as part of the Boulder batholith study form the basis of the geologic information used in our analyses and summary.

Setting

Western Montana is underlain by rocks that range in age from Archean to Quaternary. High-grade metamorphic rocks and lesser amounts of felsic plutonic rocks compose most of the Archean lithologic units exposed in cores of mountain ranges in the southwestern part of the State. Archean rocks were deformed in Paleoproterozoic time during the assembly and formation of the North American craton. A major Paleoproterozoic contractional suture zone between Archean cratonic provinces of the northern Rocky Mountains trends northeasterly across east-central Idaho and western Montana, into southern Saskatchewan. In Mesoproterozoic time, the area comprising western Montana and adjacent Idaho was the site of thick accumulations of sediment deposited in what is now known as the Belt basin. The basin trends north and extends from southwest Montana into British Columbia. The Helena embayment, an east-trending arm of the basin, projects eastward into west-central Montana; the embayment is bounded by high-angle faults on the north and south. Phanerozoic miogeoclinal rocks that cover Archean and Proterozoic rocks were complexly deformed in the Cretaceous. Large sheets of allochthonous rocks exposed in the western part of the State were thrust eastward and tectonically interacted with coeval Laramide uplifts of Precambrian basement rocks east of the overthrust belt. Batholithic rocks were also emplaced into these rocks during the Cretaceous; the Boulder batholith, the subject of this report, is one of the larger of these intrusive bodies.

The Boulder batholith is a plutonic complex consisting of a sequence of Cretaceous intrusions that evolved into more silicic compositions through time (Knopf, 1963). The emplacement sequence of the Boulder batholith is from initial more mafic plutons to a voluminous intermediate-composition main batholithic phase to a final, minor late-stage, alkali-rich felsic pluton. Early mafic plutons are elongate east-west bodies at the northern and southern borders of the Boulder batholith (fig. 2); their emplacement was controlled by reactivated east-trending structures acting primarily as tear structures and lateral ramps during Late Cretaceous thrust faulting. The most voluminous, intermediate plutonic phase of the batholithic complex has historically been called the "Butte Quartz Monzonite." However, by use of more recent plutonic classification systems, the composition of this pluton is not quartz monzonite (see discussion on Butte pluton); thus the name Butte pluton will be adopted, following the usage of Schmidt and others (1990), to prevent confusion. The Butte pluton is about 10 mi wide and 32 mi long and forms the north-northeast elongated heart of the plutonic complex (fig. 2). The shape and location of the Butte pluton were probably controlled by tension related to geometry of interacting structures during Late Cretaceous thrust faulting (Schmidt and others, 1990). Late-stage felsic plutons crosscut the Butte pluton; their location may be controlled by the Butte-Helena fault zone (fig. 2, see discussion on mode of emplacement).

Regional Tectonic Setting

The structural setting of the Boulder batholith region[1] has been dominated by recurrent movement on three sets of steep faults (fig. 2): northwest-trending, northeast-trending, and east-trending sets. The northwest-trending fault set consists of about 30 separate faults spaced 3.5–6 mi apart. Some of these faults are vertical at the surface, but most dip 50°–80° NE. Schmidt and Garihan (1986) concluded that these faults were down to the northeast during Mesoproterozoic time. They were reactivated as left-reverse, oblique-slip faults during east-west shortening of the thrust belt and adjacent Rocky Mountain foreland in the Late Cretaceous (Schmidt and Garihan, 1983). Most of these faults are restricted to the Tobacco Root and Highland Mountains, directly south of the Boulder batholith.

Faults of the northeast-trending set occur over a wide zone (120 mi) spanning both the thrust belt and the basement rocks of the foreland. O'Neill and Lopez (1985) have documented recurrent activity along this fault set, going back to at least Mesoproterozoic time; they named the fault trend the Great Falls tectonic zone (not labeled in fig. 2). McBride and others (1990) extended the zone to include thrusts in the Archean basement rocks of the Rocky Mountain foreland and showed that the thrusts had a component of right-lateral slip

[1]The following discussion of the kinematics of emplacement of the Boulder batholith is excerpted from Schmidt, Smedes, and O'Neill (1990). Minor additions to the original article herein are by O'Neill and are based on geologic observations made since that time.

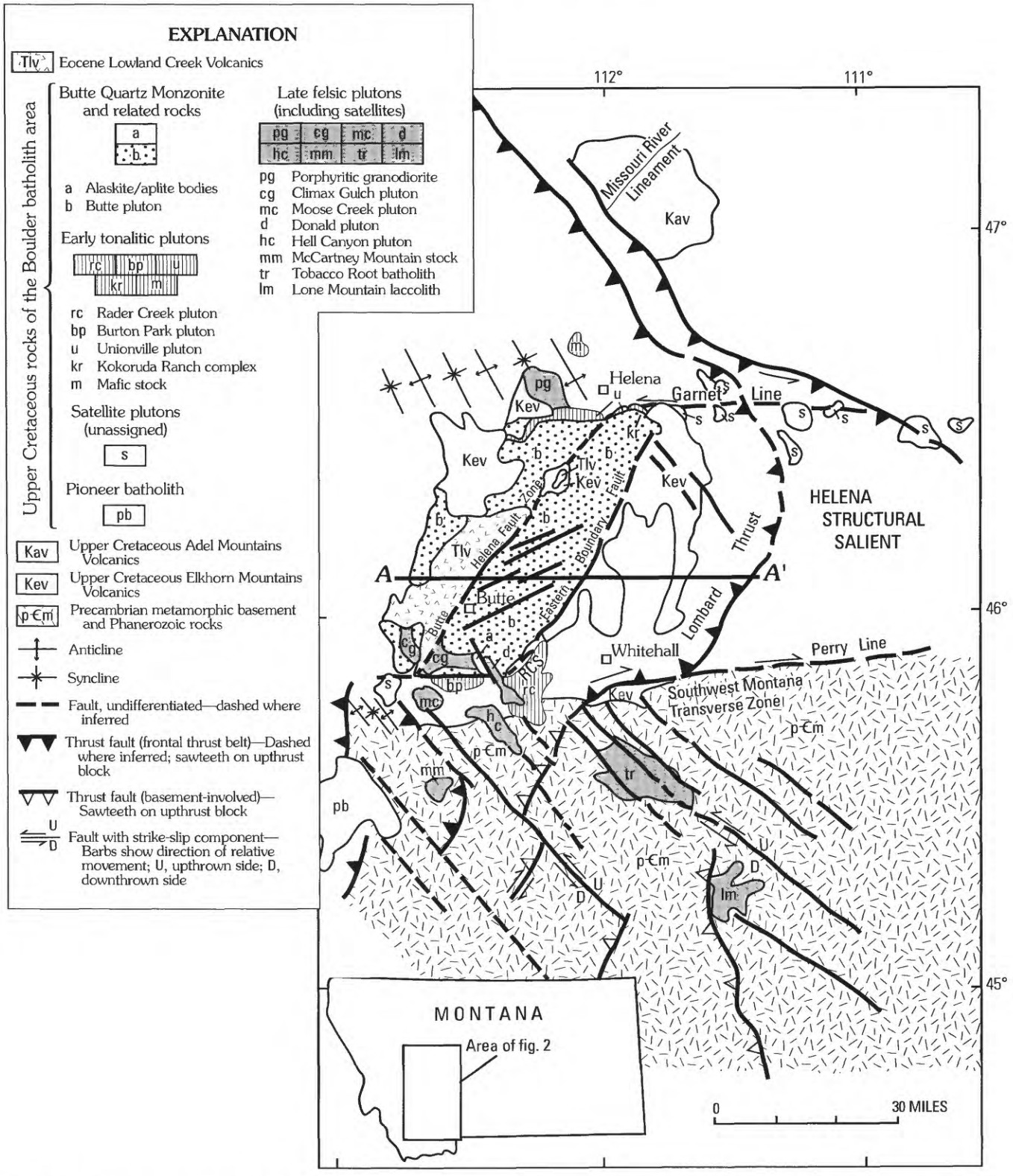

Figure 2. Tectonic map of the Boulder batholith area showing major plutonic units and faults (modified from Schmidt and others, 1990, fig. 1). Inset map shows location. Unlabeled areas are Proterozoic and Phanerozoic rocks. RCS, Rader Creek screen. Cross section *A*–*A*' is shown in figure 3.

due to easterly-directed compression during the Late Cretaceous. More recently, O'Neill (1998) has described the architecture of the Great Falls tectonic zone across western Montana; he described the zone as a Paleoproterozoic collisional orogen and continental suture whose axis is now obscured beneath the Boulder batholith.

Major east-trending Mesoproterozoic faults or fault zones are inferred to be either buried or reactivated by thrusts along the southwest Montana transverse zone at the southern margin of the Helena structural salient (fig. 2) (Robinson, 1963; Schmidt and O'Neill, 1983). The zone is likely controlled by a major down-to-the-north normal fault zone, the Perry line of Harris (1957), that marked the southern margin of the Helena embayment of the Belt basin in Mesoproterozoic time. The westward projection of the line closely coincides with the southern margin of the Boulder batholith. Another, though less distinct, east-trending Proterozoic normal fault zone has been identified in the northern Helena salient (Winston, 1986). This fault zone, the Garnet line of Winston (1986), is interpreted to mark the north edge of the Mesoproterozoic Helena embayment. Late Cretaceous sinistral shear along the segment of the Garnet line fault zone that crosses the northern boundary of the Boulder batholith has produced a series of large northwest-trending en echelon folds in the Proterozoic and Phanerozoic rocks in that region.

In summary, the upper crust in the region of the Boulder batholith is crisscrossed by three sets of deeply penetrating faults that have been recurrently active since the Proterozoic.

Contacts with Adjacent Rocks

Fifteen plutons make up the Boulder batholith (fig. 2). Tonalitic plutons are products of the earliest stage of intrusive activity and are preserved dominantly along the north and south margins of the batholith. These plutons are the most mafic bodies in the batholith and occur as northwest-trending and east-trending dike-like bodies. The intrusion of the earliest plutons appears to have been controlled by the intersection of east-trending faults that bound the Mesoproterozoic Helena embayment of the Belt basin on the north and south with the axial crustal suture zone within the Great Falls tectonic zone.

The Butte pluton, which underlies the entire study area, forms about 73 percent of the outcrop area of the Boulder batholith. It can be divided into eastern and western sectors separated by the Butte-Helena fault zone (fig. 2). In the south, the fault zone is 3 mi wide and separates the batholith from younger Lowland Creek Volcanics. In the north the zone is marked by northeast-trending late-stage plutons, small bodies of alaskite and pegmatite, and abundant late-stage fissure veins. This zone is interpreted to be one of deep-seated faulting associated with the axial suture of the Great Falls tectonic zone.

The eastern boundary of the Butte pluton has long been interpreted as having been emplaced along a preexisting northeast-trending fault that was partly obliterated by stoping. In several places the Elkhorn Mountains Volcanics are intensely sheared and recrystallized along the fault zone (Smedes, 1966; Prostka, 1966). In the north the fault appears to terminate abruptly against the east-trending Garnet line. On the south, it bends gradually westward and merges with the east-trending Perry line that marks the southern boundary of the batholith.

The east-west cross-sectional shape of the pluton is known only from gravity data of Biehler and Bonini (1969) and Burfeind (1967). The pluton is highly asymmetric and can be divided into two parts: (1) a relatively thin wedge-shaped body west of the Butte-Helena fault zone and (2) a thick, steep-sided pluton east of the fault zone (fig. 3).

Mode of Emplacement

Plutonic rocks west of the Butte-Helena fault zone appear to have been intruded as a laccolith that now has an

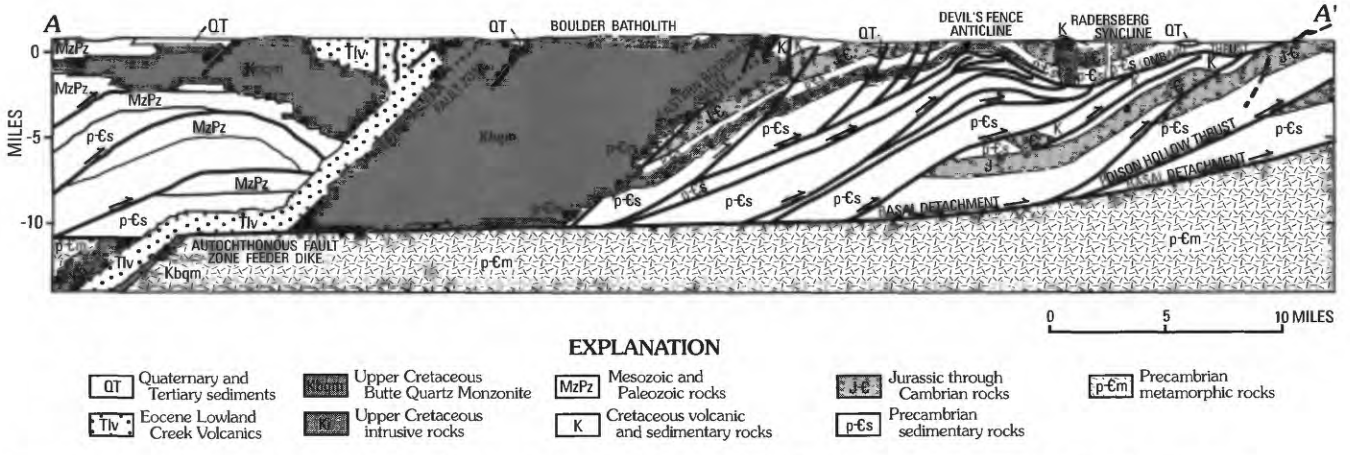

Figure 3. Regional cross section (line *A*–*A'* of fig. 2) showing interpreted relationship of main mass of Butte pluton to faults (modified from Schmidt and others, 1990, fig. 3).

extensive gently west dipping updomed roof of Elkhorn Mountains Volcanics and a few large roof pendants of pre-volcanic sedimentary rocks (Smedes and others, 1988). This part of the batholith is clearly thinner than the eastern part and probably thins gradually westward. However, quite a different mode of intrusion seems to be required for the eastern part of the pluton (figs. 2, 3), because (1) this part of the batholith is a parallelogram in map view and is bounded on four sides by faults; (2) the roof apparently never contained any rocks older than the cogenetic Elkhorn Mountains Volcanics; and (3) the floor is interpreted to be a thrust belt decollement. We suggest that a rhombohedral pull-apart opened up within the Helena salient of the thrust belt during active eastward movement of the thrust sheets. Such a cavity may have formed by interaction of the thrust sheet above the basal decollement with the east-trending faults that bound the pluton on the north and south and with the northeast-trending faults that bound the rhombohedral mass on the east and west. Emplacement may have taken place episodically as a series of sheeted dikes.

The pull-apart is centered on the Butte-Helena fault zone that in turn is a Cretaceous manifestation of recurrent faulting above the Paleoproterozoic continental suture zone named the Great Falls tectonic zone. Thin-skinned, east-directed tectonic transport occurred in rocks north and south of the suture zone; however, thick-skinned basement deformation of the Rocky Mountain foreland occurred only southeast of the Great Falls tectonic zone. Thus, east-west crustal shortening southeast of the tectonic zone included both thick- and thin-skinned deformation, whereas to the northwest only thin-skinned deformation is recorded; hence east-directed tectonic transport of the crust was greater to the southeast. The deep-seated fault lines that bound the north and south sides of the Helena embayment of the Belt basin acted as accommodation zones that allowed a pull-apart to form along the crust-penetrating suture of the Paleoproterozoic collisional orogen. A progressively opening rhombohedral pull-apart was thus outlined by northeast- and east-trending faults, and this pull-apart was progressively filled from below by Butte pluton magmas. When pull-apart ceased and the rhomb-shaped part of the Butte pluton achieved its final form, the western, laccolithic part of the Butte pluton developed as the volume of magma exceeded the room available in the pull-apart region.

Tertiary Extensional Structures

In middle Eocene time, regional extension of the crust led to renewed eruption of calc-alkaline magmas along the Butte-Helena fault zone to produce the Lowland Creek Volcanics (Tlv, figs. 2 and 3). In the early Oligocene, bimodal rhyolite-basalt volcanism of the Helena volcanic field was centered in the northwestern part of the batholith.

Igneous Rocks

Names for rock units used in the original reports (Becraft and others, 1963; Ruppel, 1963) are not used in this report in favor of using names that indicate textural and chemical character of the rocks. Because the plutonic rocks are all part of the same pluton and have the same general chemistry throughout the area, map units are defined on the basis of texture. Rock textures highlight cooling features of the pluton and are important for understanding the physical breakdown and chemical weathering of these rocks. Traditional modal data are available for the plutonic rocks, and these data are presented herein for comparison to other commonly used rock classification systems. However, because of the desirability of using the ground-water and surface-water chemistry of both the plutonic and volcanic rocks to relate rock type to other collaborative studies that are part of this project, we have chosen to discuss and compare the volcanic and plutonic rocks of the study area using their major-element chemistry. Thus, the major-element chemistry of the igneous rocks is presented and classification of the volcanic and plutonic rocks is based on systems used by De La Roche and others (1980). Using the same criteria to classify all the igneous rocks provides better comparison among rock types and includes the mafic minerals as part of the classification. Using mafic minerals as part of the classification system is pertinent to this study because mafic minerals are extremely important constituents in contributing to the acid-neutralizing potential of rocks in contact with acid-bearing water that issues both from exposed, unmined but mineralized areas, and from inactive mine workings.

Most of the rock units in the study area are Cretaceous igneous rocks. Previous work has shown that the Elkhorn Mountains Volcanics and the Boulder batholith are part of the same magmatic system (Roberts, 1953; Klepper and others, 1957; Robinson, 1963; Smedes, 1966). In general, the Elkhorn Mountains Volcanics represent magma that reached the surface and erupted, forming a volcanic and volcanogenic layered sequence; the Boulder batholith represents the parent magma that crystallized beneath the Elkhorn Mountains Volcanics (Robinson and others, 1968; Rutland and others, 1989). Only two eruptive units of the Elkhorn Mountains Volcanics are present in the area of plate 1. The Boulder batholith in the area of plate 1 includes three textural phases of the Butte pluton, the largest pluton of the Boulder batholith. Younger, Eocene and Oligocene volcanic rocks and associated dikes are not related to the Boulder batholith but are related to later regionally important igneous events.

Upper Cretaceous Elkhorn Mountains Volcanics

The Elkhorn Mountains Volcanics are from 2.2 to 3.0 mi thick and once covered about 10,000 mi^2 (Smedes, 1966), making this volcanic field one of the largest known ash-flow volcanic fields (Lipman, 1984). The Elkhorn Mountains Volcanics are folded concordantly with the pre-volcanic rocks

and were thus erupted during and after contractional deformation. They were named and described from the Elkhorn Mountains (Klepper and others, 1957) located about 15 mi east of the study area. The volcanics are informally divided into three members: a lower unit of tuff, lapilli tuff, and tuff breccia; a middle unit mainly of welded tuff; and an upper unit of well-bedded tuffaceous sedimentary rocks. Small bodies of intrusive rocks are included with the Elkhorn Mountains Volcanics because they are thought to be the same age as the volcanics rather than part of the major intrusion of the Butte pluton.

Lower Member

The lower member does not crop out in the study area or in the area of plate 1 but is found to the east in the Elkhorn Mountains (Smedes, 1966). The lower member is andesitic tuff, flow breccias, and volcaniclastic rocks and is as much as 4,900 ft thick. Andesitic ash-flow tuffaceous rocks are massive and commonly flow brecciated; some are slightly welded. Sedimentary rocks derived from these andesitic rocks range from sandstone to pebble and boulder conglomerate.

It is unlikely that the lower member was ever deposited in the study area, given that the batholith was intruded into an ever-opening pull-apart that formed after the lower member was deposited; the lower member is necessarily restricted to areas east and west of the Butte pluton.

Middle Member

The middle member is primarily dacitic welded tuff and also includes lapilli tuff, tuff breccia, and minor volcanic sandstone and conglomerate. The middle member may be as much as 8,200 ft thick (Smedes, 1966) and is the predominant member of the Elkhorn Mountains Volcanics in the study area and across the area of plate 1. Two welded tuff zones of which dacite is the most common rock type make up the middle member. Welded tuffs of the upper zone are light-greenish-gray and medium-gray rocks. Groundmass is fine to very fine grained, and phenocrysts are mostly euhedral plagioclase and hornblende. Plagioclase composition is An_{30-35} (Ruppel, 1963). Plagioclase phenocrysts range from 0.5 to 3 mm long, and the mafic minerals are generally less than 1 mm across.[2] Welded tuffs of the lower zone are brownish gray or reddish gray. The groundmass is aphanitic to very fine grained. Plagioclase phenocrysts are 1–2 mm long, and biotite grains are found in trace amounts. Small lithic fragments of volcanic rock are common. In the welded tuffs, phenocrysts are commonly aligned parallel to welding features and flattened fragments of pumice and glass. Tuff breccia and lapilli tuff are more common in the lower parts of the middle member and probably represent unwelded or partly welded tuff of the same compositions.

[2]All microscopic measurements are given in millimeters rather than inches. To convert to inches, multiply by 0.04.

Local interbedded volcanic sandstone and conglomerate contain fragments of welded tuff and probably originated by local erosion of volcanic rocks between major volcanic eruptions.

The middle member crops out as roof pendants on the Butte pluton across the western part of the study area and as a weakly folded inlier on the east side of the study area. Throughout the study area, the base of the middle member has been partly assimilated by the intrusion.

Upper Member

The upper member of the Elkhorn Mountains Volcanics is primarily volcaniclastic material reworked from the lower members; it includes some tuff layers. The upper member is as much as 1,900 ft thick (Smedes, 1966). Dark-gray, thin-bedded to laminated, fine-grained andesitic mudstone to siltstone is the dominant rock type, interbedded with lesser amounts of andesitic sandstone to conglomerate and breccia. Andesitic sandstone contains subrounded to rounded grains that are well sorted. Breccia is probably of landslide or mudflow origin. Lapilli tuff and crystal tuff, which are interbedded with the fine-grained sedimentary rocks, document on-going volcanism.

Rocks of the upper member are found in and extending out of the southwestern part of the study area above the welded tuff of the middle member, and also along the east side of the study area. The base of the upper member is generally conformable with rocks of the middle member. The overlying Lowland Creek Volcanics lie on top of the upper member of the Elkhorn Mountains Volcanics across an angular unconformity.

Chemical Composition

Becraft and others (1963) reported the chemical analyses of two samples of tuff from the upper member of the Elkhorn Mountains Volcanics and one sample of same-age intrusive porphyry. Their tuff samples are andesite and rhyodacite in composition; the intrusive porphyry is a dacite (fig. 4). Ruppel (1963) reported the analyses of two welded tuffs and a metamorphosed welded tuff, with all three samples from the middle member. The two welded tuff samples are dacites (fig. 4). The metamorphosed welded tuff is compositionally a rhyolite (fig. 4). Ruppel (1963) suggested that the tuff was altered (silicified) after its deposition, perhaps by the intrusion of the Butte pluton. Desborough, Briggs, and Mazza (1998, table 1, p. 6–7) collected four samples of unaltered bedrock of the middle member of the Elkhorn Mountains Volcanics from the study area; these samples range from lati-andesite to dacite to rhyodacite in composition (fig. 4). Desborough, Briggs, and Mazza (1998, table 3, p. 11) also sampled silicified volcanic rocks of the Elkhorn Mountains Volcanics at Jack Mountain (fig. 5).

Similar to the rocks of the Butte pluton, samples of Elkhorn Mountains Volcanics show rather consistent and typical

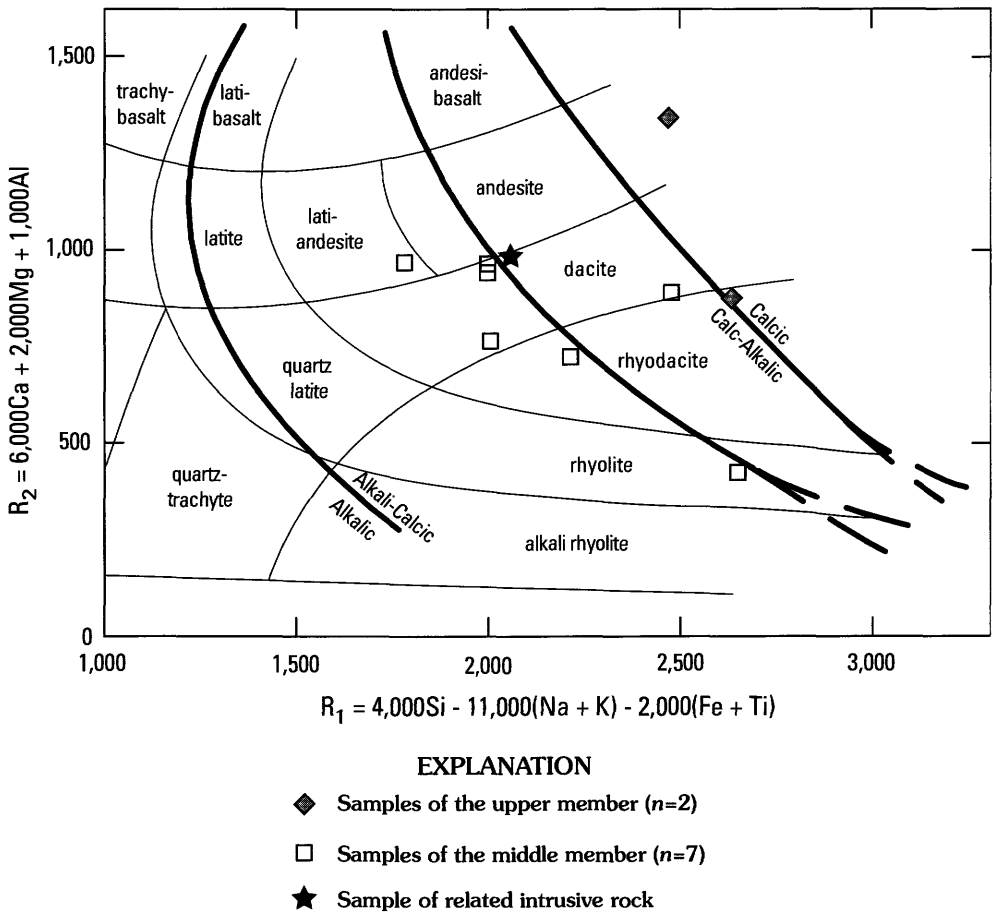

Figure 4. Classification of samples of the Elkhorn Mountains Volcanics in the study area based on the R_1R_2-diagram of De La Roche and others (1980). Analytical data from Becraft and others (1963, table 1, p. 7), Ruppel (1963, table 2, p. 16), and Desborough, Briggs, and Mazza (1998, table 1, p. 6–7).

inverse relationships between silica content and concentrations of magnesium, calcium, phosphorus, and titanium (fig. 5); aluminum and manganese also show similar inverse trends. An association of these metals with mafic minerals is likely; therefore, the least silica rich rocks of the Elkhorn Mountains Volcanics likely contain relatively more mafic minerals.

A comparison of figures 5 and 6 shows that the range and magnitude of major-element concentrations are generally similar between the representative samples of the Butte pluton and the Elkhorn Mountains Volcanics. No modal data for the Elkhorn Mountains Volcanics have been published, mainly because the fine-grained nature of these rocks precludes mineral identification and volume estimates in petrographic sections.

Metamorphism

The Butte pluton intruded into the middle and upper members of the Elkhorn Mountains Volcanics, and, near contacts with plutonic rocks, the tuffs are contact metamorphosed to cordierite hornfels facies. The hornfels are very fine grained rocks in which original textures have been destroyed, resulting in a dense impermeable rock. As for less dramatic metamorphic effects, low-grade contact metamorphism of the tuffs and welded tuffs formed quartz-sericite-alkali feldspar hornfels as much as 65 ft away from the contact. In these hornfels, Becraft and others (1963) and Ruppel (1963) observed that mafic minerals have been mostly destroyed and the remainder of the rock has been converted to sericitized feldspar phenocrysts and a groundmass of fine-grained intergrown sericite, quartz, and alkali feldspar. Pyrite and tourmaline in cavities and along fractures were introduced during or after formation of the hornfels. Wispy textures in these hornfels rocks in the western part of the study area are probably relict welding texture. Chemically, samples of this rock are much more silicic than unmetamorphosed samples (fig. 4), reflecting the importance of the hydrothermal introduction of silica as part of the metamorphism. Both the composition and texture of the hornfels considerably affect the chemical reactions between this rock and ground and surface water and the response of this rock to weathering. See section, "Acid-Neutralizing Potential of Bedrock," p. 83 .

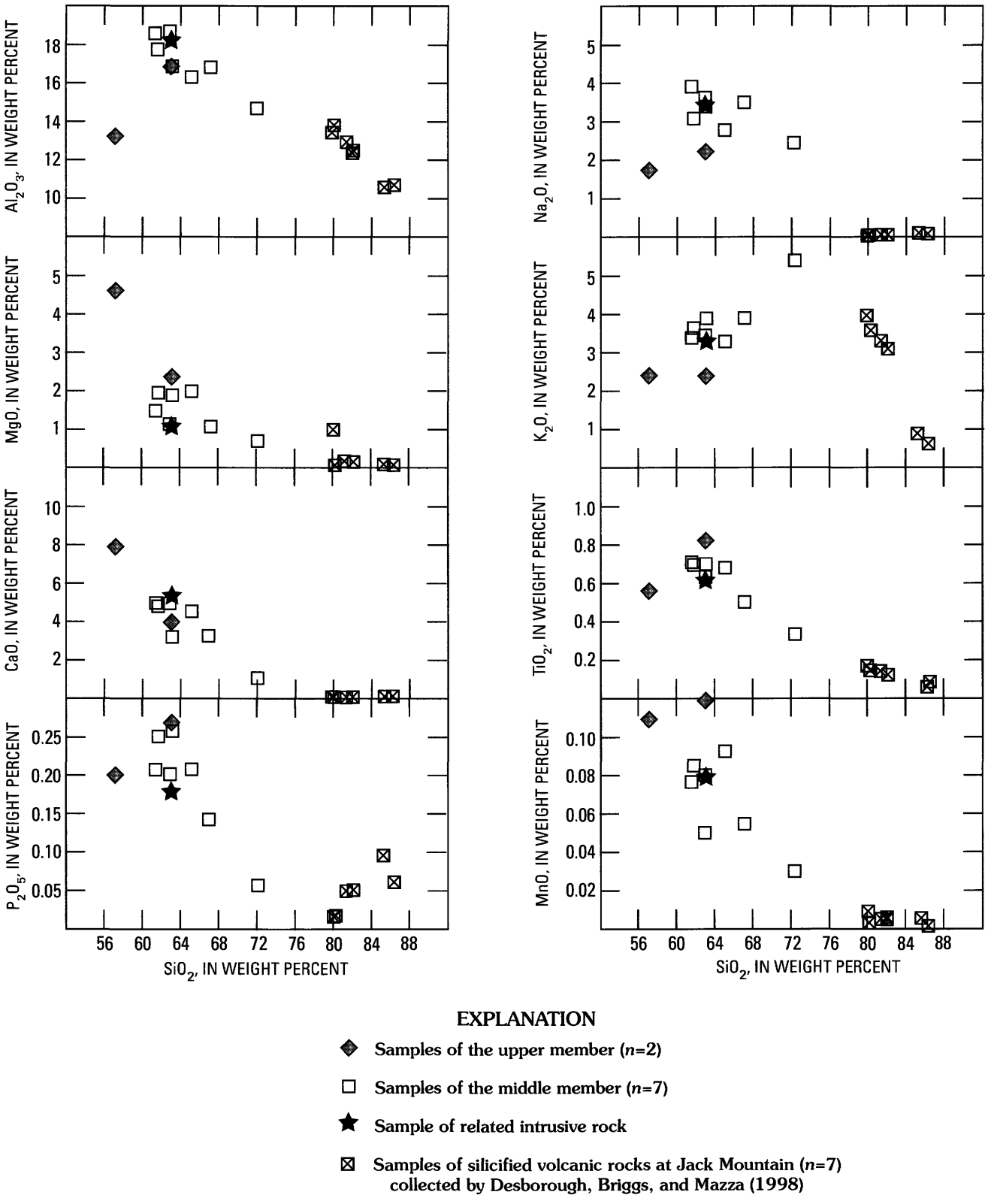

Figure 5. Harker variation diagrams showing abundances of major oxides versus SiO_2 for 17 samples of the Elkhorn Mountains Volcanics from the study area. Analytical data from Becraft and others (1963, table 1, p. 7), Ruppel (1963, table 2, p. 16), and Desborough, Briggs, and Mazza (1998, table 3, p. 11).

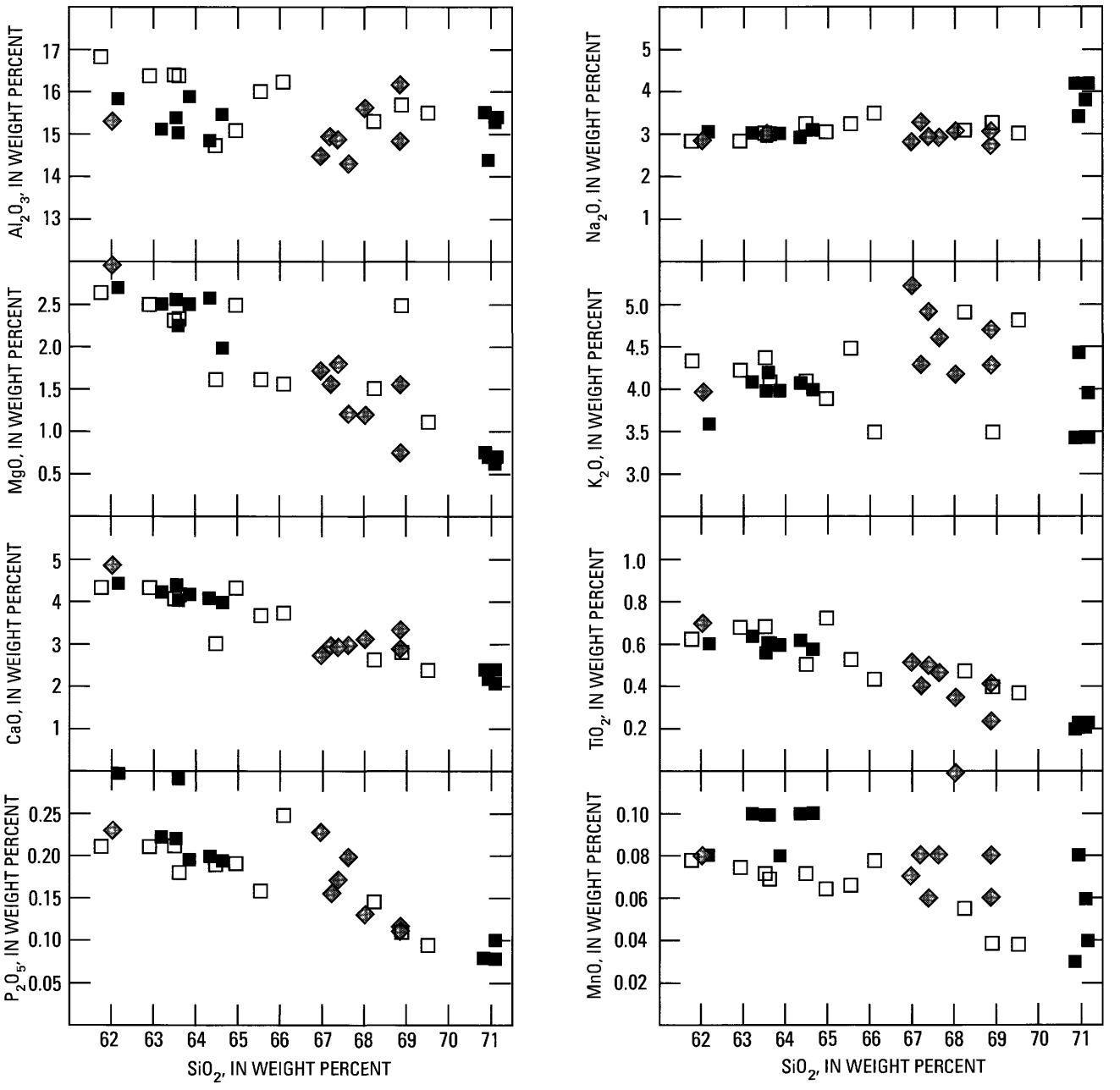

Figure 6. Harker variation diagrams showing abundances of major oxides versus SiO_2 for 30 samples of Butte pluton in the study area. Chemical data from Becraft and others (1963, table 2, p. 10), Ruppel (1963, table 3, p. 26), and Desborough, Briggs, and Mazza (1998, table 1, p. 6–7).

Ages

Age determinations of rocks of the Elkhorn Mountains Volcanics have been obtained elsewhere in the region. Vertebrate and plant fossils found in the Elkhorn Mountains Volcanics are from the Campanian Stage of the Upper Cretaceous (Smedes, 1966). Only a few isotopic ages are reported and, of these, only two have been considered reliable. These are hornblende K-Ar ages, both from the lower member, thus recording the onset of volcanism. A sample of autoclastic breccia from near the base of the lower member from a site southeast of this study area resulted in reported dates of 77.6±2.4 and 78.8±2.4 Ma (Robinson and others, 1968). Another sample from near the top of the lower member west of this study area resulted in a reported date of 77.6±2.4 Ma (Robinson and others, 1968). Fossils from welded tuffs near the top of the upper member are dated at 73 to 75 Ma and record the end of volcanism. Together these data indicate that volcanism occurred for about 5 m.y. from about 78 to 73 Ma (Robinson and others, 1968). More recent dating of Cretaceous fossil zones (Obradovich, 1993) suggests that volcanism, represented as volcaniclastic rocks of the underlying Slim Sam Formation, began about 81 Ma (Tysdal, 2000), thus extending the period of igneous activity.

Late Cretaceous Butte Pluton of the Boulder Batholith

Previous mapping in the study area by Ruppel (1963) and Becraft and others (1963) resulted in complex subdivision of granitic units based on grain size, amount of mafic minerals, outcrop color, and texture. Between the two maps, 19 map units were used to subdivide rocks of the Butte pluton. Units used for the present study are simplified to only three map units (pl. 1) for the following reasons.

Although the units designated by Ruppel and Becraft and others were used consistently where defined, they were not completely carried across both quadrangles. Additionally, gradational boundaries without identified contacts were used in some areas. Thus, distinctions among medium grained, coarse grained, and porphyritic or among the different color varieties were not made everywhere and could not be carried across the present study area without a great deal of additional field mapping.

Significantly, the previous reports make it abundantly clear that such effort is not warranted. Geochemical analyses and modal data for units show unequivocally that some units distinguished by texture or by color index could not be differentiated based on rock chemistry, and further, some units that have identical textures have different chemical signatures and modes. Thus, color was used by earlier workers to distinguish some otherwise chemically and texturally identical rocks (Becraft and others, 1963; Ruppel, 1963). Pink versus gray color in granite is, in some cases, indicative of later alteration of the rock by hydrothermal fluids. Where alteration has not occurred, the pink color may reflect magmatic conditions, in particular, the oxidation state of iron in the feldspar. The previous authors make it clear that the chemical, modal, and textural data show no indication of separate magma sources or even of separate intrusive phases of the same magma (Becraft and others, 1963; Ruppel, 1963). To avoid confusion of the classification systems in these rocks with similar chemistry and to highlight internal features of the Butte pluton in the study area, map units used on plate 1 are defined mostly on the basis of texture. Thus, the complicated map units used by Becraft and others (1963) and Ruppel (1963) are not used in this study in favor of units that were mapped consistently by previous workers and those presented here that are deemed relevant to the present study.

Based on replotting of modal data of Becraft and others (1963) and Ruppel (1963), samples from the Butte pluton plot in the granite field (fig. 7; Streckeisen, 1976) as it was originally classified (Weed, 1887; Knopf, 1957). Subsequent to the original work, these rocks were typically named quartz monzonite (Butte Quartz Monzonite of Becraft and others, 1963; Ruppel, 1963; and many others) due to a then popular igneous rock classification system (Johannsen, 1939; and see Knopf, 1957). Alternatively, based on major-element chemistry in which all constituents of the rock are considered, samples of the Butte pluton from the study area plot in the granodiorite-tonalite fields (see discussion on "Chemical Composition").

Medium- to Coarse-Grained Phase

The dominant rock type in the study area is the medium- to coarse-grained hornblende-biotite phase of the Butte pluton; this phase (Kbm) underlies as much as 90 percent of the study area but is conspicuously absent in the vicinity of Jack Mountain. Even where not exposed on the surface, this rock is not deeply buried and underlies all other exposed rocks. Thus, the chemistry, grain size, and fracture patterns of the medium- to coarse-grained phase and the presence of hornblende and biotite are the most important factors in the environmental geology of the study area. The chemical and physical characteristics of this rock type dominate all other factors in controlling ground-water flow, ground-water chemistry, and acid-neutralizing potential of bedrock in the study area.

The medium- to coarse-grained phase is light to dark gray in fresh samples; some samples are pinkish gray or brownish gray as well. Modal counts published in Becraft and others (1963) and Ruppel (1963) have been replotted in figure 7 and show a spread of compositions across the part of the granite field (monzogranite) where plagioclase and potassium feldspar are present in subequal amounts. A few samples fall in the granodiorite field owing to a predominance of plagioclase over potassium feldspar. Plagioclase composition is in the range of An_{20}-An_{50}; plagioclase crystals are commonly rimmed by zoned albite in coarser grained rocks. Quartz makes up 20–30 percent of the medium- to coarse-grained phase and is commonly strained. Mafic minerals are biotite and hornblende and represent from 5 to 14 percent of the rock. Generally,

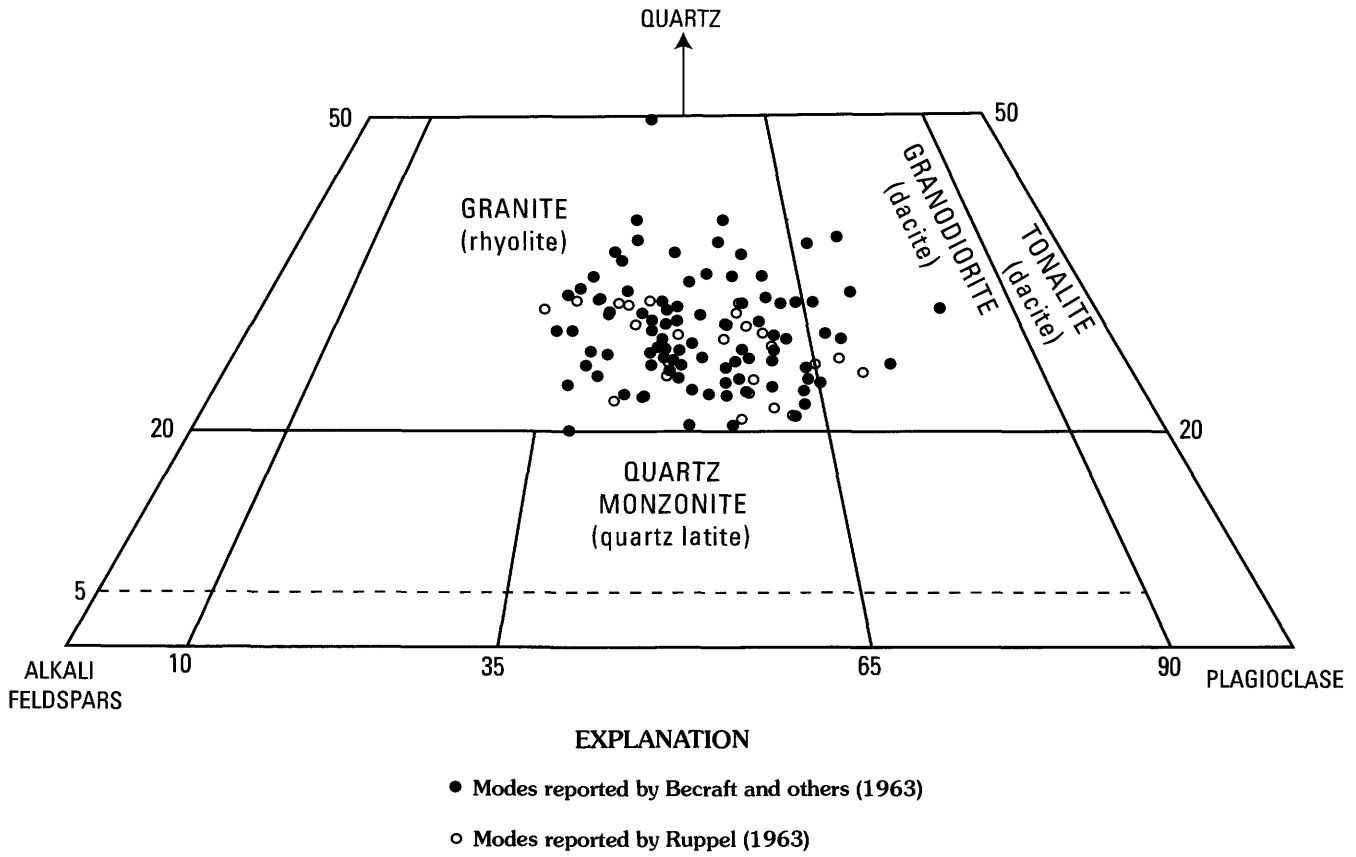

Figure 7. Modes of rocks of Butte pluton in the study area as counted from thin sections by Becraft and others (1963, fig. 3, p. 8) and Ruppel (1963, fig. 3, p. 23). Modes are plotted on modal classification diagram for plutonic rocks constructed by Streckeisen (1976); equivalent volcanic rock names are given in parentheses.

biotite slightly predominates over hornblende; biotite averages 3–7 percent and hornblende averages 1–7 percent. Relict augite is found in most samples. As much as 4 percent tourmaline is present. Sphene, magnetite, zircon, apatite, and allanite are common as trace minerals.

The medium- to coarse-grained phase is commonly equigranular, but minor areas of porphyritic texture with medium- and coarse-grained groundmass are found along the northern edge of the map area of plate 1. Based on mapping of Becraft and others (1963) and Ruppel (1963), the grain size in this unit forms a distinct pattern of coarser at deeper exposures as opposed to medium at higher positions relative to the original roof of the pluton. The porphyritic varieties noted in previous mapping are at the northern contact of the Butte pluton against the older, cogenetic Unionville pluton (Knopf, 1963). This porphyritic texture in the Butte pluton is presumably due to more rapid cooling near the roof and side of the magma body during crystallization.

Pegmatitic to aplitic segregations form knots in the medium- to coarse-grained phase, especially in the upper parts of this unit. The pegmatitic and aplitic segregations are feldspar and quartz intergrowths that can be either coarser or finer than the surrounding rock and also commonly include visible crystals of tourmaline and epidote. Some of these pegmatitic or aplitic knots have crystals terminating inward into poorly formed miarolitic cavities. Where the knots or cavities are particularly common, the rock has locally been mapped as aplite bodies by the previous workers; in this study, these rocks are interpreted to be textural and compositional phases that formed due to liquid-rich bubbles near the top of the crystallizing magma. Miarolitic cavities indicate moderate to shallow emplacement and cooling of the magma at about 2.5 mi beneath the paleosurface.

Fine-Grained Porphyritic Phase

The fine-grained porphyritic phase includes light- and dark-gray and pinkish-gray varieties and both porphyritic and equigranular varieties; this phase (Kbf) is most abundant in the study area in the vicinity of Jack Mountain. Phenocrysts are most commonly potassium feldspar, but one variety has plagioclase phenocrysts. Plagioclase composition is in the range of An_{30}-An_{50}; crystals are commonly zoned. Quartz makes up 20–30 percent of the fine-grained phase and is commonly strained. Mafic minerals are biotite and hornblende. Generally, biotite slightly predominates over hornblende; biotite averages 4–7 percent and hornblende averages 2–4 percent. Sphene, magnetite, zircon, apatite, and allanite are common trace minerals.

The porphyritic fine-grained variety is composed dominantly of rocks with groundmass crystals of about 1 mm and phenocrysts as much as 30 mm.[3] Some equigranular varieties with grain size of about 1 mm were originally mapped as separate units based on the textural difference. The groundmass in both porphyritic and equigranular varieties is formed of interlocking grains.

Other textural varieties in this unit include granophyre, porphyry, and minor aplite. In the granophyric variety, fine to very fine rosettes of quartz and graphic intergrowths of quartz and feldspar form most of the groundmass. In the porphyry variety, the groundmass is very fine and the appearance of the phenocrysts dominates the rock in hand specimen. Some small zones of aplite, rock having lower mafic mineral content and composed of a mosaic of quartz and feldspar grains, are included in this unit. In all these textural types, aplitic material forms knots and segregations associated with sparse, poorly formed miarolitic cavities. These textures indicate moderately shallow cooling at about 2.5 mi beneath the surface.

The fine-grained porphyritic variety and associated varieties are most commonly found at the highest elevations in the Butte pluton. They are located overwhelmingly near the contact of the Butte pluton with overlying roof rocks. This phase forms a chill margin to the rest of the pluton and, thus, crystallized before the coarser grained phases. In places where this relationship does not hold and the fine-grained phase appears to be surrounded by the coarser grained phases, this chill phase may represent rafts caused by the failure of the roof zone during emplacement of the still mobile coarser magma.

Aplite and Porphyry

The aplite and porphyry unit (Kba) includes rocks originally mapped as alaskite and pegmatite map units. When replotted (fig. 7), modal counts published in Becraft and others (1963) spread across the modal granite field with most samples falling in the part of the granite field (syenogranite) having higher concentration of potassium feldspar than plagioclase feldspar. These rocks have considerably higher silica content than the other phases with quartz composing 31–42 percent of the rock. Potassium feldspar makes up 30–65 percent, and sodic plagioclase makes up most of the rest of the rock. Biotite is the only common mafic mineral, and it is only present in trace amounts of less than 1 percent. Black tourmaline is common locally.

Textures in much of this unit are similar to those in the fine-grained porphyritic phase; the unit is distinguished from it on the basis of the very low mafic content. Although some sugary alaskitic textures do exist in the area, most of this unit has aplitic (fine-grained pegmatitic) or leucocratic porphyritic textures. Grain size of the aplite and porphyry matrix averages about 1 mm. However, some pegmatite with much coarser quartz and feldspar grains is also included in this unit. Fine-grained to very fine grained rosettes of quartz and graphic intergrowths of quartz and feldspar are common.

The aplite and porphyry units form tabular bodies and dikes throughout the map area. East of the study area, on the east side of the area of plate 1, aplite dikes are common. These have strongly preferred northeast trends, although other orientations are also evident. These aplite dikes formed in steep joints. Aplite is also present as segregations that form knots at different scales: many knots are characteristically small but some are so extensive and intergrown that they were mapped as separate bodies. Many of the tabular aplite bodies throughout the map area are part of the fine-grained, chilled facies that formed near the top of the magma chamber rather than the usual late-stage segregations typical of aplite.

Chemical Composition

As part of this study, Desborough, Briggs, and Mazza (1998) collected 11 samples of unaltered Butte pluton bedrock in the Basin and Cataract Creek basins. The major-element compositions of their samples appear to overlap with those of the Butte pluton samples of Ruppel (1963, p. 26), as well as all but the four most silica rich rocks of Becraft and others (1963, table 2, p. 10), as shown in figures 6 and 8. Harker variation diagrams showing the rock chemistry of Butte pluton samples from all three studies (fig. 6) reveal a fairly consistent trend for a few elements. The concentrations of magnesium, calcium, phosphorus, and titanium show an inverse relationship with silica; that is, as silica content increased in the melt, magnesium, calcium, phosphorus, and titanium decreased. Harker variation diagrams by Tilling (1974, fig. 3, p. 3883), which display more than 250 chemical analyses of Boulder batholith rocks and its satellite plutons, show this same inverse relationship between silica and magnesium, calcium, phosphorus, and titanium.

In major-element composition, no distinct difference is evident between rocks of the fine-grained porphyritic unit and rocks of the medium- to coarse-grained unit (figs. 6 and 8). This similarity provides further evidence that these two units had a common magma source and probably do not represent separate intrusive events. Because of the similar compositions, the two units should have nearly the same acid-neutralizing potential in the study area. (See section, "Acid-Neutralizing Potential of Bedrock.")

The multi-element chemistry of the 11 Butte pluton bedrock samples collected by Desborough, Briggs, and Mazza (1998, table 1, p. 6–7) was examined with correlation statistics. Although this data set is not large enough to warrant confident statistical conclusions, a few interesting relationships were found. Calcium correlated very strongly with iron and scandium (correlation coefficient (R) of >0.9), strongly with vanadium and titanium (R>0.8), and well with magnesium, phosphorus, and manganese (R>0.7). Iron and titanium

[3]All microscopic measurements are given in millimeters rather than inches. To convert to inches, multiply by 0.04.

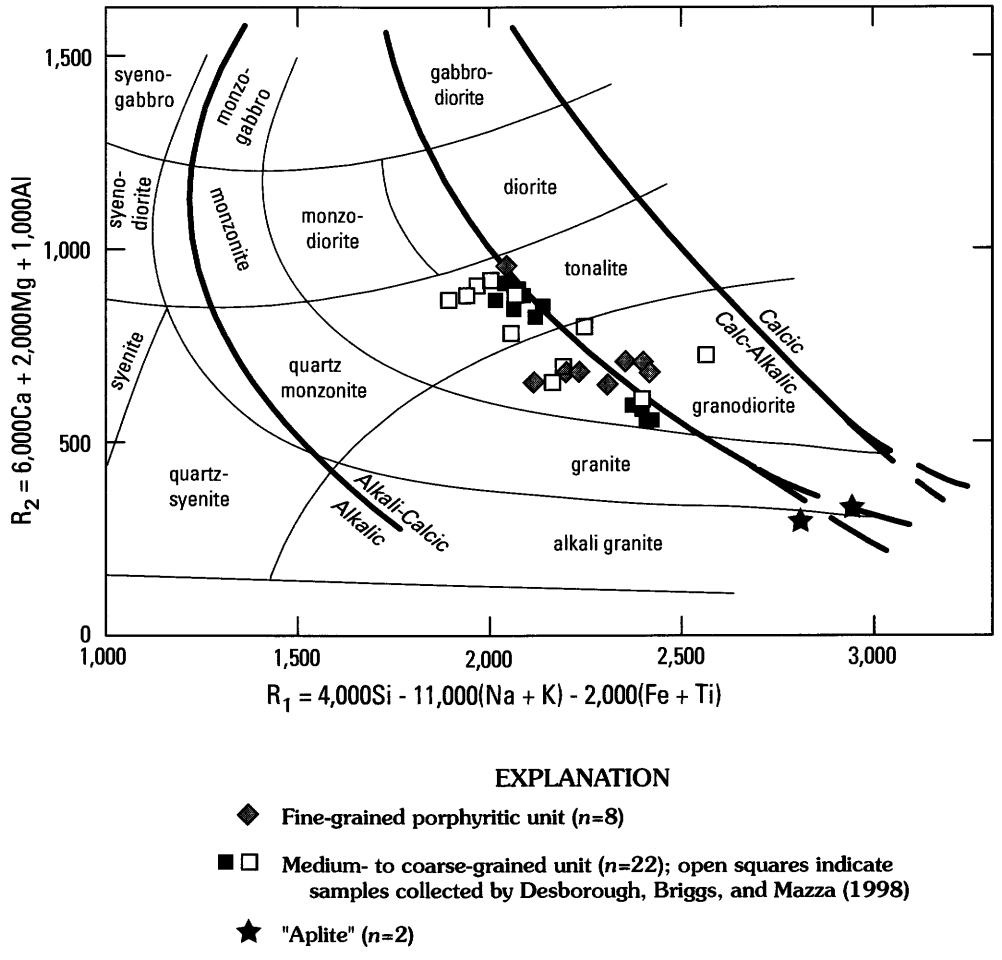

Figure 8. Classification of Butte pluton samples from the study area based on the R_1R_2-diagram of De La Roche and others (1980). Chemical data from Becraft and others (1963, table 2, p. 10, and table 5, p. 22), Ruppel (1963, table 3, p. 26), and Desborough, Briggs, and Mazza (1998, table 1, p. 6–7).

showed similar correlation matrices. A grouping of Ti-Sc-V-Ca-Fe-Y, and to a lesser extent, manganese, accounted for 30 percent of the variation in the factor analysis. The grouping of Ca-Fe-Ti, associated with magnesium and phosphorus, may be explained by mafic minerals, such as: (1) the amphiboles tremolite [ideal formula $Ca_2Mg_5Si_8O_{22}(OH)_2$], actinolite [$Ca_2(Mg, Fe)_5Si_8O_{22}(OH)_2$], and hornblende [$(Ca, Na)_{2-3}(Mg, Fe, Al)_5Si_6(Si, Al)_2O_{22}(OH)_2$]; (2) sphene [$CaTiO(SiO_4)$]; (3) biotite [$K(Mg, Fe)_3(AlSi_3O_{10}(OH)_2$]; and (4) apatite [$Ca_5(PO_4)_3(F, Cl, OH)$]. Note again the trends in figure 6, which suggest that as silica content increased in the normal crystallization of this plutonic melt, magnesium, calcium, phosphorus, and titanium concentrations decreased. Thus, silica-rich facies of the Butte pluton should contain relatively fewer mafic minerals, whereas less silica-rich facies should have relatively more mafic minerals.

Project research indicates that the mafic minerals within the Butte pluton contribute significantly to the acid-neutralizing potential of the watershed (Desborough, Briggs, Mazza, and Driscoll, 1998). Butte pluton rocks rich in mafic minerals are thought to have higher capacity to neutralize acidic waters than plutonic and volcanic facies that are more silicic and have fewer mafic minerals. The relationship between mafic minerals and acid-neutralizing potential is discussed later in this chapter and in McCafferty and others (this volume, Chapter D2).

Ages

Rocks of the Boulder batholith have been dated previously by K-Ar methods (Knopf, 1956; McDowell, 1966; Robinson and others, 1968; Tilling and others, 1968) and preliminary Pb-alpha dating has also been done (Chapman and others, 1955). Previous K-Ar ages for the Boulder batholith are cooling ages that range from 78 to 70 Ma. The Pb-alpha ages obtained by Chapman and others (1955) on the Butte pluton were 71 Ma.

New U-Pb dating using SHRIMP techniques was done in conjunction with this study. The single age, from a sample collected from the central part of the Butte pluton near the trace

of the Butte-Helena fault zone, is 74.5±0.9 Ma. This new age indicates that the span of emplacement for most of the Boulder batholith is from about 82 to 74 Ma (Lund and others, 2002).

Relationship Between Late Cretaceous-Age Volcanic and Plutonic Rocks

Comparison of Geochemical Data

Rock chemistry indicates that most of the magma that formed the Elkhorn Mountains Volcanics was related to the mafic plutons of the Boulder batholith (Tilling, 1974). Significant mafic plutons, of relatively lesser volumetric importance in the Boulder batholith, are the Unionville pluton along the northern margin of the batholith directly north of this study area, the Kokoruda Ranch Complex on the northeast corner of the batholith, and the Burton Park and Rader Creek plutons near the southern margin of the batholith (fig. 2). Thus, rock chemical information suggests that most of the early magma of this volcano-plutonic complex was erupted and relatively little of it crystallized in the crust.

Chemical analyses indicate that only ash flows of the middle member of the Elkhorn Mountains Volcanics were derived from the same magma as the Butte pluton or related silicic intrusive rocks. Chemical compositions of ash flows of the middle member plot in a silicic and potassic extension of the field plotted for the Butte pluton and related silicic plutons (compare figs. 4 and 8). Thus, the middle member of the Elkhorn Mountains Volcanics and the Butte pluton had a common source, and the middle member is probably a differentiate of the magma that formed the Butte pluton and other closely related silicic plutons (Tilling, 1974; Lambe, 1981; Rutland, 1986; Rutland and others, 1989). Further, a volumetrically small part of the volcanic rocks are related to the Butte pluton, which is overwhelmingly the most voluminous part of the Boulder batholith.

Emplacement History

The 78- to 72-Ma volcanic-plutonic episode began with eruption of volcanic ash that was water-worked and became incorporated into Upper Cretaceous volcanogenic sedimentary deposits of the Slim Sam Formation. Early, voluminous volcanism was coeval with injection of the oldest, more mafic magmas into the upper crust along older, deep-seated fault zones. Magma of this generation intruded Paleozoic and Mesozoic prevolcanic country rocks and cooled to form the mafic plutons concentrated along the northern and southern margins of the batholith; most of the magma of this generation erupted to form the lower member of the Elkhorn Mountains Volcanics. During the main stage, more silicic magmas were injected, probably as sheeted dikes, into the progressively forming structural pull-apart in the upper crust, forming the voluminous Butte pluton. Because the void created by the pull-apart was an ongoing process, apparently less magma was available to be erupted to form the middle member of the Elkhorn Mountains Volcanics. The upper member of the Elkhorn Mountains Volcanics documents the waning stages of volcanism and the return to a sedimentary environment, as much of the material in the upper member is water-worked tuff and coarse volcanogenic sedimentary rocks. The magma that formed the Butte pluton clearly intruded its own cogenetic volcanic cover rocks; that the lower member of the Elkhorn Mountains Volcanics is absent in the study area is consistent with the dynamic opening of a pull-apart and consequent tectonic transport of early, lower member volcanics to the east. Thus, the presence of the contact between the Elkhorn Mountains Volcanics and the Butte pluton in the study area suggests that the exposures of coeval volcanic-plutonic rocks are at or near the structural top of the pluton where it intrudes its volcanic cover.

Internal Geometry of Butte Pluton

Becraft and others (1963) and Ruppel (1963) described, and plate 1 illustrates, a textural pattern of finer grained rocks at the top of the Boulder batholith. The overall pattern is of an original chill zone of fine-grained rock at the roof and more slowly cooled, coarse-grained zones at depth; finer grained rocks near or at the original roof of the pluton are more common in the laccolithic part of the pluton in the west part of the area of plate 1. In some places, the coarser phases are in direct contact with the overlying roof rocks, suggesting an unsolidified, mobile interior of the magma body intruded above the level of its earlier formed chilled border. The large number of aplite dikes in the Butte pluton on the east side of the map area in the main body of the pluton probably represents late water-rich segregations that migrated into joints. Some of the aplite bodies that were mapped as irregular sheets are interpreted to be part of the chilled facies that formed near the roof of the magma chamber. This silicic, water-rich phase either chilled against the roof or was injected into joints as they formed during the contraction related to cooling of the whole pluton. The chilled phases of the roof zone also show evidence of having been stoped (cut loose and rafted in the magma) and of being assimilated by still-mobile magmas, resulting in some irregular outcrop patterns.

Tertiary Volcanic Rocks

Tertiary volcanic and intrusive rocks of the study area were mapped and classified by Becraft and others (1963) and Ruppel (1963) into "quartz latite" and "rhyolite" groups. These workers agreed with Knopf (1913, p. 41) that the "rhyolite" and "quartz latite" seem to represent two distinctly different periods of volcanic activity. Becraft and others (1963) and Ruppel (1963) correlated the "quartz latite" group with a part of the Lowland Creek Volcanics of early Eocene in age, as

defined by Smedes and others (1962) southwest of the study area. "Rhyolite" rocks in the study area have been included in the early Oligocene Helena volcanic field of Chadwick (1978).

Eocene Lowland Creek Volcanics

Smedes (1962) named and described the Lowland Creek Volcanics for a thick sequence of volcanic rocks and associated intrusive dikes and plugs exposed north and west of Butte, Mont. Lowland Creek, the type locality of these rocks, drains into the Boulder River about 7.5 mi upstream from the town of Basin. The original extent of the volcanic field was a northeast-elongate zone of about 125 mi^2, more or less centered near Lowland Creek. The northeasternmost extent of the volcanic field was just east of the study area at Jefferson City. Radiometric K-Ar age determinations indicate the volcanics are Eocene in age, 50–48 Ma (Smedes and Thomas, 1965). New $^{40}Ar/^{39}Ar$ ages suggest that some of these rocks may be as old as 52 Ma (Ispolatov and others, 1996).

Lowland Creek Volcanics are a complexly intertongued and interlayered volcanic and volcaniclastic sequence nearly 6,100 ft thick. The layered rocks, in general, consist of a basal conglomerate overlain by welded tuff deposits that compose more than half of the volcanic sequence. Lava flows and vitrophyre make up the uppermost part of the sequence.

Lowland Creek Volcanics are present only in the southernmost part of the watershed study area. Tuffaceous rocks underlie Pole Mountain northwest of Basin as well as the nose of a small ridge at the confluence of Cataract and Big Limber Creeks just east of Basin. The remaining Lowland Creek rocks occur as small plugs, phreato-magmatic breccia pipes and diatremes, and abundant northeast-trending dikes best exposed near High Ore Creek. These volcanic rocks rest on partly exhumed Butte pluton rocks as well as on the cogenetic Elkhorn Mountains Volcanics.

Based on normative quartz, potassium feldspar, and plagioclase calculated from chemical analyses, Becraft and others (1963) and Ruppel (1963) classified rocks from this group as quartz latites. Becraft and others (1963, table 7, p. 28) reported the chemical analyses of four samples of intrusive rocks of this group. Ruppel (1963, table 4, p. 49) reported the analyses of two volcanic rocks and one intrusive rock from this group. Use of the R_1R_2-diagram of De La Roche and others (1980) plots three of Becraft's samples in the rhyodacite field and one just into the rhyolite field (fig. 9); Ruppel's analyses of welded tuff and intrusive rock samples plot in the rhyodacite field (fig. 9). Ruppel's lapilli tuff sample plots well to the right of the alkali rhyolite field (fig. 9); the high silica content is probably due to silicification after deposition. In general chemical composition (refer to fig. 10), the rhyodacite welded tuff sample of Ruppel (1963) clusters with the four intrusive rocks of Becraft and others (1963). The rhyodacite intrusive rock of Ruppel (1963) appears to be compositionally intermediate between the rhyodacite of the Lowland Creek Volcanics and rhyolitic rocks of the Helena volcanic field (fig. 10).

Eocene-Oligocene Helena Volcanic Rocks

The Helena volcanic field includes rhyolitic rocks in the northern part of the Boulder batholith, as well as silicic flows west, northwest, and east of Helena at Avon, Mullan Pass, and Lava Mountain, respectively. Rocks from this field have yielded radiometric K-Ar ages between 37.3 and 35.8 Ma (Chadwick, 1978). Rocks in the northern part of the Boulder batholith, near or within the study area, have not been dated.

Rhyolitic rocks of the Helena volcanic field are present along the Continental Divide in the western and northern parts of the watershed study area (pl. 1). The rhyolite consists of volcanic flows and tuffs on the west and forms intrusive centers near the Basin Creek mine in the north. The rock is porphyritic with common sanidine and biotite phenocrysts. The rhyolite was erupted onto an erosion surface of low relief and rests unconformably on plutonic rocks of the Butte pluton, Elkhorn Mountains and Lowland Creek Volcanics, and the Eocene-Oligocene sedimentary rocks of the poorly exposed and unmapped Renova Formation.

On the R_1R_2-diagram of De La Roche and others (1980), the four published analyses for samples of the Eocene-Oligocene rhyolitic rocks of the Helena volcanic field plot in the alkali rhyolite field (fig. 9). These rocks include two samples of flows collected by Ruppel (1963), a sample of silicified rock collected from the southeast flank of Red Mountain directly north of the study area by Becraft and others (1963), and a sample of rhyolite from the top of Red Mountain reported by Clarke (1910, p. 80). In addition to higher silica content than the Eocene Lowland Creek Volcanics, the Eocene-Oligocene alkali rhyolites of the Helena volcanic field have generally lower amounts of aluminum, calcium, magnesium, and titanium, and higher sodium and potassium (fig. 10). A silica-rich sample of the Lowland Creek Volcanics, Ruppel's (1963) lapilli tuff sample (likely silicified), is chemically similar to the Helena volcanic rocks (fig. 10).

Miocene-Pliocene Volcanic Rocks

Although no volcanic rocks younger than the Helena volcanic rocks have been recognized from the central parts of the Boulder batholith, Ruppel (1963) described basalt in the northwestern part of the area of plate 1, and he included these rocks with the Elkhorn Mountains Volcanics. Basaltic flows and flow breccias rest unconformably on the Elkhorn Mountains Volcanics; basaltic intrusive rocks commonly intrude them as well. Ruppel (1963) commented that the basaltic rocks west of the Basin quadrangle are folded and faulted in a style similar to that of the Elkhorn Mountains Volcanics in the Basin quadrangle. Based largely on the structural similarity, Ruppel (1963) provisionally included the extrusive basalts with the Elkhorn Mountains Volcanics.

Basalts are known from the Avon area, directly northwest of the area of plate 1. Trombetta (1987), in his study of Helena rhyolitic rocks exposed near Avon, recognized that the basaltic rocks in this area are the youngest of the extrusive rocks and

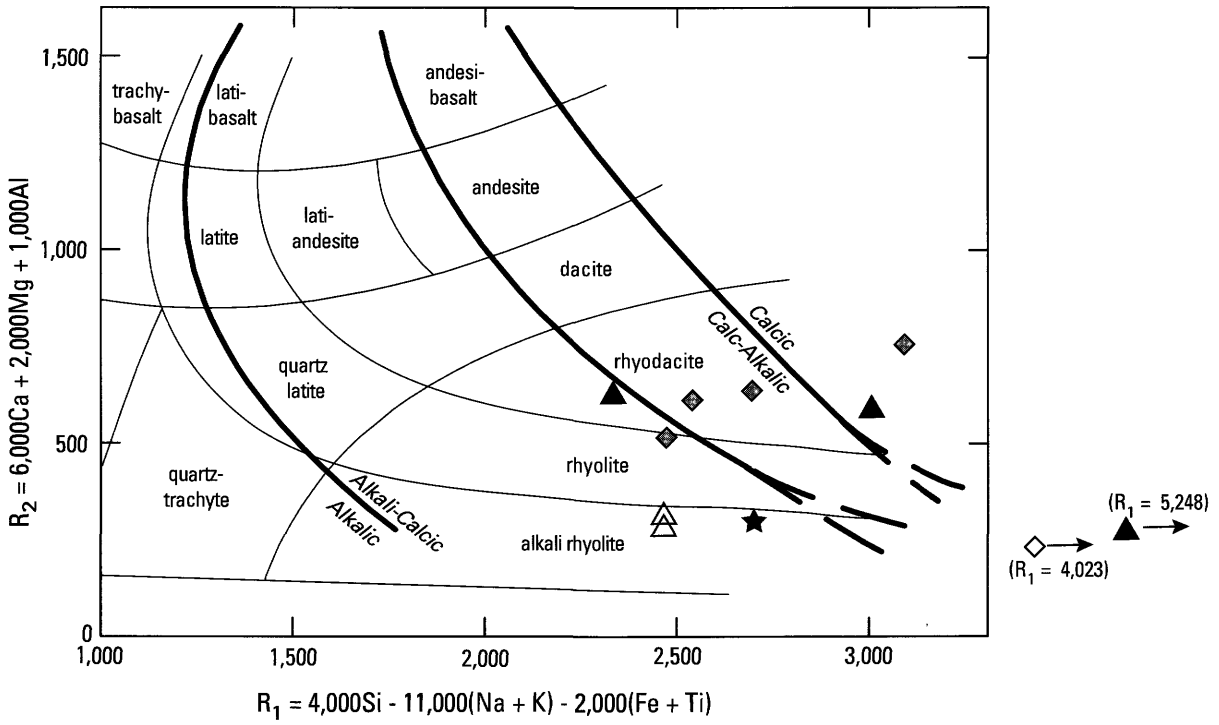

EXPLANATION

- ◈ Intrusive rocks related to Lowland Creek Volcanics, called "quartz latite" (*n*=4) and collected by Becraft and others (1963, table 7, p. 28)
- ▲ Lowland Creek Volcanics: lapilli tuff (*n*=1), welded tuff (*n*=1), and intrusive rock (*n*=1) called the "quartz latite group" and collected by Ruppel (1963, table 4, p. 49)
- △ Helena volcanics flow rocks called the "rhyolite group" (*n*=2) and collected by Ruppel (1963, table 4, p. 49)
- ◇ Altered rhyolite from the Helena volcanics from southeast slope of Red Mountain collected by Becraft and others (1963, table 8, p. 30)
- ★ Rhyolite from the Helena volcanics from top of Red Mountain, as reported by Clarke (1910, p. 80)

Figure 9. Classification of samples of Eocene Lowland Creek Volcanics and of Eocene-Oligocene volcanic rocks from the Helena volcanic field in the study area based on the R_1R_2-diagram of De La Roche and others (1980).

are not genetically related to underlying rhyolitic rocks. We have no definitive data regarding the age of the basalt flows, flow breccias, and intrusive basaltic rocks in the map area; however, on the basis of crosscutting relations observed directly northwest of the study area (Trombetta, 1987), at least some basaltic rocks are likely late Tertiary in age. No basaltic rocks are present in the study area.

Sedimentary Rocks

Lower Tertiary Sedimentary Rocks

Sedimentary rocks of early Tertiary age were not recognized in the study area by previous workers. Today, due largely to numerous new roads constructed to accommodate development of the Basin Creek mine in the northern part of the study area and extensive logging operations in the western part, new exposures of bedrock in roadcuts have allowed recognition of previously concealed sedimentary rocks. The newly recognized rocks consist of poorly cemented and layered, light-gray to tan sediment composed of sand and silt derived mainly from erosion of batholithic rocks. The newly discovered sedimentary deposits are preserved only where they are overlain by more resistant Eocene to lower Oligocene rhyolitic rocks of the Helena volcanic field in the western and northern parts of the study area.

The new exposures are extremely limited and of poor quality, and are not shown on plate 1. Along the Elk Gulch tributary of Joe Bowers Creek in the northwestern part of the study area, the upper 3–4 ft of the sedimentary unit has been exposed. The sediments are weakly layered and locally

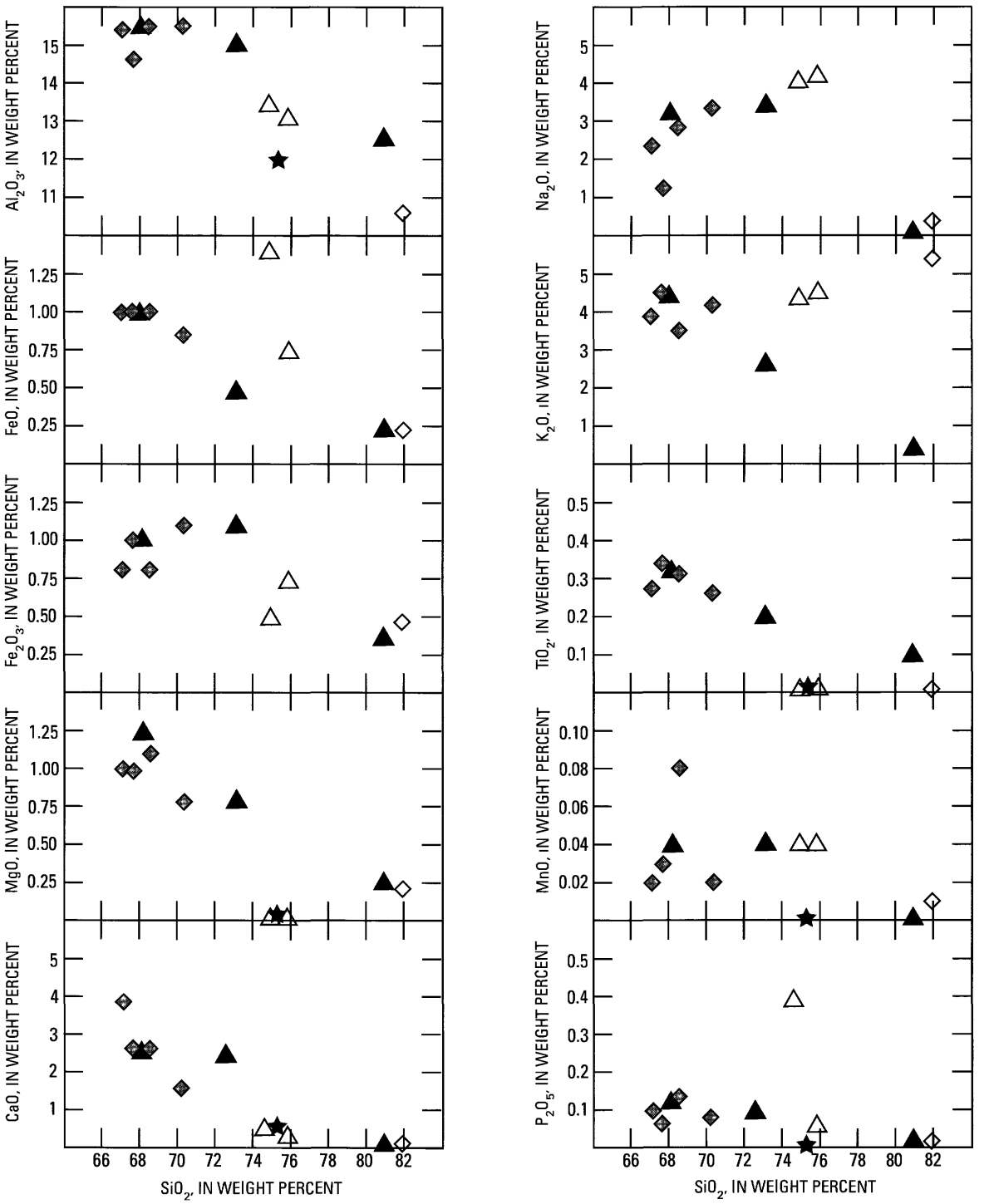

EXPLANATION

- ◈ Intrusive rocks related to Lowland Creek Volcanics, called "quartz latite" (*n*=4) and collected by Becraft and others (1963, table 7, p. 28)
- ▲ Lowland Creek Volcanics: lapilli tuff (*n*=1), welded tuff (*n*=1), and intrusive rock (*n*=1) called the "quartz latite group" and collected by Ruppel (1963, table 4, p. 49)
- △ Helena volcanics flow rocks called the "rhyolite group" (*n*=2) and collected by Ruppel (1963, table 4, p. 49)
- ◇ Altered rhyolite from the Helena volcanics from southeast slope of Red Mountain collected by Becraft and others (1963, table 8, p. 30)
- ★ Rhyolite from the Helena volcanics from top of Red Mountain, as reported by Clarke (1910, p. 80)

Figure 10. Harker variation diagrams showing abundances of major oxides versus SiO_2 for 11 samples of Eocene Lowland Creek Volcanics and of Eocene-Oligocene volcanic rocks from the Helena volcanic field in the study area.

contain cut and fill sedimentary structures. Here, the overlying rhyolite has baked the underlying sedimentary rocks, resulting in a 6-in. thick, bright-red zone of oxidation at the contact. An exploratory hole dug at the base of the exposure revealed 2 ft of loosely consolidated arkosic sand; the base of the sand was not reached.

The maximum thickness of the sedimentary rocks is not known; thickness is variable, as the unit is not everywhere present, and probably does not exceed 50 ft. Maximum road-cut thicknesses of about 15 ft are present west of the study area in the Red Rock Creek drainage basin, west of Thunderbolt Mountain and outside the area shown on plate 1. The distribution of the sediment appears to have been controlled by early Tertiary topography in this area. The sedimentary deposits appear to have filled in lower areas, while higher areas remained uncovered.

Although these sedimentary rocks were not previously mapped in the study area below the Helena volcanic rocks, somewhat anomalous geologic conditions present at this geologic horizon can be interpreted to reflect the presence of these deposits. Abundant colluvial deposits, landslides, and unusually moist and wet soil conditions associated with bogs and springs are present in many places along the lower contact of the Helena volcanic rocks. We suggest that the localized mass-wasting deposits and unusual hydrologic conditions reflect the presence of concealed, poorly consolidated, porous, and easily weathered sedimentary units at this contact.

Lower Tertiary sedimentary rocks are common in southwestern Montana but are mostly found only in present-day basins. These basin-fill sediments are part of the Bozeman Group of Robinson (1963) and have been divided into the older Eocene-Oligocene Renova Formation and the younger Miocene-Pliocene Six Mile Creek Formation. The older Renova filled sedimentary basins of unknown extent that formed in the Eocene. The Renova basins were later segmented by late Tertiary-Quaternary basin-range faulting. The Renova is known primarily from sparse outcrops along the margins of these young basins. In only one other uplifted mountain range in this region are lower Tertiary basin-fill sediments known to be preserved—the Gravelly Range south of the study area (O'Neill and Christiansen, 2002; Luikart, 1997). In the Gravelly Range, loosely consolidated sandstone and siltstone containing Eocene-Oligocene vertebrate fossils are preserved beneath resistant volcanic rock.

Quaternary Deposits

The most extensive surficial deposits in the study area are glacial accumulations of Pleistocene age. These deposits comprise mainly morainal debris and outwash. On the east the glacial drift is largely confined to the headwaters area and valley bottom of Cataract Creek. On the west, in the Basin Creek watershed, glacial till is extensive, covering gentle, east-facing slopes from Pole Mountain to the Continental Divide as well as the broad valley bottoms of Basin and Jack Creeks and their smaller tributaries. Ruppel (1963) and Becraft and others (1963), in their discussion of glaciation, concluded that the glacial deposits represent the older of two major late Pleistocene periods of glaciation in southwest Montana. The older glacial period, now commonly referred to as Bull Lake episode, ended about 120,000 years ago. Bull Lake glaciation was more extensive and reached lower elevations than the younger Pinedale episode, which was restricted to only the highest alpine areas of the region, some 18,000 to 10,000 years ago. The assignment of the glacial deposits to the older, Bull Lake period of glaciation in the study area was based largely on the 6 to 10 ft depth of weathering of the till, the lack of conspicuous, preserved glacial morphology, and the relatively low elevation of the deposits.

The till is composed mainly of locally derived plutonic and volcanic rocks. Because much of the till is deeply weathered, smaller clasts in the original till are poorly preserved and most have disintegrated into unsorted sand- and granule-size grains that now form the interstitial matrix for larger, less weathered boulders.

Glacial outwash is exposed only in the Basin Creek drainage of the study area, at the confluence of Basin and Jack Creeks, and along Basin Creek about 2 mi southeast of the confluence. The deposits consist of pebbles and cobbles interlayered with fine- to coarse-grained sand lenses. Additional deposits of relatively coarse grained outwash are concealed beneath younger, finer grained stream and bog deposits along the upper reaches of Basin Creek as well. During the course of this study, stream and flood-plain deposits along Basin Creek at Buckeye Meadow were sampled in 10 relatively closely spaced monitoring wells in the vicinity of the Buckeye mine. In this area, coarse braided stream deposits interpreted to represent, in part, glacial outwash are overlain by as much as 10 ft of thin stream sand and gravel lenses interlayered with organic-rich sand, silt, and clay deposited in levees, bogs, and backswamps (pl. 2). One well (site 4a, pl. 2) drilled in these organic-rich sediments intersected the 6,845 year old Mazama ash at 3.6 ft depth.

Less widespread surficial deposits are also present throughout the study area. These deposits include stream alluvium, localized alluvial fan deposits, colluvium, talus deposits, and localized landslides. Solifluction or down-slope creep of many of the finer grained surficial deposits appears to be occurring at the present time. Relatively gentle slopes, extensive exposures of deeply weathered, porous glacial till locally superimposed on weakly consolidated lower Tertiary sedimentary rocks, and relatively thick winter snow pack combine to produce a large area of water-logged, unstable surface conditions that engender down-slope creep of unconsolidated sediment during periods of snow melt and high runoff.

Structural Geology and Tectonics

Introduction

Fracture systems in igneous rocks are a prominent phenomenon recognized and described worldwide. Perhaps the most commonly recognized fractures are primary nondiastrophic cooling and contraction columnar joints characteristic of volcanic flows and intrusive rocks emplaced at shallow depths. Fractures can also reflect diastrophic processes that record structural and tectonic events. The Butte pluton of the Boulder batholith, well known for its locally spectacular fracture systems (fig. 11), appears to contain both nondiastrophic and diastrophic features. Prominent nondiastrophic fracture systems are well exposed because the level of erosion of the pluton is minimal, and only the outer skin of the magma body (1,500 ft or less), where cooling fractures are best developed, is exposed. The Cretaceous Boulder batholith was also intruded during Laramide time into one of the more complexly deformed tectonic regions of the American Cordillera. The Butte pluton can be considered unusual because it appears to contain both primary and secondary diastrophic structures. Primary diastrophic fractures are herein interpreted to represent structures related to the mechanism of intrusion of the pluton; colinear secondary fractures are postemplacement structures formed throughout the Tertiary and Quaternary in response to reactivation of deep-seated, earlier formed structures. The origin and orientation of the fracture systems in the pluton, including the nondiastrophic cooling features, appear to be intimately tied to the mechanism of emplacement of the igneous body.

The origin of the fracture systems presented here follows years of discussion regarding the origin of vein systems in the Butte pluton. The most recent discussion of their origin was by Woodward (1986), who correctly observed that polymetallic quartz veins developed in an east-west compressional stress field within the Sevier orogenic belt. Woodward (1986) postulated that the northeast and northwest vein systems represented conjugate shears in such a stress field, whereas east-trending fractures, which host the quartz-vein deposits in the study area as well as at Butte, were extensional fractures oriented parallel to the maximum principal stress trajectories. Although this proposal would apply to a static, cooling body intruded into an ongoing contractional environment, we do not believe it to be compatible with the mechanism of emplacement of the batholith described previously, in the section, "Mode of Emplacement."

Figure 11. Prominent fracture systems in Butte pluton. View to north from Interstate 90 about 2 mi east of Homestake Pass south of the area of plate 1.

Nondiastrophic Fracture Systems

Nine major fracture systems are recognized in the Boulder batholith. The primary age of six of these systems is established by the observation that aplite (including pegmatite and alaskite) dikes and quartz veins follow them. Three of the six primary fracture systems, best exposed in the Basin quadrangle, were interpreted by Ruppel (1963), following the terminology of Balk (1948), as nondiastrophic cooling joints: they are cross joints, longitudinal joints, and primary flat-lying joints (fig. 12). In the Boulder batholith, cross joints are steep to nearly vertical east-trending fractures spaced from about 5 to 10 ft. Longitudinal joints trend north and generally dip steeply west; spacing on these fractures is from 1 to 5 ft. These two nearly vertical joint sets have been intruded in various localities by thin dikes of aplite. Primary flat-lying joints, which mainly dip gently south, have locally been intruded by thick sheets of aplite. In coarser grained facies of the batholith, joint spacing of north-trending fractures increases to 15 ft, and east-trending fractures are spaced at intervals as much as 40 ft. Individual joints are rarely longer than about 30 ft; however, where one joint dies out, it is commonly overlapped by a parallel joint that either is entirely separate and less than 1 in. to several inches away, or is connected by a transverse joint or joint set.

Joint sets of identical orientation and character were described by Smedes (1966) from the northern Elkhorn Mountains directly east of the study area (fig. 13). In that area, the north-trending set is the better developed of the two nearly vertical sets.

The three primary, nondiastrophic fracture sets just described appear to be genetically related to the emplacement and cooling history of the batholith. Theoretical, two-dimensional calculations of the stress field in static, cooling magma bodies in the crust have been presented by Knapp and Norton (1987). Theoretical calculations of such a magma body reveal a radial and concentric stress field in which the maximum principal stress is in the radial position (fig. 14). In such a case, tension fractures related to the cooling, crystallization, and contraction of a magma body will be vertical at the top and rotate to horizontal along the sides of the crystallized, brittle pluton. Nearer to the molten center of the magma, maximum principal thermal stress trajectories are deflected to horizontal and become concentric around the cooling center. Fractures formed directly above the cooling center are flat lying or horizontal.

The east half of the Butte pluton has been interpreted to have been emplaced within an ever-widening, east-directed pull-apart in the Helena embayment that was bounded by steep fault abutments on the north, south, east, and west (figs. 2, 3). Along the roof of the crystallized, yet still cooling pluton, the stress field described by Knapp and Norton (1987) likely applies (fig. 14); that is, the maximum principal stress trajectories are vertical and the least principal stress is horizontal. However, because the inferred pull-apart emplacement mechanism is not static but an ongoing process, maximum stress is unlikely to be radial around the body; the likelihood is that it remains vertical along the sides of this particular, eastward-expanding pluton. Thus, the least principal stress must be horizontal and oriented east-west. In this kinematic scenario the intermediate stress must also be horizontal and directed normal to the confining walls on the north and south. With this configuration of stress trajectories, well-developed north-trending fractures should be a prominent joint set in the pluton. In the likelihood that growth of a pull-apart follows the conventional wisdom of strike-slip fault displacement, the

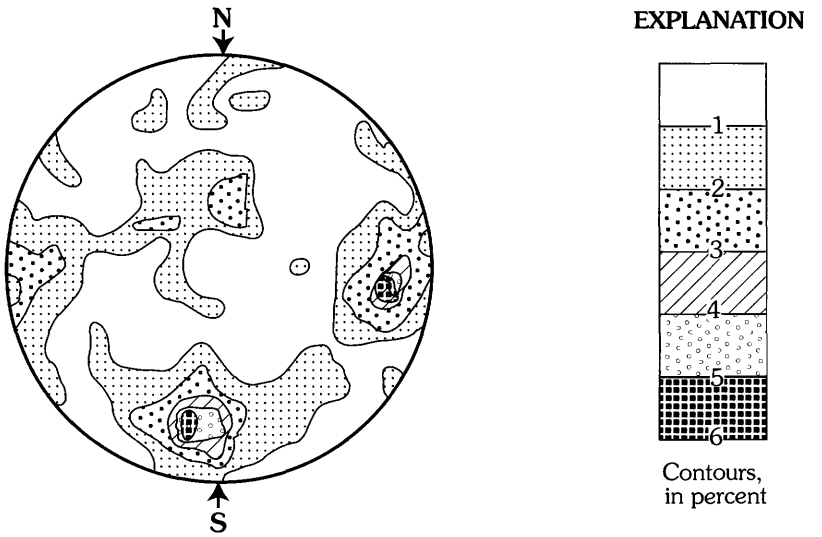

Figure 12. Contour diagram of 493 joints in Butte pluton rocks from west half of the area of plate 1, equal area projection on lower hemisphere (from Ruppel, 1963, pl. 5).

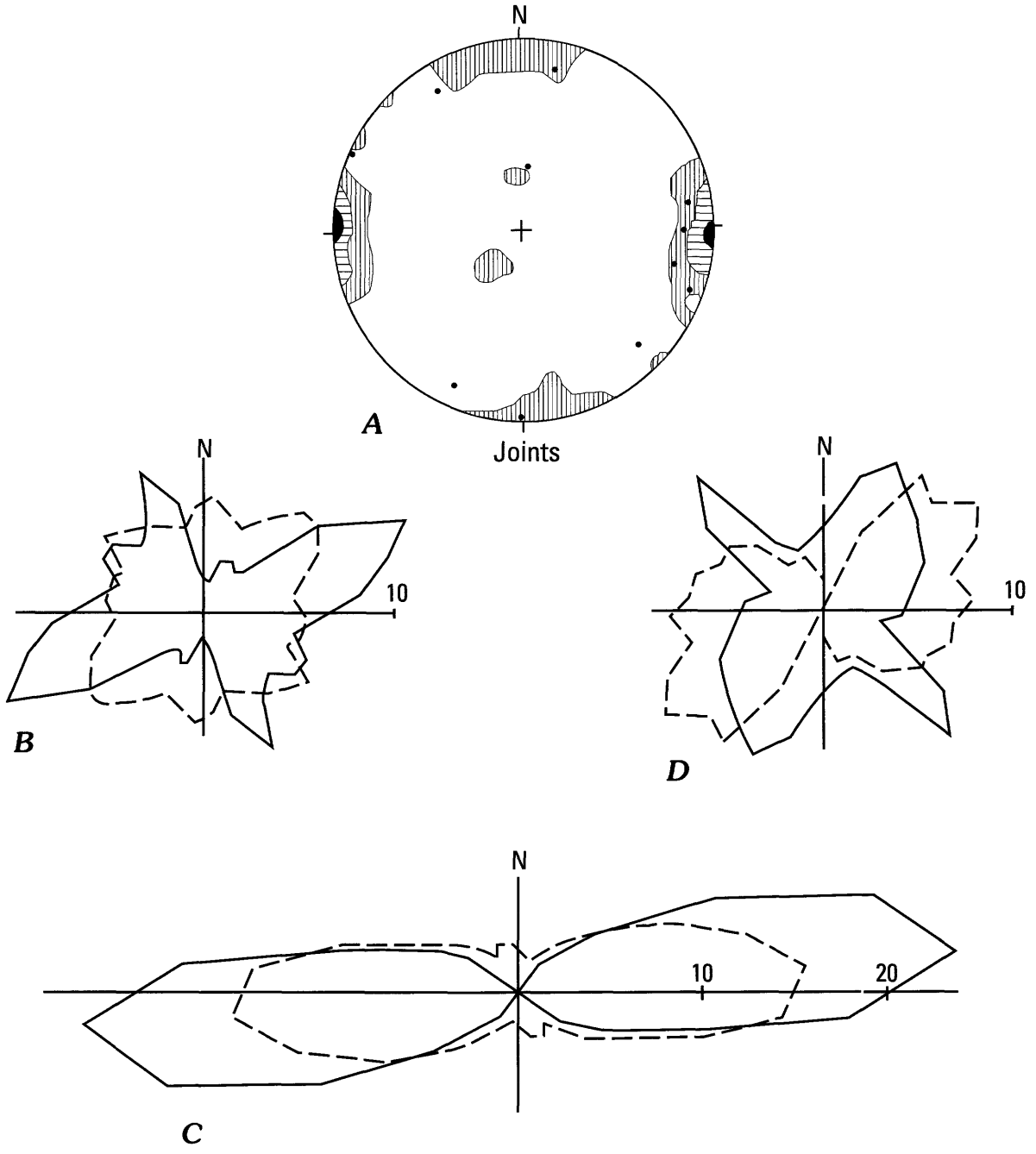

Figure 13. Summary diagrams of *A*, joints; *B*, alaskite, aplite, and pegmatite dikes; *C*, veins; and *D*, faults and lineaments in the northern Elkhorn Mountains east of the area of plate 1 (from Smedes, 1966, fig. 30). *A*, Contour diagram of poles of 283 joints in Butte pluton and point diagram of poles of 11 joints in the Kokoruda Ranch complex. Contours 2-6-10 (11) percent. Equal area projection of lower hemisphere. *B*, *C*, *D*, Each rosette is a statistical summary showing relative abundance (percent) of trends of all high-angle planar structures of a given type and is weighted according to length. *B*, Solid line, dikes in the Butte pluton (n=685); dashed line, dikes in the Kokoruda Ranch complex (n=42). *C*, Solid line, metalliferous quartz veins (n=192); dashed line, chalcedony veins (n=698). *D*, Solid line, faults (n=996); dashed line, lineaments (n=1,357).

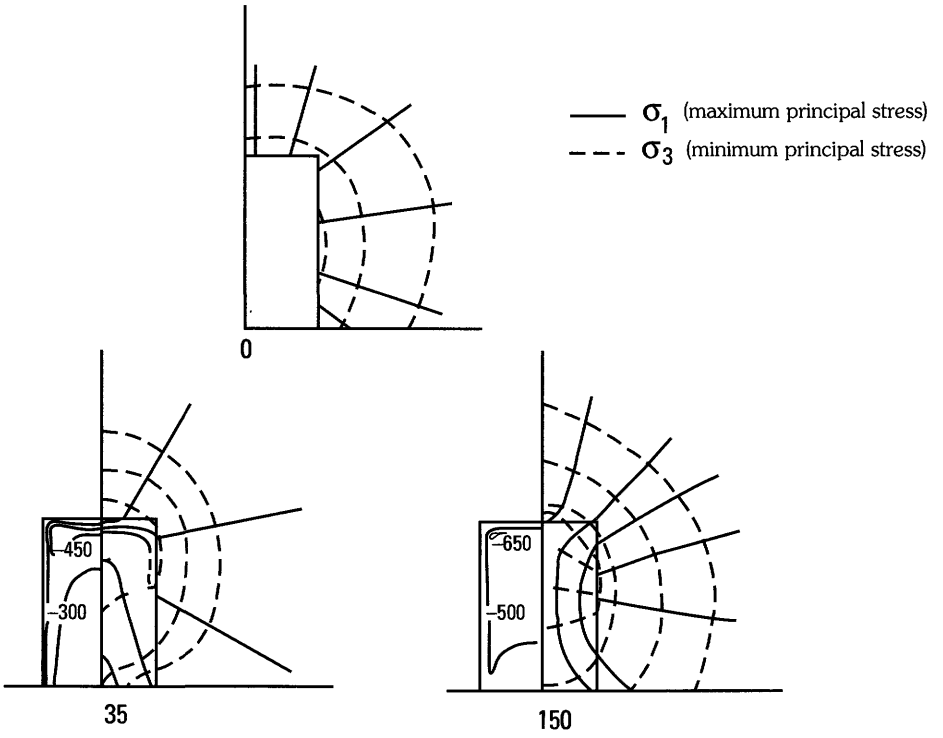

Figure 14. Principal stress trajectories and net change in temperature (°C) in the model system at 0, 35,000, and 150,000 years after pluton emplacement (from Knapp and Norton, 1987, fig. 6). Rectangular box represents hypothetical pluton measuring 3 km wide, 4.5 km high, and infinite in the third dimension. Trajectories are radial and tangential around the cooling center located at the top of the pluton at 35,000 years after emplacement.

horizontal intermediate and least principal stresses seem likely to switch positions periodically during magma emplacement. North-south least principal stress orientation should lead to the development of east-trending fractures as well.

Directly above the partly molten cooling center of the pluton, the maximum and least principal stress trajectories are deflected and switch orientations: the maximum principal stress trajectories become horizontal and the least principal stress is vertical (fig. 14). In this stress configuration, prominent horizontal or flat-lying fractures should develop. Because the cooling and crystallization of an igneous body proceeds from the outer rind toward the center, the horizontal fractures are probably the first joint system to form. The common horizontal fractures and joints, often filled with aplite, probably formed earliest, in the elastic, upper parts of the pluton directly above the cooling center where the maximum principal stress was horizontal. Vertical joints, sparsely filled with aplite, formed later in solidified regions farther away from the cooling center of the magma; these joints formed in response to horizontal tensile stresses related to the position of the least principal stress and a nonradial vertical maximum principal stress. As such, the joints formed should be of three orientations: one early-formed horizontal set and two vertical sets trending north and east. As observed by Smedes (1966), the north-trending fractures, which reflect the east-directed pull-apart mechanism, are the prominent tensile fracture in the batholith.

Given the theoretical parameters presented by Knapp and Norton (1987) and the mechanism of emplacement interpreted by Schmidt and others (1990), the orientation of the three observed primary, nondiastrophic joint sets in the Boulder batholith seems to conform with the thermal stress field postulated to occur during magma cooling within a progressively opening, east-directed pull-apart zone.

Synemplacement Diastrophic Fracture Systems

Of the six primary fracture systems in the study area the three remaining systems are diastrophic and appear to be best developed and their included fractures more numerous on the east in the Jefferson City quadrangle. These three fracture systems are best developed farther east in the northern part of the Elkhorn Mountains (figs. 13 and 15). These fracture systems are intruded by large aplite (alaskite) dikes or thin chalcedony veins, or are shear zones that contain quartz veins and polymetallic mineral deposits. That these fracture systems contain late melt fractions from the Butte pluton indicates that they are primary structural features. (See section on "Age," p. 81.)

Large aplite (alaskite) dikes that extend for many hundreds of feet are the most prominent linear features in the area. The preferred orientation of these dikes in the Jefferson City quadrangle and adjacent Elkhorn Mountains is northeast (fig. 15*A*). Becraft and others (1963) observed a bimodal

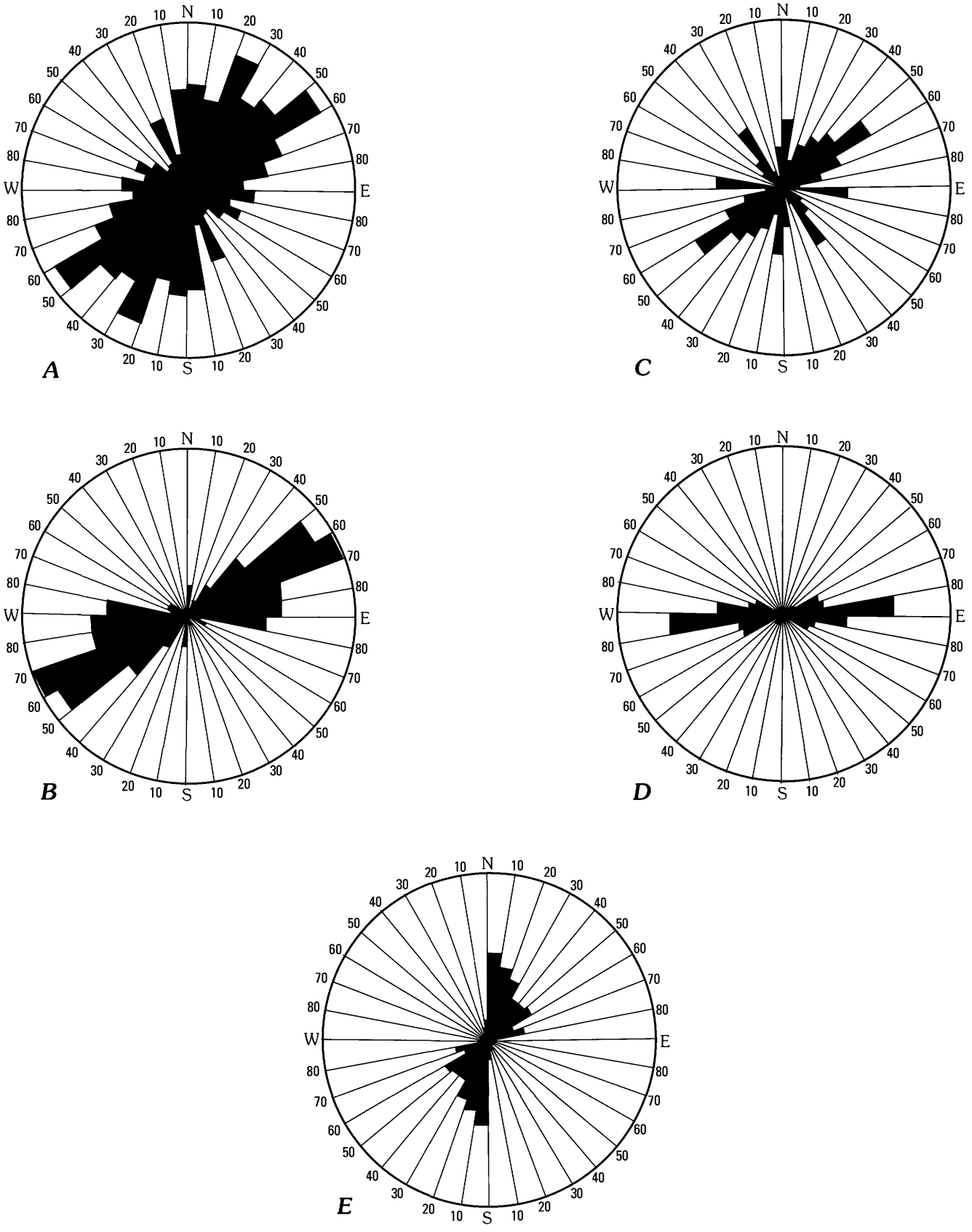

Figure 15. Trends of dikes, veins, shear zones, and nonmineralized faults in the east half of the area of plate 1 (from Becraft and others, 1963, figs. 29, 30, 31, 32, and 33). All data plotted in 10° increments; all data are from Jefferson City quadrangle. *A*, trends of 513 steeply dipping alaskite dikes. *B*, trends of 255 steeply dipping chalcedony vein zones. *C*, trends of 142 nonmineralized faults and topographically expressed lineaments. *D*, trends of 182 shear zones. *E*, trends of 177 Tertiary quartz latite dikes.

northeast trend with two rose diagram maxima at N. 25°E. and N. 55°E. Their rose diagram reveals a small but conspicuous N. 25°W. preferred orientation as well. To the northeast in the Elkhorn Mountains, Smedes (1966) observed and recorded equal numbers of northeast- and northwest-trending aplite (alaskite) dikes (fig. 13). Becraft and others (1963) also examined and described chalcedony veins that are most common in the southern part of the study area. Preferred orientation of chalcedony veins is N. 55°–65°E. (fig. 15*B*).

The most important fracture system, based on its economic significance, is marked by east-trending shear zones as much as 6 mi long (fig. 15*D*). The zones are unusual because, although they cut the overlying Elkhorn Mountains Volcanics, offset is not observed along them. Moreover, the shear zones terminate at the east edge of the batholith and do not extend into the adjacent country rock. Also, east-trending faults have not been mapped in the western, laccolithic part of the batholith. Northeast-trending dikes of the middle Eocene Lowland Creek Volcanics cut the shear zone, and they themselves are neither sheared nor altered. The east-trending shear zones have slickensided surfaces that indicate oblique-slip movement; most zones dip steeply north. The major east-trending zones in the study area host the major mineral deposits and sites of the largest mines. The Comet mine on the east in High Ore Creek and the Morning Glory mine in Cataract Creek are along one of these major east-trending zones; a second major east-trending shear is the locus of the Crystal mine in Uncle Sam Gulch and the Bullion mine along the south fork of Jack Creek (pl. 1). All these mines are point sources for acidic mine and(or) metal-rich drainage in the study area (Nimick and Cleasby, this volume, Chapter D5).

These three primary fracture systems parallel the major fault systems that controlled the location and shape of the batholith. Their genesis is interpreted to be related to the emplacement mechanism of the batholith (fig. 16). In our summary of the emplacement history of the batholith, we noted that the structural setting of the batholith is dominated by three sets of deep-seated northeast-, northwest-, and east-trending faults that first formed in Proterozoic time. All three sets were active during emplacement of the batholith and controlled not only its geographic position and its shape, but also early-formed fracture systems in the igneous mass.

Early-formed fractures directly south of the batholith are northwest-trending reverse faults that offset crystalline basement rocks of the Rocky Mountain foreland; these faults accommodated Laramide basement crustal shortening that terminated against the northeast-trending axial suture of the Great Falls tectonic zone beneath the batholith. Displacement

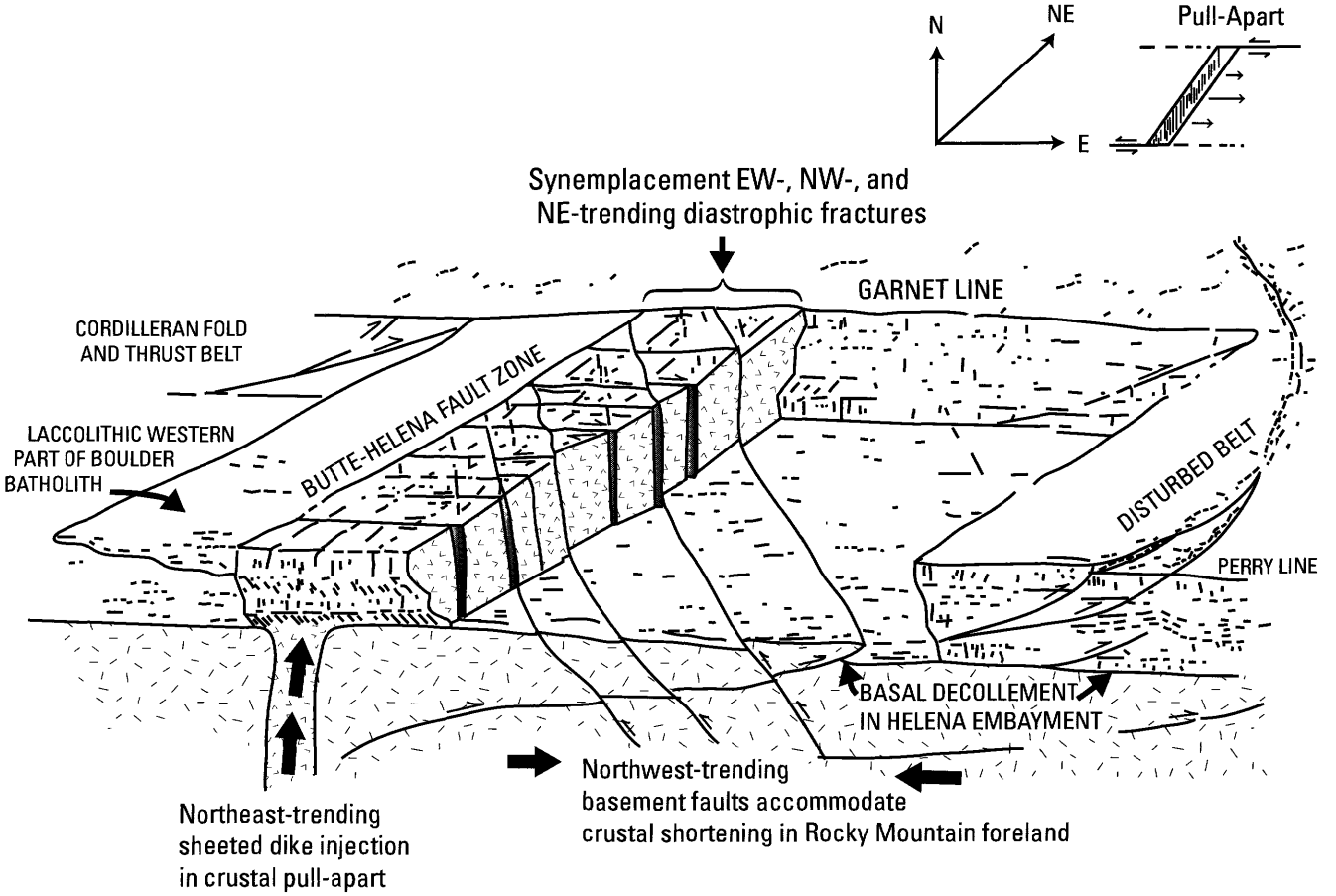

Figure 16. Schematic diagram showing relationship of deep-seated fault zones, which controlled emplacement of the Boulder batholith, to synemplacement diastrophic fractures in the Butte pluton. Butte-Helena fault is directly over central part of Great Falls tectonic zone.

of basement rocks along northwest trends at the floor of the batholith during its emplacement is inferred to have displaced crystallized, brittle batholithic rocks. The cooling, still partly molten core of the batholith would also be affected by fault movement, which would have enhanced leakage of late-stage magmatic melts into newly formed fracture systems. Northeast-trending fractures filled with alaskite dikes and chalcedony veins are interpreted to reflect synthetic and antithetic fractures formed subparallel to the Butte-Helena fault zone as the pull-apart expanded eastward.

The east-trending shear zones are subparallel to the bounding faults on the north and south. As the pull-apart widened eastward, it carried with it partly cooled, brittle batholithic rocks. The east-trending shear zones, which host the polymetallic quartz vein deposits and are restricted to the batholith, outline eastward-elongate blocks of Butte pluton rocks carried eastward during tectonism. The east-trending shear zones are interpreted to be accommodation zones within the batholith that allowed coeval, yet slightly disparate, eastward advance of the plutonic rocks during growth of the pull-apart.

Late Diastrophic Structures

Of the nine major fracture systems recognized in the batholith, the last three are secondary systems that owe their origin to reactivation of preexisting structures. Tertiary and Quaternary recurrent movement along preexisting faults and fractures in southwestern Montana has been documented by previous workers (for example, Schmidt and Garrihan, 1983; O'Neill and Lopez, 1985; O'Neill and others, 1986). In middle Eocene time, northeast-trending fracture systems were important in controlling the location of intrusion of numerous dike swarms and igneous plugs and stocks along the Great Falls tectonic zone from east-central Idaho, across southwestern Montana, including the Boulder batholith, and extending into the high plains of north-central Montana. A significant amount of faulting along northwest trends began in the Miocene that marked the initiation of Basin and Range extension in southwestern Montana (Reynolds, 1979). Directly south and southeast of the Boulder batholith, northwest-trending faults that cut the Highland Mountains have been reactivated to form a series of horsts and grabens that trend northwest into the batholith (O'Neill and others, 1986). Faults that controlled the emplacement of the batholith are precisely those that have been reactivated in Cenozoic time. As such, in the study area, primary diastrophic fracture sets that formed in the Cretaceous are colinear with younger, Tertiary and Quaternary nonmineralized fractures and faults, lineaments, and dike swarms within the batholith.

Lineaments

In the Basin and Jefferson City quadrangles, a pronounced rectilinear drainage pattern trends northeast and northwest. Because the bedrock in these linear drainages is concealed by surficial deposits, the reason for such prominent zones of weakness is not known. Two prominent drainages, the main northwest-trending stem of Basin Creek and northeast-trending Jack Creek, are examples of lineaments in the study area. That the lineaments formed after the emplacement of the Butte pluton is clear because they extend across all phases of the pluton without interruption. Northeast-trending, elongate breccia pipes and northwest-trending shear zones occur along and parallel to the lineaments and are thought to be localized along the structurally weak zones that the lineaments represent.

Dikes

Eocene Lowland Creek dikes in the eastern part of the study area and a younger belt of Oligocene rhyolitic volcanic rocks on the west show a strong northeast trend. The emplacement of these rocks is inferrred to have been controlled by structurally weak zones defined by many of the parallel lineaments.

Faults

Quaternary and Tertiary faults are not particularly conspicuous in the study area. The only significant faults are northeast- and northwest-trending structures that parallel topographic lineaments. Two northeast-trending faults are present in the northern part of the study area. The northernmost fault is the larger and parallels the Continental Divide, passing just north of Old Baldy Mountain (pl. 1). This fault cuts all bedrock units and, significantly, displaces glacial deposits, disrupts postglacial drainage patterns, and is marked by prominent scarps as much as 300 ft high. A second fault along the northwest flank of Three Brothers displaces only batholithic rocks; it does not appear to displace swamp and bog deposits along its trace. A large, northeast-trending fault zone is present in the southern part of the study area in Big Limber Gulch and High Ore Creek. This fault zone is marked by pervasive alteration of plutonic and volcanic rocks, giving the rocks an orange-red hue along the trend. The fault drops volcanic rocks of both the Elkhorn Mountains and Lowland Creek Volcanics on the northwest side relative to plutonic rocks on the southeast side. Two northwest-trending shear zones in the vicinity of Pole Mountain are zones of crushed rock bounded by sharp, nearly vertical faults.

Mineral Deposits

The mine wastes of particular interest to this study are related to Late Cretaceous quartz-vein polymetallic sulfide mineralization and alteration systems. Eocene breccia-pipe and Miocene disseminated precious-metal mineralization and associated alteration systems are also present in the study area,

and the resultant metals and areas of altered rock have also contributed to the present-day surficial environment.

Late Cretaceous Mineralized Rock

The Late Cretaceous polymetallic sulfide veins in the study area are in the Basin and Boulder districts. These districts were important primarily for their gold and silver production. Lead and zinc made up the largest volume of the metals recovered, although zinc was not recovered in the early operations because it could not be smelted and had little commercial value. Volumetrically lesser amounts of gold, silver, and copper were recovered, as reported from smelter data, but these were the metals of the most value. All these polymetallic veins have associated pyrite, which generates acid waters in oxidizing, near-surface environments.

Polymetallic deposits in the study area were discovered in the late 1860s, but most of the production probably took place from about 1883 to 1907 (see Church, Nimick, and others, this volume, Chapter B). Sporadic mining activity has been ongoing in the study area in the years following until 1997. Most of the opening up of the veins from the surface rather than by adits has been done since World War II.

Controlling Structures

Narrow brecciated and sheared zones and related joint systems host the polymetallic pyritic quartz-vein mineral deposits that are important to this study. These mineralized shear/breccia zones trend from east-west to about N. 80°E. and are nearly vertical, as discussed in the section, "Structural Geology and Tectonics." The longest zone is the Comet–Gray Eagle zone, which is about 6 mi long; it extends from Cataract Creek to the upper part of the Boulder River valley (pl. 1). Most of these zones are complex features along which different short fault segments anastomose and overlap to form the larger structure.

These mineralized veins are near the top of the Butte pluton. The veins die out upward into the volcanic rocks, perhaps indicating less open fracturing in the volcanic rocks in comparison to the plutonic rocks. Additionally, that the fluids responsible for these mineralized veins were concentrated at the top of the pluton can be inferrred from the large number of mines located near or at the top of the plutonic rocks (pl. 1). Mines at the upper contact of the pluton, such as Gray Eagle, Bluebird-Pen Yan, and Boulder Chief mines in or near the southeastern part of the study area, are associated with shear zones; but these deposits are also reportedly somewhat pod-shaped (Becraft and others, 1963). Preferential location of mineralized veins near the roof of the pluton may be a result of the Elkhorn Mountains Volcanics acting as a caprock or impermeable barrier above the pluton.

Many of the polymetallic quartz veins are cut by Eocene dikes related to the Lowland Creek Volcanics. In places, the dikes follow the trend of the veins, even splitting and complicating the vein exposures. Where parallel to veins, margins of the dikes are sheared in many cases, indicating continued fault movement along some of these shear zones from Late Cretaceous through at least Eocene time.

Polymetallic Quartz Veins

Vein material has intruded fractured and sheared zones; the veins have sharp contacts against the intruded wallrock. Vein systems range from just a few inches across to 50 ft wide. Many of the veins are complexly anastomosing systems of veins and veinlets, even branching off into horsetail structures, rather than being a single simple vein (Becraft and others, 1963). However, in general, they have a tabular geometry. A general appearance of layering is common, reflecting repeated introduction of mineralizing fluids.

Quartz is the dominant mineral in the veins. Most early quartz is milky gray, whereas quartz introduced later in the sequence is commonly white. Few open-space features such as cockscomb structure or crystal terminations are present in the quartz. Absence of these features in deposits of this type is generally considered to indicate mid-level (mesothermal) deposits formed at a depth of 1–2.5 mi (Lindgren, 1933).

Tourmaline, commonly in the form of radiating black needles, is intergrown with quartz and pyrite. Volumetrically, it is the second most important vein mineral; it was a major constituent of the early veins but decreased in prevalence in the later veins.

Pyrite is the most ubiquitous sulfide mineral; fine to medium grains are disseminated in the quartz-vein material and in the nearby wallrocks. Argentiferous galena and sphalerite were the principal ore minerals. Argentiferous galena is also disseminated in veins and wallrock, but the argentiferous sphalerite is confined to the quartz veins. Chalcopyrite is common whereas the abundance of tetrahedrite is highly variable. Arsenopyrite is also disseminated in quartz. Arsenic-rich arsenopyrite was often sorted onto dumps or left in stopes; if present in the ore, it resulted in operators being penalized at the smelters. Stibnite, bornite, cosalite, enargite, chalcocite, ruby silver, boulangerite, bournonite, and albandite also have been reported from these veins (Becraft and others, 1963).

In many deposits, pink-tinged carbonate veinlets, stringers, and networks crosscut the other vein materials and form the youngest phase of the mineralized quartz veins. The carbonate is dominantly dolomite but ranges in composition from calcite to ankerite.

Chalcedony veins and quartz-chalcedony veins are younger than the quartz veins. These are not sulfide bearing but do contain uranium minerals. In places, these veins occupy the same fracture systems as the sulfide-bearing quartz veins, but they are predominantly found on the east side of the area of plate 1, deeper in the Butte pluton, and with strongly dominant northeast trends (Becraft and others, 1963).

Alteration Envelopes

The mineralized veins are accompanied by complex and overlapping alteration zones that range from 2 to 300 ft in width. In the simple veins with well-defined boundaries, alteration zones are distributed symmetrically about the vein. Sericitic, argillic, and chloritic alteration zones are present. Nearest the vein, a narrow (1 to 4 in.) greenish-gray sericite zone developed in the wallrocks. The sericitic alteration zone consists primarily of sericite and quartz. Depending on the amount of quartz in this zone, the contact with the vein itself may be gradational or sharp. Pyrite and lesser argentiferous galena are in places finely disseminated in the sericitic zone (Becraft and others, 1963). Tourmaline is present along with quartz in some localities. Some muscovite is present in addition to sericite; it probably formed as an alteration product of biotite. Original minerals and rock textures are largely destroyed.

The typical argillic zone is dull gray white and clay rich. Original mineral outlines and rock textures are preserved. Plagioclase is altered to montmorillonite with lesser amounts of kaolinite, sericite, quartz, epidote, and calcite. Biotite is altered to montmorillonite and kaolinite with lesser amounts of illite, ilmenite, chlorite, and sericite. Potassium feldspar is only partially altered to kaolinite. The argillic zone as much as 10–15 ft wide and gradational with the sericitic zone over a narrow distance of less than 2 in. (Becraft and others, 1963).

The chloritic zone is typically wider than the sericitic and argillic zones. Original minerals are partially preserved and rock textures remain; the rock is generally nonfriable. Plagioclase is only partly argillized and is altered to sericite along fractures. Biotite and hornblende are altered to chlorite, minor clays, magnetite, ilmenite, epidote, quartz, and calcite. Potassium feldspar is only slightly altered or fresh. The chloritic zone is as much as 4–12 in. wide. It is diffusely gradational with the argillic zone over about 1 ft and is more broadly gradational with fresh rock. The persistent long Comet–Gray Eagle vein system has large alteration envelopes that are in places more than 300 ft wide.

The bulk changes of chemistry resulting from the alteration of country rocks are of particular importance in the study of the capacity of the country rocks to neutralize acid water generated by the exposure of sulfide mineral deposits to weathering and oxidation. Chemical profiles from the data of Becraft and others (1963) for alteration zones at two deposits in the area are shown in figure 17. Whereas the calcium, magnesium, and sodium concentrations are slightly decreased in the chloritic zones, the argillic and sericitic zones show marked decreases in these elements. This change in rock chemistry is due to the loss of mafic minerals during alteration processes. This loss of mafic minerals in the alteration zones affects the ability of the altered rock to neutralize acidic water. (See section, "Acid-Neutralizing Potential of Bedrock.")

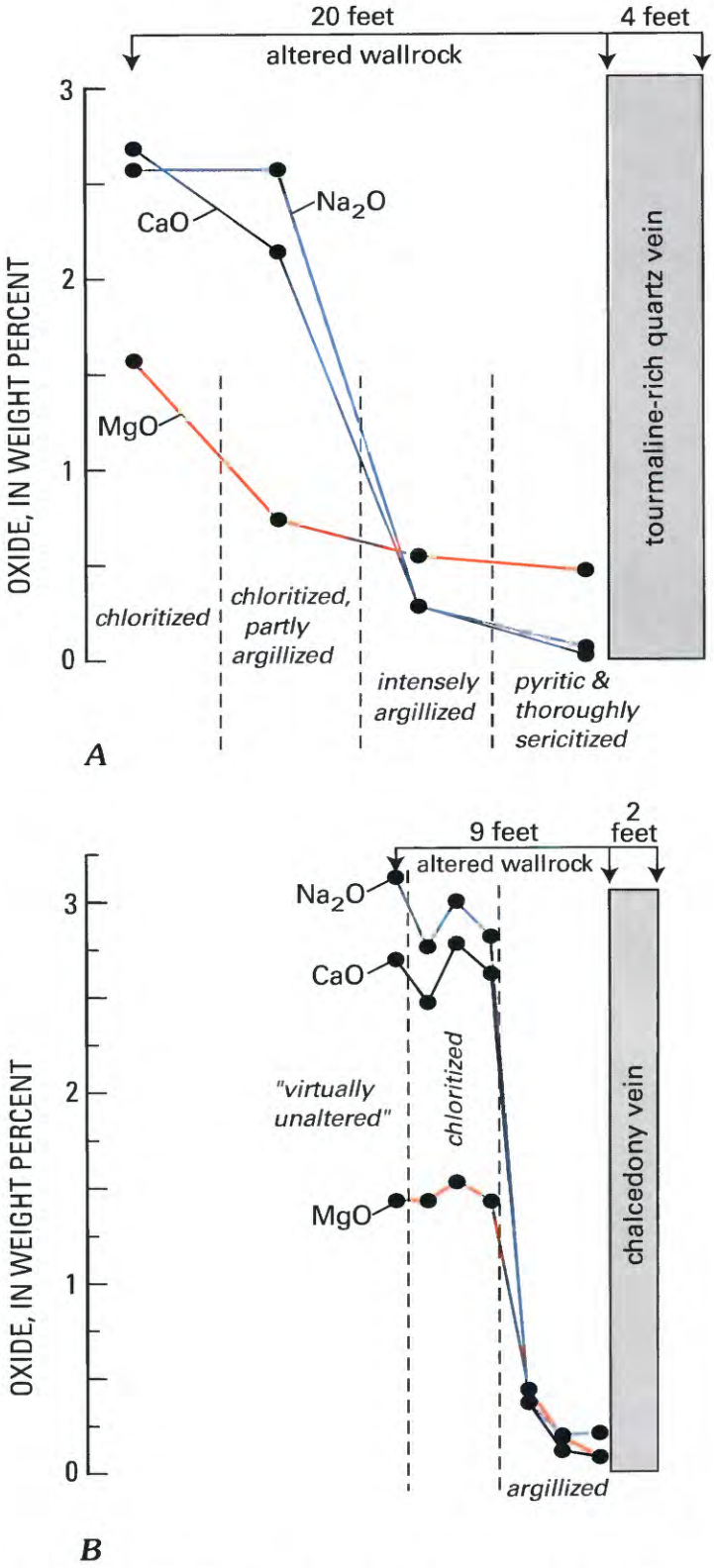

Figure 17. Variation diagram showing relationship of selected metal oxides in Butte pluton wallrocks and in alteration zones from two mines near the study area (data from Becraft and others, 1963, tables 11 and 12, p. 44 and 45). *A*, Bunker Hill mine; *B*, G. Washington mine.

Origin of Mineralizing Fluids

Observations at the Bluebird–Pen Yan mine near the eastern border of the study area, the mineralogy of pegmatitic knots and segregations present throughout the study area, the mineralogy of rocks at the roof zone of the pluton, and observations of the silicate mineralogy of the veins all bear on the question of the origin of the mineralizing fluids. At the Bluebird–Pen Yan mine, rosettes of tourmaline intergrown with pyrite are common (Winchell and Winchell, 1912). The character of samples found on the Bluebird–Pen Yan dump is that of a water-saturated, incompatible element-rich, metal-rich fluid that concentrated at the roof of the pluton. Estimates indicate that the deposits extended only about 1,300 ft below the roof of the pluton (Elliott, 1996, p. 36). A simple sulfide-mineral zonation with depth, resulting in relatively fewer precious metals at depth, has been noted (Billingsley and Grimes, 1918). Tourmaline is more prevalent in the deposits that formed at the highest parts of the Butte pluton; it is also common in the pegmatitic/aplitic segregations and knots that also formed in the upper parts of the pluton. Knopf (1913) and Billingsley and Grimes (1918) related the zoning of metals to depth below the roof of the pluton. The presence of tourmaline in all these areas and types of fluid-rich segregations in the Butte pluton suggests that the sulfide mineralizing fluids were similar to late-stage fluids that formed fluid-rich compositional and textural segregations of various sizes in rocks near the roof. This indicates that these mineral deposits are related directly to the Butte pluton and not to a younger igneous event.

Comparison to Other Veins in the Butte Pluton

Polymetallic quartz-vein deposits in the study area (Basin and Boulder mining districts) are similar to those in nearby districts. Vein deposits in mining districts in the drainages north of the study area (Knopf, 1913) are similar to those in the study area in terms of scale and mineralogy and are probably of the same origin. Districts having the most similar characteristics are Rimini to the north and Clancy to the northeast. Some deposits in the Elkhorn Mountains mining district to the east are also similar. Of the districts in the Butte pluton, the quartz-vein deposits in the study area (and at Rimini and Clancy) probably formed closest to the top of the mineralizing system and at the shallowest crustal depths. Deposits farther north, near Helena, had a thicker roof that included Mesozoic sedimentary rocks in addition to Elkhorn Mountains Volcanics. Some of the quartz-vein deposits near Helena are closely related to the emplacement of Eocene porphyritic dikes, and many appear to be more like precious-metal skarn deposits than polymetallic quartz-vein deposits.

Polymetallic precious-metal quartz-vein deposits in and near the study area are clearly simple vein deposits compared to the complex situation in the Butte district to the southwest. Although much excellent work has been done in the Butte district, timing of mineralization and origin of complexly overlapping vein and porphyry deposits have not yet been completely worked out. Current data suggest that products of early vein mineralization at Butte may turn out to have had an origin similar to that of the polymetallic quartz-vein deposits near the study area. The bulk of the mineralized rock at Butte—the porphyry copper and molybdenum deposits—is clearly younger, however; and judging by published age information (Miller, 1973), the deposits are too young to be related to the Boulder batholith. Deposits in the Butte district are distant from roof rocks, indicating a setting in which veins formed deeper within the hosting Butte pluton than veins near the study area to the north.

Tourmaline is an important constituent of the quartz-vein and alteration assemblages in deposits in the districts near Basin (including Rimini and Clancy) and in deposits considered to be the oldest and most closely related to the Butte pluton in the Elkhorn district in the Elkhorn Mountains to the east (Smedes, 1966). These districts containing tourmaline are all proximal to the roof of the Butte pluton. Interestingly, tourmaline is not reported in the vein or porphyry systems at Butte (Sales and Meyer, 1949; Becraft and others, 1963). Geologic information suggests that early vein deposits, now exposed at Butte, may have formed at a greater depth and that porphyry deposits are younger (Meyer and others, 1968; Miller, 1973) than polymetallic quartz-vein deposits in the study area.

Age

No dates are currently available for the polymetallic quartz-vein deposits of the study area. Likewise, no dates are available for the silver-rich vein deposits to the north in the Helena drainages, or for the silver-rich vein deposits that were mined early in the Butte district (prior to discovery of the rich copper-molybdenum porphyry deposits at depth). Relative age relations show that the polymetallic quartz veins are clearly older than chalcedony veins and Lowland Creek Volcanics. The best evidence for the ages of the polymetallic quartz-vein deposits in the study area is that they seem to be related to late-stage crystallization of the Butte pluton and thus probably date from about 74 Ma (Lund and others, 2002). Reported dates for thermal events related to porphyry copper-molybdenum deposits at Butte are between about 65 and 56 Ma (Miller, 1973). Thus, the porphyry systems at Butte are significantly younger than all phases of the Boulder batholith and must be unrelated to the polymetallic quartz-vein deposits that are of interest in this study.

Tertiary Mineralization

Lowland Creek Volcanics Mineralization

Diatreme-related mineral deposits in the study area are in phreato-magmatic units (Tlc) associated with Eocene Lowland Creek volcanism. The diatremes crosscut rhyodacite ignimbrite flows of the Lowland Creek Volcanics and Late Cretaceous plutonic and volcanic rocks. Some of the diatremes formed in the same north-northeast fractures as dikes (Tli) that are associated with the Lowland Creek Volcanics, and some are cut by Lowland Creek-related dikes indicating a relation to Eocene volcanism. The diatremes are primarily matrix rich breccia with sand-sized tuffaceous and quartzo-feldspathic matrix and diverse breccia fragments. The angular to sub-rounded breccia fragments include clasts of Lowland Creek Volcanics, Elkhorn Mountains Volcanics, Butte pluton, and carbonized wood (Becraft and others, 1963; Ruppel, 1963; Sillitoe and others, 1985). The composition of fragments and matrix indicate that the diatremes intruded the three rock types. The specimen that contained wood fragments indicates that the diatremes were locally open to the surface as in a maar volcano (Sillitoe and others, 1985). The diatremes are from 300 ft to about 2 mi in length and are known to continue at least 1,000 ft in depth below the present surface (Becraft and others, 1963; Sillitoe and others, 1985).

Mineralized material is in the form of disseminated sulfide minerals in the breccia matrix associated with quartz in vugs and veinlets. In places, most of the matrix itself is sulfide minerals. Multiple episodes of mineralization and brecciation are evident. Sulfide mineralogy is pyrite, sphalerite, galena, minor chalcopyrite, and rare electrum. With the exception of the absence of arsenopyrite, this mineralogy is similar to that of the earlier polymetallic quartz-vein deposits (Sillitoe and others, 1985). Other minerals occurring with the sulfides are quartz, manganocalcite, rhodochrosite, and siderite. Tourmaline is noticeably absent in deposits of this age as compared to the earlier quartz-vein deposits (Sillitoe and others, 1985). Alteration zones include central sericitization with carbonate minerals, minor silicification, and kaolinite formation in plagioclase. A more distal propylitic zone includes chlorite, montmorillonite, and carbonate (Becraft and others, 1963; Ruppel, 1963; Sillitoe and others, 1985). Preliminary $^{40}Ar/^{39}Ar$ dating from this study suggests that mineralization took place about 53 Ma (M. Kunk, unpub. data, 2000).

Recent mining of this type of deposit has occurred at the Montana Tunnels mine (Sillitoe and others, 1985) across the drainage divide 2 mi east of the study area. This was an open-pit bulk mining operation that mined lower grade disseminated gold, silver, lead, and zinc. An historical deposit called Montana Tunnels east of the study area and the much smaller Obelisk deposit on the south edge of the study area were both mined by adits for gold and silver in 1900 or before (Becraft and others, 1963).

Helena Volcanic Rocks Mineralization

Oligocene pyroclastic rhyolite tuffs of the Helena volcanic field host disseminated gold deposits at the head of the Basin Creek drainage. The volcanic rocks originated from vents aligned along an east-northeast trend, which are, from west to east, the peak southwest of the Josephine mine, the peak at Carlson mine, Luttrell Peak, and Red Mountain (Smith and others, this volume, Chapter E3). In the volcanic rocks near the vents, the circulation of localized late-stage, ore-bearing hydrothermal fluids was pervasive and resulted in disseminated gold deposits near vents. These deposits are probably about 28 m.y. old, and formed immediately following consolidation of the volcanic rocks (Chadwick, 1978).

The disseminated gold deposits formed in two types of environment. The simplest deposits are in zones of intense alteration in the rhyolite flow layers in this interbedded sequence of flow and pyroclastic layers. The more complex type of deposit is along the contact between the older rocks of the Butte pluton and the young rhyolite where hydrothermal fluids moved along the weathered surface of the older plutonic rocks and up into the base of the volcanic rocks. Some primary mineralized rock is in the weathered rocks of the Butte pluton and in the upper parts of fractures in it (Dan Adams, Pegasus Corporation, oral commun., 1999). Primary gold is in finely disseminated pyrite and possibly locally in arsenopyrite (Ruppel, 1963). Intense low-temperature argillic alteration resulted in destruction of feldspars to form clays, and in silicification in the mineralized zones. Secondary enrichment resulted from oxidation of the primary pyrite during weathering. Gold has been the only metal produced from this type of deposit, making these significantly different from older pluton-related polymetallic quartz-vein deposits in the study area.

The most recent mining of this type of deposit was at the Basin Creek mine, where bulk mining of low-grade mineralized rock was undertaken for gold in three relatively small open pits. This recent mining activity was centered over areas of high-grade gold mineralized rock and in areas of historical mining that explored deposits formed by weathering and secondary enrichment. The historical mines were Venus (Martin, this volume, Chapter D3) and Pauper's Dream and Porphyry Dike (nearby, in Tenmile Creek headwaters).

Pervasive Alteration Systems

Several areas in the study area have undergone pervasive alteration that is unrelated to known mineralized systems as shown previously (Becraft and others, 1963). A large area of hydrothermal alteration, which was not previously shown, is near Big Limber Gulch and Cataract and High Ore Creeks in the southern part of the study area (pl. 1). This alteration resulted in chloritization of biotite and destruction of plagioclase to form clay minerals. The alteration zone seems to be related to north-northeast-trending normal faults and smaller structures that controlled emplacement of late-stage

chalcedony veins as well as Eocene dikes related to the Lowland Creek Volcanics. This zone of pervasive alteration is of a much larger magnitude than the narrow alteration envelopes that formed around the Late Cretaceous polymetallic quartz-vein deposits. Additionally, the setting is quite different from areas of alteration at the top of the Butte pluton directly under the volcanic roof rocks, such as at Jack Mountain and the Occidental Plateau, where alteration is more clearly a direct magmatic process involving water-rich fluids at the top of the magma chamber. These pervasively alterated rocks in the southern part of the study area may be related to Eocene Lowland Creek volcanism rather than to the older polymetallic quartz-vein deposits.

Hydrogen and oxygen isotopic study of rocks in the Boulder batholith included rocks of the Butte pluton in the study area (Sheppard and Taylor, 1974; Tilling, 1977). Samples taken by Sheppard and Taylor (1974) near Basin were mostly in the zone of the Eocene Lowland Creek dike swarm and structures that controlled them. Sheppard and Taylor (1974) concluded that most of the alteration in the study area was the result of meteoric water that circulated after solidification of the Butte pluton. They envisioned this process taking place during the Late Cretaceous or early Tertiary. In the absence of dating of the alteration-zone mineralogy, their data and observations would also support an Eocene age for the pervasive alteration event.

The location, size, and chemistry of these pervasive zones of alteration could affect the ability of the country rocks to neutralize acidic water.

Gold Placer Deposits

Placer mining of alluvial and glacial deposits containing gold was the earliest mining in the study area (Church, Nimick, and others, this volume). Some placer mines were also in areas where weathering and oxidation resulted in secondary gold enrichment above lode or disseminated deposits. In these areas gravity separation methods were used to mine as much as 100 ft of the uppermost, strongly weathered rubble. The discovery and mining of placer deposits was an important exploration clue that indicated the presence of gold-bearing lode deposits in the study area.

Tin Placer Deposits

Tin, in the form of cassiterite, is reported in gold-bearing placers along upper reaches of Monitor, Tenmile, and Basin Creeks (pl. 1). The source of the cassiterite is believed to be the Oligocene rhyolite of the Helena volcanic field on the Continental Divide ridge near the Basin Creek mine area (Ruppel, 1963).

Acid-Neutralizing Potential of Bedrock

The acid-neutralizing potential (ANP) of bedrock is an important control on water quality in areas of inactive mines and mill tailings. In areas of polymetallic quartz-vein deposits, such as the Boulder River study area, acidic drainage water is caused chiefly by the oxidation of the common gangue mineral pyrite. Interest in understanding the surficial water-bedrock chemical interactions in the Boulder River study area was prompted by the fact that even though numerous pyrite-bearing mine-waste piles lie in the area (Metesh and others, 1994: Metesh and others, 1995; Desborough and Fey, 1997), only a few, small acidic stream reaches exist (Nimick and Cleasby, this volume, fig. 2). The Boulder River watershed appears to have a natural acid-neutralizing capacity, and that capacity must be controlled by the mineralogy of the bedrock.

Acid-neutralizing potential values reported herein are converted to "calcite equivalent" regardless of whether the acid-neutralizing mineral is calcite or other minerals. Calcite equivalent has become the standard usage for engineering practices and other purposes related to acid-neutralizing potential. For simplicity, consider that 1 g (gram) of calcite will neutralize 10,000 g (10 L (liters)) of acidic water of pH = 3.0. In another context, a cubic foot of rock with 1 weight percent of calcite could neutralize about 8.4 tons (7,660 L) of water of pH = 3.0 if all the calcite were available to react with the acidic water.

Ruppel (1963) studied about 250 thin sections of the Butte pluton and Elkhorn Mountains Volcanics in the west half of the area of plate 1, but he reported no carbonate minerals that might contribute to acid-neutralizing potential. However, large slabs (10×10 cm) of fresh plutonic rocks studied by Desborough, Briggs, and Mazza (1998), using alizarin-red chemical stain, revealed minor amounts of calcite. Calcite concentrations from approximately 0.1 to 1.6 weight percent were determined based on total carbon analyses for 15 bedrock samples. Leaching studies using acidic (pH = 2.90) mine-waste leachate showed that the acid-neutralizing potential of these bedrocks was greater than could be accounted for by the dissolution of these small amounts of calcite. A second quantitative study (Desborough, Briggs, Mazza, and Driscoll, 1998) of three samples of plutonic rocks and their separated mineral fractions, using acidic mine-waste leachate and analysis of total carbon for calculating calcite concentrations, showed that mafic minerals such as biotite, chlorite, and tremolite have significant acid-neutralizing potential. Table 1 summarizes the most significant aspects of mineralogical, chemical, and acidic leaching studies of the three samples of plutonic rocks. These samples had different concentrations of calcite, different concentrations of mafic minerals, and only minor differences in total acid-neutralizing potential. Although sample FMT020

Table 1. Acid-neutralizing potential for three samples of plutonic rocks with different calcite concentration and different concentrations of mafic minerals, and total acid-neutralizing potential.

[Data from Desborough, Briggs, Mazza, and Driscoll (1998)]

Sample No.	FMT020	FMT022	FMT032
Weight percent calcite	1.4	0.4	1.0
ANP of rock due to silicates expressed in wt. percent calcite equivalence	4.7	5.8	7.2
Weight percent mafic minerals	5.2	16.5	16.4
Total calcite equivalent ANP of rock as wt. percent calcite	6.1	6.2	8.2

had only 5.2 weight percent of mafic minerals, it had about 2.6 weight percent of chlorite, whereas the other two samples (FMT022 and FMT032) had no chlorite (table 1) but had higher concentrations of mafic minerals (16.5 and 16.4 percent, respectively). The sample with minor chlorite had significant acid-neutralizing potential because magnesium-rich chlorite (clinochlore) has more acid-neutralizing potential than the other mafic minerals, tremolite and biotite. For this reason, the range in weight percent calcite equivalent acid-neutralizing potential among the three samples studied differed by only 25 percent, whereas the concentration of mafic minerals was tripled in the chlorite-free samples.

The Elkhorn Mountains Volcanics have significant acid-neutralizing potential owing largely to abundant chlorite. Because they lie *above* the polymetallic quartz veins, they could have some impact on acid generated from veins, because water percolating through the volcanics down to mineralized zones would have increased acid-neutralizing capacity.

Rocks that have been altered by hydrothermal solutions, such as those immediately surrounding the small polymetallic quartz veins explored and (or) mined for metallic minerals during the last century, have negligible acid-neutralizing potential because mafic minerals are virtually absent. Although these veins and adjacent altered rock represent less than a few percent of the study area (Ruppel, 1963; Becraft and others, 1963), they are the localities where the mines are situated so their negligible acid-neutralizing potential is significant.

Extensive hydrothermally altered areas that are silicified and highly fractured, such as at Jack Mountain, have insignificant acid-neutralizing potential (Desborough, Briggs, and Mazza, 1998). However, this alteration includes andalusite and pyrophyllite and is thought to be unrelated to the formation of polymetallic quartz-vein deposits.

A study of mineralogy and acid-neutralizing potential of some Butte pluton and Elkhorn Mountains Volcanics was conducted to explore bedrock suitability for mine-waste repositories in the Basin Creek drainage (Desborough and Driscoll, 1998). Four sites were core drilled by the USDA Forest Service in 1998. Two were near the Bullion mine wastes and two were near the Buckeye/Enterprise mine wastes. One site near the Bullion mine-waste piles was drilled into highly silicified and fractured Elkhorn Mountains Volcanics on Jack Ridge east of Jack Mountain; acid-neutralizing potential of samples was low and equivalent to only 0.4 weight percent calcite. The cored samples in Butte pluton drilled at a site within a few hundred yards of the Bullion waste piles had much larger acid-neutralizing potential, equivalent to 2.0 weight percent calcite. The two sites cored near the Buckeye/Enterprise mine were silicified or silicified+pyrite-bearing altered Elkhorn Mountains Volcanics; their calcite equivalent acid-neutralizing potential was only about 0.5 weight percent and they were intensely fractured—characteristics undesirable for mine-waste repositories.

Cored rocks that had the highest acid-neutralizing potential (for example, near Bullion mine) had abundant magnetite in heavy-mineral concentrates made from these rocks, whereas those with low acid-neutralizing potential contained no magnetite in the heavy-mineral concentrates (Desborough and Driscoll, 1998, table 1). This difference in magnetite concentration is probably due to the destruction of magnetite during hydrothermal alteration. This observation is important because airborne magnetic data for the study area show that the hydrothermally altered areas have a much lower magnetic susceptibility than igneous bedrock unaffected by hydrothermal alteration, and it allows potential discrimination of altered, and thus low ANP, bedrock from airborne geophysical surveys (McCafferty and others, this volume, Chapter D2).

Summary

The description of the geologic framework, the new interpretation of the bedrock geology, and the discussion of the tectonic and structural history of emplacement of the Boulder batholith presented in this report focus on geologic topics that bear greatest relevance to reclamation efforts by Federal land-management agencies entrusted with the remediation of inactive mine sites in the watershed study area. The interpretive geology is portrayed in a consistent, contemporary geologic context designed to tie the geologic conditions to geochemical results for water, sediment, and ultimately to biotic habitat. Discussion of the mineralogic and textural character of the Butte pluton gives insight into the scope of the significant, widespread acid-neutralizing capacity of the bedrock and documents why acidic water is not presently more prevalent within the study area. Additionally,

recognition that the polymetallic quartz-vein deposits are restricted to rocks within 1,000 ft or less of the roof of the Butte pluton suggests that prior to mining, any acid water that may have been generated was quickly neutralized by the subjacent plutonic rocks. Recognition of weakly consolidated Eocene, largely unexposed sediments buried beneath Tertiary volcanic rocks that now underlie the Continental Divide helps explain the hydrology of topographically perched boggy and swampy areas and associated solifluction processes observed within the study area. The mechanism of emplacement of the Boulder batholith is crucial to understanding (1) the nature of the narrow, widely spaced fractures that initially controlled the locus of polymetallic quartz-vein deposits as well as (2) the pervasive, closely spaced cooling fractures that control the current hydrologic character of the plutonic rocks (McDougal and others, this volume, Chapter D9). Closely tied to the understanding of tectonic controls of emplacement of the batholith is the recognition of the propensity for recurrent movement on synemplacement fault or fracture systems and the initiation of younger faults with preferred orientations subparallel to the older structures.

Understanding the bedrock composition and geologic architecture and the characteristics and mode of emplacement of polymetallic quartz-vein deposits is intended to guide the land-management agencies in the selection of suitable repository sites where acid-neutralizing potential is present and where movement of ground water through fractures is minimal. Prior to mine development these polymetallic quartz-vein deposits were likely minor acid-producing sources surrounded by rocks with high acid-neutralizing potential.

References Cited

Balk, Robert, 1948, Structural behavior of igneous rocks: Ann Arbor, Mich., Edwards Brothers, Inc., 177 p.

Becraft, G.E., Pinckney, D.M., and Rosenblum, Sam, 1963, Geology and mineral deposits of the Jefferson City quadrangle, Jefferson and Lewis and Clark Counties, Montana: U.S. Geological Survey Professional Paper 428, 101 p., 18 plates.

Biehler, Shawn, and Bonini, W.E., 1969, A regional gravity study of the Boulder batholith, Montana, *in* Larsen, L., ed., Igneous and metamorphic geology: Geological Society of America Memoir 115, p. 401–422.

Billingsley, Paul, and Grimes, J.A., 1918, Ore deposits of the Boulder batholith of Montana: American Institute of Mining Engineers Transactions, v. 58, p. 284–361.

Burfeind, W.J., 1967, A gravity investigation of the Tobacco Root Mountains, Jefferson Basin, Boulder batholith, and adjacent areas of southwestern Montana: Bloomington, Ind., Indiana University Ph. D. dissertation, 90 p.

Chadwick, R.A., 1978, Geochronology of post-Eocene rhyolitic and basaltic volcanism in southwestern Montana: Isochron/West, no. 22, p. 25–28.

Chapman, R.W., Gotfried, D., and Waring, C.L., 1955, Age determinations on some rocks from the Boulder batholith and other batholiths of western Montana: Geological Society of America Bulletin, v. 66, p. 607–610.

Clarke, F.W., 1910, Analyses of rocks and minerals from the laboratory of the United States Geological Survey, 1880 to 1908: U.S. Geological Survey Bulletin 419, p. 80.

De La Roche, H., Leterrier, J., Grandclaude, P., and Marchal, M., 1980, A classification of volcanic and plutonic rocks using R1R2-diagram and major-element analyses—Its relationships with current nomenclature: Chemical Geology, v. 29, p. 183–210.

Desborough, G.A., Briggs, P.H., and Mazza, Nilah, 1998, Chemical and mineralogical characteristics and acid-neutralizing potential of fresh and altered rocks and soils of the Boulder River headwaters in Basin and Cataract Creeks of northern Jefferson County, Montana: U.S. Geological Survey Open-File Report 98–40, 21 p.

Desborough, G.A., Briggs, P.H., Mazza, Nilah, and Driscoll, Rhonda, 1998, Acid-neutralizing potential of minerals in intrusive rocks of the Boulder batholith in northern Jefferson County, Montana: U.S. Geological Survey Open-File Report 98–364, 21 p.

Desborough, G.A., and Driscoll, Rhonda, 1998, Mineralogical characteristics and acid-neutralizing potential of drill core samples from eight sites considered for metal-mine related waste repositories in northern Jefferson, Powell, and Lewis and Clark Counties, Montana: U.S Geological Survey Open-File Report 98–790, 6 p.

Desborough, G.A., and Fey, D.L., 1997, Preliminary characterization of acid-generating potential and toxic metal solubility of some abandoned metal-mining related wastes in the Boulder River headwaters, northern Jefferson County, Montana: U.S. Geological Survey Open-File Report 97–478, 21 p.

Elliott, J.E., 1996, Continental Divide region, *in* Tysdal, R.G., Ludington, Steve, and McCafferty, A.E., Mineral and energy resource asssessment of the Helena National Forest, west-central Montana: U.S. Geological Survey Open-File Report 96–683–A, p. F32–F36.

Hamilton, Warren, and Myers, W.B., 1967, The nature of batholiths: U.S. Geological Survey Professional Paper 554–C, 30 p.

Harris, S.A., 1957, The tectonics of Montana as related to the Belt series: Billings Geological Society, 8th Annual Field Conference Guidebook, p. 22–33.

Ispolatov, V.O., Dudas, F.O., Snee, L.W., and Harlan, S.S., 1996, Precise dating of the Lowland Creek Volcanics, west-central Montana: Geological Society of America Abstracts with Programs, v. 28, p. 484.

Johannsen, Albert, 1939, A descriptive petrography of the igneous rocks—Volume I, Introduction, textures, classifications and glossary: Chicago, Ill., University of Chicago Press, 318 p.

Klepper, M.R., Robinson, G.D., and Smedes, H.W., 1971, On the nature of the Boulder batholith of Montana: Geological Society of America Bulletin, v. 82, p. 1563–1580.

Klepper, M.R., Weeks, R.A., and Ruppel, E.T., 1957, Geology of the southern Elkhorn Mountains, Jefferson and Broadwater Counties, Montana: U.S. Geological Survey Professional Paper 292, 82 p.

Knapp, R.B., and Norton, Dennis, 1987, Preliminary numerical analysis of processes related to magma crystallization and stress evolution in cooling pluton environments: American Journal of Science, v. 281, p. 35–68.

Knopf, Adolph, 1913, Ore deposits of the Helena mining region, Montana: U.S. Geological Survey Bulletin 527, 143 p.

Knopf, Adolph, 1956, Argon-potassium determination of the age of the Boulder bathylith, Montana: American Journal of Science, v. 254, p. 744–745.

Knopf, Adolph, 1957, The Boulder bathylith of Montana: American Journal of Science, v. 255, p. 81–103.

Knopf, Adolph, 1963, Geology of the northern part of the Boulder bathylith and adjacent area, Montana: U.S. Geological Survey Miscellaneous Geologic Investigations I–381, scale 1:48,000.

Lambe, R.N., 1981, Crystallization and petrogenesis of the southern portion of the Boulder batholith, Montana: Berkeley, Calif., University of California Ph. D. dissertation, 171 p.

Lindgren, Waldemar, 1886, Relation of the coal of Montana to the older rocks; Appendix B, Eruptive rocks: Tenth Census, v. 15, p. 733–734.

Lindgren, Waldemar, 1933, Mineral deposits, 4th Edition: New York, McGraw-Hill, 930 p.

Lipman, P.W., 1984, The roots of ash flow calderas in western North America—Windows into the tops of granitic batholiths: Journal of Geophysical Research, v. 11, p. 8801–8841.

Luikart, E.J., 1997, Syn- and post-Laramide geology of the south-central Gravelly Range, southwestern Montana: Bozeman, Mont., Montana State University M.S. thesis, 96 p.

Lund, Karen, Aleinikoff, J.N., Kunk, M.J., Unruh, D.M., Zeihen, G.D., Hodges, W.C., du Bray, E.A., and O'Neill, J.M., 2002, SHRIMP U-Pb and $^{40}Ar/^{39}Ar$ age constraints for relating plutonism and mineralization in the Boulder batholith region, Montana: Economic Geology, v. 97, p. 241–267.

McBride, B.C., Schmidt, C.J., Guthrie, G.E., and Sheedlo, M.K., 1990, Multiple reactivation of a collisional boundary—An example from southwestern Montana, *in* Bartholomew, M.J., Hyndman, D.W., Mogk, D.W., and Mason, Robert, eds., Proceedings of the 8th International Conference on Basement Tectonics: Hingham, Mass., Kluwer Academic Publishers, p. 341–358.

McDowell, F., 1966, Potassium-argon dating of Cordilleran intrusives: New York, Columbia University Ph. D. dissertation, 246 p.

Metesh, J.J., Lonn, J.D., Duaime, T.E., and Wintergerst, Robert, 1994, Abandoned-inactive mines program, Deerlodge National Forest—Volume I, Basin Creek drainage: Montana Bureau of Mines and Geology Open-File Report 321, 131 p.

Metesh, J.J., Lonn, J.D., Duaime, T.E., Marvin, R.K., and Wintergerst, Robert, 1995, Abandoned-inactive mines program, Deerlodge National Forest—Volume II, Cataract Creek drainage: Montana Bureau of Mines and Geology Open-File Report 344, 201 p.

Meyer, C., Shea, E.P., Goddard, C.C., Jr., Zeihen, L.G., Guilber, J.M., Miller, R.N., McAleer, J.F., Brox, G.B., Ingersoll, R.G., Jr., Burns, G.J., and Wigal, T., 1968, Ore deposits at Butte, Montana, *in* Ridge, J.D., ed., Ore deposits of the United States, 1933–1967, Graton-Sales Volume II: American Institute of Mining, Metallurgical, and Petroleum Engineers, p. 1373–1416.

Miller, R.N., 1973, Production history of the Butte district and geological function, past and present, *in* Miller, R.N., ed., Guidebook for the Butte field meeting of Society of Economic Geologists, 1973: Butte, Mont., Society of Economic Geologists, p. F1–F10.

Nimick, D.A., and Cleasby, T.E., 1998, What streams are affected by abandoned mines—Characterization of water quality in the streams of the Boulder River watershed, Montana [abs.] *in* Science for watershed decisions on abandoned mine lands—Review of preliminary results: U.S. Geological Survey Open-File Report 98–0297, p. 9.

Obradovich, J.D., 1993, A Cretaceous time scale, *in* Caldwell, W.E.G., and Kaufman, E.G., eds., Evolution of the western Interior Basin: Geological Association of Canada Special Paper 39, p. 379–396.

O'Neill, J.M., 1998, The Great Falls tectonic zone—An Early Proterozoic collisional orogen beneath and south of the Belt basin, *in* Berg, R.B., ed., Proceedings of Belt Symposium III: Montana Bureau of Mines and Geology Special Publication 111, p. 227–234.

O'Neill, J.M., Ferris, D.C., Schmidt, C.J., and Hanneman, D.L., 1986, Recurrent movement along northwest-trending faults at the southern margin of the Belt basin, Highland Mountains, southwestern Montana, *in* Roberts, S.M., ed., Belt Supergroup: Montana Bureau of Mines and Geology Special Publication 94, p. 208–216.

O'Neill, J.M., and Lopez, D.A., 1985, Character and regional significance of the Great Falls tectonic zone, east-central Idaho and west-central Montana: American Association of Petroleum Geologists Bulletin, v. 69, p. 437–447.

Prostka, H.J., 1966, Igneous geology of the Dry Mountain quadrangle, Jefferson County, Montana: U.S. Geological Survey Bulletin 1221–F, 21 p.

Reynolds, M.W., 1979, Character and extent of basin-range faulting, western Montana and east-central Idaho, *in* Newman, G.W., and Goode, H.D., eds., Basin and range symposium and Great Basin field conference: Rocky Mountain Association of Geologists, p. 185–193.

Roberts, W.A., 1953, Notes on the alaskitic rocks in the Boulder batholith near Clancey, western Montana: Northwest Science, v. 27, p. 121–124.

Robinson, G.D., 1963, Geology of the Three Forks quadrangle, Montana, with descriptions of igneous rocks by H. Frank Barnett: U.S. Geological Survey Bulletin 988–F, 121–141 p.

Robinson, G.D., Klepper, M.R., and Obradovich, J.D., 1968, Overlapping plutonism, volcanism, and tectonism in the Boulder batholith region, western Montana *in* Coats, R.R., Hay, R.L., and Anderson, C.A., eds., Studies in volcanology: Geological Society of America Memoir 116, p. 557–576.

Ruppel, E.T., 1963, Geology of the Basin quadrangle, Jefferson, Lewis and Clark, and Powell Counties, Montana: U.S. Geological Survey Bulletin 1151, 121 p., 7 plates.

Rutland, C., 1986, The geochemistry of the Elkhorn Mountains Volcanics and its relationship to the magma chamber of the Boulder batholith: East Lansing, Mich., Michigan State University Ph. D. dissertation, 96 p.

Rutland, C., Smedes, H.W., Tilling, R.I., and Greenwood, W.R., 1989, Volcanism and plutonism at shallow crustal levels—The Elkhorn Mountains Volcanics and the Boulder batholith, southwestern Montana, *in* Hyndman, D.W. ed., Cordilleran volcanism, plutonism, and magma generation at various crustal levels, Montana and Idaho: 28th International Geological Congress, Field Trip Guidebook T337, p. 16–31.

Sales, R.H., and Meyer, C., 1949, Results from preliminary studies of vein formation at Butte, Montana: Economic Geology, v. 44, p. 465–484.

Schmidt, C.J., and Garihan, J.M., 1983, Laramide tectonic development of the Rocky Mountain foreland of southwestern Montana, *in* Lowell, J.D., ed., Rocky Mountain foreland basins and uplifts: Rocky Mountain Association of Geologists, p. 271–294.

Schmidt, C.J., and Garihan, J.M., 1986, Role of recurrent movement of northwest-trending basement faults in the tectonic evolution of southwestern Montana, *in* Aldrich, M.J., and Laughlin, A.W., eds., Proceedings of the 6th International Conference on Basement Tectonics: International Basement Tectonics Association, p. 1–15.

Schmidt, C.J., and O'Neill, J.M., 1983, Structural evolution of the southwest Montana transverse zone, *in* Powers, R.B., ed., Western overthrust belt—its geology and hydrocarbon potential—from Alaska through Mexico: Rocky Mountain Association of Geologists Special Publication, p. 193–218.

Schmidt, C.J., Smedes, H.W., and O'Neill, J.M., 1990, Syncompressional emplacement of the Boulder and Tobacco Root batholith (Montana-U.S.A.) by pull-apart along old fault zones: Geological Journal, v. 25, p. 305–318.

Sheppard, S.M.F., and Taylor, H.P., Jr., 1974, Hydrogen and oxygen isotope evidence for the origins of water in the Boulder batholith and the Butte ore deposits, Montana: Economic Geology, v. 69, p. 926–946.

Sillitoe, R.H., Grauberger, G.L., and Elliott, J.E., 1985, A diatreme-hosted gold deposit at Montana Tunnels, Montana: Economic Geology, v. 80, p. 1707–1721.

Smedes, H.W., 1962, Lowland Creek volcanics, an Oligocene formation near Butte, Montana: Journal of Geology, v. 70, p. 255–266.

Smedes, H.W., 1966, Geology and igneous petrology of the northern Elkhorn Mountains, Jefferson and Broadwater Counties, Montana: U.S. Geological Survey Professional Paper 510, 116 p.

Smedes, H.W., Klepper, M.R., Pinckney, D.M., Becraft, G.E., and Ruppel, E.T., 1962, Preliminary geologic map of the Elk Park quadrangle, Jefferson and Silver Box Counties, Montana: U.S. Geological Survey Mineral Investigations Field Studies Map MF–246, scale 1:48,000.

Smedes, H.W., Klepper, M.R., and Tilling, R.I., 1988, Preliminary map of plutonic units of the Boulder batholith, southwestern Montana: U.S. Geological Survey Open-File Report 88–283, scale 1: 200,000.

Smedes, H.W., and Thomas, H.H., 1965, Reassignment of the Lowland Creek volcanics to Eocene age: Journal of Geology, v. 73, p. 508–510.

Streckeisen, A., 1976, To each plutonic rock its proper name: Earth-Science Reviews, v. 12, p. 1–33.

Tilling, R.I., 1968, Zonal distribution of variations in structural state of alkali feldspar within the Rader Creek pluton, Boulder batholith, Montana: Journal of Petrology, v. 9, p. 331–357.

Tilling, R.I., 1973, Boulder batholith, Montana; a product of two contemporaneous but chemically distinct magma series: Geological Society of America Bulletin, v. 84, p. 3879–3900.

Tilling, R.I., 1974, Composition and time relations of plutonic and associated volcanic rocks, Boulder batholith region, Montana: Geological Society of America Bulletin, v. 85, p. 1925–1930.

Tilling, R.I., 1977, Interaction of meteoric waters with magmas of the Boulder batholith, Montana: Economic Geology, v. 72, p. 859–864.

Tilling, R.I., Klepper, M.R., and Obradovich, J.D., 1968, K-Ar ages and time span of emplacement of the Boulder batholith, Montana: American Journal of Science, v. 266, p. 671–689.

Trombetta, J.T., 1987, Evolution of the Eocene Avon volcanic complex, Powell County, Montana: Bozeman, Mont., Montana State University M.S. thesis, 97 p.

Tysdal, R.G., 1998, Revisions of Cretaceous Slim Sam Formation, western Montana: U.S. Geological Survey Professional Paper 1601–B, 8 p.

Weed, W.H., 1887, Description of the Butte, Montana special district: U.S. Geological Survey Atlas, Butte special folio 38, 14 p.

Winchell, H.V., and Winchell, A.N., 1912, Notes on the Blue Bird mine: Economic Geology, v. 7, p. 287–294.

Winston, Don, 1986, Sedimentation and tectonics of the Middle Proterozoic Belt basin and their influence on Phanerozoic compression and extension in western Montana and northern Idaho, *in* Peterson, James, ed., Paleotectonics and sedimentation: American Association of Petroleum Geologists Memoir 41, p. 87–118.

Woodward, L.A., 1986, Tectonic origin of fractures for fissure vein emplacement in the Boulder batholith and adjacent rocks, Montana: Economic Geology, v. 81, p. 1387–1395.

Geophysical Characterization of Geologic Features with Environmental Implications from Airborne Magnetic and Apparent Resistivity Data

By Anne E. McCafferty, Bradley S. Van Gosen, Bruce D. Smith, and Tracy C. Sole

Chapter D2 of
Integrated Investigations of Environmental Effects of Historical Mining in the Basin and Boulder Mining Districts, Boulder River Watershed, Jefferson County, Montana
Edited by David A. Nimick, Stanley E. Church, and Susan E. Finger

Professional Paper 1652–D2

U.S. Department of the Interior
U.S. Geological Survey

Contents

Figures

Tables

NOTE ON CONVERSIONS:
The scientific standard for measurements in this report is the metric system. To convert meters to feet, multiply by 3.28. To convert kilometers to miles, multiply by 0.62

Chapter D2
Geophysical Characterization of Geologic Features with Environmental Implications from Airborne Magnetic and Apparent Resistivity Data

By Anne E. McCafferty, Bradley S. Van Gosen, Bruce D. Smith, and Tracy C. Sole

Abstract

High-resolution magnetic and apparent resistivity data collected from airborne geophysical surveys characterize aspects of geologic features in and near the Boulder River watershed that have important environmental consequences. Physical properties of bedrock expressed in the geophysical maps as magnetic and apparent resistivity anomalies are intrinsically related to mineralogical and chemical properties that have the potential to neutralize or produce acidic metal-rich waters. In particular, assemblages of acid-consuming minerals are directly associated with varying amounts of the mineral magnetite. Magnetite is the main source for magnetic anomalies and, in part, resistivity anomalies. The recognition of the relationship of magnetite to geophysical anomalies, alteration mineral assemblages, and acid-neutralization and acid-generation potential is one of the most important results of this study. Mathematical transformations applied to the magnetic and resistivity data result in pseudo-mineral maps that display volume-percent magnetite and that facilitate direct estimates of the associated amounts of acid-consuming minerals present in most of the rock types in the Boulder River watershed. The geophysical magnetite maps infer areas in the watershed with varying degrees of acid neutralization and, in some cases, map the locations of the acid-generating rocks. Many areas with low- to zero-percent magnetite coincide with areas of known hydrothermal alteration, silica-rich rock, and (or) geologic units containing sulfide-rich mineral assemblages, such as the polymetallic quartz veins. Results suggest that about 30 percent of the volcanic and plutonic rock lacks appreciable minerals to provide neutralization for acidic water. In the absence of much subsurface drill data, the three-dimensional capability of the geophysical data provides information on the environmental properties of bedrock at depth. This study demonstrates the utility of geophysical surveying to address issues surrounding water quality, aquatic health, and selection of safe waste-rock repositories. The methods and approaches employed in this study can be applied to other watersheds with similar plutonic regimes containing acid-generating historical mines or source rocks.

Introduction

The watershed approach to study and remediate historical mining areas has many environmental and economic benefits (Buxton and others, 1997). Watersheds are much larger in area and have more diverse environmental characteristics than individual mine sites. Therefore, implementing a watershed approach requires a broader study framework than might be used at a single site. In particular, techniques that reduce the resources needed for watershed-scale data collection and facilitate data analysis over large areas are especially useful. Airborne geophysical surveying is one example of such a technique.

Several characteristics of airborne geophysical surveys make them particularly useful for studying watersheds containing historical mines. First, data are collected essentially continuously, providing the same type of information for the entire survey area. In comparison, other related field tools, such as ground geophysical surveys or geochemical sampling, may have access and logistical constraints and typically provide only a limited amount of information for discrete sites or small areas. Second, geophysical surveys provide a third dimension to surface-collected information, providing insight on geologic properties with depth. Although subsurface geology has an important bearing on a range of hydrogeologic and geochemical issues important to the study of these watersheds, adequate resources often are not available for extensive drilling. Airborne geophysical mapping is also not hindered by vegetative cover or unconsolidated deposits, which can obscure bedrock geology.

Airborne geophysical surveys traditionally have been used for mineral prospecting, for structural geology studies, and in some instances, for mapping plumes of contaminated ground water. To our knowledge, airborne geophysical surveying has not been used previously in abandoned mine land studies on watershed scales even though geophysical techniques have the potential to address several key environmental issues related to historical mining and repository siting. This study was undertaken to determine the utility of airborne geophysical surveys to assess environmental aspects of this

watershed. Results of this study define how the geophysical data relate to environmental properties for many types of rocks that crop out throughout much of southwest Montana. Therefore, we expect that these study results can be extrapolated to other mining areas with similar rock types.

During the last decade, significant research has focused on determining the environmental signature of metallic *mineral deposits* and their effect on water quality and aquatic and human health (du Bray, 1995; Wanty and others, 1999). Plumlee (1999) has provided a succinct summary on the "environmental signature" of mineral deposits and a discussion on key geologic characteristics that control the degree of impact of a mineral deposit on the environment. This report takes an analogous approach, but describes a methodology to evaluate the environmental signature of *bedrock geology* and its influence on mitigating the negative effects associated with acid-generating mineral deposits in the study area.

Purpose and Scope

The purpose of this report is to combine high-resolution airborne geophysical data with geologic information to address environmental aspects in watersheds affected by historical mining. In particular, magnetic and apparent resistivity data are used to characterize the amounts of acid-consuming mineral assemblages within specific plutonic and volcanic rock units in and near areas of historical mining. Acid-neutralizing potential is an important environmental property of bedrock that has bearing on the effects of historical mine sites on aquatic environment and selection of suitable sites for mine-waste repositories.

The area covered by the airborne survey includes most of the Boulder River watershed study area and parts of the adjacent Tenmile and Prickly Pear Creek watersheds. Where appropriate, we distinguish between the Boulder River watershed study area and the larger geophysical survey area (fig. 1).

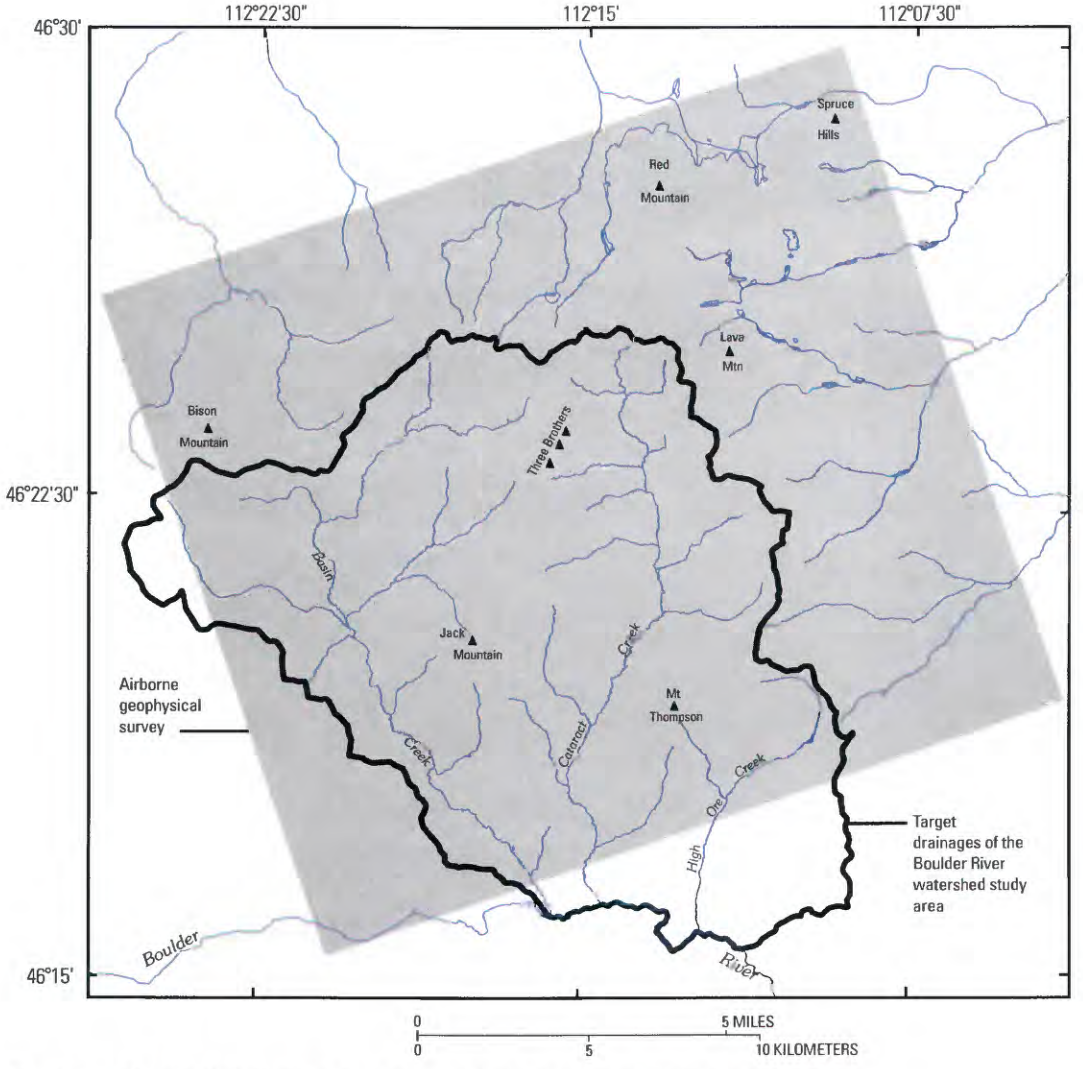

Figure 1. Boulder River watershed (part) and area of airborne geophysical survey.

Two geoenvironmental maps were produced to portray the relative degree of acid-neutralizing potential of bedrock. One map is based on geologic information and the other on airborne geophysical data. The first map was derived from rock-sample mineralogy, where acid-neutralizing potential was assigned to specific rock units based on amounts of acid-consuming minerals. The second map, derived from the geophysical data, shows acid-neutralizing potential as a function of magnetite abundance. Magnetite abundance correlates well with the abundance of acid-consuming minerals and can be estimated from the geophysical data by the application of mathematical transformations.

Finally, the study combines the geology- and geophysics-based geoenvironmental maps to spatially portray bedrock characteristics that are important controls on the impact of acid-generating mineral deposits on shallow subsurface and surface environments. The resultant map has important environmental implications for abandoned mine land issues in the Boulder River watershed.

Airborne Geophysical Survey

During December 1996, a high-resolution airborne geophysical survey was flown by helicopter over parts of the High Ore and Cataract Creek basins. The following year, a second survey was flown to augment the 1996 survey over the Basin Creek basin on the west and also over the east side of the study area. Geophysical data were acquired at the beginning of the Boulder River watershed study so that maps and derivative products could help researchers prioritize ground investigations. The two surveys were flown with identical specifications for compatibility and were digitally combined to form one data set that is analyzed in this report.

Magnetic and apparent resistivity data were collected along flightlines spaced 200 m apart and flown along an azimuth of 160°/340°. The electromagnetic (EM) field was measured with three frequencies (900, 7,200, and 56,000 Hz) using horizontal coplanar transmitting and receiving coils towed in a "bird" or sensor that varied in elevation but generally was located at approximately 30 m above the ground surface. The helicopter towed the sensor at higher altitudes in populated areas, or where higher altitudes were appropriate for safe flying, for example, over powerlines. The magnetic-field sensor was mounted 15 m above the electromagnetic sensor.

Data were collected approximately every 3 m along the flightline. The flightline data for the magnetic anomaly and resistivity data were interpolated onto a 25 m interval grid. Digital flightline data, grids, and information on other derivative geophysical products from this survey are available on CD-ROM (Smith and others, 2000).

Apparent Resistivity Data

The electromagnetic sensor measures the electrical resistivity (or the reciprocal, conductivity) of rocks. The depth of investigation for EM measurements varies inversely as a square root of frequency and earth resistivity (Telford and others, 1976) with the highest frequency (56,000 Hz) having a depth of investigation from the surface to a few to 10 m. The mid-frequency (7,200 Hz) has a depth of investigation of approximately 30 m. The lowest frequency (900 Hz) can explore as deep as 60 m.

EM measurements can be affected by noise from cultural sources such as powerlines. For example, a series of linear anomalies caused by a large powerline in the southern part of the survey area is evident in the data for all three frequencies. In comparison to the other frequencies, noise from cultural sources is elevated in the 56,000-Hz data. However, noise is minimal in the 7,200- and 900-Hz resistivity maps and only data from these two frequencies were used in this report. A map showing apparent resistivities from the 7,200-Hz data is shown in figure 2. Resistivity signatures as defined in the 7,200-Hz resistivity map were used to distinguish geologic units and structures. Data from the 900-Hz apparent resistivity were used to derive a pseudo-mineral map of magnetite.

Magnetic Data Enhancements

Aeromagnetic surveying is based on mapping variations in the local magnetic field, which are caused by changes in concentration of various magnetic minerals in surface and subsurface rocks. In order to emphasize magnetic features from sources in the shallow geologic environment, a number of data enhancement techniques were applied to the magnetic data. The purpose of the enhancements was to transform anomalies into forms that can be directly compared with important rock mineralogical properties. This section describes enhancements that (1) correctly positioned anomalies over their causative sources, (2) increased the resolution of small-scale anomalies related to near-surface magnetic sources, and (3) converted data to a model of magnetic susceptibilities for comparison with rock mineralogical properties.

Reduction-to-Pole

The study area is located at a geomagnetic latitude where magnetic anomalies are shifted slightly to the southwest from their sources (assuming induced magnetization) and are represented by an anomaly pair determined, in part, by the inclination of the present-day Earth's field. To correct anomalies for this offset in symmetry and position, a filter called reduction-to-pole (RTP) was applied to the magnetic data (fig. 3) using programs available in Phillips (1997). Application of the RTP filter results in magnetic anomalies correctly positioned over their sources and, most importantly, allows for a more accurate interpretation of magnetic source location relative to geologic features.

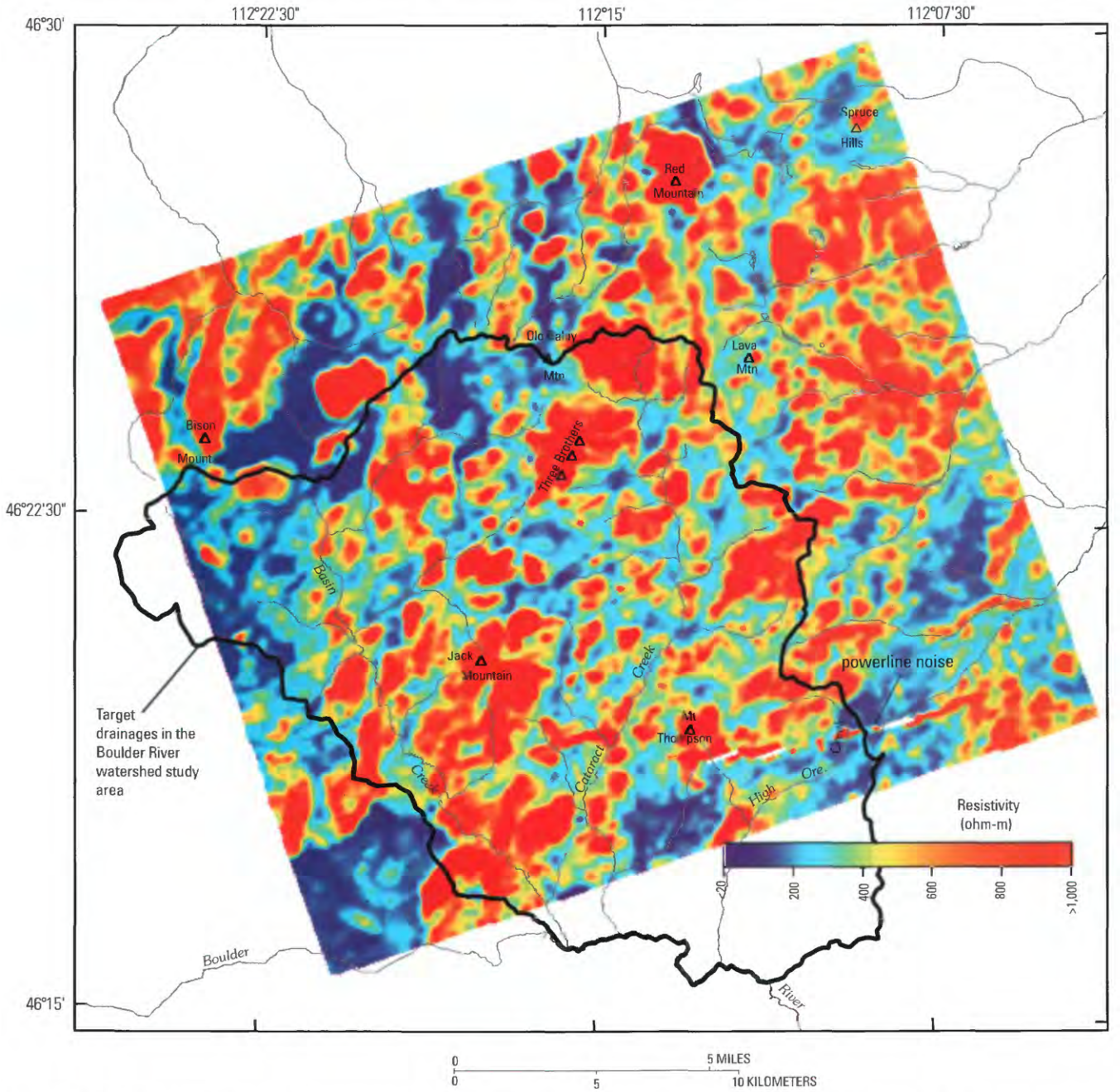

Figure 2. 7,200-Hz apparent resistivity data showing lateral variations in electrical resistivity of rocks from surface elevations to approximate depth of 30 m. Data from this map were used to define resistivity characteristics of geologic units.

High-Pass Magnetic Anomaly

To aid interpretation of anomalies related to near-surface geologic units, a "match" filter was applied to the RTP data. Match filters facilitate first approximations of magnetic fields corresponding to sources at relative depths based on ranges of wavelengths. The filter was employed using methodology developed by Syberg (1972) with computer programs in Phillips (1997). Application of the filter for this study yielded a short-wavelength anomaly field that approximates the magnetic response of a shallow magnetic source layer located within the upper 200 m of the Earth's crust (fig. 4).

We focused our analysis on the magnetic response from the shallowest depth layer, defined here as the "high-pass" magnetic anomaly, because this shallow layer is related to near-surface geologic units and processes important to this study. Additionally, the depth range of the shallowest magnetic source layer corresponds most closely to the depths of investigation of the apparent resistivity data and to the depths where acid-neutralization reactions most likely occur.

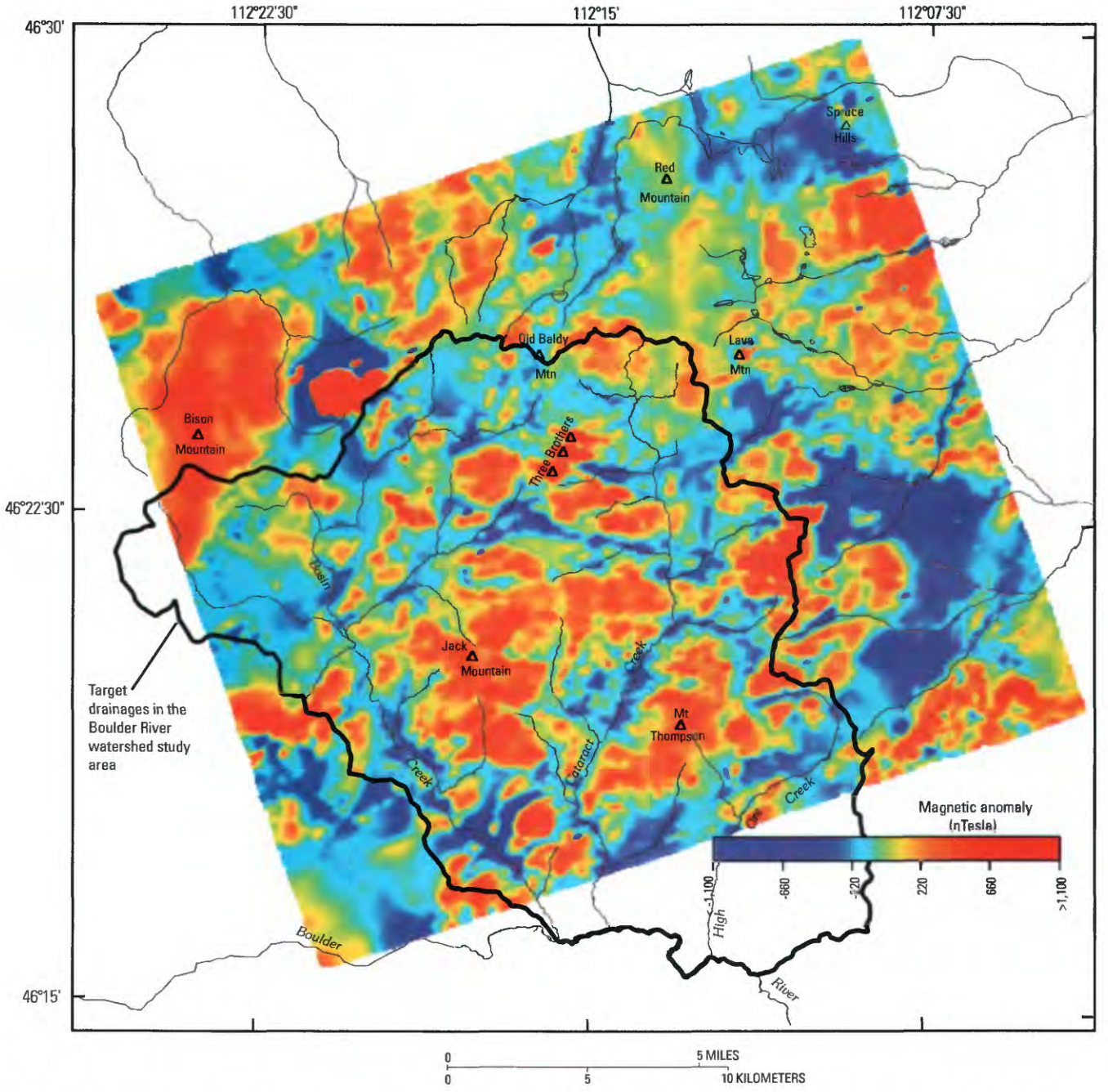

Figure 3. Reduced-to-pole magnetic anomaly map. Data in this map were filtered to enhance magnetic anomalies associated with shallow magnetic sources (fig. 4) and produce models of magnetic susceptibilities and volume-percent magnetite (fig. 5).

Magnetic Susceptibility Model

A model of magnetic susceptibility was calculated from the high-pass magnetic anomaly data to approximate the causative physical property producing the anomaly field, and also as an intermediate step toward estimating volume-percent magnetite. Magnetic susceptibility is almost entirely related to the abundance of the mineral magnetite because other magnetic minerals such as pyrrhotite, maghemite, and ilmenite are scarce in rocks exposed in the Boulder River watershed study area (Ruppel, 1963; Becraft and others, 1963). In addition, the susceptibility of magnetite is roughly 100 times the susceptibility of pyrrhotite (Dobrin and Savit, 1988). Therefore, we can be quite confident that the magnetic anomalies observed in the geophysical survey are overwhelmingly influenced by the distribution of magnetite.

Prior to estimating magnetic susceptibilities, we calculated a magnetization model from the high-pass anomaly data using a method from Blakely (1995) modified by J.D. Phillips (USGS, written commun., 2002). The method

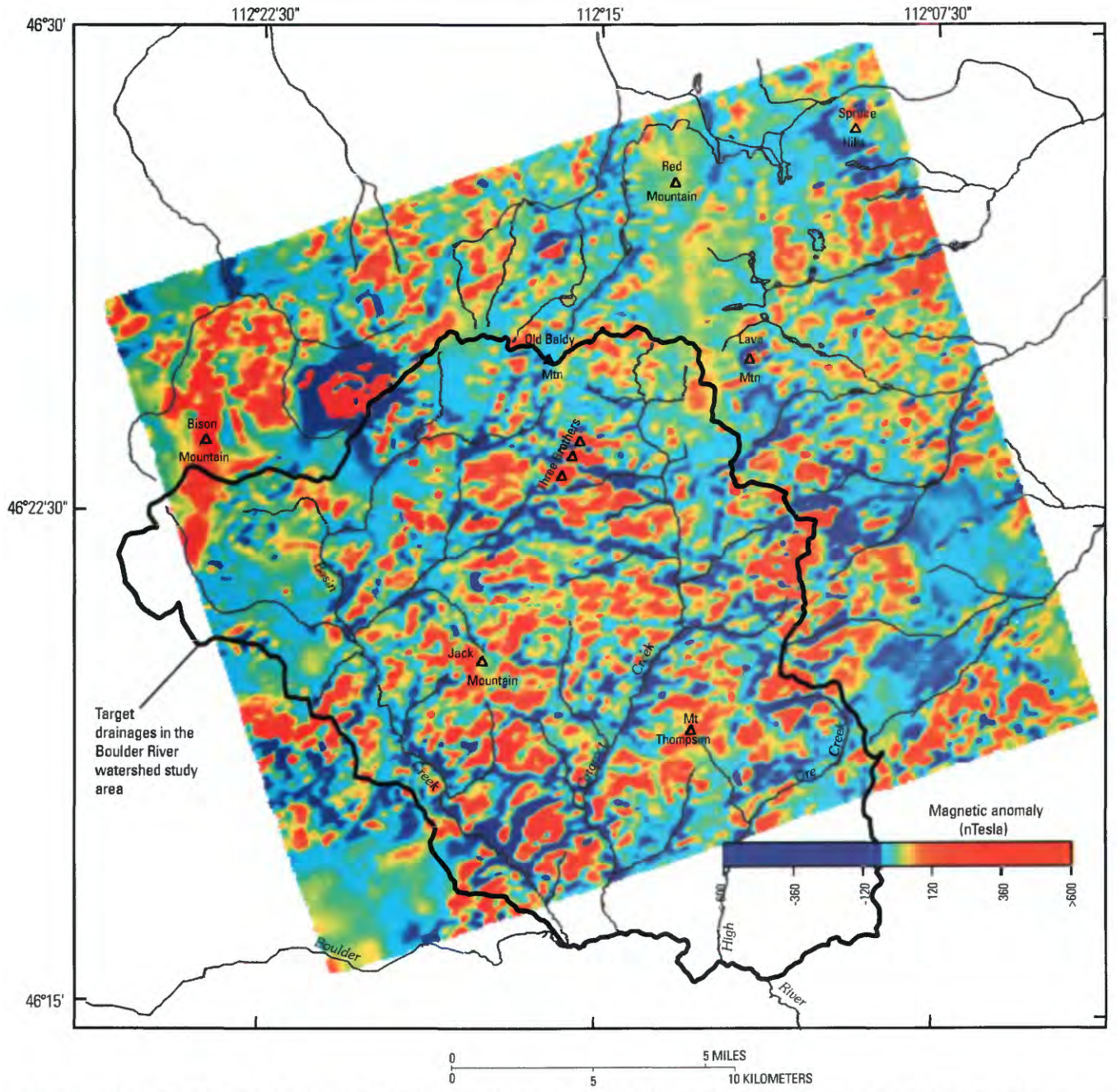

Figure 4. High-pass magnetic anomaly map calculated from reduced-to-pole magnetic anomaly data (fig. 3). Map emphasizes short-wavelength magnetic anomalies caused by lateral variations in magnetic properties of rocks exposed on the surface to approximate depths of 200 m.

inverts gridded magnetic anomaly data to magnetization estimates. For this study, we defined a 200 m thick rock layer with an upper surface represented by topography. The thickness was defined from the estimated thickness given from the matched filtering process. To obtain a first estimate of magnetization, the high-pass data were divided by an appropriate factor that produced reasonable magnetization estimates. These data were used as a first approximation to a magnetization model. The magnetic effect of the first approximation for magnetization was calculated, and the output magnetic field was scaled against the high-pass anomaly data for a best fit in terms of least squares. A difference grid was produced by subtracting the magnetic field calculated from the first approximation from the high-pass data. Magnetic values in the error grid were scaled to appropriate magnetization values and added to the first approximation to create a second approximation. This process was repeated until a minimum difference between the calculated field and high-pass magnetic field was achieved. The magnetic anomaly field resulting from the final magnetization model contained errors of less than 2 gammas for more than 95 percent of the grid. We converted magnetizations to magnetic susceptibilities by dividing the magnetization values

by the total intensity of the geomagnetic field and assuming induced magnetizations. The magnetic susceptibility model is shown in figure 5.

The range in model susceptibility values is significantly narrower than the range of susceptibilities measured in either field observations during this study, or from results of magnetic-property laboratory studies of Hanna (1969). Susceptibility measurements taken at outcrop can typically range over orders of magnitude and can do so within the same rock type over short distances (within a few centimeters in some cases). The discrepancy between field and model susceptibility values is not surprising, however, and is controlled in large

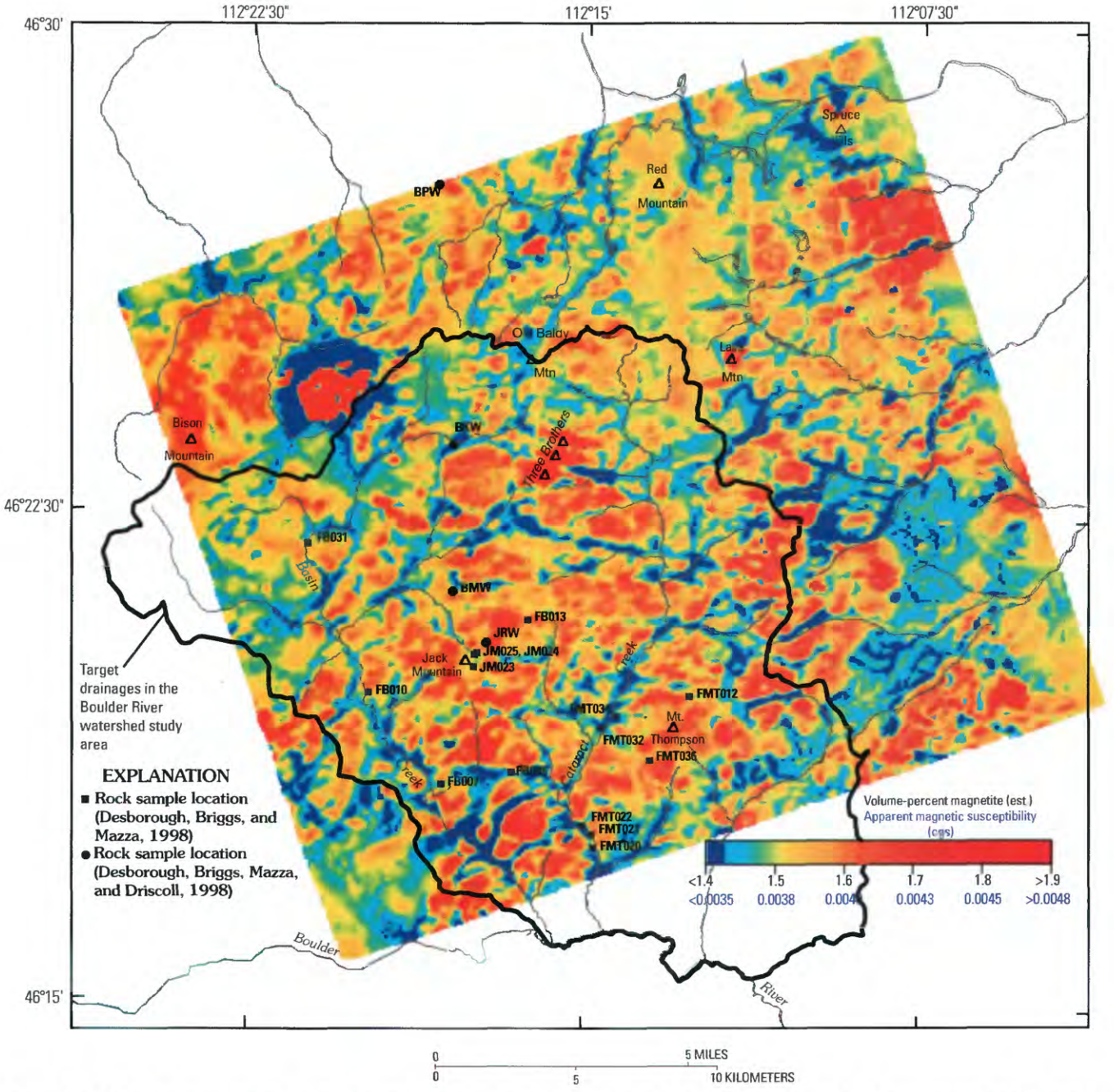

Figure 5. Magnetic susceptibility and estimated volume-percent magnetite models calculated from high-pass magnetic data (fig. 4). Magnetic susceptibility characteristics for geologic units within airborne geophysical survey are given in figure 9. Values for percent magnetite at locations of rocks analyzed for acid-neutralizing potential are given in table 2. Low values of volume-percent magnetite (<1.4 percent) are shown in blue and infer areas of rocks with low acid-neutralizing potential. In contrast, red areas infer bedrock with high magnetite content and corresponding high acid-neutralizing potential.

part by scale. Field susceptibility measurements sample only a very small volume of rock, and values can vary greatly due to relatively small changes in magnetic mineral content. In contrast, the susceptibility model based on airborne surveying represents the integrated response of magnetic properties within a much larger volume of rock (illustrated in fig. 6). Magnetic susceptibilities from the model do, however, fall within the range of susceptibilities measured in laboratory and field. The model calculations are reasonable values for the types of plutonic and volcanic lithology present in the watershed, and they produce a magnetic field that closely approximates the observed field. These factors support the assumption that the model susceptibilities provide a reasonable representation of rock magnetic properties within the near surface.

Figure 6. Sketch illustrating concept of bulk magnetic susceptibility versus magnetic susceptibility measured at outcrop. Measurements taken from an airborne magnetic sensor integrate effects from a much larger volume of rock compared to measurements taken at outcrop.

Geophysical Signatures of Geologic Features

This section presents an overview of the apparent resistivity and magnetic susceptibility signatures for approximately 40 geologic units organized under six major lithologic groups. These groups include Quaternary deposits, Eocene-Oligocene Helena volcanic rocks, Eocene Lowland Creek Volcanics, Upper Cretaceous Elkhorn Mountains Volcanics, Late Cretaceous Butte pluton granitic rocks, and Late Cretaceous polymetallic quartz veins (fig. 7). In addition, statistical approaches were used to define geophysical signatures of the polymetallic quartz veins and to quantify geophysical gradient trends related to geologic structures.

Geophysical signatures for the geologic units are presented as box plot diagrams that present summary statistics. The resistivity (fig. 8) and magnetic susceptibility (fig. 9) charts are effective visual tools to illustrate the range in physical property variation inherent in a single geologic unit, showing similarities, differences, and overlap in geophysical signature among multiple units. Interpretation of the physical property characteristics is described in terms of the geologic factors and processes that influence the range of resistivity and magnetic susceptibility values. The diagrams were produced by determining the physical property values that had overlap with a particular geologic unit from 100×100 m grids of geology (Ruppel, 1963; Becraft and others, 1963), 7,200-Hz resistivity (fig. 2), and magnetic susceptibility data (fig. 5).

Quaternary Unconsolidated Deposits

Unconsolidated deposits are mainly glacial deposits and alluvial sediments found primarily on the valley floors. Low electrical resistivities characterize the Quaternary deposits; values average approximately 180 ohm-m. In general, the surficial deposits are electrically conductive (resistivity lows) relative to bedrock because of contained water, interconnected pore space, and predominance of clays. The chemistry and amount of the contained water can be highly variable and have a significant effect on the electrical properties of rocks. For example, if interstitial water is dilute, that is, free from salinity and dissolved metals, and there is little connected pore space, high resistivities will result. Alternately, as is likely the case for most of these unconsolidated deposits, the abundant pore space is connected and the sediments are saturated, resulting in a decrease in electrical resistivity.

There is considerable overlap between the resistivity of the unconsolidated deposits and that of many other geologic units, especially the Tertiary volcanic units (fig. 8). This overlap can be attributed to similar amounts of clays, which developed either as part of hydrothermal processes or from low-temperature weathering processes. Both processes can produce clays with similar resistivity ranges (Telford and others, 1976). Local resistivity anomaly highs that occur in valley floors are interpreted to be the resistivity response of shallowly buried bedrock that projects from adjacent hill slopes.

Although resistivity anomalies are produced from electrical property changes in the unconsolidated deposits, magnetic surveying is relatively insensitive to magnetic property changes in the sediments. Rather, the magnetic anomaly map is dominated by magnetic properties in the underlying bedrock because the unconsolidated deposits are effectively magnetically transparent owing to the relatively thin mantle of unconsolidated deposits in comparison to the volumetrically large underlying bedrock (Ruppel, 1963; Becraft and others, 1963). Although magnetite is present in the unconsolidated deposits, the amount of magnetite is not sufficient to cause significant magnetic anomalies.

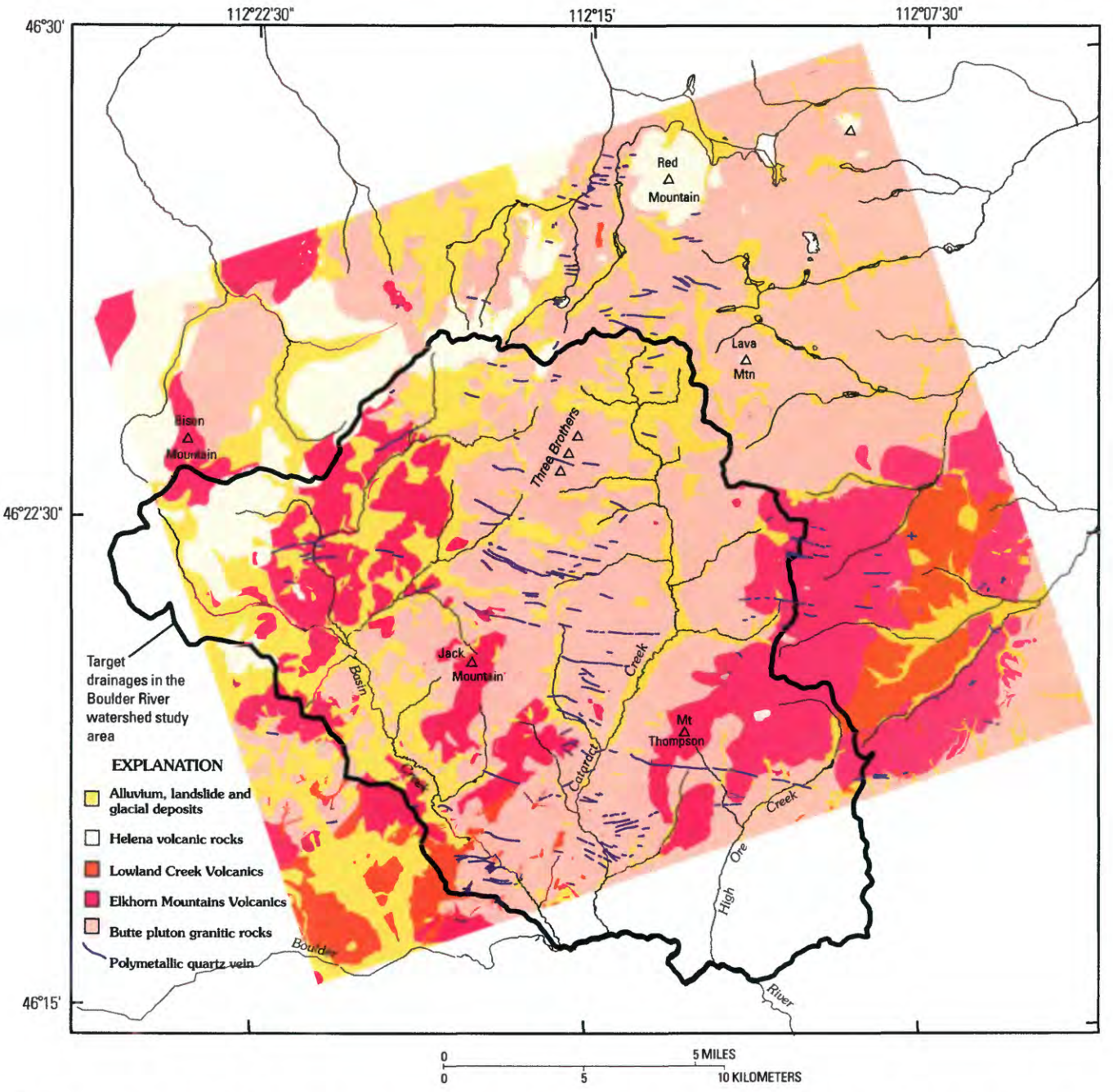

Figure 7. Main lithologic units within area of airborne geophysical survey over the Boulder River watershed study area and surrounding region. Generalized from Ruppel (1963) and Becraft and others (1963).

Eocene-Oligocene Helena Volcanic Rocks

Rocks mapped as rhyolite intrusives (Tri) in the Helena volcanic field are generally some of the most resistive rock units in the study area (fig. 8). The largest Tertiary intrusive body in the study area is exposed at Red Mountain (fig. 7). A sample of intrusive rhyolite from the top of Red Mountain contained more than 75 percent SiO_2. An altered counterpart to the fresh rhyolite collected on the southeast slope of Red Mountain contains a slightly higher (81 percent) but comparable amount of silica (Becraft and others, 1963, p. 30). The large amplitude resistivity high (fig. 2), moderately low amplitude magnetic anomaly (fig. 4), and mineralogy at Red Mountain are evidence that silica-rich fluids were introduced as part of the alteration event. Silica-rich rocks typically have low magnetic susceptibility owing to their decreased magnetite content and high electrical resistivities (Telford and others, 1976).

In contrast, intrusions that are part of the Helena volcanic field that exhibit a much different geophysical signature and show evidence of a hydrothermal event with more potassic-rich fluids exist in other parts of the airborne geophysical

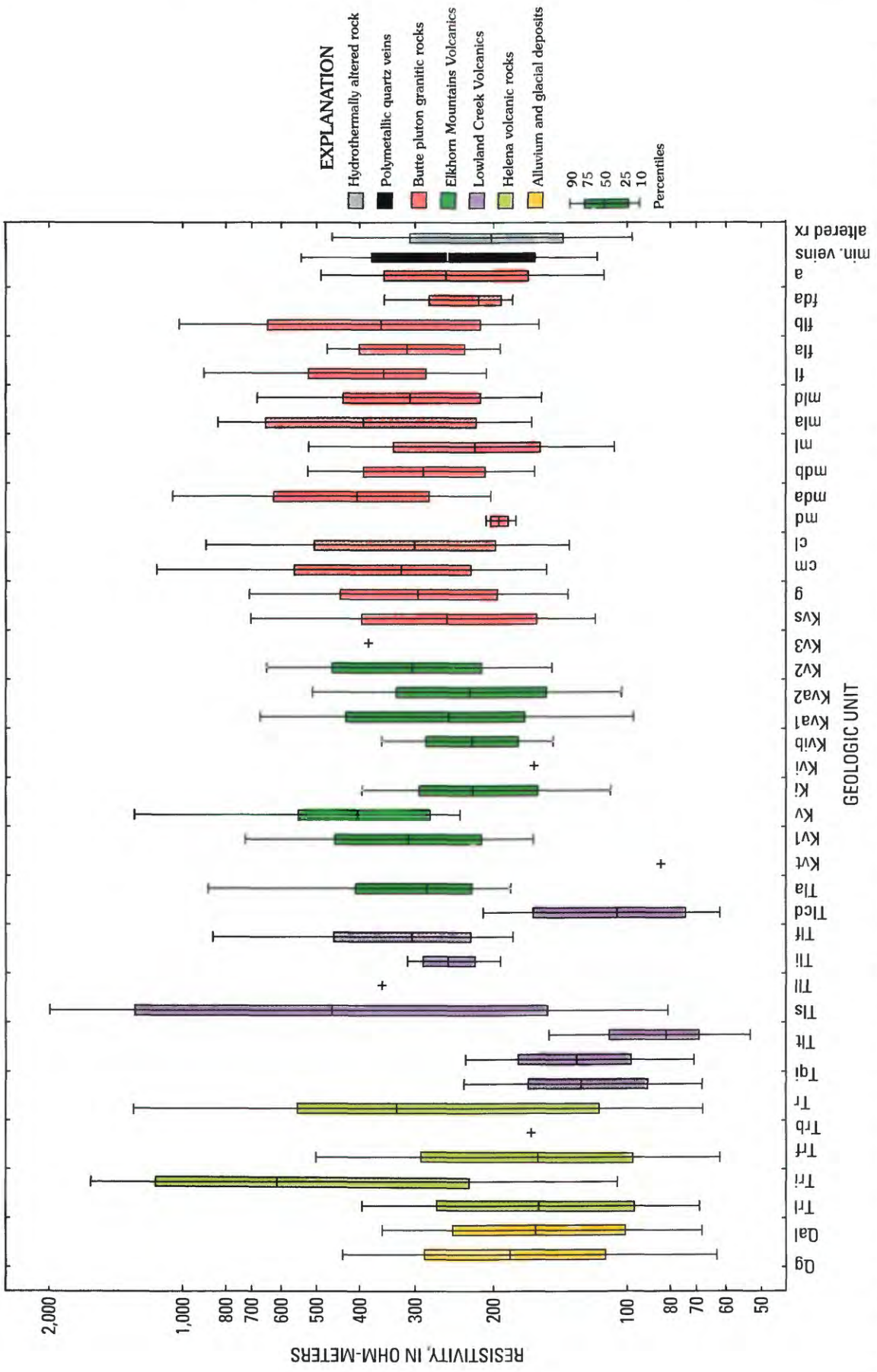

Figure 8. Electrical resistivity characteristics from 7,200-Hz resistivity grid (fig. 2) for geologic units within airborne geophysical survey. Geologic unit symbols from Ruppel (1963) and Becraft and others (1963). Unit descriptions in table 1.

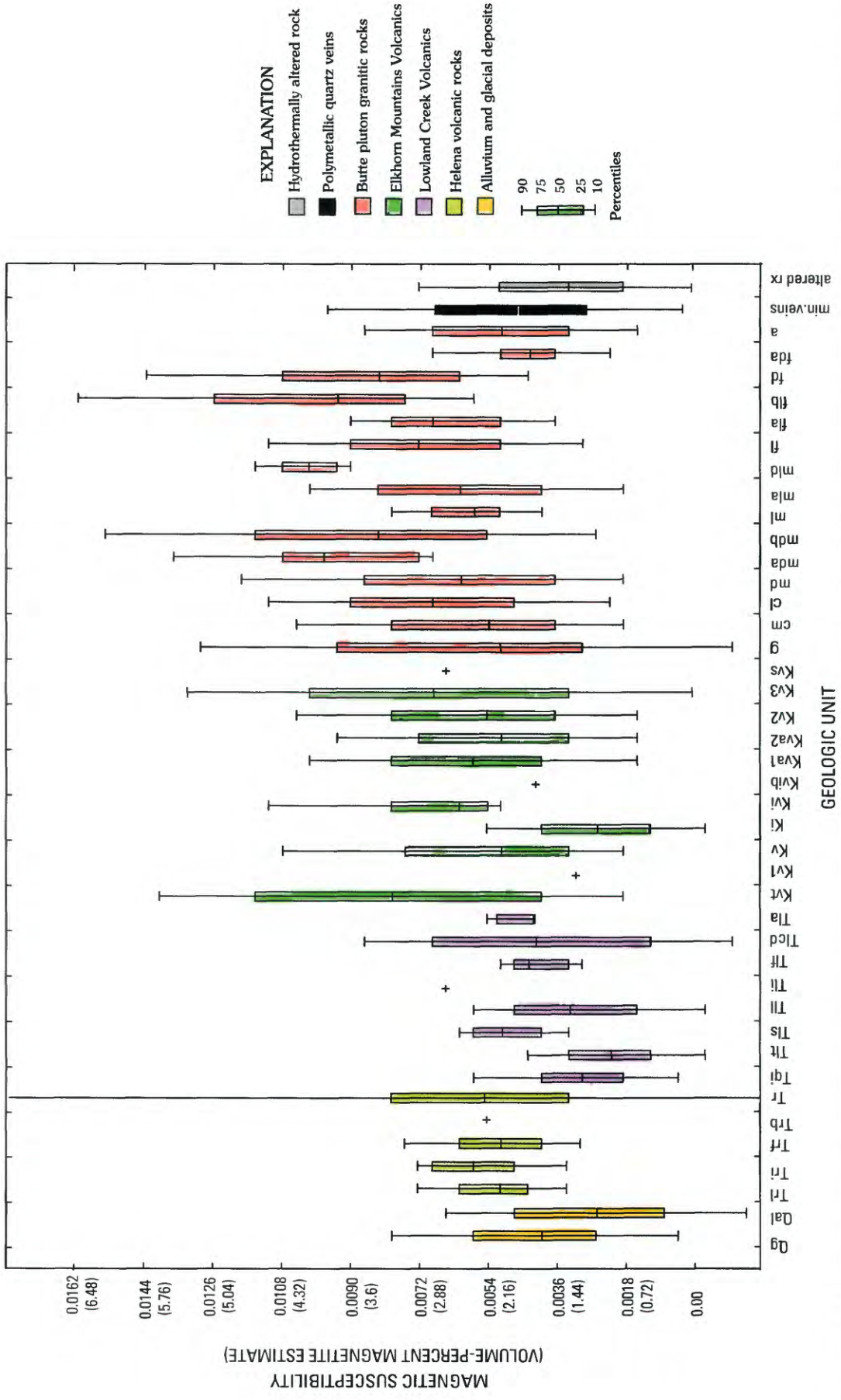

Figure 9. Magnetic susceptibility and volume-percent magnetite estimates shown in figure 5 modeled from high-pass magnetic anomaly data (fig. 4) for geologic units within airborne geophysical survey. Geologic unit descriptions from Ruppel (1963) and Becraft and others (1963) and in table 1.

survey area. The most prominent of these are located east of Bison Mountain and north of the Boulder River watershed study boundary, in the northwestern part of the airborne geophysical survey. Very large amplitude "bullseye" resistivity and magnetic anomaly highs ringed by distinct resistivity and magnetic anomaly lows (fig. 2 and fig. 3, respectively) are located here, representing both extremes in highest and lowest modeled magnetic susceptibilities and electrical resistivity values. Although undivided Tertiary rhyolite (Tr) is mapped here (Ruppel, 1963), we interpret the geophysical anomalies to represent the response of a vent area with a large intrusive body at shallow depth. Geologic evidence for other vent areas along a northeast trend occurs in this area (O'Neill and others, this volume, Chapter D1). The resistivity anomaly high is interpreted to represent the electrical response of a more silicified cap over the intrusive center. Emplacement of the inferred intrusive has significantly altered the surrounding host rock resulting in the magnetic and resistivity lows that surround the circular geophysical highs. Additionally, the resistivity lows surrounding the source suggest that the hydrothermal fluids were not silica rich. Other areas with similar geophysical signatures occur over outcrops of undivided rhyolite rocks exposed at Lava Mountain and at Spruce Hills (fig. 7).

Eocene Lowland Creek Volcanics

Resistivity values have the greatest variability in rocks that form the Eocene Lowland Creek Volcanics. Relatively high resistivity values characterize the lapilli tuff (Tll) unit of Ruppel (1963), whereas very low resistivities characterize the volcanic sandstone (Tls) unit of Ruppel (1963). Chemical analyses of a sample of Tll (Ruppel, 1963, p. 49) showed exceptionally high percentage of silica, which is in agreement with the overall high resistivities that characterize this rock (fig. 8). Extremely low apparent resistivities occur over the volcanic sandstone unit (Tls). Average resistivity for this unit is 120 ohm-m and is consistent with resistivities expected for clays (Telford and others, 1976), which suggests that clays are well developed in this unit. Additionally, sedimentary rocks typically have lower resistivities compared to igneous rocks, owing to increased porosity.

The Lowland Creek Volcanics are characterized by low magnetic susceptibility values (fig. 9). The low values are the combined response from remanent magnetization and nonmagnetic mineralogy. Total magnetization is a vector sum of induced (also called normal) magnetization (M_n) and remanent magnetization (M_r);

$$M_t = M_n + M_r$$

where normal magnetization is the product of the Earth's magnetic field (H) and magnetic susceptibility (k);

$$M_n = kH$$

The magnetic susceptibility model (fig. 5) was calculated assuming that remanent magnetization is not a dominant factor in the plutonic and volcanic rocks in the study area and that normal magnetization, which is primarily a function of magnetic susceptibility, is the main contributor to magnetic anomalies in the study area. This is true for most rock types in the study area. However, remanent magnetization is present in some units within the Lowland Creek Volcanics (Hanna, 1969), but it is of such low intensities that its contribution to total magnetization is minimal. Of more importance in explaining the magnetic anomaly lows (and low magnetic susceptibilities) that typify much of the outcrop of Lowland Creek Volcanics is the nonmagnetic mineralogy of the rocks. Average susceptibility for more than 80 outcrop measurements of Lowland Creek Volcanics is 0.00005 (cgs), which is 20 times lower than average susceptibilities of Elkhorn Mountains Volcanics, and 50 times lower in value than average susceptibilities measured in Butte pluton granitic rocks.

A large area of magnetic lows occurs over outcrops of Lowland Creek Volcanics in the vicinity of the Wickes mining district, located southeast of the Boulder River watershed, where rocks are pervasively altered (Becraft and others, 1963). The cause of the magnetic anomaly and magnetic susceptibility lows is the destruction of magnetite due to introduction of hydrothermal fluids, which have chemically removed magnetite.

Upper Cretaceous Elkhorn Mountains Volcanics

The range of resistivity and the magnetic susceptibility values for the units of Elkhorn Mountains Volcanics are similar in overall geophysical character to those of the Butte pluton units. However, some notable differences can be seen. As discussed in O'Neill and others (this volume), only the ash flow deposits of the middle member of the Elkhorn Mountains Volcanics were derived from the relatively silica rich magma that produced the Butte pluton. The other volcanic units in the group were derived from more mafic phases of the Boulder batholith, are less voluminous, and lie outside the geophysical study area.

Three units were grouped on the generalized geologic map by O'Neill and others (this volume, pl. 1) to define the middle member, Kevm; these include Kva1, Kva2, and Kv2 (table 1). The magnetic susceptibility ranges of the three map units (fig. 9) are almost identical, so a geophysical rationale exists for grouping these three units into one composite unit. Resistivity ranges for the three units also overlap (fig. 8). However, some areas of unit Kva2 have significantly higher resistivity values, suggestive of a more silica rich composition than the other two middle member map units have. Additionally, in the geology-based geoenvironmental map section (p. 110), we show that Kva2 is significantly different in chemical composition, enough to warrant a separate classification from the other units in this volcanic group.

Assuming that the middle member map units in the Elkhorn Mountains Volcanics were derived from a more silica rich phase of the Butte pluton, we expect that their magnetic susceptibilities would be lower and their resistivities higher in comparison with upper member units presumably derived

Table 1. Map symbols, descriptions, and average sum of percent calcium and iron from whole-rock chemical analyses of samples collected in and around the Boulder River watershed study area.

[Sum of calcium and iron reflects the presence of calcic and mafic mineral assemblages that provide significant ANP to low pH waters. Rocks with higher percentages of calcium and mafic minerals possess higher ANP. The chemical data are used to create the geology-based geoenvironmental map shown in figure 14. Relative ANP is defined in varying degrees: H, high; MH, moderately high; M, moderate; ML, moderately low; L, low. Leaders (--), samples not available for chemical analyses and no ANP assigned]

Geologic map symbol		Description	Percent Ca+Fe	Relative ANP
Original[1,2]	Generalized[3]			
		Quaternary alluvium and glacial deposits		
Qg[1]	Qg	glacial deposits	--	--
QTst[1]	Qg	gravel veneering strath	--	--
Qal[1]	Qal	alluvium	--	--
Qst[1]	Qal	fan gravel	--	--
		Tertiary Helena volcanic rocks; rhyolite		
Trl[1]	Trl	lapilli tuff	--	--
Tri[1,2]	Tri	intrusive	1.9[2]	L
altered Tri[2]	Tri	altered intrusive	0.6[2]	L
Trf[1,2]	Trf	flow	1.5[1]	L
Trb[1]	Trb	flow breccia	--	--
Tr[1,2]	Tr	undivided	--	--
		Tertiary Lowland Creek Volcanics; quartz latite		
Tli[1]	Tli	intrusive rocks	3.2[1,2]	ML
Tlt[1,2]	Tlt	tuff	--	--
Tls[1]	Tls	sandstone	--	--
Tll[1]	Tll	lapilli tuff	0.5[1]	L
Tlf[1]	Tlf	lava flow	--	--
Tlcd[1]	Tlcd	clastic dikes	--	--
Tla[1]	Tla	welded tuff	3.2[1]	ML
		Cretaceous Elkhorn Mountains Volcanics		
Kvt[1]	Kev	crystal tuff	--	--
Kvl[1]	Kev	lapilli tuff	--	--
Kv[1,2]	Kev	undivided volcanics	--	--
Ki[2]	Kei	rhyodacite porphyry	6.5[2]	MH
Kvi[1]	Kei	intrusive andesite	--	--
Kvib[1]	Kei	intrusive basalt	--	--
Kva1[1]	Kevm	lower dark-gray and greenish-gray welded tuff	6.3[1,4]	MH
Kva2[1]	Kevm	upper medium- and light-gray welded tuff	5.1[1]	M
altered Kva2	Kva2	upper medium- and light-gray welded tuff	1.3[4]	L
Kv2[2]	Kevm	light-greenish-gray to light-gray welded tuffs	6.1[4]	MH
Kv3[2]	Kevu	well-bedded dark-gray tuffs	9.1[2]	H
Kvs[1]	Kevu	andesitic sandstone	--	--
		Cretaceous Butte pluton granitics		
cm[2]	Kbm	undivided coarse and medium grained	6.3[2,4]	H
altered cm[4]	Kbm	undivided coarse and medium grained	2.3[2]	ML
cl[2]	Kbm	coarse-grained light-gray biotite-hornblende	5.8[2,4]	MH
cla[2]	Kbm	coarse-grained light-gray biotite-hornblende	6.5[2]	MH
md[1,2]	Kbm	medium grained dark gray	5.7[1,2,4]	MH
altered md[4]	Kbm	medium grained dark gray	1.8[2]	L

Table 1. Map symbols, descriptions, and average sum of percent calcium and iron from whole rock chemical analyses of samples collected in and around the Boulder River watershed study area.—Continued

Geologic map symbol		Description	Percent Ca+Fe	Relative ANP
Original[1,2]	Generalized[3]			
		Cretaceous Butte pluton granitics—Continued		
mda[2]	Kbm	medium grained dark gray	7.0[2]	MH
mdb[1]	Kbm	medium grained medium gray with pink tint	7.1[1]	MH
mdc[1]	Kbm	medium grained with abundant mafic minerals	6.9[1]	MH
ml[2]	Kbm	medium grained light gray	3.1[2]	ML
mla[1,2]	Kbm	medium grained light gray, reddish-brown tint	4.4[2,4]	M
mld[1]	Kbm	medium grained light gray with abundant biotite	--	--
g[1]	Kbm	fine to medium grained, dark gray	7.9[1]	H
fl[1,2]	Kbf	fine grained light gray	5.0[1,2]	M
fla[1,2]	Kbf	fine grained light gray porphyritic	--	--
flb[1,2]	Kbf	fine grained light gray with pink tint	4.6[1]	M
flc[2]	Kbf	fine grained light gray	4.3[2]	M
fd[1,2]	Kbf	fine grained dark gray	5.0[1,2]	M
fda[2]	Kbf	fine grained dark gray porphyritic	4.6[2]	M
a[2]	Kba	alaskite, aplite, and pegmatite	0.8[2]	L

[1]Ruppel, 1963. [2]Becraft and others, 1963. [3]O'Neill and others, this volume. [4]Desborough, Briggs, Mazza, and Driscoll, 1998.

from a more mafic magma. However, the geophysical data suggest that the middle member units are more similar in geophysical character to the other units than the interpretation of the rock chemistry suggests.

Late Cretaceous Butte Pluton Granitic Rocks

In comparison to other granitic plutons of similar mineralogy, the Butte pluton is characterized by lower than normal resistivity values. The relatively low resistivity values initially puzzled us given that typical resistivities for similar granitic rocks are in the thousands of ohm-meters range (Telford and others, 1976). Resistivity for most of the Butte pluton granitic rocks ranges from approximately 300 to 800 ohm-m (fig. 8). The lower than average resistivity values determined from the airborne survey imply that the pluton has been greatly affected by surficial weathering, hydrothermal alteration, and fracturing within its upper 60 m. Clays, which result from either low-temperature weathering or hydrothermal processes, tend to lower the resistivity of igneous and volcanic rocks. Consequently, altered volcanic and plutonic granitic rocks are typically less resistive (more conductive) in comparison with their fresh unaltered state. Direct current electrical resistivity soundings made from ground measurements on the Butte pluton confirm that the electrical resistivity of the first 30 m is on the order of 200 to 300 ohm-m in many places, again much lower than expected (Smith and Sole, 2000).

Studies of magnetic properties of Butte pluton granites show that these rocks possess normal polarity and that intensities of remanent magnetization are negligible (Hanna and others, 1994). The intensities present in the form of normal magnetizations are strong enough to contribute significantly to magnetic anomaly intensities. Consequently, magnetic anomalies over the pluton can be chiefly explained by magnetite content. Granite that contains more magnetite has a stronger magnetization and results in a more positive (larger amplitude) magnetic anomaly. In granite that has undergone chemical alteration, whether hydrothermal or deuteric, primary magnetite has been destroyed and the rock is associated with a more negative (lower amplitude) magnetic anomaly (Hanna, 1969). Alteration typically causes conversion of magnetite to nonmagnetic, more highly oxidized and hydrated iron-oxide minerals such as limonite (Ruppel, 1963). In cases where redox conditions are reducing, magnetite can be destroyed as its iron is reduced. The resulting ferrous iron is combined with sulfur to form pyrite (Desborough and Driscoll, 1998). Overall, the resulting geophysical effect of the alteration processes is a reduction in magnetization and a corresponding lowering of the intensity of the magnetic anomaly. A detailed analysis of magnetite content within the environmentally important Butte pluton follows in a later section.

Late Cretaceous Polymetallic Quartz Veins

Two types of veins cut the Butte pluton granitic rocks of the study area. East-trending polymetallic quartz veins host the ore deposits exploited by mining. Generally northeast trending chalcedony veins that are not mineralized also cut the granitic rocks. Geologic characteristics associated with mining the east-trending polymetallic quartz veins exert the most negative impact on the surface-water quality in the Boulder River watershed study area. Water draining from mines, adits,

and waste associated with the polymetallic veins is a major source for acidic and metal-rich surface waters (Nimick and Cleasby, this volume, Chapter D5; Kimball and others, this volume, Chapter D6). Geophysical characteristics that define these mineralized veins include low magnetic susceptibilities (fig. 9) and moderately high resistivities (fig. 8). The statistical summaries presented in the resistivity and magnetic susceptibility diagrams are useful to view the range of physical properties that characterize a particular feature, but they do not allow for a comprehensive understanding of how "distinct" or characteristic these signatures are in comparison with geophysical signatures of other geologic features.

To quantify how characteristic (or not) low magnetic susceptibilities and high resistivities are of the mineralized veins, we applied a statistical approach using methodology developed by Lee and others (2001) to the resistivity (fig. 2) and magnetic susceptibility data (fig. 5). The approach uses a ratio of probabilities, also called weights (W), to describe the statistical likelihood of a class of a particular evidential layer having a spatial association with a given prototype area. For this study, the evidential layers are the magnetic susceptibility and resistivity data, and classes are defined as values within these data. Prototypes against which we compare the evidential layers include locations of polymetallic quartz veins and nonmineralized chalcedony veins (Ruppel, 1963; Becraft and others, 1963).

Weights fall within three general categories that describe the spatial association:

a positive spatial association exists if $W > 1$;
a negative spatial association exists if $W < 1$; and
a random association is present if $W = 1$

To illustrate, a weight of 30 would suggest that a particular class, high values of resistivity, for example, within a geophysical data layer would be 30 times more likely to be associated with a particular mineral deposit than any other feature in the study region.

The geophysical signatures of nonmineralized chalcedony veins were examined to determine if the two vein types could be distinguished on a geophysical basis.

Histograms that describe the spatial association between the resistivity and magnetic susceptibility data and polymetallic quartz and chalcedony veins are shown in figure 10. Results show that moderately high resistivities, in the range of 1,750 to 2,500 ohm-m, characterize the polymetallic quartz veins. Resistivities for the nonmineralized chalcedony veins show a strong spatial association ($W > 1$) with a slightly lower resistivity range (1,050 to 1,700 ohm-m). High electrical resistivities that characterize both vein types may reflect the presence of resistive gangue minerals (quartz) and low porosity of the vein material.

Polymetallic quartz veins are characterized by very low magnetic susceptibilities (fig. 10). Model magnetic susceptibilities that characterize the mineralized veins range from –0.0059 to –0.0026 (cgs). This range of values is interpreted to be a combined effect of demagnetization of once magnetite-rich host rock from hydrothermal alteration processes and the nonmagnetic mineralogy of the vein material. In contrast to the resistivity signature, no particular magnetic susceptibilities characterize the chalcedony veins as evidenced by the random spatial associations defined by weights that fluctuate around the value of 1 (fig. 10). The lack of distinct magnetic signature of the chalcedony can be attributed to the narrower alteration envelopes surrounding the chalcedony veins compared to the wider alteration envelopes surrounding the polymetallic quartz veins (Becraft and others, 1963). Fluids associated with the emplacement of the chalcedony veins only locally altered the country rock. In contrast, fluids associated with the emplacement of the polymetallic quartz veins had a more profound effect on the wall rock, resulting in larger alteration envelopes and greater modification of host rock magnetic mineralogy (Becraft and others, 1963).

Geologic Structures and Geophysical Trends

Obvious features in the geophysical maps are linear gradients that trend over kilometers. Many gradients and narrow elongate anomalies define faults and structures that map contacts between rocks with different resistivity or magnetic properties. Faults can be expressed as linear resistivity lows if the degree of fracturing is high (equivalent to high porosity), clay has developed from weathering or alteration processes, and (or) water is present. Alternately, fault zones that contain silicified fractures, are dry, and have little clay present commonly are expressed as resistivity highs. Resistivity values can be orders of magnitude higher in dry, unfractured rock in contrast to wet and fractured rock (Olhoeft, 1985). The magnetic expression of faults depends on the magnetic properties of the adjacent rocks. If a fault juxtaposes rocks with similar magnetic properties, no magnetic expression of the geologic contact is likely. However, if a nonmagnetic rock is adjacent to a highly magnetic rock type, a distinct magnetic gradient will mark the fault contact.

Geophysical gradient trends are defined as distinct linear and curvilinear elements that can be mapped from contours in the geophysical data (Grauch, 1988). Figure 11 shows geophysical trends calculated from grids of the 7,200-Hz apparent resistivity (fig. 2) and RTP magnetic anomaly data (fig. 3). Dominant geophysical trend directions are co-linear with the orientation of three major fracture systems in the region. These orientations include a set of northeast- and northwest-trending structures, and a third east-trending set. The three principal fracture systems likely reflect deep-seated and reactivated structures related to emplacement of the Boulder batholith and to have been active recurrently since the Proterozoic (O'Neill and others, this volume).

Dominant orientations of geophysical gradients are northwest and west-northwest. The northwest-trending gradients are partly co-linear with faults and lineaments mapped by Smedes (1966) and lineaments mapped from remote sensing data within and around the Boulder River watershed study area (McDougal and others, this volume, Chapter D9). Although

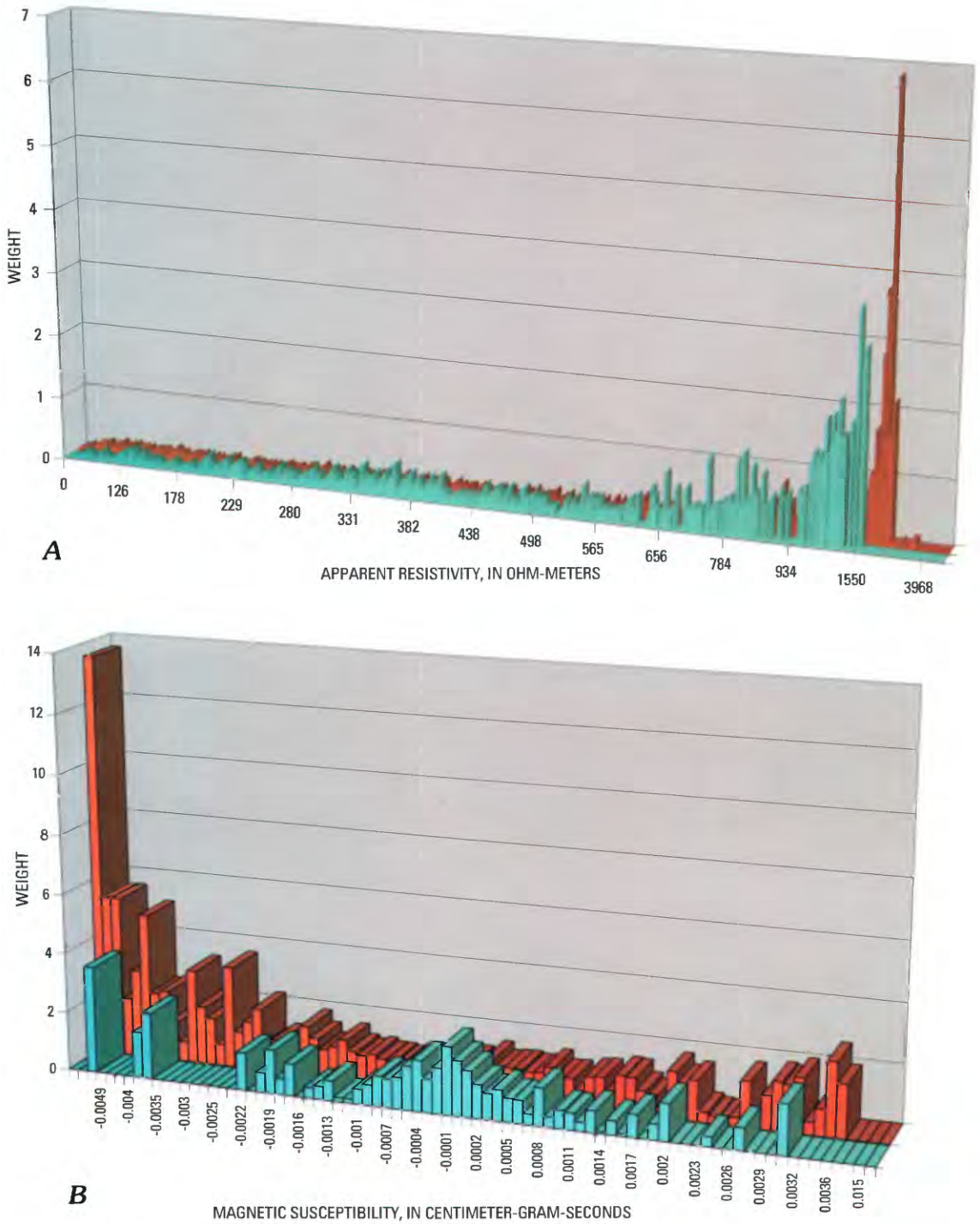

Figure 10. Statistical probabilities (weights) that describe the spatial association between *A*, resistivity, or *B*, magnetic susceptibility and mineralized polymetallic (red) or nonmineralized (blue) veins. The greater the weight, the stronger the spatial association. Low values of magnetic susceptibility, in the range of –0.0049 to –0.0022, are two to fourteen times more likely to occur over the polymetallic veins than any other geologic feature in the study. Alternately, the nonmineralized veins have no characteristic magnetic susceptibility signature; a weak to random spatial association exists as evidenced by weights around the value of 1. Results of the modeling for resistivity data show that both vein types are strongly associated with moderately high values of resistivity.

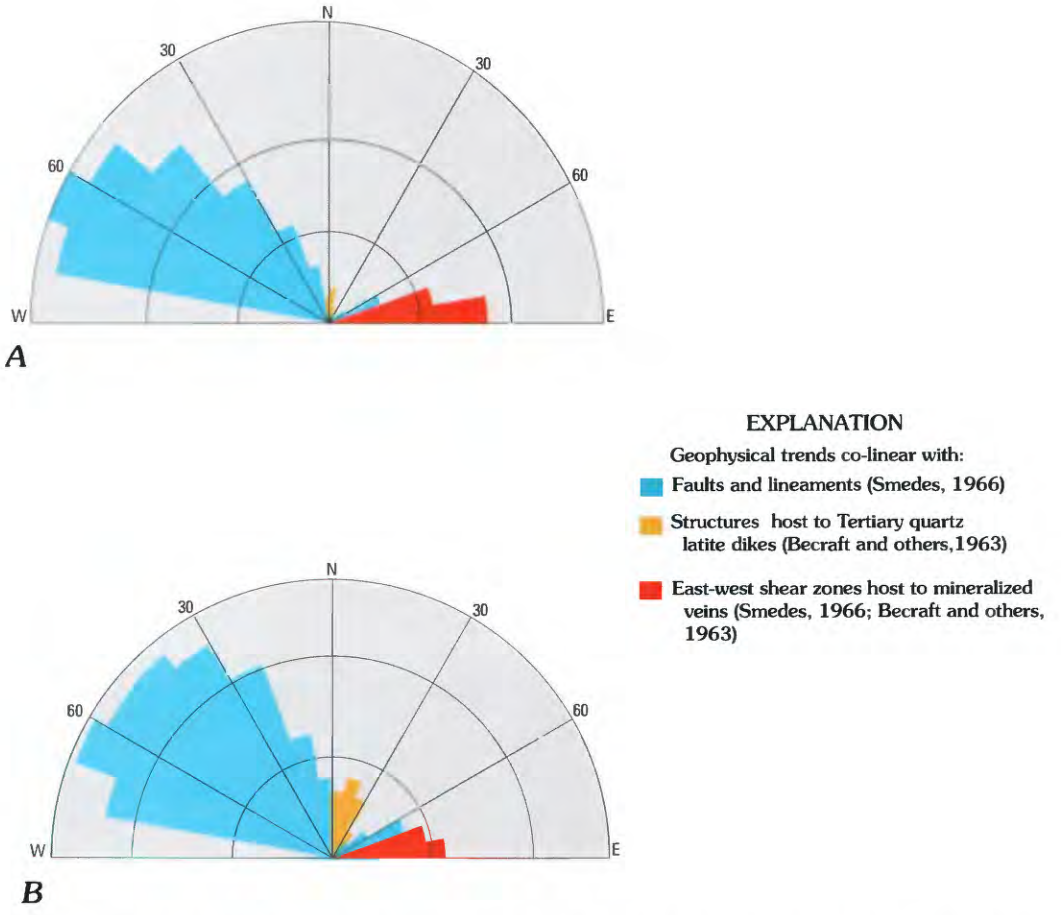

Figure 11. Geophysical gradient trends from *A*, grids of reduced-to-pole magnetic anomaly (fig. 3) and *B*, 7,200-Hz apparent resistivity data (fig. 2); both plotted in 10 increments. Colors indicate increments of geophysical trends co-linear with trends of mapped geologic features.

the mapping performed by Smedes lies outside the Boulder River watershed study, a similar structural and geologic setting exists in our study area (O'Neill and others, this volume). The less dominant geophysical gradient trend direction is northeast, which is co-linear with trends of alaskite dikes and chalcedony veins mapped in the Jefferson City quadrangle (Becraft and others, 1963).

The preferred northwesterly trend in the geophysical data is not obvious in the geology or mapped structures for the area (Ruppel, 1963; Becraft and others, 1963) but is reflected in topography. Streams form a northeast-northwest rectilinear drainage pattern in parts of the study area, and some linear magnetic and resistivity lows follow segments of this drainage network. Details pertaining to the structures along the drainages are poorly understood because the structures are partly or entirely concealed by younger volcanic rock or surficial deposits.

One interpretation for the strong northwest-trending linear magnetic lows is destruction of magnetite in shear zones. Zones of major tectonic adjustment may be expressed in magnetic maps as linear magnetic anomaly lows, especially if these zones were affected by recurrent thermal activity. Ruppel (1963) and Becraft and others (1963) interpreted the rectilinear drainage pattern to reflect structurally weak zones that have persisted as controlling structures since the Proterozoic. These zones are characterized by steeply dipping deep-seated faults that were first formed in the Proterozoic and reactivated during the emplacement of the Boulder batholith. The presence and distribution of elongate breccia pipes (Ruppel, 1963) provide supporting evidence of the northeast-trending structural zones.

East-trending resistivity and magnetic anomaly gradients define a third trend set (fig. 11). These geophysical trends parallel shear zones that host the polymetallic mineralized veins. Unlike the northwest- and northeast-trending magnetic gradients, which mostly coincide with the drainages, the east-trending shear zones cross a variety of topography. Many of the mapped mineralized veins coincide with linear magnetic anomaly lows and likely reflect the destruction of magnetite in adjacent wall rock and the nonmagnetic mineralogy of the vein material.

A fourth minor gradient trend set in the magnetic and resistivity data generally is co-linear with structures host to Tertiary dikes (Becraft and others, 1963) (this report, fig. 11).

The spatial association of linear magnetic and resistivity trends in the watershed with known geologic structures strongly implies that geophysical gradients mark locations of faults and fractures. As is evident in the resistivity and magnetic anomaly maps for the watershed (figs. 1 and 2), linear geophysical gradients greatly outnumber structures mapped at the surface (O'Neill and others, this volume, pl. 1). Implications for fractures and faults as related to the important issue of ground-water flow and quality are discussed in McDougal and others (this volume).

Geology-Based Geoenvironmental Map

Impact of a mine or mineralized terrain on the environment is controlled in large part by the geologic landscape. The environmental behavior of geology in a mineralized terrain is effectively portrayed in a study that assessed the potential impact of mining in Montana on surface water quality (Lee and others, 2001). The statewide study used geologic, geochemical, and geophysical information in conjunction with a predictive methodology to model the environmental behavior of geologic units that host metal-sulfide-rich deposits. An important aspect of the study included an effort to predict the environmental behavior of geologic units by classifying rocks in terms of acid-neutralizing or acid-generating potential, which was based on estimated amounts of calcium- or sulfide-bearing minerals expected for the various rock formations. Classifications used a ranking scheme (high, moderate, low) largely determined by knowledge provided by scientists with expertise and experience with Montana geology. The availability of new high-resolution geophysical data, detailed geologic maps, and whole-rock chemistry data in the Boulder River watershed study area allowed us to use an approach similar to the State study but at a more detailed scale.

Water quality is generally good in most of the major streams in the watershed based upon water-quality criteria established for aquatic life, although water quality is degraded downstream of some mine sites such as the Bullion, Crystal, and Comet mines (Nimick and Cleasby, this volume; Kimball and others, this volume). The effects of metal-rich, acidic mine drainage on surface water are thought to be naturally mitigated (Nimick and Cleasby, this volume) by acid-consuming minerals present in fresh granitic and volcanic rocks (Desborough, Briggs, Mazza, and Driscoll, 1998). Clearly, the mineralogy of the rocks in mine-waste piles and in those that underlie mine sites influences the quality of surface water and naturally exacerbates or mitigates the effects of high metal concentrations and acidity. We developed a geology-based geoenvironmental map portraying the rock unit characteristics to examine the spatial relation between environmental characteristics of the geology and water quality.

Acid-Neutralizing Potential

Estimating Acid-Neutralizing Potential

Acid-neutralizing potential (ANP) is an important environmental property of rock units because it can greatly influence water quality in mineralized areas such as the Boulder River watershed. However, ANP is not mapped routinely by field geologists. Therefore, a method was needed to estimate ANP from geologic information traditionally collected in the field. For this study, we combined the geologic map units of Ruppel (1963) and Becraft and others (1963), based in large part on grain size and mineralogy within formations, with rock chemistry data to develop a geoenvironmental map showing ANP.

Ruppel (1963) and Becraft and others (1963) mapped the Butte pluton granitic rocks based on mineralogy, color, and grain size. Mineralogy and color are important for estimating ANP because these qualities have direct bearing on the abundance of mafic minerals related to acid-consuming mineralogical assemblages. Grain size is important not only because different grain-size phases contain different mineral assemblages but also because grain size influences the geophysical signature and allows geophysical data to distinguish rock units, as described in a later section.

In the Boulder River watershed study area, ANP is provided by a suite of acid-consuming minerals. Calcite is present in minor amounts as interstitial fillings in fresh Butte pluton granitic rocks (Desborough, Briggs, and Mazza, 1998). Calcite is an important acid-consuming mineral because of the acid-neutralizing potential of the carbonate ion. Mafic minerals—including biotite, hornblende, tremolite, chlorite, and feldspars—are also important (Desborough, Briggs, Mazza, and Driscoll, 1998) because acid is consumed and bicarbonate ions are produced as these minerals weather. In addition, some mafic minerals, such as biotite, tremolite, and chlorite, contain hydroxide ions. Both bicarbonate and hydroxide ions can neutralize acid and thus mitigate the effects of metals in water through chemical bonding.

Quantitative data on abundance of acid-consuming minerals are not available for the mapped rock units. However, chemical data for rock units are available. Concentration data for key major elements can be used as indicators of the abundance of the acid-consuming minerals. Calcium and (or) iron are important major elements in calcite, plagioclase feldspars, and mafic minerals but not in other minerals, such as quartz or potassium feldspar, which have little acid-neutralizing potential. Therefore, calcium and iron are used as indicator elements to estimate the relative ANP of the rock units mapped by Ruppel (1963) and Becraft and others (1963).

Iron and calcium percentages were obtained from (1) chemical analyses made during the original geologic mapping efforts that provide the geologic framework for this study (Ruppel, 1963; Becraft and others, 1963) and (2) analyses of samples and core analyzed for the Boulder River watershed study (Desborough, Briggs, and Mazza, 1998; Desborough, Briggs, Mazza, and Driscoll, 1998; Desborough and Driscoll, 1998). Figure 12 shows the relation between ANP measured in leachate studies, and the sum of calcium and iron concentrations in samples of plutonic and volcanic rock units. Although traditional ANP data expressed in percent calcite equivalent are not available for these samples, results of a leach experiment that used an acidic (pH=2.9) leachate demonstrate the relation between calcium, iron, and pH.

Whole-rock chemistry data are available for 26 geologic units that cover approximately 70 percent of the geophysical survey area. Sampling is admittedly sparse and restricted to a meager one to four samples per unit. Although too few samples are available to determine statistical significance, in principle, the rocks collected were considered representative of the overall unit. Consequently, we assume that the chemical signature is generally representative for a given unit. A listing of map symbols and descriptions for geologic units referred to in this report, as well as the average sum of calcium and iron concentrations, are given in table 1.

A relative ANP rank was assigned to each map unit on the basis of calcium and iron concentration. These data also are shown in figure 13 (top chart). Geologic units not sampled and therefore not assigned environmental characteristics include unconsolidated Quaternary alluvial and glacial deposits with unknown, or perhaps heterogeneous, acid-neutralizing potential.

Relative degrees of ANP are portrayed in the geoenvironmental map (fig. 14) as shades of green—lighter hues indicate rocks with high acid-neutralizing potential (relatively high percent of mafic and calcic minerals) whereas dark green infers rocks with relatively low ANP (low percentages of mafic and calcic minerals).

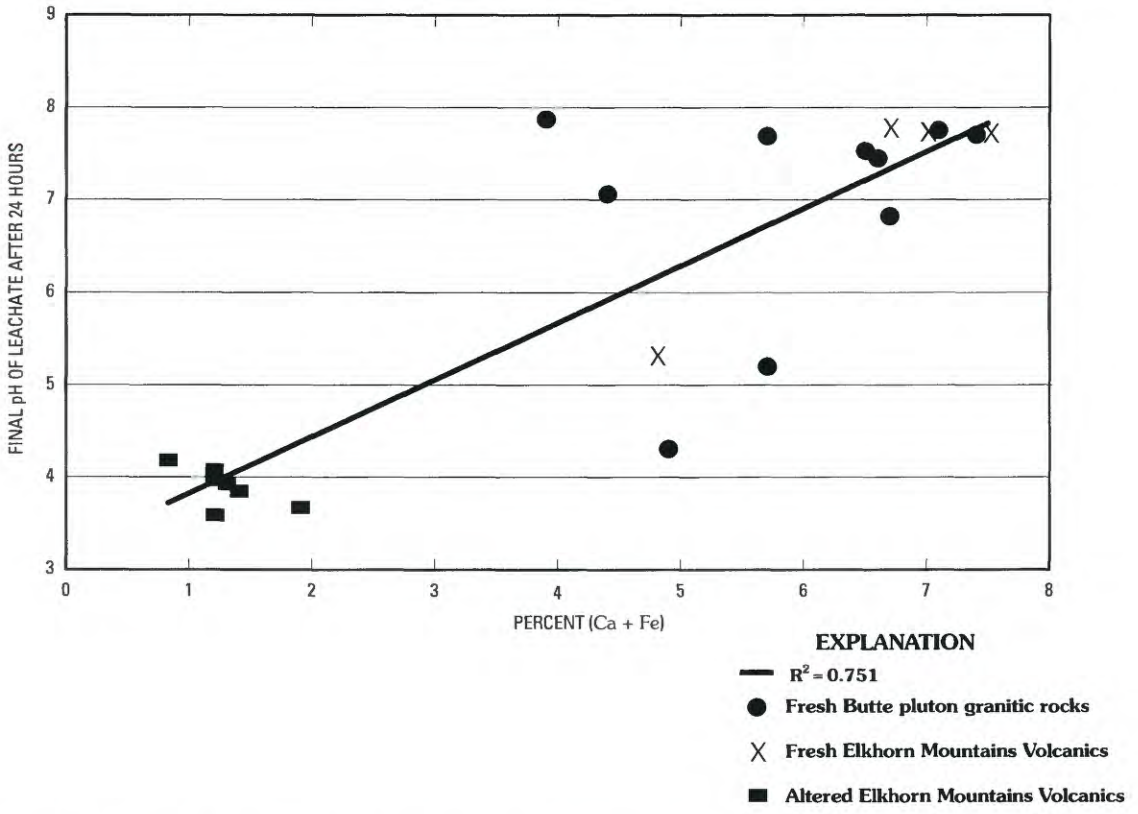

Figure 12. Relation of calcium and iron content to pH of acidic mine-waste leachate after 24 hour exposure for fresh Butte pluton granitic rocks, Elkhorn Mountains Volcanics, and altered Elkhorn Mountains Volcanics (Desborough, Briggs, and Mazza, 1998).

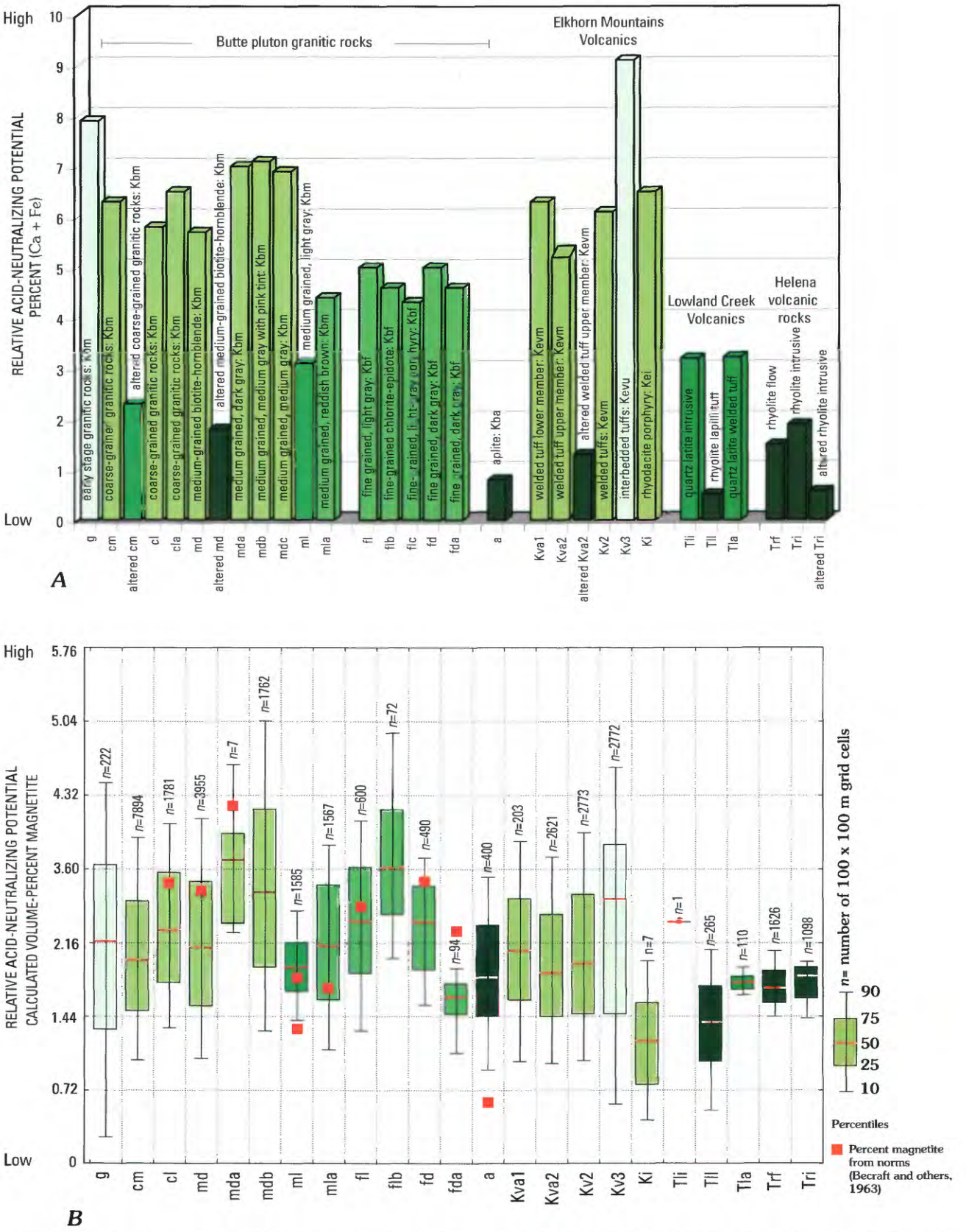

Figure 13. Relative acid-neutralizing potential of geologic units. *A*, based on whole-rock chemistry (table 1); *B*, based on volume-percent magnetite calculated from the magnetic susceptibility model (fig. 5) for the same geologic units. Geologic symbols are from Ruppel (1963) and Becraft and others (1963) and described in table 1. Red squares in *B*, percent magnetite as measured from rock samples (Becraft and others, 1963). Data from *A* were used to make the geoenvironmental map in figure 14.

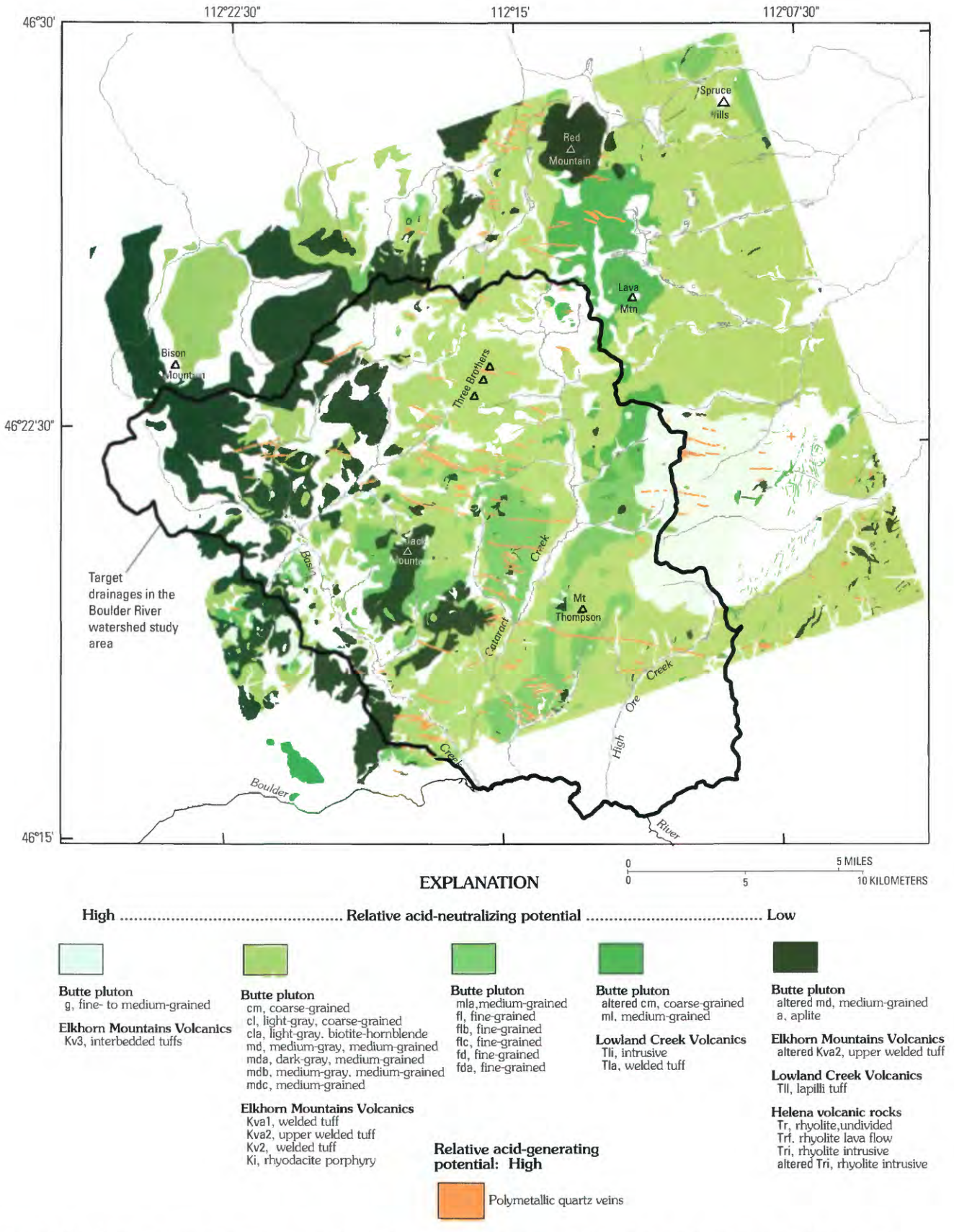

Figure 14. Geology-based geoenvironmental map showing relative acid-neutralizing potential of geologic units based on percentages of calcium and iron (table 1 and fig. 13). Acid-generating polymetallic quartz veins also shown.

Acid-Neutralizing Potential of Rock Units

The Butte pluton plays an important environmental role in the watershed. Geologically, it hosts the acid-generating polymetallic quartz vein deposits. Chemically, it contains minerals that provide significant acid-neutralization and thus has ANP comparable to that of many calcite-rich sedimentary rocks (Desborough, Briggs, and Mazza, 1998; Desborough, Briggs, Mazza, and Driscoll, 1998). This ANP likely is the reason that few streams in the Boulder River watershed study area have acidic pH (Nimick and Cleasby, this volume). Geographically, the Butte pluton is the largest pluton of the Boulder batholith, covering an area 17×51 km, which represents approximately 73 percent of the outcrop of the Boulder batholith in southwest Montana (O'Neill and others, this volume, pl. 1). It crops out in approximately 44 percent of the area covered by the geophysical survey, and 36 percent of the area within the Boulder River watershed; it also underlies younger rocks exposed at the surface.

Relative acid-neutralizing potential for the Butte pluton granitic rocks is variable but roughly correlates with age of emplacement; early-stage mafic intrusions have higher relative ANP compared to later stage silica-rich granitic phases (fig. 13). Rocks of the earliest stage of intrusion, designated as "g" in Ruppel (1963), have the highest relative ANP for all rocks in the Butte pluton and second highest relative ANP for rocks in the study area (fig. 13). The medium- to coarse-grained granitic rocks represent the most voluminous mafic phase of the pluton and are the dominant rock types in the study area, constituting more than 90 percent of the pluton outcrop. Most of the coarse- and medium-grained units contain 6–8 percent calcium and iron and are interpreted to have moderately high to high ANP (table 1). Volumetrically significant exceptions are the ml and mla units (table 1). These medium-grained units are rather widespread, making up approximately 7 percent of the area covered by the airborne survey, although much of the ml unit lies outside the Boulder River watershed in the adjacent Prickly Pear Creek watershed. Whereas most of the coarse- and medium-grained phases contain more than 6 percent iron and calcium, the ml unit is characterized by half as much iron and calcium. Both the ml and mla units are host to a number of mineralized veins. We would expect that acid- and metal-rich waters draining from veins hosted in these rocks would be neutralized, but not as quickly as similar contaminated water draining off veins hosted in the other coarse- and medium-grained phases of the pluton.

The fine-grained plutonic units (fl, flb, flc, fd, and fda) are chemically indistinguishable from each other and are characterized by iron and calcium contents that average 4.5 percent. These facies would be interpreted to have consistently lower relative ANP than most of the medium- or coarse-grained phases.

The most silica rich units in the pluton consist of aplite. The aplites represent a less mafic, more alkali rich phase interpreted to have been formed from a later stage magma (Ruppel, 1963). Aplite is interpreted to have the lowest ANP of all the granitic phases in the pluton. It is also the least voluminous unit in the Butte pluton, at less than 2 percent of mapped outcrops.

Rock samples with the highest average percentage of iron and calcium and therefore interpreted to have highest ANP are those from rocks of the Elkhorn Mountains Volcanics (fig. 13). Samples of interbedded tuffs (Becraft and others, 1963, map unit Kv3) contain an average of 9 percent calcium and iron. The area of outcrop for this unit is quite large, covering approximately 5 percent of the airborne geophysical survey area, although the majority lies outside the Boulder River watershed in the Prickly Pear Creek watershed to the east. Overall, the mineralogy of the Cretaceous volcanic units is similar to that for the Butte pluton because both are part of the same magmatic system (Roberts, 1953; Klepper and others, 1957; Robinson, 1963; Smedes, 1966). However, one unit of Elkhorn Mountains Volcanics has relatively low ANP in comparison with the other volcanics. Samples of the upper welded tuff unit (Kva2) that crops out near Jack Mountain and is presumably unaltered contain less than 2 percent calcium and iron (fig. 13), similar to the Tertiary volcanics and altered plutonic rocks with lowest ANP in the study. Altered samples of the same rock type (altered Kva2) taken near the top of Jack Mountain (Desborough, Briggs, and Mazza, 1998) show even lower percentages of calcium and iron (slightly more than 1 percent).

The acid-neutralizing effect of the Cretaceous and Tertiary volcanic units on metalliferous and acidic water draining the mineral deposits exposed by mining and waste piles is not as critical as that of the Butte plutonic rocks. This is because the Cretaceous and Tertiary volcanic rocks are located stratigraphically and topographically above the acid-generating mineralized veins. Nonetheless, water draining through and downgradient from these rock units would presumably have some mitigating effect on water quality (O'Neill and others, this volume).

Along with providing an in-place understanding of environmental characteristics of the geology, an environmental geology map can provide scientific information for other uses. For example, information provided on the map could be used to evaluate rock suitability for engineering purposes. Some units in the Elkhorn Mountains Volcanics may be suitable sources for material to line a waste-rock repository given other cost and logistic considerations. So, although the Elkhorn Mountains Volcanics do not have as direct an influence on water quality, their geologic characteristics do have implications for other uses.

Rocks with the lowest percentages of calcium and iron and interpreted to have the lowest ANP in the study include Tertiary volcanic units within the Lowland Creek Volcanics and the Helena volcanic field (fig. 13). The volcanic rocks are characterized by high silica content (Ruppel, 1963) that provides little acid neutralization.

A significant reduction in iron and calcium minerals occurs when a rock is altered by hydrothermal fluids

(Desborough, Briggs, and Mazza, 1998; Desborough and Driscoll, 1998), resulting in low ANP. Iron and calcium percentages from altered rock samples are shown in figure 13 for four rock types (cm, md, Kva2, and Tri). In all four cases, the percent of calcium plus iron is significantly lower in the altered sample (30 to 60 percent less) compared to its unaltered counterpart.

Acid-Generating Potential

Acid-generating sources in the watershed are Late Cretaceous polymetallic quartz veins and associated waste piles that contain abundant pyrite and varying amounts of other sulfide minerals (Ruppel, 1963; Becraft and others, 1963; O'Neill and others, this volume). The veins cover less than 1 percent of the surface area in the Boulder River watershed, but oxidation of mine waste caused by near-surface weathering and mining activity has produced metal-rich acidic water. The metal-laden water that enters the main drainages and tributaries (Nimick and Cleasby, this volume) adversely affects aquatic health (Farag and others, this volume, Chapter D10).

Evidence for other acid-generating sources occurs (1) in the Helena volcanic rocks near the Basin Creek mine where disseminated pyrite is associated with mineralization (Ruppel, 1963) and (2) in altered Elkhorn Mountains Volcanics rocks near the Buckeye and Enterprise mines (O'Neill and others, this volume).

Effect of Acid-Neutralizing Minerals on Aquatic Health

The presence and quantities of iron and calcium in mafic and calcic minerals that are commonly found in the plutonic and volcanic rocks in the Boulder River watershed have a bearing on water quality and aquatic health. Iron or calcium is present in biotite ($K(Mg,Fe^{+2})_3(Al,Fe^{+3})Si_3O_{10}(OH)_2$), tremolite ($Ca_2Mg_5Si_8O_{22}(OH)_2$), and chlorite ($(Mg, Fe^{+2},Fe^{+3})_6 AlSi_3O_{10}(OH)_8$). These minerals also contain hydroxide ions (OH^-), which have the ability to raise water pH and mitigate deleterious effects of metals in the water. When hydroxide ions are exposed to acidic water, they are free to combine with hydrogen ions (H^+), raising the pH of the water. Chlorite has abundant hydroxide ions and is ubiquitous in the Butte pluton rocks. Chlorite is derived from primary mafic minerals such as hornblende and formed during regional metamorphism due to heating during late magmatic activity in the Boulder batholith.

Additionally, calcium is connected to the environmental signature of a rock through the role of bicarbonate ions (HCO_3^-) in the neutralizing process. Bicarbonate forms complexes with several potentially toxic metal ions (Cd, Cu, Zn), thereby reducing the toxicity of these metals in surface water to aquatic life. One source for bicarbonate is in minor amounts of interstitial calcite in fresh Butte pluton granitic rocks (Desborough, Briggs, and Mazza, 1998).

Calcium, Iron, and Geophysical Response

For volcanic and plutonic rocks in the Boulder River watershed study area, variations in calcium and iron content correlate with quantities of other minerals that strongly influence geophysical response, specifically silica and magnetite. Although electromagnetic and magnetic surveys are not sensitive to calcium content as such, elevated amounts of calcium correspond to a decrease in silica (fig. 5 in O'Neill and others, this volume). Silica acts as an electrical insulator; electrical current does not pass easily through it. Consequently, rocks with high amounts of silica will typically produce resistivity anomaly highs. Silica-rich rocks in the watershed study area also produce lower amplitude magnetic anomalies in comparison with more mafic rock phases, primarily owing to lower magnetite content.

As discussed in the previous section, iron in volcanic and plutonic rocks is derived from a number of minerals that provide acid neutralization. Iron is a main constituent in magnetite (Fe_3O_4), which does not provide acid neutralization but is present in association with the minerals that do. In the following section, we discuss the importance of magnetite in terms of geophysical signature and relate magnetite to acid-neutralizing potential.

Geophysical Magnetite Maps

> "Cored rocks that had the highest acid-neutralizing potential (for example, near Bullion mine) had abundant magnetite in heavy-mineral concentrates made from these rocks, whereas those with low acid-neutralizing potential contained no magnetite in the heavy-mineral concentrates" (O'Neill and others, this volume).

This section investigates the hypothesis presented by our colleagues—that magnetite content may be indicative of granitic rock alteration and thereby relate to a rock's ability to provide acid neutralization. By transforming the resistivity and magnetic anomaly data to maps of magnetite distribution, we can make the geophysical magnetite maps function as proxy ANP maps. In the previous section, information from rock chemistry provided a mineralogical rationale to define acid-neutralizing potential. However, with so few rock samples and the presence of glacial, alluvial, and tree cover, variations in environmental properties of underlying bedrock were impossible to discern in the field for much of the study area. The detail provided in the geophysical survey and the ability of geophysical methods to "see" beneath much of the problematic vegetation and rock cover provide a means to continuously map major to minor variations in rock environmental properties. Information extracted from the geophysical survey can be used as an indirect measuring tool of mineralogical properties in that magnetite is used as an indicator for other important acid-consuming minerals.

Magnetite Estimates from Magnetic Susceptibility Model

Magnetic susceptibility is, to a large degree, a measure of magnetite content. For rocks whose concentrations of magnetite lie between 0.1 and 10 percent, volume percentage of magnetite (*Vm*) can be estimated from susceptibility (*k* in cgs) with the following equation:

$Vm = 400\ k$ (modified from Balsley and Buddington, 1958)

Estimates for volume percent magnetite were determined from the grid of magnetic susceptibility data using this equation. Model magnetic susceptibilities were given in relation to percent magnetite in the map shown in figure 5 and for geologic units in figure 9. Negative magnetic susceptibilities were set to zero.

Magnetite content derived from the magnetic susceptibility model was compared to magnetite content determined visually from thin sections for a limited number of rock samples. The lower chart in figure 13 shows rock sample percent magnetite for 12 rock samples (Becraft and others, 1963) compared to model susceptibilities. Analyses were available for nine Butte pluton units. Magnetite contents measured for the 12 rock samples fall either within or very near the range for a given unit (fig. 13*B*), signifying that the susceptibility model is, at the very least, a reasonable representation of magnetite distribution in the watershed.

Magnetite Estimates from 900-Hz Apparent Resistivity Data

Magnetite, because of its electrical properties, is the only mineral that causes observed negative in-phase anomalies in horizontal coplanar resistivity data. As part of the airborne survey contract with the USGS, estimates of apparent volume percent magnetite are available (Smith and others, 2000). Magnetite estimates were determined by identification of negative in-phase anomalies in the 900-Hz resistivity data and by application of a calculation based on methodology in Fraser (1981). The estimates are *apparent* because they are based on a theoretical model and provide only a relative gauge of magnetite content. Estimates for magnetite are restricted to rocks located to a maximum depth of 60 m.

The method has limitations under certain geologic conditions. The greatest constraint for use of this method in our study area relates to the low resistivities of many of the volcanic rocks. Unreliable magnetite estimates result for rocks with resistivities of less than 500 ohm-m (Fraser, 1981). For this reason, only pixels within the EM magnetite grid that coincide with resistivities greater than 500 ohm-m are shown in figure 15, with the consequence that 46 percent of the area within the airborne geophysical survey was excluded. Most of the excluded area is over rocks within the Helena and Elkhorn Mountains volcanic fields. The low resistivities of the volcanic units are attributed to the greater development of clays from surface weathering and alteration processes.

Magnetite estimates in the EM magnetite model are unrealistically low in comparison with magnetite concentrations determined from rock sample modal analyses (Becraft and others, 1963; Desborough, Briggs, and Mazza, 1998) but are interpreted to reflect *relative* amounts of magnetite within rocks located within 60 m of the surface. Attenuated (low) EM magnetite values can occur in rocks that are very magnetic, where error from strong magnetic polarization exists, and over rocks where the electromagnetic sensor height exceeds 45 m (Fraser, 1981).

Within the Boulder River watershed study area, the granitic units of the Butte pluton are characterized by high EM magnetite values and are in general agreement with high percent magnetite values calculated from the magnetic anomaly data (fig. 9). Outside the watershed boundary, in the adjacent Prickly Pear Creek watershed to the east and Tenmile Creek watershed to the north, most of the Butte pluton outcrop is associated with very low to zero-percent apparent magnetite anomalies. Much of the low percent magnetite occurs over the ml unit, west of Lava Mountain, which also has a correspondingly low magnetic signature (fig. 9) and low percent magnetite as determined from rock sample analysis (fig. 13*B*).

Relationship of Magnetite to Alteration Processes

Mineralization, metamorphism, and magmatic processes have altered the original mineralogical composition of plutonic and volcanic rocks in the study area. Locations of altered Butte plutonic rocks related to Late Cretaceous mineralization were mapped in the eastern part of the study area but are limited to narrow envelopes surrounding a select number of mineralized veins studied in detail in the Jefferson City quadrangle (Becraft and others, 1963). As part of the detailed study of polymetallic quartz veins and wall rock alteration, Becraft and others (1963) collected samples of Butte pluton granitic rocks adjacent to well-exposed mineralized veins, sampling from the veins outward to rock least affected by alteration processes. Results of our study provide an understanding of the relationship between alteration mineral assemblages and magnetite abundance. Within the alteration envelope, three zones are observed and include, from most altered to least altered, a sericitic zone, an argillic zone, and a chloritic zone. "Least altered" describes granitic rocks that appear unaffected by surface weathering or sulfide mineralization. Mineralogical analyses show that within zones of argillic alteration, magnetite is absent. This concept is illustrated in figure 16.

Evidence for alteration of the original mineralogy due to metamorphism is present in units of the Elkhorn Mountains Volcanics where chemical analyses show metamorphosed samples are more silicic (less mafic) than unmetamorphosed samples (Ruppel, 1963). Metamorphism was caused by the intrusion of the Butte pluton into the Elkhorn Mountains Volcanics. The metamorphosed samples also show a

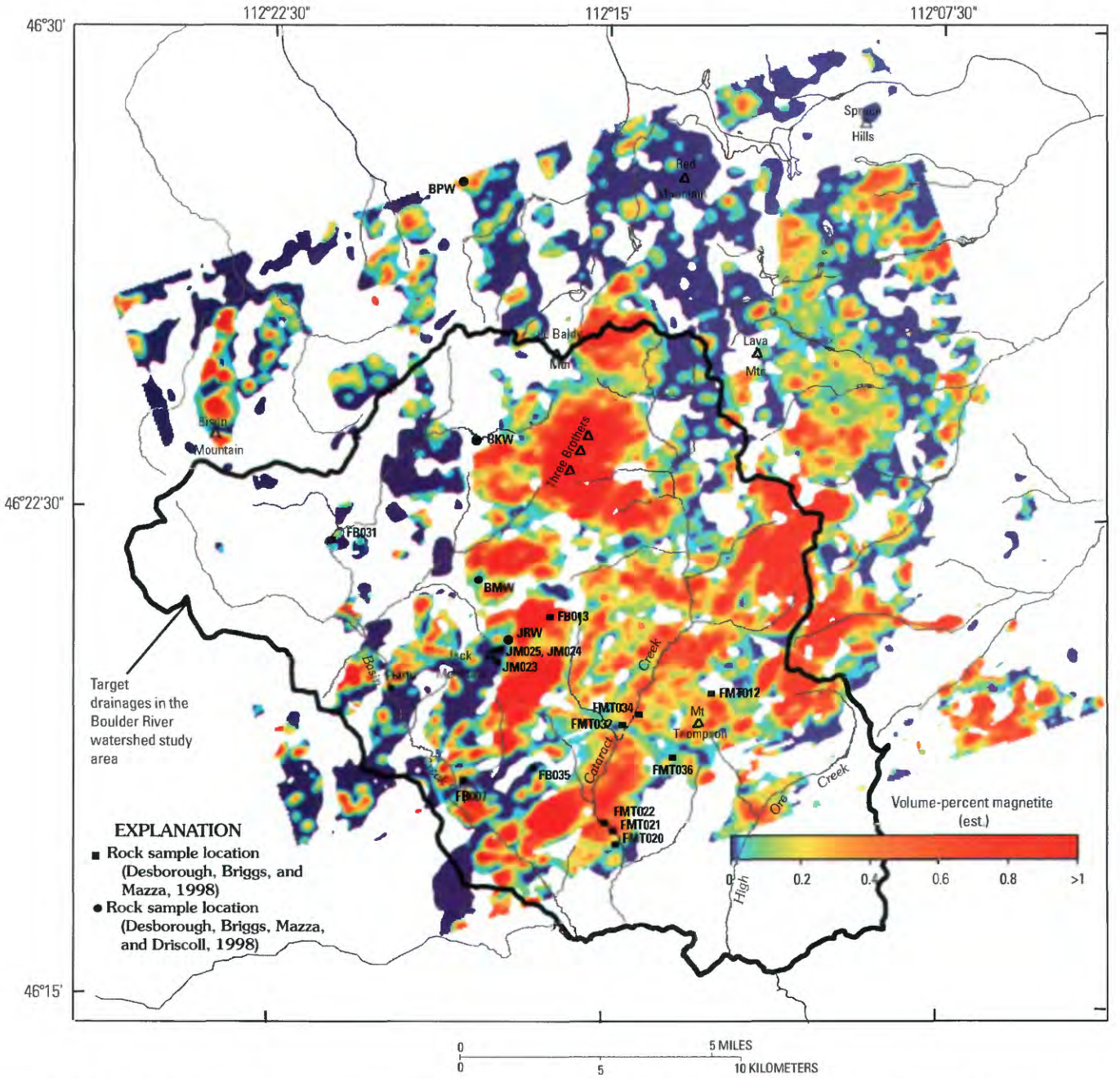

Figure 15. EM magnetite anomaly calculated from 900-Hz resistivity data where resistivity is greater than 500 ohm-m. White areas within airborne geophysical survey are characterized by low resistivities and result in unreliable EM magnetite estimates. Values for percent magnetite are given at locations of rocks analyzed for acid-neutralizing potential (table 2). Low EM magnetite estimates are combined with areas of high resistivity to map locations of silica-rich rock units with inferred low acid-neutralizing potential.

significant (30–80 percent) decrease in iron oxides, which likely reflects a decrease in magnetite content as well.

Alteration in which hydrothermal fluids were dominantly silicic rather than potassic or alkalic is present in altered rocks within the Elkhorn Mountains Volcanics. Chemical analyses of altered rocks from the top of Jack Mountain show no magnetite present in heavy-mineral concentrates (Desborough, Briggs, and Mazza, 1998).

O'Neill and others (this volume) discuss two other alteration events that altered the mineralogy of some of the Butte plutonic rocks. Several areas mapped in the southern part of the study area contain zones of alteration, but no samples were collected to determine magnetite content.

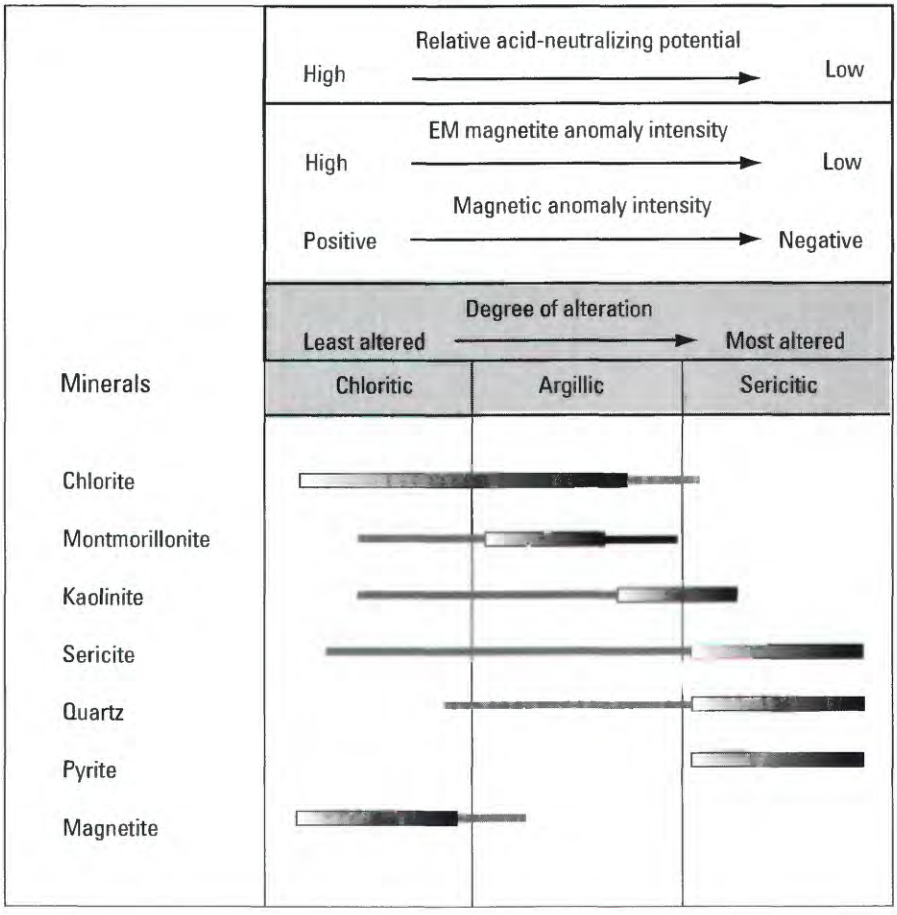

Figure 16. Persistence of minerals in alteration zones from a suite of Butte pluton rocks measured from polymetallic quartz veins (most altered) outward to granitic rocks least affected by alteration. Modified from Becraft and others (1963) to show persistence of magnetite, corresponding geophysical signatures, and relative acid-neutralizing potential. Gradient regions indicate range of relatively high mineral abundance; solid lines indicate minor amounts of minerals.

Relationship of Magnetite to Environmental Rock Properties

Magnetite provides a means to connect geophysical signatures with important environmental rock properties. Geochemical investigations conducted as part of the Boulder River watershed study illustrate the connection between the presence of magnetite and corresponding acid-neutralizing potential for Butte pluton granitic rocks and other rock types. Rock samples of fresh and altered rock collected from drill core as well as surface outcrop samples were chemically analyzed to determine mineralogical characteristics associated with acid-neutralizing potential (Desborough and Driscoll, 1998; Desborough, Briggs, and Mazza, 1998; Desborough, Briggs, Mazza, and Driscoll, 1998). Table 2 compares the results of the leachate studies to determine ANP with values for percent magnetite as calculated from the geophysical data. Localities of the leachate samples are shown on the magnetic susceptibility model (fig. 5) and the EM magnetite map (fig. 15).

Although too few samples were analyzed to provide confident statistical conclusions, we can make some relevant and consistent observations regarding presence of magnetite, acid-neutralizing potential, and geophysical signature. For the 12 samples of unaltered Butte pluton granitic rock that lie within the airborne survey area, relatively high values from the EM magnetite anomaly data (0.24–0.86 percent, with an average of 0.44 percent) correspond with high acid-neutralizing potential as calculated from whole-rock chemistry. Percent magnetite derived from the magnetic susceptibility data for fresh Butte pluton rocks ranges from 1.12 to 1.83 percent, with an average value of 1.55 percent. All samples of these fresh rocks contain magnetite in the heavy-mineral concentrates. Unfortunately, no samples of *altered* Butte pluton granitic rocks were analyzed for acid-neutralizing potential.

Percent magnetite calculated from the apparent resistivity data for unaltered Elkhorn Mountains Volcanics shows that these rocks have slightly higher EM magnetite anomaly values (average 0.09 percent) than their altered counterparts (average 0.03 percent). Magnetite estimates for sample localities

Table 2. Relative acid-neutralizing potential from analyses of surface and core rock samples collected in and around the Boulder River watershed study area.

[Volume-percent magnetite values calculated from the EM magnetite data (fig. 15) and magnetic susceptibility model (fig. 5) are given at each sample location to illustrate the relation between the presence of magnetite, geophysical data, and relative acid-neutralizing potential. Leaders (---), unreliable EM magnetite estimates owing to high rock conductivity. Geologic map symbols in parentheses are described in table 1]

Outcrop or drill core sample and acid-neutralizing analysis information						Volume-percent magnetite estimated from geophysical data	
Sample	Depth (ft)	Geologic unit	Degree of alteration	Heavy minerals	Relative ANP	900-Hz apparent resistivity	High-pass magnetic anomaly
FB007B1 FB007B2 FB007B3	Surface	Butte pluton (md)	Unaltered	[1]Magnetite, zircon, pyrite (< 1 ppm)	High	0.24	1.47
FB013	Surface	Butte pluton (cl)	Unaltered	[1]Magnetite, zircon, pyrite (< 1 ppm)	High	0.86	1.79
FB010	Surface	Butte pluton (cl)	Unaltered	[1]Magnetite, hornblende, zircon, pyrite (< 1 ppm)	High	0.29	1.49
FMT012	Surface	Elkhorn Mountains Volcanics (Kv2)	Unaltered	[1]Magnetite, pyrite (< 1 ppm)	High	---	1.78
FMT020	Surface	Butte pluton (mla)	Unaltered	[3]Magnetite	High	0.27	1.60
FMT021	Surface	Butte pluton (cl)	Unaltered	[4]Magnetite, chlorite, apatite, zircon, biotite, tremolite, pyrite (< 1 ppm)	High	0.61	1.46
FMT022	Surface	Butte pluton (cl)	Unaltered	[3]Magnetite	High	0.45	1.61
FMT031	Surface	Elkhorn Mountains Volcanics (Kva1)	Unaltered	[4]Magnetite, chlorite, apatite, zircon, biotite, tremolite, pyrite (< 1 ppm)	High	0.10	1.53
FMT032	Surface	Butte pluton (mla)	Unaltered	[3]Magnetite	High	0.27	1.50
FMT034	Surface	Butte pluton (cm)	Unaltered	[4]Magnetite, chlorite, apatite, zircon, biotite, tremolite	High	0.58	1.12
FB035	Surface	Elkhorn Mountains Volcanics (Kva1)	Unaltered	[4]Magnetite, chlorite, apatite, zircon, biotite, tremolite, pyrite (< 1 ppm)	High	0	1.56
FMT036	Surface	Elkhorn Mountains Volcanics (Kva2)	Unaltered	[4]Magnetite, chlorite, apatite, zircon, biotite, tremolite, pyrite (< 1 ppm)	High	0.18	1.76
JM023	Surface	Elkhorn Mountains Volcanics (Kva2)	Altered	[4]Pyrite	Low	0.06	1.40
JM024	Surface	Elkhorn Mountains Volcanics (Kva2)	Altered	[4]Pyrite	Low	0.05	1.39
JM025	Surface	Elkhorn Mountains Volcanics (Kva2)	Altered	[4]Pyrite	Low	0	1.51
BMW	1–40	Butte pluton (cl)	Unaltered	[2]Magnetite, zircon	High	0.37	1.63
JRW	24–66	Elkhorn Mountains Volcanics (Kva2)	Altered	[2]Zircon	Low	0.09	1.40
BKW	25–62	Elkhorn Mountains Volcanics (Kva2)	Altered	[2]None, pyrite abundant	Low	---	1.16
BPW	15–39	Butte pluton (md)	Unaltered	[2]Magnetite, zircon, pyrite	High	0.37	1.83

[1]Heavy-mineral concentrates from Desborough and Fey, 1997.

[2]Heavy-mineral concentrates from Desborough and Driscoll, 1998.

[3]Heavy-mineral concentrates from Desborough, Briggs, and Mazza, 1998.

[4]Heavy-mineral concentrates from Desborough, Briggs, Mazza, and Driscoll, 1998.

FMT012 and BKW are not available from the EM magnetite data owing to low resistivities at these locations. Magnetite estimates from the magnetic susceptibility data (fig. 5) for four samples of unaltered Elkhorn Mountains Volcanics average 1.65 percent. Alternatively, consistently lower values for (magnetic data) magnetite occur for the five samples of altered Elkhorn Mountains Volcanics (average 1.37 percent). Samples of altered Elkhorn Mountains Volcanics contain no magnetite as determined from the heavy-mineral concentrates (Desborough, Briggs, Mazza, and Driscoll, 1998; Desborough and Driscoll, 1998).

Associations between alteration mineral assemblages, magnetite, geophysical anomaly signature, and acid-neutralizing potential for alteration zones mapped in Butte pluton granitic rocks are summarized in figure 16. Magnetic susceptibility and EM magnetite anomaly intensity progressively decrease as granitic rocks are altered to argillic levels. Rocks having undergone alteration to sericitic levels are characterized by low magnetic susceptibility and EM magnetite anomalies near zero. Compositional changes in the granitic rocks caused by progressively higher degrees of alteration coincide with the absence of magnetite and chlorite. Chemically, the lack of chlorite also corresponds to a decrease in the acid-neutralizing potential of the rock (Desborough, Briggs, and Mazza, 1998; Desborough, Briggs, Mazza, and Driscoll, 1998).

Geophysical Refinement of Geoenvironmental Map

Geophysics-Based Geoenvironmental Map

A geophysics-based geoenvironmental map (fig. 17) infers locations of surface and shallow subsurface bedrock with low magnetite content. Geophysical magnetite lows were determined on geologic and statistical criteria. Solid red in figure 17 defines pixels with values of 0 percent from the EM magnetite grid (fig. 15) combined with resistivities greater than 500 ohm-m from the 900-Hz resistivity grid (not shown). Geologically, these areas coincide with mapped outcrops enriched with silica and low in magnetite from either primary mineralogy or from introduction of silica-rich hydrothermal fluids (Ruppel, 1963; Becraft and others, 1963). Examples include (1) altered rocks with known low acid-neutralizing potential such as the altered Elkhorn Mountains Volcanics at Jack Mountain (Desborough, Briggs, and Mazza, 1998) or (2) rocks interpreted to have low acid-neutralizing potential such as the silica-rich Tertiary rhyolite at Red Mountain. Other solid red areas in figure 17 are interpreted to share analogous electrical properties and map similar rock types.

Pixels with values less than 1.4 percent in the magnetic susceptibility magnetite grid (fig. 5) are shown in the red pattern in figure 17. Lowermost magnetite content (less than 1.4 percent) was defined statistically for most rock types (fig. 9). Geologically, results best characterized mapped outcrop of altered rocks (Becraft and others, 1963; O'Neill and others, this volume). Other areas corresponding to magnetic susceptibility magnetite lows include parts of the study area expected to contain altered rocks such as clusters of polymetallic quartz veins and contact zones between the Butte plutonic rocks and younger volcanic units. Many of the main streams and tributaries are coincident with linear geophysical magnetite lows, which may be sites that provide little or no neutralization to acidic water draining from the mined areas and thus may not aid mitigation of toxic metal loads to aquatic life. Coincidence of geophysical magnetite lows with polymetallic veins suggests that some of the low-percent magnetite domains are mapping locations of *acid-generating* rocks that are depleted in magnetite from intense sulfidization.

Geology- and Geophysics-Based Geoenvironmental Map

Combining the geophysics- and geology-based geoenvironmental maps provides maximum detail in bedrock acid-neutralizing potential. The combined geoenvironmental map (fig. 18) is a portrayal of the underlying geologic "landscape" that influences surface- and ground-water quality, the natural mitigation of metals and acidity, and, ultimately, the health of the ecosystem. Optimal geologic conditions are present where rocks with high acid-neutralizing potential (lightest green shades in figs. 14 and 18) do not overlap with geophysical magnetite lows or polymetallic quartz veins. Least desirable conditions may exist where polymetallic quartz veins lie within, uphill, or up gradient from rocks with low acid-neutralizing potential. These conditions identify places in the watershed that may be environmentally problematic to the mitigation of acidic metal-rich water.

Results of our study show that approximately 30 percent of the geophysical survey areas include rocks sufficiently depleted in magnetite to have low acid-neutralizing potential. Approximately 20 percent of the Butte pluton rocks within the Boulder River watershed study area are defined with low acid-neutralizing potential. From an environmental context, these areas characterize rocks that should not provide significant mitigation to acidic water draining downhill or down gradient from mined or undisturbed mineralized rocks. We also expect that, in areas containing altered Butte pluton, the potential for mitigation of metals toxic to aquatic life is reduced due to lack of calcic and mafic minerals to provide bicarbonate and hydroxide ions.

Large, contiguous areas of geophysical magnetite lows occur over volcanic rocks in the Eocene Lowland Creek and Eocene-Oligocene Helena volcanic fields. The largest area covered by geophysical magnetic lows is located in the southeastern part of the study area over silicic rocks within the Lowland Creek volcanic field (figs. 7 and 17). The geophysical data were especially useful in these rocks as no

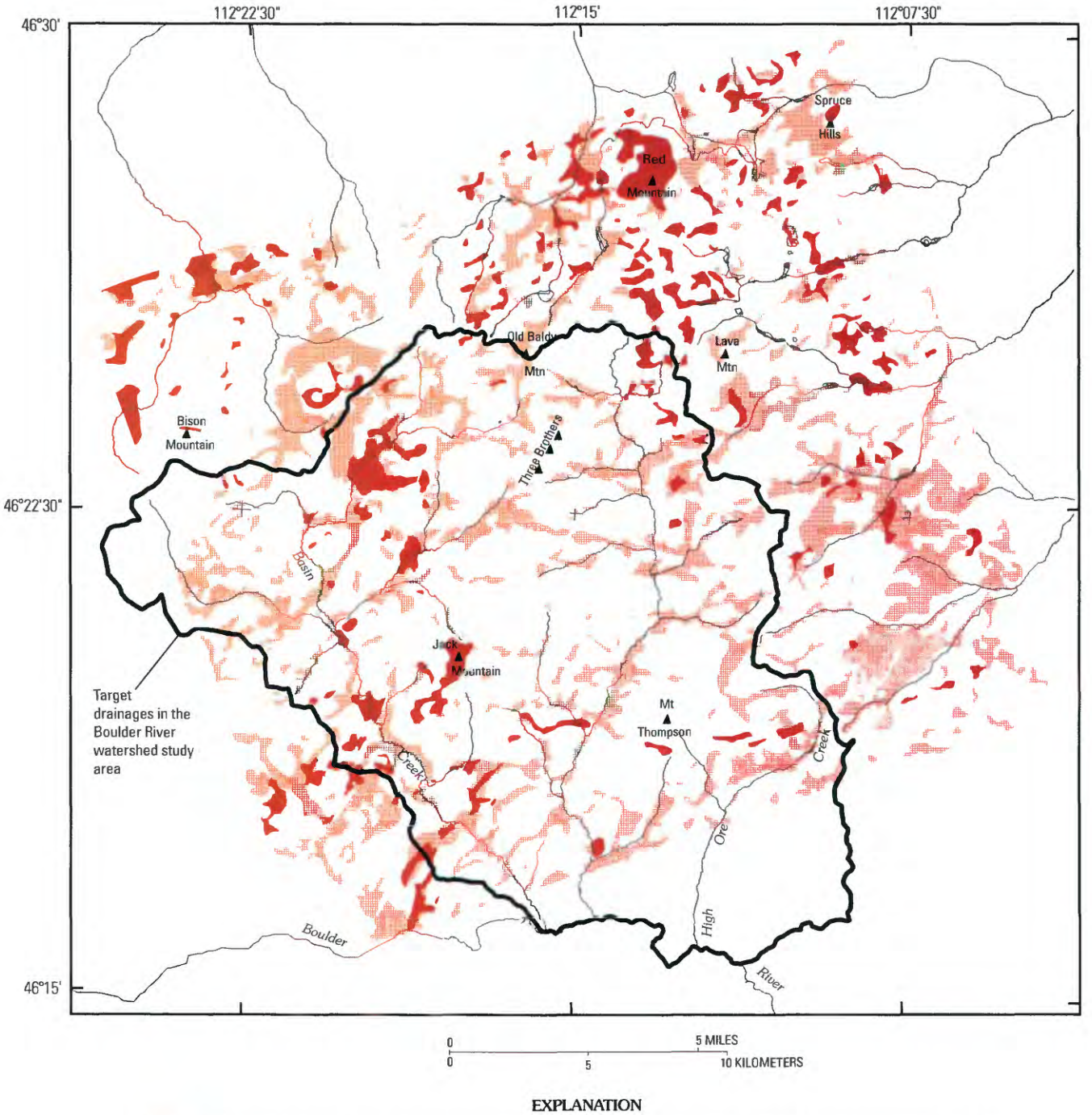

Figure 17. Geophysics-based geoenvironmental map showing locations of inferred low acid-neutralizing potential based on low values of volume-percent magnetite calculated from airborne geophysical data.

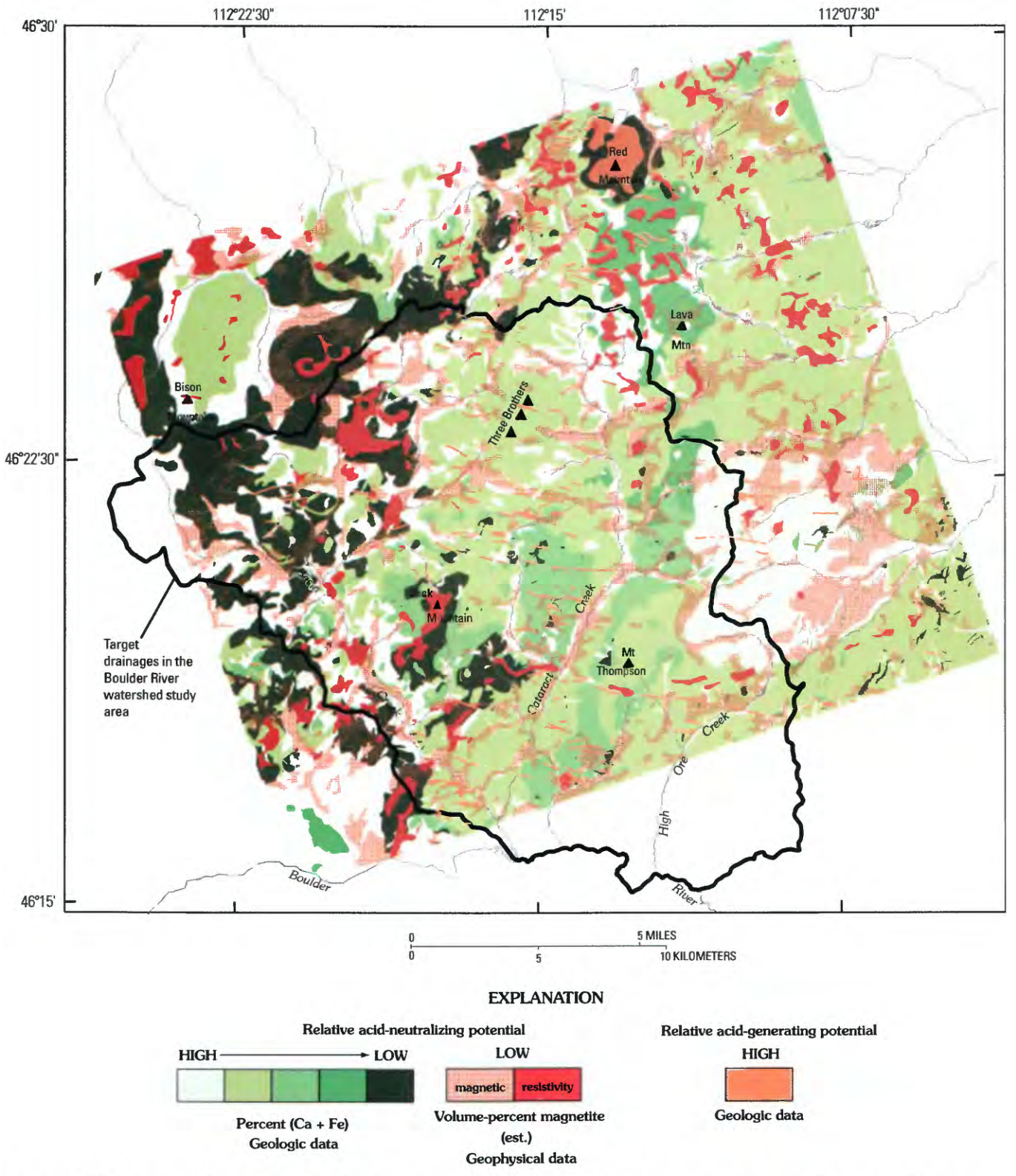

Figure 18. Combined geology- and geophysics-based geoenvironmental map showing relative acid-neutralizing and acid-generating potential of rocks inferred from rock mineralogy (fig. 14) and volume-percent magnetite calculated from airborne magnetic and apparent resistivity data (fig. 17). White areas, no data available.

mineralogical data were available to determine amounts of acid-consuming minerals. Other large areas, in association with geophysical magnetite lows, occur within Tertiary volcanic rocks in the northern part of the study area. Evidence that these rocks are also low in acid-neutralizing potential is present in low calcium and iron (fig. 13) and high silica content.

Implications for Siting of Waste-Rock Repositories

Maps that portray pertinent environmental geologic characteristics, such as the map derived from this study (fig. 18), could be an information layer used in decision-making processes for locating geologically favorable waste-rock repositories. Cleanup of inactive mines is an important goal of State and Federal land-management agencies. The primary environmental impact of inactive mines is degraded surface-water quality in streams (Nimick and Cleasby, this volume) and resultant impairment of aquatic habitat caused by metals (Farag and others, this volume). Mine waste and mill tailings are the main contributor of metals to surface drainages in the study area (Church, Unruh, and others, this volume; Nimick and Cleasby, this volume). Therefore, an important component of any restoration plan will be finding one or more suitable repository sites where mill tailings and mine wastes could be consolidated and safely stored.

In the early stages of the project (1996–1999), providing information to land managers regarding geologically suitable repository sites for mine waste and mill tailings was a priority. The USDA Forest Service together with geophysicists, geologists, and geochemists from the U.S. Geological Survey evaluated particular sites chosen by both groups to determine their suitability for storing the mine wastes in the watershed. However, during the course of the study, the unexpected bankruptcy of Pegasus Mining and the existing presence of the Luttrell pit at their mining operation (Smith and others, this volume, Chapter E3) made the process of repository siting moot. The USDA Forest Service and U.S. Environmental Protection Agency have a joint agreement to move mine waste from the Boulder River watershed and adjacent Tenmile Creek watershed into the Luttrell pit, located along the Continental Divide between the two watersheds.

Although not a current issue in the Boulder River watershed, repository siting within the larger context of the Departments of the Interior and Agriculture efforts to coordinate restoration activities at other Federal lands affected by inactive mines is a current issue being faced in many watersheds in the western United States. Exercises to characterize the environmental properties of geologic units, such as the techniques presented here, provide a scientific strategy for repository siting in other areas where safe mine-waste storage is an issue. For example, placing a repository in rock that is located at or near a ground-water recharge area in bedrocks with little or no ANP could potentially result in disruption or destabilization of underground portions of a repository and contamination of surface and shallow ground water. If a land-use manager is restricted to a particular tract of ground in which to bury metal-sulfide waste rock, the environmental geology map can be one layer, among others, that provides geologic guidance as to which "host" rocks provide the better environmental controls.

Summary

This report presents an empirical approach to extend the knowledge of geologic characteristics that exert fundamental controls on the natural environment with depth. In particular, high-resolution airborne geophysical data are used to map the surface and shallow subsurface distribution of acid-neutralizing minerals in igneous bedrock.

Enhancement techniques applied to the aeromagnetic anomaly data result in maps that emphasize magnetic rock properties in the uppermost surface to shallow subsurface. The statistical summaries describing the magnetic susceptibility and apparent resistivity signature for approximately 40 geologic units allow for comparison of geophysical variability within and across geologic units and provide a basis for discussion of important factors controlling the anomaly signature. Geophysical analyses show that the polymetallic quartz veins are distinctively characterized by very low magnetic susceptibilities and moderately high resistivities. Trends of geophysical gradients are co-linear with mapped structures and faults.

The geology-based geoenvironmental map, derived from mineralogical and geochemical data, shows variability in relative acid-neutralizing potential as a function of mafic and calcic mineral abundance. Representative rock samples used to produce the geology-based geoenvironmental map are limited in number but considered sufficient to provide an understanding of acid-neutralizing potential. Granitic and most volcanic rocks that are fresh or unaltered have abundant mafic and calcic minerals with significant acid-neutralizing potential. In contrast, rocks that are silica rich and (or) have been intensely altered by hydrothermal solutions have negligible amounts of mafic minerals, insignificant amounts of calcite, and little acid-neutralizing capacity. Known sources for acidic metal-rich water in the Boulder River watershed are the Late Cretaceous polymetallic quartz veins and associated mine waste. Potential acid-generating source rock may include areas of Tertiary volcanic rocks containing disseminated pyrite.

This study demonstrates that magnetite acts as a relative gauge for corresponding amounts of mafic and calcic minerals in igneous rocks that provide significant acid neutralization to acidic and metal-rich waters. In fresh (unaltered) Tertiary and Cretaceous granitic and volcanic rocks, magnetite is a common accessory mineral (Ruppel, 1963; Becraft and others, 1963) and is associated with mineral assemblages that provide relative degrees of acid neutralization (Desborough, Briggs, and Mazza, 1998; Desborough, Briggs, Mazza, and Driscoll,

1998). Where the igneous rocks are altered, the rock is devoid of magnetite and there is a corresponding depletion in acid-neutralizing potential.

Magnetite is ubiquitous in nearly all the Cretaceous- and Tertiary-age volcanic and plutonic rocks exposed in the Boulder River watershed. Although magnetite is a minor mineral constituent, it provides an easily measured property that can be correlated to measurable percentages of important acid-neutralizing minerals.

Mathematical filters convert magnetic anomaly and apparent resistivity data to pseudo-mineral maps to show surface and shallow subsurface distribution of magnetite. Magnetite is the main source for magnetic anomalies and contributes to the resistivity response of a rock. Magnetite estimates from the magnetic susceptibility model data are within realistic ranges when compared to values determined from rock samples. Estimates from the apparent resistivity data, however, are consistently lower in comparison with magnetite measurements from rock samples but are used in this report to reflect *relative* amounts of magnetite within rocks.

The geophysical magnetite models outline areas interpreted to indicate near-surface rocks lacking or depleted in magnetite. The magnetite depletion can be the result of high-temperature alteration of primary minerals or a silica-rich mineral composition. Absence of magnetite corresponds to low amounts of acid-consuming minerals. In some cases, low values in the geophysical magnetite data correspond with locations of acid-generating source rock such as sulfide-metal-rich veins. Alternately, areas with high values of magnetite from the geophysical models are interpreted to represent rocks associated with significant amounts of acid-consuming minerals.

The geophysical refinement to the geology-based geoenvironmental map results in an improved understanding of the spatial distribution of bedrock environmental characteristics. This report provides a summary of the geophysical signatures and geoenvironmental characteristics of volcanic and plutonic units, many of which extend well beyond the Boulder River watershed study area and crop out commonly throughout southwest Montana. Consequently, the methodology described here can be applied to watersheds that are geologically similar to the study area and which have water-quality degradation caused by historical mining like that in the Boulder River watershed.

References Cited

Balsley, J.R., and Buddington, A.F., 1958, Iron-titanium oxide minerals, rocks, and aeromagnetic anomalies of the Adirondack area, New York: Economic Geology, v. 53, no. 7, p. 777–805.

Becraft, G.E., Pinckney, D.M., and Rosenblum, Sam, 1963, Geology and mineral deposits of the Jefferson City quadrangle, Jefferson, and Lewis and Clark Counties, Montana: U.S. Geological Survey Professional Paper 428, 101 p.

Blakely, R.J., 1995, Potential theory in gravity and magnetic applications: London, Cambridge University Press.

Buxton, H.T., Nimick, D.A., von Guerard, Paul, Church, S.E., Frazier, Ann, Gray, J.R., Lipin, B.R., Marsh, S.P., Woodward, Daniel, Kimball, Briant, Finger, Susan, Ischinger, Lee, Fordham, J.C., Power, M.S., Bunck, Christine, and Jones, J.W., 1997, A science-based, watershed strategy to support effective remediation of abandoned mine lands: Proceedings of the Fourth International Conference on Acid Rock Drainage, Vancouver, B.C., May 31–June 6, 1997, p. 1869–1880.

Desborough, G.A., Briggs, P.H., and Mazza, Nilah, 1998, Chemical and mineralogical characteristics and acid-neutralizing potential of fresh and altered rocks and soils of the Boulder River headwaters in Basin and cataract Creeks of northern Jefferson County, Montana: U.S. Geological Survey Open-File Report 98–40, 21 p.

Desborough, G.A., Briggs, P.H., Mazza, Nilah, and Driscoll, Rhonda, 1998, Acid-neutralizing potential of minerals in intrusive rocks of the Boulder batholith in northern Jefferson County, Montana: U.S. Geological Survey Open-File Report 98–0364, 21 p.

Desborough, G.A., and Driscoll, Rhonda, 1998, Mineralogical characteristics and acid-neutralizing potential of drill core samples from eight sites considered for metal mine related waste repositories in northern Jefferson, Powell, and Lewis and Clark counties, Montana: U.S. Geological Survey Open-File Report 98–790, 6 p.

Dobrin, M.B., and Savit, C.H., 1988, Introduction to geophysical prospecting, Fourth Edition: New York, McGraw Hill, 867 p.

du Bray, E.A., 1995, Preliminary compilation of descriptive geoenvironmental mineral deposit models: U.S. Geological Survey Open-File Report 95–0831, 272 p.

Fraser, D.C., 1981, Magnetite mapping with a multicoil airborne electromagnetic system: Geophysics, v. 46, no. 11, p. 1579–1593.

Grauch, V.J.S., 1988, Statistical evaluation of linear trends in a compilation of aeromagnetic data from the southwestern U.S.: Geological Society of America Abstracts with Programs, v. 10, no. 7, p. A327.

Hanna, W.F., 1969, Negative aeromagnetic anomalies over mineralized areas of the Boulder batholith, Montana: U.S. Geological Survey Professional Paper 650–D, p. 159–167.

Hanna, W.F., Hassemer, J.H., Elliott, J.E., Wallace, C.A., and Snyder, S.L., 1994, Maps showing gravity and aeromagnetic anomalies in the Butte 1°×2° quadrangle, Montana: U.S. Geological Survey Miscellaneous Investigations Series Map I–2050–I, scale 1:250,000.

Klepper, M.R., Weeks, R.A., and Ruppel, E.T., 1957, Geology of the southern Elkhorn Mountains, Jefferson and Broadwater Counties, Montana: U.S. Geological Survey Professional Paper 292, 82 p.

Lee, G.K., McCafferty, A.E., Alminas, H.V., Bankey, Viki, Frishman, David, Knepper, D.H. Jr., Kulik, D.M., Marsh, S.P., Phillips, J.D., Pitkin, J.A., Smith, S.M., Stoeser, D.B., Tysdal, R.G., and Van Gosen, B.S., 2001, Montana geoenvironmental explorer: U.S. Geological Survey Digital Data Series DDS–65.

Olhoeft, G.R., 1985, Low-frequency electrical properties: Geophysics, v. 50, no. 12, p. 2492–2503.

Phillips, J.D., 1997, Potential-field geophysical software for the PC, version 2.2: U.S. Geological Survey Open-File Report 97–725, 34 p.

Plumlee, G.S., 2000, The environmental geology of mineral deposits, *in* Plumlee, G.S., and Logsdon, J.J., eds., The environmental geochemistry of mineral deposits—Part A, Processes, techniques, and health issues: Society of Economic Geologists, Reviews in Economic Geology, v. 6A, p. 77–116.

Roberts, W.A., 1953, Notes on the alaskite rocks in the Boulder batholith near Clancy, western Montana: Northwest Science, v. 27, p. 121–124.

Robinson, G.D., 1963, Geology of the Three Forks quadrangle, Montana, with descriptions of igneous rocks by H. Frank Barnett: U.S. Geological Survey Bulletin 988–F, p. 121–141.

Ruppel, E.T., 1963, Geology of the Basin quadrangle, Jefferson, Lewis and Clark, and Powell Counties, Montana: U.S. Geological Survey Bulletin 1151, 121 p.

Smedes, H.W., 1966, Geology and igneous petrology of the northern Elkhorn Mountains, Jefferson and Broadwater Counties, Montana: U.S. Geological Survey Professional Paper 510, 116 p.

Smith, B.D., Labson, V.F., and Hill, Pat, 2000, Airborne geophysical survey in the Boulder River watershed, Jefferson and Lewis and Clark counties, Montana: U.S. Geological Survey Open-File Report 00–240, one CD-ROM.

Smith, B.D., and Sole, T.C., 2000, Schlumberger DC resistivity soundings in the Boulder watershed, Jefferson and Lewis and Clark Counties, Montana: U.S. Geological Survey Open-File Report 00–0110, available at URL http://pubs.usgs.gov/of/2000/ofr-00-0110/.

Syberg, F.J.R., 1972, A Fourier method for the regional-residual problem of potential fields: Geophysical Prospecting, v. 20, p. 47–75.

Telford, W.M., Geldart, L.P., Sheriff, R.E., and Keys, D.A., 1976, Applied geophysics: Cambridge, U.K., Cambridge University Press.

Wanty, R.B., Berger, B.R., and Plumlee, G.S., 1999, Geoenvironmental models, *in* Fabbri, A.G., ed., Proceedings, 1998 NATO Advanced Studies Institute Workshop on Geoenvironmental Models of Mineral Deposits: Dordrecht; Boston, L. Kluwer Academic Publishers.

Mine Inventory

By E. Paul Martin

Chapter D3 of

Integrated Investigations of Environmental Effects of Historical Mining in the Basin and Boulder Mining Districts, Boulder River Watershed, Jefferson County, Montana

Edited by David A. Nimick, Stanley E. Church, and Susan E. Finger

Professional Paper 1652–D3

U.S. Department of the Interior
U.S. Geological Survey

Contents

Figures

Tables

Chapter D3
Mine Inventory

By E. Paul Martin

Abstract

An inventory of inactive and historical mines and mine-related sites in the Boulder River watershed study area was compiled from existing State and Federal sources. Site locations were spatially verified using digital orthophoto quadrangles to ensure an accurate geographically referenced inventory. The inventory also provides, where available, descriptive information, compiled from published sources, that supports the environmental evaluation of the effect of historical mining in the study area. This information includes the presence and the pH of flowing water from an adit, the presence and estimated volume of mine waste and mill tailings, and estimates of past production. These data provide site-specific information about potential anthropogenic contributions of deposit-related trace elements observed within the watershed.

Introduction

This chapter describes the mine inventory compiled for the Boulder River watershed study area. One of the most important facets of characterizing watersheds affected by historical mines is determining the location of as well as information about the mines, mills, and other mine-related sites. Every site in the watershed represents a potential source of deposit-related trace elements that could affect water quality and ecosystem health through direct drainage, seepage, erosion, or runoff. Within the Boulder River watershed, abundant and comprehensive data are available from several previous investigations. However, these data had not previously been compiled into one database, and many of the inventoried sites had only approximate locations.

The objective of this inventory is to create a database of mine-related sites that are accurately positioned and attributed in order to provide information to answer important questions about mine-site and stream remediation. The inventory combines geographically referenced locations and descriptive information in a format that lays the foundation for answering environmental and remediation questions using geographic information system (GIS) technology. The inventory comprises significant mines and mine-related sites in the Basin Creek, Cataract Creek, and High Ore Creek basins (major tributaries of the Boulder River), and in the areas drained by the portion of the Boulder River from the mouth of Basin Creek to High Ore Creek. (See Church, Nimick, and others, this volume, Chapter B, fig. 2.)

Methodology

The process used to determine the representative location for a mine-related site included the following steps. Data from the State of Montana, United States Department of Agriculture (USDA) Forest Service, Bureau of Land Management (BLM), and U.S. Geological Survey (USGS) databases provided an initial site data and localities list. These data were combined into one digital layer, and each site location was resolved to one representative point based on 1993 and 1998 digital orthophoto quadrangles (DOQs). Some mine-related sites contained multiple adits, shafts, and prospects, yet only one point location was captured to "best" represent the inventory site. Also, in some cases, the site location had to be determined strictly from a written description because not all of the historical data were georeferenced. Using digital orthophoto quadrangle (DOQ) image plots containing the resolved mine locations, USDA Forest Service and USGS personnel in Montana verified and revised the localities of the mine-related sites based on limited site visits, survey plats, and local knowledge of the area. Field inventories conducted by the Montana Bureau of Mines and Geology (Metesh and others, 1994, 1995, 1996; Marvin and others, 1997; Roby and others, 1960), the Montana Department of State Lands (1995), the Montana Department of Environmental Quality (1997), and the U.S. Geological Survey (Elliott and others, 1992) represent the sources for the descriptive data.

Data

Figure 1 shows 143 mine-related sites included in the inventory. Factors for inclusion or exclusion in the inventory focused on a site's contribution to environmental degradation, the physical hazard risk, past production volumes, and simply whether a site had a known name. The number for each site in figure 1 references a unique identifier for the study. Within the

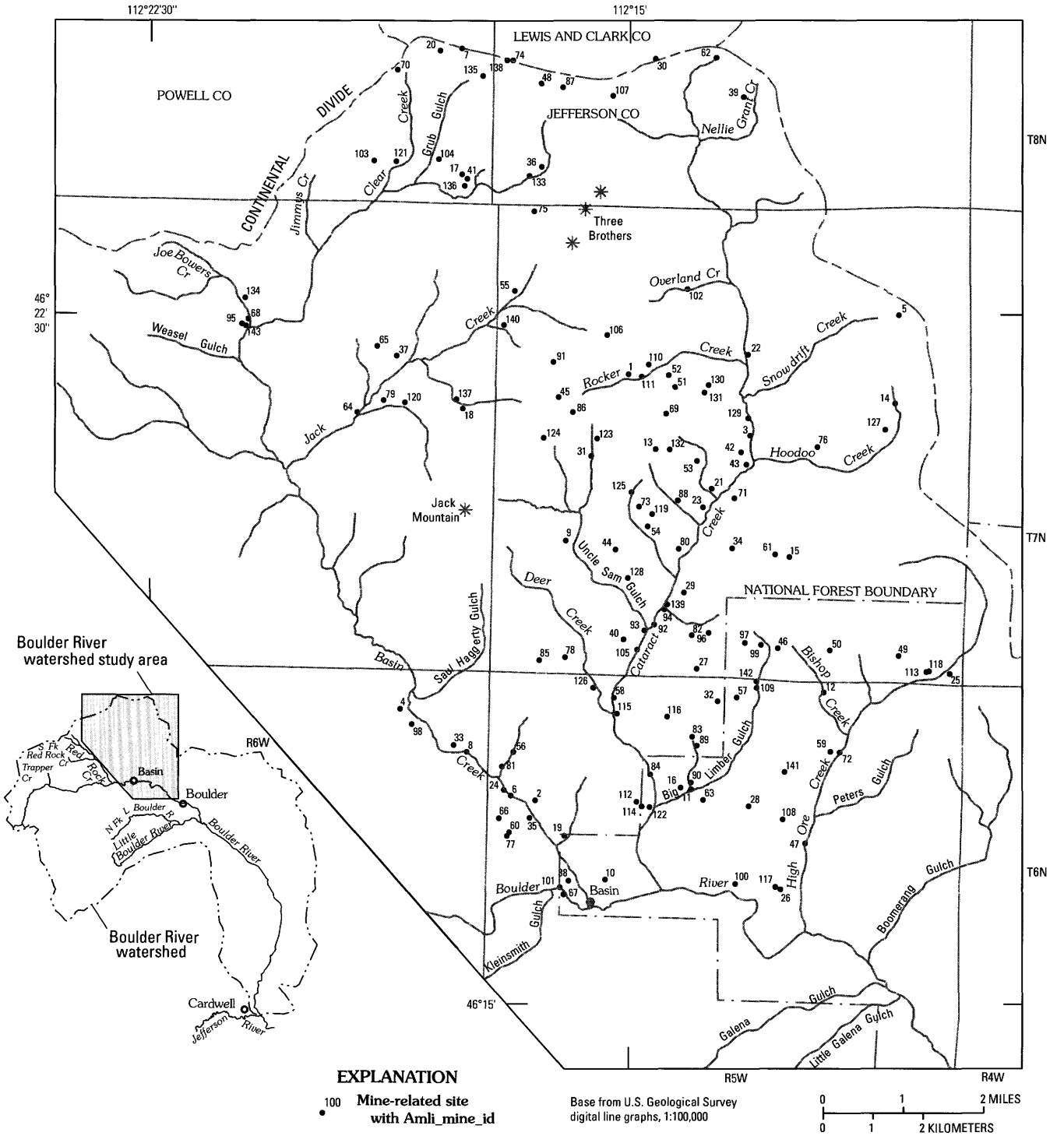

Figure 1. Mine inventory for Boulder River watershed study area.

mines database, this identifier is an item called Amli_mine_id and allows mine-related sites to be associated with scientific data and selected field sample sites. (See Rich and others, this volume, Chapter G, for a complete explanation of this relationship and how to access the mine inventory and project databases.)

Table 1 presents the descriptive information for each site in the inventory. The name field is self-explanatory. The next fields are the unique identifier just referenced and the geographic coordinates. The location status field provides a relative measure of how accurately the site has been positioned. The shafts and adits fields give an indication of the extent of

Table 1. Site-specific data for mines and prospects in the Boulder River watershed study area.

[Amli_mine_id in the database is Site No. (fig. 1); verif., verified; apprx., approximated; gpm, gallons per minute; undeterm., value not known; quantities expressed in units used in original data; tons, 2,000 pounds; yd^3, cubic yard; --, no data. Blank spaces for flow rate and pH reflect the logical extension of a value of zero for the number of flowing adits or "no data" for the number of flowing adits. Production: very large, greater than $5,000,000 or greater than 250,000 tons of ore; large, $500,000 to $5,000,000 or 25,000 to 250,000 tons of ore; medium, $50,000 to $499,000 or 2,500 to 24,000 tons of ore; small, less than $50,000 or less than 2,500 tons of ore. Production data from Elliott and others (1992)]

Site name	Site No. (fig. 1)	W. longitude	N. latitude	Location status	Shafts	Adits	No. of flowing adits	Flow rate	pH	Mill existence	Dump quantity	Tailings quantity	Past production
Ada	1	112 15 4.451	46 21 45.312	verif.	1	8	multiple	west adit, <0.5 gpm east adit, --	6.67 2.57	no	1,500 tons	--	medium
Adelaide	2	112 16 25.629	46 17 9.374	verif.	--	2	0			no	--	--	undeterm.
Apollo	3	112 13 9.840	46 21 6.840	verif.	--	1	--			--	--	--	small
Aurora	4	112 18 33.120	46 18 6.840	verif.	--	5	0			no	--	--	small
Bakama	5	112 10 52.765	46 22 25.637	verif.	--	1	0			--	--	--	small
Basin Belle	6	112 16 48.482	46 17 12.195	verif.	--	2	0			no	2,000 tons	--	small
Basin Creek	7	112 17 45.423	46 25 17.565	apprx.	--	--	--			--	--	--	very large
Basin Creek Placer	8	112 17 30.120	46 17 39.840	apprx.	--	--	--			--	--	--	--
Basin Gold & Silver	9	112 16 0.840	46 19 57.000	apprx.	--	--	--			--	--	--	--
Basin Mill/Atwater Complex	10	112 15 18.860	46 16 18.769	verif.	--	--	--			yes	--	--	--
Big Limber	11	112 13 59.880	46 17 17.880	apprx.	--	--	--			--	--	--	--
Bishop Creek	12	112 11 57.715	46 18 21.774	apprx.	--	1	1	--	--	--	--	--	--
Black Bear	13	112 14 38.040	46 20 57.120	verif.	1	2	2	--	--	no	3,000 tons	--	small
Blue Diamond-Occidental	14	112 10 55.075	46 21 28.896	verif.	--	3	2	Blue Diamond = 2 gpm Occidental = 7 gpm	6.55 --	no	1,000 tons 900 tons	--	undeterm.
Boulder Chief	15	112 12 31.599	46 19 48.616	verif.	1	2	1	0.1 gpm	2.63	yes	14,225 yd^3	138 yd^3	small
Boulder Vestal	16	112 14 9.592	46 17 18.893	apprx.	--	1	--			--	--	--	small
Buckeye	17	112 17 41.413	46 23 50.974	verif.	1	multiple	0			yes	6,130 yd^3	20,750 yd^3	medium
Bullion	18	112 17 39.106	46 21 21.458	verif.	1	4	2 (1 sampled)	7 gpm	2.58	yes	42,150 yd^3	4,200 yd^3	medium
Buster	19	112 15 57.829	46 16 46.635	apprx.	--	--	--			--	--	--	undeterm.
Carlson	20	112 18 5.700	46 25 11.959	verif.	--	--	--			--	--	--	--
Cataract	21	112 13 50.880	46 20 24.000	verif.	2	3	2	--	--	yes	--	--	--
Cataract Creek Placer	22	112 13 13.080	46 21 59.040	verif.	--	--	--			--	--	--	--
Cataract Tailings	23	112 13 53.040	46 20 17.160	verif.	--	--	--			--	--	1,000 tons	--
Columbus	24	112 16 54.822	46 17 15.693	verif.	--	3	0			no	--	--	--
Comet	25	112 10 0.120	46 18 34.920	verif.	2	--	--			yes	214,000 yd^3	500,000 yd^3	very large
Comstock Group	26	112 12 35.015	46 16 14.072	verif.	--	1	--			--	--	--	small
Condor Lodes	27	112 13 56.585	46 18 35.971	verif.	1	1	--			--	--	--	undeterm.
Copper King Prospect	28	112 13 6.094	46 17 7.453	apprx.	--	--	--			--	--	--	small
Cracker	29	112 14 9.960	46 19 24.960	verif.	--	1	1	12 gpm	7.39	no	4,000 tons	--	small
Crescent	30	112 14 44.160	46 25 18.120	verif.	2	1	1	5 gpm	3.15	yes	8,460 yd^3	840 yd^3	small
Crystal	31	112 15 38.160	46 20 52.080	verif.	multiple	2	1	36 gpm	3.21	no	--	--	large

Table 1. Site-specific data for mines and prospects in the Boulder River watershed study area.—Continued

Site name	Site No. (fig. 1)	W. longitude	N. latitude	Location status	Shafts	Adits	No. of flowing adits	Flow rate	pH	Mill existence	Dump quantity	Tailings quantity	Past production
Custer	32	112 13 36.840	46 18 15.120	verif.	1	1	0			--	--	--	medium
Daily West	33	112 17 42.458	46 17 44.402	verif.	--	2	0			--	300 tons	--	small
Della Prospect	34	112 13 25.155	46 19 53.847	verif.	--	--	--			--	--	--	undeterm.
Doris	35	112 16 30.609	46 16 57.986	verif.	--	2	0			--	4,470 yd^3	--	small
Double Shaft	36	112 16 28.823	46 23 58.126	verif.	4	--	--			no	--	--	undeterm.
Dumortierite Prospect	37	112 18 41.650	46 21 54.704	apprx.	--	--	--			no	--	--	small
East Katie	38	112 15 52.972	46 16 17.553	verif.	1	--	--			--	--	--	small
Eldorado and Plateau	39	112 13 21.000	46 24 45.000	verif.	4	1	0			no	--	--	small
Elmer	40	112 15 5.425	46 18 54.133	verif.	--	1	0			--	--	--	undeterm.
Enterprise	41	112 17 38.340	46 23 49.534	verif.	1	1	1	--	3.18	--	22,930 yd^3	--	small
Eva May	42	112 13 18.335	46 20 55.908	verif.	1	1	1	5 gpm	6.67	yes	92,000 yd^3	11,000 yd^3	large
Eva May Tailings	43	112 13 13.080	46 20 48.120	verif.	--	--	--			--	--	--	--
Evening Star & Golden Assets	44	112 15 14.117	46 19 51.716	verif.	--	--	--			--	--	--	--
First Shot	45	112 16 9.840	46 21 29.880	verif.	--	--	--			--	--	--	small
Freeburg	46	112 12 41.160	46 18 49.781	verif.	--	--	--			--	--	--	--
Golconda/Reliance	47	112 12 10.840	46 16 43.878	verif.	--	2	--			no	--	--	small
Golden Glow/Lula Bell	48	112 16 30.561	46 24 51.941	verif.	--	2	--			no	--	--	undeterm.
Golden Thread	49	112 10 48.290	46 18 45.904	apprx.	--	--	--			--	--	--	small
Gray Eagle	50	112 11 52.627	46 18 49.037	verif.	1	4	1	--	6.98	--	73,000 yd^3	--	large
Gray Lead	51	112 14 20.989	46 21 37.343	verif.	--	2	1	3 gpm	7.39	yes	--	800 tons	small
Great Shield Uranium	52	112 14 26.880	46 21 45.000	apprx.	--	--	--			--	--	--	--
Hanna	53	112 13 59.160	46 20 49.920	apprx.	--	--	--			--	--	--	undeterm.
Hattie Ferguson	54	112 14 50.102	46 19 57.704	verif.	1	4	2	0.5 gpm 2.9 gpm	7.02 7.09	no	--	--	medium
Hawkeye	55	112 16 52.292	46 22 37.938	verif.	--	1	1	--	--	no	--	--	undeterm.
Hector	56	112 16 46.352	46 17 40.388	verif.	--	2	--			no	100 tons	--	undeterm.
Hiawatha	57	112 13 18.836	46 18 17.682	verif.	1	3	--			--	--	--	medium
Hidden Treasure	58	112 15 13.599	46 18 16.391	apprx.	--	--	--			--	--	--	small
High Ore	59	112 11 50.459	46 17 43.494	verif.	--	1	--			--	--	--	small
Highland	60	112 16 49.280	46 16 48.478	verif.	--	5	--			--	--	--	--
Ida M.	61	112 12 44.629	46 19 50.040	verif.	0	1	1	2 gpm	5.43	no	--	--	small
Ida May	62	112 13 46.999	46 25 10.141	verif.	1	0	0			--	--	--	small
Independence	63	112 13 49.080	46 17 11.040	apprx.	--	--	--			--	--	--	--
Jack Creek Mill Tailings	64	112 19 17.659	46 21 17.864	verif.	--	--	--			--	--	23,000 yd^3	--
Jack Creek Ridge	65	112 18 59.886	46 22 0.864	verif.	--	--	--			--	--	--	--
Jessie	66	112 16 59.117	46 16 57.573	verif.	--	--	--			--	--	--	--

Table 1. Site-specific data for mines and prospects in the Boulder River watershed study area.—Continued

Site name	Site No. (fig. 1)	W. longitude	N. latitude	Location status	Shafts	Adits	No. of flowing adits	Flow rate	pH	Mill existence	Dump quantity	Tailings quantity	Past production
Jib Tailings	67	112 15 57.820	46 16 8.780	verif.	--	--	--			--	--	--	--
Joe Bower's	68	112 21 1.080	46 22 17.040	verif.	0	1	1	--	high	--	removed	--	undeterm.
John T.	69	112 14 29.040	46 21 20.160	verif.	--	1	0			--	--	--	small
Josephine	70	112 18 45.000	46 24 59.040	verif.	2	1	1	--	5.8	--	21,680 yd^3	--	small
Jumbo	71	112 13 23.880	46 20 26.160	apprx.	--	1	0			--	--	--	undeterm.
King Cole	72	112 11 41.753	46 17 43.032	verif.	--	2	--			no	medium	--	small
Klondyke	73	112 14 52.937	46 20 19.782	verif.	1	multiple	0			--	--	--	small
Lady Hennessey	74	112 16 57.197	46 25 7.853	verif.	2	multiple	--			--	--	--	small
Lady Leith	75	112 16 35.182	46 23 29.229	verif.	2	6	2	--	neutral	no	3,505 yd^3	--	small
Lizzie Osborne	76	112 12 6.840	46 21 0.000	verif.	--	2	0			--	--	--	undeterm.
Lotta	77	112 16 51.330	46 16 46.110	verif.	--	1	--			--	--	--	--
Louise	78	112 15 59.693	46 18 41.946	verif.	--	1	0			--	--	--	undeterm.
Lower Bullion Mill and Smelter	79	112 18 53.460	46 21 26.044	verif.	--	--	--			yes	--	--	--
Lower Hattie Ferguson	80	112 14 15.198	46 19 52.803	verif.	0	1	1	<1 gpm	6.87	--	2,000 tons	--	undeterm.
Lower Hector	81	112 16 57.000	46 17 30.840	verif.	--	1	--			no	<10 yd^3	--	undeterm.
Lower Vera & Marie	82	112 14 1.827	46 18 57.349	apprx.	--	--	--			--	--	--	--
Manhattan	83	112 13 59.689	46 17 51.642	verif.	--	--	1	--	--	--	--	--	undeterm.
Mantle	84	112 14 34.427	46 17 27.187	verif.	2	2	--			yes	large	--	small
Marguerita	85	112 16 23.880	46 18 39.960	verif.	1	1	--			--	--	--	small
Mary Anne	86	112 15 56.160	46 21 20.160	verif.	--	--	0			--	--	--	--
May Lillie	87	112 16 10.316	46 24 49.437	verif.	--	--	--			--	--	--	--
Mike #14	88	112 14 16.713	46 20 24.161	verif.	--	1	0			--	--	--	undeterm.
Minneapolis	89	112 13 55.339	46 17 46.085	verif.	--	2	1	--	--	no	--	--	small
Minneapolis Placer & Prospect	90	112 14 0.217	46 17 22.178	verif.	--	1	0			no	--	--	--
Morning	91	112 16 15.206	46 21 52.699	verif.	3	3	2	--	6.31 6.31	no	1,300 tons	--	small
Morning Glory	92	112 14 36.960	46 19 4.080	verif.	1	3	0			no	29,000 yd^3	7,200 yd^3	medium
Morning Glory Tailings	93	112 14 45.960	46 19 0.120	verif.	--	--	0			yes	--	6000 tons	--
Morning Marie	94	112 14 27.820	46 19 13.807	verif.	1	1	1	<0.5 gpm	--	no	--	--	undeterm.
Morning Star	95	112 21 6.849	46 22 13.742	verif.	--	3	--			no	--	--	small
Mountain Chief	96	112 13 46.034	46 18 59.199	apprx.	1	1	1	--	--	yes	500 tons	--	small
Mt. Thompson	97	112 13 12.000	46 18 52.920	verif.	--	3	0			--	--	--	small
N462741	98	112 18 21.795	46 17 57.227	apprx.	--	--	--			--	--	--	--
North Waldy	99	112 12 56.880	46 18 51.840	verif.	--	1	1	1 gpm	7.43	no	small	--	undeterm.
Obelisk	100	112 13 17.468	46 16 17.113	verif.	1	2	0			yes	--	--	small
Old Basin Mill Site	101	112 16 0.962	46 16 13.243	verif.	--	--	--			yes	--	--	--

Table 1. Site-specific data for mines and prospects in the Boulder River watershed study area.—Continued

Site name	Site No. (fig. 1)	W. longitude	N. latitude	Location status	Shafts	Adits	No. of flowing adits	Flow rate	pH	Mill existence	Dump quantity	Tailings quantity	Past production
Overland Creek	102	112 14 11.040	46 22 41.880	verif.	2	--	--			no	--	--	undeterm.
Pearl	103	112 19 5.880	46 24 0.000	apprx.	1	--	--			no	--	--	--
Perry Parks Placer	104	112 18 5.194	46 24 2.017	verif.	--	--	--			--	placer dredgings	--	--
Phantom	105	112 14 52.515	46 18 47.624	verif.	--	1	1	0.5 gpm	7.43	no	200 tons	--	undeterm.
Piermont No.1 East/North Ada	106	112 15 25.453	46 22 10.349	verif.	2	--	--			no	--	--	undeterm.
Quartz Creek	107	112 15 23.410	46 24 44.553	verif.	--	1	0			--	--	--	undeterm.
Queen of the Hills	108	112 12 34.270	46 16 59.234	apprx.	--	--	--			--	--	--	small
Red Wing	109	112 12 58.139	46 18 24.187	verif.	--	2	1	0.2 gpm	7.74	no	--	--	small
Rocker	110	112 14 45.960	46 21 51.840	verif.	--	2	1	<1 gpm	3.35	no	1,500 tons	--	undeterm.
Rocker Extension	111	112 14 52.080	46 21 43.920	verif.	--	1	1	2 gpm	8.56	no	350 tons	--	undeterm.
Rose	112	112 14 45.161	46 17 8.054	verif.	--	--	--			--	--	--	small
Rumley	113	112 10 21.954	46 18 36.010	apprx.	1	--	--			--	--	--	medium
Ruth	114	112 14 42.157	46 17 6.384	verif.	--	--	--			--	--	--	undeterm.
Saturday Night	115	112 15 10.514	46 18 6.066	verif.	1	1	0			--	--	--	small
Seattle	116	112 14 23.534	46 18 4.564	verif.	--	multiple	0			--	--	--	undeterm.
Silmont Claims	117	112 12 39.795	46 16 15.526	verif.	--	--	0			--	--	--	--
Silver Hill	118	112 10 19.489	46 18 36.448	verif.	1	--	--			--	--	--	small
Sirius	119	112 14 40.518	46 20 15.110	verif.	1	1	1	1.5 gpm	4.44	no	5,000 tons	--	small
Smelter Creek Adit	120	112 18 33.120	46 21 24.840	verif.	--	--	--			--	--	--	--
Solar (Solar Pearl)	121	112 18 44.970	46 24 0.036	apprx.	2	1	--			no	--	--	small
South Mantle	122	112 14 38.810	46 17 6.117	verif.	--	3	--			no	--	--	small
Sparkling Water	123	112 15 32.870	46 21 3.327	verif.	--	--	0			--	--	--	undeterm.
St. Lawrence	124	112 16 22.963	46 21 3.636	verif.	2	--	--			--	--	--	undeterm.
St. Nick	125	112 15 0.131	46 20 29.061	verif.	1	--	--			--	--	--	undeterm.
Slyvan	126	112 15 32.825	46 18 22.638	verif.	--	3	--			--	--	--	undeterm.
Totten (Billie T.)	127	112 11 3.840	46 21 11.880	verif.	--	1	--			--	--	--	small
Uncle Sam	128	112 15 2.133	46 19 33.894	verif.	1	multiple	0			no	--	--	medium
Unnamed #1	129	112 13 12.000	46 21 18.000	verif.	--	1	1	--	--	no	500 tons	--	undeterm.
Unnamed #2	130	112 13 49.515	46 21 38.995	verif.	--	1	1	1 gpm	7.05	no	250 tons	--	undeterm.
Unnamed #3	131	112 13 53.480	46 21 34.194	verif.	3	2	1	<1 gpm	6.11	no	--	--	undeterm.
Unnamed #4	132	112 14 25.080	46 20 57.120	verif.	--	1	1	1 gpm	7.24	no	--	--	undeterm.
Unnamed Placer	133	112 16 40.080	46 23 52.08	verif.	--	--	--			--	--	--	--
Unnamed Placer	134	112 21 4.445	46 22 30.735	verif.	--	--	--			--	--	--	--
Unnamed Uranium	135	112 17 25.080	46 24 56.160	apprx.	--	--	--			--	--	--	--
Upper Buckeye Mill Tailings	136	112 17 40.770	46 23 44.869	verif.	--	--	--			yes	--	20,750 yd^3	--
Upper Bullion Mill Tailings	137	112 17 45.313	46 21 27.448	verif.	--	--	--			yes	--	4,200 yd^3	--
Venus	138	112 17 2.588	46 25 6.468	apprx.	--	--	--			--	--	--	small
Vera & Marie	139	112 14 25.080	46 19 17.040	verif.	2	2	--			no	1,500 tons	--	small
Vindicator	140	112 17 2.040	46 22 15.960	verif.	--	multiple	multiple	--	6.68	no	--	--	small
Virginia	141	112 12 32.677	46 17 29.805	apprx.	--	--	0			--	--	--	small
Waldy	142	112 12 58.339	46 18 28.426	verif.	--	1	1	5 gpm	7.93	no	small	--	undeterm.
Winters Camp	143	112 21 3.021	46 22 12.487	verif.	1	4	1	--	--	no	--	--	undeterm.

the workings at that site. The number of flowing adits, the flow rate, and the pH of the discharge represent important point-source information. In numerous cases, either the site did not have a flowing adit or data were not available for the flow rate and pH. The mill existence field indicates the historical presence or absence of a mill at the site. The dump quantity and tailings quantity fields provide a measure of the amount of waste rock or mill tailings at each site (again, the sources did not necessarily document this descriptor for every site). The past production field shows each site's output in relative terms. The following provides a measure of the value or magnitude of production based either upon the value of the ore shipped (expressed in units of $1,000) or tonnage produced (expressed in units of 1,000 tons): very large, greater than $5,000,000 or greater than 250,000 tons of ore; large, $500,000–$5,000,000 or 25,000–250,000 tons of ore; medium, $50,000–$499,000 or 2,500–24,000 tons of ore; small, less than $50,000 or less than 2,500 tons of ore; no or undetermined production. Monetary figures represent value at time of production (Elliott and others, 1992).

Discussion

The Boulder River watershed study area contains numerous prospects and smaller mine-related localities not inventoried for this study. Whereas the potential exists for any one of these sites to adversely affect ecosystem health, the data sources and field investigations suggest that this inventory is comprehensive in terms of identifying the significant historical mines and mine-related sites.

Some historical mine sites contain large underground workings or have multiple shafts and adits over an area. Regardless of complexity, the inventory represents each site with a single location.

The decision to encode the location status field in table 1 with "verified" or "approximate" was determined by a comparison of the source description and field diagrams with the DOQs and locations symbolized on existing maps. A verified value means that USDA Forest Service and USGS personnel in Montana checked the mine-related location and agreed on its position with a high degree of confidence.

The values in table 1 represent a choice of values from multiple sources. Discounting the unique identifier, the geographic coordinates, and the location status, the values for any particular column do not necessarily originate from the same source. For example, the number of adits for the Ada mine originates from source A, and the number of adits for the Bullion mine originates from source B. Likewise for any particular mine, the values for each of the columns may derive from different sources. All data sources are referenced herein.

References Cited

Elliott, J.E., Loen, J.S., Wise, K.K., and Blaskowski, M.J., 1992, Maps showing locations of mines and prospects in the Butte 1 degree × 2 degree quadrangle, western Montana: U.S. Geological Survey Miscellaneous Investigations Series Map I–2050–C, 2 plates, scale 1:250,000, and pamphlet, 147 p.

Marvin, R.K., Metesh, J.J., Bowlers, T.P., Lonn, J.D., Watson, J.E., Madison, J.P., and Hargrave, P.A., 1997, Abandoned-inactive mines program, U.S. Bureau of Land Management: Montana Bureau of Mines and Geology Open-File Report 348, 506 p.

Metesh, J.J., Lonn, J.D., Duaime, T.E., and Wintergerst, Robert, 1994, Abandoned-inactive mines program, Deerlodge National Forest—Volume I, Basin Creek drainage: Montana Bureau of Mines and Geology Open-File Report 321, 131 p.

Metesh, J.J., Lonn, J.D., Duaime, T.E., Marvin, R.K., and Wintergerst, Robert, 1995, Abandoned-inactive mines program, Deerlodge National Forest—Volume II, Cataract Creek drainage: Montana Bureau of Mines and Geology Open-File Report 344, 201 p.

Metesh, J.J., Lonn, J.D., Marvin, R.K., Madison, J.P., and Wintergerst, Robert, 1996, Abandoned-inactive mines program, Deerlodge National Forest—Volume V, Jefferson River drainage: Montana Bureau of Mines and Geology Open-File Report 347, 179 p.

Montana Department of Environmental Quality, 1997, Watershed analysis of abandoned hardrock mine priority sites 1997: Prepared by Pioneer Technical Services, Inc., Butte, Mont., and Integrated Geoscience, Inc., Helena, Mont., for the Mine Waste Cleanup Bureau, variously paginated.

Montana Department of State Lands, 1995, Abandoned hardrock mine priority sites, 1995 summary report: Prepared by Pioneer Technical Services, Inc., Butte, Mont., for the Abandoned Mine Reclamation Bureau, variously paginated.

Roby, R.N., Ackerman, W.C., Fulkerson, F.B., and Crowley, F.A., 1960, Mines and mineral deposits (except fuels), Jefferson County, Montana: Montana Bureau of Mines and Geology Bulletin 16, 120 p.

U.S. Geological Survey/USDA Forest Service – published maps and map/field materials:

Basin quadrangle - 1:24,000-scale – 1985 provisional edition.

Basin quadrangle – 1:24,000-scale – 1996 USGS/USFS edition.

Bison Mountain – 1:24,000-scale – 1985 provisional edition.

Chessman Reservoir – 1:24,000-scale – 1985 provisional edition.

Mount Thompson – 1:24,000-scale – 1985 provisional edition.

Mount Thompson – 1:24,000-scale – 1996 USGS/USFS edition.

Three Brothers – 1:24,000-scale – 1985 provisional edition.

Thunderbolt Creek – 1:24,000-scale – 1985 provisional edition.

Thunderbolt Creek – 1:24,000-scale – 1996 USGS/USFS edition.

Metal Leaching in Mine-Waste Materials and Two Schemes for Classification of Potential Environmental Effects of Mine-Waste Piles

By David L. Fey and George A. Desborough

Chapter D4 of
Integrated Investigations of Environmental Effects of Historical Mining in the Basin and Boulder Mining Districts, Boulder River Watershed, Jefferson County, Montana
Edited by David A. Nimick, Stanley E. Church, and Susan E. Finger

Professional Paper 1652–D4

U.S. Department of the Interior
U.S. Geological Survey

Contents

Figures

Tables

Chapter D4
Metal Leaching in Mine-Waste Materials and Two Schemes for Classification of Potential Environmental Effects of Mine-Waste Piles

By David L. Fey and George A. Desborough

Abstract

Surface waste material was collected from 19 metal-mining-related dumps at 10 sites in the Boulder River watershed study area. Leach and acidity analyses of waste material provided a foundation for the development of two classification schemes for evaluating the potential environmental effect of mine-waste piles. Mineralogical and geochemical analyses of a vertical core of tailings at a mill site showed a distinction in the amount of deposit-related elements between surface and buried waste material.

Mineralogy of bulk surface samples was determined primarily by X-ray diffraction. Anglesite and jarosite were present in about 80 percent of the waste piles. Sphalerite and arsenopyrite, both common primary minerals in the mineral deposits, were not present in the mine-waste samples. Goslarite (a zinc sulfate) and scorodite (iron arsenate) were identified in the field. Total-digestion inductively coupled plasma–atomic emission spectroscopy (ICP-AES) elemental and X-ray diffraction analyses of a core from the Buckeye flotation tailings revealed that most of the pile contained oxidized tailings composed of secondary minerals produced during weathering and sparse to no original sulfide minerals; the bottom of the core contained a layer of primary sulfide minerals. Comparison of concentrations in the sulfide and oxidized layers in this core demonstrated that significant leaching of deposit-related trace elements had occurred in the oxidized layer, with some elements migrating downward.

The surface samples were subjected to two leaching techniques to determine the concentration of water-soluble, deposit-related trace elements in the dump materials. Net acid production, an indication of the ability of a material to produce acid when oxidized over a long period of time, was also determined. The sum of the concentrations of deposit-related elements (Ag+As+Cd+Cu+Pb+Zn) in these leachates, when plotted against either the leachate pH or the net acid-production value, provided two schemes for classifying these mine wastes. Metal-mining wastes in the study area had classifications ranging from low potential to high potential for causing environmental degradation. The leach and acidity tests showed that material with net acid potential greater than 20 pounds $CaCO_3$ per ton equivalent will release high concentrations of iron, arsenic, cadmium, copper, lead, and zinc, and produce leachates with low pH.

The two classification schemes derived from the chemical and waste-pile-size data provide a means to compare the potential of the waste piles in a watershed to cause environmental degradation. These methods are meant to provide numerical means of evaluating and comparing wastes, but do not incorporate such factors as proximity to ground or surface water, presence of surface water, or draining adit water flowing over or infiltrating into the piles. These factors must be considered by land managers along with the classification results.

Introduction

Metal-mining-related wastes in the Boulder River watershed study area cause detrimental effects on water quality because of acid generation and toxic-metal solubilization (Nimick and Cleasby, this volume, Chapter D5; Cannon and others, this volume, Chapter E1). Mining-related wastes also contribute to contamination of streambed sediment through the fluvial transport and deposition of tailings and the settling of metal-rich colloidal material (Church, Unruh, and others, this volume, Chapter D8).

Veins enriched in base and precious metals were explored and mined in the Basin, Cataract, and High Ore Creek basins for a period of more than 70 years. Extracted minerals included galena, sphalerite, pyrite, chalcopyrite, tetrahedrite, and arsenopyrite. Most of the metal-mining waste sites in the study area were identified and described by the Montana Bureau of Mines and Geology (Metesh and others, 1994; Metesh and others, 1995; Marvin and others, 1996). In 1997, we collected composite surface samples from sites in the Basin and Cataract Creek basins to identify, characterize, and classify waste sources.

Purpose and Scope

The purpose of this chapter is to describe various geochemical and mineralogical studies to help understand and assess the potential geochemical effect of mine-waste piles in the Boulder River watershed study area. Material from the surface of waste piles was sampled and analyzed to determine the minerals and elements present in waste piles. A core was collected from one waste pile to determine whether surface samples have different trace-element composition and mineralogy from samples collected at depths. Finally, chemical and physical attributes of waste piles were combined to construct two classification schemes to rank the potential environmental hazard of runoff from mine-waste piles. The goals of this part of the Boulder River watershed study were to:

- Characterize the mineralogy and geochemistry of mine wastes
- Demonstrate the geochemical differences between surface and subsurface material in mine-waste piles
- Develop a classification scheme or schemes to assess the potential environmental effect of runoff from mine waste
- Apply the classification schemes to the sampled mine-waste piles.

Sample Collection and Preparation

Bulk Surface Samples

Mine-waste samples (exploration waste, dump material, or mill tailings) were collected from the surface of 19 waste piles at 10 sites in the Boulder River watershed study area. Surface material was collected for analysis because it is what is exposed to air, rain, and snowmelt runoff infiltration. Material from each site was collected from 30 or more randomly selected 3-ft cells across the top and sides of a dump to a depth of approximately 3 in. using four to six randomly selected 2–3 oz scoops per cell. This collection method is designed to reduce the sampling error (also called the fundamental error; Smith and others, 2000). Samples were dry sieved in the field to obtain a minus-0.08 in. (<2 mm) fraction. The minus-0.08 in. fraction was deemed to be the most reactive to water in short-term exposures. Coarser material was discarded. The resulting composite sample typically contained 2–4 lb of mine waste. The minus-0.08 in. fraction was split in the laboratory using a Jones splitter. One fraction was further split into a ½ lb sample that was used for (1) bulk chemical analysis (after sieving to minus-80 mesh (<190 μm) and grinding to minus-200 mesh (<75 μm)); (2) X-ray diffraction (XRD) analysis to determine mineralogy; (3) analysis of heavy-mineral concentrates to identify high-density minerals; (4) leaching tests to determine amounts of soluble deposit-related elements; and (5) net acid production (NAP) tests (after grinding to minus-200 mesh (<75 μm)).

Two-Inch Diameter Vertical Core

At the Buckeye mill tailings site, we also drove a 2-in. PVC pipe about 6 ft through the thickest part of the tailings. In the laboratory, core samples were described and subdivided into subsamples (by depth) according to visually identified differences in mineralogy, organic content, and apparent oxidation zones. The subsample material was sieved to minus-100 mesh (<150 μm), analyzed for bulk chemistry, and examined with XRD for mineralogy. Analyses from this core illustrate the leaching of trace elements as sulfidic waste weathers; they are discussed in more detail in the section on effects of weathering on dump surface material and in Cannon and others (this volume).

Location of Mine-Waste Sites

We sampled and analyzed material from selected sites likely to have moderate to high impact on the environment, and to which we had access (either public land or private land with permission). We did not sample all possible waste sites, and so the rankings derived from the classification schemes discussed herein serve as applied examples of those schemes, and not a definitive ranking of all mine-waste sites in the study area.

Metesh and others (1995) inventoried 37 waste sites from historical records in the Basin Creek basin and visited 28. They sampled 14 sites. Of those 14, we visited and sampled 5 sites. Our sampling plan was based on assessing which sites were likely to contribute adversely to the quality of water and sediment in the study area. Some sites were deemed too small, too distant from any surface water (for example, the Morning mine), or too inaccessible for remediation (Hector mine). Other sites showed no significant impact on nearby streambed sediment (for example, Lady Lieth and Winter's Camp mines), and so were not sampled. Metesh and others (1995) inventoried 57 sites in the Cataract Creek basin, visited 54, and sampled 27. We collected samples at five sites, using the criteria just listed to screen sites. The Crescent mine is accessible only by foot, and although it has visible mine discharge, it had negligible effect on sediment in upper Cataract Creek, based on streambed sediment analyses (Church, Unruh, and others, this volume). Similarly, effect on sediment of Hoodoo Creek (tributary to Cataract Creek) from the Blue Diamond–Occidental mine was minimal. The Phantom mine-waste pile on Cataract Creek was very small (200 tons). One site not sampled but which should have been was the Morning Glory tailings. This site is on the west bank of Cataract Creek and contained approximately 6,000 tons of material (Metesh and

others, 1995). However, Metesh and others (1995) concluded that the pile did not appear to contribute to the degradation of Cataract Creek, and that the mineralogy of the material suggested little potential for metals to be released.

We collected 19 bulk surface samples from mine-waste piles at 10 mine sites located in the Basin and Cataract Creek basins (fig. 1). The estimated sizes of the waste piles are in table 1.

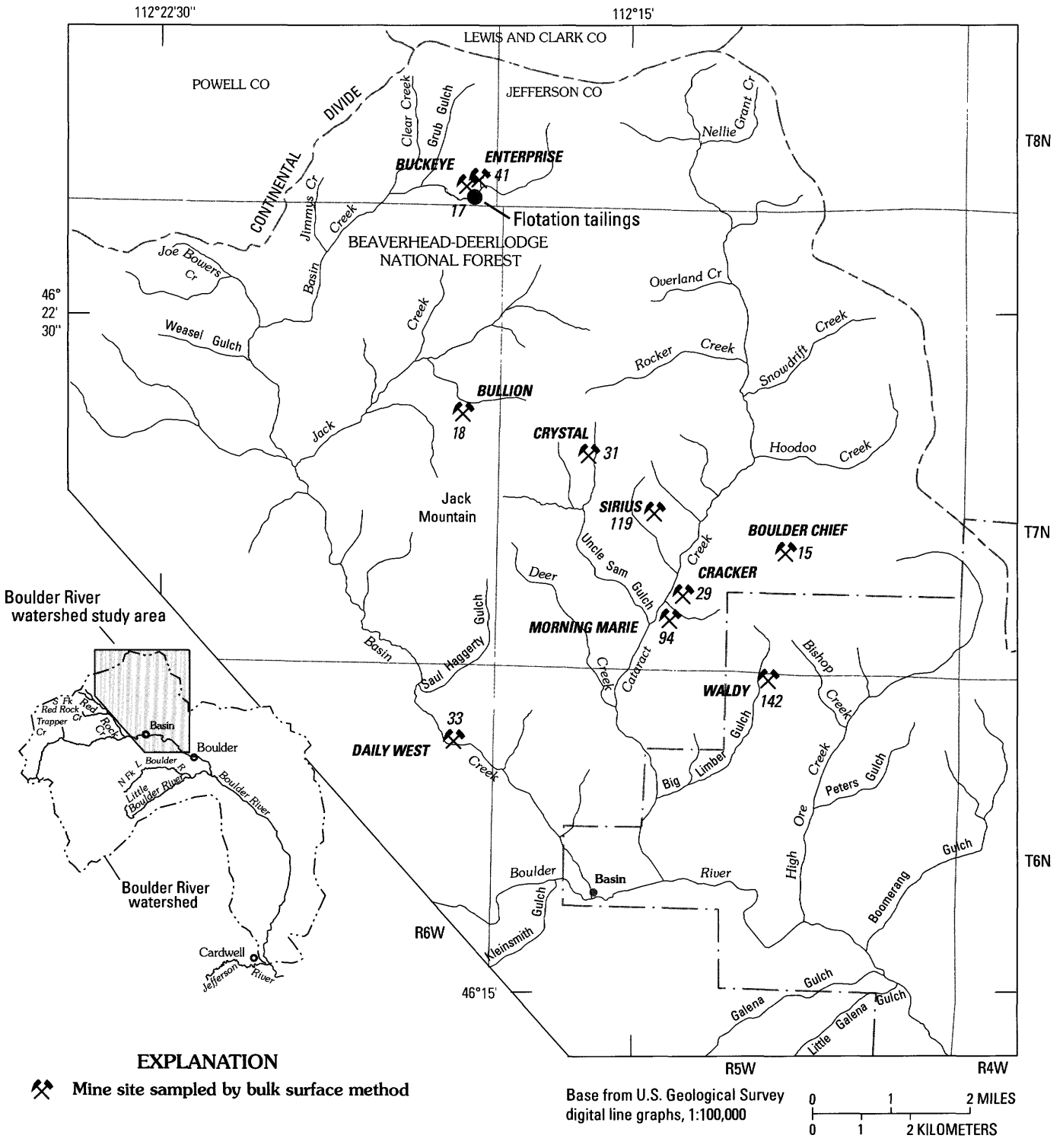

Figure 1. Boulder River watershed study area, and localities of bulk surface mine-waste samples (sites numbered as in Martin, this volume, Chapter D3).

Table 1. Site numbers, site names, sample descriptions, and estimated size of mine-waste piles sampled in the Boulder River watershed study area.

[Site numbers are from Martin (this volume, table 1)]

	Site No. and name	Sample description, bulk surface sample	Estimated size (tons)
41	Enterprise mine	Brown waste from Enterprise mine	5,000
17	Buckeye mine	Light-gray waste from Buckeye mine	10,000
		Light-gray tailings from flat near creek	8,400
18	Bullion mine	Uppermost dump, upper adit	6,000
		Middle dump, middle adit	7,000
		Lower dump, lower adit	12,000
		Small dump near lowest adit	500
		Upper tailings impoundment	1,200
		Lower tailings impoundment	3,600
15	Boulder Chief mine	Waste above adit from open cut	3,500
		Waste from below mine adit	3,500
142	Waldy mine	Waste dump at adit	700
94	Morning Marie mine	Waste piles from adit	1,000
29	Cracker mine	Waste from adit	4,000
33	Daily West mine	Yellow waste near creek bed	300
119	Sirius mine	Waste dump at adit	5,000
31	Crystal mine	Altered rock along east side of open cut	20,000
		Altered rock along west side of open cut	10,000
		Waste at ore bins near creek	4,000

In the Basin Creek basin, we visited the following sites and collected samples as noted:

- Buckeye mine area near the head of Basin Creek; two samples
- Enterprise mine area (just upstream of the Buckeye mine on Basin Creek); one sample
- Bullion mine area, above a small tributary to Jack Creek (the Bullion mine tributary); six samples
- Daily West mine, along Basin Creek about 3 mi upstream from the town of Basin; one sample.

In the Cataract Creek drainage basin, we visited the following sites and collected samples as noted:

- Crystal mine, near the head of Uncle Sam Gulch (tributary of Cataract Creek); three samples
- Sirius mine; one sample
- Morning Marie mine, along Cataract Creek upstream of Uncle Sam Gulch; one sample
- Cracker mine, along Cataract Creek upstream of Uncle Sam Gulch; one sample
- Boulder Chief mine, about 1½ mi east of Cataract Creek and 1½ mi south of Hoodoo Creek; two samples
- Waldy mine, in Big Limber Gulch about 2 mi upstream from Cataract Creek; one sample.

The High Ore Creek basin is also in the study area. However, we did not collect samples from the Comet mine, the largest mining operation in that drainage, because it was scheduled for remediation.

Figure 2. View of lower (largest) waste dump at Bullion mine, looking north. Distance across dump is about 200 feet (60 m). Loading chute seen at center of picture. Mill was below dump, to the north.

Geochemistry and Mineralogy of Mine Wastes

Mineralogy

Minerals in the bulk surface samples of mine waste were determined by X-ray diffraction (copper radiation) of 2-oz samples of the minus-0.08-in. (<2 mm) fraction after pulverizing in a Spex mill to minus-200 mesh (<75 µm). Both anglesite and jarosite were present in about 80 percent of the samples. Whereas anglesite is chemically simple ($PbSO_4$), jarosite may be chemically complex. Studies of members of the alunite-jarosite family of minerals by Scott (1987) showed that the general formula for jarosite is $AB_3(XO_4)_2(OH)_6$; the large cation (A) may be Na, K, Ag, NH_4, H_3O, Ca, Pb, Ba, Sr, or Ce, and the B sites may be occupied by Al, Fe, Cu, or Zn. The anion (XO_4) may be SO_4, PO_4, AsO_4, SbO_4, CrO_4, or SiO_4. For our samples, the dominant X-ray diffraction pattern was that of the jarosite family, with SO_4 as the major anion with some possible AsO_4 substitution where arsenic was abundant. The major cations appeared to be K, Pb, and H_3O based on scanning electron microscopy and energy-dispersive X-ray fluorescence analysis.

Heavy-mineral concentrates were obtained by mechanical panning of a 1-oz fraction of each minus-0.08 in. (<2mm) split in order to concentrate high-density minerals such as pyrite, galena, and sphalerite. These minerals were identified by X-ray diffraction, X-ray fluorescence, and optical microscopy. Although sphalerite (ZnS) and arsenopyrite (FeAsS) are common primary hydrothermal minerals in the ore deposits of the study area (Billingsley and Grimes, 1918), we found no arsenopyrite in the heavy-mineral concentrates from any sample and only trace amounts of sphalerite in one sample.

White botryoidal crusts of goslarite ($ZnSO_4 \cdot 7H_2O$) were found underneath an overhang on the largest waste pile at the Bullion mine (fig. 3). Thus, we suspect that zinc resides chiefly in this soluble zinc sulfate, and possibly in gunningite ($(Zn, Mn)SO_4 \cdot H_2O$). Scorodite, a highly water-soluble iron arsenate ($FeAsO_4 \cdot 2H_2O$), was abundant on the surface of one waste pile at the head of Jack Creek, about 1 mile north of the Bullion mine. Scorodite is the most commonly occurring oxidized secondary mineral derived from arsenopyrite. The absence of primary zinc- and arsenic-bearing minerals and the presence of these two secondary minerals suggest that most of the zinc- and arsenic-bearing primary sulfide minerals had been converted to more soluble sulfate or arsenate phases by weathering. This weathering took place since the cessation of mining, a period of 50–100 years.

Figure 3. Soluble salt goslarite ($ZnSO_4 \cdot 7H_2O$) coating mine waste, Bullion mine. This easily dissolved mineral formed in place from leaching of zinc from waste pile; it was protected here from rain by an overhanging cut in the waste pile. Field of view in photograph is about 1 ft across.

Mixed-Acid Digestion Method

A mixed-acid digestion technique was used to provide bulk analyses of surface mine-waste samples and the core subsamples. We used the results to illustrate the geochemical difference between dump surface material (mostly oxidized) and material at depth (partially oxidized or unoxidized). A 0.2 g portion of material was subjected to a mixed-acid digestion using, in sequence, HCl, HNO_3, $HClO_4$, and HF acids (Crock and others, 1983; Briggs, 1996). The resulting solution was analyzed for 40 elements using inductively coupled plasma–atomic emission spectroscopy (ICP-AES). The digestion dissolves sulfides and most silicates and oxides; resistant or refractory minerals such as zircon, spinels, and some tin oxides are only partially dissolved. Samples of standard reference material (SRM) were digested and analyzed with the mine-waste samples. These standards were SRM-2704, SRM-2709, SRM-2710, and SRM-2711, available from the National Institute of Standards and Technology. Analytical results for the bulk surface materials are in Fey, Desborough, and Finney (2000), and results for the 2-in. core from the Buckeye site are in Cannon and others (this volume) and the database (Rich and others, this volume, Chapter G). A statistical summary of mean values, median values, and standard deviations for multiple analyses of the reference materials, and comparisons with certified values appear in Fey, Unruh, and Church (1999).

Passive Leach Method

A passive leach procedure was also applied to the bulk surface mine-waste materials, and the results were used in one of the waste classification schemes discussed herein. A 100-g sample was exposed to 2 L of laboratory deionized water (pH of 5.0±0.2) in an open 4-L beaker. Samples were left at rest for 1 hour and then gently stirred for 5 seconds to prevent stratification of the leachate. The pH of the leachate was measured after 24 hours, and then a 60-mL sample of the leachate was filtered through a Gelman 0.45-µm filter using a disposable 60-mL syringe (Desborough and Fey, 1997), acidified with six drops of ultra-pure HNO_3, and refrigerated prior to analysis by ICP-AES. The data for the passive leach procedure are in Desborough and Fey (1997).

EPA-1312 Leach Method (Synthetic Precipitation Leach Procedure–SPLP)

This procedure was used on the bulk surface mine-waste materials, and the results were used in one of the waste classification schemes discussed below. A 100-g sample of mine waste was placed in a 2.3-L polyethylene bottle. Two liters of an extract solution were added, resulting in a 1:20 sample/extract ratio, with 300 cm^3 of headspace. The extract solution was made from deionized water acidified to a pH of 4.2 with

a 1-percent aqueous solution of 60/40 v/v H_2SO_4/HNO_3. The capped bottles were placed on an end-over-end (tumbling) rotating agitator at 30 rpm for 18 hours. The leachates were then pressure filtered through a 0.7-µm filter (USEPA, 1986). A 100-mL aliquot of filtered solution was acidified with ultra-pure HNO_3 and analyzed for 25 elements by ICP-AES (Briggs and Fey, 1996) and for sulfate (as sulfur) by ICP-AES. Specific conductance and pH were determined on the unacidified bulk filtered leachate. All data are in Fey, Desborough, and Finney (2000).

Net Acid Production (NAP) Method

This test was applied to the bulk surface mine-waste materials, and the results are used in one of the classification schemes herein. A 1.0-g sample of pulverized, minus-200 mesh material was digested with a solution of 30 volume-percent hydrogen peroxide to oxidize pyrite and pyrrhotite, thereby producing sulfuric acid (Lapakko and Lawrence, 1993). The produced acidic solution reacted with the bulk sample, releasing additional acidity from water-soluble salts (present as a result of wetting-drying cycles on the mine-waste pile). The solution also reacted with acid-consuming minerals such as carbonates, biotite, chlorite, and epidote. The solutions were heated to near-boiling for 1 hour, cooled, and filtered. The filtrate was then titrated to a pH of 7 with 0.1M NaOH. A calculated net acid production (NAP) is expressed in terms of lb-equivalent $CaCO_3$ per ton of mine waste. This NAP is meant to represent the net long-term or total potential of a material to produce acid over an unspecified period of weathering. The NAP analyses are in table 2.

Effects of Weathering on Dump Surface Material

In this study, we collected surface samples at 10 waste sites. Factors that can influence the resulting analytical values are numerous. One factor is the surface inhomogeneity of the material sampled. We addressed that factor by collecting many subsamples from at least 30 cells across the surfaces of waste piles and mixing them into one composite sample. Another factor leading to variation is inhomogeneity on a vertical scale within a waste pile. The surface zone typically is composed of oxidized material that has been exposed to the environment for 50 years or more. The concentrations of deposit-related trace elements are usually lower in surface waste material than in material from deeper inside a pile due to accelerated weathering and leaching at the surface. Other concerns related to differential weathering of dumps include slope aspect (north-facing or south-facing) and top versus sides, but we did not address these particular distinctions in this study. Material from below the surface is less likely to be completely oxidized, and material from deep within a pile can contain a large proportion of the original sulfide minerals. Hence, surface sampling is likely to produce a sample biased towards lower metal content, but one that represents the material that determines the chemical composition of surface runoff. Deep sampling would provide a sample that yields a higher metal content and that better represents the long-term potential for future metal release. However, deep sampling is both technically difficult and expensive. We collected a 6-ft long core from the thickest part of the Buckeye tailings, and through geochemical analyses, we show the distinction between surface sampling and depth sampling. The *processes* of element mobility and dispersion of metals represented by this core are discussed in Cannon and others (this volume).

Production records from Roby and others (1960) indicate that ore was last produced at the Buckeye mine in 1939. Rossillon and Haynes (1999) suggested that reprocessing of ores using flotation took place in the early 1940s, resulting in the waste we investigated from the flood plain near the Buckeye mine. Thus, the study of this core examines the results of a 60-year experiment, showing the effect of annual saturation and weathering of mine wastes in a temperate environment. The 2-in. core provided an opportunity to examine the tailings chemistry vertically from the present surface to a depth of about 6 ft. Throughout most of the flood-plain area that is covered by waste, the tailings were thin (generally less than 2 ft thick) and oxidized. The 6-ft core encountered a layer of unoxidized sulfidic tailing about 20 in. thick at a depth of 3 ft (fig. 4). The sulfide zone was near the bottom of the tailings deposit, resting on stream-deposited sand and gravel in a buried wetland. Although some initial inhomogeneity may have existed in the deposition of these reprocessed tailings, they all were likely deposited as sulfidic material; the difference in chemistry between the oxidized and sulfidic tailings now likely reflects the relative mobility of metals as they were weathered and oxidized from the original sulfide minerals. We analyzed, by mixed-acid digestion and XRD, 26 subsamples from this core: 14 from the upper, oxidized zone, 8 from the sulfide zone, and 4 from the contaminated flood-plain sediment beneath the tailings. We distinguished the zones in the core by visual inspection, descriptions of the core intervals, and mineralogy of the subsamples. The oxidized zone contained no visible sulfides and no pyrite based on XRD (although traces of sphalerite were found by XRD of samples concentrated by panning). The sulfide tailings zone had visible sulfides, and pyrite was identified by XRD. Sample descriptions, mineralogy by XRD, and concentrations of selected elements in mixed-acid digestions are in table 1 of Cannon and others (this volume).

The analyses for silver, lead, copper, zinc, cadmium, and arsenic are summarized in the box plot in figure 5. The median values are instructive to demonstrate the relative mobilities of the elements. The median silver values for the oxidized and the sulfide tailings were nearly identical (67 ppm vs. 70 ppm). This indicates that silver was not mobile in this surficial weathering environment. Lead shows a 33 percent decrease from the sulfide to the oxidized zone (15,000 ppm

Table 2. Site numbers, names, pH of passive leach, net acid production (NAP), sum of five trace elements (As+Cd+Cu+Pb+Zn) in both leaches; iron, sulfate, and specific conductance of EPA-1312 leach, and classification scores of wastes by Method 1 and Method 2.

Site	Site No. and name	pH, passive leach standard units	NAP, lb/ton	Specific conductance, 1312 leach µS/cm	Sulfate, 1312 leach mg/L	Sum of metals, passive leach µg/L	Sum of metals, 1312 leach µg/L	Dissolved iron, 1312 leach µg/L	Rank by Method 1 scale 1-9	Rank by Method 2 scale 3-10
41	Enterprise mine	3.75	12	106	16	100	330	190	5	5
17	Buckeye mine	3.33	42	240	44	2,500	11,000	1,700	8	10
		3.25	10	210	37	13,000	13,000	1,200	9	9
18	Bullion mine	2.94	34	597	120	4,100	5,700	9,700	8	10
		3.08	36	315	130	6,000	7,100	5,400	9	10
		3.74	8	230	85	3,600	5,400	130	7	8
		3.62	8	107	21	42	190	120	4	3
		3.92	6	60	8.8	150	480	210	4	4
		3.90	6	61	7.9	230	650	360	5	5
15	Boulder Chief mine	6.78	0	119	15	41	66	80	3	5
		3.23	12	333	67	6,600	11,000	1,000	9	9
142	Waldy mine	6.60	4	202	55	27	28	33	2	4
94	Morning Marie mine	3.65	6	96	18	100	200	22	4	4
29	Cracker mine	3.46	26	185	47	7,800	14,000	34	9	8
33	Daily West mine	2.75	68	1,090	280	36,000	34,000	22,000	7	8
119	Sirius mine	3.33	16	240	55	2,000	9,400	620	8	7
31	Crystal mine	5.93	0	87	31	750	710	190	6	5
		4.76	2	60	24	270	260	26	5	5
		3.84	8	78	29	1,800	3,100	37	6	6

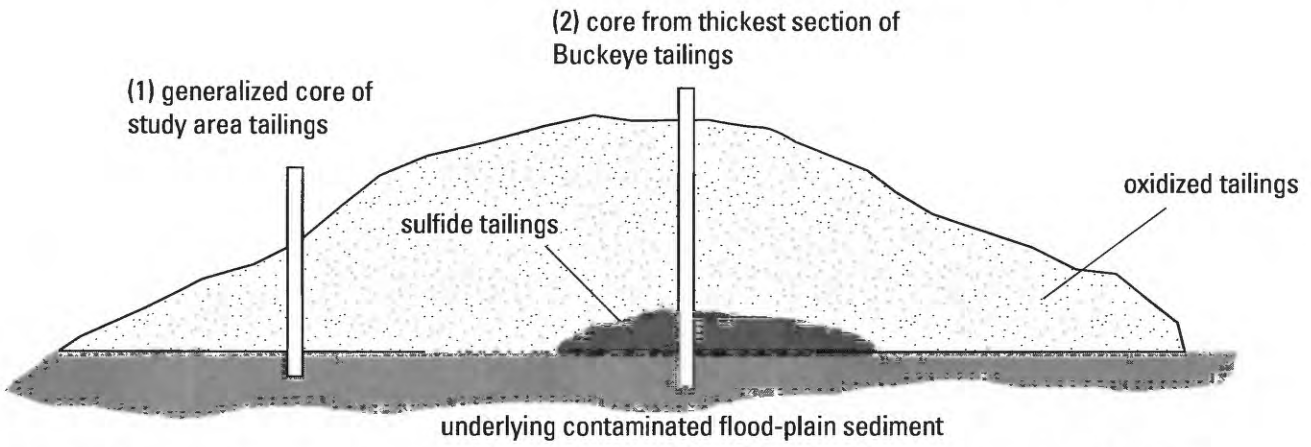

Figure 4. Generalized cross section of tailings sampled by cores at Buckeye flotation mill. Tailings consisted predominantly of oxidized waste material and were sampled as per core number 1. At thickest part of Buckeye flotation tailings, a sulfide layer remaining at depth was sampled as per core number 2. Copper, zinc, cadmium, and arsenic can migrate and are removed by annual flooding of the site during spring runoff (Cannon and others, this volume).

vs. 10,000 ppm). This means that some lead was lost from the oxidized tailings (Cannon and others, this volume). Note that anglesite (lead sulfate, a weathering product) was present in all of the oxidized tailing samples.

Copper, zinc, and cadmium all show dramatic differences between the sulfide and oxidized tailings zones. The median copper value for the sulfide tailings was 2,800 ppm, whereas it was only 88 ppm in the oxidized tailings. The median copper value from a premining baseline core taken at site 7B from the meadow south of Basin Creek was 29 ppm (Church, Unruh, and others, this volume, table 3); the oxidized tailings zone in our core contained barely three times the copper concentration over the local background. These results show that the majority of copper originally present in the tailings

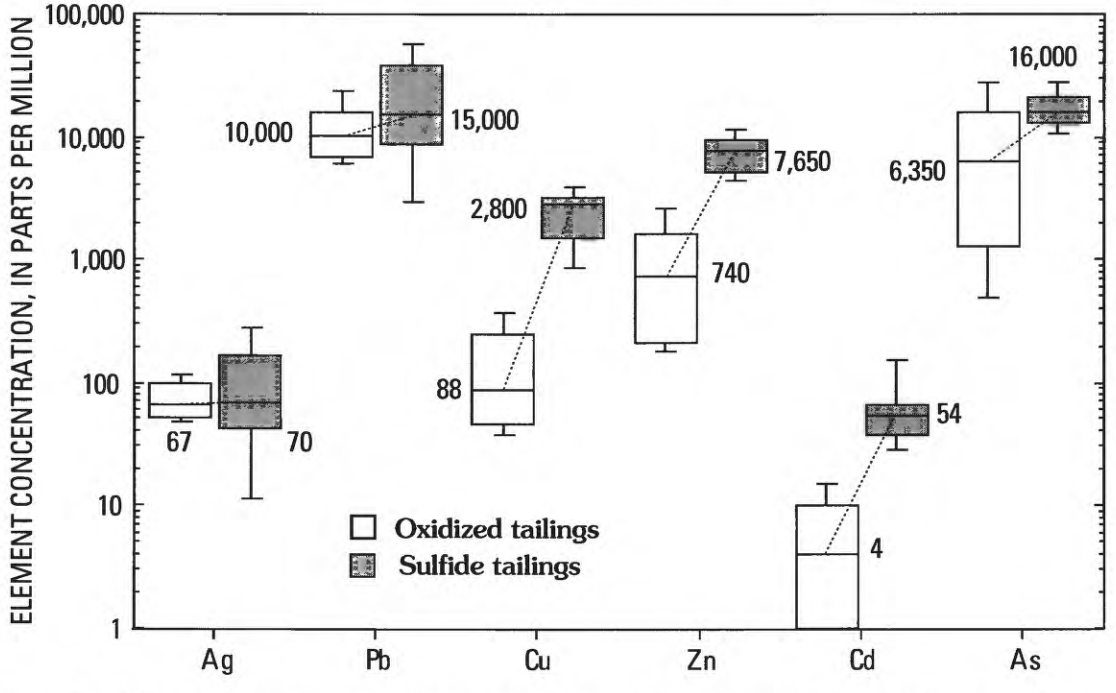

Figure 5. Box plots of silver, lead, copper, zinc, cadmium, and arsenic concentrations in tailings core from Buckeye mine site. Upper bar represents 90th percentile of population; upper line of box represents 75th percentile; middle line represents 50th percentile (median); lower line represents 25th percentile; lower bar represents 10th percentile. Numbers by the boxes are median values. Plot shows that silver is essentially immobile, lead is slightly mobile, and that copper, zinc, cadmium, and arsenic can be mobilized by near-surface weathering processes.

was leached from the oxidized zone. The median values for zinc were 7,650 ppm and 740 ppm, respectively. The zinc concentration in the oxidized tailings was only 10 percent of the concentration in the sulfide tailings, so we conclude that zinc, like copper, was weathered out of and dispersed from the upper tailings. The local background concentration for zinc, also taken from the core at site 7B, was 190 ppm. Cadmium is geochemically similar to zinc and showed a similar response. The median value for cadmium in the sulfide tailings was 54 ppm, whereas in the oxidized tailing it was 4 ppm. Similar to zinc, the cadmium concentration in the oxide tailings zone was about 10 percent the concentration contained in the sulfide tailings zone. It is important to note that the trace-element concentrations in the sulfide tailings zone probably do not represent the original concentrations, as some losses from weathering may have occurred in the sulfide tailings zone as well. For example, anglesite (lead sulfate, a weathering product) was also present in most of the sulfide tailings subsamples, indicating that weathering processes were active in the subsurface sulfide tailings zone.

Arsenic concentrations in the oxidized zone were highly variable, but the median value was lower than in the sulfide zone. The median values were 6,350 and 16,000 ppm, respectively. The lowest concentration of arsenic in the oxidized tailings was only 500 ppm. Concentrations of arsenic in the contaminated flood-plain sediment below the sulfide tailings were relatively high (about 2,000 ppm). Together, these observations suggest that much but not all of the arsenic had been leached from the oxidized tailings, that arsenic was somewhat mobile in the sulfidic tailings, and that some of the mobilized arsenic accumulated in the flood-plain sediment.

These geochemical results demonstrate two important issues. First, surface material on mine-waste piles has undergone weathering by surface processes. Second, collection of surface samples leads to analyses that underestimate the deposit-related metals in the mine-waste dumps (except silver, which appears to be chemically immobile).

Classification Schemes for Mine-Waste Piles

One of the objectives of collecting and studying mine waste from the study area was to develop and apply a classification method, based on chemical and physical parameters, to help land managers prioritize mine-waste sites in terms of removal or remediation. Values for total-metal content, water-soluble metals, mineralogy, net acid production, pH of leach solutions, and size all are important in describing a particular material's tendency to affect water that it contacts. Over the course of the study, we developed two methods to classify mine-waste piles in the Boulder River watershed study area.

The first method (Method 1) was described in Desborough and Fey (1997) and utilized the pH of the passive leach solutions, the sum of dissolved deposit-related elements (ΣDE) (ΣAs+Cd+Cu+Pb+Zn in µg/L) in the passive leach solutions, and the estimated size (in tons) of the waste dump. Four classes were defined for the acidity component: for pH > 6.0, class 0; for pH between 4.5 and 6.0, class 1; for pH between 3.5 and 4.5, class 2; and for pH <3.5, class 3. Similarly, for the sum of dissolved elements, four classes were defined: for ΣDE <500 µg/L, class 0; for ΣDE between 500 and <1,000 µg/L, class 1; for ΣDE between 1,000 and 5,000 µg/L, class 2; and for ΣDE >5,000 µg/L, class 3. The size factor has three classes: for size <500 tons, class 1; for size between 500 and 2,500 tons, class 2; and for size >2,500 tons, class 3. These size classes were defined for this study; other watersheds may have waste piles with far greater ranges in size. The sum of the class numbers for each parameter (pH, ΣDE, size) gives a classification number between 1 (low potential for water-quality degradation) and 9 (high potential). The classification numbers based on Method 1 for the waste piles are listed in table 2.

A second ranking method (Method 2) has been developed that considers the effects of (1) the net acid production (NAP), (2) the sum of dissolved deposit-related elements (also ΣAs+Cd+Cu+Pb+Zn) in the leach solution following the EPA-1312 leach method, (3) the concentration of dissolved iron in the EPA-1312 solution, and (4) estimated size. This ranking method was described in Fey, Desborough, and Church (2000). The approach is similar to Method 1, which utilized element concentration data from the passive leach. The difference is that Method 2 does not consider the pH of the passive leach solution (a short-term snapshot of hydrogen ion activity mostly resulting from the dissolution of water-soluble salts) as the "acidity parameter," but rather utilizes the total long-term net acid production (NAP), as determined by the hydrogen-peroxide oxidation of sulfides in the sample.

There are two chemical components to Method 2: a plot of ΣDE from the EPA-1312 leach solutions against the NAP, and a plot of dissolved iron from the EPA-1312 leach solutions against the NAP. A plot of the NAP, expressed as lb $CaCO_3$ per ton, versus the ΣDE from the EPA-1312 leach solutions was developed from data for about 110 mine-waste samples collected from the Animas River study area in Colorado, and the Boulder River watershed study area (Fey, Desborough, and Church, 2000). Only the samples from the Boulder River study area are shown here (fig. 6). We delineated four classes of samples: Group 1, which has low NAP (<20 lb $CaCO_3$/ton) and <1,000 µg/L ΣDE; Group 2, which has low NAP and moderate ΣDE (between 1,000 and 5,000 µg/L); Group 3, which has low NAP and high ΣDE (>5,000 µg/L); and Group 4, which has high NAP (>20 lb $CaCO_3$/ton) and high ΣDE (>5,000 µg/L). No samples plotted in the lower right-hand area in the diagram of high NAP and low ΣDE.

The second chemical indicator considered in Method 2 was the dissolved iron content of the EPA-1312 leach solutions. Iron is an important constituent in the mine wastes and the leach solutions because considerable amounts of pyrite (or its oxyhydroxide weathering products) are found in many mine wastes. Fey, Desborough, and Church (2000) showed that samples from the Boulder River watershed study area can

contain as much as 0.05 percent of their iron in water-soluble form. Dissolved iron in water results in well-defined acute and chronic toxicity, regardless of alkalinity (Colorado Department of Health, 1984). Therefore, we added dissolved iron as one of parameters in the ranking criteria. Because the dissolved iron concentration of a leachate can overwhelm the signal from the ΣDE, we plot it on a separate figure (fig. 7). We classified the data points into three groups: Group 1, having NAP less than 20 lb $CaCO_3$/ton and dissolved iron less than 1,000 µg/L; Group 2, having NAP less than 20 lb $CaCO_3$/ton and dissolved iron greater than 1,000 µg/L; and Group 3, having NAP greater than 20 lb $CaCO_3$/ton and dissolved iron greater than 1,000 µg/L. Figure 7 shows these classes. Only one out of twenty-one samples plotted in the lower right hand portion of the diagram, representing the unusual condition of relatively high acidity and a low dissolved iron concentration. This sample was from the Cracker waste pile.

The size classes were the same as for Method 1: for size <500 tons, class 1; for size between 500 and 2,500 tons, class 2; and for size >2,500 tons, class 3. Figures 6 and 7 combine to show that if the NAP is above 20 lb $CaCO_3$/ton, the mine waste is likely to produce high concentrations of dissolved trace elements in leach solutions.

Method 2 sums the class numbers for the sum of dissolved metals and NAP (four classes), dissolved iron and NAP (three classes), and the size (three classes). The sum of these three criteria then yields an estimate of a mine-waste pile's potential to adversely affect water quality, with a rank of 3 indicating little potential and a rank of 10 indicating the highest potential. The classification numbers based on Method 2 for the waste piles are listed in table 2.

Classification of Mine-Waste Piles in the Boulder River Watershed

We apply here both classification schemes to the bulk surface samples that we collected from mine sites in the Boulder River watershed study area (fig. 8). The sample sites are depicted with symbols of three different colors, representing the relative potential for the materials to affect water quality.

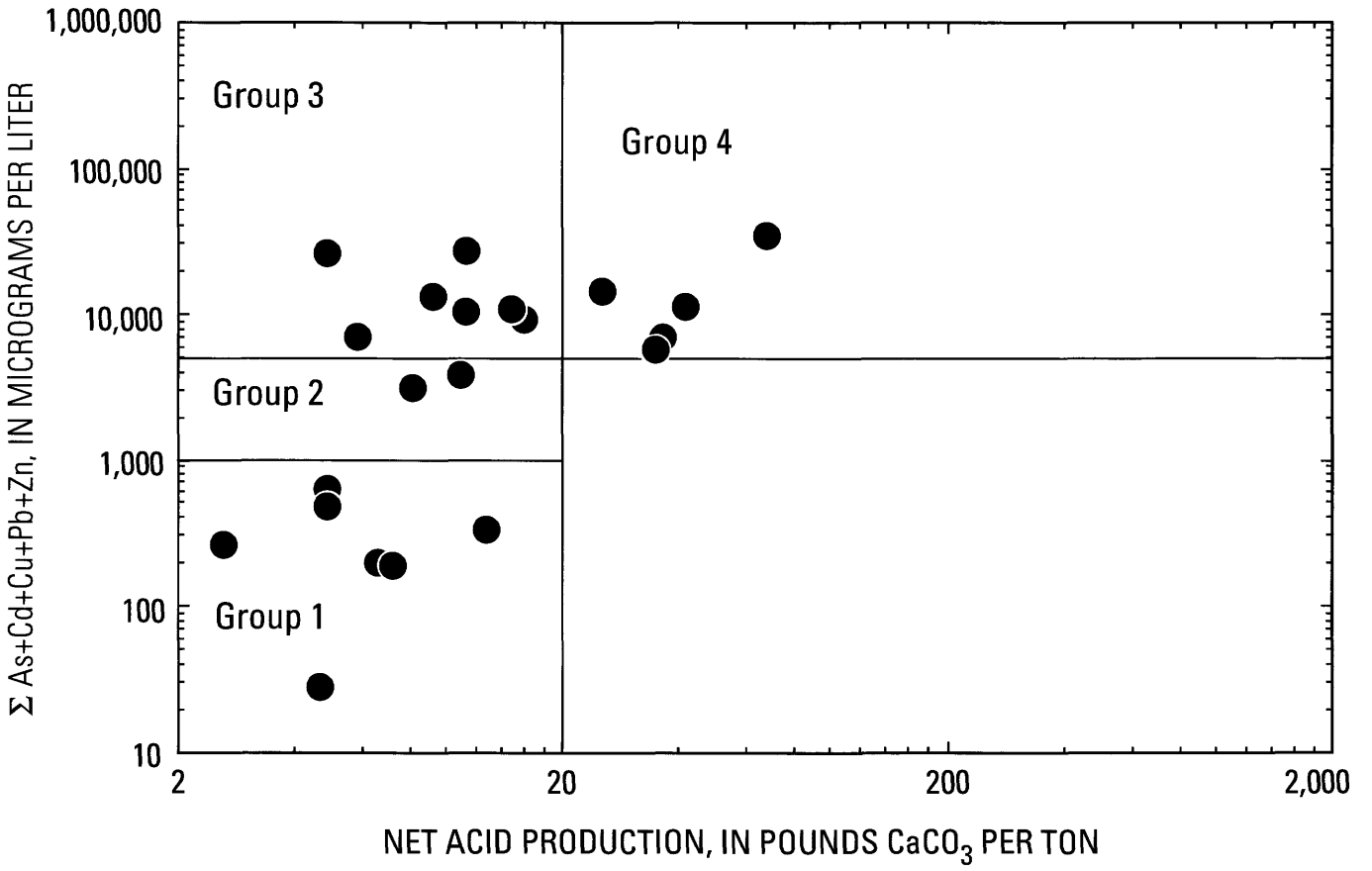

Figure 6. Net acid production (NAP) of waste samples versus the sum of dissolved concentrations of As+Cd+Cu+Pb+Zn from EPA-1312 leach solutions. NAP is a measure of long-term acid producing potential of waste material. Samples with NAP greater than 20 lb/ ton $CaCO_3$ equivalent generally have the sum of metals greater than 5,000 µg/L for mine wastes from the type of polymetallic vein deposit in the Boulder River watershed.

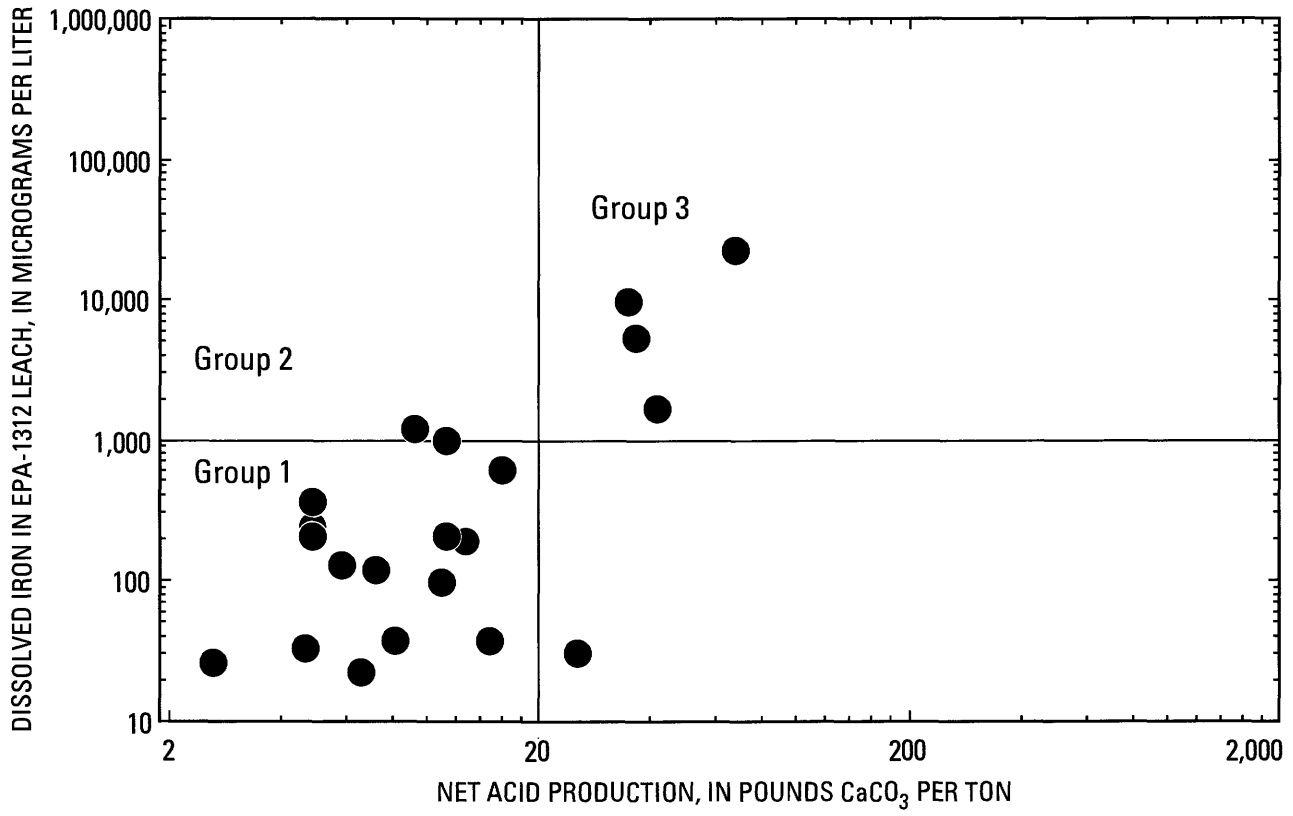

Figure 7. Net acid production (NAP) of waste samples versus dissolved iron from EPA-1312 leach solutions. Samples with NAP greater than 20 lb/ ton $CaCO_3$ equivalent generally have dissolved iron greater than 1,000 µg/L for wastes from the type of polymetallic vein deposit in the Boulder River watershed.

In this illustration, the size of the waste pile has been incorporated into the color of symbol used.

The classification results reveal that the Buckeye mine-waste pile had the highest potential for affecting the nearby environment. With Method 1 this pile scored 8 on a scale of 1 to 9. On the basis of Method 2 the Buckeye mine-waste pile scored 10 on a scale of 3 to 10. Flotation tailings from the reprocessed gravity tailings of the Buckeye mine, deposited on the north side of Basin Creek, also presented a significant problem. These tailings scored 9/9 and 8/10, respectively, on the basis of Method 1 and Method 2. The waste pile at the Enterprise mine, near the Buckeye mine/mill complex, scored a moderate 5/9 and 5/10.

At the Bullion mine, there were three large waste piles, termed the upper, middle, and lower waste sites. The upper and middle waste piles scored high. On the basis of Method 1, they scored 8/9 and 9/9; using Method 2, both scored high, 10/10. The lower waste pile of the Bullion mine complex was the largest, and also scored high. Its classification scores were 7/9 and 8/10. During a rainfall event on August 2, 1999, overland flow was observed at the Bullion mine site. After an initial decrease, dissolved zinc concentrations increased by about three fold in the Bullion Mine tributary, presumably from the dissolution of easily soluble zinc salts (Lambing and others, this volume, Chapter D7). This observation confirms that mine-waste piles can have a direct, short-term effect on water quality in receiving streams.

In addition to the three large waste piles, two former tailings impoundments were farther downstream along Bullion Mine tributary. These tailings were different from the unmilled mine wastes in the three large dumps; the difference is reflected in the classification scores. The tailings had been leached of much of their original metal content (table 2), and so their classification scores were moderate. The upper tailings impoundment scored 4/9 and 4/10, and the lower tailings impoundment scored 5/9 and 5/10. A small (500 ton) dump near the two former tailings impoundments had classification scores of 4/9 and 3/10.

Along Uncle Sam Gulch, waste from ore bins upstream from the adit at the Crystal mine scored moderately high (6/9 and 6/10). Material collected from the large exploration cut in the hilltop above the mine had very low acidity and low leachable metals. The scores for this surface material were 6/9 and 6/10 (east side) and 5/9 and 5/10 (west side). After a rainfall event on August 4–5, 1999, zinc concentrations in Uncle Sam Gulch increased by a factor of about 1.8 (Lambing and others, this volume).

The Sirius mine had low acidity, moderately high summed metal content, and low dissolved iron. Its scores were 8/9 and 7/10. The Cracker mine dump was close to Cataract

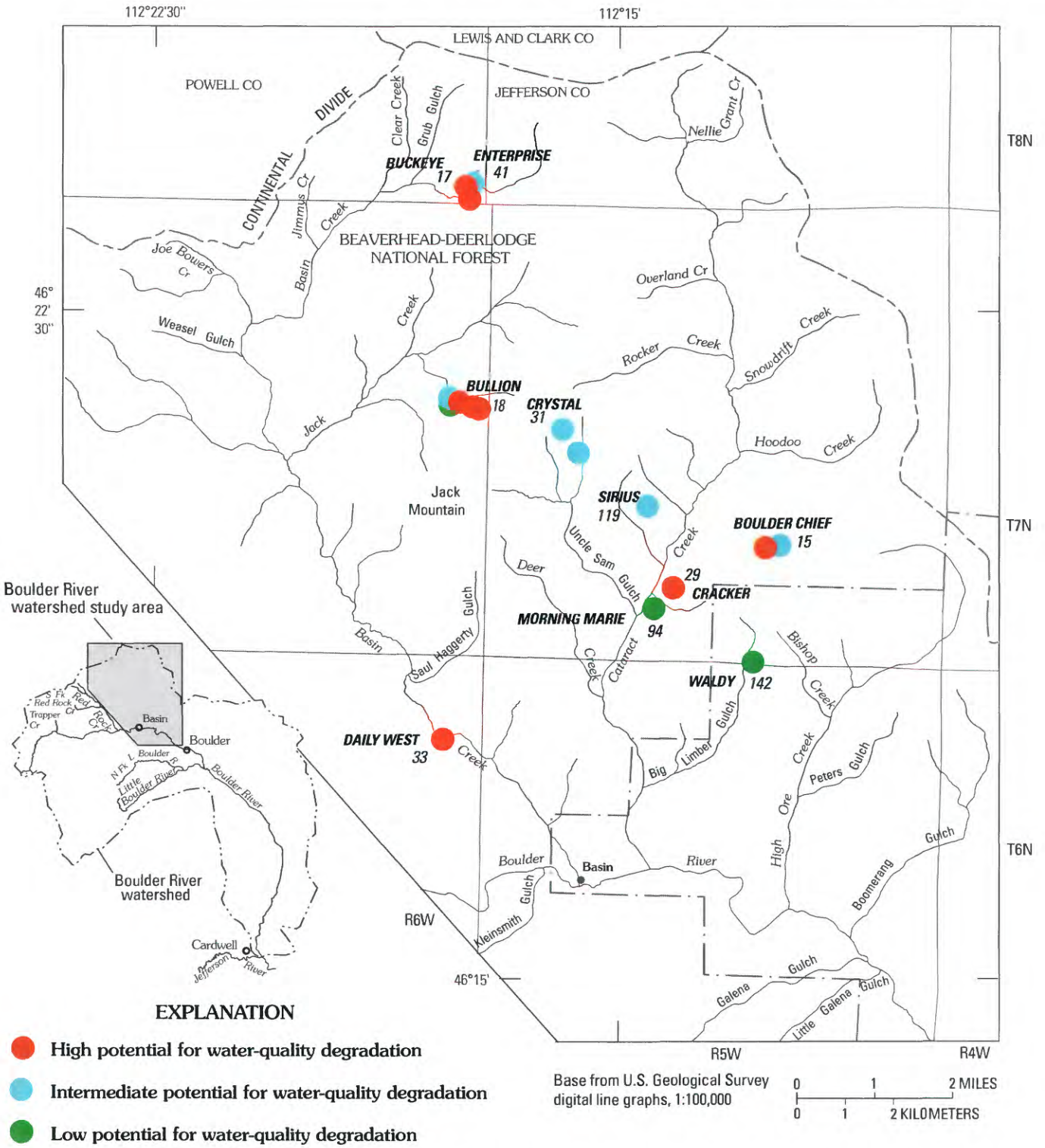

Figure 8. Boulder River watershed study area with mine-waste piles ranked by water-quality degradation potential. Green sites, low potential; blue sites, intermediate potential; red sites, highest potential for water quality degradation. This ranking using chemical data and size does not incorporate nonquantified data such as presence of draining adits, surface water in contact with dumps, or distance to streams. Sites numbered as in Martin, this volume.

Creek, contained moderately large tonnage (4,000 tons), and had low dissolved iron but high summed dissolved trace elements. The classification scores were 9/9 and 8/10. The Daily West dump, despite its small size, has the most available soluble acid and metals of any of the wastes studied in this report. In addition, the waste pile is located in the flood plain of Basin Creek. The classification scores were high (7/9 and 8/10) but would have been higher if the dump were larger.

The waste from below the adit of the Boulder Chief mine was classified high, with scores of 9/9 and 8/10. This site was situated more than ½ mi from the nearest first-order tributary, and Cataract Creek was more than 1 mi away. However, the metal-loading study for Cataract Creek detected input from the Boulder Chief mine (Kimball and others, this volume, Chapter D6).

The waste piles from both the Morning Marie (Cataract Creek) and Waldy (Big Limber Gulch) mines were small, and had low acidity, low dissolved summed metals, and low dissolved iron. The scores from the two classification methods were 4/9 and 4/10 for the Morning Marie waste pile and 2/9 and 4/10 for the Waldy waste pile.

An important factor not included in this numerical ranking model is the proximity to a stream of a particular waste dump. Assigning a numerical value to this factor is difficult, as several aspects may influence the severity of the impact from waste material. Water draining from an adit and over a waste pile, or surface water flowing over or through the waste and directly into a nearby creek constitutes a direct flow path for impact of that waste pile on stream water. This should be a primary, non-numerical factor to be considered in ranking waste dumps for removal. Proximity to a stream or body of water is also important, as storm or snowmelt runoff can easily transport acid and dissolved metals or metal-sorbing colloidal materials directly to surface water. In two studies of waste-material impact on surface water in the Animas River, Colo., watershed, Nash (1999a, 1999b) emphasized the importance of field observations of these kinds of flow paths. Knowledge of local ground water, the influence of fracture control on ground-water flow, and waste permeability is also important.

Summary and Conclusions

Metal-mining waste was collected by bulk surface sampling at 10 sites in the Boulder River watershed study area. Mineralogical analyses revealed that 80 percent of the samples contained anglesite and jarosite. Primary sulfide minerals were rare: only trace amounts of sphalerite and no arsenopyrite, although these minerals had been reported as abundant by early reports. The minerals goslarite (a zinc sulfate) and scorodite (iron arsenate) were found in the field. Mineralogical and whole-sample analyses of core samples from the thickest part of the flotation tailings at the Buckeye site demonstrated the relative mobilities of six deposit-related elements over a 60+ year period of annual weathering cycles. Silver is essentially chemically immobile, lead is nearly immobile, and copper, zinc, cadmium, and arsenic can be mobilized in the surface weathering environment.

Two classification methods for mine-waste piles were developed. These schemes were based on geochemical data derived from two leach methods and waste-pile size. The geochemical parameters were pH and soluble metal content (As+Cd+Cu+Pb+Zn) from a passive leach, and NAP, soluble metal and soluble iron content from an EPA-1312 leach. Applying these methods to the Boulder River watershed study area reveals that waste piles from the Buckeye mine/mill, the Bullion mine/mill, the Daily West mine, the Cracker mine, and the Boulder Chief mine had high potential for environmental degradation. Wastes from the Crystal mine and the Sirius mine had an intermediate potential, and wastes from the Morning Marie and the Waldy mines had low potential for environmental degradation.

References Cited

Billingsley, P., and Grimes, J.A., 1918, Ore deposits of the Boulder batholith: American Institute of Mining and Metallurgical Engineers Transactions, v. 58, p. 284–361.

Briggs, P.H., 1996, Forty elements by inductively coupled-plasma atomic emission spectrometry, *in* Arbogast, B.F., ed., Analytical methods manual for the Mineral Resources Program: U.S. Geological Survey Open-File Report 96–525, p. 77–94.

Briggs, P.H., and Fey, D.L., 1996, Twenty-four elements in natural and acid mine waters by inductively coupled plasma-atomic emission spectrometry, *in* Arbogast, B.F., ed., Analytical methods manual for the Mineral Resource Surveys Program, U.S. Geological Survey: U.S. Geological Survey Open-File Report 96–525, p. 95–101.

Colorado Department of Health, 1984, Basic standards and methodologies: 3.1.0 (5CCR 1002.8).

Crock, J.G., Lichte, F.E., and Briggs, P.H., 1983, Determination of elements in National Bureau of Standards geologic reference materials SRM 278 obsidian and SRM 688 basalt by inductively coupled plasma-atomic emission spectroscopy: Geostandards Newsletter, v. 7, p. 335–340.

Desborough, G.A., and Fey, D.L., 1997, Preliminary characterization of acid-generating potential and toxic metal solubility of some abandoned metal-mining related wastes in the Boulder River headwaters, northern Jefferson County, Montana: U.S. Geological Survey Open-File Report 97–478, 21 p.

Fey, D.L., Desborough, G.A., and Church, S.E., 2000, Comparison of two leach procedures applied to metal-mining related wastes in Colorado and Montana and a relative ranking method for mine wastes, *in* ICARD 2000; Proceedings of the Fifth International Conference on Acid Rock Drainage, Volume 2: Society for Mining, Metallurgy, and Exploration, Inc., p. 1477–1487.

Fey, D.L., Desborough, G.A., and Finney, C.J., 2000, Analytical results for total-digestions, EPA–1312 leach, and net acid production for twenty-three abandoned metal-mining related wastes in the Boulder River watershed, Northern Jefferson County, Montana: U.S. Geological Survey Open-File Report 00–114, 17 p.

Fey, D.L., Unruh, D.M., and Church, S.E., 1999, Chemical data and lead isotopic compositions in stream-sediment samples from the Boulder River watershed, Jefferson County, Montana: U. S. Geological Survey Open-File Report 99–575, 147 p.

Lapakko, K., and Lawrence, L.W., 1993, Modification of the net acid production (NAP) test, *in* Proceedings of the Seventeenth Annual British Columbia Mine Reclamation Symposium, Port Hardy, British Columbia, May 4–7, 1993: p. 145–159.

Marvin, R.K., Metesh, J.J., Bowler, T.P., Lonn, J.D., Watson, J.E., Madison, J.P., and Hargrave, P.A., 1997, Abandoned-inactive mines program, U.S. Bureau of Land Management: Montana Bureau of Mines and Geology Open-File Report 348, 506 p.

Metesh, J.J., Lonn, J.D., Duaime, T.E., and Wintergerst, Robert, 1994, Abandoned-inactive mines program, Deerlodge National Forest—Volume I, Basin Creek drainage: Montana Bureau of Mines and Geology Open-File Report 321, 131 p.

Metesh, J.J., Lonn, J.D., Duaime, T.E., Marvin, R.K., and Wintergerst, Robert, 1995, Abandoned-inactive mines program, Deerlodge National Forest—Volume II, Cataract Creek drainage: Montana Bureau of Mines and Geology Open-File Report 344, 201 p.

Nash, J.T., 1999a, Geochemical investigations and interim recommendations for priority abandoned mine sites on USDA Forest Service lands, Mineral Creek watershed, San Juan County, Colorado: U.S. Geological Survey Open-File Report 99–170, 40 p.

Nash, J.T., 1999b, Geochemical investigations and interim recommendations for priority abandoned mine sites, BLM lands, Upper Animas River watershed, San Juan County, Colorado: U.S. Geological Survey Open-File Report 99–323, 45 p.

Roby, R.N., Ackerman, W.C., Fulkerson, F.B., and Crowley, F.A., 1960, Mines and mineral deposits (except fuels), Jefferson County, Montana: Montana Bureau of Mines and Geology Bulletin 16, 122 p.

Rossillon, M., and Haynes, T., 1999, Basin Creek Mine Reclamation Heritage Resource Inventory 1998, Volume I: Butte, Mont., Renewable Technologies, Inc., 126 p. [Submitted to Beaverhead-Deerlodge National Forest, Dillon, Montana.]

Scott, K.M., 1987, Solid solution in, and classification of, gossan-derived members of the alunite-jarosite family, northwest Queensland, Australia: American Mineralogist, v. 72, p. 178–187.

Smith, K.S., Ramsey, C.A., and Hageman, P.L., 2000, Sampling strategy for the rapid screening of mine-waste dumps on abandoned mine lands, *in* ICARD 2000; Proceedings of the Fifth International Conference on Acid Rock Drainage, Volume 2: Society for Mining, Metallurgy, and Exploration, Inc., p. 1456–1462.

U.S. Environmental Protection Agency (USEPA), 1986, Test methods for evaluating solid waste, Volumes I and II (SW–846) Third Edition, November, Updates are available through Revision 2B, published April 4, 1995.

Trace Elements in Water in Streams Affected by Historical Mining

By David A. Nimick and Thomas E. Cleasby

Chapter D5 of
Integrated Investigations of Environmental Effects of Historical Mining in the Basin and Boulder Mining Districts, Boulder River Watershed, Jefferson County, Montana
Edited by David A. Nimick, Stanley E. Church, and Susan E. Finger

Professional Paper 1652–D5

U.S. Department of the Interior
U.S. Geological Survey

Contents

Figures

Tables

Chapter D5
Trace Elements in Water in Streams Affected by Historical Mining

By David A. Nimick and Thomas E. Cleasby

Abstract

Investigation of trace elements in water of the Boulder River watershed provided information to (1) delineate stream reaches having elevated concentrations of trace elements, (2) determine sources of the trace elements, (3) understand the transport of dissolved and particulate forms of trace elements, (4) evaluate the potential for trace-element toxicity to biota, and (5) establish a long-term water-quality monitoring plan. Water-quality data collected in and near the watershed during 1996–2000, as well as historical data, were used for the assessment.

Concentrations of trace elements associated with ore deposits in the watershed varied greatly, with the highest concentrations occurring in small streams downstream from a few inactive mines. Cadmium, copper, lead, and zinc concentrations in streams affected by historical mining commonly were higher than aquatic-life standards. Concentrations exceeded acute aquatic-life standards by as much as 200-fold. Few stream reaches had acidic pH (less than 6.5). Of all of the inactive mines in the watershed, the Bullion, Crystal, and Comet mine sites produced most of the trace-element load to the watershed and had the largest effect on trace-element concentrations in streams. Cataract Creek, which drains the Crystal mine, contributed larger dissolved trace-element loads to the Boulder River than either Basin or High Ore Creeks, which drain the Bullion and Comet mines, respectively.

Introduction

More than 140 inactive mines and 15 mills are scattered throughout the Basin, Cataract, and High Ore Creek basins in the Boulder River watershed study area (fig. 1), but knowledge about the individual or cumulative effects of these sites on streams in the watershed is limited. Water is the main transport mechanism for trace elements derived from historical hard-rock mining areas and serves as the habitat for aquatic organisms that may be exposed to potentially toxic concentrations. Therefore, assessing the distribution, magnitude, and sources of trace elements in water is an integral component of any study of the environmental effects on aquatic ecosystems in watersheds that contain inactive mines. Understanding the distribution and magnitude of trace elements in streams throughout an affected watershed is important for prioritizing remediation activities and establishing restoration goals. Characterization of trace-element sources and pathways is essential for planning effective and cost-efficient remediation. Integrating water-quality data with streambed-sediment data and biological measures of aquatic health then allows assessment of the vulnerability of aquatic ecosystems to the effects of historical mining in the study area.

Purpose and Scope

This report assesses the concentrations, sources, and loads of mining-related trace elements in streams draining historical mining areas in the Boulder River watershed near the town of Basin in southwestern Montana. Trace elements of particular interest were those which are associated with the ore deposits in the watershed and which can pose a toxic risk to aquatic life. Trace-element concentrations and associated physical and chemical data were determined for water samples from 64 sites during 1996–2000. These data are presented in the database (Rich and others, this volume, Chapter G and accompanying CD-ROM). In addition, we utilized water-quality data presented by Kimball and others (this volume, Chapter D6) and historical water-quality data (Nimick and Cleasby, 2000, table 4).

To help us characterize environmental conditions in streams of the Boulder River watershed, we set goals of determining the seasonal and spatial distribution of trace-element concentrations in surface water throughout the watershed, and then identifying the significant mining- and nonmining-related source(s) of those trace elements. Source areas were determined from concentration gradients showing downstream changes in trace-element concentrations in water and from trace-element loads revealing areas where major increases occurred in the mass of elements transported. We distinguished mining- and nonmining-related sources of trace

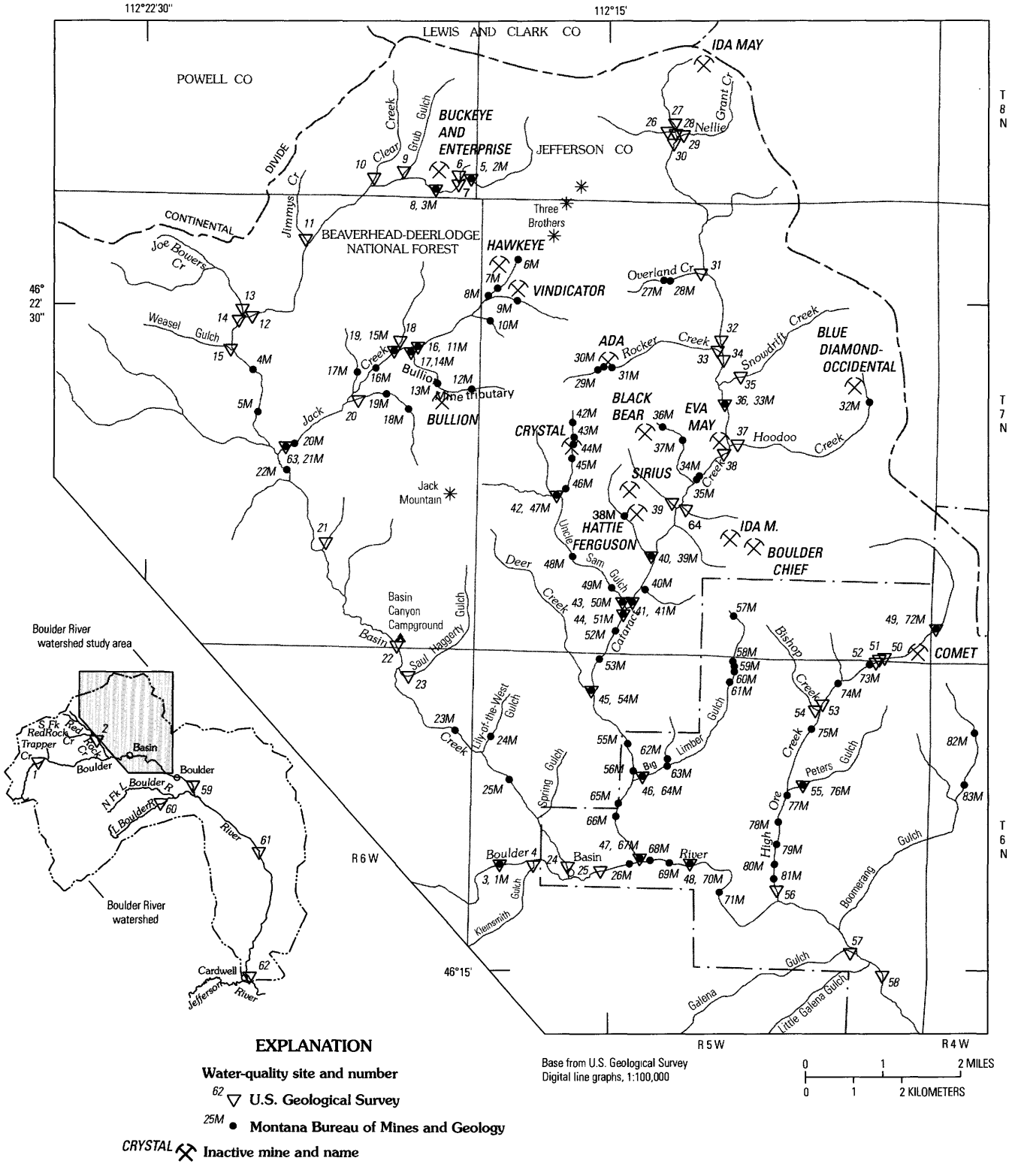

Figure 1. Water-quality sites and selected inactive mines in Boulder River watershed study area, Montana.

elements in mineralized watersheds by comparing water-quality data to the location of mined areas and geologic units.

The water-sampling program conducted during this study had four objectives. The first objective was to determine what mining-related trace elements occurred at concentrations that were potentially toxic to aquatic organisms. To accomplish this objective, we analyzed samples from selected sites during the early part of the study for a large suite of trace elements. The second objective was to characterize the range of concentrations of the potentially toxic trace elements throughout the watershed both spatially and seasonally. To accomplish this objective, samples were collected once during high-flow conditions and once during low-flow conditions at many sites throughout the watershed. To efficiently evaluate many sites in the watershed, samples from some sites were analyzed only for total-recoverable zinc, because zinc is associated with the watershed's ore deposits and occurs more frequently in detectable concentrations in surface water than the other deposit-related trace elements. The third objective was to characterize trace-element loads at five key sites in the watershed during a complete hydrologic cycle. For this objective, samples were collected 13 times during 1996–97 over a wide range of flow conditions. The fourth objective was to establish a water-quality monitoring program to determine long-term seasonal and annual variations near areas where remediation activities had been planned by State and Federal agencies. This last part of the water-sampling program was initiated in 1997 before any remediation started, so that pre-remediation conditions could be documented. Sampling at five key sites in the watershed continued during 1998–2000 but at a lower frequency than in 1997. Long-term monitoring sites also were established downstream from the Bullion, Crystal, Comet, and Buckeye mines as well as the reach of Cataract Creek between Uncle Sam Gulch and Hoodoo Creek. Results for this fourth objective are reported in this chapter for the five key sites as well as for the Comet mine by Gelinas and Tupling (this volume, Chapter E2) and for the Buckeye and Enterprise mines by Cannon and others (this volume, Chapter E1).

Trace elements of particular concern for this study were those typically associated with polymetallic veins (Becraft and others, 1963; Ruppel, 1963), which were the primary rocks mined in the watershed. These trace elements include antimony, arsenic, cadmium, copper, gold, iron, lead, silver, and zinc. In contrast, trace elements that are not associated with polymetallic vein systems are called rock-forming trace elements and include chromium, strontium, vanadium, and the rare-earth elements.

Previous Investigations

The first systematic assessment of the effects of historical mining on water quality in the Boulder River watershed took place in the 1970s (summarized by Ken Knudson, consulting biologist, Helena, Mont., written commun., 1984). Results showed that trace-element concentrations were higher in High Ore Creek than in Basin or Cataract Creeks. No streamflow data were collected and therefore loads could not be calculated. In 1985, Phillips and Hill (1986) sampled 14 sites during spring runoff. Results indicated that, although concentrations were high in High Ore Creek (as noted by Knudson, written commun., 1984), the load of trace elements contributed by Cataract Creek to the Boulder River was greater than the load from High Ore Creek because of the much larger streamflow in Cataract Creek. The Montana Bureau of Mines and Geology collected water-quality samples from numerous sites throughout the watershed as part of the inventories of inactive mines completed in the mid-1990s for the USDA Forest Service (Metesh and others, 1994, 1995, 1996) and Bureau of Land Management (Marvin and others, 1997). Data from these mine-inventory reports were useful for characterizing the range and distribution of trace-element concentrations throughout the watershed because many sites were sampled.

Data Collection

Water-quality samples for this study were collected from 64 sites (fig. 1) between October 1996 and October 2000. Water-quality sites were located throughout the study area on both small and large streams and at locations upstream and downstream from selected inactive mines. We also collected samples at three sites on the Boulder River (sites 59, 61, and 62) downstream from the study area to determine the extent of trace-element enrichment from the Basin and Boulder mining districts.

Reference sites were selected in drainages that had a geologic setting similar to that of the study area except without mineralized rocks. We sampled these sites to establish a reference for water-quality comparison with mineralized areas. No sites were available in unmined, mineralized zones to indicate natural background conditions in the study area. Reference sites (fig. 1) included the Boulder River upstream from the Boulder River watershed study area (site 1), Red Rock Creek (site 2), and the Little Boulder River (site 60).

The area upstream from site 1 is underlain by Late Cretaceous plutonic rocks of the Boulder batholith as well as the Late Cretaceous Elkhorn Mountains Volcanics and Eocene Lowland Creek Volcanics (Wallace, 1987). Little historical mining took place in this area of the Boulder River watershed (Elliott and others, 1992). The areas upstream from site 2 (Red Rock Creek) and site 60 (Little Boulder River) are underlain by Late Cretaceous plutonic rocks of the Boulder batholith and the Elkhorn Mountains Volcanics (Wallace, 1987). Elliott and others (1992) did not indicate any historical mines or prospects in these two areas, but small producing historical mines did exist in the Little Boulder River basin upstream from the sampling site. However, with the exception of one placer mine, these mines and prospects are not close to the Little Boulder River.

Methods of data collection and analysis, as well as quality-assurance data, are in Nimick and Cleasby (2000).

The types of data collected included streamflow, field measurements of physical and chemical properties, suspended-sediment concentration, and analytical results for major ions, nutrients, and dissolved and total-recoverable trace elements. Streamflow was measured according to methods described by Rantz and others (1982). Water samples typically were collected from multiple verticals across the stream using depth- and width-integration methods. These methods provide a vertically and laterally discharge-weighted sample that is representative of the entire flow through the cross section of a stream. Grab samples were collected when streamflow was too low to allow use of a depth-integrating sampler. Sampling equipment consisted of standard USGS depth-integrating suspended-sediment samplers (models DH-81, DH-48, and D-74TM), which are either constructed of plastic or coated with a nonmetallic epoxy paint; both types are equipped with interchangeable nylon nozzles for sampling a wide range of stream depths and velocities.

General Water Chemistry

Without elevated trace-element concentrations, the water in almost all streams in the Boulder River watershed study area generally is not toxic to aquatic organisms and water quality would be considered good. Concentrations of dissolved solids were low (generally less than 120 mg/L), presumably because the granitic and volcanic rocks in the watershed weather relatively slowly, producing few solutes, and because ground water has a relatively short residence time in the local flow paths in the bedrock (McDougal and others, this volume, Chapter D9). Dissolved solids concentrations were higher, ranging as high as 273 mg/L, in streams such as Bullion Mine tributary, Uncle Sam Gulch, and High Ore Creek where mine-drainage effects were most pronounced.

The major-ion chemistry of streams varied depending on the geology of their drainage basins and the relative amount of mine drainage they received. The Boulder River above Kleinsmith Gulch (site 3) and the Little Boulder River (site 60) had a calcium-sodium bicarbonate type water. Basin Creek had a similar water type during high flow, but during low-flow conditions, the water was a calcium-magnesium bicarbonate-sulfate type, with the addition of sulfate indicating the effects of mine drainage. Streams that are upstream from most mining and drain the interior of the study area, such as Jack Creek above the Bullion Mine tributary, High Ore Creek above the Comet mine, and Cataract Creek above Uncle Sam Gulch, had a calcium bicarbonate type water. Cataract Creek downstream from Uncle Sam Gulch also had calcium bicarbonate type water, although the proportion of sulfate was greater than it was upstream. High Ore Creek at the mouth had calcium sulfate-bicarbonate water, showing the effects of mine drainage.

Hardness is an important property of water because the toxicity of some trace elements increases as hardness decreases. Hardness values were relatively low (12–87 mg/L) year-round in most streams throughout the study area. Values in High Ore Creek downstream from the Comet mine and Galena Gulch were higher, ranging from 44 to 180 mg/L. Hardness values typically were lowest during high flow, such as during spring runoff, owing to dilution; they were highest during low flow.

We measured the concentration of suspended sediment routinely in samples collected for this study during 1996–2000 because transport of trace elements in the particulate fraction can be important, particularly during high flow (fig. 2). Suspended-sediment concentrations typically were low (generally less than 7 mg/L) during low flow in streams both upstream and downstream of mined areas. Concentrations of suspended sediment were slightly higher in streams such as the Bullion Mine tributary (site 17), Uncle Sam Gulch (site 43), and High Ore Creek (site 56) that were most affected by mining. Low-flow suspended-sediment concentrations were as high as 15 mg/L in these streams, likely resulting from the presence of colloidal material produced during neutralization of acidic mine drainage. Suspended-sediment concentrations during high-flow conditions were higher, ranging as high as

Figure 2. Flood-plain tailings eroding at Jack Creek during snowmelt runoff upstream from site 19, May 1997.

76 mg/L in the Boulder River above Kleinsmith Gulch (site 3) and lower Basin and Cataract Creeks (sites 24 and 47). In High Ore Creek, the maximum concentration (86 mg/L) was similar except for a March 1999 sample (308 mg/L) that likely was affected by remediation activities. High-flow suspended-sediment concentrations generally were higher in the Bullion Mine tributary (site 17), Jack Creek (site 19), Uncle Sam Gulch (site 43), and the Boulder River below Little Galena Gulch (site 58), where maximum values ranged from 99 to 174 mg/L.

Water-Quality Standards

One of the most important reasons for characterizing water quality in streams affected by historical mining is to determine whether trace elements occur at concentrations that may be toxic to aquatic organisms. The relative magnitude of trace-element concentrations in water in various stream reaches can be evaluated by comparing measured concentrations with State and Federal aquatic-life standards. Except for aluminum, standards issued by the State of Montana (Montana Department of Environmental Quality, 1999) are applicable to the total-recoverable concentration of each trace element, whereas Federal standards (U.S. Environmental Protection Agency, 1999) are applicable to the dissolved concentration. Dissolved concentrations are defined by the regulatory agencies as the concentration in a 0.45-µm filtrate. For aluminum, the Montana standards are applicable to the dissolved concentration and the U.S. Environmental Protection Agency (EPA) standards are applicable to the total-recoverable (unfiltered) concentration. Aquatic-life standards for some metals (such as cadmium, copper, lead, and zinc) that are found regularly in the Boulder River watershed are dependent on hardness. Table 1 shows the range of hardness values measured in different streams in the watershed and the corresponding range of hardness-adjusted values for the State and Federal acute and chronic aquatic-life standards. In general, the lower values of the aquatic-life standards applied when streamflow was high because hardness values in the Boulder River watershed were lowest during these high-flow periods. Metals generally are more toxic to aquatic organisms than to humans. Human-health standards (Montana Department of Environmental Quality, 1999) for cadmium (5 µg/L), copper (1,300 µg/L), lead (15 µg/L), and zinc (2,100 µg/L) typically are higher than the hardness-adjusted aquatic-life standards for the watershed.

Table 1. Aquatic-life standards for selected trace elements in the Boulder River watershed.

[Abbreviations: µg/L, micrograms per liter; µm, micrometer; mg/L, milligrams per liter]

Constituent	Boulder River, Basin Creek, and Cataract Creek		High Ore Creek[1]	
	Minimum	Maximum	Minimum	Maximum
Hardness (mg/L)	12	87	44	180
	Acute aquatic-life standard (µg/L)[2]			
Aluminum[3,4]	750	750	750	750
Arsenic[3]	340	340	340	340
Cadmium	1.0/0.5	3.9/3.7	1.8/1.8	8.8/8.1
Copper	3.8/1.8	12/12	6.5/6.2	24/23
Lead	14/6.0	68/55	29/26	173/122
Zinc	37/19	106/104	60/58	197/193
	Chronic aquatic-life standard (µg/L)[2]			
Aluminum[3]	87	87	87	87
Arsenic[3]	150	150	150	150
Cadmium	0.8/0.4	2.2/2.0	1.3/1.2	3.9/3.5
Copper	2.9/1.5	8.3/8.0	4.6/4.4	15/15
Lead	0.5/0.2	2.7/2.2	1.1/1.0	6.7/4.7
Zinc	37/20	106/105	60/59	197/194

[1]Includes Galena Gulch, in which the geology is similar to High Ore Creek.

[2]The first number is the Montana aquatic-life standard (Montana Department of Environmental Quality, 1999). The second number is the EPA standard (U.S. Environmental Protection Agency, 1999). Except for aluminum, Montana aquatic-life standards refer to total-recoverable concentrations, whereas EPA aquatic-life standards refer to dissolved (0.45-µm filtration) concentrations. For aluminum, the Montana standards refer to dissolved (0.45-µm filtration) concentrations and EPA standards refer to total-recoverable concentrations. When hardness is less than 25 mg/L, the Montana standard computed for a hardness of 25 mg/L applies.

[3]Aquatic-life standards for aluminum and arsenic are not dependent on hardness. Only one value is listed because the Montana and EPA standards are the same.

[4]Montana and EPA standards for aluminum apply when pH values are between 6.5 and 9.0.

Arsenic is not as toxic to aquatic organisms as the other trace elements at similar concentrations, and human-health standards for arsenic are lower than aquatic-life standards. The Montana human-health standard of 18 µg/L (Montana Department of Environmental Quality, 1999), the EPA maximum contaminant level of 50 µg/L (U.S. Environmental Protection Agency, 1999), and the proposed maximum contaminant level of 10 µg/L are much lower than the acute and chronic aquatic-life standards for arsenic (340 and 150 µg/L, respectively).

Trace Elements in Water

We characterized the magnitude and extent of trace elements in surface water in the Boulder River watershed by systematic sampling of streams throughout the study area during a wide range of hydrologic conditions, comparing metal concentrations to aquatic-life standards, estimating annual loading of trace elements to the main streams in the watershed, and analyzing concentration data for temporal trends. We also made water-quality measurements in reference streams draining subbasins underlain by unmineralized rock of the same or similar lithologic units as those in the Boulder River watershed study area.

Water samples initially were analyzed for a broad suite of trace elements. Concentrations of some elements, such as beryllium, chromium, mercury, nickel, and silver, consistently were near or less than the minimum reporting level of the analytical laboratory or less than the applicable aquatic-life standard; routine analysis for these trace elements therefore was discontinued early in the study. Other elements, particularly the metals cadmium, copper, lead, and zinc, had concentrations greater than the applicable aquatic-life standards at many sites downstream from inactive mines. Therefore, this report focuses on these metals, as well as arsenic, which is pervasive throughout the watershed. Historical water-quality data collected during 1991–97 from inventories of inactive mines (Metesh and others, 1994, 1995, 1996; Marvin and others, 1997; summarized in Nimick and Cleasby, 2000, table 4) and other investigations also were used to characterize study-area streams.

The data described herein were collected either as part of a periodic sampling program (most of the 1996–2000 data) or as part of a one-time sampling event (most of the historical data). These types of sampling programs are designed to provide a broad overview of water-quality conditions in a watershed or a record of water quality at one or more sites over a long time period. Other water-quality sampling programs with different purposes also were conducted during this investigation of the Boulder River watershed. Although an integral part of the watershed study, results of these programs are reported elsewhere in this volume. These other sampling programs included synoptic-sampling studies of closely spaced sites along specific stream reaches where more detailed information on trace-element loading was needed (Cannon and others, this volume, Chapter E1; Kimball and others, this volume, Chapter D6) and hourly sampling during 1- to 2-day periods at selected sites to document effects of diel (24-hour) cycles or storm runoff on trace-element concentrations (Lambing and others, this volume, Chapter D7).

Ribbon Maps

Ribbon maps are used in this chapter to display the large amount of trace-element data collected and compiled during this study for water-quality sites throughout the watershed. These maps use colors to indicate the approximate range in concentration of a specific constituent in different stream reaches and different hydrologic conditions. The maps also are useful for assessing exceedances of water-quality criteria throughout the watershed (table 1). A common assessment method in some studies is to compare each trace-element concentration in a water-quality sample to a specific standard. Summarizing this type of information for many samples from multiple sites would be tedious, especially when some criteria, such as aquatic-life standards for metals, vary depending on hardness. Ribbon maps, on the other hand, provide a way to summarize and display this information if the concentration ranges used in the maps bracket values for water-quality criteria. Although the ribbon maps are less specific and less precise than tabulated data, they may be more useful for evaluating exceedances on a watershed scale. A ribbon map can be used to display the range of all the data for the constituent, only data for a specific period, or only data for specific hydrologic conditions.

Ribbon maps were constructed for arsenic, cadmium, copper, lead, and zinc concentrations in water. The color coding for each map is similar. The concentration ranges represented by each color are the same for the dissolved (0.45-µm filtration) and total-recoverable concentration maps for an individual trace element but differ among the trace elements. The only exception is for cadmium, where the concentration ranges represented by blue and green are not the same on the dissolved and total-recoverable maps because the lower minimum reporting level for the analytical method for dissolved cadmium provided more definition relative to the aquatic-life standards.

The concentration ranges depicted by color coding on the ribbon maps are considered approximate because the data were limited, most sites were sampled only once or a few times, and samples were collected over a 10-year period (1991–2000) and at different streamflow conditions. Therefore, the data likely did not represent the full range of concentrations. Similarly, concentrations at some sampling sites extended over more than one concentration range. At these sites, the median concentration value for the available data was used to designate the appropriate concentration range for the site. Minimum reporting levels for historical data were higher than for the 1996–2000 data. At sites where only historical

data less than the minimum reporting level were available, the assumption was made that concentrations at the site were in the lowest (blue) concentration range. Owing to the limited number of sampling sites, the exact location where a trace-element concentration changed from one concentration range to the next was roughly estimated based on likely dilution effects from tributary inflows; therefore, the location of these color changes is considered approximate. Despite these limitations, ribbon maps have the benefit of summarizing data from many water samples and thereby provide an overall picture of trace-element concentrations in various stream reaches of the watershed.

Separate ribbon maps were constructed for dissolved and total-recoverable trace-element concentrations because the importance of these two fractions is different during different streamflow conditions. Dissolved concentrations of some trace elements tended to be higher during low flow than during high flow because the effect of dilution is minimal during low flow. In contrast, total-recoverable concentrations tended to be higher during high flow (particularly for arsenic, copper, and lead) because trace-element-enriched streambed sediment is entrained during high flow. In addition, during low flow, little particulate or colloidal material was transported by most streams in the study area, and total-recoverable concentrations were approximately equal to the dissolved concentrations. Therefore, ribbon maps show either dissolved concentrations during low flow or total-recoverable concentrations during high flow. Because streamflow data were not available for some of the concentration data and because of the difficulty in determining whether flow was high or low for any given site in a particular year, we defined high flow as occurring during April–June and low flow during July–March. On the basis of the 58-year streamflow record for the Boulder River near Boulder (USGS streamflow-gauging station number 06033000, site 59), spring runoff (streamflow greater than 150 ft^3/s at this site) generally occurs between mid-April and June. Runoff periods during 1996–2000 are shown in Church, Nimick, and others (this volume, Chapter B, fig. 3).

For all ribbon maps, concentrations increase as the color changes from blue through green and yellow to orange and red. Reaches colored blue had concentrations either less than most water-quality criteria or less than the laboratory minimum reporting level applicable to most of the water-quality samples collected during 1996–2000. Concentration ranges represented by green and yellow were chosen to broadly represent applicable water-quality criteria. For arsenic, the applicable criteria were the Montana human-health standard (18 µg/L) and the EPA maximum contaminant level (50 µg/L). For metals, the freshwater acute and chronic aquatic-life standards (table 1) were used to define concentration ranges. Aquatic-life standards (table 1) are dependent on hardness, which generally is dependent on streamflow. Standards based on the measured hardness in the Boulder River and Basin and Cataract Creeks were used because these basins constitute most of the study area. Hardness values in High Ore Creek tended to be higher than in the other study area streams (table 1); therefore, the aquatic-life standards were somewhat higher than the color-coded values. Green reaches had concentrations within or near the range of the Montana and EPA chronic aquatic-life standards. Concentrations in the yellow reaches were higher and ranged from about the maximum of the chronic standards up to about the maximum values of the acute standards. For arsenic, green reaches had detectable concentrations less than the Montana human-health standard, and yellow reaches had concentrations between the Montana human-health standard and the EPA maximum contaminant level. For zinc, acute and chronic aquatic-life standards were nearly equal (table 1); consequently, green color-coding was not used. Orange reaches had trace-element concentrations that almost always exceeded the maximum value of the acute standard (maximum contaminant level for arsenic) and ranged up to 10 times the maximum value of this standard. Red reaches had concentrations that exceeded this standard by more than 10 times. Data used to construct the ribbon maps consisted of data for 1996–2000 collected for this study (Rich and others, this volume, Chapter G and accompanying CD-ROM) and data for 1991–97 compiled from the Ground Water Information Center database at the Montana Bureau of Mines and Geology (Nimick and Cleasby, 2000, table 4).

pH

In many mining-affected watersheds, streams have low pH values owing to acidic mine drainage. However, few stream reaches in the Boulder River watershed were acidic (fig. 3), and pH values were near-neutral to slightly alkaline everywhere except in isolated circumstances, where acid discharge from inactive mines affected small streams. The primary acidic (pH values less than 6.5) reaches were in Uncle Sam Gulch downstream from the Crystal mine and the Bullion Mine tributary (fig. 4) downstream from the Bullion mine. Rocker Creek downstream from the Ada mine also was somewhat acidic (pH of 5.8). Although other inactive mine sites had acidic drainage, the paucity of acidic stream reaches in the watershed likely results from acid-neutralizing capacity provided by mafic minerals and secondary calcite in the granitic rocks of the Boulder batholith (Desborough and Fey, 1997; Desborough, Briggs, and Mazza, 1998; Desborough and others, 1998; Desborough and Driscoll, 1998).

Trace-Element Partitioning

Trace elements transported in a stream are either dissolved or in a particulate form. This partitioning is important for studies of streams affected by mine drainage because toxicity depends greatly on the chemical form of each trace element, with the dissolved form typically being more toxic than particulate forms (Brown and others, 1974; Erickson and others, 1996). Dissolved species of trace elements are analyzed in filtered water samples whereas concentrations of particulate forms are determined by the difference between

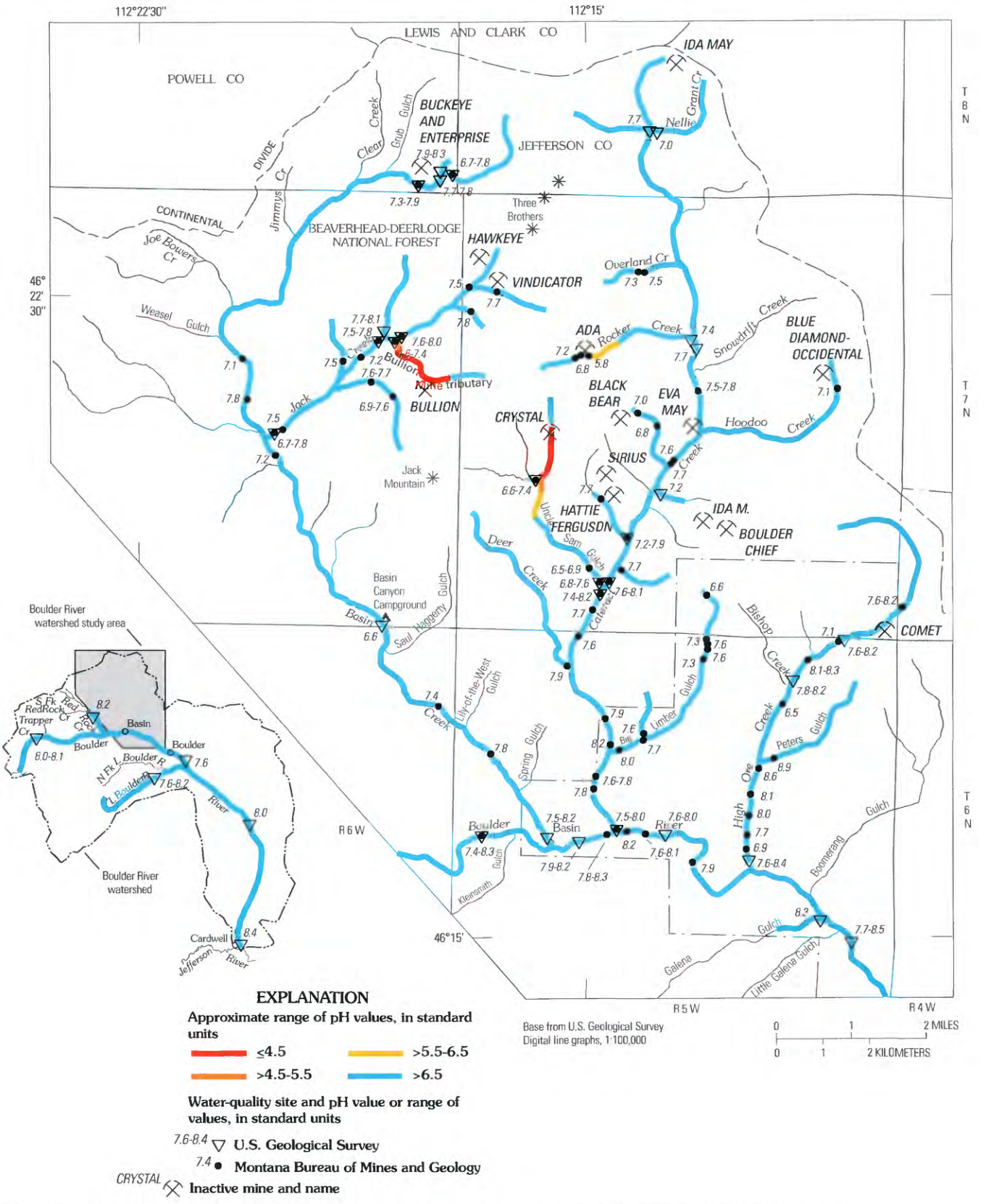

Figure 3. Approximate values of pH during low-streamflow conditions (July–March), 1991–2000. Site locations and numbers are shown in figure 1. Values of pH for Bullion Mine tributary and Uncle Sam Gulch were defined by data from Kimball and others (this volume) and are not shown.

Figure 4. Acidic water in Bullion Mine tributary, August 1998. Bullion mine is on bare hillslope (top center of photograph).

total-recoverable (unfiltered) and filtered concentrations. Dissolved species include ionic forms (for example, Zn^{2+}) and aqueous ion pairs (for example, $ZnHCO_3^+$). These forms are not retained by normal filtration, which typically uses a 0.45-µm pore-size filter, or by ultrafiltration, which typically uses a 10,000-Dalton nominal (about 0.001-µm) pore-size filter. Particulate forms include colloidal material and coarser particles that can settle to the streambed. Colloidal material is too fine to settle unless it aggregates and often is defined operationally as particles ranging in size from 0.001 to 1 µm (Rees and Ranville, 1990). Large quantities of colloidal material, typically oxyhydroxides of aluminum, iron, and manganese, form as acidic inflows are neutralized in the receiving stream (Chapman and others, 1983; Kimball and others, 1995; Schemel and others, 2000). The colloidal material aggregates, settles to the streambed, and coats the streambed material, which subsequently can be entrained and transported downstream during high flow (Church and others, 1997). Although 0.45-µm filtration is commonly used to separate the dissolved and particulate fractions in water-quality studies, trace-element concentrations in a 0.45-µm filtrate may be higher than the actual dissolved fraction because some colloids can pass through the filter (Kimball and others, 1995). Ultrafiltration can be used to determine concentrations of actual dissolved trace elements (Kimball and others, 1995). In this study, aliquots of selected water samples collected in 1996–98 were filtered through 0.45-µm and 10,000-Dalton pore-size filters to determine the possible presence and role of the colloidal fraction in transporting trace elements (D.A. Nimick, unpub. data).

The general pattern of trace-element partitioning among unfiltered samples (total-recoverable concentrations) and 10,000-Dalton and 0.45-µm filtrates from the Boulder River watershed depended primarily on the trace element and, to a lesser extent, on the proximity of the sampling site to principal source areas. Limited data indicate that aluminum and iron were almost entirely associated with colloidal or particulate material in streams both upstream and downstream from historical mining areas in the study area. Many total-recoverable aluminum and several total-recoverable iron concentrations were at least 100 µg/L or higher, whereas concentrations of aluminum and iron in ultrafiltrates typically were much lower. Limited data also indicate that cadmium and zinc partitioned mostly to the dissolved (ultrafiltrate) phase, particularly during low flow. In contrast, lead partitioned almost exclusively to the colloidal or particulate fraction during most flow conditions. Large amounts of arsenic and copper also partitioned to the solid phase but, unlike lead, arsenic and copper also were present in substantial proportions in the dissolved phase. During high flow, the partitioning of many trace elements shifted with increased proportions of each trace element in the particulate or colloidal phase because of entrainment of streambed sediment.

Differences in concentrations between 0.45-µm filtrates and ultrafiltrates varied between trace elements. Iron concentrations typically were two- to three-fold (or more) higher in 0.45-µm filtrates than in ultrafiltrates, indicating a substantial portion of colloidal iron in most streams. In contrast, concentrations of arsenic, cadmium, and zinc in 0.45-µm filtrates typically were similar or only 10–20 percent higher than in ultrafiltrates, indicating that only small amounts of these trace elements were present as colloidal material even though colloidal iron was present. Thus, concentration data for 0.45-µm filtrates generally can be assumed to be representative of dissolved arsenic, cadmium, and zinc concentrations.

Partitioning of copper in 0.45-µm filtrates and ultrafiltrates is not known because of copper contamination introduced during the 0.001-µm filtration. Partitioning of lead also is not known because concentrations in one or both filtrates typically were less than the minimum reporting level. On the basis of these evaluations, data for 0.45-µm filtrates are used in this report to define dissolved concentrations of trace elements.

Relation of Streamflow and Concentration

Streamflow is an important factor in controlling trace-element concentrations as well as the proportion of dissolved and colloidal or particulate trace elements being transported (fig. 5). In many streams, dissolved (filtered) concentrations typically decrease as streamflow increases owing to dilution. Total-recoverable concentrations typically increase during high flow because colloidal and particulate material is entrained from the streambed or eroded from streambanks. However, these general relations are not universal. Therefore, the streamflow-concentration relations need to be determined for each trace element.

The relation between streamflow and dissolved (0.45-µm filtration) trace-element concentrations is shown in figure 6 for five sites in the Boulder River watershed. At one site (site 56, High Ore Creek), data are segregated into a pre- and a post-remediation period to illustrate remediation effects on water quality. At Boulder River below Little Galena Gulch (site 58), Cataract Creek (site 47), and High Ore Creek (site 56, pre-remediation), dissolved cadmium and zinc concentrations decreased as streamflow increased during snowmelt runoff. This relation is expected because cadmium and zinc are likely to exist in the dissolved phase (Smith, 1999). For High Ore Creek (site 56) this generalization applies to the period before September 1997, when remediation activities began at the Comet mine (Gelinas and Tupling, this volume). The decrease in dissolved cadmium and zinc concentrations with increased streamflow at these three sites suggests that the sources of these metals were relatively constant, for example from ground-water or adit discharge, as opposed to leaching of mine wastes or tailings either in piles or in fluvial deposits, where loading would be expected to increase during snowmelt or storm runoff. This relation did not hold for Boulder River above Kleinsmith Gulch (site 3) or for Basin Creek (site 24). At these sites, cadmium and zinc concentrations did not change appreciably with increased streamflow, perhaps because upstream loading of these metals was relatively insignificant and concentrations were controlled more by desorption from streambed sediment. Dissolved arsenic concentrations generally did not vary with streamflow at most sites, probably because concentrations were low and, as shown in a later section, because arsenic is derived from the entire watershed and not primarily from the mined areas. In High Ore Creek, post-remediation dissolved arsenic concentrations during low flow are higher than pre-remediation concentrations and decrease with increased streamflow. Dissolved copper concentrations increased at all five sites as streamflow increased. This pattern, which is the reverse of the pattern for cadmium and zinc at sites 58, 47, and 56 (pre-remediation), likely is an artifact of filter pore size. Copper is more likely to exist in the particulate or colloidal phase than in the dissolved phase (Smith, 1999). Colloidal material is more readily

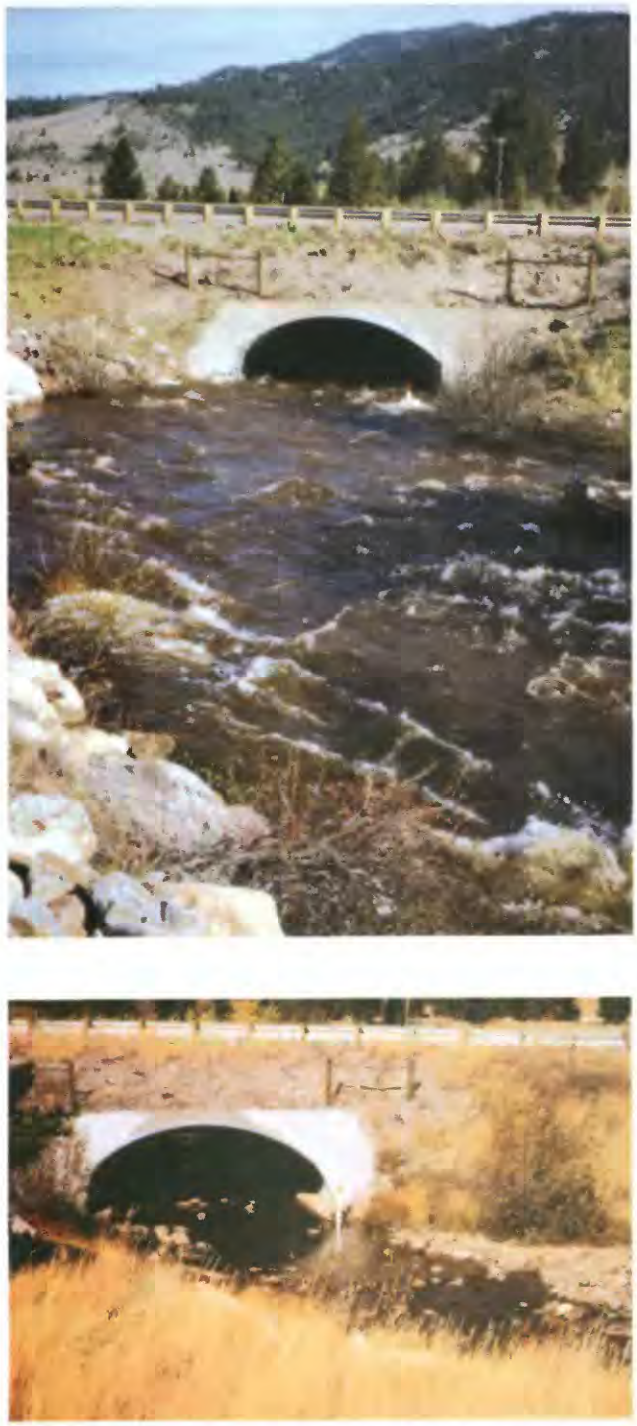

Figure 5. Cataract Creek at Basin (site 47) during high-streamflow conditions, June 1997 (top), and low-streamflow conditions, October 1996 (bottom).

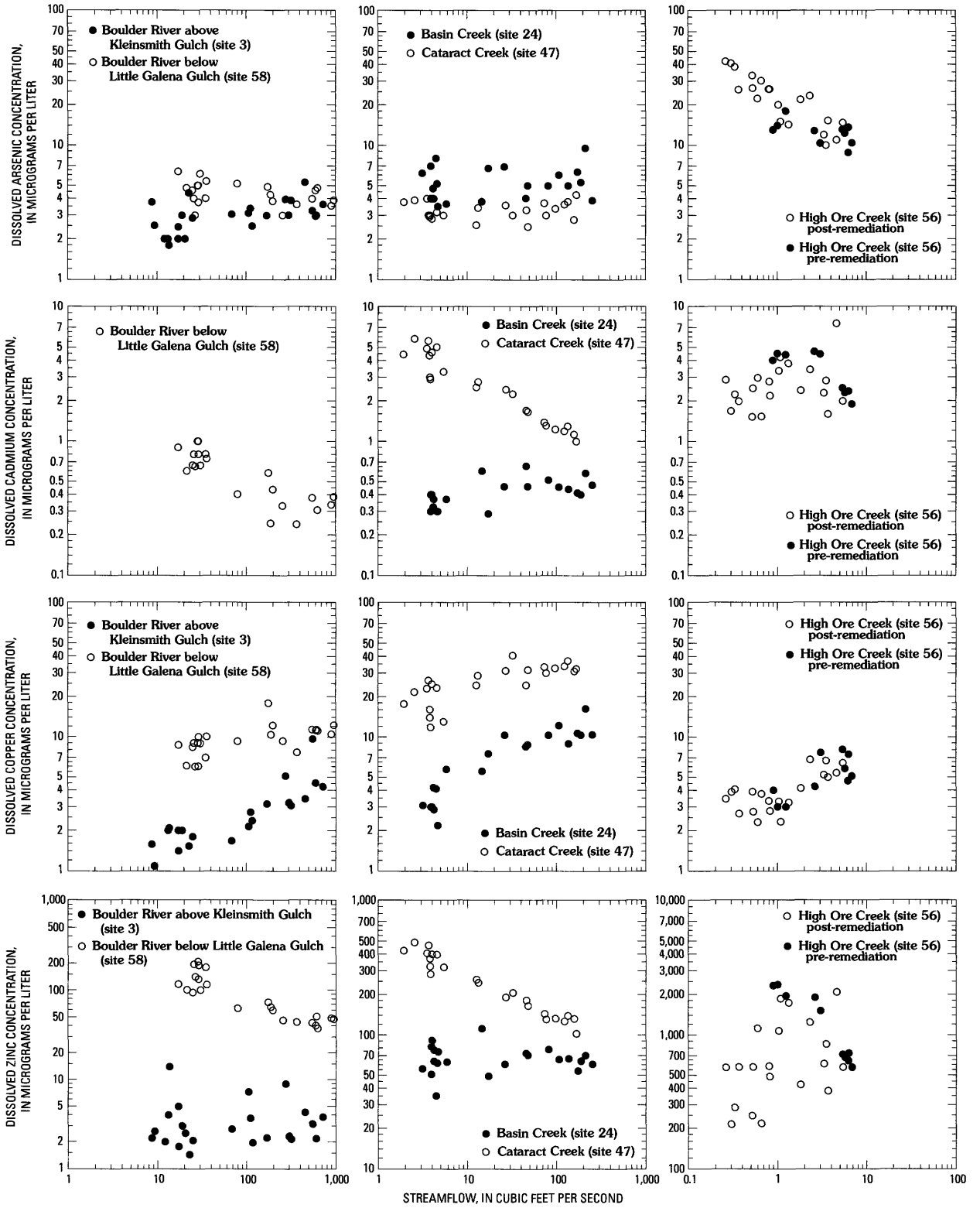

Figure 6. Relation of streamflow to dissolved (0.45-µm filtration) trace-element concentrations at five sites, 1996–2000. Dissolved cadmium concentrations for the Boulder River above Kleinsmith Gulch (site 3) were less than the minimum reporting levels and are not shown.

entrained from the streambed during high flows than during low flows and, thus, more colloids would move in suspension in the water column during high flow. Because some colloidal material can pass through the 0.45-μm filter used in this study, copper concentrations in 0.45-μm filtrates would be expected to increase as streamflow increases.

The relation between streamflow and dissolved and total-recoverable concentrations is not the same for each trace element during low-flow and high-flow conditions. Figure 7 shows the relation between streamflow and dissolved and total-recoverable trace-element concentrations for Cataract Creek (site 47). These relations are typical for other watershed streams with elevated trace-element concentrations. Total-recoverable and dissolved concentrations of aluminum and iron increased greatly with streamflow. Copper and manganese total-recoverable concentrations increased moderately with increasing flow. Although dissolved copper increased as total recoverable copper increased, dissolved manganese remained relatively constant as flows changed and total-recoverable manganese increased. The patterns for arsenic and lead are somewhat similar to that of manganese. Dissolved arsenic concentrations were consistently low (2–5 μg/L) during all flow conditions, but total-recoverable arsenic concentrations increased about 10-fold during high flow. Similarly, dissolved lead concentrations were consistently low (<1–1 μg/L), but total-recoverable concentrations increased as much as 20-fold during high flow. These increases in total-recoverable arsenic and lead concentrations indicate that arsenic and lead may be associated with the hydrous metal oxide coatings on streambed sediment and transported when colloids are resuspended during high flow (Church, Unruh, and others, this volume, Chapter D8). Total-recoverable concentrations of cadmium and zinc were only slightly higher than dissolved concentrations, indicating that, although suspended sediment was enriched in cadmium and zinc (Church, Unruh, and others, this volume, fig. 12), the amount of particulate cadmium and zinc in the water column was small relative to the dissolved fraction. This relation demonstrates that these metals strongly partition to the dissolved phase.

Seasonal differences in streamflow are an important factor affecting the severity and timing of aquatic toxicity. The importance of understanding these factors is demonstrated in figure 7 using aluminum, cadmium, copper, lead, and zinc data for Cataract Creek (site 47). These graphs show the EPA hardness-adjusted aquatic-life standards for each water sample. Total-recoverable copper concentrations increased from 13 to 90 μg/L and total-recoverable lead concentrations increased from less than 1 to 22 μg/L as streamflow increased from 1.9 to 168 ft^3/s. In contrast, hardness (not shown) and the aquatic-life standards for copper and lead decreased as streamflow increased. Similar to copper and lead, total-recoverable aluminum concentrations also increased with streamflow from 12 to 952 μg/L and exceeded the acute aquatic-life standard during high flow. The implication of these trends is that the toxicity of copper and lead is much greater during high flow. For cadmium and zinc, concentrations decreased about three- to four-fold as streamflow increased. The aquatic-life standards for cadmium and zinc also decreased as streamflow increased, but the decreases in these standards were somewhat less than for concentration. Therefore, the degree of aquatic toxicity for cadmium and zinc was slightly greater during low flow, although the difference between high-flow and low-flow toxicity for cadmium and zinc was not nearly as great as it was for copper and lead. Part of the convergence of the aquatic-life standards and concentrations of cadmium and zinc at high-flow results from the regulatory restriction that hardness-adjusted aquatic standards do not continue to decrease as hardness decreases to values less than 25 mg/L, which happened every spring during snowmelt runoff in Cataract Creek.

Trace-Element Concentrations

Trace-element concentrations in streams of the Boulder River watershed varied greatly, with the highest concentrations occurring in small streams downstream from just a few of the inactive mines in the watershed. The lowest concentrations generally were in stream reaches upstream from areas of historical mining or in headwater streams where small inactive mines had little effect. Cadmium, copper, lead, and zinc concentrations commonly exceeded chronic aquatic-life standards. The highest concentrations were in streams downstream from three large inactive mines: the Crystal mine (fig. 8) in a tributary to Cataract Creek, the Bullion mine (fig. 9) in a tributary to Jack Creek, and the Comet mine in High Ore Creek (Gelinas and Tupling, this volume, fig. 3). Downstream from these three mines, the chronic aquatic-life standard for at least one metal associated with the watershed's ore deposits was exceeded at all sampling sites, including sites in the Boulder River between Basin Creek and the Jefferson River.

The magnitude and distribution of trace elements in water are shown by ribbon maps for zinc, cadmium, copper, lead, and arsenic. Of these, zinc probably provides the best overall indicator for several reasons. First, concentration data for dissolved and total-recoverable zinc are available for more sites than for other trace elements. Second, zinc is a mobile metal that occurs at many sites in concentrations well above the minimum reporting level; however, concentrations of zinc are relatively low in areas unaffected by mining. Finally, exceedances of aquatic-life standards typically are larger for zinc than for other trace elements. Therefore, zinc is very useful for assessing the effects of mine drainage in the watershed. For some sites, only total-recoverable zinc concentration data were available; these data also were used to construct the dissolved zinc ribbon map because zinc occurs primarily in the dissolved phase and the total-recoverable concentrations provide an upper limit on the dissolved zinc concentrations at the sites with limited or no dissolved zinc data.

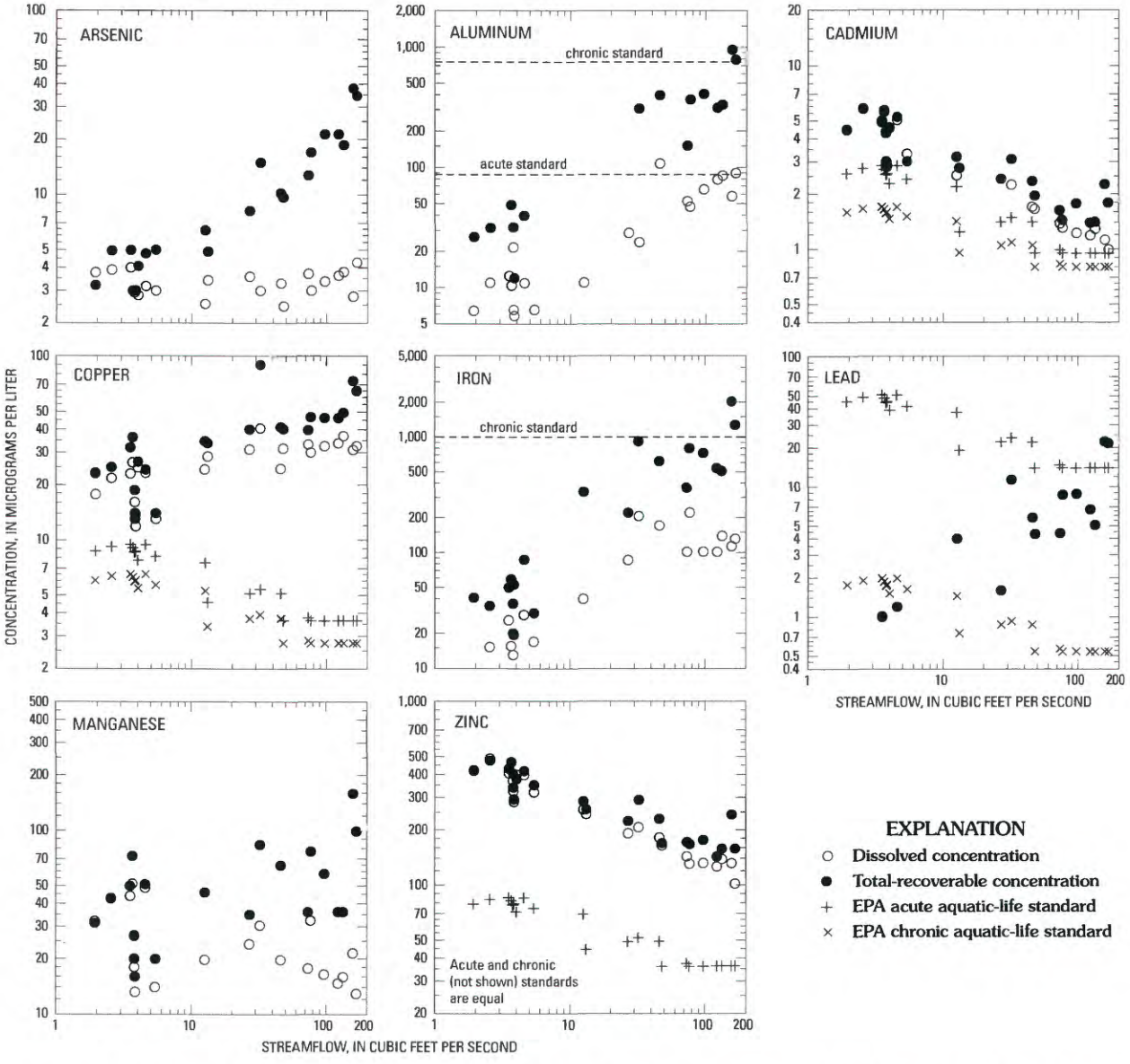

Figure 7. Relation of streamflow to dissolved (0.45-µm filtration) and total-recoverable trace-element concentrations in Cataract Creek (site 47), 1996–2000. Dissolved lead data are not shown because concentrations were equal to or less than minimum reporting level of 1 µg/L. U.S. Environmental Protection Agency (EPA) aquatic-life standards vary with hardness for cadmium, copper, lead, and zinc; standards for manganese have not been established. Standards for arsenic are not shown because they are much higher than measured concentrations.

Zinc

Dissolved zinc concentrations during low flow (fig. 10) ranged from <1 µg/L at some sites to 21,000 µg/L in Uncle Sam Gulch below the Crystal mine (site 44M). At sites in areas upstream from historical mining and in many headwater areas that were mined, dissolved zinc concentrations generally were <50 µg/L, and at most sites, the concentrations were <10 µg/L.

Three inactive mines (Crystal, Bullion, and Comet) had a profound effect on zinc concentrations in the watershed. Downstream from these mines, zinc concentrations were as high as 50–200 times the acute aquatic-life standard (19–197 µg/L, table 1). Discharge from the adit at the Crystal mine increased dissolved zinc concentrations in Uncle Sam Gulch from 12 µg/L upstream from the mine to 58,600 µg/L downstream from the mine (Kimball and others, this volume). Zinc concentrations were elevated throughout Uncle Sam Gulch, although dilution from tributaries decreased dissolved concentrations during low flow to 1,750–5,730 µg/L at the mouth (site 43). The Bullion Mine tributary (site 17) had dissolved zinc concentrations ranging from 2,130 to 5,820 µg/L, which elevated concentrations in Jack Creek to 205–405 µg/L at the mouth. The Comet mine site had a similar effect

Figure 8. Crystal mine, June 1997. Acidic discharge drains from adit (out of view near lower right of photograph) to Uncle Sam Gulch on far left.

Figure 9. Bullion mine, June 1997. Primary adits are on hillslope denuded by mine wastes above Bullion Mine tributary, which flows from right to left at edge of trees at center right of photograph. Acid discharge from one adit flows downslope in lower right corner.

on High Ore Creek. Upstream from the Comet mine (site 49), zinc concentrations were low, ranging from <1 to 54 µg/L. However, at all sites on High Ore Creek downstream from the mine, dissolved zinc concentrations were much higher, ranging from 388 to 5,214 µg/L prior to the start of remediation activities (Gelinas and Tupling, this volume).

The effect of drainage from each of these three mines extended far downstream (fig. 10). For example, the zinc loading from Uncle Sam Gulch affected concentrations in Cataract Creek downstream to its mouth. Dissolved zinc concentrations during low flow, from 191 to 634 µg/L at the mouth, were always higher than the acute aquatic-life standard (19–104 µg/L, table 1) in this lower reach of Cataract Creek. Zinc loading from Bullion Mine tributary increased dissolved zinc concentrations in Jack Creek from 12.3–33 µg/L (site 16) to between 205 and 1,280 µg/L

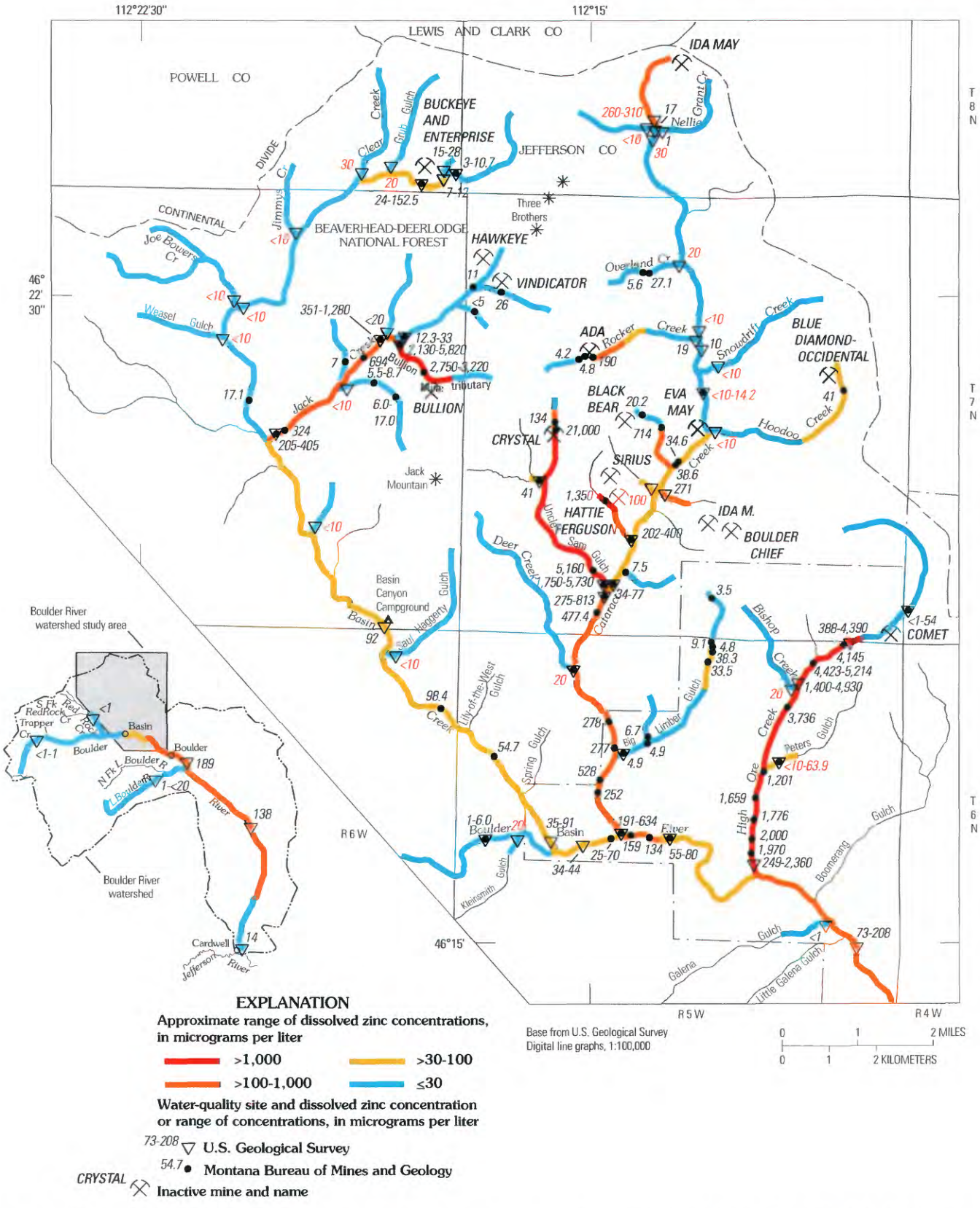

Figure 10. Approximate concentrations of dissolved zinc during low-streamflow conditions (July–March), 1991–2000. Site locations and numbers are shown in figure 1. Values in red are supplemental total-recoverable zinc concentrations for sites where dissolved zinc data are limited or do not exist. Concentration data from Kimball and others (this volume), although not shown, were used to define color coding for Bullion Mine tributary and Uncle Sam Gulch.

(sites 19 and 63) and, farther downstream, to 35–91 µg/L at the mouth of Basin Creek (site 24). Fluvial tailings along Jack Creek (Church, Unruh, and others, this volume) upstream and downstream from site 19 might be an additional source of zinc and other trace elements at downstream sampling sites.

The effect of drainage from these three mines continued downstream into the Boulder River, where dissolved zinc concentrations during low flow increased incrementally downstream from Basin, Cataract, and High Ore Creeks. Upstream from Basin Creek, concentrations in the Boulder River were 1–6 µg/L, whereas concentrations ranged from 25 to 70 µg/L between Basin and Cataract Creeks. Between Cataract and High Ore Creeks, concentrations were higher, ranging from 55 to 159 µg/L. Finally, downstream from High Ore Creek, concentrations in the Boulder River ranged from 73 to 208 µg/L. On the basis of one sampling episode during low flow, dissolved zinc concentrations exceeded the acute aquatic-life standard downstream from the Basin and Boulder mining districts almost to the Jefferson River (fig. 10).

Other inactive mines contributed dissolved zinc to streams in the Boulder River watershed during low flow but not to the same degree as in those reaches affected by the Crystal, Bullion, and Comet mines. In the Cataract Creek basin upstream from Uncle Sam Gulch, dissolved zinc concentrations were 100 µg/L or higher in four unnamed tributaries between Uncle Sam Gulch and Hoodoo Creek, in Rocker Creek downstream from the Ada mine, and in the headwater portion of Cataract Creek downstream from the Ida May mine. In upper Basin Creek, the Buckeye and Enterprise mines were a source of trace elements (Cannon and others, this volume). Dissolved zinc concentrations in upper Basin Creek downstream from these mines (site 8) generally were less than about 40 µg/L. Similarly, mines in upper Big Limber Gulch and Hoodoo Creek in the Cataract Creek basin appear to be the cause of slightly elevated dissolved zinc concentrations during low flow (fig. 10).

Total-recoverable zinc concentrations during high flow (fig. 11) tended to be lower than dissolved concentrations during low flow, particularly in reaches where zinc concentrations were elevated. Concentrations in Basin Creek downstream from the Buckeye and Enterprise mines were an exception to this generalization. In this reach, loading of zinc and other trace elements was substantial during spring runoff, resulting in higher concentrations during high flow (Cannon and others, this volume). In reaches relatively unaffected by historical mining, such as Cataract Creek upstream from Hoodoo Creek, total-recoverable zinc concentrations were low during high flow (generally less than 50 µg/L) but slightly higher than low-flow dissolved concentrations.

Cadmium

The spatial distribution of dissolved cadmium concentrations during low flow (fig. 12) was similar to the distribution of dissolved zinc concentrations, indicating that sources of cadmium and zinc were similar. Cadmium concentrations exceeded the acute aquatic-life standard (0.4–3.9 µg/L, table 1) in many of the same reaches where zinc exceeded this standard, particularly in headwater areas near inactive mines. However, in comparison to zinc, dissolved cadmium concentrations were not as elevated above the acute aquatic-life standard. This is shown by the lesser extent of yellow-, orange-, and red-colored reaches on the dissolved cadmium ribbon map (fig. 12) compared to the zinc map (fig. 10). Uncle Sam Gulch and the Bullion Mine tributary are the only red reaches on the cadmium ribbon map, whereas other stream reaches are red on the zinc map. Because the relative degree of exceedance of the aquatic-life standard was smaller for cadmium concentrations than zinc concentrations, exceedances of the cadmium standards did not extend as far downstream below major sources as did exceedances of the zinc standard. For instance, dissolved cadmium concentrations at the mouth of Basin Creek barely exceeded 0.4 µg/L (fig. 12). Although cadmium concentrations in the Boulder River increased incrementally downstream through the study area, aquatic-life standards were only exceeded downstream from Cataract Creek. Similar to zinc, total-recoverable cadmium concentrations during high flow (fig. 13) generally were lower than dissolved concentrations during low flow except in Basin Creek downstream from the Buckeye and Enterprise mines.

Copper

Dissolved copper concentrations during low flow (fig. 14) exceeded the acute aquatic-life standard (1.8–12 µg/L, table 1) by more than 10 times (red color) downstream from the Bullion and Crystal mines in the Bullion Mine tributary and Uncle Sam Gulch, respectively. In contrast, concentrations in High Ore Creek downstream from the Comet mine were much lower (2–8 µg/L). Although High Ore Creek is colored green on the dissolved copper ribbon map, indicating exceedance of the chronic criteria for other parts of the watershed where hardness values are lower, none of the low-flow concentrations actually exceeded the hardness-adjusted standard. The small amount of copper relative to zinc and cadmium that leaches from the Comet mine area probably results from the different ore body at this site compared to the polymetallic veins that compose ore bodies near the Crystal and Bullion mines (O'Neill and others, this volume, Chapter D1). The copper loading from the Bullion Mine tributary increased copper concentrations in Jack Creek and, farther downstream, in Basin Creek. Similarly, the copper loading from Uncle Sam Gulch affected Cataract Creek downstream to its mouth. Similar to cadmium and zinc, dissolved copper concentrations in the Boulder River were enriched downstream from Basin Creek; concentrations generally ranged between the acute and chronic aquatic-life standards. Dissolved copper concentrations in the Boulder River were highest in the reach between Cataract and High Ore Creeks and decreased downstream from High Ore Creek. Total-recoverable copper concentrations during high flow (fig. 15) typically were higher than dissolved copper concentrations during low flow, most

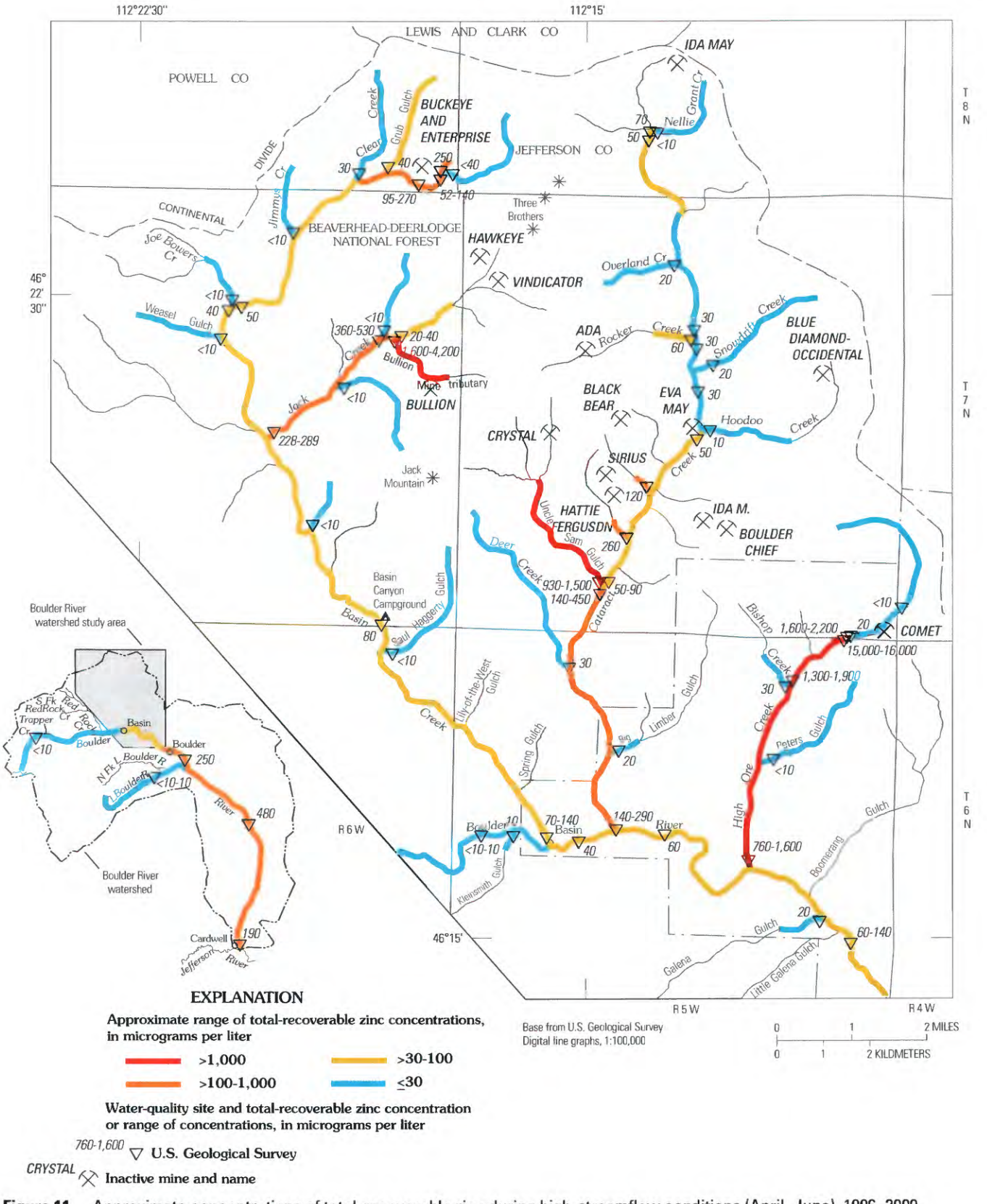

Figure 11. Approximate concentrations of total-recoverable zinc during high-streamflow conditions (April–June), 1996–2000. Site locations and numbers are shown in figure 1.

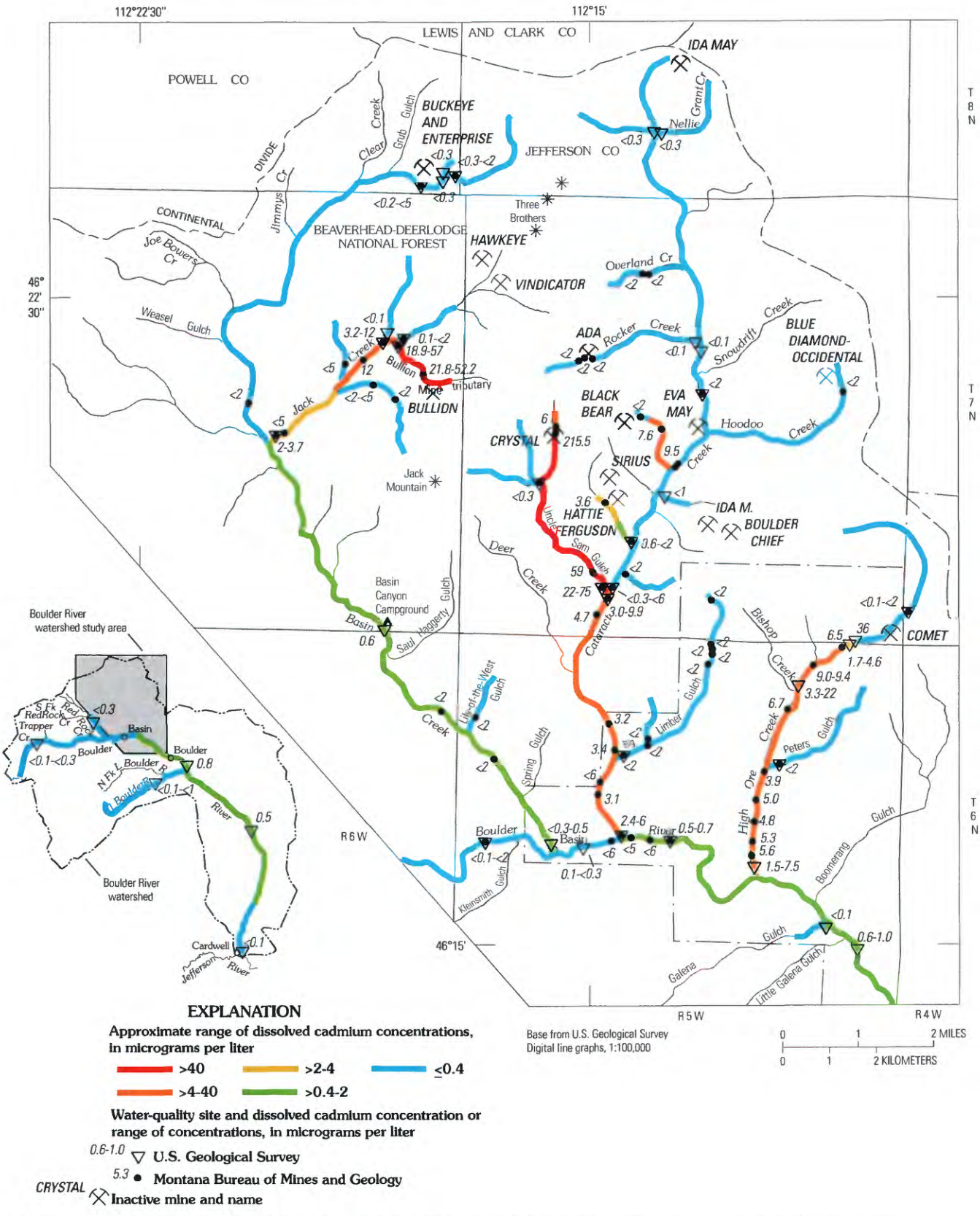

Figure 12. Approximate concentrations of dissolved cadmium during low-streamflow conditions (July–March), 1991–2000. Site locations and numbers are shown in figure 1.

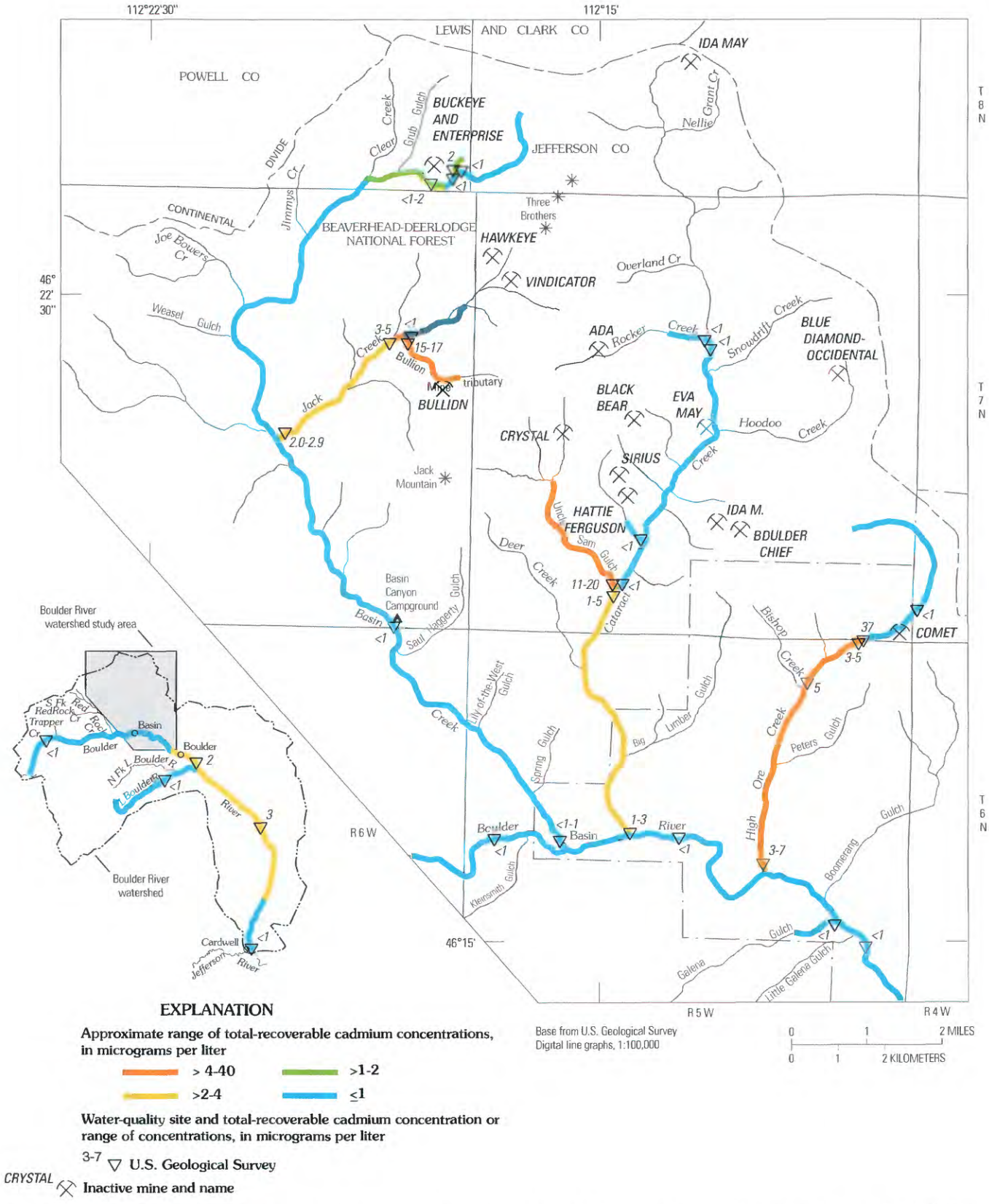

Figure 13. Approximate concentrations of total-recoverable cadmium during high-streamflow conditions (April–June), 1996–2000. Site locations and numbers are shown in figure 1.

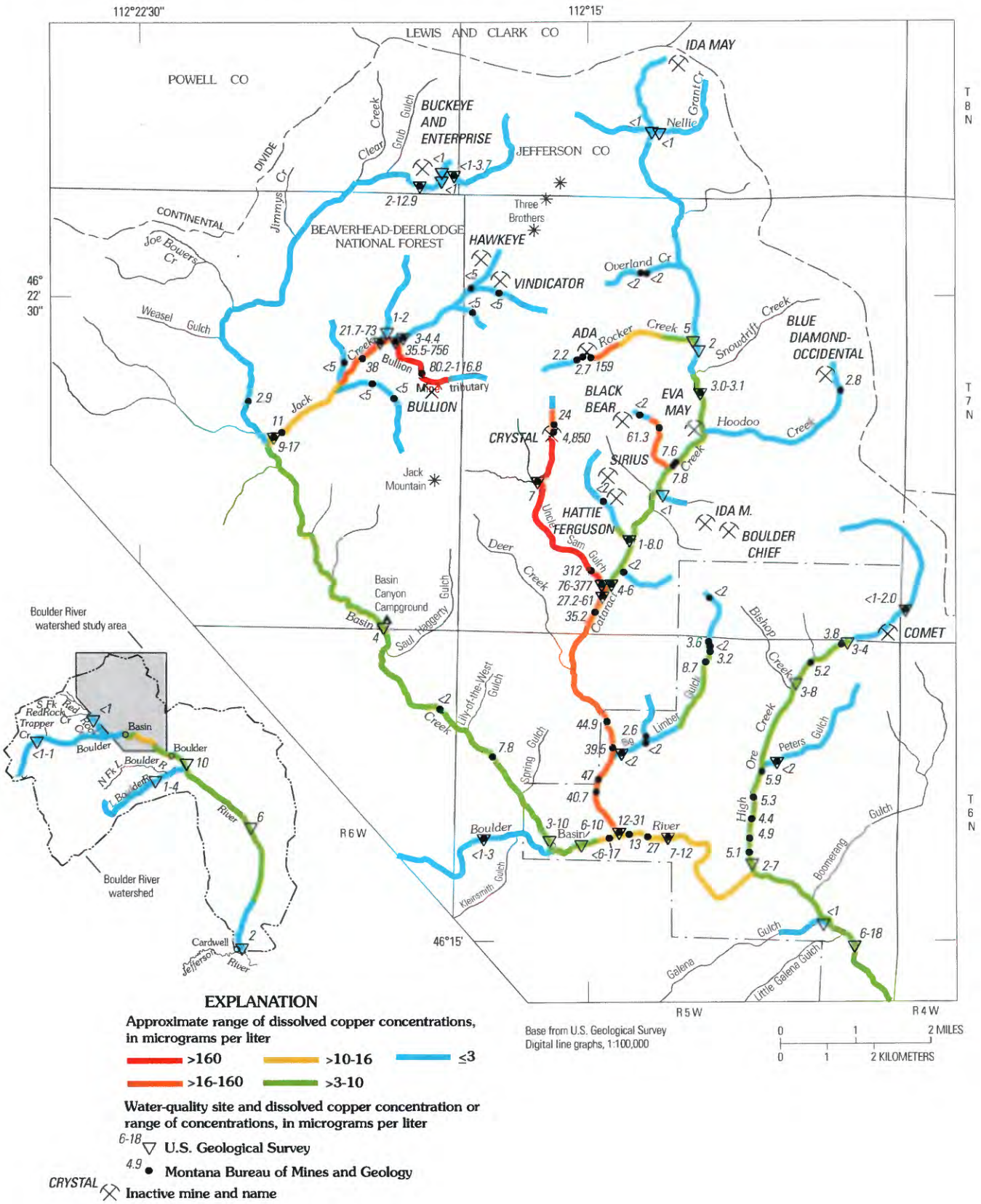

Figure 14. Approximate concentrations of dissolved copper during low-streamflow conditions (July–March), 1991–2000. Site locations and numbers are shown in figure 1. Concentration data from Kimball and others (this volume), although not shown, were used to define color coding for Bullion Mine tributary and Uncle Sam Gulch.

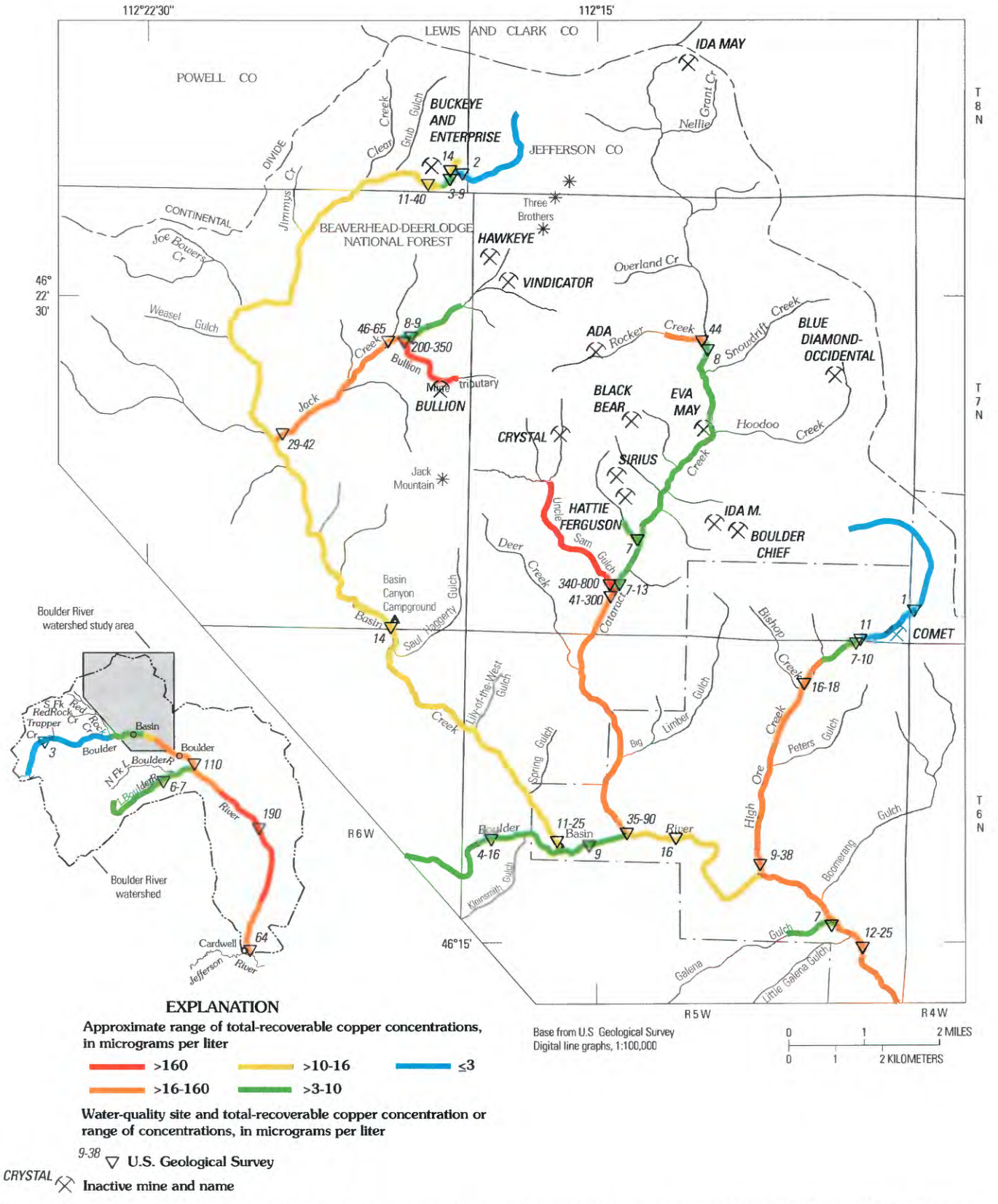

Figure 15. Approximate concentrations of total-recoverable copper during high-streamflow conditions (April–June), 1996–2000. Site locations and numbers are shown in figure 1.

likely because copper partitions more strongly than zinc or cadmium to the particulate phase, thus enriching stream sediment, which is transported during high flow.

Lead

Dissolved lead concentrations in almost all parts of the study area were less than the minimum reporting level and are not shown on a ribbon map. The only sites where dissolved lead concentrations were typically higher than the minimum reporting level during low flow were the Bullion Mine tributary (site 17), where concentrations ranged from <1 to 8.7 µg/L, and Uncle Sam Gulch just downstream from the Crystal mine (site 44M), where the concentration was 78.6 µg/L. Both sites had acidic pH values (fig. 3).

Similar to copper, total-recoverable lead concentrations during high flow (fig. 16) were higher than during low flow because lead partitions strongly to the colloidal or particulate phase. Total-recoverable lead concentrations generally ranged between the chronic and acute aquatic-life standards (yellow color) throughout most of the watershed downstream from not only the Bullion, Crystal, and Comet mines, but also the Buckeye and Enterprise mines on upper Basin Creek and the Eva May mine on upper Cataract Creek.

Arsenic

Dissolved arsenic was present at low concentrations in both mined and unmined parts of the study area and in reference streams in other parts of the watershed. Concentrations during low flow (fig. 17) were not substantially elevated in any stream. Dissolved concentrations were much lower than the chronic aquatic-life standard (150 µg/L) throughout the watershed and exceeded the Montana human-health standard (18 µg/L) only locally. Dissolved arsenic concentrations generally ranged from 1 to 5 µg/L at almost all sampling sites in the study area, as well as in areas upstream from historical mining (sites 1, 2, 49, and 60, fig. 1). Few sites had concentrations less than the minimum reporting level (1 µg/L). Concentrations in lower Basin Creek as well as in the Boulder River downstream from the study area were slightly higher, ranging as high as 9 µg/L. These higher concentrations in Basin Creek appear to come from mining- and nonmining-related sources near the Buckeye and Enterprise mines (Cannon and others, this volume) as well as in Jack Creek, and possibly other tributaries. The higher dissolved arsenic concentrations in the Boulder River downstream from the study area appear to result from sources near or downstream from Boulder. Three stream reaches had concentrations higher than the Montana human-health standard of 18 µg/L: Basin Creek downstream from the Buckeye and Enterprise mines (site 8), an unnamed and unmined tributary to Uncle Sam Gulch (site 42), and High Ore Creek downstream from the Comet mine (sites 52, 53, and 56). Mine wastes, mill tailings, and fluvial deposits appear to be the source of arsenic in High Ore Creek (Gelinas and Tupling, this volume). However, arsenic in Basin Creek near the Buckeye and Enterprise mines appears to be derived not only from mined areas, where the median arsenic concentration in mine wastes exceeds 1 weight percent (Church, Unruh, and others, this volume, table 2), but also from unmined areas (Cannon and others, this volume). The unnamed tributary to Uncle Sam Gulch drains an unmined area; therefore, the arsenic, which presumably is leaching naturally from arsenic-rich geologic sources, in this drainage is nonmining related.

The spatial pattern of total-recoverable arsenic concentrations during high flow (fig. 18) was much different from the pattern for low-flow dissolved concentrations. The high-flow total-recoverable concentrations were higher than low-flow dissolved concentrations (fig. 17) at almost all sites having data for both flow conditions. No other trace element, with the exception of lead, had such a large difference between the low-flow dissolved and high-flow total-recoverable concentrations. The maximum dissolved arsenic concentration in the watershed during low flow was 44 µg/L, whereas the maximum total-recoverable concentration during high flow was 760 µg/L. The chronic aquatic-life standard (150 µg/L) was equaled or exceeded at one or more sites downstream from the Buckeye, Bullion, Crystal, or Comet mines. Whereas the effect of historical mining areas is not readily apparent in the dissolved arsenic map (fig. 17), the effect is very apparent in the total-recoverable map (fig. 18). Because arsenic in mine drainage adsorbs to streambed sediment quickly (Smith, 1999), dissolved concentrations during low flow are low. However, during high flow, arsenic-rich sediment is entrained within the water column and produces the high total-recoverable concentrations observed during this study. This same process also is the cause of the high concentrations of total-recoverable lead during high-flow conditions in the watershed.

Aluminum

Aluminum is not discussed in detail and ribbon maps are not presented because aluminum concentrations, unlike concentrations of other trace elements, do not appear to be overly toxic in the watershed. The toxicity of aluminum in neutral to alkaline surface water is not well understood (U.S. Environmental Protection Agency, 1999, p. 19), and therefore the established aquatic-life standards may be conservative. Typically, the primary concern regarding aluminum toxicity is not in reaches with neutral to slightly alkaline pH but rather in reaches that are mixing zones where acidic water rich in dissolved aluminum is neutralized, resulting in the formation of aluminum hydroxide colloids. These colloids can then coat the streambed and the gills of aquatic organisms.

Dissolved aluminum concentrations during low flow were consistently low in almost all streams. Concentrations only exceeded the chronic aquatic-life standard of 87 µg/L in the Bullion Mine tributary and the upper and middle reaches

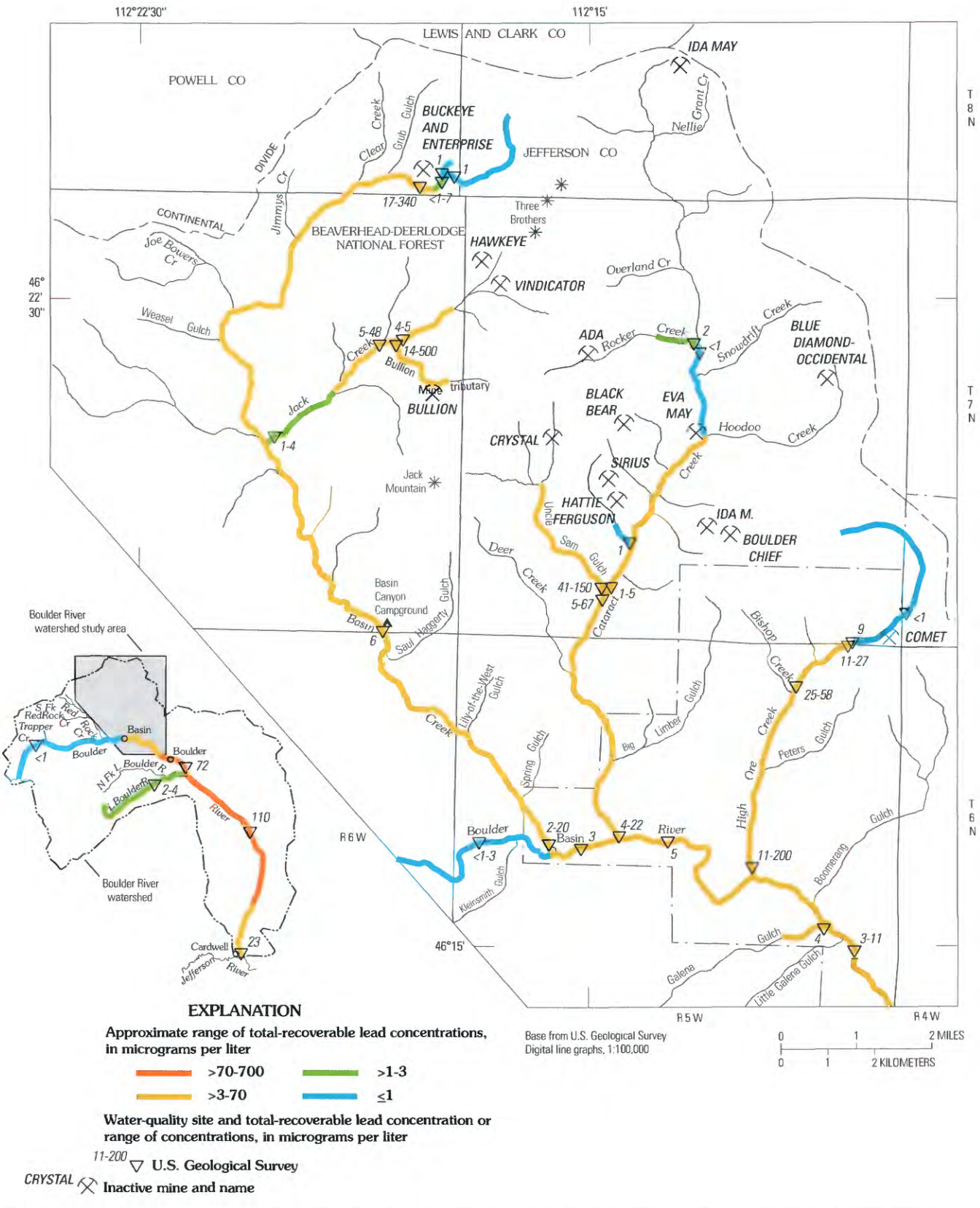

Figure 16. Approximate concentrations of total-recoverable lead during high-streamflow conditions (April–June), 1996–2000. Site locations and numbers are shown in figure 1.

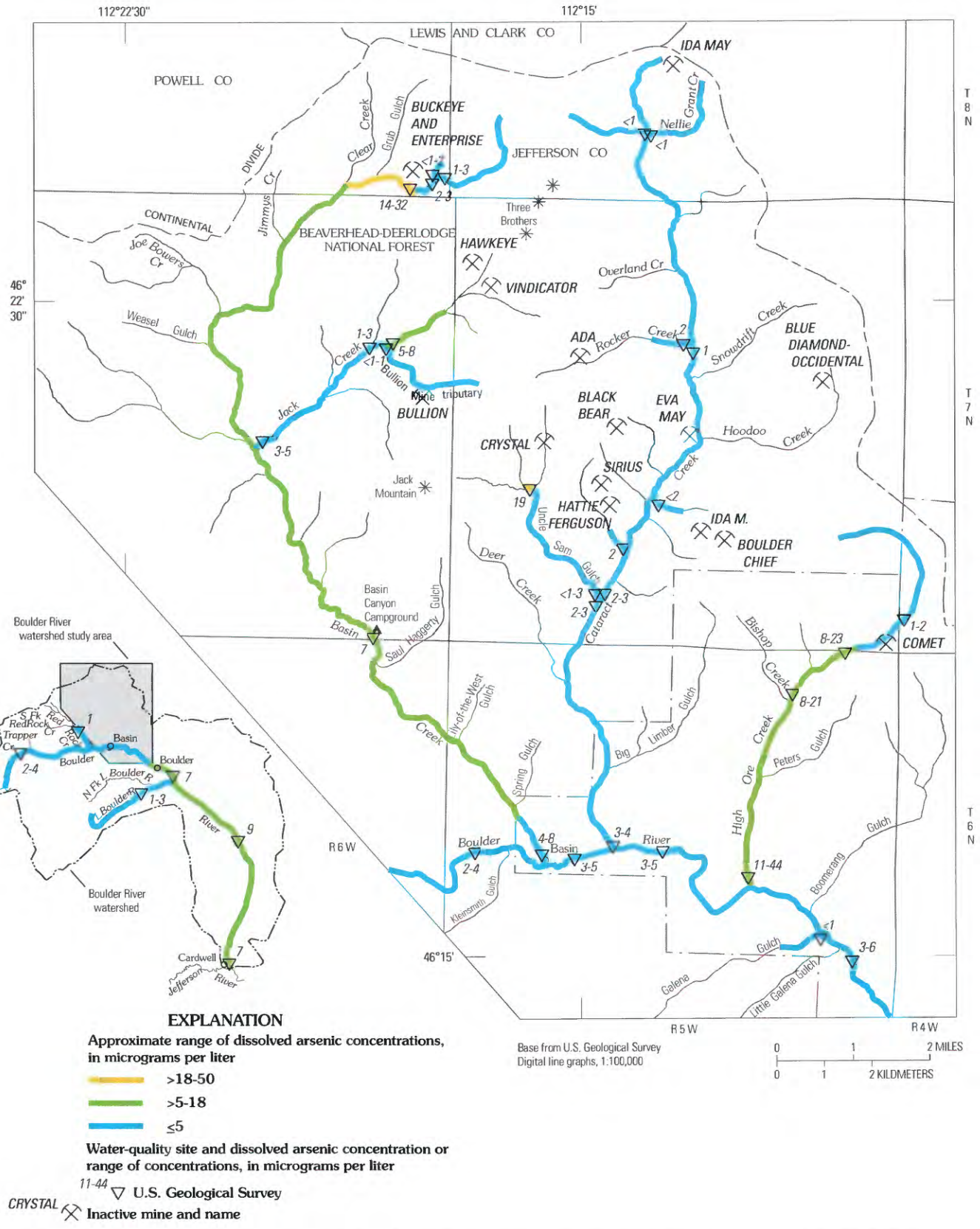

Figure 17. Approximate concentrations of dissolved arsenic during low-streamflow conditions (July–March), 1996–2000. Site locations and numbers are shown in figure 1.

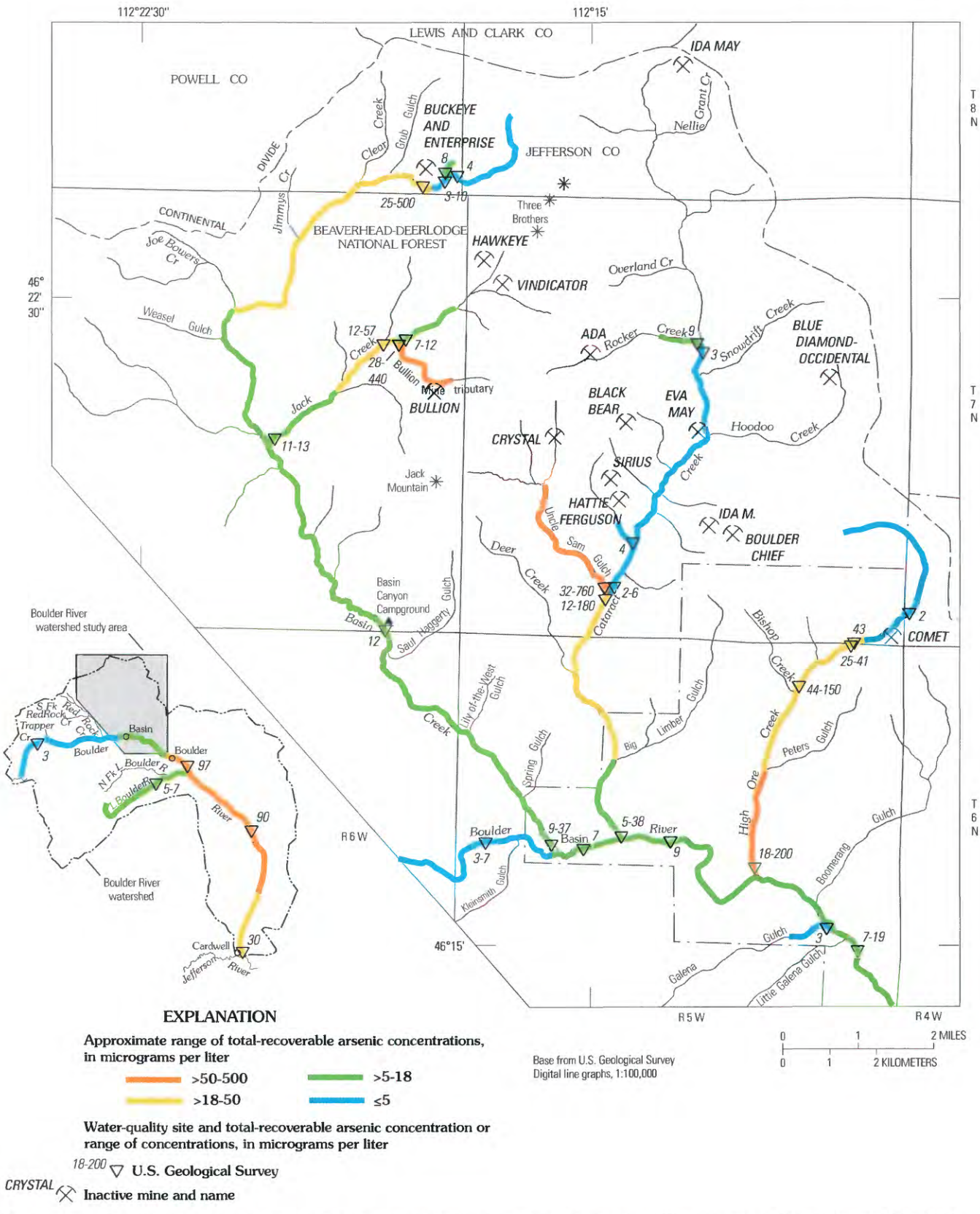

Figure 18. Approximate concentrations of total-recoverable arsenic during high-streamflow conditions (April–June), 1996–2000. Site locations and numbers are shown in figure 1.

of Uncle Sam Gulch on the basis of data collected by Kimball and others (this volume) and data for sites 17 and 43 (Rich and others, this volume). These reaches generally were acidic, and therefore dissolved concentrations of aluminum and other metals would be expected to be elevated. Total-recoverable aluminum concentrations during low flow typically were somewhat higher than dissolved concentrations, and exceeded the chronic aquatic-life standard at sites in Basin Creek (site 8), Jack Creek (site 19), Uncle Sam Gulch and Cataract Creek (sites 43 and 44), and High Ore Creek (site 56) downstream from the Buckeye, Bullion, Crystal, and Comet mines, respectively. The maximum total-recoverable low-flow concentration at these sites was 570 µg/L, which did not exceed the acute aquatic-life standard of 750 µg/L.

Total-recoverable aluminum concentrations typically were highest during high flow, exceeding the acute aquatic-life standard (750 µg/L) in some samples from many sites, including some sites in streams upstream from mining activities. For example, the median total-recoverable aluminum concentration during high-flow conditions in the Boulder River was the same (560 µg/L) upstream (site 3) and downstream (site 58) from the study area. This value also was higher than the median high-flow total-recoverable concentrations (370–445 µg/L) at the mouths of Basin, Cataract, and High Ore Creeks. These data indicate that the primary source of aluminum was not related to historical mining. In addition, although total-recoverable aluminum concentrations exceeded the acute and chronic aquatic-life standards in many parts of the watershed during high flow, the distribution of total-recoverable aluminum does not correlate well with stream reaches where aquatic health is thought to be impaired (Farag and others, this volume, Chapter D10).

Concentration Trends During 1996–2000

Temporal trends in trace-element concentrations can be caused by changes in hydrologic conditions over multi-year periods (for example, several dry years followed by several wet years) or by changes in loading resulting from remediation activities in mined areas. Changes due to varying hydrologic conditions do not necessarily imply that contaminant supply has changed, but rather just indicates fluctuating delivery and transport rates. Actual trends caused by a physical change in either contaminant supply or delivery process are more readily detected by statistically accounting for the effect of flow variation. Trace-element concentration data collected during 1996–2000 for this study at five key sites in the study area were analyzed statistically for trends. Generally, a 4-year period is too short to demonstrate systematic trends. However, some preliminary trends are discernible in the concentration data.

Temporal profiles of dissolved zinc concentrations during 1996–2000 are depicted in figure 19 for five sites in the watershed. These graphs show the full range of concentration variation over the sampling period, seasonal patterns related to streamflow, and year-to-year patterns over the 4-year period. Trend tests were performed on these data sets to estimate the probability that the data exhibit a temporal trend. Because apparent trends are sometimes indicated by the seasonal change in concentration caused by streamflow variations, concentration data frequently are adjusted prior to the trend test to account for the variation due to streamflow. In this case, streamflow adjustment was incorporated into the trend test by using a linear regression of streamflow and concentration. The residuals from this regression were then evaluated for temporal trends (table 2) using the non-parametric Kendall's tau correlation (Helsel and Hirsch, 1992).

Variations in dissolved zinc concentrations in the Boulder River above Kleinsmith Gulch during 1996–2000 indicated no statistical trend. As a result, the magnitude of zinc load for a given flow did not vary appreciably during the study period. Presumably, loading of other trace elements from similar areas underlain by unmineralized rock upstream from the study area may also have shown little change. Similarly, dissolved zinc data for Basin and Cataract Creeks appear to have had no trend during 1996–2000. The absence of zinc concentration trends is consistent with the lack of remediation activity in the Basin and Cataract Creek basins. In contrast, dissolved zinc concentrations for High Ore Creek and the Boulder River below Little Galena Gulch exhibited a decreasing trend during 1996–2000. These trends and the related remediation activities conducted in 1997–2000 in the High Ore Creek valley are discussed in a subsequent chapter (Gelinas and Tupling, this volume).

Sources of Trace Elements

Mining-Related Sources

Although the Boulder River watershed has more than 140 inactive mines and 15 mills (Martin, this volume, Chapter D3), only a few are significant sources of trace elements to streams. The downstream concentration profiles depicted in the ribbon maps (figs. 10–18) clearly show the influence of the Comet, Crystal, and Bullion mines (and, to a lesser extent, the Buckeye and Enterprise mines) on trace-element concentrations in the watershed. Ribbon maps depicting trace-element concentrations in streambed sediment also show the influence of these mines (Church, Unruh, and others, this volume). Waste rock was present at each of these mines, and mill tailings were present at three of these mines. Runoff from and erosion of these mine wastes likely contributed to the trace-element load discharged from these sites. Analysis of metal leaching from selected waste piles demonstrated that mine-waste materials at the Bullion and Buckeye mines had a high potential to impact streamwater quality (Fey and

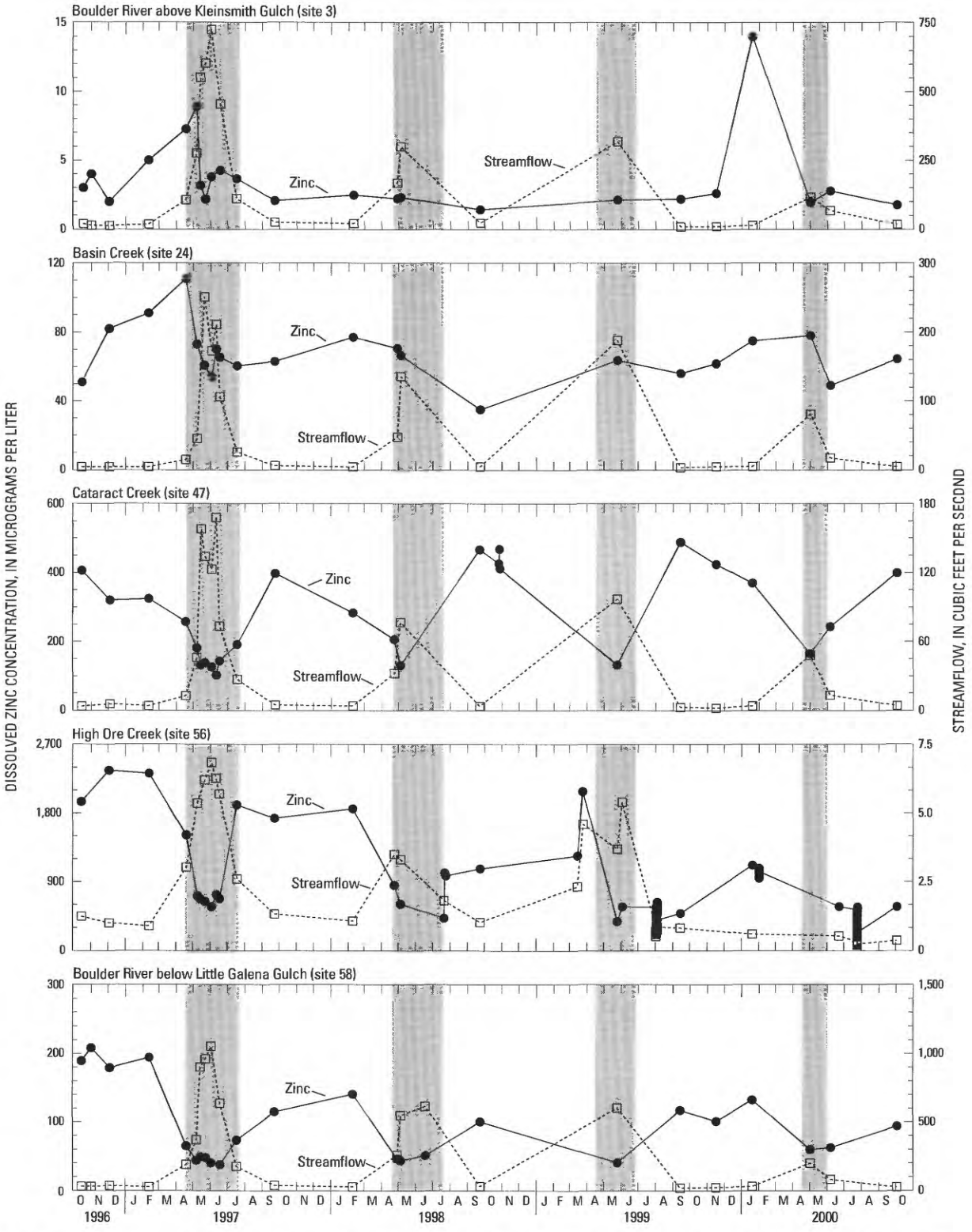

Figure 19. Temporal profiles of dissolved zinc concentration and streamflow at five sites, 1996–2000. Shaded areas indicate periods of high streamflow during spring runoff. Lines connecting the data points are for visual generalization of temporal patterns and do not imply actual knowledge of concentrations or streamflow between sampling dates.

Table 2. Results of linear regression and Kendall's correlation for trend tests of dissolved zinc concentration for five sites in the Boulder River watershed.

Site number (fig. 1)	Station name	Linear regression of dissolved zinc concentration and streamflow		Kendall's correlation, residuals and time data pairs[1]		Conclusion[2]
		Slope	R^2	τ	p value	
3	Boulder River above Kleinsmith Gulch	0.207	0.006	–0.059	0.692	No trend.
24	Basin Creek	200	.001	–.039	.780	No trend.
47	Cataract Creek	–3.04	.952	–.028	.853	No trend.
56	High Ore Creek	.134	.007	–.362	.0081	Decreasing trend.
58	Boulder River below Little Galena Gulch.	–2.32	.803	–.536	.0002	Decreasing trend.

[1]The p value indicates the probability of obtaining the computed τ value if no temporal trend in the data exists. Thus, small p values (generally less than about 0.05) indicate temporal trends, whereas large p values indicate no temporal trends. Decreasing trends are associated with negative values of τ.

[2]Trend tests are based on a short-term (4-year) dataset; consequently, conclusions regarding trend are considered preliminary.

Desborough, this volume). At the Crystal mine, adit discharge was sufficient to make this mine the most significant source of trace elements in the watershed. Detailed investigations of trace-element sources are reported for the Crystal and Bullion mines (Kimball and others, this volume) and the Buckeye and Enterprise mines (Cannon and others, this volume). Remediation activities started in late 1997 in the Comet mine area in the High Ore Creek basin; consequently, a detailed investigation of trace-element sources was not conducted there for this study.

The ribbon maps (figs. 10–18) show that effects from historical mining exist in stream reaches other than those affected by the Comet, Crystal, Bullion, Buckeye, and Enterprise mines. In particular, inactive mines along Cataract Creek and in tributaries to Cataract Creek contribute sufficient copper, zinc, and, in some cases, cadmium to increase concentrations in these reaches to levels near aquatic-life standards.

Premining Background Sources

Watersheds that experienced historical mining activity also contain undisturbed mineralized rocks that might weather and contribute acid and trace elements to streams. These mineralized rocks can be either mineral deposits or surrounding rock affected by hydrothermal alteration. Differentiating between trace-element loads derived from undisturbed geologic sources and mining-affected sources is essential for the mining-related contribution to be put in perspective. In addition, land managers can use information on the relative contributions of trace elements from undisturbed geologic sources and mining-related sources in a watershed for prioritizing subbasins for remediation and for establishing post-remediation water-quality goals.

In the Boulder River watershed, sources of cadmium, copper, lead, and zinc in undisturbed areas appear to be small because concentrations of these metals in water are not elevated at reference sites upstream from mining activities or even in some headwater drainages with inactive mines. This conclusion is reasonable for two reasons. First, mineralized veins and surrounding zones affected by hydrothermal alteration, which contain pyrite and other sulfide minerals that are the source of trace elements associated with ore deposits, have limited areal extent in the watershed. Second, the acid-neutralizing capacity provided by mafic minerals and secondary calcite in the Boulder batholith limits the migration of acidic, metal-rich water produced by oxidation of the veins and altered rock (Desborough, Briggs, Mazza, and Driscoll, 1998; Desborough, Briggs, and Mazza, 1998). However, premining water-quality data do not exist for stream reaches downstream from mined areas; hence, the reasons stated are somewhat speculative. Arsenic, on the other hand, appears to have small but pervasive sources throughout the undisturbed parts of the watershed.

Trace-Element Loading to the Boulder River

Early biological studies in the watershed (Vincent, 1975; Nelson, 1976) postulated that trace-element loads from Basin, Cataract, and High Ore Creeks affected fisheries in the Boulder River. We determined the relative importance of each of the three major tributaries as contributors of dissolved trace elements to the Boulder River by estimating the annual streamflow and loads of dissolved trace elements during water year 1997 (October 1996 through September 1997). This loading analysis used only data for water year 1997 (fig. 20) because data were collected less frequently in subsequent years and because remediation activities began at the Comet mine along High Ore Creek in late 1997, which affected trace-element loads from this stream to the Boulder River (Gelinas and Tupling, this volume).

The annual loads of dissolved trace elements from Basin Creek (site 24), Cataract Creek (site 47), and High Ore Creek (site 56), and at sites on the Boulder River upstream (site 3) and downstream (site 58) of these tributary streams, were estimated in a multi-step process utilizing water-quality data for 13 sample sets collected between October 1996 and September

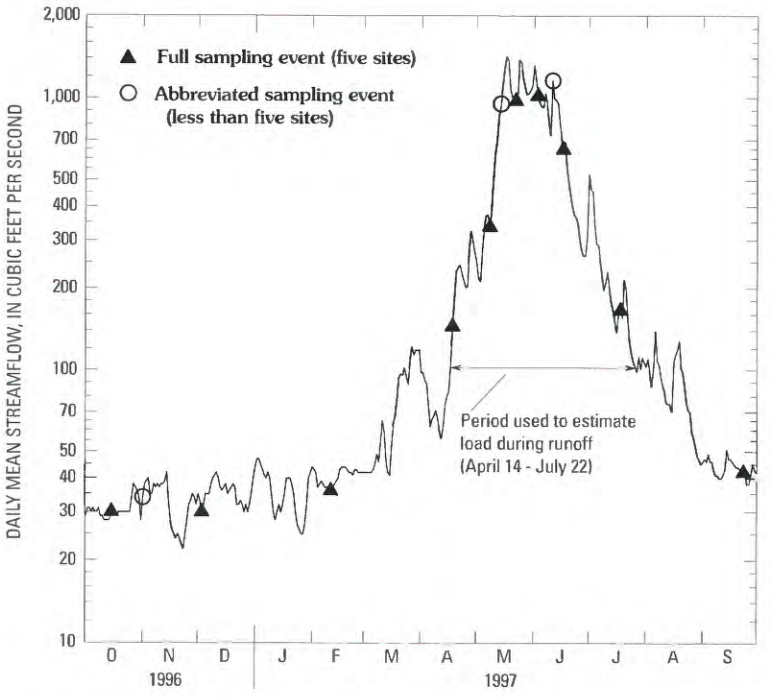

Figure 20. Hydrograph for Boulder River at Boulder (site 59) and sampling dates for water-quality data used for analysis of trace-element loading at five sites, water year 1997.

1997 and the daily mean streamflow record for a nearby site on the Boulder River (site 59, USGS streamflow-gauging station 06033000; Shields and others, 1998). First, a regression model relating daily mean streamflow at the gauging station to instantaneous streamflow measured at the time of sampling was developed for each sampling site. Second, the flow relation for each site was applied to the daily mean flows at the gauging station to construct a daily flow record for water year 1997 for each site. Third, a set of regression models relating instantaneous streamflow at the time of sampling to the concentration of each trace element was developed. Fourth, these regression models were used with the estimated daily streamflow values for each site to estimate daily trace-element concentrations. Fifth, daily loads for each trace element were estimated by multiplying estimated daily streamflow and concentration. Finally, daily loads were summed for the year to estimate the annual loads for water year 1997 at each site (table 3).

Basin, Cataract, and High Ore Creeks together contributed 33 percent of the annual streamflow in the Boulder River (site 58) at the downstream end of the study area (fig. 21), roughly in proportion to their total drainage area compared to the drainage area upstream from the Boulder River below Little Galena Gulch. The dissolved arsenic load contributed by the three tributaries was 38 percent of the load at site 58, about the same proportion as streamflow, indicating that the mineralized rocks in the study area contribute little if any excess dissolved arsenic. In contrast, the three tributaries contribute nearly all the dissolved cadmium load (89 percent) and zinc load (83 percent) and more than half of the dissolved copper load (56 percent). On an annual basis, Cataract Creek contributes more cadmium, copper, and zinc to the Boulder River than Basin and High Ore Creeks. The contribution of cadmium and copper from Cataract Creek was more than twice as large as the load from Basin Creek, and from 6 to almost 40 times greater than the load from High Ore Creek. The load of dissolved zinc from Cataract Creek was almost 1.5 to 2 times as large as the loads from Basin and High Ore Creeks. High Ore Creek contributed little dissolved copper, accounting for only 1 percent of the load at site 58. Most of the dissolved trace-element load in Basin and Cataract Creeks was transported during runoff. In contrast, the High Ore Creek basin, which has lower mountains and therefore less snowmelt runoff from its headwaters, contributed almost half of its streamflow and trace-element load outside of the snowmelt runoff period.

Figure 21. Boulder River below Little Galena Gulch (site 58) during spring runoff, June 1997.

Table 3. Estimated annual streamflow and annual loads of dissolved trace elements for five sites in the Boulder River watershed, water year 1997.

[Numbers in parentheses are negative. Period used to estimate load during runoff for 1997 was April 14 to July 22. >, greater than; <, less than; --, not applicable]

Station name	Site number (see fig. 1)	Streamflow			Dissolved arsenic		
		Annual stream-flow (acre-feet)	Percent of streamflow at site 58	Percent of streamflow during runoff period	Annual load, in tons	Percent of load at site 58	Percent of load during runoff period
Boulder River above Klein-smith Gulch.	3	31.7×10^6	67	83	0.422	57	87
Basin Creek	24	8.32×10^6	18	86	.173	23	88
Cataract Creek	47	6.40×10^6	14	84	.082	11	83
High Ore Creek	56	0.596×10^6	1	55	.029	4	51
Unaccounted for[1]	--	0.0456×10^6	(<1)	--	.033	4	--
Boulder River below Little Galena Gulch.	58	47.0×10^6	100	82	.739	100	80

Site number (fig. 1)	Dissolved cadmium			Dissolved copper			Dissolved zinc		
	Annual load, in tons	Percent of load at site 58	Percent of load during runoff period	Annual load, in tons	Percent of load at site 58	Percent of load during runoff period	Annual load, in tons	Percent of load at site 58	Percent of load during runoff period
3	<0.012	<17	81	0.521	27	87	0.47	4	85
24	.015	21	88	.334	18	94	2.05	19	84
47	.041	58	65	.710	37	88	4.13	38	63
56	.007	10	5	.011	1	67	2.96	27	36
--	>.004	>6	--	.324	17	--	1.37	12	--
58	.071	100	70	1.90	100	84	11.0	100	60

[1]Unaccounted for streamflow and loads were calculated by subtracting the sum of the values for sites 3, 24, 47, and 56 from the value for site 58. The resulting value could represent unsampled inflows or be an artifact of the analysis. Percents may not total to exactly 100 due to rounding.

Summary

Concentrations, sources, and loads of trace elements in streams affected by historical mining in the Boulder River watershed near Basin in southwestern Montana were investigated during this study. Study results are essential for land managers to plan effective and cost-efficient remediation, prioritize remediation activities, and establish restoration goals. Specific objectives were to determine which trace elements associated with ore deposits in the watershed occurred at levels that potentially could be toxic to aquatic organisms, characterize trace-element concentrations throughout the watershed, identify primary source areas by quantifying trace-element loads at key sites in the watershed, and establish a water-quality monitoring program to determine long-term seasonal and annual variations near areas where remediation activities were likely. The study focused on those trace elements associated with the polymetallic veins exploited by historical mining.

The magnitude and extent of trace elements in the Boulder River watershed were assessed by systematic sampling of streams throughout the area during a wide range of hydrologic conditions, comparison of trace-element concentrations to aquatic-life standards, estimation of annual loading of trace elements to the main streams in the watershed, and analysis of concentration data for temporal trends. Water-quality measurements also were made in reference streams draining unmineralized subbasins underlain by the same or similar lithologic units. Almost all streams in the Boulder River watershed had near-neutral to alkaline pH and, except for elevated trace-element concentrations, generally good water quality.

Trace-element concentrations in streams of the Boulder River watershed varied greatly; the highest concentrations occur in small streams downstream from a few of the inactive mines in the watershed, and the lowest concentrations are generally in stream reaches upstream from areas of historical mining or in headwater streams where small inactive mines had little effect. Cadmium, copper, lead, and zinc concentrations commonly exceeded chronic aquatic-life standards. Zinc exceeded these standards to a greater degree than did the other metals. The highest concentrations were in streams downstream from three large inactive mines: the Crystal mine in Uncle Sam Gulch, the Comet mine in High Ore Creek, and the Bullion mine in a tributary to Jack Creek. Downstream from these three mines, the chronic aquatic-life standard for at least one trace element associated with the metal ore deposits in the watershed was exceeded at all sampling sites, including sites in the Boulder River between Basin Creek and the Jefferson River. Because hardness decreases while concentrations increase, the toxicity of copper and lead was much higher during high flow compared to low flow. Toxicity of cadmium and zinc also was slightly higher during high flow compared to low flow.

In the Boulder River watershed, sources of cadmium, copper, lead, and zinc in undisturbed areas appear to be small; however, arsenic is pervasive at low concentrations throughout the watershed. Basin, Cataract, and High Ore Creeks together contributed 33 and 38 percent of the annual streamflow and dissolved arsenic, respectively, at the downstream Boulder River site, roughly in proportion to their percentage of the total drainage area. In contrast, the three tributaries contributed nearly all the dissolved cadmium (89 percent) and zinc (83 percent) as well as more than half of the dissolved copper (56 percent). On an annual basis, Cataract Creek contributed more cadmium, copper, and zinc than either Basin Creek or High Ore Creek.

References Cited

Becraft, G.E., Pinckney, D.M., and Rosenblum, Sam, 1963, Geology and mineral deposits of the Jefferson City quadrangle, Jefferson and Lewis and Clark Counties, Montana: U.S. Geological Survey Professional Paper 428, 101 p.

Brown, V.M., Shaw, T.L., and Shurben, D.G., 1974, Aspects of water quality and the toxicity of copper to rainbow trout: Water Research, v. 8, p. 797–803.

Chapman, B.M., Jones, D.R., and Jung, R.F., 1983, Processes controlling metal ion attenuation in acid mine drainage streams: Geochimica et Cosmochimica Acta, v. 47, p. 1957–1973.

Church, S.E., Kimball, B.A., Fey, D.L., Ferderer, D.A., Yager, T.J., and Vaughn, R.B., 1997, Source, transport, and partitioning of metals between water, colloids, and bed sediments of the Animas River, Colorado: U.S. Geological Survey Open-File Report 97–151, 136 p.

Desborough, G.A., Briggs, P.H., and Mazza, Nilah, 1998, Chemical and mineralogical characteristics and acid-neutralizing potential of fresh and altered rocks and soils of the Boulder River headwaters in Basin and Cataract Creeks of northern Jefferson County, Montana: U.S. Geological Survey Open-File Report 98–40, 21 p.

Desborough, G.A., Briggs, P.H., Mazza, Nilah, and Driscoll, Rhonda, 1998, Acid-neutralizing potential of minerals in intrusive rocks of the Boulder batholith in northern Jefferson County, Montana: U.S. Geological Survey Open-File Report 98–364, 21 p.

Desborough, G.A., and Driscoll, Rhonda, 1998, Mineralogical characteristics and acid-neutralizing potential of drill core samples from eight sites considered from metal-mine related waste repositories in northern Jefferson, Powell, and Lewis and Clark Counties, Montana: U.S. Geological Survey Open-File Report 98–790, 6 p.

Desborough, G.A., and Fey, D.L., 1997, Preliminary characterization of acid-generating potential and toxic metal solubility of some abandoned metal-mining related wastes in the Boulder River headwaters, northern Jefferson County, Montana: U.S. Geological Survey Open-File Report 97–478, 21 p.

Elliott, J.E., Loen, J.S., Wise, K.K., and Blaskowski, M.J., 1992, Maps showing locations of mines and prospects in the Butte 1°×2° quadrangle, western Montana: U.S. Geological Survey Miscellaneous Investigations Series Map I–2050–C, 147 p., scale 1:250,000.

Erickson, R.J., Benoit, D.A., Mattson, V.R., Nelson, H.P., and Leonard, E.N., 1996, The effects of water chemistry on the toxicity of copper to fathead minnows: Environmental Toxicology and Chemistry, v. 15, p. 181–193.

Helsel, D.R., and Hirsch, R.M., 1992, Statistical methods in water resources: Amsterdam, Elsevier, 522 p.

Kimball, B.A., Callender, Edward, and Axtmann, E.V., 1995, Effects of colloids on metal transport in a river receiving acid mine drainage, upper Arkansas River, Colorado, U.S.A.: Applied Geochemistry, v. 10, p. 285–306.

Marvin, R.K., Metesh, J.J., Bowler, T.P., Lonn, J.D., Watson, J.E., Madison, J.P., and Hargrave, P.A., 1997, Abandoned-inactive mines program, U.S. Bureau of Land Management: Montana Bureau of Mines and Geology Open-File Report 348, 506 p.

Metesh, J.J., Lonn, J.D., Duaime, T.E., and Wintergerst, Robert, 1994, Abandoned-inactive mines program, Deerlodge National Forest—Volume I, Basin Creek drainage: Montana Bureau of Mines and Geology Open-File Report 321, 131 p.

Metesh, J.J., Lonn, J.D., Duaime, T.E., Marvin, R.K., and Wintergerst, Robert, 1995, Abandoned-inactive mines program, Deerlodge National Forest—Volume II, Cataract Creek drainage: Montana Bureau of Mines and Geology Open-File Report 344, 201 p.

Metesh, J.J., Lonn, J.D., Marvin, R.K., Madison, J.P., and Wintergerst, Robert, 1996, Abandoned-inactive mines program, Deerlodge National Forest—Volume V, Jefferson River drainage: Montana Bureau of Mines and Geology Open-File Report 347, 179 p.

Montana Department of Environmental Quality, 1999, Montana numeric water quality standards: Helena, Mont., Planning Prevention and Assistance Division, Standards and Economic Analysis Section Circular WQB-7, 41 p.

Nelson, F.A., 1976, The effects of metals on trout populations in the upper Boulder River, Montana: Bozeman, Mont., Montana State University M.S. thesis, 60 p.

Nimick, D.A., and Cleasby, T.E., 2000, Water-quality data for streams in the Boulder River watershed, Jefferson County, Montana: U.S. Geological Survey Open-File Report 00–99, 70 p.

Phillips, Glen, and Hill, Kurt, 1986, Evaluation of sources and toxicity of copper and zinc in the Boulder River drainage, Jefferson County—1985: Montana Department of Fish, Wildlife and Parks, Pollution Control Information Series Technical Report 4, 28 p.

Rantz, S.E., and others, 1982, Measurement and computation of streamflow—Volume 1, Measurement of stage and discharge: U.S. Geological Survey Water-Supply Paper 2175, p. 1–284.

Rees, T.F., and Ranville, J.F., 1990, Collection and analysis of colloidal particles transported in the Mississippi River, U.S.A.: Journal of Contaminant Hydrology, v. 6, p. 241–250.

Ruppel, E.T., 1963, Geology of the Basin quadrangle, Jefferson, Lewis and Clark, and Powell Counties, Montana: U.S. Geological Survey Bulletin 1151, 121 p.

Schemel, L.E., Kimball, B.A., and Bencala, K.E., 2000, Colloid formation and metal transport through two mixing zones affected by acid mine drainage near Silverton, Colorado: Applied Geochemistry, v. 15, p. 1003–1018.

Shields, R.R., White, M.K., Ladd, P.B., Chambers, C.L., and Dodge, K.A., 1998, Water resources data, Montana, water year 1997: U.S. Geological Survey Water-Data Report MT–97–1, 474 p.

Smith, K.S., 1999, Metal sorption on mineral surfaces, An overview with examples relating to mineral deposits, *in* Plumlee, G.S., and Logsdon, M.J., eds., The environmental geochemistry of mineral deposits—Part A, Processes, techniques, and health issues: Society of Economic Geologists, Reviews in Economic Geology, v. 6A, p. 161–182.

U.S. Environmental Protection Agency, 1999, National recommended water quality criteria—Correction: Washington, D.C., Office of Water, EPA 822-Z-99-001, 25 p.

Vincent, E.R., 1975, Southwest Montana fisheries investigation, Inventory of waters of the project area: Montana Department of Fish and Game, Fisheries Division, Project no. F-9-R-23, Job no. 1-a, 12 p.

Wallace, C.A., 1987, Generalized geologic map of the Butte 1°×2° quadrangle, Montana: U.S. Geological Survey Miscellaneous Field Studies Map MF-1925, scale 1:250,000.

Quantification of Metal Loading by Tracer Injection and Synoptic Sampling, 1997–98

By Briant A. Kimball, Robert L. Runkel, Thomas E. Cleasby, and David A. Nimick

Chapter D6 of
Integrated Investigations of Environmental Effects of Historical Mining in the Basin and Boulder Mining Districts, Boulder River Watershed, Jefferson County, Montana
Edited by David A. Nimick, Stanley E. Church, and Susan E. Finger

Professional Paper 1652–D6

U.S. Department of the Interior
U.S. Geological Survey

Contents

Figures

Tables

METRIC CONVERSION FACTORS AND ABBREVIATIONS

Multiply	By	To obtain
foot (ft)	0.30481	meter (m)
cubic foot per second (ft^3/s)	28.317	liter per second (L/s)
pound (lb)	.45	kilogram (kg)

Temperature in degree Celsius (°C) can be converted to temperature in degree Fahrenheit (°F) by using the following equation:

$$°F = 9/5°C+32.$$

The following terms and abbreviations also are used in this report:

kilograms per day (kg/day)
milligram per liter (mg/L)
microgram per liter (μg/L)
millimoles per liter (mM/L)
milliliters per minute (mL/min)
milligram per second (mg/s)

Chapter D6
Quantification of Metal Loading by Tracer Injection and Synoptic Sampling, 1997–98

By Briant A. Kimball, Robert L. Runkel, Thomas E. Cleasby, and David A. Nimick

Abstract

Determination of the best sites for remediation of mine drainage requires an understanding of metal contributions from all sources in a watershed. A hydrologic framework to study metal loading in selected streams of the Boulder River watershed of Montana was established by a series of mass-loading studies of three impacted stream reaches. Each study used the tracer-dilution method in conjunction with synoptic sampling to determine the spatial distribution of discharge and concentration. Discharge and concentration data were then used to develop mass-loading profiles for the various metals of interest. Discharge and load profiles (1) identify the principal sources of load to the streams; (2) demonstrate the importance of unsampled, dispersed subsurface inflows; and (3) estimate the amount of attenuation. The two major sources of metal loading to the streams are the Crystal mine adit discharge in Uncle Sam Gulch and the Bullion mine adit in the Bullion Mine tributary. Other sources are small in comparison to these two. Along the 40,905-foot study reach of Cataract Creek, 21.2 kilograms per day of zinc were added to the stream. About 75 percent of this load came from Uncle Sam Gulch, a principal tributary. By comparison, the adit discharge from the Bullion mine accounted for 2.8 kilograms per day of zinc, which was only about 20 percent of the zinc load coming from the Crystal mine adit in Uncle Sam Gulch.

About 34 percent of the zinc load in Cataract Creek occurred as unsampled inflow, including part of the load from Uncle Sam Gulch. Along the study reach, about 34 percent of the zinc load was removed to the stream bed. Similar details are available for other metals in each of the three streams studied. This watershed approach provides a detailed snapshot of metal load for the watershed to support remediation decisions, and quantifies processes affecting metal transport.

Introduction

Land-management agencies in the Boulder River watershed of Montana are charged with the task of reclaiming abandoned mine lands. Numerous inactive mines contribute substantial metal loads and acidic waters to the streams that drain the Boulder River watershed. The affected streams are headwater systems that gain substantial amounts of water as they flow down valley. Sources of additional water range from well-defined tributary inflows to diffuse ground-water inflows that are not visible. The water quality associated with these sources also varies dramatically, from dilute mountain springs to metal-rich water emanating from mineralized areas. The challenge facing land-management agencies is thus one of source determination: For a given stream, what sources of water are most detrimental to water quality? This question is of paramount importance to land managers who must implement remedial actions subject to fiscal constraints.

The approach used in these studies to address the problem of source determination is based on two well-established techniques: the tracer-dilution method and synoptic sampling. The tracer-dilution method provides estimates of stream discharge that are in turn used to quantify the amount of water entering the stream through tributary and ground-water inflow. Synoptic sampling of instream and inflow chemistry provides a spatially detailed "snapshot" of stream-water quality. When used in unison, these techniques provide a description of the watershed that includes both discharge and concentration. Discharge and concentration data can then be used to determine the mass loading associated with various sources of water. Sources representing the greatest contributions in terms of mass loading can then be the target of remedial action.

Purpose and Scope

The purpose of this chapter is to describe the application of the combined tracer-dilution and synoptic-sampling method to selected stream reaches within the Boulder River watershed. Application of the method results in a set of mass-loading curves that illustrate the spatial distribution of the various inflow sources and the effects of the sources on instream water quality. The mass-loading curves are used to answer three basic questions. First, which sources have the greatest effect on stream-water quality in terms of the greatest contributions to constituent loads? Sources determined to be substantial in

terms of mass loading could be the subject of further study and candidates for remedial action. Second, are there substantial inflows that are primarily composed of diffuse ground-water inflow? Stream subreaches that are dominated by ground-water loading may not be amenable to remediation due to the lack of a well-defined surface-water inflow. Third, is there substantial instream attenuation of metal loads? Attenuation of metal loads by geochemical processes should be considered as part of the remedial design.

This chapter begins with a detailed account of the studies conducted on individual stream reaches within the watershed and the associated mass-loading curves. These studies were conducted over two field seasons (1997–98) during low flow. Despite the focus on the low-flow period, differences in the flow regimes arise as a result of yearly variability. The studies in Uncle Sam Gulch and the Bullion Mine tributary were conducted during a 2-week period in 1998.

Methods

The combined tracer-dilution and synoptic-sampling method has been applied to many streams in the Rocky Mountains (Bencala and McKnight, 1987; Kimball, Broshears, and others, 1994; Kimball, 1997; Kimball and others, 1999, 2001, 2002). The studies described herein were undertaken during low-flow conditions (generally August and September). Application of the method to low-flow conditions is an appropriate focus for two reasons. First, the mass-loading profile at low flow reflects the importance of metal sources that enter the stream on a continuous basis. Remedial actions that address the sources identified at low flow will, therefore, improve water quality during the entire year. Second, the pattern of metal loading at low flow indicates which sources contribute to high concentrations during the winter months when the most toxic conditions likely occur (Besser and Leib, 1999). During the winter months, the extent of dilution of mine drainage is less than during higher flow, and limits of toxicity are more likely to be exceeded (Besser and others, 2001). Although dissolved metal loads are greater during snowmelt runoff, true dissolved metal concentrations generally are lower (Nimick and Cleasby, this volume, Chapter D5) and the risk to aquatic life is not as great.

Tracer Injections and Stream Discharge

Quantifying discharge in mountain streams by the traditional velocity-area method[1] (Rantz and others, 1982) is compromised because of the roughness of the streambed and the variability caused by pools and riffles (Jarrett, 1992). Further, a substantial percentage of discharge may flow through porous areas of the streambed that make up the hyporheic zone (Zellweger and others, 1989). Measurement of discharge with the velocity-area method does not account for flow through the hyporheic zone[2], and discharge estimated by that method may result in an underestimate of metal loads (Zellweger and others, 1989; Kimball, 1997). Another limitation of the velocity-area method for the characterization of metal loads is the time and personnel requirements associated with each discharge measurement. In the studies described herein, numerous (about 30–50) instream samples were collected during a single day to characterize stream chemistry at steady state. Velocity-area discharge measurements made in conjunction with sample collection at a large number of sites are limiting, if not impossible.

The tracer-dilution method is an alternative means of estimating discharge (Kilpatrick and Cobb, 1985). The tracer-dilution method uses an inert tracer that is continuously injected into the stream at a constant rate and concentration. With sufficient time, all parts of the stream, including side pools and the hyporheic zone, will become saturated with the tracer. Instream concentrations at a specific distance downstream will become constant (Kimball, 1997). When the stream reaches this condition during a tracer-injection, it is at a "plateau concentration." Decreases in plateau concentration along the length of the stream reflect the dilution of tracer by additional water entering the channel from surface and ground-water inflows. This dilution allows for the calculation of discharge at each stream site. Application of the tracer-dilution method addresses both of the problems previously noted: (1) the tracer enters porous areas of the streambed such that flow through the hyporheic zone also is measured; and (2) collection of tracer samples when plateau concentrations are achieved provides the ability to obtain discharge estimates at numerous stream sites.

Successful implementation of the tracer-dilution method is dependent on two factors. First and foremost, the injected tracer must be transported through the stream reach in a conservative manner; concentrations of the tracer should be unaffected by biogeochemical reactions. Previous studies have documented the transport and chemistry of inorganic salt tracers (Bencala and others, 1990; Broshears and others, 1993; Zellweger, 1994). Because of the conservative behavior of chloride in most natural waters and the availability of inexpensive sodium chloride salt, NaCl was used in the studies described herein. A second important factor is the ability to maintain a constant rate of injection during the study. For the studies described here, tracer injections were controlled with precision metering pumps linked to a Campbell CR-10 data logger. Use of the data logger provides a means to maintain a constant injection rate as battery voltage decreases. Additional details on specific tracer injections are included in the "Subbasin Studies" section.

[1]Velocity-area discharge method. Physical measurement of discharge made by dividing a cross section of the flowing stream into at least 20 area increments and measuring velocity at the center of each increment. The sum gives the total discharge at that cross section.

[2]Hyporheic zone. That area of the streambed alluvium that contains at least 10 percent stream water as a result of exchange with the stream.

Kilpatrick and Cobb (1985) presented a simple mass-balance equation that considers the concentration and injection rate of the added tracer. Discharge at the first synoptic site downstream from the injection is given by:

$$Q_D = \frac{Q_{INJ}C_{INJ}}{C_D - C_0} \quad (1)$$

where Q_{INJ} = the injection rate,
C_{INJ} = the injectate concentration,
C_D = the tracer concentration at the plateau, and
C_0 = the naturally occurring concentration of the tracer upstream from the injection.

This equation is based on two assumptions: that (1) negligible inflow enters the stream between the injection site and the first synoptic site, and (2) the injection concentration is much greater than C_0. Discharge estimates at the remaining synoptic sites are given by:

$$Q_D = \frac{Q_U C_U - C_L}{C_D - C_L} \quad (2)$$

where C_L = tracer concentration in the inflow waters entering a specified subreach,
C_U = the plateau tracer concentration for the synoptic site immediately upstream, and
Q_U = the stream discharge for the synoptic site immediately upstream.

Inflow chloride concentrations in some subreaches represent well-defined surface inflows that are easily sampled. In other subreaches, inflow waters may be primarily diffuse ground-water inflows that are difficult or impossible to sample. These subreaches require estimation of the chloride inflow concentration, a process that can lead to uncertainty in discharge calculations. For the three studies described here, chloride values in subreaches that are dominated by unsampled ground-water inflow had to be estimated. The uniformity in surface-inflow chloride concentrations has a negligible effect on discharge estimates. Note that the problem of estimating chloride for systems with variable background concentrations may be avoided by conducting a pre-synoptic sampling of the stream (Kimball and others, 2001). At the start and end of the injection, samples generally are collected manually at intervals of 5 or 10 minutes at three to five sites, chosen from among the synoptic sampling sites, to define the arrival and departure of the tracer. During the plateau period, hourly samples are taken by automatic samplers at the same sites, which are called transport sites. These samples provide information for transport modeling and allow for resolving temporal effects from storms that could occur during synoptic sampling.

Synoptic Sampling and Analytical Methods

The spatial distribution of metal sources may be characterized by synoptic sampling. Under ideal conditions, samples at all of the sampling locations would be collected simultaneously, providing a description of stream-water quality at steady state. Personnel limitations generally preclude simultaneous sample collection, but the synoptic studies described in the following text provide an approximate means of describing steady-state conditions. This approximation is achieved by the collection of samples throughout a relatively short period (less than 8 hr) and by conducting the studies during low-flow conditions such that the effects of diurnal flow variation are minimized. By approximating steady-state conditions, synoptic sampling provides a spatially intensive "snapshot" of chemistry and discharge that is used to quantify instream loads.

During a synoptic study, samples are collected at several stream and inflow sites. Stream sites along the study reach are spaced such that they bracket the sampled inflows and areas of likely subsurface inflow. Subreaches that are bracketed by two adjacent stream sites are referred to as stream segments. The intent of this bracketing is to capture the changes in load that are attributable to visible surface inflow and (or) diffuse subsurface inflow within each segment. At this level of spatial detail, changes in stream chemistry and discharge between stream sampling sites reflect a net metal load for specific segments, although the loads cannot always be attributed to specific sources.

For each of the following studies, stream and inflow samples were collected at numerous predetermined locations, beginning at the downstream end of the study reach and ending upstream of the tracer-injection. This downstream-to-upstream sampling order was followed in order to avoid disturbing streambed materials. Inflow and stream sites that were considered well mixed were sampled by using grab techniques. Stream sites that were not well mixed were sampled by equal width integration[3] (Ward and Harr, 1990). Water temperature was measured on site and the collected samples were transported to a central location for further processing. Samples were processed at a central location to measure pH and specific conductance and to divide the sample into the following bottles: a raw (unfiltered) unacidified sample (RU), a raw acidified sample (RA), a filtered unacidified sample (FU), a filtered acidified sample (FA), and a ultrafiltered acidified sample (UFA).

Specific conductance and pH were determined from the RU sample within hours of sample collection. Filtration included tangential-flow filtration through 0.45-µm membranes (FU and FA samples) and ultrafiltration by using a 10,000-Dalton molecular weight membrane (UFA sample).

[3]Equal-width integration. Sample collected by moving a depth-integrating sampler, like a USGS DH-81, down and up at a constant rate at equal increments of width across a stream. Thus, those parts of the stream that have greater discharge will fill the bottle the most.

Metal concentrations for the RA, FA, and UFA samples were determined by inductively coupled plasma–atomic emission spectrometry (Lichte and others, 1987). Anion concentrations were determined from FU samples by using ion chromatography (Kimball and others, 1999). Ferrous iron was determined colorimetrically from the UFA samples (Kimball and others, 1992), and total alkalinity was determined by titration.

Use of two filter sizes provides for three different operationally defined concentrations for each metal. The unfiltered sample (RA) provides a measure of the total-recoverable metal concentration (dissolved + colloidal), and the ultrafiltrate concentration (UFA) is considered the dissolved metal concentration. The 0.45-µm concentration (FA) is used for comparison purposes. Colloidal metal concentrations are defined as the difference between the total-recoverable (RA) and the ultrafiltrate metal concentrations (UFA) for stream samples (Kimball and others, 1995).

Principal Components Analysis

An important objective of synoptic sampling is to recognize patterns or chemical characteristics that indicate the sources of mine drainage. Water-rock interactions with different mineral assemblages in source areas create distinct chemical signatures among the inflows. The signatures may produce groups of inflow samples that are distinguished by their similarities. Groups of stream samples may be linked to inflow groups, indicating which inflows influence stream chemistry. Distinctions among inflow groups also may lead to an understanding of differences in drainage from mined and nonmined areas.

Patterns in the chemistry, including the pH, of synoptic samples are displayed by using Principal Components Analysis (PCA). A principal component represents a transformed axis that is a linear combination of the original variables (Daultrey, 1976; Davis, 1986). The transformation to a new axis is not statistical, but is simply a rotation (in multi-dimensional space) that orients the data points so that we observe the greatest amount of difference (or variance) among them. The rotation does not change the relation of one sample to another; it only changes how we view the samples. For example, if the surface of a framed picture were given x, y, and z coordinates to represent its surface morphology, PCA would rotate the picture so that one would be looking at it straight on instead of at some angle. The x and y variables (height and width of the picture) are much greater than the depth (which would mostly be due to the frame). Conceptually, PCA rotates chemical data in a similar manner, and this helps one visualize the greatest distinctions among groups of samples. It also emphasizes distinct outlier samples. The first two principal components generally show enough of the variance in a data set to distinguish groups among the samples. Each sample is related to a principal component by its score on that component, which is the coordinate of the original data point on the new principal component axis.

PCA also can emphasize the physical and chemical processes that are responsible for the distinctions among groups of samples. Each chemical constituent has a correlation to the new principal components, called a loading in the jargon of PCA. These correlations can be expressed as arrows or vectors on a plot of sample scores. By combining the classification information of scores with the process information from loadings, a biplot is created. Biplots are used to present results of PCA for each mass-loading study.

Chemical reactions and mixing processes often result in linear relations among chemical constituents. To emphasize the linear relations among variables, the chemical concentration of each constituent, expressed in millimoles per liter, was log transformed. This improves correlations that may be related to stoichiometries of particular chemical reactions. It is the products of chemical reactions that end up as dissolved constituents in the stream and are sampled in a water-quality study. Mole ratios of those products provide mass-balance evidence of the water-rock reactions that may account for the observed chemistry. PCA calculations were carried out with the U.S. Geological Survey Statpac programs that include special scaling options to improve the biplot (Grundy and Miesch, 1987).

Constituent Loads

Given estimates of stream discharge and metal concentration, solute load at each stream site can be quantified as the simple product of discharge and concentration. This calculation leads to a longitudinal profile of the sampled instream load. Any change in load between a pair of stream sites accounts for the gain or loss of solute load for that segment. Gains in solute load imply the existence of a source for the solute that reaches the stream between the two stream sites. Instream load also can decrease within a stream segment, indicating a net loss of the solute as a result of chemical or biological processes. The sum of all the increases in load between sampling sites along the study reach produces cumulative instream load. At the end of the study reach, the cumulative instream load is an estimate of the total load of solute added to the stream; this estimate is likely a minimum estimate because it only measures the net loading between sites. Some of the load in that stream segment could be lost through attenuation within an individual stream segment.

The change in discharge between stream sites is used in a second approach to calculating loads. The change in discharge between two stream sites, multiplied by solute concentration of an inflow sample, provides an estimate of the inflow load for a stream segment. The sum of the inflow loads for all sampled inflows provides a longitudinal profile of the cumulative inflow load, which indicates how well the sampled inflows account for the load measured within the stream. The cumulative instream and cumulative inflow profiles are equivalent if the sampled inflows are representative of the inflows that enter the stream. This situation rarely occurs, however, because

inflows to streams include both surface and subsurface inflow. Greater subsurface concentrations would cause the profile of cumulative instream load to be more than the profile of cumulative inflow load.

Load profiles provide not only information to evaluate the location and magnitude of metal loading to the stream, but also help in understanding and quantifying watershed processes. The loading profile is a view from the stream; it accounts for the loads that actually reach the stream. A particular mine adit away from the stream may have a greater load at its adit, but if that load is attenuated before it reaches the stream, it is not accounted for within the load profile. Thus, inflow samples are obtained near the stream to represent the net delivery of metals to the stream from various sources. The three ways to account for loads from the watershed are based on instream and inflow loads. First, the sampled instream load provides information about the relative importance of metal sources in terms of which stream segments contribute the greatest loads. The level of detail from synoptic sampling allows individual increases, measured in each stream segment, to be viewed in the context of the whole watershed. Second, the difference between the cumulative instream and cumulative inflow loads provides information about the location of unsampled, or possible ground-water inflows. Third, the difference between the cumulative instream load and the sampled instream load provides information about the extent of attenuation of solutes. All this information is available on the scale of individual stream segments and the scale of the entire study reach.

Subbasin Studies

Complete chemical data for synoptic samples that were collected in each of the subbasin studies are presented in the database on CD-ROM. A description of sampling sites and summaries of chemical data are presented here for each subbasin. Locations of all the mines discussed in this chapter are in Martin (this volume, Chapter D3).

Cataract Creek Basin

Study Area and Experimental Design

The experimental design of the tracer-injection study in Cataract Creek is described in Cleasby and others (2000). The study reach started 3,000 ft upstream from Hoodoo Creek and ended at the confluence with the Boulder River (fig. 1); the total distance is more than 40,000 ft and was divided into 44 stream segments. Inflow samples were collected in 20 of the stream segments; 23 inflows were sampled in all. Downstream distance for each of the segments and inflows, along with site descriptions, are listed in table 1.

A sodium chloride tracer with a chloride concentration of 133,200 mg/L was injected at a rate of 435 mL/min. This provided a clear chloride signal that was elevated above background concentrations (fig. 2). Because the inflow chloride concentrations were low, but not constant, equation 2 was used to calculate discharge (fig. 2). The increase in discharge along the study reach was 12.5 ft^3/s. Discharge increased by 4.8 ft^3/s in those segments that had no inflow samples; this was 38 percent of the total increase in discharge, which was a considerable ground-water component to the increase in flow. The path of the creek generally follows the structural control of a major fault (O'Neill and others, this volume, Chapter D1, pl. 1), and the reach is predicted to be a gaining reach based on the lineament and fracture-density analysis of McDougal and others (this volume, Chapter D9).

Chemical Characterization of Synoptic Samples

Synoptic sampling of inflows provides a range of chemistry that affects the stream and provides a context for the changes in stream chemistry and solute loads. In a watershed affected by mine drainage that has outcrops of rocks with acid-neutralizing capacity, inflow chemistry can range from acidic and metal-rich to alkaline and essentially metal-free. Both kinds of inflow chemistries can affect the stream chemistry.

Stream water in Cataract Creek was a calcium bicarbonate type, reflecting the chemical weathering of bedrock in the watershed (Nimick and Cleasby, this volume, Chapter D5). The tracer overwhelmed baseline concentrations of sodium and chloride in the stream. The baseline concentrations of inflows, however, were approximately 3 mg/L sodium and 0.3 mg/L chloride. This baseline chloride concentration was about 10 times lower than the chloride concentration at the final stream sampling site (fig. 2). The alkalinity of Cataract Creek remained nearly constant along the entire reach (fig. 3). Concentration of the other major ions increased slightly downstream from Uncle Sam Gulch; changes in calcium and sulfate were the greatest (fig. 3). Calcium concentrations upstream from Uncle Sam Gulch averaged 12.4 mg/L, and 15.0 mg/L downstream; sulfate concentrations averaged 9.1 mg/L upstream and 16.8 mg/L downstream. The greater change in sulfate mostly represents the mine-drainage inputs from Uncle Sam Gulch.

Several metals occurred with measurable concentrations. Aluminum, copper, iron, manganese, and zinc concentrations were substantially above detection limits. Cadmium, nickel, and lead concentrations mostly were near limits of detection. Although no great variation occurred in major-ion concentrations or pH along the study reach, substantial differences did occur in metal concentrations upstream and downstream from Uncle Sam Gulch, with higher concentrations occurring downstream (fig. 4). Concentrations of aluminum, copper, and zinc that were less than the detection limits are not plotted; therefore, the lines are not all continuous. Average

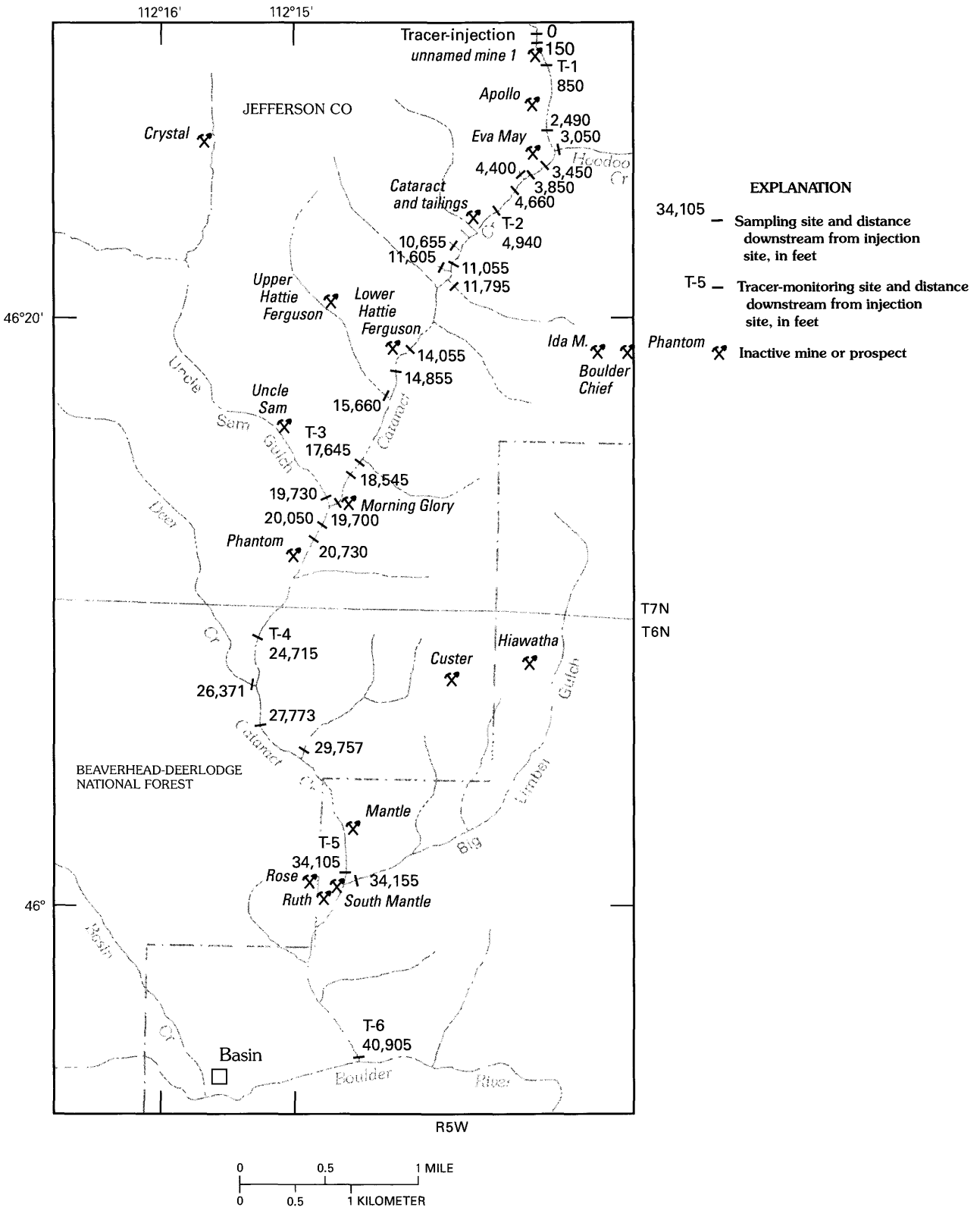

Figure 1. Location of study reach, selected inactive mines or prospects, and selected sampling sites, Cataract Creek drainage (modified from Cleasby and others, 2000).

Table 1. Segment number, distance along study reach, source, site description, and selected water-quality characteristics of water from synoptic sampling sites, Cataract Creek, August 13, 1997.

[Dist, distance, in feet along the study reach; source: S, stream; RBI, right-bank inflow; LBI, left-bank inflow; Q, discharge, in liters per second; T, temperature, in degrees Celsius; pH, in standard units; Ksc, specific conductance, in microsiemens per centimeter; Cl, chloride, in milligrams per liter]

Segment number	Dist	Source	Site description	Q	pH	Ksc	Cl
S01	150	S	First site below injection	117	7.71	110	8.28
T01	160	RBI	Right-bank inflow	4.0	7.62	70	<.1
S02	850	S	T1 transport site in canyon	121	7.85	108	8.26
S03	1,370	S	Above right-bank mine dump	124	7.82	106	8.08
T02	1,615	RBI	Right-bank inflow from mine dump	4.0	7.59	190	<.1
S04	1,690	S	Below mine dump at Apollo mine	130	7.87	107	7.72
T03	1,691	RBI	Right-bank inflow	0.1	7.81	175	<.1
S05	2,490	S	Above mine dump at Eva May mine	130	7.83	107	7.74
T04	3,050	LBI	Hoodoo Creek on left bank	40.0	7.75	106	<.1
S06	3,450	S	Below Hoodoo Creek	170	7.82	106	5.99
S07	3,850	S	Above Eva May mine tailings	174	7.83	105	5.85
T05	4,400	RBI	Eva May tailings inflow	8.0	7.48	100	<.1
S08	4,660	S	Adjacent to Eva May tailings pile	182	7.83	106	5.61
S09	4,940	S	T2 transport site below Eva May mine	185	7.73	107	5.52
T06	4,941	RBI	From pipe under road	2.0	7.71	92	<.1
S10	5,940	S	Below curve with overbank tailings	187	7.74	108	5.46
S11	6,800	S	Along bend	189	7.74	107	5.42
S12	7,900	S	Below old cabin	191	7.80	108	5.37
S13	8,700	S	Below mine dump, at Cataract mine tailings	193	7.71	108	5.31
T07	8,820	RBI	Below Cataract mine dump	5.0	7.26	65	<.1
S14	9,220	S	Adjacent to Cataract mine tailings	198	7.66	108	5.20
T08	9,225	RBI	Cataract mine tailings with iron stains	3.5	7.20	88	<.1
S15	10,380	S	End of large flood plain	205	7.52	110	5.02
T09	10,655	RBI	Right-bank inflow	10.0	7.51	57	<.1
S16	11,055	S	Adjacent to ponded water on right bank	215	7.38	109	4.81
T10	11,605	RBI	Inflow with iron stains	4.5	6.61	130	<.1
T11	11,795	LBI	Boulder Chief and Ida M. mines	4.5	7.57	122	<.1
S17	12,115	S	Above large clear-cut area	224	7.68	109	4.63
T12	12,120	LBI	Left-bank inflow	7.0	7.63	143	<.1
S18	13,255	S	Above Lower Hattie Ferguson mine	231	7.77	111	4.49
S19	14,055	S	Below Lower Hattie Ferguson mine	236	7.82	113	4.42
S20	14,855	S	Above left-bank inflow	239	7.81	113	4.37
T13	14,860	LBI	Left-bank inflow	3.0	7.89	84	<.1
S21	15,655	S	Below Upper Hattie Ferguson mine	242	7.44	112	4.31
T14	15,660	RBI	Upper Hattie Ferguson mine	4.0	7.59	116	<.1
T15	15,845	RBI	Right-bank inflow	4.0	7.45	135	<.1
S22	16,845	S	Below inflows	250	7.81	113	4.19
S23	17,645	S	T3 transport site below logging-road ford	261	7.72	114	4.05
S24	18,545	S	Above biological sampling site	270	7.80	116	3.93
S25	19,245	S	Above Morning Glory mine	276	7.64	116	3.85
S26	19,700	S	Below Morning Glory mine	276	7.83	116	3.92
T16	19,730	RBI	Uncle Sam Gulch	50.0	7.32	134	<.1
S27	20,050	S	Below Uncle Sam Gulch	326	7.63	119	3.30
S28	20,730	S	Below cabin and tailings pile on right bank	336	7.81	118	3.22
S29	21,130	S	Check for reaction below Uncle Sam Gulch	336	7.61	118	3.22
T17	21,315	LBI	Waste-rock piles on both banks	2.0	8.10	409	<.1
S30	21,715	S	Along cascades below small mine dumps	338	7.83	118	3.21
S31	22,315	S	Above rock wall	338	7.80	118	3.21

Table 1. Segment number, distance along study reach, source, site description, and selected water-quality characteristics of water from synoptic sampling sites, Cataract Creek, August 13, 1997.—Continued

Segment number	Dist	Source	Site description	Q	pH	Ksc	Cl
T18	22,565	LBI	Left-bank inflow	0.1	7.77	222	< .1
T19	22,715	LBI	Left-bank inflow	0.1	7.19	220	< .1
S32	22,915	S	Below small inflow	338	7.65	120	3.21
S33	23,715	S	At old lean-to	342	7.74	123	3.18
T20	24,495	RBI	Draining oxbows	3.0	7.20	279	< .1
S34	24,715	S	T4 transport site above canyon	345	7.65	123	3.16
S35	25,215	S	Above start of canyon	349	7.70	124	3.13
S36	26,335	S	Above Deer Creek	349		126	3.13

Segment number	Dist	Source	Site description	Q	T	pH	Ksc	Cl
T21	26,370	RB	Deer Creek	11.0	11.5	8.14	188	<.1
S37	26,590	S	Below Deer Creek	360	13.5	7.88	126	3.05
S38	26,970	S	Below large concrete bridge	361	13.5	8.01	126	3.04
S39	27,775	S	Below second wooden bridge	364	13.5	8.23	126	3.02
T22	29,760	LB	Left-bank inflow	13.0	11.5	8.48	500	<.1
S40	29,970	S	Below old cabin on right bank	377	13.5	7.40	126	2.99
S41	31,470	S	Along cascade reach	382	13.5	7.82	128	2.96
S42	32,970	S	Wide section of canyon	387	13.5		128	2.93
S43	34,105	S	T5 transport site above Big Limber Gulch	394	13.5	7.84	128	2.89
T23	34,155	LB	Big Limber Creek	36.0	14.5	8.00	280	<.1
S44	34,355	S	Below Big Limber Creek	430	14.0	7.84	130	2.79
S45	40,905	S	T6 transport site Cataract Creek at mouth	472	14.8	7.83	131	2.59

concentrations of total-recoverable aluminum increased from less than 50 to about 80 µg/L at S27 (fig. 4*A*). All of the filtered copper concentrations were less than detection, and only a few sites downstream from Uncle Sam Gulch had total-recoverable concentrations greater than detection (fig. 4*B*). Copper concentrations of Uncle Sam Gulch and Big Limber Gulch were greater than 100 µg/L. Total-recoverable concentrations of iron decreased from 300 to 249 µg/L (fig. 4*C*). Filtered and total-recoverable zinc concentrations were near detection limits from the injection site to the area of the Eva May mine tailings (S08). Downstream from S08, zinc concentrations were measurable all the way to S26, upstream from Uncle Sam Gulch. Downstream from Uncle Sam Gulch, filtered zinc concentration increased an average of 34 to 461 µg/L (fig. 4*D*). Concentrations of total manganese increased from an average of 12 to 75 µg/L at S27, and had a pattern similar to that of zinc. Concentrations of cadmium, lead, and nickel were too low to observe patterns.

Nimick and Cleasby (this volume, Chapter D5) indicate those parts of Cataract Creek where metal concentrations exceeded instream aquatic life standards for acute and chronic toxicity. The tracer-study results are comparable to their findings.

The importance of the iron and aluminum colloids is seen by their impact on other metals. Total-recoverable copper concentrations were substantially higher downstream from Uncle Sam Gulch, most likely because copper was sorbed to the iron colloids (fig. 4*B*). Total-recoverable zinc concentrations increased from near the detection limit to an average of 461 µg/L downstream from Uncle Sam Gulch, and about 14 percent of that total-recoverable zinc was transported in the colloidal phase (fig. 4*D*). The presence of copper and zinc in the colloidal material could have effects on the chronic toxicity of the stream (Clements, 1994; Besser and others, 2001). The colloidal concentrations contribute to the high concentrations of copper and zinc in the bed sediments downstream from Uncle Sam Gulch (Church and others, this volume, Chapter D8).

On the basis of principal components analysis (Kimball and others, 2001), differences in chemical composition among inflows along Cataract Creek distinguish five groups among the synoptic samples (fig. 5). Three of these groups represent both stream and inflow samples, and two include only inflows. The combination of stream and inflow samples in a group may explain two conditions. First, for stream samples collected upstream of mine-drainage inflows, the chemical character of the stream samples should resemble

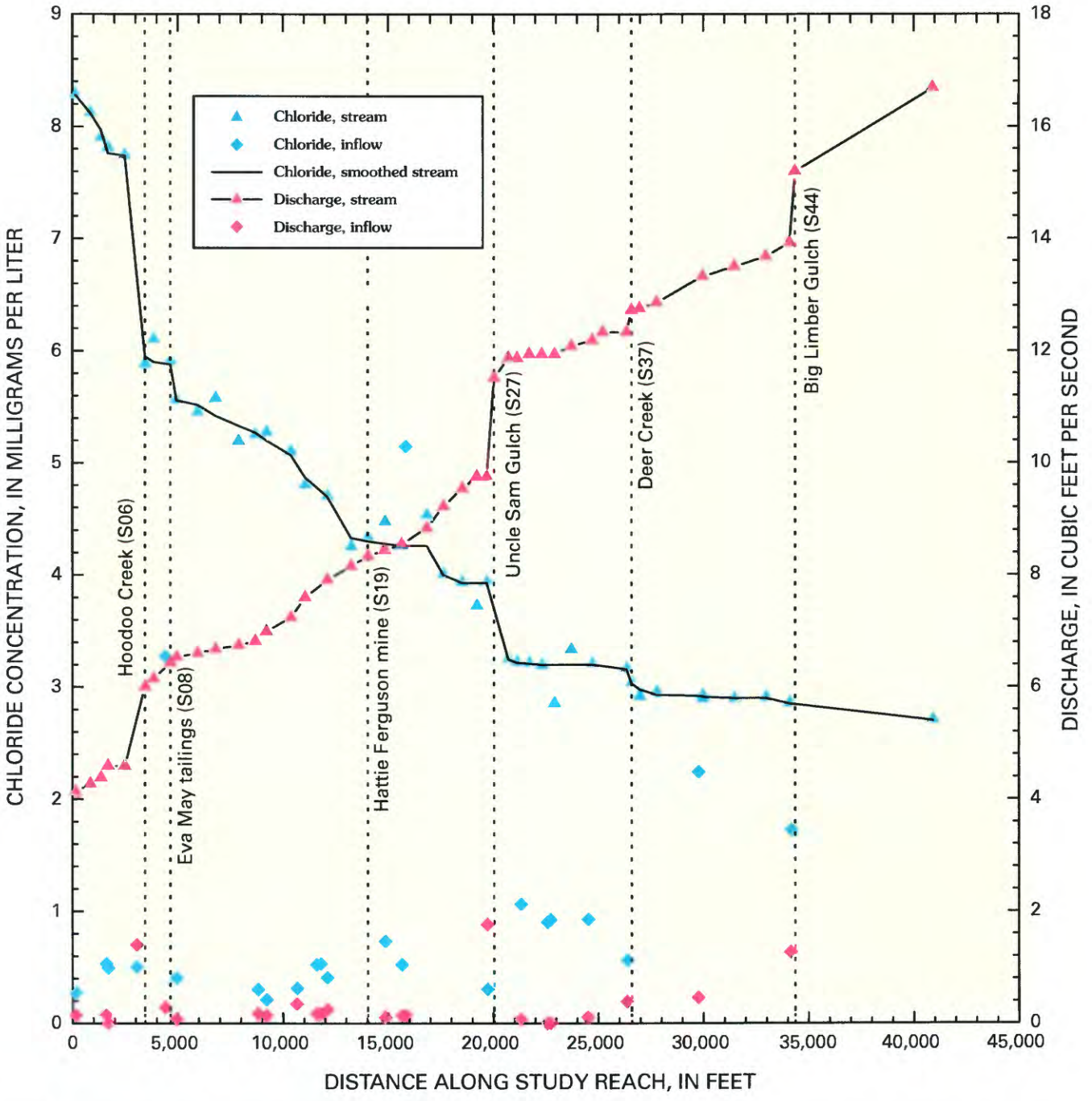

Figure 2. Injected chloride concentration and calculated discharge, Cataract Creek, August 1997. Numbers are segment numbers, table 1.

inflows that drain the same unaltered bedrock in the catchment. Second, where an inflow dramatically changes the character of the stream water, that inflow may determine the character of stream samples for some distance downstream until additional inflows or instream chemical reactions cause further change.

The vectors indicate the chemical differences among groups of samples (fig. 5). For example, samples that plot to the upper left are higher in metals, while samples that plot to the upper right have higher concentrations of the alkaline-earth metals and sulfate. Group 1 represents samples somewhat affected by mining, and includes samples upstream from Hoodoo Creek and inflow T08 (table 2). Group 2 includes most stream sites upstream from Uncle Sam Gulch and most of the inflows along that reach. These samples plot in the direction of slightly greater metal concentrations than group 1, and several of these inflows are draining areas that include tailings. Group 2 represents inflows and stream sites upstream from Uncle Sam Gulch that have higher concentrations of alkaline-earth metals and sulfate. Group 3 represents the

Table 2. Average composition of groups from principal components analysis of synoptic samples, Cataract Creek, August 1997.

[pH, in standard units; all concentrations in milligrams per liter]

Solute	Group 1 Limited effects of mining, upstream from Hoodoo Creek	Group 2 Stream samples upstream from Uncle Sam Gulch	Group 3 Stream samples downstream from Uncle Sam Gulch	Group 4 Inflows affected by alkaline-earth weathering	Group 5 Inflows from Big Limber Gulch area
Number of samples	13	24	20	9	2
pH	7.70	7.63	7.76	7.64	8.29
Sulfate	10.8	12.7	13.3	29.9	38.3
Calcium	12.5	13.7	14.6	33.4	48.3
Magnesium	2.43	2.68	2.92	5.74	9.46
Aluminum	.040	.043	.039	.025	.001
Cadmium	.003	.005	.003	.005	.001
Copper	.019	.021	.022	.028	.003
Iron	.222	.248	.311	.086	.004
Manganese	.033	.047	.062	.145	.031
Nickel	.003	.004	.003	.001	.001
Lead	.002	.003	.002	.001	.001
Strontium	.095	.118	.105	.233	.370
Zinc	.154	.243	.234	.173	.001

change in composition downstream from Uncle Sam Gulch. The sample from Uncle Sam Gulch, T16, was the only inflow sample in group 3. It is grouped with the downstream samples because it has a great influence on the chemistry of those stream samples. Stream samples in group 3 plot between the stream samples of group 2 and inflow T16; this indicates the change that resulted from the inflow of Uncle Sam Gulch. The vectors around T16 indicate that it is mostly a shift in cadmium, copper, manganese, and zinc. Groups 4 and 5 include only inflow samples, representing higher concentrations of alkaline-earth metals and sulfate, but not contributing metals.

Load Profiles

A summary of the net change in load for each segment is listed in table 3, along with a summary of calculations for the whole study reach. Cumulative instream loads provide the best estimate of the total loading for an element in a study reach. The cumulative instream load for the selected constituents in table 3 varies considerably. Sulfate load was the greatest, more than 720 kg/day, while copper load was only 2 kg/day. Among the metals, zinc had the greatest cumulative load, with 17 kg/day. The details of this loading are illustrated in load profiles and bar charts showing summaries of surface inflow, unsampled inflow, and net losses for individual stream segments (figs. 6–11).

There are differences among the profiles of metal and sulfate loading along the study reach of Cataract Creek. The two extreme profiles were those of sulfate (fig. 6) and zinc (fig. 7). The profile of sulfate shows loading in many stream segments all along the study reach. The resulting profile is a broad gradual increase in the cumulative instream load, punctuated by the tributary inflows at Hoodoo Creek (S06), Uncle Sam Gulch (S27), and Big Limber Gulch (S44). The most plausible cause of this profile is the contribution from weathering reactions throughout the watershed. Sulfate most likely has a mineralogical residence in sulfide minerals associated with alteration in the watershed. However, it is most likely more widespread than the metals associated with ore deposits.

At the other extreme, zinc loading was dominated by a large loading in one stream segment, the inflow of Uncle Sam Gulch (fig. 7). There were a few other, much smaller loads from stream segments, but none compares with the loading from Uncle Sam Gulch. This pattern results from the adit drainage of the Crystal mine into Uncle Sam Gulch (Nimick and Cleasby, this volume, Chapter D5).

These two patterns of sulfate and zinc load profiles represent different mixtures of weathering processes and mine drainage in the watershed. Profiles of other metals have some differences from these two that mostly result from the conservative or reactive behavior of the metals once they have been added to the stream. Manganese loading was similar to that of zinc, and the load from the segment containing Uncle Sam Gulch (S27) dominated the profile (fig. 8). Downstream from Uncle Sam Gulch, the manganese load decreased slightly, but no transfer of manganese to the colloidal phase took place. Instead, manganese was lost to the streambed, probably through sorption to streambed materials. A similar pattern was observed for manganese in Little Cottonwood Creek, Utah, where the pH was comparable to that of Cataract Creek (Kimball and others, 2001).

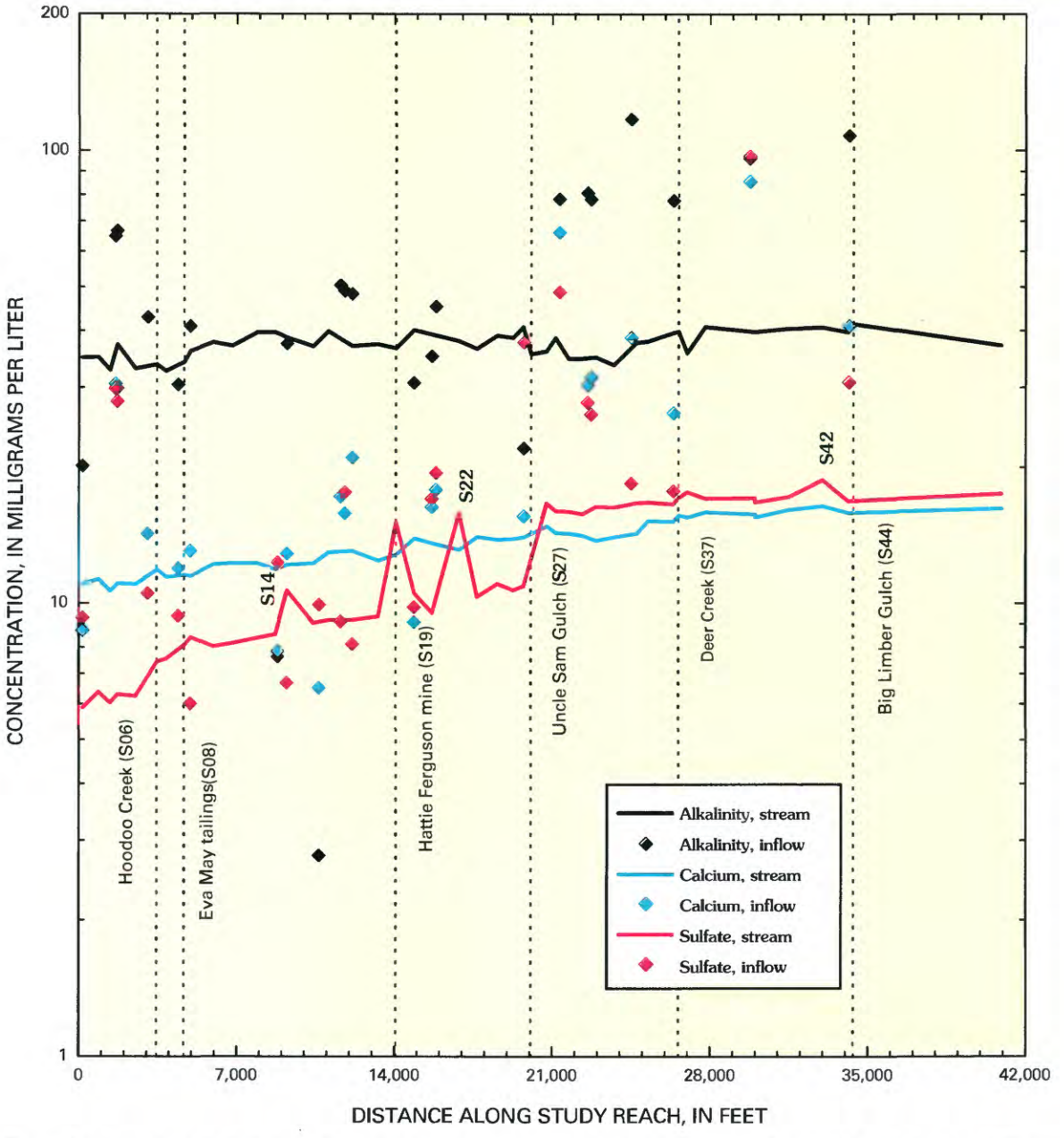

Figure 3. Variation of alkalinity, calcium, and sulfate concentrations with distance, Cataract Creek, August 1997.

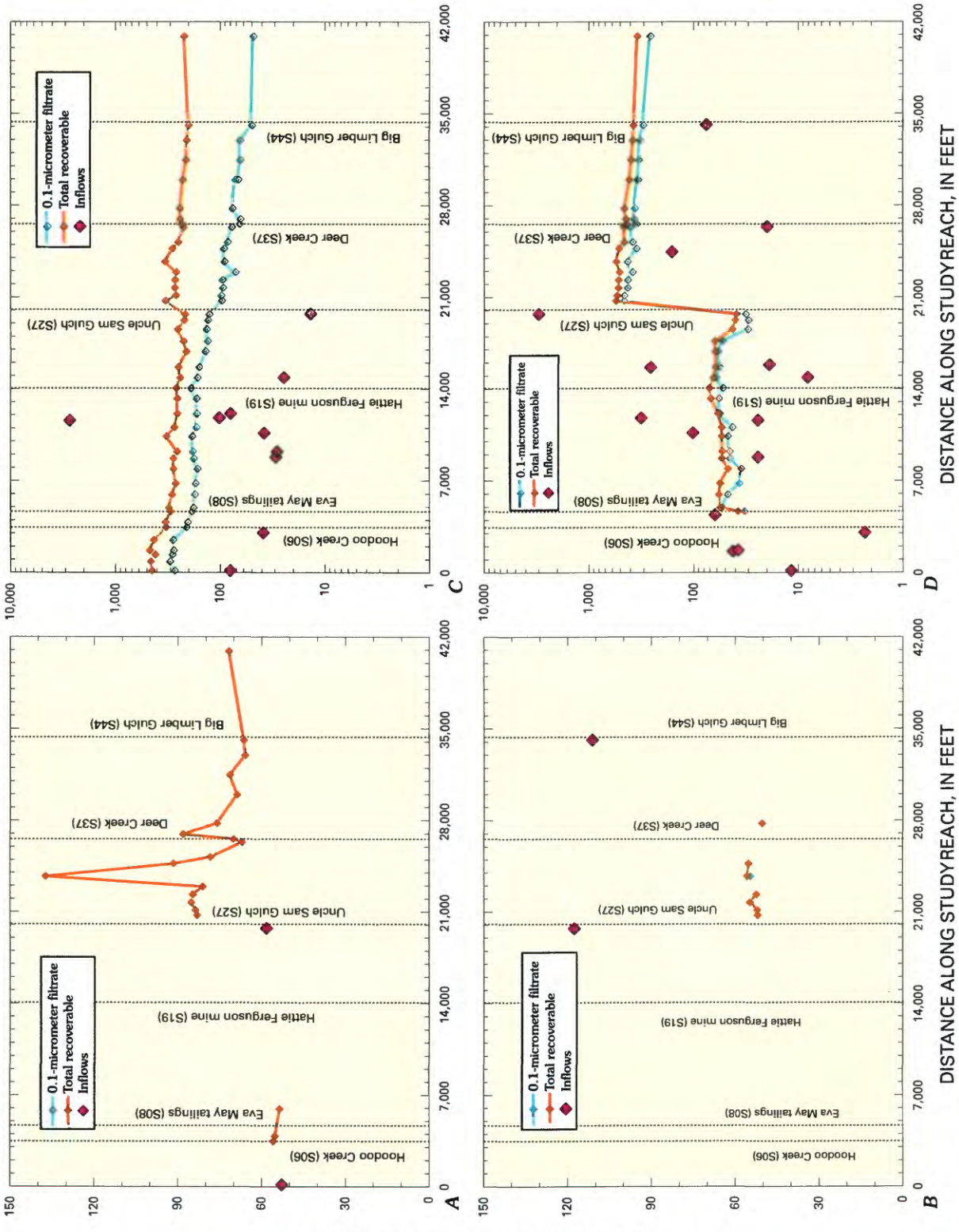

Figure 4. *Variation of A, aluminum; B, copper; C, iron; and D, zinc concentrations with distance, Cataract Creek, August 1997.*

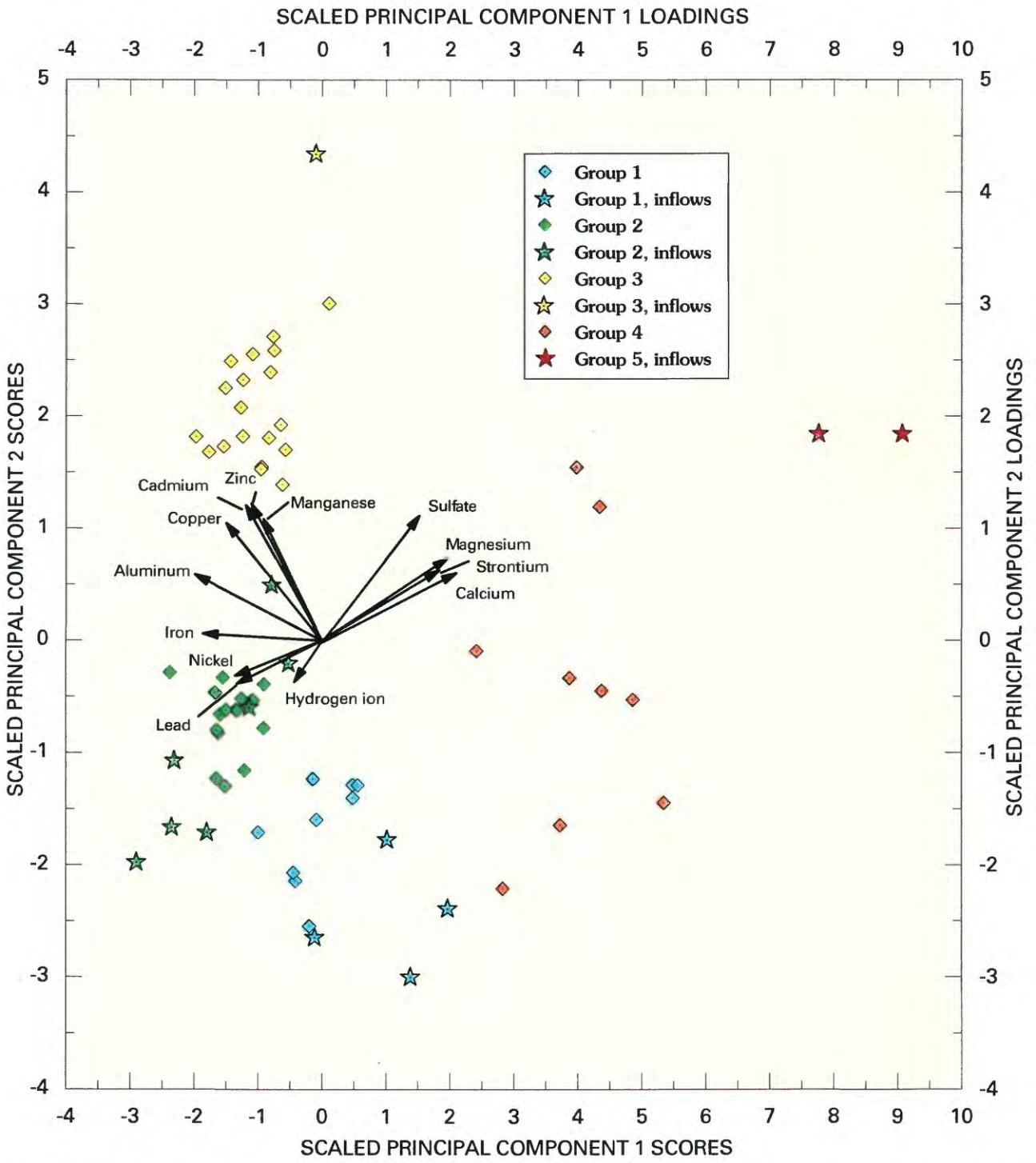

Figure 5. Biplot of principal component scores for synoptic samples and loadings for chemical constituents, Cataract Creek, August 1997.

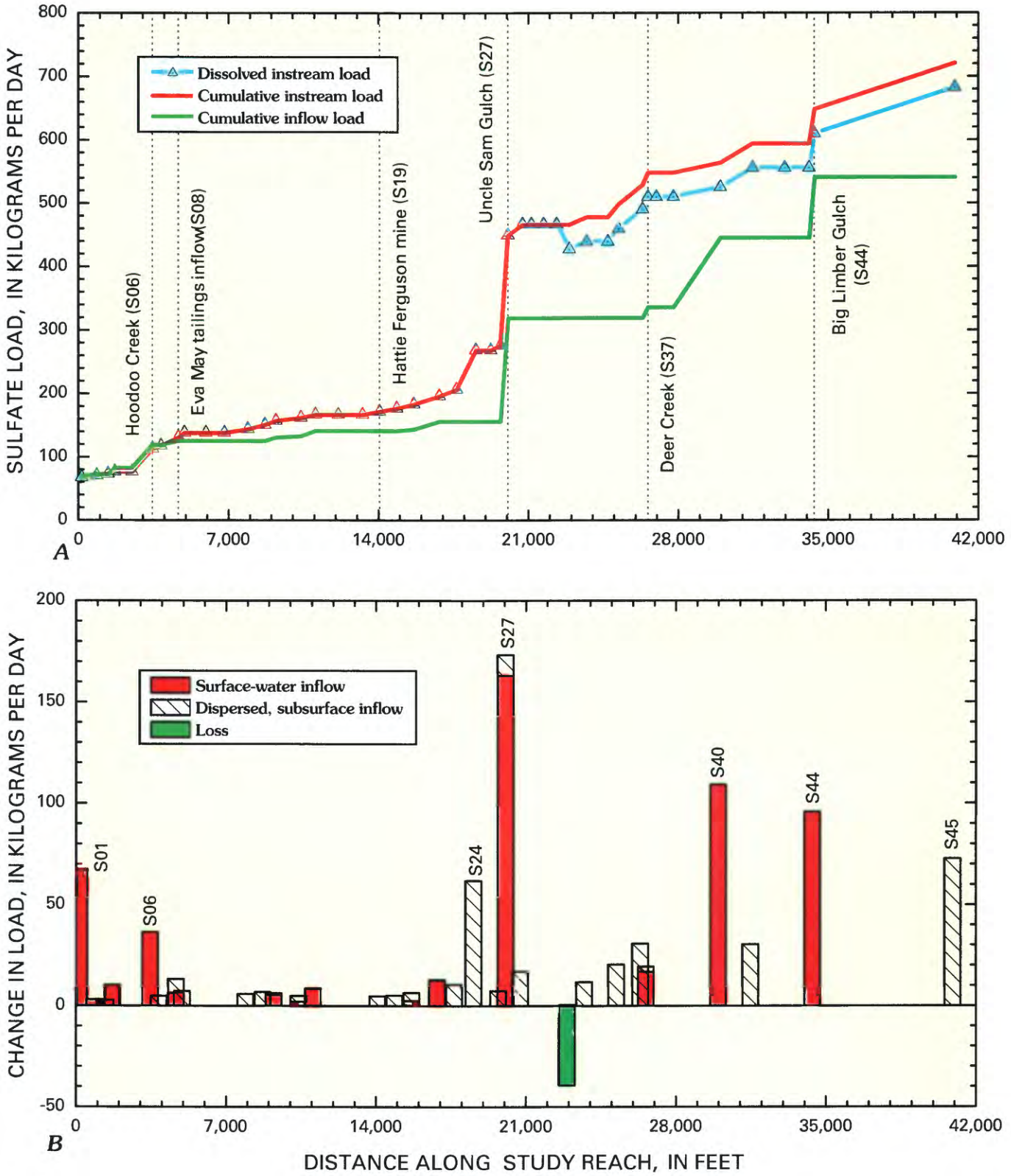

Figure 6. Variation of *A*, sulfate load with distance, and *B*, changes in load for individual stream segments, Cataract Creek, August 1997.

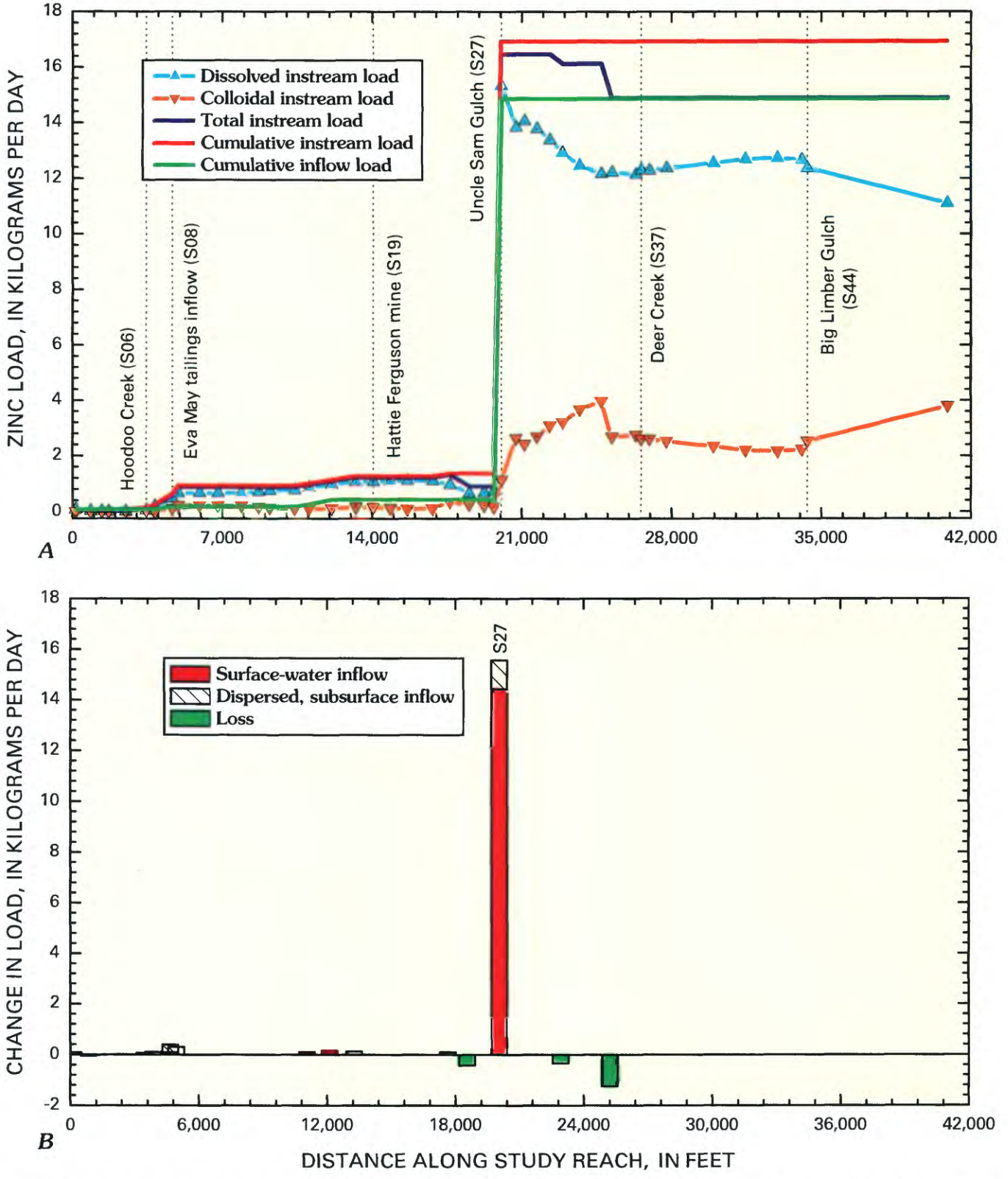

Figure 7. Variation of *A*, zinc load with distance, and *B*, changes in load for individual stream segments, Cataract Creek, August 1997.

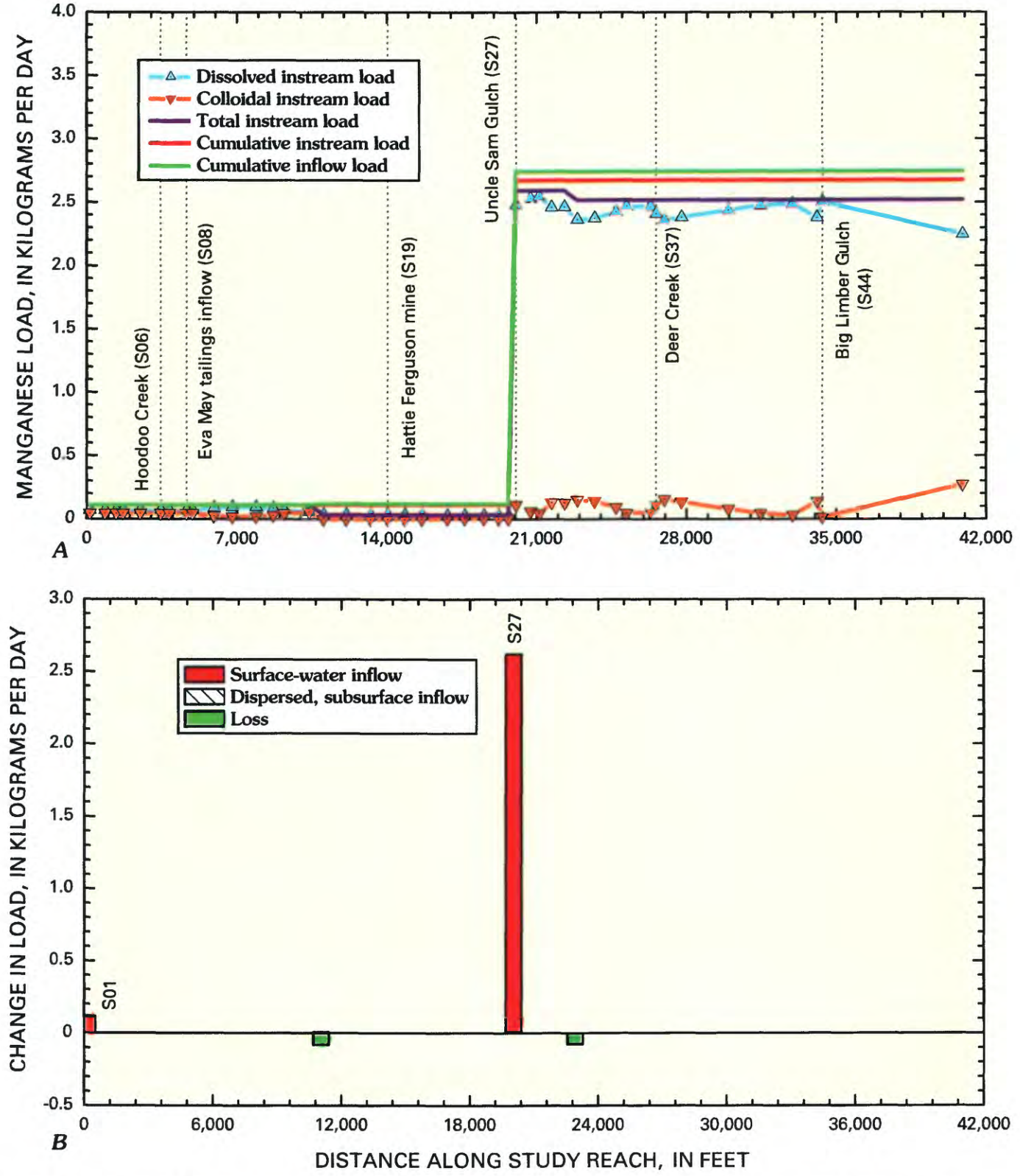

Figure 8. Variation of *A*, manganese load with distance, and *B*, changes in load for individual stream segments, Cataract Creek, August 1997.

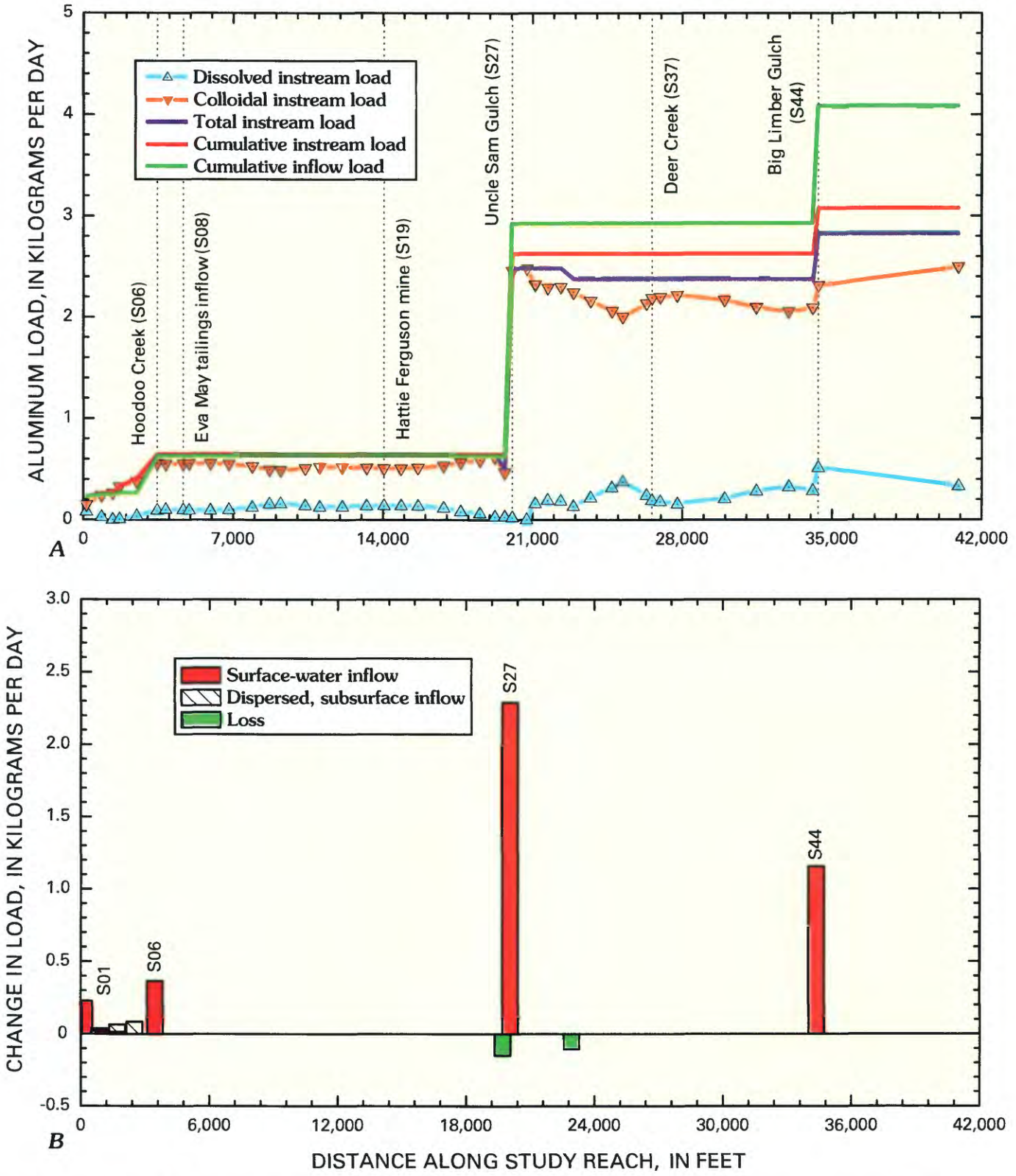

Figure 9. Variation of *A*, aluminum load with distance, and *B*, changes in load for individual stream segments, Cataract Creek, August 1997.

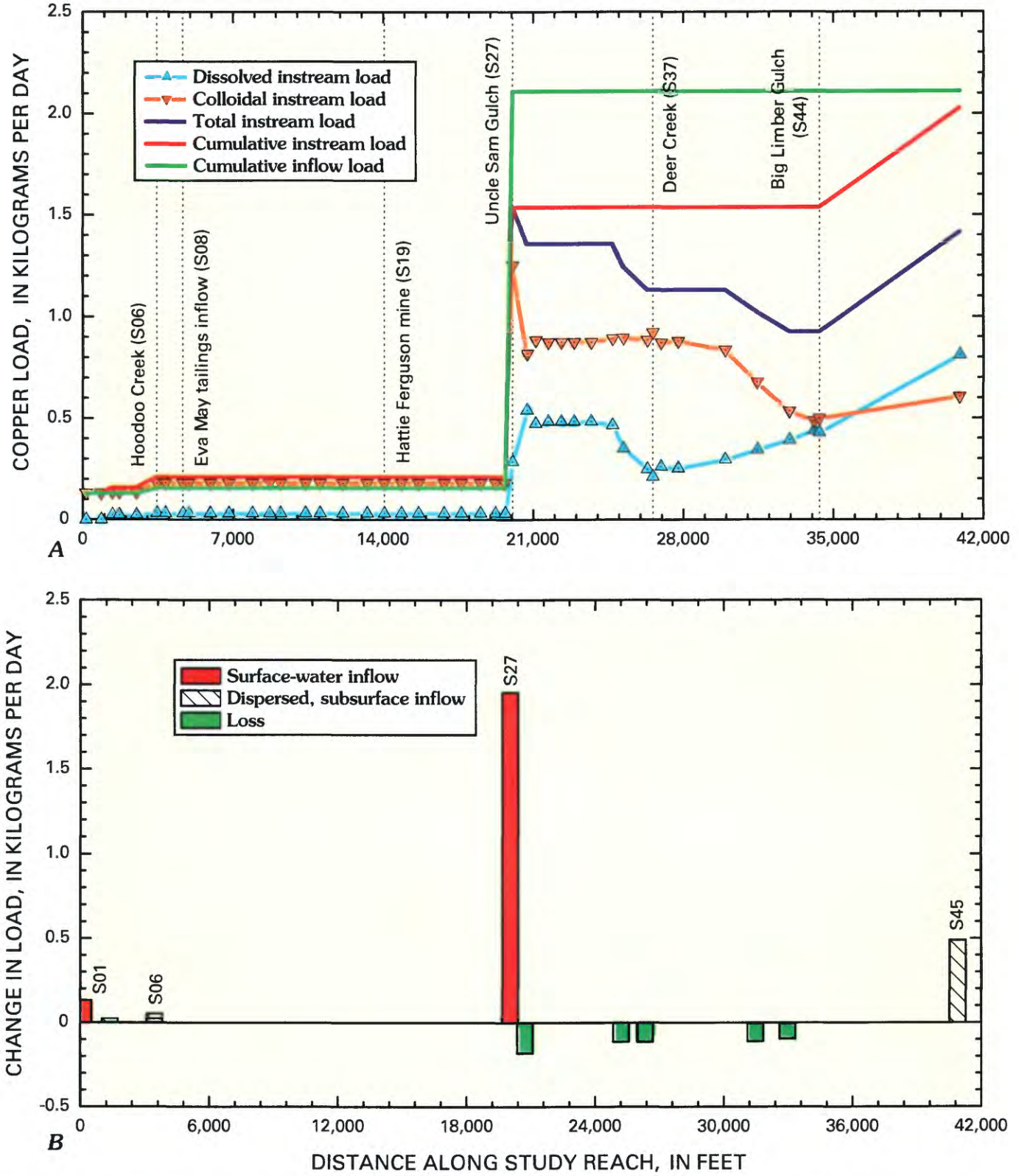

Figure 10. Variation of *A*, copper load with distance, and *B*, changes in load for individual stream segments, Cataract Creek, August 1997.

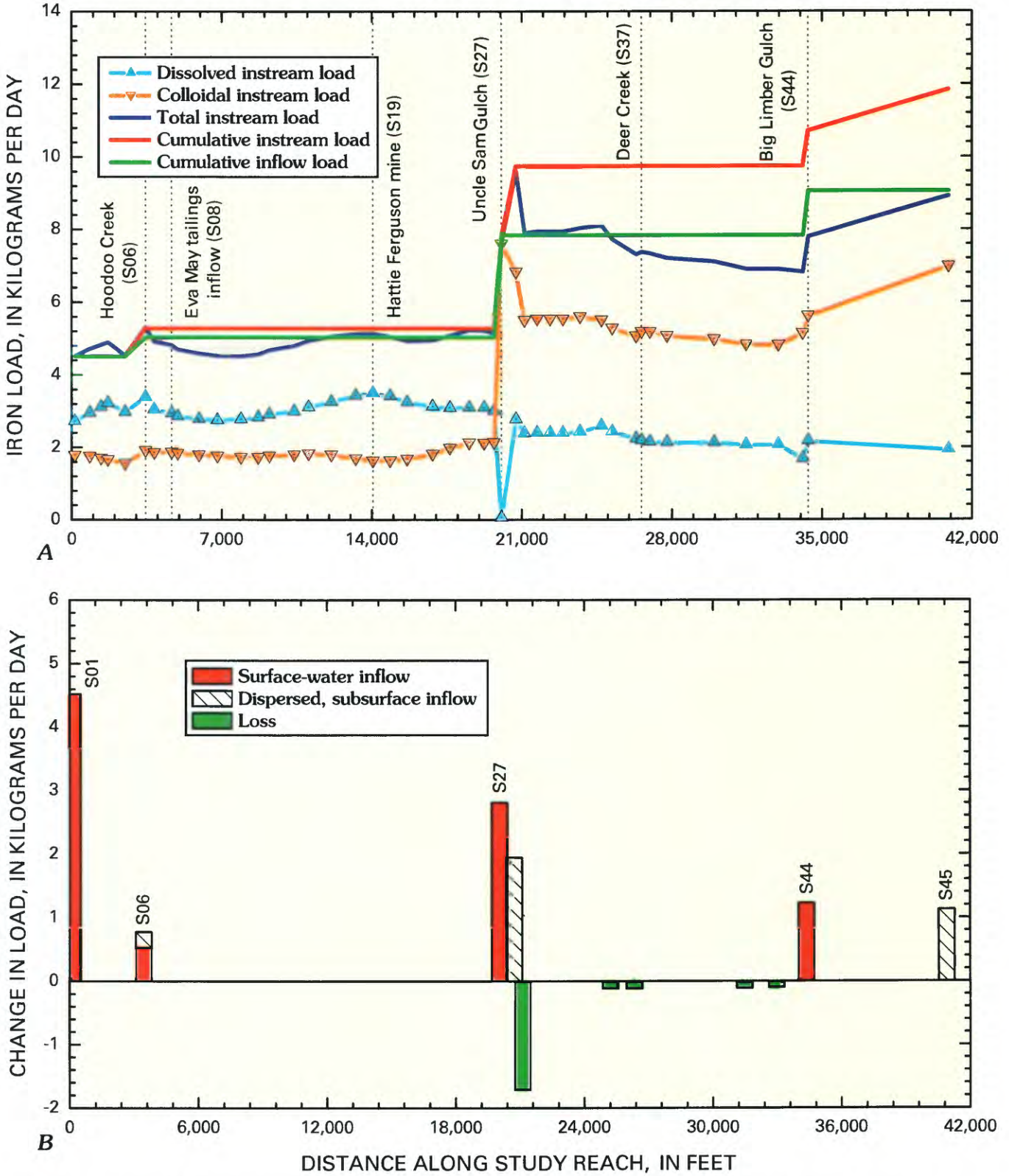

Figure 11. Variation of *A*, iron load with distance, and *B*, changes in load for individual stream segments, Cataract Creek, August 1997.

Loading profiles of aluminum, copper, and iron were mixtures between the sulfate and zinc profiles. Substantial loads of aluminum entered the stream at Uncle Sam Gulch (S27) and segment S44 (fig. 9*A*). Most of the aluminum that entered the stream at Uncle Sam Gulch was transported downstream as colloidal aluminum (figs. 4*A*, 9*A*). Copper loading mostly occurred at Uncle Sam Gulch (segment S27; fig. 10). Downstream from there, the copper was mostly present as colloidal copper, but there appeared to be some transformation between dissolved and colloidal phases in response to downstream inflows. There was a loss of copper load to the streambed between Uncle Sam Gulch and Big Limber Gulch, which, in part, was due to loss in the iron colloids.

The iron profile (fig. 11*A*) indicates a relatively small increase in load from Uncle Sam Gulch (segment S27); the greatest loading was from upstream sources (segment S01). Because iron is reactive in mine-drainage settings, there very likely was attenuation of iron concentrations as water traveled from sources at adits or seeps to the stream (Kimball, Broshears, and others, 1994). Unsampled inflow of iron occurred in segment S28, downstream from Uncle Sam Gulch. This corresponds to unsampled inflow of sulfate (fig. 6*B*), and could indicate weathering of pyrite in tailings piles along the stream in that area. Because most of the iron load was colloidal, losses such as that downstream from segment S28 very likely involved the transformation of dissolved to colloidal iron and then settling of aggregated colloids and (or) entrapment in the algae covering streambed cobbles, as indicated by Church, Unruh, and others (this volume, Chapter D8).

Locations of Major Loading

The cumulative instream load listed in table 3 is the best estimate of the total metal loading along the study reach. Although differences are seen among metal loading profiles, their similarities identify the locations where most of the metal loading occurs. Locations of the major contributions to Cataract Creek are indicated in table 3 by color shading. There were five locations where most of the loading occurred. The greatest loading occurred with the inflow of Uncle Sam Gulch (S27). This inflow accounted for 64 percent of the aluminum load, 66 percent of the copper load, 21 percent of the iron load, 96 percent of the manganese load, 92 percent of the zinc load, and 24 percent of the sulfate load (table 3). Iron (38 percent) and manganese (4 percent) loads were important at the beginning of the study reach (segment S01). The other constituents were also present (table 3). The Eva May tailings (segment S08) contributed to the load of zinc (2 percent). The inflow of Big Limber Gulch (segment S44) accounted for aluminum (14 percent), iron (8 percent), and sulfate (8 percent). Mines and mineralized rock in that drainage could account for these loads (O'Neill and others, this volume, pl. 1; McCafferty and others, this volume). Finally, loads of copper (24 percent), iron (10 percent), and sulfate (10 percent) increased in the large segment represented by the sample at the mouth of Cataract Creek (S45). Little is known about possible sources in this segment.

Unsampled Inflow

The principal locations of unsampled inflow include Uncle Sam Gulch (S17), segment S28 downstream from Uncle Sam Gulch, and segment S45 between Big Limber Gulch and the mouth of Cataract Creek. The unsampled inflow from Uncle Sam Gulch consisted of sulfate (fig. 6*B*) and zinc (fig. 7*B*). Downstream from Uncle Sam Gulch, a substantial tailings pile lies along Cataract Creek in segment S28, and this could be the source of iron and sulfate loading to the stream in that segment. Little is known about the last stream segment, S45, where there was unsampled inflow of copper, iron, and sulfate because there was no access to the stream along that reach.

Attenuation of Load

Along the length of the study reach, substantial attenuation only occurred for copper (30 percent) and iron (25 percent, table 3); most of the constituents were transported to the Boulder River once they entered Cataract Creek. Attenuation of copper and iron occurred downstream from Uncle Sam Gulch (figs. 10*B* and 11*B*), after the load had greatly increased. This was likely a result of the loss of colloidal iron to the streambed through settling of aggregated colloids or through entrapment by algae on the streambed cobbles.

Uncle Sam Gulch Subbasin

Results of the tracer-injection study in Cataract Creek indicated that Uncle Sam Gulch was the principal source of metal loading to the stream. A tracer-injection study was done during low-flow conditions in late August 1998 to investigate the source of metals and the patterns of metal loading.

Study Area and Experimental Design

The study reach began upstream from the Crystal mine, near the headwaters of the stream, and continued to the mouth of Uncle Sam Gulch, where the stream discharges into lower Cataract Creek (fig. 12). Synoptic sampling sites defined 36 stream segments. Stream segment numbers are listed in table 4, but the detailed descriptions of these sites are found in the database (Rich and others, this volume, Chapter G). Fourteen inflows were sampled in 13 of these segments.

A sodium chloride solution of 161,200 mg/L chloride was injected at a rate of 92 mL/min for a 48.7-hour period starting at 16:50 MDT on August 27, 1998. During the course of the injection, difficulties with the pumps complicated the interpretation of the chloride profile downstream from the injection.

Table 3. Change in load for individual stream segments and summary of load calculations, Cataract Creek, August 1997.

[Distance, in feet along the study reach; Al, aluminum; Cu, copper; Fe, iron; Mn; manganese; Zn, zinc; SO_4, sulfate; all values of load are in kilograms per day; percentages are percent of cumulative instream load; color of cell indicates rank of load: red, first; orange, second; yellow, third; green, fourth; blue, fifth; negative values of load indicated in red type with parentheses]

Segment number	Site descriptions	Distance	Al	Cu	Fe	Mn	Zn	SO_4
S01	First site below injection	150	0.227	0.131	4.52	0.116	0.078	67.6
S02	T1 transport site in canyon	850	0.038				(0.038)	3.09
S03	Above right-bank mine dump	1,370		0.028			(0.016)	2.80
S04	Below mine dump at Apollo mine	1,690	0.066					3.53
S05	Above mine dump at Eva May mine	2,490	0.084				0.007	
S06	Below Hoodoo Creek	3,450	0.234	0.053	0.778		0.068	36.3
S07	Above Eva May mine tailings	3,850					0.107	4.87
S08	Adjacent to Eva May tailings pile	4,660					0.386	13.2
S09	T2 transport site below Eva May mine	4,940					0.299	7.25
S10	Below curve with overbank tailings	5,940						
S11	Along bend	6,800						
S12	Below old cabin	7,900						5.89
S13	Below mine dump, at Cataract mine tailings	8,700						6.85
S14	Adjacent to Cataract mine tailings	9,220						6.27
S15	End of large flood plain	10,380						4.92
S16	Adjacent to ponded water on right bank	11,055				(0.081)	0.083	4.82
S17	Above large clear-cut area	12,115					0.132	
S18	Above Lower Hattie Ferguson mine	13,255					0.127	
S19	Below Lower Hattie Ferguson mine	14,055						4.78
S20	Above left-bank inflow	14,855						5.14
S21	Below Upper Hattie Ferguson mine	15,655						6.51
S22	Below inflows, checking water inflow	16,845						12.9
S23	T3 transport site below logging-road	17,645					0.103	10.5
S24	Above biological sampling site	18,545					(0.418)	62.0
S25	Above Morning Glory mine	19,245						
S26	Above Uncle Sam Gulch, below Morning Glory mine	19,700	(0.149)					7.39
S27	Below Uncle Sam Gulch	20,050	1.98	1.33	2.52	2.56	15.6	173
S28	Below cabin and tailings pile on right bank	20,730		(0.180)	1.95			17.0
S29	Check for reaction below Uncle Sam Gulch	21,130			(1.71)			
S30	Along cascades below small mine dump	21,715						
S31	Above rock wall	22,315						
S32	Below small inflow	22,915	(0.105)			(0.076)	(0.342)	(39.4)
S33	At old lean-to	23,715						11.8
S34	T4 transport site above canyon	24,715						
S35	Above start of canyon	25,215		(0.113)			(1.24)	20.3
S36	Above Deer Creek	26,335		(0.113)				30.7
S37	Below Deer Creek	26,590						19.3
S38	Below large concrete bridge	26,970						
S39	Below second wooden bridge	27,775						
S40	Below old cabin on right bank	29,970						15.6
S41	Along cascade reach	31,470		(0.110)				30.4
S42	Wide section of canyon	32,970		(0.096)				
S43	T5 transport site above Big Limber Gulch	34,105						
S44	Below Big Limber Gulch	34,355	0.448		0.971			54.3
S45	Cataract Creek at mouth	40,905		0.489	1.13			72.7
	Cumulative instream load		3.08	2.03	11.9	2.68	17.0	722
	Cumulative inflow load		4.08	2.11	9.09	2.75	14.9	540
	Percent inflow		132	104	77	103	88	75
	Unsampled inflow		< 0	< 0	2.77	< 0	2.09	182
	Percent unsampled		< 1	< 1	23	< 1	12	25
	Attenuation		0.254	0.612	2.92	0.157	2.05	39.4
	Percent attenuation		8	30	25	6	12	5

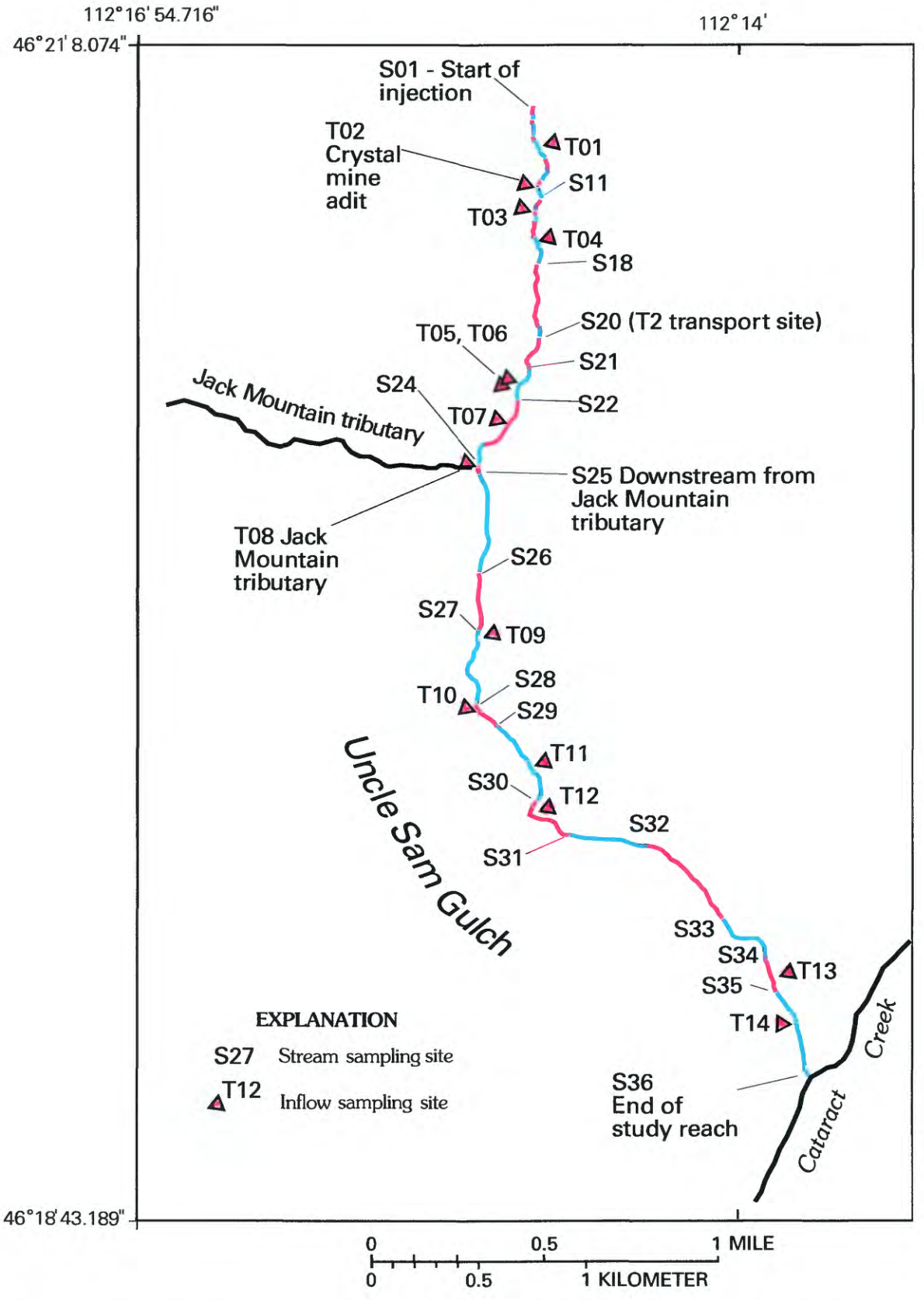

Figure 12. Location of stream segments (indicated by alternating colors) and inflows for synoptic sampling, Uncle Sam Gulch, August 1998.

Table 4. Segment number, source, distance along study reach, site description, and field data for water from synoptic sampling sites, Uncle Sam Gulch, August 29, 1998.

[Dist, distance, in feet along the study reach; source: S, stream; LBI, left bank inflow, RBI, right bank inflow; pH, in standard units; Ksc, specific conductance, in microsiemens per centimeter; Q, discharge, in liters per second; Cl, chloride, in milligrams per liter]

Segment number	Dist	Source	Description	Site identifier	pH	Ksc	Q	Cl
S01	0	S	Upstream from injection	SAM0	7.18	45	0.07	4.00
S02	278	S	First site below injection	SAM278	7.26	45	0.07	4.29
S03	305	S	Stream site, no description	SAM305	7.45	220	0.09	50.1
S04	592	S	Channel converges	SAM592	7.47	1,045	0.10	279
S05	702	S	Below several small tailings piles	SAM702	7.43	2,340	0.27	650
S06	780	S	T1 transport site	SAM780	7.24	2,210	0.28	606
T01	792	LBI	Left bank tributary from old prospect	SAM792	7.04	78	0.03	3.94
S07	957	S	At steep waste rock pile	SAM957	7.29	1,838	0.31	509
S08	1,152	S	Below deep cuts eroding banks	SAM1152	7.29	1,535	0.28	390
S09	1,314	S	At toe of waste rock pile	SAM1314	7.13	1,356	0.37	345
S10	1,399	S	Above Crystal adit discharge	SAM1399	7.05	1,302	0.43	325
T02	1,413	RBI	Right bank Crystal adit inflow	SAM1413	3.21	1,164	2.27	4.84
S11	1,461	S	Below Crystal mine adit	SAM1461	3.27	1,195	2.70	50.7
S12	1,560	S	Below Crystal waste rock pile	SAM1560	3.25	1,204	2.71	54.6
S13	1,661	S	At edge of treatment pond	SAM1661	3.23	1,210	2.71	51.6
S14	1,764	S	At treatment pond pipe	SAM1764	3.20	1,195	2.74	53.7
T03	1,829	RBI	Right bank inflow from waste rock	SAM1829	2.83	1,563	0.04	7.50
S15	1,866	S	Below obvious mining disturbance	SAM1866	3.19	1,205	2.77	54.4
S16	2,026	S	Below mining disturbance (2)	SAM2026	3.17	1,189	2.81	52.4
S17	2,273	S	Below mining disturbance (3)	SAM2273	3.14	1,182	2.89	51.2
T04	2,286	LBI	Left bank tributary, low conductance	SAM2286	7.26	56	0.25	3.41
S18	2,727	S	Below left bank inflow	SAM2727	3.22	1,065	3.14	40.9
S19	3,170	S	Stream near road	SAM3170	3.30	878	3.90	25.0
S20	3,777	S	T2 transport site—edge of clear cut	SAM3777	3.32	774	4.48	20.0
S21	4,365	S	Stream at lower conductance	SAM4365	3.44	732	4.71	20.2
T05	4,650	RBI	Right bank tributary	SAM4650	6.97	80	0.19	5.40
T06	4,763	RBI	Right bank seep with iron precipitate	SAM4763	6.71	123	0.37	6.66
S22	4,915	S	At boggy area along right bank	SAM4915	3.48	686	5.28	21.3
T07	5,264	RBI	Right bank tributary near road	SAM5264	6.83	139	0.47	6.80
S23	5,830	S	T3 transport site	SAM5830	3.53	642	5.75	24.1
S24	6,068	S	Upstream from Jack Mountain tributary	SAM6068	3.58	621	5.65	22.1
T08	6,088	RBI	Jack Mountain tributary (right bank)	SAM6088	7.17	63	10.12	4.21
S25	6,213	S	Below Jack Mountain tributary	SAM6213	4.81	243	15.76	10.1
S26	7,417	S	At heavy vegetation, low gradient	SAM7417	4.91	229	17.14	10.5
S27	8,270	S	At small clearing near road	SAM8270	5.13	222	17.41	9.86
T09	8,374	LBI	Left bank inflow from marshy area	SAM8374	6.95	116	1.22	4.85
S28	9,200	S	T4-Upstream from old cabin	SAM9200	6.62	211	18.63	5.05
T10	9,400	RBI	Right bank tributary by cabin	SAM9400	7.61	91	1.60	6.22
S29	9,588	S	Near road below cabin inflow	SAM9588	6.74	201	20.23	8.34
T11	10,289	LBI	Left bank tributary	SAM10289	7.24	147	0.77	5.56
S30	10,856	S	Split in stream	SAM10856	7.14	194	20.99	8.00
T12	11,006	LBI	Left bank tributary	SAM11006	7.50	114	3.43	5.82
S31	11,724	S	Stream below dilution inflow	SAM11724	6.89	183	24.42	7.54
S32	12,795	S	Below tailings	SAM12795	7.28	181	25.51	7.38
S33	14,540	S	T5 transport site—upstream end of culvert	SAM14540	7.29	177	26.42	7.37
S34	15,314	S	Below power line crossing	SAM15314	7.32	176	27.08	7.22
T13	15,671	LBI	Left bank tributary	SAM15671	7.84	165	5.58	5.44
S35	15,971	S	Below tributary near road	SAM15971	7.36	184	32.65	6.93
T14	16,471	RBI	Right bank tributary draining wet area	SAM16471	7.74	217	4.14	0.94
S36	17,095	S	Uncle Sam at mouth	SAM17095	6.62	180	36.80	6.79

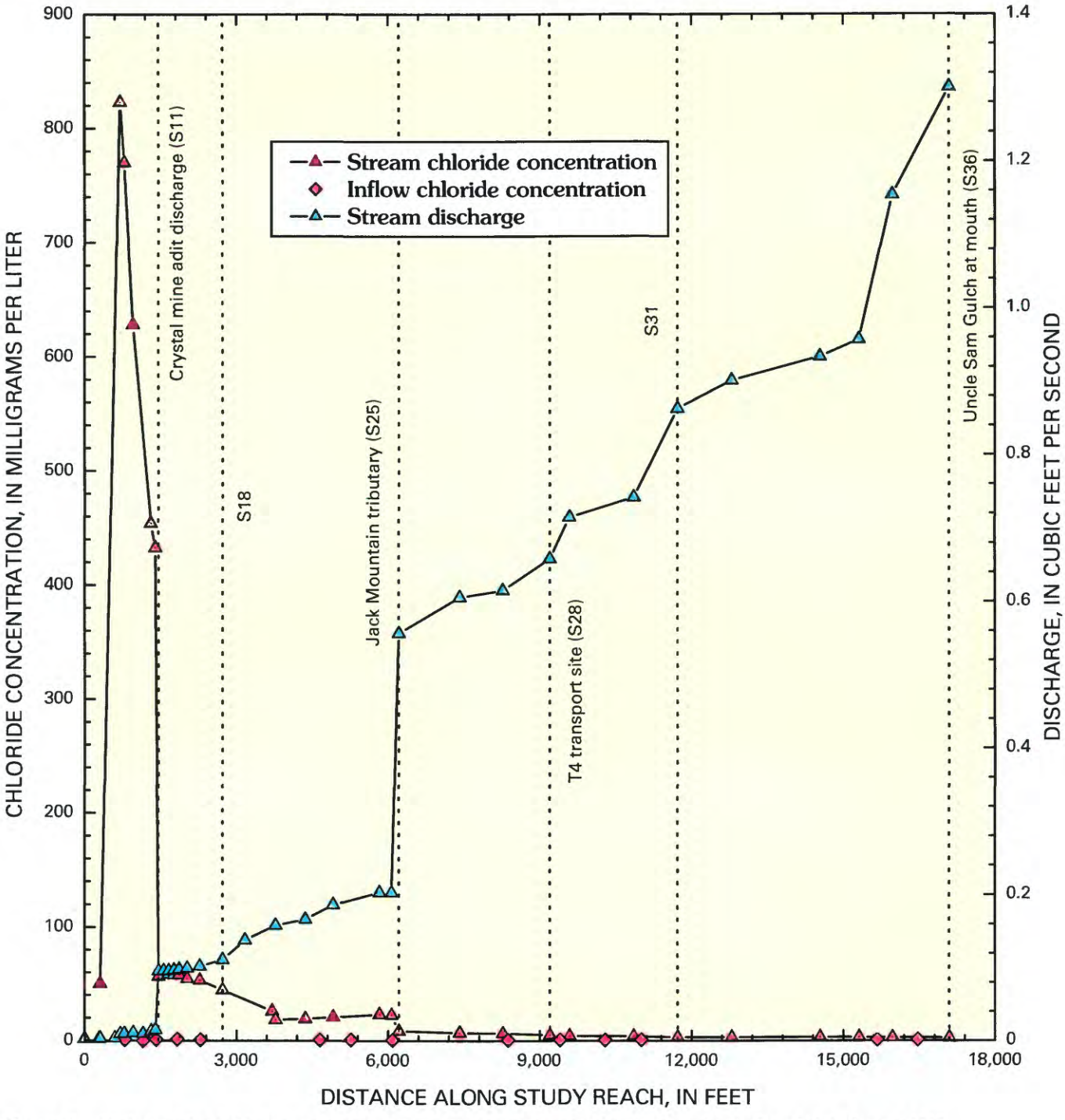

Figure 13. Variation of chloride concentration and calculated discharge with distance, Uncle Sam Gulch, August 1998.

Although the decrease of chloride concentration appeared to be systematic, a "wave" of chloride moved through the study reach during the synoptic sampling, indicated by the increase of chloride at the first few sampling sites (fig. 13). Because of these complications, chloride and sulfate ratios around inflows, along with velocity-area discharge measurements, were used to calculate the increase of flow due to individual inflows. The resulting calculated discharge ranged from 0.004 to 1.3 ft^3/s (fig. 13). Most of this increase was from Jack Mountain tributary (T8). Discharge increased only 0.07 ft^3/s in those segments that had no sampled inflow, only 10 percent of the total increase, and so the explicit amount of ground-water inflow was small.

Chemical Characterization of Synoptic Samples

Changes in stream-water chemistry along Uncle Sam Gulch were distinct and occurred over short distances in response to acidic and neutral inflows. The abrupt changes of pH along the study reach indicate where the changes occurred (fig. 14). Upstream from the Crystal mine, pH was greater than 7.0, sulfate concentration was less than 25 mg/L, and metal concentrations were relatively low (fig. 15). With the addition of the adit drainage (T2), and the spring from the mine waste-rock pile (T3), pH dropped substantially, to less than 3.5, and sulfate increased to greater than 550 mg/L. Metal concentrations increased to greater than 10,000 µg/L aluminum, 10,000 µg/L copper, 40,000 µg/L iron, and 60,000 µg/L zinc (fig. 15). Baseline sediment chemistry also indicates the impact from mining (Church, Unruh, and others, this volume, figs. 4–10). Inflow from Jack Mountain tributary increased the pH to 4.81 in segment S25, and pH continued to increase to 5.13 by the end of segment S27. Farther downstream, after additional neutral inflows at T9 and T10, the pH increased to 6.74 at segment S29. Within the reach of increasing pH, from segment S25 to S27, dissolved concentrations of the metals decreased and colloidal concentrations increased. Iron colloids, however, started forming upstream from the inflow of Jack Mountain tributary; the total-recoverable iron was greater than the two filtered concentrations (fig. 15*C*). At the higher pH there was a steady formation of aluminum and iron colloids as water moved downstream (fig. 15*A*, *C*). As the colloids formed, dissolved copper concentrations decreased and most of the copper became associated with the colloidal phase (fig. 15*B*). Concentrations of dissolved zinc exceeded chronic water-quality criteria at all sites downstream from the Crystal mine adit, as noted by Nimick and Cleasby (this volume, Chapter D5).

Table 5. Average chemical composition of groups from principal components analysis of synoptic samples, Uncle Sam Gulch, August 1998.

[LD, less than detection limit; all values in milligrams per liter, except pH, which is in standard units]

Number of samples or solute	Group 1 Stream from S1 to S3, upstream from acid inflows	Group 1 Unaffected inflows	Group 2 Stream site S4, unaffected by acid inflows	Group 2 Inflows unaffected by mining	Group 3 Stream from S5 to S10, affected bull-dozed area	Group 4 Stream from S11 to S18, affected by Crystal mine adit	Group 4 Most acidic inflow, including Crystal mine adit	Group 5 Stream between S19 and S24	Group 6 Stream between S25 and S31	Group 7 Stream between S32 and S36
Number of samples	3	2	1	10	6	6	2	6	7	5
pH	7.30	7.15	7.47	7.26	7.24	3.21	3.02	3.44	6.03	7.17
Calcium	5.44	9.29	9.84	17.3	23.6	54.3	62.0	35.2	17.6	18.2
Magnesium	.957	1.47	1.67	3.18	3.84	15.5	19.7	9.43	4.24	4.07
Sulfate	6.11	9.31	10.0	15.9	10.1	507	706	293	78.4	53.1
Aluminum	.121	.032	.045	.017	.037	12.4	17.3	7.86	1.83	.683
Cadmium	.002	.002	.003	.004	.006	.771	.891	.453	.119	.072
Copper	.007	.008	.015	.027	.023	12.4	15.6	7.36	1.93	.731
Iron	1.11	.242	.499	.139	.232	36.0	43.0	10.5	1.03	.284
Manganese	.067	.069	.084	.409	.075	11.9	16.4	7.19	1.87	.949
Nickel	.001	LD	.001	LD	.001	.054	.065	.030	.008	.006
Lead	.009	LD	.001	LD	.001	.243	.134	.188	.042	.001
Strontium	.066	.070	.121	.131	.271	.267	.270	.212	.126	.134
Zinc	.047	.085	.121	.157	.232	56.7	71.4	33.7	8.92	5.60

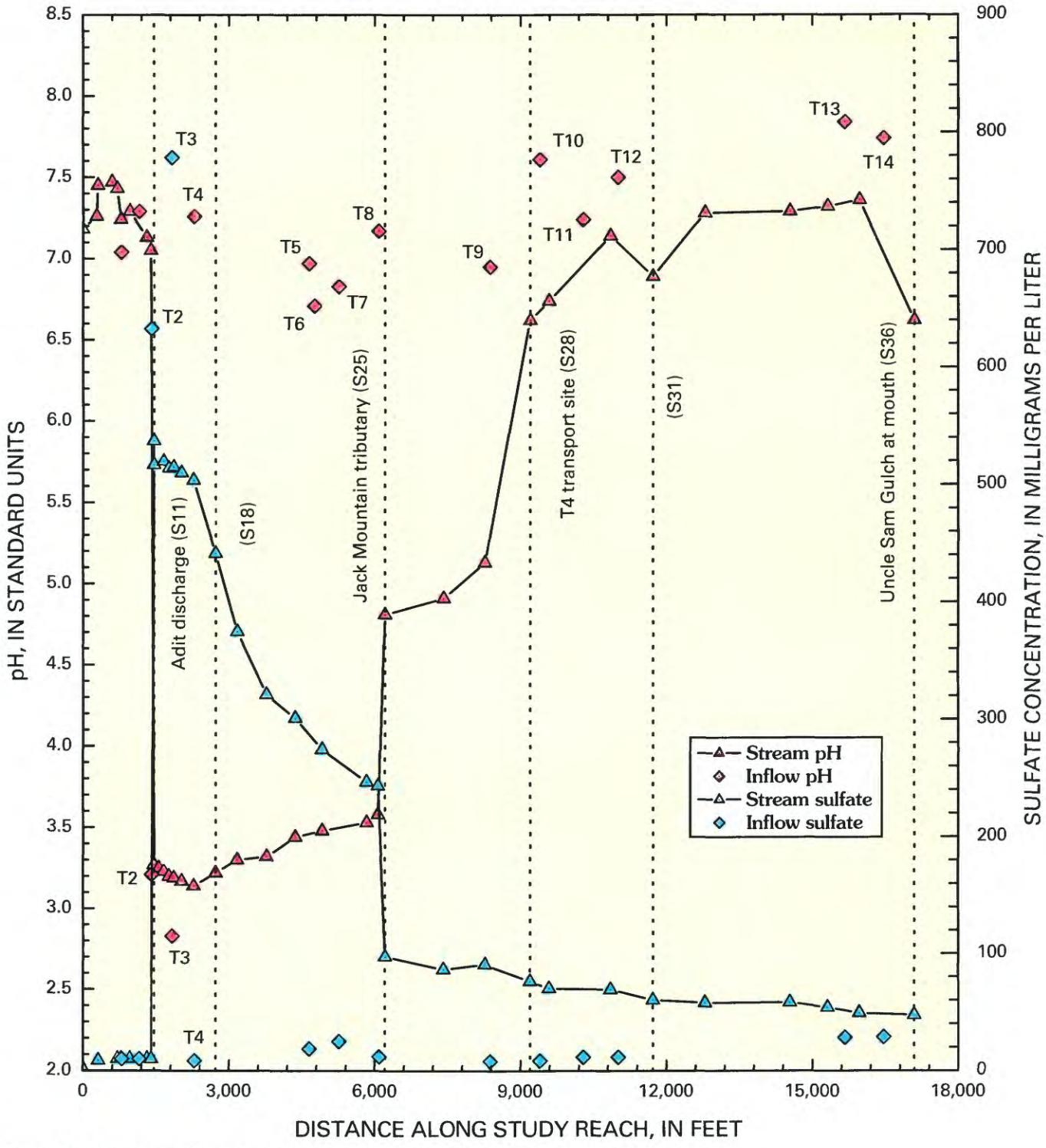

Figure 14. Variation of pH and sulfate with distance, Uncle Sam Gulch, August 1998.

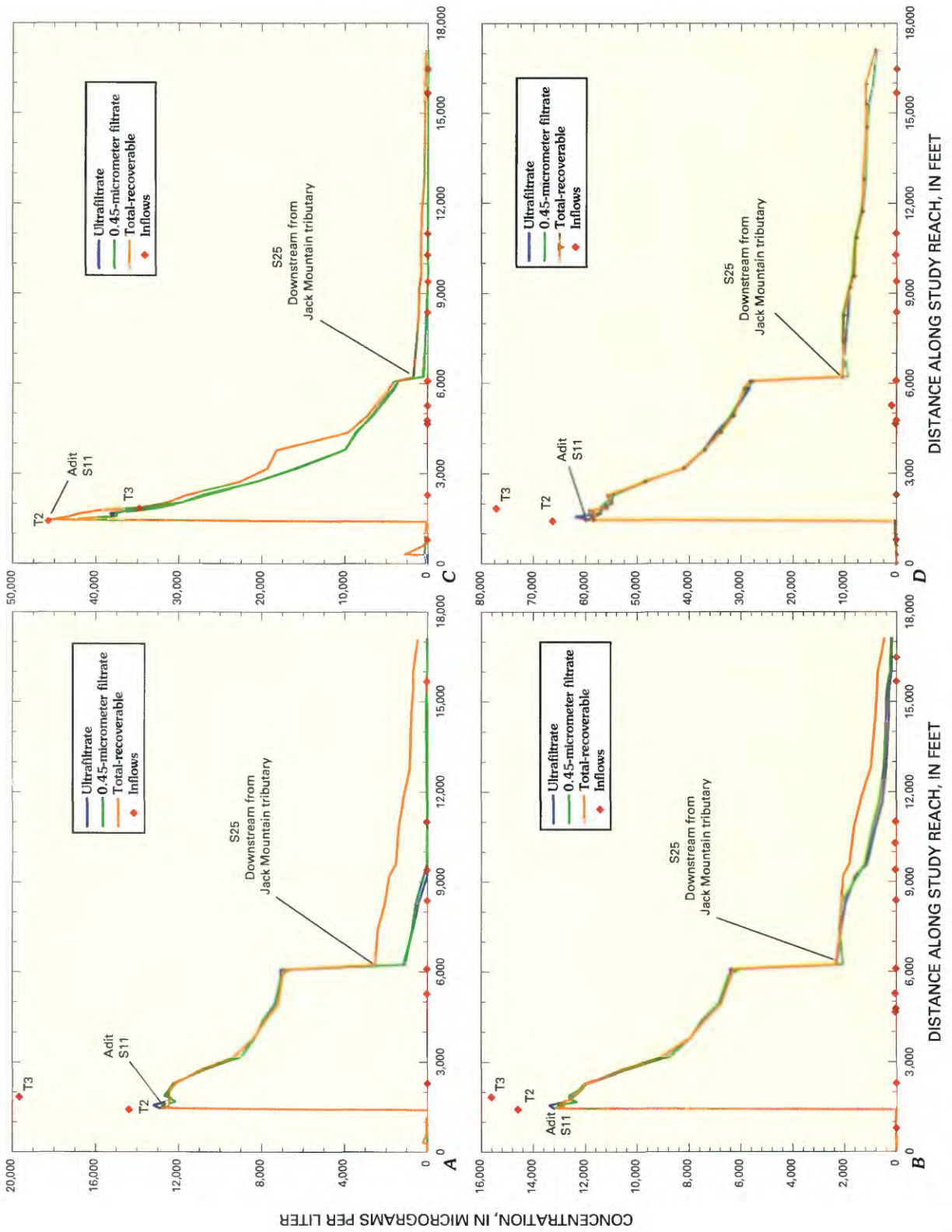

Figure 15. Variation of *A*, aluminum, *B*, copper, *C*, iron, and *D*, zinc concentrations with distance, Uncle Sam Gulch, August 1998.

These substantial changes in stream chemistry and the variability of inflows resulted in a classification of seven groups of samples by PCA (fig. 16). Six of the groups represent variations in stream-water chemistry, with associated inflows, and one represents inflows unaffected by mining or alteration (table 5). The biplot provides a reasonable interpretation of the chemical variation among synoptic samples from Uncle Sam Gulch. Two sets of stream sites (groups 1 and 3) are unaffected by discharge from the Crystal mine adit and plot to the right on the biplot (fig. 16). All the vectors indicate increasing concentrations to the right; the vectors for metals from the mine are very similar and so they are only identified as a group. Samples to the left of the biplot are opposite all the vectors, and have the lowest concentrations. Group 1 contains two inflow samples (T01 and T04) that resulted from the same weathering reactions that produced the stream-water chemistry upstream from segment S04. An extensive amount of disturbance resulted from bulldozing of soil up the mountain on the right bank of the stream. Inflow water that drained the disturbed area contributed high calcium, sulfate, and some zinc (group 3). With the inflow of adit discharge and water from the waste-rock pile (inflows T02 and T03), the chemistry shifted to reflect the acidic, metal-rich character of those inflows (group 4), far to the right of the biplot. Variations among stream samples in groups 5, 6, and 7 represent dilution by the non-mining inflows as water moved downstream. With greater dilution, the chemical character of the stream water becomes increasingly more like the inflows of group 2; samples plot progressively to the left downstream. Thus, in groups 5, 6, and 7 segment numbers increase from right to left, indicating a sequential dilution. The large jump from group 5 to 6 results from the inflow of Jack Mountain tributary (T08), which is one of the group 2 inflows (fig. 16).

Load Profiles

Colloids were responsible for much of the metal transport in Uncle Sam Gulch (fig. 15). Load profiles reflect dynamic changes between dissolved and colloidal phases along the study reach (figs. 17–25). A summary of load calculations for each solute is listed in table 6. A distinction is evident between the loading profile of strontium and those of the other metals. Although the Crystal mine adit in stream segment S11 contributed a substantial load of strontium, it was not the largest loading among the stream segments (fig. 17). Similar to the strontium profile in Cataract Creek, the profile in Uncle Sam Gulch most likely represents weathering from non-mined sources. However, all the metals and sulfate had similar loading profiles in segment S01. Downstream from the Crystal mine adit, however, individual profiles of metal loading differed because of the conservative or reactive nature of the different metals.

The pattern of strontium loading indicated more segments contributing to the load than most other constituents (fig. 17; table 6). Although drainage from the Crystal mine adit in segment S11 contributes a substantial strontium load, other segments were equally important. Unlike the sulfate loading in Cataract Creek, sulfate loading in Uncle Sam Gulch was derived substantially from one source, the Crystal mine adit in segment S11 (fig. 18). Other locations of sulfate loading throughout the watershed were minor (fig. 18*B*). A small amount of unsampled inflow occurred in segments S19, S20, and S26, but most of the sulfate loading was accounted for by the sampled inflows. One similarity between profiles of sulfate and strontium was the increase in load in the last two stream segments of the study reach (segments S35 and S36). The source of these loads may be a large fault that intersects the stream in segment S35 (O'Neill and others, this volume, pl. 1). Some of the metal loads also increased in segment S35, near the end of the study reach.

Downstream from the inflow of the Crystal mine adit, cadmium, manganese, nickel, and zinc were mostly conservative. These metals had fewer sources than strontium and sulfate. The principal source of cadmium load was the inflow from the Crystal mine adit (fig. 19). At segment S35, near the confluence with Cataract Creek, there was a substantial increase in cadmium load, which was all in the colloidal phase. Profiles of manganese (fig. 20) and zinc (fig. 21) load were similar to that of cadmium. The principal source of loading for both metals was inflow from the Crystal mine adit (T02, segment S11). Manganese load increased slightly with the inflow of Jack Mountain tributary. Manganese load decreased downstream from segment S30, but zinc load did not. Zinc had unsampled inflow at segment S19 and segment S26, one segment downstream from Jack Mountain tributary. The instream load of both metals was substantial at the confluence with Cataract Creek, which is consistent with the contribution of Uncle Sam Gulch on the loads in Cataract Creek (figs. 7 and 8).

Other metals were reactive downstream from the Crystal mine adit (S11). Iron was the most reactive (fig. 22); aluminum (fig. 23), copper (fig. 24), and lead (fig. 25) were reactive downstream from the inflow of Jack Mountain tributary (S25). The adit of the Crystal mine was essentially the only measurable source of iron load along the study reach; however, sources downstream from the adit could have been masked by a net negative change in iron load within individual stream segments due to loss from the water column (fig. 22). Downstream from the adit inflow the profile of iron load differed from profiles of the other solutes because of a continuous decrease in total iron load. Upstream from Jack Mountain tributary, the iron load was mostly in the dissolved phase and decreased by about 80 percent from segment S11 to segment S24. Downstream from Jack Mountain tributary, there was essentially a complete transformation of iron from the dissolved to the colloidal phase, and the colloidal phase was dominant all the way to the confluence with Cataract Creek. Downstream from Jack Mountain tributary, ferrihydrite is probably the iron phase being precipitated at the higher pH (Bigham and Nordstrom, 2000). Loss of iron load along the

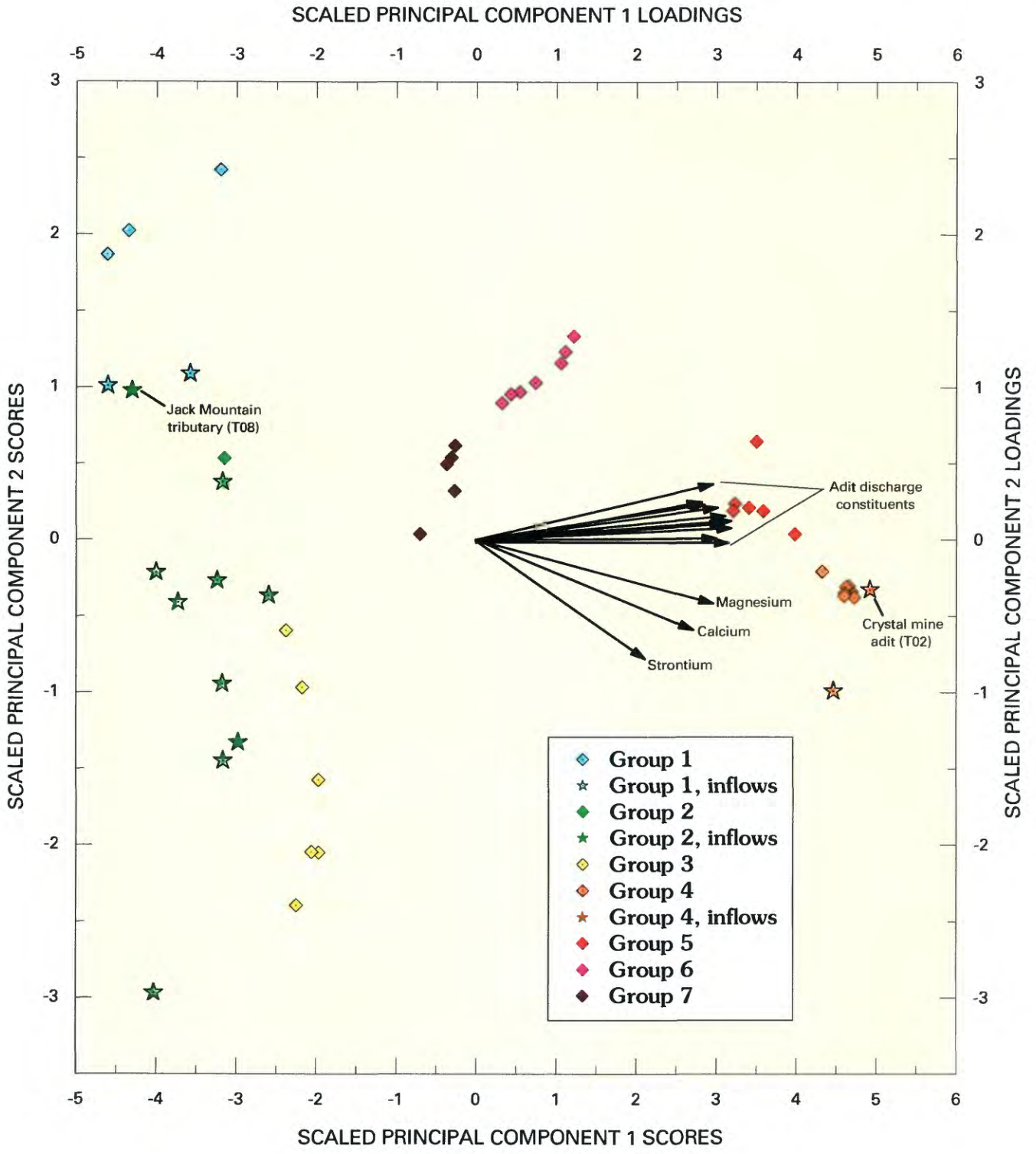

Figure 16. Biplot of principal component scores for synoptic samples and loadings for chemical constituents, Uncle Sam Gulch, August 1998.

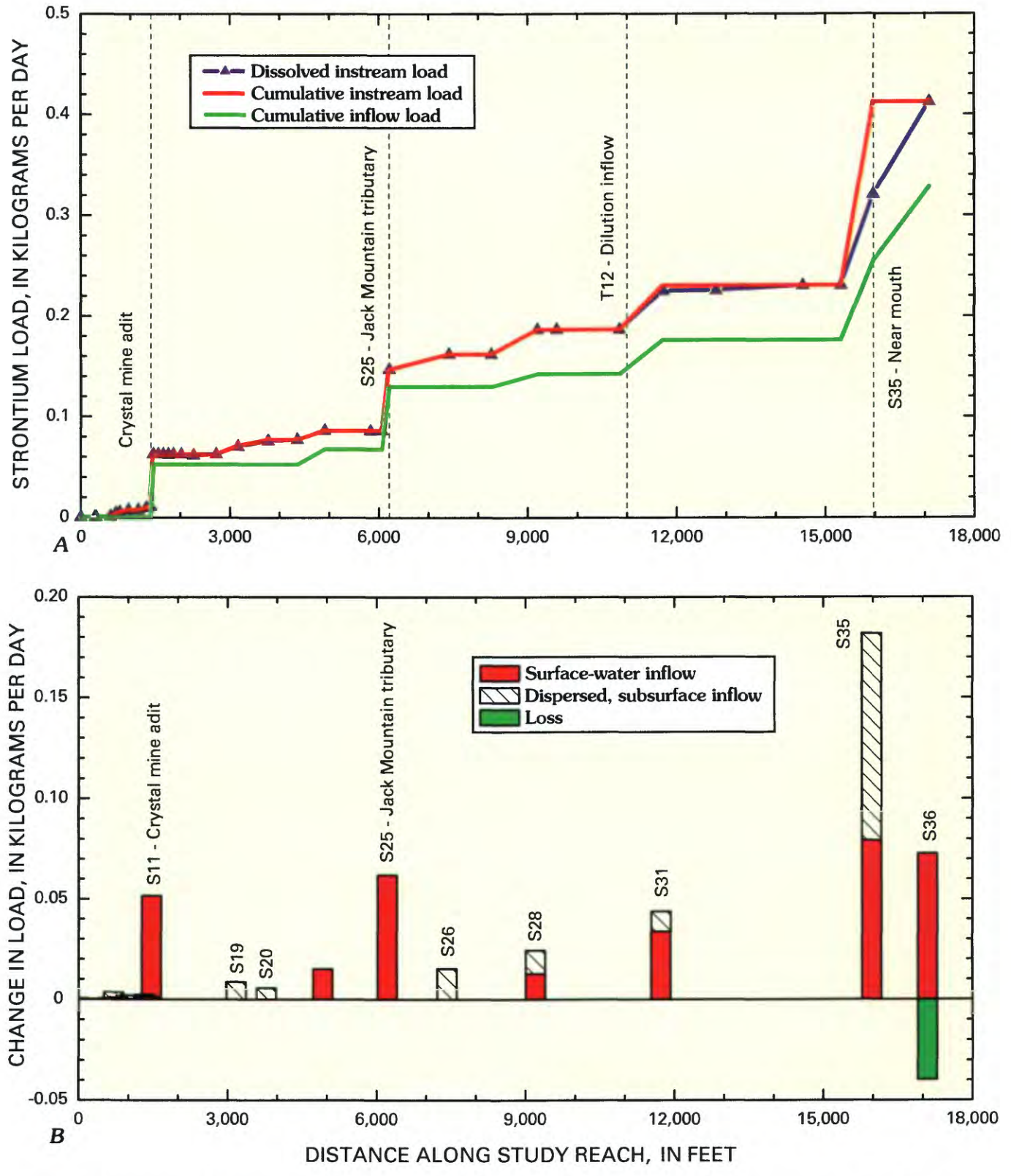

Figure 17. Variation of *A*, strontium load with distance, and *B*, changes in load for individual stream segments, Uncle Sam Gulch, August 1998.

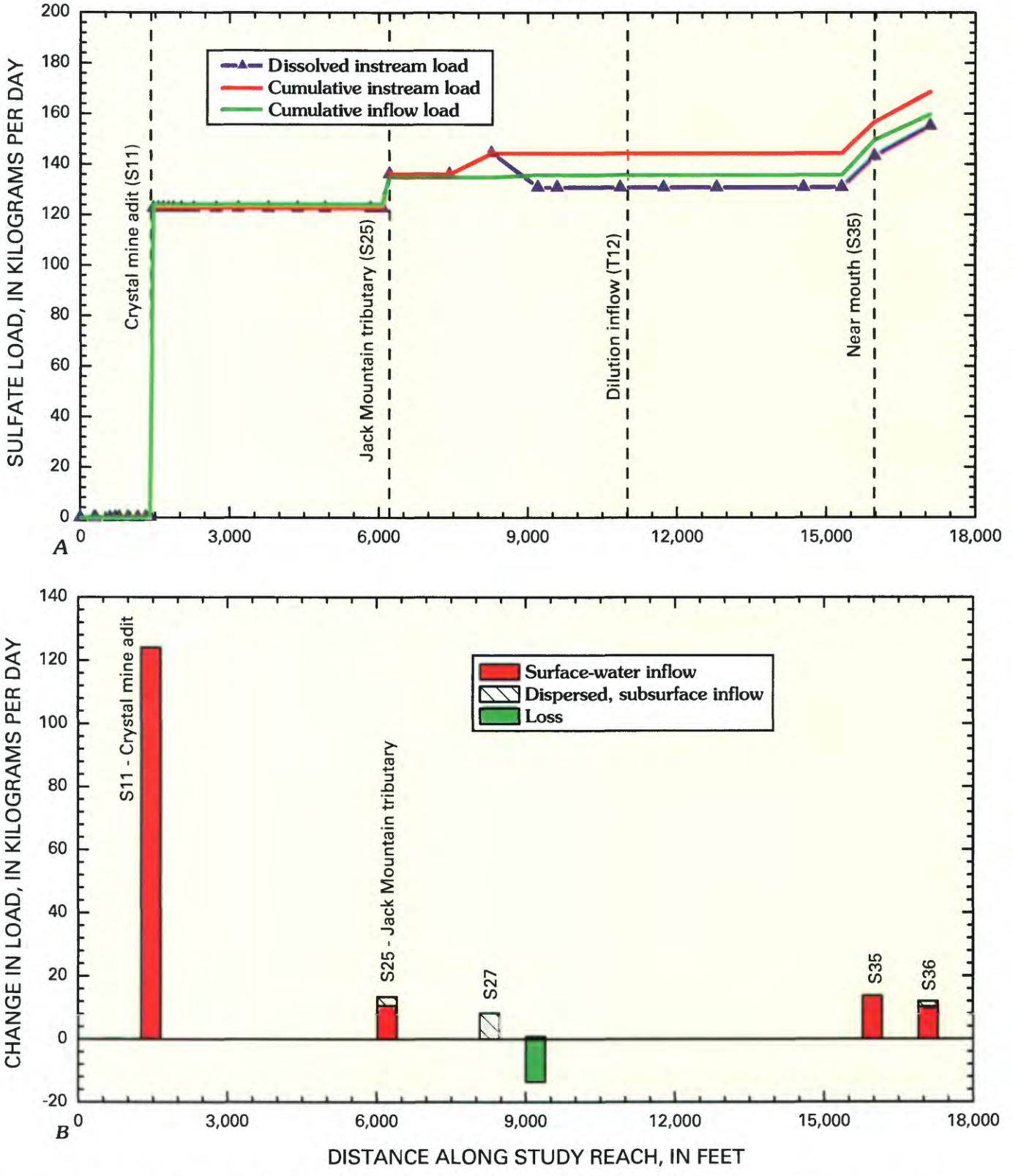

Figure 18. Variation of *A*, sulfate load with distance, and *B*, changes in load for individual stream segments, Uncle Sam Gulch, August 1998.

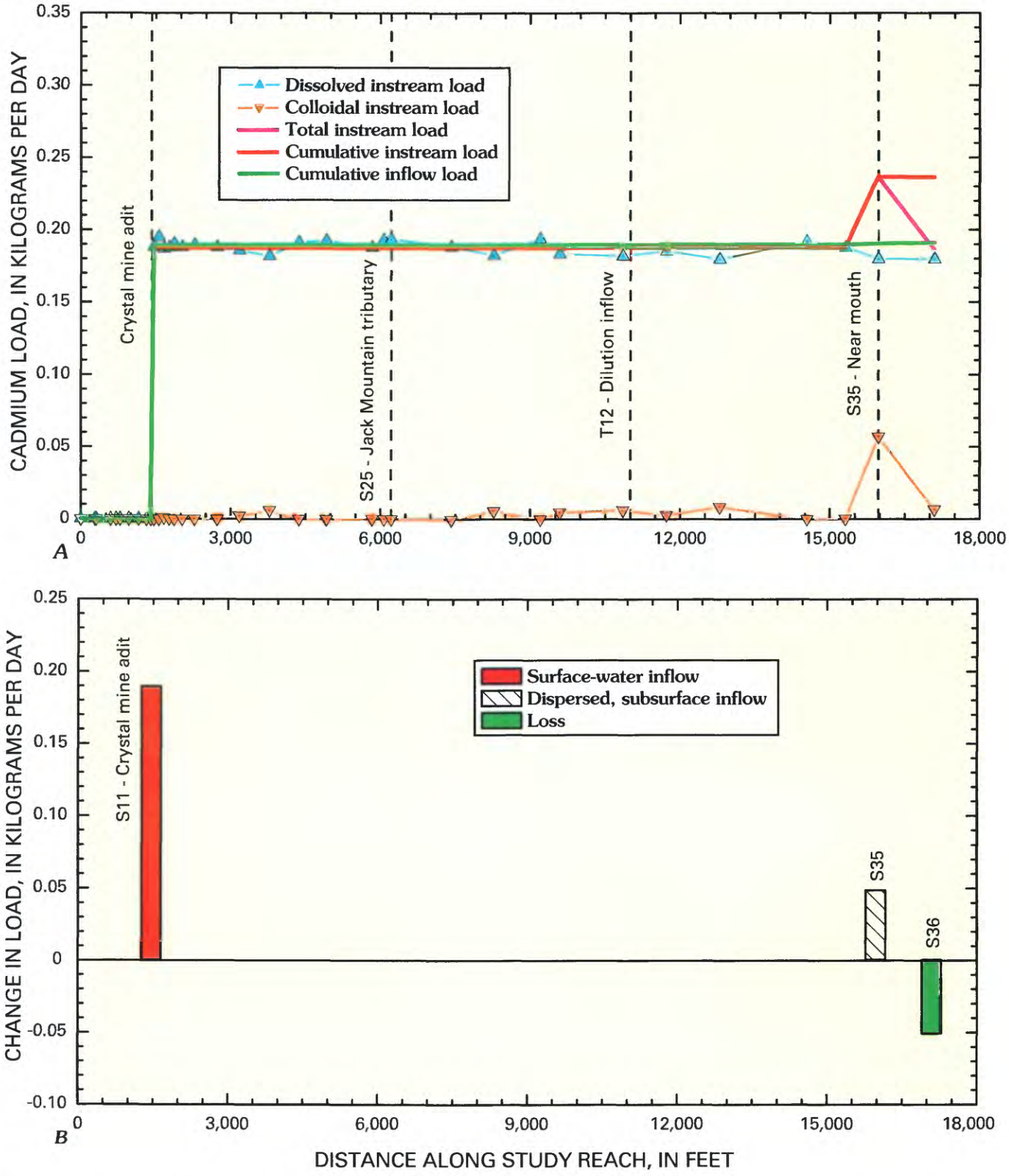

Figure 19. Variation of *A*, cadmium load with distance, and *B*, changes in load for individual stream segments, Uncle Sam Gulch, August 1998.

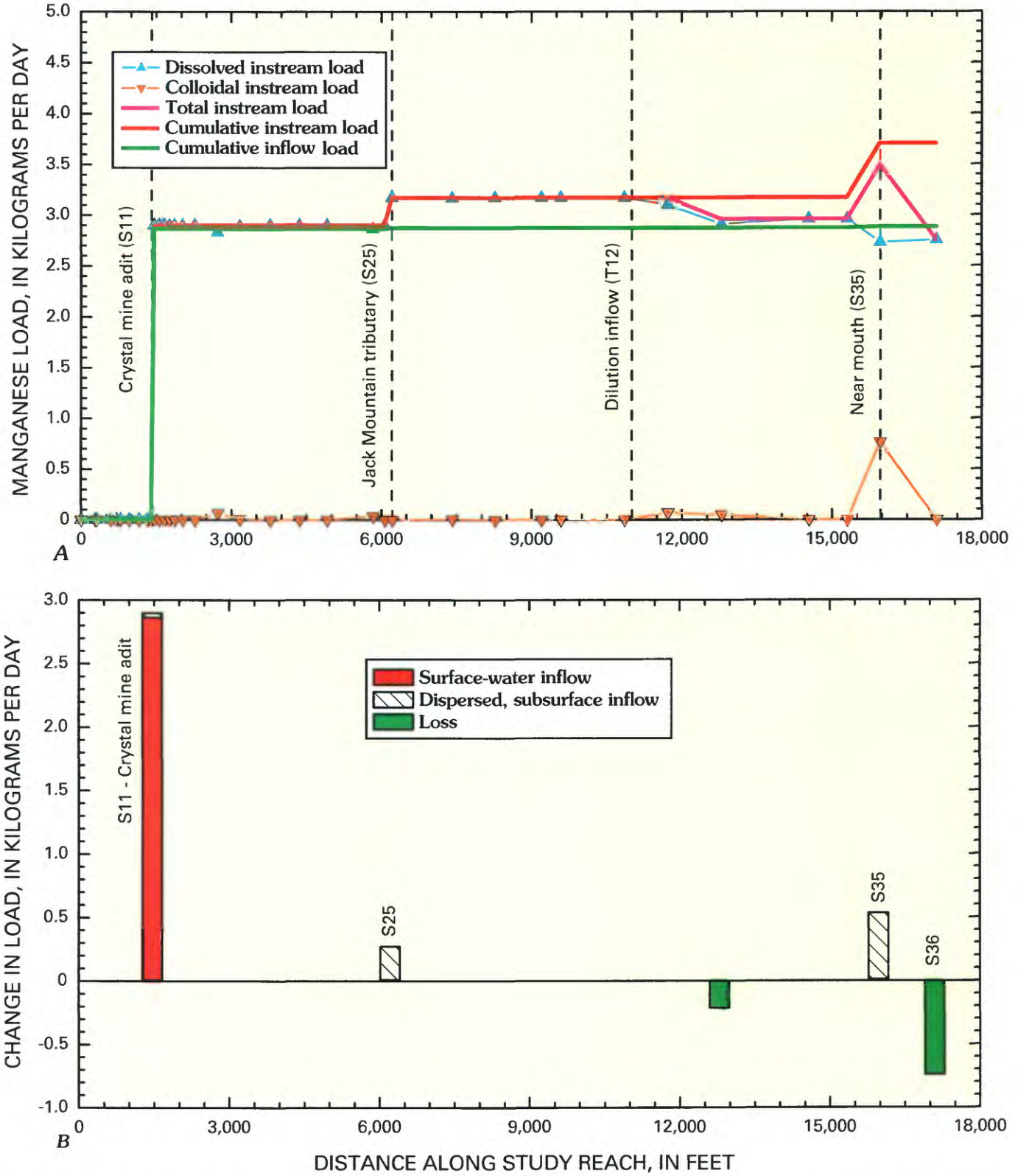

Figure 20. Variation of *A*, manganese load with distance, and *B*, changes in load for individual stream segments, Uncle Sam Gulch, August 1998.

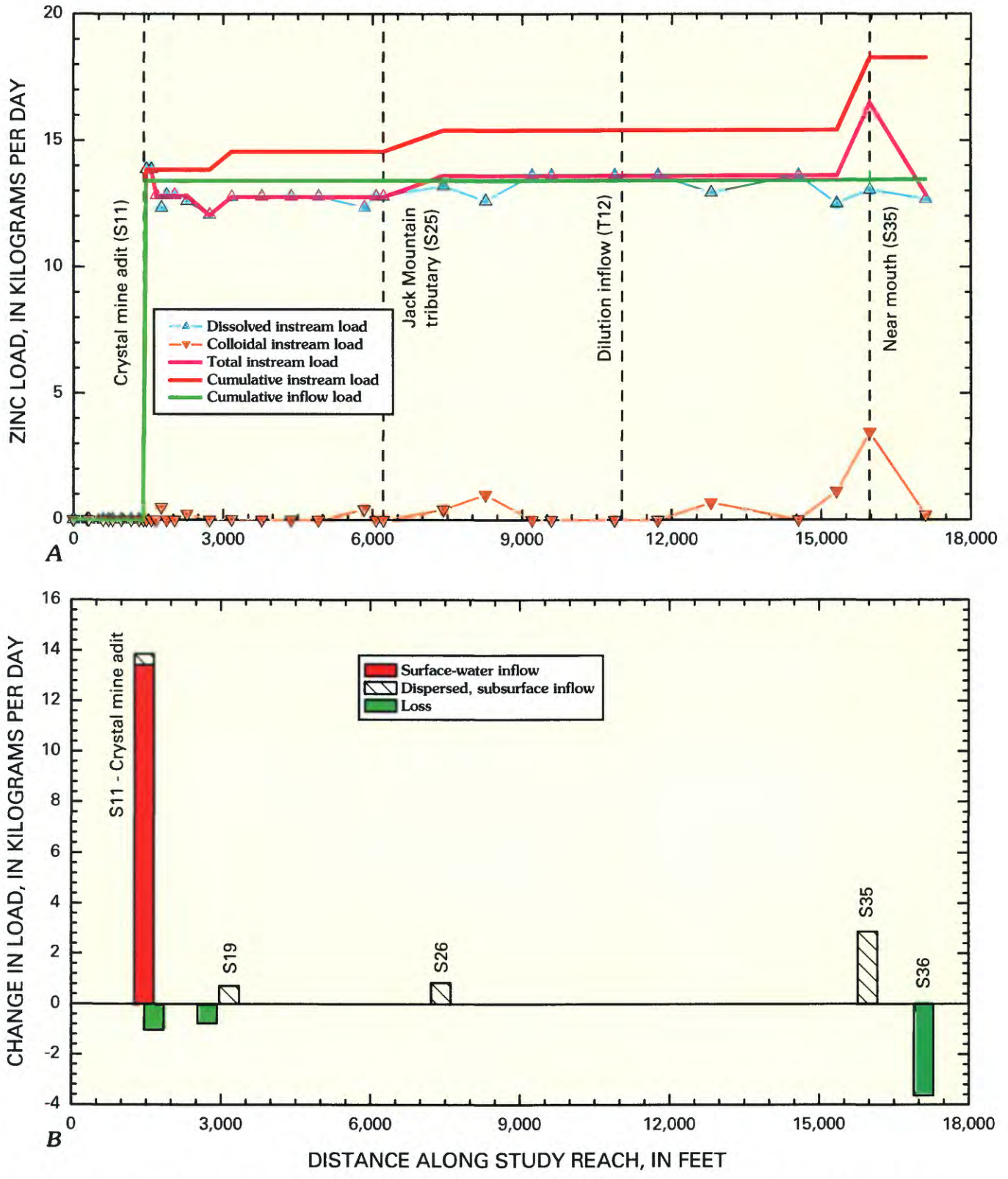

Figure 21. Variation of *A*, zinc load with distance, and *B*, changes in load for individual stream segments, Uncle Sam Gulch, August 1998.

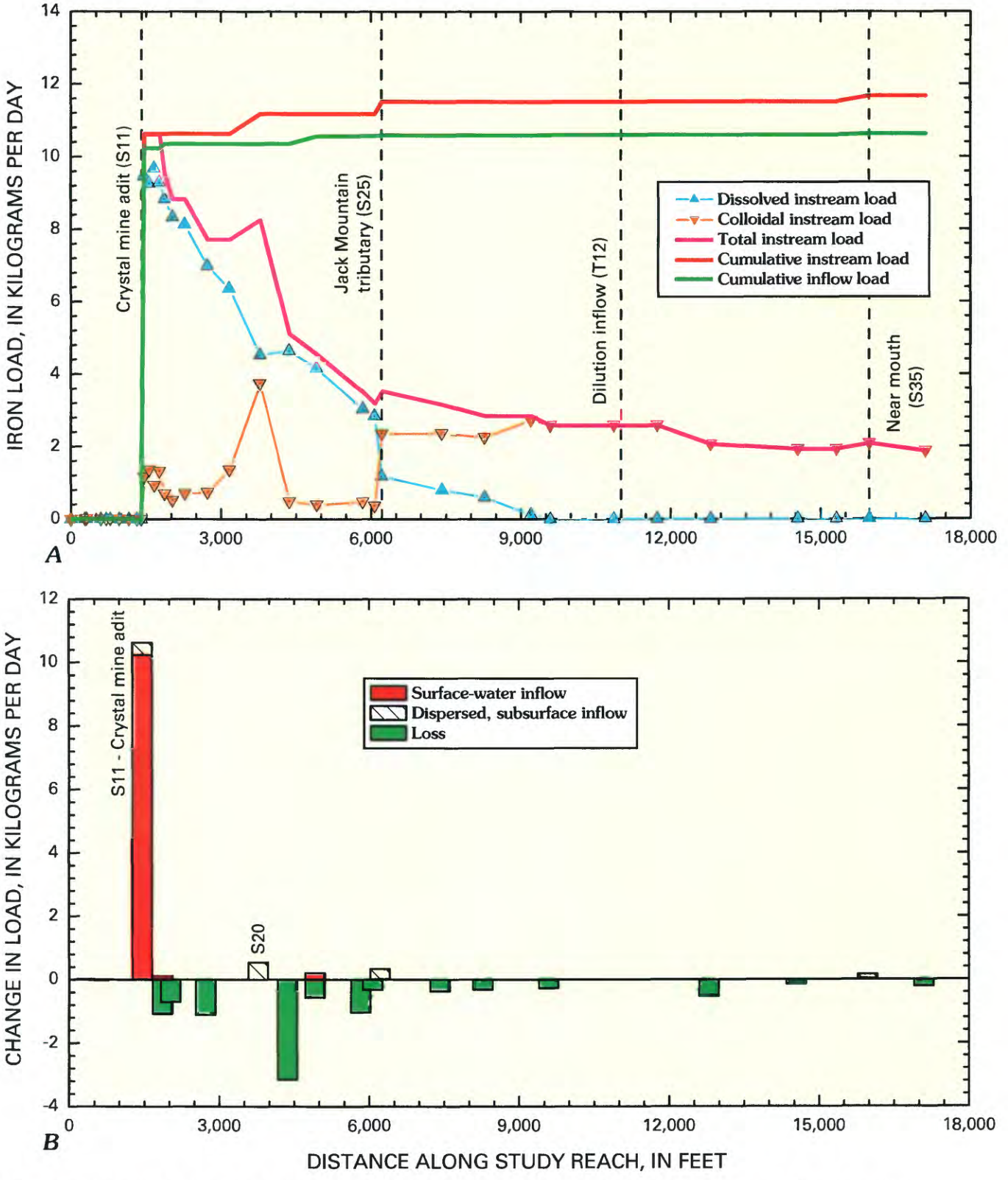

Figure 22. Variation of *A*, iron load with distance, and *B*, changes in load for individual stream segments, Uncle Sam Gulch, August 1998.

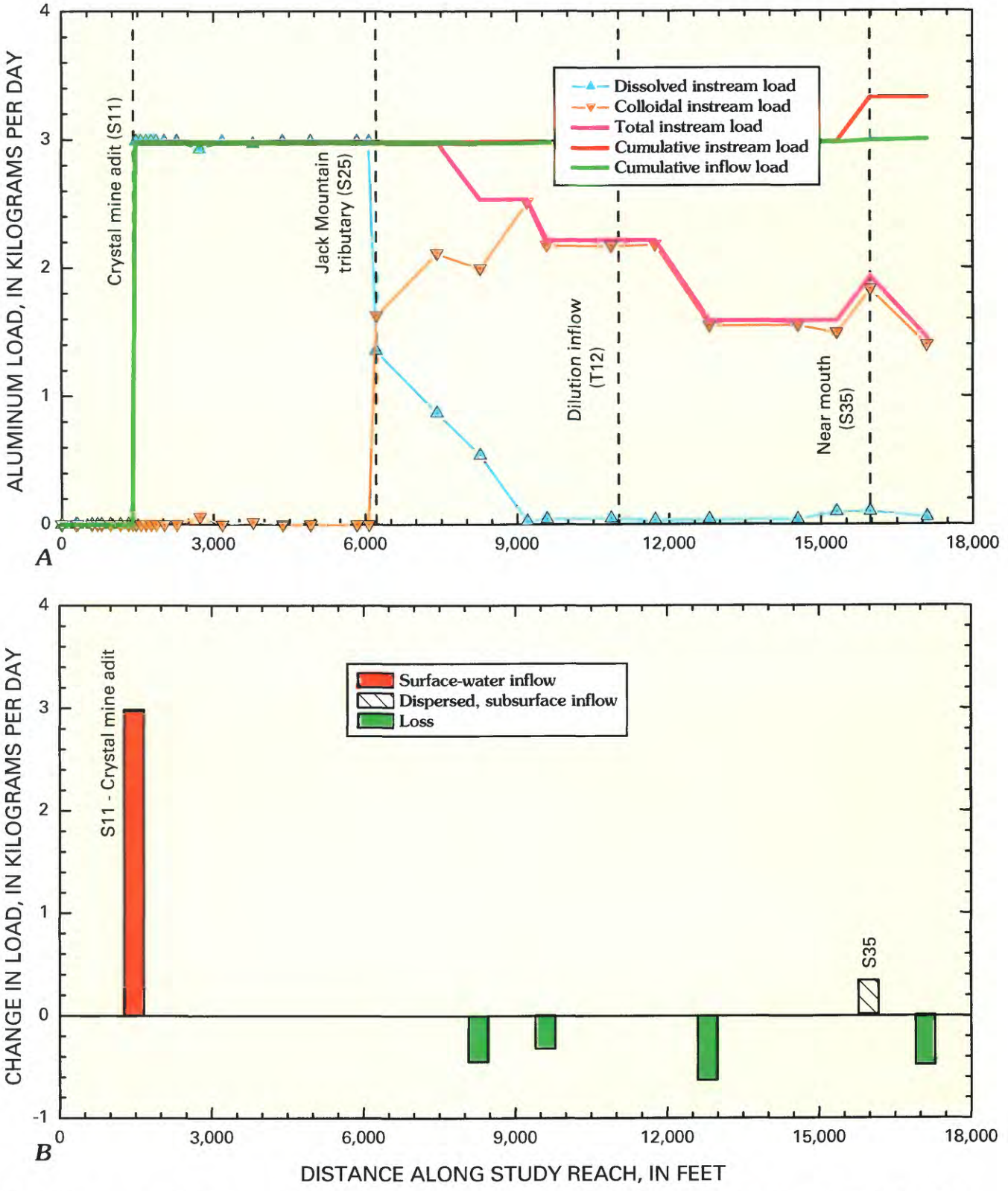

Figure 23. Variation of *A*, aluminum load with distance, and *B*, changes in load for individual stream segments, Uncle Sam Gulch, August 1998.

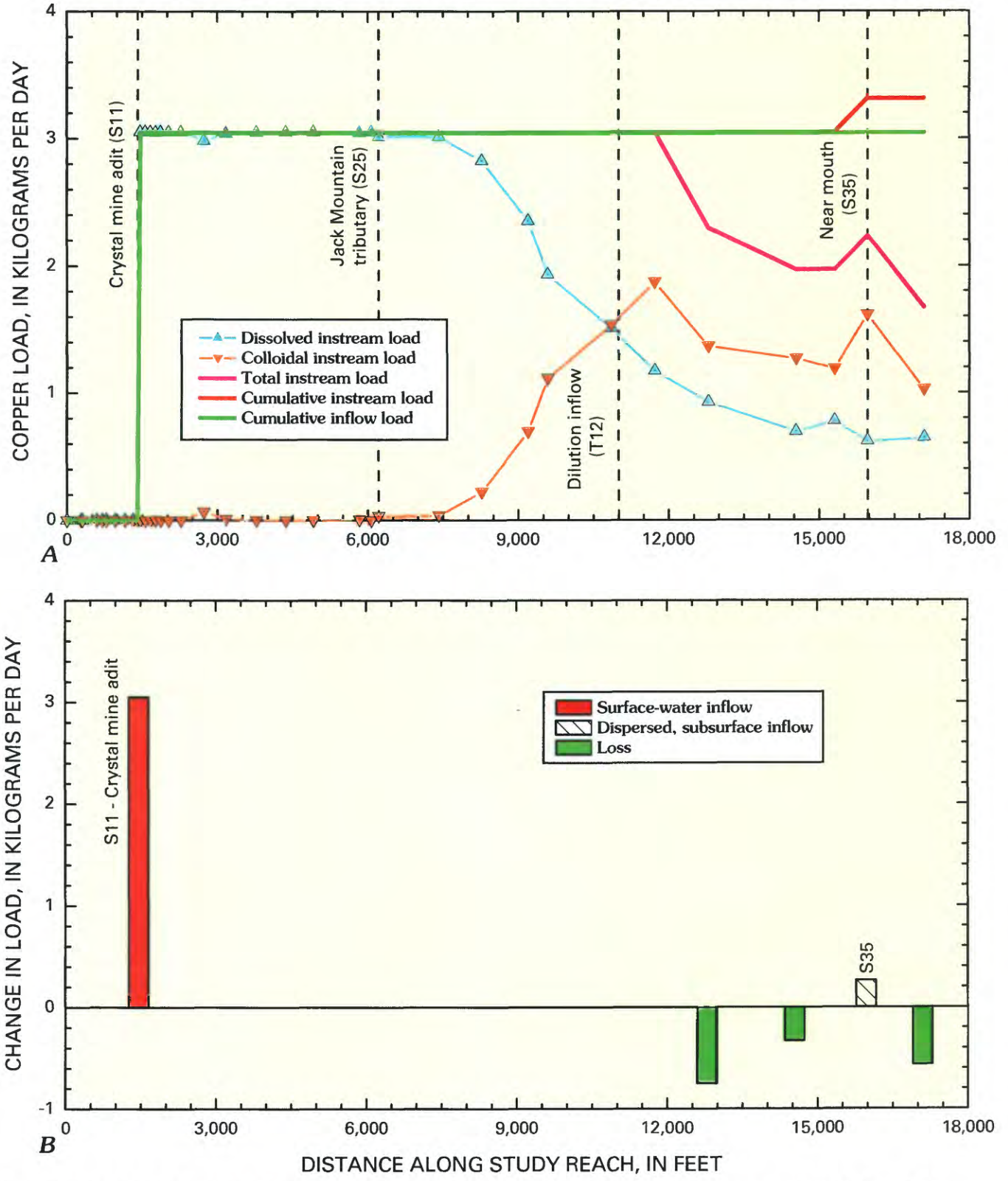

Figure 24. Variation of *A*, copper load with distance, and *B*, changes in load for individual stream segments, Uncle Sam Gulch, August 1998.

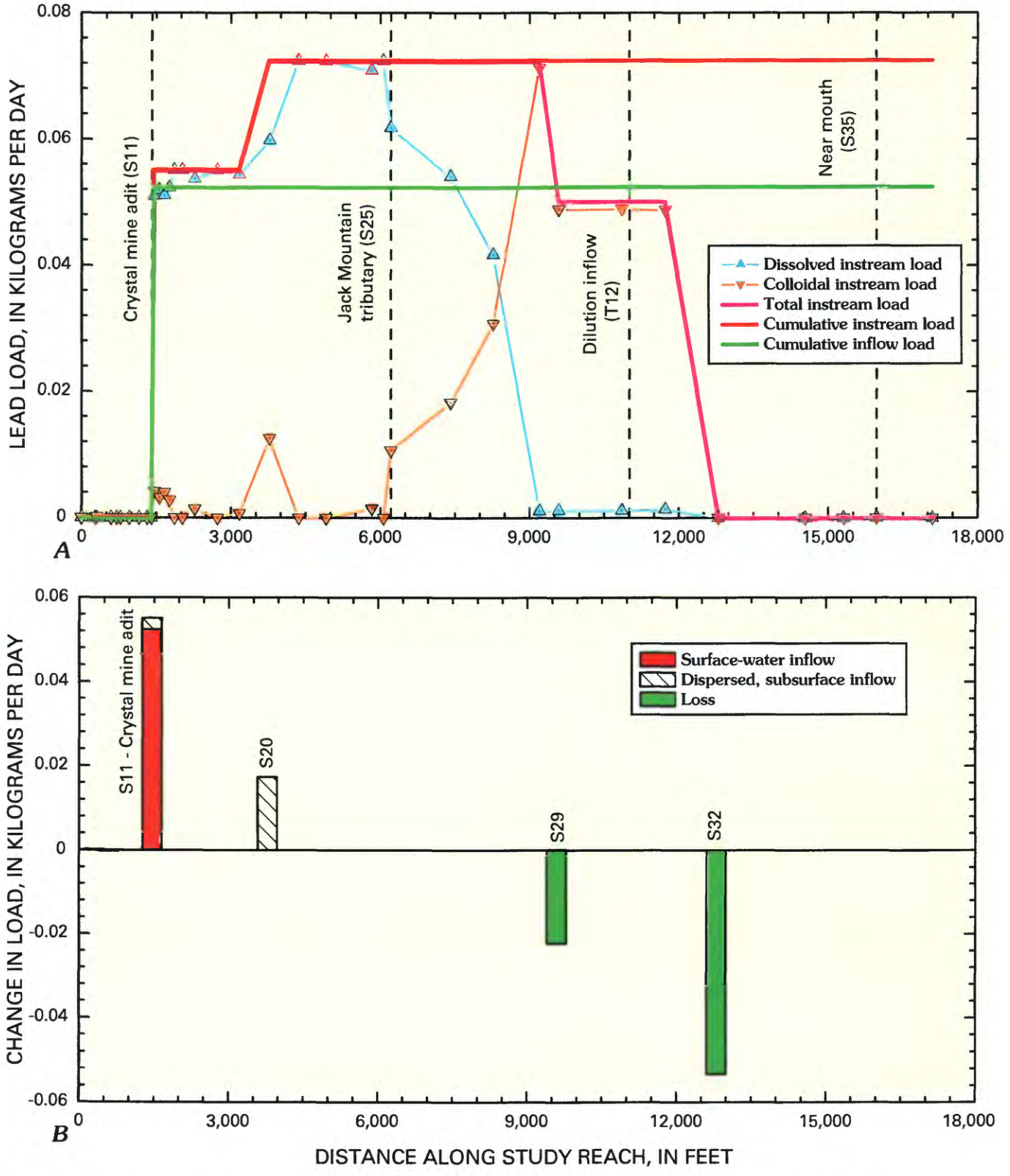

Figure 25. Variation of *A*, lead load with distance, and *B*, changes in load for individual stream segments, Uncle Sam Gulch, August 1998.

Table 6. Change in load for individual stream segments and summary of load calculations for selected solutes, Uncle Sam Gulch, August 1998.

[Distance, in meters along the study reach; Al, aluminum; Cu, copper; Fe, iron; Pb, lead; Mn, manganese; Sr, strontium; Zn, zinc; SO_4, sulfate; cumulative instream load, cumulative inflow load, unsampled load, and attenuation in kilograms per day; numbers in red with parentheses indicate a loss of load; color of cell indicates the segments with the greatest load: red, largest load; orange, second largest; yellow; third; green, fourth; blue, fifth]

Segment number	Distance	Al	Cu	Fe	Pb	Mn	Sr	Zn	SO_4
S01	0	0.000	0.000	0.001	0.000	0.000	0.000	0.000	0.010
S02	278	.000	(.000)	.001		.000		(.000)	.039
S03	305	.001	.000	.019	.000	.001	.000	.001	.019
S04	592	(.001)	.000	(.017)	(.000)	(.000)	.001	.000	.019
S05	702	.001	.001	.004	.000	.002	.003	.004	.151
S06	780						.001		
S07	957		(.000)				.002	.001	.026
S08	1,152	(.000)	(.000)	(.004)		(.001)		(.001)	(.030)
S09	1,314	(.001)	.000	.001		.000	.002	.003	.081
S10	1,399	.001					.001	(.001)	.043
S11	1,461	2.99	3.05	10.6	.055	2.90	.052	13.9	122
S12	1,560								
S13	1,661							(1.02)	
S14	1,764								
S15	1,866			(1.08)					
S16	2,026			(.702)					
S17	2,273								
S18	2,727			(1.11)				(.772)	
S19	3,170						.009	.715	
S20	3,777			0.547	.017		.006		
S21	4,365			(3.15)					
S22	4,915			(.567)			.009		
S23	5,830			(1.03)					
S24	6,068			(.320)					
S25	6,213			.337		.272	.061		13.5
S26	7,417			(.368)			.015	.841	
S27	8,270	(.447)		(.313)					8.25
S28	9,200						.024		(13.6)
S29	9,588	(.320)		(.263)	(.022)				
S30	10,856								
S31	11,724						.044		
S32	12,795	(.629)	(.751)	(.524)	(.053)	(.212)			
S33	14,540		(.327)	(.140)					
S34	15,314								
S35	15,971	.342	.265	0.160		2.87	.182	2.87	12.3
S36	17,095	(.479)	(.561)	(.212)		(.740)	(.040)	(3.63)	12.0
Cumulative instream load		3.33	3.32	11.7	.073	3.71	.412	18.3	169
Cumulative inflow load		3.00	3.05	10.6	.053	2.88	.328	13.5	160
Percent inflow load		90	92	91	72	78	80	74	94
Unsampled inflow		.329	.268	1.06	.020	.823	.084	4.85	9.33
Percent unsampled inflow		10	8	9	28	22	20	26	6
Attenuation		1.88	1.64	9.81	.073	.953	.000	5.43	13.6
Percent attenuation		56	49	84	100	26	0	30	8

study reach is consistent with the relatively small contribution of iron load from Uncle Sam Gulch to Cataract Creek (fig. 11).

Most of the aluminum load also entered the stream in the adit discharge of the Crystal mine (fig. 23). One additional increase was measurable in segment S35, and it was unsampled inflow for aluminum as it was for other metals. Higher pH downstream from Jack Mountain tributary caused a complete change in aluminum load from the dissolved to the colloidal phase. Unlike the transformation of iron, this change in aluminum phase occurred along the next 2,000 ft of stream. The colloidal aluminum load subsequently decreased downstream to about half the amount present before the transformation.

Copper loading resembled that of aluminum; the major source was the adit inflow from the Crystal mine, and load decreased substantially downstream from Jack Mountain tributary (fig. 24). For copper, the decrease in load was not as abrupt as for iron. Instead, there was a gradual transformation from dissolved to colloidal copper after sorption to iron and perhaps aluminum colloids between segments S25 and S29. The percentage of total-recoverable copper that is in the colloidal form increased systematically with pH, in a manner very similar to a sorption isotherm (Smith, 1999). The increase in copper load at segment S35 was an increase in colloidal, rather than dissolved, copper. The unsampled inflow of copper likely occurred as dissolved copper that was sorbed to iron colloids during the time of transport through the stream segment.

The loading profile of lead differed from those of the other metals because some of the loading occurred downstream from the inflow from the Crystal mine adit (segment S20), and not just from the adit inflow (fig. 25). The greatest increase occurred in segment S20, from unsampled inflow. Downstream from Jack Mountain tributary, the lead load decreased, but in a pattern more like copper indicating gradual sorption rather than precipitation. In stream segment S32, essentially the entire lead load was gone from the water column, possibly due to the increase of instream pH in this segment. The loss of lead is consistent with the increase of lead concentration in the bed sediments (Church and others, this volume, fig. 5).

Locations of Major Loading

Inflow from the Crystal mine adit at segment S11 dominated the loading of all the constituents except strontium (table 6). Loading from the adit accounted for more than 90 percent of the aluminum, copper, and iron; more than 70 percent of the lead, manganese, zinc, and sulfate; but only 13 percent of the strontium load. Segment S35, which was almost to the mouth of Uncle Sam Gulch, was the next most substantial source for loads for several constituents. This is the location of a major fault and several veins that have not been mined (O'Neill and others, this volume, pl. 1). Segment S20 was a source for 23 percent of the lead load. The inflow of Jack Mountain tributary, accounted for by segment S25, was a source for iron, manganese, strontium, and sulfate.

Unsampled Inflow

Unsampled inflow was less than 30 percent for all the constituents. The greatest amount of unsampled inflow was for lead (28 percent), manganese (22 percent), and strontium (20 percent). For lead (fig. 25*B*), the unsampled inflow occurred in segment S20 (fig. 25*B*). The source of this loading is unknown, but likely is associated with ground water from the Crystal mine or the waste-rock pile. Unsampled inflow for manganese (fig. 20*B*) occurred in segments S25 and S35, and for strontium (fig. 17*B*) it mostly occurred in segment S35, but there were several segments with a small amount of unsampled inflow. The small amount of unsampled inflow for zinc and sulfate reflects a general lack of widespread alteration of rocks in the watershed.

Attenuation of Load

Most of the attenuation of metals in Uncle Sam Gulch occurred downstream from Jack Mountain tributary. About 50 percent of the aluminum (fig. 23*A*) and copper (fig 24*A*), more than 80 percent of the iron (fig. 22*A*), and all of the lead (fig. 25*A*) that entered Uncle Sam Gulch were removed from the water column by the end of the study reach (table 6). This metal attenuation resulted in the accumulation of colloidal floc on the streambed. In the Animas River watershed, Church and others (1997) quantified a large increase in the load of colloidal floc that was transported, or flushed, by high flows during snowmelt runoff. About 30 percent of the manganese and zinc loads were removed (table 6), but only 8 percent of the sulfate load and less than 1 percent of the strontium load were removed.

The attenuation of iron started immediately downstream from the adit inflow (fig. 22). The geochemical behavior of iron makes its loading profile different from that of other metals. The profile indicates that only segment S11 was a major source of loading; the net gain for all but three other segments was negative or near zero. This does not mean, however, that there were no contributions from other stream segments. Because the transformation of dissolved to colloidal iron occurred rapidly with respect to transport of the metals in the stream (Kimball, Broshears, and others, 1994), most of the colloidal iron can be lost through aggregation, settling, and filtering through the streambed within the same stream segment where it enters (Grundl and Delwiche, 1993; Packman and others, 2000). Thus, there could have been contributions or iron load in other stream segments, but if the iron entering the stream is rapidly transformed to colloidal iron and removed from the water column, there is no accounting of that mass loading at this stream-segment scale.

Load profiles help to quantify the mass transfer of chemical reactions in the stream. Changes in load indicate the timing and mechanisms of precipitation and sorption reactions in the context of stream transport (Kimball, Bencala, and Broshears, 1994). The dominant reactions affecting metals downstream from Jack Mountain tributary were the formation of iron and

aluminum colloids. At the low pH upstream from Jack Mountain tributary, Desborough and others (2000) determined that the iron precipitate was schwertmannite. Bigham and Nordstrom (2000) discussed the steps in the formation of schwertmannite, and the final step is represented as:

$$8Fe^{3+}+SO_4^{-2}+14H_2O=Fe_8O_8(OH)_6(SO_4)+22H^+ \quad (3)$$

Downstream from Jack Mountain tributary, at a higher pH, the precipitate was ferrihydrite:

$$Fe^{3+}+3OH^-=Fe(OH)_{3,s} \quad (4)$$

The change may be due to a more positive surface charge on the iron colloid at low pH, favoring anion sorption. Attenuation of aluminum, on the other hand, begins with a transformation from dissolved to colloidal aluminum, probably through the formation of polynuclear aluminum complexes at low temperature (Baes and Mesmer, 1976):

$$xAl^{3+}+yH_2O\Leftrightarrow Al_x(OH)_y^{(3x-y)+}+H^+ \quad (5)$$

Downstream from the inflow of Jack Mountain tributary where the pH increased above 5.5, this transformation begins (fig. 24). As the complex grows it becomes too large to pass through the 10,000 Dalton filter and can be considered colloidal. A crystalline mineral phase, like gibbsite ($Al(OH)_{3,s}$), would occur with aging on the streambed.

Loads of dissolved iron and dissolved aluminum were transformed from the dissolved to the colloidal phase in segments S25 through S28, downstream from Jack Mountain tributary (fig. 26). In each successive stream segment the total load was constant; before the loss of any load, only the portion of the colloidal phase increased. By adding in the amount of the colloidal phases lost to the streambed, the mass balance was still constant. After transport to segment S28, both aluminum and iron were completely transformed to the colloidal phase. Once the colloidal iron was present, dissolved copper started to change to colloidal copper, most likely from sorption to the iron solids. Often it is not possible to distinguish if copper is removed by sorption or coprecipitation (Fulghum and others, 1988), but these data clearly point toward sorption, rather than coprecipitation, as the mechanism of copper removal, because copper was transformed only after the iron colloid had formed. At segment S30, the dissolved and colloidal copper loads were nearly equal, and by segment S32 there was a loss of copper load to the streambed. By accounting for the dissolved, colloidal, and lost copper loads, the total copper remained constant and the mass balance indicates that the mass transfer between phases occurred in the water column.

Comparison of copper mass transfer (figs. 24 and 26) clearly indicates that the transformation of copper from the dissolved to the colloidal phase occurred after the formation of the aluminum and iron colloids. The moles of copper sorbed were less than one tenth of the moles of aluminum or iron formed, but this was a substantial quantity of mass transfer. Webster and others (1998) have shown that a high sulfate percentage in iron hydroxides increases the sorption capacity of the iron phase; schwertmannite has a higher sulfate percentage. This profile and timing strongly indicate that the process for copper removal is sorption rather than coprecipitation, according to a general reaction, using ferrihydrite:

$$Cu^{2+}+2H^+\equiv Fe(OH)_{3,s}\Leftrightarrow 2H^++Cu^{2+}\equiv Fe(OH)_{3,s} \quad (6)$$

where ≡ indicates bonding to a solid surface. Runkel and others (1999) have simulated sorption of copper to iron colloids in a mine-drainage stream, showing that it is a reversible reaction.

Bullion Mine Tributary Subbasin

Mine drainage that affects a small tributary of Jack Creek, called the Bullion Mine tributary in this report, originates from the same ore body that was mined at the Crystal mine in Uncle Sam Gulch (fig. 12). The adit of the Bullion mine discharges to the Bullion Mine tributary where it is a small stream, and the impact of the mine drainage is substantial. A mass-loading study was done during low-flow conditions in early September 1998 to investigate the source of metals and the patterns of metal loading.

Study Area and Experimental Design

Stream samples defined 33 segments and bracketed a total of 11 inflows along the study reach (fig. 27). Site numbers and descriptions of stream and inflow sites are listed in table 7 for reference; detailed field and chemical data for these sites are in the database (Rich and others, this volume). A sodium chloride solution, with 79,040 mg/L chloride, was injected into the Bullion Mine tributary at a rate of 0.0017 L/s for 36 hours, starting at 10:00 MDT on August 30, 1998. Chloride concentration decreased systematically downstream from the injection, indicating those stream segments that contributed water to the stream (fig. 28). Calculated discharge ranged from 0.12 to 0.80 ft^3/s (fig. 28). The largest inflow was Jack Creek (site T11) with a calculated discharge of 0.52 ft^3/s. Jack Creek represented 65 percent of the total streamflow. Stream segments that had sampled inflows accounted for 88 percent of the total increase in streamflow, and discharge increased 0.20 ft^3/s in those segments that had no sampled inflow. This indicates that a minimum of 12 percent of the total increase in streamflow was unsampled inflow, on the basis of tracer information.

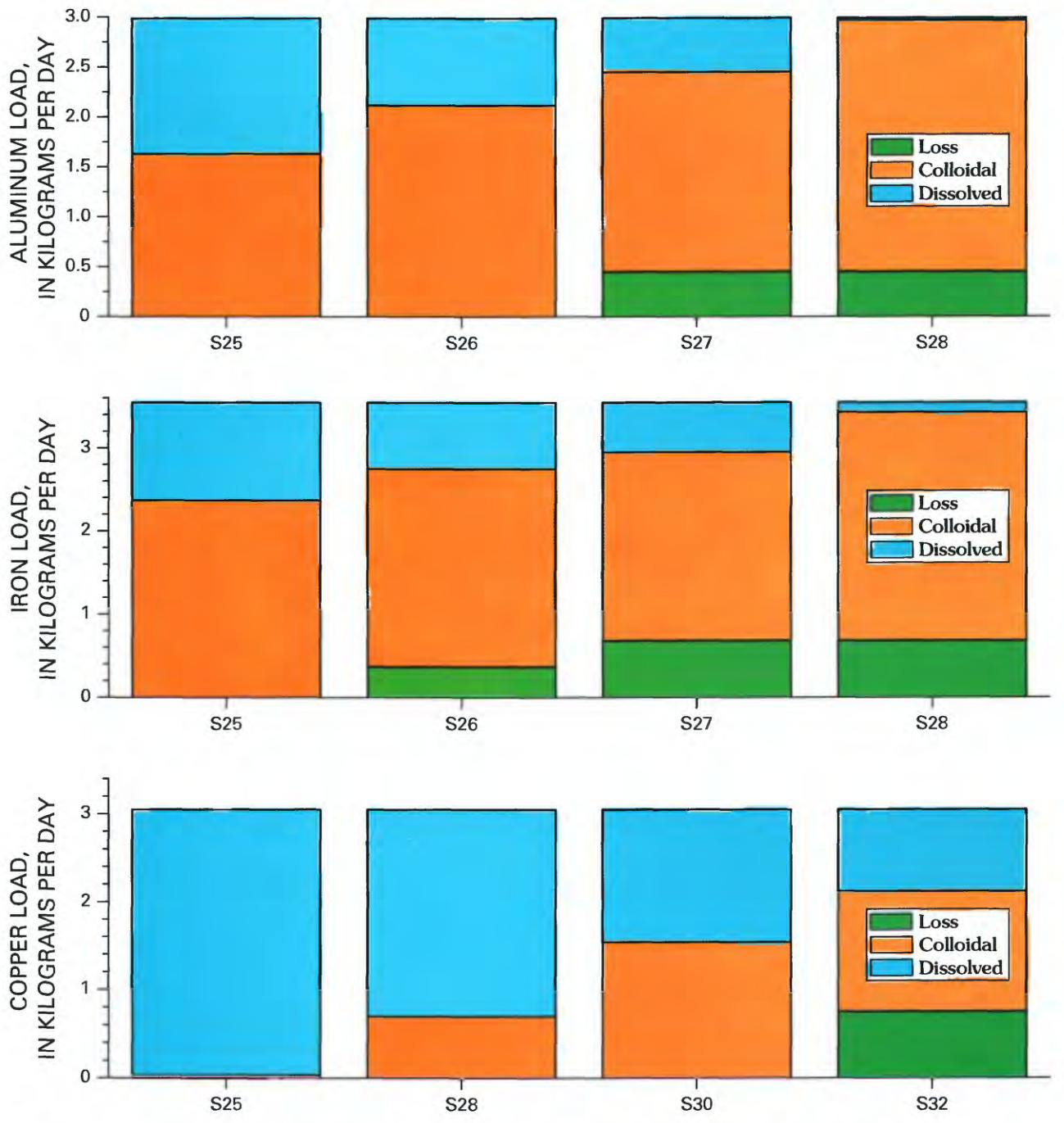

Figure 26. Mass transfer of metals between dissolved and colloidal phases, Uncle Sam Gulch, August 1998.

Table 7. Segment number, distance along study reach, source, site description, site number, and field and chemical data for water from synoptic sampling sites, Bullion Mine tributary, September 1, 1998.

[Dist, distance, in feet along the study reach; source: S, stream; LBI, left bank inflow; RBI, right bank inflow; pH, in standard units; Ksc, specific conductance, in microsiemens per centimeter; Q, discharge, in liters per second; Cl, chloride, in milligrams per liter]

Segment number	Dist	Source	Description	Site Number	pH	Ksc	Q	Cl
S01	0	S	Above injection site	Bull0	6.82	67	3.3	0.28
S02	150	S	Below injection site	Bull150	7.07	171	3.3	33.5
S03	235	S	T1 transport site below injection	Bull235	7.08	168	3.3	31.8
S04	296	S	At start of mining disturbance	Bull296	6.89	167	3.3	32.0
S05	341	S	Above acidic inflows	Bull341	6.88	169	3.4	31.1
T01	346	LBI	Left bank inflow from mine	Bull346	2.78	1,827	0.17	2.94
T02	359	LBI	Second acid inflow	Bull355	2.83	1,829	0.35	3.46
S06	383	S	Below acidic inflows—log jam	Bull383	3.61	419	3.9	26.9
S07	437	S	Stream below acidic inflows	Bull437	3.55	439	3.9	26.5
S08	485	S	Below rock dam in small pond	Bull485	3.63	443	4.0	26.2
S09	540	S	At pine over creek	Bull540	3.60	448	4.0	26.1
T03	582	LBI	Left bank inflow	Bull582	3.52	1,185	0.20	1.54
S10	627	S	Below high conductance inflow	Bull627	3.52	473	4.2	24.5
S11	726	S	Upstream from bedrock control	Bull726	3.58	418	4.2	24.8
T04	733	LBI	Left bank near end of tailings	Bull733	4.61	532	0.02	0.73
S12	793	S	Downstream of log at meander	Bull793	3.52	478	4.2	24.2
S13	856	S	At large boulder control	Bull856	3.56	477	4.2	23.4
S14	945	S	Stream	Bull945	3.52	476	4.3	23.3
S15	1,025	S	Above breached settling dam	Bull1025	3.56	476	4.4	22.4
S16	1,109	S	At breached dam	Bull1109	3.58	478	4.5	23.2
S17	1,197	S	At convergence of stream channels	Bull1197	3.63	475	4.5	22.7
S18	1,264	S	Stream	Bull1264	3.75	468	4.5	22.4
S19	1,404	S	At meander bend	Bull1404	3.71	471	4.5	22.1
S20	1,522	S	At log jam	Bull1522	3.66	458	4.6	21.9
T05	1,554	RBI	Right bank tributary	Bull1554	6.72	81	0.00	0.26
S21	1,672	S	Pool upstream from log jam	Bull1672	3.73	454	4.6	21.3
S22	1,808	S	Upstream from rock falls	Bull1808	3.68	456	4.7	21.3
T06	1,874	LBI	First high pH left bank inflow	Bull1874	6.79	190	0.00	0.41
S23	1,990	S	Below high pH inflow	Bull1990	3.73	450	4.7	20.9
T07	1,992	LBI	Second high pH left bank inflow	Bull1992	6.83	129	0.45	0.27
S24	2,155	S	T2 transport site	Bull2155	3.85	413	5.2	18.8
T08	2,157	LBI	Left bank tributary	Bull2157	6.40	162	0.37	0.36
T09	2,191	RBI	Right bank tributary	Bull2191	6.50	67	0.37	0.20
S25	2,278	S	At narrow point in canyon	Bull2278	4.14	360	5.9	16.5
S26	2,585	S	Stream	Bull2585	4.11	357	5.9	16.7
S27	2,951	S	Stream	Bull2951	4.39	349	6.1	16.3
S28	3,457	S	Downstream from steep gradient	Bull3457	4.20	348	6.1	16.2
S29	3,958	S	Stream	Bull3958	4.32	338	6.3	15.3
S30	4,729	S	Stream	Bull4729	4.34	319	6.6	14.9
T10	5,245	LBI	Left bank inflow	Bull5245	6.33	54	0.32	0.20
S31	5,338	S	T3 transport site—near mouth	Bull5338	4.64	310	6.9	13.9
T11	5,339	RBI	Jack Creek	Bull5339	6.77		15	0.22
S32	5,454	S	Jack Creek below Bullion Mine tributary	Bull5454	6.60	152	22	4.17
S33	6,019	S	Jack Creek above tailings impoundment	Bull6019	6.70	151	23	4.00

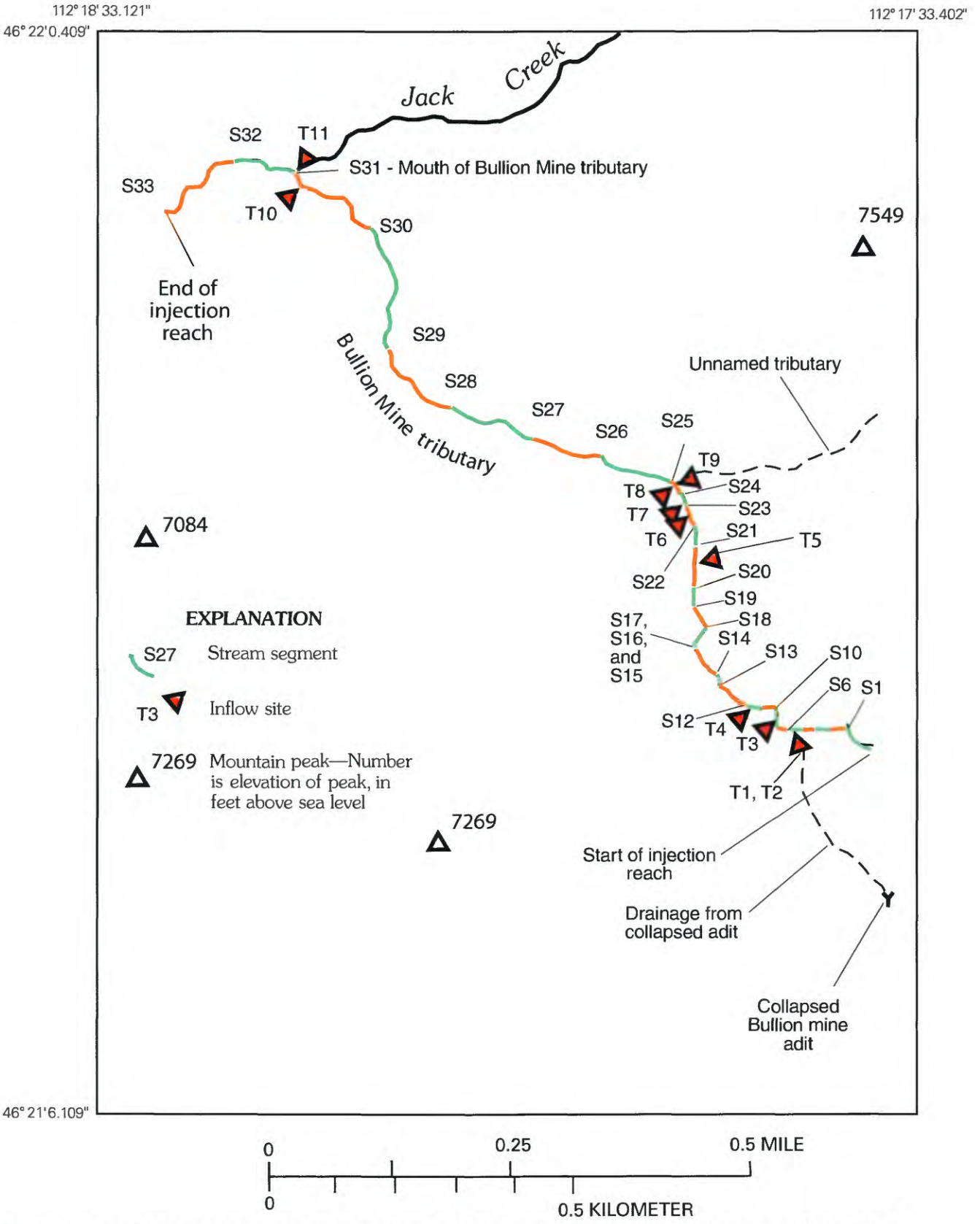

Figure 27. Location of stream segments (indicated by alternating colors) and inflows for synoptic sampling, Bullion Mine tributary, September 1998.

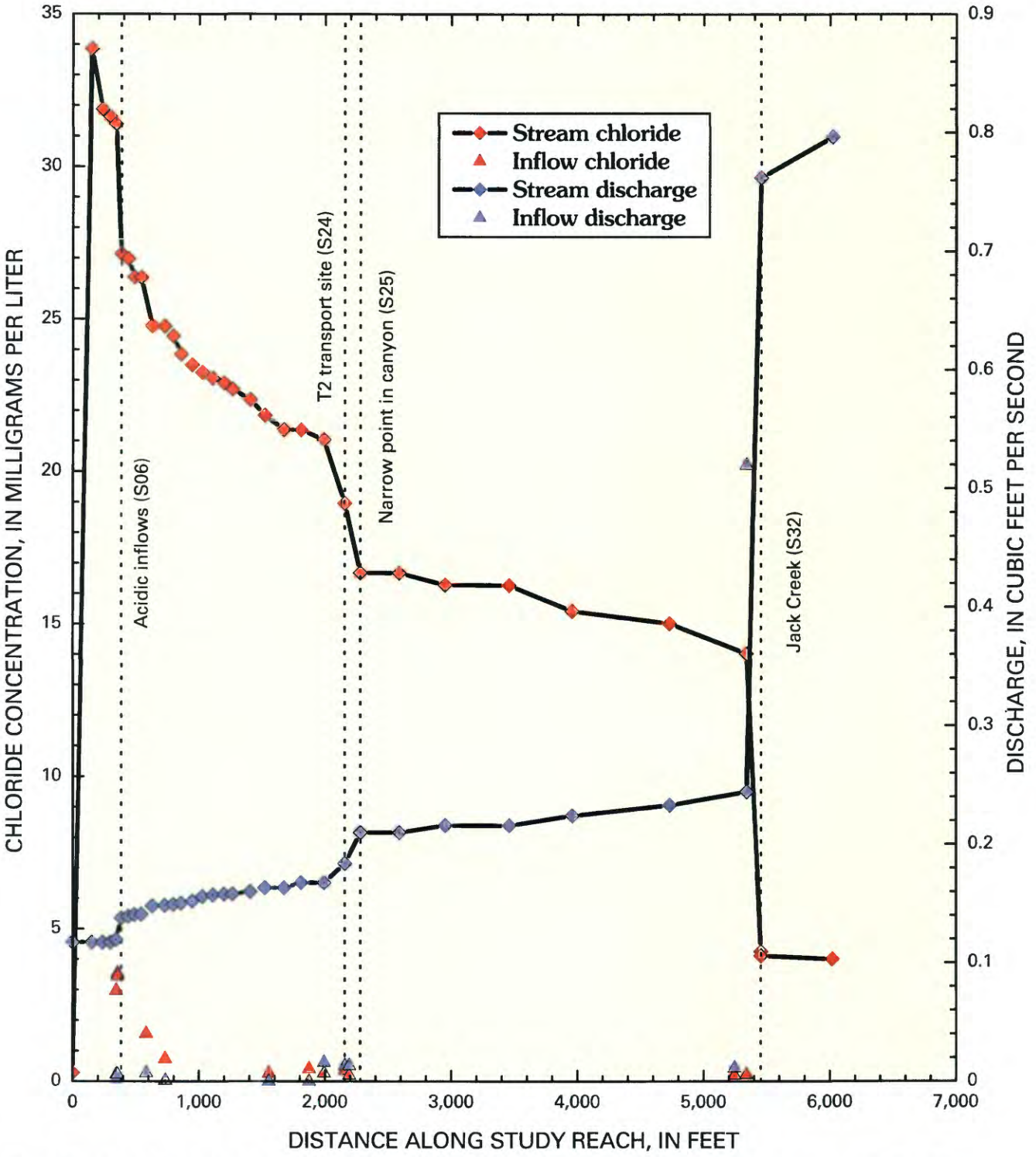

Figure 28. Variation of chloride concentration and calculated discharge with distance along the study reach, Bullion Mine tributary, September 1998.

Chemical Characterization of Synoptic Samples

The impact of inflows from the Bullion mine adit was evident from the variation of pH along the study reach in the Bullion Mine tributary (fig. 29). Three acidic inflows (T01, T02, and T03) caused a large decrease in pH (Metesh and others, 1994). Within this same area of the stream are old mill tailings that may affect the stream chemistry, along with the drainage from the collapsed adit (Fey and others, 2000). Near-neutral pH inflows at T05 through T09 only raised the pH slightly. Downstream from the confluence with Jack Creek, the pH returned to neutral, as indicated by Nimick and Cleasby (this volume, fig. 2). Changes in dissolved and colloidal metal concentrations occurred at the same locations as the changes in pH (fig. 30). The greatest increase in concentration for each of the metals was at segment S06, downstream from inflows T01 and T02. Both the filtered concentrations and the total-recoverable concentrations of aluminum, copper, and zinc increased (fig. 30*A*, *C*, *D*), indicating that these metals were present as truly dissolved metals at this low pH. The concentration decreased at segment S25 owing to inflows. At this point, there were small differences between filtered and total-recoverable concentrations, indicating colloidal concentrations. Concentrations of these metals remained nearly constant until the inflow of Jack Creek, where concentration decreased substantially (segment S32), and aluminum and copper were transformed to colloidal concentrations. Only a small part of the zinc was transformed to the colloidal form. Nimick and Cleasby (this volume) have noted where concentrations of zinc exceeded water-quality criteria at sites downstream from the Bullion mine adit inflows.

Most of the iron occurred as colloidal solids (fig. 30*B*), as indicated by the large difference between the total-recoverable and the ultrafiltrate concentrations. At site S06, downstream from the first acidic inflow, the colloidal iron concentration was 11 mg/L and the dissolved concentration was 5 mg/L. From that point on downstream, the water was noticeably cloudy due to colloidal solids (fig. 31), which were most likely schwertmannite due to the low pH of the stream. Downstream from the inflow of Jack Creek, iron concentrations were lower, but a greater percentage of the total-recoverable iron occurred as colloidal iron.

The difference between iron and the other metals resulted from the low pH of the Bullion Mine tributary (fig. 29). At S06, the pH was 3.61, which was sufficiently high for iron precipitation, but too low for the precipitation of aluminum (Nordstrom and Ball, 1986; Bigham and Nordstrom, 2000). This pH also was too low for any substantial sorption of copper or zinc to the iron colloids (Smith, 1999). Downstream from Jack Creek, at segment S32, the pH increased to 6.60, causing substantial formation of aluminum colloids and sorption of copper (fig. 30*A*, *C*), but the pH was not high enough for sorption of zinc (fig. 30*D*). At this higher pH, however, a clear distinction existed between unfiltered and 0.45-µm filtered concentrations of aluminum, copper, and zinc. This indicates a continuum of colloid sizes, and that the 0.45-µm membrane was not effective in separating the colloidal and dissolved concentrations, as observed in many other streams affected by acid mine drainage (Kimball and others, 1992; Kimball and others, 1995).

Clear chemical distinctions among stream and inflow samples were distinguished by principal components analysis into seven groups (table 8). Inflows were part of four different groups. The most dilute inflows were grouped with the stream samples that were upstream from any mining influence. All these samples represent the results of weathering catchment bedrock that is unaffected by alteration or mining (group 1). One of these inflows was Jack Creek (T10), which drains a much larger area than the Bullion Mine tributary but results in this same dilute chemical composition as the most upstream samples in the Bullion Mine tributary (table 8). A second set of inflows (group 7) differed from the dilute inflows because they had higher calcium and sulfate concentrations, possibly reflecting some effects of mine waste or a change in the mineralogy that they drain. A third group of inflows (group 6) includes the acidic inflows that had such a strong effect on the stream.

Three groups of stream samples occurred downstream from the acidic inflows. Group 2 was immediately downstream from T01 and T02, and reflects the change to acidic, metal-rich stream water. In the biplot (fig. 32), this group generally lies along a line between inflows T01 and T02 and the dilute samples of group 1. Downstream from inflow T03 a change occurred in the stream-water chemistry to higher concentrations of calcium and sulfate, and group 3 plots to the upper right of group 2 in the direction of inflow T03 (group 3). Downstream from inflows T08 and T09, a change to a higher pH occurred, and concentrations of several metals decreased (group 4). Segments S32 and S33 (group 5), downstream from Jack Creek, were quite different because of the dilution by Jack Creek and the instream chemical reactions that occurred in the mixing zone. Thus, changes in stream chemistry were quite systematic in response to the inflows. Details of these changes among groups will be illustrated by profiles of metal loading.

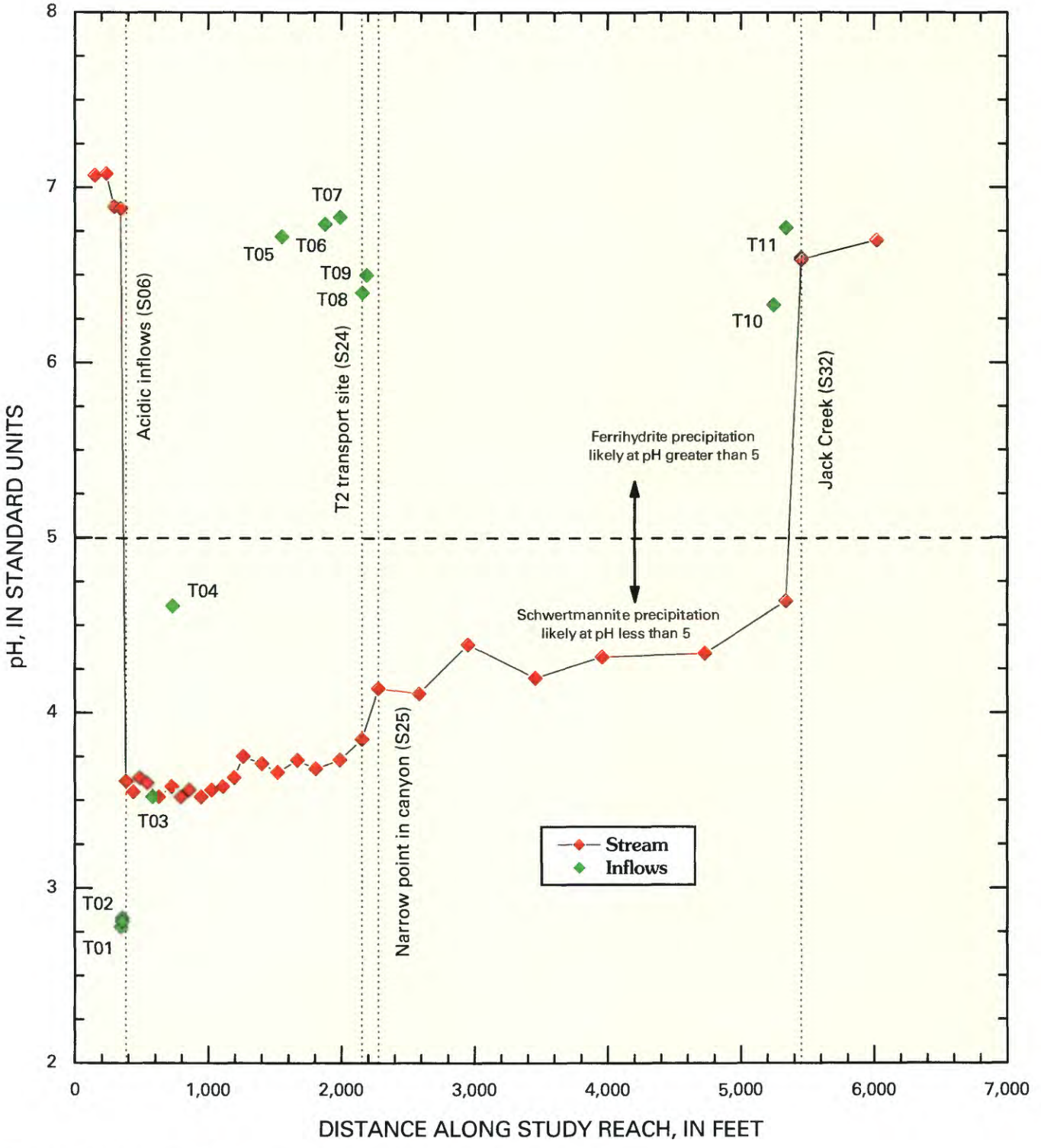

Figure 29. Variation of pH with distance, Bullion Mine tributary, September 1998.

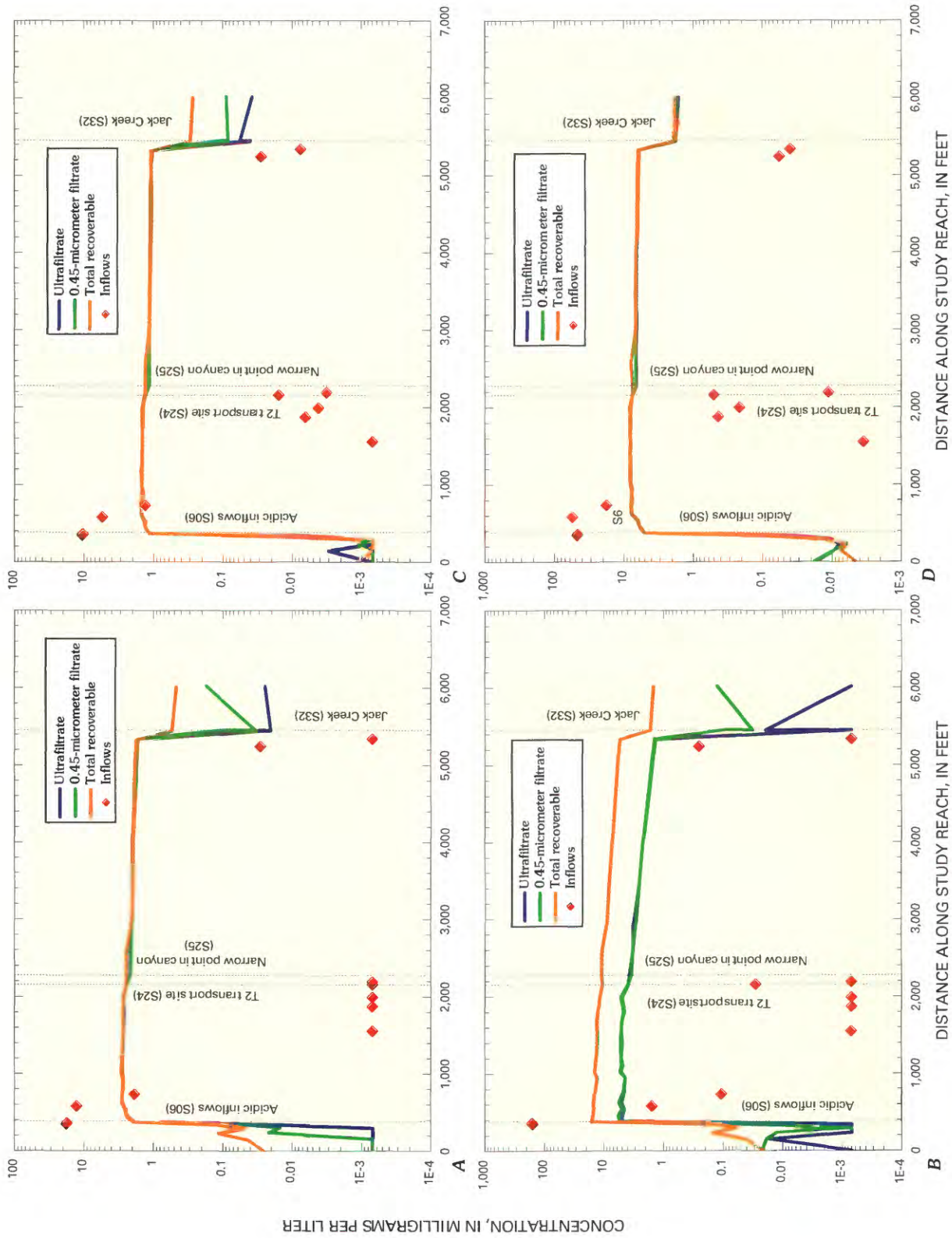

Figure 30. Variation of *A*, aluminum; *B*, iron; *C*, copper; and *D*, zinc concentrations with distance, Bullion Mine tributary, September 1998.

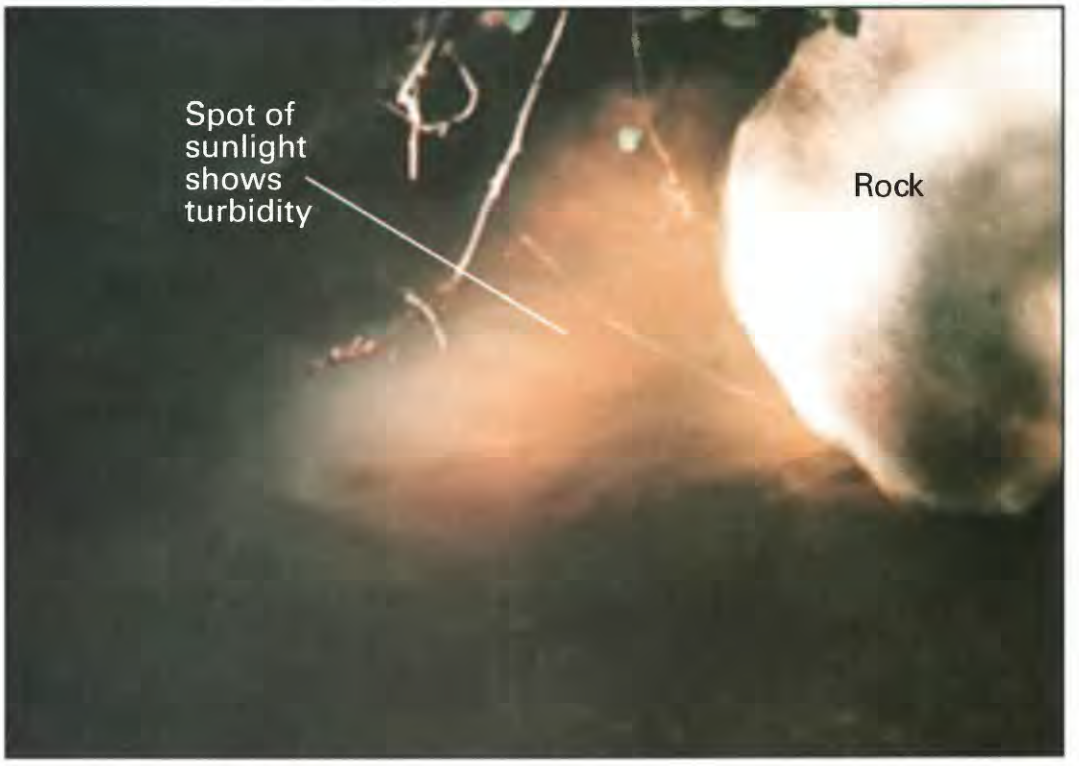

Figure 31. Bullion Mine tributary showing turbid nature of stream water owing to colloidal suspension of solids, September 1998. Length of photo area is about 1 m.

Table 8. Median composition of groups from principal components analysis for synoptic sampling sites, Bullion Mine tributary, September 1998.

[pH, in standard units; Dis, dissolved; LD, less than detection; Col, colloidal; all concentrations in milligrams per liter; -, no data]

Number of samples or solute	Phase	Group 1 Unaffected stream sites	Group 1 Unaffected inflows	Group 2 Stream after inflows T1 and T2	Group 3 Stream after inflow T3 to inflow T8	Group 3 Inflow T4, acidic, but higher pH	Group 4 Stream from S25 to S28	Group 5 Jack Creek samples	Group 6 Drainage from Bullion mine adit	Group 7 Inflows T6, T7, and T8 with higher pH
Number of samples		5	4	6	16	1	4	2	3	3
pH	Dis	6.89	6.61	3.62	3.65	4.61	4.17	6.65	2.82	6.79
Calcium	Dis	7.88	9.50	19.0	24.9	63.7	25.1	15.5	89.2	21.2
Magnesium	Dis	1.73	2.31	5.91	7.47	15.2	7.03	3.93	33.7	4.76
Sodium	Dis	21.2	2.72	17.9	15.8	4.23	12.8	4.91	5.27	2.76
Chloride	Dis	31.8	.210	26.2	22.4	0.730	16.4	4.08	2.94	0.360
Sulfate	Dis	7.43	5.11	131	160	273	136	41.4	1,100	36.1
Aluminum	Dis	LD	.013	2.18	2.80	1.89	2.12	.024	17.9	LD
	Col	.049	-	.048	.043	-	.177	.483	-	-
Cadmium	Dis	.002	.002	.068	.087	.151	.073	.019	.556	.007
	Col	LD	-	.001	LD	-	.004	.002	-	-
Copper	Dis	LD	.004	1.20	1.46	1.31	1.15	.043	10.6	.011
	Col	LD	-	.004	LD	-	.069	.235	-	-
Iron	Dis	LD	.005	4.74	5.01	.107	3.24	.005	158	.004
	Col	.061	-	10.4	8.48	-	6.56	1.58	-	-
Lead	Dis	LD	LD	.029	.042	.111	.031	LD	.382	LD
	Col	LD	-	LD	.007	-	.009	LD	-	-
Manganese	Dis	.001	.001	3.02	3.82	4.37	3.00	.645	25.1	.017
	Col	.002	-	.015	LD	-	.165	.016	-	-
Nickel	Dis	LD	LD	.014	.020	.049	.016	.002	.142	LD
	Col	LD	-	.002	.002	-	.005	.003	-	-
Strontium	Dis	.063	.068	.095	.115	.258	.119	.088	.310	.095
Zinc	Dis	.011	.022	6.06	7.90	17.7	6.66	1.68	47.4	.446
	Col	LD	-	LD	.004	-	.479	.181	-	-

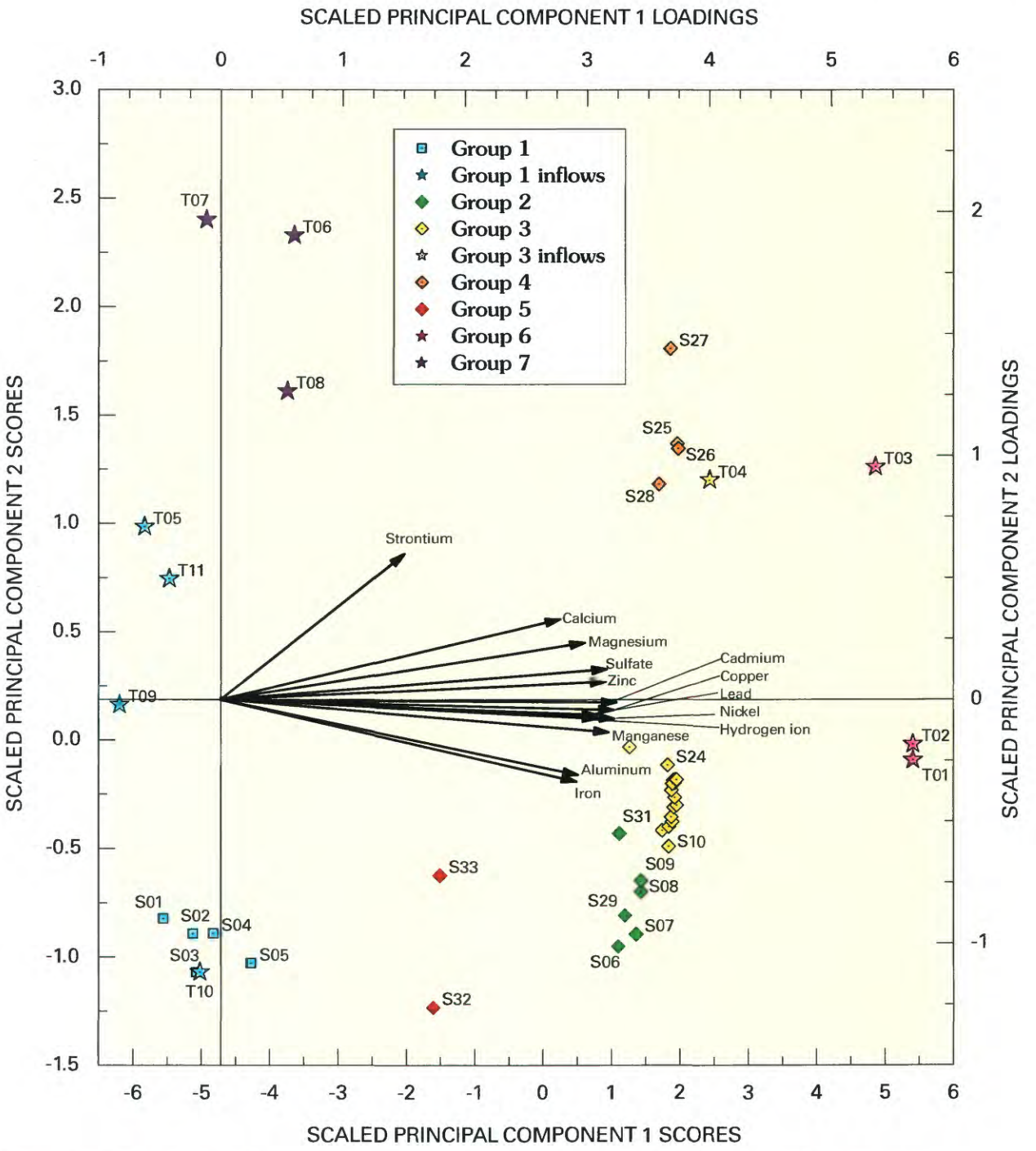

Figure 32. Biplot of principal component scores for synoptic samples and loadings for chemical constituents, Bullion Mine tributary, September 1998.

Load Profiles

Loading profiles of metals in the Bullion Mine tributary are comparable to those in Uncle Sam Gulch, mostly because of the distinct sources of metals and the chemical reactions that transformed metals downstream from neutral-pH inflows. Changes in the load for each individual stream segment are illustrated in figures 33 through 42; and a summary of load calculations is shown in table 9. There were three characteristic patterns of loading profiles among the solutes in the Bullion Mine tributary: (1) solutes that were conservative all along the study reach, (2) solutes that were conservative and then reactive transport downstream from Jack Creek, and (3) solutes that was reactive along the entire study reach.

Cadmium (fig. 33), manganese (fig. 34), zinc (fig. 35), and sulfate (fig. 36) were mostly conservative along the entire study reach. For each of these solutes, the greatest loading occurred downstream from the acidic inflows in segments S06 and S10, and for manganese and zinc additional loading occurred in segment S25 (table 9). Because this latter increase in load occurred as an increase of colloidal manganese and zinc (figs. 34*A* and 35*A*), it may have been caused by stirring up of the streambed colloids during sampling. However, a clear increase in strontium load was observed in that same stream segment (fig. 37), and strontium load would not likely increase from stirring up of the bottom. Downstream from segment S25, there was some loss of manganese load to the streambed in segment S27, and a similar small amount occurred downstream from the confluence with Jack Creek at segment S32.

Aluminum (fig. 38), copper (fig. 39), and nickel (fig. 40) loads were similar to cadmium, manganese, zinc, and sulfate except that downstream from the confluence with Jack Creek (S32), they were more reactive. Their loads changed from almost completely dissolved in the Bullion Mine tributary to almost completely colloidal in Jack Creek. This is consistent with the change in pH from less than 5.0 to greater than 6.0 that occurred as the two streams mixed (fig. 29).

Iron (fig. 41) and lead (fig. 42) were reactive along the entire study reach. Load profiles for dissolved and colloidal iron indicate the importance of the acidic inflow at T01 (fig. 41*A*). Because cadmium, copper, and iron reactions and loss to the streambed occurred on a time scale of transport within individual stream segments, their net instream load is less than the inflow load or is negative. Thus, the cumulative instream load is less than the cumulative inflow load (table 9). For example, the inflow load of iron increased 7.17 kg/day for segment S06, but instream load increased only 5.46 kg/day. The difference of 1.71 kg/day would be the amount of iron precipitation to the streambed. Travel time through the segment was less than 2 minutes, pointing out the rapid reaction of the iron precipitation and aggregation to form colloidal particles (Grundl and Delwiche, 1993; Kimball, Broshears, and others, 1994). Downstream from Jack Creek, a complete transformation of dissolved to colloidal iron occurred (fig. 41*A*); colloidal iron load increased by 0.72 kg/day and the dissolved load decreased by 0.81 kg/day; the difference was from additional loss to the streambed.

The lead profile (fig. 42) also indicated reactive transport through the study reach. Total load clearly increased at each of the acidic inflows. Some of the lead changed between dissolved and colloidal phases in response to increases in pH downstream from site S25. Downstream from Jack Creek, all the lead was removed from the water column to the streambed, sorbed to the iron colloids.

Locations of Major Loading

Similarities among the loading profiles indicate two principal locations of the metal loading along the Bullion Mine tributary. The greatest loading for all the constituents except strontium was in segment S06 (table 9). Segment S10 also received substantial loading. Inflows T01, T02, and T03, which are in segments S06 and S10, drain the Bullion mine adit, and their surface flow was traced back to the collapsed adit. From segment S15 to segment S25, metal loading was minimal. At segment S25, loads increased for several of the metals (table 9). This could be due to the narrowing of the canyon at that point (table 8), which may have forced some subsurface water into the stream channel.

Unsampled Inflow

Because the Bullion mine adit was the primary source of metals in the watershed, there was relatively little unsampled inflow in the Bullion Mine tributary (table 9). Unsampled inflow generally occurred at the same locations as the principal surface-water loadings, indicating that some of the flow from the adit had seeped into the ground but was still contributing to the load. Nickel and lead had the highest percentages of unsampled inflow (table 9).

Attenuation of Load

Downstream from the principal inflows of metals at T01, T02, and T03, attenuation of most of the metals was relatively slight. For cadmium, manganese, zinc, sulfate, copper, nickel, and iron, the inflow load exceeded the instream load at S06, which most likely means that there was some removal of these solutes that is not accounted for in the calculation of attenuation in table 9. At the low pH of Bullion Mine tributary, the removal of sulfate with iron could indicate the formation of schwertmannite as the streambed precipitate (Bigham and Nordstrom, 2000).

Colloidal iron was lost from the water column during transport downstream (fig. 41). The loss most likely involves a sequence of aggregation in the water column and then entrapment by biofilm on the streambed cobbles (Besser and others, 2001). Packman and others (2000) have proposed that colloids can be strained from the water column by the streambed as hyporheic exchange of water takes place during transport.

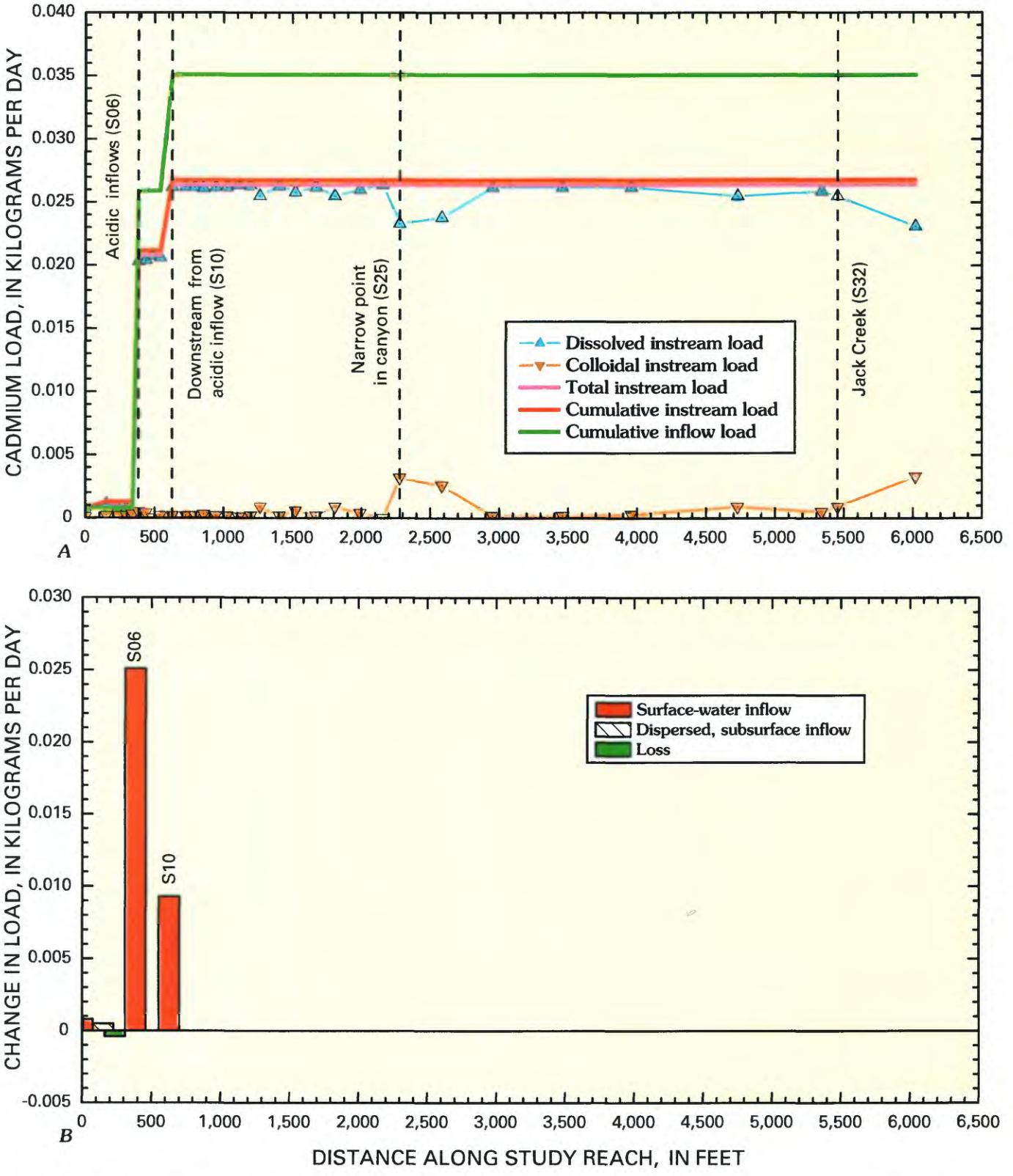

Figure 33. Variation of *A*, cadmium load with distance, and *B*, changes in load for individual stream segments, Bullion Mine tributary, September 1998.

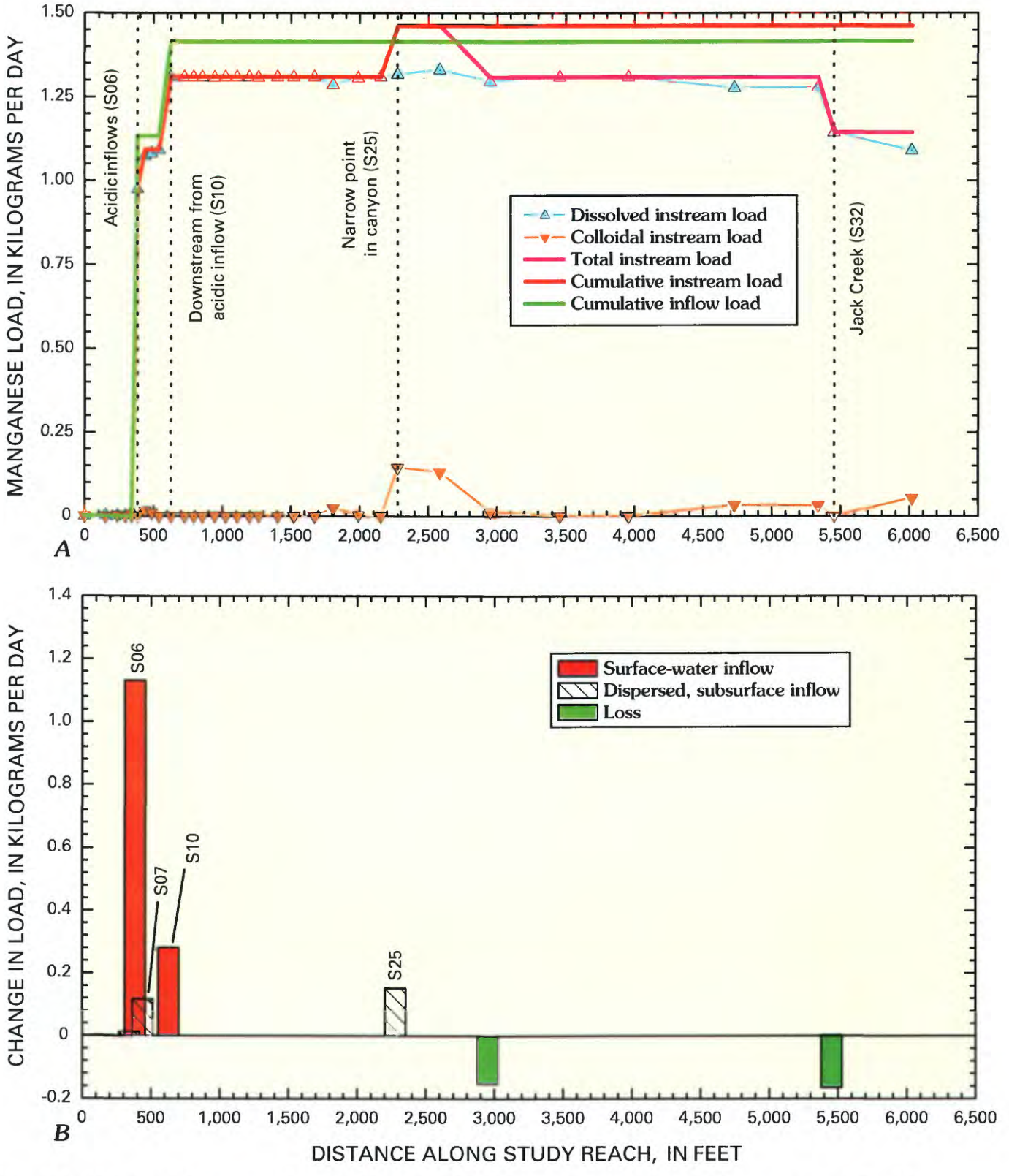

Figure 34. Variation of *A*, manganese load with distance, and *B*, changes in load for individual stream segments, Bullion Mine tributary, September 1998.

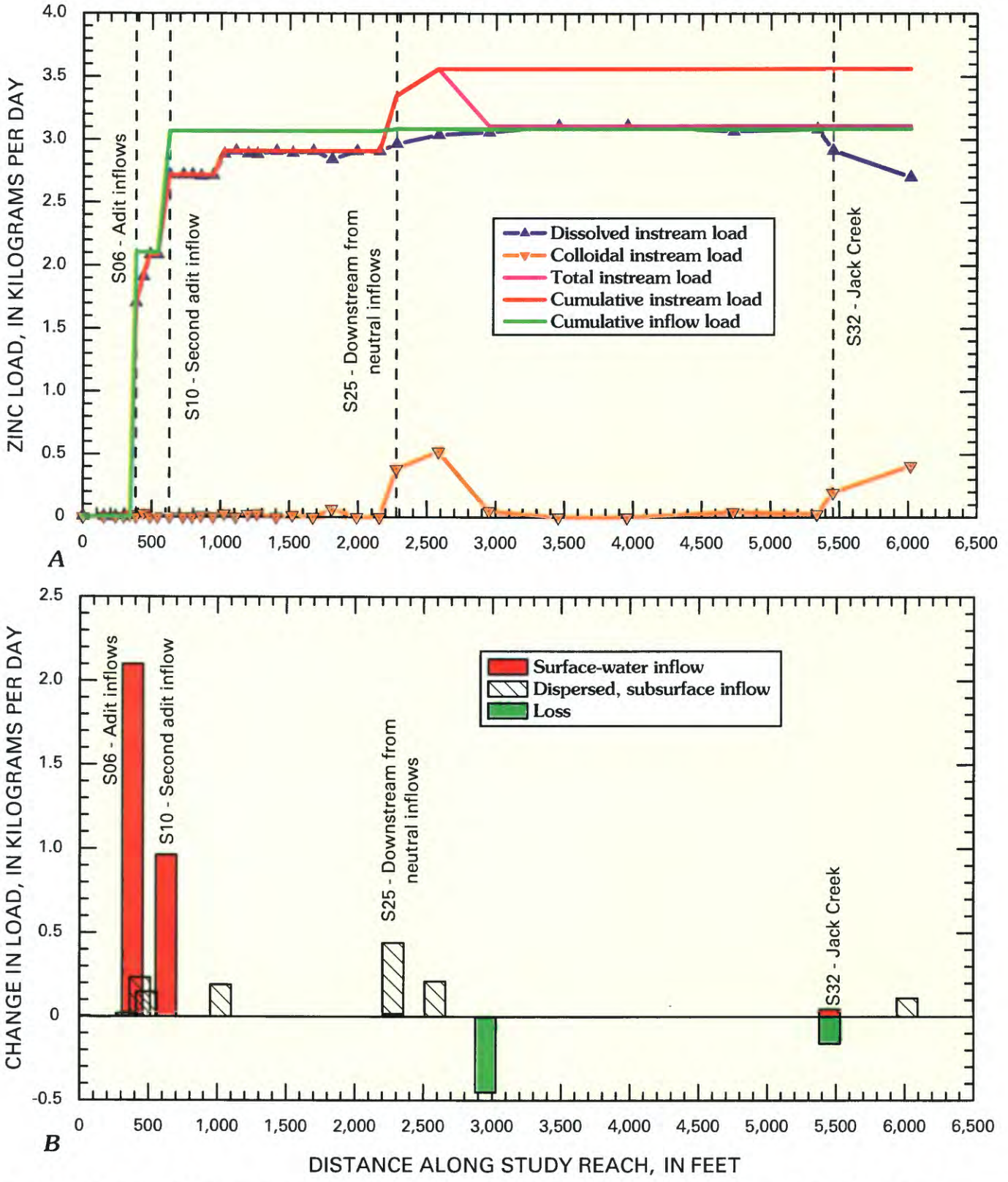

Figure 35. Variation of *A*, zinc load with distance, and *B*, changes in load for individual stream segments, Bullion Mine tributary, September 1998.

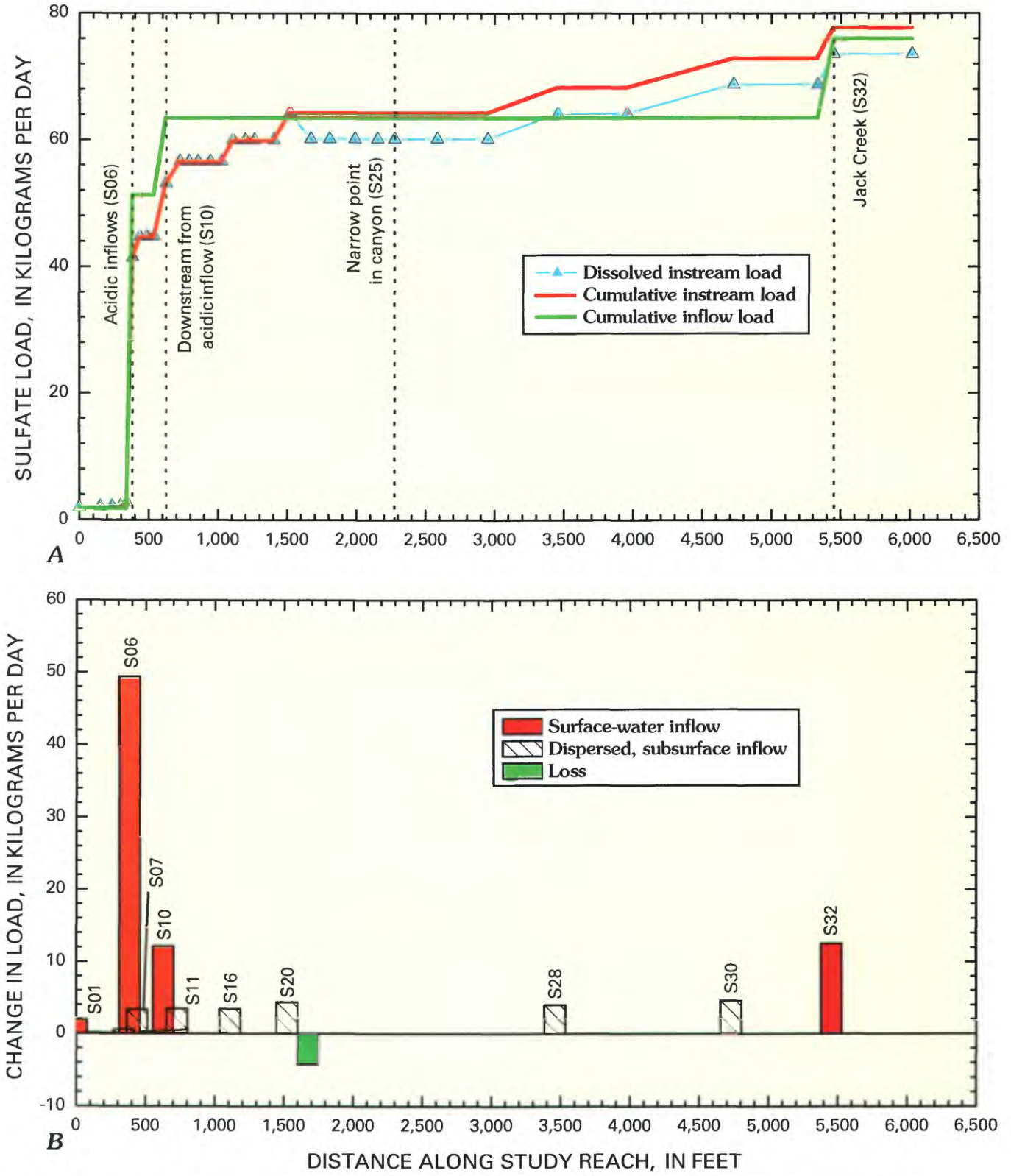

Figure 36. Variation of *A*, sulfate load with distance, and *B*, changes in load for individual stream segments, Bullion Mine tributary, September 1998.

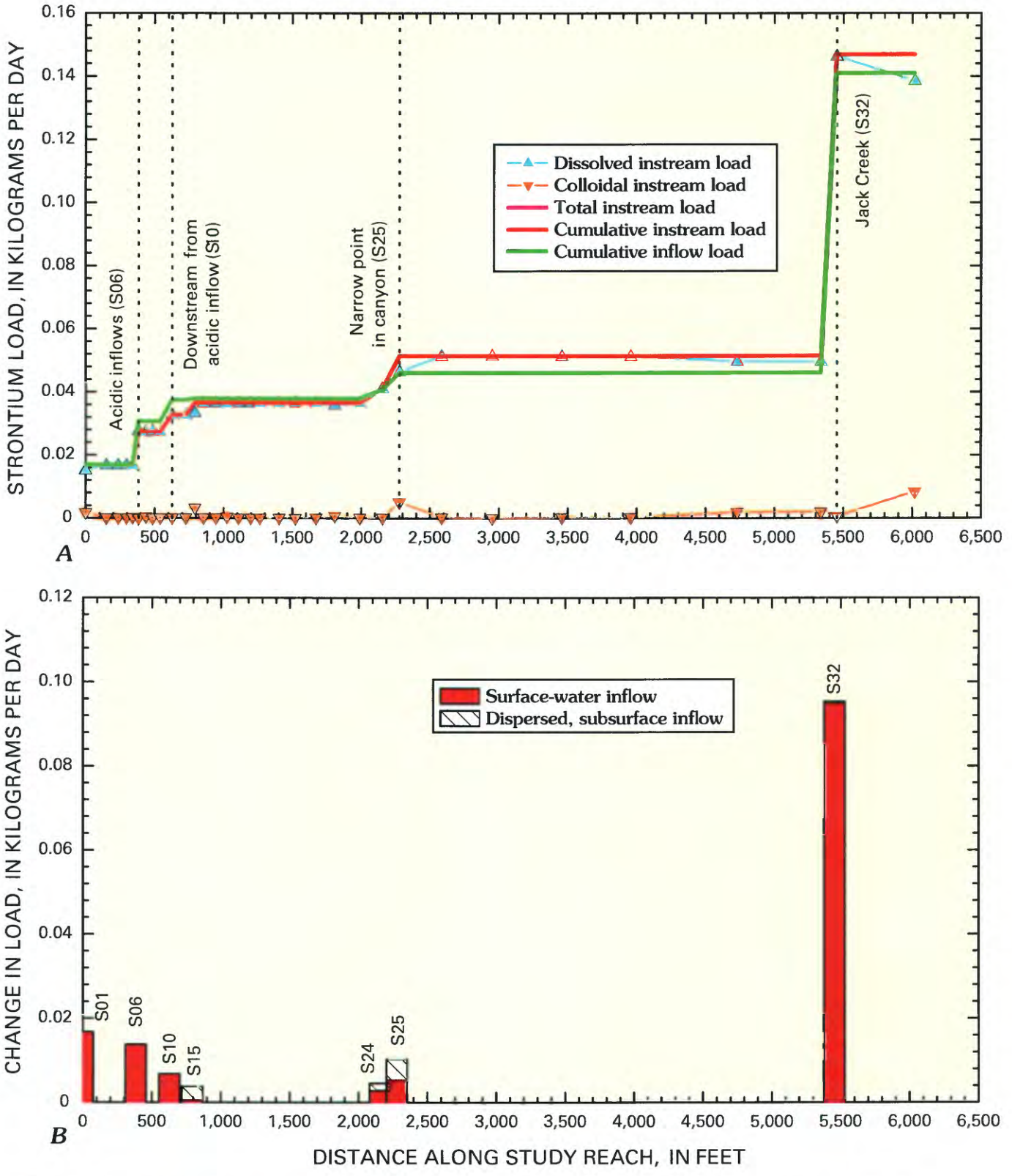

Figure 37. Variation of *A*, strontium load with distance, and *B*, changes in load for individual stream segments, Bullion Mine tributary, September 1998.

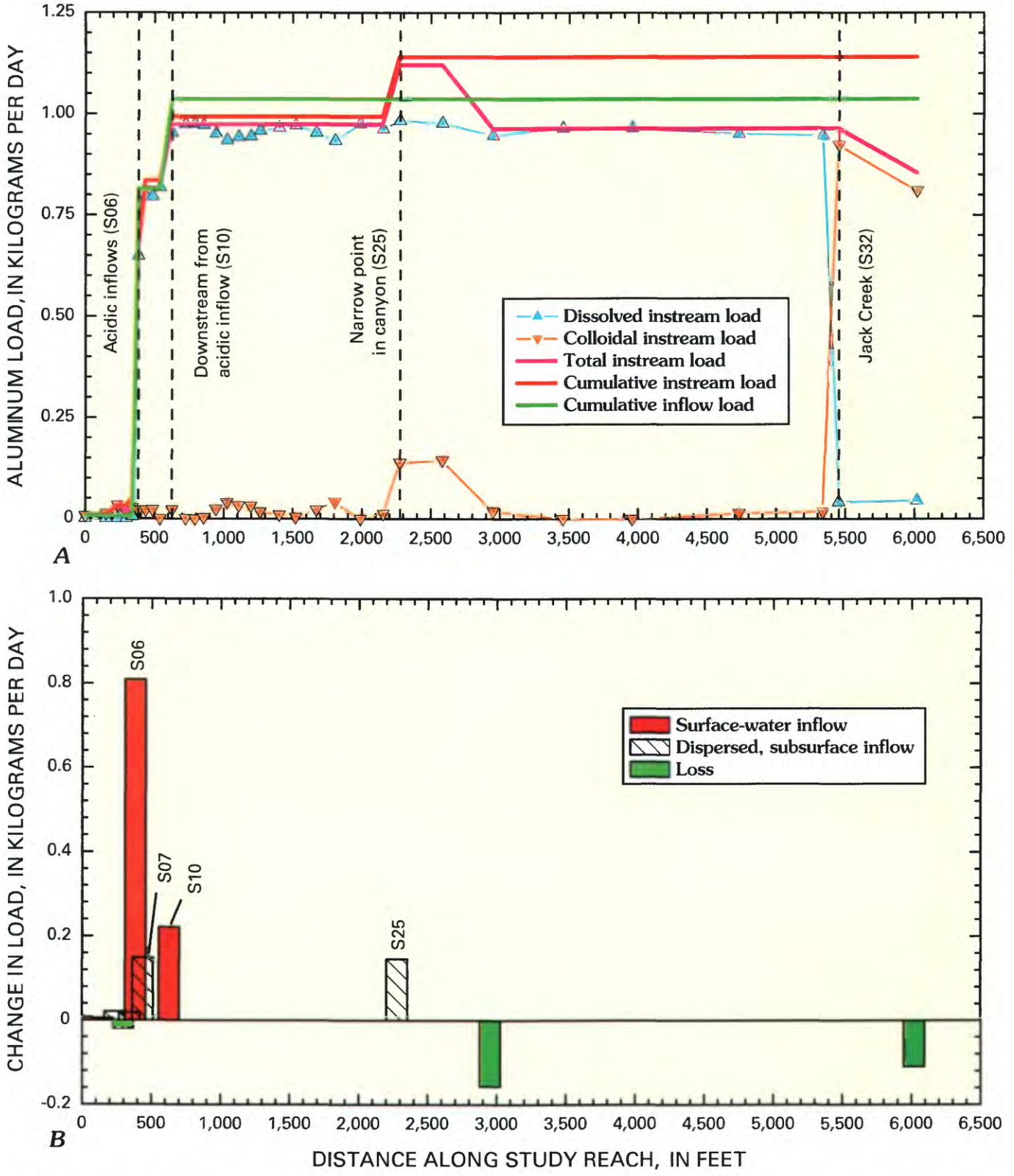

Figure 38. Variation of *A*, aluminum load with distance, and *B*, changes in load for individual stream segments, Bullion Mine tributary, September 1998.

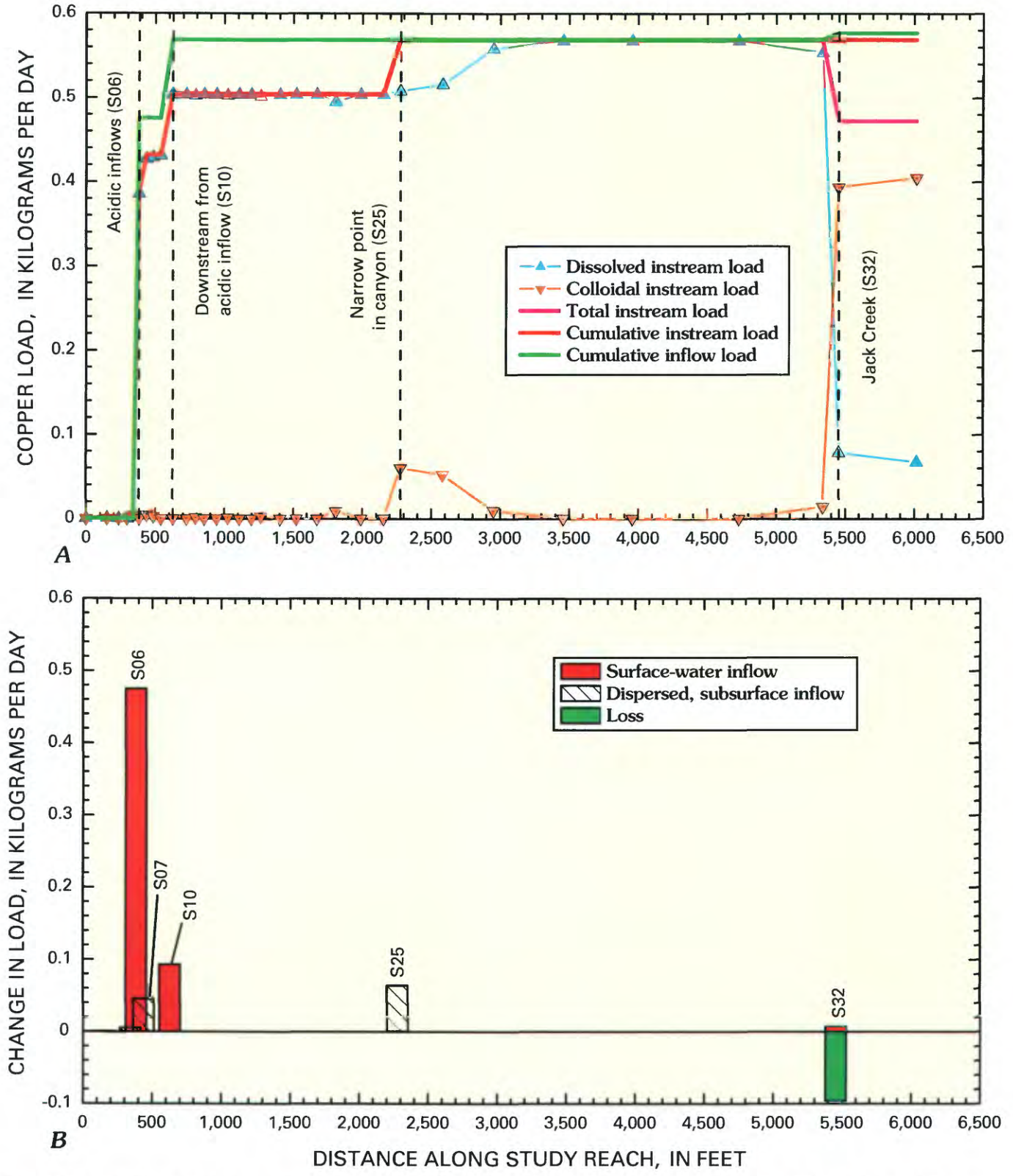

Figure 39. Variation of *A*, copper load with distance, and *B*, changes in load for individual stream segments, Bullion Mine tributary, September 1998.

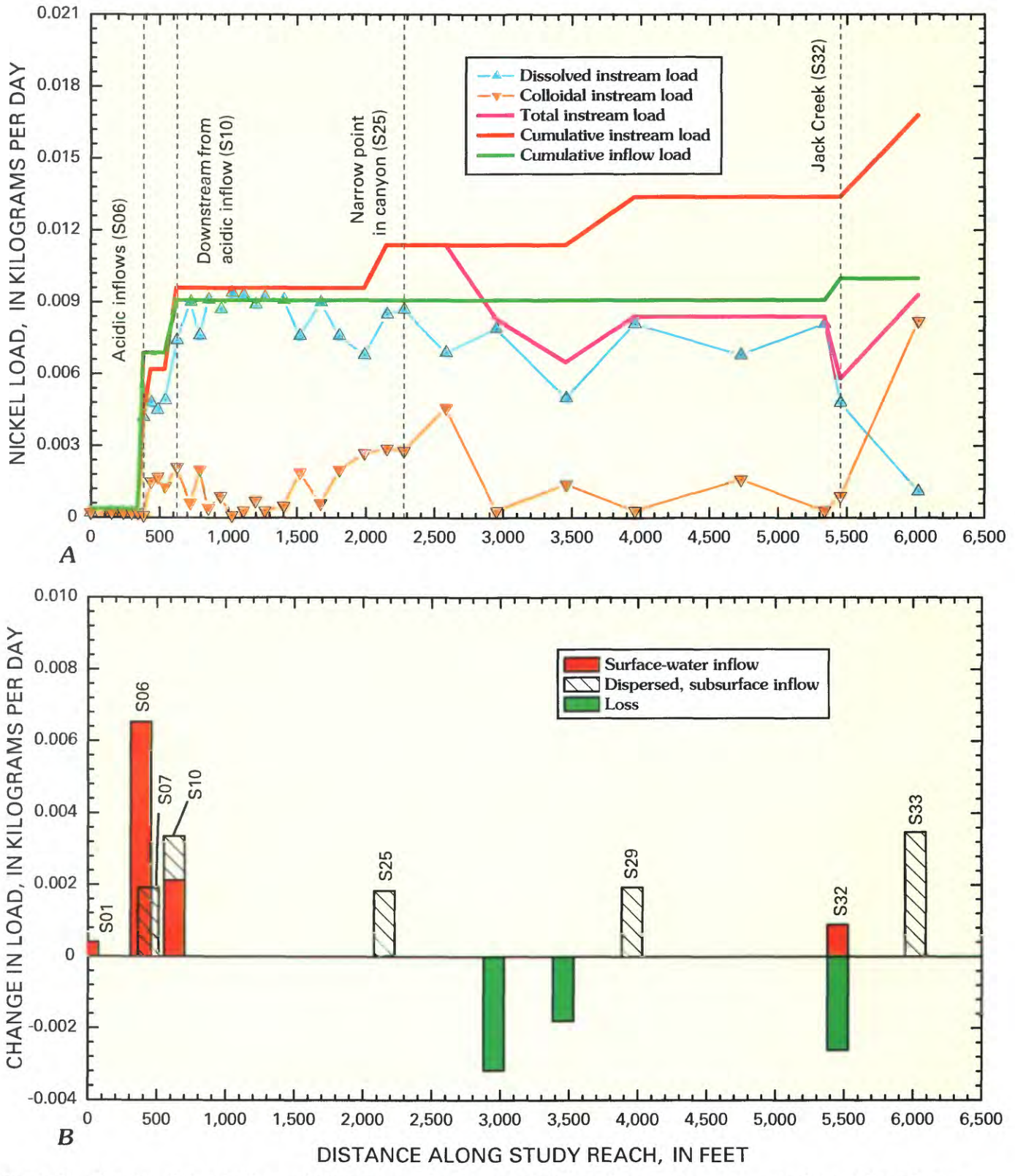

Figure 40. Variation of *A*, nickel load with distance, and *B*, changes in load for individual stream segments, Bullion Mine tributary, September 1998.

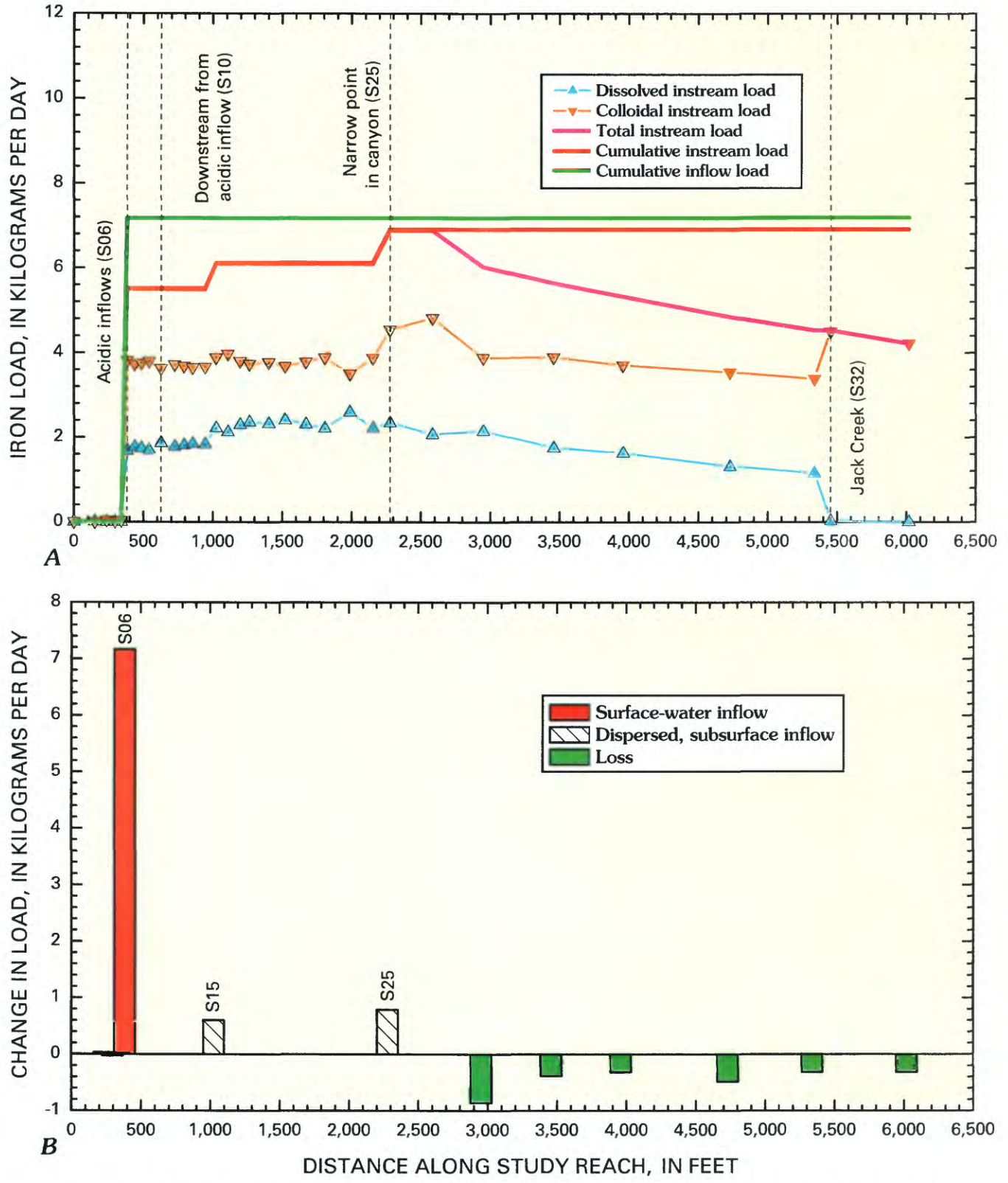

Figure 41. Variation of *A*, iron load with distance, and *B*, changes in load for individual stream segments, Bullion Mine tributary, September 1998.

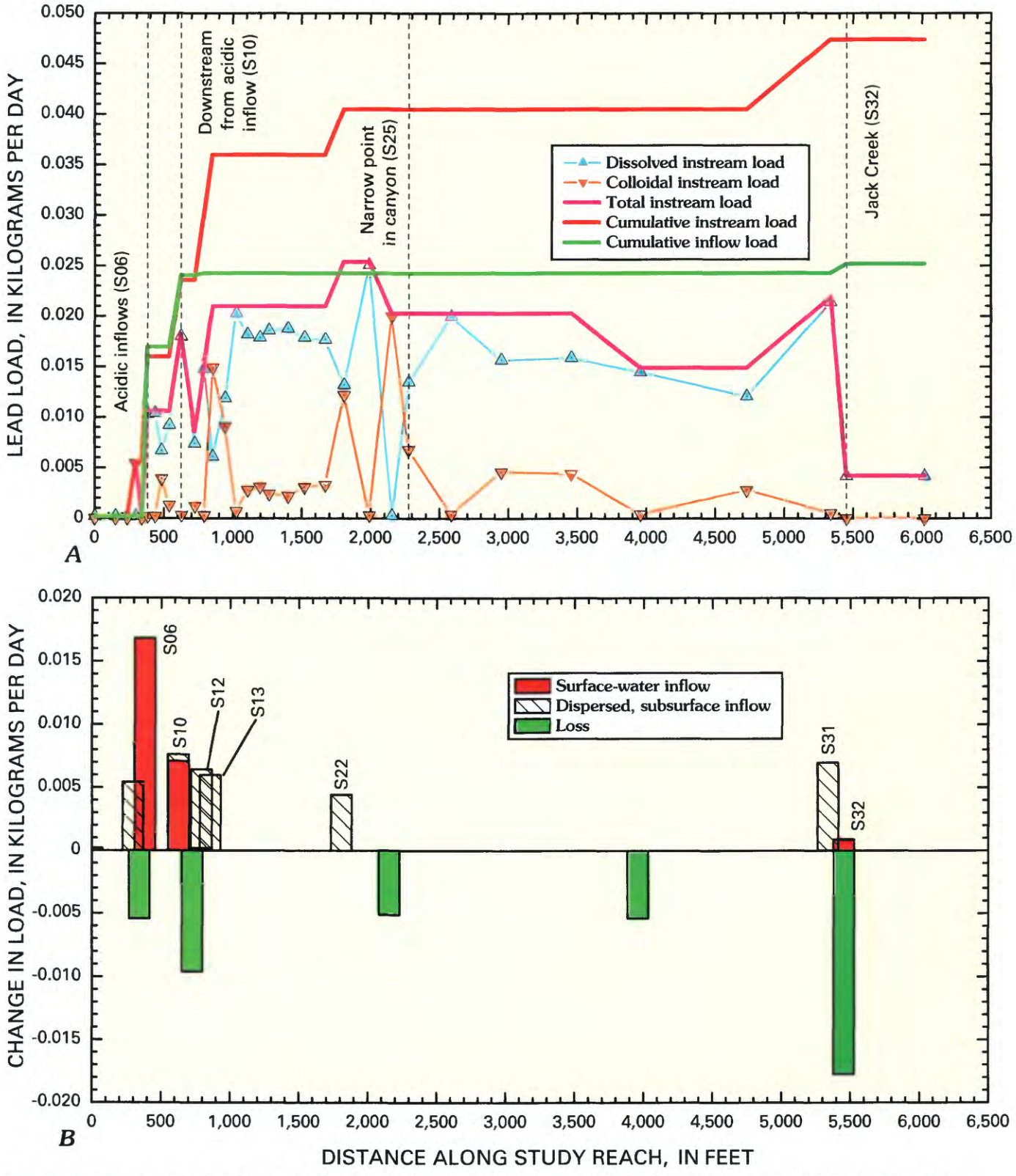

Figure 42. Variation of *A*, lead load with distance, and *B*, changes in load for individual stream segments, Bullion Mine tributary, September 1998.

Table 9. Change in load for individual stream segments and summary of load calculations for selected solutes, Bullion Mine tributary, September 1998.

[Distance, in feet along the study reach; Al, aluminum; Cu, copper; Fe, iron; Mn, manganese; Ni, nickel; Pb, lead; Sr, strontium; Zn, zinc; SO_4, sulfate; cumulative instream load, cumulative inflow load, unsampled load, and attenuation in kilograms per day; numbers in red with parentheses indicate a loss of load; cell color indicates the segments with the greatest load: red, largest load; orange, second largest; yellow, third; green, fourth; blue, fifth]

Segment number	Distance	Al	Cd	Cu	Fe	Mn	Ni	Pb	Sr	Zn	SO_4
S01	0	0.007	0.001	0.000	0.006	0.001	0.000	0.000	0.017	0.005	1.92
S02	150	.005	.000	.001	.006	.002				(.002)	.126
S03	235	.021	(.000)	(.001)	.032					(.000)	.112
S04	296	(.019)			(.026)	(.001)		.005		.001	
S05	341	.019		.005	.020	.013		(.005)		.024	.573
S06	383	.637	.020	.380	5.46	.961	.004	.010	.011	1.68	38.7
S07	437	.149		.045		.117	.002			.233	3.33
S08	485									.148	
S09	540										
S10	627	.158	.006	.073		.218	.003	.008	.005	.634	8.38
S11	726							(.010)			3.44
S12	793							.006	.004		
S13	856							.006			
S14	945										
S15	1,025				.603					.191	
S16	1,109										3.41
S17	1,197										
S18	1,264										
S19	1,404										
S20	1,522										4.37
S21	1,672										(4.24)
S22	1,808							.004			
S23	1,990										
S24	2,155						.002	(.005)	.005		
S25	2,278	.147		.064	.789	.152			.010	.441	
S26	2,585									.211	
S27	2,951	(.157)			(.859)	(.152)	(.003)			(.451)	
S28	3,457				(.383)		(.002)				4.00
S29	3,958				(.316)		.002	(.005)			
S30	4,729				(.482)						4.61
S31	5,338				(.315)			0.007			
S32	5,454			(.096)		(.165)	(.003)	(.018)	.095		4.81
S33	6,019	(.109)			(.313)		.003				
Cumulative instream load		1.14	.027	.569	6.92	1.46	.017	.047	.147	3.56	77.8
Cumulative inflow load		1.04	.035	.577	7.19	1.42	.010	.025	.141	3.08	76.0
Percent inflow load		91	131	101	104	97	59	53	96	87	98
Unsampled inflow		.105	(.008)	(.008)	(.270)	.047	.007	.022	.006	.480	1.80
Percent unsampled load		9.2	(31)	(1.4)	(3.9)	3.2	41	47	4.0	13	2.3
Attenuation		.286	.000	.096	2.69	.318	.008	.043	.000	.454	4.24
Percent attenuation		25	1.4	17	39	22	45	91	.0	13	5

Downstream from the inflow of Jack Creek, substantial attenuation occurred for copper, manganese, nickel, and lead (figs. 39, 34, 40, and 42). These metals most likely sorbed to iron and aluminum colloids. As the colloidal material was removed, the metal loads decreased. Cadmium, zinc, aluminum, and iron (figs. 33, 35, 38, and 41) were transformed from dissolved to colloidal phases but were not substantially removed from the water column; their total-recoverable concentrations remained nearly constant.

Discussion

On the basis of the three tracer-injection studies, we can make some generalizations about sources of metals within the Boulder River watershed and discuss the major processes that affect the metal transport. Because copper and zinc adversely affect the aquatic life, this discussion will focus on those two metals.

Sources of Metals

Surface-water inflows were the principal source of the copper and zinc loads. Unsampled inflow of copper was 23 percent of the total cumulative load in Cataract Creek, but only 8 percent in Uncle Sam Gulch, and less than detection in the Bullion Mine tributary (tables 3, 6, and 9). Unsampled inflow of copper in Cataract Creek occurred only in the last large stream segment between Big Limber Creek and the mouth (fig. 10*B*). Because access for sampling was not given, we do not know if a source in that segment could have been sampled. Unsampled inflow for zinc load ranged from 12 to 26 percent in the three study reaches, indicating that most of the zinc loads also were surface-water inflows.

This surface-water inflow is dominated by drainage from the Crystal and Bullion mine adits in both Basin and Cataract Creeks at low flow (tables 3, 6, and 9). Nimick and Cleasby (this volume) had a similar conclusion, based on more widespread watershed sampling. Other sources of metals in these watersheds are minimal in comparison to these adit drainages. The tracer-injection studies were conducted at different times and under slightly different conditions, but they provide a picture of loading during base-flow conditions that can be compared among the streams. Loading of copper and zinc from the Bullion Mine adit was 0.50 and 2.69 kg/day, respectively. By comparison, loading from the Crystal Mine adit was 3.05 and 13.9 kg/day for copper and zinc; or about five times greater. Loadings of copper and zinc reaching the Boulder River from Cataract Creek are greater than loads from Basin Creek (Nimick and Cleasby, this volume), which is consistent with these differences in loading.

Processes Affecting Metals

Metal attenuation, particularly in Uncle Sam Gulch and the Bullion Mine tributary, resulted from inflows of near-neutral pH water downstream from the principal metal sources. Those elements that are more reactive in the streams, principally aluminum, copper, iron, and lead, were lost to the streambed in Uncle Sam Gulch. Although they were not lost to the same extent in the study reach of the Bullion Mine tributary, they were affected by attenuation downstream from the confluence with Jack Creek. Attenuation may continue in Basin Creek (Nimick and Cleasby, this volume). A substantial amount of the manganese and zinc that entered the streams from both mine adits was transported all the way to the Boulder River and likely affects aquatic health there.

Metals that are lost to the streambed can be flushed downstream during periods of snowmelt runoff or storms (Church and others, 1997). Thus, attenuation of the metals does not mean that the metals are no longer a concern for aquatic health. As part of the streambed material, these metals can enter food pathways to aquatic organisms (Farag and others, this volume, Chapter D10). This has also been documented in other streams affected by mine drainage (Clements, 1994; Besser and others, 2001).

Implications

Loading profiles that have been documented from the tracer-injection studies have important implications for possible remediation. When metal loading in a watershed is dominated by several discrete sources, and those sources contribute a high percentage of the total loads, the most effective approach to remediation would obviously be to focus on those identified sources. Remediation efforts of the many smaller sources of metals would have only limited impact on stream recovery. The lack of regional alteration that can produce widespread metal loading also simplifies remediation options.

Summary

Tracer-injection and synoptic sampling methods were used to quantify the locations and magnitude of loading to selected reaches of three streams in the Boulder River watershed study area in Montana. Tracer studies helped identify the location of major sources of metal loading to the streams, the extent of loading from subsurface sources, and the extent of attenuation downstream from the sources. Along the 40,905-ft study reach of Cataract Creek, 21.2 kg/day of zinc were added to the stream. About 75 percent of this load came from Uncle Sam Gulch, a principal tributary. The major source of metal loading to Uncle Sam Gulch was the Crystal mine adit discharge. The Bullion Mine adit discharge was the principal source to the Bullion Mine tributary of Jack Creek. Other sources were small in comparison to these two. The adit

discharge from the Bullion mine accounted for 2.8 kg/day of zinc, which was only about 20 percent of the zinc load coming from the Crystal mine adit in Uncle Sam Gulch. Both adit discharges drain the same mineral deposit and contribute acidic, metal-rich water to the receiving streams. Most of the loading was from identifiable surface inflows, but part of the total load of each metal was contributed by subsurface inflow. During transport in Uncle Sam Gulch and the Bullion Mine tributary, much of the iron and aluminum was transformed from dissolved to colloidal phases downstream from the inflows of neutral-pH tributaries. This colloidal material affects the transport of other metals that sorb to the colloids. Deposition of this material on the streambeds provides a route for metals to enter the food web and create a condition of chronic toxicity for fish downstream. These two mine-adit sources likely have the most impact on the aquatic health of the Boulder River watershed.

References Cited

Baes, C.F., Jr., and Mesmer, R.E., 1976, The hydrolysis of cations: New York, John Wiley, 489 p.

Bencala, K.E., and McKnight, D.M., 1987, Identifying in-stream variability—Sampling iron in an acidic stream, *in* Averett, R.C., and McKnight, D.M., eds., Chemical quality of water and the hydrologic cycle: Chelsea, Mich., Lewis Publishers, Inc., p. 255–269.

Bencala, K.E., McKnight, D.M., and Zellweger, G.W., 1990, Characterization of transport in an acidic and metal-rich mountain stream based on a lithium tracer injection and simulations of transient storage: Water Resources Research, v. 26, p. 989–1000.

Besser, J.M., Brumbaugh, W.G., May, T.W., Church, S.E., and Kimball, B.A., 2001, Bioavailability of metals in stream food webs and hazards to brook trout (*Salvelinus fontinalis*) in the Upper Animas River watershed, Colorado: Archive of Environmental Contamination and Toxicology, v. 40, p. 48–59.

Besser, J.M., and Leib, K.J., 1999, Modeling frequency of occurrence of toxic concentrations of zinc and copper in the Upper Animas River, *in* Morganwalp, D.W., and Buxton, H.T., eds., U.S. Geological Survey Toxic Substances Hydrology Program—Proceedings of the Technical Meeting, Charleston, S.C., March 8–12, 1999, Volume 1, Contamination from hardrock mining: U.S. Geological Survey Water-Resources Investigations Report 99–4018A, p. 75–81.

Bigham, J.M., and Nordstrom, D.K., 2000, Iron and aluminum hydroxysulfates from acid sulfate waters, *in* Alpers, C.N., Jambor, J.L., and Nordstrom, D.K., eds., Sulfate minerals—Crystallography, geochemistry, and environmental significance: Mineralogical Society of America, Reviews in Mineralogy and Geochemistry, v. 40, p. 351–403.

Broshears, R.E., Bencala, K.E., Kimball, B.A., and McKnight, D.M., 1993, Tracer-dilution experiments and solute-transport simulations for a mountain stream, Saint Kevin Gulch, Colorado: U.S. Geological Survey Water-Resources Investigations Report 92–4081, 18 p.

Church, S.E., Kimball, B.A., Fey, D.L., Ferderer, D.A., Yager, T.J., and Vaughn, R.B., 1997, Source, transport, and partitioning of metals between water, colloids, and bed sediments of the Animas River, Colorado: U.S. Geological Survey Open-File Report 97–151, 135 p.

Cleasby, T.E., Nimick, D.A., and Kimball, B.A., 2000, Quantification of metal loads by tracer-injection and synoptic sampling methods in Cataract Creek, Jefferson County, Montana, August 1997: U.S. Geological Survey Water-Resources Investigations Report 00–4237, 39 p.

Clements, W.H., 1994, Benthic invertebrate community responses to heavy metals in the Upper Arkansas River basin, Colorado: Journal of the North American Benthological Society, v. 13, no. 1, p. 30–44.

Davis, J.C., 1986, Statistics and data analysis in geology, Second Edition: New York, John Wiley, 646 p.

Daultrey, S., 1976, Principal components analysis: Concepts and Techniques in Modern Geography 8, Institute of British Geographers, 50 p.

Desborough, G.A., Leinz, R.W., Sutley, S.J., Briggs, P.H., Swayze, G.A., Smith, K.S., and Breit, George, 2000, Leaching studies of schwertmannite-rich precipitates from the Animas River headwaters, Colorado, and Boulder River headwaters, Montana: U.S. Geological Survey Open-File Report 00–004, 16 p.

Fey, D.L., Church, S.E., and Finney, C.A., 2000, Analytical results for Bullion Mine and Crystal mine waste samples and bed sediments from a small tributary to Jack Creek and from Uncle Sam Gulch, Boulder River watershed, Montana: U.S. Geological Survey Open-File Report 00–031, 63 p.

Fulghum, J.E., Bryan, S.R., Linton, R.W., Bauer, C.F., and Griffis, D.P., 1988, Discrimination between adsorption and coprecipitation in aquatic particle standards by surface analysis techniques—Lead distributions in calcium carbonates: Environmental Science & Technology, v. 22, p. 463–467.

Grundl, T., and Delwiche, J., 1993, Kinetics of ferric oxyhydroxide precipitation: Journal of Contaminant Hydrology, v. 14, p. 71–97.

Grundy, W.D., and Miesch, A.T., 1987, Brief descriptions of STATPAC and related statistical programs for the IBM personal computer—Documentation: U.S. Geological Survey Open-File Report 87–411–A, 34 p.

Jarrett, R.D., 1992, Hydraulics of mountain rivers, *in* Yen, B.C., ed., Channel flow resistance centennial of Manning's formula: International Conference of the Centennial of Manning's and Kuichling's Rational Formula, Littleton, Colo., Water Resources Publications, p. 287–298.

Kilpatrick, F.A., and Cobb, E.D., 1985, Measurement of discharge using tracers: U.S. Geological Survey Techniques of Water-Resources Investigations, book 3, chapter A16.

Kimball, B.A., 1997, Use of tracer injections and synoptic sampling to measure metal loading from acid mine drainage: U.S. Geological Survey Fact Sheet FS–245–96.

Kimball, B.A., Bencala, K.E., and Broshears, R.E., 1994, Geochemical processes in the context of hydrologic transport—Reactions of metals in St. Kevin Gulch, Colorado, *in* Dutton, A., ed., Toxic substances in the hydrologic sciences: Minneapolis, Minn., American Institute of Hydrology, p. 80–94.

Kimball, B.A., Broshears, R.E., Bencala, K.E., and McKnight, D.M., 1994, Coupling of hydrologic transport and chemical reactions in a stream affected by acid mine drainage: Environmental Science & Technology, v. 28, p. 2065–2073.

Kimball, B.A., Callender, Edward, and Axtmann, E.V., 1995, Effects of colloids on metal transport in a river receiving acid mine drainage, Upper Arkansas River, Colorado, U.S.A.: Applied Geochemistry, v. 10, p. 285–306.

Kimball, B.A., McKnight, D.M., Wetherbee, G.A., and Harnish, R.A., 1992, Mechanisms of iron photoreduction in a metal-rich, acidic stream, St. Kevin Gulch, Colorado, U.S.A.: Chemical Geology, v. 96, p. 227–239.

Kimball, B.A., Nimick, D.A., Gerner, L.J., and Runkel, R.L., 1999, Quantification of metal loading in Fisher Creek by tracer injection and synoptic sampling, Park County, Montana, August 1997: U.S. Geological Survey Water-Resources Investigations Report 99–4119, 40 p.

Kimball, B.A., Runkel, R.L., and Gerner, L.J., 2001, Quantification of mine-drainage inflows to Little Cottonwood Creek, Utah, using a tracer-injection and synoptic-sampling study: Environmental Geology, v. 40, p. 1390–1404.

Kimball, B.A., Runkel, R.L., Walton-Day, K., and Bencala, K.E., 2002, Assessment of metal loads in watersheds affected by acid mine drainage by using tracer injection and synoptic sampling—Cement Creek, Colorado, U.S.A.: Applied Geochemistry, v. 17, p. 1183–1207.

Lichte, F.E., Golightly, D.W., and Lamothe, P.J., 1987, Inductively coupled plasma–atomic emission spectrometry, Chapter B *in* Baedecker, P.A., ed., Methods for geochemical analysis: U.S. Geological Survey Bulletin 1770, p. B1–B10.

Metesh, J.J., Lonn, J.D., Duaime, T.E., and Wintergerst, Robert, 1994, Abandoned-inactive mines program, Deerlodge National Forest—Volume I, Basin Creek drainage: Montana Bureau of Mines and Geology Open-File Report 321, 131 p.

Nordstrom, D.K., and Ball, J.W., 1986, The geochemical behavior of aluminum in acidified surface waters: Science, v. 232, p. 54–56.

Packman, A.I., Brooks, N.H., and Morgan, J.J., 2000, A physicochemical model for colloid exchange between a stream and a sand streambed with bed forms: Water Resources Research, v. 36, no. 8, p. 2351–2361.

Rantz, S.E., and others, 1982, Measurement and computation of streamflow—Volume 1, Measurement of stage and discharge: U.S. Geological Survey Water-Supply Paper 2175, 2 vols., 631 p.

Runkel, R.L., Kimball, B.A., McKnight, D.M., and Bencala, K.E., 1999, Reactive solute transport in streams—A surface complexation approach for trace metal sorption: Water Resources Research, v. 35, no. 12, p. 3829–3840.

Smith, K.S., 1999, Metal sorption on mineral surfaces—An overview with examples relating to mineral deposits, *in* Plumlee, G.S., and Logsdon, M.J., eds., The environmental geochemistry of mineral deposits—Part A, Processes, techniques, and health issues: Littleton, Colo., Society of Economic Geologists, Reviews in Economic Geology, v. 6A, p. 161–162.

Ward, J.R., and Harr, C.A., 1990, Methods for collection and processing of surface-water and bed-material samples for physical and chemical analyses: U.S. Geological Survey Open-File Report 90–140, 71 p.

Webster, J.G., Swedlund, P.J., and Webster, K.S., 1998, Trace metal adsorption onto an acid mine drainage iron (III) oxy hydroxy sulfate: Environmental Science & Technology, v. 32, no. 10, p. 1361–1368.

Zellweger, G.W., 1994, Testing and comparison of four ionic tracers to measure stream flow loss by multiple tracer injection: Hydrological Processes, v. 8, p. 155–165.

Zellweger, G.W., Avanzino, R.J., and Bencala, K.E., 1989, Comparison of tracer-dilution and current-meter discharge measurements in a small gravel-bed stream, Little Lost Man Creek, California: U.S. Geological Survey Water-Resources Investigations Report 89-4150, 20 p.

Short-Term Variation of Trace-Element Concentrations during Base Flow and Rainfall Runoff in Small Basins, August 1999

By John H. Lambing, David A. Nimick, and Thomas E. Cleasby

Chapter D7 of
Integrated Investigations of Environmental Effects of Historical Mining in the Basin and Boulder Mining Districts, Boulder River Watershed, Jefferson County, Montana
Edited by David A. Nimick, Stanley E. Church, and Susan E. Finger

Professional Paper 1652–D7

U.S. Department of the Interior
U.S. Geological Survey

Contents

Figures

CONVERSION FACTORS, VERTICAL DATUM, ABBREVIATED UNITS

Multiply	By	To obtain
cubic foot per second (ft^3/s)	0.028317	cubic meter per second

Temperature can be converted to degrees Celsius (°C) or degrees Fahrenheit (°F) by the following equations:

$°C = 5/9 (°F - 32)$

$°F = 9/5 °C + 32$

Sea level: In this report, "sea level" refers to the National Geodetic Vertical Datum of 1929 (NGVD of 1929)—a geodetic datum derived from a general adjustment of the first-order level nets of both the United States and Canada, formerly called Sea Level Datum of 1929.

µg/L	microgram per liter
µg/L/hour	microgram per liter per hour
µm	micrometer
µS/cm	microsiemens per centimeter at 25 degrees Celsius
mg/L	milligram per liter

Chapter D7
Short-Term Variation of Trace-Element Concentrations during Base Flow and Rainfall Runoff in Small Basins, August 1999

By John H. Lambing, David A. Nimick, and Thomas E. Cleasby

Abstract

Water-quality data for the Boulder River watershed of southwest Montana indicated that dissolved zinc concentrations vary cyclically throughout the day during base flow. To provide insight into the pattern and magnitude of trace-element concentration changes during a 24-hour (diel) cycle, water samples were collected hourly in three small tributary basins of the Boulder River watershed that drain abandoned mine lands. Hourly zinc variations were examined at five sites in High Ore, Jack, and Cataract Creeks; arsenic, copper, and manganese also were analyzed at the High Ore Creek site. Dissolved zinc concentrations in High Ore Creek varied by about 400 µg/L (micrograms per liter) during a 24-hour cycle, representing about a three-fold change in concentration. Another type of short-term variation in zinc concentrations was documented when rainstorms produced runoff over mine wastes during the sampling of base flow at four sites. Within 1 to 5 hours following the onset of intense rain, dissolved zinc concentrations increased rapidly at all four sites, ranging from a 670 µg/L increase in Cataract Creek below Uncle Sam Gulch to a 6,200 µg/L increase in a tributary below the Bullion mine. Short-term variations of trace-element concentrations caused by either diel cycles or rainfall runoff can potentially affect interpretation of trace-element sources, long-term trends, and biological risk.

Introduction

Periodic sampling conducted during 1997–99 to describe water-quality conditions on a watershed scale (Nimick and Cleasby, this volume, Chapter D5) provided insufficient data to characterize two important phenomena: diel (24-hour) variation in trace-element concentrations during base flow and changes induced by short-duration rainstorm events. Diel cycles have been noted in other streams affected by metals (McKnight and others, 1988; Brick and Moore, 1996; Nimick and Cleasby, 2001) and arsenic (Fuller and Davis, 1989) derived from mine wastes, as well as naturally occurring arsenic (Nimick and others, 1998). The specific mechanism causing diel concentration changes is not known, but the effect likely results from a combination of geochemical, biological, and physical processes that affect the partitioning of trace elements between the dissolved and solid phases. Such processes that occur regularly during the course of a 24-hour cycle could produce systematic temporal patterns in trace-element concentrations, thereby causing analytical results to vary depending on the time of day that samples are collected. Water-quality data collected for Cataract Creek (Cleasby and others, 2000) and High Ore Creek (Nimick and Cleasby, 2000) indicated that relatively large variations of dissolved zinc concentrations were occurring at different times of the day during base flow. This phenomenon warranted further investigation because diel concentration changes might affect synoptic load calculations and subsequent interpretation of trace-element sources, detection of long-term trends, and reliable evaluations of the effectiveness of remediation efforts. In addition, diel cycles in concentrations of potentially toxic constituents could affect assessment of biological exposure risks.

Short-term and potentially large variations in trace-element concentrations also can be caused by rainfall runoff that flushes trace elements from mine wastes into stream channels. This type of pulse event has been documented in mining areas where waste rock or mill tailings are exposed, or where historical floods have redistributed tailings along the flood plain (Lambing, 1991; Nimick and Moore, 1991; Smith and others, 1998). Because of the inherent difficulty in sampling short-lived and localized storm events, little quantitative information exists on the duration and magnitude of elevated trace-element concentrations that can occur in response to the overland flushing of mine waste. Tailings erosion and transport, however, can be an extremely important influence in mining-impacted watersheds, as this mechanism of metal delivery to the stream is presumed to be responsible for fishkills noted in other mining areas (Lambing, 1991; U.S. Environmental Protection Agency, 1999).

Hourly sampling was conducted at five sites in three tributary basins of the Boulder River watershed during August 1999 (fig. 1) to quantify short-term variation in trace-element concentrations associated with diel cycles. Dissolved zinc was chosen as the primary trace element for analysis because it typically is present at detectable concentrations in the tributary basins, is known to display diel cycles (Brick and Moore, 1996), and can be toxic to aquatic life. Although the study was not originally designed to sample rainstorm runoff, rainstorms over two of the three basins produced runoff during sampling that provided a unique opportunity to characterize an important hydrologic condition that occurs irregularly, is short-lived, and is logistically difficult to sample.

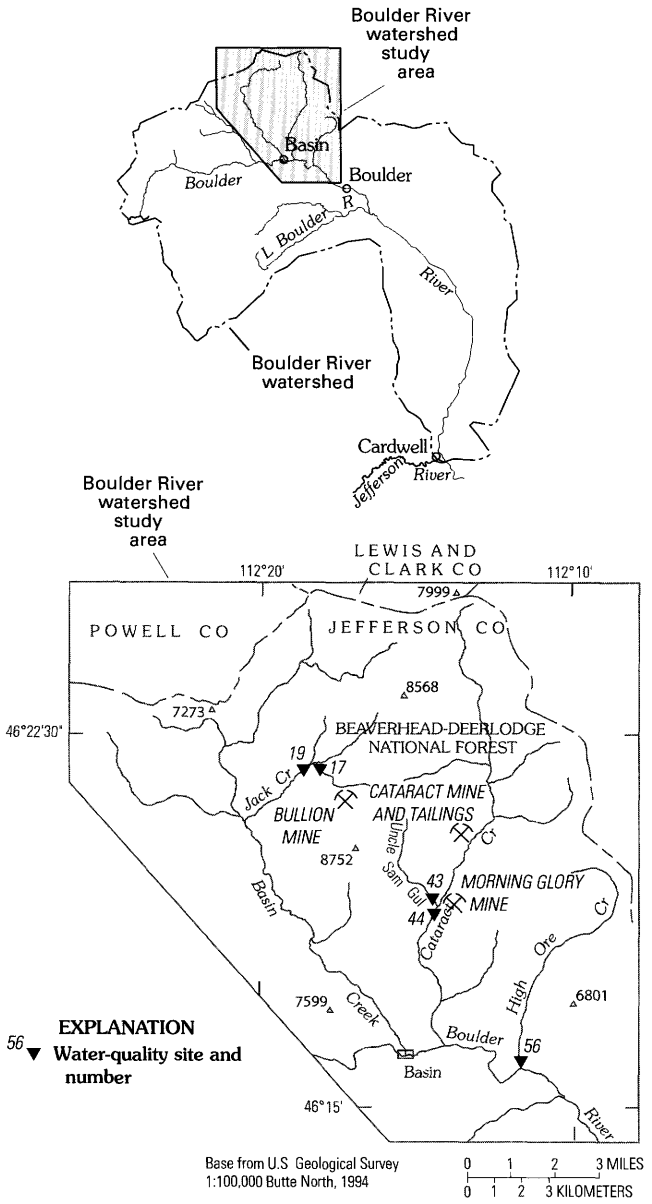

Figure 1. Location of study area and sampling sites. Site numbers are those assigned by Nimick and Cleasby (this volume). Altitude shown in feet.

Purpose and Scope

The original purpose of this investigation was to collect data on diel changes in trace-element concentrations during base flow at five sites in three small basins—Jack, Cataract, and High Ore Creeks—that drain abandoned mine lands in the Boulder River watershed study area (fig. 1). The intent was to utilize these data to define temporal patterns and quantify magnitudes of trace-element concentration changes. This information could help to resolve whether load variations determined from synoptic sampling represented source inputs or sampling artifacts. Samples were collected hourly over 1.5- to 2-day periods to document the changes in dissolved zinc concentrations during base-flow conditions. Samples from the High Ore Creek site also were analyzed for dissolved arsenic, copper, and manganese to examine if concentrations of other trace elements exhibited diel cycles. In addition, field parameters known to exhibit diel cycles in aquatic environments (streamflow, pH, dissolved oxygen, specific conductance, and water temperature) were measured hourly to identify associations with zinc concentrations that could be potentially useful for understanding the process or processes controlling diel variations.

During the collection of hourly samples in the Jack and Cataract Creek basins, localized rainstorms produced runoff that interrupted base flow. However, the hourly samples of runoff collected during and following these rainstorms provided data characterizing the variations of dissolved zinc concentrations in response to a short-duration storm. The investigation was thus effectively expanded to include an assessment of rainfall runoff over mine wastes. Consequently, this report documents short-term changes in zinc concentrations and related parameters resulting from two distinct processes.

Methods

Automated pumping samplers were used to collect water-quality samples at hourly intervals at each site. The intake of each sampler was placed in a riffle near midstream where the stream was well mixed. Samples were processed within 4 hours of collection according to procedures described by Wilde and others (1998). Samples were filtered through a 0.1-μm (micrometer) plate filter and acidified using ultrapure nitric acid. Field measurements of pH, dissolved oxygen, specific conductance, and water temperature were recorded hourly at each site with a multiparameter meter according to procedures described in Wagner and others (2000). At each site, the meter was submerged in the stream near the intake of the pumping sampler.

Several different methods were used for the measurement of streamflow during this study. Streamflow was determined hourly in High Ore Creek by tracer dilution methods using procedures described by Kimball (1997). Samples for trace-element analyses from High Ore Creek were collected

upstream from the tracer-injection point and were unaffected by the chloride solution. At the other four sites, streamflow values were determined periodically either by current-meter measurements (Cataract and Jack Creek sites) or with a Parshall flume (Uncle Sam Gulch and Bullion Mine tributary sites).

Most samples were analyzed for dissolved zinc by the U.S. Geological Survey (USGS) National Water Quality Laboratory in Denver, Colo. Most samples from the High Ore Creek site also were analyzed by the USGS for other selected trace elements (arsenic, cadmium, copper, and manganese) and for chloride (to calculate hourly streamflow values). Dissolved trace elements were determined by inductively coupled plasma–mass spectrometry, and dissolved chloride was determined by ion chromatography. Analytical procedures are described in Garbarino and Taylor (1996) and Fishman (1993).

Diel Variation of Trace-Element Concentrations during Base Flow

During sampling in the Jack and Cataract Creek basins, rainfall runoff prevented full characterization of diel cycles under base-flow conditions. No significant rainfall or overland runoff was observed during sampling in the High Ore Creek basin; consequently, data for this site represent the most complete description of the base-flow diel cycle of trace-element concentrations. Hourly data for High Ore Creek were examined to determine temporal patterns and the magnitude of dissolved trace-element concentration changes, with zinc being the primary element evaluated.

High Ore Creek

The diel variation of dissolved zinc concentrations in High Ore Creek (site 56, fig. 1) over a 53-hour period during August 2–4, 1999, is shown at the bottom of figure 2. The variation over the approximately 2-day period was relatively consistent, displaying a distinct symmetry in both magnitude and timing during the daily rise and fall of concentrations. The difference between the minimum and maximum zinc concentrations was about 400 µg/L during the period of sampling. The minimum concentrations were about 210 µg/L and occurred in the early evening at about 1700 hours. The maximum concentrations also were similar on both days, ranging from about 580 to 630 µg/ L. The maximum concentrations represented about a three-fold increase over the minimum and lasted about 2 hours in the early morning shortly after sunrise (from about 0600 to 0800 hours). Concentrations increased relatively gradually on the rising limb, followed by a more rapid concentration decrease on the falling limb. The average rate of concentration change during the falling limb (about 45 µg/L/hour) was slightly greater than that during the rising limb (about 30 µg/L/hour).

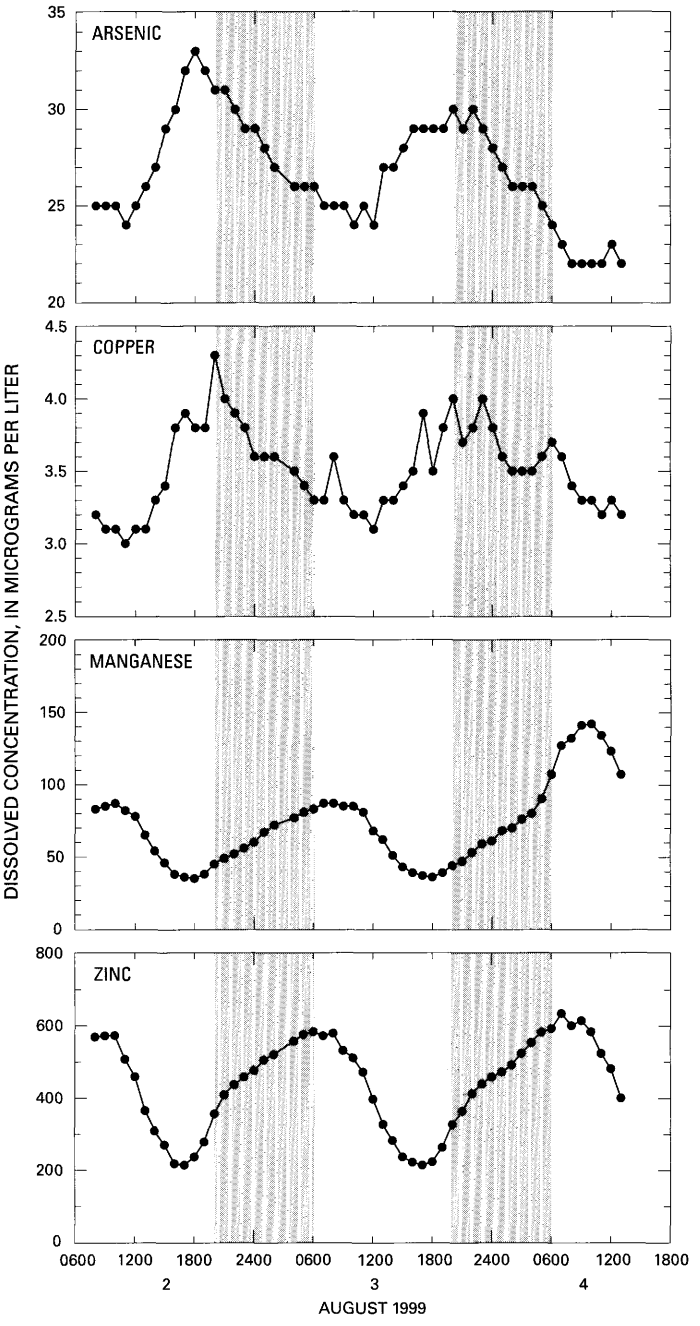

Figure 2. Diel variation of dissolved (0.1-µm filtration) arsenic, copper, manganese, and zinc concentrations in High Ore Creek (site 56), August 2–4, 1999.

In addition to zinc, diel variations of dissolved arsenic, copper, and manganese concentrations are shown in figure 2 to allow comparison of temporal patterns and magnitude of change. These data for base-flow conditions in High Ore Creek indicate that diel cycles exist to varying degrees for each of the four trace elements shown. In general, two patterns are evident: manganese and zinc display similar timing of concentration changes during the day, while arsenic and copper have nearly the opposite timing of concentration maxima and minima relative to zinc. Manganese is the most similar to zinc in the proportional magnitude of its diel

cycle. For example, the diel range of zinc concentrations was approximately three-fold (about 200 to 600 µg/L) and the maximum and minimum concentrations generally occurred at about 0700 and 1700 hours, respectively. Similarly, the diel range for manganese concentrations (35 to 87 µg/L for the first-day cycle) was about 2.5-fold for most of the sampling period, although an anomalous increase in manganese concentrations during the last few hours of the second day may not be representative of the typical diel pattern. The maximum and minimum dissolved manganese concentrations occurred at about 0800 and 1800 hours, respectively. In contrast, the diel range for arsenic and copper concentrations was somewhat less than for manganese or zinc, varying only about 1.5-fold between the minimum and maximum concentrations. Concentrations of arsenic and copper also were substantially lower, with arsenic ranging from 22 to 33 µg/L and copper ranging from about 3 to 4 µg/L. The differences in timing of the diel concentration cycles for arsenic and copper relative to those for manganese and zinc indicate that either different processes are driving the concentration changes, or that the instream supply of arsenic and copper, possibly attached to colloids or metal-hydroxide coatings on streambed sediment, is more limited and cannot support a large shift in partitioning between the dissolved and particulate phases under the ambient physical and chemical conditions in the stream.

Other Streams

Base-flow conditions at the other four sites (sites 17, 19, 43, and 44, fig. 1) lasted only for about the first 10 to 12 hours of hourly sampling before the onset of rainfall runoff (between about 1600 and 1800 hours on August 2 and 4). Zinc concentration data for these short pre-rainfall sampling periods generally follow the same pattern observed at High Ore Creek: maximum values occurred in early morning, followed by decreasing values through late morning and afternoon. The magnitude of the variations, however, was minor compared to that for High Ore Creek.

In the Jack Creek basin, the differences between the minimum and maximum zinc concentrations during the pre-rainfall period (about 0600 to 1800 hours on August 2) were about 250 to 300 µg/L at both the Bullion Mine tributary (from 3,900 to 4,150 µg/L) and Jack Creek mainstem (from 722 to 1,010 µg/L). Although the magnitude of variation was similar at both sites, the pre-rainfall concentration difference represented only about a 6 percent change at the Bullion Mine tributary, but more than a 40 percent change at the Jack Creek site. The limited variability in diel zinc concentrations at the Bullion Mine tributary may be due to the low ambient pH (about 5.2 during base flow), which could prevent geochemical partitioning between the dissolved and particulate phases.

In the Cataract Creek basin, differences between the minimum and maximum concentrations during the pre-rainfall period (about 0700 to 1800 hours on August 4) were 660 µg/L (from 4,330 to 4,990 µg/L) in Uncle Sam Gulch and about 100 µg/L (from 628 to 731 µg/L) in Cataract Creek. These concentration differences represent about a 15 percent variation at both sites.

Because the pre-rainfall data for the Jack and Cataract Creek basins span the period from about 0600 to 1800 hours, the full range of the zinc diel cycle likely was encompassed because that general time interval included the diel minimum and maximum values at High Ore Creek. If this assumption is correct, then the diel changes in zinc concentrations in the Jack and Cataract Creek basins are proportionally much less than the 3-fold change observed for High Ore Creek.

Correlation of Zinc Concentrations with Field Parameters

The correlation of diel variations of dissolved zinc concentrations and selected field parameters in High Ore Creek (fig. 3) was examined to provide insight into possible causes of the diel zinc cycles. Field parameters such as streamflow, pH, dissolved oxygen, specific conductance, and water temperature are easily measured, are known to exhibit diel cycles, and might be associated with geochemical processes that control the diel zinc cycle. In addition, identification of strong correlations between field parameters and zinc concentrations could provide a basis for developing either mathematical methods or sampling strategies to minimize the effect of diel variations on data sets used to interpret trace-element sources, long-term trends, and biological risk.

The strength of relations was evaluated by the coefficient of determination (R^2), which expresses the proportion of total variation in the dependent variable (Y) that is explained by regression with the independent variable (X). Also, the closeness in patterns of change and timing of maximum and minimum values was considered indicative of whether diel fluctuations in zinc concentrations have a strong likelihood of a direct geochemical association with the field parameter.

Streamflow

Concurrent diel variations in streamflow and dissolved zinc concentration in High Ore Creek are shown in figure 3*A*. Streamflow during the 2-day period showed a nearly 1.5-fold diel variation, ranging from about 0.6 to 0.9 ft^3/s (cubic feet per second). In many streams, flow increases commonly are associated with dilution and decreasing solute concentrations, but the timing of the diel streamflow variations in High Ore Creek relative to those of dissolved zinc concentrations does not support a dilution effect. Rather, the timing of peak dissolved zinc concentrations (around 0600 to 0800 hours) coincides with the rising limb of the diel flow increase.

The relation between streamflow and dissolved zinc concentration in High Ore Creek was weak ($R^2 = 0.29$) and had a positive slope, indicating that dissolved zinc concentrations increase as flow increases. Dissolved metal concentrations that increase with flow have been observed in other streams

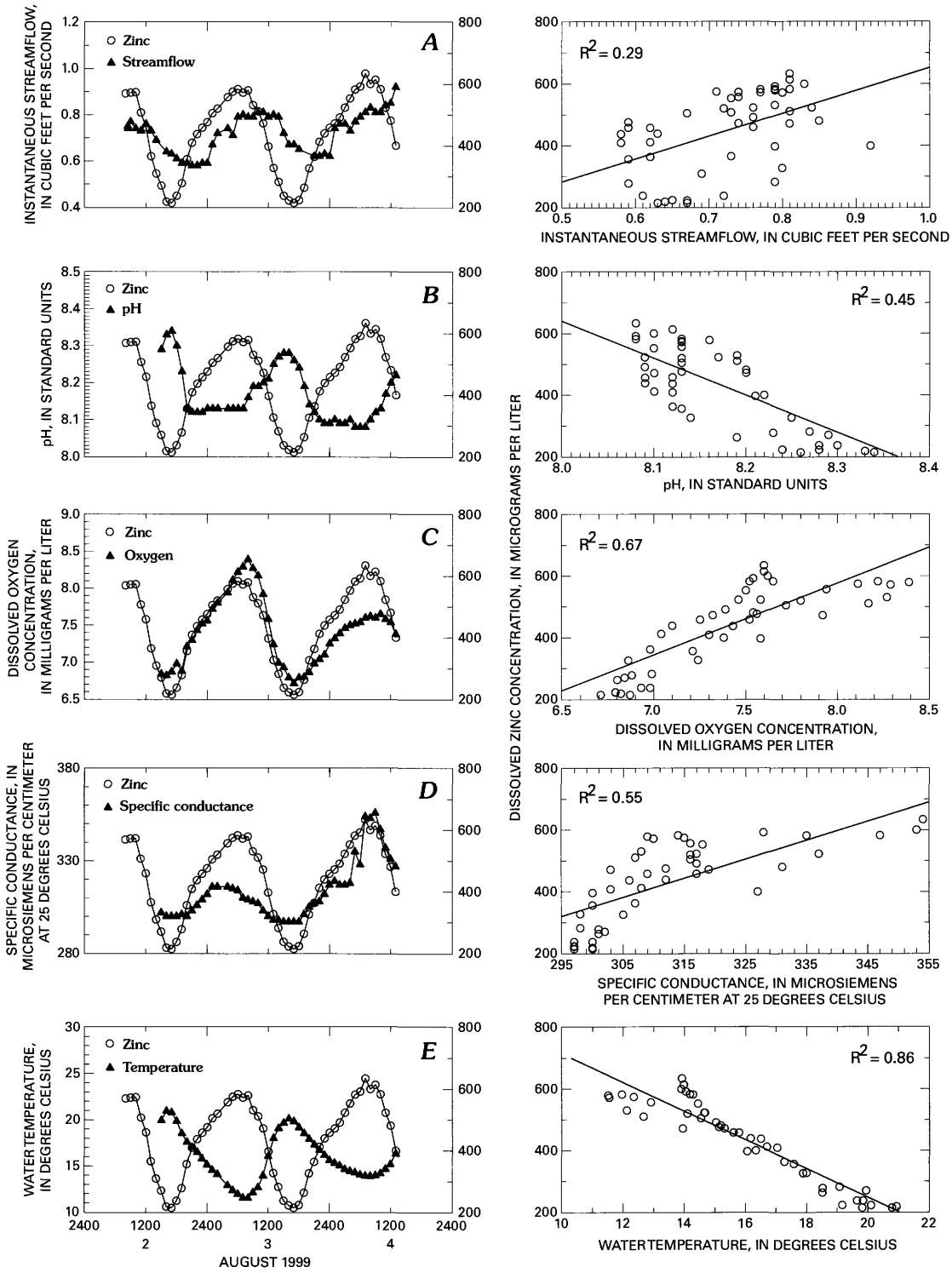

Figure 3. Diel variation and correlation of dissolved (0.1-µm filtration) zinc concentrations in High Ore Creek (site 56), August 2–4, 1999, with selected field parameters. *A*, streamflow; *B*, pH; *C*, dissolved oxygen; *D*, specific conductance; *E*, water temperature.

that are contaminated with mine and mill wastes (J.H. Lambing, unpub. data, 2000). Such increases in dissolved zinc concentration may result from entrainment of zinc-enriched tailings during runoff, followed by dissolution of weakly sorbed particulate zinc to a soluble form. The diel sampling in High Ore Creek, however, was conducted during base flow. In the absence of overland runoff to entrain zinc-enriched tailings, an instream source of zinc is more likely to be causing the diel cycle.

A possible flow-related explanation for a zinc diel cycle is associated with the ground water residing in the alluvium below and adjacent to the stream channel. If ground water

was enriched in dissolved zinc, then an instream zinc diel cycle could result as diel variations in evapotranspiration from the flood plain change the amount of ground water discharging to the stream throughout the day. For example, if ground-water discharge to the stream is greater at night because less ground water is discharged to the atmosphere by evaporation and transpiration, then the instream flow and concentration of dissolved zinc could simultaneously increase. The concurrent increase in streamflow and zinc concentration during an approximately 6-hour period from about midnight to 0600 hours (fig. 3*A*) may support this concept. However, the temporal patterns of streamflow and concentration are not sufficiently in unison to assume that ground-water inflow could be solely responsible for the zinc diel cycle. Also, the ground water was not sampled; therefore, the potential for zinc enrichment by ground water is only speculated.

pH

Concurrent diel variations in pH and dissolved zinc concentration in High Ore Creek are shown in figure 3*B*. The minimum pH values generally are reached within a few hours after sunset (about 2000 hours), similar to when minimum values for streamflow are observed. Unlike streamflow, however, pH is maintained at a relatively constant value throughout the night. Near sunrise (about 0600 hours), pH begins to rise, almost simultaneously as zinc concentrations begin to fall. Values of pH reach a maximum around mid-afternoon, which corresponds well with minimum zinc concentrations. The increase in pH from the nighttime minimum was relatively minor in High Ore Creek, representing less than 0.3 of a pH unit (range of 8.08 to 8.34). The maximum pH value was maintained only for about 2–4 hours, unlike the nighttime minimum that was maintained for about 10–12 hours. Although the pH minimum was maintained as an extended plateau rather than continuing to decline, the time interval spanning the minimum pH values coincided fairly well with the interval of increasing zinc concentrations.

The relation between pH and dissolved zinc concentration was slightly stronger ($R^2 = 0.45$) than that for streamflow and dissolved zinc, with a negative slope indicating that dissolved zinc concentrations increase as pH decreases. This inverse correlation is typical of the solubility exhibited by many metals. The lower pH during the night possibly could solubilize particulate zinc from the instream colloidal fraction or streambed sediment to achieve a cyclical nighttime increase. If this is the case, however, the increased zinc solubility is occurring over a very narrow range of pH values.

Dissolved Oxygen

Concurrent diel variations in dissolved oxygen and dissolved zinc concentrations in High Ore Creek are shown in figure 3*C*. Dissolved oxygen concentrations varied by less than 2 mg/L (milligrams per liter), ranging from about 6.7 to 8.4 mg/L. The maximum dissolved oxygen concentration occurred around 0800 hours, while the minimum occurred near 1700 hours. The dissolved oxygen concentrations likely were responding primarily to water temperature because concentrations began dropping in mid-morning as the water warmed and oxygen solubility decreased. This pattern of decreasing dissolved oxygen concentrations during the day generally is the opposite of biologically productive streams with substantial photosynthetic activity. Metal concentrations in the stream probably inhibit aquatic plant growth, thereby suppressing photosynthetic oxygen production. The temporal patterns of dissolved oxygen and zinc concentrations had generally similar symmetry and their maximum and minimum concentrations coincided within 1 hour of each other.

The relation between dissolved oxygen and dissolved zinc concentrations in High Ore Creek was fairly strong ($R^2 = 0.67$) and displayed a positive slope, indicating that dissolved zinc concentrations increase as dissolved oxygen concentrations increase. The strength of the relation and the relatively close match in diel variation indicate that dissolved oxygen concentration might be a useful surrogate for estimating diel cycles in zinc concentrations. However, the relation might have been merely coincidental because the oxygen variations were responding almost entirely to water temperature. In addition, the multiple biological and physical factors influencing dissolved oxygen concentrations may complicate straightforward interpretation of diel effects.

Specific Conductance

Concurrent diel variations in specific conductance and dissolved zinc concentrations in High Ore Creek are shown in figure 3*D*. Specific conductance, which commonly correlates well with major-ion concentrations, was examined to indicate if a correlation also existed for trace concentrations typical of most metals. The maximum specific conductance values generally occurred within several hours of the maximum zinc concentrations, thereby indicating that major-ion solutes may respond to the same physical or geochemical process influencing zinc concentrations. The relation between specific conductance and dissolved zinc concentrations in High Ore Creek was moderately strong ($R^2 = 0.55$) and had a positive slope, indicating that zinc concentrations increase as conductance increases. Specific conductance values generally increased through the night, which corresponds to the pattern observed for dissolved zinc concentrations and, to a lesser extent, for streamflow. However, the diel patterns for specific conductance, streamflow, and dissolved zinc concentrations in High Ore Creek are not sufficiently in unison to support the concept that constituent-enriched ground water flowing to the stream is primarily responsible for driving the diel concentration cycle.

An abrupt increase in specific conductance occurred during the second day of the sampling period from about 0500 to 0900 on August 4, followed by a rapid decrease for the next 4 hours until the end of sampling. These values appear to be anomalous relative to the preceding diel patterns. If

the values for the last 9 hours of sampling are omitted, the R^2 for the regression relation between specific conductance and dissolved zinc concentrations increases to 0.75. Although this stronger correlation may indicate a more direct link between processes driving diel cycles in both major ions and dissolved zinc, the several-hour lag between conductance and zinc minima and maxima implies that other mechanisms may be exerting primary control over the diel zinc concentration cycle. Of note regarding the anomalously high conductance values during the last 9 hours of sampling is that a nearly identical pattern was observed for dissolved manganese (fig. 2). Other trace elements and field parameters did not display this anomalous pattern.

Water Temperature

Concurrent diel variations in water temperature and dissolved zinc concentration in High Ore Creek are shown in figure 3*E*. The relation between water temperature and dissolved zinc concentrations in High Ore Creek was very strong ($R^2 = 0.86$) and substantially better than the relation between zinc and any of the other field parameters. The negative slope of the relation indicates that dissolved zinc concentrations increase as water temperatures decrease. The timing of temperature maxima and zinc minima is nearly concurrent, which would be expected based on the strong inverse correlation. Maximum temperatures occurred in late afternoon, which closely matched the timing of minimum dissolved zinc concentrations (about 1700 hours). Similarly, minimum temperatures occurred in early morning within an hour or so of the maximum dissolved zinc concentrations (about 0700 hours).

A possible temperature-related explanation for a zinc diel cycle is geochemical adsorption-desorption reactions acting on zinc-enriched colloids or streambed sediments. Studies of solution equilibria using thermodynamic principles (Machesky, 1990; Barrow, 1992; Trivedi and Axe, 2000) indicate that cation adsorption onto particulate material increases as temperature increases, and decreases as the temperature decreases. Thus, during the night and early morning when water temperatures decrease, adsorption of divalent metals such as zinc would decrease, thereby resulting in higher dissolved zinc concentrations as the water cools. This pattern of increasing zinc concentration was observed in High Ore Creek throughout the night until shortly after sunrise: dissolved zinc concentrations reached a maximum in the early morning (0600 to 0800 hours) within an hour or so of the minimum water temperature (0700 to 0800 hours). As water temperature increased throughout the morning and afternoon, adsorption onto colloids or streambed sediment would increase and progressively remove zinc from solution, thereby causing a corresponding decrease in dissolved zinc concentration during the afternoon. This conceptual process was consistent with observed data, whereby dissolved zinc concentrations reached a minimum coincident with maximum water temperatures.

Variation of Zinc Concentrations during Rainfall Runoff

Localized rainstorms over parts of the Boulder River watershed on August 2 and 4, 1999, created short-term overland runoff that affected streamflow conditions during the diel sampling investigation. As a result of increased flows, the base-flow diel cycle for dissolved zinc concentrations was obscured by both dilution effects and the inputs of additional zinc via runoff over wastes from inactive mines. Data from the hourly samples provide a temporally intensive characterization of changes in zinc concentrations over an approximately 1.5-day period in the Jack and Cataract Creek basins. The magnitude and duration of zinc concentration changes during rainfall runoff also may indicate how other metals associated with mine wastes or tailings might respond during short-term flushing events.

Rainfall volumes, intensity, and duration were not measured during the storms. However, changes in streamflow were periodically documented during the sampling period by stage readings and current-meter flow measurements. Because of the short period of runoff and the relatively minor increases in streamflow, the zinc loads derived from rainfall runoff were presumed to be small relative to loads transported by the much larger and sustained runoff during spring snowmelt. However, because instream dilution is minimal during low-flow conditions, increases in trace-element concentrations during rainfall runoff may be greater than those during either spring snowmelt runoff or base-flow diel cycles. Data from such a hydrologic condition, therefore, provide a valuable reference to short-term changes in biological exposure risks.

Jack Creek Basin

In the Jack Creek basin, streamflows in Bullion Mine tributary and Jack Creek below Bullion Mine tributary (sites 17 and 19, fig. 1) were affected by rainfall runoff during the diel sampling period. Variations in dissolved zinc concentrations at both sites over a 36-hour period during August 2–3, 1999, are shown in figure 4.

At about 1800 hours on August 2, heavy rain began falling in the Jack Creek basin and lasted for about 4 hours. Within an hour after the start of the rainstorm, overland runoff was observed. The largest measured streamflow in Jack Creek during the sampling period was 2.22 ft^3/s, but streamflow was estimated by stage readings to have increased 5-fold from about 1 to 5 ft^3/s. Although flows were not measured during runoff in Bullion Mine tributary, overland runoff also was observed at this nearby site, presumably increasing flow in a manner similar to that of Jack Creek. The initial effect of this runoff was a rapid decrease of about 1,000 µg/L in dissolved zinc concentrations in Bullion Mine tributary during the first 2–3 hours of heavy rain (fig. 4). The zinc concentration also decreased rapidly by about 400 µg/L in Jack Creek,

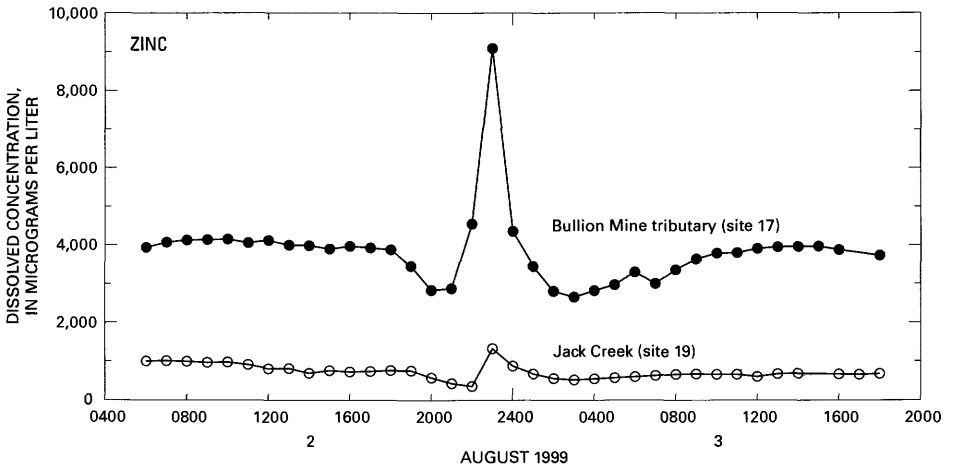

Figure 4. Variation of dissolved (0.1-µm filtration) zinc concentrations during rainfall runoff in Bullion Mine tributary (site 17) and Jack Creek below Bullion Mine tributary (site 19), August 2–3, 1999. Heavy rain began falling at about 1800 hours on August 2.

beginning about an hour after the decline began in the Bullion Mine tributary and continuing during the 2–3 hour period of initial rainfall runoff. The decreases in dissolved zinc concentrations at both sites were likely the result of dilution from overland runoff draining from upland headwater areas containing relatively few sources of waste rock or tailings.

After the initial 2–3 hours of runoff and concentration decreases at both sites, dissolved zinc concentrations increased rapidly over the following 1–2 hours, presumably resulting from dissolution of soluble zinc sulfate salts such as goslarite (Fey and Desborough, this volume, Chapter D4, fig. 3) from waste rock and tailings at the Bullion mine. At the Bullion Mine tributary, zinc concentrations increased by about 6,200 µg/L (from 2,880 to 9,100 µg/L) during a 2-hour period. At Jack Creek, zinc concentrations increased by nearly 1,000 µg/L (from 346 µg/L to 1,320 µg/L) during a 1-hour period. Because the timing of both concentration peaks was nearly identical (fig. 4), inflow from the Bullion Mine tributary likely contributed most of the zinc to Jack Creek during this rainfall event. It is not known how far downstream the peak concentrations measured in the Jack Creek mainstem below Bullion Mine tributary were maintained until dilution from other tributaries or overland runoff from non-mined areas caused concentrations to decrease.

Dissolved zinc concentrations at both sites decreased from their peaks as sharply as they had risen. The temporal pattern of declining zinc concentrations was very similar at both sites, with concentrations decreasing for the next 4 hours to values similar to those observed during the initial periods of runoff (fig. 4). After reaching a post-peak minimum concentration at both sites at about 0300 hours on August 3, zinc concentrations gradually began increasing over the next several hours before stabilizing at near pre-rainfall values.

Cataract Creek Basin

In the Cataract Creek basin, streamflows in Uncle Sam Gulch and Cataract Creek below Uncle Sam Gulch (sites 43 and 44, fig. 1) also were affected by rainfall runoff during the diel sampling period. Variations in dissolved zinc concentrations at both sites over a 35-hour period during August 4–5, 1999, are shown in figure 5.

Beginning at about 1800 hours on August 4, a gradual but steady increase in dissolved zinc concentrations began in Cataract Creek and lasted for about 6 hours. A light rain was falling at the time. During this same period, zinc concentrations increased and decreased irregularly in Uncle Sam Gulch, possibly indicating sporadic runoff volumes and accompanying dilution effects, or variable quality of runoff from different parts of the basin. A relatively large increase in dissolved zinc concentration occurred in Cataract Creek between 2400 and 0100 hours on August 5, but only a small increase occurred in Uncle Sam Gulch during this time. The concentration increases in Cataract Creek likely originated from sources upstream from Uncle Sam Gulch, such as the Morning Glory mine or Cataract mine and tailings (fig. 1).

Shortly after the onset of heavy rain during the night, zinc concentrations increased irregularly between about 2400 and 0500 hours at both sites on Uncle Sam Gulch and Cataract Creek. The sharpest increase occurred between 0300 and 0500 hours in Uncle Sam Gulch. Zinc concentrations during the 5-hour period increased by about 3,100 µg/L (from 4,040 to 7,130 µg/L) in Uncle Sam Gulch and about 670 µg/L (from 779 to 1,450 µg/L) in Cataract Creek, with concentrations at both sites peaking at the same time and at nearly identical proportions (nearly a 2-fold increase). The uniformity in timing and proportionality of concentration increases at the two sites strongly indicates that Uncle Sam Gulch was the primary source of zinc input to Cataract Creek during this runoff event.

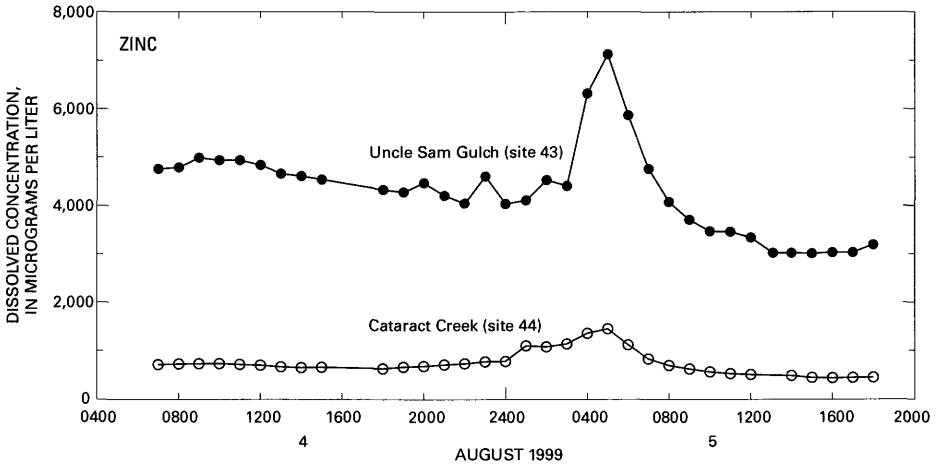

Figure 5. Variation of dissolved (0.1-μm filtration) zinc concentrations during rainfall runoff in Uncle Sam Gulch (site 43) and Cataract Creek below Uncle Sam Gulch (site 44), August 4–5, 1999. Rain began falling about 1800 hours on August 4.

It is not known how far downstream the peak concentration of dissolved zinc in Cataract Creek was maintained.

Dissolved zinc concentrations at both sites decreased from their peak concentrations as rapidly as they had risen. Within 3 hours of their peaks, concentrations in Cataract Creek and Uncle Sam Gulch decreased to levels similar to those measured during the pre-rainfall period. Concentrations continued to gradually decrease at both sites for several hours, eventually stabilizing within about 8–10 hours after the peak.

Implications of Short-Term Variation in Trace-Element Concentrations

Efforts to characterize trace-element concentrations in streams draining abandoned mine lands typically rely upon data collected at widely dispersed locations and over a broad range of hydrologic conditions. These data are used to establish baseline conditions, indicate the locations of major sources of trace-element inputs, detect long-term trends for evaluating remediation effectiveness, evaluate potential risks to aquatic biota, and provide information on how streamflow conditions and season influence concentrations. But if short-term variability of metal or other constituent concentrations is substantial and persistent, interpretations of source inputs, trends, or biological exposure risks may be susceptible to error due to inadequate characterization by routine sampling strategies where samples are widely spaced in time. Large diel cycles in trace-element concentrations, and rapid concentration increases caused by rainfall runoff, pose difficulties in assessments of trace-element sources or long-term trends, and thereby produce uncertainty for resource managers attempting to prioritize areas for cleanup, design remedial treatments, or evaluate remediation effectiveness. The information obtained during these short-term sampling episodes in the Boulder River watershed may not quantitatively relate to other similar sites, but the patterns of variation observed can provide an awareness of potential factors to consider when studies to characterize streams draining abandoned mine lands are being planned.

Diel cycles of zinc or other trace-element concentrations can complicate comparison of loads determined during synoptic sampling because of the difficulty in resolving whether load differences between successive sites are the result of actual inputs or simply an artifact of sampling time. Synoptic sampling to identify spatially discrete source areas (for example, Kimball and others, this volume, Chapter D6) commonly is conducted during base flow when a steady-state input of constituent loads is assumed. However, if the steady-state assumption is not met and concentrations at a site vary widely during the course of a day, then comparisons of load differences between sites may under- or over-estimate actual inputs if successive sites are sampled many hours apart and at different phases of a diel concentration cycle. Under this condition, interpretations of some trace-element sources could be invalidated. In High Ore Creek, the diel variation (fig. 2) was small for copper (about 1 μg/L) and moderate for arsenic (about 10 μg/L). Consequently, the effect on synoptic load calculations and source interpretations for these elements is relatively small. The larger diel variations for manganese (about 80 μg/L) and zinc (about 400 μg/L) could affect interpretations of synoptic loads and inputs along stream reaches. Therefore, unless the diel effect is accounted for by either design of a synoptic sampling schedule that minimizes time differences between successive sites, or by mathematical normalization of analytical results, the only stream reaches that can reliably be considered as a source of trace-element input are those where between-site concentration differences exceed the diel rate of change.

Similar to the effect on synoptic load determinations, evaluations of long-term trends at a site could be complicated

in streams having large diel variations if samples collected periodically over multiple years were obtained at different times of the day. The variable sampling times would result in different phases of the diel cycle being sampled and a potentially wide range of concentrations representing base-flow conditions. The wide range of time-dependent concentrations caused by the natural variability of diel concentration cycles could obscure the presence of an actual trend, or mistakenly indicate a trend where none exists.

If same-time sampling over multiple years is not practical, a possible approach to facilitate interpretation of diel variation is to develop a means to mathematically normalize ambient concentrations. Although water temperature may not be the sole, or even predominant, control on diel cycling of dissolved zinc concentrations, its strong correlation with dissolved zinc concentrations makes it a potentially good surrogate to normalize sample concentrations to an equivalent concentration at a standard reference temperature. Because concentrations of zinc can vary widely from site to site, a diel-adjustment method needs to be independent of the magnitude of concentration. Presumably, such a method would be based on a proportional rate of change of concentration relative to temperature or other surrogate parameters. With further study, mathematical-adjustment methods might be developed that are process-based and applicable to a wide range of stream conditions.

In terms of biological exposure, diel cycles of trace-element concentrations could have sustained but difficult-to-detect impacts on aquatic biota. A chronic stress conceivably could be imposed on aquatic biota if trace-element concentrations regularly exceeded aquatic-life standards, even if only for portions of each day. Characterization of short-lived exceedances may be difficult, however, using data obtained from routine sampling strategies that assume a discrete value measured in a sample represents a consistent level of exposure throughout the day.

A hypothetical example of the effect of diel zinc loading from High Ore Creek on dissolved zinc concentrations in the Boulder River during base flow is illustrated in figure 6. In this example, estimated diel variations of dissolved zinc concentrations in the Boulder River resulting solely from the inflow of High Ore Creek have been constructed from mass-balance calculations using the diel variations in zinc load from High Ore Creek and the instream flow and background zinc concentration in the Boulder River (Nimick and Cleasby, 2000). This estimate of the diel loading effect indicates a maximum increase of about 20 µg/L (from about 10 to 30 µg/L) of dissolved zinc in the Boulder River resulting from the inflow of this one tributary. Although this level of increase is not sufficient to cause exceedances of aquatic-life criteria for zinc, similar diel effects from loading of other trace elements, cumulative diel effects from multiple tributaries draining abandoned mine lands, or more substantial loading effects from storm runoff during low flow could cause receiving streams and their biota to be adversely impacted on short-term time scales that are difficult to document.

Data from the sampling of rainfall runoff provide clear evidence that runoff from waste rock or tailings into streams can result in rapid and large increases of dissolved zinc concentrations that are sufficient to greatly increase biological risk in the vicinity of source areas. The sharp increases noted for dissolved zinc presumably could occur for other trace elements that are prevalent in mine wastes of the Boulder River watershed. This local increase is likely maintained for some distance downstream, although the magnitude and spatial extent have not been quantified. Sampling such episodes of trace-element input to quantify the magnitude, spatial extent, and duration of biological risk can be very difficult logistically due to the short-lived and localized nature of storm runoff. Opportunistic sampling such as occurred in this study, or the use of automated pumping samplers triggered by a continuously monitored surrogate, may be the only feasible means to

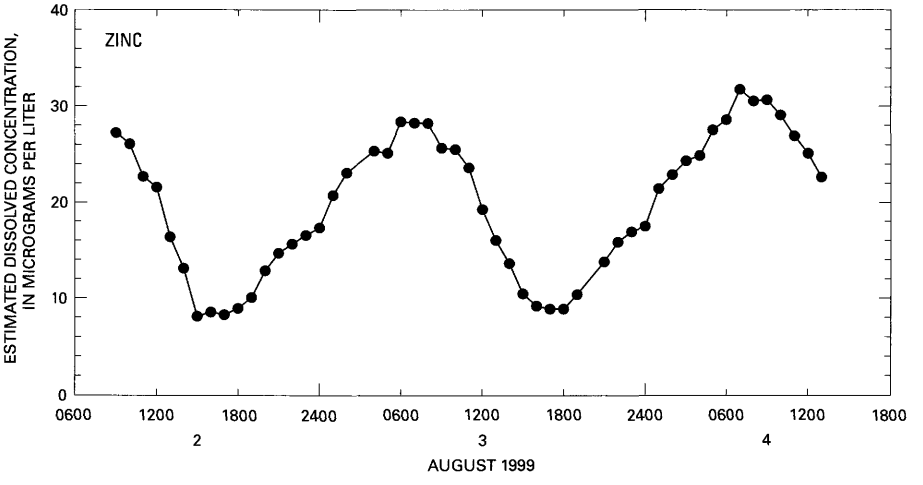

Figure 6. Hypothetical diel variation of dissolved (0.1-µm filtration) zinc concentrations in Boulder River resulting from inflow of High Ore Creek.

characterize the site-specific responses to the flushing of trace elements from abandoned mine lands into streams.

Whether the cause of short-term variation in trace-element concentrations is a diel cycle or localized rainfall runoff, the downstream cumulative effect is of concern. Depending on the magnitude of loads delivered and the dilution capacity of the receiving stream, cyclical diel peak loads in tributaries or the flushing of waste rock and tailings by rainfall runoff may sufficiently impact the chemistry of both local and more distant stream reaches to temporarily exceed thresholds for biological impairment. The short-term variation of zinc concentrations may not have much practical consequence for evaluating biological risk in those tributaries where aquatic-life criteria for acute toxicity are consistently exceeded. But inflows from such impacted tributaries may have pronounced effects downstream in Basin Creek or the Boulder River mainstem, both of which support a trout fishery (Farag and others, this volume). Biological risks, including possible lethality, would be especially pronounced for the pulse of trace elements delivered by rainfall runoff during low flows when concentrations increase to a greater extent and more rapidly than from the diel cycle.

Summary

Variations in trace-element concentrations on a 24-hour (diel) basis in streams draining historical mining areas can, if sufficiently large and persistent, affect interpretations of trace-element sources, long-term trends, and biological risk. In this study, hourly samples were collected at five sites in August 1999 to quantify short-term variation of dissolved trace-element concentrations associated with base-flow diel cycles in three small basins that drain abandoned mine lands in the Boulder River watershed. The zinc diel cycle in High Ore Creek over a 53-hour period during base flow was relatively consistent, with zinc concentrations varying by about 400 µg/L between the maximum and minimum. Maximum concentrations (about 580 to 630 µg/L) occurred shortly after sunrise (between 0600 to 0800 hours) and represented about a three-fold increase over the minimum concentration (about 210 µg/L), which occurred in the early evening at about 1700 hours. The maximum rate of zinc concentration change was about 45 µg/L/hour on the falling limb of the diel cycle. At High Ore Creek, samples also were analyzed for dissolved arsenic, copper, and manganese, all of which exhibited diel cycles to varying degrees. The manganese cycle was the most similar to zinc in both symmetry and proportionality of concentration differences (about a 2.5-fold range in concentration). The diel cycles for arsenic and copper were proportionally smaller (about a 1.5-fold range in concentration), and the timings of concentration minima and maxima were nearly opposite to those for zinc and manganese.

Selected field parameters (streamflow, pH, dissolved oxygen, specific conductance, and water temperature) also were measured hourly to identify correlations that might provide insight into possible geochemical associations with the zinc diel cycle. Zinc concentrations generally increased as streamflow increased; therefore, dilution was not indicated to be the cause of the diel cycle. An inverse correlation between pH and dissolved zinc concentrations exhibited fairly good concurrence in the timing of maxima and minima, possibly indicating a geochemical association. The correlation between water temperature and dissolved zinc concentration was stronger than that observed for any of the other field parameters; dissolved zinc concentrations increased as water temperatures decreased. The inverse symmetry of diel variations for dissolved zinc concentrations and water temperature coincided closely in time. This observation corresponds well to solution equilibria using thermodynamic principles, which indicates that zinc can undergo adsorption-desorption reactions with particulate material (colloids and streambed sediment) as water temperature changes. With further study, it might be possible to utilize one or more field parameters as surrogates to normalize zinc concentrations to minimize the effect of diel variation on data sets used to interpret trace-element sources, long-term trends, and biological risk.

During the diel sampling period, rainstorms over the Jack and Cataract Creek basins produced runoff that obscured the base-flow diel cycles but provided a unique opportunity to document zinc variations during rainfall runoff. Rapid increases in dissolved zinc concentrations over 1–5 hour intervals ranged from about 670 µg/L in Cataract Creek below Uncle Sam Gulch to about 6,200 µg/L in Bullion Mine tributary of the Jack Creek basin. Data from this sampling provide clear evidence that runoff from waste rock or tailings into streams can result in rapid and large increases of dissolved trace-element concentrations that are sufficient to increase the potential for biological risk in the vicinity of source areas.

Whether the cause of short-term variation of instream trace-element concentrations is a diel cycle or localized rainfall runoff, data reported herein show that the cumulative effect of trace-element loading from mining-affected tributaries on downstream reaches is of concern. Depending on the magnitude of loads delivered and the dilution capacity of receiving streams, impacts to water quality may be sufficient to exceed thresholds for biological impairment or lethality, both locally and for extended distances downstream from the trace-element source.

References Cited

Barrow, N.J., 1992, A brief discussion of the effect of temperature on the reaction of inorganic ions with soil: Journal of Soil Science, v. 43, p. 37–45.

Brick, C.M., and Moore, J.N., 1996, Diel variation of trace metals in the upper Clark Fork River, Montana: Environmental Science and Technology, v. 30, p. 1953–1960.

Cleasby, T.E., Nimick, D.A., and Kimball, B.A., 2000, Quantification of metal loads by tracer-injection and synoptic-sampling methods in Cataract Creek, Jefferson County, Montana, August 1997: U.S. Geological Survey Water-Resources Investigations Report 00–4237, 39 p.

Fishman, M.J., 1993, Methods of analysis by the U.S. Geological Survey National Water Quality Laboratory—Determination of inorganic and organic constituents in water and fluvial sediments: U.S. Geological Survey Open-File Report 93–125, 217 p.

Fuller, C.C., and Davis, J.A., 1989, Influence of coupling of sorption and photosynthetic processes on trace element cycles in natural waters: Nature, v. 340, p. 52–54.

Garbarino, J.R., and Taylor, H.E., 1996, Inductively coupled plasma-mass spectrometric method for the determination of dissolved trace elements in natural water: U.S. Geological Survey Open-File Report 94–358, 49 p.

Kimball, B.A., 1997, Use of tracer injections and synoptic sampling to measure metal loading from acid mine drainage: U.S. Geological Survey Fact Sheet FS–245–96, 8 p.

Lambing, J.H., 1991, Water-quality and transport characteristics of suspended sediment and trace elements in streamflow of the upper Clark Fork basin from Galen to Missoula, Montana, 1985–90: U.S. Geological Survey Water-Resources Investigations Report 91–4139, 73 p.

Machesky, M.L., 1990, Influence of temperature on ion adsorption by hydrous metal oxides, *in* Melchior, D.C., and Bassett, R.L., eds., Chemical modeling of aqueous systems II: Washington, D.C., American Chemical Society Symposium Series 416, p. 283–292.

McKnight, D.M., Kimball, B.A., and Bencala, K.E., 1988, Iron photoreduction and oxidation in an acidic mountain stream: Science, v. 240, p. 637–640.

Nimick, D.A., and Cleasby, T.E., 2000, Water-quality data for streams in the Boulder River watershed, Jefferson County, Montana: U.S. Geological Survey Open-File Report 00–99, 70 p.

Nimick, D.A., and Cleasby, T.E., 2001, Quantification of metal loads by tracer injection and synoptic sampling in Daisy Creek and the Stillwater River, Park County, Montana: U.S. Geological Survey Water-Resources Investigations Report 00–4261, 51 p.

Nimick, D.A., and Moore, J.N., 1991, Prediction of water-soluble metal concentrations in fluvially deposited tailings sediment, upper Clark Fork valley, Montana, U.S.A.: Applied Geochemistry, v. 6, p. 635–646.

Nimick, D.A., Moore, J.N., Dalby, C.E., and Savka, M.W., 1998, The fate of geothermal arsenic in the Madison and Missouri Rivers, Montana and Wyoming: Water Resources Research, v. 34, p. 3051–3067.

Smith, J.D., Lambing, J.H., Nimick, D.A., Parrett, Charles, Ramey, Michael, and Schafer, William, 1998, Geomorphology, flood-plain tailings, and metal transport in the upper Clark Fork valley, Montana: U.S. Geological Survey Water-Resources Investigations Report 98–4170, 56 p.

Trivedi, P. and Axe, L., 2000, Modeling Cd and Zn sorption to hydrous metal oxides: Environmental Science and Technology, v. 34, p. 2215–2223.

U.S. Environmental Protection Agency, 1999, Ecological risk assessment, Clark Fork River operable unit, Milltown sediments/ Clark Fork River Superfund Site, Public Review Draft, Volume 1: Prepared by ISSI Consulting Group, Inc., Denver, Colo., for USEPA Region VIII, December 1999, variously paged.

Wagner, R.J., Mattraw, H.C., Ritz, G.C., and Smith, B.A., 2000, Guidelines and standard procedures for continuous water-quality monitors—Site selection, field operation, calibration, record computation, and reporting: U.S. Geological Survey Water-Resources Investigations Report 00–4252, 53 p.

Wilde, F.D., Radtke, D.B., Gibs, Jacob, and Iwatsubo, R.T., 1998, National field manual for the collection of water-quality data: U.S. Geological Survey Techniques of Water-Resources Investigations, book 9, Chapters A1–A9.

Trace Elements and Lead Isotopes in Streambed Sediment in Streams Affected by Historical Mining

By Stanley E. Church, Daniel M. Unruh, David L. Fey, and Tracy C. Sole

Chapter D8 of
Integrated Investigations of Environmental Effects of Historical Mining in the Basin and Boulder Mining Districts, Boulder River Watershed, Jefferson County, Montana
Edited by David A. Nimick, Stanley E. Church, and Susan E. Finger

Professional Paper 1652–D8

U.S. Department of the Interior
U.S. Geological Survey

Contents

Figures

Tables

Chapter D8
Trace Elements and Lead Isotopes in Streambed Sediment in Streams Affected by Historical Mining

By Stanley E. Church, Daniel M. Unruh, David L. Fey, and Tracy C. Sole

Abstract

Assessment of deposit-related and rock-forming trace elements in streambed sediment in the Boulder River watershed has provided the data necessary to delineate stream reaches having elevated contaminant concentrations in tributary streams, to determine anthropogenic sources of contaminated streambed sediment, to understand the transport of dissolved and particulate trace elements, and to establish the streambed-sediment framework needed to evaluate toxicity to aquatic biota. Concentrations of the suite of deposit-related trace elements—copper, lead, zinc, arsenic, silver, cadmium, and antimony—were elevated in modern streambed sediment in the Boulder River downstream from the confluence with Basin, Cataract, and High Ore Creeks. The major sources of these contaminants were tied directly to historical mining. All major tributary basins, Basin Creek, Jack Creek, Cataract Creek, Uncle Sam Gulch, and High Ore Creek, and the Boulder River downstream from the confluence of Basin Creek, had concentrations of leachable copper, lead, and arsenic in modern streambed sediment that exceeded the apparent effects threshold for aquatic biota. In the Boulder River, these effects can be traced for a distance of about 55 river miles downstream to the confluence with the Jefferson River. Concentrations of cadmium and zinc exceeded the apparent effects threshold in streambed sediment in the Boulder River downstream from the confluences of Cataract and High Ore Creeks. Everywhere within the three basins downstream from the major mines, the concentrations of all the deposit-related trace elements exceeded the screening level concentration for aquatic biota.

Comparison of the concentrations of this suite of deposit-related trace elements in streambed sediment today with that in premining streambed sediment from terrace deposits in the flood plains of these streams showed that the concentrations of the deposit-related trace elements were substantially elevated, from several to more than 100 times that prior to historical mining. Lead isotopic data from these two media indicated that the effect of mineralized rock on the streambed-sediment geochemistry prior to mining was small, but nevertheless greater than the concentrations of deposit-related trace elements in tributaries unaffected by historical mining or mineralized rock.

Two different sources of deposit lead were defined by the lead isotopic data, one representing the polymetallic vein deposits in both the Basin and Cataract Creek basins, and a second at the Comet mine in the High Ore Creek basin. Calculations of the extent of the contamination of the streambed sediment in the Boulder River indicate about 35 percent of the lead contamination was introduced by streambed sediment from Basin Creek and the Jib Mill, about 15 percent was derived from Cataract Creek, and about 50 percent was from High Ore Creek. Contaminants carried in streambed sediment from High Ore Creek dominated the concentrations of deposit-related trace elements in stream sediment of the Boulder River below the confluence downstream to the Jefferson River. Data from suspended sediment, when compared with that from the streambed sediment, indicated that copper and zinc were being actively and differentially transported in the suspended-sediment phase relative to arsenic and lead.

Introduction

Streambed-sediment geochemical studies have been used in mineral exploration programs for more than 50 years, using the principle that the presence of elevated trace-element concentrations at a locality or localities may be an indication of undiscovered mineral deposits upstream. Erosion of these mineral deposits or the altered rock surrounding them provides evidence of their presence at specific sites in the watershed. In the case of historical mining districts such as the Basin and Boulder districts discussed here, no historical data exist to indicate either what the concentrations of several important trace elements in water or streambed sediment might have been prior to mining, or whether aquatic life was present in or downstream of these historical mine and mill sites. This report examines the concentrations and sources of selected trace elements in streambed sediment in the Boulder River and its major tributaries near the town of Basin in southwestern Montana.

Ruppel (1963) and Becraft and others (1963) described the mineralogy of the veins that were mined in the Boulder River watershed study area. In general, the miners exploited polymetallic quartz veins containing pyrite, galena, sphalerite, chalcopyrite, arsenopyrite, and minor amounts of tetrahedrite. For purposes of this report, we focus on the distribution of a subset of trace elements that are specifically associated with these polymetallic vein deposits: copper, lead, zinc, arsenic, silver, cadmium, antimony, and gold. We refer to this trace-element suite as the deposit-related trace elements. In contrast, trace elements that are not associated with and enriched in the polymetallic vein deposits are herein referred to as rock-forming trace elements and include chromium, cobalt, strontium, titanium, vanadium, the rare-earth elements, and many others.

Fundamental time-frame differences are present in the data obtained from different sample media collected in the Boulder River watershed study. Water-quality data provide an instantaneous measure of the concentrations of constituents in the water column in a dynamic system. Concentrations of dissolved trace elements in water varied widely depending on streamflow conditions, ground- and surface-water flow, daily variations caused by plant uptake, and instream geochemical reactions (Nimick and Cleasby, this volume, Chapter D5; Lambing and others, this volume, Chapter D7; Kimball and others, this volume, Chapter D6). Suspended-sediment samples, which also included colloidal material, provided data on the concentrations of trace elements in the sediment fraction being transported in the water column. In contrast, streambed-sediment samples integrated conditions at a sample site over a longer time period because the streambed deposits were composed of detrital material transported and deposited during high flow as well as additional material that accumulated at the site during low-flow conditions (Church, Nimick, and others, this volume, Chapter B, fig. 3). This additional material included colloidal material composed of amorphous oxyhydroxides of aluminum, iron, and manganese that either coated these detrital grains or coalesced and settled to the streambed. These coatings and colloids contained and continued to sorb the deposit-related trace elements, effectively lowering their dissolved concentrations in water. Both processes, grain coating and colloidal settling, and continued sorption by these reactive aluminum, iron, and manganese oxyhydroxide surfaces, enriched the streambed sediment with deposit-related trace elements. This enrichment process continued throughout low-flow periods and caused concentrations of the deposit-related trace elements to increase with time during low-flow conditions for a period of several months each year following spring runoff.

Purpose and Scope

Major objectives of this study were four-fold.

- The primary goal was to characterize one aspect of the current aquatic environmental conditions in the Boulder River watershed—that is, to determine the present-day spatial distribution of deposit-related trace elements in streambed sediment throughout the watershed. This objective was achieved through geochemical analysis of streambed-sediment samples collected at 63 sites throughout the basin during low flow over the 3-year period from 1996 through 1998.
- A second objective was to identify those mining sites that provide the major contributions of deposit-related trace elements to the streams. This objective was achieved through spatial analysis of contributions of these deposit-related trace elements from mine sites to streambed sediment in specific stream reaches.
- A third objective was to determine the premining geochemical baseline—that is, the concentrations of the deposit-related trace elements in streambed sediment that predate historical mining. Determination of the premining geochemical baseline was necessary to define the minimum concentrations of the deposit-related trace elements that feasible remediation efforts might be expected to achieve. This goal was achieved by sampling of streambed sediment in tributaries located upstream from past mining activities and by sampling premining fluvial deposits in old stream terraces. However, we were limited by the distribution, preservation, and recognition of, as well as access to, these old stream-terrace deposits downstream from historical mining sites. Dendrochronology and historical records have been used to provide a chronology for these terrace deposits (Unruh and others, 2000).
- A fourth objective was to quantify the deposit-related trace-element contribution to the streambed sediment today from historical mine sites within the watershed. The data sets could then be used to evaluate the elevated deposit-related trace-element concentrations found in water and their potential detrimental effects on aquatic habitat in the Boulder River study area (Nimick and Cleasby, this volume; Farag and others, this volume, Chapter D10; Finger, Farag, and others, this volume, Chapter C).

Previous Geochemical Investigations

Analytical results for major- and trace-element concentrations in streambed sediment have been reported from two previous studies: the Butte 1° × 2° study (McDanal and others, 1985; Elliott and others, 1992) conducted from 1975 to 1983, and the National Uranium Resource Evaluation (NURE) program conducted from 1976 to 1977 (Aamodt, 1978; Broxton, 1980; Van Eeckhout, 1981). In both studies, streambed sediment was collected from small, first-order tributaries, as indicated on 1:24,000-scale topographic maps, with drainage areas of about 1 to 4 or more mi^2, in order to evaluate the sources

of deposit-related trace elements for mineral exploration. Not all first-order tributary streams within the Boulder River study area were sampled in the NURE or the Butte 1° × 2° studies. Analytical results from the NURE studies were used to develop regional geochemical maps for copper, lead, and zinc; and results from the Butte 1° × 2° study were used to develop the regional geochemical map for arsenic. These geochemical maps provide a regional geochemical baseline circa the late 1970s for the Boulder River watershed study area. Sample localities are shown in figure 1. These regional geochemical maps showed the effects of past mining on the first-order tributary drainages and defined an area within the study area with elevated concentrations of copper, lead, zinc, and arsenic. The regional geochemical maps were used to focus the current study on critically affected stream reaches.

The NURE data (Broxton, 1980; Van Eeckhout, 1981) also indicated that the Boulder batholith contained elevated concentrations of uranium. The uranium is in pitchblende in chalcedony veins that occur with the base- and precious-metal polymetallic veins in the Boulder batholith in the study area (Ruppel, 1963; Becraft and others, 1963). No new data have been collected on the occurrence and distribution of the uranium-bearing minerals in these veins.

Sample Collection and Preparation

Streambed Sediment

Streambed-sediment samples were collected from 38, 31, and 18 sites, respectively, in October 1996, July 1997, and July 1998 at a total of 63 separate localities on Basin, Cataract, High Ore, and Jack Creeks, Uncle Sam Gulch, and the Boulder and Little Boulder Rivers, or their first-order tributaries (fig. 1). Some samples were collected from outside the study area to sample basins with the same geology, to determine the geochemical baseline in unmineralized streams, and to evaluate the downstream limits of effects in the Boulder River. Streambed-sediment samples were collected during low-flow conditions, thus ensuring collection of colloidal material in the streambed sediment. At each sampling site, streambed-sediment samples were collected, using a plastic scoop, from the surfaces of fluvial sediment deposits in pool or low-velocity areas on both sides of the stream along a 100–150 foot reach. The samples were composited, wet sieved with ambient stream water to pass through a 10-mesh (<2 mm) stainless steel screen, and collected in a plastic gold pan. About 6.5 lb of material was sealed in plastic containers at the site. During the 1996 sampling, a few streambed-sediment samples from the first-order tributary basins were collected to both augment and verify previous work conducted in the NURE and Butte 1° × 2° regional geochemical studies (fig. 1). Seven pairs of streambed-sediment samples, one each from the north and south sides of the Boulder River, were collected upstream and downstream of the confluences of Basin, Cataract, and High Ore Creeks (sites *5S*, *6S*, *8S*, *9S*, *11S*, *12S*, and *13S*; fig. 1).

In the laboratory, the samples were air dried and sieved to minus 100-mesh (<150 μm) to correspond directly with the procedure used in the NURE study (the Butte 1° × 2° study used minus-80-mesh sediment), and split for analysis (Fey, Unruh, and Church, 1999). The sample material analyzed constitutes the very fine sand, silt, and clay size fractions of the fluvial sediment in the active stream channel. Results are in the database (Rich and others, this volume, Chapter G).

Low-flow conditions in the watershed, defined as less than 150 ft^3/s at U.S. Geological Survey gauging station 06033300 located 2 mi east of Boulder, started in mid-July in each of the 3 years streambed sediment was sampled (Church, Nimick, and others, this volume, fig. 3). The 1996 samples were collected about 3 months after the onset of low flow, whereas the 1997 and 1998 samples were collected shortly after the spring-runoff period. The samples collected in the latter 2 years are therefore not directly comparable to the data from the 1996 data set because of differences in the time period after runoff for accumulation of colloidal components at the sampling sites. In general, the latter two data sets contain lower concentrations of the deposit-related trace elements, although they exhibit the same trends as were found in the 1996 data set. In construction of the trace-element maps, the 1996 data were used wherever possible. This choice particularly affects sites *7S*, *10S*, and *14S* on the Boulder River (fig. 1).

Suspended Sediment

In May 1997 during spring runoff, D.A. Nimick collected suspended-sediment samples from six localities (fig. 1) using a DH-74-TM sampler and width- and depth-integrated sampling procedures. Approximately 8 L of water were collected. After the suspended sediment settled in plastic containers, it was collected and air dried for analysis (Fey, Unruh, and Church, 1999).

Premining Sediment

Stream terraces were sampled at a number of localities (fig. 2) in the study area using either trenches or cores through stream deposits preserved in cutbanks along the creeks and river (Unruh and others, 2000). The terrace deposits were generally composed of poorly sorted fluvial silt, sand, and gravel containing lithic clasts ranging in size up to 12 in. in diameter (fig. 3). Because no discernible stratigraphy was preserved in the gravel deposits, samples were taken in 6- to 12-in. intervals throughout the exposed terrace section. We dug back into the terrace deposit at least 8 in., carefully removing any materials that might have been deposited on the surface or cut bank of the terrace by historical floods that might have contaminated the sample. We removed unvegetated sand and gravel deposited on top of the terrace deposits unless covered by a

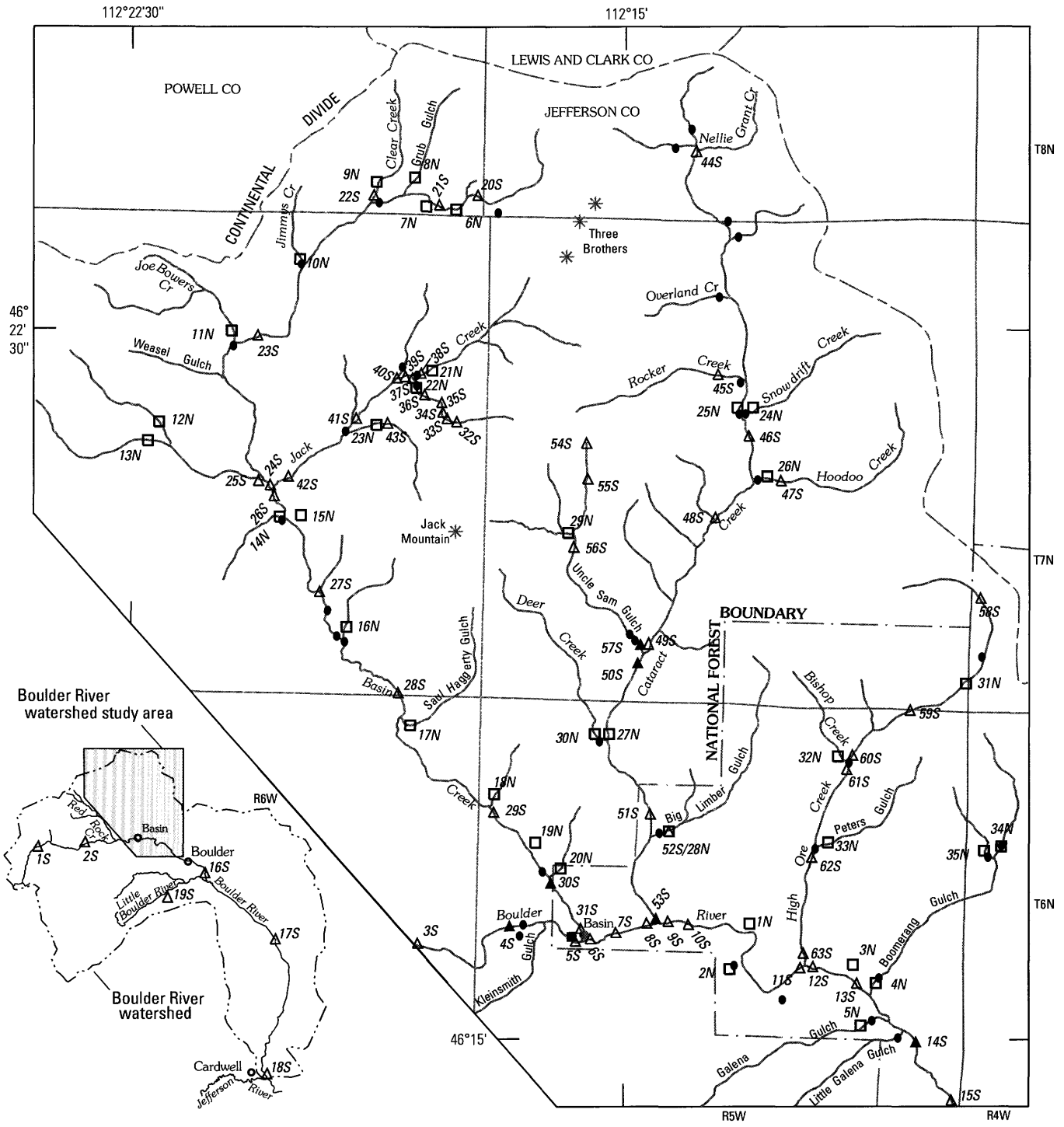

EXPLANATION

- 21S △ Streambed-sediment locality sampled by U.S. Geological Survey
- 30S ▲ Suspended-sediment locality sampled by U.S. Geological Survey
- 1N □ Streambed-sediment locality sampled during NURE program
- • Streambed-sediment locality sampled by U.S. Geological Survey, Butte 1° x 2° study
- ■ Jib Mill site

Figure 1. Localities where suspended-sediment and streambed-sediment samples were collected during current study, and where streambed-sediment samples were collected in Butte 1° x 2° and NURE studies during the 1970s. Some small tributaries sampled during Butte 1° x 2° study are not shown. Prior to this study, no samples were collected from the major tributaries or Boulder River. The Jib Mill site is also shown.

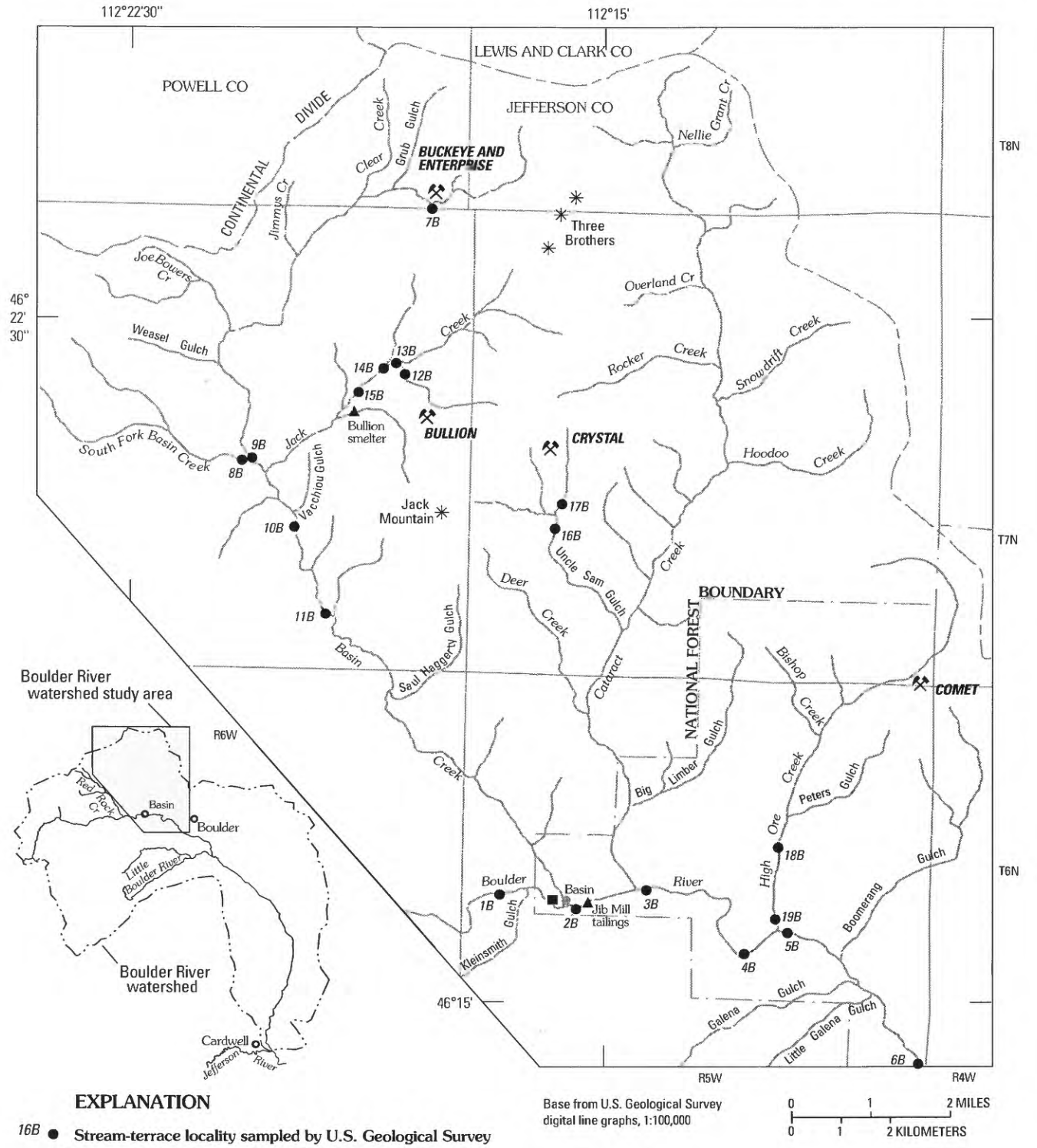

Figure 2. Localities where stream-terrace sites were sampled for premining streambed sediment to determine premining geochemical baseline. Also shown are several mine and mill sites sampled for this study that were localities of the primary point sources of contamination reaching the streams. Fluvial tailings deposits and selected mine sites were also sampled.

Figure 3. Stream-terrace deposit sites. *A*, Terrace sampled on Basin Creek (near site *10B*). Notice mottled iron staining in layer below the well-developed soil horizon and above the gravel indicating postdepositional oxidization and possible movement of iron in the terrace sediments. *B*, Terrace site sampled at beaver dam impoundment on upper Jack Creek downstream from Bullion Mine tributary (site *14B*). Note thick deposit of fluvial tailings from blowout of the mill tailings dams at the Bullion mine. Core sample was taken using a 2-in.-diameter PVC pipe near base of a 99-year-old Lodgepole pine buried in the dam during construction. *C*, Flood-plain gravel deposit on Uncle Sam Gulch downstream from Crystal mine (site *17B*). The premining baseline core (foreground) was taken between two large stabilizing roots of a 252-year-old Ponderosa pine harvested in 1983. Stainless steel coring probe used for the 1-in. diameter cores is lying on top of stump. Note contaminated water and streambed sediment in Uncle Sam Gulch (background). *D*, fluvial deposits from near site *6B*, downstream from High Ore Creek on the Boulder River. Uppermost layer above white zone and in root zone contaminated by post-mining overbank sediment. Cottonwood growing on river bank at this locality gave dendrochronological age of 60 years.

well-developed soil horizon to prevent contamination by recently deposited gravel and silt. We took a minimum of three samples at each site to provide some measure of reproducibility of the analytical data, or to discern a geochemical trend in the data from the site. Where the analytical results were not consistent between samples collected at the same site, not all the results were used to estimate the premining geochemical baseline. The gravel samples were dry sieved in the field to pass a 2-mm stainless steel screen, and sent to the laboratory for further processing.

In the laboratory, the samples were air dried if needed, sieved to pass 100-mesh (<150 μm), and split to ensure homogeneity (Fey, Unruh, and Church, 1999). The sample material analyzed constitutes the very fine sand, silt, and clay size fractions of the premining fluvial sediment; results are in Unruh and others (2000) and in the database (Rich and others, this volume).

Sample Analysis

Geochemical Methods

Geochemical data for the streambed-sediment, suspended-sediment, and terrace samples were determined using inductively coupled plasma–atomic emission spectrometry (ICP-AES) from a mixed mineral-acid total digestion (Briggs, 1996; Church, 1981) and from a partial-digestion method using 2M HCl-1 percent H_2O_2 (Fey, Unruh, and Church, 1999). This partial digestion or leach was designed to dissolve the aluminum, iron, and manganese oxyhydroxide component of the streambed sediment and isolate the deposit-related trace elements contained in this component of the streambed sediment from those trace elements in the rock-forming phases of the streambed sediment found in the total digestions of the residual phases (Rich and others, this volume). Total-digestion data were used for the geochemical maps (figs. 8–9) so that the data collected in this study are comparable with those from previous studies (figs. 4–7), whereas the partial-digestion data have been used to make the concentration versus distance diagrams (figs. 11–14) that showed the streambed-sediment geochemistry profiles. All analytical results are available in the database (Rich and others, this volume).

Lead Isotopic Methods

Lead isotopic analyses of the streambed sediment were done on the partial-digestion solutions using standard lead isotopic methods (Fey, Unruh, and Church, 1999; Unruh and others, 2000). Results are reported in terms of the lead isotope ratio to ^{204}Pb, the isotope of lead that has no radioactive parent. All analytical results are in the database (Rich and others, this volume).

Dendrochronology and the Historical Record

We used historical data and dendrochronology to constrain the ages of premining gravel in terrace deposits used to determine the premining geochemical baseline. The dendrochronological data provide minimum ages for the terrace deposits whereas the historical data provide ages of structures or events within the mining district. Historical data for the Basin and Cataract mining districts were reviewed by Rossillon and Haynes (1999), who provided this work under contract with the USDA Forest Service.

Dendrochronological analysis was conducted by the Laboratory of Tree-Ring Research, University of Arizona, Tucson, Ariz.; the results are in Unruh and others (2000). Dates from live trees provided a minimum age of the terrace. Dates from dead standing trees sampled also provided only a minimum age, but with a larger uncertainty. Construction of a dendrochronological record from live trees to allow dating of dead trees was not achieved. The climate of the basin was sufficiently constant through time that a distinctive tree-ring structure versus time curve could not be constructed (Jeff Dean, Laboratory of Tree-Ring Research, University of Arizona, written commun., 1999). Development of a mature soil horizon on terraces was used in a qualitative sense to estimate the relative age and maturity of stream-terrace deposits.

Trace Elements in Streambed Sediment

Deposit-related trace elements derived from acidic drainage and mine waste as well as from mineralized but unmined sources typically accumulate in the streambed sediment downstream from inactive, historical mines. In the Boulder River watershed study area, these trace elements were concentrated in the colloidal phase and the grain coatings of the streambed sediment. As seen from the data, the difference between the concentrations of the deposit-related trace elements in the total-digestion data and data from the residual silicates clearly showed that the deposit-related trace elements were concentrated in and associated with the iron oxyhydroxide component of the streambed sediment. Downstream concentration profiles for streambed sediment, constructed using the partial-digestion data, were used to delineate stream reaches that had elevated deposit-related trace-element concentrations, to locate sources of contaminated material, and to help understand the transport of dissolved and particulate trace elements. In addition, we used concentration data to evaluate the potential toxicity of deposit-related trace elements in streambed sediment to biota (Farag and others, this volume).

The measured concentrations of deposit-related trace elements in the streambed sediment varied with the velocity of the flow regime. The colloidal component and the suspended sediment tended to settle out of suspension in low-velocity reaches in the stream or river. Thus, the deposit-related trace-element concentrations were susceptible to temporal

variability caused by sorption to grain coatings and colloids, and by deposition of the suspended sediment during low flow. They were also dependent upon the frequency of summer storms because the increased flow may mobilize some fraction of the colloidal component that had settled to the streambed. In general, one would not expect temporal variability to affect spatial variation of the geochemical signature obtained from a streambed-sediment survey within a watershed as long as the entire sample suite was collected over a short time frame (barring a summer rainstorm during the sample collection period). No such rainfall event occurred during any of the three streambed-sediment sampling efforts in the Boulder River watershed (Church, Nimick, and others, this volume, fig. 3).

Downstream profiles of deposit-related trace-element concentrations in streambed sediment in the Boulder River watershed study area were similar to the concentration profiles observed for surface water for copper, lead, zinc, and cadmium (Nimick and Cleasby, this volume). The highest concentrations of leachable and total deposit-related trace elements in streambed sediment occurred immediately downstream from the large mines, the Buckeye, Bullion, Crystal, and Comet mines (fig. 2), whereas concentrations of these deposit-related trace elements were near average crustal abundance values in rocks underlying subbasins where mineral deposits have not been found. Copper, lead, zinc, arsenic, cadmium, and antimony were concentrated in the leachable phase, indicating sorption to the hydrous aluminum, iron, and manganese grain coatings and colloids in streambed sediment. Concentrations of trace elements not associated with the mineral deposits (for example, chromium, cobalt, strontium, titanium, vanadium, and the rare-earth elements) were similar throughout the watershed where underlain by the same rock type.

Geochemical Mapping Using Streambed-Sediment Data

Estimating the Premining Geochemical Baseline from Regional Geochemical Data

The geochemical baseline for the Boulder River watershed study area today was evaluated using geochemical data from small tributaries from both the current and previous studies. Data from these small tributaries where the drainage basin is underlain by unmineralized rocks of the Boulder batholith and the Elkhorn Mountains Volcanics (O'Neill and others, this volume, Chapter D1) provided but one measure of the geochemical baseline prior to historical mining. Tributary streams sampled in the earlier studies that had near-crustal-abundance trace-element concentrations were generally not resampled. Reference sites located in drainages that had a geologic setting similar to the study area were sampled outside the study area to provide data for comparison with mineralized areas. At site *1S* on the upper Boulder River (fig. 1), the drainage basin is underlain by Cretaceous plutonic rocks of the Boulder batholith and the coeval Elkhorn Mountains Volcanics (Wallace, 1987). Elliott and others (1992) indicated one large past-producing mine, several small historical mines with no known production, and several prospects in the headwaters of the Boulder River substantially upstream of the sampling site. At site *19S* on the Little Boulder River (fig. 1), the basin is underlain by Cretaceous plutonic rocks of the Boulder batholith and the coeval Elkhorn Mountains Volcanics (Wallace, 1987). Elliott and others (1992) indicated that a small gold placer, several prospects, and several small past-producing historical mines were located in the Little Boulder River basin upstream of the sampling site. With the exception of the placer mine, these mines and prospects were not close to the Little Boulder River. At site *2S* (fig. 1), the drainage basin is underlain by Cretaceous plutonic rocks of the Boulder batholith and the coeval Elkhorn Mountains Volcanics on the north side of the Boulder River, but by the younger Lowland Creek Volcanics of Eocene age on the south side of the Boulder River (Wallace, 1987). Elliott and others (1992) indicated little past mining in this area of the Boulder River watershed.

Thirty-five streambed-sediment sites from the NURE study (Aamodt, 1978; Broxton, 1980; Van Eeckhout, 1981) were located within the Boulder River watershed study area (fig. 1). Many of these sites were on first-order tributary streams shown on 1:24,000-scale topographic maps (fig. 1). Results for copper, lead, and zinc from 16 streambed-sediment samples from the NURE study and 11 samples collected from the Boulder River watershed study area are summarized in table 1. Samples were restricted to those collected from tributary drainages generally underlain by rocks of the Butte pluton that appeared to have little or minimal effects from past mining activities. Arsenic was not analyzed, and only a few cadmium and silver concentrations were determined or were above the limit of detection in streambed sediment analyzed during the NURE study. Median and mean concentrations for this suite of trace elements are in reasonable agreement between the two data sets. The standard deviation of the data sets is small when compared to the median value. The median and mean concentrations of the deposit-related trace elements are near or below average crustal abundance values for cadmium, copper, and silver, and were elevated above crustal abundance values for arsenic, lead, and zinc (table 1). We used the median values determined from these two studies to define one measure of the premining geochemical baseline in the Boulder River watershed and to compare with enrichment for this same suite of trace elements downstream from inactive mine sites in the Boulder River watershed study area.

Regional Geochemical Mapping—The Late 1970s Geochemical Baseline

Regional geochemical maps of the study area were constructed from the streambed-sediment data from first-order

Table 1. Trace-element data from streambed sediment from tributary drainages that have little impact from past mining in the Boulder River watershed, Montana.

[<, value below specific limit of detection (ICP-AES; this study); n.a., not analyzed; --, no data calculated; No. of sites does not include censored arsenic values in the new data set or censored zinc values in the NURE data set; crustal abundance data from Fortescue (1992)]

	Copper ppm	Lead ppm	Zinc ppm	Arsenic ppm	Cadmium ppm	Silver ppm
			New Boulder study			
Median	21	47	150	35	< 2	< 2
Mean	23	50	164	32	< 2	< 2
Std. dev.	12	24	65	12	--	--
No. of sites	11	11	11	10	--	--
			NURE study			
Median	46	31	147	n.a.	<5	<5
Mean	45	37	146	n.a.	<5	<5
Std. dev.	18	16	54	n.a.	--	--
No. of sites	16	16	12	--	--	--
			Boulder River watershed geochemical baseline			
Median	32	35	150	35	<2	<2
Mean	36	42	155	32	<2	<2
Std. dev.	19	21	59	12	--	--
Crustal abundance	68	13	76	1.8	0.16	0.08

tributary drainages sampled in the NURE or Butte 1° x 2° studies using the procedures described in Smith (1994) and Smith and others (1997). The data sets for copper, lead, zinc, and arsenic were each gridded using 3,281-ft (1,000-m) cells from a block of data with a large margin surrounding the Boulder River watershed study area to ensure that the interpolation of the geochemical data surface was not affected by "edge effects." Contoured geochemical maps were constructed from the gridded data using approximate multiples of crustal abundance (Fortescue, 1992; table 1) for four of the deposit-related trace elements. Sample localities appear in figure 1. The maps were trimmed to produce the regional geochemical base maps (figs. 4–7). Data from both regional geochemical studies were used to focus the investigations of the environmental effect of past mining activities in the study area. No regional geochemical maps were constructed for silver and cadmium because the data were censored below the detection limit of 2 ppm, which was substantially above the crustal abundance value (table 1).

Current Studies of Streambed Sediment—Definition of Sources of Contaminants

Total-digestion streambed-sediment data collected from the main tributaries (Basin, Cataract, High Ore, and Jack Creeks, and Uncle Sam Gulch) during this study have been used to produce the ribbon maps superposed on the regional geochemical base maps of the Boulder River watershed study area (figs. 4–7) to provide the basic framework for the interpretation of the distribution of the deposit-related trace elements. The deposit-related trace elements were derived from the weathering of both altered and unaltered rock (O'Neill and others, this volume; McCafferty and others, this volume, Chapter D2) as well as mine waste and mill tailings (Fey and Desborough, this volume, Chapter D4; Martin, this volume, Chapter D3). Ribbon maps for silver and cadmium are presented as figures 8 and 9. Values on the ribbon reflect the concentration of the deposit-related trace element measured at the nearest downstream sample site. Exceptions to this procedure have been made where additional field data supported these changes: (1) data from site *4S* on the Boulder River were assumed to apply downstream to the Jib Mill site (figs. 1 and 2); (2) data from site *46S* on upper Cataract Creek were assumed to apply to the reach of Cataract Creek upstream from the Eva May mine (near the confluence with Hoodoo Creek) to site *46S*; (3) data from site *51S* were assumed to apply to the reach between site *51S* and the confluence with Big Limber Gulch; and (4) data from site *58S*, in the headwaters of High Ore Creek, were assumed to apply to the entire reach upstream from the Comet mine. Data from sites *7S, 10S*, and *14S* on the Boulder River, which were collected in 1997 and 1998, were collected much earlier in the summer following the onset of low-flow conditions than those streambed-sediment samples collected from the Boulder River in 1996, so whenever in conflict with the data from the 1996 sampling, the 1997-98 data were not used to construct the

ribbon maps. Leachable iron concentrations determined using the partial-digestion data have been used to show that iron-rich sediment accumulates downstream from the major mine sites in the watershed (fig. 10). Some of the areas of high leachable iron concentrations were downstream from mine sites and corresponded to areas of low pH observed in the stream reaches at low flow (Nimick and Cleasby, this volume, fig. 3).

Rock-forming trace elements, such as chromium, cobalt, strontium, vanadium, titanium, and the rare-earth elements, showed no abrupt changes in concentration in the streambed sediment downstream from the major mines in the watershed in either the NURE, Butte 1° × 2°, or our data sets. This indicated that the source of the deposit-related trace-element enrichment found in some streambed-sediment samples downstream from historical mining sites in the study area was associated with past mining of the mineral deposits, as was shown in studies in other watersheds affected by historical mining activity (for example, Church and others, 1993, 1997). In the terrace deposits, as will be shown later, premining geochemical baseline data (with the exception of one site) did not show such profound enrichment of the deposit-related trace elements.

Streambed sediment was sampled at several localities in the Boulder River watershed for 2 or 3 consecutive years to evaluate the temporal stability of the geochemical maps. The data set was not sufficiently large to provide a rigorous statistical test, but it was sufficient to provide a general overview of the stability of the geochemical maps. In general, rock-forming trace-element concentrations were stable at the ±10 percent level, whereas the deposit-related trace elements, which were controlled by the percentage of colloidal material in the streambed sediment, varied substantially between the 1996 and the 1997 and 1998 data sets as discussed in paragraph 1 of this section. Data used for the geochemical profile diagrams (figs. 11–13) and streambed-sediment ribbon maps (figs. 4–10) were primarily from samples collected during the 1996 field season. The concentrations of the deposit-related trace elements in the 1997–98 data sets generally were lower than those in the 1996 data set because of the difference in time frames for accumulation of colloids at these sites.

Geochemical Baseline Maps from Streambed Sediment, 1996–1999

Studies of streambed sediment affected by mine drainage in other watersheds (Church and others, 1993, 1997; Kimball and others, 1995; Nordstrom and Alpers, 1999; Smith, 1999; Desborough and others, 2000) have shown that trace elements were sorbed to grain coatings and to iron and aluminum colloids, that is, hydrous iron oxyhydroxides (for example, ferrihydrite), iron oxysulphates (for example, schwertmannite), and aluminum oxysulphates. The results from the present study indicate that the mineralogical residence site for the sorbed deposit-related trace elements was the grain coatings and colloids formed in the water column during mixing of the acidic drainage with more neutral water. Enrichment of iron from colloidal transport and settling on the streambed is a function of the pH of the water, sorption of deposit-related trace elements to the grain coatings and colloids, and the velocity of the stream. The enrichment of colloidal iron is shown on the ribbon map of leachable iron (fig. 10). Strongly elevated concentrations of leachable iron occurred in the stream reaches below the Comet, Crystal, and Bullion mines. The elevated concentrations of metals in Hoodoo and Rocker Creeks also may reflect past mining activity. Strongly elevated concentrations of leachable iron in upper Cataract Creek (fig. 10) appear to be related to wetland areas in the headwaters. Comparison of the partial-digestion data to crustal abundance is problematic because published crustal abundance data were determined from total-digestion results. Therefore, in the discussion following, enrichments of the deposit-related trace elements are expressed using the total-digestion data, whereas discussions of mechanisms of enrichment are drawn from the partial-digestion data. Partial-digestion concentrations were generally lower than the total-digestion concentrations because the deposit-related trace elements in rock-forming particles and sulfide grains, with the exception of galena, were not dissolved by the partial digestion.

Deposit-related trace elements were concentrated in the reaches of the major tributaries and creeks where leachable iron concentrations were generally greater than the 75th percentile (2.0 wt. percent or 20,000 ppm iron) downstream from major mine sites in the Boulder River watershed study area. Copper concentrations in streambed sediment below the Crystal and the Comet mines exceeded 20 times crustal abundance and affected Uncle Sam Gulch and Cataract Creek, and High Ore Creek, respectively, to their confluence with the Boulder River (fig. 4). Elevated concentrations of lead occurred in streambed sediment immediately downstream from the Buckeye and Bullion mine sites and affected upper Basin and Jack Creeks downstream to their confluence (fig. 5). In the stream reaches downstream from the Crystal mine, lead concentrations of greater than 140 times crustal abundance affected Uncle Sam Gulch and Cataract Creek for several miles downstream from the mine site to the confluence with the Boulder River. Streambed sediment in Cataract Creek between the confluence of Hoodoo Creek and Uncle Sam Gulch downstream from the Eva May mine had an elevated lead concentration in excess of 19 times crustal abundance. Lead concentrations exceeded 400 times crustal abundance in streambed sediment in High Ore Creek downstream from the Comet mine and in the Boulder River for at least 2 miles downstream from the confluence with High Ore Creek (fig. 5).

In general, the distribution of arsenic (fig. 7) and silver (fig. 8) in streambed sediment follows that of lead, although silver was more quickly attenuated than lead by instream processes. Elevated concentrations of zinc (fig. 6) and cadmium (fig. 9) were more dispersed downstream from the major mine sites than were copper, lead, arsenic, and silver, which reflect the tendency of cadmium and zinc to sorb less strongly than copper, lead, arsenic, and silver to the hydrous iron oxide

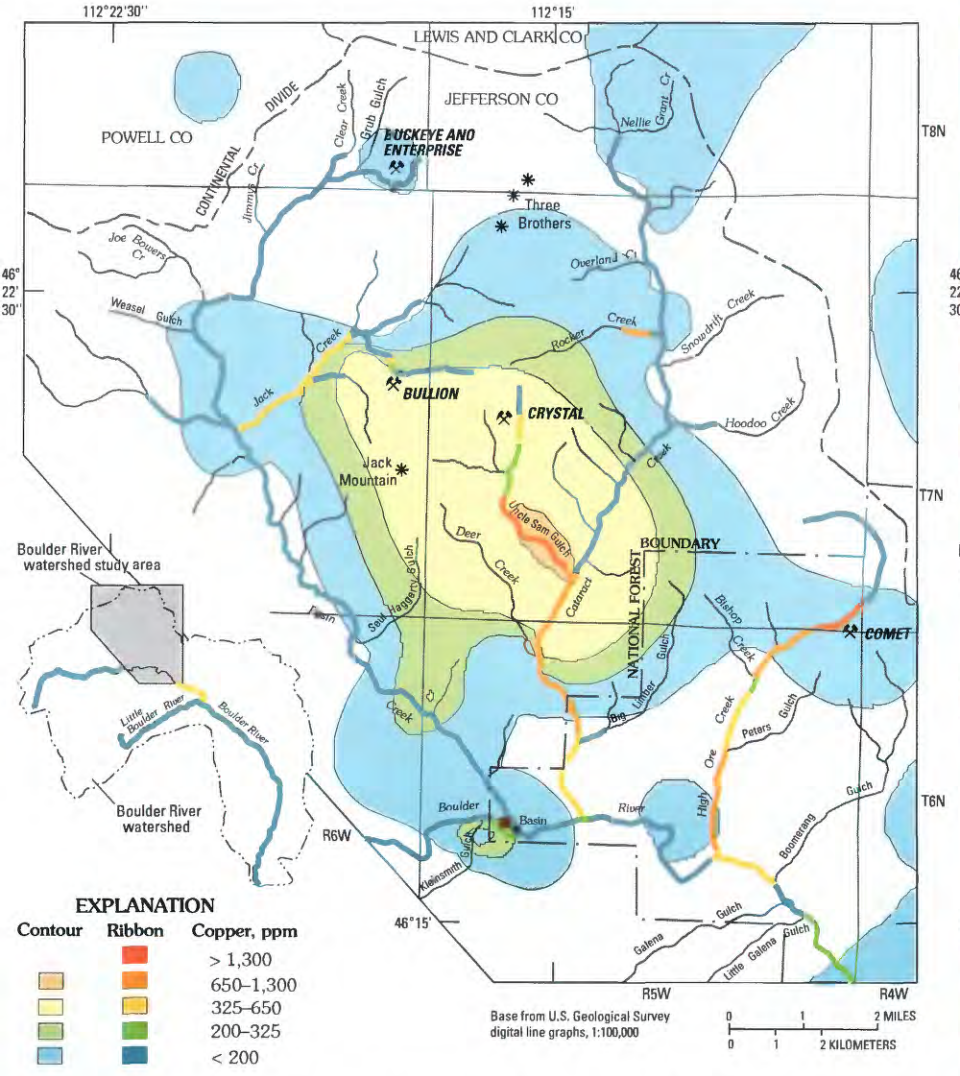

Figure 4. Regional geochemistry for copper from total-digestion data from NURE streambed-sediment data (Broxton, 1980) showing contrast with copper concentrations in streambed sediment from major tributaries. White, sample density insufficient to allow projection of geochemical surface using a 3,281-ft (1,000-m) grid-cell density. Dark-red square, Jib Mill site.

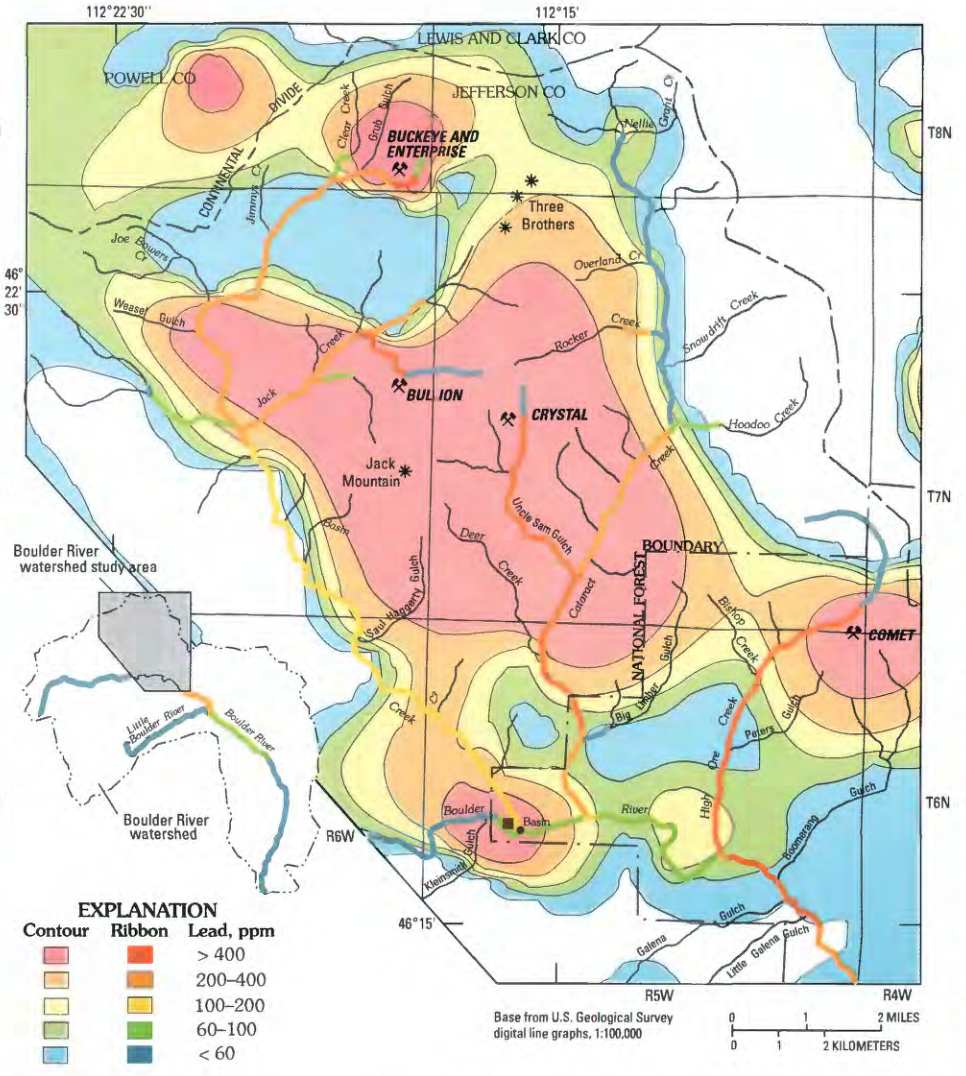

Figure 5. Regional geochemistry for lead from total-digestion data from NURE streambed-sediment data (Broxton, 1980) showing contrast with lead concentrations in streambed sediment from major tributaries. White, sample density insufficient to allow projection of geochemical surface using a 3,281-ft (1,000-m) grid-cell density. Dark-red square, Jib Mill site.

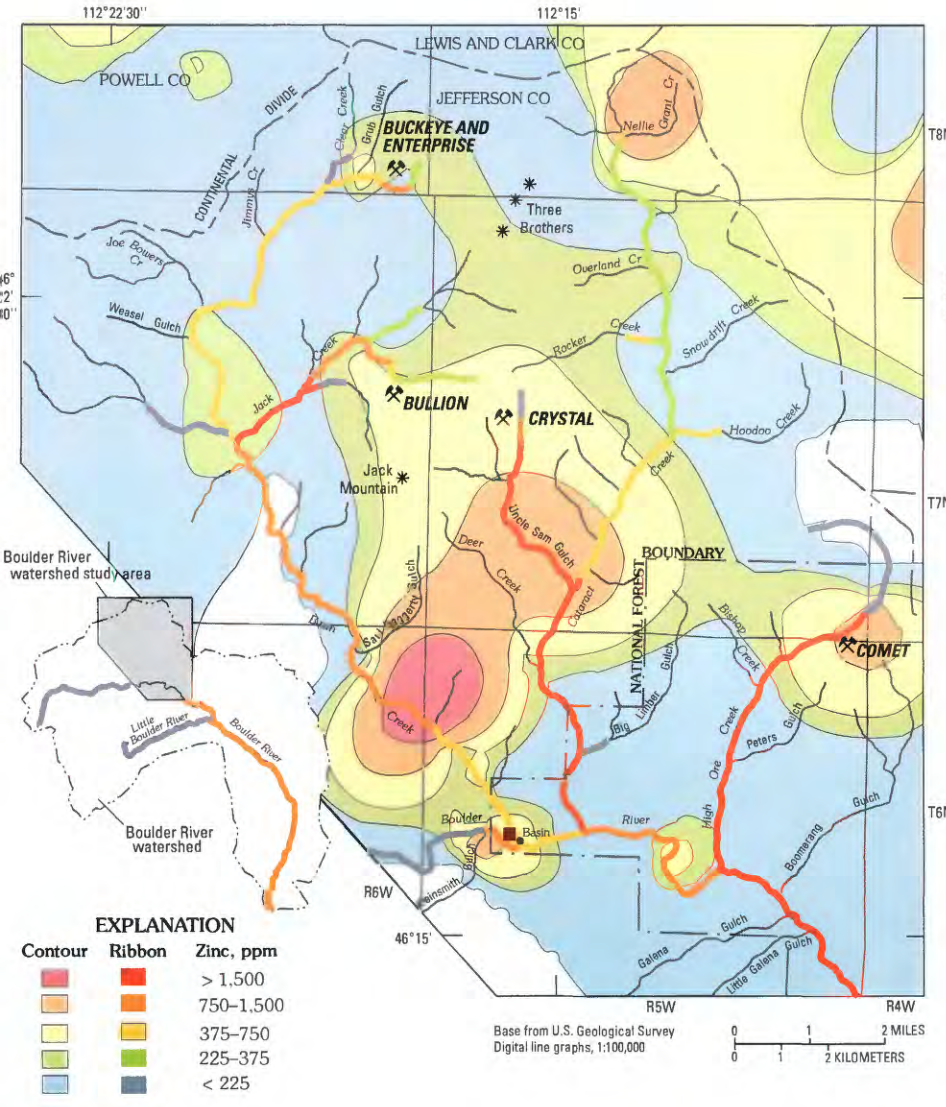

Figure 6. Regional geochemistry for zinc from total-digestion data from NURE streambed-sediment data (Broxton, 1980) showing contrast with zinc concentrations in streambed sediment from major tributaries. White, sample density insufficient to allow projection of geochemical surface using a 3,281-ft (1,000-m) grid-cell density. Dark-red square, Jib Mill site.

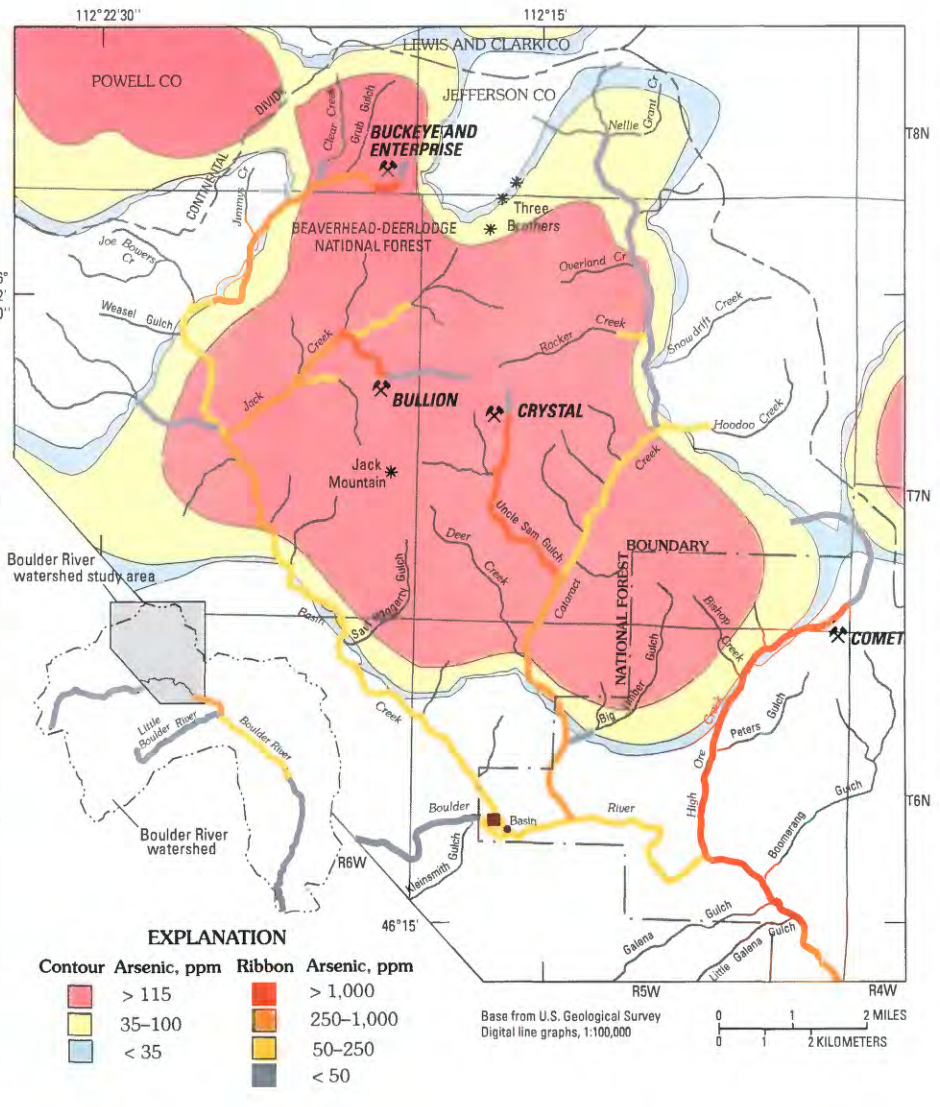

Figure 7. Regional geochemistry for total arsenic from analysis of streambed sediment from Butte 1° x 2° study (McDanal and others, 1985) showing contrast with arsenic concentrations in streambed sediment from major tributaries. White, sample density insufficient to allow projection of geochemical surface using a 3,281-ft (1,000-m) grid-cell density. Dark-red square, Jib Mill site.

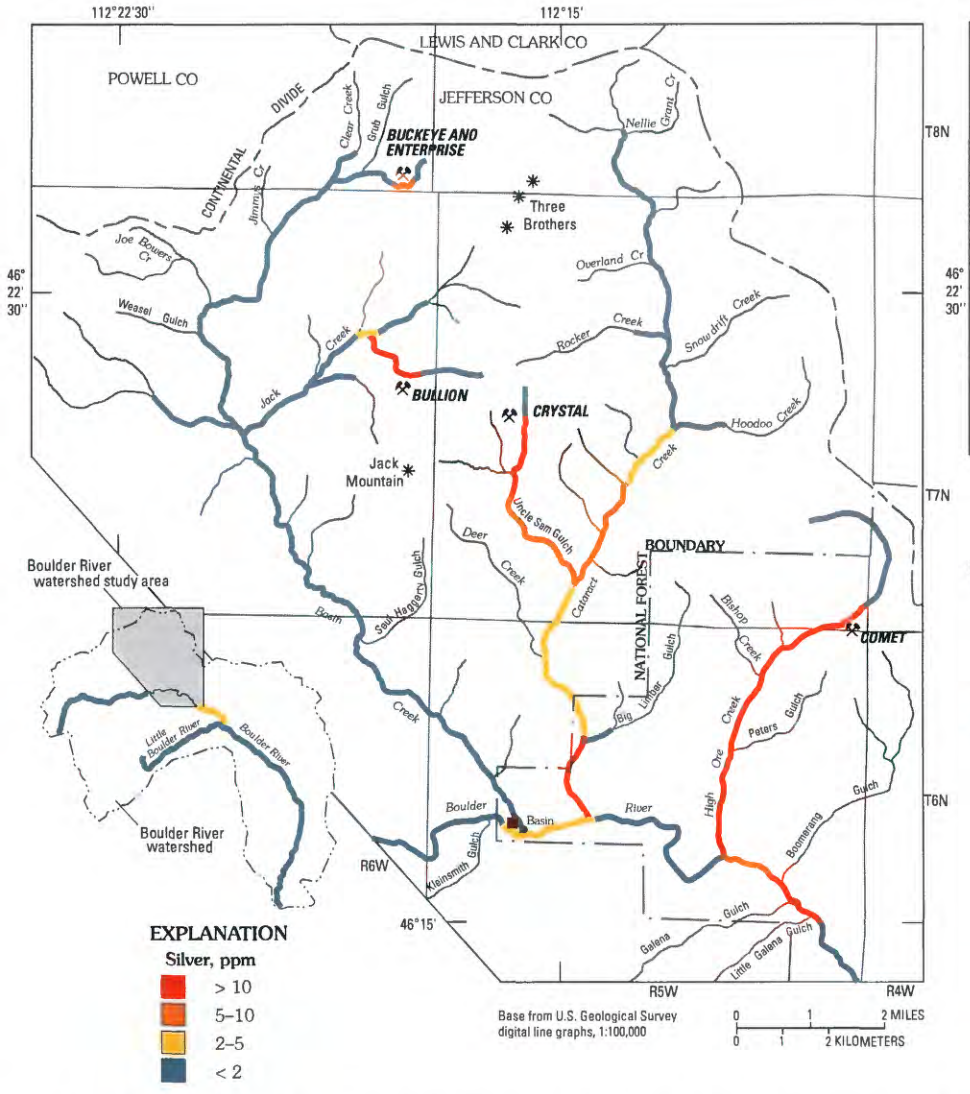

Figure 8. Concentrations of silver from total-digestion data from streambed sediment collected from major tributaries during current study. Dark-red square, Jib Mill site.

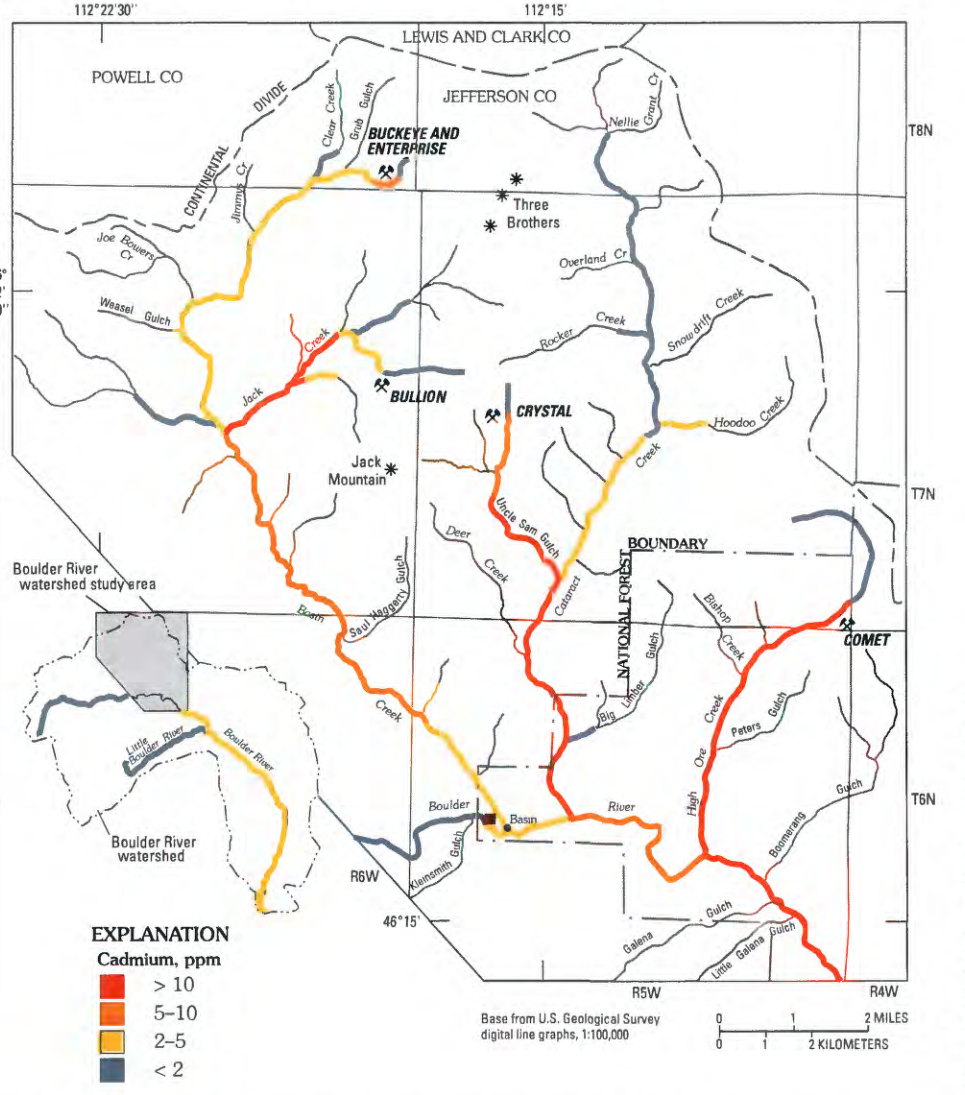

Figure 9. Concentrations of cadmium from total-digestion data from streambed sediment collected from major tributaries during current study. Dark-red square, Jib Mill site.

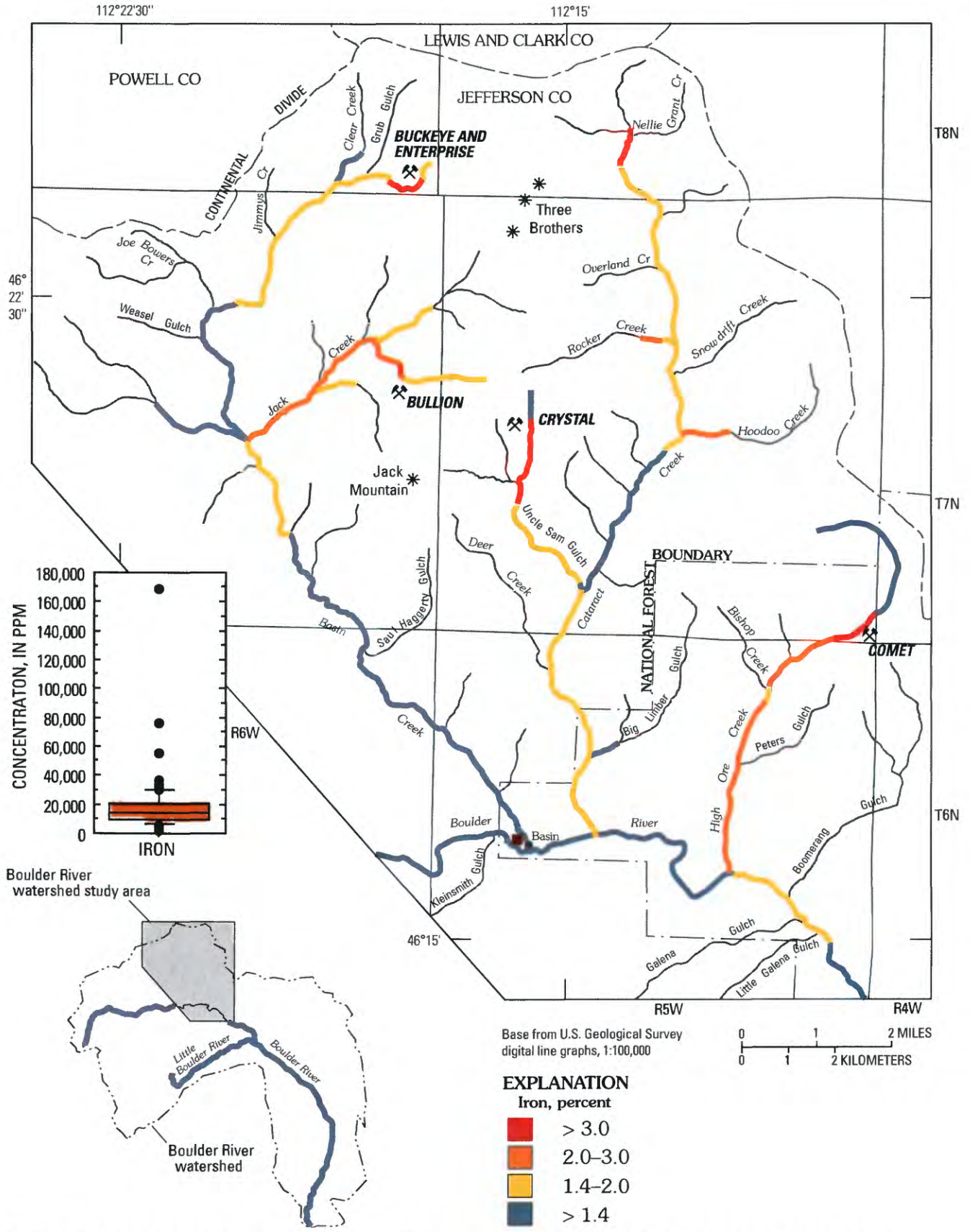

Figure 10. Concentrations of leachable iron in streambed sediment from major tributaries (leachate data). Box plot shows distribution of leachable iron data; 75th percentile is 2.0 weight percent or 20,000 ppm, the 90th percentile is 3.0 weight percent, or 30,000 ppm. Dark-red square, Jib Mill site.

phases (Smith, 1999; Schemel and others, 2000). These same trends were seen in comparison of dissolved cadmium and zinc data with lead and arsenic in surface water (Nimick and Cleasby, this volume). Elevated cadmium and zinc concentrations (10 to more than 20 times crustal abundance) from the Bullion mine affected the lower reaches of Jack Creek and Basin Creek downstream from the confluence of Jack Creek. Elevated cadmium and zinc concentrations from the Crystal mine affected Uncle Sam Gulch and Cataract Creek downstream from Uncle Sam Gulch. The Boulder River had also been affected downstream from Cataract Creek. High Ore Creek downstream from the breached tailings dam at the Comet mine (Gelinas and Tupling, this volume, Chapter E2) had elevated concentrations of cadmium and zinc that affected streambed sediment in High Ore Creek as well as the Boulder River for about 2 miles downstream from the confluence.

Partial-digestion data for copper, lead, zinc, arsenic, silver, cadmium, and antimony are plotted as a function of river distance in figures 11–13. Distance is expressed in miles downstream from the confluence of Basin Creek with the Boulder River, which was assigned an arbitrary value of 15 miles (25 km). Samples from the principal tributary streams are plotted relative to the distance upstream from the confluence of the tributary with the stream it intersects. Streambed-sediment data from other tributary streams not affected by mining are not shown, but they are summarized in table 1. The tie lines show the substantial influx of deposit-related trace elements in the stream from particular mine sites as well as the dispersive effect of downstream transport and dilution by uncontaminated sediment from other tributary basins. This dispersive effect can also be seen on the ribbon maps (figs. 4–10). The concentrations of the deposit-related trace elements in the seven pairs of streambed-sediment samples from the north and south sides of the Boulder River (sites *5S*, *6S*, *8S*, *9S*, *11S*, *12S*, and *13S*; fig. 1) were averaged to produce the ribbon maps and the geochemical profile diagrams (figs. 4–10, 11–13). The data from the Boulder River streambed sediment are plotted on all of the geochemical profile diagrams (figs. 11–13) so that the streambed-sediment contribution from each of the three principal tributaries to the Boulder River can be evaluated. Additional amounts of deposit-related trace elements were being contributed by both the dissolved and suspended loads (Nimick and Cleasby, this volume).

Major sources of mine waste sampled during this study (fig. 2) are also indicated on the geochemical profile diagrams. From the study of mine sites, Fey and Desborough (this volume) identified and ranked several major mine sites that contained substantial concentrations of deposit-related trace elements. Statistical data for deposit-related trace-element concentrations from five sites are summarized in table 2. Samples from three of the sites, Bullion, Buckeye, and Comet, represent a large enough number of mill tailings samples to be statistically meaningful. We use the 75th percentile as an estimate of the concentration of the contaminants in figures 11–13 because mixing with soil and streambed sediment in many of the samples had reduced the concentrations of the deposit-related trace elements. Therefore, the median value was judged to not be a good indicator of the concentration of the deposit-related trace elements from the source.

Basin Creek

Geochemical data for leachable copper, lead, zinc, arsenic, silver, cadmium, and antimony from streambed sediment from the Basin Creek geochemical profile are in figure 11. In addition to the data from the Boulder River, three stream reaches are distinguished on this diagram: (1) Basin Creek, a major contaminated tributary of the Boulder River, (2) Jack Creek, and (3) the unnamed tributary to Jack Creek that drains the Bullion mine, hereafter referred to as Bullion Mine tributary (fig. 2). Three major anthropogenic sources of deposit-related trace elements lie along Basin Creek: the Buckeye and Enterprise mines in the headwaters of Basin Creek, the Bullion mine in the headwaters of the Bullion Mine tributary, and the Bullion smelter reservoir on lower Jack Creek (site *15B*, fig. 2). Mill tailings and mine waste from both the Buckeye and Enterprise mine sites and the Bullion mine site received high rankings. Both were recommended for remedial action (Fey and Desborough, this volume).

Exposed sulfidic wastes from the Buckeye and Enterprise mines caused an increase in deposit-related trace-element concentrations in streambed sediment (site *21S* at about river mi 2; fig. 11) in the upper reaches of Basin Creek (Cannon and others, this volume, Chapter E1). Metesh and others (1994) reported surface water draining from this site with a pH of 3.12. Cannon and others (this volume) reported pH values of 3.1 to 4.1 that varied by season at this site. Copper, lead, zinc, and arsenic in the total-digestion data from site *21S* below the Buckeye and Enterprise mines were enriched by factors of 4.1, 46, 4.5, and 129 respectively over the geochemical baseline (table 1). Concentrations of the deposit-related trace elements in streambed sediment decreased steadily until upstream from the confluence with Jack Creek at site *24S* (river mi 7.5). The Bullion mine (fig. 2), on the Bullion Mine tributary of Jack Creek, was the major source of streambed-sediment contamination in Jack Creek (river mi 6). Metesh and others (1994) reported mine adit drainage at this site with a pH of 2.58, and Desborough and others (2000) reported schwertmannite, a hydrous iron sulfate, in streambed sediment below the Bullion mine. Schwertmannite forms in acidic waters in the pH range of 2.8 to 4.5 (Bigham and others, 1996). Concentrations of copper, lead, zinc, and arsenic were enriched in streambed sediment below the Bullion mine (site *33S*) by factors of 10, 25, 4.6, and 66 respectively (table 1). Fluvial tailings in overbank deposits downstream (*35S–37S*), presumably deposited after the breach of the tailings impoundments at the mine site, had deposit-related trace-element concentrations that substantially exceeded the enrichment factors found downstream (*34S–36S*) along Bullion Mine tributary. The addition of sediment from upper Jack Creek was responsible for the dilution of the deposit-related trace-element concentrations in streambed sediment immediately downstream from the confluence

Table 2. Statistical summaries of the mine waste data.

[75th percentile was used as the best estimate of the composition of the contaminant]

Statistical data	Copper ppm	Lead ppm	Zinc ppm	Arsenic ppm	Cadmium ppm	Silver ppm
Jib Mill tailings[1] (n = 18)						
Minimum	250	200	110	280	< 2	< 2
25th percentile	310	300	200	360	< 2	< 2
Median	360	330	250	400	< 2	< 2
75th percentile	**470**	**360**	**340**	**460**	**< 2**	**< 2**
Maximum	790	470	520	550	< 2	< 2
Bullion Mill tailings[2] (n = 155)						
Minimum	44	190	61	230	1	6
25th percentile	92	1,900	130	2,000	8	21
Median	140	2,600	170	2,500	11	27
75th percentile	**280**	**4,700**	**250**	**4,600**	**20**	**50**
Maximum	2,700	16,000	18,000	13,000	150	130
Buckeye Mill tailings[3] (n = 67)						
Minimum	28	120	76	210	3	3
25th percentile	100	2,200	160	6,400	33	22
Median	160	9,800	250	13,000	69	56
75th percentile	**260**	**17,000**	**450**	**20,000**	**118**	**87**
Maximum	4,800	93,000	28,000	63,000	370	290
Crystal mine wastes[2] (n = 9)						
Minimum	190	510	360	840	< 2	6
25th percentile	220	830	630	1,500	< 2	7
Median	400	1,000	640	2,400	< 2	9
75th percentile	**660**	**1,500**	**770**	**3,400**	**< 2**	**13**
Maximum	1,600	2,300	8,000	11,000	< 2	26
Comet Mill tailings[4] (n = 149)						
Minimum	30	90	200	67	2	8
25th percentile	500	4,600	1,400	3,900	11	65
Median	830	9,200	2,400	6,000	20	110
75th percentile	**1,300**	**15,000**	**5,300**	**8,000**	**57**	**160**
Maximum	4,300	59,000	50,000	22,000	740	460

[1]Unruh and others (2000).
[2]Fey and others (2000).
[3]Fey, Church, and Finney (1999).
[4]Fey and Church (1998).

of Bullion Mine tributary with Jack Creek. Impoundment of these tailings and streambed sediment in an abandoned beaver pond at site *14B* just downstream from the confluence with the Bullion Mine tributary, and in an old reservoir at site *15B* (upstream from site *41S*), which was built to provide water for the Bullion smelter that operated from 1904 to 1906 (Rossillon and Haynes, 1999), trapped contaminated sediment in the lower reaches of Jack Creek.

Jack Creek provided a large contribution to the streambed sediment in Basin Creek, as can be seen by the major increase in deposit-related trace-element concentrations at the confluence of Jack Creek with Basin Creek at about river mi 7.6 (site *26S*, fig. 11). Deposit-related trace-element concentrations decreased slowly downstream in streambed sediment of Jack Creek from the confluence with the Bullion Mine tributary to the confluence with Basin Creek. The streambed sediment in Jack Creek was highly enriched in leachable iron (fig. 10) resulting from the acid mine drainage from the Bullion mine (Kimball and others, this volume).

The effect of deposit-related trace elements from the Bullion mine on the streambed sediment concentrations of copper, zinc, arsenic, and cadmium in Basin Creek downstream from the confluence with Jack Creek substantially overwhelmed the deposit-related trace-element concentrations in the streambed

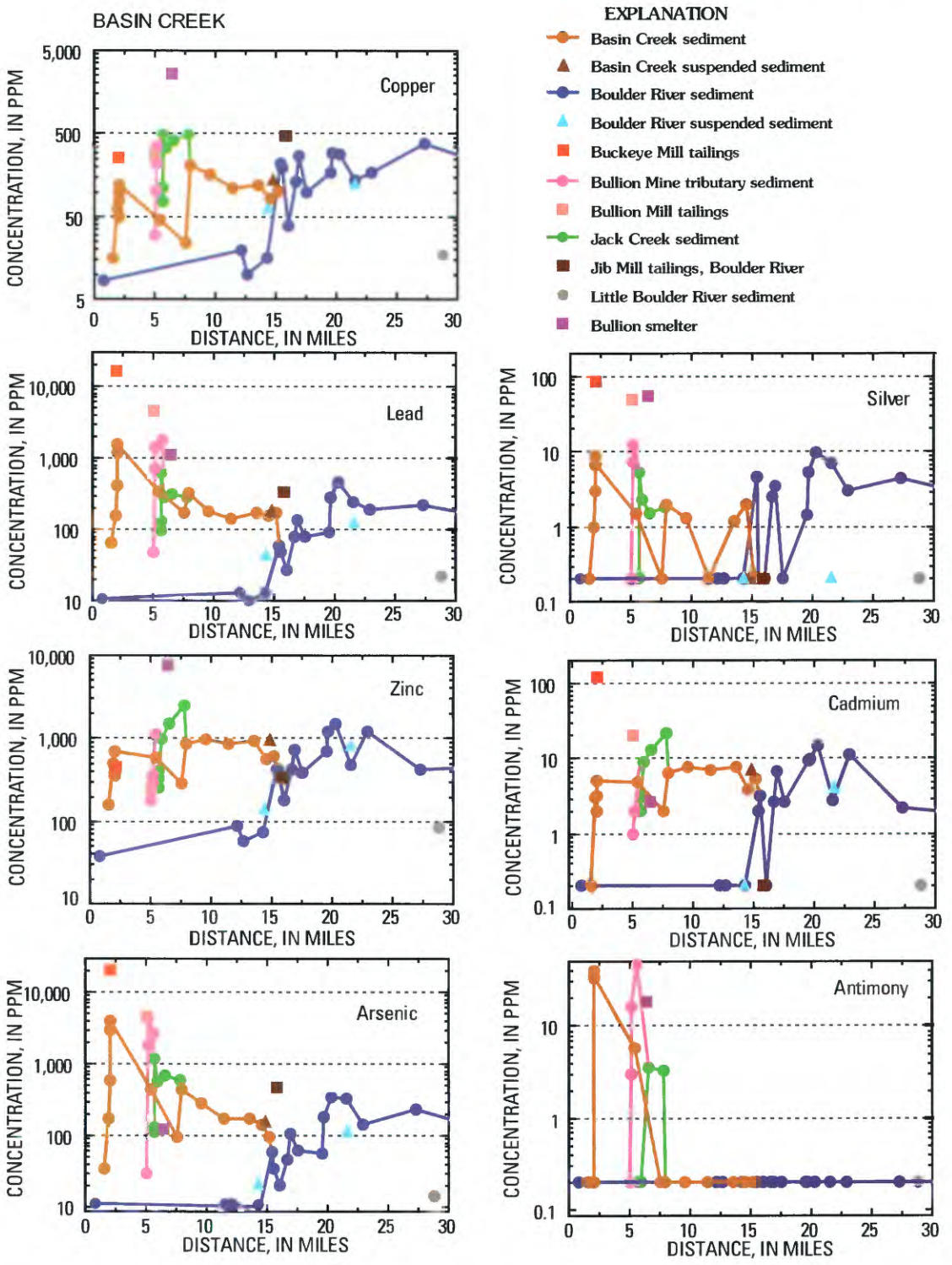

Figure 11. Concentrations of copper, lead, zinc, arsenic, silver, cadmium, and antimony determined in the partial digestion of streambed sediment from Basin Creek and its tributaries, and their effect on streambed sediment of Boulder River. Trace-element concentrations determined for major sources within the watershed are also shown. Data plotted against distance; upstream always to left regardless of actual direction stream flows. Samples that represent streambed sediment from active stream or river channel are indicated by discrete solid symbols and connected by tie lines. Concentrations of antimony, cadmium, and silver are censored at 2 ppm and arsenic at 5 ppm.

sediment that were derived from the Buckeye and Enterprise mines. Concentrations of three trace elements increased substantially downstream from the confluence of Jack Creek with Basin Creek (sites *24S* and *26S*): copper from 29 to 130 ppm, zinc from 380 to 580 ppm, and arsenic from 140 to 330 ppm, in the total-digestion data and copper from 24 to 210 ppm, zinc from 290 to 840 ppm, and arsenic from 98 to 430 ppm in the partial-digestion data. Lead concentrations in the streambed sediment remained relatively constant at about 200 ppm in the total-digestion data, but lead concentrations increased in the partial-digestion data from 170 to 320 ppm. Differences in the total-digestion data and the partial-digestion data probably are not analytical but are more likely the result of the difference in sample size used for the analytical procedure (0.2 g for the total digestion versus 2.0 g for the partial digestion; Fey, Unruh, and Church, 1999). These differences between data sets are generally not large or very important in an absolute sense because the data always exhibit the same trends. The differences are largely the result of the "nugget effect," that is, an observed difference when elements are concentrated in a single grain, in this case the deposit-related trace elements in the iron colloids.

Downstream from the confluence of Basin Creek with Jack Creek, deposit-related trace-element concentrations were diluted by uncontaminated streambed sediment that had lower concentrations of deposit-related trace elements entering Basin Creek from other tributary drainages. At the confluence of Basin Creek and Boulder River (site *31S*), copper, lead, and arsenic concentrations in streambed sediment decreased from 130 to 93 ppm, from 210 to 160 ppm, and from 330 ppm to 110 ppm, respectively. Zinc concentrations increased slightly downstream from the confluence with Jack Creek from 580 to 600 ppm. Concentrations of leachable zinc in streambed sediment were about 900 ppm downstream and decreased near the confluence with the Boulder River to about 600 ppm.

As shown in figure 11, the data from the suspended sediment from the Boulder River upstream from the confluence with Basin Creek (*4S*) and from Basin Creek just upstream from the confluence (*30S*) with the Boulder River indicated that the total concentration of deposit-related trace elements in the suspended sediment was very similar to that found in the leachable phase of the streambed sediment in the stream reach where the suspended sediment was sampled. Such a correlation would be expected since the suspended sediments are dominated by the colloidal components extracted during the partial digestion. Concentrations of deposit-related trace elements were elevated relative to where they were collected because the suspended-sediment samples, which were collected in May 1997, represented streambed sediment that had accumulated upstream during low flow in 1996.

Cataract Creek

In addition to the data from the streambed-sediment study, extensive water-quality data have been collected (Nimick and Cleasby, this volume) and a metal-loading study conducted on Cataract Creek (Kimball and others, this volume; Cleasby and others, 2000). The results of the metal-loading study clearly showed little effect on the streambed-sediment geochemistry of Cataract Creek by past mining upstream from the Eva May mine, located near the confluence of Hoodoo Creek (river mi 10.5, fig. 12). Rocker Creek was contaminated by past mining in its headwaters (probably from the Ada mine), but little of that deposit-related trace-element contamination was transported into Cataract Creek as streambed sediment as evidenced by the NURE data from lower Rocker Creek (Broxton, 1980). The contamination likely was trapped in the low gradient reach of Rocker Creek upstream from the confluence and diluted by the relatively uncontaminated streambed sediment in Cataract Creek upstream from the Eva May mine site. In the reach from the Hoodoo Creek confluence (using the data from site *46S*, river mi 10) downstream to Uncle Sam Gulch (site *49S*, river mi 12.5), streambed-sediment concentrations of copper increased from 47 to 190 ppm, lead from 47 to 240 ppm, zinc from 280 to 610 ppm, and arsenic from 63 to 150 ppm. In the leachable phase, partial-digestion data for copper increased from 44 to 110 ppm, lead from 49 to 220 ppm, zinc from 250 to 440 ppm, arsenic from 41 to 96 ppm, silver from <1 to 5 ppm, and cadmium from 1.5 to 2.7 ppm. The increase in the deposit-related trace-element concentrations in the streambed sediment, by about a factor of four in this stream reach, was not caused by streambed sediment from Hoodoo Creek or by the influx of tailings from the Eva May mine site, even though direct field evidence showed transport of tailings from the Eva May mine site into Cataract Creek. The August 1997 metal-loading study (Kimball and others, this volume; Cleasby and others, 2000) indicated that the Cataract mine and mill tailings sites and the upper and lower Hattie Ferguson mine sites were probable sources of deposit-related trace elements in this reach. Additional sources of mine waste on private property, to which we did not have access, were located along Cataract Creek near the stream bank, such as the Morning Glory mine (Martin, this volume).

The Crystal mine (fig. 2, table 2), located in the headwaters of Uncle Sam Gulch (fig. 12, river mi 10), was the major source of deposit-related trace elements in the streambed sediment of Cataract Creek (table 2). Mine wastes from the Crystal mine were ranked as a moderate source of deposit-related trace elements (Fey and Desborough, this volume). Copper, lead, zinc, arsenic, silver, and cadmium concentrations in streambed sediment increased dramatically directly below the mine (sites *54S* and *55S*, river mi 10.5). Additional enrichments of copper and zinc occur at the confluence of Uncle Sam Gulch with Cataract Creek (site *57S*, river mi 12.5), but lead and arsenic concentrations decrease. Desborough and others (2000) reported the presence of schwertmannite in streambed sediment from Uncle Sam Gulch immediately downstream from the Crystal mine adit. The pH of Uncle Sam Gulch downstream from the Crystal mine was 3.2–3.5 (Metesh and others, 1995; Nimick and Cleasby, 2000), which is within the pH stability field of

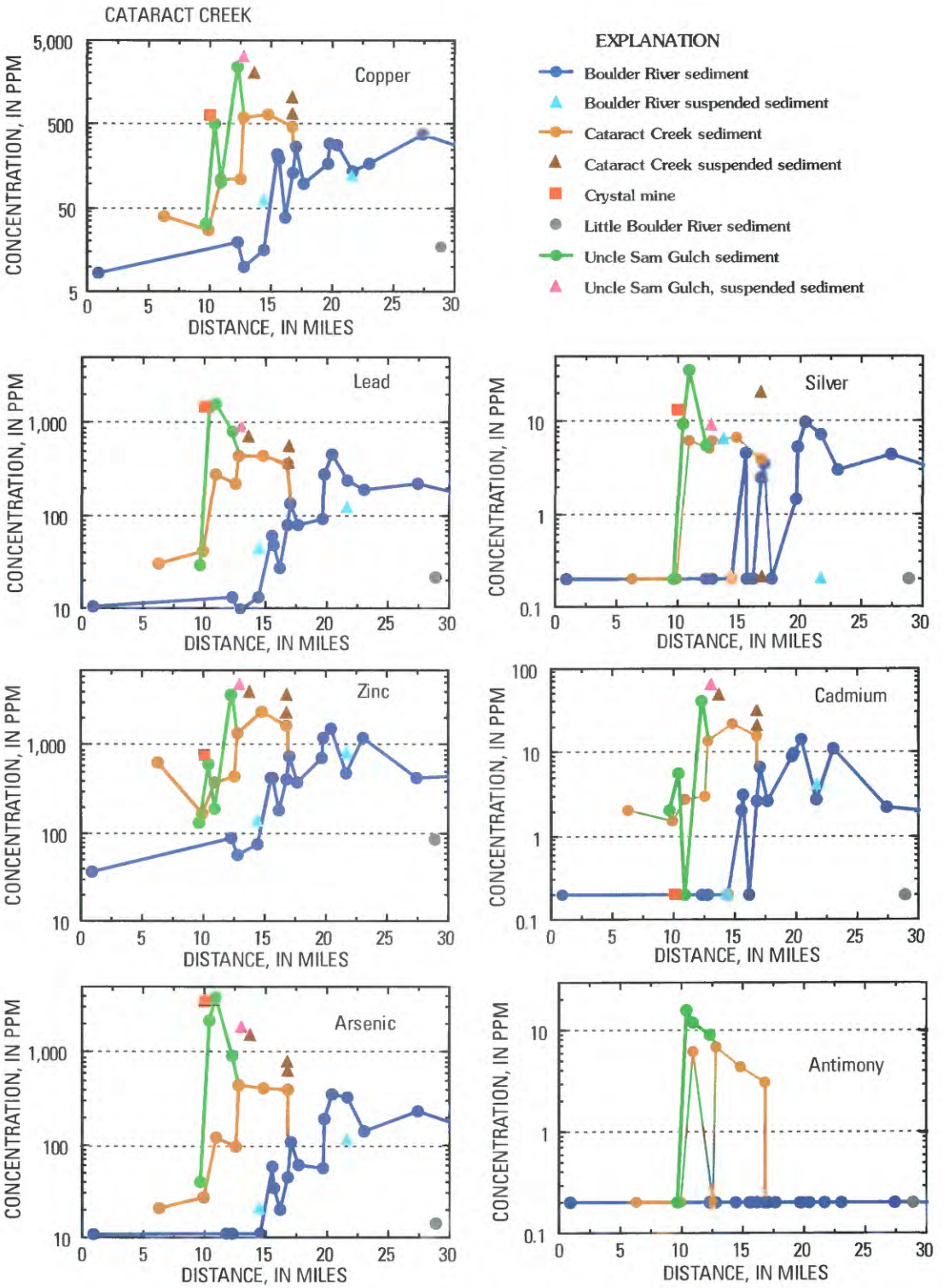

Figure 12. Concentrations of copper, lead, zinc, arsenic, silver, cadmium, and antimony determined in the partial digestion of streambed sediment from Cataract Creek and its tributaries, and their effect on streambed sediment of Boulder River. Trace-element concentrations determined for major sources within the watershed are also shown. Data are plotted against distance; upstream always to left regardless of actual direction stream flows. Samples that represent streambed sediment from active stream or river channel are indicated by discrete solid symbols and connected by tie lines. Concentrations of antimony, cadmium, and silver are censored at 2 ppm and arsenic at 5 ppm.

schwertmannite (Bigham and others, 1996); pH increased to 7.3 ± 0.2 at the confluence with Cataract Creek at low flow (Nimick and Cleasby, this volume, fig. 3). The enrichment of deposit-related trace elements in the streambed sediment of Uncle Sam Gulch upstream from the confluence with Cataract Creek at site *57S* is as follows: copper, 72; lead, 26; and zinc, 25; and arsenic, 37 times the geochemical baseline (table 1). Suspended-sediment concentrations collected from site *57S* (river mi 12.5) exceeded the concentrations of deposit-related trace elements in streambed sediment with enrichment factors of 93 for copper, 24 for lead, 32 for zinc, and 49 for arsenic relative to the geochemical baseline (table 1). Suspended-sediment concentrations decreased by a factor of 2 to 3.5 at site *57S*. Enrichment factors in the streambed sediment at site *53S* are as follows: copper, 14 fold; lead, 13 fold; zinc, 6.7 fold; and arsenic, 17 fold. Relative to the suspended-sediment concentrations at site *53S*, the concentrations in the suspended sediment were similar for lead, arsenic, and silver, but enriched by a factor of 2 for copper, a factor of 3 for zinc, and a factor of 3.5 for cadmium. These enrichment factors indicate that differential transport of these three deposit-related trace elements occurred in the suspended-sediment load.

The streambed sediment contributed by Uncle Sam Gulch increased the concentrations of deposit-related trace elements in streambed sediment in Cataract Creek downstream from the confluence (site *50S*, river mi 12.6). Copper was enriched from 6 to 20, lead from 7 to 14, zinc from 4 to 15, and arsenic from 4 to 16 times the geochemical baseline (table 1). Deposit-related trace-element concentrations in suspended sediment at site *50S* were substantially elevated upstream from the concentrations in streambed sediment, which indicated that much of the deposit-related trace-element load was transported in the suspended sediment as colloids. Little change was evident in the concentrations of copper (420 ppm, a 13-fold enrichment), lead (320 ppm, a 9-fold enrichment), zinc (1,450 ppm, a 10-fold enrichment) and arsenic (460 ppm, a 13-fold enrichment) in streambed sediment in Cataract Creek between Uncle Sam Gulch (site *50S*) and the Boulder River (site *53S*). We interpret these data to indicate that the Crystal mine site on Uncle Sam Gulch was the major source of contaminants in Cataract Creek. Results from the metal-loading study (Cleasby and others, 2000; Kimball and others, this volume) showed that Uncle Sam Gulch was the source of 92 percent of the zinc load and 66 percent of the copper load in Cataract Creek.

High Ore Creek

The major source of deposit-related trace elements in streambed sediment of High Ore Creek was the Comet mine (Fey and Church, 1998), an open-pit mine with extensive underground workings located near the headwaters (fig. 2). A tailings dam constructed across the drainage adjacent to the Comet mine was breached (Gelinas and Tupling, this volume). Mill tailings had washed downstream from the mine site, contaminating the High Ore Creek watershed (river mi 16; Rich and others, this volume). The tailings in the breached impoundment were removed in 1998 by the Montana Department of Environmental Quality and stored in the open pit at the Comet mine. The downstream fluvial tailings were removed by the U.S. Bureau of Land Management during the course of this study (Gelinas and Tupling, this volume). Downstream of the breached tailings dam, streambed sediment had deposit-related trace-element concentrations of 2,000 ppm copper, 5,700 ppm lead, 17,000 ppm zinc, 8,100 ppm arsenic, 52 ppm silver, and 150 ppm cadmium (site *59S*, river mi 20; fig. 13). Enrichment relative to the geochemical baseline values (table 1) was: copper, more than 60-fold; zinc, more than 110-fold; lead, more than 160-fold, and arsenic, cadmium, and silver by more than 200-fold. Sediment from Bishop Creek, the major tributary entering High Ore Creek between sites *60S* and *61S* (river mi 17), resulted in some dilution of the deposit-related trace elements in streambed sediment of High Ore Creek. Deposit-related trace-element concentrations in streambed sediment at the mouth of High Ore Creek (site *63S*, river mi 21) were reduced to about 740 ppm copper, 1,600 ppm lead, 10,000 ppm zinc, 4,300 ppm arsenic, 34 ppm silver, and 69 ppm cadmium in October 1996 when High Ore Creek was first sampled. In general, copper was diluted by a factor of 2.7, lead by a factor of 3.6, zinc by a factor of 1.7, and arsenic by a factor of 1.9. Overbank deposits of fluvial tailings from the Comet mine, identified on the basis of the lead isotopic signature (Rich and others, this volume), were found on a low terrace at site *14S* on the Boulder River. These deposits probably formed during the breach of the mill tailings dam at the Comet mine site. High Ore Creek was a minor source of streambed sediment, but it was a major source of deposit-related trace-element contaminants to the streambed sediment of the Boulder River.

Boulder River

Streambed-sediment samples were collected systematically at sites along the Boulder River upstream, through, and downstream of the Basin and Boulder mining districts, about 100 ft upstream and downstream from the confluences of Basin, Cataract, and High Ore Creeks. At sites *5S, 6S, 8S, 9S, 11S, 12S*, and *13S*, samples were collected from both the north and south sides of the Boulder River. Only the average values from these sites are shown in figure 14*A*. The objective of this sampling plan was to evaluate the efficiency of mixing of sediment from the major tributaries and the effect of flow and velocity on the accumulation of colloidal material on the streambed of the Boulder River. Samples from the north and south sides of the Boulder River had major differences in concentrations: higher concentrations of leachable iron and deposit-related trace elements occurred in streambed sediment deposited on the lower velocity side of the reach where colloidal particles settled. Basin, Cataract, and High Ore Creeks enter the Boulder River from the north. As shown by the data (Rich and others, this volume), mixing in the fluvial system at a distance of 100 ft downstream from the confluence was not complete at that distance from any of the three confluences.

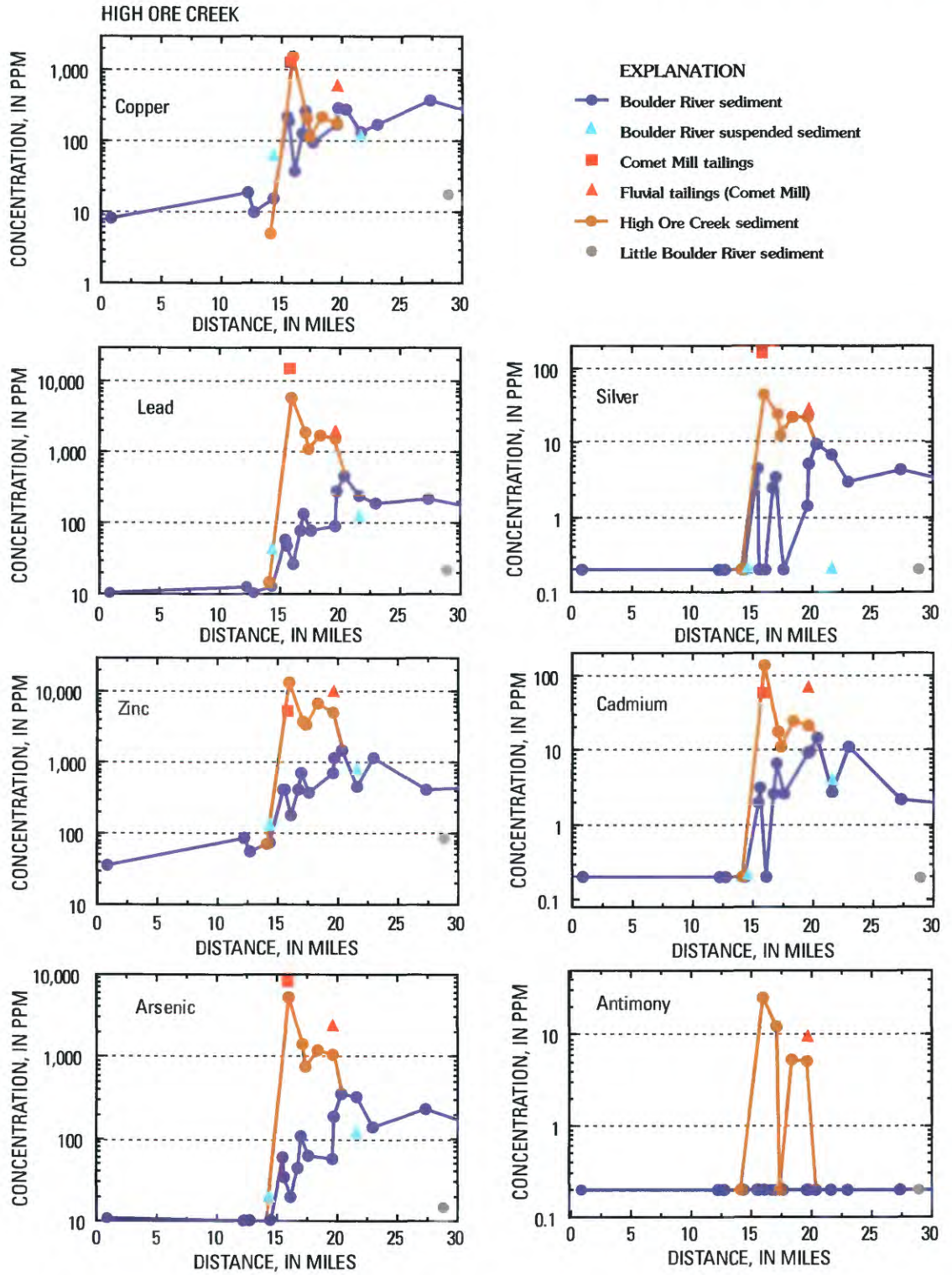

Figure 13. Concentrations of copper, lead, zinc, arsenic, silver, cadmium, and antimony determined in the partial digestion of streambed sediment from High Ore Creek and its tributaries, and their effect on streambed sediment of Boulder River. Trace-element concentrations determined for major sources within the watershed are also shown. Data are plotted against distance; upstream always to left regardless of actual direction stream flows. Samples that represent streambed sediment from active stream or river channel are indicated by discrete solid symbols and connected by tie lines. Concentrations of antimony, cadmium, and silver are censored at 2 ppm and arsenic at 5 ppm.

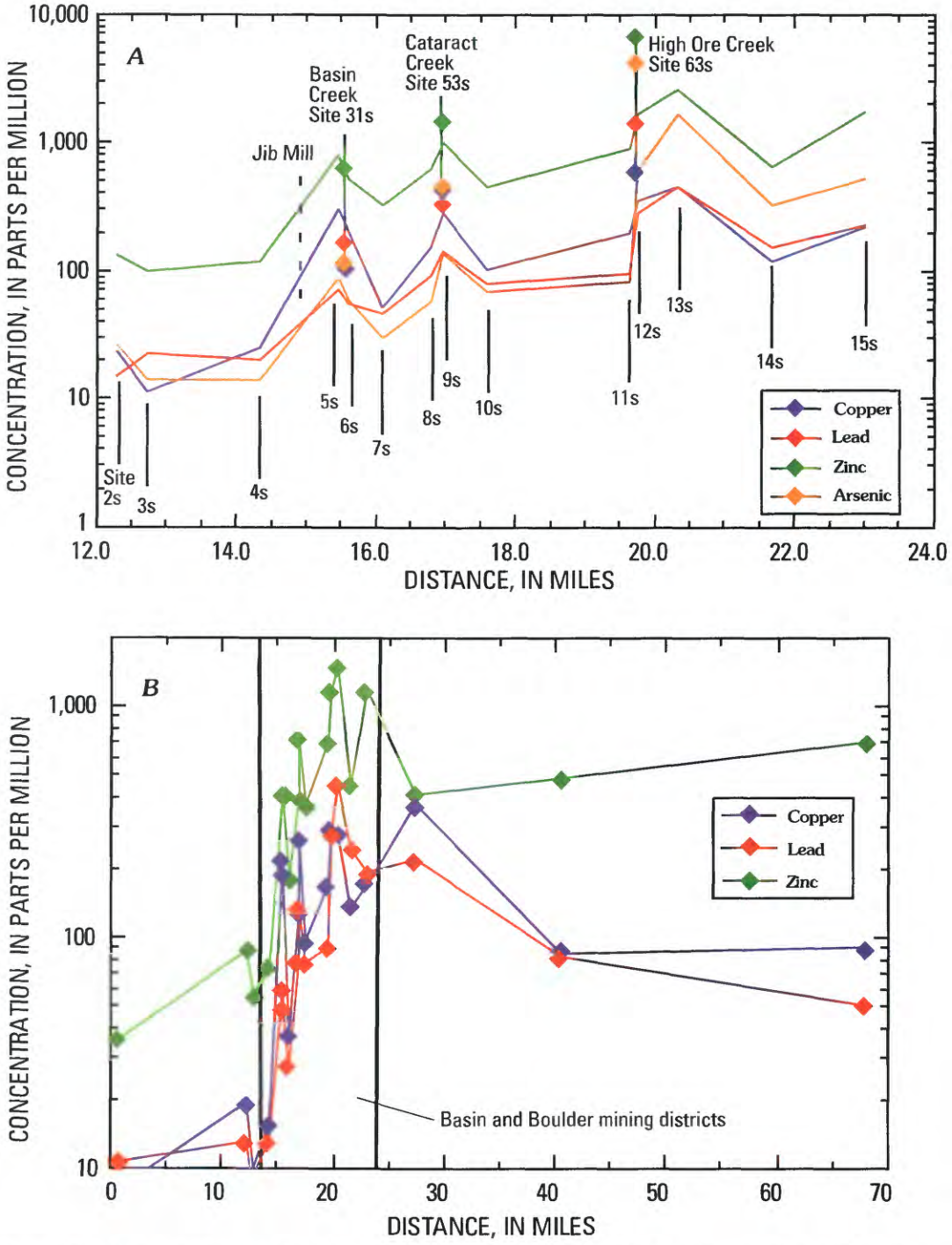

Figure 14. Concentration profiles of copper, zinc, lead, and arsenic. *A*, Determined in the total digestion of streambed sediment in Boulder River. Data plotted against distance, upstream always to left. Data for samples from both north and south sides of river at sites *5S*, *6S*, *8S*, *9S*, *11S*, *12S*, and *13S* have been averaged to provide a continuous profile of element concentrations in Boulder River streambed sediment. Concentration data from Basin Creek (site *31S*), Cataract Creek (site *53S*), and High Ore Creek (site *63S*) are shown as diamonds to indicate concentrations of these deposit-related trace elements in streambed sediment that was added by the three major tributaries. Concentrations of arsenic are censored at 5 ppm. *B*, Determined from partial digestion of streambed sediment in Boulder River. Arsenic profile (not shown) closely mimics that of lead.

Concentrations of copper, lead, zinc, and arsenic were not systematically higher on either the north or the south side of the Boulder River.

The distributions of copper, lead, zinc, and arsenic in Boulder River streambed sediment showed similar abundance patterns; concentrations increased downstream from each of the confluences (fig. 14*A*). Variation between sites downstream of the confluences was within the variation we would expect from stream-sediment sampling. The increase in concentrations at site *5S*, upstream from the confluence of Basin Creek, can be explained by contributions from the Jib Mill site and several small prospects in the area between sites *4S* and *5S* (fig. 1). Downstream from the confluence with Basin Creek (site *6S*), the deposit-related trace-element concentrations decreased slightly. This is reasonable in view of the fact that the deposit-related trace-element concentrations in Basin Creek at site *31S* were similar for arsenic and zinc and lower for copper than those in the Boulder River at site *5S* (fig. 14*A*). Only lead appeared to be significantly enriched in Basin Creek relative to the Boulder River. Downstream from the Basin Creek confluence, deposit-related trace-element concentrations in Boulder River streambed sediment decreased by more than a factor of two (except lead) at site *7S* (river mi 16.2). Samples from site *7S* were collected in 1997 from a deep pool that had accumulated significantly more detrital sediment relative to other sites sampled on the Boulder River. Thus, the decrease in deposit-related trace-element concentrations at this site was atypical of the other sites used for comparison. A minor increase in deposit-related trace-element concentrations occurred between sites *6S* and *8S*; it was not significant.

Deposit-related trace-element enrichment between sites *10S* and *11S* (both upstream from High Ore Creek) appears to be confined primarily to copper and zinc. The downstream enrichment of the more soluble metals suggested that the enrichment at site *11S* was most likely due to sedimentation of colloidal particles and sorption processes within the Boulder River rather than enrichment from an outside source. Samples from site *10S* were collected in 1997.

Deposit-related trace-element concentrations increased dramatically immediately downstream from High Ore Creek (site *12S*, fig. 14*A*) and continued to increase for at least 0.5 mile to site *13S* (river mi 20.7). Deposit-related trace-element concentrations then decreased significantly at site *14S* (1997 data; river mi 21.7), but increased at site *15S* (river mi 23). We had difficulty in obtaining sample material at site *14S*, which was on the outside of a meander where streambed sediment did not tend to accumulate. The data between sites *13S* and *15S* showed a gradual decrease in concentration; these data were used to define the concentration trend for the ribbon maps (figs. 4–9).

The effect of historical mining within the Basin mining district on the concentrations of copper, lead, and zinc in streambed sediment of the Boulder River is clear from fig. 14*B*. Note the substantial increase in concentrations of these deposit-related trace elements in the streambed sediment of the Boulder River as it flowed through the Basin and Boulder mining districts. Note also that lead concentrations were diluted as a function of distance downstream from the mining districts (that is, downstream from river mi 40). Arsenic also showed the same trend as lead but is not plotted in figure 14*B*. Concentrations of both copper and zinc increased downstream, albeit at different rates. Both metals have been shown to be toxic to fish in the watershed (Farag and others, this volume). This phenomenon also was observed in the Animas River watershed (Church and others, 1997) and in the Arkansas River watershed (Church and others, 1993; Kimball and others, 1995); it reflects the transport, sorption, and subsequent deposition of colloidal particles from the water column to the streambed sediment. The effect of historical mining activity on aquatic habitat may extend for many river miles downstream from a historical mining district.

Summary

One of the primary goals of this study was to characterize the deposit-related trace-element distributions and show the impact of historical mining on streambed sediment in the Boulder River watershed study area. The data presented clearly indicate significant enrichment of the deposit-related trace elements copper, lead, zinc, arsenic, silver, cadmium, and antimony in streambed sediment in the major tributary streams downstream from historical mine sites. We have identified the major sources of the deposit-related contaminants: Jack Creek downstream from the Bullion mine and upper Basin Creek downstream from the Buckeye mine are the most severely affected reaches in the Basin Creek basin. Uncle Sam Gulch immediately downstream from the Crystal mine is the most severely affected tributary on Cataract Creek, and it affected Cataract Creek from the confluence with Uncle Sam Gulch to the Boulder River. High Ore Creek is severely affected from the Comet mine to its confluence with the Boulder River. The Boulder River has been impacted by streambed sediment from all three of the major tributaries as well as by milling of ore at the Jib Mill site on the Boulder River near the Basin Creek confluence. Thus we have identified the major point sources of contamination within the Boulder River watershed and fulfilled the second goal of this study. Differential transport of copper and zinc in the suspended sediment and deposition of colloids in the low-velocity zones of the Boulder River have resulted in irregularly dispersed deposits of contaminated streambed sediment in the Boulder River downstream from the confluences of the three major tributaries.

Premining Geochemical Baseline

Determination of the sources of deposit-related trace elements in the streambed sediment and terrace deposits requires careful evaluation of all possible sources. In addition to those identified at some historical mine sites as just described, these other sources include the unaltered rocks in the Boulder River

watershed study area, the altered areas in the Butte pluton, and the unmined vein deposits that still exist within the study area. Of these, only the hydrothermally altered zones have not been discussed. The geologic character of hydrothermal alteration in the Butte pluton clearly indicates that unmined sources of elevated deposit-related trace-element concentrations are limited. O'Neill and others (this volume) summarize alteration studies of earlier workers. Polymetallic veins were emplaced along shear zones subsequent to cooling of the Butte pluton. The total width of the veins and the alteration zones is measured in terms of a few feet (maximum width about 50 ft). Argillic and sericitic alteration occurred on the outer fringes of the veins where chlorite replaces mafic minerals in the pluton. Silica replacement and deposition were characteristic along vein walls, and sulfide minerals were restricted to the mineralized veins. Becraft and others (1963) defined areas of alteration in the Butte pluton that were not associated with the mineralization that produced the polymetallic vein deposits. McCafferty and others (this volume) mapped the distribution of the chlorite-rich, magnetite-poor altered rocks in the pluton and showed that they parallel known structural features in the Boulder batholith (O'Neill and others, this volume; McDougal and others, this volume, Chapter D9). Sources of deposit-related trace elements, other than the veins exploited by historical mining, were therefore largely restricted to those mineralized veins that had not been mined. Because of the limited extent of geologic sources for elevated concentrations of deposit-related trace elements, the most logical sources of contamination are the fluvial deposits of postmining age along stream reaches in the watershed. Therefore, minimum values were used when the depth profile plots of the geochemical data from stream terrace deposits suggested that the samples might have been contaminated by postmining fluvial processes.

Determination of the premining geochemical baseline in the historical mining districts within the study area was a necessary goal of this project so that we could define minimum target concentrations for the deposit-related trace elements that feasible remediation efforts might be expected to achieve. Elevated deposit-related trace-element concentrations in mining districts commonly are found in soils and streambed deposits prior to mining. The fundamental and difficult question to answer in historical mining districts is: What were these baseline concentrations of the deposit-related trace elements prior to mining? To evaluate the data collected from these localities (fig. 2), concentration profiles of eight major and trace elements (iron, manganese, copper, lead, zinc, arsenic, silver, and cadmium) were graphed, and the concentration-versus-depth profiles examined and interpreted from sample descriptions of sediment grains (Unruh and others, 2000; Rich and others, this volume). Depth profile plots of the data for six of these elements from several of the sites studied appear as figures 15–18 together with plots of the enrichment ratio for copper, lead, zinc, and arsenic (that is, the observed concentration of the deposit-related trace element divided by the geochemical baseline value for the trace element; data from table 1). Site descriptions, age control, and premining geochemical baseline data for six deposit-related trace elements are summarized in table 3. Identification and interpretation of the geochemical data from premining terraces that contained streambed sediment unaffected by either subsequent erosion and deposition, ground-water movement, or infiltration of contaminated surface waters in the streams resulted in the following general observations:

1. Gravels sampled from terraces that have no vegetation or established soil profile are young, that is, postmining (circa 1870; Ruppel, 1963), and have consistently proven to be contaminated by deposit-related trace elements . These included samples from sites *2B* and *3B* on the Boulder River, site *11B* on Basin Creek, site *13B* on Jack Creek, site *16B* on Uncle Sam Gulch, and sites *18B* and *19B* on High Ore Creek (fig. 2).

2. Samples from other terraces showed evidence of contamination, either from onlap deposition of sediment on the terrace, or by infiltration of contaminated surface waters in the streams. In this case, the data showed distinct trends of deposit-related trace-element enrichment as a function of depth. As one approached the low-flow-water-level depth in the core, concentrations of the deposit-related trace elements increased (for example, see site *2B*, fig. 18).

3. Ground-water movement may also have caused changes in deposit-related trace-element concentrations that vary as a function of element mobility. The deposit-related trace elements are listed in table 3 in inferred increasing element mobility from left to right (Fey and Desborough, this volume). Iron and manganese profiles with depth were used as a qualitative measure of ground-water movement of deposit-related trace elements in the cores (figs. 15–18). Precipitation of iron-oxide coatings on grain surfaces was used as an independent indicator of this process and was also indicated in the figures (for example, site *7B*, fig. 15). Ribbon maps (figs. 19–22) show premining concentrations of copper, lead, zinc, and arsenic in streambed sediment for the major tributaries and the Boulder River. Stream reaches with no data are also indicated on the maps. Premining geochemical background concentrations for both silver and cadmium in streambed sediment were below the limit of detection (< 2 ppm) everywhere within the study area.

Basin Creek

Premining geochemical baseline data for the deposit-related trace elements in streambed sediment were determined successfully at sites *7B* through *10B* (figs. 2 and 15). Additional data determined from streambed sediment that underlies the mill tailings at the Buckeye mine site on upper Basin Creek were also used to determine the premining geochemical baseline (Rich and others, this volume; Cannon and others, this volume). At site *7B*, ground-water movement in the upper 2 ft of the core had resulted in movement of the deposit-related trace elements. Only those data from samples below 2.5 ft in depth showed a consistent pattern and were used to

Table 3. Descriptions of sites sampled for possible premining geochemical baseline, age control, and determination of premining concentrations of selected deposit-related trace elements at those sites.

[Site localities in figure 2; LFWL = low-flow water level in adjacent stream; age data from Laboratory for Tree-ring Research, Univ. of Arizona, Tucson, Ariz., reported in Unruh and others (2000); nd, no data; description of Mazama ash at site B-7 in O'Neill and others, this volume, plate 2]

Site	Description	Age control	No. samples	Ag ppm	As ppm	Pb ppm	Cu ppm	Zn ppm	Cd ppm
		Boulder River							
1B	Terrace gravel, about 2 ft above LFWL, minimal vegetation.	nd	1	< 2	57	40	100	110	< 2
2B	Terrace gravel, about 4 ft above LFWL, no vegetation.	nd	1	< 2	24	34	52	150	< 2
3B	Discontinuous terrace gravel deposits along north bank of river.	nd	nd	--	--	--	--	--	--
4B	Terrace gravel, about 15 ft above LFWL.	nd	3	< 2	36	67	67	100	< 2
5B	Terrace gravel, about 12 ft above LFWL.	nd	1	< 2	46	74	43	140	< 2
6B	Terrace gravel, about 8 ft above LFWL, well-developed soil profile.	Live cottonwood, 60 years old; sediments pre-1940.	3	< 2	59	70	70	210	< 2
		Basin Creek							
Buckeye Mill site	Sediments from cores beneath fluvial tailings at mill site.	nd	4	< 2	31	39	53	180	2
7B	Core taken in meadow south of Buckeye mill site, soil about 1 ft above LFWL.	Mazama ash encountered at base of core; sediment circa 6,845 years B.P.	5	< 2	26	79	29	190	< 2
8B	Core from stream terrace, South Fork of Basin Creek, well-developed soil profile.	nd	8	< 2	23	63	24	110	< 2
9B	Core from stream terrace on Basin Creek, about 6 ft above LFWL, good soil profile.	nd	4	< 2	28	52	39	200	2
10B	Core from stream terrace on Basin Creek, about 3 ft above LFWL, good soil profile.	nd	7	< 2	31	57	19	150	< 2
11B	Terrace gravel, about 4 ft above LFWL, no vegetation.	nd	nd	--	--	--	--	--	--
Bullion Mill site	Sediments from cores beneath fluvial tailings at mill site.	nd		< 2	120	110	85	150	< 2
12B	Core from stream terrace, about 2 ft above LFWL, well-developed soil profile.	nd	4	< 2	53	35	56	250	< 2
13B	Core from stream terrace, about 3 ft above LFWL, no vegetation.	nd	nd	--	--	--	--	--	--
14B	Core from sediments beneath beaver dam. Beaver pond flooded with mill tailings. There is no historical record of this flood event.	Live Lodgepole pine, 99 years old, pre-1900; dead tree in dam, 87 years old, sediment is pre-1840 if one assumes that the tree was killed in forest fire of 1934.	3	< 2	130	58	34	210	2
15B	Core from reservoir built for Bullion smelter, which was on county tax rolls 1903-1905; smelter operated 1904-1906 (Rossillon and Haynes, 1999).	Dead tree 251 years old, pre-1652 sediment assuming tree was cut down in 1903 at time of dam construction.	1	< 2	110	60	72	--	--

Table 3. Descriptions of sites sampled for possible premining geochemical baseline, age control, and determination of premining concentrations of selected deposit-related trace elements at those sites.—Continued

Site	Description	Age control	No. samples	Ag ppm	As ppm	Pb ppm	Cu ppm	Zn ppm	Cd ppm
		Cataract Creek							
16B	Core from stream terrace near miner's cabin, surface covered with mill tailings.	nd	nd	--	--	--	--	--	--
17B	Core from stream gravels taken beneath old tree, terrace about 1 ft above LFWL.	3-ft diameter Ponderosa pine cut down in 1983, 252 years old, sediment pre-1731.	4	< 2	220	190	110	--	--
		High Ore Creek							
Comet Mill site	Sediments from cores beneath fluvial tailings downstream from mill site.	nd	4	< 2	32	48	32	160	< 2
18B	Core through fluvial tailing deposit, no vegetation.	nd	1	< 2	120	220	130	--	--
19B	Core through terrace deposit, 3 ft above LFWL, no vegetation.	nd	nd						
		Summary							
Median values		nd		< 2	46	60	53	160	< 2

determine the premining geochemical baseline values at this site. The enrichment ratio did not exceed 3.5 in this section of the core for any of the deposit-related trace elements. At about 4 ft depth at this site in a separate core, we encountered Mazama ash, which was dated at 6,845 years B.P. (O'Neill and others, this volume, pl. 2). The montaine basin where this sample was taken was dammed by a terminal glacial moraine downstream from the Buckeye mill tailings site and the basin filled with postglacial sediment. Downstream on the South Fork of Basin Creek at site *8B*, none of the deposit-related trace elements exceeded an enrichment ratio of two and all data were used (not shown in fig. 15). At site *9B*, on the main channel of Basin Creek upstream from the confluence with the South Fork of Basin Creek, we found an abrupt transition between sediment indicating premining geochemical baseline and sediment that had been contaminated by historical mining. Samples from below 2.7 ft depth were used to indicate premining geochemical baseline values and had enrichment ratios of 2 or less. In contrast, sediment from above 2.5 ft depth showed evidence of ground-water movement of the deposit-related trace elements; copper, lead, arsenic, and cadmium were generally enriched in the sediment in this upper section of the core by a factor of more than 5. Zinc, which was relatively more mobile, and to some extent copper, have been leached out of the core particularly at the upper level above 1 ft depth. At site *10B*, on Basin Creek downstream from the confluence with Jack Creek, all the data from the terrace deposits at this site were used. Profile plots of deposit-related trace-element concentrations were relatively constant in spite of the fact that we observed iron-oxide coatings on the grains below 2.5 ft and manganese had moved in this terrace deposit. At site *10B*, enrichment factors were always less than 2. Site *11B* was from a low terrace gravel with no vegetative cover. All data indicate that the streambed sediment from this terrace was contaminated and postmining in age. Because site *11B* was the farthest downstream site on Basin Creek, we used the data from site *10B* for the premining geochemical baseline in streambed sediment for the reach downstream from site *10B* when preparing the premining geochemical ribbon maps (figs. 19–22).

On Jack Creek, we investigated terrace deposits at sites *12B* through *15B* (fig. 2). We also obtained data from the cores taken through the tailings below the Bullion mine site (Rich and others, this volume). At site *12B*, we sampled contaminated fluvial sediment that overlies uncontaminated streambed sediment (fig. 16). Enrichment factors for the deposit-related trace elements in the lower section of the core below 6 in. did not exceed 2, whereas above that depth in the core, they were highly variable, approaching 4 to 5 for the more mobile deposit-related trace elements copper and zinc. The mill tailings dam at the Bullion mine site was breached and flotation mill tailings flushed downstream in an event of unknown age. Fluvial tailings deposits exposed along Bullion Mine tributary have had much of the original content of copper and zinc leached out (Rich and others, this volume). The core from site *12B* was one locality where these metals have been sorbed by the older sediment. Site *13B* (not shown in fig. 16) was in a young terrace with no vegetation on the surface of the terrace. All the streambed sediment in this terrace was deposited after the onset of mining and was contaminated. At site *14B*, we cored beneath the dam of an abandoned beaver pond that had been flooded during the breach of the mill tailings dam (fig. 3*B*). The minimum age of the premining streambed

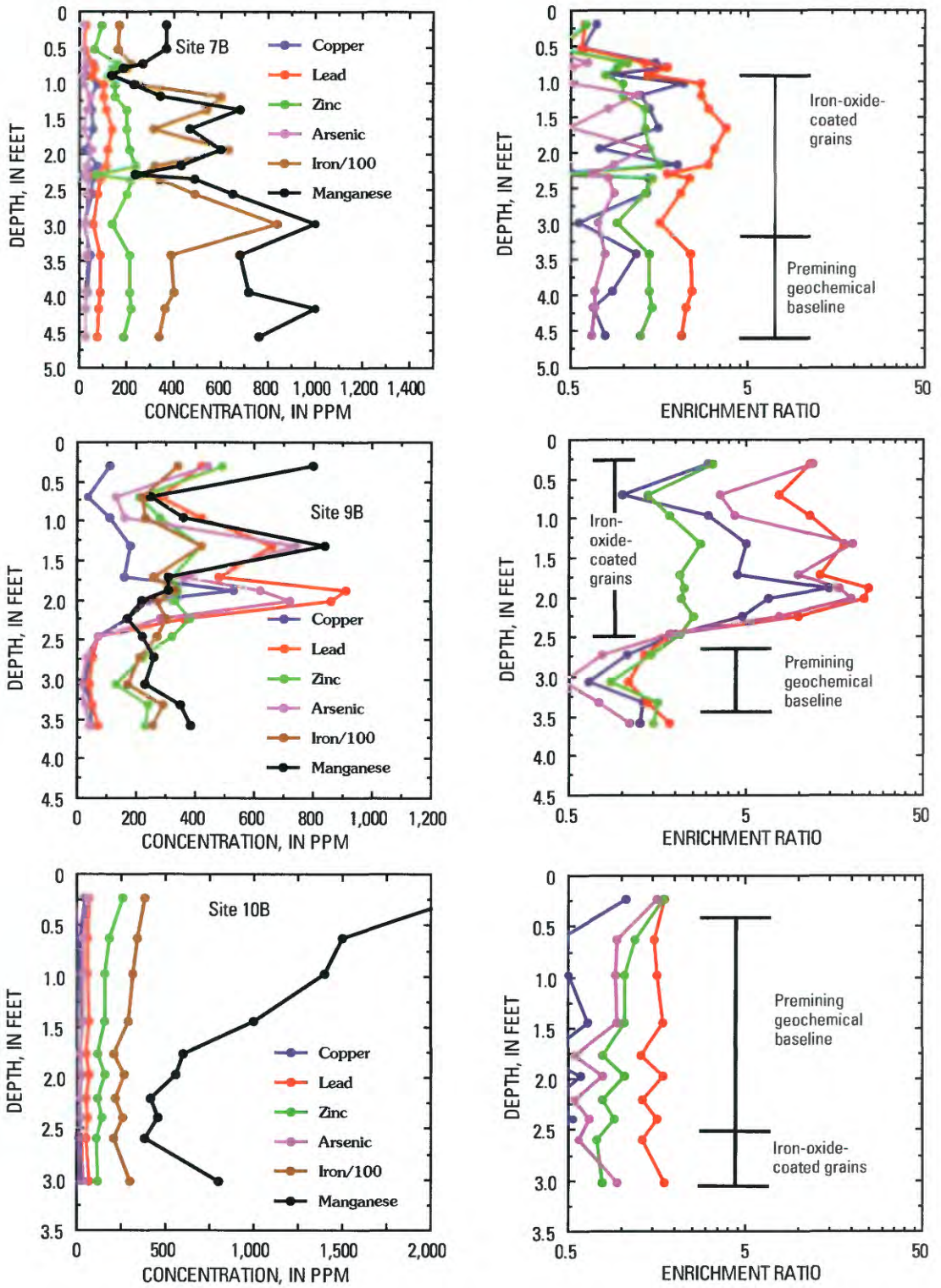

Figure 15. Plots of geochemical data for the elements copper, lead, zinc, arsenic, iron, and manganese from cores taken at sites *7B*, *9B*, and *10B* (fig. 2) for determination of premining geochemical baseline in streambed sediment from Basin Creek basin. Uppermost soil interval was not analyzed; top is ground surface. Presence of iron-oxide coatings on grains was interpreted to be indicative of ground-water movement of deposit-related trace elements that would compromise geochemical baseline concentration data. Intervals in each core used for determination of the premining geochemical baseline are indicated; data are summarized in table 3. Geochemical data from core at site *8B* were very similar to that from site *10B*. Site *11B* yielded no usable data.

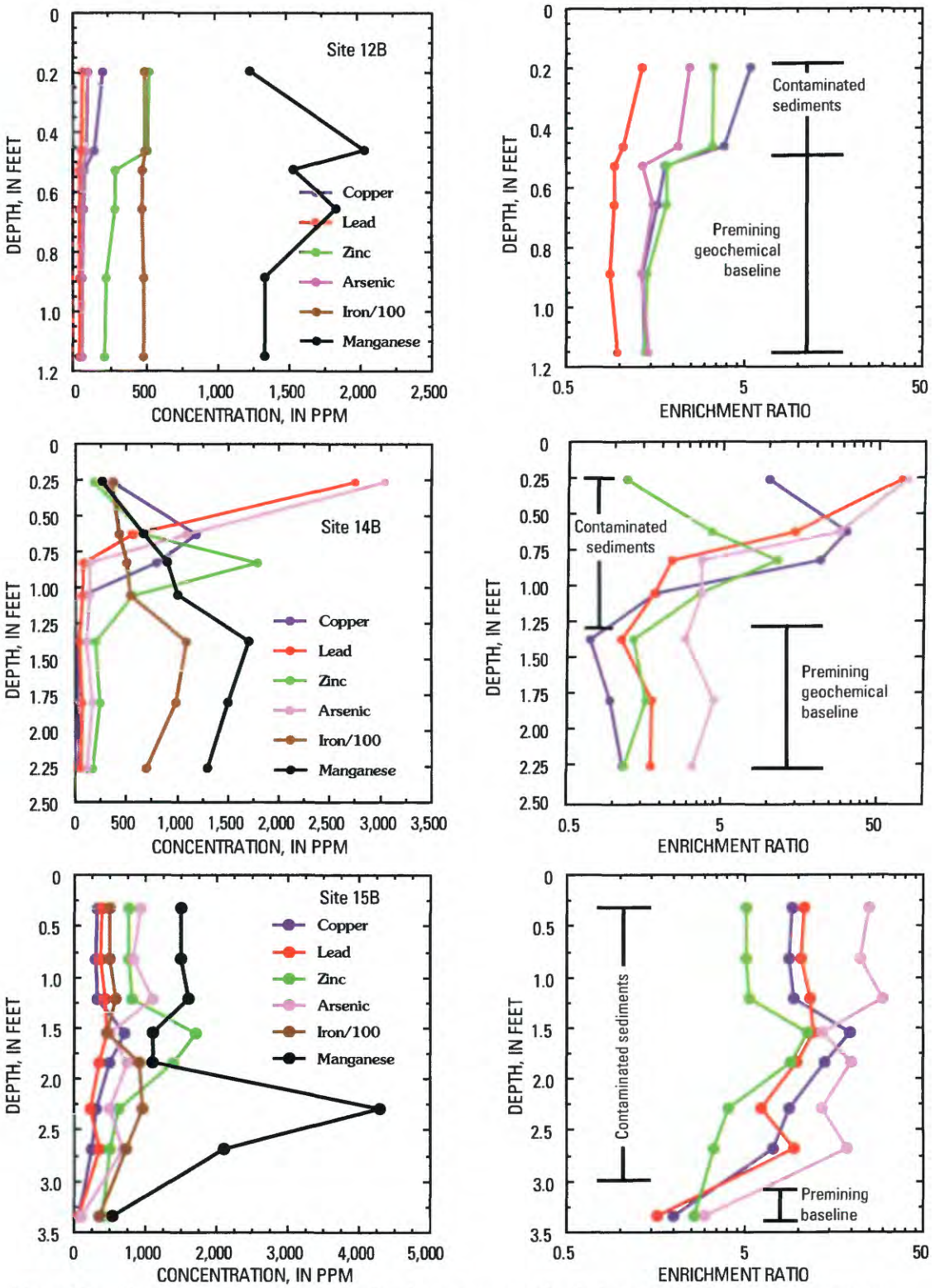

Figure 16. Plots of geochemical data for the elements copper, lead, zinc, arsenic, iron, and manganese from cores taken at sites *12B*, *14B*, and *15B* (fig. 2) for determination of premining geochemical baseline in streambed sediment from Jack Creek basin. Uppermost soil interval was not analyzed; top is ground surface. Presence of iron-oxide coatings on grains was interpreted to be indicative of ground-water movement of deposit-related trace elements that would compromise geochemical baseline data. Intervals in each core used for determination of the premining geochemical baseline are indicated; data are summarized in table 3. All data from site *13B* indicated that only contaminated sediment was present in this core. We used only the minimum value from the geochemical data from site *15B*, which should be considered an estimate of the premining geochemical baseline in this reservoir.

sediment in this core below the beaver dam is 99 years on the basis of the tree-ring count of a dead Lodgepole pine(?) growing in and partially buried by the beaver dam. Concentrations of the deposit-related trace elements decrease abruptly at a depth of 1.3 ft. Enrichment ratios in the lower section of the core for copper, lead, and zinc were less than 2 and for arsenic were between 3 and 4. At site *15B*, we sampled streambed sediment trapped in a water reservoir on Jack Creek built in 1903 to supply the Bullion smelter. According to Rossillon and Haynes (1999), the Bullion smelter operated between 1904 and 1906. The sediment sample was taken adjacent to a Douglas-fir stump dated at 251 years. Because the stump was within a few hundred feet of the dam and Douglas-fir are sparse in this Lodgepole pine forest, the tree was probably cut down at the time of construction in 1903 for use in the dam, which was built entirely of Douglas-fir logs. Only the lowermost sample interval was used to estimate the premining geochemical baseline at the site (pre-1652). All other samples in the core through reservoir sediment had elevated enrichment factors for copper, lead, and arsenic that exceeded 5. Zinc was leached out of the sediment in the reservoir impoundment and showed variable enrichment ratios. This reservoir constitutes a large, reversible source of fluvial mine tailings that will contaminate water and streambed sediment in Jack Creek for many decades unless remediated.

Cataract Creek

The concentrations of deposit-related trace elements in streambed sediment of Cataract Creek upstream from the confluence with Uncle Sam Gulch were not investigated because most of the area is on private property and because data from streambed sediment collected in the stream indicated only a small enrichment in deposit-related trace-element concentrations. One potential source of contaminants, the Eva May mine, had been partially remediated prior to this study. No sites where terrace gravel would accumulate due to the steepness of the gradient of this reach of Cataract Creek were identified downstream from the confluence of Uncle Sam Gulch. In Uncle Sam Gulch, no usable data were obtained from the core from site *16B* (fig. 2). At site *17B*, located in a clear-cut in the flood plain of Uncle Sam Gulch, streambed sediment was cored from between the roots of a 3-ft diameter Ponderosa pine that had been cut down in 1983 (Robert Wintergerst, USDA Forest Service, written commun., 1998). The tree was 252 years old, indicating that the streambed sediment predates the onset of mining by more than a century (circa 1731). Instead of the expected low values, concentrations of copper, lead, zinc, arsenic, and cadmium were elevated and varied with depth (fig. 17). Only silver had a low concentration approaching the local geochemical baseline (table 1). Iron concentrations were constant and were not enriched, whereas manganese concentrations were highly variable and showed enrichment near the top of the core above 1 ft in depth (that is, above the ground-water table). Arsenic and copper were enriched above 1 ft in depth, whereas zinc was enriched below that zone with enrichment factors exceeding 10. Copper concentrations between 1.5 and 2.3 ft were enriched by factors of 2–4, arsenic and lead by factors of 5–7, and zinc was enriched by about a factor of 7 over three of the cored intervals. These data represented the best estimate of the premining geochemical baseline in Uncle Sam Gulch prior to mining. We interpret these data to indicate that the vein exploited at the Crystal mine probably was exposed at the surface and that deposit-related trace elements were being actively eroded into the stream at the site prior to discovery about 1883 (Rossillon and Haynes, 1999).

High Ore Creek

The premining geochemical baseline was not successfully determined at either site *18B* or *19B* (fig. 2). At both sites, the terrace gravel had no vegetation cover on the surface and proved to be contaminated young terrace gravel. At site *18B*, we used the minimum concentrations from the base of the core, although these concentrations are merely an estimate of what the premining geochemical baseline might have been (fig. 17). Cadmium and zinc concentrations were clearly contaminated by ground-water movement of these two metals. Additional premining geochemical baseline data were obtained from streambed sediment cored from beneath the fluvial mill tailings below the Comet mine site and are summarized in table 3.

Boulder River

Six terrace gravel sites were sampled along the Boulder River (sites *1B* through *6B*; fig. 2); the data for three of these sites, *2B*, *4B*, and *6B*, illustrate the results (fig. 18). Site *3B* contained no usable data and was postmining in age. At sites *1B*, *2B*, and *5B*, the lowermost samples had elevated deposit-related trace-element concentrations (fig. 18). Whether this was (1) the result of surficial contamination by young sediment with the existing sand and gravel on the banks, which were not removed because we failed to dig back far enough into the gravel deposit, or (2) the result of movement of metals and colloids into the gravel deposits from the contaminated surface waters was not tested. At sites *1B*, *2B*, and *5B*, only the data from the least contaminated interval were used. This was the top interval at sites *1B* and *5B*, and the middle interval at site *2B* (fig. 18). Site *2B* is located immediately downstream from the Jib Mill site (fig. 2) and likely contained overbank deposits contaminated by mill tailings on top of the terrace gravel. As will be shown in "Lead Isotopic Results," lead isotope data from site *2B* prove the value of this approach. The concentrations of the deposit-related trace elements in the upper intervals from sites *1B* and *5B* were very similar to those from site *6B* and are not shown in figure 18. Sites *4B* and *6B* were both large, vegetated terrace deposits that gave very consistent results. The terrace at site *6B* is a minimum

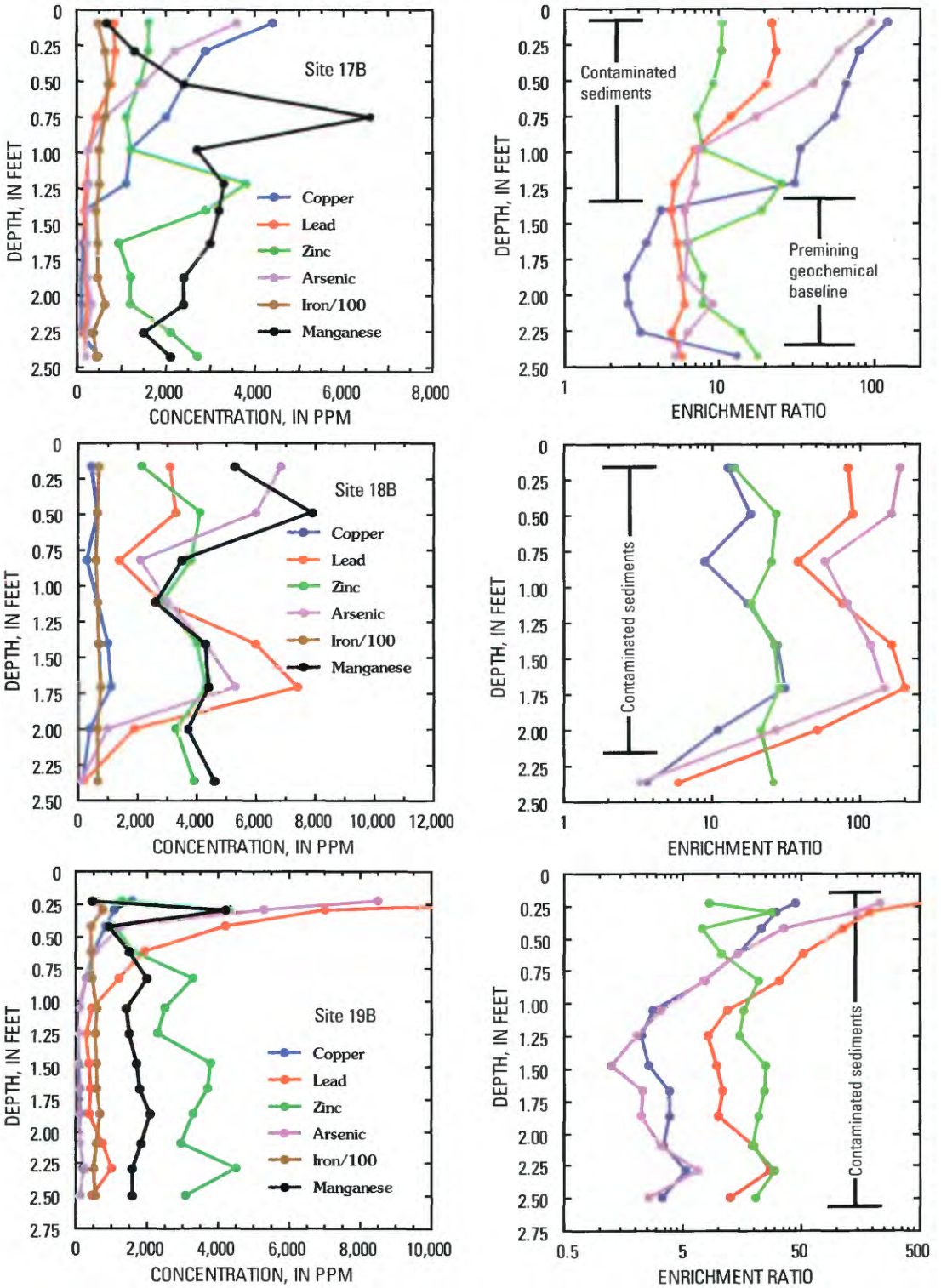

Figure 17. Plots of geochemical data for the elements copper, lead, zinc, arsenic, iron, and manganese from cores taken at site *17B* (fig. 2) for determination of premining geochemical baseline in streambed sediment from Uncle Sam Gulch basin, and at sites *18B* and *19B* in High Ore Creek basin. Uppermost soil interval was not analyzed; top is ground surface. Presence of iron-oxide coatings on grains was interpreted to be indicative of ground-water movement of deposit-related trace elements that would compromise geochemical baseline data. Intervals in each core used for determination of the premining geochemical baseline are indicated on the figures; data are summarized in table 3. Samples for site *16B* were contaminated. No convincing evidence for a premining baseline was determined in High Ore Creek basin from cores taken at sites *18B* and *19B*.

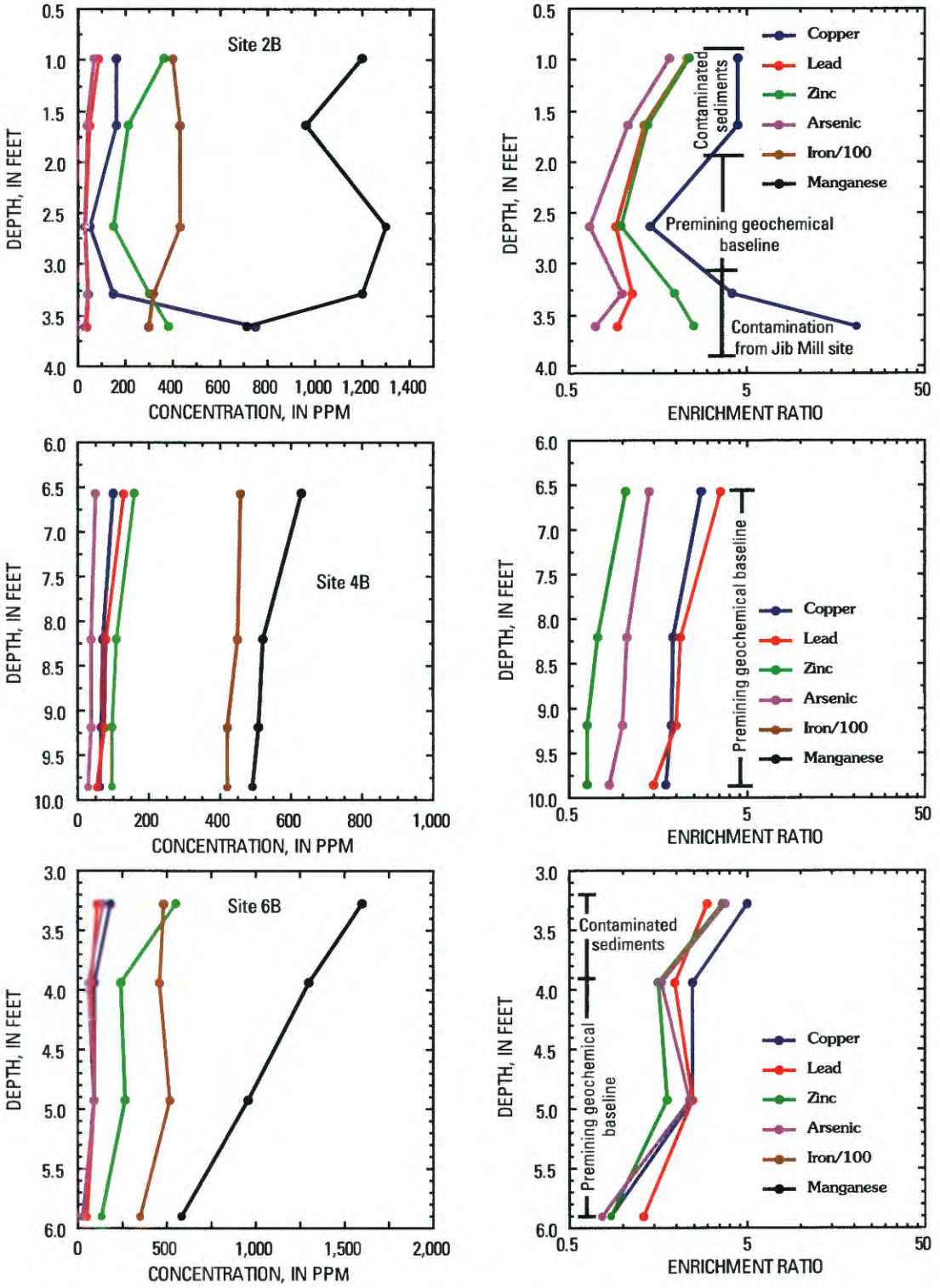

Figure 18. Plots of geochemical data for the elements copper, lead, zinc, arsenic, iron, and manganese from cores taken at sites *2B*, *4B*, and *6B* (fig. 2) for determination of premining geochemical baseline in streambed sediment from Boulder River watershed in the Basin and Boulder mining districts. Uppermost soil interval was not analyzed; top is ground surface. Presence of iron-oxide coatings on grains was interpreted to be indicative of ground-water movement of deposit-related trace elements that would compromise geochemical baseline data. Intervals in each core used for determination of premining geochemical baseline are indicated on the figures; data are summarized in table 3. All samples from site *3B* were contaminated.

of 60 years old, on the basis of dendrochronological age of a large cottonwood tree that was growing on the terrace deposit. Samples were taken from the exposed root zone in the terrace cut bank. The uppermost interval was composed of a silt layer and may represent a flood deposit rather than local terrace gravel. Including the data from the silt layer does not significantly affect the premining geochemical baseline ribbon maps of figures 19–22.

Boulder River Watershed

Ribbon maps of the premining geochemical baseline for the watershed are shown in figures 19–22. The data used are both in table 3 and taken from the current geochemical maps in areas where past mining had little effect (figs. 4–7). The same concentration intervals were used as in the previous maps to facilitate comparisons of the conditions in the Boulder River watershed today with those prior to mining (Rich and others, this volume). Premining geochemical baselines for all the deposit-related trace elements were in the lowest two concentration ranges everywhere except downstream from the Crystal mine site in Uncle Sam Gulch.

In contrast to the data from unmined and probably unmineralized tributaries in table 1, the premining geochemical baseline determined from terrace deposits in the Basin and Boulder mining districts was higher than reported in table 1. Premining geochemical baseline concentrations for copper ranged from 19 to 150 ppm with a median value of 53 ppm; lead ranged from 34 to 220 ppm with a median value of 60 ppm; zinc ranged from 100 to 250 ppm with a median value of 160 ppm; arsenic ranged from 23 to 220 with a median value of 46 ppm (35 ppm in table 1); silver was always < 2 ppm; and cadmium ranged from <2 to 2 ppm with a consensus value of <2 ppm. These median values are 65 percent higher for copper, 60 percent higher for lead, 30 percent higher for arsenic, but only 6 percent higher for zinc than those given in table 1. The agreement between the two methods for determination of the premining geochemical baseline is remarkable. Use of either set of geochemical baseline values would make little difference in terms of evaluating the toxic effect of historical mining on aquatic life in the three major tributaries in the Boulder River watershed study area. The data demonstrate the feasibility of using terrace deposits of premining age to determine streambed-sediment geochemistry prior to the onset of mining in a historical mining district. The independent determination of premining geochemical baseline from premining terrace deposits fulfills the third goal of this study. The two methods for the determination of premining geochemical baselines, that is, the use of premining sediments preserved in terrace deposits, and the use of stream sediment from unaffected tributaries in a historical mining district, provide compelling evidence that the watershed would have supported aquatic life prior to mining.

Lead Isotopic Results

Lead isotopic analyses of all streambed sediment, sediment cores, and selected premining terrace sediment were completed to determine if metals in the present-day streambed-sediment samples were derived from past mining activities. Four isotopes of lead exist in nature, three of which change directly as a function of time through the radioactive decay of uranium and thorium: ^{206}Pb is the daughter product of decay of ^{238}U, ^{207}Pb is the daughter product of decay of ^{235}U, and ^{208}Pb is the daughter product of decay of ^{232}Th. However, ^{204}Pb has no radioactive parent. Thus, the isotopic composition of lead in rocks in the Earth's crust (that is, $^{206}Pb/^{204}Pb$, $^{207}Pb/^{204}Pb$, and $^{208}Pb/^{204}Pb$) changes regularly with time as uranium and thorium undergo radioactive decay. When mineral deposits are formed, lead is separated from the parent uranium and thorium isotopes and the lead isotopic composition of the hydrothermal fluid is "frozen" into the sulfide minerals, usually in galena, within the mineral deposit. This mineral deposit lead isotope signature will then differ from that of the host rocks underlying a watershed because the lead in the host rocks continues to change with time whereas the lead in the mineral deposit remains fixed.

The isotopic composition of lead in streambed sediment reflects mixtures of lead from many discrete sources: the mineral deposits, unmined altered rock surrounding those deposits, the unmineralized rocks underlying the watershed, mine-waste dumps near mine adits, and mill tailings produced during the processing of ore. Physical transport of detrital material derived from erosion and mixing of all these materials combine to make up the streambed sediment. In addition, aqueous or colloidal transport of deposit-related trace elements from mined sites to the stream, and precipitation by mixing, sorption to the colloids and grain coatings, and subsequent settling of the colloids to the streambed also contribute deposit-related trace elements to the streambed.

In order for the lead isotopic data to be useful, it must be possible (1) to measure the isotopic compositions of all suspected sources of lead as well as the premining geochemical baseline, and (2) to determine the lead isotopic composition of the contaminant. Moreover, (3) the lead-isotopic composition of the contaminants must be distinct from that of uncontaminated or premining geochemical baseline (Church and others, 1997).

The lead isotopic values in the present study area form single arrays on lead isotopic correlation plots (that is, $^{206}Pb/^{204}Pb$ versus $^{207}Pb/^{204}Pb$ and $^{206}Pb/^{204}Pb$ versus $^{208}Pb/^{204}Pb$ plots). This was because the lead in most of the streambed-sediment samples was contained in minerals derived from the Butte pluton of the Boulder batholith or the associated Elkhorn Mountains Volcanics. The variations observed among the samples reflect variations in U/Pb among the different rocks and ores, which were derived from a common source during melting that formed the batholith and subsequent mineralization (O'Neill and others, this volume; Lund and others,

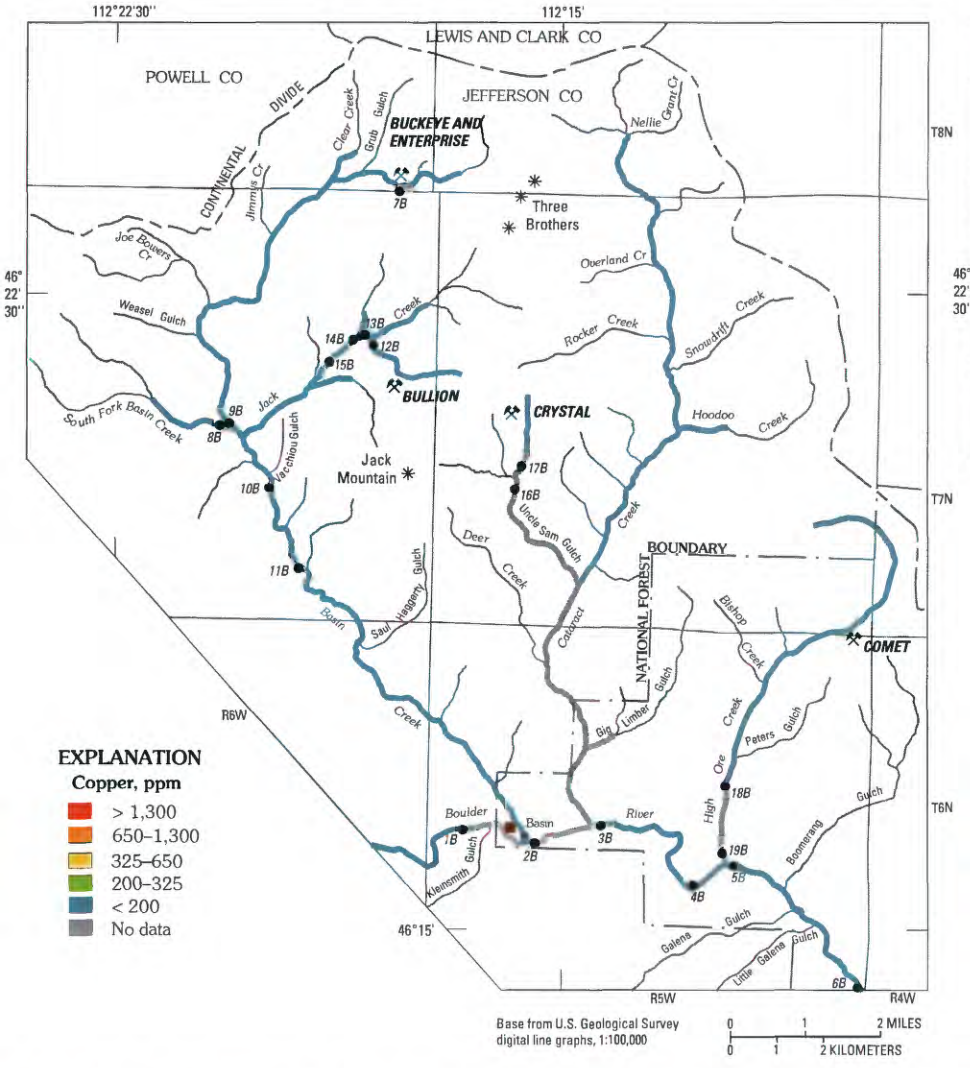

Figure 19. Concentrations of copper (ppm) in premining streambed sediment (solid dot) of Boulder River watershed study area. Stream reaches shown in gray, no data. Concentration intervals are same as in figure 4. Note that all stream reaches where we determined premining geochemical baseline have concentrations of copper below 200 ppm, that is, less than six times baseline value of 32 ppm (table 1). Dark-red square, Jib Mill site.

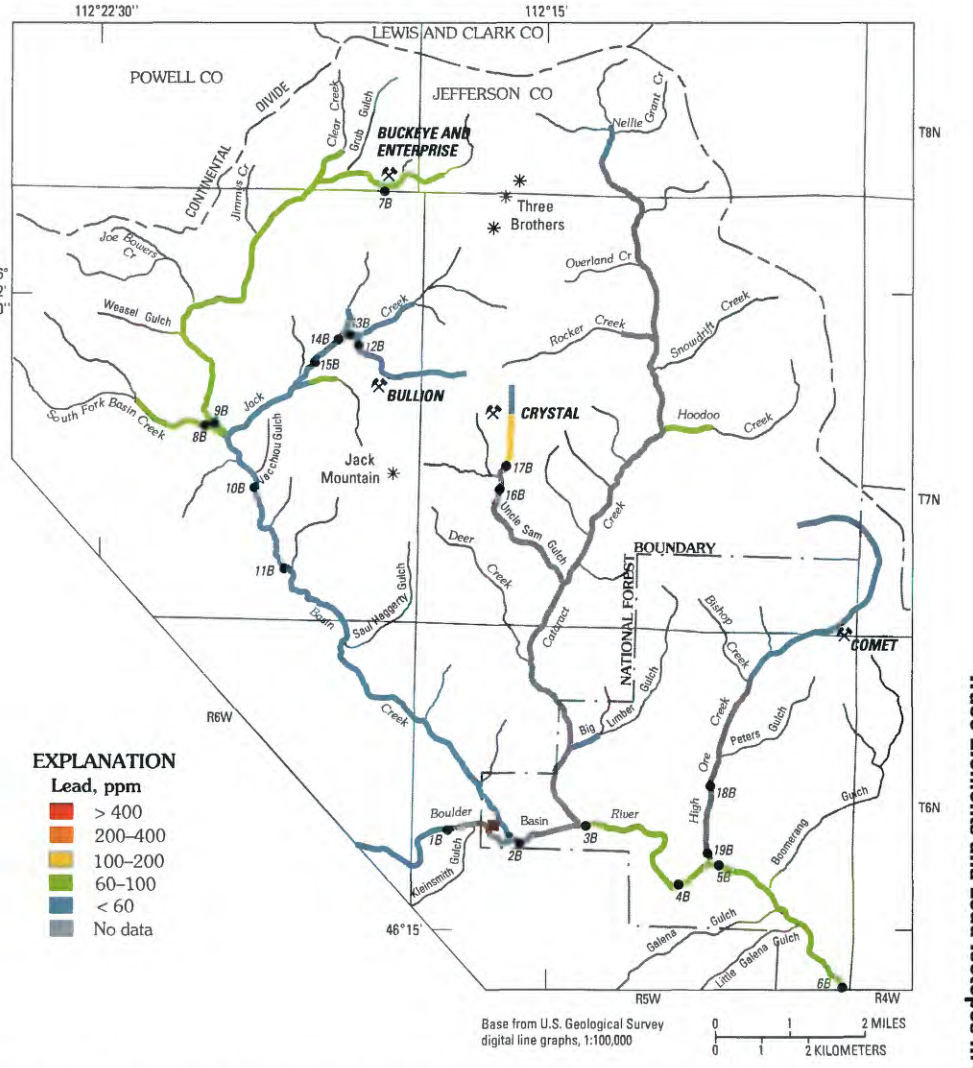

Figure 20. Concentrations of lead (ppm) in premining streambed sediment (solid dot) of Boulder River watershed study area. Stream reaches shown in gray, no data. Concentration intervals are same as in figure 5. Note that many stream reaches where we have been able to determine premining geochemical baseline have concentrations of lead below 80 ppm, that is, about twice the baseline value of 35 ppm (table 1), with the exception of the reach downstream from Crystal mine in Uncle Sam Gulch at site *17B*. Dark-red square, Jib Mill site.

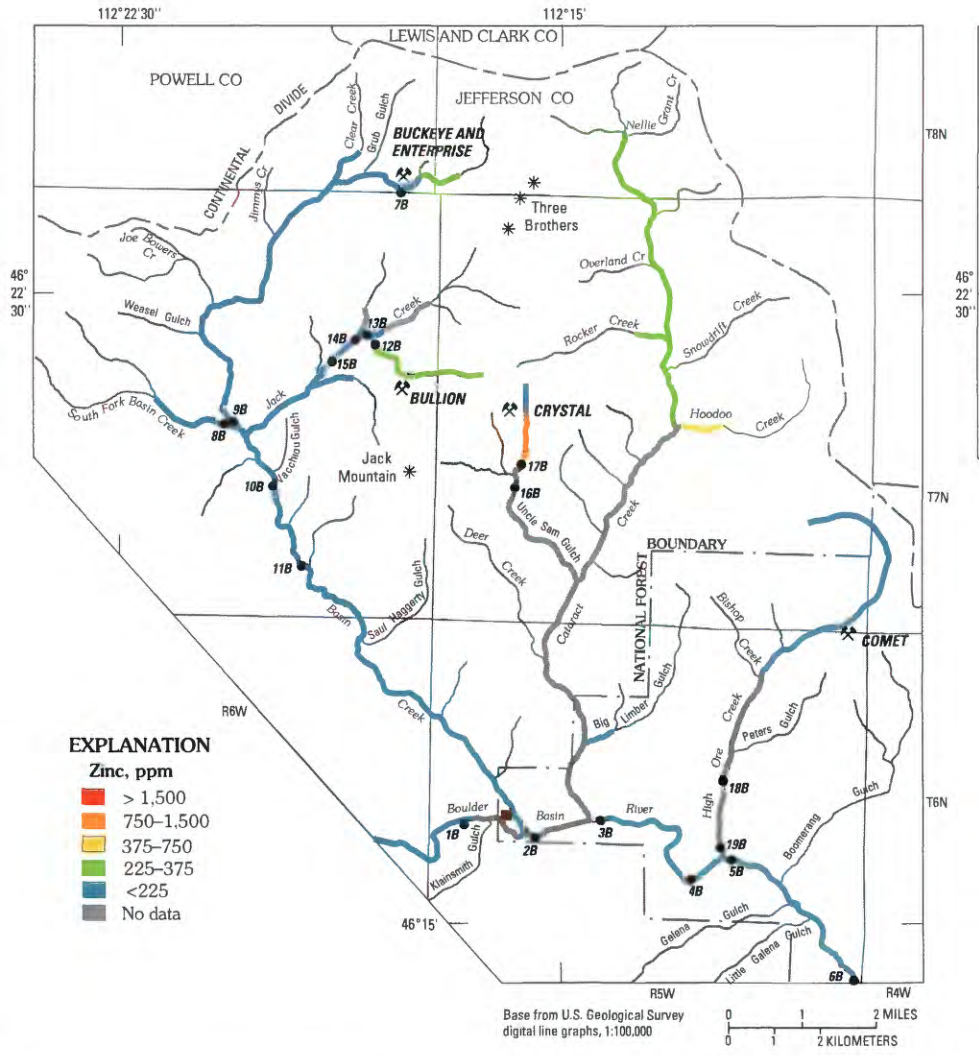

Figure 21. Concentrations of zinc (ppm) in premining streambed sediment (solid dot) of Boulder River watershed study area. Stream reaches shown in gray, no data. Concentration intervals are same as in figure 6. Note that many stream reaches where we have been able to determine premining geochemical baseline have concentrations of zinc below 200 ppm, that is, less than 1.5 times the baseline value of 150 ppm (table 1), with the exception of the reach downstream from Crystal mine in Uncle Sam Gulch at site *17B*. Dark-red square, Jib Mill site.

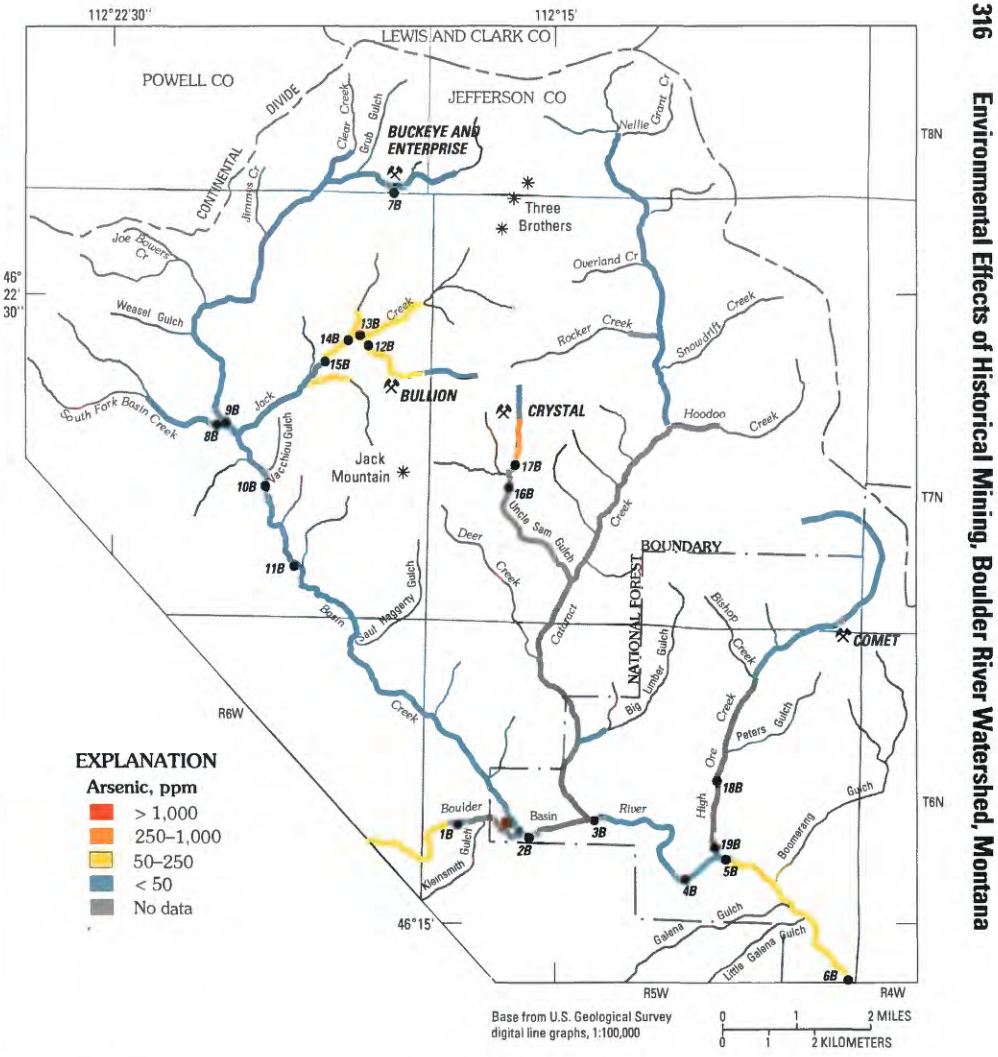

Figure 22. Concentrations of arsenic (ppm) in premining streambed sediment (solid dot) of Boulder River watershed study area. Reaches shown in gray, no data. Concentration intervals the same as in figure 7. Note that many stream reaches where we have been able to determine premining geochemical baseline have concentrations of arsenic below 50 ppm (table 1; arsenic has a median value of 35 ppm). However, downstream from Bullion and Crystal mines, arsenic concentrations were elevated. Dark-red square, Jib Mill site.

2002). Consequently, the lead isotopic data will be represented exclusively using $^{206}Pb/^{204}Pb$ values throughout the ensuing discussion.

Lead isotopic data showed an inverse relationship with lead concentrations (fig. 23). The highest $^{206}Pb/^{204}Pb$ values from drainage basins underlain largely by rocks of the Butte pluton of the Boulder batholith (18.1–18.2) and lowest lead concentration values (<60 ppm) were found among some of the premining streambed-sediment samples collected either from tributaries upstream from major mines or from the Boulder River upstream from Basin Creek. Streambed-sediment samples from sites *3S* and *4S* (between river miles 12.5 and 14.5, fig. 24*A*) along the Boulder River showed anomalously high $^{206}Pb/^{204}Pb$ values of 18.3–18.4. These streambed-sediment samples were collected downstream from where the Boulder River cuts through a large dike of Eocene Lowland Creek Volcanics (O'Neill and others, this volume, pl. 1). These Eocene rocks are younger than and have a different source than the Boulder batholith. As a result, they had a more radiogenic lead isotopic composition; that is, they had a higher $^{206}Pb/^{204}Pb$ value than the rocks that make up the majority of the Boulder River watershed study area. Lead isotopic data from these two sites were used as an estimate of the uncontaminated streambed sediment in the Boulder River immediately upstream from the Jib Mill and Basin Creek, but they were not used to calculate average premining baseline lead isotopic values in streambed sediment anywhere else within the study area (table 4).

The lead data in figure 23 clearly indicated two principal sources of deposit-related lead. Streambed-sediment samples containing high concentrations of lead (for example, samples from High Ore Creek with lead concentrations >1,000 ppm) showed a relatively constant $^{206}Pb/^{204}Pb$ value of 18.06. We interpret this value to represent the $^{206}Pb/^{204}Pb$ value of deposit-related contaminant lead from the Comet mine in this drainage. In contrast, the highest concentrations of lead in the Basin and Cataract Creek basins were characterized by a $^{206}Pb/^{204}Pb$ value of 17.90–17.93. Because sampling was limited at each of the mines in the Basin and Cataract Creek basins, we used the average of the highest lead samples (that is, lead concentrations greater than 1,000 ppm and $^{206}Pb/^{204}Pb$ value of 17.91) collected from these two basins to represent the lead isotopic composition of the contaminant lead for both the Basin and Cataract Creek basins (fig. 23, table 4). Comparison of the deposit lead signatures from the mining districts with the data from the geochemical baseline site *2B* downstream from the Jib Mill ($^{206}Pb/^{204}Pb$ value of 17.73) is clear evidence that the low lead isotopic value from this site is not from mines in the Basin and Boulder mining districts.

One unfortunate aspect of the relationship among virtually all samples to a common source is that the total range of $^{206}Pb/^{204}Pb$ values among the samples was only about 1.7 percent, varying from $^{206}Pb/^{204}Pb$ of 17.9 to 18.2 (fig. 23, excluding the streambed sediment apparently derived from the Eocene Lowland Creek Volcanics). This means that, when even comparatively small amounts of deposit-related lead are added to the streambed sediment, the $^{206}Pb/^{204}Pb$ value of the streambed sediment will rapidly approach that of the deposit lead. Consequently, we were not able to resolve the small isotopic differences created by the addition of deposit lead from other downstream sources within the study area.

Lead isotopic data from modern streambed-sediment samples and from the premining terrace appear as figures 24–27; data are in the database (Rich and others, this volume). Individual mine localities are indicated in the figures, plotted by distance (river mi).

Basin Creek

The lead isotopic compositions of streambed sediment from Basin Creek are compared with those of the Boulder River in figure 24*A*. All Basin Creek streambed-sediment samples had lower $^{206}Pb/^{204}Pb$ values than those of the Boulder River upstream from the Basin mining district. As Basin Creek flowed past the Buckeye mine, the $^{206}Pb/^{204}Pb$ value decreased from 18.0 to 17.9. The $^{206}Pb/^{204}Pb$ progressively increased downstream as a result of both settling out of colloidal phases rich in deposit-related trace elements and dilution by streambed sediment derived from nonmineralized rock in the Basin Creek basin. At the confluence with Jack Creek, the $^{206}Pb/^{204}Pb$ value decreased from 18.0 to 17.92 as a result of contaminant lead contributed by Jack Creek. Downstream of this confluence to the confluence of Basin Creek with the Boulder River, the $^{206}Pb/^{204}Pb$ value progressively increased as a result of dilution by streambed sediment from unmineralized subbasins drained by other tributaries to Basin Creek (fig. 24*A*, *B*).

The effects of the Buckeye and Bullion mines on the $^{206}Pb/^{204}Pb$ value and the lead concentrations in the streambed sediment of upper Basin Creek and the Bullion Mine tributary, respectively, are readily apparent (fig. 24B, C). Lead isotopic values decreased and lead concentrations increased significantly as the streams flowed past these mine sites. The lead concentration and isotopic values in streambed sediment upstream from these mines (sites *20S* and *32S*) were similar to those found in premining streambed sediment from terrace samples collected along these streams.

In contrast, the streambed-sediment samples from Jack Creek collected upstream from the confluence with the Bullion Mine tributary (site *38S*) had elevated lead concentrations and comparatively low $^{206}Pb/^{204}Pb$ values. These results suggest that either historical mining activity or exposed mineralized rock also influenced the deposit-related trace-element concentrations and lead isotopic characteristics of upper Jack Creek. In any case, the $^{206}Pb/^{204}Pb$ value of streambed sediment in Jack Creek was already so similar to those of the contaminant sources ($^{206}Pb/^{204}Pb$ of 17.91–17.92) upstream from the confluence with the Bullion Mine tributary that the addition of streambed sediment from the Bullion Mine tributary was not discernible in the lead isotopic data (fig. 24*B*). However, the addition of leachable lead from the Bullion Mine tributary to Jack Creek had a large effect on the concentration of lead as

Table 4. Estimates of contaminant and premining baseline lead isotopic compositions from Boulder River watershed study area.

[Data are from Fey, Unruh, and Church (1999) and Unruh and others (2000); data are in database, Rich and others, this volume]

Sample	Site	Sample type	Pb ppm	$^{206}Pb/^{204}Pb$
Baseline, Boulder River upstream from Basin Creek				
97-BM-115	3S	Streambed sediment	20	18.263
98-BMS-113	3S	Streambed sediment	24	18.318
96-BM-121	4S	Streambed sediment	20	18.425
Mean Value			21	18.389
Baseline, Boulder River downstream from Basin Creek				
96-BM-107	22S	Streambed sediment	61	18.185
97-BM-102s1	32S	Streambed sediment	59	18.079
97-BM-120	44S	Streambed sediment	36	18.213
97-BM-108s1	54S	Streambed sediment	34	18.055
98-BMS-115	58S	Streambed sediment	31	18.227
99BMB-102a	1B	Stream terrace	48	18.190
99BMB-103c	2B	Stream terrace	34	18.123
99BMB-108a	5B	Stream terrace	51	18.114
98BMB-406a-e	7B	Stream terrace	33	18.096
98BMB-401cdfh	8B	Stream terrace	39	18.126
98BMB-402jkl	9B	Stream terrace	33	18.099
98BMB-403eghi	10B	Stream terrace	36	18.122
98BMB-407b-f	12B	Stream terrace	33	18.163
97BMB(S)-122efgh	13B	Stream terrace	42	18.094
97BMF-131(9fg13ef)		Core through fluvial tailings, Comet Mill.	33	18.101
Mean Value			40	18.132
Deposit–related lead, Basin and Cataract Creeks				
96-BM-136	21S	Streambed sediment	1,600	17.895
96-BM-115	34S	Streambed sediment	1,400	17.927
97-BM-104G	35S	Fluvial tailings	12,000	17.925
96-BM-114		Bullion smelter waste	1,300	17.897
97-BM-106G	37S	Fluvial tailings	2,600	17.923
96-BM-116	55S	Streambed sediment	1,900	17.921
96-BM-118	57S	Streambed sediment	920	17.925
Mean Value				17.916
Deposit–related lead, High Ore Creek				
96-BM-101	59S	Streambed sediment	5,700	18.069
96-BM-102	60S	Streambed sediment	1,900	18.062
96-BM-102d	60S	Streambed sediment	2,000	18.064
Mean Value				18.065

well as other deposit-related trace elements in streambed sediment downstream from the confluence with the Bullion Mine tributary (fig. 11).

With the exception of the two most-upstream samples (sites *20S* and *32S*), the streambed-sediment samples from both Jack and Basin Creeks showed elevated lead concentrations and low $^{206}Pb/^{204}Pb$ relative to streambed sediment from premining terraces (fig. 24*B*, *C*). Although the $^{206}Pb/^{204}Pb$ value and lead concentration in streambed sediment from Basin Creek progressively approached those of the premining samples as a function of distance downstream, the contaminants in Basin Creek still exerted a significant influence on streambed-sediment geochemistry at the confluence with the Boulder River (river mi 15, fig. 24*A*).

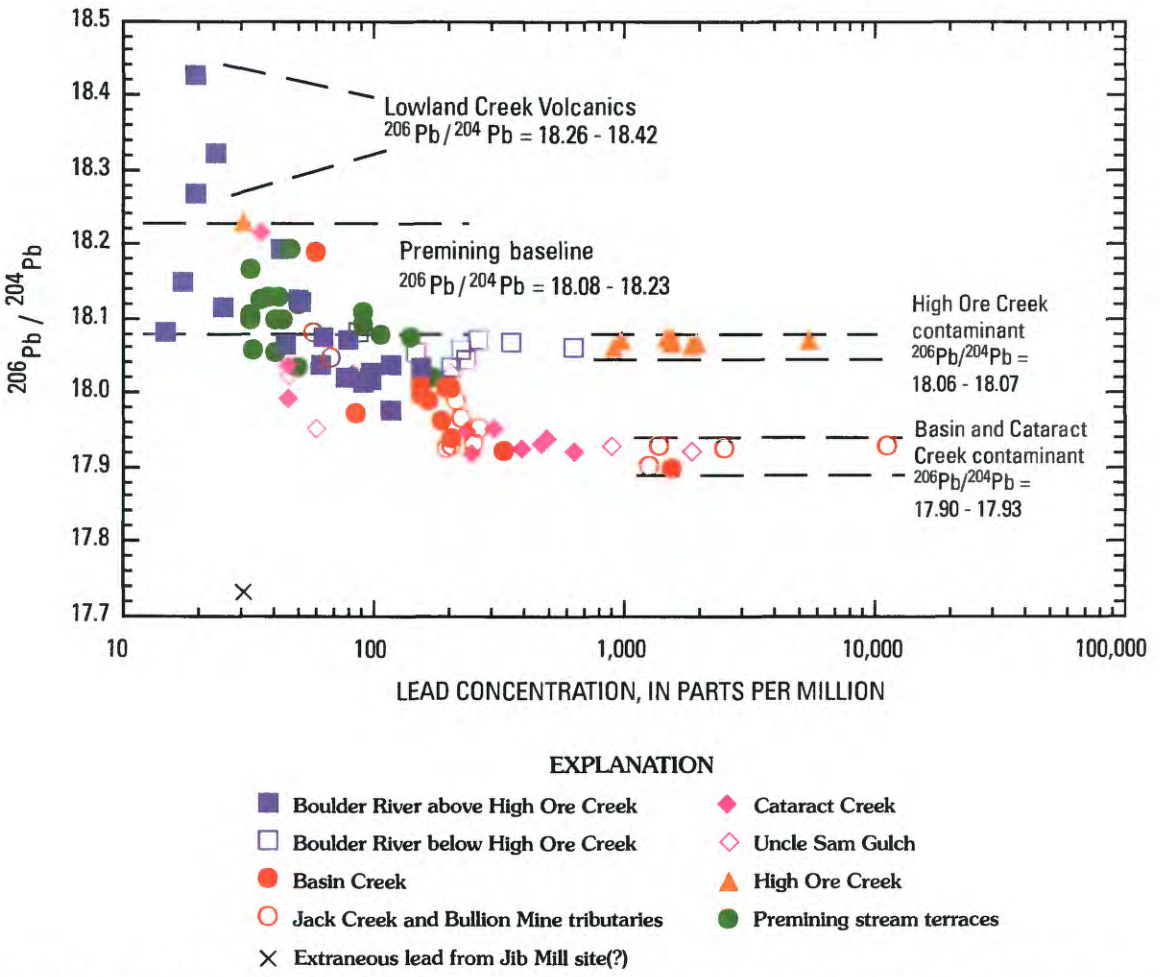

Figure 23. Plot of concentration of lead versus isotopic composition of lead ($^{206}Pb/^{204}Pb$) showing the dominant effect of mixing of contaminant lead derived from mining on isotopic composition of leachable lead in streambed sediment. Analytical error for lead isotopic data is smaller than the symbol. Note limited range in lead isotopic compositions.

Cataract Creek

The $^{206}Pb/^{204}Pb$ values in Cataract Creek streambed sediment decreased progressively downstream from premining baseline values at river mi 6 (fig. 25*A*, site *44S*) to essentially contaminant values at the confluence with Uncle Sam Gulch (river mi 13, sites *49S* and *50S*). Deposit-related trace-element-rich streambed sediment derived from tributaries such as Hoodoo and Rocker Creeks and mines such as the Eva May, Cataract, and Hattie Ferguson in upper Cataract Creek (Martin, this volume) contributed to the deposit-like lead isotopic signature in the streambed sediment at site *49S* (river mi 12.5). Consequently, the effect of streambed sediment derived from Uncle Sam Gulch on the $^{206}Pb/^{204}Pb$ value downstream from the confluence with Cataract Creek was nearly undiscernible in the lead isotope data. Only a slight decrease in the $^{206}Pb/^{204}Pb$ value and an increase in lead concentration in streambed sediment were observed downstream from the confluence (fig. 25*B, C*). The interpretation of the data from site *50S* was further complicated by the fact that mine waste from the Morning Glory was in and along Cataract Creek over an extended area upstream and downstream from the confluence with Uncle Sam Gulch (Martin, this volume).

The influence from the Crystal mine on the deposit-related trace-element load in the streambed sediment of Uncle Sam Gulch is clearly evident in figure 25*B, C*. The lead concentration increased from 34 ppm upstream from the Crystal mine to 1,900 ppm downstream, whereas $^{206}Pb/^{204}Pb$ value decreased from 18.06 to 17.92. The $^{206}Pb/^{204}Pb$ value remained relatively constant all the way downstream to the confluence with Cataract Creek and lead concentrations decreased by about a factor of 2. Downstream from the confluence with Uncle Sam Gulch, lead in the streambed sediment of Cataract Creek decreased only slightly toward premining baseline values; the $^{206}Pb/^{204}Pb$ value increased to 17.95 whereas lead concentrations decreased to 310 ppm upstream from the confluence of Cataract Creek with the Boulder River. Although the lead isotopic composition of deposit lead in Cataract Creek

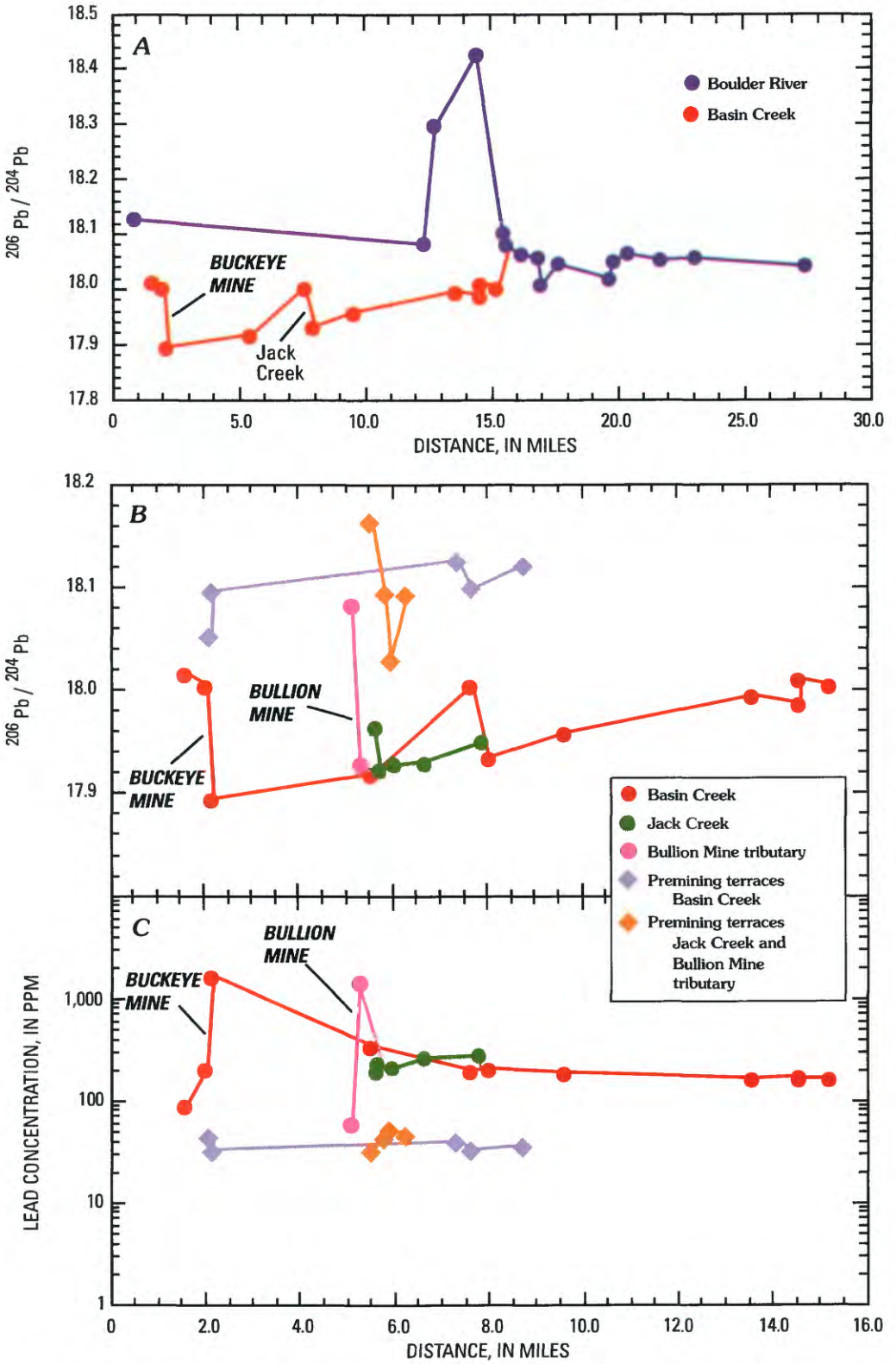

Figure 24. Profile plots of lead isotopic composition (*A*, *B*) and lead concentration (*C*) determined in streambed sediment. *A*, $^{206}Pb/^{204}Pb$ versus distance on Boulder River and Basin Creek. *B*, $^{206}Pb/^{204}Pb$ versus distance on Basin Creek, Jack Creek, and the Bullion Mine tributary. *C*, Concentration of lead in streambed sediment on Basin Creek, Jack Creek, and the Bullion Mine tributary versus distance.

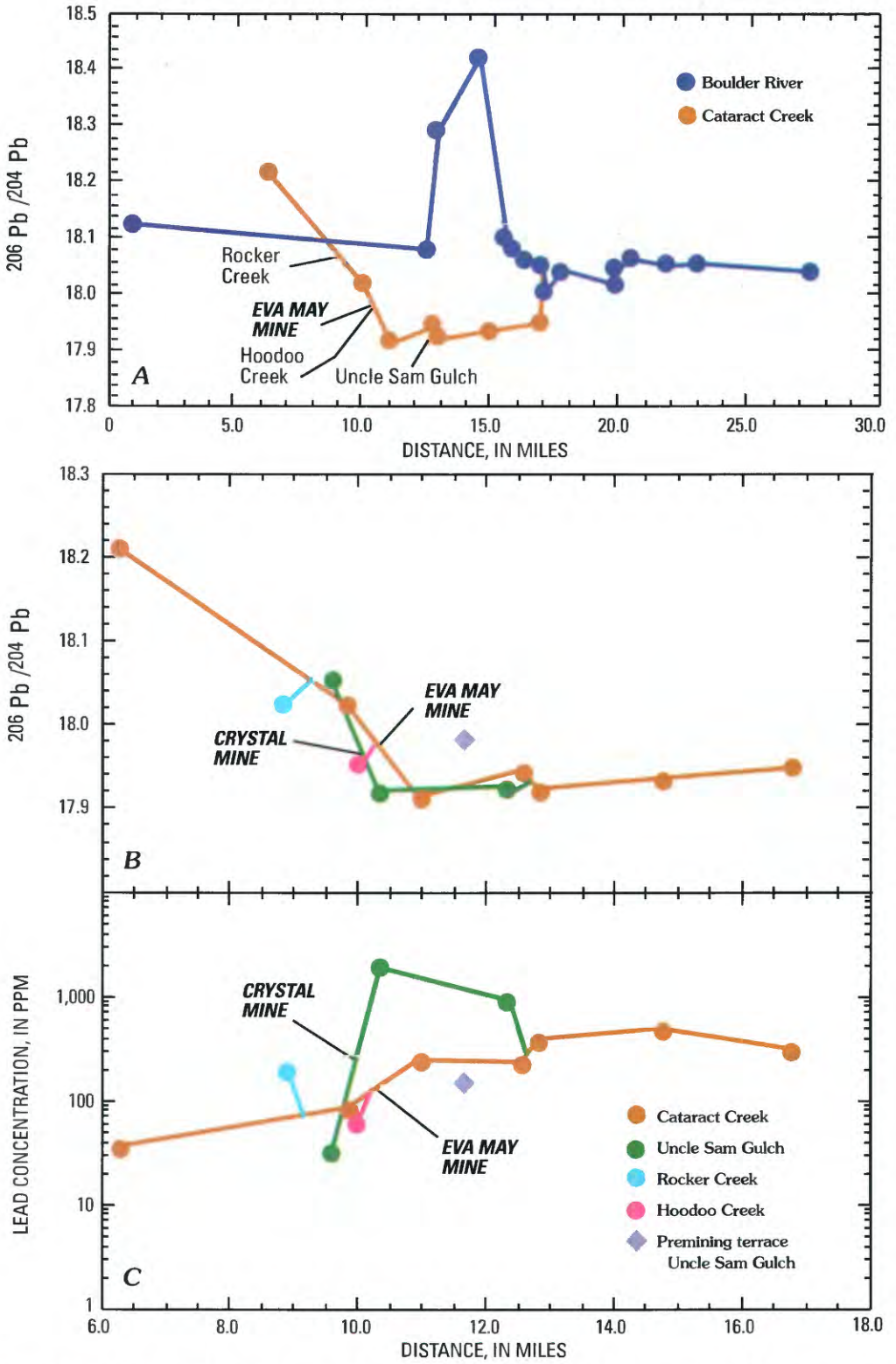

Figure 25. Profile plots of lead isotopic composition (*A*, *B*) and lead concentration (*C*) determined in streambed sediment. *A*, $^{206}Pb/^{204}Pb$ versus distance on Boulder River and Cataract Creek. *B*, $^{206}Pb/^{204}Pb$ versus distance on Cataract Creek and Uncle Sam Gulch. *C*, Concentration of lead in streambed sediment of Cataract Creek and Uncle Sam Gulch versus distance. Note small difference in lead isotopic composition versus the great difference in lead concentration in premining versus modern streambed sediment in Uncle Sam Gulch.

near the Eva May mine site and in Hoodoo Creek was identical to that from the Crystal mine, the very large increase in lead concentration in streambed sediment today downstream from the confluence with Uncle Sam Gulch indicated that the Crystal mine was the major source of contaminants in the Cataract Creek basin.

As mentioned previously, we were not able to obtain any premining stream-terrace samples from Cataract Creek. Lead isotopic data obtained from a single premining terrace sample (*17B*) on Uncle Sam Gulch are shown in figure 25*B, C*. The lower than normal $^{206}Pb/^{204}Pb$ value of 17.99 was in accord with higher than normal deposit-related trace-element concentrations observed at this site (fig. 17). The data indicate that a significant amount of lead was in the streambed sediment prior to mining if the sample from the base of the core at site *17B* was not contaminated by past mining.

High Ore Creek

The Comet mine site on High Ore Creek (river mi 15.9) contributed the bulk of the deposit-related trace elements to streambed sediment in this basin. The $^{206}Pb/^{204}Pb$ value decreased markedly from 18.23 in streambed sediment upstream to 18.07 downstream from the mine (fig. 26*A, B*). Lead concentrations (fig. 26*C*) increased dramatically from about 30 ppm to 5,700 ppm over this same interval. Downstream from the Comet mine, the $^{206}Pb/^{204}Pb$ value remained relatively constant at 18.06–18.07 to the confluence with the Boulder River. Lead concentrations decreased from 1,600 to 1,000 ppm but were still strongly elevated relative to premining concentrations (table 1). Note that the composition of contaminant deposit lead from the Basin and Cataract Creeks was lower than that from the Comet mine, so the lead isotopic composition of streambed sediment in the Boulder River increased to the deposit-lead value at the Comet mine (table 4, fig. 23) downstream from the confluence with High Ore Creek.

Samples from two of the cores that penetrated through the fluvial tailings immediately downstream from the Comet mine (fig. 2) have been used to estimate premining baseline values for streambed sediment in High Ore Creek. One of the samples had a $^{206}Pb/^{204}Pb$ value of 18.10 and contained 33 ppm lead, very similar to premining baseline values throughout the study area. The other had an elevated lead concentration (110 ppm) and somewhat lower $^{206}Pb/^{204}Pb$ value of 18.08. Because these samples were overlain by tailings, the possibility that lead migration through the sediment column may have affected even the sample with the lowest lead concentration must be considered. In any case, present-day lead concentrations in streambed sediment in High Ore Creek prior to the removal actions, which began in 1997, appeared to be 30–150 times those in streambed sediment prior to mining (tables 1 and 4).

Boulder River

Lead isotopic data for the entire 70-mile segment of the Boulder River are summarized in figure 27*A*. The $^{206}Pb/^{204}Pb$ values were lowest through the historical mining district and progressively increased downstream from the district. At a distance of approximately 45 miles downstream from the Basin and Boulder mining districts (site *18S*; river mi 68), the $^{206}Pb/^{204}Pb$ finally approached the baseline value at site *1S* in the Boulder River (river mi 0.5). However, if the $^{206}Pb/^{204}Pb$ value of 18.27 in streambed sediment from the Little Boulder River was a reasonable indication of sediment unaffected by mining activity (site *19S*, river mi 30), then we would conclude that the contribution of deposit lead was still evident at site *18S*, forty-five miles downstream from the Basin and Boulder mining districts near the confluence with the Jefferson River (fig. 27).

The effects of each of the tributaries on the $^{206}Pb/^{204}Pb$ value and lead concentration of Boulder River streambed sediment can be evaluated from figure 27. Lead derived from the Jib Mill (and associated tailings) and Basin Creek caused a pronounced decrease in the $^{206}Pb/^{204}Pb$ value and an increase in lead concentration in Boulder River streambed sediment. It was not possible to isolate the contributions from these two sources because mill tailings apparently derived from the Jib Mill were found downstream of the confluence of Basin Creek and the Boulder River. Furthermore, numerous small prospects in the area, as well as construction debris from a railroad grade and interstate highway, have all caused at least some disruption to the normal sedimentation processes, if not a direct contribution to the sediment load in the Boulder River. Lead isotope data from site *2B* (fig. 2) demonstrated that the use of the minimum concentration from the core at this site was the correct approach to determination of the uncontaminated geochemical baseline in stream-terrace deposits. Geochemical data from the site (fig. 18) indicate a minimum in all deposit-related trace-element concentrations at a depth of 2.6 ft. The $^{206}Pb/^{204}Pb$ from the three lowest sampled intervals was 17.726, which plotted below the field of the deposit leads from the Basin and Boulder mining districts (fig. 23), indicating an extraneous source of lead and copper associated with the Jib Mill. In contrast, the sample from the 2.6 ft depth had a concentration of 34 ppm and a $^{206}Pb/^{204}Pb$ value of 18.123, which plots in the field of uncontaminated sediment from the study area (fig. 23).

Streambed sediment derived from Cataract Creek caused an abrupt increase in both the $^{206}Pb/^{204}Pb$ and lead concentration in the streambed-sediment sample collected immediately downstream (site *9S*, fig. 1, river mi 17) of the confluence of Cataract Creek with the Boulder River. The lead concentration in the Boulder River streambed sediment decreased at site *10S* (river mi 17.5) to values close to those obtained just upstream from the confluence (site *8S*).

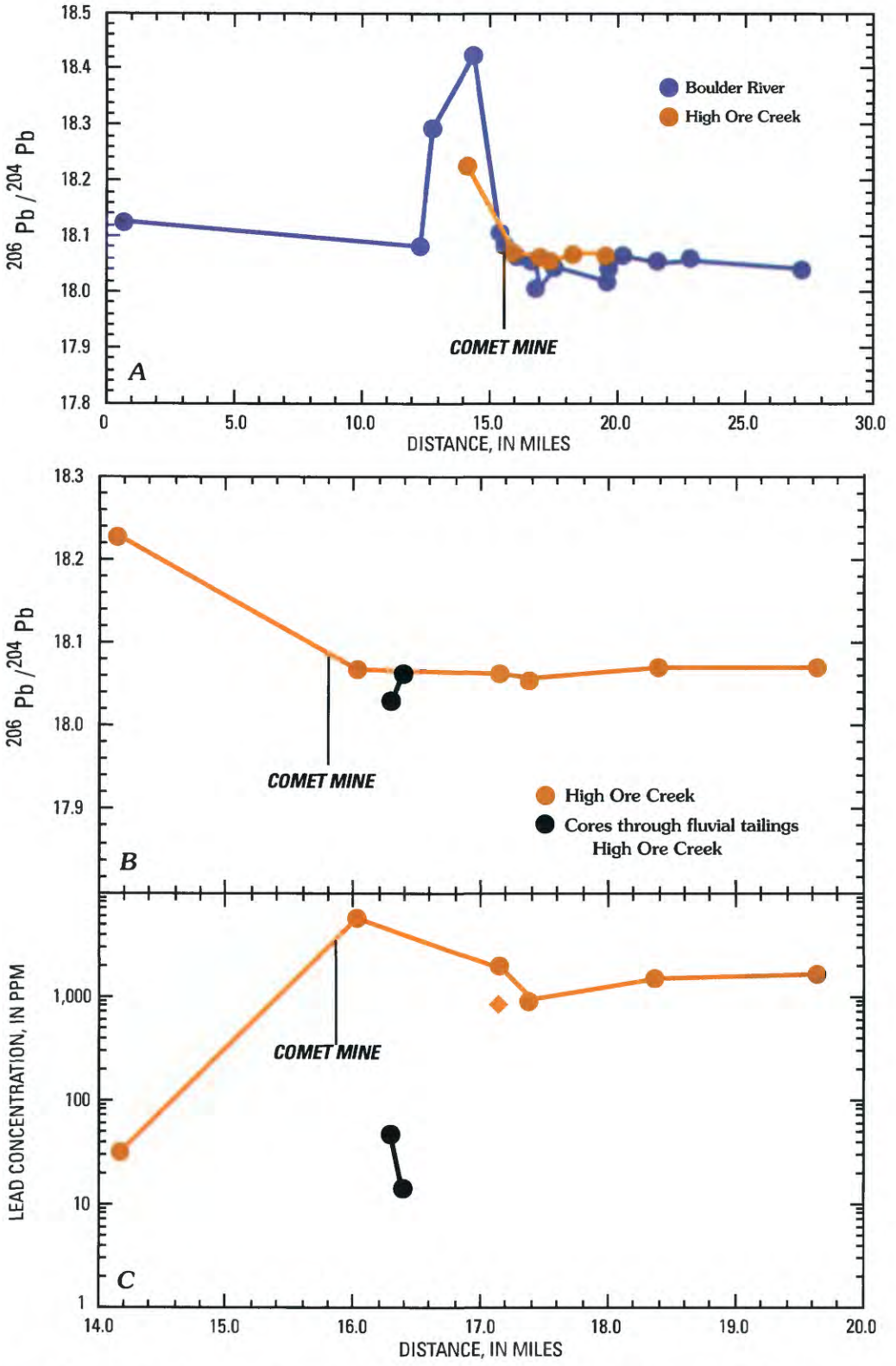

Figure 26. Profile plots of lead isotopic composition (*A, B*) and lead concentration (*C*) determined in streambed sediment. *A*, $^{206}Pb/^{204}Pb$ versus distance on Boulder River and High Ore Creek. *B*, $^{206}Pb/^{204}Pb$ versus distance on High Ore Creek. *C*, Concentration of lead in streambed sediment from High Ore Creek versus distance. Note small difference in lead isotopic composition relative to the large difference in lead concentration in premining versus modern streambed sediment in High Ore Creek.

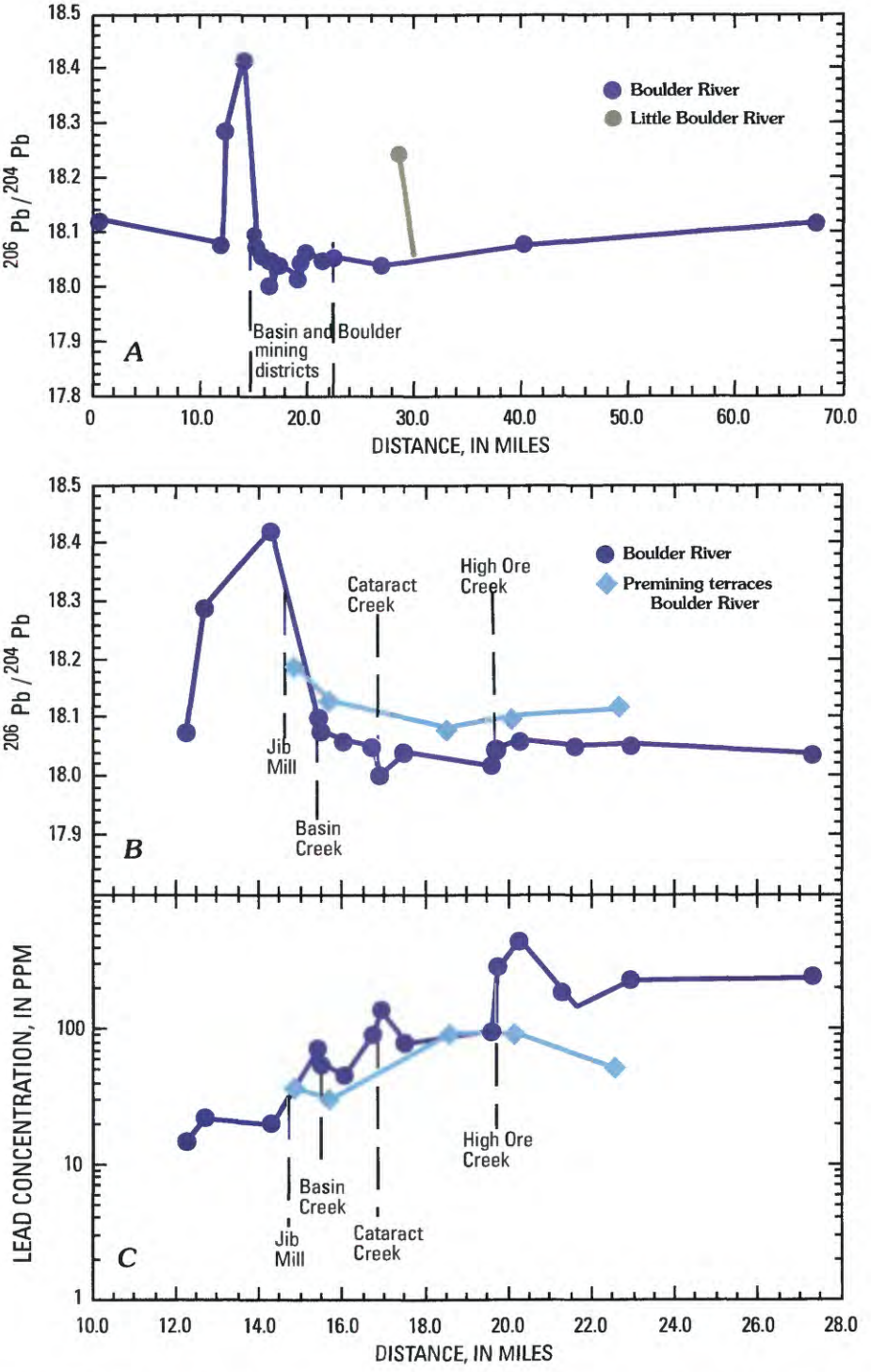

Figure 27. Profile plots of lead isotopic composition (*A*, *B*) and lead concentration (*C*) determined in streambed sediment. *A*, $^{206}Pb/^{204}Pb$ versus distance on Boulder River. *B*, $^{206}Pb/^{204}Pb$ at larger-scale intervals for streambed sediment on Boulder River and premining terrace deposits (sites in fig. 18). *C*, Concentration of lead in streambed sediment today and in streambed sediment from premining terrace samples versus distance on Boulder River.

At the confluence with High Ore Creek, lead concentrations in Boulder River streambed sediment increased by more than a factor of two and remained elevated through river mi 28 (fig. 27*C*). The $^{206}Pb/^{204}Pb$ values increased slightly from 18.02 to 18.05 and remained relatively constant at the latter value through river mi 28, indicating a predominance of the lead from the Comet mine in the streambed sediment of the Boulder River downstream from the confluence with High Ore Creek.

Throughout the Basin and Boulder mining districts, all $^{206}Pb/^{204}Pb$ values in modern streambed sediment were uniformly lower than those from the streambed sediment from premining terraces (fig. 27*B*), probably because of contamination from historical mines, mills, and smelters in the mining districts. This is in spite of the fact that the lead concentrations, at least upstream from High Ore Creek, were quite similar between the premining and present-day data sets (fig. 27*C*). Significant increases in lead concentrations in present-day streambed sediment in the Boulder River were apparent downstream from the confluence of all three tributary streams, but were most pronounced downstream from the confluence with High Ore Creek (fig. 27*C*).

Calculation of the Effect of Historical Mining on the Streambed Sediment in the Boulder River

Bulk mixing calculations were used to estimate the contribution of contaminated streambed sediment from each of the three basins to the streambed sediment of the Boulder River. These calculations, however, assume uniform, well-mixed end members, which we have shown was not the case from our sampling of the north and south banks of the Boulder River downstream from the confluences of the three principal tributaries. Sampling variability also adds an additional source of error that had not been evaluated because replicate samples were not collected in any one year during this study. Furthermore, the calculation errors associated with the small spread of the entire lead isotopic data set result in some mathematical limitations. However, the calculations are useful to evaluate the scale of the heterogeneity in the sampling and to portray the overwhelming effect that the contamination from past mining in the three basins had on the fine-grained (<150 µm) streambed sediment and contaminant loads in the Boulder River. Comparisons of the data for copper and zinc, which were transported largely in the dissolved and suspended phases (Nimick and Cleasby, this volume; Kimball and others, this volume), with the data for lead and arsenic, which were transported largely as colloidal components of the streambed sediment and as grain coatings on detritus in the streambed sediment, are useful in our understanding of the transport of contaminants in the suspended- and streambed-sediment loads. The data also provided valuable information on the mixing zones downstream from stream confluences.

The effect of the deposit-related trace elements in the streambed sediment was estimated on the basis of the increase in trace-element concentrations in the streambed sediment of the Boulder River using the following equation, assuming bulk mixing:

$$P_S = [(C_A - C_B) / (C_A - C_C)] \times 100 \quad (1)$$

where P_S is the percent of the total sediment contributed by tributary C to the receiving stream at site B,

C_A is the concentration of the trace element in streambed sediment in the river upstream from the confluence with the tributary C,

C_B is the concentration of the trace element in streambed sediment in the river downstream from the confluence with the tributary and

C_C is the concentration of the trace element in the tributary stream C at its confluence.

The amount of a deposit-related trace-element contaminant in streambed sediment in the river that was contributed by the tributary was estimated from the following equation, also assuming bulk mixing:

$$P_C = P_S \times C_C / C_B \quad (2)$$

where P_C is the percent contaminant contributed by the tributary and P_S, C_C, and C_B are defined as in eq. 1.

An independent method of estimating P_C for lead was obtained from the lead isotopic data (Church and others, 1997) using the following equation:

$$P_{Pb} = [(R_A - R_B) / (R_A - R_C)] \times 100 \quad (3)$$

where P_{Pb} is the percent lead contributed by the tributary C to the river,

R_A is the $^{206}Pb/^{204}Pb$ in the river upstream of the confluence with tributary C,

R_B is the $^{206}Pb/^{204}Pb$ in the river downstream of the confluence with the tributary, and

R_C is the $^{206}Pb/^{204}Pb$ in tributary C upstream from the confluence.

Values used for A, B, and C in these equations are indicated in table 5.

Although this method is based on mass and is therefore independent of trace-element concentrations and the mechanisms of transport, estimates may be uncertain as a result of the small isotopic differences found among R_A, R_B, and R_C relative to the precision of the individual measurements of these lead isotopic ratios. This was especially true for very small contributions (that is, $R_A \approx R_B$) and very large contributions (that is, $R_B \approx R_C$) from C. It was also true in the situation where contributions of C to previously contaminated sediment are similar (that is, $R_A \approx R_B \approx R_C$).

Calculations were made, using equations 1, 2, and 3 and the 1996 total-digestion data, to determine the effects of each of the three main tributaries on the streambed-sediment geochemistry of the Boulder River. These results are summarized in table 5. Calculations were made for several site "*B*"

Table 5. Calculated copper, zinc, arsenic, and lead contributions from Basin, Cataract, and High Ore Creeks to Boulder River.

[Total-digestion data are from samples collected in 1996; P_S, P_C, and P_{Pb} are defined from equations 1–3 (in text) and are expressed in percent. Columns in order of element mobility as defined in Fey and Desborough, this volume. Bold type values, good agreement between the different methods of calculation for amount of contaminants contributed by each tributary to Boulder River. Sites are referred to as A, B, or C, as defined in text]

Basin Creek and Jib Mill contributions to Boulder River															
	Site	Cu ppm	Zn ppm	As ppm	Pb ppm	$^{206}Pb/^{204}Pb$	P_SCu	P_SZn	P_SAs	P_SPb	P_CCu	P_CZn	P_CAs	P_CPb	P_{Pb}
A	4S	25	120	14	20	18.425									
C	31S	93	600	110	160	18.005									
B	6S	205	530	60	57	18.078	265	85	**48**	26	120	97	**88**	**74**	**83**
B	8S	150	635	59	92	18.054	184	107	**46**	**51**	114	101	**87**	**89**	**88**
A	5S	305	820	89	72	18.102									
C	31S	93	600	110	160	18.005									
B	6S	205	530	60	57	18.078	47	132	-138	-17	21	149	-253	-48	25

Cataract Creek contributions to Boulder River															
	Site	Cu ppm	Zn ppm	As ppm	Pb ppm	$^{206}Pb/^{204}Pb$	P_SCu	P_SZn	P_SAs	P_SPb	P_CCu	P_CZn	P_CAs	P_CPb	P_{Pb}
A	8S	150	635	59	92	18.054									
C	53S	560	2,600	380	310	17.949									
B	9S	285	1,015	135	140	18.006	33	19	**24**	**22**	65	**50**	67	**49**	**46**

High Ore Creek contributions to Boulder River															
	Site	Cu ppm	Zn ppm	As ppm	Pb ppm	$^{206}Pb/^{204}Pb$	P_SCu	P_SZn	P_SAs	P_SPb	P_CCu	P_CZn	P_CAs	P_CPb	P_{Pb}
A	11S	195	890	81	97	18.019									
C	63S	740	10,000	4,300	1,600	18.068									
B	12S	350	1,650	605	285	18.048	28	**8**	**12**	**13**	60	51	**88**	70	59
B	13S	455	2,600	1,665	460	18.063	48	19	38	24	78	72	**97**	**84**	**90**
B	15S	220	1,700	530	230	18.056	5	**9**	**11**	**9**	15	52	**86**	62	76

localities to evaluate the effects of the tributaries both immediately downstream from the confluence and farther downstream. We used the concentrations and $^{206}Pb/^{204}Pb$ value of the tributary sample closest to the confluence of the Boulder River as site "*C*" (sites *31S*, *53S*, and *63S*; figs. 1 and 14).

The choice of sites upstream of the confluence (that is, site "*A*") for each of the tributaries was somewhat problematic because the downstream concentration profiles (fig. 14*B*) do not progressively increase in the Boulder River. Whereas it would have been simple to dismiss this irregularity as due to sample heterogeneity, we interpreted the data as a transport phenomenon in the Boulder River. Sediment collected immediately upstream and downstream from the confluences have previously been shown to be quite heterogeneous depending upon the side of the river on which the sample was collected. Also, samples collected midway between tributary confluences generally showed atypically low deposit-related trace-element concentrations that may not be representative of the river segment between the tributaries because these sites were collected in 1997 and 1998, so year-to-year variation was also present in the data set. Consequently, we used the 1996 total-digestion data from the sites immediately upstream of each of the confluences of Cataract and High Ore Creeks as "site *A*" for these two tributaries (table 5).

The effects of streambed sediment derived from Basin Creek on the Boulder River were distinguished from the effects of mill tailings contributed by the Jib Mill on the basis of the lead isotopic data measured in the terrace at site *2B*. However, because the Jib Mill site is private property and was not sampled, we cannot quantitatively separate the contributions from Basin Creek and the Jib Mill site. We have chosen site *4S* as site "*A*" for the calculations for Basin Creek (table 5, fig. 1). The marked increase in deposit-related trace-element concentrations between sites *4S* and *5S* and the calculations in table 5 suggest that the Jib Mill contributed significant amounts of copper and zinc and more modest amounts of arsenic and lead to the streambed sediment of the Boulder River. This observation from the streambed-sediment data calculations was supported by the analysis of the chemical data from core *2B* (fig. 18) sampled downstream from the Jib Mill, which showed increased concentrations of copper and zinc in the lower portions of the core, and by the lead isotopic data from this section of the core, which indicated that ore from outside the Basin and Boulder mining districts was processed at the Jib Mill (fig. 23). The percent sediment contribution (eq. 1) calculated for Basin Creek from the arsenic data agreed well using either site *6S* or *8S* as the downstream site (48 and 46 percent respectively, table 5) and compared well with calculations using the lead data from site *8S* (51 percent). Calculations of the percent contaminant for both lead and arsenic (eq. 2) agreed well using both downstream sites ranging between 74 and 89 percent. These values also agreed well with the calculated percentage of deposit lead (83 and 88 percent) from the lead isotope data (eq. 3). All calculations indicated an unaccounted-for contribution of copper and zinc, which we attribute to the Jib Mill site (see data from site *2B*, fig. 18).

Calculations for the percent sediment (eq. 1) and the percent contaminant (eq. 2) using the copper and zinc data were much higher, ranging from about 97 to 120 percent for $P_C Cu$ and $P_C Zn$. However, calculated copper contributions ($P_S Cu$) were very large, ranging from 184 to 265 percent (table 5). We interpret these data to indicate that a large component of copper was being contributed from an unsampled location between *4S* and *5S*, probably the Jib Mill site. Basin Creek (site *31S*) was apparently a lesser contributor of deposit-related trace-element contamination to the Boulder River than the Jib Mill site.

The effects of streambed sediment contributed by Cataract Creek to the Boulder River have been calculated using the data from sites *8S*, *9S*, and *53S* (table 5, fig. 1). Concentrations of all four deposit-related trace elements increased significantly in streambed sediment downstream of the confluence with Cataract Creek at site *9S*. Calculations of the percentage of contaminant ($P_C Pb$) and the percentage of deposit lead (P_{Pb}) for site *9S* were also in good agreement at 49 and 46 percent respectively. The calculated percent sediment increased using the 1996 total-digestion data for zinc, lead, arsenic, and copper from 19 to 33 percent of the sediment contributed by Cataract Creek (table 5). The calculated percent contaminant increased in a similar fashion ranging from 49 to 67 percent. Higher values for arsenic and copper indicate preferential transport of these two trace elements in the water or suspended sediment of Cataract Creek.

The effects of streambed sediment contributed by High Ore Creek to the Boulder River have been calculated using the data from sites *11S*, *12S*, and *63S* (table 5, fig. 1). Calculations for site *12S*, immediately downstream from High Ore Creek (figs. 1 and 14*B*) suggested that, whereas the percent sediment contributed by High Ore Creek was in the range of 8 to 13 percent using the zinc, arsenic, and lead concentrations ($P_S Zn$, $P_S As$, and $P_S Pb$), 51 to 88 percent of the contaminants in streambed sediment of the Boulder River were contributed by the streambed sediment from High Ore Creek (table 5, fig. 1). At site *13S* approximately 0.6 mi downstream from High Ore Creek where the differences between concentration and lead isotopic data were reduced between the two different sites from the north and south sides of the river, calculated contaminant contributions from High Ore Creek ranged from 72 to 97 percent for all deposit-related trace elements and 90 percent deposit-lead contaminant. At site *15S*, about 3.3 mi downstream, the calculated percentages using the arsenic, lead, and the lead isotopic data were 86, 62, and 76 percent respectively, whereas the calculations for zinc and copper were substantially lower, 52 and 15 percent respectively.

Evidence for preferential transport of copper and zinc relative to lead (shown previously in fig. 14*A*) and the inconsistent results for these two elements as shown in table 5 indicated that the lead isotopic data generally represented the best estimates of overall deposit-related trace-element contributions to the streambed sediment in the Boulder River. In most instances, the percent contribution calculated from the arsenic and lead concentration data was in reasonably good agreement

with that calculated from the $^{206}Pb/^{204}Pb$ data. Calculations of streambed-sediment contributions from Cataract and High Ore Creeks were probably best estimated from the arsenic and lead data. However, reliable estimates for the Basin Creek contribution cannot be made because of the influence of the Jib Mill at the confluence.

The effects of the three tributaries on the lead in the streambed sediment of the Boulder River are summarized in more detail in figure 28. The effect of past mining on the streambed sediment in the Boulder River increased progressively as the Boulder River flowed through the Basin and Cataract mining districts. It is evident from figures 28 and 29 that High Ore Creek contributed the largest fraction of deposit-related lead to the Boulder River. Downstream from High Ore Creek through site *15S*, about 3.3 mi downstream from High Ore Creek, more than 70 percent of the lead in the streambed sediment was traced to deposit lead from historical mining activity in the Boulder River watershed study area.

Estimates of the percentage of deposit-related lead at any site within the area can be made using $^{206}Pb/^{204}Pb$ data and equation 3. The appropriate R_A and R_C values are in table 4, and the R_B values were those measured at the individual sites. The calculated percent deposit-lead values (P_{Pb} values, eq. 3) are shown as a ribbon map, figure 29. Because we expressed the lead isotopic data in terms of percent contaminant deposit lead, the two different identified isotopic signatures for the deposit leads, one from Basin Creek and Cataract Creek basins, and a second from High Ore Creek basin (fig. 23), were normalized out of the data in figure 28. In using these data, however, we were not able to distinguish between deposit-related lead that had weathered from outcrops of mineralized rock and lead introduced into the stream from historical mining wastes or mill tailings. Consequently, although the calculated P_{Pb} values may closely approximate contaminant lead contributions downstream from major mines, these values are not, in a strict sense, percentages of lead introduced by historical mining. However, in the absence of data indicating a large, undefined source of deposit-related trace elements in the study area, the calculated percentages provided a good estimate of the contaminants introduced into the aquatic habitat today by past mining practices.

The highest percentages of deposit-related lead were found downstream of the major mines in the area. Concentrations of lead in streambed sediment from Basin Creek decreased to some extent as shown by higher $^{206}Pb/^{204}Pb$ values downstream from both the Buckeye mine and the confluence with Jack Creek, but 50–75 percent of the lead present in the streambed sediment of Basin Creek at its confluence with the Boulder River was deposit-related lead.

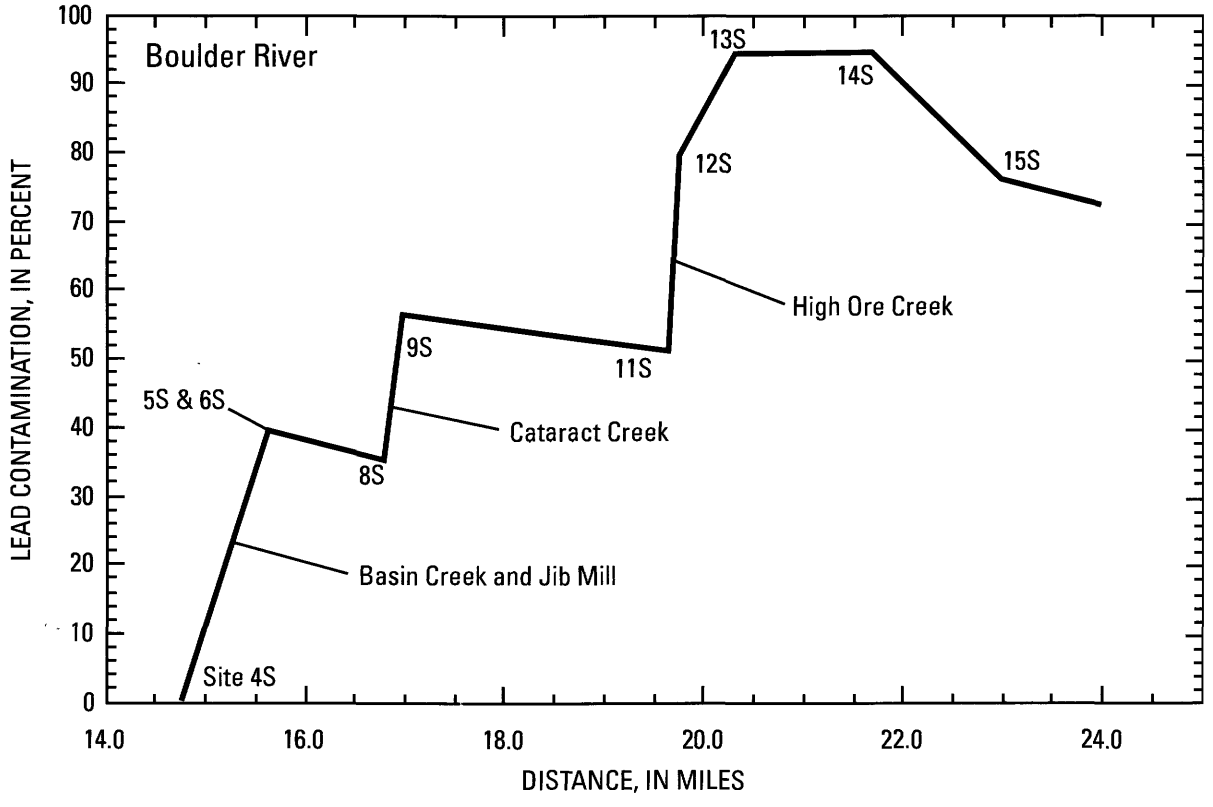

Figure 28. Plot of the calculated percent deposit-lead contamination added to the streambed sediment of the Boulder River by the addition of tailings from the Jib Mill site and streambed sediment from Basin Creek, from streambed sediment from Cataract Creek, and from streambed sediment from High Ore Creek.

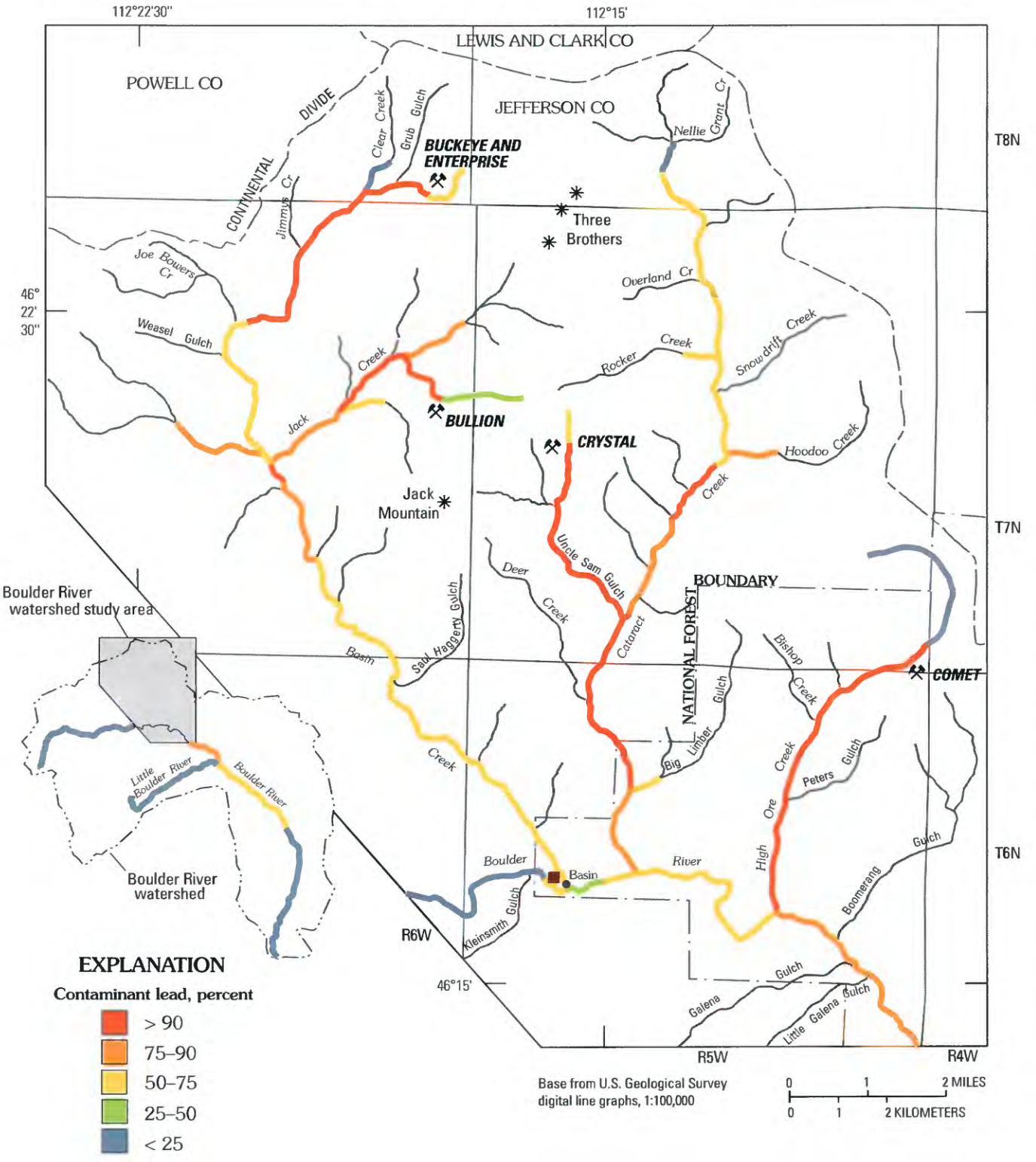

Figure 29. Ribbon map showing calculated percentages of deposit lead in streambed sediment today (table 5). Dark-red square, Jib Mill site.

The highest proportions of deposit-related lead in the Cataract Creek drainage were found downstream from the Eva May mine site, in Uncle Sam Gulch downstream from the Crystal mine, and in Cataract Creek downstream from Uncle Sam Gulch. The $^{206}Pb/^{204}Pb$ values in streambed sediment downstream from this confluence increased only slightly before Cataract Creek enters the Boulder River.

The Comet mine on High Ore Creek represents the dominant source of deposit-related lead in this basin. The calculated percentages of deposit-related lead remain greater than 90 percent from the Comet mine to the confluence with the Boulder River.

Downstream from site *15S* on the Boulder River, calculations become very tentative owing to the lack of data from surrounding rocks or streambed sediment from other tributaries to the Boulder River. The Little Boulder River, a principal tributary that enters the Boulder River just downstream from site *16S* (river mi 28) had $^{206}Pb/^{204}Pb$ values similar to or slightly higher than those of premining baseline values estimated in table 4. If we assume that the estimated premining baseline values in table 4 are valid downstream from site *15S* and that no other sources of deposit-related lead occur downstream, then calculations can be made as for figures 28 and 29. Results suggest that as much as 80, 50, and 13 percent of the lead in streambed sediment of the Boulder River at sites *16S* (river mi 27), *17S* (river mi 41), and *18S* (river mi 68) respectively is deposit-related lead. Thus, we have quantified the contaminant contributions of the major tributaries to the Boulder River, fulfilling the fourth goal of the study.

Comparison of the Boulder River Watershed Streambed-Sediment Data with Sediment-Quality Guidelines

Sediment-quality guidelines for trace-element concentrations in streambed sediment have only recently been defined and are not currently regulated. Various measures of biologic response to elevated concentrations of deposit-related trace elements in sediment are summarized in table 6 (Jones and others, 1997; MacDonald and others, 2000). Different definitions are used to define the effect of sediment-borne contaminants on aquatic life (see the footnotes, table 6). For the purposes of this discussion, we adopt the terminology used in MacDonald and others (2000). The Threshold Effect Concentration (TEC) is defined as the "contaminant concentration below which harmful effects on sediment-dwelling organisms were not expected," whereas the Probable Effect Concentration (PEC) is defined as the "contaminant concentration above which harmful effects on sediment-dwelling organisms were expected to occur frequently" (MacDonald and others, 2000, p. 21). For the elements antimony and silver, no TEC or PEC values have been determined. For these elements, we use the Screening Level Concentration (SLC) values (table 6), defined as "the highest concentration that can be tolerated by approximately 95 percent of the benthic fauna"(EPA, 1996).

For most of the deposit-related trace elements investigated in this watershed, the ranges of the TEC (or SLC) and PEC concentrations were significantly below those found in the streambed sediment from the Boulder River watershed study area. Leachable concentrations of the potentially toxic trace elements investigated in this study are those concentrations either sorbed or loosely bound in the iron-oxyhydroxide fraction of the streambed sediment. Leachable trace-element concentrations were compared with the sediment-quality guidelines at four sites on the Boulder River, at the mouths of the three major tributaries, and below the major mine sites (table 7). Concentrations of arsenic and lead exceeded the PEC sediment-quality guidelines in streambed sediment throughout the Basin, Cataract, and High Ore Creek basins and in the streambed sediment in the Boulder River immediately downstream from their confluences except at site 6S for lead downstream of the Basin Creek confluence. Copper concentrations exceeded PEC values in Basin Creek below the Bullion Mine tributary, in Uncle Sam Gulch and Cataract Creek downstream to the confluence in the Boulder River, and in the Boulder River downstream from Basin Creek to the confluence with the Little Boulder River (river mi 27). Copper concentrations exceeded the TEC everywhere in the study area downstream from historical mining. Zinc and cadmium concentrations exceeded the PEC in streambed sediment downstream from the Buckeye mine on Basin Creek, and exceeded the TEC elsewhere throughout the Basin Creek basin downstream from historical mining. Zinc and cadmium concentrations in streambed sediment exceeded the PEC everywhere in the Cataract Creek and High Ore Creek basins. Zinc exceeded the PEC and cadmium exceeded the TEC in the streambed sediment of the Boulder River downstream from the confluence with the Little Boulder River because of the sorption of zinc to freshly precipitated colloidal fraction of the streambed sediment (see fig. 14*B*). Silver and antimony concentrations exceeded the SLC values in streambed sediment everywhere within the study area downstream from historical mining sites where the concentrations in streambed sediment exceed the analytical limits of detection.

Table 6. Summary of screening level concentrations proposed as possible measures for sediment-quality guidelines.

[Concentrations in parts per million, ppm; --, no value recommended; bold values are recommended consensus values]

	ARCS[1]		Ontario MOE[4]		EPA-IV SLC[5]	OSWER SLC[6]	Range of SLC[7]	Range of AET[8]	Consensus TEC[9]	Consensus PEC[10]
	TEC[2]	PEC[3]	Low	Severe						
Antimony	--	--	--	--	12	--	12	--	--	--
Arsenic	12.1	57	6	33	7.24	8.2	7–12	33–57	**9.79**	**33.0**
Cadmium	0.592	11.7	0.6	10	1	1.2	0.6–1.0	10–12	**0.99**	**4.98**
Copper	28	77.7	16	110	18.7	34	16–34	78–110	**31.6**	**149**
Iron	--	--	20,000	40,000	--	--	20,000	40,000	--	--
Lead	34.2	396	31	250	30.2	47	30–47	250–400	**35.8**	**128**
Silver	--	--	--	--	2	--	2	--	--	--
Zinc	159	1,532	120	820	124	150	120–160	820–1,532	**121**	**459**

[1]ARCS - Assessment and Remediation of Contaminated Sediments Project, EPA Region IV, Great Lakes Program (U.S. EPA, 1996).

[2]TEC -Threshold Effect Concentration, the contaminant concentration below which harmful effects on sediment-dwelling organisms were not expected.

[3]PEC - Probable Effect Concentration, the contaminant concentration above which harmful effects on sediment-dwelling organisms were expected to occur frequently.

[4]Ontario MOE - Low, the lowest effect level of screening level concentration (5th percentile); Severe, severe effect level of screening level concentration (95th percentile; Persuad and others, 1993).

[5]EPA-IV - Ecological screening values for sediments (U.S. EPA, 1995).

[6]OSWER - Office of Solid Waste and Emergency Response (U.S. EPA, 1996) screening level concentrations.

[7]SLC - Screening Level Concentration, the highest concentration of a contaminant that can be tolerated by approximately 95 percent of the benthic fauna.

[8]AET - Apparent Effects Threshold, that concentration above which statistically significant biologic effects always occur.

[9]Consensus-based TEC from MacDonald and others (2000); predicted TEC shown accurately predicts no toxic effect more than 80 percent of the time (n=347) for all trace elements in table except for arsenic where the TEC shown accurately predicts no toxic effect 74 percent of the time (n=150).

[10]Consensus-based PEC from MacDonald and others (2000); predicted PEC shown accurately predicts a toxic effect 90 percent or more of the time (n=347) for all trace elements in table except for arsenic where the PEC shown accurately predicts a toxic effect 76.9 percent of the time (n=150).

Table 7. Sites where the leachable deposit-related trace-element concentrations in streambed sediment from the study area exceed recommended screening levels.

[Concentrations of trace elements copper, lead, zinc, arsenic, and cadmium are in italics where they exceed the TEC and in bold where they exceed the PEC concentration (from table 6, consensus-based values); and for silver and antimony, concentrations are in italics where they exceed the SLC concentration (from table 6, U.S. EPA-IV Screening Level Concentrations)]

Location	Site	Cu ppm	Pb ppm	Zn ppm	As ppm	Cd ppm	Ag ppm	Sb ppm
Boulder River upstream from Basin Creek	4S	25	20	120	*14*	<1	<1	<3
Basin Creek downstream from Buckeye Mill.	21S	*120*	***1,600***	***680***	***4,000***	***5***	*6.9*	*34*
Bullion Mine tributary downstream from the Bullion mine.	34S	***340***	***1,400***	*350*	***4,400***	*1.6*	*12*	*16*
Jack Creek at confluence	24S	24	***170***	*290*	***98***	*2*	<1	<3
Basin Creek at confluence	31S	*93*	***162***	***585***	***125***	***5.3***	<1	<3
Boulder River downstream from the confluence with Basin Creek.	6S	***190***	*49*	*425*	***35***	*3.1*	<1	<3
Uncle Sam Gulch at confluence	57S	***2,400***	***790***	***3,700***	***900***	***41***	*5.4*	*9.2*
Cataract Creek at confluence	53S	***420***	***320***	***1,450***	***460***	***15***	*3.7*	3
Boulder River downstream from the confluence with Cataract Creek.	9S	***235***	***135***	***725***	***105***	*4.7*	*3.1*	<3
High Ore Creek downstream from the Comet Mill.	59S	***1,600***	***5,900***	***14,000***	***5,300***	***140***	*45*	*25*
High Ore Creek	63S	***540***	***1,400***	***6,100***	***4,200***	***21***	*22*	4.9
Boulder River downstream from the confluence with High Ore Creek.	13S	***285***	***460***	***1,500***	***350***	***14.5***	*9.6*	<3
Boulder River upstream from the confluence with Little Boulder River.	16S	***380***	***220***	*420*	***230***	*2.2*	*4.3*	<3
Little Boulder River	19S	17	22	85	*14*	<1	<1	<3
Boulder River at river mi 40	17S	*86*	*83*	***490***	***57***	*1.4*	*1.3*	<3
Boulder River at confluence with Jefferson River.	18S	*92*	*50*	***700***	*15*	*4.7*	*<1*	<3

Summary

Assessment of deposit-related and rock-forming trace elements in streambed sediment in the Boulder River watershed has provided the data necessary to delineate stream reaches having elevated contaminant concentrations that exceeded recommended action levels for streambed sediment, to determine anthropogenic sources of deposit-related trace elements that contaminated sediment, to understand the transport of dissolved and particulate trace elements, and to establish the streambed-sediment framework needed to evaluate toxicity to aquatic biota.

Concentrations of the suite of deposit-related trace elements copper, lead, zinc, arsenic, silver, cadmium, and antimony were elevated in modern streambed sediment in the Boulder River downstream from the confluence with Basin, Cataract, and High Ore Creeks. The major sources of these contaminants can be tied directly to historical mining at the Buckeye and Enterprise mines in upper Basin Creek, the Bullion mine on a small tributary of Jack Creek and sediment trapped in beaver ponds and a small reservoir on Jack Creek, the area of Cataract Creek just upstream from the confluence with Uncle Sam Gulch, the Crystal mine in upper Uncle Sam Gulch, and the Comet mine in upper High Ore Creek. The Jib Mill site immediately upstream from the confluence of Basin Creek with the Boulder River was also implicated as a source of these contaminants, especially of elevated concentrations of copper in the Boulder River at the confluence with Basin Creek.

Downstream from the confluence of Basin Creek, concentrations of leachable arsenic and copper exceeded the probable effect concentration, and lead, zinc, silver, cadmium, and antimony exceeded the threshold effect concentration, in modern streambed sediment of the Boulder River. Downstream from the confluence with Cataract Creek to the confluence with the Little Boulder River, streambed sediment in the Boulder River contained concentrations of copper, lead, zinc, arsenic, and at most sites, cadmium that exceeded the probable effect concentration in streambed sediment. All of the major tributary basins, Basin Creek, Jack Creek, Cataract Creek, Uncle Sam Gulch, and High Ore Creek, also

had concentrations of copper, lead, and arsenic in streambed sediment downstream of these major mines to their confluence that exceeded the probable effects concentration. Everywhere within the three basins downstream from the major mines, the concentrations of all the deposit-related trace elements exceeded the sediment-quality guidelines (table 7).

Comparison of the concentrations of this suite of deposit-related trace elements in streambed sediment today with that in premining streambed sediment from terrace deposits in the flood plains of these streams showed that the concentrations of the deposit-related trace elements were substantially elevated in streambed sediment today, from several to more than 100 times that prior to historical mining activities. Lead isotopic data from these two media indicate that the effect of mineralized rock on the streambed-sediment geochemistry prior to mining was small relative to what we can see today.

Two different sources of deposit lead were defined by the lead isotopic data, one representing the polymetallic vein deposits in both the Basin and Cataract Creek basins, and a second at the Comet mine in the High Ore Creek basin. Calculations of the extent of the contamination caused by historical mining activity using both the arsenic and lead concentration data and the lead isotopic data gave similar results. In contrast, calculations using the copper and zinc data gave higher percentages, some exceeding 100 percent. These results indicate that the copper and zinc were being actively and differentially transported in the suspended-sediment phase and were being precipitated to the streambed sediment as a function of velocity of the stream reach often miles downstream from their source. The contribution of contaminant lead, as shown in figure 28, to streambed sediment of the Boulder River from Basin Creek was about 35 percent and from Cataract Creek about 15 percent. However, the contribution of contaminant lead to streambed sediment of the Boulder River from High Ore Creek was about 50 percent. The contamination from High Ore Creek dominated the concentrations of deposit-related trace elements in stream sediment of the Boulder River below the confluence downstream to the Jefferson River.

References Cited

Aamodt, P.L., 1978, Uranium hydrogeochemical and stream sediment pilot study of the Boulder batholith, Montana: Grand Junction, Colo., U.S. Dept. of Energy, GJBX-56(78), 118 p.

Becraft, G.E., Pinckney, D.M., and Rosenblum, Sam, 1963, Geology and mineral deposits of the Jefferson City Quadrangle, Jefferson and Lewis and Clark Counties, Montana: U.S. Geological Survey Professional Paper 428, 101 p.

Bigham, J.M., Schwertmann, U., Traina, S.J., Winland, R.L., and Wolf, M., 1996, Schwertmannite and the chemical modeling of iron in acid sulfate waters: Geochemica et Cosmochimica Acta, v. 60, p. 2111–2121.

Briggs, P.H., 1996, Forty elements by inductively coupled plasma-atomic emission spectroscopy, *in* Arbogast, B.F., ed., Analytical methods manual for the Mineral Resources Program, U.S. Geological Survey: U.S. Geological Survey Open-File Report 96–525, p. 77–94.

Broxton, W.W., 1980, Uranium hydrogeochemical and stream sediment reconnaissance data release for the Butte NTMS quadrangle, Montana, including concentrations of forty-two additional elements: Grand Junction, Colo., U.S. Dept. of Energy, GJBX-129(80), 207 p.

Church, S.E., 1981, Multielement analysis of fifty-four geochemical reference samples using inductively coupled plasma-atomic emission spectrometry: Geostandards Newsletter, v. 5, p. 133–160.

Church, S.E., Holmes, C.E., Briggs, P.H., Vaughn, R.B., Cathcart, James, and Marot, Margaret, 1993, Geochemical and lead-isotope data from stream and lake sediments, and cores from the upper Arkansas River drainage—Effects of mining at Leadville, Colorado, on heavy-metal concentrations in the Arkansas River: U.S. Geological Survey Open-File Report 93–534, 61 p.

Church, S.E., Kimball, B.A., Fey, D.L., Ferderer, D.A., Yager, T.J., and Vaughn, R.B., 1997, Source, transport, and partitioning of metals between water, colloids, and bed sediments of the Animas River, Colorado: U.S. Geological Survey Open-File Report 97–151, 136 p.

Cleasby, T.E., Nimick, D.A., and Kimball, B.A., 2000, Quantification of metal loads by tracer-injection and synoptic-sampling methods in Cataract Creek, Jefferson County, Montana, August 1997: U.S. Geological Survey Water-Resources Investigations Report 00–4237, 39 p.

Desborough, G.A., Leinz, Reinhardt, Sutley, Stephen, Briggs, P.H., Swayze, G.A., Smith, K.S., and Breit, George, 2000, Leaching studies of schwertmannite-rich precipitates from the Animas River headwaters, Colorado and Boulder River headwaters, Montana: U.S. Geological Survey Open-File Report 00–004, 16 p.

Elliott, J.E., Loen, J.S., Wise, K.K., and Blaskowski, M.J., 1992, Maps showing locations of mines and prospects in the Butte 1° × 2° quadrangle, western Montana: U.S. Geological Survey Miscellaneous Investigations Series Map I–2050–C, 147 p., 2 sheets, scale 1:250,000.

Fey, D.L., and Church, S.E., 1998, Analytical results for 42 fluvial tailings cores and 7 stream-sediment samples from High Ore Creek, northern Jefferson County, Montana: U.S. Geological Survey Open-File Report 98–215, 49 p.

Fey, D.L., Church, S.E., and Finney, C.A., 1999, Analytical results for 35 mine-waste tailings cores and six stream-sediment samples, and an estimate of the volume of contaminated material at the Buckeye meadow on upper Basin Creek, northern Jefferson County, Montana: U.S. Geological Survey Open-File Report 99–537, 59 p.

Fey, D.L., Church, S.E., and Finney, C.A., 2000, Analytical results for Bullion mine and Crystal mine waste samples and bed sediments from a small tributary to Jack Creek and from Uncle Sam Gulch, Boulder River watershed, Montana: U.S. Geological Survey Open-File Report 00–031, 63 p.

Fey, D.L., Unruh, D.M., and Church, S.E., 1999, Chemical data and lead isotopic compositions in stream-sediment samples from the Boulder River watershed, Jefferson County, Montana: U.S. Geological Survey Open-File Report 99–575, 147 p.

Fortescue, J.A.C., 1992, Landscape geochemistry: retrospect and prospect—1990: Applied Geochemistry, v. 7, p. 1–53.

Jones, D.S., Suter, G.W., II, and Hull, R.N., 1997, Toxicological benchmarks for screening contaminants of potential concern for effects on sediment-associated biota; 1997 revision: Department of Energy Report ES/ER/TM-95/R4, 30 p., unpaginated appendices.

Kimball, B.A., Callendar, E., and Axtmann, E.V., 1995, Effects of colloids on metal transport in a river receiving acid mine drainage, upper Arkansas River, Colorado, U.S.A.: Applied Geochemistry, v. 10, p. 285–306.

Lund, Karen, Aleinikoff, J.N., Kunk, M.J., Unruh, D.M., Zeihen, G.D., Hodges, W.C., duBray, E.A., and O'Neill, J.M., 2002, SHRIMP U-Pb and $^{40}Ar/^{39}Ar$ age constraints for relating plutonism and mineralization in the Boulder batholith region, Montana: Economic Geology, v. 97, p. 241–267.

MacDonald, D.D., Ingersoll, C.G., and Berger, T.A., 2000, Development and evaluation of consensus-based sediment quality guidelines for freshwater ecosystems: Archives of Environmental Contamination and Toxicology, v. 39, p. 20–31.

McDanal, S.K., Campbell, W.L., Fox, J.P., and Lee, G.K., 1985, Magnetic tape containing analytical results for rocks, soils, stream sediments, and heavy-mineral concentrate samples: U.S. Geological Survey Report USGS-GD-85-006; available from U.S. Department of Commerce, National Technical Information Service, Springfield, Virginia 22151.

Metesh, J.J., Lonn, J.D., Duaime, T.E., and Wintergerst, Robert, 1994, Abandoned-inactive mines program, Deerlodge National Forest—Volume I, Basin Creek Drainage: Montana Bureau of Mines and Geology Open-File Report 321, 131 p.

Metesh, J.J., Lonn, J.D., Duaime, T.E., and Wintergerst, Robert, 1995, Abandoned-inactive mines program, Deerlodge National Forest—Volume II, Cataract Creek Drainage: Montana Bureau of Mines and Geology Open-File Report 344, 201 p.

Nimick, D.A., and Cleasby, T.E., 2000, Water-quality data for streams in the Boulder River watershed, Jefferson County, Montana: U.S. Geological Survey Open-File Report 00–99, 70 p.

Nordstrom, D.K., and Alpers, C.N., 1999, Geochemistry of mine waters, *in* Plumlee, G.S., and Logsdon, M.J., eds., The environmental geochemistry of mineral deposits—Part A, Processes, techniques, and health issues: Society of Economic Geologists, Reviews in Economic Geology, v. 6A, p. 133–160.

OSWER (Office of Solid Waste and Emergency Response, Environmental Protection Agency), 1996, Ecotox thresholds: ECO Update, v. 3, p. 1–12.

Persuad, D., Jaaugmagi, R., and Hayton, A., 1993, Guidelines for the protection and management of aquatic sediment quality in Ontario: Ontario Ministry of the Environment and Energy, 30 p.

Rossillon, Mitzi, and Haynes, Tom, 1999, Basin Creek mine reclamation heritage resource inventory 1998, unpublished report prepared for the Beaverhead-Deerlodge National Forest, Dillon, Mont., 126 p.

Ruppel, E.T., 1963, geology of the Basin quadrangle, Jefferson, Lewis and Clark, and Powell Counties, Montana: U.S. Geological Survey Bulletin 1151, 121 p.

Schemel, L.E., Kimball, B.A., and Bencala, K.E., 2000, Colloid formation and metal transport through two mixing zones affected by acid mine drainage near Silverton, Colorado: Applied Geochemistry, v. 15, p. 1003–1018.

Smith, K.S., 1999, Metal sorption on mineral surfaces—An overview with examples relating to mineral deposits, *in* Plumlee, G.S., and Logsdon, M.J., eds., The environmental geochemistry of mineral deposits—Part A, Processes, techniques, and health issues: Society of Economic Geologists, Reviews in Economic Geology, v. 6A, p. 161–182.

Smith, S.M., 1994, Geochemical maps of copper, lead, and zinc, upper Arkansas River drainage basin, Colorado: U.S. Geological Survey Open-File Report 94–408, 15 p.

Smith, S.M., Church, S.E., and Green, G.N., 1997, Effects of geology and mining activity on sediment geochemistry of the Arkansas River drainage basin, Colorado: Explore, no. 96, p. 6–10, 14.

Unruh, D.M., Fey, D.L., and Church, S.E., 2000, Chemical data and lead isotopic compositions of geochemical baseline samples from streambed sediments and smelter slag, lead isotopic compositions in fluvial tailings, and dendrochronology results from the Boulder River watershed, Jefferson County, Montana: U.S. Geological Survey Open-File Report 00–38, 75 p.

U.S. Environmental Protection Agency, 1995, National sediment inventory; Documentation of derivation of freshwater sediment quality: Washington, D.C., Office of Water, EPA Report.

U.S. Environmental Protection Agency, 1996, Calculation and evaluation of sediment effect concentrations for the amphipod Hyalella azteca and the midge Chironomus riparius: Chicago, Ill., Great Lakes National Program Office, EPA Report 905-R96-008.

Van Eeckhout, E.M., 1981, Utilizing the geochemical data from the National Uranium Resource Evaluation (NURE) Program; an evaluation of the Butte Montana quadrangle, Montana: Grand Junction, Colo., U.S. Dept. of Energy, GJBX-58(81), 67 p.

Wallace, C.A., 1987, Generalized geologic map of the Butte 1°× 2° quadrangle, Montana: U.S. Geological Survey Miscellaneous Field Studies Map MF–1925, scale 1:250,000.

Hydrogeology of the Boulder River Watershed Study Area and Examination of the Regional Ground-Water Flow System Using Interpreted Fracture Mapping from Remote Sensing Data

By Robert R. McDougal, M.R. Cannon, Bruce D. Smith, and David A. Ruppert

Chapter D9 of
Integrated Investigations of Environmental Effects of Historical Mining in the Basin and Boulder Mining Districts, Boulder River Watershed, Jefferson County, Montana
Edited by David A. Nimick, Stanley E. Church, and Susan E. Finger

Professional Paper 1652–D9

U.S. Department of the Interior
U.S. Geological Survey

Contents

Figures

Tables

Chapter D9
Hydrogeology of the Boulder River Watershed Study Area and Examination of the Regional Ground-Water Flow System Using Interpreted Fracture Mapping from Remote Sensing Data

By Robert R. McDougal, M.R. Cannon, Bruce D. Smith, and David A. Ruppert[1]

Abstract

This investigation describes the shallow unconsolidated and upper fracture-controlled ground-water flow regimes in the Boulder River watershed, and uses remote sensing data to map linear surface features that are interpreted as fractures and are assumed to be associated with regional fracture controlled subsurface flow. Ground water in the Boulder River watershed occurs primarily in saturated unconsolidated deposits and the upper portion of a fractured bedrock aquifer. The hydraulic properties of the bedrock aquifer, at depth, are largely unknown. However, along fault zones, mineralized zones, and some large fractures, the hydraulic conductivity may be significant. A conceptual model of ground-water flow was developed based on hydrogeologic characteristics of aquifers investigated near the inactive Buckeye, Bullion, and Crystal mines, and on observations of ground-water discharge from granitic, volcanic, and unconsolidated rock units throughout the Basin Creek and Cataract Creek drainages. The direction of shallow ground-water flow can be modeled as the gradient of topographic slope. Deeper ground-water flow likely is a function of fracture width, continuity, and interconnectivity, and likely is partly controlled by the heterogeneous and anisotropic orientation of fractures. Four remote sensing data sets, used as base images, provided a range of spatial resolutions for linear feature mapping. Endpoint data from mapped linear features, used in a 2-D orientation analysis, enabled us to determine primary orientations of lineaments from rose diagrams and to produce contour maps of linear feature characteristics. A contour map of combined linear feature spatial frequency and intersections was compared with a map of wetland-soils areas to identify correlated areas of high fracture occurrence and areas where the potentiometric surface is close to the land surface. The mapped lineaments show a consistent east-west primary orientation. The greatest linear feature spatial frequency, length, and frequency of intersections occurred on the Continental Divide at the northern boundary of the Boulder River watershed study area. The observation of highest interpreted fracture frequency on the Continental Divide is significant in that this area may provide potential recharge for fracture-controlled ground water. The comparison of highest interpreted fracture frequency with areas of mapped shallow ground water shows a correlation in several locations between potential areas of recharge to the fractured granitic aquifer and areas of discharge, or wet soils. The description of the ground-water regime and the identification of areas of high interpreted fracture frequency are components of the ground-water system that should be considered in the design of strategies for mine remediation.

Introduction

The Boulder River watershed is representative of mountainous terrains in the western United States where ground water occurs in unconsolidated Quaternary alluvial and colluvial deposits, and in fractures in underlying plutonic rocks. The crystalline bedrock aquifers commonly have significantly lower hydraulic conductivity and storage potential than the unconsolidated aquifers, except where substantial secondary fracture permeability exists.

Based on field observations near the inactive Buckeye, Bullion, and Crystal mines, and on observations of ground-water discharge from granitic, volcanic, and unconsolidated rock units throughout the Basin Creek and Cataract Creek drainages (fig. 1), the hydraulic characteristics and flow regimes of the upper part of the ground-water system in the Boulder River watershed are relatively well understood. The hydraulic properties of the fractured bedrock aquifer and its

[1]United States Department of Agriculture (USDA) Forest Service, Beaverhead-Deerlodge National Forest, Butte, Mont.

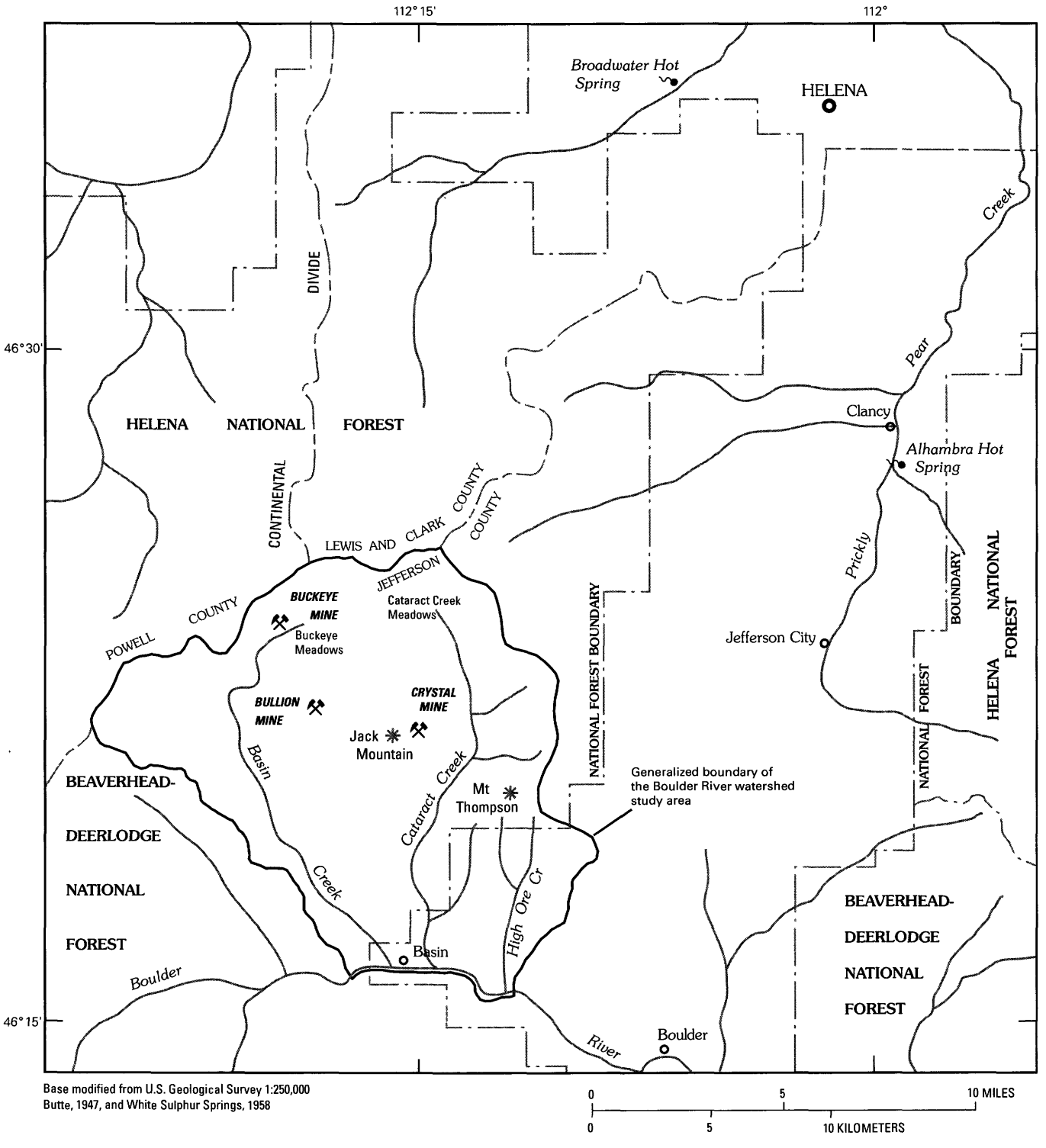

Figure 1. Site map for hydrogeologic study of the Boulder River watershed.

contribution to the regional ground-water system, however, have not been well characterized. Similarly, the relative importance of shallow (local) and deep (regional) ground-water flow as pathways for transporting metals from mining-related and natural sources to streams in the watershed is not well understood. Detailed synoptic streamflow measurements indicated that ground water discharges to streams in several locations in the study area (Kimball and others, this volume, Chapter D6).

This investigation describes the shallow unconsolidated, and upper fracture-controlled ground-water flow regimes within the Boulder River watershed study area, and uses remote sensing data to map linear surface features in approximately 528 mi^2 of the watershed and surrounding area. The mapped linear features identified in this study are interpreted to represent the surface expression of faults, joints, and other fractures in the Butte pluton and overlying volcanic rocks. The regional and subregional structurally controlled ground-water flow regimes are assumed to be associated with the orientation of these linear features.

Previous studies have shown that mineral deposits and hydrothermal fluid flow in many mining districts occur along linear trends that can range in length from tens of feet to tens of miles in length (Rowan and Wetlaufer, 1975). Remote sensing data, such as Landsat Thematic Mapper (TM) data, have successfully been used to evaluate the relationship between mineral deposits and linear structural features (Sabins, 1987). Concepts from these previous studies have been applied in this study to examine the potential relation between fracture systems and ground-water flow. The statistical analysis of linear feature orientation presented here is intended to provide a general view of the potential regional flow directions in the bedrock aquifer by identifying primary azimuths of mapped linear features. To identify and map all structural features from remotely sensed data is not possible, because of ground resolution limitations, vegetation cover, and alluvial or colluvial cover. It is also not possible, in most cases, to differentiate types of linear features. That is, is the linear feature the surface expression of a fault, fracture, joint, or mineralized vein? Mapped linear features from these data sets provide a representation of the spatial distribution and orientation of bedrock fractures, and that of fractures in overlying volcanic rocks. Therefore, maps of this type should be interpreted as a statistical sample of the naturally occurring linear features in a region (Knepper, 1996).

Purpose and Scope

The purpose of this investigation is to provide a conceptual representation of the ground-water system in the Boulder River watershed study area. The objectives of the study are to

- Develop a conceptual model of ground-water flow for the purpose of describing the relative magnitude of ground-water flow systems in various rock units.
- Map linear features from remote sensing imagery. The linear features are assumed to represent the spatial distribution, spatial frequency, and orientation of faults, joints, and fractures associated with structurally controlled ground-water flow.
- Compare a contour map of combined linear feature spatial frequency and intersections with a wet soils coverage representing areas of inferred shallow ground water. Areas that have high fracture frequency and wet soils may be areas of recharge or discharge for fracture-controlled ground-water flow.
- Evaluate how the ground-water flow systems may affect mine-site remediation in the watershed.

Hydrogeologic Setting

Igneous rocks of the Cretaceous Elkhorn Mountains Volcanics and cogenetic Boulder batholith, and Tertiary volcanic rocks, crop out over most of the Boulder River watershed study area and adjacent areas (O'Neill and others, this volume, Chapter D1). In places, the igneous rocks are overlain by unconsolidated surficial deposits of various origin, including glacial drift, stream alluvium, bog deposits, and mass-wasting deposits. Hydrogeologic characteristics of the thin and porous surficial deposits are vastly different from those of the underlying massive, low-permeability igneous rocks. Characteristics such as permeability, fracture density, degree of weathering, and thickness and extent of geologic units have a major control on location and magnitude of ground-water flow systems in the region.

Elkhorn Mountains Volcanics

The Elkhorn Mountains Volcanics are present on many of the higher ridges and peaks in the northwestern part of the study area, on Jack Mountain in the central part of the study area, and in the Mount Thompson area near the headwaters of High Ore Creek. Primary permeability of the volcanic rocks is very low; however, where the rocks were examined on Jack Mountain and in the northern part of the Basin Creek drainage, they were highly fractured with many open and intersecting fractures. Samples of Elkhorn Mountains Volcanics collected on Jack Mountain by Desborough and others (1998) were intensely fractured at intervals of about 4 in. or less and were silicified. Core holes drilled on Jack Mountain (Maxim Technologies, Inc., 1999) revealed that fractures in the subsurface generally were clay filled, and a slug test in one of the holes indicated a hydraulic conductivity of 0.3 ft/day. Nearly all hydraulic conductivity of the volcanic rocks is a result of the intense fracturing. Based on observed fracture systems, the Elkhorn Mountains Volcanics in the northern and central parts of the study area have small ground-water storage capacity with low to moderate hydraulic conductivity, largely dependent on the degree of clay filling in the fractures.

Boulder Batholith

Plutonic, granodioritic rocks of the Butte pluton of the Boulder batholith underlie most of the study area and extend for many miles beyond the study area boundary. Nearly all permeability of the Butte pluton is the result of fracturing and near-surface weathering. Plutonic rocks in outcrop generally are highly fractured and have three prominent sets of closely spaced joints. Observations of nearly 500 joints in the plutonic rocks documented a prominent joint set that trends about east and dips steeply north, a set that trends about north and most commonly dips steeply west, and a set that trends east and most commonly dips gently south (Ruppel, 1963). The joints are spaced from a few inches to many feet apart. In the Basin 7.5-minute quadrangle, the north-trending steep joints are from about 1 to 5 ft apart and the east-trending steep joints are from 5 to 10 ft apart. Individual joints are rarely more than 30 ft long, but where one joint dies out it commonly is overlapped by a parallel joint that is entirely separate or that is connected by a linking transverse joint (Ruppel, 1963).

Outcrops of the Butte pluton are characterized by large open fractures caused by weathering along existing joints (O'Neill and others, this volume, fig. 11). In many areas, joints in the rocks have sufficiently weathered to leave large, free-standing, rounded boulders. Weathering of the plutonic rocks decreases rapidly with depth, which is clearly evident in many road cuts, mine workings, excavations, and drill holes. In areas examined, the upper 5 ft of rock typically contain open joints. From about 5 to 50 ft in depth, the plutonic rock grades from slightly weathered to unaltered rock; most joints become tight; and many are filled with clay. Below about 50 ft, rocks of the Butte pluton typically are fractured, although most fractures are extremely tight, and weathering is observed only on some fracture surfaces. Exceptions to these general characteristics are found along fault zones, mineralized zones, and some large fractures.

Hydraulic conductivity of the granodioritic rocks of the Butte pluton typically is very low. At a core hole drilled south of the Bullion mine, hydraulic conductivity measured from a slug test was about 0.02 ft/day (Maxim Technologies Inc., 1999). At another core hole on the Continental Divide 2.5 mi north of the study area, the hydraulic conductivity of the plutonic rocks was about 0.04 ft/day, as determined from a slug test (Maxim Technologies Inc., 1999). Water wells drilled into the granodioritic rocks typically have small yields, although well yields are highly variable and range from 0 to as much as 100 gallons per minute (Montana Department of Natural Resources and Conservation, unpublished data). Well yield is highly dependent on degree of fracturing and connection of the fractures to sources of recharge.

Tertiary Volcanics

Tertiary volcanic rocks are present in relatively small areas of the Boulder River watershed study area and include quartz latite of Eocene age and rhyolite of Oligocene-Eocene age. Quartz latite of the Lowland Creek Volcanics is present in several small outcrops near the town of Basin; rhyolitic rocks crop out near the Continental Divide in the northwestern part of the study area (O'Neill and others, this volume). Most of the joints in the Tertiary volcanic rocks are primary joints and partings resulting from flowage and cooling (Ruppel, 1963). Columnar joints are common in outcrops of rhyolite and quartz latite welded tuff. Platy jointing parallel to flow laminae is common in rhyolite and results in weathered outcrops that have the appearance of rock rubble. Typically, the permeability and hydraulic conductivity of these types of volcanic rocks are relatively low (Freeze and Cherry, 1979). However, in areas where fracturing occurs, there can be a wide range of secondary permeability that largely is dependent on the degree of fracturing and amount of clay in fractures.

Unconsolidated Deposits

Unconsolidated deposits, consisting chiefly of Quaternary glacial deposits and stream alluvium, mantle a large part of the bedrock surface in the upper valleys of Basin Creek and Cataract Creek. Glacial deposits in the study area include bouldery till, outwash, and lake sediments, with till being by far the most abundant (O'Neill and others, this volume). The glacial deposits are reported to be early Wisconsin in age, equivalent to the Bull Lake stage of glaciation in the Wind River Mountains of Wyoming (Ruppel, 1963). Other young unconsolidated deposits include small areas of colluvium, talus, landslide, and bog deposits. Thickness of unconsolidated deposits ranges from less than 1 ft to more than 31 ft in some stream valleys as observed in road cuts and drill holes in the study area.

In the northwest part of the study area, arkosic sand and silt deposits underlie Oligocene-Eocene volcanic rocks, with weakly consolidated early Tertiary sedimentary rocks also present. Due to the weakly consolidated character of these rocks, anomalous hydrologic conditions exist along the Continental Divide at the base of the rhyolitic volcanic rocks. Unusually moist and wet soil conditions associated with bogs and springs are typical along the base of the rhyolitic volcanics (O'Neill and others, this volume).

Most surficial unconsolidated deposits are fairly thin, whereas the weakly consolidated Tertiary deposits may be as much as 45 ft thick. These deposits are important local aquifers because of their relatively large hydraulic conductivity and porosity. All of these deposits are readily recharged by precipitation, and many small springs and seeps discharge from unconsolidated deposits near or along their contact with underlying bedrock. Discharge from the springs typically varies from peak flow in the spring or early summer to low flow or no flow by late summer. These flow characteristics are typical of springs fed by local ground-water flow systems. Hydraulic conductivity of unconsolidated deposits, measured from slug tests at nine wells near the Buckeye mine, ranged

from 0.03 to 40 ft/day, with a median of 0.2 ft/day (Cannon and others, this volume, Chapter E1, table 5). The lowest measured hydraulic conductivity values were in till; the highest value was in alluvial sand.

Ground-Water Recharge and Discharge

Recharge to aquifers primarily occurs from snowmelt and large precipitation events in spring and early summer. Recharge likely occurs on most topographic highs, and greater amounts of recharge are in areas with the highest precipitation and highest hydraulic conductivity. The water table is near land surface in much of the study area, including high-elevation ridges and slopes, as observed from wells and springs. Discharge in the form of numerous small springs and seeps occurs in topographic lows, at abrupt breaks in slope, and at geologic contacts where there is a downward decrease in hydraulic conductivity. Ground-water flow paths in the upper aquifers, from recharge to discharge areas, are generally short—commonly less than a few thousand feet. Most active ground-water circulation occurs in unconsolidated deposits and the upper 50 ft of fractured bedrock.

Nearly all discharges observed in mine workings, road cuts, exploration pits, and natural springs were characterized as discharge from local ground-water flow systems based on characteristics such as topographic position, seasonal variation in flow, water quality, and geologic source. Water contained in fractures within the upper 50 ft of plutonic rocks generally is part of the local ground-water flow system and, on a macroscopic scale, flow direction in the rock is likely controlled largely by topography.

Discharge from regional flow systems was not observed within the study area. A very small part of annual recharge likely enters deep, regional flow systems through some fault and large fracture zones. Regional ground-water flow would be constrained by the very low hydraulic conductivity of the granodioritic bedrock, and would occur only as the result of secondary permeability along faults and fractures. Direction of flow within the regional system is presumably controlled by geologic structure and topography. Possible discharge areas for regional flow originating in the study area are Broadwater hot springs on the north end of the Butte pluton west of Helena and the Prickly Pear Creek valley east of the study area, in the vicinity of Alhambra hot springs (fig. 1).

Base-flow discharge of streams that drain the study area is sustained by ground-water flow from unconsolidated deposits and the upper zone of fractured and weathered bedrock. The small ground-water discharge available from the shallow aquifers and the lack of regional ground-water discharge to the streams are evident in the small base flow and steep recession curves of stream hydrographs (Church, Nimick, and others, this volume, Chapter B, fig. 3). Base flow of Basin Creek, Cataract Creek, and High Ore Creek, determined from winter measurements made from 1996 to 2000, averaged 0.11 ft^3/s from each square mile of drainage area. The base-flow discharge is equivalent to 1.5 in. of runoff per year from the entire drainage area.

Methods of Investigation

Conceptual Model of Ground-Water Flow

Theoretical and mathematical ground-water flow concepts documented by Hubbert (1940), Toth (1963), and Freeze and Witherspoon (1966, 1967) form the basis of modern ground-water modeling. Data requirements for model development include (1) hydraulic conductivity distribution of the geologic units within the drainage basin, (2) geometry of the basin, including variations in topography and location of basin boundaries, and (3) configuration of the water table as determined from measurements of water levels in wells and by the measurement of elevation of recharge and discharge areas. A conceptual model of steady-state ground-water flow in the Boulder River watershed was constructed through the application of theoretical ground-water flow concepts to observed hydrogeologic properties of rocks and topographic and hydrologic characteristics of the study area. Included in the model are representations of typical flow regimes within the watershed.

Linear Feature Mapping

Four data sets, Landsat Thematic Mapper (TM), India Remote Sensing satellite (IRS 1-C) panchromatic, U.S. Geological Survey Digital Orthophoto Quads (DOQ), and U.S. Geological Survey Digital Elevation Models (DEM), were used to generate base images for mapping linear features. The different spatial resolutions of these data sets facilitated identification of linear features at various scales, ranging in length from a few hundred feet to several miles. All image processing and enhancement was performed using ENVI® (Environment for Visualizing Images, Research Systems Inc., 1998).

Images produced from the Landsat TM data[2] (94 ft (30 m)[3] spatial resolution) were processed to enhance linear surface features by applying directional convolution filters to the images to emphasize north-south-, east-west-, northeast-southwest-, and northwest-southeast-trending linear features, and features adjacent to these principal directions (fig. 2). In all of the images where directional filters were used (TM, IRS, and DOQ), a user-defined addback value of 75 percent of the original image was selected. A principal components (PC) transformation was applied to maximize the variance of the TM multispectral data. This process is useful for identifying less correlated information in the data set which may

[2]The Landsat 5 scene was obtained from EROS Data Center and is part of the Multi-Resolution Land Characteristics (MRLC) data set. Entity ID number: MBP03902806281994. Image acquisition date: June 28, 1994. Path 39, row 28.

[3]The spatial resolution of remote sensing data is usually reported in metric units.

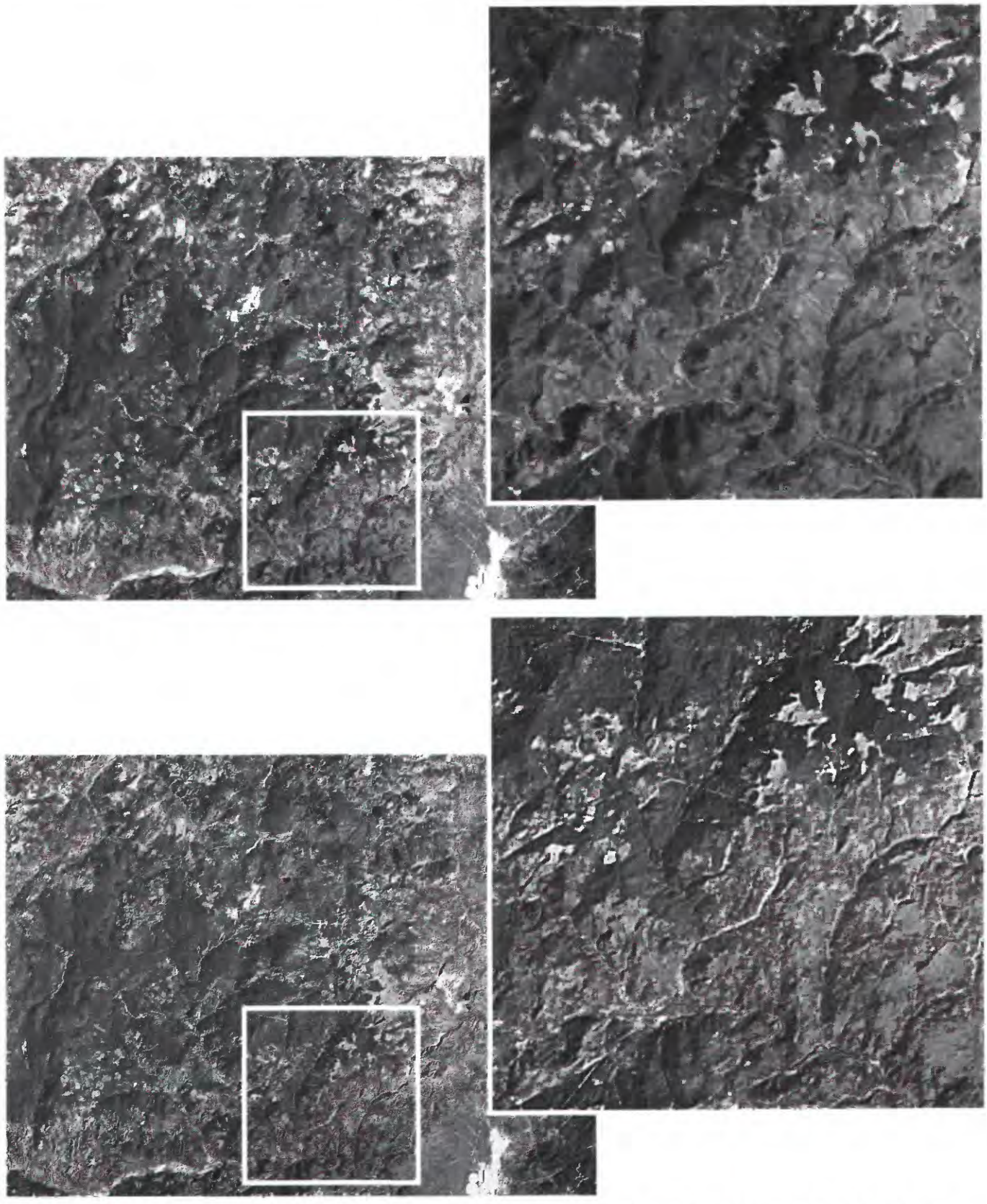

Figure 2. Comparison of unfiltered Landsat Thematic Mapper (TM) band 4 image (top) and TM band 4 image filtered to enhance northeast-trending features (bottom). In each image pair, the white outline is enlarged in the upper right view.

be overwhelmed by the highly correlated topographic and albedo effects (Sabins, 1987). After inspection of the six resulting principal component images, PC-3 was selected because it provided the most suitable base image for mapping. Directional filters were applied to the image, as previously described, to enhance linear features (fig. 3). Lineaments considered to represent faults, fractures, or other geologic structures were mapped from each TM base image and included in a vector coverage. The endpoint map and image coordinates for each vector were recorded. The same mapping procedure was used for all the other data sets.

The IRS panchromatic data[4] (16 ft (5 m) spatial resolution) were filtered to reduce the effects of nonperiodic banding in the image. This noise is the result of sensitivity variations in the IRS satellite's "push-broom" detector array. A bit error filter (Eliason and McEwen, 1990) was used to minimize the resulting noise. The residual banding, however, could not be completely removed without degrading the image. The resulting image was directionally filtered to enhance linear features as previously described (fig. 4). Because of the northeast-southwest trend of the residual banding, the image was not used to map linear features oriented in this direction.

Six DOQ images[5] (3.3 ft (1 m) spatial resolution), corresponding to the 7.5-minute topographic quadrangles covering the study area, were directionally filtered as previously described. The resulting images, having the highest spatial resolution, were used to identify the smallest mappable linear features.

When linear features are mapped from satellite or aerial imagery, an important consideration is that visual bias will be introduced by the direction of solar illumination. Linear features that are oriented parallel to the direction of solar illumination are often not as easily identified as those oriented perpendicular to this direction, where shadowing becomes more prominent. To minimize this effect, a DEM (33 ft (10 m) spatial resolution) was used to produce two shaded relief images that could be artificially illuminated from any selected direction, and using any selected sun elevation angle (fig. 5). The solar illumination azimuths are 124° for the TM data, 148° for the IRS data, and 120° for the DOQ data. Based on this predominantly southeastern illumination direction of the data sets, the shaded relief images were illuminated from 0° and 45°, with a solar elevation angle of 45°.

The geographic coordinates (recorded as Universal Transverse Mercator (UTM) coordinates) of the endpoints of each mapped vector were used to calculate the azimuth and length of each linear feature. These data were used in a 2-D orientation analysis (Rockworks™, Rockware ® Inc., 1999) to determine primary orientations of lineaments from rose diagrams and to produce contour maps of linear feature characteristics. Rose diagrams are polar histograms, which represent the two-dimensional (horizontal plane) orientations of mapped linear features. The statistical parameters of sample size (N), maximum percentage, mean percentage, vector mean azimuth (direction), standard deviation, confidence interval, and R-magnitude were calculated for each diagram. The maximum percentage is the histogram class with the greatest frequency, while the mean percentage is the class containing the average frequency. The confidence interval represents the interval on either side of the mean azimuth that most likely (using a 95 percent confidence level) contains the true mean direction. The R-magnitude values are standardized to range from 0 to 1 and are a measure of the magnitude of the azimuth mean. Data sets with a large dispersion about the mean have small values for R (values near 0), and data sets that are tightly grouped around the mean have a large value for R (values near 1).

Rose diagrams were produced to display the primary orientations of linear features. Petals in each rose diagram were either sized proportional to the length of the lineaments (total length of linear features within a 10° class range) or sized proportional to the spatial frequency of the lineaments within a 10° class range. The linear feature data were filtered using length groupings of 3.3–1,640 ft (1–500 m)[6], 1,640–3,281 ft (500–1,000 m), 3,281–9,843 ft (1,000–3,000 m), and 9,843–26,247 ft (3,000–8,000 m). Length-proportional rose diagrams were produced for each length group. The length groupings are meant to compare the orientations of short, short to medium, medium to long, and long length ranges of linear features.

The northeast-trending Butte-Helena fault zone divides the study area roughly into a southeastern region of synemplaced diastrophic fractures of the Butte pluton, and a western laccolithic region (O'Neill and others, this volume). The study area was divided into four quadrants (fig. 6), and rose diagrams of linear feature spatial frequency were plotted for each quadrant. Linear features were assigned to the quadrant that contained the midpoint of the linear feature. The rose diagrams corresponding to the four quadrants are intended to illustrate differences in linear feature orientation associated with differing geologic subregions and environments.

Contour maps of the spatial frequency, length, occurrence of intersections, combined spatial frequency and intersections, and combined spatial frequency and length were produced by interpolating the linear feature data using the kriging[7] gridding method (Surfer 7 ®, Golden Software, Inc.). In a spatial frequency grid, the value assigned to each grid cell represents the number of linear features that lie in the cell. This number includes lines that originate in the cell, end in the cell, and pass through the cell. In a length grid, the value for each

[4]IRS-1C Pan Image acquired from Space Imaging Inc. path/row/section: 252/036/A & 252/036/B. acquisition date: 7-16-97(a) & 11-13-97(b).

[5]This data set is from the National Technical Means (NTM) declassified archives. The images, as received, have been degraded to 3.3 ft (1 m) spatial resolution.

[6]The linear feature data were originally recorded as endpoints in UTM coordinates, and the length groupings were based on calculated lengths from the metric coordinates. Therefore, metric units are also shown here.

[7]Kriging is a geostatistical gridding method that is often used to produce contour maps from irregularly spaced data. Kriging attempts to express trends suggested in the data by taking into account what is known about the spatial characteristics of the data (Isaaks and Srivastava, 1989).

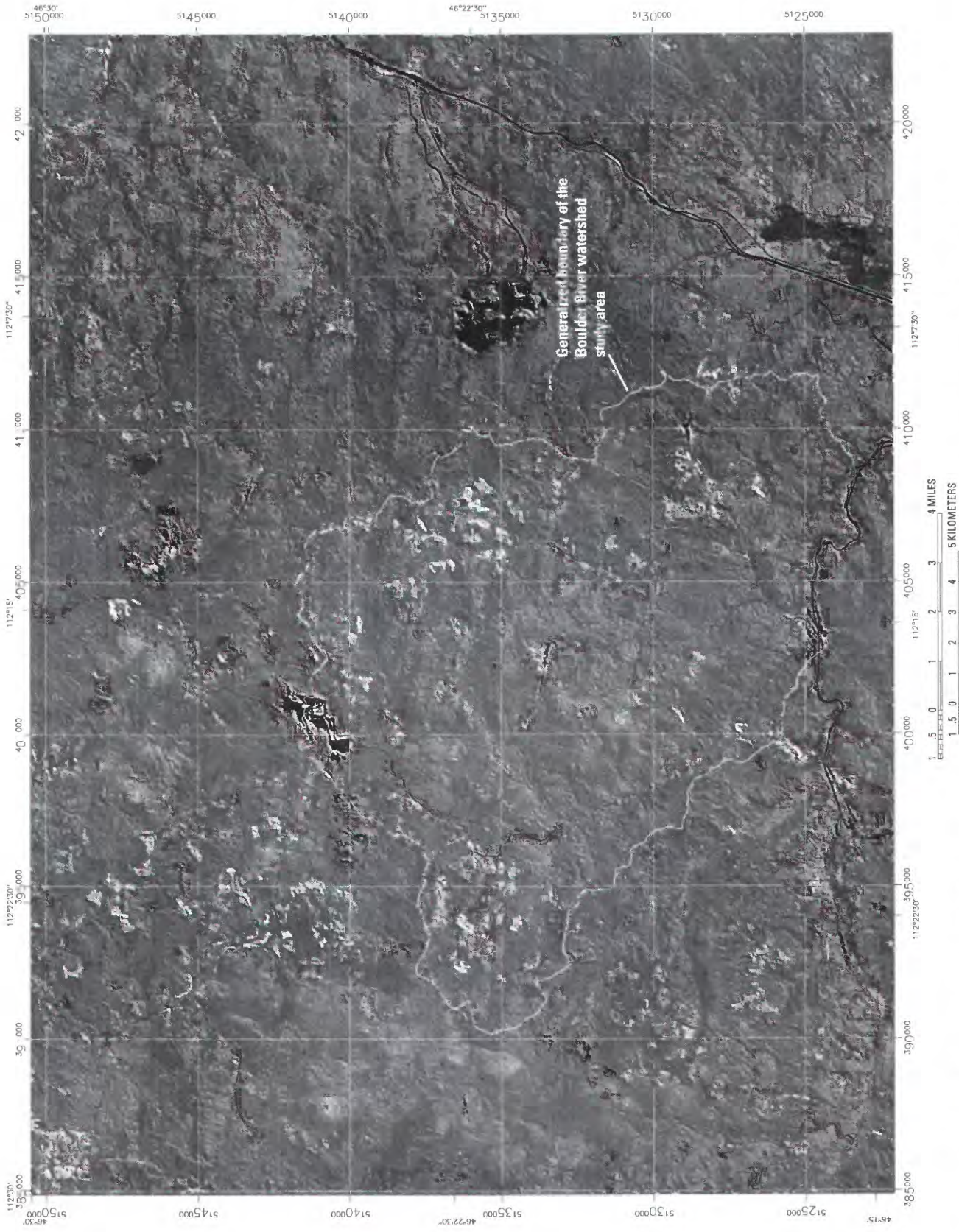

Figure 3. Landsat Thematic Mapper (TM) Principal Component (PC) 3, directionally filtered to enhance northeast-trending linear features.

Figure 4. IRS-1C satellite image directionally filtered to enhance linear features and a bit error filter applied to remove residual noise (16 ft or 5 m spatial resolution).

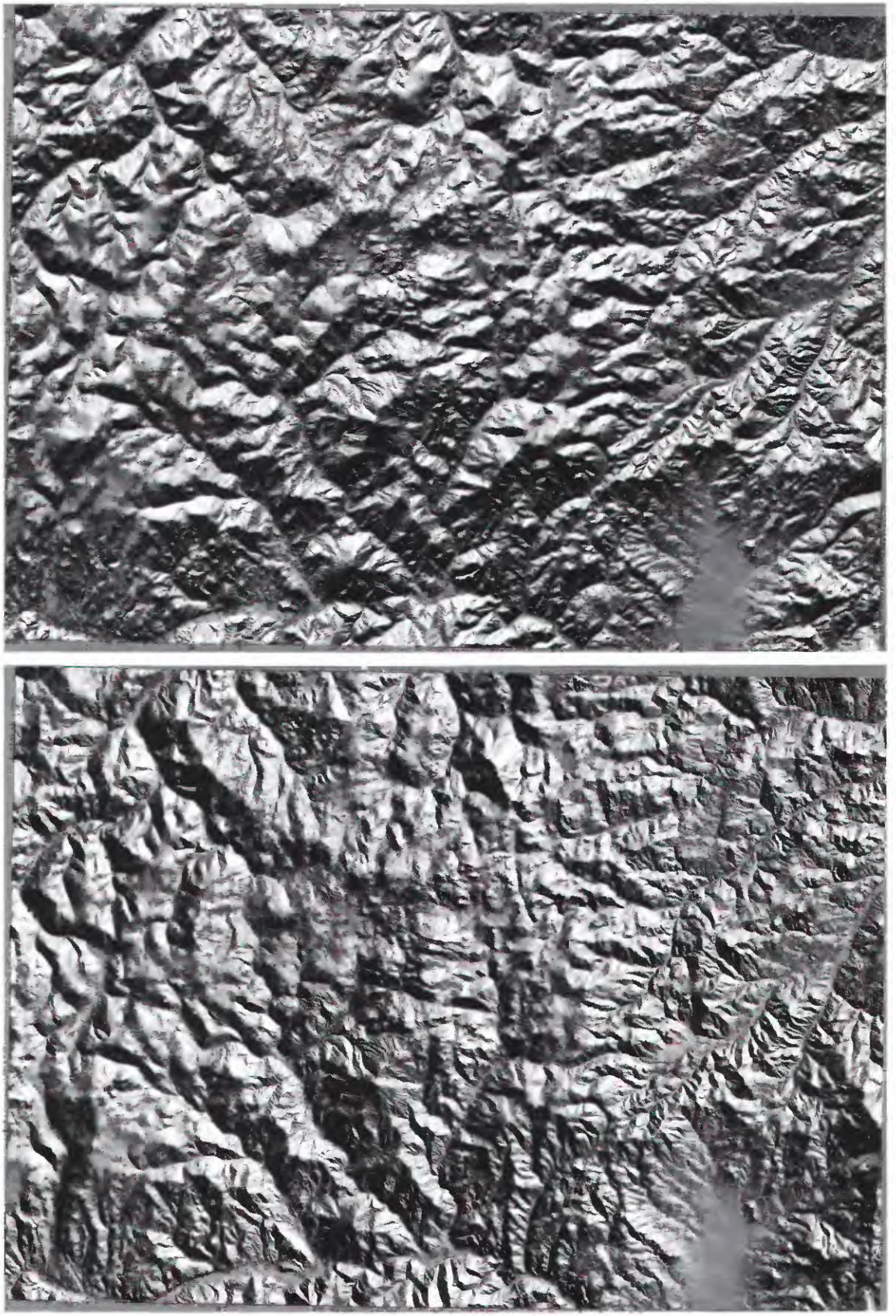

Figure 5. Shaded relief Digital Elevation Model (DEM) images artificially illuminated from 0° azimuth (top) and 45° azimuth (bottom) (area shown corresponds to previous figures).

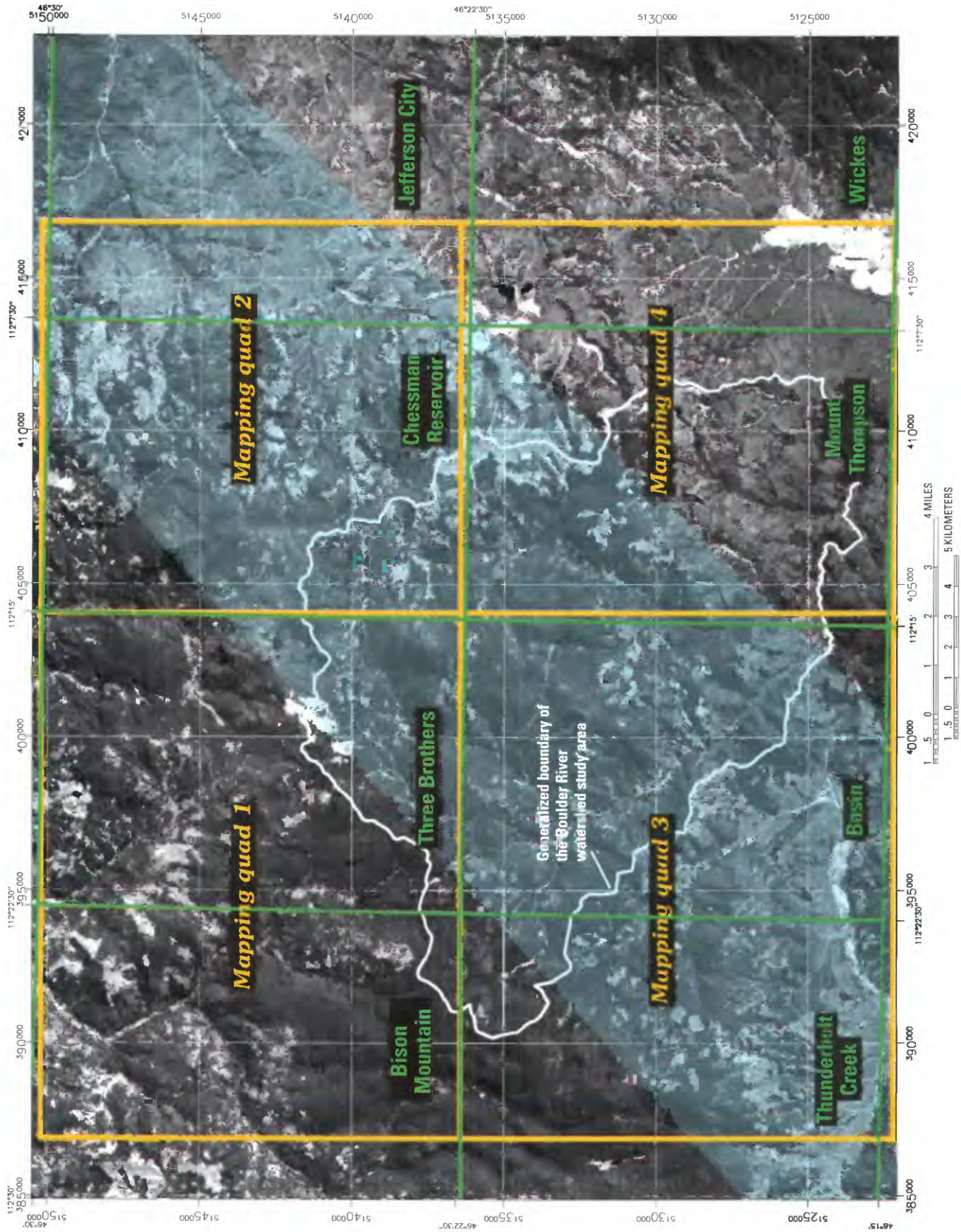

Figure 6. Site map showing USGS 7.5-minute quadrangle (1:24,000 scale) boundaries (green), linear feature mapping quads (yellow), and approximate area of the Butte-Helena fault zone (blue).

cell represents the total lengths, added together, of all linear features that pass through the cell. The total length of each linear feature is calculated, not just the length of the section of the feature that lies within the cell. In an intersection grid, the value for each cell represents the number of intersections of linear features that occur within the cell. Each contour map was made using a grid cell size of 2,500 ft on each side. This grid cell size was selected, based on the results of various test dimensions, to minimize false map features produced by the gridding algorithm.

Contour maps combining spatial frequency and intersection data, and spatial frequency and length data were produced to show where these features occur together. Values for linear feature spatial frequency, intersections, and length were normalized, that is, the values from each data set were divided by their maximum value so that all values would range from 0 to 1. The data were then combined to produce the values that were contoured in the combination maps. In terms of ground-water flow, areas with greater combined spatial frequency and intersections may identify where greater hydraulic connection in the bedrock aquifer exists, assuming fractures are hydraulically conductive. Areas where greater spatial frequency and linear feature length are coincident represent deeper ground-water circulation. Longer linear features likely represent fractures extending to greater depths, and therefore, deeper ground-water circulation, again assuming that the fractures are hydraulically conductive.

The contour map depicting linear feature spatial frequency and intersections was combined with a map of shallow ground water and wetland areas. This map is a derivative product from a land-type inventory of the Beaverhead-Deerlodge National Forest (D. Ruppert, unpub. data, 1980); it shows areas where ground water occurs at or near the land surface. Some of the water associated with areas of high water tables has been observed on the ground and on aerial photos as originating from seeps and springs oriented along linear features. These linear features are interpreted as being associated with bedrock structures. The purpose of combining these maps is to identify where zones of inferred high fracture frequency and areas where the potentiometric surface is close to the land surface coincide. These correlated areas may represent recharge to or discharge from fractured rock.

Results and Analysis

Conceptual Model of Ground-Water Flow

Geologic units in the Boulder River watershed study area can be grouped, based on their relative hydraulic conductivity, into three hydrogeologic units that correspond to three layers of a conceptual ground-water flow model (fig. 7). The upper model layer represents unconsolidated deposits and has the largest hydraulic conductivity. The second model layer represents the upper fractured and weathered zone in the granodioritic bedrock: it has a smaller hydraulic conductivity than the unconsolidated deposits but a much greater hydraulic conductivity than underlying unweathered Butte pluton. Fractured rocks of Elkhorn Mountains Volcanics and Tertiary volcanics also are included in the second model layer of rocks having intermediate hydraulic conductivity. The third or lowest layer of the conceptual model represents the very low hydraulic conductivity of the Butte pluton. The crystalline rocks are likely fractured at depth, but fracture permeability undoubtedly decreases with depth. The exception to this low permeability might occur in fault zones where hydraulic conductivity in fractures might increase. This three-layer conceptual model oversimplifies the hydraulic properties of rocks in the study area; however, it preserves important hydraulic characteristics, which are that hydraulic conductivity is greatest in the upper unconsolidated alluvium and generally decreases with depth. The hydrogeologic properties of the Butte pluton are the primary factors that limit development of regional ground-water flow systems in the study area.

Topography determines the upper geometry of the ground-water basin and is a major control on direction of ground-water flow in a basin such as the Boulder River watershed, where at depth no extensive high permeability unit exists. The steep hummocky terrain of the study area, combined with the decrease in hydraulic conductivity of geologic units with depth, results in the formation of mostly shallow, localized ground-water flow systems (Toth, 1963; Freeze and Witherspoon, 1967). Direction of shallow ground-water flow in the study area can be modeled as the gradient of topographic slope. Mathematical analysis (Freeze and Witherspoon, 1967) has shown that changes in topographic slope, combined with decreasing hydraulic conductivity with depth, will focus ground-water discharge at breaks in slope and at geologic contacts, similar to those observed in the Boulder River watershed. A conceptual three-layer model of decreasing hydraulic conductivity with depth also is consistent with the generally shallow depths to ground water observed in the study area. In the conceptual model of ground water just outlined, the upper layer of rocks has the greatest hydraulic conductivity and transports the greatest amount of ground water per unit volume of aquifer on an annual cycle. The second layer of rocks, having intermediate hydraulic conductivity, transports a smaller amount of ground water than the upper layer. The third layer of rocks, in which hydraulic conductivity is very low, transports the least amount of water annually, even though the amount of water stored within this unit may be large.

The ground-water flow regimes included in the conceptual model (fig. 7) are typical of conditions in the watershed; the views are meant to represent various settings for ground- and surface-water interaction and to depict the geologic controls on basin hydraulics. Figure 7*A* illustrates an area where principal recharge is through unconsolidated alluvium, with secondary recharge through surface fractures. Ground-water discharge in this flow regime is to springs that occur at the

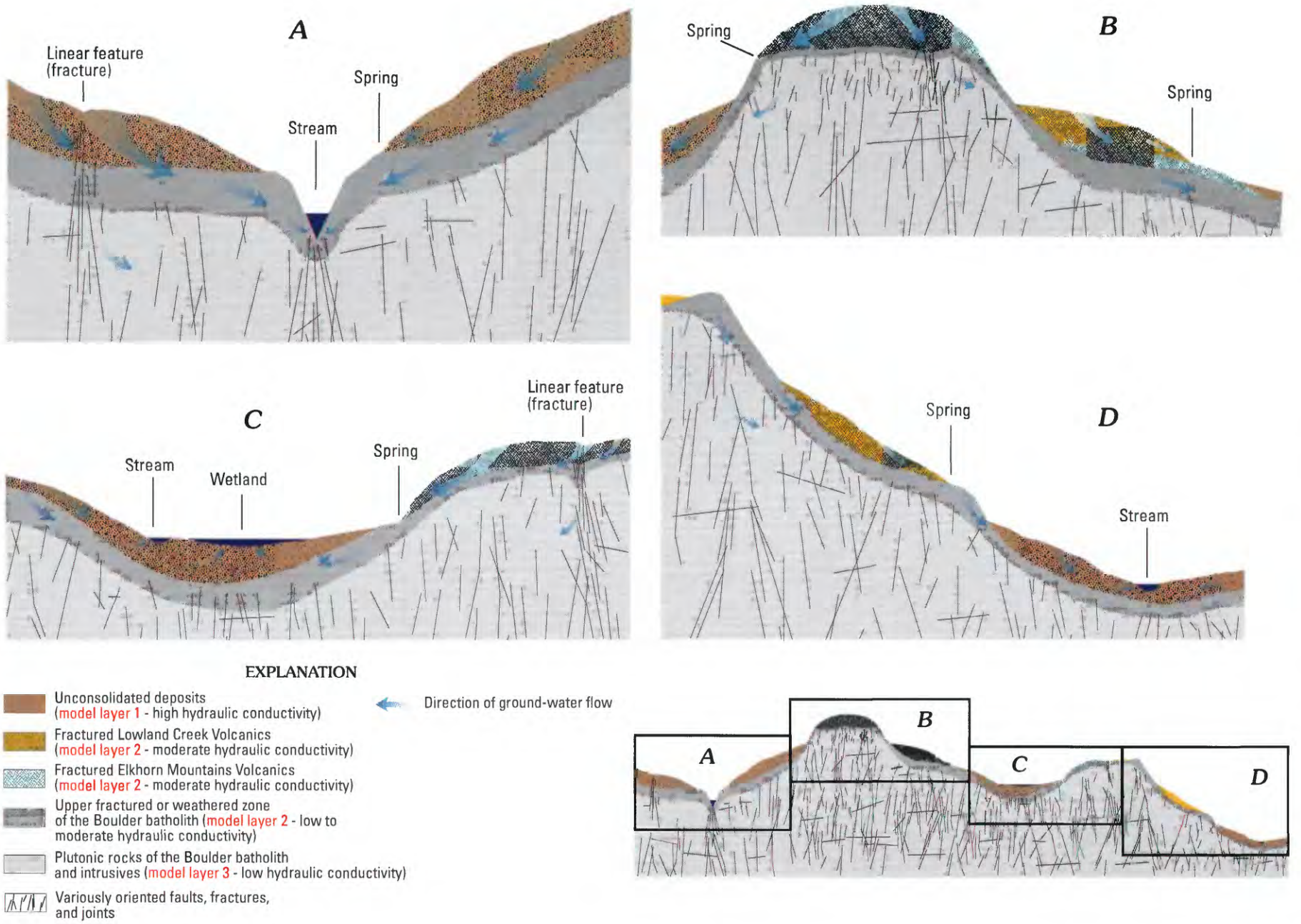

Figure 7. Conceptual ground-water model and depiction of flow regimes in the Boulder River watershed (cross sections are for purposes of illustration and are not to scale). Areas corresponding to views are noted in text.

contact between unconsolidated alluvium and plutonic rocks, and to a channel whose location was likely controlled by bedrock fractures. Cataract Creek near the confluence of Uncle Sam Gulch is an example of this type of stream.

Figure 7*B* illustrates a flow regime where ground-water recharge occurs at a topographic high, in fractured Elkhorn Mountains Volcanics (analogous to conditions at Jack Mountain), and in the fractured Lowland Creek Volcanics. Ground-water discharge in this regime is to springs at the contact between the Cretaceous and Tertiary volcanics, and the contact of the Elkhorn Mountains Volcanics and underlying plutonic rocks.

The flow regime in Figure 7*C* depicts ground-water recharge occurring in unconsolidated alluvium, fractured Elkhorn Mountains Volcanics, and throughgoing fractures in volcanic and plutonic rocks. Discharge is to wetlands and adjacent streams in glacial valley fill (analogous to Buckeye Meadows), and to springs that occur at breaks in slope and the contact between volcanic and plutonic rocks.

Figure 7*D* illustrates a ground-water flow regime where recharge occurs in exposed fractured and weathered plutonic rocks, fractured Lowland Creek Volcanics, and unconsolidated alluvium. Discharge in this regime is to springs located at the contact between Tertiary volcanics and plutonic rocks, and to streams in unconsolidated alluvium. Examples of this flow regime are the lower Basin Creek valley, upstream from the town of Basin, and upper Cataract Creek meadows.

Linear Feature Analysis

Linear features were mapped within the Boulder River watershed study area and in areas surrounding the study area (fig. 8). A total of 563 features were mapped. These linear features are interpreted as representing the surface expression of faults, joints, other fractures, and mineralized veins. Statistical summaries of length and orientation are in tables 1 and 2. The mapped linear features range in length from 671 ft to 26,070 ft, with a mean of 4,902 ft. The mean orientation (azimuth) of all mapped features is 79.92°. The primary and secondary orientations and other minor trends of linear features are summarized in table 3.

A rose diagram summarizing the orientations of all mapped linear features is shown in figure 9*A*. Figure 9*B* has a similar rose diagram in which the orientations were weighted according to each feature's length. Both rose diagrams show two primary trend sets with azimuths of 65° and 105°. The length weighted rose diagram was compared to rose diagrams of lineament and fault orientation analysis results from a previous study (Smedes, 1966) of the northern Elkhorn Mountains (adjacent to and northeast of the area of this study). These diagrams show the orientation of 996 faults and 1,357 lineaments that were mapped from field observations and aerial photos, and weighted by length. The comparison with linear feature orientations (fig. 9*B*) shows a correlated trend of faults to the northeast, and of lineaments to the east-northeast. There is little correlation in the prominent trend of fault orientation to the southeast. However, the average angle of illumination of the remote sensing base images, as described preceding, is co-linear with this trend, and linear features oriented in this direction would be less discernible.

The length filtered rose diagrams indicate that short to moderate-length linear features (fig. 10*A* and 10*B*) generally trend to the northeast and east-northeast. The moderate- to long length features, ranging from 3,280 to 26,250 ft (1,000 to 8,000 m) (fig. 10*C* and 10*D*) also have two primary trend sets, with a predominant orientation to the east-southeast and a secondary orientation to the east-northeast.

The mapped lineaments grouped by quadrant (fig. 11*A–D*) have a consistent east-west primary mean azimuth direction similar to that seen in the length filtered rose diagrams. The primary and secondary orientations in the quadrant-grouped diagrams are typically about 100°–110° and 70°–80°. A minor orientation in figure 11*A* and 11*C* is 20°–30°, and in figure 11*D* is 30°–40°. In a previous study of the Jefferson City 15-minute quadrangle (Becraft and others, 1963), a northeast primary trend of nonmineralized faults and topographically expressed lineaments (fig. 11*E*) was observed. Minor trends are at 0°–10°, 90°–100°, and 140°–150°. The Jefferson City 15-minute quadrangle corresponds to the eastern part of this study (quadrants 2 and 4, fig. 6). In order to compare trends from the same area, linear features from quadrants 2 and 4 were combined and the rose diagram from Becraft and others (1963) was overlaid (fig. 11*E*). There are correlated trends to the northeast and east, and to a lesser extent, to the southeast. The trend at 0°–10° shown in the rose diagram from Becraft and others (1963) is not well correlated.

Mapping quadrant 1 (fig. 6) covers an area corresponding with a portion of the laccolithic western part of the Boulder batholith, northwest of the Butte-Helena fault zone (O'Neill and others, this volume, fig. 16). Part of the area is overlain with Elkhorn Mountains Volcanics. Mapping quadrant 4 is southeast of the Butte-Helena fault zone and includes areas of the Butte pluton, Elkhorn Mountains Volcanics, and Lowland

Table 1. Summary statistics for mapped linear features.

Mean	4,902 ft
Standard error	157 ft
Median	3,600 ft
Mode	3,678 ft
Standard deviation	3,713 ft
Range	25,400 ft
Minimum	671 ft
Maximum	26,070 ft
Sum	2,759,538 ft
Count	563

Table 2. Summary statistics for orientations of mapped linear features.

[--, when length filtering is deactivated, minimum and maximum length are not applicable]

Rose diagram	Calculation method	Length filtering	Minimum length (feet)	Maximum length (feet)	Sample size	Maximum percentage	Mean percentage	Mean azimuth (degrees)	Relative standard deviation (percent)	Confidence interval (degrees)	R-magnitude
fig. 9*A*	Frequency	Deactivated	--	--	563	13.3	5.6	79.92	3.54	3.13	0.80
fig. 9*B*	Length	Deactivated	--	--	563	18.3	5.6	83.79	4.51	3.03	0.81
fig. 10*A*	Length	Activated	3.3	1,640	51	15.9	7.7	63.20	5.06	8.90	0.85
fig. 10*B*	Length	Activated	1,640	3,281	192	11.6	5.6	77.17	3.56	5.33	0.80
fig. 10*C*	Length	Activated	3,281	9,843	264	15.8	5.9	84.32	3.31	4.82	0.78
fig. 10*D*	Length	Activated	9,843	26,247	56	30.3	9.1	88.32	9.27	7.20	0.89
fig. 11*A* Quadrant 1	Frequency	Deactivated	--	--	196	12.8	5.6	74.30	3.65	5.57	0.78
fig. 11*B* Quadrant 2	Frequency	Deactivated	--	--	150	18.7	5.6	85.55	5.14	5.20	0.85
fig. 11*C* Quadrant 3	Frequency	Deactivated	--	--	99	16.2	5.9	79.90	3.82	8.27	0.76
fig. 11*D* Quadrant 4	Frequency	Deactivated	--	--	118	14.4	5.9	81.72	3.80	6.64	0.81

Table 3. Summary of main orientations of mapped linear features.

	Mean azimuth (degrees)	Primary orientation (degrees)	Secondary orientation (degrees)	Other minor trends (degrees)
All linear features	79.92	100-110	70-80	20-30
All linear features weighted by length.	83.79	100-110	70-80	30-40
Length filtered				
3.3-1,640 ft (1-500 m)	63.20	20-40	50-60	70-80
1,640-3,281 ft (500-1,000 m)	77.17	60-70	90-110	20-30
3,281-9,843 ft (1,000-3,000 m)	84.32	100-110	60-80	30-40
9,843-26,247 ft (3,000-8,000 m)	88.32	90-110	60-70	30-40
Grouped by quadrant				
Quadrant 1 (NW)	74.30	100-110	70-80	20-30
Quadrant 2 (NE)	85.55	100-110	60-80	130-140
Quadrant 3 (SW)	79.90	90-100	20-30	50-80
Quadrant 4 (SE)	81.72	70-80	100-120	30-40

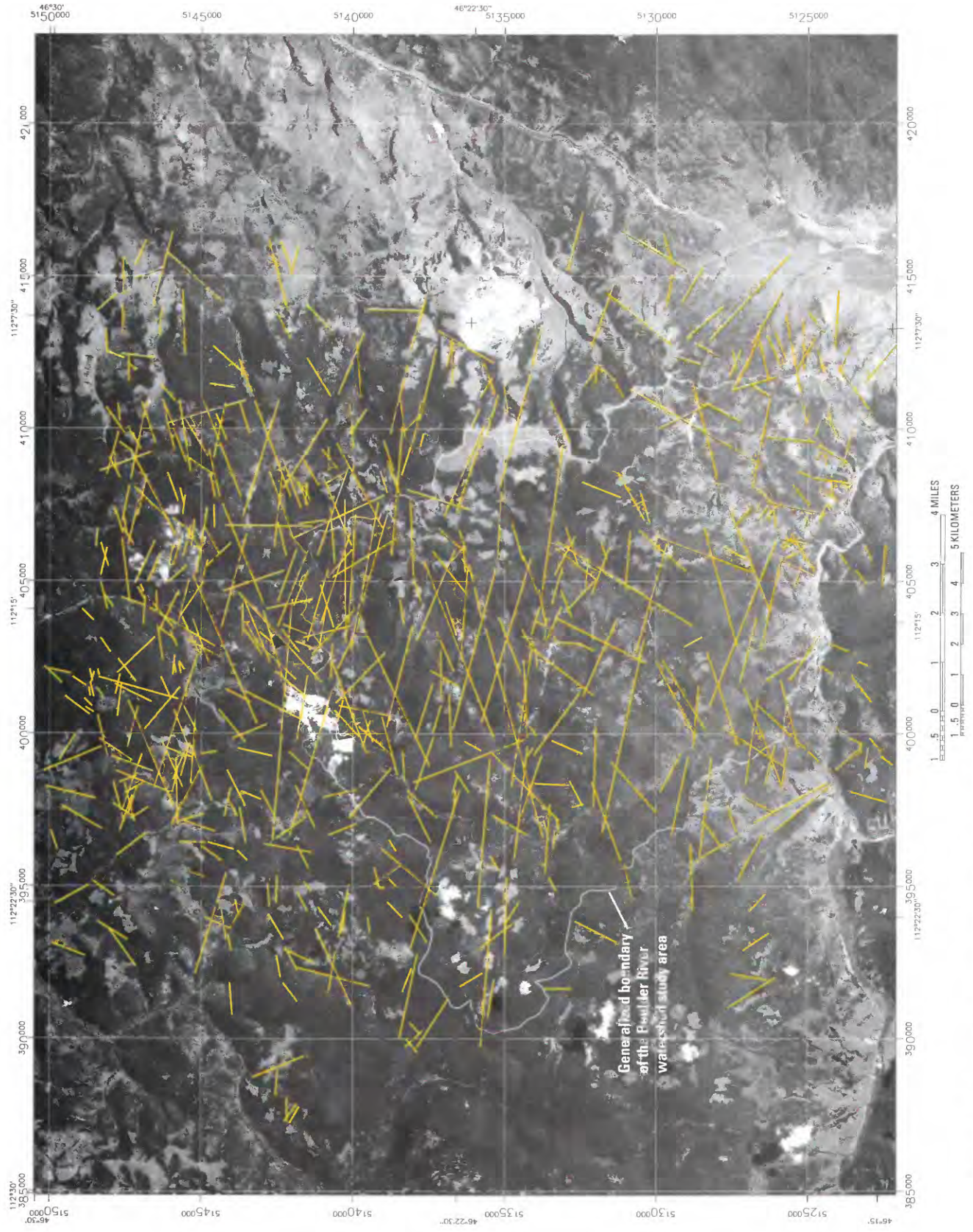

Figure 8. Mapped linear features, Boulder River watershed study area and adjacent region.

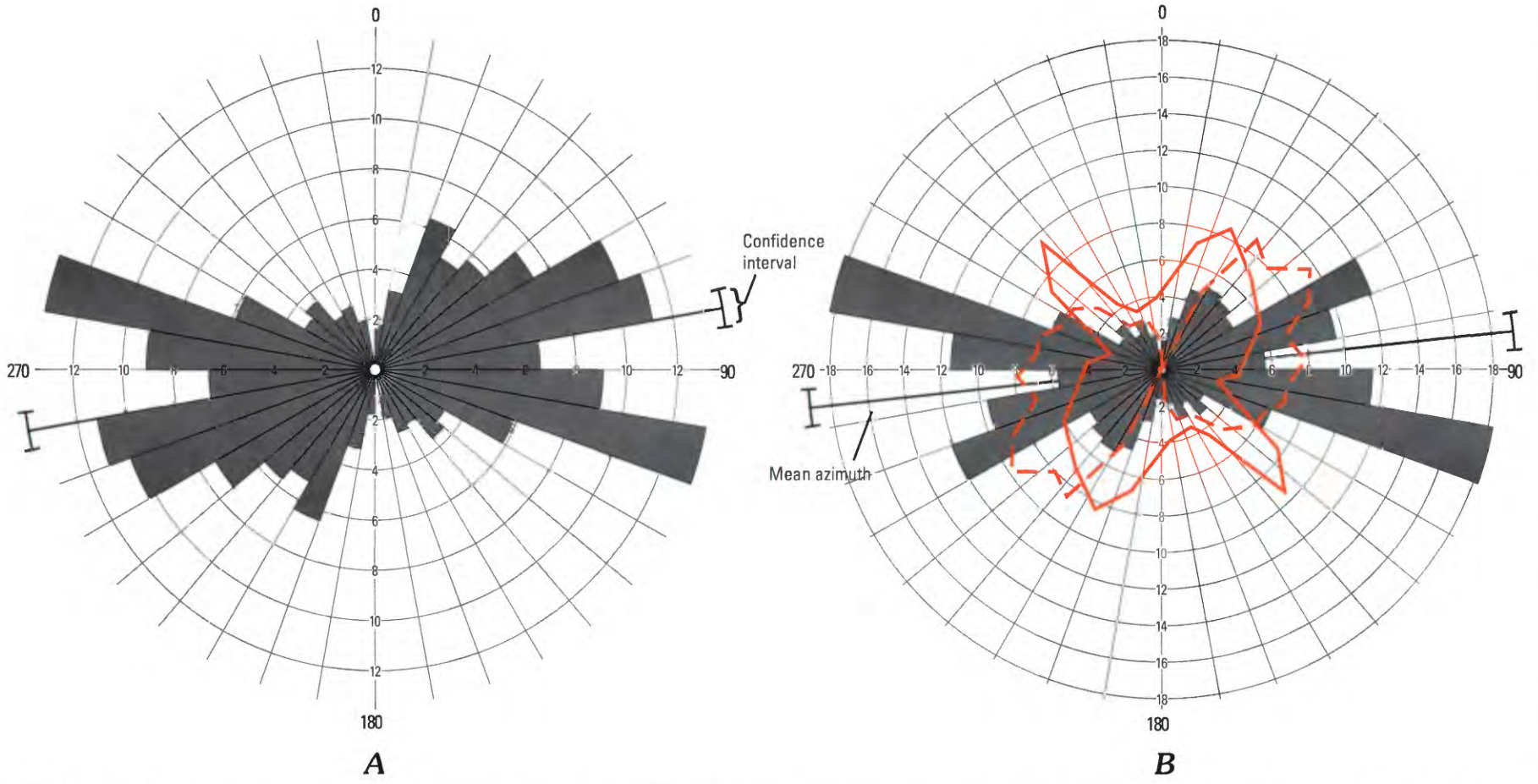

Figure 9. Rose diagrams representing *A*, orientations of all linear features, and *B*, all linear features weighted by length. The confidence interval represents the interval on either side of the mean azimuth that most likely (using a 95 percent confidence level) contains the true mean direction. Rose diagrams from a previous study (Smedes, 1966) of the northern Elkhorn Mountains showing the orientation of 996 faults (solid red line) and 1,357 lineaments (dashed red line) are shown in view B.

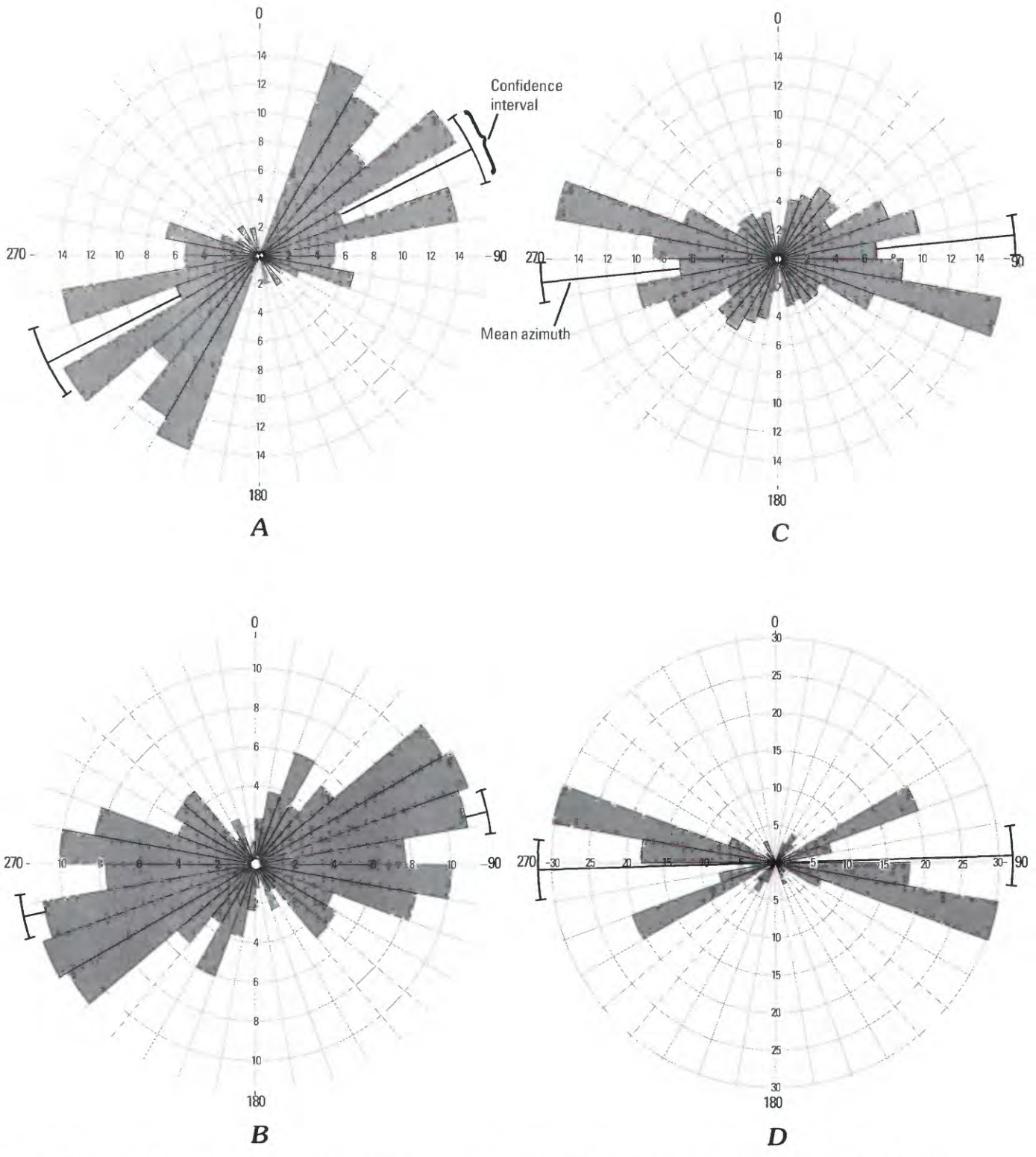

Figure 10. Length filtered rose diagrams of linear features *A*, 3.3–1,640 ft (1–500 m) in length; *B*, 1,640–3,281 ft (500–1,000 m) in length; *C*, 3,281–9,843 ft (1,000–3,000 m) in length; *D*, 9,843–26,247 ft (3,000–8,000 m) in length. The mean azimuth and confidence interval are shown for each diagram.

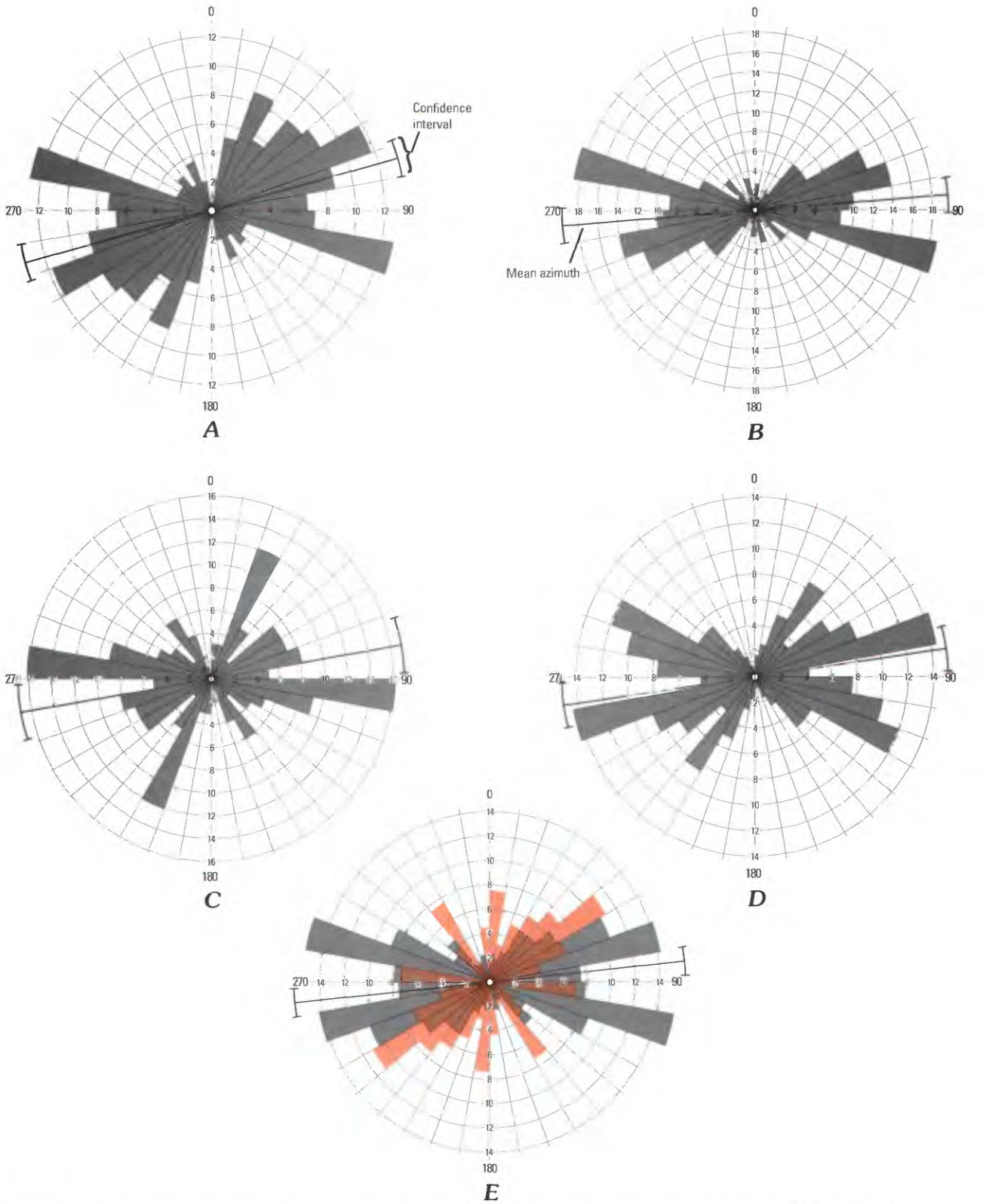

Figure 11. Rose diagrams showing linear feature orientation arranged by quadrants shown in figure 6. *A*, quadrant 1; *B*, quadrant 2; *C*, quadrant 3; *D*, quadrant 4. The mean azimuth and confidence interval are shown for each diagram. *E*, rose diagram (red) from a previous study (Becraft and others, 1963) in the Jefferson City 15-minute quadrangle of the trends of 142 nonmineralized faults and topographically expressed lineaments overlaid on combined linear feature orientation of quadrants 2 and 4.

Creek Volcanics. The trends of mapped linear features for these two quadrants are similar (fig. 11*A* and 11*D*), with the exception of a minor trend oriented to the north-northwest in quadrant 1. The similarity of linear feature orientation in these two quadrants suggests a consistent pattern of fracturing northwest and southeast of the Butte-Helena fault zone.

Quadrant 2 and quadrant 3 (fig. 6) represent the northeastern and southwestern portion, respectively, of the Butte-Helena fault zone within the study area. Linear features in the northeast quadrant (fig. 11*B*) show two primary trend sets similar to the orientation of spatial frequency distribution for the entire study area (fig. 9*A*). The southwest quadrant (fig. 11*C*) has primary east-west (90°–100°) and north-northeast (20°–30°) orientations, with minor classes trending east-northeast (50°–80°) and southeast (140°–160°). These orientation classes are consistent with the synemplaced diastrophic fracture orientations of the Butte pluton (O'Neill and others, this volume). Because of the more dispersed orientations in this quadrant, fracture-controlled ground-water flow directions would also be expected to be more diffuse.

Within the Boulder River watershed study area, the greatest occurrence of linear feature spatial frequency, length, and intersection frequency (figs. 12–14) was mapped near the Continental Divide at the northern boundary of the study area between Old Baldy and Lava Mountains. Other areas of high linear feature spatial frequency are indicated in the central part of the watershed near the Crystal mine, in the north part of the watershed near the Buckeye mine, and in the south part of the watershed east of Basin (fig. 12). Longer linear features also occur in the central part of the watershed near the Crystal and Bullion mines and in the southern part of the watershed (fig. 13). Combined contour maps of linear feature spatial frequency and intersections (fig. 15), and spatial frequency and length (fig. 16) show similar results, with an area of high combined spatial frequency and length west of the Bullion mine.

Areas of relatively dense linear features overlap with areas of mapped shallow ground water (fig. 17) in several locations. An instance is seen in the northern part of the watershed between Old Baldy Mountain and Lava Mountain. Old Baldy Mountain is mapped as an area of high linear feature spatial frequency and is flanked on the east and south by areas where the water table is near the land surface. Similar occurrences of this correlation are seen in the central part of the watershed near the Crystal and Bullion mines, and in the northwest part of the study area near Basin Creek. Areas of high linear feature spatial frequency on either flank of the Continental Divide and in other topographically high areas likely have enhanced ground-water recharge through the fractures in volcanic and plutonic rocks. Adjacent areas of inferred shallow ground water represent potential discharge in unconsolidated alluvium, fractured volcanics, and fractured plutonic rocks.

Conclusions and Discussion

Based on field observations at the Buckeye, Bullion, and Crystal mines and the ground-water flow concepts outlined here, ground-water flow to mines in the Boulder River watershed study area is primarily local in origin. Ground-water flow to underground workings, such as those at the Bullion and Crystal mines, primarily comes from infiltration of shallow ground water from rocks above the mine workings and from interception of surface runoff into mine trenches and pits. Ground water that enters mine workings through lateral flow from fractured plutonic rocks is a relatively small percentage of the total water entering mines. Remediation efforts that eliminate ponded surface water near mine workings and reduce infiltration and surface runoff to caved adits and trenches would significantly reduce the quantity of shallow ground water entering mine workings. The relatively small amount of ground water that enters underground mine workings from deeper fractures in plutonic rocks probably could not be eliminated or even significantly reduced through any surface remediation efforts. Given the probable long residence times for deep circulation and relatively high acid-neutralizing potential (Desborough and others, 1998) of the plutonic rocks, fracture-controlled ground water at depth likely would not adversely affect surface water quality in the watershed.

The primary surface-water flow direction (Basin Creek, Cataract Creek, and High Ore Creek) in the watershed is to the south into the Boulder River. Shallow ground water in the unconsolidated aquifer likely follows a similar flow direction, which is primarily topographically controlled. However, the predominant east-west orientation, and the orientation of other minor trends, of mapped linear features, assumed associated with fractures, may have a significant influence on structurally controlled shallow ground-water flow directions. The orientation of bedrock linear structural features likely affects the flow direction of deeply circulating regional ground-water flow. The rose diagrams presented in this study indicate that the orientations of mapped linear features at the surface are co-linear with the orientation of geophysical gradients in the subsurface (McCafferty and others, this volume). This suggests that some linear structures extend to considerable depth, and that ground-water storage at depth is potentially large.

The high linear feature frequency indicated in areas along the Continental Divide is significant in that these areas represent potential recharge to fracture-controlled ground water in both the Boulder River watershed and the Tenmile Creek watershed to the north. The higher occurrence of mapped linear features could identify potential recharge sources for fracture-controlled ground water, consistent with the conceptual model presented in this study.

The results of this study provide a conceptual understanding of the ground-water and surface-water relationships in the watershed, identify possible fracture-controlled ground-water recharge areas associated with near-surface structures, and map areas of greatest linear feature spatial frequency. These components should be considered in any mine-site restoration strategy or in identifying suitable locations for mine-waste repositories.

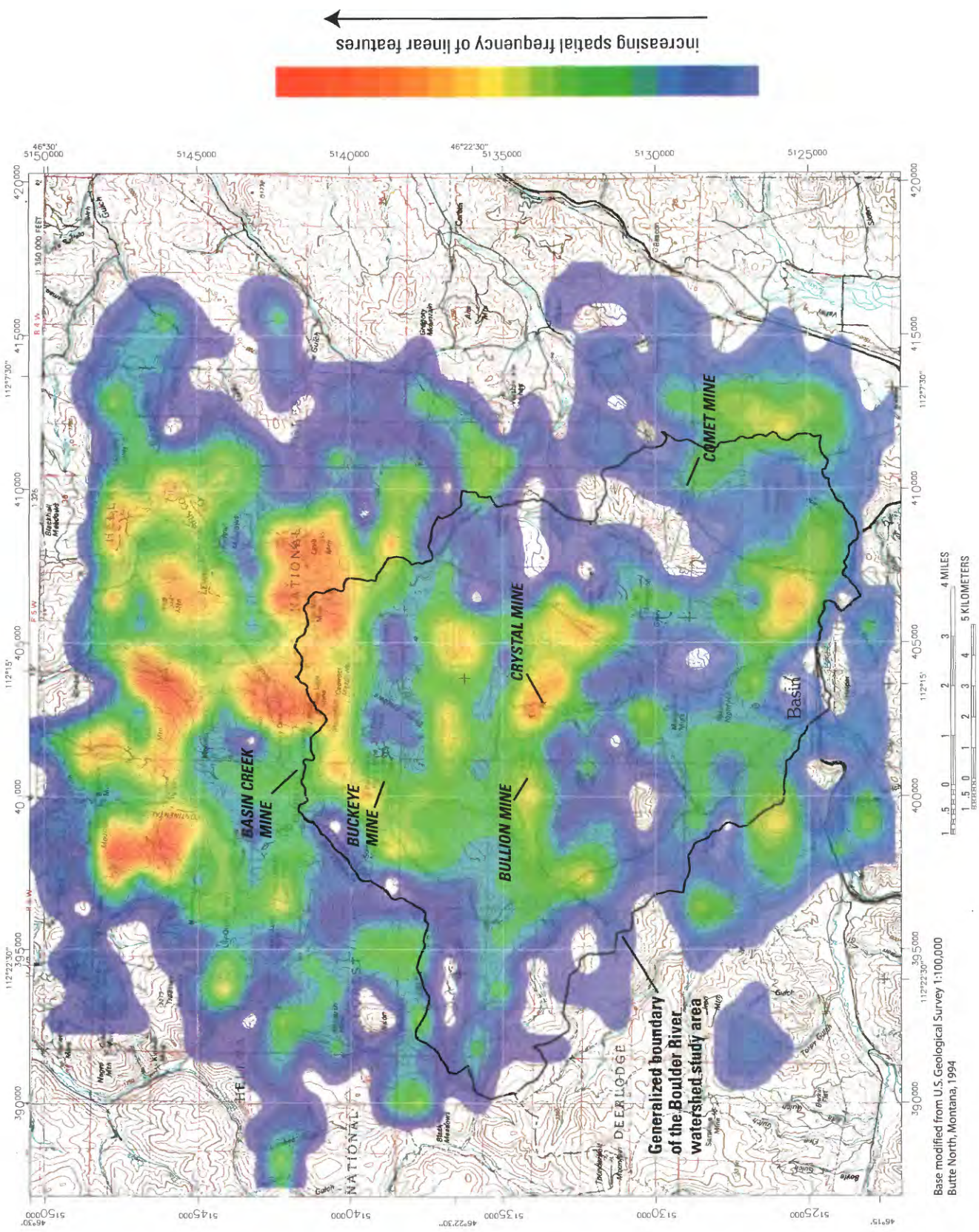

Figure 12. Contour map of linear feature spatial frequency (2,500 ft grid cell size) in the Boulder River watershed region.

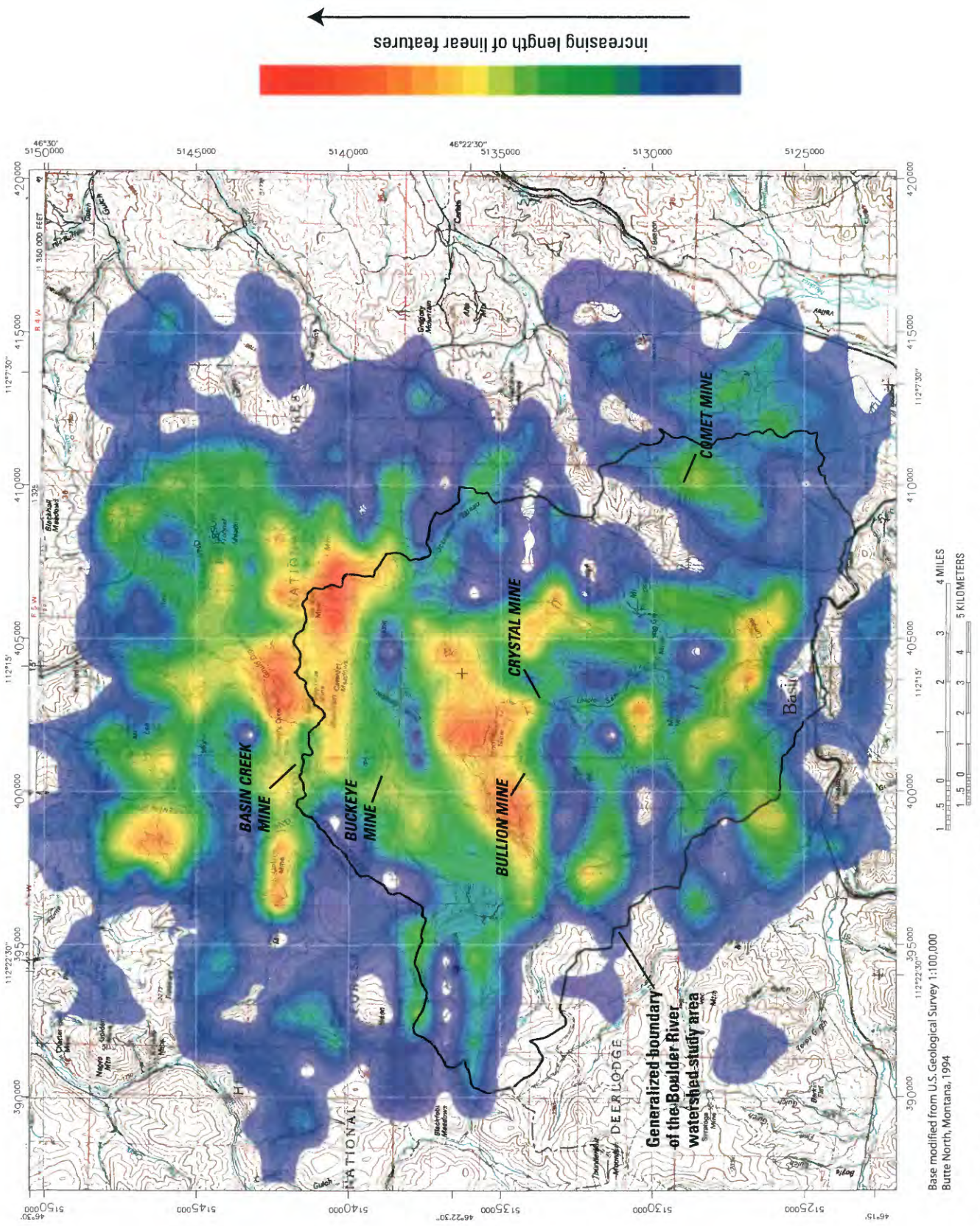

Figure 13. Contour map of linear feature length (2,500 ft grid cell size) in the Boulder River watershed region.

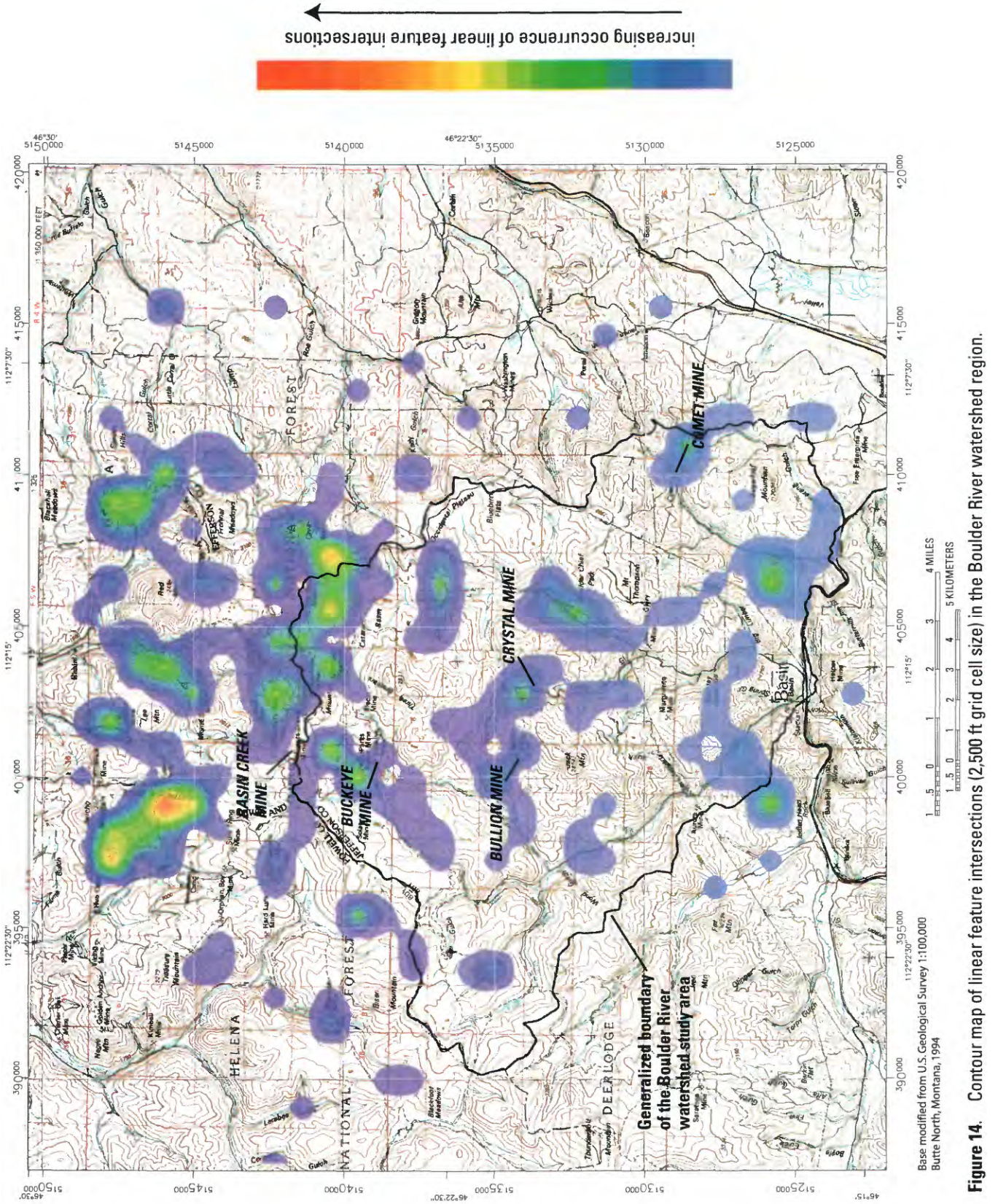

Figure 14. Contour map of linear feature intersections (2,500 ft grid cell size) in the Boulder River watershed region.

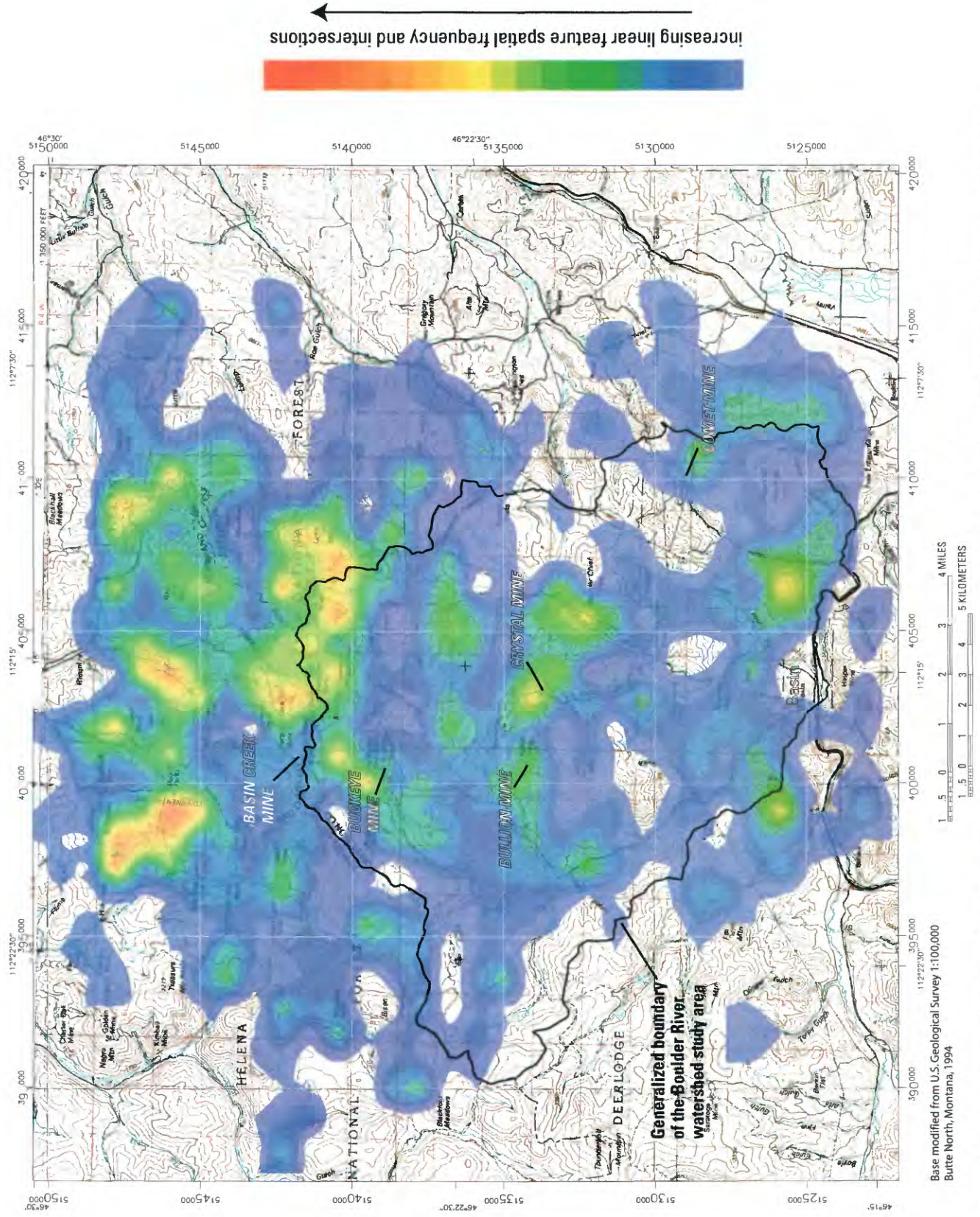

Figure 15. Contour map of combined linear feature spatial frequency and intersections (2,500 ft grid cell size) in the Boulder River watershed region.

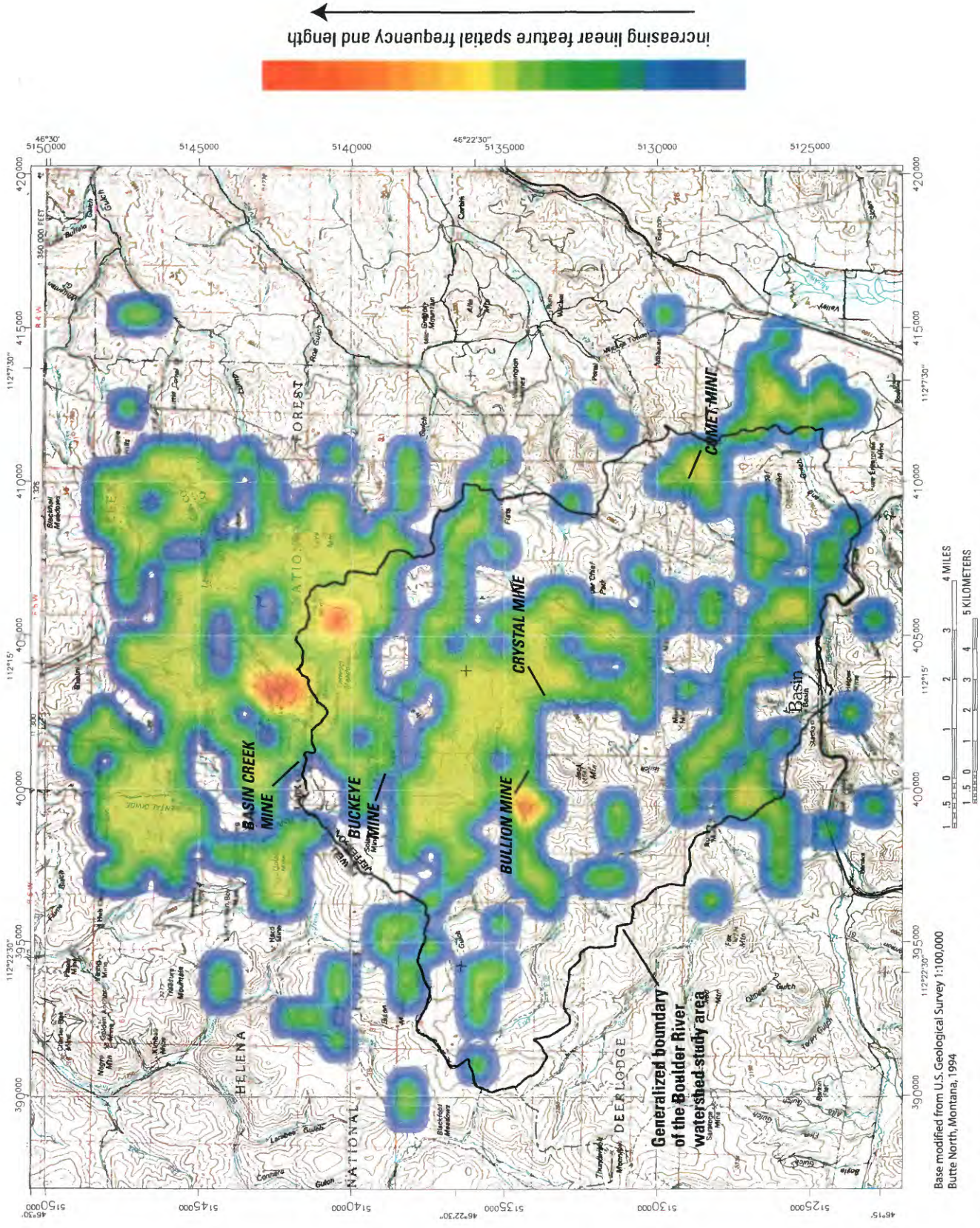

Figure 16. Contour map of combined linear feature spatial frequency and total length (2,500 ft grid cell size) in the Boulder River watershed region.

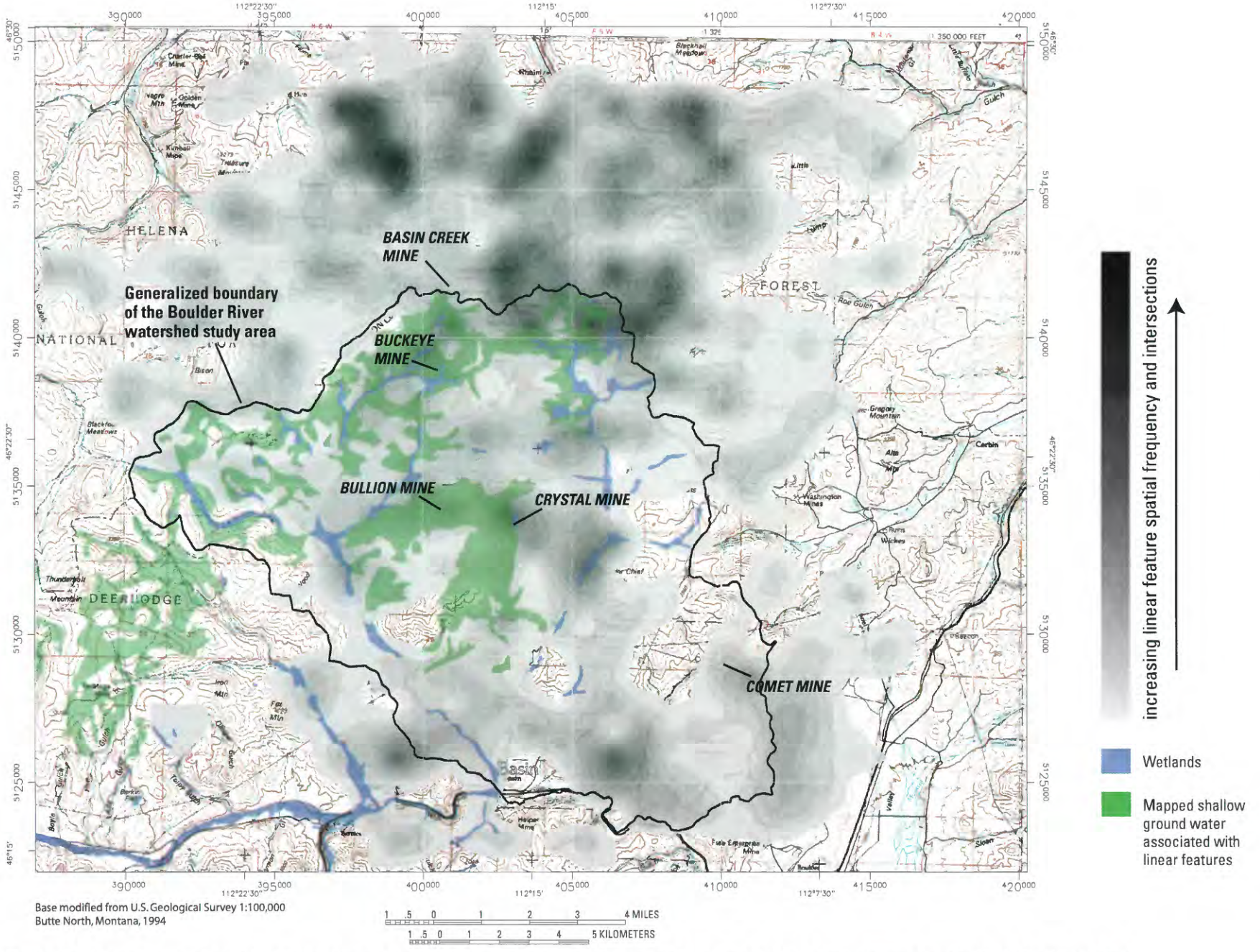

Figure 17. Contour map of combined linear feature spatial frequency and intersections, and areas of mapped shallow ground water (2,500 ft grid cell size).

References Cited

Becraft, G.E., Pinckney, D.M., and Rosenblum, Sam, 1963, Geology and mineral deposits of the Jefferson City quadrangle, Jefferson and Lewis and Clark Counties, Montana: U.S. Geological Survey Professional Paper 428, 101 p., 18 plates.

Desborough, G.A., Briggs, P.H., and Mazza, N., 1998, Chemical and mineralogical characteristics and acid-neutralizing potential of fresh and altered rocks and soils of the Boulder River headwaters in Basin and Cataract Creeks of Northern Jefferson County, Montana: U.S. Geological Survey Open-File Report 98–40, 21 p.

Eliason, E.M., and McEwen, A.S., 1990, Adaptive box filters for removal of random noise from digital images: Photogrammetric Engineering & Remote Sensing, v. 56, no. 4, p. 453.

Freeze, R.A., and Cherry, J.A., 1979, Groundwater: Englewood Cliffs, N.J., Prentice-Hall, Inc., 604 p.

Freeze, R.A., and Witherspoon, P.A., 1966, Theoretical analysis of regional groundwater flow—I, Analytical and numerical solutions to the mathematical model: Water Resources Research, v. 2, no. 4, p. 641–656.

Freeze, R.A., and Witherspoon, P.A., 1967, Theoretical analysis of regional groundwater flow—II, Effect of water table configuration and subsurface permeability variation: Water Resources Research, v. 3, no. 2, p. 623–634.

Hubbert, M.K., 1940, The theory of ground-water motion: Journal of Geology, v. 48, no. 8, pt. I, p. 785–944.

Isaaks, E.H., and Srivastava, R.M., 1989, An introduction to applied geostatistics: New York, Oxford, 561 p.

Knepper, D.H., 1996, Interpreted linear features from Landsat Thematic Mapper images, Southern Ute Indian Reservation, Colorado, *in* Geology and resources of the Paradox Basin, Utah: Utah Geological Association Guidebook 25.

Maxim Technologies Inc., 1999, Final engineering evaluation of potential repository sites, Beaverhead-Deerlodge and Helena National Forests, Lewis and Clark, Powell, and Jefferson Counties, Montana: Helena, Mont., prepared for USDA Forest Service, Region I, Missoula, Mont., variously paged.

Research Systems, Inc., 1998, Boulder, Colorado, ENVI, The Environment for Visualizing Images.

Rockware, Inc., 1999, Golden, Colorado, RockWorks99.

Rowan, L.C., and Wetlaufer, P.H., 1975, Iron-absorption band analysis for the discrimination of iron-rich zones: U.S. Geological Survey, Type III Final Report, Contract S-70243-AG.

Ruppel, E.T., 1963, Geology of the Basin quadrangle, Jefferson, Lewis and Clark, and Powell Counties, Montana: U.S. Geological Survey Bulletin 1151, 121 p., 7 plates.

Sabins, F. F., 1987, Remote sensing principles and interpretation, Second Edition: New York, Freeman.

Smedes, H.W., 1966, Geology and igneous petrology of the northern Elkhorn Mountains, Jefferson and Broadwater Counties, Montana: U.S. Geological Survey Professional Paper 510, 116 p.

Toth, J., 1963, A theoretical analysis of groundwater flow in small drainage basins: Journal of Geophysical Research, v. 68, no. 16, p. 4795–4812.

Aquatic Health and Exposure Pathways of Trace Elements

By Aïda M. Farag, David A. Nimick, Briant A. Kimball, Stanley E. Church, Don Skaar, William G. Brumbaugh, Christer Hogstrand, and Elizabeth MacConnell

Chapter D10 of

Integrated Investigations of Environmental Effects of Historical Mining in the Basin and Boulder Mining Districts, Boulder River Watershed, Jefferson County, Montana

Edited by David A. Nimick, Stanley E. Church, and Susan E. Finger

Professional Paper 1652–D10

U.S. Department of the Interior
U.S. Geological Survey

Contents

Figures

Tables

Chapter D10
Aquatic Health and Exposure Pathways of Trace Elements

By Aïda M. Farag, David A. Nimick, Briant A. Kimball, Stanley E. Church, Don Skaar,[1] William G. Brumbaugh, Christer Hogstrand,[2] and Elizabeth MacConnell[3]

Abstract

Historical mine adits, mill tailings, and waste-rock dumps in the Boulder River watershed, Montana, are sources of trace elements to streams. Biological studies were undertaken to characterize the aquatic health of fisheries and the exposure pathway of these trace elements in watershed streams. Aquatic health was assessed by measuring the survivability of hatchery fish, measuring the biomass and density of resident fish, and documenting the physiology of fish exposed to trace elements. Pathways of exposure were assessed by determining trace-element concentrations in water, sediment, biofilm, invertebrates, and fish tissues and by defining relations among these components.

Instream survivability experiments at sites that had no resident trout and were downstream from inactive mines indicated that elevated concentrations of filtered cadmium, copper, and zinc were associated with increased mortality as well as hypertrophy (swelling), degeneration (dying), and necrosis of epithelial cells in gills of hatchery trout. In lower Cataract Creek, a site farther downstream, the health of resident trout was impaired. A decrease in the number of trout per acre indicated population-level effects; and increased metallothionein, increased products of lipid peroxidation, and elevated concentrations of trace elements in fish tissues indicated individual-level effects.

The concentrations of cadmium, copper, and zinc in water and those of arsenic, cadmium, copper, lead, and zinc in sediment in some watershed streams were sufficient to affect aquatic life. Concentrations of arsenic, copper, cadmium, lead, and zinc in invertebrates from lower Cataract Creek (63, 339, 59, 34, and 2,410 µg/g (dry weight, respectively)) were greater than concentrations in invertebrates from the Clark Fork River watershed, Montana (19, 174, 2.3, 15, and 648, respectively), where these trace elements were associated with reduced survival, growth, and health of cutthroat trout fed diets composed of the Clark Fork River invertebrates. The concentrations of all trace elements, except cadmium, in colloids and biofilm were significantly correlated, which suggests that transfer of trace elements associated with colloids to biological portions of biofilm is an important pathway in which trace elements associated with abiotic components are first presented to biotic components. The interrelationship of trace elements accumulating in the abiotic and biotic components sampled suggests that copper, cadmium, and zinc concentrations increased in fish tissues as a result of direct exposure from water and sediment contact and indirect exposure through the food chain. Apparently, trace elements have made contact with biota through these two pathways and have thereby compromised the overall aquatic health of the Boulder River watershed.

Introduction

Environmental effects of historical mining in a watershed typically are manifested as impairment of the health of aquatic life in streams. The health of fisheries usually is considered an important aquatic life issue because fish represent the top of the food chain in streams and because fish are a resource of considerable interest to land managers and the public. Aquatic health of the fisheries in a watershed can be defined in multiple ways. For example, direct measures of the reduced survivability of fish or reduced levels of fish biomass or density may indicate the inability of a watershed to support an optimal population size. However, to explain possible mechanisms of this population-level impairment and to establish a cause-and-effect relationship between a stressor (for example, concentrations in tissues or "tissue dose" of trace elements) and the effects at the population level (for example, reduced biomass/density), the health of individual fish must be studied. Understanding the pathways of trace-element exposure can further establish the cause-and-effect relationship between stressors and the particular concentrations accumulated in the aquatic components (biofilm, invertebrates, and fish). Interpretation of trace-element concentrations in these components can help define the overall health of the aquatic life in a watershed and provide a baseline for comparisons following remediation activities.

In the Boulder River watershed, Basin, Cataract, and High Ore Creeks (fig. 1) have elevated trace-element

[1]Montana Fish, Wildlife, and Parks, Helena, Montana.

[2]Kings College, London, England.

[3]U.S. Fish and Wildlife Service, Bozeman, Montana.

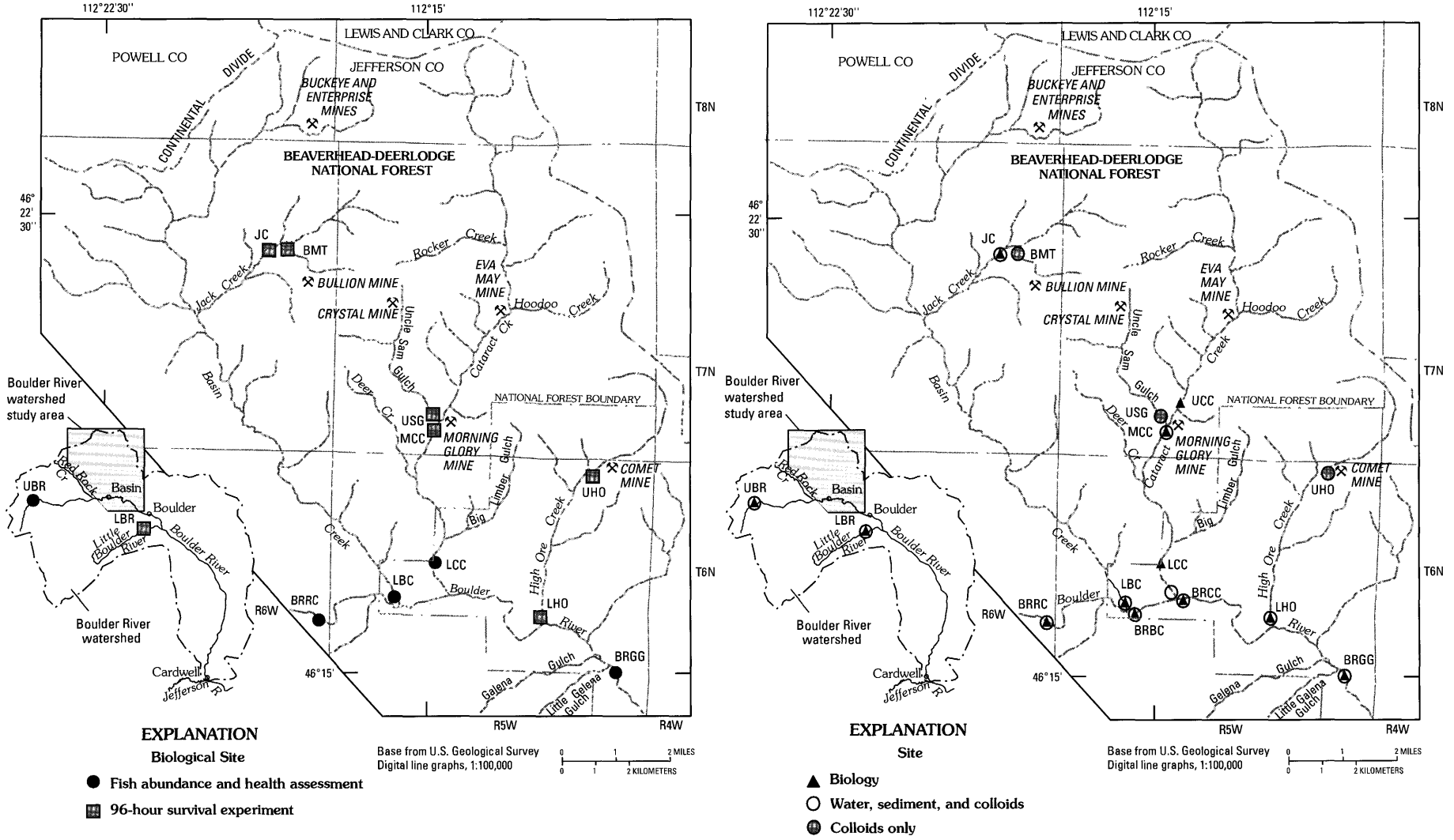

Figure 1. Biological sampling sites used for assessing aquatic health (left) and exposure pathways (right) in Boulder River watershed, Montana.

concentrations in water and streambed sediment, and trace-element loads from these streams affect trace-element concentrations in the Boulder River (Church, Unruh, and others, this volume, Chapter D8; Nimick and Cleasby, this volume, Chapter D5). All species of fish are absent from stream reaches downstream from a few draining mine adits in the watershed, but populations of brook trout (*Salvelinus fontinalis*), rainbow trout (*Oncorhynchus mykiss*), and cutthroat trout (*Oncorhynchus clarki*) reside farther downstream (Robert Wintergerst, United States Department of Agriculture (USDA) Forest Service, Missoula, Mont., oral commun., 1997). Additionally, viable populations of native, genetically pure, westslope cutthroat trout (*Oncorhynchus clarkii lewisi*) exist in High Ore Creek upstream from the Comet mine (fig. 1).

Purpose and Scope

This report examines the aquatic health of fisheries and the exposure pathways of trace elements in streams draining historical mining areas of the Boulder River watershed near Basin in southwestern Montana. Multiple investigations were conducted to fulfill the following biological objectives:

- Determine the survivability of westslope cutthroat trout in stream reaches that lacked fish
- Determine the biomass, density, and health of resident fish
- Characterize the pathway and partitioning of trace elements in water, sediment, biofilm, benthic macroinvertebrates, and fish
- Define the role of water, colloids, and sediment in the transfer of trace elements to aquatic life.

The first objective, to determine the survivability of westslope cutthroat trout in stream reaches that lacked fish, was important for documenting the maximum trace-element concentrations that would not be acutely toxic to fish. Some fishless reaches in Jack Creek, Uncle Sam Gulch, and High Ore Creek coincided with trace-element concentrations of filtered Cd (cadmium) greater than 50 µg/L (micrograms per liter) and as much as 5,000 µg/L of filtered Zn (zinc) in water (Nimick and Cleasby, this volume, figs. 11 and 14). Instream experiments to determine the survivability of cutthroat trout were conducted at seven sites (table 1; fig. 1). Additionally, the concentrations of whole-body ions (such as calcium, potassium, sodium) and histological changes in fish that occurred during the survival studies were investigated because they could provide insight about the mechanisms causing acute toxicity. Whole body calcium, potassium, and sodium could

Table 1. Biological sampling sites, Boulder River watershed.

Site ID (fig. 1)	Site name	Reference site	Assessments			
			Fish	Biofilm, invertebrates	Survival experiment	
					1998	1999
LBR	Little Boulder River	x		x	x	x
BMT	Bullion Mine tributary				x	x
JC	Jack Creek downstream from Bullion Mine tributary.			x	x	x
USG	Uncle Sam Gulch				x	x
UCC	Cataract Creek upstream from Uncle Sam Gulch.			x		
MCC	Cataract Creek downstream from Uncle Sam Gulch.			x	x	x
LCC	Cataract Creek at mouth		x	x		
UHO	High Ore Creek downstream from Comet mine.					x
LHO	High Ore Creek at mouth			x	x	x
LBC	Basin Creek near mouth		x	x		
UBR	Boulder River upstream from Trapper Creek.	x	x	x		
BRRC	Boulder River downstream from Red Rock Creek.	x	x	x		
BRBC	Boulder River downstream from Basin Creek.			x		
BRCC	Boulder River downstream from Cataract Creek.			x		
BRGG	Boulder River downstream from Galena Gulch.		x	x		

indicate upsets in ionoregulatory status as a result of metal exposure. Histological examinations could provide insight about acute changes in tissues, especially gills, which might result during the survivability experiments.

Our second objective was to determine the biomass, density, and health of fish in streams and in the mainstem of the study area. Trace-element exposure can affect aquatic biota and the overall ecological health of a river system (Farag and others, 1995). No assessments of individual fish health had been previously performed in the Boulder River. Surveys of fish biomass and density, measures of physiological function, and trace-element concentrations in tissues at five sites (table 1; fig. 1) were used to provide a picture of exposure related to physiological malfunction and any resulting decrease in fish populations. In addition, we used measures of metallothionein and products of lipid peroxidation (see results for definitions of these measurements) to define physiological malfunction. Then we interpreted these physiological malfunction data with data on trace-element concentrations in tissues and with data on fish biomass and density to determine the overall ecological health of sites in our study area within the Boulder River watershed.

Our third and fourth objectives were established to define the exposure pathways of trace elements. These objectives were to characterize the pathway and partitioning of trace elements in water, sediment, biofilm (also referred to *aufwuchs*, and consists of abiotic and biotic materials that form a surface layer on rocks in streams), invertebrates, and fish, and to define the influence of water, colloids, and sediment in the transfer of trace elements to aquatic life. To meet these objectives, we collected samples for trace-element analysis from both abiotic and biotic components throughout the watershed. Biofilm and benthic macroinvertebrates were collected from 12 sites; fish tissues were collected from 5 sites (table 1; fig. 1).

Previous Studies

Although aquatic health had not been previously rigorously studied in the Boulder River watershed, investigations of the effects of mining on aquatic life in the Boulder River began in 1975. Nelson (1976) found reductions in the survival of fish eggs during an egg bioassay and reductions in fish populations at sites on the Boulder River below Cataract Creek and High Ore Creek. Gardner (1977) found that the invertebrate community diversity in the Boulder River at a station downstream from High Ore Creek was reduced compared to an upstream station on the Boulder River located downstream from Red Rock Creek. In both studies, the differences between sites upstream and downstream of High Ore Creek were attributed to the greater concentrations of zinc in the water at the site below High Ore Creek.

In the 1990s, other investigations of the watershed were initiated to define the fitness of aquatic life in the Boulder River watershed. Gless (1990) designated Basin Creek a "stream of concern," Cataract Creek as "degraded," and High Ore Creek as "extremely degraded." These classifications were based on elevated concentrations of arsenic in the water column and the rare presence of aquatic life in some stream reaches. Gless (1990) observed iron stains and dead vegetation as high as 4.5 ft above the stream banks of Cataract Creek. Martin (1992) documented elevated concentrations of cadmium, copper, and zinc in water, sediment, aquatic invertebrates, and fish in the Cataract Creek drainage and related these concentrations to the sources of trace elements in the drainage.

Acknowledgments

The authors thank Thomas E. Cleasby for assistance with water-sample and fish-tissue collections; Jack Goldstein, Dave Harper, and Brad Mueller for assistance during collections of biology samples and performance of toxicity experiments; Michèle Williams for assistance with measurements of lipid peroxidation; Ron Spoon and Kurt Hill for assistance during biomass/density and habitat assessments; and Mark Ellesieck and Darren Rhea for statistical assistance and graphics.

Methods

Aquatic Health

Assessing aquatic health of fisheries involved investigations that measured survivability of hatchery trout in instream experiments, measured fish biomass and density, assessed fish physiology, and statistical analysis of the data. Farag and others (2003) have provided more complete details of the methods described herein.

Survival Experiments

The survival of westslope cutthroat trout from the Washoe Park State Fish Hatchery, Anaconda, Mont., was determined with 96-hr in-situ experiments at five sites downstream from large inactive mine sites in Basin and Cataract Creek basins and in lower High Ore Creek (fig. 1) during low-flow conditions in 1998. We repeated the experiment in 1999 and added a sixth site in upper High Ore Creek. This site was added because of its close proximity to the Comet mine site, where remediation efforts were underway (Gelinas and Tupling, this volume, Chapter E2). This site also was in close proximity to a native population of westslope cutthroat trout living upstream of the Comet mine. A site on the Little Boulder River (fig. 1, LBR), which lacked significant historical mine activity, was selected as a reference site.

Twenty Age-1 fish were placed at each site, with five fish in each of four 4-L polyethylene enclosures. We investigated the whole-body ion status of sampled fish during 1998 to determine if ionoregulatory failure due to elevated

concentrations of trace elements in the water column was the cause of death. During 1999, additional experimental fish were held at each site, and the tissues were processed by standard histological methods and examined by light microscopy.

Water quality was monitored at each site during the 96-hr survival experiments. Specific conductance, pH, and dissolved oxygen were measured onsite, and water samples were analyzed for total hardness and filtered and total-recoverable trace elements (Lambing and others, this volume, Chapter D7; Nimick and Cleasby, this volume).

Fish Biomass, Density, and Physiology

Five sites were selected to study resident fish population and physiology. The three tributary sites were upper Boulder River (UBR, reference site), lower Cataract Creek (LCC), and lower Basin Creek (LBC) (fig. 1). The two mainstem sites were the Boulder River downstream from Red Rock Creek (BRRC, reference) and downstream from Galena Gulch (BRGG). The differences in flow between the tributary and mainstem sites required that different methods be used to study populations in these two types of sites. Multiple-pass depletion was used to estimate populations in the smaller, tributary sites, and mark-recapture techniques were used to estimate populations in the mainstem sites (Zippen, 1958). Fish were collected by electrofishing. Total lengths and weights were recorded, and scales were collected to define the length at age.

Using methods described by Platts and others (1983), depth, velocity, substrate, and microhabitat features were measured at sites sampled for fish abundance. Weighted usable area was calculated from these parameters using the PHABSIM models (Platts and others, 1983). Calculated weighted usable area was used to differentiate the available habitat among sites. Suitability indices (SI) for all brook trout life stages were from Chapman (1995), rainbow trout fry SI values were from Raleigh and others (1984), and rainbow trout juvenile and adult SI values came from Ken Bovee (oral commun., 1997) for the South Platte River, Colo. Water-quality conditions were monitored periodically between October 1996 and September 1999 at the five fish-health-assessment sites (Nimick and Cleasby, this volume).

Thirteen to twenty-five rainbow trout of 8 ± 1.7 inches (mean $\pm$ 1 σ) and 0.20 ± 0.14 pounds were collected from each site for physiological analyses during low flow in 1997. Each fish was pithed, and a necropsy was performed immediately to define any gross abnormalities (for example, nodules on internal organs, discolored or frayed gills; Goede, 1989). Samples of gill and liver were dissected from each fish and immediately frozen with liquid nitrogen. Five additional rainbow trout (same size as preceding) were collected from each site and frozen for measurements of whole-body trace-element concentrations. At least five composite samples of each tissue from each site were prepared in the laboratory by combining tissues from two to five fish. To define the physiological condition of fish from the sites, concentrations of tissue trace elements, products of lipid peroxidation, and metallothionein were measured in aliquants of the composite samples. Arsenic, cadmium, copper, lead, and zinc were measured in gills, livers, and whole fish ($n \geq 5$ for each tissue type). Quality control included measurements of predigestion spikes, postdigestion spikes, digestion replicates, and reference tissue samples.

Statistical Analyses

Data for tissue trace-element concentrations, metallothionein, products of lipid peroxidation, length at age, and fish biomass/density estimates were analyzed with one-way analysis of variance (SAS Institute, 1989). We tested the data for equality of variances with the Levene test after transforming the data when necessary. Means were compared using a Fischer least significant difference test with a statistical criterion of $\alpha = 0.05$. We did not statistically analyze the survival data.

Exposure Pathways

We collected water, sediment, biofilm, and invertebrates from 12 sites within the Boulder River watershed (table 1) to examine the pathway of metals in abiotic and biotic components of streams. Five sites were on the mainstem Boulder River (UBR, BRRC, BRBC, BRCC, and BRGG) and seven sites were on tributaries (UBR, LHO, LCC, MCC, UCC, LBC, and JC; fig. 1). BRRC was a reference for the mainstem sites. Data from UBR (characteristics were similar to tributaries) and LBR were combined as a reference for the tributary sites. Once the boundaries of a site were established, we collected samples of biofilm and invertebrates at four riffle localities at the site ($n = 4$). Methods of sample collection and data analysis are summarized herein. A more complete description of these methods is in Farag and others (work in progress).

Water samples were collected periodically during 1996–99 at all sites. Water temperature, specific conductance, pH, and streamflow were measured at the time of sampling (Nimick and Cleasby, this volume). Water samples were analyzed for total-recoverable (unfiltered) and filtered (0.45-µm pore-size) trace-element concentrations. We determined colloidal concentrations of trace elements in the water column indirectly by subtracting an ultrafiltered trace-element concentration (0.1-µm, or 10,000 Dalton, pore size) from a total-recoverable trace-element concentration. A composite sediment sample was collected at each site over a 100–150 ft reach by means of a plastic scoop (Church, Unruh, and others, this volume). We collected biofilm by gently scraping the surface of rocks collected from the near-shore streambed. Macroinvertebrates were sampled with a 3-mm mesh net attached to a 2×4-ft frame. The substrate in approximately 65 ft^2 of riffle upstream from the net was overturned, and the dislodged macroinvertebrates were collected in the net. Fish were collected as described in the preceding section. (See "Fish Biomass, Density, and Physiology.")

Statistics

Concentrations of trace elements measured in water, sediment, biofilm, invertebrates, gill, liver, and whole fish collected from the test sites were compared to concentrations in samples collected from the reference sites. Data from multiple reference sites were combined into one group and are referred to as the pooled reference (REF). Multiple reference sites were not sampled for gill, liver, and whole fish. Data for all sites were tested for homogeneity of variance and transformed when necessary. Under the assumption of equal variances, an Analysis of Variance (ANOVA) was performed to test for differences between means. If any difference was detected, Dunnett's one-tailed t-test (Dunnett, 1955) was used to make comparisons between each experimental site and the reference site for each trace element. Regressions also were performed to define correlations of trace-element accumulation among water, sediment, colloids, biofilm, and fish.

Results

Aquatic Health

Survival Experiments

Survival of caged westslope cutthroat trout at 96 hours was less at all test sites (table 1) than at the Little Boulder River reference site during 1998 and 1999 (fig. 2). Except survival at the lower High Ore Creek site, which was 33 percent during 1999, survival at 96 hr was 0 percent at all experimental sites during both years. In most cases, survival was affected in 24 to 48 hr during 1999. Fish died more quickly at Jack Creek and middle Cataract Creek during 1999 as compared to 1998. In the two most extreme cases, cutthroat trout placed in Uncle Sam Gulch and the Bullion Mine tributary died in 5 and 8 hr, respectively, during 1999. Survival was reduced to 5 percent at upper High Ore Creek at 72 hr, and the experiment at this site was ended at that time.

The concentrations of whole-body ions in fish in 1998 did not differ significantly among sites (reference site included).

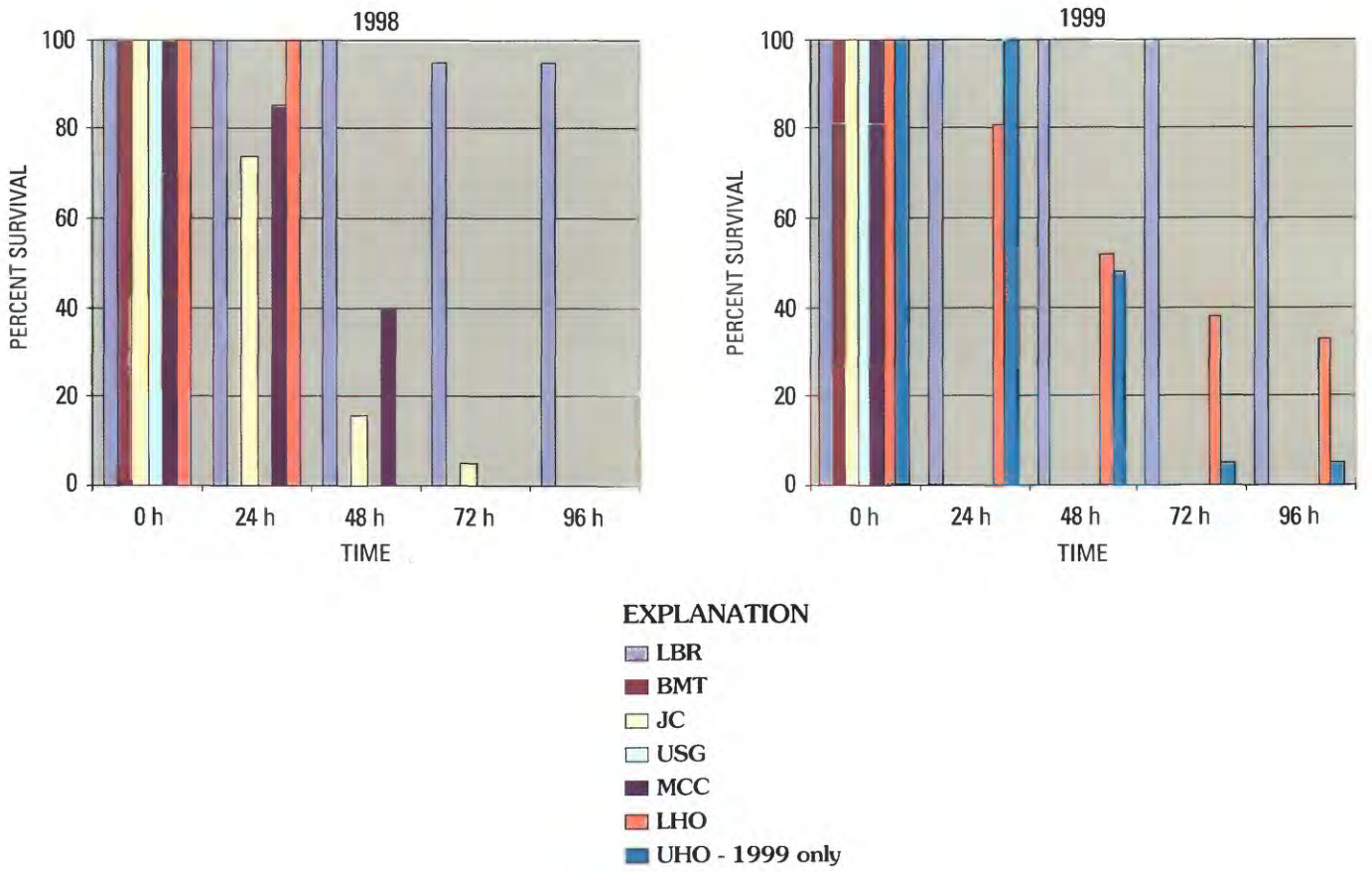

Figure 2. Survival of hatchery cutthroat trout placed in various tributaries of Boulder River for as long as 96 hr during 1998 and 1999.

Concentrations of ions ranged from 22,500 to 24,900 µg Ca/g, 12,000 to 15,100 µg K/g, and 2,050 to 3,180 µg Na/g, with the highest concentrations noted in fish from Uncle Sam Gulch. The histological analyses during 1999 indicated that degeneration (dying) and necrosis (death) of gill epithelia was the most significant tissue lesion. Excessive mucus production and hypertrophy (swelling) also were noted in gill epithelia of fish from the test sites (fig. 3). Spongiosis, a condition of edema and necrosis, was also observed in the nares (nasal sensory organ) of fish held in the test sites. Additionally, excessive mucus was noted in the skin of fish from all test sites. There was some hypertrophy in the gill lamellae and abundant mucus in the nares of fish held at the reference site, but these changes were less severe than those at the test sites. The proliferation of epithelial cells noted in gills of fish from both the upper and lower High Ore Creek sites indicates that toxicity was less acute at these sites, consistent with the longer times to death at these sites in 1999. Additionally, the pseudobranch of fish from lower High Ore Creek contained cystic (fluid-filled) areas, an abnormal condition not noted at other sites. We noted dark longitudinal coloration in the skin at death for fish at the High Ore Creek sites. This discoloration was about 0.5 cm wide and was observed across the length of the fish. Correspondingly, an increased accumulation of melanocytes was noted in the skin of fish collected from lower High Ore Creek.

Water Chemistry—Survival Experiments

Water chemistry was variable in stream reaches where 96-hr survival experiments were performed in 1998 and 1999. The onsite experiments were performed between mid-July and early August, but streamflow conditions were different each year. During the 1999 experiments, streams had low-flow conditions typical of late summer, whereas the 1998 experiments were conducted near the end of spring runoff. Streamflow was higher during the 1998 experiments, and trace-element concentrations generally were lower in 1998 than in 1999. In both years, almost all the cadmium and zinc was in the filtered (0.45 µm) fraction, and copper was divided about equally between the filtered and particulate phases. Therefore, filtered concentrations of cadmium, copper, and zinc are presented (table 2). Concentrations of arsenic and lead generally were low relative to concentrations of the other trace elements (<3 µg As/L except LHO and UHO with 22–33 µg As/L; <1 µg/L for Pb/L except BMT with 3.1 µg Pb/L), and the data are not presented. The pH values were neutral to slightly basic (7.0–8.3) except for the site on Bullion Mine tributary, where pH was 5.2–5.4. The temperature range was 11°–21°C for all sites.

The relationship between trace-element concentrations and mortality followed a consistent pattern; higher concentrations resulted in greater and more rapid mortality. At the reference site on the Little Boulder River (LBR), hardness (48–56 mg/L) and trace-element concentrations (<0.3 µg Cd/L, 2 µg Cu/L, 2–5 µg Zn/L) were low. Water-quality conditions at this reference site were similar in 1998 and 1999. However, streamflow was 4–8 times higher during the experiments in 1998 than in 1999 in the Jack and Cataract Creek drainages. Consequently, constituent concentrations were higher in 1999 at the four sites in these two drainages (BMT, JC, USG, MCC). In 1999, concentrations of cadmium, copper, and zinc were about 100 percent higher and hardness values were about 50 percent higher than the corresponding 1998 levels at each site. Hardness measured generally higher at the two High Ore Creek sites (LHO and UHO 130–140 mg/L) compared to all other sites. Concentrations of trace elements were similar at the two sites on High Ore Creek in 1999 and somewhat higher at lower High Ore Creek in 1998 compared to 1999, apparently as a result of streamflow (table 2).

Results of hourly sampling in 1999 indicated that filtered zinc concentrations typically varied at many sites (Lambing and others, this volume). These variations resulted from normal diel concentration cycles and from the effect of storm runoff, which occurred during the toxicity experiments in Jack Creek in 1999. Diel cycles resulting in 2- to 3-fold changes in dissolved cadmium and zinc concentrations have been documented at several sites in and near the study area and are thought to be caused by the effect of water temperature and pH on the partitioning of cadmium and zinc between dissolved and sorbed phases (Fuller and Davis, 1989; Lambing and others, this volume). Therefore, a wide range of concentrations may occur daily at each site.

Fish Biomass and Density Estimates

Of the three tributaries studied, the combined biomass of all species of trout observed (on either an areal or a lineal basis) was the smallest at the lower Cataract Creek site (table 3). There were 12 ± 3.5 lb/acre at lower Cataract Creek versus 60±4.9 lb/acre at the upper Boulder River site and 37±1.9 lb/acre at the lower Basin Creek site. Brook and rainbow trout were the two trout species found in the tributaries; brook trout were the most common species of fish at the upper Boulder River site, whereas rainbow trout were the most common species of fish present at the lower Cataract Creek site. However, both species were present in about equal numbers in lower Basin Creek. The species composition in lower Cataract Creek and lower Basin Creek seemed to generally reflect the composition of the nearest mainstem sites; the Boulder River site near Red Rock Creek had a similar composition to that in lower Basin Creek, and the Boulder River site near Galena Gulch was similar to that in lower Cataract Creek. Although there was a trend of less biomass at the Boulder River site near Galena Gulch (BRGG) compared to the reference site upstream from the affected study reach (BRRC), the difference was not significant (table 3). There were no significant differences among lengths at age calculated from scales of rainbow trout samples from the three tributary sites (fig. 4), nor was there a difference in length at age between fish sampled from the mainstem sites (data are not presented). The observations for density (number per 1,000 ft) have the same pattern as biomass results for all sites (table 3).

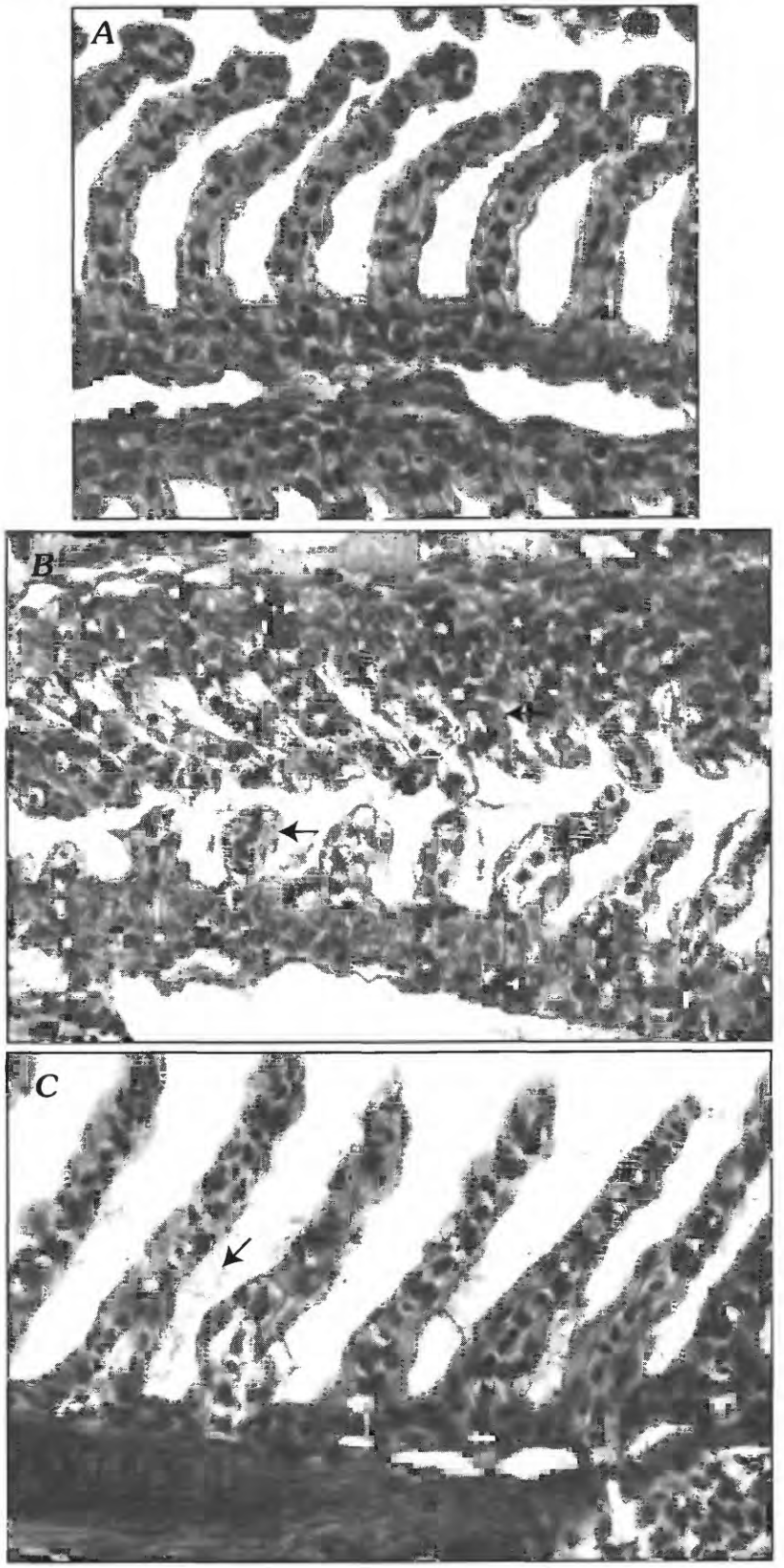

Figure 3. Gill tissue of trout held during the 1999, 96-hr survival experiment. *A*, Gill section of a cutthroat trout held at Little Boulder River site (reference). Section is 5 µm thick, stained with hematoxylin and eosin, × 250. *B*, Gill section of a trout held at Middle Cataract Creek site. Top arrow points to hypertrophied cells; bottom arrow points to degenerate epithelial cell. Section is 5 µm thick, stained with hematoxylin and eosin, x 250. *C*, Gill section of a trout held at upper High Ore Creek site. Arrow points to excessive mucus. Section is 5 µm thick, stained with hematoxylin and eosin, x 250.

Table 2. Physical and chemical data for stream sites during the 96-hour survival experiments.

[Trace-element concentrations are for filtered samples; median values are listed when multiple samples were collected during an experiment]

Site (fig. 1)	Sample date	Cadmium (µg/L)	Copper (µg/L)	Zinc (µg/L)	pH (standard units)	Hardness (mg $CaCO_3$/L)	Streamflow (ft^3/s)
LBR – Reference	7/21/98	<0.3	2.0	2.0	7.9-8.1	48	6.4
	8/2/99	<0.3	2.4	2.5	8.0-8.2	56	2.5
BMT	7/21/98	20	113	2,160	7.4	39	1.1
	8/2/99	38	557	3,970	5.2-5.4	66	0.02
	8/3/99	35	314	3,920	5.9	--	--
JC	7/21/98	3.4	33	377	7.7-7.8	29	32.5
	8/2/99	8.0	51	656	7.0-7.4	44	1.1
USG	7/21/98	22	84	1,830	7.6	41	4.9
	8/2/99	75	377	5,730	7.3	--	--
	8/4/99	59	206	4,840	7.5	63	0.71
MCC	7/21/98	4.4	34	391	7.8-8.2	36	20.5
	8/2/99	9.6	48	714	7.9	--	--
	8/4/99	9.3	48	651	7.8-7.9	48	4.6
UHO	8/3/99	2.5	3.7	550	8.2	140	0.35
LHO	7/21/98	3.7	5.0	987	8.1-8.3	130	1.8
	8/2/99	2.0	3.6	459	8.1-8.3	140	0.71

Fish species observed at the five fish-abundance sites during 1997–99 included three native species (longnose sucker *Catostomus catostomus*, mottled sculpin *Cottus bairdi*, and mountain whitefish *Prosopium williamsoni*) and four non-native species (Yellowstone cutthroat trout, rainbow trout *Salmo gairderi*, eastern brook trout *Salvelinus fontinalis*, and brown trout *Salmo trutta*). The mainstem sites had a greater number of species than did the tributary sites. Most of the brown trout and mountain whitefish captured in the mainstem (in 1998 and 1999) were in spawning condition and may have migrated from sites farther downstream. Mottled sculpin were found at the upper Boulder and the lower Basin Creek tributaries, and mountain whitefish were found at lower Basin Creek. Neither mottled sculpin nor whitefish were found at lower Cataract Creek. None of the rainbow, cutthroat, or brook trout collected from the tributary sites appeared to be spawning.

Habitat Characterization of Fish Abundance Sites

The habitat of the tributary sites differed in many ways. The lower Cataract Creek site had a higher stream gradient (2.7 percent) than the other tributary sites (2.0 and 1.1 percent for UBR and LBC, respectively) as well as a higher percent of habitat described as riffles (94 percent as compared to 70 percent for UBR and 60 percent for LBC). Lower Cataract Creek had the widest bankfull channel width (80 ft) and a corresponding lower mean depth and velocity than the other sites. All sites were similar in having a fair amount of canopy cover (13.4–19.8 percent), little woody debris (0.1–1.4 percent), low levels of embeddedness (1.3–1.4 percent), and small amounts of undercut bank (1–4 percent) or overhanging vegetation (1–4 percent). For the mainstem sites, the Boulder River near Galena Gulch had a much higher percentage of riffles (84 percent) than the Boulder River near Red Rock Creek (38 percent), even though the Boulder River near Galena Gulch site had a slightly lower gradient (0.8 percent vs. 1.2 percent). Both sites were characterized as having no pool habitat, and the sites were also similar in the amount of canopy cover, woody debris, embeddedness, bank cover, undercut banks, and overhanging vegetation. Mean velocity at the Boulder River near Red Rock Creek site was slightly higher (1.04 ft/s) than that at the Boulder River near Galena Gulch (0.99 ft/s). Boulder River near Galena Gulch is a larger stream, having a bankfull channel width of 114 ft, compared to only 68.6 ft for the Boulder River near Red Rock Creek. Microhabitat was quantified in terms of weighted usable area from one set of measurements taken along 10 or 11 transects at each site in late September–early October 1998. Large amounts of available habitat are reflected by large amounts of weighted usable area. Therefore, observed excessive differences in weighted usable area among sites would suggest that habitat is responsible for differences in biomass/density estimates. For both brook and rainbow trout, the weighted usable area in the tributaries was greatest in lower Basin Creek for fry and

Table 3. Size ranges and biomass/density estimates of brook, rainbow, and cutthroat trout in tributaries and mainstem of the Boulder River.

[The estimates were performed during late July (1997) and early October (1998 and 1999), and numbers are reported with standard error in parentheses; "*" indicates significant difference from reference at $p = 0.05$]

Site (fig. 1)	Size range (inches)	No./1,000 ft	No./acre	Pounds/acre
		Tributaries		
UBR – Reference				
1997	2.7-12.4	214 (53)	551 (137)	57 (13)
1998	2.0-9.6	212.4 (19)	547 (49)	53 (4.6)
1999	2.4-10.2	325 (19)	837 (50)	70 (4.0)
Mean			645 (96)	60.0 (4.9)
LBC				
1997	1.6-13.2	144 (23)	404 (63)	55 (7.7)
1998	2.0-10.5	210 (8)	591 (22)	55 (2.8)
1999	1.7-11.1	381 (13)	1,070 (35)	61 (1.9)
Mean			688 (198)	56.8 (1.9)
LCC				
1997	2.7-8.3	41 (14)	74 (25)	5.2 (1.8)
1998	1.4-8.6	142 (12)	257 (21)	14 (1.2)
1999	3.3-8.6	94 (3)	171 (5)	17 (0.5)
Mean			167 (152)*	12 (3.5)*
		Boulder River		
BRRC – Reference				
1998	4.2-11.8	148 (30)	275 (18) (37)	31 (6.1)
1999	3.9-12.5	219 (15)	180 (37)	50 (5.4)
Mean			227 (48)	40 (9.3)
BRGG				
1998	4.2-12.6	177 (10)	200 (15)	19 (1.1)
1999	4.3-13.8	227 (17)	156 (9)	27 (2.5)
Mean			178 (22)	225 (4.2)

juveniles, and greatest for adults in upper Boulder River. Lower Cataract Creek had the lowest weighted usable area for each life stage (table 4). In the mainstem, weighted usable area for juveniles and adults was greatest for both species in Boulder River near Galena Gulch, but the weighted usable area for fry was greatest for both species at Boulder River near Red Rock Creek.

Water Chemistry—Resident Fish Biomass/Density and Health

Data from water samples collected in 1996–97 at the five biomass/density and fish-health sites indicated that filtered and total-recoverable concentrations of Al, Sb, As, Ba, Be, Cr, Co, Fe, Mn, Hg, Mo, Ni, U, Ag, and U (Nimick and Cleasby, this volume) were either less than method-detection levels or less than concentrations established by the U.S. Environmental Protection Agency (1999, 2001) to protect aquatic life. In contrast, concentrations of Cd, Cu, Pb, and Zn (table 4) frequently were elevated at sites downstream of the historical mining activity (LBC, LCC, and BRGG).

Trace-element concentrations generally were low (table 5) during all flow conditions at the sites (UBR and BRRC) upstream of historical mining activities. At Boulder River near Red Rock Creek, concentrations of copper exceeded the acute and chronic aquatic-life standard in 2 of 4 samples measured for filtered and 6 of 10 samples measured for total-recoverable copper during high flow. Some total-recoverable lead concentrations also exceeded the chronic but not acute aquatic-life standard at Boulder River near Red Rock Creek. Trace-element concentrations were higher at the other three sites. The highest concentrations of trace elements occurred at the lower Cataract Creek site, where

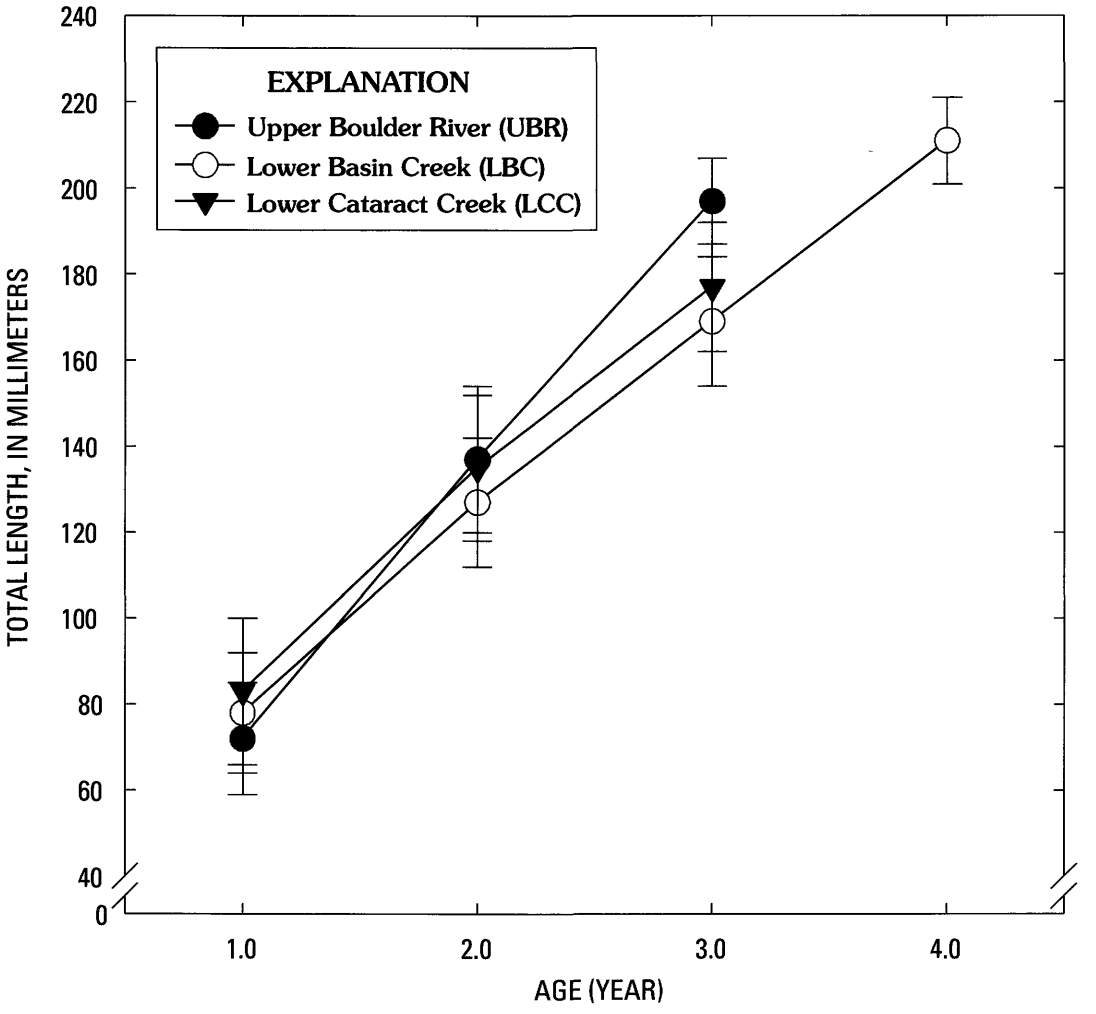

Figure 4. Comparisons of growth of trout in three tributaries in Boulder River watershed. Means are presented as symbols and ± standard deviations are represented with bars.

filtered cadmium, copper, and zinc concentrations exceeded acute standards in every sample. Filtered zinc concentrations also exceeded acute standards in all samples from lower Basin Creek and Boulder River near Galena Gulch. Concentrations of cadmium and copper frequently exceeded standards during high flow at these two sites and at Boulder River near Galena Gulch during low flow as well.

Concentrations of filtered cadmium and zinc at the lower Cataract Creek site were similar to concentrations associated with mortality in the 96-hr survival experiments. Median concentrations (table 5) at this site were higher than at middle

Table 4. Weighted usable area (ft^2 WUA) per 1,000 ft^2 of stream for brook and rainbow trout fry, juveniles, and adults.

[WUA based on the product of suitability index values for depth, velocity, and substrate; Fry (<2 inches), Juveniles (2–8 inches), and Adults (>8 inches)]

Site (fig. 1)	Brook trout			Rainbow trout		
	Fry	Juvenile	Adult	Fry	Juvenile	Adult
UBR	4.6	5.6	27.2	20.6	9.6	3.7
LBC	5.2	5.6	25.7	23.6	15.6	3.1
LCC	4.5	5.6	19.7	17.8	8.6	2.1
BRRC	4.1	2.5	14.5	12.4	16.0	5.3
BRGG	2.2	2.5	21.3	18.1	23.3	6.0

Table 5. Physical and chemical data for stream sites where fish health was assessed, Boulder River watershed, Montana, 1996–99.

[Median filtered (filt.) and total-recoverable (total) trace-element concentrations are listed, and *n* represents the number of samples collected on different dates throughout the flow condition]

Site (fig. 1)	*n*	Streamflow (ft^3/s)	pH	Hardness (mg/L as $CaCO_3$)	Filtered trace-element concentration, median (µg/L)									
					Arsenic		Cadmium		Copper		Lead		Zinc	
					Total	Filt.	Total	Filt.	Total	Filt.	Total	Filt.	Total	Filt.
High-flow conditions														
UBR	2	14-81	7.6-8.1	21-38	4.0	2.5	<1	<0.3	3	1.5	<1	<1	<10	1
BRRC	10	106-724	7.6-8.2	22-50	5.5	3.3	<1	<0.3	5	3.3	1.1	<1	11	3
LBC	10	14-251	7.0-8.0	12-35	11	4.0	<1	0.4	12	8.7	2.6	<1	81	61
LCC	11	14-170	6.8-8.0	18-54	17	3.4	1.8	1.3	46	33	6.7	<1	177	139
BRGG	11	177-1,049	7.5-8.2	19-48	12	4.0	<1	0.3	20	11	5.9	<1	73	46
Low-flow conditions														
UBR	2	4-4	8.0	52-53	2.5	2.0	<1	<0.3	1.5	<1	<1	<1	<10	<1
BRRC	8	7-25	7.4-8.3	54-61	3.0	2.4	<1	<0.3	1.4	1.7	<1	<1	<10	2.3
LBC	7	4-7	7.5-8.2	39-42	7.0	4.0	<1	0.4	4.0	3.0	<1	<1	66	63
LCC	7	4-7	7.5-8.3	59-69	4.8	3.0	5.0	4.9	24	22	<1	<1	419	397
BRGG	8	18-35	7.7-8.5	61-68	6.0	5.0	<1	0.8	10	9.0	<1	<1	180	160

Cataract Creek and Jack Creek during the 1998 experiments in which 100 percent mortality was observed at 96 hr. Filtered trace-element concentrations at the other four fish-assessment sites during low flow were considerably less than the concentrations associated with mortality in the survival experiments (tables 2 and 5).

Tissue Trace Elements

Concentrations of most trace elements in the livers of resident rainbow trout were greatest in fish from lower Cataract Creek (table 6). Concentrations in the livers of rainbow trout from lower Cataract Creek were higher than 1,000 µg Cu/g, 60 µg Cd/g, and 13 µg As/g (dry wt). Concentrations of trace elements in the livers of fish from lower Basin Creek and Boulder River near Galena Gulch also were elevated above those measured at the reference sites (UBR and BRRC). In general, the pattern of metal accumulation in livers was LCC > LBC ≥ BRGG > BRRC ≥ UBR (table 6). In an exception to this pattern, the greatest concentration of lead was in fish from Boulder River near Galena Gulch.

The pattern of trace-element concentrations in livers was similar to the pattern in gills (table 6). The greatest concentrations of copper, cadmium, and zinc were in the gills of fish from lower Cataract Creek (>20 µg Cu/g, >60 µg Cd/g, and >700 µg Zn/g) (table 6). Whereas lesser concentrations of copper and greater amounts of zinc occurred in the gill compared to the liver, the concentrations of cadmium in livers and gills of fish from lower Cataract Creek were nearly identical. As was noted for liver, the greatest concentrations of lead were in gills from fish at Boulder River near Galena Gulch. However, unlike liver, there was no significant accumulation of arsenic in the gills.

The pattern of trace-element accumulation described for livers and gills was similar in whole fish. Again, the greatest concentrations of most trace elements in whole fish were in samples from lower Cataract Creek, where 22 µg Cu/g, 4.9 µg Cd/g, and 8 µg As/g were measured (table 6). Although less cadmium was observed in the whole body versus liver and gill, the mean cadmium concentration in whole fish from lower Cataract Creek was 4.9 µg/g. There was no significant accumulation of lead in whole fish.

Metallothionein

Physiological malfunction can be defined with measurements of metallothioneins and products of lipid peroxidation (Farag and others, 1994, 1995). These measurements have been associated with reduced growth in laboratory experiments (metallothioneins: Dixon and Sprague, 1981; Roch and McCarter, 1984; Marr and others, 1995; lipid peroxidation: Woodward and others, 1995) and with exposure to trace elements (metallothioneins: Dixon and Sprague, 1981; Roch and

Table 6. Mean trace-element concentrations in fish, 1998.

[Means followed by the same letter (within a tissue) are not significantly different at $p = 0.05$; standard error of the mean is in parentheses]

Site (fig. 1)	Trace-element concentration, mean (µg/g dry weight)[1]				
	Arsenic	Cadmium	Copper	Lead	Zinc
			Gill		
UBR	2.7 (0.4)^{a}	0.79 (0.04)^{a}	5.6 (1.9)^{ab}	0.3 (0.9)^{a}	667 (162)^{a}
LBC	3.1 (0.5)^{a}	30.1 (0.2)^{b}	7.7 (0.1)^{b}	1.2 (0.1)^{b}	845 (148)^{abc}
LCC	2.8 (0.4)^{a}	71.4 (3.9)^{c}	21.5 (1.9)^{c}	1.3 (0.1)^{bc}	744 (103)^{abc}
BRRC	1.3 (0.4)^{b}	3.2 (1.6)^{a}	4.3 (0.1)^{a}	0.4 (0.2)^{a}	404 (89)^{b}
BRGG	1.3 (0.04)^{b}	25.7 (1.2)^{b}	5.6 (0.2)^{ab}	1.7 (0.2)^{c}	1,070 (179)^{c}
			Liver		
UBR	2.7 (0.3)^{a}	1.5 (0.2)^{a}	125 (22)^{a}	0.60 (0.01)^{a}	110 (3)
LBC	7.2 (1.0)^{b}	29.2 (2.3)^{b}	488 (83)^{b}	0.29 (0.03)^{b}	174 (3)
LCC	13.8 (0.5)^{c}	70.6 (4.9)^{c}	1,010 (100)^{c}	0.37 (0.03)^{b}	262 (13)
BRRC	2.0 (0.4)^{a}	7.1 (2.4)^{a}	319 (106)^{a}	0.09 (0.03)^{a}	126 (8)
BRGG	4.8 (0.4)^{d}	20.7 (2.7)^{d}	548 (74)^{d}	0.54 (0.08)^{c}	204 (14)
			Whole fish		
UBR	1.7 (0.6)^{ac}	0.15 (0.01)^{a}	5.2 (0.2)	<0.25	104 (4.4)
LBC	6.0 (1.7)^{ab}	2.7 (0.4)^{b}	13 (1.1)	2.1 (1.1)	318 (24)
LCC	8.0 (1.2)^{b}	4.9 (0.3)^{c}	22 (2.1)	1.2 (0.28)	353 (9.8)
BRRC	0.9 (0.1)^{c}	0.16 (0.02)^{a}	7.7 (0.8)	0.26 (0.01)	105 (8.1)
BRGG	3.5 (1.0)^{abc}	2.4 (0.3)^{b}	14.3 (0.7)	0.88 (0.05)	309 (28)

[1]Different letters designate a significant difference among sites at $p<0.05$ within a trace element for mainstem and tributaries.

McCarter, 1984; Marr and others, 1995; lipid peroxidation: Wills, 1985; Stern, 1985; DiGiulio and others, 1989).

Metallothioneins are proteins that bind metals, such as copper, cadmium, and zinc (Hogstrand and Haux, 1991; Stegeman and others, 1992). Because metallothionein synthesis and concentrations increase when fish are exposed to metals, the induction of these proteins indicates metal exposure in fish. The induction of metallothioneins in trout also has been associated with slowed growth of trout that maintain induced metallothionein concentrations (Marr and others, 1995). Therefore, elevated metallothionein concentrations also may indicate reduced fitness of trout.

Concentrations of metallothionein were greatest in the livers of rainbow trout from lower Cataract Creek (921 µg/g). The mean concentration of metallothionein in livers of fish from lower Cataract Creek was significantly greater than that in livers of fish from the reference site on the upper Boulder River (UBR, table 7). A trend toward greater metallothionein appeared in livers of fish from lower Basin Creek compared to the reference site, but this finding was not significant. The gills generally had small concentrations of metallothionein, and concentrations in gills measured at lower Basin Creek were less than those collected from lower Cataract Creek and Boulder River near Galena Gulch. Concentrations of metallothionein in livers or gills of fish from the mainstem sites (BRRC and BRRG) showed no significant differences.

Table 7. Metallothionein concentrations in gill and liver samples of resident rainbow trout, 1997.

[Values are reported as mean with 2 σ error in parentheses; means followed by the same letter (within a tissue) are not significantly different at $p = 0.05$; $n = 5$ for all sites except BRGG, where $n = 6$; metallothionein concentration in µg/g wet weight]

Site (fig. 1)	Metallothionein (µg/g)	
	Gill	Liver
Tributaries		
UBR – Reference	9.37[ab] (0.63)	31.2[a] (7.70)
LBC	7.61[a] (1.00)	597[ab] (289)
LCC	12.0[b] (1.18)	921[b] (216)
Boulder River		
BRGG – Reference	12.4[b] (0.52)	271[ab] (195)
BRGG	11.1[ab] (1.15)	293[ab] (60.5)

Lipid Peroxidation

Elevated concentrations of products of lipid peroxidation indicate cell death and tissue damage (Farag and others, 1995). Cell membranes are composed of polyunsaturated fatty-acid side chains and generally have a fluid composition. However, these side chains are targets of lipid peroxidation, a process that changes the structural integrity of the cell membrane and may ultimately result in cell death and tissue damage (Halliwell and Gutteridge, 1985; Wills, 1985). Trace elements that exist in more than one valence state, such as copper, may initiate lipid peroxidation (Wills, 1985). Trace elements may also initiate lipid peroxidation because they inhibit antioxidant enzymes such as glutathione peroxidase and transferase (Reddy and others, 1981). The amounts of products of lipid peroxidation measured with 340-nm excitation in the livers of rainbow trout from lower Cataract Creek were significant compared to amounts measured in livers of rainbow trout from upper Boulder River (table 8). No difference in the mean amount of products of lipid peroxidation was found in livers of fish from the two mainstem sites (BRRC and BRGG). There was no significant difference in lipid peroxidation in the gills of fish among tributary or mainstem sites. Products of lipid peroxidation also were measured with 360-nm excitation. Although a trend appeared of increased products of lipid peroxidation measured with 360-nm excitation, the difference was not significant (data not presented).

Exposure Pathways

Water

In stream water, concentrations of arsenic and lead were greatest at lower High Ore Creek (table 9, total recoverable of 64 µg/L and 54 µg/L respectively) during high flow. Copper concentrations also were greater at most sites during high flow, although the highest total-recoverable concentrations at any site occurred during low flow at Jack Creek (140 µg/L). Unlike arsenic and lead, the concentrations of cadmium and zinc were greater during low rather than high

Table 8. Lipid peroxidation of tissues sampled from resident rainbow trout, 1997.

[Values are reported as mean with 2 σ error SEM in parentheses; means followed by the same letter (within a tissue) are not significantly different at $p = 0.05$; $n = 5$ for all sites except site BRGG, where $n = 6$]

Site (fig. 1)	Relative intensity[1]	
	Gill	Liver
Tributaries		
UBR – Reference	73.1[a] (8.19)	114[a] (5.31)
LBC	66.4[a] (6.91)	115[a] (11.7)
LCC	73.8[a] (3.77)	141[b] (7.28)
Boulder River		
BRRC – Reference	79.2[a] (6.57)	125[ab] (11.9)
BRGG	73.1[a] (4.09)	127[ab] (4.63)

[1]Note: Lipid peroxidation is expressed as the fluorometric measurement (relative intensity) of a chloroform extract of tissue. The relative intensity was measured at 340-nm excitation and 435-nm emission when 0.05 µg/mL of quinine sulfate measured 322 with settings to measure gill and 136 with settings to measure liver (Farag and others, 2003). Different letters designate a significant difference among sites at $p<0.05$ within a trace element for mainstem and tributaries.

Table 9. Median trace-element concentrations in water, 1996–99.

[*n* = number of samples collected on different dates throughout the flow condition; Tot = total recoverable concentration; Filt = concentration in 0.45-µm filtrate; REF 1 = pooled value for LBR and UBR site and REF 2 = BRRC]

Site (fig. 1)		*n*	Streamflow (ft^3/s)	Hardness (mg/L $CaCO_3$)	Trace-element concentration, median (µg/L)									
					Arsenic		Cadmium		Copper		Lead		Zinc	
					Tot	Filt	Tot	Filt	Tot	Filt	Tot	Filt	Tot	Filt
High-flow conditions														
Tributaries														
	LBR	2	69-94	19	6.0	3.0	<1	<0.1	6.5	2.0	3.0	<1	<10	3.5
Ref 1	UBR	2	15-83	21-38	4.0	2.5	<1	<0.3	3	1.5	<1	<1	<10	1
	LHO	15	1.8-6.8	74-150	64	13	4.9	2.4	17	5.8	54	<1	177	139
	LCC	11	13-168	18-54	17	3.4	1.8	1.3	46	33	6.7	<1	1,290	678
	MCC	7	17-186	18-37	15	3.0	3.3	2.3	62	33	13	<1	322	231
	UCC	6	15-121	17-37	3.5	2.3	<1	<0.3	8.9	7.2	3.0	<1	58	43
	LBC	10	15-251	12-35	12	5.2	5.2	.5	14	10	4.7	4.7	93	66
	JC	6	4.4-35	19-38	32	3.0	3.5	3.2	59	32	9.6	<1	397	352
Mainstem														
Ref 2	BRRC	10	106-725	22-50	5.4	3.3	<1	<0.3	5.0	3.3	1.2	<1	11	3.4
	BRBC	2	94-436	24-47	7.0	4.4	<1	<0.3	9.2	7.2	1.9	<1	39	29
	BRCC	2	106-513	24-47	8.2	4.1	<1	.4	15	11	2.5	<1	66	94
	BRGG	11	175-1,050	19-48	12	4.0	<1	.3	23	12	8.5	<1	100	51
Low-flow conditions														
Tributaries														
	LBR	6	2.4-6.3	37-56	2.0	2.0	<1	<0.1	5.0	2.0	<1	<1	<10	2.0
REF 1	UBR	2	2.3-3.8	52-53	2.5	2.0	<1	<0.3	1.5	<1	<1	<1	<10	<1
	LHO	8	0.52-1.3	140-170	33	17	4.5	3.9	4.6	3.1	6.8	<1	1,970	1,800
	LCC	8	1.9-5.4	59-69	4.0	3.1	5.0	4.7	24	20	<1	<1	420	402
	MCC	5	3.6-4.6	48-57	3.5	2.0	9.4	8.9	82	53	2.0	<1	765	727
	UCC	4	2.8-5.0	43-52	2.7	2.4	<1	.3	4.6	4.5	<1	<1	64	60
	LBC	8	3.1-5.8	39-42	7.1	4.6	<1	.4	4.1	3.0	<1	<1	73	62
	JC	4	.86-1.2	44-51	18	1.9	12	11	140	69	4.1	<1	1,270	1,200
Mainstem														
REF 2	BRRC	9	8.6-25	54-61	3.0	2.5	<1	<0.3	1.4	1.6	<1	<1	<10	2.5
	BRBC	2	25-28	55-59	4.0	3.5	<1	<0.3	9.4	7.9	<1	<1	44	41
	BRCC	2	26-33	57-60	4.2	3.7	<1	.6	12	9.2	<1	<1	86	80
	BRGG	9	17-36	61-68	6.0	5.0	<1	.8	10	8.9	<1	<1	149	140

flow. Zinc concentrations were greatest at lower High Ore Creek during low flow (1,970 µg/L) (table 9). The greatest concentrations of cadmium were measured at Jack Creek (12 µg Cd/L) and middle Cataract Creek (9.4 µg Cd/L) during low flow. The pH ranged from 7.0 to 8.5 at all sites regardless of flow (Nimick and Cleasby, this volume).

Colloids

The presence of colloids in the water column is indicated most clearly by the high concentration of colloidal iron (table 10) and, to a lesser extent, aluminum (data not presented) at most sites including the reference sites. These data support the conclusion of Church, Unruh, and others (this volume) that, based on an analysis of suspended sediment collected during high flow in 1997, much of the sediment in watershed streams is iron oxyhydroxide colloidal material. This colloidal material has a large capacity for sorbing trace elements, and the degree of metal enrichment varies among sites.

The general pattern of partitioning of trace elements between dissolved (0.001 µm) and colloidal fractions in the water column depended primarily on the trace element and, to a lesser extent, on the proximity of the sampling site to a source of trace elements. Almost all iron and lead were present in the colloidal fraction, whereas cadmium and zinc were primarily dissolved. Large amounts of arsenic and copper also partitioned to the colloidal phase, but unlike lead, arsenic and copper also existed in the dissolved phase.

The spatial pattern of colloidal trace-element concentrations generally was the same as for trace-element concentrations in water and sediment in that the highest colloidal concentrations were directly downstream from inactive mines. Trace-element-rich acidic water draining from mines in the Boulder watershed study area is neutralized in mixing zones in streams, producing substantial loads of metal-rich colloids rich in trace elements. These colloids then can be transported long distances downstream (Kimball and others, this volume, Chapter D6). Substantial colloid loads occurred in the Bullion Mine tributary (BMT) and Jack Creek (JC) downstream from the Bullion mine, in Uncle Sam Gulch (USG) and Cataract Creek (MCC) downstream from the Crystal mine, and in High Ore Creek (UHO and LHO) downstream from the Comet mine (table 10). For the 12 main sampling sites, the highest concentrations of colloidal trace elements were at lower High Ore Creek (0.5 µg/L Cd, 8.2 µg/L Pb, and 322 µg/L Zn) and Jack Creek (24 µg/L As and 74 µg/L Cu). Concentrations at sites nearer inactive mines (BMT, USG, and UHO) were even higher, and often exceeded 1 mg/L for iron and zinc (table 10). Colloidal concentrations of arsenic, copper, lead, and zinc increased in the Boulder River in a step-wise downstream pattern as each of the three mining-affected tributaries entered the mainstem.

Table 10. Mean trace-element concentrations in colloids and ultrafiltrates during low-flow conditions, 1996–98.

[Dis = dissolved concentration in ultrafiltrate; Col = concentration in colloidal fraction; REF 1 = pooled value for LBR and UBR site; REF 2 = BBRC; *, ancillary sampling site near an inactive mine]

Site (fig. 1)		n	Trace-element concentration, mean (µg/L)											
			Arsenic		Cadmium		Copper		Iron		Lead		Zinc	
			Dis	Col	Dis	Col	Dis	Col	Dis	Col	Dis	Col	Dis	Col
Tributaries														
	LBR	2	<3	1.0	0.1	0.4	2.5	<3	<50	225	0.4	<1	<2	<10
REF 1	UBR	3	2.6	1.4	<0.1	<0.3	<1	1.2	<50	193	0.4	<1	<2	<10
	LHO	3	14	14	4.2	0.5	2.5	3.2	<50	197	0.5	8.2	1,750	322
	LCC	3	3.2	2.2	4.0	<0.3	16	15	<50	95	0.3	1.2	329	22
	MCC	4	<3	3.5	6.5	<0.3	27.5	38	<50	204	0.5	1.7	546	73
	UCC	3	<3	1.5	0.3	0.2	5.3	<1	<50	135	0.3	<1	56	5
	LBC	3	5.6	4.6	0.4	0.1	5.1	2.6	<50	107	0.1	1.8	54	11
	JC	3	<3	24	9.0	0.3	41	74	33	857	0.5	4.5	942	88
	BMT*	3	<1	27	45	1	469	87	748	1,940	2	13	5,000	270
	USG*	3	<1	6	43	1	141	256	<10	196	0.5	8	3,520	350
	UHO*	1	8	102	6	<0.3	1	9	<1	1,600	<1	44	4,390	710
Mainstem														
REF 2	BRRC	2	3.6	1.5	<0.1	0.4	2.5	<2	48	490	0.3	0.4	2	3
	BRBC	3	4.4	1.2	0.2	0.4	8.4	1.2	39	316	0.3	0.2	35	5
	BRCC	3	4.5	1.5	0.5	<0.3	10	2.8	<50	270	0.4	0.1	65	15
	BRGG	3	5.0	7.0	0.7	0.3	8.0	8.7	<50	283	0.5	0.6	112	41

Sediment

In streambed sediment, the concentrations of all trace elements except copper were highest at lower High Ore Creek (740 µg As/g, 14 µg Cd/g, 1,100 µg Pb/g, and 3,400 µg Zn/g) (table 11). The concentrations of arsenic, cadmium, and zinc in Cataract and Basin Creeks were 2 to 5 times less than concentrations in lower High Ore Creek but were still much higher than the concentrations at the reference site on the upper Boulder River (UBR). The concentrations of cadmium were similar in Cataract Creek (9.3 µg/g at MCC and 11 µg/g at LCC) compared to lower High Ore Creek. The highest copper concentrations were in Cataract Creek (450 µg/g at MCC, 440 µg/g at LCC) followed by Jack Creek (180 µg/g at JC) and High Ore Creek (140 µg/g at LHO).

In the Boulder River, trace-element concentrations in sediment generally were less than in the tributaries. However, concentrations of all trace elements, except cadmium at BRBC, were greater at the three downstream mainstem sites compared to the reference site (BRRC). For instance, arsenic concentrations were 99 µg/g at Boulder River near Galena Gulch, far higher than the 8.3 µg/g measured at Boulder River near Red Rock Creek upstream from the area of historical mining.

Biofilm

Trace-element concentrations in biofilm decreased at sites farthest downstream from historical mining areas (table 12). The greatest concentrations of cadmium, copper, and lead were in Jack Creek (all data presented as $\mu g/g \pm \sigma$; 70±5; 4,620±860; 885±84 respectively) followed by middle Cataract Creek (60±22; 1,940±850; 660±150 respectively), then lower High Ore Creek (41±3; 321±9; 1,100±30 respectively). The concentrations of these trace elements decreased substantially downstream in Basin Creek (LBC) but were still 18–23 times greater than the concentration for the combined reference (REF 1) used for the tributary sites. Concentrations of these trace elements in biofilm were significantly less at lower Cataract Creek compared to the middle Cataract Creek site. However, the downstream site in Cataract Creek (LCC) yielded elevated concentrations of trace elements compared to the combined reference. Biofilm from upper Cataract Creek (UCC) had concentrations of trace elements less than those of lower Cataract Creek but greater (though not significantly) than the combined reference. The concentrations of cadmium and lead but not copper were significantly elevated in biofilm from lower High Ore Creek compared to the combined reference.

Table 11. Leachable trace-element concentrations in composite streambed sediment, 1998.

[REF 1 = pooled value for LBR and UBR site and REF 2 = BRRC]

Site (fig. 1)		Arsenic (µg/g)	Cadmium (µg/g)	Copper (µg/g)	Lead (µg/g)	Zinc (µg/g)
Tributaries	LBR	20	<1	13	26	100
	UBR	13	<1	7.8	10	40
	REF 1	17	<1	10	18	70
	LHO	740	14	140	1,100	3,400
	LCC	580	11	440	390	1,300
	MCC	250	9.3	450	280	930
	UCC	96	3.0	110	220	440
	LBC	140	3.9	98	150	640
	JC	330	4.2	180	190	490
Mainstem	BRRC REF 2	8.3	<1	16	13	74
	BRBC	20	<1	38	27	180
	BRCC	55	3.2	110	80	430
	BRGG	99	2.8	84	99	490

Biofilm from lower High Ore Creek had the greatest concentrations of arsenic and zinc (all data presented as µg/g±σ, 3,300±400 and 18,100±1,700 respectively) followed by Jack Creek (2,600±170 and 6,210±170 respectively) and middle Cataract Creek (1,700±700 and 6,000±2,240 respectively). Concentrations of arsenic and zinc decreased farther downstream at lower Cataract Creek and lower Basin Creek but were still greater than 26 times the concentrations at the reference site.

Elevated concentrations of trace elements persisted in the mainstem of the Boulder River. The arsenic concentration in biofilm at Boulder River near Galena Gulch was 262 µg/g. The zinc concentrations at Boulder River near Galena Gulch were similar to the concentrations measured at lower Cataract Creek (3,200±250 versus 3,870±420), although the concentrations of arsenic in biofilm from the mainstem downstream from Cataract Creek (BRCC) were less than that from lower Cataract Creek (67±3 versus 731±67). The concentrations of trace elements in biofilm from the Boulder River downstream from Basin Creek and downstream from Cataract Creek also were elevated compared to concentrations at the reference site (BRRC, REF 2).

Benthic Macroinvertebrates

The concentrations of trace elements were generally less in benthic macroinvertebrates compared to the biofilm, but invertebrates from many of the test sites had concentrations greater than at the reference site (tables 12 and 13). This trend was apparent at sites throughout the watershed even in the absence of extensive statistical significance. Furthermore, some of the greatest concentrations of cadmium, copper, and lead were observed in the lower portion of Cataract Creek (all data presented as µg/g± σ, 59±5; 340±130; 34±16 respectively). In general, though concentrations of trace elements persisted in invertebrates from sites on the Boulder River, they were less than concentrations of invertebrates from the tributaries. One exception to this observation was lead; invertebrates from Boulder River near Galena Gulch had the greatest mean concentration of lead measured in the watershed. These results demonstrate that trace elements were being transported downstream and were transferred to the food chain.

Fish Tissues

As stated in a preceding section (see "Fish Biomass, Density, and Physiology"), mean concentrations of trace elements, especially arsenic, cadmium, and copper, were greatest in gill, liver, and whole fish from lower Cataract Creek (table 6). The concentrations of cadmium in the gill, liver, and whole fish from lower Cataract Creek were magnitudes greater than that found in the reference, upper Boulder River (90 times for gill, 47 times for liver, 33 times for whole fish). Likewise, the concentrations of copper in fish from lower Cataract Creek ranged from 4 to 8 times the concentrations in fish from the reference. Although concentrations of trace elements were less in fish from the mainstem, elevated arsenic, cadmium, and zinc were measured in fish as far downstream as Boulder River near Galena Gulch.

Table 12. Mean trace-element concentrations in biofilm, 1998.

[Standard error of the mean is in parentheses, and *n* = sample size; REF 1 = pooled value for LBR and UBR sites, REF 2 = BRRC]

Site (fig. 1)		n	Trace-element concentration, mean (µg/g dry weight)[1]				
			Arsenic	Cadmium	Copper	Lead	Zinc
Tributaries	LBR	4	17.7 (1.4)	1.0 (0.1)	25 (4)	12 (3)	99 (15)
	UBR	4	17.8 (2.0)	0.7 (0.1)	15 (2)	12 (1)	62 (8)
	REF 1	8	17.7 (1.1)^{a}	0.8 (0.1)^{a}	20 (3)^{a}	12 (1)^{a}	81 (11)^{a}
	LHO	4	3,300 (400)^{d}	41.2 (2.7)^{bcd}	321 (9)^{ab*}	1,100 (30)^{e}	18,100 (1,700)^{c}
	LCC	4	731 (67)^{ab*}	30.6 (4.5)^{abcd*}	853 (96)^{ab*}	389 (46)^{bc}	3,870 (420)^{ab*}
	MCC	4	1,700 (700)^{bc}	60 (22)^{cd}	1,940 (850)^{b}	660 (150)^{cd}	6,000 (2,240)^{b}
	UCC	4	130 (13)^{a}	23 (12)^{abc*}	260 (56)^{ab*}	256 (89)^{ab*}	2,360 (660)^{ab*}
	LBC	4	475 (77)^{ab*}	16.6 (2.7)^{ab*}	369 (62)^{ab*}	281 (29)^{ab*}	2,320 (350)^{ab*}
	JC	4	2,600 (170)^{cd}	70.3 (4.5)^{d}	4,620 (860)^{c}	885 (84)^{de}	6,210 (170)^{b}
Mainstem	REF 2	4	15.3 (1.2)^{a}	0.54 (0.06)^{a}	23 (2)^{a}	12.2 (0.9)^{a}	141 (34)^{a}
	BRBC	4	37.6 (4.1)^{a*}	3.3 (0.5)^{a*}	89 (14)^{b}	32.3 (2.3)^{ab*}	619 (95)^{ab*}
	BRCC	4	67.1 (2.9)^{b}	10.5 (2.4)^{b}	170 (18)^{c}	50.0 (7.5)^{b}	1,240 (180)^{b}
	BRGG	4	262 (12)^{c}	17.4 (1.5)^{c}	270 (16)^{d}	278 (9)^{c}	3,200 (250)^{c}

[1]Different letters designate a significant difference at $p<0.05$ within a trace element for mainstem and tributary sites; * indicates a significant difference at $p<0.05$ between specified site and reference *only*.

Table 13. Mean trace-element concentrations in invertebrates, 1998.

[Standard error of the mean (2 σ) is in parentheses; *n* = sample size; REF 1 = pooled value for LBR and UBR sites; and REF 2 = BRRC]

Site (fig. 1)		n	Trace-element concentration, mean (µg/g dry weight)[1]				
			Arsenic	Cadmium	Copper	Lead	Zinc
Tributaries	LBR	4	2.3 (0.3)	3.7 (0.4)**	38 (1)**	1.2 (0.2)	340 (27)**
	UBR	4	3.7 (1.0)	0.9 (0.2)**	30 (1)**	1.0 (0.3)	235 (18)**
	REF 1	8	3.0 (0.5)^{a}	2.3 (0.6)^{a}	34 (2)^{a}	1.2 (0.2)^{a}	288 (25)^{a}
	LHO	4	60 (11)^{bc}	16.7 (0.8)^{b}	74 (4)^{ab*}	36 (6)^{b}	3,090 (75)^{d}
	LCC	4	63 (27)^{bc}	59.3 (5.4)^{d}	340 (130)^{c}	34 (16)^{b}	2,410 (420)^{cd}
	MCC	4	80.1 (7.3)^{c}	35.0 (5.4)^{c}	268 (35)^{bc}	24.1 (2.0)^{ab*}	2,070 (290)^{bc}
	UCC	4	7.5 (2.9)^{ab}	15.9 (3.2)^{b}	77 (4)^{ab*}	11.2 (4.4)^{ab*}	1,050 (200)^{a*}
	LBC	4	21.5 (1.4)^{abc*}	18.1 (1.3)^{b}	92 (6)^{abc*}	12.4 (0.7)^{ab*}	929 (80)^{a*}
	JC	4	77 (29)^{c}	10.0 (2.8)^{ab*}	319 (89)^{bc}	12.6 (9.9)^{ab*}	580 (144)^{a}
Mainstem	REF 2	4	4.6 (0.3)^{a}	1.1 (0.3)^{a}	29 (1)^{a}	1.6 (0.1)^{a}	237 (11)^{a}
	BRBC	4	5.3 (0.3)^{a}	10.6 (5.7)^{ab*}	85 (5)^{b}	3.3 (0.4)^{a*}	584 (81)^{b}
	BRCC	4	13.1 (2.0)^{ab*}	16.2 (2.1)^{b}	111 (7)^{b}	8.5 (1.5)^{a*}	977 (127)^{c}
	BRGG	4	26.7 (8.8)^{b}	11.7 (3.0)^{ab*}	98 (16)^{b}	38 (18)^{a*}	669 (66)^{bc}

[1]Different letters designate a significant difference at $p<0.05$ within a trace element for mainstem and tributary sites.

* indicates a significant difference at $p<0.05$ between specified site and reference *only*.

**indicates a significant difference at $p<0.05$ between pooled reference sites.

Relationships among Components

Significant correlations were observed among the metal concentrations measured in the various abiotic and biotic components sampled in the Boulder River watershed. The concentrations of all trace elements, except lead, measured in low-flow total, filtered, or dissolved water correlated with concentrations in biological components (table 14). Significant correlations between water and biology were more frequent for cadmium, copper, and zinc than for arsenic. Copper and zinc measured in total, filtered, or dissolved water correlated with colloids, biofilm, and macroinvertebrates. However, arsenic in total water rather than filtered or dissolved correlated more significantly with colloids and biofilm. Because $r \leq 0.884$ for biofilm and total arsenic, the amount of variation explained by the corresponding r^2 values (not listed) is less for arsenic than was generally observed for cadmium, copper, and zinc. No significant correlations were observed between arsenic in water and arsenic in fish, although cadmium, copper, and zinc in water were significantly correlated to fish tissues. Copper in the water was directly correlated to gill, liver, and whole fish; cadmium was directly correlated to gill and liver; and zinc was directly correlated to liver. Therefore, cadmium, copper, and zinc accumulated in various levels of the food chain and directly in fish from the water column.

Some significant correlations were found between trace elements in water and sediment, but *r* values ranged from 0.537 to 0.877 and correspond to generally smaller r^2 values. These small r^2 values indicate that these correlations explain less variation than was generally observed between trace elements in water and biology. Some of the strongest correlations between trace elements in water and sediment were observed for zinc and cadmium in low-flow dissolved water ($r = 0.877$ and 0.857, respectively).

Concentrations in sediment correlated directly with biology for all trace elements. Trace elements in sediment correlated with biofilm and (or) macroinvertebrates for all trace elements, and the *r* ranged from 0.667 to 0.952. The strongest correlations were for zinc in biofilm ($r = 0.952$) and macroinvertebrates ($r = 0.899$). Additionally, cadmium and copper concentrations in sediment were correlated directly to gill, liver, and whole fish ($r \geq 0.922$). Arsenic concentrations in sediment were correlated directly to concentrations in liver and whole fish ($r = 0.978$ and $r = 0.882$, respectively). Zinc concentrations in sediment were correlated to zinc concentrations in liver ($r = 0.953$). These results indicate that sediment, in addition to water, appears to provide a source of trace elements to aquatic resources in the Boulder River watershed.

Concentrations of trace elements in colloids were correlated to concentrations in biofilm for all trace elements, except cadmium, at $p \geq 0.01$ with $r \geq 0.900$ for copper, lead, and zinc and $r = 0.819$ for arsenic. The corresponding r^2 values for most of the correlations indicate that much of the variation in the data is explained. Concentrations of arsenic, copper, and zinc in colloids also were correlated to macroinvertebrates but at $p \geq 0.05$ rather than $p \geq 0.01$, and the corresponding *r* values were ≤ 0.760. Colloids also correlated directly with liver and whole fish for copper and with whole fish for lead.

Biofilm and macroinvertebrates were correlated to one another for arsenic, copper, lead, and zinc. However, all r were <0.828 and indicated small corresponding values for r^2; as a result, small amounts of variation were explained. Biofilm

Table 14. Correlation coefficients for trace-element concentrations measured in water, sediment, colloids, biofilm, benthic macroinvertebrates, fish gill, fish liver, and whole fish, 1996–99.

[Concentrations in water: Total = total recoverable concentration, Filt = concentration in 0.45-µm filtrate, Dis = dissolved concentration in ultrafiltrate, LF = low flow; Inverts = benthic macroinvertebrates; probability values in parentheses; n_1 = number of water, sediment, colloid, biofilm, and invertebrate samples included in correlations with fish tissues; n_2 = number of gill, liver, or whole fish concentrations used in the same correlations. Bold type, significance at $p<0.01$; underline at $p<0.05$; standard type designates significance at $p<0.10$. Correlations not significant above $p<0.10$ not presented]

	n	Total LF	Filt LF	Dis	Sediment	Colloids	Biofilm	n_1	n_2	Gill	Liver	Whole fish
Arsenic												
Total LF	12							5	5	--	--	--
Filt LF	12	**0.852** (0.0004)						5	5	--	--	--
Dis	12	0.764 (0.0273)	**0.976** (<0.0001)					5	5	--	--	--
Sediment	12	0.754 (0.0047)	**0.677** (0.0156)	--				5	5	--	**0.978** (0.004)	0.882 (0.048)
Colloids	12	**0.771** (0.0033)	--	--	0.522 (0.0816)			5	5	--	--	--
Biofilm	12	**0.884** (0.0001)	0.619 (0.0318)	--	**0.809** (0.0962)	**0.819** (0.0011)		5	5	--	**0.971** (0.006)	**0.994** (0.001)
Inverts	12	0.522 (0.0817)	--	--	**0.769** (0.0035)	0.647 (0.0231)	**0.828** (0.0009)	5	5	--	**0.965** (0.008)	0.898 (0.039)
Gill	5										--	--
Liver	5									--		**0.960** (0.0090)
Whole fish	5									--	--	
Cadmium												
Total LF	4							1	5	0.888 (0.044)	0.916 (0.029)	--
Filt LF	9	**0.998** (<0.0001)						3	5	0.928 (0.023)	0.943 (0.016)	0.855 (0.065)
Dis	10	**0.986** (<0.0001)	**0.984** (<0.0001)					3	5	0.941 (0.017)	0.954 (0.012)	0.873 (0.053)
Sediment	8	0.537 (0.0717)	0.771 (0.0254)	0.857 (0.0032)				3	5	0.990 (0.001)	**0.996** (0.001)	0.952 (0.013)
Colloids	8	--	--	--	--			3	5	--	--	--
Biofilm	12	**0.943** (<0.0001)	**0.960** (<0.0001)	**0.932** (0.0003)	**0.852** (0.0072)	--	--	5	5	**0.971** (0.006)	0.942 (0.017)	**0.996** (0.001)
Inverts	12	--	0.733 (0.0246)	0.656 (0.0456)	0.687 (0.0596)	--	--	5	5	**0.983** (0.003)	**0.993** (0.001)	0.938 (0.019)
Gill	5										**0.994** (0.001)	**0.985** (0.002)
Liver	5									--		**0.964** (0.008)
Whole fish	5									--	--	
Copper												
Total LF	12							5	5	0.929 (0.023)	0.952 (0.013)	0.940 (0.018)
Filt LF	12	**0.986** (<0.0001)						5	5	0.908 (0.033)	0.957 (0.011)	0.943 (0.016)
Dis	11	**0.975** (<0.0001)	**0.987** (<0.0001)					4	5	0.897 (0.039)	**0.990** (0.001)	**0.984** (0.003)

Table 14. Correlation coefficients for trace-element concentrations measured in water, sediment, colloids, biofilm, benthic macroinvertebrates, fish gill, fish liver, and whole fish, 1996–99.—Continued

	n	Total	Filt LF	Dis	Sediment	Colloids	Biofilm	n_1	n_2	Gill	Liver	Whole fish
Sediment	12	--	0.611 (0.0350)	0.605 (0.0350)				5	5	**0.989** (0.002)	0.946 (0.015)	0.922 (0.026)
Colloids	9	**0.994** (<0.0001)	**0.974** (<0.0001)	**0.972** (<0.0001)	--			4	5	0.853 (0.066)	0.931 (0.021)	0.932 (0.021)
Biofilm	12	**0.983** (<0.0001)	**0.949** (<0.0001)	**0.951** (<0.0001)	--	**0.992** (<0.0001)		5	5	0.942 (0.017)	**0.966** (0.008)	0.968 (0.007)
Inverts	12	**0.770** (0.0034)	**0.830** (0.0008)	**0.867** (0.0003)	**0.859** (0.0003)	0.760 (0.0174)	**0.761** (0.0041)	5	5	**0.981** (0.003)	0.953 (0.012)	0.940 (0.020)
Gill	5										0.888 (0.045)	0.857 (0.063)
Liver	5									--		0.991 (0.001)
Whole fish	5									--	--	
Lead												
Total LF	3							0	5			
Filt LF	0							0	5			
Dis	12	--						0	5			
Sediment	12	--		--				5	5	--	--	--
Colloids	9	--		0.591 (0.0941)	**0.875** (0.0020)			4	5	--	--	0.951 (0.013)
Biofilm	12	--		--	**0.808** (0.0015)	**0.920** (0.0004)		5	5	0.889 (0.044)	--	--
Inverts	12	--		--	0.667 (0.0178)	--	0.640 (0.0249)	5	5	0.921 (0.026)	--	--
Gill	5										--	--
Liver	5									--		--
Whole fish	5									--	--	
Zinc												
Total LF	9							3	5	--	0.948 (0.014)	--
Filt LF	12	**1.000** (<0.0001)						5	5	--	0.946 (0.015)	--
Dis	10	**0.995** (<0.0001)	**0.922** (<0.0001)					4	5	--	0.945 (0.015)	--
Sediment	12	**0.835** (0.0007)	**0.827** (0.0009)	**0.877** (0.0009)				5	5	--	0.953 (0.012)	0.876 (0.051)
Colloids	10	**0.928** (<0.0001)	**0.918** (0.0002)	**0.957** (<0.0001)	**0.930** (<0.0001)		--	4	5	0.847 (0.070)	--	--
Biofilm	12	**0.946** (<0.0001)	**0.941** (<0.0001)	**0.969** (<0.0001)	**0.952** (<0.0001)	**0.983** (<0.0001)		5	5	--	**0.967** (0.007)	**0.970** (0.006)
Inverts	12	0.694 (0.0124)	0.691 (0.0128)	0.699 (0.0246)	**0.899** (<0.0001)	0.709 (0.0218)	**0.804** (0.0016)	5	5	--	0.911 (0.031)	--
Gill	5										--	--
Liver	5									--		0.904 (0.035)
Whole fish	5									--	--	

and invertebrates were directly correlated with gill, liver, and whole fish for cadmium, and copper; liver and whole fish for arsenic; liver for zinc; and gill for lead. Concentrations of all trace elements, except lead, in liver correlated with those measured in whole fish. Concentrations in gill were also correlated to liver concentrations for cadmium. However, concentrations between gill and whole fish were not correlated for any of the metals measured.

Discussion

This study provides evidence that populations of fish are unlikely to survive in close proximity to some inactive mine sites in Basin, Cataract, and High Ore Creeks. Limited survival in some stream reaches of these basins appears to be related to elevated concentrations of trace elements present in the water column. Furthermore, the health and biomass/density of resident fish in lower Cataract Creek may be compromised as a result of exposure routes that include water, sediment, and diet. In addition, one route in the dietary pathway may begin with colloids suspended in the water column.

Aquatic Health

The multiple tools we used to investigate the effects of historical mining in the Boulder River watershed allow us to define where trace elements affect the aquatic health of the watershed. In the most extreme cases, where concentrations of trace elements were greatest in the water column, population-level effects existed and fish survival was poor. The relation between trace-element concentrations and mortality was consistent, and greater trace-element concentrations were associated with greater and more rapid mortality.

The association between fish mortality and the elevated concentrations of trace elements in the water provides evidence that trace elements caused the observed mortalities. Water-quality criteria have been established by the U.S. Environmental Protection Agency (1999, 2001) for the chronic and acute protection of aquatic life. Although the water-quality criteria are hardness dependent, we can calculate standards for the average hardness measured at various sites in this watershed. The acute aquatic-life standards are 12 µg Cu/L and 82 µg Zn/L in Basin and Cataract Creeks at a hardness of 66 mg/L. The toxicity of some metals is alleviated by elevated hardness in the water. (See Finger, Farag, and others, this volume, Chapter C, for more complete discussion.) Therefore, the greater hardness values at lower High Ore Creek (LHO, 140 mg/L) may explain why survival was slightly better in this stream.

The hypertrophy noted in gills of fish in this study is consistent with the edema noted previously in the secondary lamellae of rainbow trout exposed to 40 mg Zn/L for 3 hr (Skidmore and Tovell, 1972). Skidmore and Tovell (1972) also observed severe curling of the secondary lamellae, a finding not unlike the "twisting" that was noted in the gills of fish collected from middle Cataract Creek (MCC), where concentrations of zinc ranged from 400 to 700 µg/L. Cutthroat trout near death experienced excess mucus production in this study. Handy and Eddy (1991) suggested that excess mucus production is part of a "general stress response" in rainbow trout. Therefore, ionoregulatory upset (though we could not measure this upset directly) was the likely cause of hypertrophy (swelling), degeneration (dying), and necrosis (death) of epithelial cells in the gills. And, mucus production occurred simultaneously as a general response to stress.

The concentrations of cadmium, copper, and zinc in water at lower Cataract Creek are near the concentrations reported at middle Cataract Creek site, where mortality was observed during in-place experiments. Therefore, resident fish in lower Cataract Creek may have acclimated to the elevated concentrations of trace elements. Simultaneously, a metabolic cost of acclimation may be expressed at lower Cataract Creek as acclimation coincides with a decreased mass (though not decreased growth) of trout in lower Cataract Creek.

Metallothioneins are proteins that bind trace elements such as copper, cadmium, and zinc and may play a role in the acclimation of fish to trace elements (Stegeman and others, 1992). Marr and others (1995) demonstrated that a physiological cost of acclimation exists for brown trout in the Clark Fork River, Mont., where trout acclimated to trace elements in the river had elevated concentrations of metallothionein in their livers and grew less than trout not acclimated to the trace elements. Furthermore, Dixon and Sprague (1981) concluded that decreased growth was a result of the metabolic costs associated with acclimation to copper in the laboratory. Trout from lower Cataract Creek had elevated metallothionein in their livers. Similar to Marr and others (1995), metallothionein was greatest in the livers of fish that also had the greatest concentrations of trace elements in the liver.

Further evidence of the compromised health of resident fish in lower Cataract Creek was the greater amounts of products of lipid peroxidation in the livers. Peroxidation of fatty-acid side chains in cell membranes can change the structural integrity of cell membranes and may lead to cell death and tissue damage (Halliwell and Gutteridge, 1985; Wills, 1985). These findings imply that the livers of trout in lower Cataract Creek were compromised and this state was associated with elevated concentrations of trace elements in the liver. The concentrations of arsenic, copper, cadmium, lead, and zinc in livers of trout from lower Cataract Creek also were elevated above the concentrations in the livers of fish from the reference site (UBR). In fact, the >1,000 µg Cu/g in the livers of fish from lower Cataract Creek was much greater than the upper limit of an effect concentration of 480 µg Cu/g suggested by Farag and others (1995) for the Clark Fork River, Mont.

The extent of the reduced fish biomass and density at lower Cataract Creek cannot be explained by habitat differences. The mass of trout per 1,000 ft in lower Cataract Creek was only 28 percent of the mass calculated for the reference

site (UBR). This biomass difference between lower Cataract Creek and the reference site was much greater than the difference in weighted usable area. For all three lifestages (fry, juvenile, and adult), lower Cataract Creek had an average of 91 and 78 percent of the weighted usable area that the reference site had for brook and rainbow trout, respectively. That habitat differences are sufficient to explain the reduced biomass/density at lower Cataract Creek is thus unlikely.

We observed decreases in the density and mass per 1,000 ft at lower Cataract Creek but did not observe differences among sites in the lengths-at-age. However, the lower density of trout at lower Cataract Creek may have masked the growth-suppressing effects of trace elements. A situation of less competition for resources may result when fish are present in lower densities. Jenkins and others (1999) found that growth of individual brown trout increased as a result of lower densities. During electrofishing activities on Cataract Creek, we only collected fish from what we observed to be the most energy-efficient feeding locations, which may have allowed for good growth (Bachman, 1984).

We also documented elevated concentrations of arsenic, cadmium, copper, lead, and zinc in the tissues of trout from lower Basin Creek (LBC) and Boulder River at Galena Gulch (BRGG). Lowe and others (1985) and Schmitt and Brumbaugh (1990) reported the 85th percentile (values for which 85 percent of samples are below) of 1.1 µg As/g, 0.33 µg Cd/g, 5.0 µg Cu/g, 1.31 µg Pb/g, and 201 µg Zn/g of whole fish collected from more than 100 stations across the United States (80 percent moisture was assumed to calculate µg/g dry weight). The mean concentrations of trace elements in whole fish collected from lower Cataract Creek, lower Basin Creek, and Boulder River near Galena Gulch exceed these 85th percentiles. Therefore, cadmium was >121, >60, and >60 times, respectively, than the 85th percentiles for lower Cataract Creek, lower Basin Creek, and Boulder River near Galena Gulch, respectively. Also, the amount of arsenic in whole fish from lower Cataract Creek, lower Basin Creek, and Boulder River near Galena Gulch was 8, 6, and >3 times, respectively, greater than the 85th percentiles.

Although the concentrations of trace elements in fish from lower Basin Creek and Boulder River near Galena Gulch were greater than in fish sampled from across the country (Lowe and others, 1985; Schmitt and Brumbaugh, 1990), the concentrations were not as great as those noted in lower Cataract Creek. Moreover, we did not observe significant changes in mass of trout per acre, metallothionein, or lipid peroxidation at lower Basin Creek or Boulder River near Galena Gulch (tables 3, 7, and 8). Therefore, the impacts of trace elements at these two sites were less than the impacts at lower Cataract Creek. This study provides a baseline of data for future monitoring. Monitoring plans that include lower Basin Creek and Boulder River near Galena Gulch, as remediation proceeds in Basin and High Ore Creeks, could document improved conditions or else changes caused by inadvertent releases of trace elements downstream when the tailings are disturbed.

The target organ of arsenic toxicity is the skin (Goyer, 1986), and arsenic is elevated in sediment, invertebrates, and fish at Boulder River near Galena Gulch (tables 5, 10, and 11). The dark coloration and the increased accumulation of melanocytes observed in the skin of fish held at lower High Ore Creek (located upstream of BRGG) during the onsite 96-hr survival experiments may have been caused by the elevated arsenic present at this site. Obvious changes in coloration were observed during the necropsy evaluations, but histological evaluations would be necessary to observe more subtle changes such as increased numbers of melanocytes. Additionally, color changes during necropsies may not always be observed because melanocyte regulation and control are lost immediately at death. For these reasons, we suggest that histological analyses be added to future assessments of aquatic health in an effort to document any tissue pathology more completely.

Exposure Pathways

Another goal of this study was to characterize the pathway and partitioning of trace elements into water, sediment, biofilm, benthic macroinvertebrates, and fish. This pathway documents the routes of trace-element exposure to fish that appear to have caused the impaired health status that we observed. Not only were trace elements elevated in all three of the tributaries of concern (Basin, Cataract, and High Ore Creeks), but also, trace elements accumulated in all components and accumulated to the greatest extent at sites nearest inactive mines. Furthermore, the pathway has resulted in concentrations of trace elements in water and sediment that may adversely affect the aquatic health in the Boulder River watershed.

Median concentrations of cadmium, copper, and zinc in stream water at most sites exceeded acute and chronic aquatic-life standards (U.S. Environmental Protection Agency, 1999, 2001). In the Boulder River watershed, hardness generally was < 50 mg $CaCO_3$ /L at all sites except lower High Ore Creek. At 50 mg/L hardness, a conservative estimate for the Boulder River watershed, the standards are (acute/chronic) 1.0/0.15 µg Cd/L, 7.0/5.0 µg Cu/L, and 66/65 µg Zn/L. These general guidelines suggest that the water quality of most of the tributary sites and even some of the mainstem sites (zinc at BRCC and BRGG) was sufficiently degraded to cause detrimental effects to aquatic life.

As was observed in the water column, cadmium, copper, and zinc were elevated in sediment throughout the Boulder River watershed. Additionally, arsenic and lead persisted in the sediment though concentrations of these trace elements generally were not elevated in the filtered fraction of the water column. Although sediment-quality criteria have not been established, several researchers have suggested concentrations to be used as sediment-quality guidelines. MacDonald and others (2000) determined that guidelines of 33 µg As/g, 4.98 µg Cd/g, 149 µg Cu/g, 128 µg Pb/g, and 459 µg Zn/g

would protect benthic macroinvertebrates from toxicity of these trace elements. These consensus-based guidelines for freshwater sediment correctly predicted no toxicity for invertebrates during the majority of laboratory investigations (correct prediction 74 percent for As, 80 percent for cadmium, 82 percent Cu, lead, and zinc). In the Boulder River watershed, sediment from all tributary sites exceeded the consensus-based guidelines for arsenic and lead, and the consensus-based guideline for arsenic was exceeded on the mainstem as far downstream as Boulder River near Galena Gulch. All tributary sites with the exception of upper Cataract Creek exceeded the consensus-based guideline for zinc. And several of the tributary sites exceeded the consensus-based guidelines for cadmium and copper. Therefore, this study suggests that the pathway of trace elements in the Boulder River watershed would lead to invertebrate toxicity in the watershed. This finding that invertebrate toxicity may be present in the Boulder River watershed is supported further by Boyle and Gustina (2000). These researchers defined the invertebrate community structure at some of the same sites investigated during this study and observed a depleted number of Ephemeroptera-Plecoptera-Tricoptera (EPT) taxa in High Ore Creek, lower Cataract Creek, and Jack Creek.

Colloids and biofilm appear to play a critical role in the pathway of trace elements to the food chain. Colloidal iron oxyhydroxides are formed immediately downstream of mine drainage mixing zones and are involved in the downstream transport of copper, lead, and zinc (Schemel and others, 2000). The association of colloids and trace elements is dynamic, and the trace elements may adsorb or desorb frequently as pH changes in mixing zones during transport. Therefore, the formation of iron colloids may play an important role in the transport of trace elements downstream and in the transfer of trace elements to biofilm.

During transport downstream, colloids commonly are trapped by biofilm on rock surfaces. Newman and McIntosh (1989) questioned the bioavailability of trace elements associated with iron oxyhydroxides. However, we suggest that the transfer of trace elements associated with iron colloids to biological components of biofilm is an important pathway where trace elements associated with abiotic components are first presented to biotic components. Significant accumulations may occur if only small portions of these trace elements are bioavailable. The significant correlations we observed between concentrations of arsenic, copper, lead, and zinc in colloids and biofilm support the hypothesis that colloids transport trace elements, at least in part, to biofilm. And, we have documented that arsenic, in addition to copper, lead, and zinc, as documented by Schemel and others (2000), likely is transported downstream by colloids. Furthermore, trace elements in biofilm are associated with both the abiotic and biotic components present in biofilm (Newman and others, 1983, 1985). This association suggests that biofilm is a critical link in the movement of trace elements directly into the food chain.

Biofilm also may accumulate trace elements by means other than the exposure received from colloids. This appears especially evident for cadmium and zinc. The concentrations of these trace elements were greater in filtered water in comparison to concentrations in colloids. We observed strong correlations between dissolved metal in water and biofilm for cadmium but not between colloids and biofilm. This suggests that water may be the primary source of the cadmium in biofilm. Dissolved zinc concentrations were greater than zinc concentrations in colloids, and the correlations were strong among water, colloids, sediment, and biofilm for zinc. This suggests that biofilm may receive zinc from water, colloids, and sediment.

Large concentrations of trace elements were observed in biofilm throughout the Boulder River watershed. In fact, arsenic and copper concentrations were greater in the Boulder River watershed than in the Coeur d'Alene River watershed in Idaho (Farag and others, 1998). The largest arsenic concentration in biofilm from the Coeur d'Alene River watershed was 155 µg/g at Cataldo, just downstream of the boundary for a Natural Resource Damage Assessment, while arsenic concentrations of 3,300 µg/g and 2,600 µg/g were found at High Ore Creek and Jack Creek, respectively. Zinc and cadmium concentrations were similar between some sites in the Coeur d'Alene and Boulder River watersheds. For example, there was slightly more zinc in the biofilm collected from High Ore Creek (18,100 µg/g) than was observed at Pinehurst (11,600 µg/g), a site within the boundary for the Natural Resource Damage Assessment of the Coeur d'Alene River watershed. Also, cadmium concentrations were similar at Jack Creek (70 µg/L) and at Nine Mile, a site defined as a significant source of trace elements for the Coeur d'Alene River watershed. We note that concentrations of lead found in the Coeur d'Alene River watershed are still among the greatest documented. The concentrations of lead in biofilm from many sites in the Boulder River watershed were higher than concentrations at the reference site (for example, 1,100 µg/g at High Ore compared to 12.1 µg/g at the reference site), but lead concentrations in biofilm from the Coeur d'Alene River watershed were magnitudes greater (for example, 27,200 µg/g at Nine Mile).

Not only were concentrations of trace elements in invertebrates elevated throughout the Boulder River watershed when they were compared to reference concentrations, but they were also elevated compared to composite invertebrate samples collected from other sites in the West where historical mining activities have occurred. In fact, the concentrations of arsenic, cadmium, copper, lead, and zinc in invertebrates from lower Cataract Creek (63, 59, 340, 34, and 2,410 µg/g, respectively) were greater than the concentrations in invertebrates from the Clark Fork River watershed (19, 2.3, 174, 15, and 648, respectively) that were associated with reduced survival, growth, and health of cutthroat trout fed diets composed of these invertebrates from the Clark Fork River watershed (Farag and others, 1994; Woodward and others, 1995).

Silver Bow Creek is a tributary of the Clark Fork River in western Montana. Historically, mine tailings were deposited along Silver Bow Creek, and some of the greatest

concentrations of trace elements in invertebrates in the Clark Fork River watershed were recorded in this stream. Arsenic concentrations in invertebrates from Jack Creek (77 µg/g) were 2 times the concentrations measured in invertebrates from Silver Bow Creek (34 µg/g before remediation of the area). And, zinc concentrations in invertebrates at lower High Ore Creek and lower Cataract Creek (3,090 and 2,410 µg/g, respectively) were greater than the amount of zinc measured in invertebrates from Silver Bow Creek (1,660 µg/g; Poulton and others, 1995). However, copper concentrations at Silver Bow Creek were considerably greater (1,380 µg/g) than those observed in invertebrates from the Boulder River watershed (for example, 340 µg/g, LCC).

As we noted in the case of biofilm, the concentrations of some trace elements in macroinvertebrates from the Boulder River watershed exceeded the concentrations in the Coeur d'Alene River watershed. Concentrations of arsenic and copper in invertebrates from Jack Creek (77 and 319 µg/g, respectively) were greater than in invertebrates collected from the Coeur d'Alene River watershed near Pinehurst (42 and 34 µg/g, respectively). However, the mean concentration of lead in invertebrates from the Coeur d'Alene River watershed at Cataldo was 292 µg/g, and as was noted with biofilm, this concentration of lead is magnitudes greater than those measured in invertebrates collected in the Boulder River watershed. Some of the largest concentrations of lead in aquatic life in the intermountain western United States continue to be documented in the Coeur d'Alene River watershed.

The pattern of accumulation in the components measured during this study differed from patterns previously observed. During a pathway investigation of the Coeur d'Alene River watershed, Farag and others (1998) found that the pattern of trace-element concentrations (from greatest to least) to be as follows: biofilm and sediment > macroinvertebrates > whole fish. However, during this investigation of the Boulder River watershed, the order of concentrations was biofilm > macroinvertebrates ≥ sediment > fish tissues > water and colloids. In fact, the concentrations of trace elements in biofilm during this study were often greater than the concentrations in sediment. This could result from the entrapment of colloid-bound trace elements by the biofilm, and this entrapment may tend to integrate the water-column concentrations over time.

The final goal of this study was to define the influence of water, colloids, and sediment in the transfer of trace elements to aquatic life. A clear interdependency among the components measured during this study exists, and all components that were measured appear to be important in the movement of trace elements up the food chain. The numerous significant correlations of trace-element concentrations among the various components support this interpretation. However, the primary pathway varied with the trace element. For example, copper, cadmium, and zinc appear to have moved directly to biota (biofilm, invertebrates, and (or) fish tissues) from water and sediment. In fact, not only did trace-element concentrations in biofilm increase with concentrations in water and sediment, but concentrations of trace elements in fish tissues also increased directly with concentrations in water and sediment. Therefore, concentrations of these trace elements appear to have increased in fish tissues as a result of direct exposure from water and sediment contact and indirect exposure through the food chain. The pathway of arsenic was slightly different, because, although arsenic accumulated in colloids and biofilm directly from water, arsenic did not accumulate in fish tissues directly from the water. The movement of lead into biological components appeared to be the result of a pathway that began with sediment because there were no correlations for lead between water and the other components.

Correlations between water and sediment were less significant than expected; two possible explanations for this observation arise. First, colloids present in the water and on sediment particles may affect the concentrations and diminish the strength of correlations. Iron colloids also are likely to be present in biofilm, and concentrations of most trace elements in biofilm were correlated with water and (or) sediment. If colloids made up a significant portion of the biofilm, these correlations of water and sediment with biofilm may have resulted in part from the significant colloid presence. A second possibility is the spatial aspect of the process by which trace elements are transferred from the water column to sediment. The process occurs as colloids form in mixing zones and then trace elements react with the colloids; this all occurs during transport downstream. Thus, a sample at a single site may not reflect the whole process, and correlations may not be good. Where a sequence of samples was collected in Uncle Sam Gulch during a metal-loading study (Kimball and others, this volume), the process was evident, but any single sample would not have indicated the process.

In summary, the pathway of trace elements to fish in the Boulder River watershed clearly included water, sediment, biofilm, and benthic macroinvertebrates. Trace elements accumulated in all of these components and to the greatest extent at sites nearest historical mining activities. The concentrations of trace elements in water and sediment routinely were such that aquatic life was affected at several sites in the watershed. Finally, the interrelationship of the trace elements accumulating in the various components suggests that fish were exposed to trace elements both directly from water and sediment and indirectly through the food chain.

Summary

Water quality in Bullion Mine tributary, Jack Creek, middle Cataract Creek, Uncle Sam Gulch, and to a lesser degree lower and upper High Ore Creek may have rendered the survival of trout unlikely at these sites and may have acted as a barrier that limited fish migration to upstream reaches in the Boulder River watershed. Additionally, because biomass/density was decreased, and metallothionein, products of lipid peroxidation, and tissue trace-element concentrations were simultaneously increased in resident fish at lower Cataract

Creek, we conclude that the aquatic health of lower Cataract Creek was compromised. Furthermore, the association of elevated trace-element concentrations in tissue, water, and sediment has led us to conclude that trace elements were the cause of the compromised aquatic health in lower Cataract Creek. Therefore, resident fish populations would benefit greatly if remediation efforts were directed to minimize the concentrations of trace elements in the water, sediment, and biota of lower Cataract Creek downstream from Uncle Sam Gulch.

The concentrations of trace elements in water and sediment routinely were such that aquatic life was affected at several sites in the watershed. And, the concentrations of arsenic, cadmium, copper, lead, and zinc in invertebrates from lower Cataract Creek were greater than the concentrations in invertebrates from some sites in the Clark Fork River watershed, Montana, where high trace-element concentrations were associated with reduced survival, growth, and health of cutthroat trout fed diets composed of these Clark Fork River invertebrates (Farag and others, 1994; Woodward and others, 1995). Arsenic concentrations in invertebrates from Jack Creek and zinc concentrations in invertebrates from lower High Ore Creek and lower Cataract Creek were greater than the concentrations of these trace elements in invertebrates from Silver Bow Creek, a tributary with some of the greatest invertebrate trace-element concentrations in the Clark Fork River watershed.

Finally, the interrelationship of the trace elements accumulating in the components measured suggests that fish were exposed to trace elements both directly from water and sediment and indirectly through the food chain. It appears that trace elements have contacted biota through these two pathways to compromise the overall aquatic health of the Boulder River watershed. One first step in the food-chain pathway seems to be associated with trace elements transferring from colloids to biofilm.

References Cited

Bachman, R.A., 1984, Foraging behavior of free-ranging wild and hatchery brown trout in a stream: Transactions of the American Fisheries Society, v. 113, p. 1–32.

Boyle, T.P., and Gustina, G.W., 2000, A strategy for use of multivariate methods of analysis of benthic macroinvertebrate communities to assess mine-related ecological stress, *in* ICARD 2000; Proceedings of the Fifth International Conference on Acid Rock Drainage, Volume 2: Society for Mining, Metallurgy, and Exploration, Inc., p. 1425–1432.

Chapman, D., 1995, Assessment of injury to fish populations-Clark Fork River NPL Sites, Mont., *in* Appendices A-H, Aquatic Resources Injury Assessment Report: State of Montana, Natural Resources Damage Program.

DiGiulio, R.T., Washburn, P.C., Wenning, R.J., Winston, G.W., and Jewell, C.S., 1989, Biochemical responses in aquatic animals—A review of determinants of oxidative stress: Environmental Toxicology and Chemistry, v. 8, p. 1103–1123.

Dixon, D.G., and Sprague, J.B., 1981, Copper bioaccumulation and hepatoprotein synthesis during acclimation to copper by juvenile rainbow trout: Aquatic Toxicology, v. 1, p. 69–81.

Dunnett, C.W., 1955, A multiple comparison procedure for comparing several treatments with a control: Journal of the American Statistical Association, v. 50, p. 1096–1121.

Farag, A.M., Boese, C.J., Woodward, D.F., and Bergman, H.L., 1994, Physiological changes and tissue metal accumulation in rainbow trout exposed to foodborne and waterborne metals: Environmental Toxicology and Chemistry, v. 13, p. 2021–2029.

Farag, A.M., Skaar, Don, Nimick, D.A., MacConnell, Elizabeth, and Hogstrand, Christer, 2003, Characterizing aquatic health using fish mortality, physiology, and population estimates in streams with elevated concentrations of arsenic, cadmium, copper, lead, and zinc in the Boulder River watershed, Montana: Transactions of the American Fisheries Society, v. 132, p. 450–467.

Farag, A.M., Stansbury, M.A., Hogstrand, Christer, MacConnell, Elizabeth, and Bergman, H.L., 1995, The physiological impairment of free ranging brown trout exposed to metals in the Clark Fork River, Montana: Canadian Journal of Fisheries and Aquatic Sciences, v. 52, p. 2038–2050.

Farag, A.M., Woodward, D.F., Goldstein, J.N., Brumbaugh, W.G., and Meyer, J.S., 1998, Concentrations of metals associated with mining waste in sediments, biofilm, benthic macroinvertebrates, and fish from the Coeur d'Alene River Basin, Idaho: Archives of Environmental Contamination and Toxicology, v. 34, p. 119–127.

Fuller, C.C., and Davis, J.A., 1989, Influence of coupling of sorption and photosynthetic processes on trace element cycles in natural waters: Nature, v. 340, p. 52–54.

Gardner, W.M., 1977, The effects of heavy metals on the distribution and abundance of aquatic insects in the Boulder River, Montana: Bozeman, Mont., Montana State University M.S. thesis, 84 p.

Gless, E.E., 1990, Biological and chemical baseline studies along the Boulder River and its tributaries in Jefferson County, Montana: Report to the Jefferson County Commissioners, January 1990.

Goede, R.W., 1989, Fish health/condition assessment procedures part 1: Utah Division of Wildlife Resources, Fisheries Experiment Station, Logan, Utah.

Goyer, R.A., 1986, Toxic effects of metals, *in* Klaassen, C.T., Amdur, M.O., and Doull, J., eds., Toxicology: New York, Macmillan, p. 583–635.

Halliwell, C., and Gutteridge, J.M.C., eds., 1985, Free radicals in biology and medicine: Oxford, Clarendon Press, p. 139–170.

Handy, R.D., and Eddy, F.B., 1991, The absence of mucus on the secondary lamellae of unstressed rainbow trout, *Oncorhynchus mykiss* (Walbaum): Journal of Fish Biology, v. 38, p. 153–155.

Hogstrand, C., and Haux, C., 1991, Binding and detoxification of heavy metals in lower vertebrates with reference to metallothionein: Comparative Biochemistry and Physiology, v. 100C, p. 137–141.

Jenkins, T.M., Diehl, S., Kratz, K.W., and Cooper, S.D., 1999, Effects of population density on individual growth of brown trout in streams: Ecology, v. 80, p. 941–956.

Lowe, T.P., May, T.W., Brumbaugh, W.G., and Kane, D.A., 1985, National Contaminant Biomonitoring Program—Concentrations of seven elements in freshwater fish, 1978–1981: Archives of Environmental Contamination and Toxicology, v. 14, p. 363–388.

MacDonald, D.D., Ingersoll, C.G., and Berger, T., 2000, Development and evaluation of consensus-based sediment quality guidelines for freshwater ecosystems: Archives of Environmental Contamination and Toxicology, v. 39, p. 20–31.

Marr, J.C.A., Bergman, H.L., Lipton, J., and Hogstrand, C., 1995, Differences in relative sensitivity of naïve and metals-acclimated brown and rainbow trout exposed to metals representative of the Clark Fork River, Montana: Canadian Journal of Fisheries and Aquatic Sciences, v. 52, p. 2016–2030.

Martin, D.S., 1992, Acid mine/rock drainage effects on water quality, sediments, invertebrates and fish located in Uncle Sam Gulch, Cataract Creek and the Boulder River, northern Jefferson County, Montana: Butte, Mont., Montana College of Mineral Science and Technology M.S. thesis, 117 p.

Nelson, F.A., 1976, The effects of metals on trout populations in the upper Boulder River, Montana: Bozeman, Mont., Montana State University M.S. thesis, 60 p.

Newman, M.C., and McIntosh, A.W., 1989, Appropriateness of aufwuchs as a monitor of bioaccumulation: Environmental Pollution, v. 60, p. 83-100.

Newman, M.C., Alberts, J.J., and Greenhut, V.A., 1985, Geochemical factors complicating the use of aufwuchs to monitor bioaccumulation of arsenic, cadmium, chromium, copper and zinc: Water Research, v. 19, p. 1157–1165.

Newman, M.C., McIntosh, A.W., and Greenhut, V.A., 1983, Geochemical factors complicating the use of aufwuchs as a biomonitor for lead levels in two New Jersey reservoirs: Water Research, v. 17, p. 625–630.

Platts, W.S., Megahan, W.F., and Minshall, G.W., 1983, Methods for evaluating stream, riparian, and biotic conditions: U.S. Department of Agriculture, Intermountain Forest and Range Experiment Station, General Technical Report INT-138, Ogden, Utah.

Poulton, B.C., Monda, D.P., Woodward, D.F., Wildhaber, M.L., and Brumbaugh, W.G., 1995, Relations between benthic community structure and metals concentrations in aquatic macroinvertebrates, Clark Fork River, Montana: Journal of Freshwater Ecology, v. 10, p. 277–293.

Raleigh, R.F., Hickman, T., Solomon, R.C., and Nelson, P.C., 1984, Habitat suitability information; Rainbow trout: U.S. Fish and Wildlife Service, Washington, D.C. GWS/OBS-82/10.60.

Reddy, C.C., Scholz, R.W., and Massaro, E.J., 1981, Cadmium, methylmercury, mercury, and lead inhibition of calf liver glutathione s-transferase exhibiting selenium-independent glutathione peroxidase activity: Toxicology and Applied Pharmacology, v. 61, p. 460–468.

Roch, M., and McCarter, J.A., 1984, Metallothionein induction, growth, and survival of chinook salmon exposed to zinc, copper, and cadmium: Bulletin of Environmental Contamination and Toxicology, v. 32, p. 478–485.

Schemel, L.E., Kimball, B.A., and Bencala, K.E., 2000, Colloid formation and metal transport through two mixing zones affected by acid mine drainage near Silverton, Colorado: Applied Geochemistry, v. 15, p. 1003–1018.

Schmitt, D.J., and Brumbaugh, W.G., 1990, National Contaminant Biomonitoring Program; Concentrations of arsenic, cadmium, copper, lead, mercury, selenium, and zinc in U.S. freshwater fish, 1976–1984: Archives of Environmental Contamination and Toxicology, v. 19, p. 731–747.

Skidmore, J.F., and Tovell, P.W.A., 1972, Toxic effects of zinc sulphate on the gills of rainbow trout: Water Research, v. 6, p. 217–230.

SAS Institute, 1989, SAS/STAT user's guide, Version 6, Fourth Edition, Volume 2: Cary, N.C., SAS Institute.

Stegeman, J.J., Brouwer, M., DiGulio, R.T., Förlin, L., Fowler, B.A., Sanders, B.M., and Van Veld, P.A., 1992, Molecular responses to environmental contamination—Enzyme and protein systems as indicators of chemical exposure and effect, *in* Hugget, R.J., Kimerle, R.A., Merhrle, P.M., Jr., and Bergman, H.L., eds., Biomarkers—Biochemical, physiological, and histological markers of anthropogenic stress: Chelsea, Mich., Lewis Publishers, p. 235–335.

Stern, A., 1985, Red cell oxidative damage, *in* Sies, H., ed., Oxidative stress in tissues: New York, Academic Press, p. 331–349.

U.S. Environmental Protection Agency, 1999, National recommended water quality criteria—Correction: Washington, D.C., Office of Water, EPA 822–Z–99–001, 25 p.

U.S. Environmental Protection Agency, 2001, 2001 update of ambient water quality criteria for cadmium: Washington, D.C., Office of Water, EPA 822–R–01–001, 35 p.

Wills, E.D., 1985, The role of dietary components in oxidative stress in tissue, *in* Sies, H., ed., Oxidative stress in tissues: New York, Academic Press, p. 197–218.

Woodward, D.F., Farag, A.M., Brumbaugh, W.G., Smith, C.E., and Bergman, H.L., 1995, Metals-contaminated benthic invertebrates in the Clark Fork River, Montana—Effects on age-0 brown trout and rainbow trout: Canadian Journal of Fisheries and Aquatic Sciences, v. 52, p. 1994–2004.

Zippen, C., 1958, The removal method of population estimation: Journal of Wildlife Management, v. 22, p. 82–90.

Understanding Trace-Element Sources and Transport to Upper Basin Creek in the Vicinity of the Buckeye and Enterprise Mines

By M.R. Cannon, Stanley E. Church, David L. Fey, Robert R. McDougal, Bruce D. Smith, and David A. Nimick

Chapter E1 of
Integrated Investigations of Environmental Effects of Historical Mining in the Basin and Boulder Mining Districts, Boulder River Watershed, Jefferson County, Montana
Edited by David A. Nimick, Stanley E. Church, and Susan E. Finger

In cooperation with the
United States Department of Agriculture (USDA) Forest Service

Professional Paper 1652–E1

U.S. Department of the Interior
U.S. Geological Survey

Contents

Figures

Tables

CONVERSION FACTORS AND DATUM

Multiply	By	To obtain
	Length	
foot (ft)	0.3048	meter (m)
inch (in.)	2.54	centimeter (cm)
	25.4	millimeter (mm)
mile (mi)	1.609	kilometer (km)
	Area	
acre	0.4047	hectare
square foot (ft^2)	0.09290	square meter
square mile (mi^2)	2.589	square kilometer
	Volume	
cubic foot (ft^3)	28.3168	liter
cubic yard (yd^3)	0.7646	cubic meter
	Flow	
cubic foot per day (ft^3/d)	0.028317	cubic meter per day
cubic foot per second (ft^3/s)	0.028317	cubic meter per second
	Hydraulic Conductivity	
foot per day	0.3048	meter per day
	Transmissivity	
foot squared per day (ft^2/d)	0.0929	meter squared per day

Temperature can be converted to degrees Celsius (°C) or degrees Fahrenheit (°F) by the following equations:

$$°C = 5/9 (°F - 32)$$
$$°F = 9/5 (°C) + 32$$

Vertical coordinate information is referenced to the National Geodetic Vertical Datum of 1929 (NGVD29); horizontal coordinate information is referenced to the North American Datum of 1927 (NAD27).

Chapter E1
Understanding Trace-Element Sources and Transport to Upper Basin Creek in the Vicinity of the Buckeye and Enterprise Mines

By M.R. Cannon, Stanley E. Church, David L. Fey, Robert R. McDougal, Bruce D. Smith, and David A. Nimick

Abstract

The Buckeye mine and adjacent Enterprise mine, located about 10 miles north of Basin, Montana, were intermittently operated in the late 1800s and early 1900s. Upper Basin Creek flows next to acid-generating pyritic rocks and the tailings left from the mining and milling operations. Overland runoff from the mine area is rich in trace elements and measurably affects water quality in upper Basin Creek, primarily during spring snowmelt and high streamflow. Detailed studies of the sources of trace elements and modes of transport to upper Basin Creek were needed to aid in designing remediation.

Geochemical analyses of core samples from areas of mill tailings identified zones containing the highest concentrations of trace elements. Geophysical surveys identified areas of high conductivity that could result from ground water containing high concentrations of dissolved solids. Ground-water samples from test wells identified areas containing high concentrations of dissolved aluminum, arsenic, cadmium, copper, iron, lead, manganese, and zinc.

During spring runoff, dissolved trace-element loads measured in upper Basin Creek were largely derived from small tributary inflows draining the area of the Buckeye and Enterprise mines. Runoff from the mine area caused concentrations of copper, lead, and zinc in upper Basin Creek to exceed the State of Montana aquatic-life standards. For all trace elements except arsenic, ground water contributed only a small part of the dissolved trace-element load to upper Basin Creek.

Introduction

The Buckeye and Enterprise mines in the upper Basin Creek area of west-central Montana are two of many inactive or abandoned metal mines that were intermittently operated in the late 1800s and early 1900s. Wastes left from the mining and processing of ore include pyritic rocks and tailings from gravity and flotation mills. Most of the flotation-mill tailings were deposited in the flood plain of upper Basin Creek, on lands now administered by the Beaverhead-Deerlodge National Forest (fig. 1). Upper Basin Creek, which flows along the southern margin of the mill tailings, receives surface-water and ground-water discharge from the tailings and areas around the mines. That discharge is rich in trace elements and measurably affects water quality in Basin Creek. State of Montana water-quality standards for aquatic life are exceeded in Basin Creek, downstream from these mines, during times of high runoff.

The United States Department of Agriculture (USDA) Forest Service and U.S. Environmental Protection Agency identified the need for remediation of the Buckeye and Enterprise mine area; however, the size of the affected area and the number of potential trace-element sources made the planning of remediation complex. The site contained multiple potential sources of trace elements, which could be transported via surface- and ground-water pathways to upper Basin Creek. Potential sources of trace elements included an adit that discharged acidic water, piles of waste rock near the mines, tailings from an early mill that were located on a hillslope adjacent to the Basin Creek valley floor, and flotation-mill tailings on the flood plain of upper Basin Creek.

Purpose and Scope

The purpose of this report is to present data and results from a comprehensive investigation of trace-element sources and transport to upper Basin Creek from surface and ground water near the Buckeye and Enterprise mines. The investigation was conducted by the U.S. Geological Survey in 1998–99. Prior to the comprehensive investigation near the mines, surface water and streambed sediment were sampled to determine the extent, magnitude, and seasonal patterns of trace-element

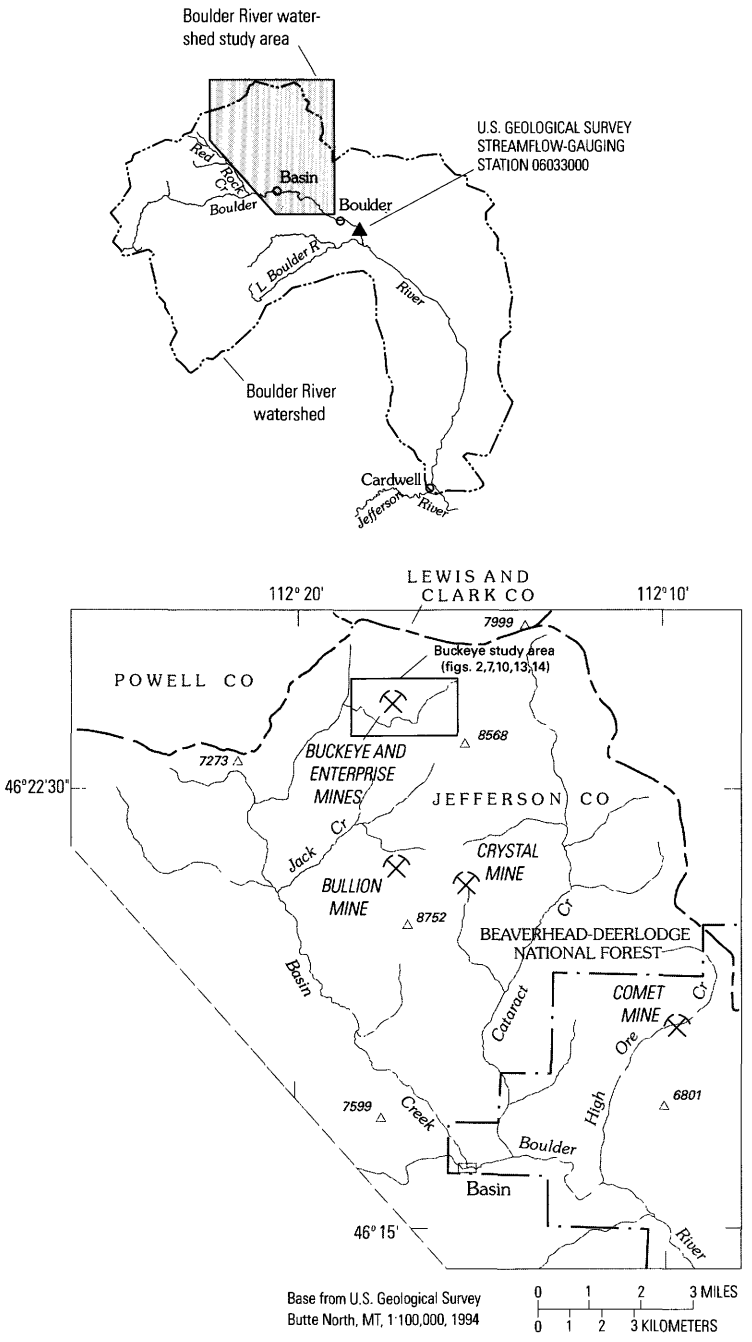

Figure 1. Location of Buckeye and Enterprise mines near upper Basin Creek, Mont. Altitude in feet.

concentrations in a large part of the Basin Creek drainage (Nimick and Cleasby, 2000; Fey, Unruh, and Church, 1999). Results of those samples indicated that the area of the Buckeye and Enterprise mines was contributing trace elements to upper Basin Creek through the transport of acidic, trace-element-rich water and sediment. Seasonal samples from upper Basin Creek indicated that the greatest concentrations and loads of trace elements occurred during spring runoff and much smaller concentrations occurred during low streamflow. Those initial water and sediment samples from upper Basin Creek clearly showed a need for a more thorough characterization of trace-element sources and mechanisms of transport to the stream.

The scope of the investigation was limited to public lands in upper Basin Creek that are adjacent to the Buckeye and Enterprise mines. To better understand the sources of trace elements and mechanisms for transport to upper Basin Creek, a multidisciplinary approach was used that examined (1) geochemistry of mill tailings and streambed sediment, (2) geophysical properties of tailings, alluvial sediments, and pore water, (3) ground-water flow and quality, and (4) surface-water flow and quality. Results of the investigation were used to aid in the development of efficient and cost-effective remediation plans for the mine site and adjacent area of public lands. Remediation activities at the site were conducted in 2000–01 by the USDA Forest Service.

Description of Study Area

The Buckeye and Enterprise mines are located in upper Basin Creek about 10 mi north of the town of Basin in Jefferson County, Mont. (fig. 1). The Buckeye mine was intermittently operated from 1868 to 1908, although the principal period of mining activity was from 1896 to 1903 (Ruppel, 1963). The ore vein, which contained gold-bearing pyrite and minor quantities of silver-bearing galena, was worked through shafts that were sunk to a depth of 100–200 ft. The adjacent Enterprise mine was operated at about the same time, but was closed before 1900. The Enterprise mine had a 400-ft vertical shaft that accessed an ore vein similar to the one at the Buckeye mine. The 5-ft thick Buckeye ore vein and the adjacent smaller veins are nearly vertical and apparently occupy fault zones trending N. 85° W. within the Butte quartz monzonite (Ruppel, 1963). During the time of mine operation, ore from the mines was processed by a gravity mill located at the Buckeye site. In the 1940s during World War II, a flotation mill was built on the flood plain of Basin Creek (fig. 2) to reprocess the old tailings from the gravity mill (Roby and others, 1960; Metesh and others, 1994). An estimated 5,000 cubic yards of flotation tailings and sandy material accumulated in the Basin Creek flood plain (Fey, Church, and Finney, 1999) as a result of activities at the flotation mill. These flood-plain tailings occupied about 3.3 acres in an irregularly shaped area of about 200 by 750 ft.

Altitudes within the study area range from about 7,020 ft along Basin Creek at the west end of the study area to 7,100 ft at the mine workings. Basin Creek drops about 20 ft as it meanders for a distance of about 4,300 ft from east to west through the study area. Because of its relatively high altitude, the area receives nearly 30 in. of precipitation per year, much of it falling as snow from late October through May (U.S. Department of Agriculture, 1981).

Sources of Trace Elements

Several potential sources of trace elements were present at the Buckeye and Enterprise mines and adjacent area. Sources included a mine adit discharging water, piles of pyritic waste rock on private property, and dispersed deposits of mill tailings on public land along upper Basin Creek. The size of the area affected by elevated concentrations of trace elements such as arsenic, cadmium, copper, lead, and zinc that are associated with the mineral deposit was unknown. To assess the lateral and vertical extent of the affected area, detailed geochemical studies were conducted on the mill tailings and soils on the flood plain of upper Basin Creek, and geophysical surveys were used to examine properties of subsurface materials along upper Basin Creek and the surrounding area.

Figure 2. Flotation mill active during the 1940s and associated tailings on flood plain of Basin Creek at Buckeye and Enterprise mines, October 1996. Buckeye mine is behind mill near clearing in trees. Enterprise mine is in trees on right side of photograph.

Flotation-Mill Tailings

The distribution, thickness, and volume of flotation-mill tailings as well as underlying fluvial sediment with elevated trace-element concentrations were estimated by Fey, Church, and Finney (1999) from 35 shallow cores collected from the flood plain of upper Basin Creek (fig. 3) in 1997. These cores were 1 inch in diameter and typically as much as 24 inches in length. The cores were subdivided into 196 samples on the basis of visual identification of differences in mineralogy, organic content, and degree of oxidation. Each sample was analyzed by geochemical and binocular-microscopic methods. Trace-element concentrations and mineralogy determined from these analyses were used to distinguish contaminated and uncontaminated material and to estimate the volume of the contaminated material (Fey, Church, and Finney, 1999). Further investigation of the mill tailings was warranted to determine the source of trace elements in underlying ground water, whether the tailings had potential for further oxidation and associated release of acid and trace elements, and what processes cause lateral and vertical dispersion of trace elements in the tailings and across the flood plain.

Geochemistry of Tailings

The geochemistry of the flotation-mill tailings was examined by detailed analysis of a core (2 inches in diameter and 79 in. long) collected from the thickest part of the mill tailings in July 1998. This core, as well as a nearby exploratory trench (approximately 10 ft long and 7 ft deep), revealed a zone of oxidized waste that graded downward into unoxidized, pyrite-rich waste near the base of the tailings. The core was subdivided into 27 samples. Sample descriptions as well as geochemical and mineralogical data from the core are in table 1. The data indicate four distinct sections corresponding to the oxidized zone (the upper 22 in.), the partly oxidized zone (22–41 in.), the unoxidized pyritic zone (41–62 in.), and buried soil developed in flood-plain sediment (62–79 in.). At the base of the mill tailings, buried wetland grasses overlie the top organic-rich layer of the buried soil. Geochemical and mineralogical data for the 2-in. core are used to demonstrate how the tailings weathered and how trace elements were mobilized, redistributed within the core, and, in some cases, leached out of the tailings. The mechanisms by which trace elements were released by weathering and dispersed through the flood plain can be understood by examination of the differences in element concentrations (from the 1-in. cores) in total- and leach-digestions as well as the distribution of primary and secondary minerals and their relative abundance within the cores.

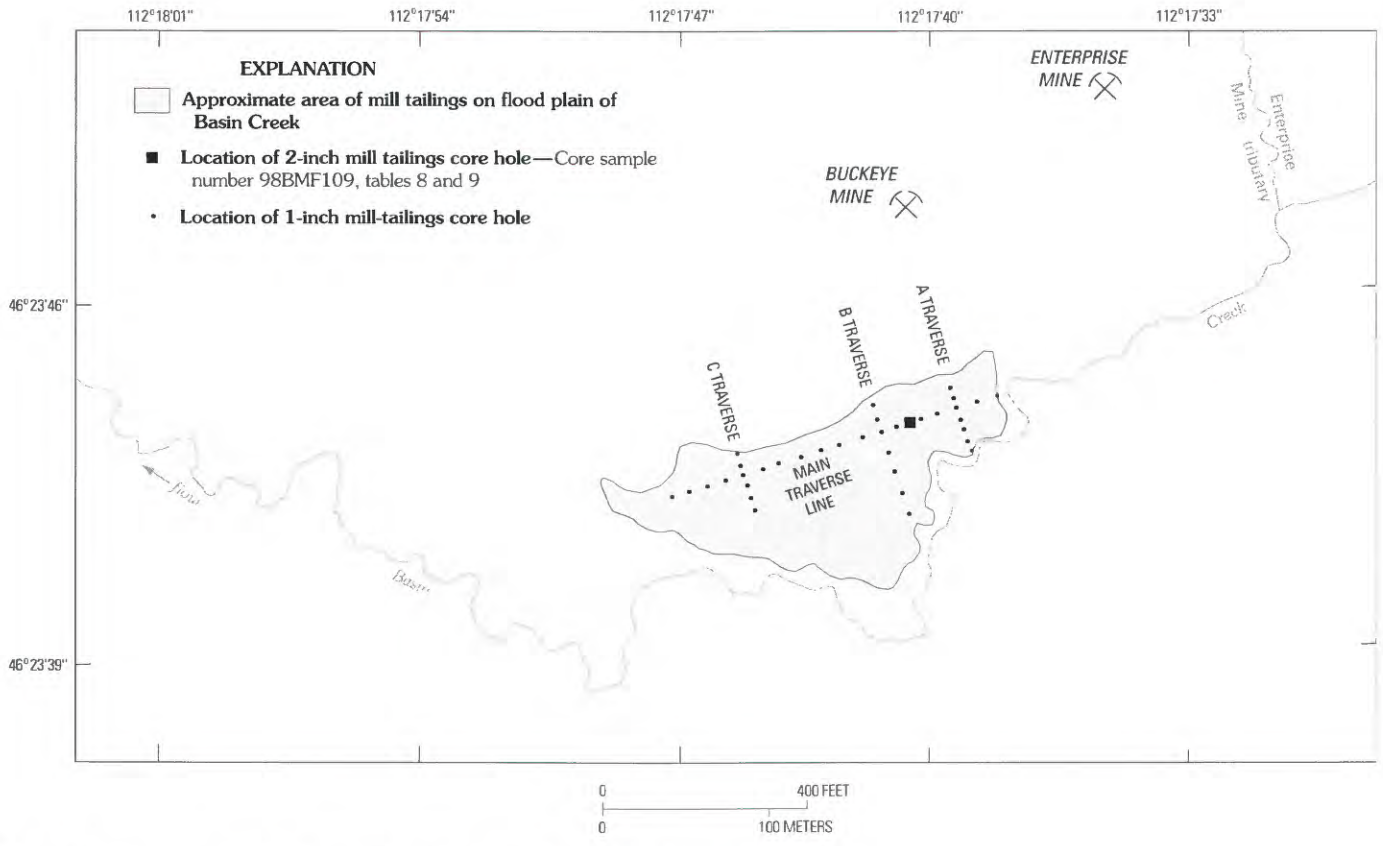

Figure 3. Location of mill tailings and core holes on flood plain of upper Basin Creek.

Total-Digestion Data

The samples from the 2-in. core were processed using a total-digestion procedure that used a mixture of strong acids (Fey and others, 2000). Concentrations of major elements such as calcium, sodium, iron, and aluminum clearly show the difference between mill tailings and the underlying buried soil and reflect differences in the mineralogy of these two units (table 1). These differences in element concentrations are caused by the large difference in proportions of the deposit-related minerals found in the rocks that were milled and the rock-forming minerals typically found in the premining flood-plain sediment beneath the tailings. Other differences in element concentrations were caused by oxidation of the abundant sulfide minerals (such as pyrite) in the tailings and leaching of the oxidation byproducts. Calcium and sodium were present in the tailings at very low concentrations, but in the underlying soil zone they were present at concentrations one to two orders of magnitude higher. This pattern largely reflects the original compositions of the tailings and underlying buried soil, with much smaller amounts of feldspar and other rock-forming minerals in the tailings compared to the soil. Aluminum exhibited a somewhat similar but less distinct pattern. Aluminum concentrations were lower in the tailings (1.6–4.4 percent) and higher in the underlying soil (5.2–9.0 percent), again reflecting the larger proportion of rock-forming minerals in the buried soil.

Within the tailings, variations in iron and aluminum concentrations with depth reflect processes that affected the tailings after their deposition on the flood plain. Iron is hosted primarily in pyrite, which likely was distributed fairly uniformly throughout the original tailings. However, iron concentrations in the core were lower in the oxidized zone (less than 1 percent) and higher in the unoxidized pyritic zone (2.6–5.6 percent). This pattern likely developed because pyrite and other sulfide minerals in the upper part of the tailings pile were oxidized and their constituents leached from the oxidized zone. The wide range in iron concentrations within just the unoxidized pyritic zone reflects the variable amount of quartz, the dominant silicate mineral in the tailings, which diluted the amount of pyrite present in individual layers sampled in the zone. Aluminum concentrations were higher in the oxidized zone (3.5–4.4 percent) than in the unoxidized pyritic zone (1.7–3.6 percent). The aluminum distribution is also a result of the leaching of the sulfide-oxidation byproducts. As these components were removed, aluminum, which was not leached, was concentrated in the oxidized zone, primarily in kaolinite that formed during weathering.

Similar to the major elements, the distribution of trace elements in the core (fig. 4) reflects the original mineralogy as well as subsequent processes that differentially mobilized and sequestered the trace elements. Strontium and silver concentrations, like calcium, sodium, and iron concentrations, reflect the original composition of the tailings and buried soil. In the tailings, strontium concentrations were low and silver concentrations were high, whereas this pattern was reversed in the buried soil. Strontium represents the rock-forming trace elements typical of the underlying premining flood-plain sediment, whereas silver represents the deposit-related trace elements that were concentrated in the tailings.

Arsenic, cadmium, copper, lead, and zinc are the trace elements that pose risk to aquatic life in Basin Creek (Farag and others, this volume, Chapter D10). These elements were enriched in the tailings (fig. 4*B*, *C*) but had distinctly different mobilities during oxidation and weathering in place. Silver is a relatively immobile trace element during oxidation and weathering. The uniform distribution of silver through the tailings (fig. 4*C*) indicates that the tailings had a fairly uniform composition as they were dumped from the flotation mill and that, initially, the tailings in the core likely were homogeneous. Therefore, comparing the distributions of the trace elements of concern to the distribution of silver provides useful information about the weathering processes. Lead, like silver, is relatively immobile (fig. 4*C*). Arsenic (fig. 4*C*) is more mobile during weathering than silver and lead but less mobile than cadmium, copper, and zinc (fig. 4*B*). Moderate to large increases in concentrations of trace elements occurred at the boundary between the oxidized zone and the partly oxidized zone (22 in. depth) and, for most trace elements, at the boundary between the partly oxidized zone and the unoxidized pyritic zone (41 in.). Concentrations also were high, particularly for arsenic, cadmium, copper, and zinc, near the top layer of the buried soil (64.3 in.). These increases were produced by downward leaching of the trace elements mobilized by sulfide oxidation in the oxidized zone. Some of the leached trace elements were sequestered as organic complexes at the top of the buried soil, which presumably had very low trace-element concentrations prior to deposition of the tailings. Below the organic material in the buried soil, concentrations of trace elements of concern decreased markedly over a distance of a few inches (fig. 4). Concentrations of arsenic, which behaves as an anion, and zinc, which remains mobile up to a pH of about 8, decreased gradually with depth reflecting their greater mobility and greater penetration into the buried soil horizon.

Leachate Data

The samples from the 2-in. core also were processed using a passive-leach procedure (Fey and others, 2000). Deionized water was used as the leachate and was mixed at a 20:1 mass ratio with the sample. The samples were leached for 24 hours without agitation to simulate the dissolution reactions that probably would occur when sulfidic tailings are exposed to surface water. Data are in table 2 and figure 5. Leachate from all intervals in the core was acidic, indicating that sulfide oxidation was occurring and that acid and trace elements would be mobile in the tailings and at least parts of the buried soil. The pH of the leachate solutions was slightly higher in the oxidized zone (pH from 3.41 to 3.68) than in the partly oxidized zone and unoxidized pyritic zone (pH from 2.53 to 3.09). In the buried soil below the tailings, the pH increased with depth. Specific conductance and sulfate concentration

Table 1. Mineralogy and concentrations of selected major and trace elements in core intervals from a 2-in. diameter core in

[Core intervals expressed as the midpoint of the depth in the core from the surface (corrected for compaction). Major-element concentrations expressed in weight percent (parts per hundred); trace-element concentrations expressed in parts per million; minerals identified by XRD listed in order of decreasing abundance; cm, centimeter; mm, millimeter; ppm, parts per million; tr., trace; XRD, X-ray diffraction; <, less than minimum reporting level; --, not analyzed]

Sample No.	Depth (mid-point, in inches)	Sample description	High-density minerals, identified by XRD	Minerals, in addition to quartz and mica identified by XRD	Aluminum (weight percent)
		Oxidized zone			
98BMF109-Aa	1.8	Light-gray/pale-yellow tailings, medium sand	anglesite, tr.sphalerite	orthoclase	4.4
98BMF109-Ab	5.3	Coarse tailings, sand sized to 1 mm	anglesite, tr.sphalerite	anglesite, kaolinite	4.3
98BMF109-Ac	8.6	Unsorted tailings with clay-size matrix	anglesite, tr.sphalerite	anglesite, kaolinite	4.2
98BMF109-Ad	11.8	Unsorted tailings with clay-size matrix	anglesite, tr.sphalerite	anglesite, kaolinite	4.2
98BMF109-Ba[1]	15.0	Light-gray tailings, poorly sorted into	anglesite, tr.sphalerite	anglesite, kaolinite	3.8
98BMF109-Bb[1]	17.9	0.52-cm thick beds, coarse grains to 2 mm.	anglesite, tr.sphalerite, gold	anglesite, orthoclase	3.5
98BMF109-Bc[1]	20.8		anglesite, tr.sphalerite	anglesite	3.6
		Partly oxidized zone			
98BMF109-Ca	23.2	Pale-yellow fine-grained tailings, 90 percent "clay" size.	anglesite	anglesite	4.0
98BMF109-Da	25.4	Pale-yellow/cream tailings, coarse- and fine-grained.	anglesite	anglesite	2.8
98BMF109-Ea	28.2	Pale yellow/gray, coarse and fine grained	anglesite	anglesite	2.5
98BMF109-Fa	31.1	Bright-yellow sand, unsorted tailings	anglesite	anglesite	1.9
98BMF109-Ga	34.4	Pale-yellow cream tailings with lenses of sulfide grain, layered.	anglesite	anglesite	2.2
98BMF109-Ha	37.5	Light-gray light-yellow fine to coarse oxidized sulfide tailings.	anglesite	anglesite	1.8
98BMF109-Ia	39.7	Yellow, medium sand tailings	anglesite	anglesite, scorodite	1.6
		Unoxidized pyritic zone			
98BMF109-Ja	42.4	Cream and dark-gray, sulfides, fine sand	pyrite, anglesite	anglesite, pyrite	3.3
98BMF109-Ka	45.5	Light- and dark-gray, sulfides, fine sand	pyrite, anglesite	pyrite, anglesite, sphalerite	2.6
98BMF109-La	48.8	Fine sand with gray sulfides	pyrite, anglesite	sphalerite, pyrite, anglesite	1.8
98BMF109-Ma	52.2	Pale-yellow tailings, some gray sulfides, medium to coarse sand, moderately sorted.	pyrite, anglesite	pyrite, anglesite	1.7
98BMF109-Mb	54.9	Pale-yellow tailings, some gray sulfides, medium to coarse sand, moderately sorted.	pyrite, anglesite	pyrite, anglesite	2.0
98BMF109-Na	57.1	Light-dark-gray tailings, fine sand, pyrite	pyrite, anglesite	pyrite, anglesite	3.2
98BMF109-Oa	59.9	Cream, poorly sorted fine-sand size tailings	pyrite	pyrite, anglesite	3.6
		Buried soil			
98BMF109-P	62.0	Organic layer	--	--	
98BMF109-Qa	64.3	Soil, dark brown at top	tr. pyrite	halloysite, plagioclase	5.2
98BMF109-Qb	67.8	Light brown at bottom	none	montmorillonite, kaolinite, plagioclase	7.6
98BMF109-Qc	71.5	Soil	none	montmorillonite, kaolinite, plagioclase	9.0
98BMF109-Qd	75.0	Soil	zircon, tr. hornblende	montmorillonite, kaolinite, plagioclase	8.9
98BMF109-Qe	78.0	Soil	zircon, tr. hornblende	montmorillonite, kaolinite, plagioclase	8.7

mill tailings along upper Basin Creek.

Calcium (weight percent)	Iron (weight percent)	Potassium (weight percent)	Sodium (weight percent)	Arsenic (ppm)	Cadmium (ppm)	Copper (ppm)	Lead (ppm)	Manganese (ppm)	Silver (ppm)	Strontium (ppm)	Zinc (ppm)
Oxidized zone											
0.02	0.86	2.1	0.05	1,600	2	54	6,100	140	52	25	280
.02	.82	2.1	.04	1,700	<2	35	7,500	140	48	24	210
.02	.80	2.0	.04	1,300	<2	47	6,900	130	48	26	260
.01	.78	2.0	.03	1,400	<2	43	7,400	140	62	21	180
.009	.63	1.8	.02	500	<2	38	5,000	120	42	15	170
.009	.57	1.6	.01	480	<2	66	8,300	120	92	9	240
.01	.62	1.7	.009	640	<2	60	7,000	120	64	7	210
Partly oxidized zone											
.01	1.8	1.9	.02	13,000	9	110	37,000	190	190	20	1,400
.008	1.6	1.3	.007	11,000	9	110	22,000	140	110	12	1,500
.009	1.6	1.2	.007	13,000	7	200	14,000	120	110	13	1,200
<.005	2.8	.89	<.005	26,000	10	270	12,000	94	64	8	1,600
.008	2.3	1.0	.009	21,000	15	360	15,000	120	98	14	2,600
.006	1.7	.86	<.005	16,000	13	250	16,000	99	70	14	2,300
<.005	4.4	.75	<.005	44,000	19	400	20,000	86	88	9	3,000
Unoxidized pyritic zone											
.009	4.0	1.6	.01	18,000	48	2,900	58,000	180	300	16	6,900
.01	5.6	1.2	.01	31,000	70	3,200	52,000	160	220	10	9,800
<.005	4.6	.88	<.005	22,000	60	2,000	26,000	110	120	6	9,000
<.005	3.1	.78	<.005	14,000	27	790	12,000	92	52	6	4,400
.006	2.6	.94	<.005	13,000	31	1,000	9,100	92	34	8	4,700
.02	4.3	1.5	.01	20,000	64	4,300	19,000	140	80	20	8,400
.01	3.6	1.7	.02	13,000	44	2,700	8,600	130	59	18	5,600
Buried soil											
--	--	--	--	--	--	--	--	--	--	--	--
.27	1.8	.60	.26	9,400	190	3,200	500	190	2	59	12,000
.56	2.1	.98	.52	2,500	17	43	110	350	<2	110	6,400
1.1	3.7	1.4	.80	2,300	2	50	160	680	<2	220	3,300
1.0	4.2	1.4	.80	2,300	7	75	160	700	<2	190	1,100
1.2	3.8	1.7	1.1	1,900	9	90	440	610	<2	230	820

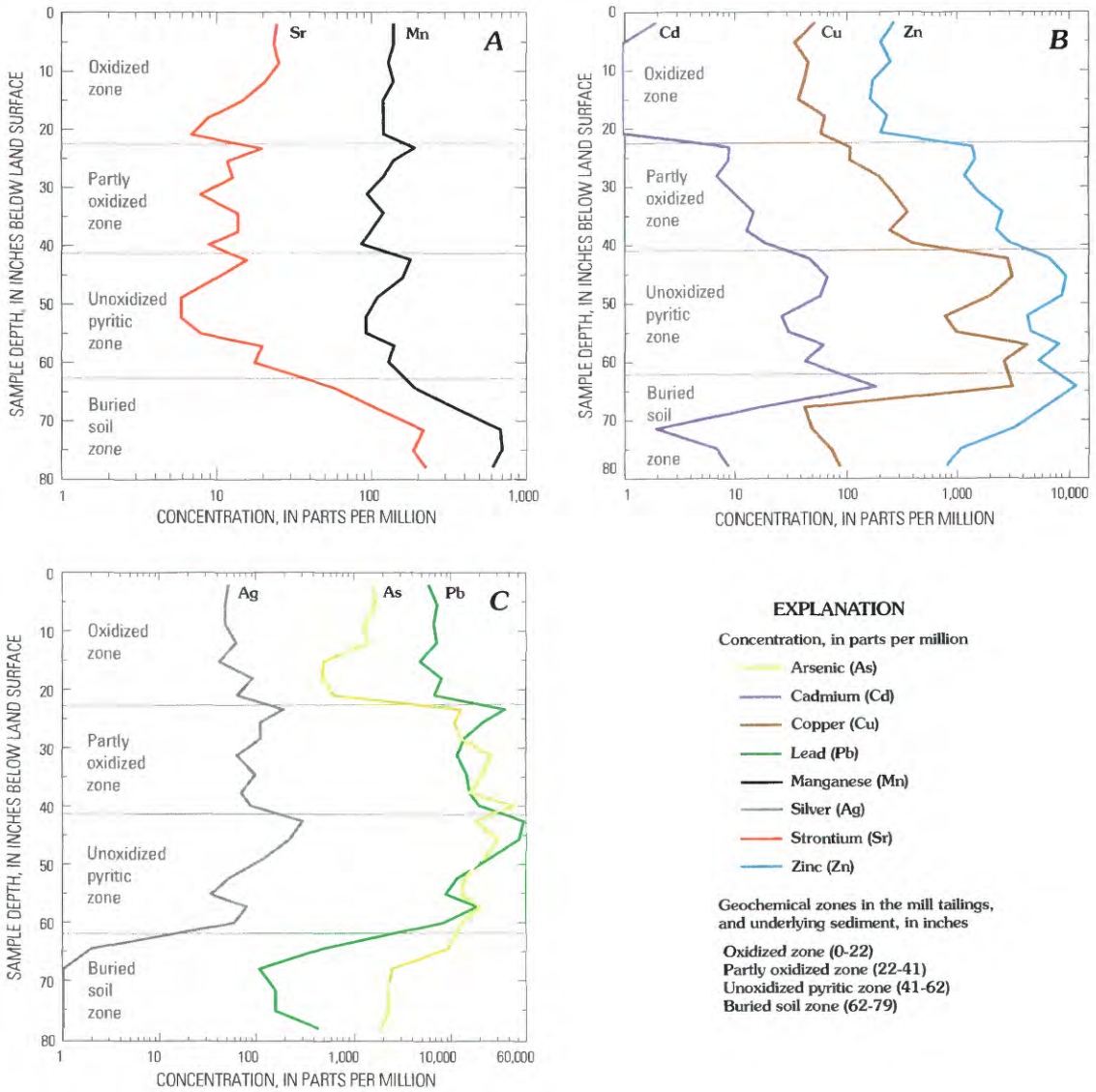

Figure 4. Relation of selected trace-element concentrations in total digests to depth in the 2-in. core through mill tailings, upper Basin Creek. Concentrations of silver in samples below 64.3 in. were less than minimum reporting level of 2 parts per million and are not shown. *A*, strontium, manganese; *B*, cadmium, copper, zinc; *C*, silver, arsenic, lead.

in the leachate were well correlated (fig. 5, $R^2 = 0.88$). Both sulfate concentration and specific conductance increased in the leachate with depth in the tailings and decreased in the buried soil. Iron concentrations in the leachate were low in the oxidized zone and high in the unoxidized pyritic zone. Iron concentrations in the oxidized zone were low because the iron had been leached out of the oxidized zone as shown by the total-digestion data.

Leachate data reflect the mobility of trace elements during oxidization of the tailings, with arsenic being the most mobile (concentration increase of about three orders of magnitude through the tailings); cadmium, copper, and zinc less mobile; and antimony, lead, and silver least mobile (fig. 5). The presence of native sulfur (identified visually) and the very soluble hydrous iron arsenate, scorodite, in the partly oxidized zone (table 1) indicates that the mobility of the trace elements was limited with depth by low permeability in tailings. The immobility of lead is clearly shown by the presence of anglesite (lead sulfate, which is relatively insoluble) in the oxidized and partly oxidized zones (table 1). No jarosite (iron-rich, hydrous potassium aluminum sulfate) was observed in the core, perhaps because insufficient potassium was available to form this mineral. Muscovite, which contains potassium, was sparse in the flotation wastes, so mobile potassium was not readily available to form jarosite. Deposit-related trace elements generally were sequestered at the top of the buried soil horizon immediately below the organic layer (62 in.), with the exception of manganese, zinc, and arsenic, which had elevated concentrations throughout the buried soil (fig. 5).

Table 2. Specific conductance, pH, and concentrations of sulfate and selected trace elements in leachate from various depth intervals of core samples collected from the mill tailings along upper Basin Creek.

[Core intervals expressed as the midpoint of the depth in the 2-in. diameter core from land surface (corrected for compaction). ICP, inductively coupled plasma; µg/L, micrograms per liter; µS/cm, microsiemens per centimeter at 25 degrees Celsius; mg/L, milligrams per liter; <, less than minimum reporting level; --, not analyzed (organic layer)]

Sample No.	Depth (mid-point, in inches)	Specific conduc-tance of leachate (µS/cm)	pH of leachate	ICP[1] Sulfate (mg/L)	ICP[2] Aluminum (µg/L)	ICP[3] Antimony (µg/L)	ICP[3] Arsenic (µg/L)	ICP[3] Cadmium (µg/L)	ICP[1] Copper (µg/L)	ICP[2] Iron (µg/L)	ICP[3] Lead (µg/L)	ICP[2] Manganese (µg/L)	ICP[2] Silver (µg/L)	ICP[1] Strontium (µg/L)	ICP[1] Zinc (µg/L)
Oxidized zone															
98BMF109-Aa	1.8	189	3.41	35	200	150	71	15	440	44	12,000	33	22	18	3,400
98BMF109-Ab	5.3	127	3.56	26	98	150	69	13	450	9.2	15,000	18	10	13	2,500
98BMF109-Ac	8.6	111	3.63	23	73	54	25	9.8	640	5.0	17,000	11	5.4	12	1,800
98BMF109-Ad	11.8	124	3.62	23	120	100	38	7.5	670	14	18,000	5.3	6	12	1,300
98BMF109-Ba	15.0	116	3.68	23	96	240	28	9.3	710	58	18,000	5.7	15	8.9	1,900
98BMF109-Bb	17.9	122	3.67	23	120	500	67	8.2	490	68	18,000	5.2	24	8.2	1,600
98BMF109-Bc	20.8	131	3.62	24	56	580	81	7.8	390	82	18,000	3.7	17	5.3	1,700
Partly oxidized zone															
98BMF109-Ca	23.2	610	3.09	97	590	1,600	250	41	2,000	2,200	9,500	14	530	4.0	8,400
98BMF109-Da	25.4	760	2.94	120	560	1,500	210	51	3,500	5,100	7,400	17	240	2.6	13,000
98BMF109-Ea	28.2	900	2.90	160	730	1,700	230	66	5,600	10,000	6,100	23	68	4.0	18,000
98BMF109-Fa	31.1	1,330	2.77	260	820	1,900	370	100	11,000	25,000	5,000	32	55	3.5	31,000
98BMF109-Ga	34.4	1,350	2.75	240	570	2,100	630	99	11,000	18,000	4,700	31	69	5.1	32,000
98BMF109-Ha	37.5	860	2.82	160	150	1,700	1,800	67	7,700	8,300	5,400	21	40	4.0	22,000
98BMF109-Ia	39.7	1,320	2.73	230	190	1,200	5,200	88	10,000	13,000	4,800	27	41	3.4	31,000
Unoxidized pyritic zone															
98BMF109-Ja	42.4	3,280	2.53	900	1,600	1,700	24,000	1,000	87,000	94,000	3,000	280	3	15	280,000
98BMF109-Ka	45.5	2,170	2.82	770	780	1,200	18,000	1,500	88,000	83,000	3,500	300	<2	3.4	310,000
98BMF109-La	48.8	1,330	3.02	440	210	720	12,000	900	46,000	45,000	4,100	190	<2	2.1	170,000
98BMF109-Ma	52.2	1,050	2.95	270	210	380	8,400	490	22,000	23,000	4,400	120	<2	6.7	83,000
98BMF109-Mb	54.9	1,350	2.90	350	480	330	7,400	640	35,000	26,000	4,000	180	<2	7.6	120,000
98BMF109-Na	57.1	2,590	2.76	900	3,400	600	14,000	1,700	140,000	100,000	3,200	540	<2	7.0	270,000
98BMF109-Oa	59.9	2,100	2.79	670	4,200	530	15,000	1,200	96,000	74,000	4,000	530	<2	5.3	180,000
Buried soil															
98BMF109-P	62.0	--	--	--	--	--	--	--	--	--	--	--	--	--	--
98BMF109-Qa	64.3	4,400	2.84	2,200	200,000	71	65,000	9,700	120,000	19,000	780	5,300	<2	120	720,000
98BMF109-Qb	67.8	1,830	3.43	840	46,000	11	6,600	580	440	1,500	130	8,600	<2	260	320,000
98BMF109-Qc	71.5	760	3.88	330	3,500	11	2,100	28	45	180	44	12,000	<2	380	86,000
98BMF109-Qd	75.0	370	4.14	140	740	3.5	3,600	51	36	65	13	7,200	<2	310	12,000
98BMF109-Qe	78.0	290	4.15	110	580	14	1,200	85	26	50	35	5,900	<2	270	7,600

[1]Inductively coupled plasma-atomic emission spectrometry (ICP-AES) data. [2]Inductively coupled plasma-mass spectrometry (ICP-MS) used at low concentrations; inductively coupled plasma-atomic emission spectrometry data used at higher concentrations. [3]Inductively coupled plasma-mass spectrometry data.

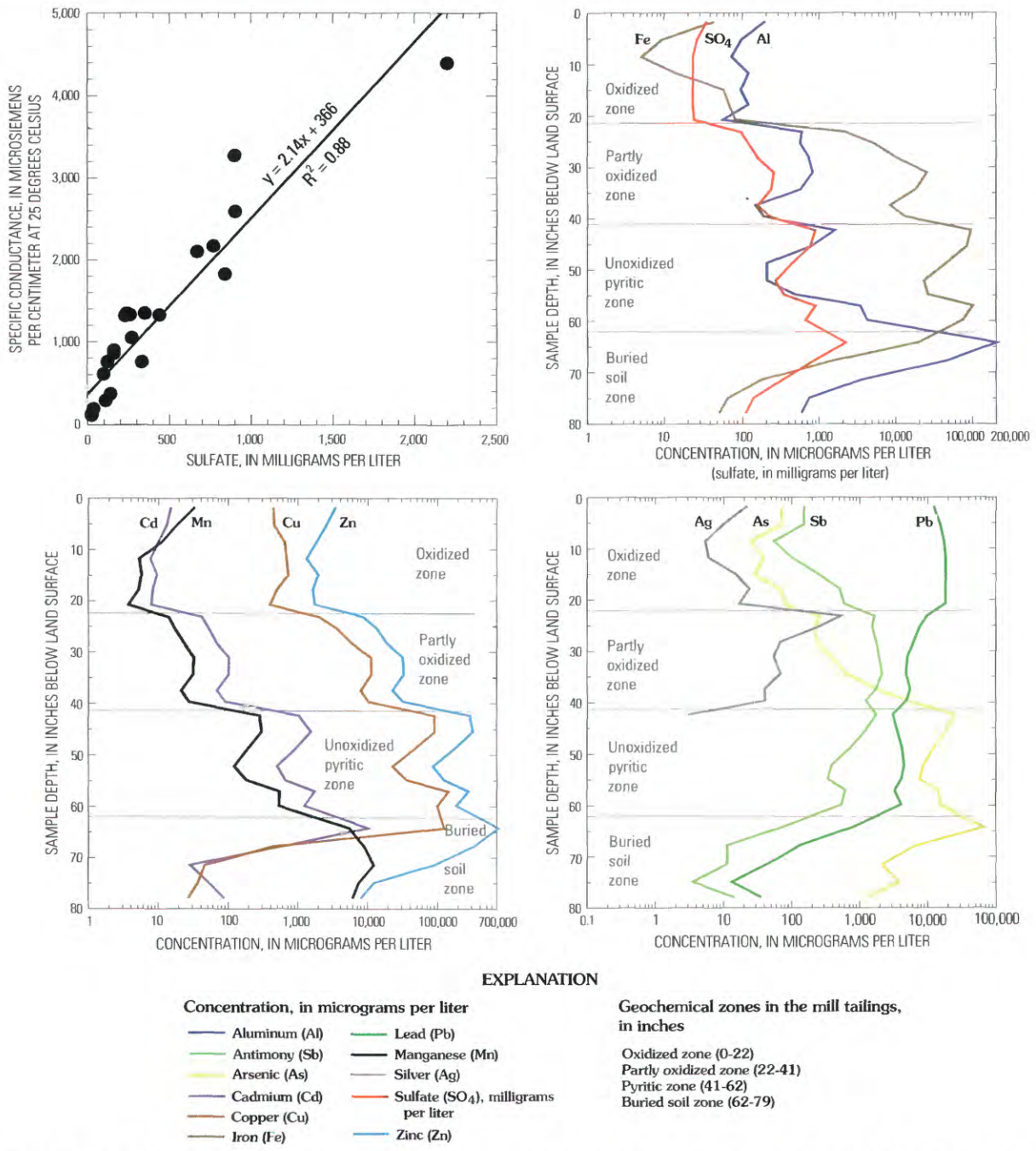

Figure 5. Relation of selected trace-element and sulfate concentrations in leachate to depth in the 2-in. core through mill tailings, upper Basin Creek. Sample numbers and analytical results are presented in table 2 and in Rich and others (this volume, Chapter G). Concentrations of silver in samples below 45.5 in. were less than minimum reporting level of 2 micrograms per liter and are not shown.

Arsenopyrite

Early descriptions of ore from the Buckeye and Enterprise mines identified arsenopyrite as a significant mineral. However, no arsenopyrite was identified by X-ray diffraction of bulk samples or the high-density-mineral concentrates from the 2-in. core (table 1). Arsenopyrite generally is absent from most of the mine wastes present in the Basin mining district (Desborough and Fey, 1997). In addition, no arsenic minerals were identified in the unoxidized pyritic zone (table 1) that would account for the arsenic concentrations of 11,000–44,000 parts per million (ppm) (1.1 to 4.4 percent) in the partly oxidized zone (fig. 4; table 1). Too much arsenic is present in the pyritic zone of the core to be incorporated into pyrite and, therefore, the arsenic must be hosted in another mineral. Arsenic could possibly be present as an amorphous phase in the pyritic zone and, therefore, not detected by X-ray diffraction (XRD).

Dispersion of Tailings on the Flood Plain

Descriptions of the 1-in. core samples (Fey, Church, and Finney, 1999) indicated that the majority of these samples looked more like flood-plain sediment than like tailings, even though many of the samples had high concentrations of the deposit-related trace elements. These observations indicate that the tailings were subjected to various weathering and dispersion processes after their deposition in the 1940s. Tailings likely were mobilized and transported away from the original pile by physical processes (wind or water erosion) and then redeposited and mixed with sediment on the flood plain or transported to Basin Creek. In addition, trace elements have been mobilized and leached by water from the tailings by chemical processes. Portions of these trace elements then were precipitated or adsorbed before reaching Basin Creek, thus increasing trace-element concentrations in flood-plain sediment. The effects of this physical and chemical dispersion on the flood-plain surface can be examined using the total-digestion geochemical data from both the 1-in.-diameter cores (fig. 3; Fey, Church, and Finney, 1999) and the 2-in.-diameter core (table 1). The 1-in. cores provide spatial data over a large part of the flood-plain area affected by tailings, whereas the 2-in. core provides detailed vertical information.

The contrast in silver and strontium concentrations provides a useful tool to differentiate between tailings and underlying premining flood-plain sediment and to understand physical and chemical dispersion processes. The contrast in concentrations was clear in the 2-in. core (fig. 4), in which tailings had low strontium (6–26 ppm) and high silver concentrations (34–300 ppm) while premining flood-plain sediment (buried soil) had high strontium (59–420 ppm) and low silver (<2–2 ppm) concentrations. However, only 11 of the 196 one-inch core samples had strontium concentrations less than 30 ppm and silver concentrations greater than 2 ppm. These 11 samples likely contained essentially pure tailings because the 11 samples were from the cores collected nearest the 2-in. core, which was located in the thickest part and presumably near the center of the tailings pile. The proportion of tailings in the other 185 one-inch core samples apparently was much less. Figure 6 shows box plots of strontium and silver concentrations for each of the 1-in. cores from the main traverse line (fig. 3). The coincidence of low strontium concentrations and high silver concentrations for the two 1-in. cores next to the 2-in. core near the center of the mill-tailings pile is apparent. Cores farther away from the 2-in. core had higher strontium and lower silver concentrations, indicating that the material at these sites was mostly flood plain sediment unaffected by tailings.

Figure 7 shows the relation between concentrations of strontium and other trace elements in the top layers of each of the 1-in. cores. The data are ordered from left to right in the graph on the basis of increasing strontium concentration, which also indicates a greater proportion of flood-plain sediment relative to tailings. In figure 7*A*, silver and lead, which behave similarly and were shown to be less chemically mobile in the 2-in. core (fig. 4*C* and 5), show marked decrease in concentration as strontium concentration increases. This pattern suggests that silver and lead were dispersed primarily by physical transport of tailings away from the original pile. In contrast, concentrations of arsenic, cadmium, copper, and zinc (fig. 7*B*, *C*) do not decrease as markedly as lead and silver concentration. These elements were shown to be more easily mobilized by chemical processes from the oxidized tailings than were lead and silver (figs. 4 and 5). Therefore, these elements most likely were dispersed to a greater extent by a chemical process involving mobilization, transport, and redeposition within the tailings area. Manganese, however, shows different behavior (fig. 7*D*): its concentration increases slightly as strontium concentration increases. This trend is opposite the concentration trend exhibited by most other trace elements and suggests that manganese is not derived from the tailings but from another source, such as ground water, that could affect all portions of the flood plain.

Shallow Subsurface Sources

Surface-geophysical surveys were conducted during the summers of 1998 and 1999 to examine the location and extent of shallow subsurface materials with high electrical conductivity, which could be related to elevated trace-element concentrations in the mill tailings along upper Basin Creek and the surrounding area. Defining the extent of potentially contaminated ground water also was a primary purpose of the geophysical investigations. Shallow subsurface materials were examined with a combination of electromagnetic, magnetic, and direct-current resistivity methods.

An electromagnetic (EM) survey was used to map the distribution of conductive materials in the mill tailings and in the underlying and surrounding valley-fill sediments and bedrock. Generally, in this type of environment, areas of high conductivity are caused by the presence of wet clays in soils or by high dissolved-solids concentrations in ground water. Magnetic metallic objects such as buried pipes, cables, or milling artifacts can cause conductive anomalies. A total-field magnetic reconnaissance survey was used to locate any metallic objects in the subsurface and differentiate them from areas with wet clays or high dissolved-solids concentration. Buried metallic objects are distinguishable because they are both conductive and magnetic.

Direct-current (DC) resistivity soundings were made on the tailings and adjacent areas to examine the vertical distribution of conductive material and to estimate the depth to bedrock beneath the tailings. Resistivity data were converted to the reciprocal values with units of conductivity so that they could be correlated directly with the electromagnetic (EM) data.

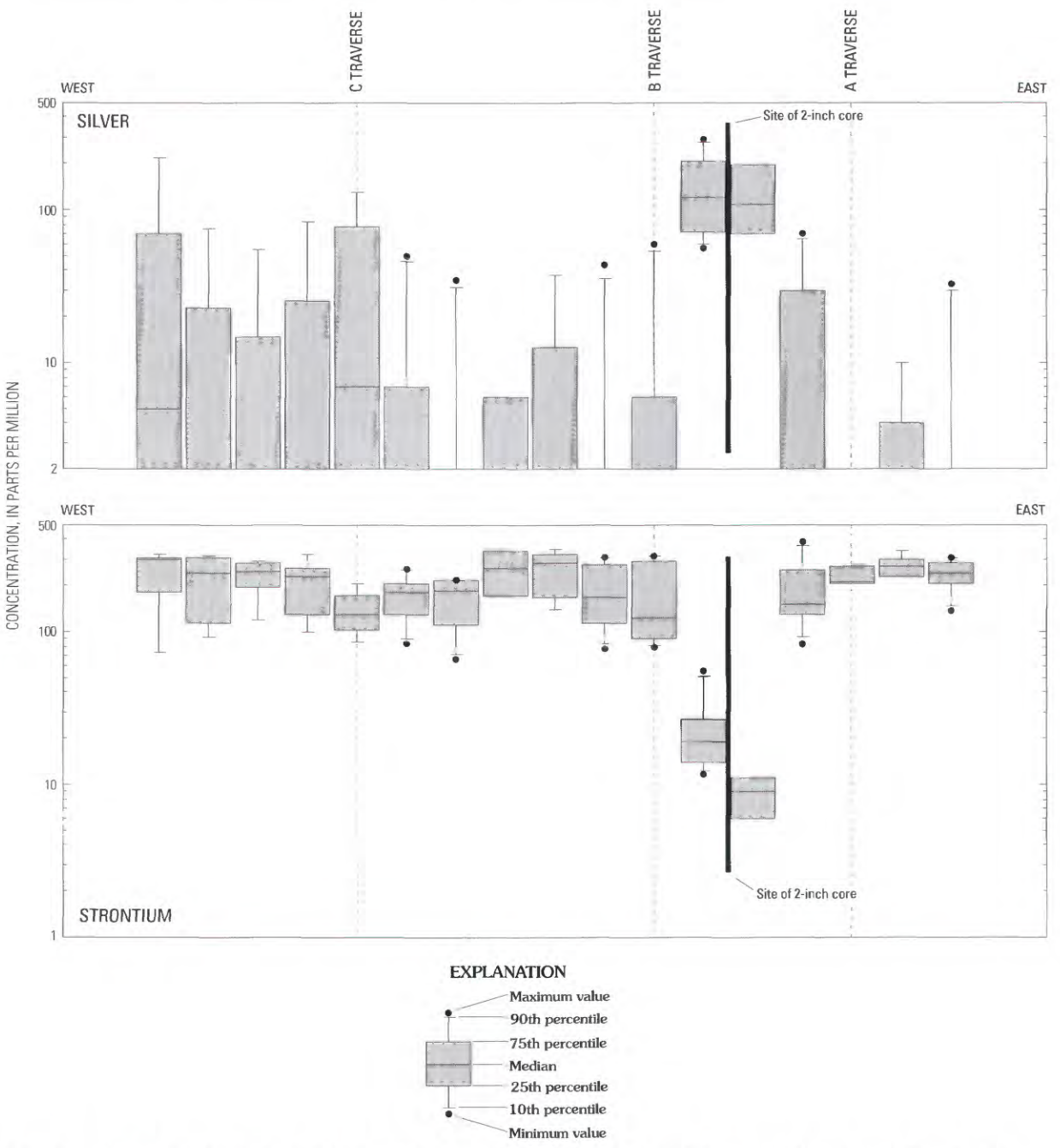

Figure 6. Range and distribution of silver and strontium concentrations in total digestions of 1-in. cores along main traverse through mill tailings, upper Basin Creek. Minimum concentration shown for silver is minimum reporting level of 2 parts per million. Location of main traverse line and sample sites shown in figure 3. Each core was divided into four to seven samples. Data are in Fey, Church, and Finney (1999).

Electromagnetic Survey of Conductive Materials

An electromagnetic (EM-34) survey conducted in 1998 and electromagnetic (EM-31) surveys conducted in 1998–99 were used to map subsurface conductivity of the mill tailings and the surrounding meadows and forested areas. These surveys measured the distribution of conductive materials in the subsurface at depths from about 10 to 100 ft. Measurements of conductivity at varying depths were achieved by use of two different EM instruments, with a horizontal and vertical transmitter/receiver dipole orientation for each instrument. In the horizontal magnetic dipole (HMD) orientation, the transmitter and receiver coils are perpendicular to the ground. In the vertical magnetic dipole (VMD) orientation, the transmitter and receiver coils are positioned parallel to the ground, resulting in a greater depth of exploration. The

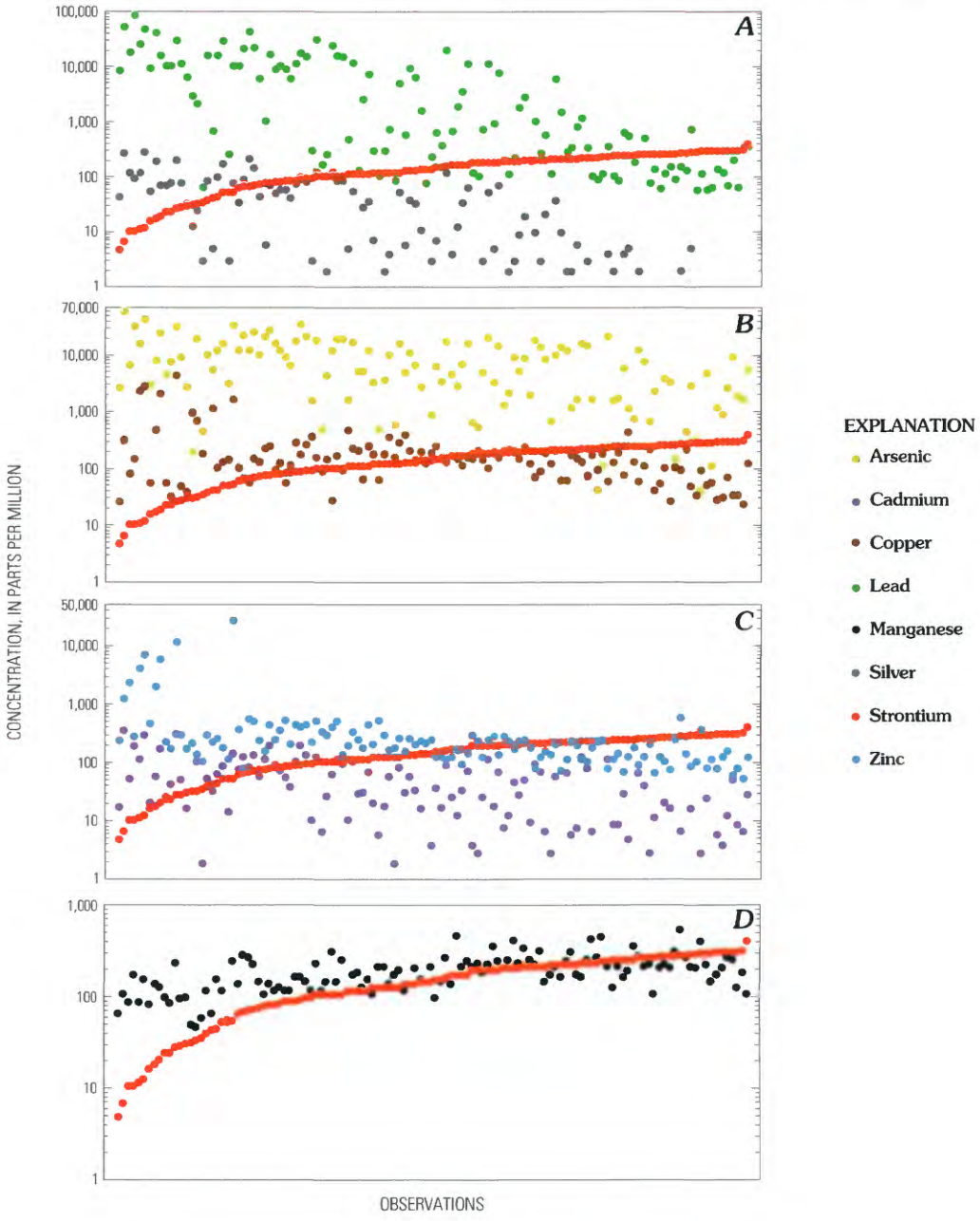

Figure 7. Relation of strontium and selected trace-element concentrations in total digests of 1-in. cores through mill tailings, upper Basin Creek. *A*, silver and lead; *B*, arsenic and copper; *C*, cadmium and zinc; *D*, manganese. Only data for samples from the contaminated zones of these cores are shown to reduce amount of data plotted. Contaminated zones were defined by Fey, Church, and Finney (1999) and included upper portion of each core where concentration of cadmium, copper, lead, silver, or zinc exceeded average crustal abundance values by about 10–50 times, depending on the trace element. Cadmium and silver concentrations reported as less than 2 parts per million are not plotted.

Geonics EM-34 has variable coil spacing that ranges from 33 ft (10 m) to 131 ft (40 m). For this survey, the EM-34 spacing was set at 33 ft, resulting in an approximate exploration depth of 49 ft in the VMD orientation, and an approximate depth of 25 ft (McNeill, 1980) in the HMD orientation. The Geonics EM-31 has a fixed intercoil spacing of 12 ft, which results in an exploration depth of approximately 20 ft in the VMD orientation, and approximately 10 ft in the HMD orientation. Data collected by each of these instruments will hereinafter be referred to based on their relative exploration depths, deep (EM-34) and shallow (EM-31). A survey grid (fig. 8) that covered the tailings and adjacent area was constructed with an origin point near the thickest part of the tailings.

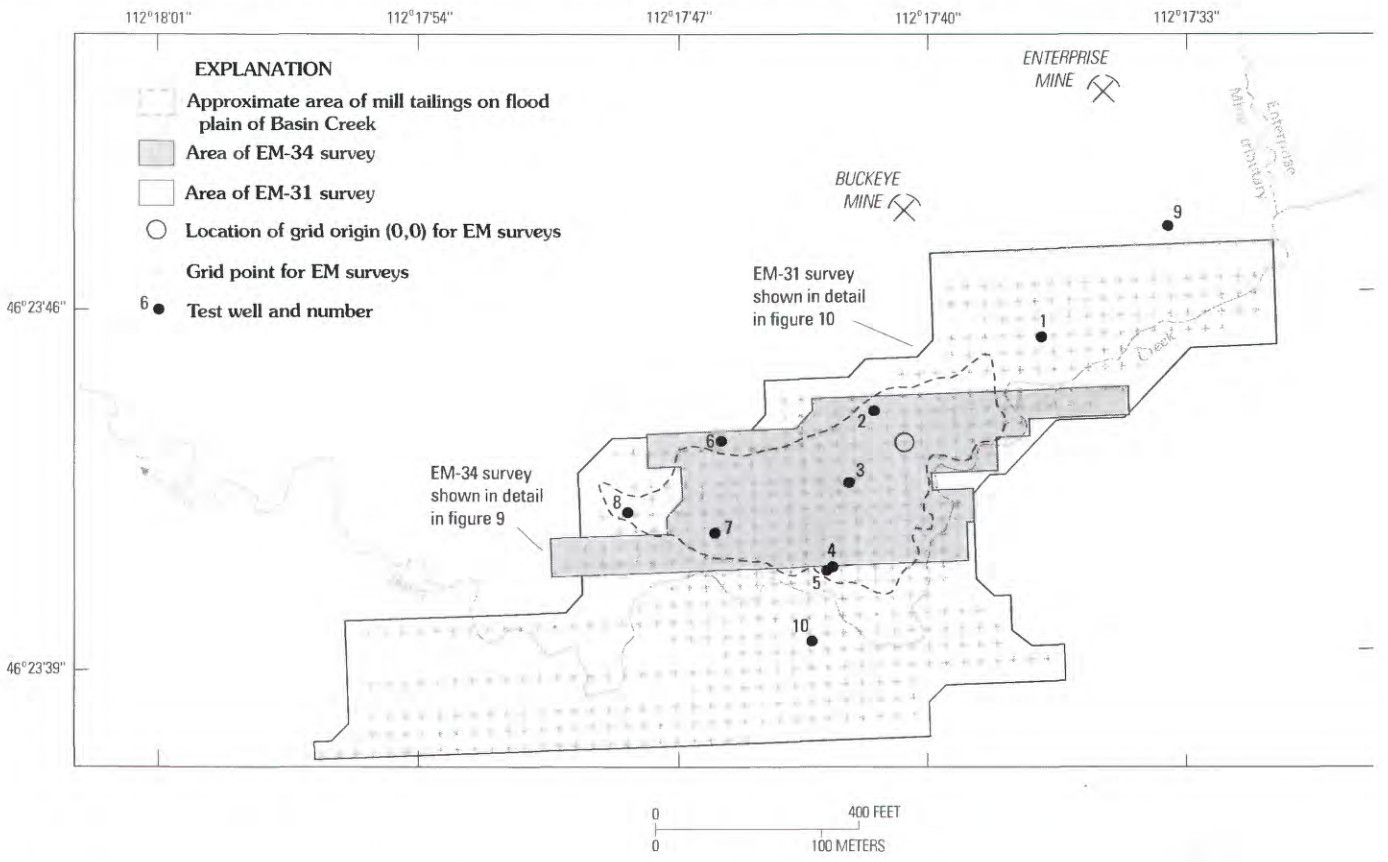

Figure 8. Location of electromagnetic (EM) survey grid and test wells.

Contours of the deep and shallow survey data show a high positive apparent-conductivity anomaly near the survey-grid origin (figs. 9*B* and 10). The 2-in. core collected near the conductivity anomaly encountered several layers about 1 in. thick of oxidized and unoxidized sulfides (table 1). Laboratory measurements of sulfide layers from the core show that the conductivity is on the order of 1,000 millisiemens per meter (mS/m) (D.V. Smith, written commun., 1999). The anomaly near the grid origin likely is the result of these highly conductive sulfide layers.

Contours of the deep VMD data show a negative conductivity anomaly near the survey-grid origin (fig. 9*A*). Buried magnetic metallic objects or lateral heterogeneities in layered deposits typically can result in similar responses. Another possibility is that the conductivity values, indicated in the core analysis, are high enough to allow for the low-induction-number approximation to be invalid. At high conductivity values (greater than 100 mS/m), the approximation of the linear relationship between instrument response and terrain conductivity becomes invalid and the reading becomes negative. This effect typically is more pronounced in the VMD orientation (McNeill, 1980).

The shallow contour maps (fig. 10) show three areas where subsurface conductivities substantially increase. First, an anomaly interpreted as a body of conductive material extends from the area of the survey-grid origin to the southwest toward Basin Creek (fig. 10*A*). This anomaly, in terms of depth, position, and conductivity, is consistent with the potentiometric surface and direction of ground-water flow at the mill-tailings site on the flood plain (fig. 14, presented in ground-water section). Second, the shallow contour map of VMD data shows an area of high conductivity in the northeast part of the survey area, south of the Enterprise mine. The higher conductivity observed in this area may be the result of elevated concentrations of major ions and trace elements in the ground water. A seep of red-colored water in the area of this anomaly was observed in July 1999. Third, an area of relatively high conductivity (fig. 10*A*) is indicated southwest of and on the other side of Basin Creek from the mill tailings in an area of wet meadows. Lithologic and geochemical data from cores or boreholes in this area are not available, but the conductivity could be the result of mill tailings deposited in this area during high streamflow. However, the higher conductivity more likely is caused by the presence of conductive clays or organic material, or both, in the meadow soil.

Magnetic Survey of Shallow Anomalies

During the summer of 1999, a total-field magnetic survey of the north-south and east-west base lines (fig. 11) was conducted using a proton precession magnetometer (Telford and others, 1990). Three measurements were taken at 33-ft (10-m)

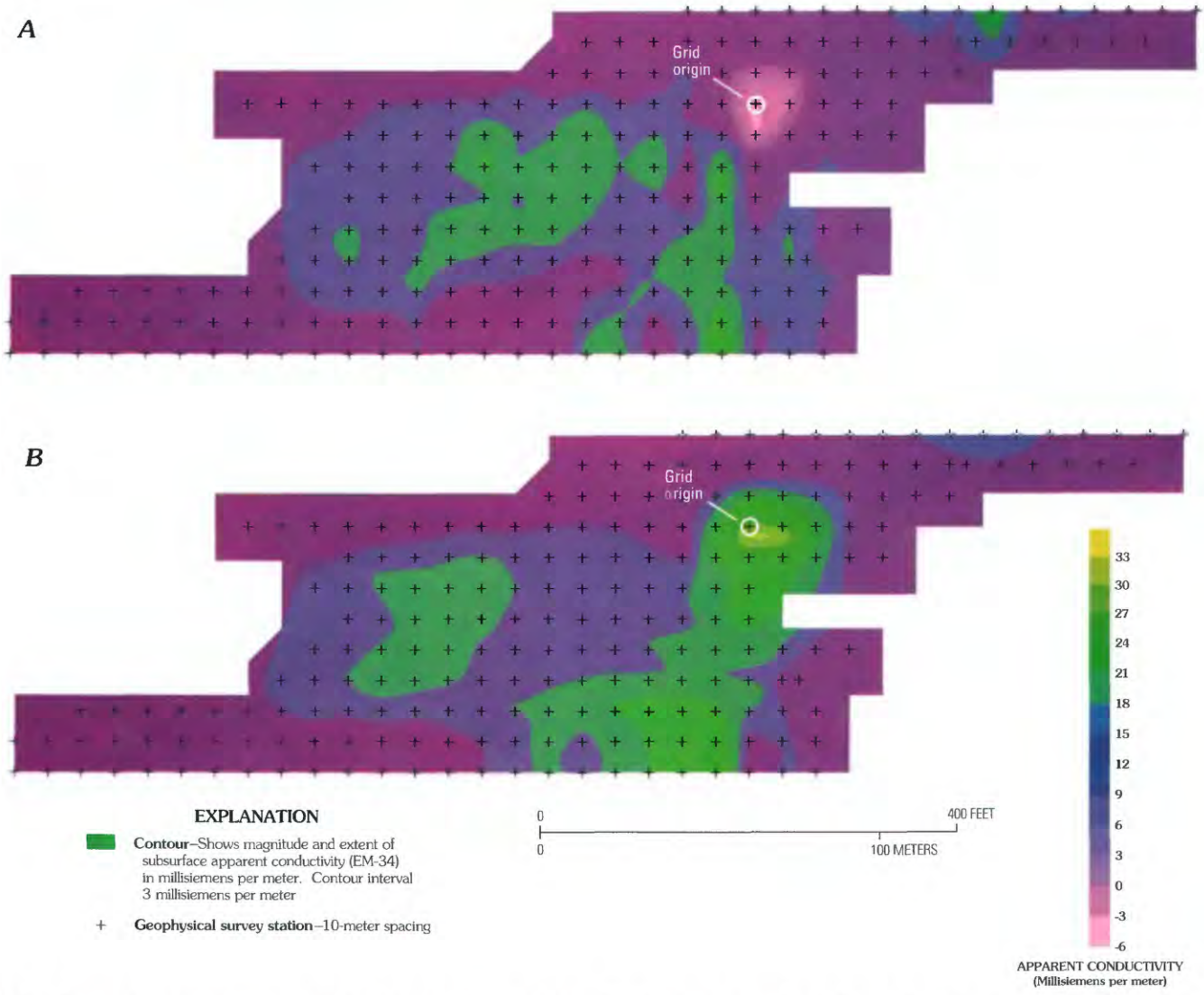

Figure 9. Deep subsurface apparent conductivity measured using an EM-34 along upper Basin Creek. *A*, vertical magnetic dipole; *B*, horizontal magnetic dipole.

intervals and averaged to account for temporal variations in the Earth's magnetic field. This survey was intended to detect buried magnetic metallic objects that might cause the local EM anomalies.

Of particular interest was the area near the grid origin where EM results indicated an area of high conductivity caused either by a buried conductive metallic object or by lateral heterogeneity in the layered mill tailings. The total-field magnetic survey indicated several metallic objects near the surface that caused local magnetic anomalies along the north-south magnetic survey line. However, no substantial magnetic anomalies were found along the east-west line, and no substantial magnetic anomalies were found in the area of the grid origin (fig. 12). Therefore, buried magnetic metallic objects are not a likely source of the high conductivity anomalies in the area of the grid origin. The likely source of the high conductivities is a zone of layered sulfides in the mill tailings.

Direct-Current Resistivity Soundings of Conductive Materials

Direct-current (DC) resistivity soundings were conducted in eight locations using an SAS DC resistivity system made by ABEM Instrument AB, Sweden, and a Schlumberger electrode array (Smith and Sole, 2000). Seven of these soundings were made on and near the main area of mill tailings (fig. 11) to provide detailed information about the subsurface variations and to possibly define the depth to bedrock. One additional sounding was made in an area of exposed granite bedrock about 2 mi northwest of the tailings (not shown in fig. 11) to directly measure the resistivity of bedrock. The sounding data (McDougal and Smith, 2000) were interpreted using software from Interpex (RESIX-IP version 2.14; Interpex, 1993).

Subsurface conductivity as interpreted from the DC soundings is shown in figure 13. Data from soundings DCS-1

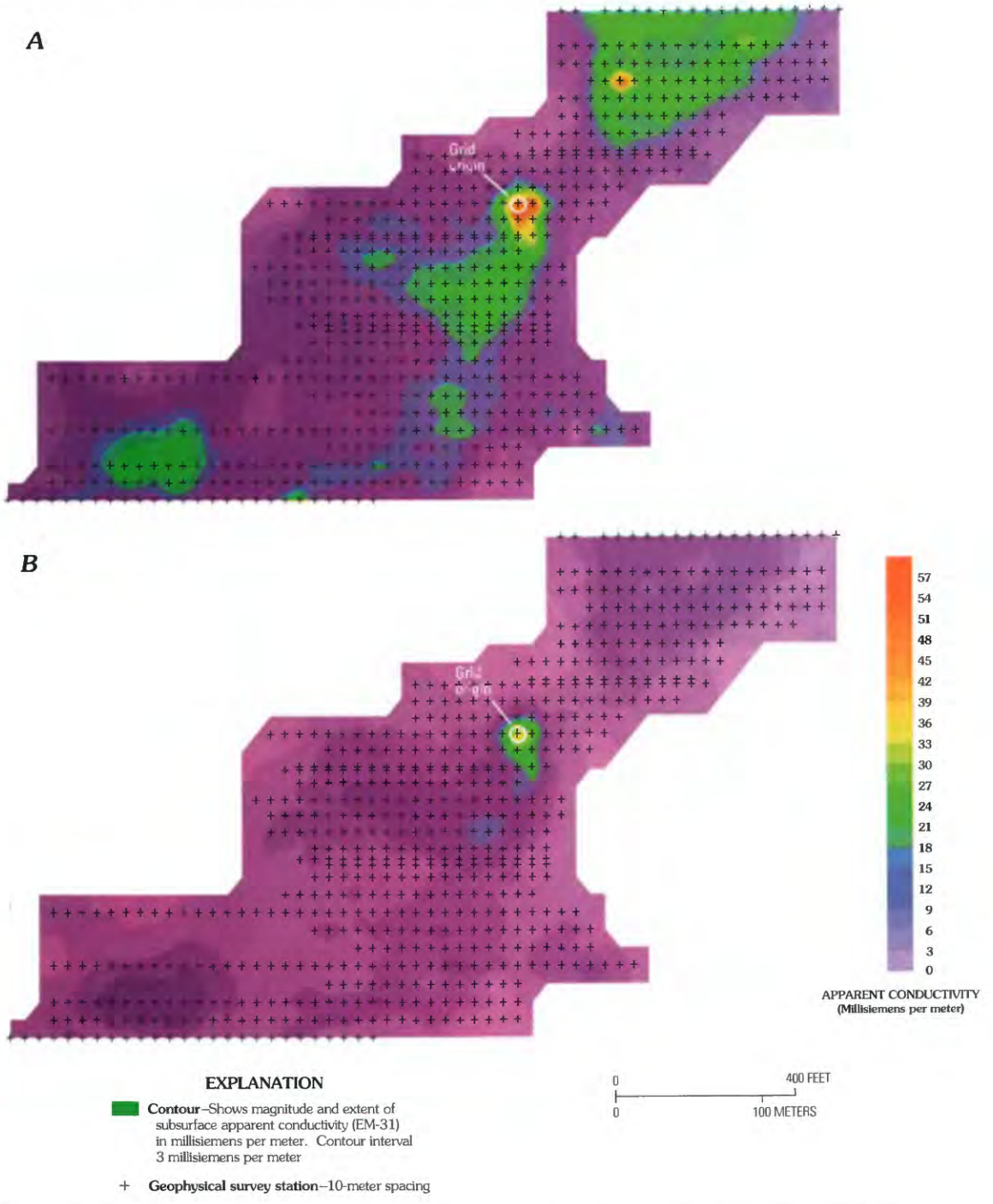

Figure 10. Shallow subsurface apparent conductivity measured using an EM-31 along upper Basin Creek. *A*, vertical magnetic dipole; *B*, horizontal magnetic dipole.

and DCS-3 (fig. 11) were not used because lateral heterogeneities affected the interpretation. For each sounding, the estimated subsurface conductivity was assumed to be located at the midpoint of the interpreted subsurface layer. The layer thickness increases at an approximately logarithmic rate because the resolution decreases at a similar rate. Consequently, the depths to points of estimated subsurface conductivity (sounding data points, fig. 13) increase logarithmically. The estimate of the conductivity of the last layer should be taken as relatively resistive or conductive because the soundings did not approach a constant value asymptotically at large electrode spacings.

A conductive anomaly at a depth of about 25 ft exists in the center of the section (fig. 13) at DCS-2. The anomaly is interpreted to be a body of conductive material, most likely ground water with high dissolved-solids concentrations. A

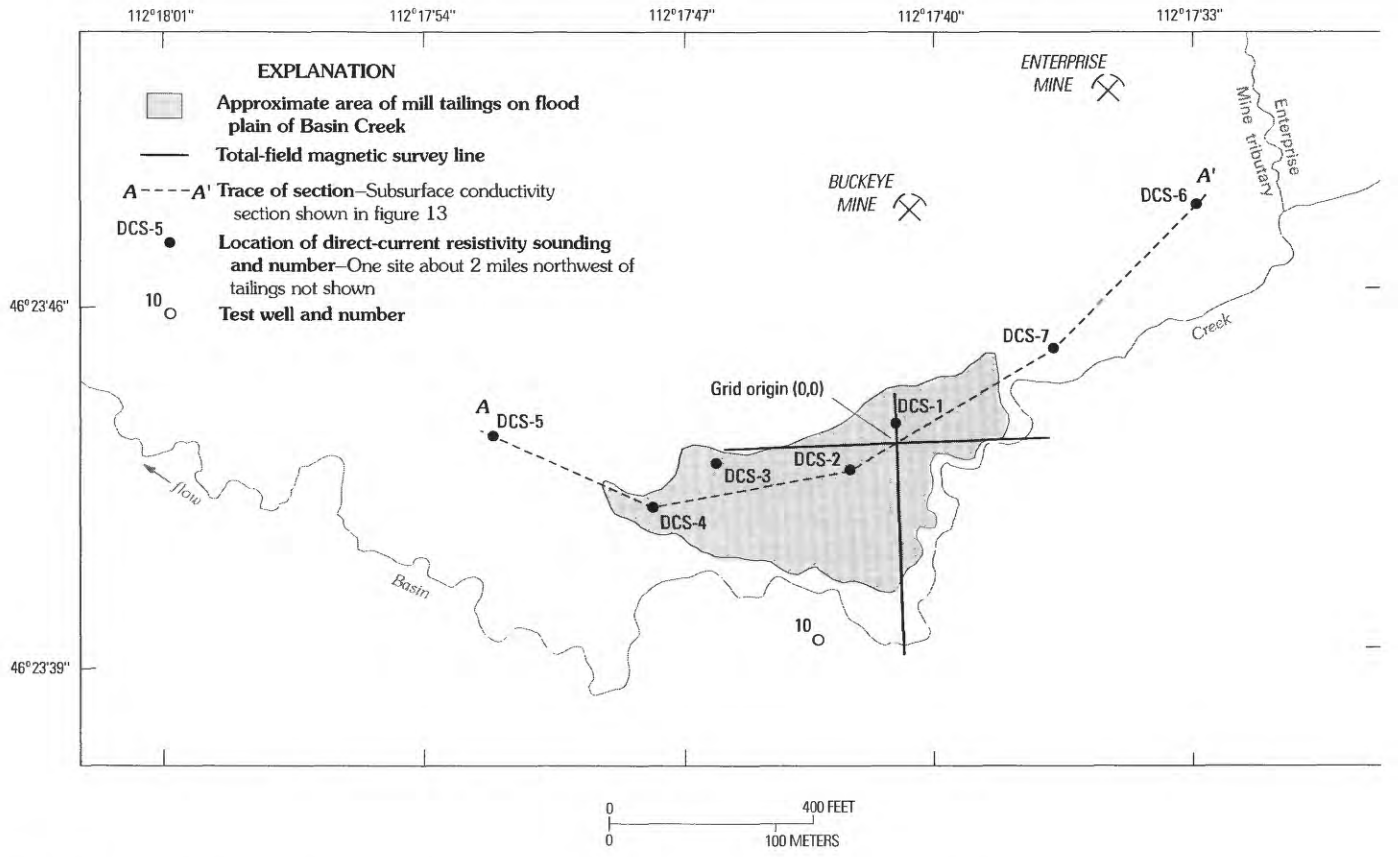

Figure 11. Location of total-field magnetic survey lines and direct-current (DC) resistivity soundings.

relatively high subsurface conductivity anomaly also exists at DCS-6. This anomaly is located between the Enterprise mine and upper Basin Creek.

The sounding made on a nearby bedrock outcrop to the northwest of the tailings (DCS-8) showed that the conductivity of shallow bedrock is about 5 mS/m. None of the subsurface conductivities are this low except perhaps for DCS-2, DCS-4, and DCS-5 (fig. 13). Consequently, granite underlying the mill tailings, with similar electrical properties as the outcropping area, may lie more than 98 ft deep. However, the granite in the stream valley likely is more weathered and has a higher volume of water than the outcrop area of DCS-8. Also, the underlying granite aquifer could have fractures that contain clays or that have water with high dissolved-solids content, which would produce higher conductivities and consequently place its depth at less than 98 ft.

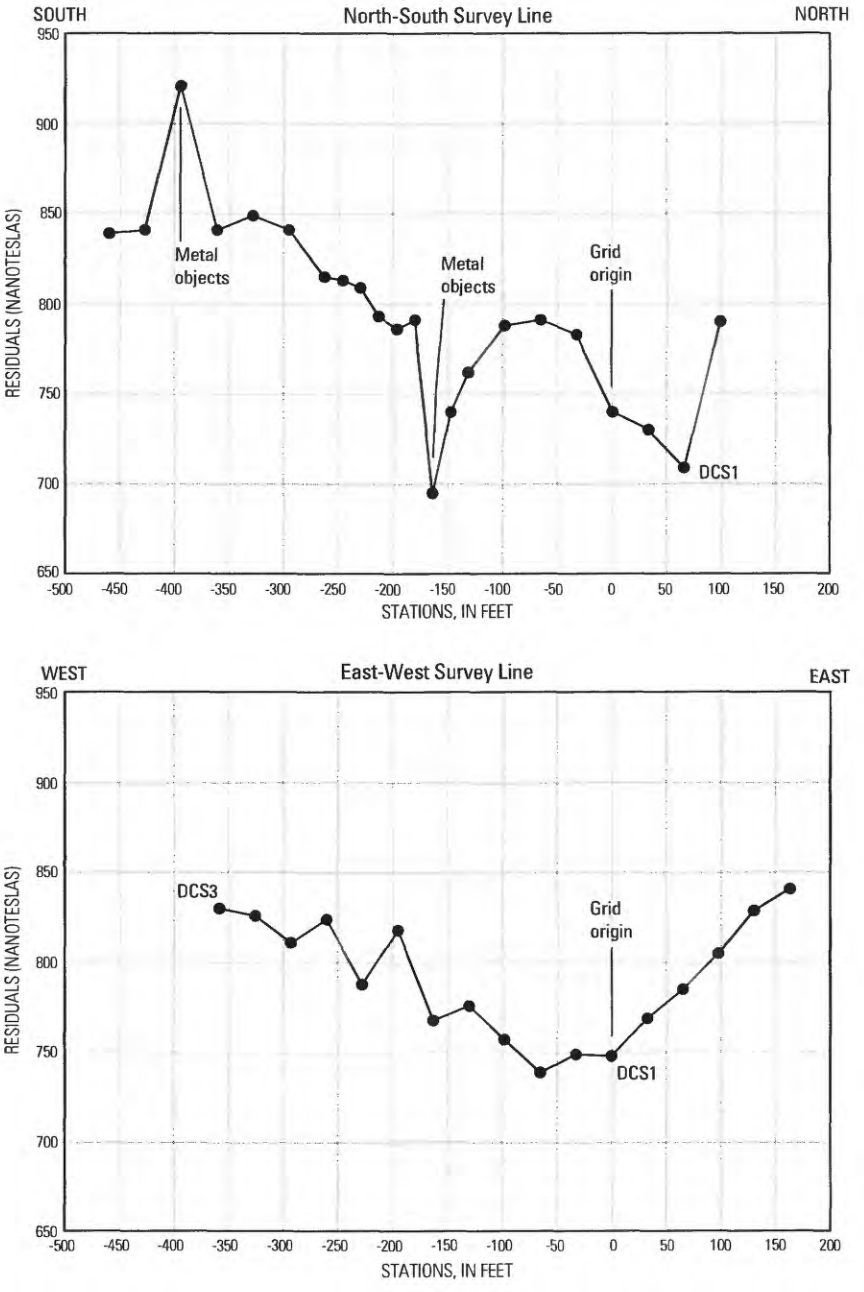

Figure 12. Results of total-field magnetic survey.

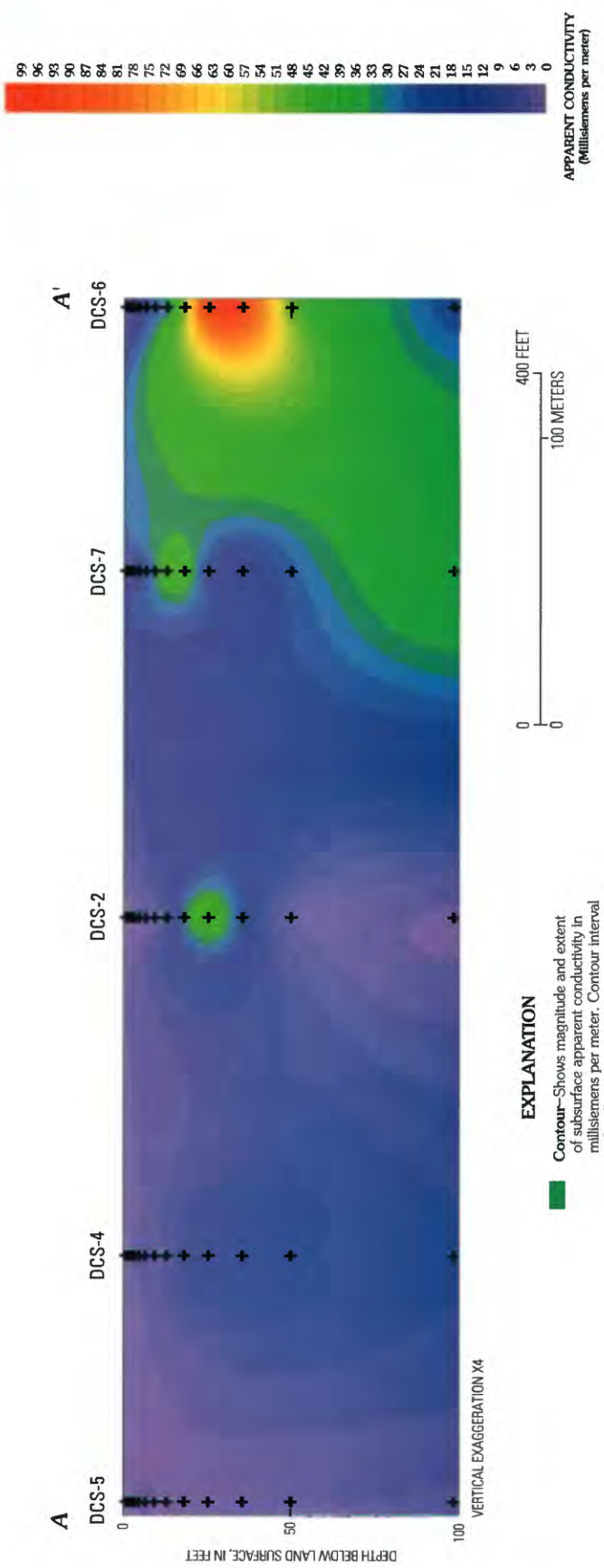

Figure 13. Subsurface conductivity from direct-current resistivity soundings. Trace of section shown in figure 11.

Transport of Trace Elements to Upper Basin Creek

Ground-water movement and surface-water runoff are the primary means of transport of trace elements from sources in the area of the Buckeye and Enterprise mines to upper Basin Creek. Studies were made of the local ground-water flow systems, quality of ground water, surface-water runoff, and quality of surface water to evaluate trace-element loads transported to upper Basin Creek by ground and surface water.

Ground Water

Ground-water resources along the upper Basin Creek valley and the area of the Buckeye and Enterprise mines were examined to identify aquifers and determine their characteristics, define ground-water and surface-water interaction along upper Basin Creek, and evaluate effects of acidic drainage on quality of ground water. Trace-element loads entering Basin Creek from acidic ground water in the study area were estimated to evaluate the effects of ground-water discharge on trace-element concentrations and loads in upper Basin Creek.

General Geohydrologic Setting

Two distinct aquifers, with vastly different hydraulic characteristics and flow systems, exist in the study area. One aquifer is a fractured bedrock system, composed of fractured, weathered, and mineralized granitic rocks of the Boulder batholith; the second aquifer is an unconsolidated porous system composed of till, alluvium, colluvium, organic-rich wetland deposits, and volcanic ash. The unconsolidated deposits underlie the flood plain of Basin Creek and overlie granitic rocks of the Boulder batholith.

Bedrock underlying the study area was originally mapped as Butte quartz monzonite of Late Cretaceous or Paleocene age (Ruppel, 1963). Recent studies have classified the Butte pluton as a medium- to coarse-grained hornblende-biotite granodiorite-tonalite (O'Neill and others, this volume, Chapter D1). Fractures in the bedrock are numerous and include several steeply dipping sets of joints and one gently dipping set. Ruppel (1963) reported that one prominent joint set trends about east and dips steeply north, and one set trends about north and dips steeply west. Individual joints in the rock are rarely more than 30 ft long, but where one joint dies out, it commonly is overlapped by a parallel joint that either is entirely separate from the other, or that is connected by a linking transverse joint. Joints are open and weathered where they are exposed in outcrops. However, with increasing depth, joints typically become tighter and less weathered or contain clay.

Hydraulic conductivity of the bedrock aquifer is directly related to the number, size, clay content, and degree of connection of joints. Hydraulic conductivity is greatest near the bedrock surface and decreases substantially within 5–50 ft of the surface, based on observations of fractures in outcrops, road cuts, core holes, and wells in the Boulder batholith. Most ground-water flow within the bedrock aquifer is in the uppermost fractured and weathered zone. Deeper fractures within the batholith can be saturated, as observed in a 100-ft-deep core hole 4 mi southeast of the study area, but fracture width and hydraulic conductivity generally are very small. Recharge from precipitation and snowmelt readily infiltrates the upper zone of weathered rock; shallow ground water follows the general topographic gradient and discharges to nearby seeps, springs, and streams. Discharge from the weathered bedrock commonly is observed at abrupt changes in topographic slope and at the contact between highly weathered and jointed rock and underlying rock that is less weathered. In the Buckeye study area, ground-water flow in the bedrock aquifer follows short flow paths from areas of recharge on slopes near the mines to areas of discharge along the valley margins and into sediments of the upper Basin Creek valley. Ground-water discharge, in the form of large seeps, was observed near the base of the bedrock hillsides south and southwest of the Buckeye and Enterprise mines. The ground-water discharge observed at this site is consistent with the conceptual model of ground-water flow as presented by McDougal and others (this volume, Chapter D9).

Saturated unconsolidated deposits that include till, alluvium, colluvium, wetland deposits, and volcanic ash form a heterogeneous aquifer that is hydraulically connected to Basin Creek. The unconsolidated deposits that compose the flood plain range from less than 1 ft to more than 30 ft thick and are overlain by mill tailings near the Buckeye mine. Bouldery till makes up a large part of the unconsolidated deposits. The till is exposed near the valley margin south of Basin Creek and along the stream banks about 1,200 ft downstream from the Buckeye flotation-mill tailings. Till overlies bedrock within much of the Basin Creek valley, and a small moraine at the lower end of the study area likely formed a natural dam to postglacial Basin Creek. Sediments that accumulated upstream from the moraine included stream-laid silt, sand, and gravel; organic-rich silt and clay; and volcanic ash from the eruption of Mount Mazama, about 6,845 years before present. Geologic and hydrologic characteristics of the unconsolidated-deposits aquifer were explored with shallow test wells.

Test Wells

Nine test wells (fig. 14; table 3) were drilled in the study area by Maxim Technologies Inc., under a contract with the USDA Forest Service. The wells were drilled into the unconsolidated deposits in the flood plain of Basin Creek to characterize the aquifer, to determine directions of ground-water flow, and to measure the quality of ground water. Seven of the test wells were installed in the area mantled by or adjacent to mill tailings. The test wells were installed using hollow-stem auger methods and were constructed of 2-in. diameter PVC (polyvinyl chloride) casing and screen, with 6-in. diameter

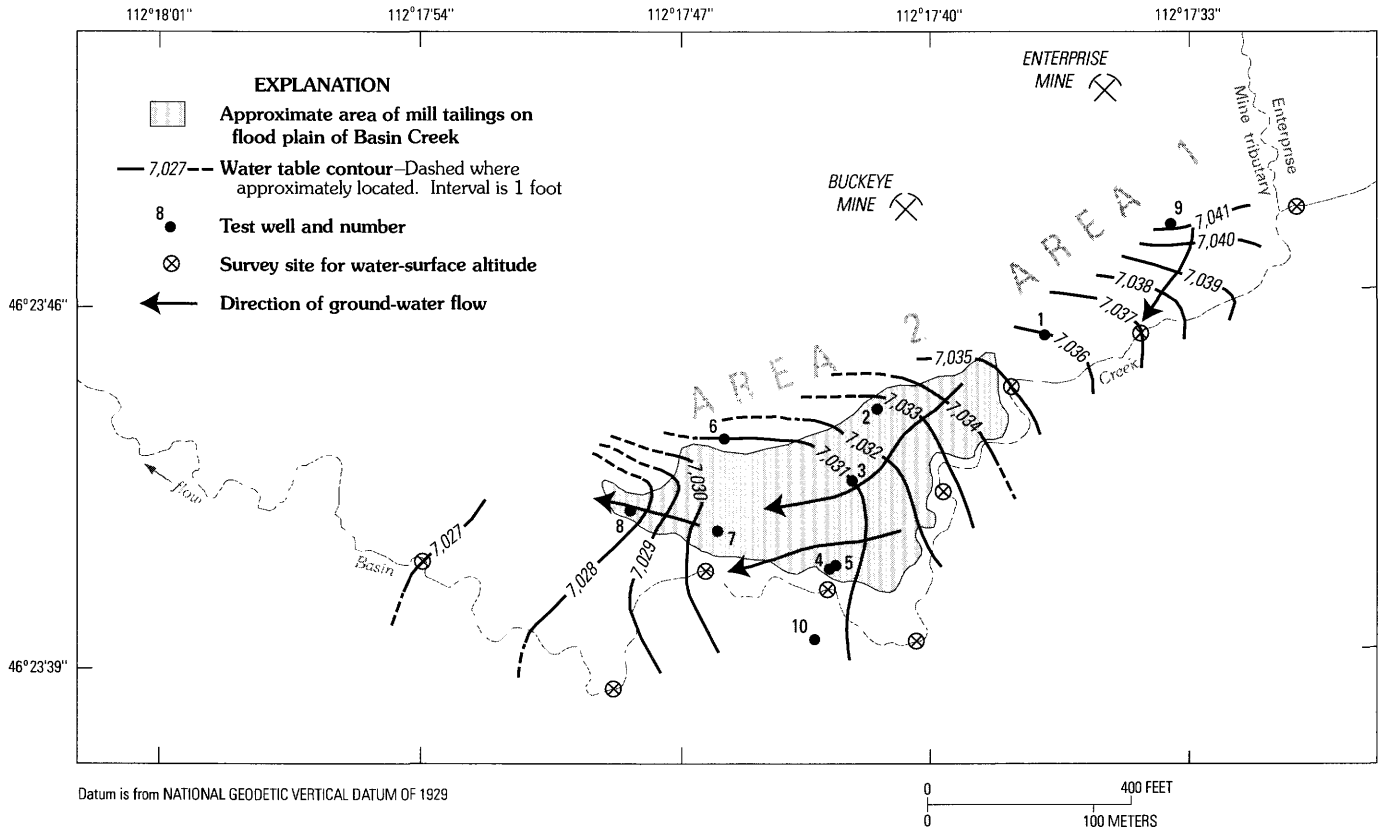

Figure 14. Location of test wells and configuration of water table, August 3, 1999.

Table 3. Well-completion data for test wells near upper Basin Creek.

[Data from Maxim Technologies, Inc., unpub. data, 1998]

Well No. (fig. 14)	Latitude N.	Longitude W.	Altitude of land surface (feet)	Drilled depth of well (feet)	Screen interval (feet)	Height of casing above land surface (feet)	Interval of bentonite seal (feet below land surface)
1	462344	1121737	7,038.6	10.8	5.6-10.6	2.8	0-3.6
2	462343	1121741	7,039.7	24.8	16.7-21.7	2.8	0-14.0
3	462342	1121742	7,034.8	11.0	5.5-10.5	3.0	0-3.7
4	462340	1121743	7,032.5	31.0	26-31	3.1	0-23.8
5	462340	1121742	7,032.8	8.5	3.5-8.5	3.0	0-2.2
6	462342	1121746	7,032.5	10.0	4.5-9.5	3.2	0-3.7
7	462341	1121746	7,032.3	11.0	5.5-10.5	2.9	0-4.7
8	462342	1121748	7,032.0	13.0	5.5-10.5	2.8	0-4.4
9	462347	1121733	7,043.6	17.0	10-15	2.3	0-8.9
10	462339	1121743	7,034.2	5.0	4-5	2.2	none[1]

[1]Sealed with cuttings.

steel protective casing at the surface. Each well screen was packed with silica filter sand and the entire annular space above the sand was sealed with bentonite. One additional shallow well (well 10) was drilled south of Basin Creek using a hand auger. Well 10 was installed in an area where an electromagnetic survey indicated moderately high values of conductivity and the possibility of ground water affected by acidic drainage from the Buckeye mill-tailings site.

Water Levels and Flow Directions

Water levels in test wells were measured periodically between December 1998 and August 1999 (table 4). Water-level data show that the water table is near land surface under the Basin Creek flood plain and in the area containing flotation-mill tailings. During part of the year, ground water saturates much of the mill tailings along Basin Creek. Water levels generally are highest in May and June, which also is when snowmelt and rain generally increase water depth and streamflow in upper Basin Creek. At well 6, measurements made in May and June documented water levels above land surface. Ground water was observed seeping from the ground in the vicinity of well 6 during that time.

A contour map showing the configuration of the water table (fig. 14) and direction of shallow ground-water flow was prepared using water-level measurements made on August 3, 1999. Water-level data for the contour map were collected from 10 wells and from water-surface altitudes of Basin Creek, surveyed at nine locations within the study area. Water-surface altitudes in Basin Creek were similar to water-table altitudes measured in shallow wells (wells 5 and 7) near the stream, indicating hydraulic connection between the stream and flood-plain sediments.

In the upstream part of the study area in the vicinity of wells 1 and 9, ground water flows southwesterly toward Basin Creek. Ground water probably moves from the vicinity of the Enterprise mine toward wells 1 and 9, and to Basin Creek, as inferred from the topographic slope in that area.

Water-level data from wells 2 through 8 indicate that ground water follows a curved flow path as it moves south and west through the area of mill tailings on the flood plain of Basin Creek. Ground water moves southward from the general area of the Buckeye mine toward wells 2 and 3 and then moves predominantly westward along the flood plain in the area of wells 4, 7, and 8. During low streamflow conditions (July through March), little or no ground water discharges to Basin Creek adjacent to or immediately downstream from the mill tailings. In the area of wells 4, 5, 7, and 10, water-level data indicate that some water may be moving from Basin Creek into the flood-plain deposits.

During higher streamflow conditions (generally late April, May, and June), water levels in wells are at their peak for the year. Based on synoptic streamflow measurements in May 1999, the high water table during spring and early summer does not cause a measurably larger discharge of ground water directly into Basin Creek than during low flow, probably because the stream also is at a higher stage at that time. It was observed that during higher water levels, water seeps out of the ground in the western and northwestern parts of the tailings deposits and that seepage drains into small tributaries flowing into Basin Creek.

Hydraulic properties of the unconsolidated-deposits aquifer were estimated from aquifer tests conducted at the nine test wells. Aquifer tests were made using a slug-injection method; changes in head were measured with a submersible pressure transducer and programmable data logger. Aquifer test data were analyzed using the curve-matching method of Cooper and others (1967). Results of aquifer tests are presented in table 5. Hydraulic conductivity values determined from the aquifer tests ranged over 3 orders of magnitude, from 0.03 to 40 ft/d. The median hydraulic conductivity was a relatively small 0.22 ft/d, reflecting the large amount of silt and clay in the sediments underlying the Basin Creek flood plain.

During low flow, discharge of ground water from the unconsolidated-deposits aquifer to Basin Creek is minimal. The water-table configuration and flow directions drawn from water-level data collected in August 1999 (fig. 14) show that ground water discharges to Basin Creek in the stream reach upstream from the mill tailings (area 1, fig. 14), but not in the area of mill tailings (area 2, fig. 14). Ground-water discharge to Basin Creek or rate of ground-water flow through sediments underlying the Basin Creek flood plain can be estimated from the gradient of the water table, cross-sectional area of the aquifer, and hydraulic conductivity of the sediments. The rate of ground-water discharge into Basin Creek within area 1 is about 25 ft^3/d, assuming an average gradient of 0.017, an aquifer cross-sectional area of 6,900 ft^2 (15 ft × 460 ft), and an average hydraulic conductivity of 0.21 ft/d (wells 1 and 9). The calculated rate of ground-water discharge within area 1 applies to discharge from the northwest side of Basin Creek and does not include discharge from the south side of the stream.

During low flow, Basin Creek receives little or no ground-water discharge through the area of mill tailings (area 2, fig. 14). Water-table contours in figure 14 indicate that near Basin Creek, ground water flows predominantly to the west, nearly parallel with the stream. The rate of ground-water flow through the upper 15 ft of sediments in the vicinity of wells 3 through 8 during low flow is about 220 ft^3/d. The calculated flow rate is for the cross section between Basin Creek and well 6, and assumes a gradient of 0.007 (4 ft/570 ft), an aquifer cross-sectional area of 3,750 ft^2 (15 ft × 250 ft), and an average hydraulic conductivity of 8.6 ft/d (average for wells 3–8, table 3).

Water Quality and Trace-Element Loads

Quality of ground water in deposits underlying the Basin Creek flood plain was determined by analysis of samples collected at 10 test wells (fig. 14). Seven of the ten test wells (wells 2-8) were in the area of mill tailings, one well (well 10) was south of Basin Creek, and two wells (wells 1 and 9) were

Table 4. Water levels, pH, and specific conductance of ground water from test wells near upper Basin Creek.

[µS/cm, microsiemens per centimeter at 25 degrees Celsius; --, no data]

Well No. (fig. 14)	Date	Water level, below or above (+) land surface (feet)	pH (standard units)	Specific conductance (µS/cm)
1	12-01-98	2.51	4.7	758
	02-23-99	2.62	3.8	768
	04-19-99	.41	--	--
	05-20-99	.16	--	--
	05-24-99	--	4.0	529
	06-07-99	--	3.4	556
	06-14-99	.18	--	--
	08-03-99	2.65	--	--
2	12-01-98	7.66	8.4	505
	02-23-99	7.83	8.2	447
	04-19-99	6.38	--	--
	05-20-99	5.02	--	--
	05-24-99	--	7.4	416
	06-07-99	--	7.2	414
	06-14-99	5.28	--	--
	08-03-99	7.10	--	--
3	12-01-98	3.78	4.9	1,260
	02-23-99	3.86	3.6	1,690
	04-19-99	2.98	--	--
	05-20-99	2.90	--	--
	05-24-99	--	4.2	1,200
	06-07-99	--	5.9	1,110
	06-14-99	3.12	--	--
	08-03-99	3.82	--	--
4	12-01-98	1.54	7.4	516
	02-23-99	1.65	8.0	443
	04-19-99	.91	--	--
	05-20-99	.68	--	--
	05-24-99	--	7.8	445
	06-07-99	--	7.8	409
	06-14-99	.95	--	--
	08-03-99	1.60	--	--
5	12-01-98	1.90	5.8	147
	02-23-99	2.03	6.0	136
	04-19-99	1.21	--	--
	05-20-99	.90	--	--
	05-24-99	--	3.6	1,530
	06-07-99	--	3.7	1,800
	06-14-99	1.24	--	--
	08-03-99	2.03	--	--
6	12-01-98	1.46	6.6	388
	02-23-99	1.52	6.5	364
	04-19-99	.43	--	--
	05-20-99	+.21	--	--
	05-24-99	--	6.4	371
	06-07-99	--	6.9	386

Table 4. Water levels, pH, and specific conductance of ground water from test wells near upper Basin Creek.—Continued

Well No. (fig. 14)	Date	Water level, below or above (+) land surface (feet)	pH (standard units)	Specific conductance (µS/cm)
6 (cont.)	06-14-99	+.22	--	--
	08-03-99	1.54	--	--
7	12-01-98	1.74	5.9	342
	02-23-99	1.88	5.4	290
	04-19-99	1.12	--	--
	05-20-99	1.02	--	--
	05-24-99	--	5.7	256
	06-07-99	--	6.6	330
	06-14-99	1.20	--	--
	08-03-99	1.85	--	--
8	12-01-98	4.58	6.3	381
	02-23-99	4.62	6.5	273
	04-19-99	4.01	--	--
	05-20-99	3.16	--	--
	05-24-99	--	6.2	390
	06-07-99	--	7.1	427
	06-14-99	3.48	--	--
	08-03-99	4.44	--	--
9	12-01-98	2.26	7.0	920
	02-23-99	2.29	6.9	924
	04-19-99	1.03	--	--
	05-20-99	.49	--	--
	05-24-99	--	6.6	903
	06-07-99	--	6.1	911
	06-14-99	.76	--	--
	08-03-99	2.43	--	--
10	07-30-99	--	6.5	167
	08-03-99	3.45	--	--

northeast of the mill tailings between Basin Creek and the Enterprise mine (fig. 14). Before the wells were sampled for chemical analysis in June and July 1999, they were purged on three occasions with a hand bailer. The wells were purged and sampled for pH and specific conductance in December 1998, and February and May 1999 (table 4).

Water samples were collected from wells 1–9 on June 7, 1999, and from well 10 on July 30, 1999, and analyzed for common ions and dissolved (0.45-micrometer (µm) filtration) trace elements (table 6). Samples from wells 1, 3, and 5 had relatively low pH and elevated concentrations of dissolved trace elements, indicating effects from acid drainage. Well 1, which is located northeast of the mill tailings, had water with a pH of 3.4 when sampled in June 1999. Water from well 1 had relatively high concentrations of dissolved aluminum, cadmium, copper, lead, manganese, and zinc (table 6). The largest dissolved lead concentration analyzed from the 10 wells was 36 micrograms per liter (µg/L) from well 1.

Water from well 3, located near the center of the mill tailings, had a pH of 5.9 when sampled in June 1999, although a sample taken in February 1999 had a pH of 3.6 (tables 4 and 6). Water from well 3 had high dissolved concentrations of dissolved aluminum, arsenic, iron, manganese, and zinc. The

Table 5. Hydraulic properties of unconsolidated deposits along upper Basin Creek.

[ft/d, foot per day; ft^2/d, foot squared per day]

Well No. (fig. 14)	Transmissivity (ft^2/d)	Hydraulic conductivity (ft/d)	Average horizontal hydraulic gradient in area of well (August 1999)	Geologic description of unconsolidated deposits in screen interval
1	1.0	0.20	0.010	Silty sand, sandy clay.
2	.19	.04	.018	Sandy, gravelly clay (till).
3	3.0	.60	.005	Sandy silt.
4	.25	.05	.003	Silty sand, sandy clay.
5	200	40	.003	Silty fine to coarse sand, sandy clay.
6	.16	.03	.018	Clayey sand, silty sand, gravel, weathered rock.
7	8.3	1.7	.015	Silty, clayey sand.
8	46	9.2	.015	Silty sand, gravel, cobbles.
9	1.1	.22	.024	Silty sand with some gravel.

largest arsenic concentration analyzed from the 10 wells was 19,000 µg/L from well 3.

Water from well 5 had a pH of 3.7 and relatively high concentrations of dissolved aluminum, arsenic, cadmium, copper, lead, manganese, and zinc. Of the 10 wells sampled, well 5 had the highest concentrations of aluminum (55,200 µg/L), cadmium (220 µg/L), copper (2,290 µg/L), and zinc (49,100 µg/L).

Wells 2, 4, 6, 7, and 8 were completed in the area of mill tailings between the Buckeye mine and Basin Creek. Water samples collected from these five wells in June 1999 had pH values that ranged from 6.6 at well 7 to 7.8 at well 4. Concentrations of dissolved aluminum, cadmium, copper, lead, and zinc were relatively low in water samples from wells 2, 4, and 6. Wells 2 and 4 are the deepest of the 10 wells and are completed in parts of the aquifer not directly affected by acid drainage. Well 6 is located at the northwestern margin of the mill tailings, upgradient from flow paths in the mill tailings, and also is not directly affected by acid drainage. Water from well 7 had relatively high concentrations of dissolved arsenic (680 µg/L) and iron (27,000 µg/L). Well 8 had a large concentration of dissolved zinc (10,300 µg/L).

Well 9, located south of the Enterprise mine, had a dissolved zinc concentration of 292 µg/L when sampled in June 1999. Well 10, located south of Basin Creek in an area not disturbed by mining, had relatively low concentrations of dissolved trace elements, except for arsenic (45 µg/L) and iron (15,000 µg/L).

Loads of trace elements reaching Basin Creek from shallow ground water can be estimated from trace-element concentrations sampled at wells and rates of ground-water flow through the upper part of the aquifer. For the stream reach upstream from the mill tailings (area 1, fig. 14), calculated ground-water discharge into Basin Creek is about 25 ft^3/d during low flow. The calculated ground-water discharge applies to the upper 15 ft of deposits, which contains most of the poor-quality water from acid drainage. Estimated trace-element loads to Basin Creek in area 1 are shown in table 7 and are based on the average trace-element concentrations at wells 1 and 9. Within area 2 of Basin Creek, ground-water flow predominantly is to the west, parallel to Basin Creek. During low flow, the dissolved trace-element load in ground water is not discharging directly to Basin Creek adjacent to the mill tailings (area 2) but likely enters Basin Creek downstream, probably within a zone from 500 to 1,200 ft west of the mill tailings. Flood-plain deposits are pinched off by a glacial moraine about 1,200 ft down valley from the mill tailings, favoring the discharge of ground water from the flood-plain deposits into Basin Creek in that area. Trace-element loads to Basin Creek from area 2 (table 7) are based on the average trace-element concentration at wells 3, 5, 6, 7, and 8 and the rate of ground-water discharge of about 220 ft^3/d during low flow.

Downstream increases in trace-element loads measured in upper Basin Creek through the Buckeye study area during low flow also can be used to evaluate the ground-water contribution to trace-element loads in Basin Creek. Water samples collected upstream (site 4B, fig. 15) and downstream (site 22B) from the mine area during low flow on October 16, 1998, showed substantial increases in some concentrations of dissolved aluminum, arsenic, manganese, and zinc (table 8). Dissolved aluminum increased from 2.3 µg/L above the mines to 12 µg/L below the mines, dissolved arsenic increased from 1 µg/L to 14 µg/L, dissolved manganese increased from 8 µg/L to 52 µg/ L, and dissolved zinc increased from 7 µg/L to 26 µg/L. Combining streamflow measurements with trace-element concentrations to compute instantaneous loads (table 9) indicated that dissolved aluminum load increased from 2.4 grams per day (g/d) above the mines to 19.4 g/d below the mines, dissolved arsenic load increased from 1.0 g/d to 22.6 g/d, dissolved copper load increased from <1 g/d to 3.2 g/d, dissolved manganese load increased from 8.4 g/d to 84.0 g/d, and dissolved zinc load increased from 7.4 g/d to 42.0 g/d.

Table 6. Concentrations of major ions and dissolved trace elements in ground water near upper Basin Creek.

[µg/L, micrograms per liter; µS/cm, microsiemens per centimeter at 25 degrees Celsius; mg/L, milligrams per liter; <, less than minimum reporting level]

Well No. (fig. 14)	Date	Specific conductance, field (µS/cm)	pH, field (standard units)	Alkalinity, laboratory (mg/L as $CaCO_3$)	Calcium, dissolved (mg/L)	Magnesium, dissolved (mg/L)	Sodium, dissolved (mg/L)	Potassium, dissolved (mg/L)	Sulfate, dissolved (mg/L as SO_4)
1	06-07-99	556	3.4	<1	64	11	5.3	2.4	270
2	06-07-99	414	7.2	79	43	14	17	4.5	120
3	06-07-99	1,110	5.9	<1	160	32	21	1.4	1,100
4	06-07-99	409	7.8	213	46	11	25	7.9	6.2
5	06-07-99	1,800	3.7	<1	240	36	17	1	1,100
6	06-07-99	386	6.9	125	44	9.5	14	5.3	56
7	06-07-99	330	6.6	16	31	8.1	4.9	1.5	100
8	06-07-99	427	7.1	29	45	11	9	<.1	160
9	06-07-99	911	6.1	94	140	27	16	6.5	390
10	07-30-99	167	6.5	64	14	4.6	5.9	.8	<0.1

Well No. (fig. 14)	Chloride, dissolved (mg/L)	Dissolved solids, sum of constituents (mg/L)	Aluminum, dissolved (µg/L)	Arsenic, dissolved (µg/L)	Cadmium, dissolved (µg/L)	Copper, dissolved (µg/L)	Iron, dissolved (µg/L)	Lead, dissolved (µg/L)	Manganese, dissolved (µg/L)	Zinc, dissolved (µg/L)
1	0.7	350	4,780	4	40	820	1,300	36	6,060	4,850
2	1.5	250	4	6	<1	1	55	<1	1,310	9
3	1.6	1,300	307	19,000	<1	2	130,000	3	7,080	12,200
4	4.4	230	3	26	<1	<1	310	<1	256	1
5	8.8	1,400	55,200	68	220	2,290	1,400	20	6,770	49,100
6	3.6	220	2	2	<1	<1	5,900	<1	3,770	9
7	1	190	8	680	<1	<1	27,000	<1	2,230	9
8	2.3	250	272	28	5	1	9,200	<1	2,290	10,300
9	.8	630	2	15	5	1	1,300	<1	1,140	292
10	.9	65	18	45	<1	<1	15,000	<1	135	2

Table 7. Estimated dissolved trace-element loads discharged to upper Basin Creek during low flow from shallow ground water in the vicinity of the Buckeye and Enterprise mines.

[g/d, grams per day]

Trace element	Load from area 1 (g/d)	Load from area 2[1] (g/d)
Aluminum	1.69	69.5
Arsenic	.007	24.7
Cadmium	.016	[2].28
Copper	.290	[2]2.85
Iron	.920	216
Lead	[2].025	[2].031
Manganese	2.55	27.6
Zinc	1.82	89.1

[1]Load from area 2 likely enters upper Basin Creek downstream from tailings area.

[2]For values that were reported as less than the minimum reporting level of 1 µg/L, the value of 1 µg/L was used to calculate an average trace-element concentration.

The increased load of trace elements in Basin Creek in the Buckeye study area during this base-flow period likely is primarily from ground-water discharge. These trace-element-load data collected during low flow support the calculations of ground-water discharge and verify that the volume of trace-element-rich ground water that enters Basin Creek near the mines is small. However, this ground-water discharge has a marked effect on concentrations in the stream due to the large concentrations of trace elements in the ground water and the small streamflow in Basin Creek. The loads contributed by ground water in areas 1 and 2 (table 7) can account for essentially all of the load increase during low flow in the study reach below the mines.

Dissolved trace elements entering Basin Creek from ground water generally do not cause the trace-element concentrations in Basin Creek to exceed the State of Montana acute aquatic-life standards during low flow. Dissolved and total-recoverable zinc concentrations (26 and 42 µg/L) at site 22B below the Buckeye mine (sample of October 16, 1998) were near the chronic and acute aquatic-life standard of 40 µg/L (Montana Department of Environmental Quality, 1999).

During spring snowmelt and resulting high streamflow, ground water with high dissolved trace-element concentrations (table 6) discharges from the mill tailings and increases the trace-element load in Basin Creek. The water table is at or near land surface during snowmelt. Shallow ground water and overland runoff leach the entire thickness of tailings and carry dissolved trace elements toward Basin Creek. Ground water seeps out of the upper part of the saturated tailings, combines with overland runoff, and flows into very small tributaries which discharge into Basin Creek. Shallow ground water also discharges directly to Basin Creek through diffuse bank seepage. Trace-element concentrations of these small tributaries were sampled during high runoff in May 1999 and are discussed in subsequent sections of this report.

Streambed Sediment in Basin Creek

Streambed-sediment samples were collected at six sites along Basin Creek (fig. 15) (Fey, Unruh, and Church, 1999). The minus-80-mesh (<0.18 mm) fraction was analyzed for leachable trace elements (Rich and others, this volume) to determine the location and magnitude of potential effects from the mine area. Trace-element concentrations in streambed-sediment samples are influenced by the input of material eroded upstream of the sample site as well as by the formation and subsequent deposition of colloidal material on the streambed during periods of low streamflow. Downstream increases in the concentrations of iron and trace elements are readily apparent in the streambed-sediment data summarized in table 10 and indicate that the Buckeye and Enterprise mine area is a source of iron and trace elements transported to Basin Creek and deposited on the streambed. The concentrations of antimony, arsenic, lead, and silver increase dramatically in the downstream direction, particularly between sites 21bS and 21cS, which are adjacent to the central part of the flotation-mill tailings. The location of these increases indicates the importance of the flotation-mill tailings as a source of trace elements that presumably have been transported via both surface water and ground water to Basin Creek. Ferricrete deposits (iron-hydroxide-cemented lithic deposits) on the north bank of Basin Creek at sites 21bS and 21cS provide additional evidence that iron has been transported by ground water from the mill-tailings area to Basin Creek. In contrast to antimony, arsenic, lead, and silver, the increases in concentrations of cadmium, copper, and zinc in streambed sediment are less dramatic, probably because these latter trace elements partition less strongly to the colloidal and particulate phases (Church and others, 1997; Schemel and others, 2000; Nimick and Cleasby, this volume, Chapter D5).

Surface Water

Basin Creek, a tributary of the Boulder River, drains the Buckeye study area and surrounding lands. Upper Basin Creek enters the study area from the east, is joined by a small south-flowing tributary near the Enterprise mine, and flows westerly through the study area (fig. 15). At the tributary confluence (near site 4B) above the Buckeye mine, upper Basin Creek has a drainage area of 1.51 mi^2; land-surface altitudes within this drainage area range from about 7,060 to 8,568 ft. The small south-flowing tributary (Enterprise Mine tributary) that joins upper Basin Creek in the eastern part of the study area (site 3T) has a drainage area of 0.32 mi^2 and land-surface altitudes that range from 7,060 to 7,580 ft. The combined drainage area of upper Basin Creek at the mouth of this tributary is 1.83 mi^2.

Table 8. Streamflow and water-quality data for upper Basin Creek, 1996–99.

[ft^3/s, cubic feet per second; °C, degrees Celsius; µg/L, micrograms per liter; µS/cm, microsiemens per centimeter at 25 degrees Celsius; mg/L, milligrams per liter; mm, millimeter; --, no data; <, less than minimum reporting level]

Site No. (fig. 15)	Site No.[1]	Station name	Date	Time	Streamflow, instantaneous (ft^3/s)	Specific conductance, field (µS/cm)	Temperature, water (°C)	pH, field (standard units)	Sediment, suspended (mg/L)	Sediment, suspended, diameter (percent finer than 0.062 mm)	Hardness (mg/L as $CaCO_3$)
4B	5	Basin Creek above Buckeye mine, near Basin	10-16-96	1030	--	78	--	--	--	--	--
			09-25-98	1345	0.44	79	5.0	7.6	29	99	32
			10-16-98	1045	.43	76	1.0	7.8	1	80	31
			05-28-99	1010	7.9	37	2.0	8.1	--	--	16
			09-13-99	1115	.34	79	5.0	7.8	--	--	--
3T	6	Enterprise Mine tributary near Basin	10-16-98	1055	.05	87	1.0	8.3	1	67	36
			05-28-99	1030	1.7	42	6.0	7.1	--	--	16
			09-13-99	1030	.009	104	4.0	7.9	--	--	--
6B	7	Basin Creek below Enterprise Mine tributary, near Basin	05-27-97	1130	12	42	4.0	--	--	--	--
			04-30-98	1100	5.0	55	0.0	7.0	8	66	23
			05-07-98	1315	10	45	--	7.7	48	46	18
			10-16-98	1340	.48	75	.5	7.7	1	75	31
			05-28-99	0945	9.2	39	2.5	7.2	--	--	16
			09-13-99	1130	.37	80	5.0	7.8	--	--	--
22B	8	Basin Creek below Buckeye mine, near Basin	10-16-96	1010	.51	82	0.0	7.3	1	62	34
			05-27-97	1045	15	44	5.0	7.1	10	36	16
			04-30-98	1015	6.3	57	3.0	7.3	16	32	23
			05-07-98	1445	17	49	3.0	7.0	74	77	17
			09-25-98	1215	.49	80	8.0	7.8	4	79	32
			10-16-98	1315	.66	75	.5	7.6	4	82	27
			05-28-99	0840	13	39	2.0	6.7	--	--	16
			09-13-99	1250	.35	82	11.0	7.9	--	--	--

[1]Site number previously published in Nimick and Cleasby (2000).

Table 8. Streamflow and water-quality data for upper Basin Creek, 1996–99.—Continued

Site No. (fig. 15)	Date	Calcium (mg/L)	Magnesium (mg/L)	Sodium (mg/L)	Potassium (mg/L)	Alkalinity, laboratory (mg/L as $CaCO_3$)	Sulfate (mg/L as SO_4)	Chloride (mg/L)	Fluoride (mg/L)	Silica (mg/L)	Dissolved solids, calculated (mg/L)
4B	10-16-96	--	--	--	--	--	--	--	--	--	--
	09-25-98	9.5	2.1	2.2	1.1	32	6.8	0.19	<0.10	14	55
	10-16-98	9.0	2.1	2.0	1.1	31	6.7	.24	<.10	14	53
	05-28-99	4.8	1.0	1.1	.68	15	2.7	.24	--	--	--
	09-13-99	--	--	--	--	--	--	--	--	--	--
3T	10-16-98	10	2.6	2.5	1.0	35	7.1	.26	<.10	11	55
	05-28-99	4.8	1.0	1.3	.64	11	6.6	.84	--	--	--
	09-13-99	--	--	--	--	--	--	--	--	--	--
6B	05-27-97	--	--	--	--	--	--	--	--	--	--
	04-30-98	6.7	1.5	1.3	1.0	19	6.5	.23	<.10	8.9	38
	05-07-98	5.4	1.2	1.1	.77	14	5.8	.27	<.10	7.2	31
	10-16-98	9.0	2.1	2.1	.94	31	6.8	.21	<.10	13	53
	05-28-99	4.8	1.0	1.2	.67	14	3.5	.21	--	--	--
	09-13-99	--	--	--	--	--	--	--	--	--	--
22B	10-16-96	10	2.3	2.3	1.0	32	8.7	.30	<.10	13	57
	05-27-97	4.8	1.1	1.2	.67	12	7.6	.19	<.10	9.6	33
	04-30-98	6.8	1.5	1.3	1.2	20	7.1	.28	<.10	8.9	40
	05-07-98	5.0	1.1	1.1	.91	10	8.7	.22	<.10	7.8	32
	09-25-98	9.3	2.2	2.2	.99	31	7.8	.19	<.10	14	56
	10-16-98	7.7	1.8	2.0	.83	29	7.5	.22	<.10	13	51
	05-28-99	4.7	1.0	1.2	.68	13	4.7	.22	--	--	--
	09-13-99	--	--	--	--	--	--	--	--	--	--

Table 8. Streamflow and water-quality data for upper Basin Creek, 1996–99.—Continued

Site No. (fig. 15)	Date	Aluminum, dissolved (µg/L)	Aluminum, total recoverable (µg/L)	Antimony, dissolved (µg/L)	Arsenic, dissolved (µg/L)	Arsenic, total recoverable (µg/L)	Barium, dissolved (µg/L)	Beryllium, dissolved (µg/L)	Cadmium, dissolved (µg/L)	Cadmium, total recoverable (µg/L)	Chromium, dissolved (µg/L)	Chromium, total recoverable (µg/L)
4B	10-16-96	--	--	--	--	--	--	--	--	--	--	--
	09-25-98	8.3	1,300	<1	3	4	8.1	<1	<0.3	<1	<1	--
	10-16-98	2.3	17	<1	1	2	4.7	<1	<.3	<1	<1	--
	05-28-99	52	185	--	2	4	--	--	<.3	<1	--	--
	09-13-99	--	--	--	--	--	--	--	--	--	--	--
3T	10-16-98	3.8	21	<1	<1	3	5.5	<1	<.3	<1	<1	--
	05-28-99	160	440	--	3	8	--	--	1.9	2	--	--
	09-13-99	--	--	--	--	--	--	--	--	--	--	--
6B	05-27-97	--	--	--	--	--	--	--	--	--	--	--
	04-30-98	149	350	<1	3	5	6.1	<1	<.3	<1	<1	--
	05-07-98	102	900	<1	7	10	5.5	<1	.5	<1	<1	--
	10-16-98	13	<10	<1	2	2	4.7	<1	<.3	<1	<1	--
	05-28-99	66	220	--	2	3	--	--	.4	<1	--	--
	09-13-99	--	--	--	--	--	--	--	--	--	--	--
22B	10-16-96	22	--	3	16	19	5.0	<1	.2	<1	<1	<1
	05-27-97	225	430	2	13	36	6.1	<1	1.2	1	<1	<1
	04-30-98	154	430	3	29	52	7.9	<1	.8	<1	<1	--
	05-07-98	219	1,300	7	38	500	8.3	<1	1.4	2	<1	--
	09-25-98	13	90	4	21	24	5.8	<1	<.3	<1	<1	--
	10-16-98	12	72	2	14	30	4.3	<1	<.3	<1	<1	--
	05-28-99	120	300	--	10	25	--	--	.6	<1	--	--
	09-13-99	--	--	--	--	--	--	--	--	--	--	--

Table 8. Streamflow and water-quality data for upper Basin Creek, 1996–99.—Continued

Site No. (fig. 15)	Date	Cobalt, dissolved (µg/L)	Copper, dissolved (µg/L)	Copper, total recoverable (µg/L)	Iron, dissolved (µg/L)	Iron, total recoverable (µg/L)	Lead, dissolved (µg/L)	Lead, total recoverable (µg/L)	Lithium, dissolved (µg/L)	Manganese, dissolved (µg/L)	Manganese, total recoverable (µg/L)
4B	10-16-96	--	--	--	--	--	--	--	--	--	--
	09-25-98	<1	<1	3	17	1,200	<1	7	--	13	46
	10-16-98	<1	<1	<1	48	71	<1	<1	--	8	<10
	05-28-99	--	2	2	61	240	<1	1	--	3	11
	09-13-99	--	--	--	--	--	--	--	--	--	--
3T	10-16-98	<1	<1	<1	50	190	<1	<1	--	54	73
	05-28-99	--	11	14	79	460	<1	1	--	178	220
	09-13-99	--	--	--	--	--	--	--	--	--	--
6B	05-27-97	--	--	--	--	--	--	--	--	--	--
	04-30-98	<1	9	9	190	600	<1	1	--	184	200
	05-07-98	<1	5	7	160	2,000	<1	7	--	229	330
	10-16-98	<1	<1	<1	103	130	<1	<1	--	28	26
	05-28-99	--	4	3	54	230	<1	<1	--	39	43
	09-13-99	--	--	--	--	--	--	--	--	--	--
22B	10-16-96	<1	2	4	130	170	<1	3	<4	65	70
	05-27-97	<1	18	18	180	530	10	24	<4	136	140
	04-30-98	<1	11	12	240	880	7.7	28	--	187	200
	05-07-98	<1	18	40	240	3,200	23	340	--	306	410
	09-25-98	<1	2	3	93	250	<1	2	--	48	55
	10-16-98	<1	2	3	88	380	<1	9	--	52	74
	05-28-99	--	9	11	100	350	5.4	17	--	85	91
	09-13-99	--	--	--	--	--	--	--	--	--	--

Table 8. Streamflow and water-quality data for upper Basin Creek, 1996–99.—Continued

Site No. (fig. 15)	Date	Mercury, dissolved (µg/L)	Mercury, total recoverable (µg/L)	Molybdenum, dissolved (µg/L)	Nickel, dissolved (µg/L)	Nickel, total recoverable (µg/L)	Silver, dissolved (µg/L)	Silver, total recoverable (µg/L)	Uranium, dissolved (µg/L)	Zinc, dissolved (µg/L)	Zinc, total recoverable (µg/L)
4B	10-16-96	--	--	--	--	--	--	--	--	--	<10
	09-25-98	--	--	<1	<1	--	<1	--	<1	3	20
	10-16-98	--	--	<1	<1	--	<1	--	<1	7	10
	05-28-99	--	--	--	--	--	--	--	--	6	<40
	09-13-99	--	--	--	--	--	--	--	--	--	--
3T	10-16-98	--	--	<1	<1	--	<1	--	<1	15	21
	05-28-99	--	--	--	--	--	--	--	--	234	250
	09-13-99	--	--	--	--	--	--	--	--	--	--
6B	05-27-97	--	--	--	--	--	--	--	--	--	100
	04-30-98	--	--	<1	1	--	<1	--	<1	129	130
	05-07-98	--	--	<1	1	--	<1	--	<1	109	140
	10-16-98	--	--	<1	<1	--	<1	--	<1	12	15
	05-28-99	--	--	--	--	--	--	--	--	49	52
	09-13-99	--	--	--	--	--	--	--	--	--	--
22B	10-16-96	<0.1	<0.1	<1	<1	<1	<1	<1	<1	39	40
	05-27-97	--	<.1	<1	<1	<1	<1	<1	<1	173	180
	04-30-98	--	--	<1	1	--	<1	--	<1	140	150
	05-07-98	--	--	<1	<1	--	<1	--	<1	218	270
	09-25-98	--	--	<1	<1	--	<1	--	<1	24	30
	10-16-98	--	--	<1	<1	--	<1	--	<1	26	42
	05-28-99	--	--	--	--	--	--	--	--	90	95
	09-13-99	--	--	--	--	--	--	--	--	--	--

Table 9. Dissolved trace-element loads in upper Basin Creek upstream and downstream of the Buckeye and Enterprise mines, October 16, 1998.

[g/d, grams per day; <, less than]

Trace element	Instantaneous load upstream[1] (g/d)	Instantaneous load downstream[1] (g/d)
Aluminum	2.4	19.4
Arsenic	1.0	22.6
Cadmium	[2]<.4	<.5
Copper	[2]<1	3.2
Iron	50.5	142
Lead	[2]<1.2	[2]<1.6
Manganese	8.4	84.0
Zinc	7.4	42.0

[1]Site 4B used to represent load upstream of the mines, instantaneous streamflow was 0.43 ft^3/s; site 22B used to represent load downstream, instantaneous streamflow was 0.66 ft^3/s.

[2]For concentrations that were reported as less than the minimum reporting level, the value of 1 µg/L for lead and copper and 0.3 µg/L for cadmium was used to calculate a maximum value for the load.

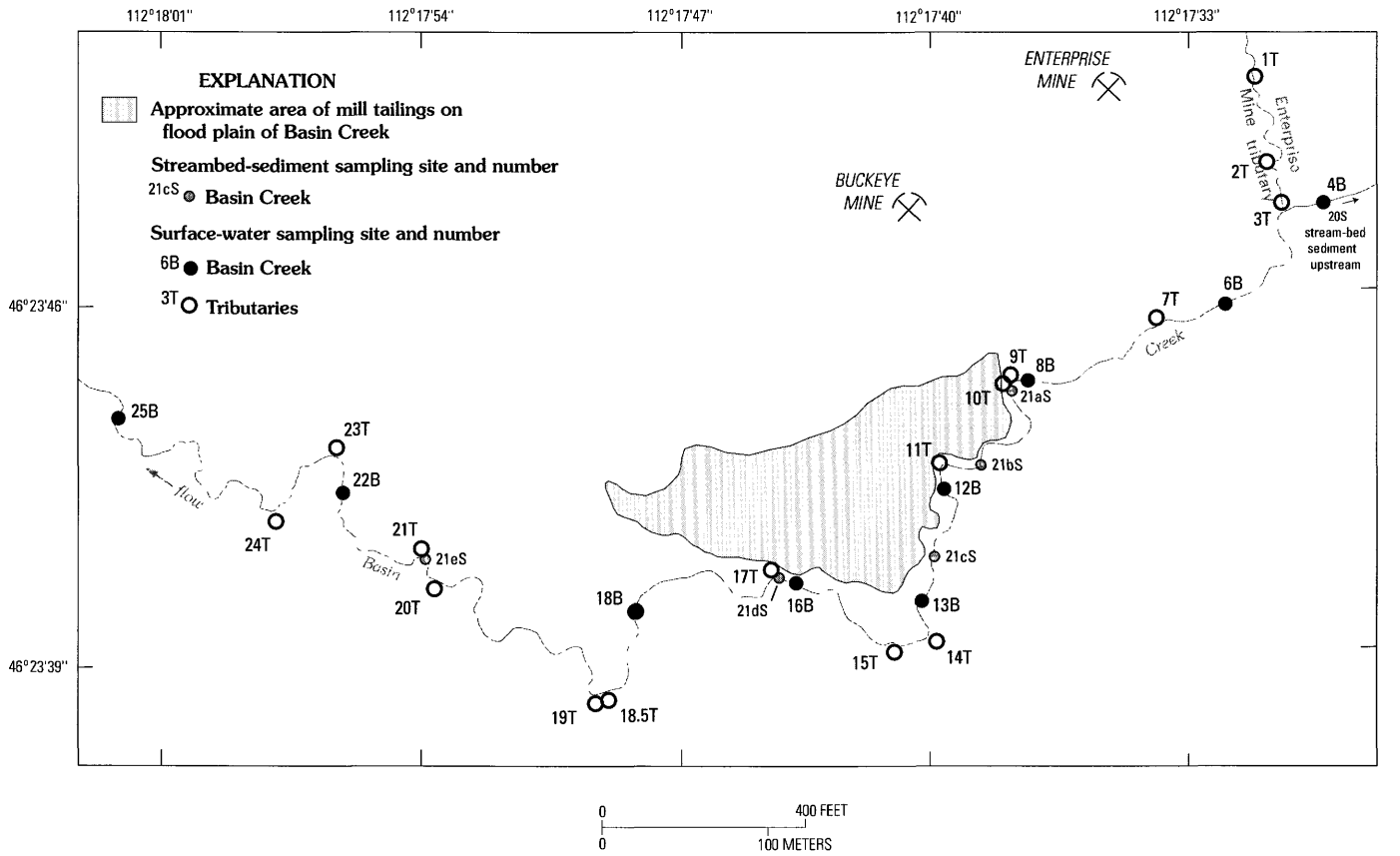

Figure 15. Location of streambed-sediment and surface-water sampling sites, upper Basin Creek.

Table 10. Concentrations of leachable iron and selected trace elements in streambed-sediment samples, upper Basin Creek.[1]

[A 2M HCl, 1-percent H_2O_2 solution was applied to streambed-sediment samples which dissolved amorphous iron oxyhydroxide phases. Concentrations in parts per million (micrograms/gram); <, less than minimum reporting level]

Site No. (fig. 15)	Date	Antimony	Arsenic	Cadmium	Copper	Iron	Lead	Silver	Zinc
20S	July 1998	<3	34	<1	16	16,000	64	<1	160
21aS	July 1997	<3	170	2.8	61	22,000	160	1.4	500
21bS	July 1997	<3	600	1.7	50	21,000	410	3.0	390
21cS	July 1997	33	3,000	2.1	79	20,000	1,200	6.5	350
21dS	July 1997	40	3,000	3.2	99	28,000	1,600	8.6	460
21eS	October 1996	34	4,000	5.0	120	33,000	1,600	6.9	680

[1]Data from Fey, Unruh, and Church (1999, table 7).

As upper Basin Creek flows through the study area to site 22B, it receives drainage from an additional 0.71 mi^2 area, of which 0.634 mi^2 is situated south of Basin Creek and 0.076 mi^2 is situated in the vicinity of the Buckeye and Enterprise mines on the north side of Basin Creek. The total drainage area of Basin Creek below Buckeye mine (to site 22B) is 2.54 mi^2.

Flow Characteristics of Basin Creek

Streamflow in Basin Creek near the Buckeye and Enterprise mines was measured periodically at sites 4B, 6B, and 22B between October 1996 and September 1999 (table 8). The highest measured flows were in May 1997, 1998, and 1999. The maximum measured streamflow in Basin Creek was 17 ft^3/s at site 22B below the Buckeye mine on May 7, 1998. The lowest flows were measured on September 13, 1999, when streamflow in Basin Creek below the Buckeye mine was 0.35 ft^3/s. Monthly distribution of annual runoff of Basin Creek can be estimated from long-term records for the streamflow-gauging station Boulder River at Boulder, Mont. (station number 06033000). Based on 1929–98 streamflow records for the Boulder River gauge, mean monthly streamflow is greatest in May and second greatest in June (U.S. Geological Survey, issued annually). May accounts for nearly 34 percent of the mean annual streamflow and June accounts for nearly 29 percent (fig. 16). For the period August through March, each month accounts for less than 5 percent of the mean annual streamflow of the Boulder River. The monthly streamflow pattern of Basin Creek in the study area likely is similar to the monthly streamflow pattern of the Boulder River.

Water Quality and Synoptic Sampling

Analyses of water samples collected from upper Basin Creek, at various dates and streamflow conditions, documented higher concentrations of dissolved trace elements at higher streamflows (table 8). For example, dissolved zinc concentrations in Basin Creek below the Buckeye mine (site 22B) ranged from 24 µg/L during low flow on September 25, 1998, to 218 µg/L during high flow on May 7, 1998. The relationship between dissolved zinc concentration and streamflow in Basin Creek below the Buckeye mine is shown in figure 17. A similar pattern of higher concentration of dissolved trace elements with larger streamflow was observed for aluminum, cadmium, copper, lead, and manganese.

Dissolved trace-element concentrations that are higher in Basin Creek at high streamflow than at low streamflow indicate that substantial amounts of dissolved trace elements sufficient to overcome dilution effects are delivered to the stream during high flow. Observations of streamflow and overland runoff made at the study area during periods of snowmelt in April and May 1999 indicated that tailings and waste rock are probable sources of dissolved trace elements (fig. 18). On April 19, 1999, upper Basin Creek contained considerable ice, snow, and slush, restricting flow in the stream and creating ponds of water on the flood plain and mill tailings. These ponds were saturating the mill tailings, and ground-water levels were rising to near land surface, as indicated by water levels in test wells located on the flood plain (fig. 14; table 4). On May 20, 1999, snow was rapidly melting and overland runoff was considerable from areas around the Buckeye and Enterprise mines and from the mill tailings. Runoff from the mines and tailings was discharging directly

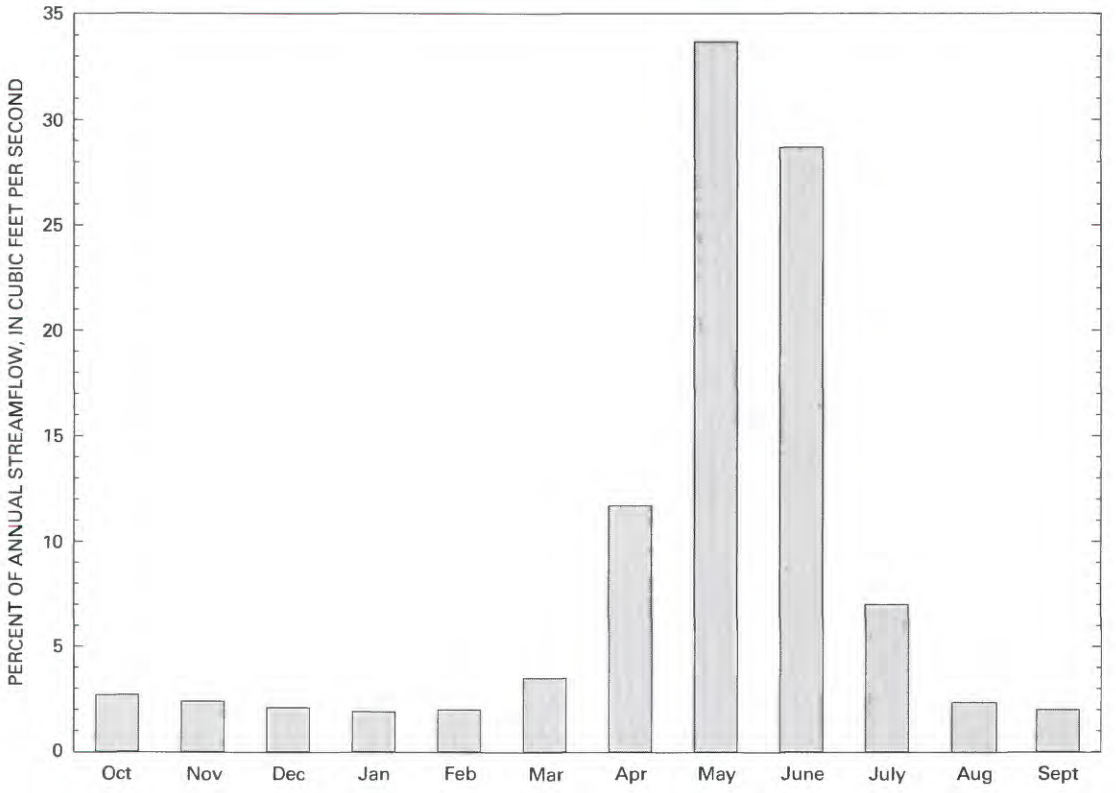

Figure 16. Monthly distribution of mean annual streamflow of Boulder River (streamflow-gauging station 06033000, fig. 1).

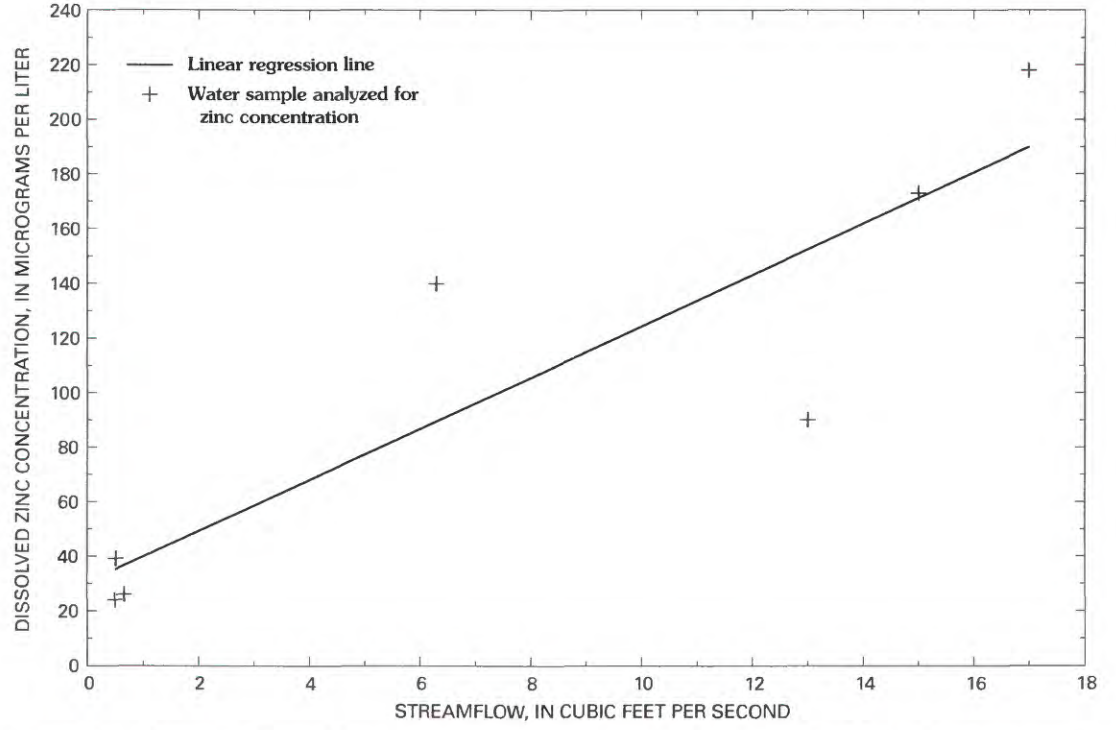

Figure 17. Relation of dissolved zinc concentration and streamflow for Basin Creek below Buckeye mine, 1996–99.

Figure 18. Snowmelt runoff from flotation-mill tailings entering upper Basin Creek near site 12B, May 27, 1999.

into Basin Creek; some of the runoff had a pH value as low as 3.08, as measured onsite with a portable pH meter.

Water quality was sampled and streamflow was measured in upper Basin Creek and all tributaries on May 28, 1999, to determine concentrations and loads of trace elements at numerous sites in upper Basin Creek near the Buckeye and Enterprise mines during high streamflow in order to identify the primary sources of trace elements. Water-quality samples were collected and streamflow measured at 25 sites in a short period between 0800 and 1130 hours under uniform hydrologic conditions to provide a synoptic characterization of downstream changes. Physical properties measured in the field at the time of streamflow measurement were water temperature, specific conductance, and pH. Tributaries to Basin Creek were identified as entering from the right bank (bank with mining wastes) or left bank (bank with no mining wastes). Water analyses included major ions as well as dissolved and total-recoverable trace elements. Dissolved trace elements were determined from samples filtered through 0.1-µm membrane filters. Water-quality and streamflow data for all sites are listed in table 11, and site locations appear in figure 15.

During the synoptic sampling of May 28, 1999, streamflow in Basin Creek ranged from 7.9 ft^3/s above the Buckeye mine (site 4B) to 12 ft^3/s at the most downstream site (25B). Tributary inflows ranged from 0.005 ft^3/s (site 9T) to 1.65 ft^3/s (site 3T, Enterprise Mine tributary). A plot of the measured streamflow in Basin Creek and its tributaries shows that nearly all increases in flow in Basin Creek during a runoff condition could be accounted for by tributary inflow (fig. 19). Some small changes in streamflow between measurement sites may be attributed to ground water; however, the changes are so small that they are within the measurement error of the methods used to measure streamflow. The difference between the measured streamflow in Basin Creek at site 25B and the sum of the measured streamflow at site 4B plus all tributary inflows was 0.44 ft^3/s, or 3.6 percent of the streamflow at site 25B.

The quality of water sampled at the 25 synoptic sites (fig. 15) ranged from good-quality water typical of local, undisturbed mountain streams to acidic, trace-element-rich runoff that exceeds Montana aquatic-life standards for acute toxicity. Sites with good-quality water that could be considered as reference sites representative of undisturbed areas were Enterprise Mine tributary above the Enterprise mine (site 1T), Basin Creek above Buckeye mine (site 4B), and several tributaries to Basin Creek from the left bank (sites 14T, 18.5T, and 19T). Water from these undisturbed sites is characterized by nearly neutral pH, hardness values of 16 milligrams per liter (mg/L) or less, and low dissolved metal concentrations (dissolved cadmium <0.3 µg/L; dissolved copper from 1.8 to 2.9 µg/L; dissolved lead from <0.3 to 0.7 µg/L; and dissolved zinc from 1.4 to 3.0 µg/L).

Water from tributaries that drained waste rock or mill tailings had high concentrations of dissolved trace elements (table 11) when sampled on May 28, 1999. The highest concentrations of dissolved trace elements were: aluminum, 34,800 µg/L at site 7T; arsenic, 985 µg/L at site 17T; cadmium, 142 µg/L at site 2T; copper, 1,700 µg/L at site 7T; iron, 12,000 µg/L at site 17T; lead, 6,470 µg/L at site 11T; manganese, 23,500 µg/L at site 7T; and zinc, 17,800 µg/L at site 2T. Tributaries draining waste rock near the Enterprise and Buckeye mines (sites 2T, 7T, 9T) had the highest concentrations of dissolved aluminum, cadmium, copper, manganese, and

Table 11. Synoptic streamflow and water-quality data for upper Basin Creek and tributaries, May 28, 1999.

[Right bank, bank containing mining wastes; left bank, bank with no mining wastes. E, estimated; ft^3/s, cubic feet per second; °C, degrees Celsius; µg/L, micrograms per liter; µS/cm, microsiemens per centimeter at 25 degrees Celsius; mg/L, milligrams per liter; <, less than minimum reporting level; --, no data]

Site No. (fig. 15)	Site description	Streamflow, instantaneous (ft^3/s)	Temperature, water (°C)	Specific conductance (µS/cm)	pH, field (standard units)	Hardness, total (mg/L as $CaCO_3$)	Calcium, dissolved (mg/L)	Magnesium, dissolved (mg/L)
1T	Enterprise Mine tributary	1.52	4.0	29	7.7	12	3.7	0.8
2T	Tributary to Enterprise Mine tributary	.012	16.5	702	4.0	240	70	16
3T	Enterprise Mine tributary	1.65	6.0	42	7.1	16	4.8	1.0
4B	Basin Creek above Buckeye mine	7.87	2.0	37	8.1	16	4.8	1.0
6B	Basin Creek below Enterprise Mine tributary	9.22	2.5	38	7.2	16	4.8	1.0
7T	Basin Creek tributary, right bank	.018	10.0	849	3.4	148	38	13
8B	Basin Creek	9.89	3.0	40	7.3	17	4.9	1.1
9T	Basin Creek tributary, right bank	.005	9.0	566	3.9	153	47	8.9
10T	Basin Creek tributary, right bank	.014	6.5	383	4.1	125	41	5.8
11T	Basin Creek tributary, right bank	.018	5.5	375	3.3	30	9.5	1.6
12B	Basin Creek	10.7	2.0	41	7.3	17	4.9	1.1
13B	Basin Creek	10.2	4.0	42	7.2	17	5.0	1.1
14T	Basin Creek tributary, left bank	.58	8.0	39	6.9	16	4.8	.9
15T	Basin Creek tributary, left bank	.01	5.0	30	6.1	11	3.4	.7
16B	Basin Creek	11.1	3.0	42	7.0	16	4.8	1.1
17T	Basin Creek tributary, right bank	.021	14	504	3.1	31	9.5	1.7
18B	Basin Creek	10.8	3.0	42	7.0	17	5.0	1.1
18.5T	Basin Creek tributary, left bank	.175	--	42	6.7	15	4.5	.9
19T	Basin Creek tributary, two inflow points from left bank	1.18	5.0	25	6.2	9	2.6	.6
20T	Basin Creek tributary, left bank	.020	7.0	32	6.0	12	3.6	.8
21T	Basin Creek tributary, right bank	.066	8.5	25	5.1	5	1.6	.3
22B	Basin Creek below Buckeye mine	12.5	2.0	39	6.7	16	4.7	1.0
23T	Basin Creek tributary, right bank	.015	7.0	28	5.7	8	2.5	.5
24T	Basin Creek tributary, three inflow points from left bank	.156	.5	23	6.1	8	2.2	.6
25B	Basin Creek	12.2	1.5	39	7.0	16	4.6	1.0

Table 11. Synoptic streamflow and water-quality data for upper Basin Creek and tributaries, May 28, 1999.—Continued

Site No. (fig. 15)	Sodium, dissolved (mg/L)	Potassium, dissolved (mg/L)	Sulfate, dissolved (mg/L as SO_4)	Chloride, dissolved (mg/L)	Alkalinity, laboratory (mg/L as $CaCO_3$)	Alumi-num, dissolved (µg/L)	Alumi-num, total recov-erable (µg/L)	Arsenic, dissolved (µg/L)	Arsenic, total recov-erable (µg/L)	Cadmium, dissolved (µg/L)
1T	1.2	0.6	1.5	0.2	12	76	231	2.3	2.3	<0.3
2T	3.7	3.6	370	.6	<1	9,980	10,300	45	50	142
3T	1.3	.6	6.6	.8	11	159	444	2.8	7.5	1.9
4B	1.1	.7	2.7	.2	15	52	185	2.2	3.8	<.3
6B	1.2	.7	3.5	.2	14	66	221	2.1	3.3	.4
7T	5.6	1.5	496	1.3	<1	34,800	32,800	123	146	107
8B	1.2	.7	4.6	.2	11	124	272	2.4	3.2	.6
9T	4.3	2.3	290	1.2	<1	14,600	14,200	271	447	57
10T	3.6	2.0	180	.5	<1	5,130	5,360	118	183	24
11T	4.4	1.7	94	.6	<1	1,350	1,800	280	5,190	23
12B	1.2	.7	4.8	.2	14	143	299	3.4	7.6	.7
13B	1.2	.7	5.2	.2	14	127	318	4.2	16	1.0
14T	1.7	.9	2.6	2.2	13	29	48	4.0	6.2	<.3
15T	1.3	.6	3.4	.3	9.2	57	136	22	32	<.3
16B	1.2	.7	--	<.1	<1	112	323	5.3	20	.7
17T	3.0	1.8	127	.5	<1	1,780	1,880	985	2,270	38
18B	1.2	.7	5.2	.2	14	126	305	7.9	23	.8
18.5T	1.7	1.0	3.0	.3	14	140	59	3.1	2.9	<.3
19T	1.1	.9	2.3	.2	9.0	64	148	1.6	3.2	<.3
20T	1.0	1.0	1.6	.4	12	78	99	33	33	<.3
21T	1.5	.7	--	--	--	94	--	182	--	1.2
22B	1.2	.7	4.7	.2	13	117	303	9.7	25	.6
23T	2.0	1.0	5.5	.6	5.5	94	205	153	220	1.3
24T	1.1	1.0	2.2	.3	8.2	69	97	15	17	<.3
25B	1.2	.7	4.6	.2	13	123	289	10	24	.6

Table 11. Synoptic streamflow and water-quality data for upper Basin Creek and tributaries, May 28, 1999.—Continued

Site No. (fig. 15)	Cadmium, total recoverable (µg/L)	Copper, dissolved (µg/L)	Copper, total recoverable (µg/L)	Iron, dissolved (µg/L)	Iron, total recoverable (µg/L)	Lead, dissolved (µg/L)	Lead, total recoverable (µg/L)	Manganese, dissolved (µg/L)	Manganese, total recoverable (µg/L)	Zinc, dissolved (µg/L)	Zinc, total recoverable (µg/L)
1T	<1	2.8	2.8	64	208	<0.3	<1	2.1	14	1.4	<40
2T	141	740	792	402	384	17	17	11,900	11,100	17,800	17,200
3T	2.1	11	14	79	465	<.3	1.1	178	217	234	254
4B	<1	2.1	1.8	61	240	<.3	1.1	3.4	10	5.9	<40
6B	<1	3.7	3.5	54	230	<.3	<1	39	43	49	52
7T	127	1,700	1,740	5,020	4,450	26	28	23,500	20,900	15,900	14,400
8B	<1	7.5	7.7	70	256	.5	1.2	102	105	89	103
9T	67	1,090	1,060	3,190	3,050	481	470	7,520	7,060	6,930	6,470
10T	24	478	524	362	430	586	552	2,590	2,460	2,860	2,840
11T	24	434	526	1,490	7,970	6,470	10,100	1,010	995	3,020	3,020
12B	<1	8.5	9.9	77	268	2.4	5.8	102	105	94	110
13B	<1	10	12	60	278	3.9	14	113	116	108	110
14T	<1	1.8	1.7	126	300	<.3	<1	6.5	10	2.2	<40
15T	<1	5.2	6.5	98	229	3.2	9.7	21	29	18	E30
16B	<1	9.3	12	70	353	3.0	14	105	112	99	121
17T	41	757	790	12,000	12,900	3,160	3,000	907	876	5,520	5,550
18B	<1	10	12	95	323	7.3	21	103	107	106	111
18.5T	<1	2.9	2.6	--	--	.7	<1	14	5.0	2.9	<40
19T	<1	2.1	2.4	118	267	<.3	<1	11	11	3.0	<40
20T	<1	7.1	7.4	147	165	5.9	6.3	20	22	29	42
21T	--	26.1	--	166	--	46	--	63	--	157	--
22B	<1	9.4	11	101	355	5.4	17	85	90	90	95
23T	1.6	40	44	194	588	9.4	28	64	64	197	203
24T	<1	4.5	5.0	79	97	2.3	2.9	7.0	6.2	25	E28
25B	<1	9.2	11	107	360	5.0	16	84	88	88	94

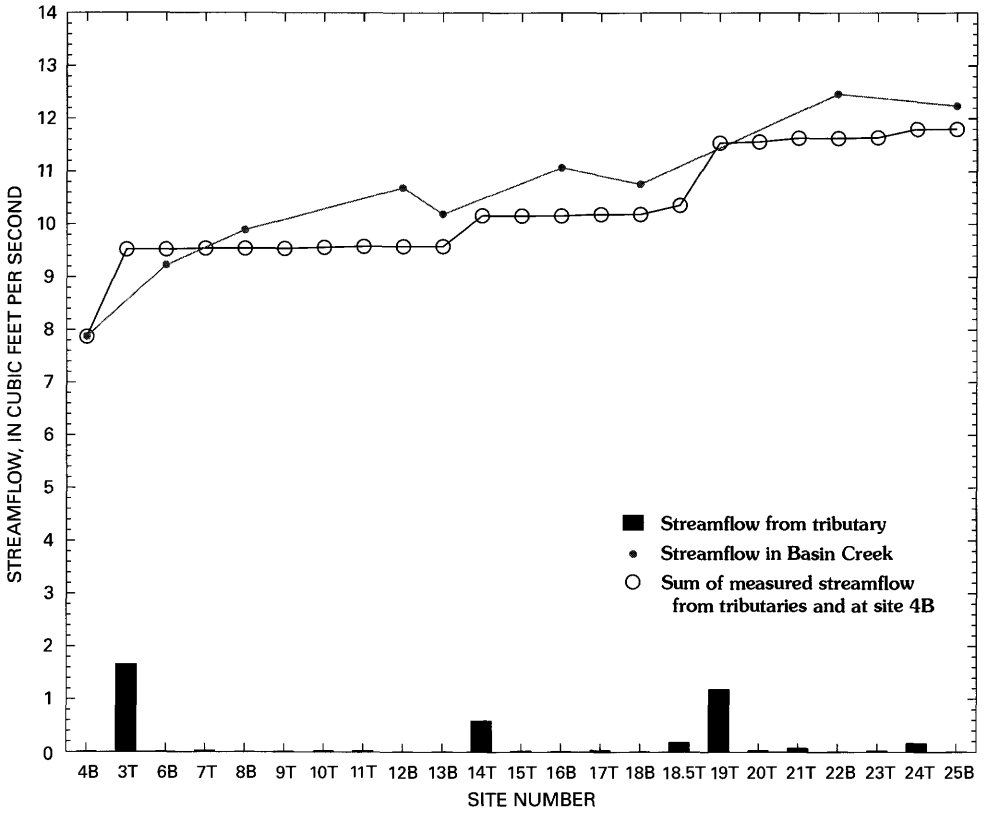

Figure 19. Streamflow in upper Basin Creek, May 28, 1999.

zinc; tributaries draining mill tailings (sites 11T, 17T), had the highest concentrations of dissolved arsenic and lead. Tributary 21T, which drains from the northern margin of the mill tailings and enters Basin Creek downstream from the mill tailings, also had high concentrations of dissolved arsenic and lead.

Total-recoverable trace-element concentrations were similar to dissolved concentrations for most samples, indicating that the soluble phase was more predominant than the particulate phase, even during runoff conditions. Small differences between dissolved and total-recoverable concentrations were observed for cadmium, copper and zinc. Some of the largest differences between dissolved and total-recoverable concentrations were observed for aluminum, arsenic, iron, and lead. The large differences between dissolved and total-recoverable concentrations indicate that aluminum, arsenic, iron, and lead were being removed from solution and forming colloidal precipitates, which likely settle to the streambed. These observations are consistent with the data from the streambed sediments (table 10), which show large concentration increases for arsenic and lead from upstream of the Enterprise mine to downstream of the mill tailings.

Metals entering Basin Creek from tributaries during the runoff conditions of May 1999 caused increased concentrations that exceeded several aquatic-life standards for the State of Montana. Total-recoverable copper concentrations exceeded the acute aquatic-life standard of 3.8 µg/L for the reach of Basin Creek between sites 8B and 25B. Total-recoverable lead concentrations exceeded the chronic aquatic-life standard of 0.54 µg/L in the reach of Basin Creek between sites 12B and 25B. Total-recoverable zinc concentrations exceeded the acute aquatic-life standard of 37 µg/L for the reach between sites 6B and 25B. The extent to which these metal concentrations exceeded aquatic-life standards farther downstream in Basin Creek is unknown.

Trace-Element Loads in Basin Creek

Instantaneous loads of dissolved trace elements were calculated using streamflow and trace-element concentration data from each site sampled during the synoptic measurements on May 28, 1999. Trace-element loads (table 12) are reported in grams per day (g/d), and were calculated by multiplying streamflow (ft^3/s) times dissolved trace-element concentration (µg/L) times a units-conversion factor of 2.4466. For cadmium and lead concentrations that were less than the minimum reporting level, loads were calculated using the value for the minimum reporting level, and these loads are reported as less-than values in table 12.

Streamflow measurements and water-quality samples collected during snowmelt runoff on May 28, 1999, showed large increases in dissolved trace-element loads in Basin Creek through the area of the Buckeye and Enterprise mines. Streamflow in Basin Creek increased from 7.87 ft^3/s upstream of the Buckeye mine (site 4B) to 12.2 ft^3/s at the most downstream

Table 12. Dissolved trace-element loads for upper Basin Creek and tributaries, May 28, 1999.

[Right bank, bank containing mining wastes; left bank, bank with no mining wastes; ft^3/s, cubic feet per second; g/d, grams per day; <, less than; >, greater than]

Site No. (fig. 15)	Site description	Time	Streamflow, instantaneous (ft^3/s)	Alumi-num load (g/d)	Arsenic load (g/d)	Cad-mium load (g/d)	Copper load (g/d)	Iron load (g/d)	Lead load (g/d)	Manga-nese load (g/d)	Zinc load (g/d)
1T	Enterprise Mine tributary	1105	1.52	282	8.59	<1.12	10.6	239	<1.12	7.88	5.03
2T	Tributary to Enterprise Mine tributary	1050	.012	293	1.31	4.16	21.7	11.8	.50	350	522
3T	Enterprise Mine tributary	1130	1.65	643	11.4	7.50	43.4	318	<1.21	719	946
4B	Basin Creek above Buckeye mine	1010	7.87	1,002	41.6	<5.78	41.3	1,166	<5.78	64.5	113
6B	Basin Creek below Enterprise Mine tributary	0945	9.22	1,499	46.2	9.02	83.0	1,218	<6.77	879	1,096
7T	Basin Creek tributary, right bank	0925	.018	1,533	5.40	4.73	75.0	221	1.17	1,036	702
8B	Basin Creek	0920	9.89	2,993	58.6	14.5	181	1,685	12.1	2,457	2,157
9T	Basin Creek tributary, right bank	0915	.005	178	3.32	.70	13.3	39.0	5.89	91.9	84.8
10T	Basin Creek tributary, right bank	0900	.014	176	4.04	.82	16.4	12.4	20.1	88.6	98.1
11T	Basin Creek tributary, right bank	0840	.018	59.6	12.4	1.00	19.1	65.6	285	44.6	133
12B	Basin Creek	0815	10.7	3,743	89.7	18.3	223	2,024	61.5	2,663	2,449
13B	Basin Creek	1105	10.2	3,163	104	25.1	255	1,486	96.7	2,822	2,691
14T	Basin Creek tributary, left bank	1055	.58	41.4	5.73	<.42	2.62	179	<.42	9.23	3.18
15T	Basin Creek tributary, left bank	1045	.01	1.40	.54	<.01	.13	2.39	.08	.52	.45
16B	Basin Creek	1015	11.1	3,042	145	19.0	251	1,887	80.8	2,832	2,671
17T	Basin Creek tributary, right bank	0955	.021	91.3	50.6	1.94	38.9	617	162	46.6	283
18B	Basin Creek	0935	10.8	3,315	209	21.1	276	2,498	193	2,717	2,778
18.5T	Basin Creek tributary, left bank	0935	.175	59.8	1.34	<.13	1.25	126	.30	5.85	1.26
19T	Basin Creek tributary, two inflow points from left bank	0915	1.18	185	4.50	<.87	6.13	341	<.87	30.9	8.61
20T	Basin Creek tributary, left bank	0900	.020	3.82	1.60	<.01	.35	7.19	.29	.98	1.44
21T	Basin Creek tributary, right bank	0855	.066	15.2	29.3	.19	4.21	26.9	7.43	10.1	25.4
22B	Basin Creek below Buckeye Mine	0840	12.5	3,572	295	18.3	287	3,078	166	2,597	2,753
23T	Basin Creek tributary, right bank	0830	.015	3.46	5.60	.05	1.46	7.11	.34	2.34	7.22
24T	Basin Creek tributary, three inflow points from left bank	0820	.156	26.4	5.69	<.11	1.71	30.3	.88	2.67	9.59
25B	Basin Creek	0800	12.2	3,676	306	18.6	276	3,192	149	2,516	2,643
INCREASE BETWEEN SITES 4B AND 25B		--	4.3	2,674	264	>12.8	235	2,026	>143	2,450	2,530

NOTE: Loads were computed from unrounded streamflow values to obtain greater resolution of small differences between sites.

measurement site (site 25B), which is an increase of 4.3 ft^3/s or 55 percent. Figures 20–27 illustrate downstream changes of dissolved trace-element loads and streamflow for each of the eight trace elements analyzed in the synoptic samples from May 28, 1999. Loads are depicted for Basin Creek, individual tributaries, and the cumulative sum of the trace-element loads from site 4B plus tributaries.

Comparison of dissolved trace-element loads within Basin Creek with the cumulative sum of dissolved trace-element loads from tributaries indicated that dissolved trace-element loads in Basin Creek at the downstream end of the study area (site 25B) were largely derived from tributary inflows draining the Buckeye and Enterprise mines during runoff conditions. Comparison of the loads in Basin Creek and its tributaries also indicated that ground water and diffuse streambank seepage contributed only a small part of the dissolved trace-element load to Basin Creek during runoff. Arsenic was the only trace element to indicate that a substantial component of the load was from ground-water discharge or seepage from saturated stream banks directly into Basin Creek during runoff. Arsenic is widespread in surface and ground water in the area, including water draining from the south side (left bank) of Basin Creek, as indicated by water-quality samples from well 10 and tributaries 14T, 19T, and 24T (tables 6, 11, and 12). Part of the arsenic load in ground water thus likely originates on the south side of Basin Creek, in the area not disturbed by mining, because of the naturally occurring arsenic in that area.

The sum of measured loads of dissolved lead from all sampled tributaries was substantially larger than the loads in Basin Creek at downstream site 25B. The sum of measured loads of dissolved lead from the tributaries was more than three times as large as the load of dissolved lead at site 25B (fig. 25). The sum of measured loads of dissolved aluminum and cadmium from the tributaries ranged from about 10 to 30 percent, respectively, larger than the load at site 25B (figs. 20 and 22). Load inputs greater than the instream loads of Basin Creek indicate that dissolved aluminum, cadmium, and lead from tributaries were precipitating or forming colloids within Basin Creek and subsequently settling to the streambed.

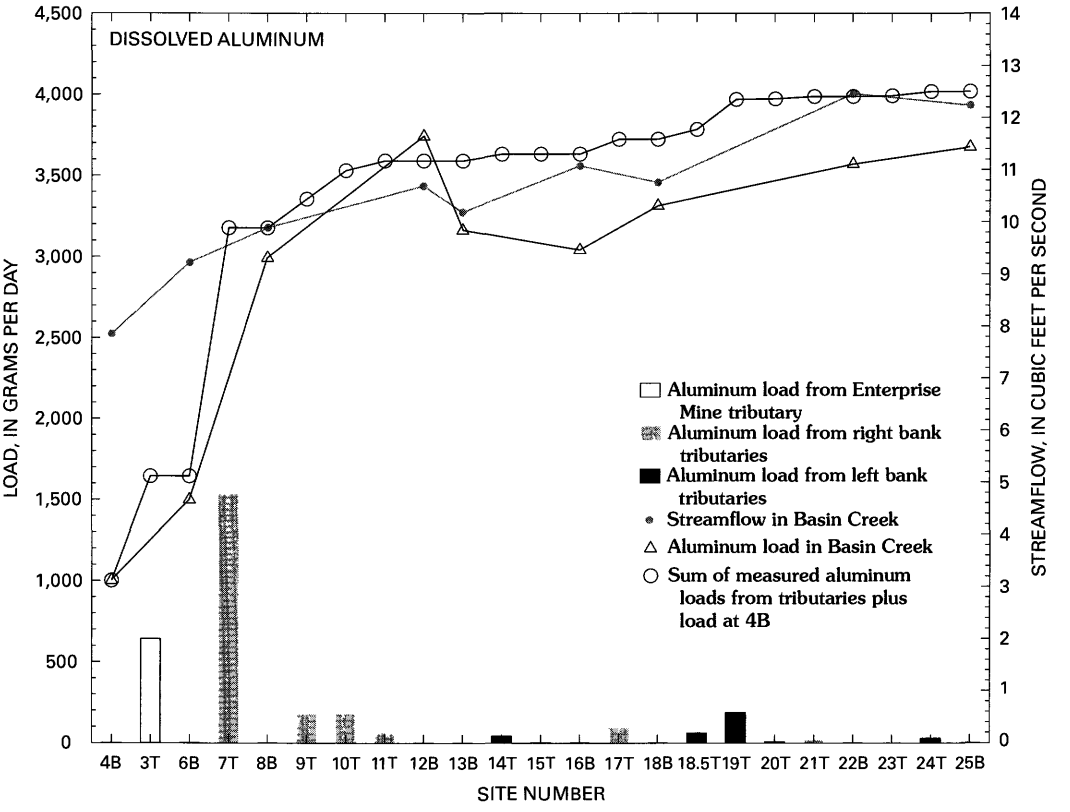

Figure 20. Dissolved aluminum load in upper Basin Creek, May 28, 1999.

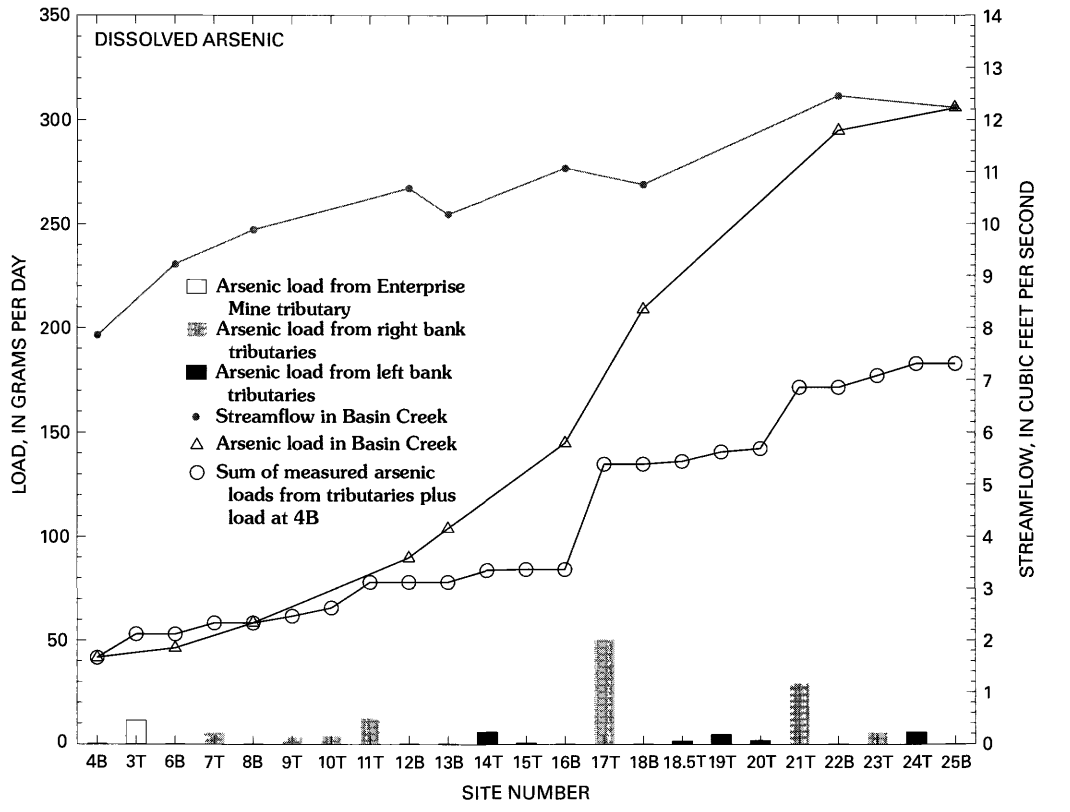

Figure 21. Dissolved arsenic load in upper Basin Creek, May 28, 1999.

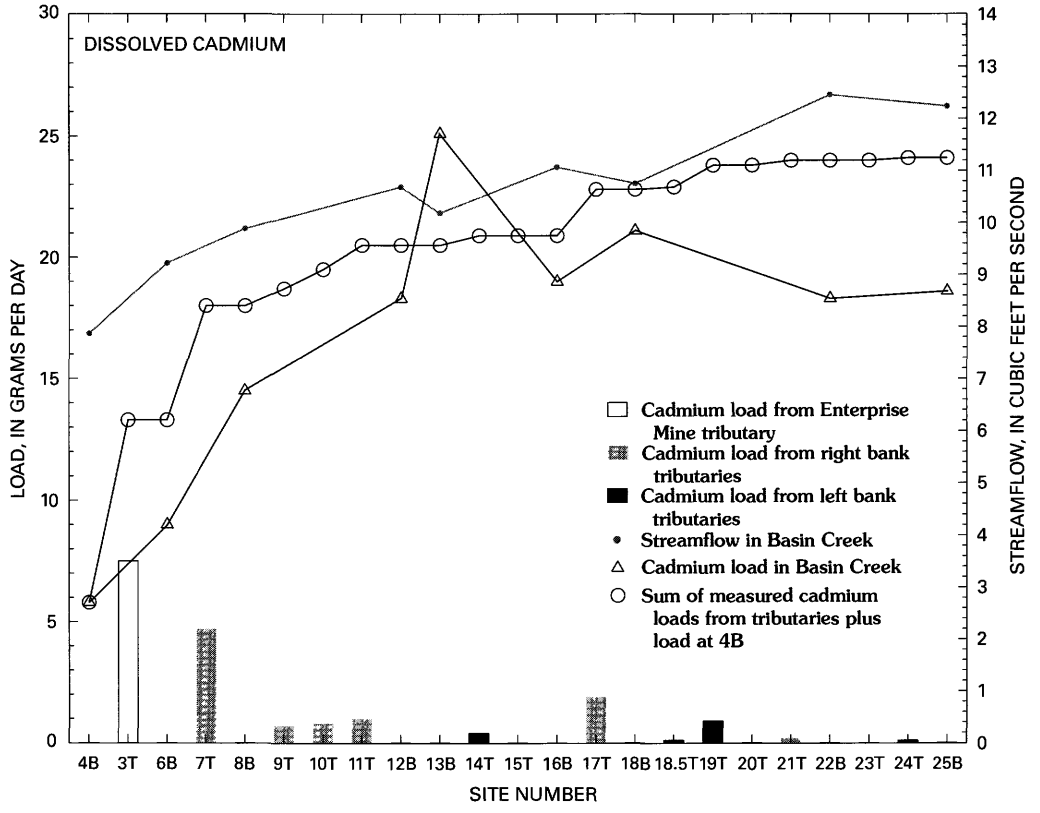

Figure 22. Dissolved cadmium load in upper Basin Creek, May 28, 1999. For cadmium concentrations that were less than minimum reporting level of 0.3 µg/L, load values are plotted using minimum reporting level.

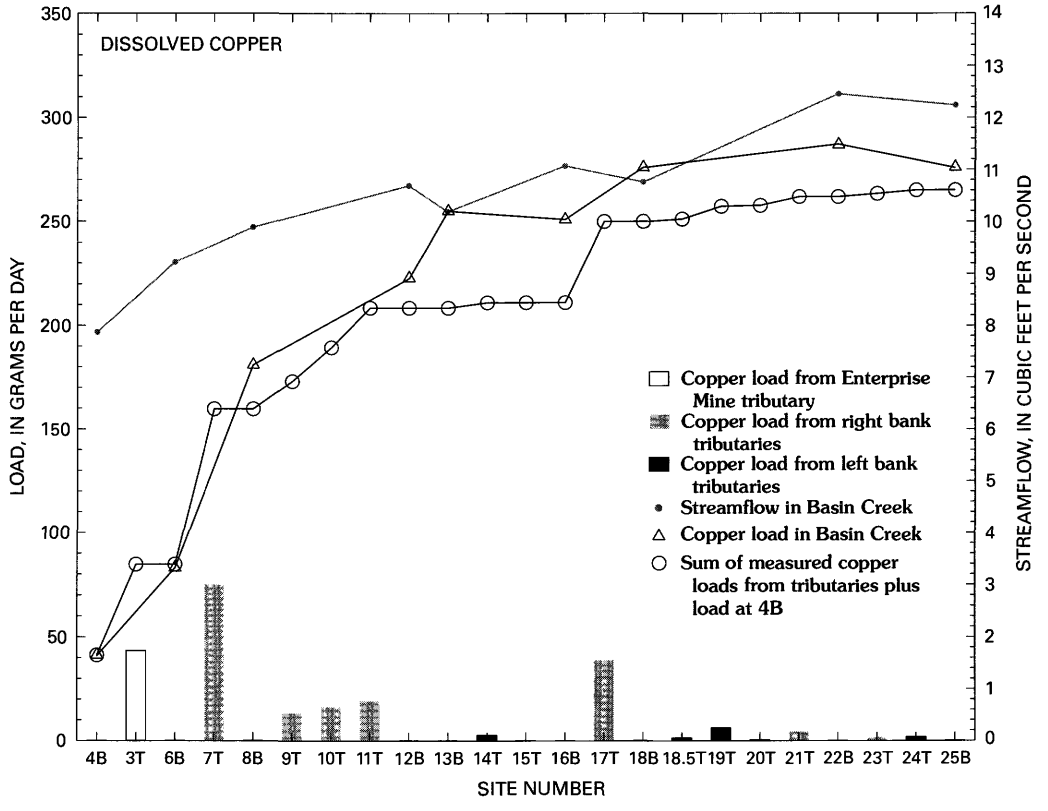

Figure 23. Dissolved copper load in upper Basin Creek, May 28, 1999.

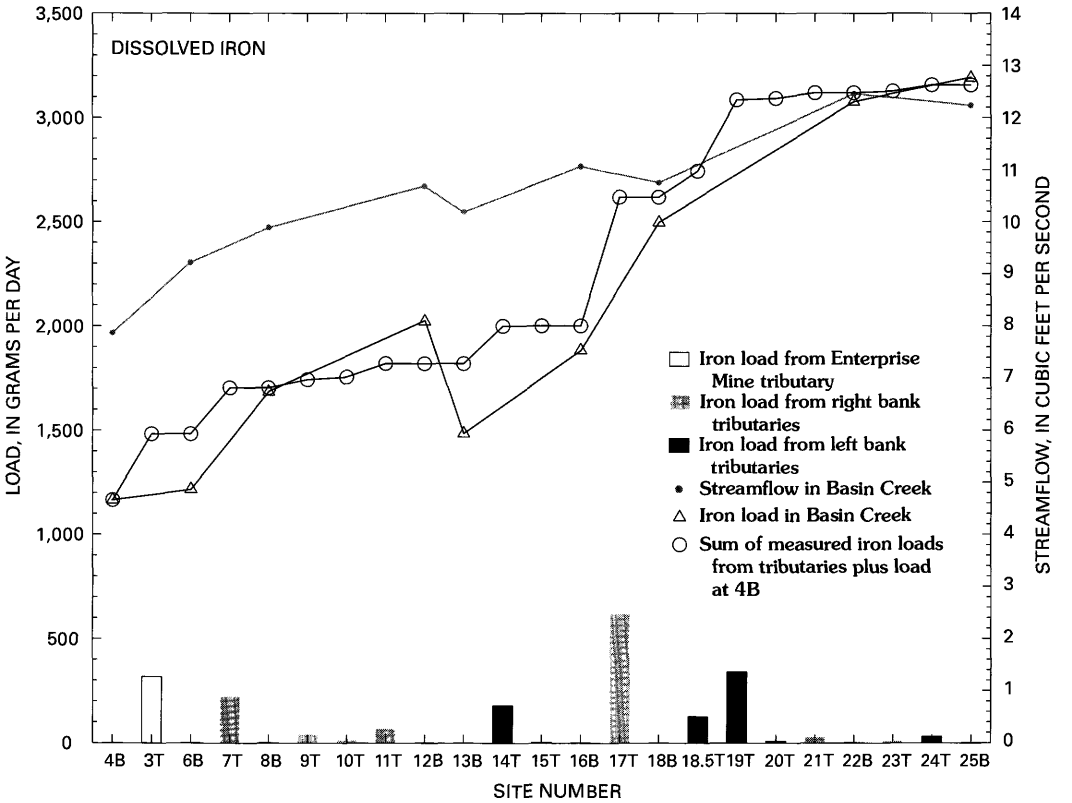

Figure 24. Dissolved iron load in upper Basin Creek, May 28, 1999.

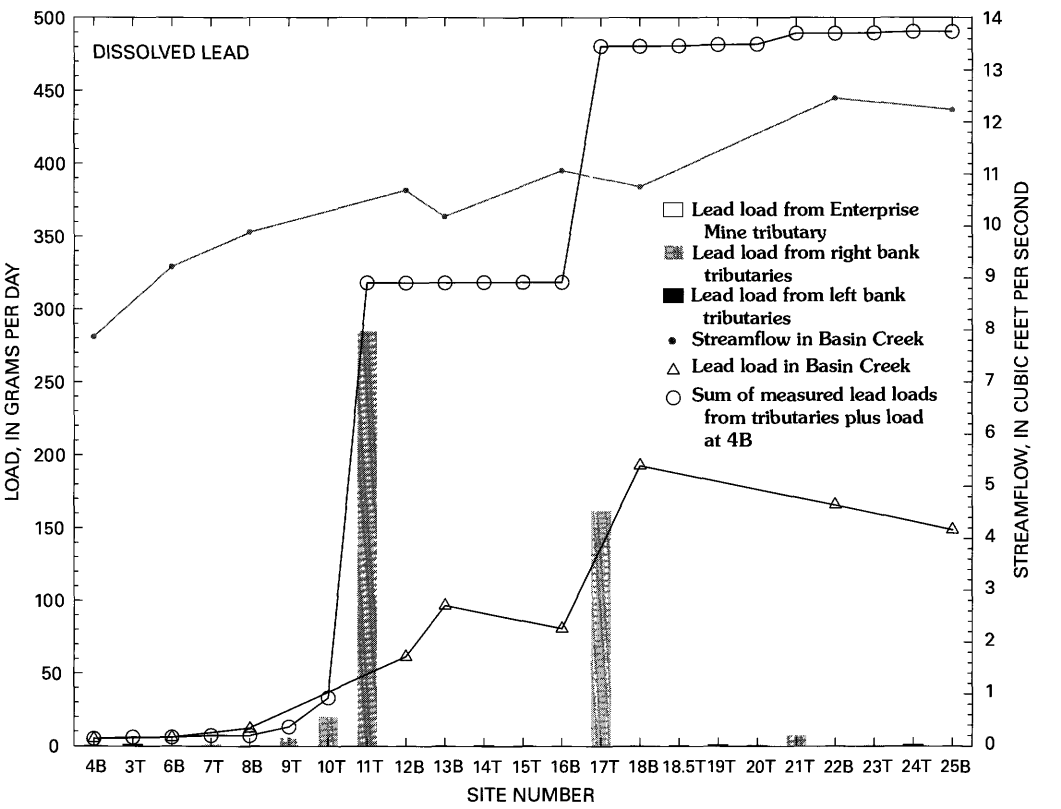

Figure 25. Dissolved lead load in upper Basin Creek, May 28, 1999. For lead concentrations that were less than minimum reporting level of 0.3 µg/L, load values are plotted using minimum reporting level.

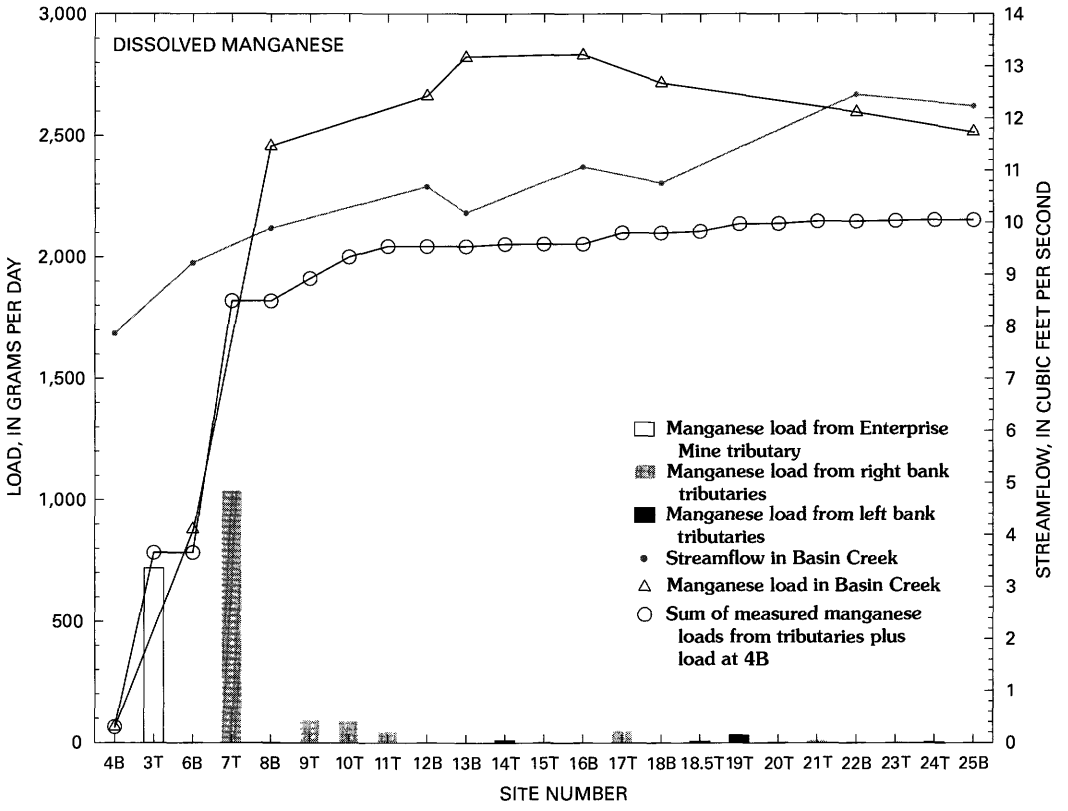

Figure 26. Dissolved manganese load in upper Basin Creek, May 28, 1999.

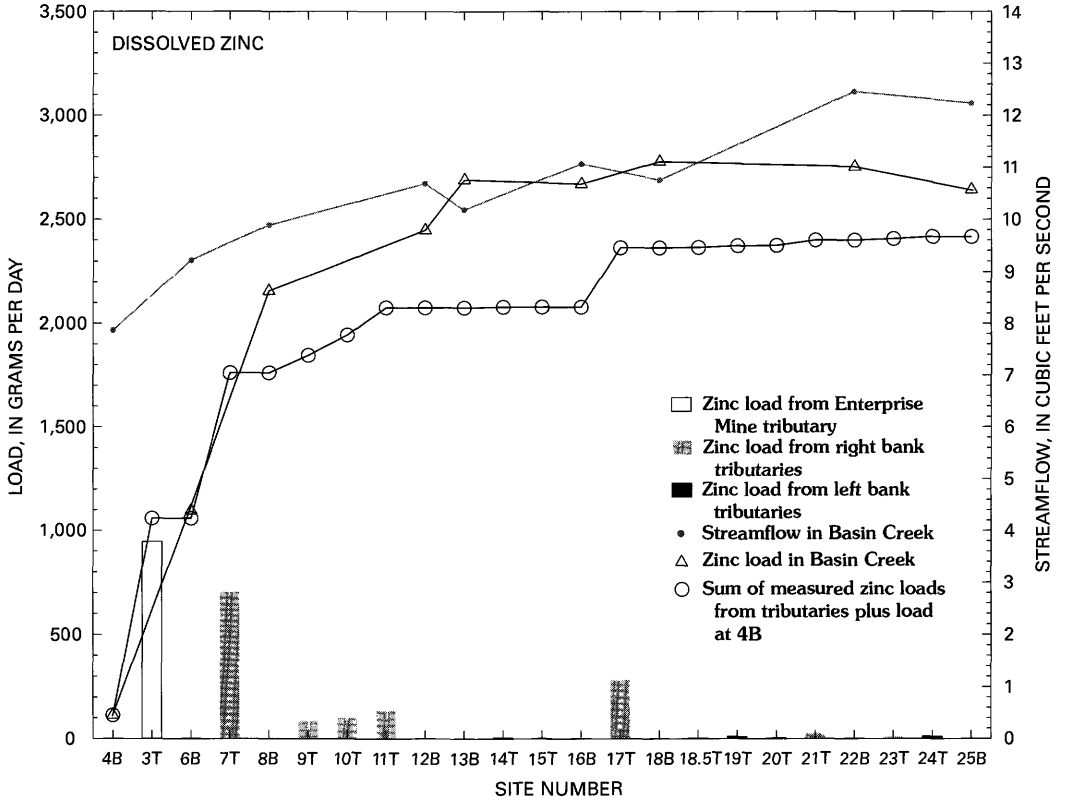

Figure 27. Dissolved zinc load in upper Basin Creek, May 28, 1999.

Summary and Conclusions

The Buckeye and Enterprise mines are located in upper Basin Creek about 10 mi north of the town of Basin in Jefferson County, Mont. Pyritic ore from the mines was processed by a gravity mill located at the Buckeye mine site; gravity-mill tailings were later reprocessed through a flotation mill located on the flood plain of Basin Creek. Flotation-mill tailings on the flood plain occupy an area of about 3.3 acres and have a volume of about 5,000 cubic yards.

Basin Creek flows along the southern margin of the mill tailings and receives surface- and ground-water runoff from the mine areas and tailings, predominantly during spring snowmelt. The runoff from the mine areas and mill tailings measurably affects the quality of water in Basin Creek. The USDA Forest Service and U.S. Environmental Protection Agency have identified the need for remediation of the Buckeye and Enterprise mine area. To effectively remediate the impacts of historical mine wastes on Basin Creek and to measure the effectiveness of proposed mine-waste cleanup, it was necessary to determine sources of trace elements and their pathways of transport to the stream.

Chemical analyses of core samples from mill tailings, soils beneath the tailings, and leachate from samples prepared from a core showed four distinct geochemical zones: an oxidized and leached zone (the upper 22 in.), a partly oxidized zone (22–41 in.), an unoxidized pyritic zone (41–62 in.), and the buried soil horizon (62–79 in.). The unoxidized pyritic zone contained the highest concentrations of trace elements, whereas concentrations of most trace elements rapidly decreased with depth in the buried soil beneath the tailings.

Surface geophysical surveys, including electromagnetic, direct-current resistivity, and total-field magnetic methods, were used to examine the location and extent of high conductivity possibly related to trace-element contamination. Subsurface conductivity was mapped using EM-31 and EM-34 terrain conductivity measuring systems. The conductivity surveys measured the variation in subsurface conductivity from about 10 to 100 ft. Areas of high conductivity can result from sediments containing wet clay or high dissolved-solids concentrations in ground water. Direct-current resistivity soundings were used to quantify subsurface conductivity variations and to estimate the depth to bedrock. Total-field magnetic measurements were used to identify magnetic metals in the subsurface.

The EM surveys identified three areas of relatively high apparent conductivity and detected a conductive plume extending from the northeast part of the mill tailings to the southwest, toward the stream. This plume correlates well with the potentiometric surface and direction of ground-water flow, and with water-quality data from the monitoring wells in and around the tailings. The electromagnetic data also indicate that ground water with a high dissolved-solids concentration probably has migrated downward. Conductive zones also were identified south of the Enterprise mine and in an area of wet meadows southwest of the Buckeye tailings.

Total-field magnetic measurements indicated that buried magnetic objects were not a likely source of high conductivity near the EM survey grid origin. Therefore, the high conductivity anomaly is likely the result of the highly conductive sulfide layers that were observed in core samples from the same area.

Data from the direct-current soundings are interpreted to be a body of conductive material, most likely ground water with a high dissolved-solids content near the center of the Buckeye tailings and below the Enterprise tailings near well 9. The anomaly is slightly deeper than shown in the EM surveys, which may indicate downward movement of dissolved solids. Direct-current resistivity soundings also indicate that depth to bedrock is likely greater than 98 ft.

Two aquifers exist in the study area. One aquifer is fractured bedrock of the Boulder batholith, and the second aquifer is unconsolidated deposits consisting of till, alluvium, colluvium, organic-rich swamp deposits, and volcanic ash. The unconsolidated deposits range from less than 1 ft to more than 30 ft thick and are overlain by mill tailings in the vicinity of the Buckeye mine. The unconsolidated-deposits aquifer overlies granitic rocks and is hydraulically connected to Basin Creek. Test wells were installed in the unconsolidated-deposits aquifer to determine direction of ground-water flow, hydraulic characteristics, and water quality.

Ground water containing high concentrations of dissolved aluminum, arsenic, cadmium, copper, iron, lead, manganese, and zinc underlies the area of mill tailings and some of the area between the Enterprise mine and Basin Creek. Discharge of trace-element-laden ground water from the mine and mill-tailings areas into upper Basin Creek is small during low flow, but appears to account for essentially all of the instream load increase in upper Basin Creek during low flow. Trace-element loads from ground water elevate the concentrations of trace elements in upper Basin Creek, although the State of Montana aquatic-life standards generally are not exceeded during low flow. At times of snowmelt runoff, ground-water levels are near land surface over much of the mill-tailings area, and ground water saturates the tailings. This ground water, containing high concentrations of dissolved trace elements, seeps out of the tailings and into small tributaries that drain into Basin Creek.

Analyses of water samples collected from upper Basin Creek and tributaries, at various dates and streamflow conditions, documented higher concentrations of dissolved trace elements at higher streamflows. To determine concentrations and loads of trace elements in Basin Creek near the Buckeye and Enterprise mines during high streamflow for the purpose of identifying major sources, synoptic water-quality samples were collected for analysis and streamflow measurements were made in upper Basin Creek and all tributaries on May 28, 1999. Water quality was sampled and streamflow was measured at 25 sites, between 0800 and 1150 hours, under uniform hydrologic conditions. Water samples were analyzed for water temperature, specific conductance, pH, common ions,

hardness, alkalinity, dissolved trace elements, and total-recoverable trace elements. The quality of water sampled at the 25 synoptic sites ranged from good-quality water typical of local, undisturbed mountain streams to trace-element-rich runoff that exceeded State of Montana aquatic-life standards for acute toxicity. The highest measured concentrations of dissolved trace elements were aluminum, 34,800 µg/L at site 7T; arsenic, 985 µg/L at site 17T; cadmium, 142 µg/L at site 2T; copper, 1,700 µg/L at site 7T; iron; 12,000 µg/L at site 17T; lead, 6,470 µg/L at site 11T; manganese, 23,500 µg/L at site 7T; and zinc, 17,800 µg/L at site 2T.

Tributaries draining waste rock near the Enterprise and Buckeye mines (sites 2T, 7T, 9T) had the highest concentrations of dissolved aluminum, cadmium, copper, manganese, and zinc; tributaries draining the mill tailings (sites 11T, 17T), had the highest concentrations of dissolved arsenic and lead. One tributary (21T), which drains from the northern margin of the mill tailings and enters Basin Creek downstream from the tailings, also had high concentrations of dissolved arsenic and lead.

During the May 1999 synoptic sampling, dissolved trace-element loads in Basin Creek at the downstream end of the study area (site 25B) were largely derived from tributary inflows draining the area of the Buckeye and Enterprise mines. For all trace elements except arsenic, ground water contributed only a small part of the dissolved load to Basin Creek during that period of snowmelt runoff. The sum of measured loads of dissolved aluminum, cadmium, and lead from tributaries was moderately to substantially larger than the sum of the loads in Basin Creek at downstream site 25B, indicating that these elements were precipitating or forming colloids within Basin Creek and subsequently settling to the streambed.

Metals entering Basin Creek from tributaries caused some of the State of Montana aquatic-life standards to be exceeded during runoff conditions of the synoptic sampling in May 1999. Copper exceeded the acute aquatic-life standard for the entire reach of Basin Creek between sites 8B and 25B. Lead exceeded the chronic aquatic-life standard in the reach of Basin Creek between sites 12B and 25B. Zinc exceeded the acute aquatic-life standard for the reach between sites 6B and 25B. The extent to which these metal concentrations exceeded aquatic-life standards farther downstream in Basin Creek is unknown.

References Cited

Church, S.E., Kimball, B.A., Fey, D.L., Ferderer, D.A., Yager, T.J., and Vaughn, R.B., 1997, Source, transport, and partitioning of metals between water, colloids, and bed sediments of the Animas River, Colorado: U.S. Geological Survey Open-File Report 97–151, 135 p.

Cooper, H.H., Jr., Bredehoeft, J.D., and Papadopulos, I.S., 1967, Response of a finite diameter well to an instantaneous charge of water: Water Resources Research, v. 3, no. 1, p. 263–269.

Desborough, G.A., and Fey, D.L., 1997, Preliminary characterization of acid-generating potential and toxic metal solubility of some abandoned metal-mining related wastes in the Boulder River headwaters, northern Jefferson County, Montana: U.S. Geological Survey Open-File Report 97–478, 21 p.

Fey, D.L., Church, S.E., and Finney, C.J., 1999, Analytical results for 35 mine-waste tailings cores and six bed-sediment samples, and an estimate of the volume of contaminated material at Buckeye meadow on upper Basin Creek, northern Jefferson County, Montana: U.S. Geological Survey Open-File Report 99–537, 59 p.

Fey, D.L., Desborough, G.A., and Church, S.E., 2000, Comparison of two leach procedures applied to metal-mining related wastes in Colorado and Montana and a relative ranking method for mine wastes, *in* ICARD 2000; Proceedings of the Fifth International Conference on Acid Rock Drainage, Volume 2: Society for Mining, Metallurgy, and Exploration, Inc., p. 1477–1487.

Fey, D.L., Unruh, D.M., and Church, S.E., 1999, Chemical data and lead isotopic compositions in stream-sediment samples from the Boulder River watershed, Jefferson County, Montana: U.S. Geological Survey Open-File Report 99–575, 147 p.

Interpex, 1993, RESIX-IP version 2.0 users manual: Golden, Colo., Interpex Limited, 150 p.

McDougal, R.R., and Smith, B.D., 2000, Ground geophysical study of the Buckeye mine tailings, Boulder watershed, Montana: U.S. Geological Survey Open-file Report 00–0371, 56 p.

McNeill, J.D., 1980, Electromagnetic terrain conductivity measurement at low induction numbers: Mississauga, Ontario, Canada, Geonics Limited, Technical Note TN-6.

Metesh, J.J., Lonn, J.D., Duaime, T.E., and Wintergerst, Robert, 1994, Abandoned-inactive mines program, Deerlodge National Forest—Volume I, Basin Creek drainage: Montana Bureau of Mines and Geology Open-File Report 321, 131 p.

Montana Department of Environmental Quality, 1999, Montana numeric water quality standards: Helena, Mont., Planning, Preservation, and Assistance Division, Standards and Economic Analysis Section Circular WQB-7, 41 p.

Nimick, D.A., and Cleasby, T.E., 2000, Water-quality data for streams in the Boulder River watershed, Jefferson County, Montana: U.S. Geological Survey Open-File Report 00–99, 70 p.

Roby, R.N., Ackerman, W.C., Fulkerson, F.B., and Crowley, F.A., 1960, Mines and mineral deposits (except fuels), Jefferson County, Montana: Montana Bureau of Mines and Geology Bulletin 16, 122 p.

Ruppel, E.T., 1963, Geology of the Basin quadrangle, Jefferson, Lewis and Clark, and Powell Counties, Montana: U.S. Geological Survey Bulletin 1151, 121 p.

Schemel, L.E., Kimball, B.A., and Bencala, K.E., 2000, Colloid formation and metal transport through two mixing zones affected by acid mine drainage near Silverton, Colorado: Applied Geochemistry, v. 15, p. 1003–1018.

Smith, B.D., and Sole, T.C., 2000, Schlumberger DC resistivity soundings in the Boulder watershed, Jefferson and Lewis and Clark Counties, Montana: U.S. Geological Survey Open-File Report 00–110, 31 p.

Telford, W.M., Geldart, L.P., and Sheriff, R.E., 1990, Applied geophysics, Second Edition: New York, Cambridge University Press, 770 p.

U.S. Department of Agriculture, Soil Conservation Service, 1981, Average annual precipitation Montana, based on 1941–1970 base period: Prepared in cooperation with Montana Department of Natural Resources and Conservation, Water Resources Division, Helena, Mont., 13 p.

U.S. Geological Survey, issued annually, Water resources data, Montana: Helena, Mont., U.S. Geological Survey Water-Data Report, pages vary.

Monitoring Remediation—Have Mine-Waste and Mill-Tailings Removal and Flood-Plain Restoration Been Successful in the High Ore Creek Valley?

By Sharon L. Gelinas and Robert Tupling

Chapter E2 of
Integrated Investigations of Environmental Effects of Historical Mining in the Basin and Boulder Mining Districts, Boulder River Watershed, Jefferson County, Montana
Edited by David A. Nimick, Stanley E. Church, and Susan E. Finger

Professional Paper 1652–E2

U.S. Department of the Interior
U.S. Geological Survey

Contents

Figures

Tables

CONVERSION FACTORS

Multiply	By	To obtain
acre	4,047	square meter
cubic foot per second (ft^3/s)	0.028317	cubic meter per second
cubic yard (yd^3)	0.7646	cubic meter
foot (ft)	0.8048	meter
mile (mi)	1.61	kilometers
ounce (oz)	28.35	gram
pound (lb)	453.6	gram

Chapter E2
Monitoring Remediation—Have Mine-Waste and Mill-Tailings Removal and Flood-Plain Restoration Been Successful in the High Ore Creek Valley?

By Sharon L. Gelinas[1] and Robert Tupling[2]

Abstract

Mining activity in the High Ore Creek basin produced mine wastes and mill tailings that resided in waste dumps or were dispersed along the flood plain by fluvial transport. These sources of arsenic and metals degraded water quality, contaminated streambed sediment, and negatively affected the health of aquatic biota. Comet mine, the largest mine in the basin, produced the majority of the waste rock and mill tailings. Evaluation of environmental data collected by the Montana Department of State Lands, the Montana Bureau of Mines and Geology, and the U.S. Geological Survey led to large-scale remediation in the High Ore Creek valley that included both removal actions and in-place treatments. Monitoring data collected before and after remediation provide a basis for documenting the effects of cleanup actions on trace-element concentrations.

A preliminary evaluation of pre- and post-remediation data indicates that dissolved zinc concentrations have decreased in High Ore Creek. Dissolved arsenic concentrations apparently have increased, presumably owing to desorption and leaching associated with liming of waste materials. Multivariate analysis of variance (MANOVA) has shown that post-remediation dissolved zinc concentrations at the mouth of High Ore Creek and in the Boulder River below Little Galena Gulch decreased significantly from pre-remediation concentrations, although concentrations in High Ore Creek are not yet stable. Continued monitoring can determine the effects of remediation on trace-element concentrations in High Ore Creek and the Boulder River ecosystem.

Introduction

Historical mining in the High Ore Creek basin produced wastes enriched in trace elements. Consequent environmental effects were sufficiently severe to warrant some of the first abandoned mine lands (AML) remediation activities in Montana. Waste rock and mill tailings produced at the Comet mine (fig. 1), one of the largest in the Boulder River watershed, were deposited across High Ore Creek. Erosion of these materials by the stream resulted in extensive deposition of tailings on the High Ore Creek valley floor and the Boulder River flood plain (Marvin and others, 1997). Leaching of acid and trace elements, such as arsenic and metals, from these mine wastes degraded water quality sufficiently to effectively eliminate fish from High Ore Creek and impaired fisheries in the Boulder River (Farag and others, this volume, Chapter D10; Pioneer Technical Services, Inc., 1999). The Comet mine area was given a high priority for cleanup by the State of Montana (Montana Department of State Lands, 1995) because of impacts to water quality and the local fisheries. Large-scale remediation efforts were initiated by State and Federal agencies in 1997 to improve riparian and aquatic conditions in High Ore Creek.

The Comet mine, located near the headwaters, was the largest and most productive mine in the High Ore Creek basin. It produced about 3,117,770 oz of silver; 42,440 oz of gold; 2,235,680 lb of copper; 28,535,230 lb of lead; and 23,486,020 lb of zinc during its intermittent operation from 1880 to 1941 (Marvin and others, 1997). The mining operation included 18,000 ft of underground workings, a 900-ft shaft, and a large open pit (Elliott and others, 1992). Ore was processed onsite. In 1931, a new mill was built near the Comet mine to process the ore from this and other nearby mines. However, the mill closed a short time after the Comet mine ceased operations in 1941 (Becraft and others, 1963).

Large quantities of waste rock and mill tailings were left in and near High Ore Creek after the mine closed. One dump containing about 150,000 yd^3 of mine waste rock was located in an upland area east of the open pit; this dump covered 3.4 acres. Two other dumps together containing about 227,000 yd^3 and covering 5.0 acres were left in the High Ore Creek valley. In addition, two impoundments containing about 196,500 yd^3 of mill tailings covering 5.5 acres were located in the valley bottom, blocking the premining stream channel (Pioneer Technical Services, Inc., 1997).

[1]Environmental Careers Organization, Boston, Mass.

[2]Montana Tech of the University of Montana, Butte, Mont.

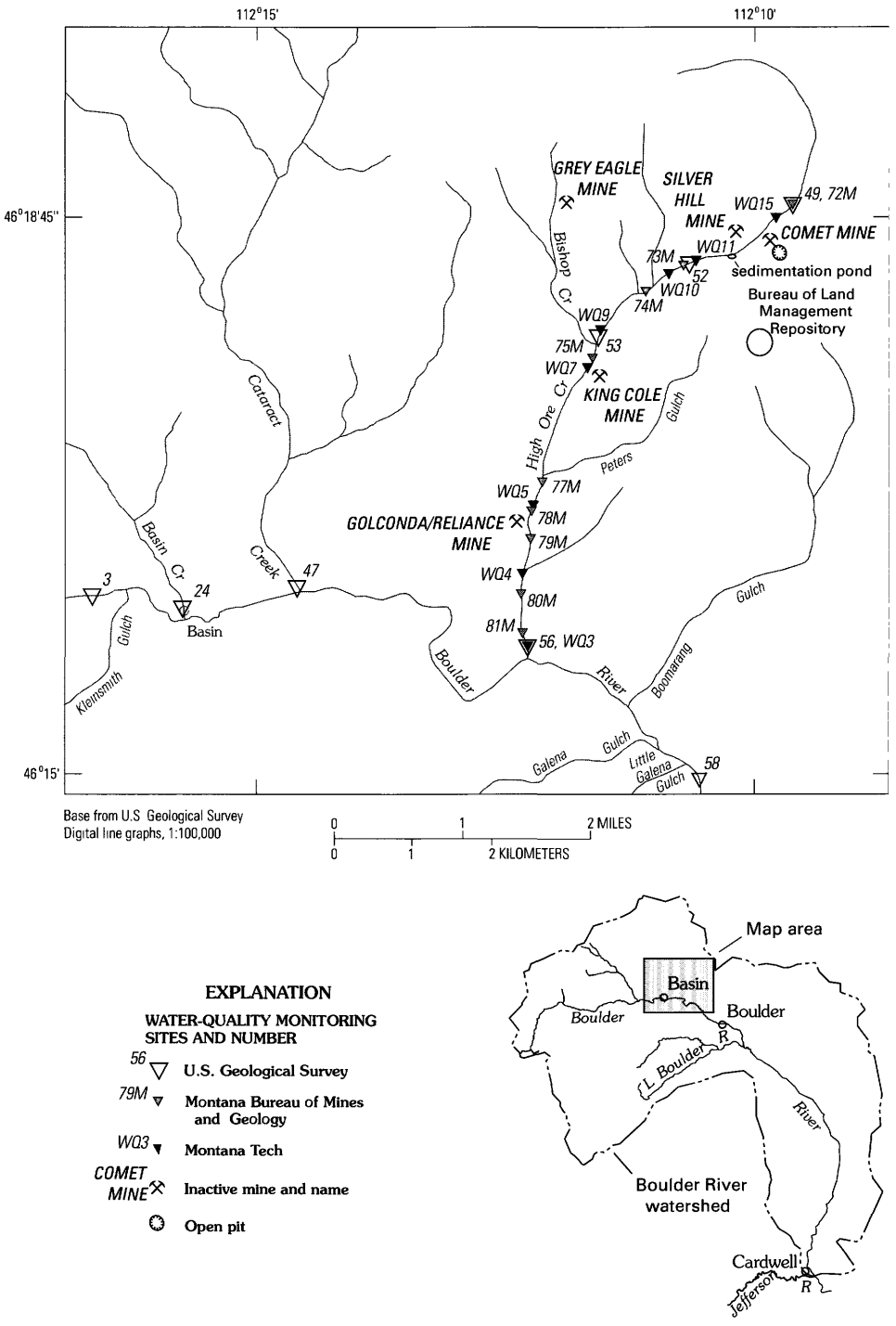

Figure 1. Location of High Ore Creek, Mont., with water-quality monitoring sites and locations of inactive mines.

In addition to the Comet mine, several small mines were located in the High Ore Creek basin (fig. 1; Martin, this volume, Chapter D3, fig. 1). The Grey Eagle mine was the largest of these smaller mines, producing primarily silver (about 2,090 oz) from 1897 to 1941 from about 10,000 ft of underground workings (Elliott and others, 1992; Marvin and others, 1997). The Silver Hill mine adjoined the Comet mine and had underground workings with one shaft (Elliott and others, 1992). The Golconda/Reliance and King Cole mines, located adjacent to High Ore Creek downstream from the Comet mine, produced mainly silver, copper, and lead (Marvin and others, 1997).

At the smaller mines in the High Ore Creek basin, waste rock was the primary mining waste left after mining ceased, because the ore was processed at the Comet mill or transported out of the basin. Six dumps containing about 2,000 yd^3 of

mine waste rock were located at the Silver Hill mine (Pioneer Technical Services, Inc., 1997). One dump, approximately 73,000 yd^3 in size, was located at the Grey Eagle mine (Montana Department of State Lands, 1995). One dump (about 4,300 yd^3 covering 0.26 acres) was located on the east bank of High Ore Creek at the King Cole mine. Two dumps (about 1,500 yd^3 covering 0.22 acres), one on either side of High Ore Creek, were located at the Golconda/Reliance mine (Marvin and others, 1997).

Purpose and Scope

The purpose of this chapter is to describe the pre-remediation environmental setting and cleanup activities and to present a preliminary evaluation of the remediation based on post-remediation monitoring data. The pre-remediation environmental setting was determined from data compiled from the Montana Department of State Lands, the Montana Bureau of Mines and Geology (MBMG), and this study. Water-quality data collected from 1993 through 2000 at nine MBMG sites, four U.S. Geological Survey (USGS) sites, and nine Montana Tech (Montana Tech of the University of Montana) sites were used to evaluate remediation success.

Pre-Remediation Environmental Setting

The Montana Department of State Lands (1995) and Marvin and others (1997) inventoried mine wastes at inactive mines to identify and prioritize mine sites with environmental hazards. Site inventories included sampling tailings, waste rock, adit discharge, seeps, stream water, and streambed sediment. These inventory investigations, along with Boulder River watershed characterization data collected by the USGS, describe in detail the pre-remediation environmental conditions in the High Ore Creek basin.

Trace elements such as arsenic, cadmium, copper, lead, manganese, mercury, silver, and zinc generally existed at elevated concentrations in the waste-rock dumps and tailings impoundments at the Comet mine (Church, Unruh, and others, this volume, Chapter D8, table 2), and in the waste rock at the Silver Hill, Grey Eagle, King Cole and Golconda/Reliance mines. These elevated concentrations were much higher than premining baseline data determined by Church, Unruh, and others (this volume, table 3). Water flowing through waste rock and mill tailings produced acid mine drainage. The potential to produce acid mine drainage was determined by acid-base accounting. If the sum of the potential acidity and the potential neutralizing capacity was negative, then the site was considered a potential acid producer. Two of the waste-rock dumps and one tailings impoundment at the Comet mine site and the waste rock at the Silver Hill and Golconda/Reliance mines were considered potential acid producers (Montana Department of State Lands, 1995; Pioneer Technical Services Inc., 1997, 1999).

Streamside tailings as much as several feet thick covered the banks and flood plain of High Ore Creek for several hundred feet downstream from the Comet mine. Farther downstream, the tailings became thinner and discontinuous. An estimated 32,000 yd^3 of tailings covered more than 21 acres of the High Ore Creek flood plain (Marvin and others, 1997; Pioneer Technical Services, Inc., 1999). Analysis of 42 fluvial tailings cores showed elevated concentrations of arsenic, cadmium, copper, lead, silver, and zinc along High Ore Creek between the Comet mine and the Boulder River. A substantial fraction (from 25 to 100 percent) of the trace elements were in the leachable phase (Fey and Church, 1998; Rich and others, this volume, Chapter G).

Streambed sediment had elevated concentrations of arsenic, cadmium, copper, lead, silver, and zinc. Copper concentrations were more than 50 times greater than estimated background levels, whereas arsenic, cadmium, lead, and zinc concentrations were more than 100 times greater than estimated background levels. Concentrations in streambed sediment decreased downstream in High Ore Creek, particularly below the confluence with Bishop Creek. At the mouth of High Ore Creek, the median concentrations in samples collected during 1996–98 were 4,300 ppm (parts per million) arsenic, 30 ppm cadmium, 480 ppm copper, 1,600 ppm lead, and 6,800 ppm zinc. In contrast, median concentrations in streambed-sediment samples collected in the Boulder River watershed from areas unaffected by mining were 35 ppm arsenic, <2 ppm cadmium, 32 ppm copper, 35 ppm lead, and 150 ppm zinc (Fey and others, 1999; Church, Unruh, and others, this volume; Rich and others, this volume).

Concentrations of dissolved cadmium and zinc in water from High Ore Creek during 1993–97 were elevated and consistently exceeded aquatic-life standards, while concentrations of dissolved copper and lead commonly were less than these standards. During pre-remediation low-flow conditions, average concentrations of dissolved cadmium and zinc (site 56, fig. 1) were 4.3 and 2,050 µg/L (micrograms per liter), respectively, which exceeded the State of Montana chronic aquatic-life standards of 3.5 and 177 µg/L, respectively (average hardness of stream samples collected during pre-remediation low flow used for calculating standards). During pre-remediation spring runoff, average dissolved concentrations of cadmium and zinc were 2.6 and 789 µg/L, respectively (Rich and others, this volume), which exceeded the State of Montana acute aquatic-life standards of 2.3 and 111 µg/L, respectively (average hardness during pre-remediation high flow used for calculating standards). Although trace-element concentrations were high in High Ore Creek, pH was consistently greater than 7.

Dissolved cadmium and zinc concentrations decreased downstream from the Comet mine during high- and low-flow conditions. Dilution by tributary inflow appears to have been a major factor in the decreases. Limited data for Bishop Creek and Peters Gulch showed low trace-element concentrations in

these tributaries. During low flow, total-recoverable zinc concentrations in the two tributaries were 20 and 40 µg/L, respectively, whereas concentrations were 30 and <10 µg/L, respectively, during spring runoff (Rich and others, this volume).

Although zinc concentrations in Bishop Creek were low relative to the mainstem, the Grey Eagle mine is a possible source that could contribute trace elements to High Ore Creek during high flow (Pioneer Technical Services, Inc , 1999). Overland runoff and high flows can transport sediment enriched with trace elements from waste-rock dumps at the Grey Eagle mine downstream to High Ore Creek. Similarly, the waste rock at the King Cole and Golconda/Reliance mines also might have degraded water quality by contributing sediment during high flow (Marvin and others, 1997).

Upstream from the Comet mine, High Ore Creek contains a pristine fisheries environment, which includes a native population of westslope cutthroat trout and a diverse population of macroinvertebrates (Gless, 1990; Pioneer Technical Services, Inc., 1999). The waste rock and tailings in the High Ore Creek valley bottom at the Comet mine blocked fish passage and thereby isolated the westslope cutthroat trout from the rest of the Boulder River watershed where introduced species of trout occur. Presumably, westslope cutthroat trout inhabited all of High Ore Creek before mining.

Downstream from the Comet mine, High Ore Creek was considered extremely degraded by Gless (1990) based on the limited diversity of the macroinvertebrate population and elevated arsenic concentrations in water. This part of the stream did not support a fishery (Pioneer Technical Services, Inc., 1999; Farag and others, this volume). In addition, studies by Nelson (1976), Knudson (Ken Knudson, consulting biologist, Helena, Mont., written commun., 1984), and Phillips and Hill (1986) demonstrated that fish populations decreased in the Boulder River downstream from High Ore Creek owing to degraded water quality resulting primarily from high trace-element concentrations.

At the mouth of High Ore Creek, biological data indicated that trace elements were accumulating in biofilm, macroinvertebrates, and fish (Farag and others, this volume). During an experiment exposing fish to ambient stream water, survival rates of juvenile westslope cutthroat trout were very low owing to elevated concentrations of copper and zinc (Farag and others, this volume). Elevated arsenic concentrations caused dark coloration and an increased number of melanocytes on fish skin (Farag and others, this volume).

In summary, the pre-remediation environmental data showed that the large amount of waste rock and tailings near the Comet mine and acid drainage from these wastes caused elevated trace-element concentrations in water from High Ore Creek and in flood-plain and streambed-sediment deposits along High Ore Creek downstream to the Boulder River. In addition, waste rock near the Grey Eagle and Golconda/Reliance mines could have contributed to the elevated trace-element concentrations in water and in flood-plain and streambed-sediment deposits.

Remediation Along the High Ore Creek Valley

Based on chemical and biological environmental data, the Comet mine wastes and mill tailings (figs. 2, 3) were

Figure 2. Mill tailings in High Ore Creek valley at Comet mine site before large-scale remediation activities, October 1996. Photograph by D.A. Nimick.

Figure 3. Comet Mill and open-pit mine before large-scale remediation activities, October 1996. Photograph by D.A. Nimick.

considered a high priority by the State of Montana and the Bureau of Land Management (BLM) for remediation. The Montana Department of Environmental Quality (MDEQ) started preliminary remediation work at the Comet mine site in 1995. Initially, the efficiency of the existing sediment pond was improved, a new treatment pond was constructed below the sediment pond, and other erosion-control barriers were installed (Pioneer Technical Services, Inc., 1997). Large-scale remediation efforts began in September 1997. From September to December 1997, waste rock and mill tailings filling the original channel and adjacent valley bottom of High Ore Creek and 1 ft of the underlying native soil near the mine were excavated and moved to the existing open pit, which was used as an unlined repository (figs. 4, 5). From May through July 1998, other waste-rock materials were amended onsite with lime. During the second phase, planned to start in 2001, about 1,700 ft of High Ore Creek will be reconstructed to restore the channel to its approximate premining position and

Figure 4. High Ore Creek valley at Comet mine site after remediation activities, August 1998. The creek has been redirected and the area regraded. Photograph by D.A. Nimick.

Figure 5. Comet Mill and mine site after remediation activities, August 1998. Waste rock and tailings have been removed, and the open pit has been used as a repository. Photograph by D.A. Nimick.

condition through the Comet mine site. Upon completion of this project, approximately 430,500 yd^3 of waste will have been removed (Pioneer Technical Services, Inc., 1997).

Because High Ore Creek had been eroding and transporting mill tailings from the Comet mine site for many years, the area downstream from the Comet mine to the Boulder River also was targeted for remediation. In fall 1999, the BLM restored 3.73 mi of High Ore Creek on BLM and private land by removing about 5,800 yd^3 of waste rock and about 28,000 yd^3 of mill tailings from the valley bottom (Pioneer Technical Services, Inc., 1999). Upstream from Bishop Creek, flood-plain and streambed-sediment deposits were removed, the High Ore Creek channel was reconstructed, and clean material was imported to backfill the excavated areas (fig. 6). Downstream from Bishop Creek, waste rock and flood-plain deposits were either removed or amended in place with lime, but the

Figure 6. Reconstructed reach of High Ore Creek downstream from Comet mine site, December 1999. Photograph by J.H. Lambing.

stream channel was not disturbed. All excavated wastes were placed in an unlined repository (fig. 1) with a multi-layered cap, south of the Comet mine (Pioneer Technical Services, Inc., 1999).

Evaluation of Remediation

The long-term pattern of trace-element concentrations in High Ore Creek will determine whether the remediation in the basin has been successful. Decreasing concentrations over time should eventually result in improved riparian and aquatic conditions. Trace-element concentrations were assessed by graphing temporal trends for four sites, by comparing longitudinal concentration profiles for similar flow conditions before and after cleanup, and by statistical analysis.

Temporal Trends

Water-quality samples were collected at or near four USGS sites (fig. 7) on High Ore Creek from September 1993 through October 2000 (Marvin and others, 1997; Nimick and Cleasby, 2000; Tupling, 2001; Rich and others, this volume). Data for these samples show the initial effect of the MDEQ and BLM remediation projects. Dissolved and total-recoverable copper and lead concentrations commonly were less than aquatic-life standards both before and after remediation and are not discussed here in further detail. Dissolved and total-recoverable cadmium, manganese, and zinc concentrations had

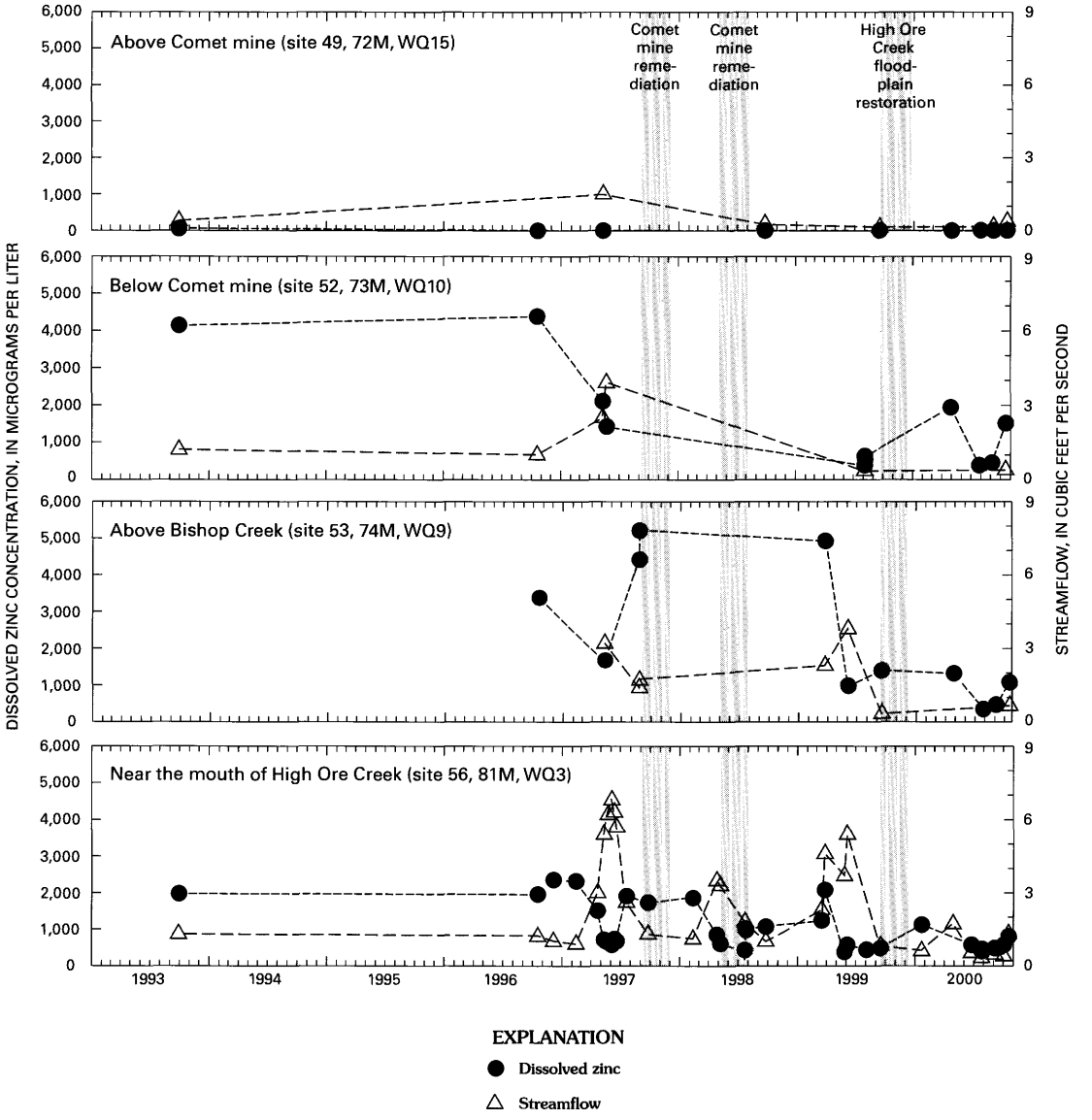

Figure 7. Dissolved zinc concentrations and streamflow in four reaches of High Ore Creek, 1993–2000. Data from Marvin and others (1997), Nimick and Cleasby (2000), Tupling (2001), and Rich and others (this volume). Zinc concentrations reported as less than the minimum reporting level of 1 µg/L are plotted as 1 µg/L.

similar patterns of temporal variation. Dissolved zinc concentrations, discussed here, illustrate the effects of remediation.

Dissolved zinc concentrations upstream from the Comet mine site (site 49) did not change from 1997 through 2000 and were consistently low (less than 55 µg/L). However, dissolved zinc concentrations at two sites (sites 52 and 53) between the Comet mine and Bishop Creek generally decreased after the beginning of large-scale cleanup in 1997 (fig. 7). Dissolved zinc concentrations near the mouth of High Ore Creek (site 56) also appear to have decreased after the beginning of large-scale cleanup. Samples collected on March 25, 1999, at sites 53 and 56 reflect early spring snowmelt runoff, which had anomalously high concentrations of dissolved zinc as well as other trace elements and suspended sediment (not shown in fig. 7). Sampling was not conducted during similar snowmelt runoff conditions prior to large-scale remediation activities. Therefore, the effect of remediation activities on zinc concentrations during early snowmelt runoff cannot be evaluated.

Pre- and Post-Remediation Concentration Profiles

An objective way to look at the effects of the Comet mine remediation is to compare pre- and post-remediation trace-element concentrations along High Ore Creek during similar flow conditions. Data collected by MBMG in September 1993 (Marvin and others, 1997) and Montana Tech in April 2000 (table 1; Tupling, 2001) as part of a post-reclamation study funded by the BLM clearly show the effects of cleanup (fig. 8). Based on limited data, streamflow in April 2000 (1.7 ft^3/s at site WQ3, fig. 1) probably was similar to the flow in September 1993 (1.3 ft^3/s at site 81M, fig. 1). Again, dissolved zinc is discussed here to illustrate a pattern that was similar for dissolved cadmium and manganese. Figure 8 shows that dissolved zinc concentrations represented by two sample sets collected during similar hydrologic conditions decreased at essentially all sampling sites between 1993 and 2000. The largest decreases between 1993 and 2000 occurred at sites in the reach between the Comet and King Cole mines. However, the increase in dissolved zinc concentrations downstream from the Comet mine site in 2000 relative to site WQ15 above the mine indicates that the mine site is still a source of dissolved zinc to High Ore Creek. From Bishop Creek to the mouth of High Ore Creek, concentrations in 2000 remained essentially uniform, unlike in 1993 when concentration increases occurred downstream from Peters Gulch and the Golconda/Reliance mine sites.

Concentrations of dissolved zinc exhibit diel cycles in High Ore Creek, with concentrations fluctuating by as much as a factor of 3 between early morning and late afternoon (Lambing and others, this volume, Chapter D7). These cycles potentially could have a large effect on comparisons of concentration data, such as those in figure 8, collected on different sampling dates. Sites downstream from Peters Gulch (fig. 8) were sampled at about the same time of day during the September 1993 and April 2000 sampling episodes. Although the same sites were not sampled each year, the sampling time for each site sampled in 2000 was within 60 minutes of the sampling time for nearest site sampled in 1993. Temporal concentration variations attributable to diel cycles during a 60-minute period are only a fraction of the total diel variation and, therefore, would not be large enough to eliminate or reverse the apparent decrease in concentration shown by the post-remediation data in figure 8. Sites between Peters Gulch and the Comet mine were not sampled at similar times during the two sampling episodes. Sites were sampled in mid- to late morning in September 1993, when concentrations would be near their maximum diel values, whereas sites were sampled in mid- to late afternoon in April 2000, when concentrations would be near the diel minimum values. Therefore, the apparent decrease in concentration shown in figure 8 may be much less than shown. These data demonstrate the importance of understanding diel cycles when trends in trace-element concentrations are being assessed.

In contrast to dissolved zinc, dissolved arsenic concentrations apparently increased since large-scale remediation began in 1997. In particular, concentrations at the mouth of High Ore Creek (site 56) not only have increased from pre-remediation levels, but values that typically were less than the State of Montana human-health standard of 18 µg/L have increased to post-remediation values that typically are higher than this standard (fig. 9). One explanation for this phenomenon is that sorption onto particulates, which is an important control on arsenic mobilization, has decreased. Sorption is dependent on pH, and arsenic desorption increases as pH increases (Pierce and Moore, 1982). However, the pH of High Ore Creek does not appear to have increased after remediation began (fig. 9), so the arsenic probably is not derived from desorption of arsenic from streambed sediment. A more likely explanation of these increases in dissolved arsenic in the stream is that the lime used to amend waste rock at the mine site and flood-plain deposits downstream from Bishop Creek resulted in an increase in pH in these materials. The higher pH likely mobilized arsenic, which then leached into High Ore Creek.

Statistical Analysis

A preliminary statistical analysis of water-quality data was done by segregating available data into two sets representing pre- and post-remediation periods. Data for September 1997 were designated as the last pre-remediation sampling data. Multivariate analysis of variance (MANOVA) was used to compare the combined means of the logarithmically transformed trace-element concentrations and streamflow values. Dissolved zinc concentrations were used to represent the general differences between pre- and post-remediation metal concentrations.

Data for five monitoring sites in the Boulder River watershed (fig. 1, sites 3, 24, 47, 56, and 58) were used to evaluate the preliminary effects of the Comet mine cleanup

Table 1. Trace-element data for High Ore Creek, April 28, 2000.[1]

[ft^3/s, cubic feet per second; µg/L, micrograms per liter; <, less than minimum reporting level; —, no data]

Site No.	Station name	Stream-flow, instan-taneous (ft^3/s)	Arsenic, dis-solved (µg/L)	Arsenic, total recov-erable (µg/L)	Cad-mium, dis-solved (µg/L)	Cad-mium, total recov-erable (µg/L)	Copper, dis-solved (µg/L)	Copper, total recov-erable (µg/L)	Lead, dis-solved (µg/L)	Lead, total recov-erable (µg/L)	Zinc, dis-solved (µg/L))	Zinc, total recov-erable (µg/L)
WQ3	High Ore Creek near mouth	1.7	21.8	47.7	2.76	3.78	3.1	10.8	<2	44.3	792	1,010
WQ4	High Ore Creek at cabin residence	—	19.9	57.9	2.67	3.92	3.56	12.1	<2	52.5	768	1,070
WQ5	High Ore Creek downstream from Peters Gulch	—	19.0	61.6	2.66	4.11	4.02	12.8	<2	58.7	768	1,060
WQ7	High Ore Creek downstream from Bishop Creek.	—	13.5	40.8	2.51	3.48	2.04	9.98	<2	57.9	767	959
WQ9	High Ore Creek upstream from Bishop Creek	—	18.6	48.0	3.97	4.92	2.59	10.1	<2	44.6	1,320	1,470
WQ10	High Ore Creek downstream from reconstruc-tion.	—	14.5	18.4	5.82	5.94	<2	3.1	<2	6.42	1,940	1,910
WQ11	High Ore Creek downstream from Comet mine and above reconstruction.	—	11.4	15.8	6.44	6.22	<2	2.84	<2	5.85	2,190	2,220
WQ15	High Ore Creek upstream from Comet mine	—	1.69	2.1	<2	<2	<2	<2	<2	<2	4.22	11.9

[1]Data from Tupling (2001).

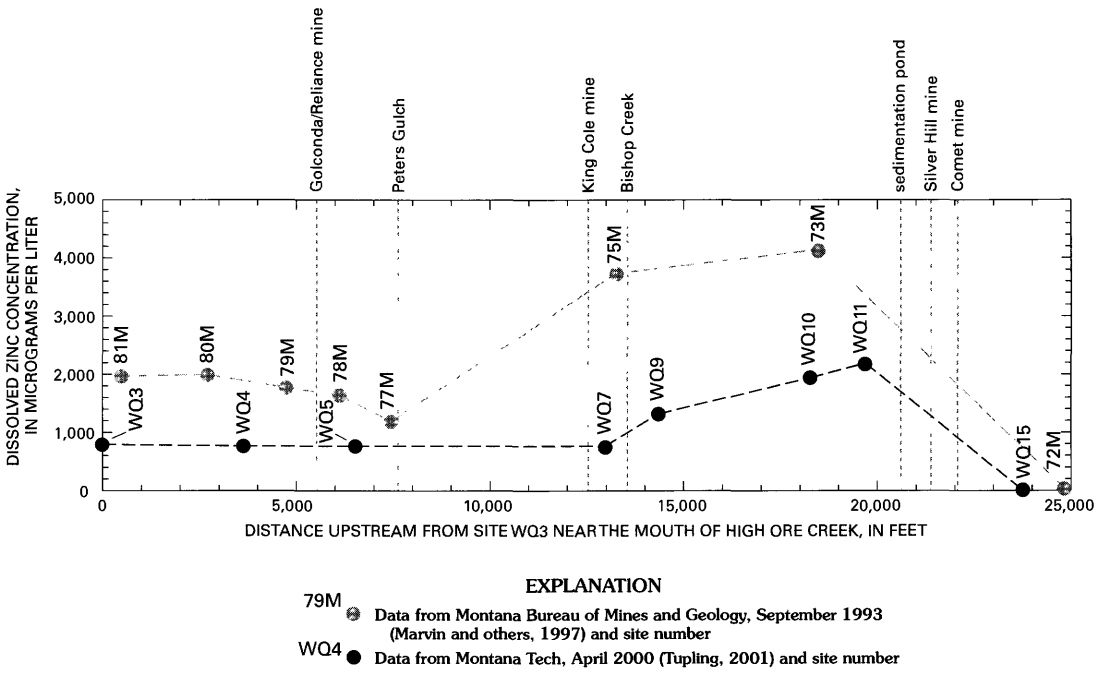

Figure 8. Dissolved zinc concentrations in High Ore Creek, September 1993 and April 2000.

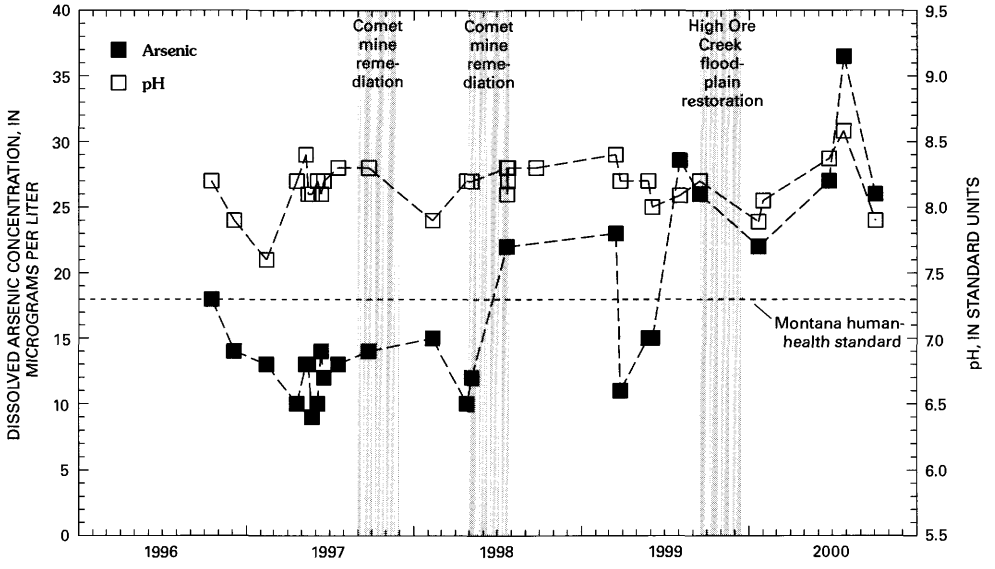

Figure 9. Dissolved arsenic concentrations and pH at mouth of High Ore Creek (site 56), 1996–2000.

on the Boulder River and High Ore Creek relative to other tributaries and upstream portions of the watershed. Results of the MANOVA tests determined that the combined means of dissolved zinc concentrations and streamflow at three sites unaffected by remediation (sites 3, 24, and 47) were not significantly different between the two time periods (before and after September 1997) (table 2). In contrast, High Ore Creek (site 56) and the Boulder River below Little Galena Gulch (site 58) had significantly different means between the two periods, indicating that dissolved zinc concentrations had changed.

Figure 10 shows ordinary least squares regression relations between streamflow and dissolved zinc concentrations for both pre- and post-remediation at the five Boulder River watershed sites. Basin Creek and Cataract Creek showed very little change in the relation between the two time periods. The upper site on the Boulder River (site 3) displayed some variation, but maintained consistently low concentrations. The most downstream site on the Boulder River (site 58) displayed a clear post-remediation downward shift in zinc concentrations at low streamflows (less than 100 ft^3/s), but tended to converge with the pre-remediation relation at higher flows (greater than 100 ft^3/s). One notable feature is that High Ore Creek post-remediation data are highly scattered, indicating that dissolved zinc concentrations have not stabilized since remediation activity ended. With time, a stronger relation between streamflow and concentration might be expected to develop as remediated areas physically stabilize and hydrologic and geochemical equilibrium is established. Continued monitoring, especially at High Ore Creek and the Boulder River below Little Galena Gulch, would provide the necessary data to better demonstrate and quantify the overall change in trace-element concentrations and, ultimately, to determine the degree to which remediation was successful in improving the health of aquatic biota.

Summary

Inactive historical mines and a mill in the High Ore Creek valley produced wastes enriched in trace elements that degraded water quality and eliminated fish in High Ore Creek downstream from the Comet mine. These environmental effects were sufficiently severe to warrant remediation activities for abandoned mine lands in the basin. Pre-remediation environmental data showed that waste rock, mill tailings, fluvial tailings deposits, and streambed sediment contained elevated trace-element concentrations. MDEQ removed waste rock and tailings at the Comet mine site in 1997–98 and plans to finish reclaiming the mine site in 2001. BLM removed Comet mill tailings from the flood plain upstream from Bishop Creek, reconstructed the stream channel, and amended the waste rock and mill tailings with lime downstream from Bishop Creek.

A preliminary evaluation of pre- and post-remediation water-quality data from four sites along High Ore Creek has shown decreased dissolved zinc concentrations through time at the three sites below the Comet mine since large-scale remediation started. Downstream profiles of dissolved zinc concentrations at multiple sites along High Ore Creek in 1993 and 2000 showed consistently lower concentrations in 2000 throughout the entire reach of High Ore Creek below the Comet mine. In contrast, dissolved arsenic concentrations apparently have increased since remediation started, most likely owing to desorption and leaching associated with the pH effects of liming. Comparison of pre- and post-remediation regression relations between streamflow and dissolved zinc concentrations at five sites throughout the Boulder River watershed indicate that zinc concentrations at the mouth of High Ore Creek and the Boulder River below Little Galena Gulch have decreased since remediation started, although concentrations in High Ore Creek are not yet stable. Continued environmental monitoring would provide the necessary data to demonstrate and quantify the change in trace-element concentrations that can ultimately determine whether remediation was successful.

Table 2. Results of multivariate analysis of variance of dissolved zinc concentrations and streamflow for selected sites in Boulder River watershed for 1993–97 and 1997–2000 periods.

Site No.	Station name	Level of significance (*p*-value)[1]	Conclusion ($\alpha = 0.05$)
3	Boulder River above Kleinsmith Gulch, near Basin	0.154	Means were equal.
24	Basin Creek at Basin	.403	Means were equal.
47	Cataract Creek at Basin	.340	Means were equal.
56	High Ore Creek near Basin	.010	Means were not equal.
58	Boulder River below Little Galena Gulch, near Boulder	.003	Means were not equal.

[1]A p-value less than 0.05 indicates a significant difference between means.

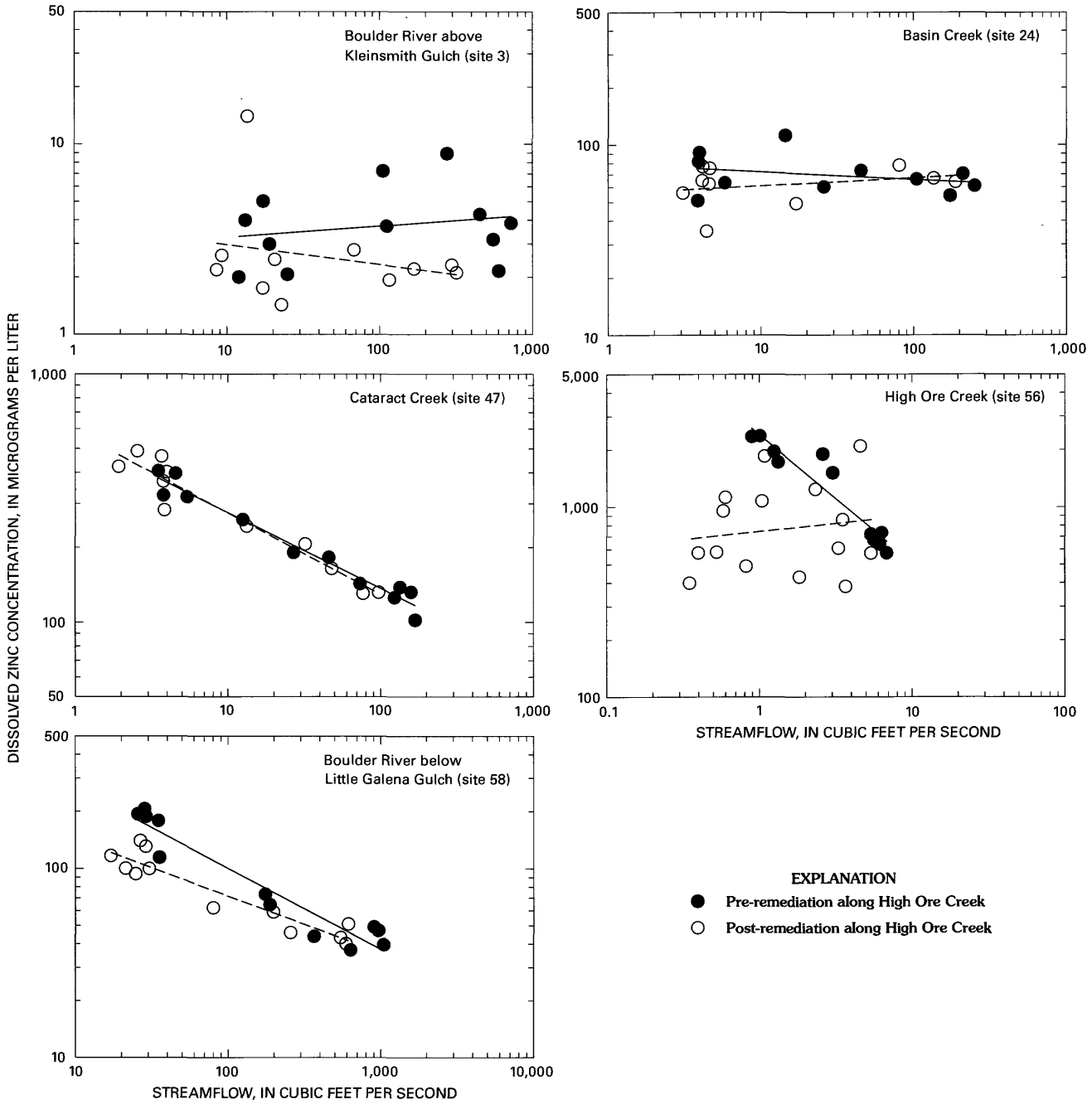

Figure 10. Regression relation of dissolved zinc concentrations and streamflow for pre- and post-remediation periods at five long-term monitoring sites in Boulder River watershed, 1996–2000.

References Cited

Becraft, G.E., Pinckney, D.M., and Rosenblum, Sam, 1963, Geology and mineral deposits of the Jefferson City quadrangle, Jefferson and Lewis and Clark Counties, Montana: U.S. Geological Survey Professional Paper 428, 100 p.

Elliott, J.E., Loen, J.S., Wise, K.K., and Blaskowski, M.J., 1992, Maps showing locations of mines and prospects in the Butte 1 degree × 2 degree quadrangle, western Montana: U.S. Geological Survey Miscellaneous Investigations Series Map I– 2050–C, 2 sheets, scale 1:250,000.

Fey, D.L., and Church, S.E., 1998, Analytical results for 42 fluvial tailings cores and 7 stream sediment samples from High Ore Creek, northern Jefferson County, Montana: U.S. Geological Survey Open-File Report 98–215, 49 p.

Fey, D.L., Unruh, D.M., and Church, S.E., 1999, Chemical data and lead isotopic compositions in stream-sediment samples from the Boulder River watershed, Jefferson County, Montana: U.S. Geological Survey Open-File Report 99–575, 147 p.

Gless, E.E., 1990, Biological and chemical baseline studies along the Boulder River and its tributaries in Jefferson County, Montana: Prepared by E.E. Gless, Montana College of Mineral Science and Technology, Butte, Mont., as a report to the Jefferson County Commissioners, variously paged.

Marvin, R.K., Metesh, J.J., Bowler, T.P., Lonn, J.D., Watson, J.E., Madison, J.P., and Hargrave, P.A., 1997, Abandoned-inactive mines program, U.S. Bureau of Land Management: Montana Bureau of Mines and Geology Open-File Report 348, 506 p.

Montana Department of State Lands, 1995, Abandoned hardrock mine priority sites, 1995, summary report: Helena, Mont., prepared for Abandoned Mine Reclamation Bureau by Pioneer Technical Services, Inc., Butte, Mont., variously paged.

Nelson, F.A., 1976, The effects of metals on trout populations in the Upper Boulder River, Montana: Bozeman, Mont., Montana State University M.S. thesis, 60 p.

Nimick, D.A., and Cleasby, T.E., 2000, Water-quality data for streams in the Boulder River watershed, Jefferson County, Montana: U.S. Geological Survey Open-File Report 00–99, 70 p.

Phillips, Glenn, and Hill, Kurt, 1986, Evaluations of sources and toxicity of copper and zinc in the Boulder River drainage, Jefferson County–1985: Montana Department of Fish, Wildlife and Parks, Pollution Control Information Series, Technical Report 4, 28 p.

Pierce, M.L., and Moore, C.B., 1982, Adsorption of arsenite and arsenate on amorphous iron hydroxides: Water Research, v. 16, p. 1247–1253.

Pioneer Technical Services, Inc., 1997, Final expanded evaluation/cost analysis for the Comet mine site: Butte, Mont., prepared for Montana Department of Environmental Quality, Abandoned Mine Reclamation Bureau, variously paged.

Pioneer Technical Services, Inc., 1999, Final expanded engineering evaluation/cost analysis for the High Ore Creek stream side tailings reclamation project: Butte, Mont., prepared for Montana Department of Environmental Quality, Abandoned Mine Reclamation Bureau, variously paged.

Tupling, Robert, 2001, Reclamation of the High Ore Creek watershed: Butte, Mont., Montana Tech of the University of Montana M.S. thesis, 133 p.

Geologic, Geophysical, and Seismic Characterization of the Luttrell Pit as a Mine-Waste Repository

By Bruce D. Smith, Robert R. McDougal, and Karen Lund

Chapter E3 of

Integrated Investigations of Environmental Effects of Historical Mining in the Basin and Boulder Mining Districts, Boulder River Watershed, Jefferson County, Montana

Edited by David A. Nimick, Stanley E. Church, and Susan E. Finger

In cooperation with the
U.S. Environmental Protection Agency

Professional Paper 1652–E3

U.S. Department of the Interior
U.S. Geological Survey

Contents

Figures

Chapter E3
Geologic, Geophysical, and Seismic Characterization of the Luttrell Pit as a Mine-Waste Repository

By Bruce D. Smith, Robert R. McDougal, and Karen Lund

Abstract

Integrated geologic and geophysical studies conducted near the Luttrell pit at the former Basin Creek mine provide geotechnical information that characterizes the area of the mine-waste repository. The geologic setting, fracture patterns, potential ground-water flow paths, and historical seismicity were examined using mining company records, geologic and geophysical data, and remote sensing images. Interpretation and analysis of airborne geophysical data suggest a much greater structural and lithologic complexity than indicated by the geologic mapping. The bedrock in the immediate area of the Luttrell pit does not have high acid-neutralizing potential as interpreted from the airborne geophysical data. Although the region is an area of high seismic activity, little historical seismic activity has been recorded near the pit. Regional stress suggests that northeast-trending fractures may be preferentially open but local stress conditions at the mine-waste repository are unknown. Although faults in the area were active before and after mineralization, no recent movement was evident in the structures exposed by the pit mining. Structures inferred from geologic mapping, from airborne geophysical data, and from lineaments mapped using remote sensing images define a northeast-trending structural zone located 0.25 miles south of the pit. This zone may influence the local flow of ground water in fractures and would be a possible area for bedrock ground-water monitoring. The potential for enhanced ground-water recharge or discharge may be greater in areas where the geophysical data indicate high electrical conductivity and mapping indicates the presence of linear features or structures.

Introduction

Mine wastes and mill tailings produced during historical mining activities commonly were discarded with little regard for any potential effect on the landscape and resources. Runoff from or direct erosion of these wastes is a primary cause of environmental degradation in many watersheds, like the Boulder River watershed, that have been affected by historical mining. Repositories are a common type of facility used to consolidate and contain mining wastes. Repository-siting studies are therefore an important component of investigations designed to characterize abandoned mine lands prior to remediation activities.

Siting of repositories requires consideration of a complex array of environmental, economic, engineering, and political factors. As a part of the overall siting investigation, geotechnical studies (geology, geophysics, seismicity, and linear feature mapping) can provide important information for assessing each of these factors. Geologic information provides the basic framework for understanding the underpinnings of the repository and is critical for understanding the hydrogeology and potential fate of any contaminants released from the repository. Geologic information also provides information on the presence of faults and potential seismicity of the area. Geophysical data are useful for examining the subsurface geology of an area in greater detail than is possible from surface mapping. Geophysics and geochemistry provide a means to estimate surface and subsurface acid-neutralizing potential. Linear feature mapping using remote sensing images provides additional detail not easily obtained from traditional geologic mapping.

In the late 1990s, land-management agencies considered several potential repository sites near major historical mines in the Boulder River watershed for consolidation of mine wastes. Initial studies of some of these sites demonstrated that the region's granitic bedrock could neutralize potential releases of acidic leachate (Desborough and Driscoll, 1998). However, further investigation of these sites was curtailed when the opportunity arose to utilize an open pit at the former Basin Creek mine. The Luttrell pit is centrally located (fig. 1) as well as sufficiently large to contain historical mining wastes from several drainage basins. The agencies initiated investigations to identify and evaluate geotechnical characteristics that would affect site engineering. Reported here are results from those studies which have implications for the potential fate of contaminant releases and the possibility of earthquake activity destabilizing the repository.

Purpose and Scope

This report describes and interprets selected geotechnical characteristics in the area of the Luttrell pit mine-waste repository, which are important considerations in engineering design. In particular, the goals of the report are to

- Describe the geology, alteration, mineralization history, joints, and faults
- Examine airborne geophysical data to determine the nature of subsurface rocks and geologic structures
- Provide preliminary conclusions about possible seismic hazards, and
- Interpret linear features from remote sensing images to identify possible structures that could control groundwater flow paths to or from the repository site.

Setting

The Luttrell pit was one of three open pits at the Basin Creek mine, which is located on the Continental Divide near the northern boundary of the Boulder River watershed study area (fig. 1). The site is near the headwaters of several drainage basins (fig. 1) where historical mining has occurred.

Gold was mined by underground and open-pit heap-leach operations in various locations within 1 mi of the Luttrell pit (fig. 1) intermittently from about 1892 to 1991. From 1915 to 1926, the Basin Creek underground mine was operated by the Anaconda Minerals Company. During 1988 and 1989, Pangea Resources Ltd. conducted the first open-pit heap-leach operations, called the Columbia and Paupers pits, in the general location of the Paupers Dream mine southwest of the Luttrell pit. Pegasus Gold Corporation purchased the mine operations in 1989 and formed Basin Creek Mining, Inc. (a wholly owned subsidiary). The Paupers and Columbia pits were backfilled during mining of the Luttrell pit and subsequently capped with clay from the site (Dan Adams, Basin Creek Mine, Inc., oral commun., 1999); the Luttrell pit had not been backfilled when mining ceased in 1991.

Based on the results of our work and other studies, use of the Luttrell pit as a mine-waste repository began in 1999. During 1999 and 2000 approximately 140,000 loose cubic yards of mine-waste material was placed in individual cells. Each cell has a composite liner and a leachate collection and removal system (URS, Greiner Woodward Clyde, written commun., November 1999). The repository has room for additional wastes that will be removed from nearby inactive mines and mills in the future.

Methods

The geologic description in this chapter was compiled from published mapping (Ruppel, 1963), unpublished data primarily from Pegasus Gold Corporation reports, and observations made during geologic field investigations (O'Neill and others, this volume, Chapter D1). M.W. Reynolds (Thamke, 2000) compiled geologic mapping of bedrock in the Helena area including the Luttrell pit area.

Airborne magnetic and electromagnetic surveys were flown over the site in 1996 and 1997 (Smith, McCafferty, and McDougal, 2000; McCafferty and others, this volume, Chapter D2). The airborne geophysical data along flightlines have been gridded with a 120-ft cell size, which is about 1/5 of the flightline spacing (Smith, Labson, and Hill, 2000). This cell size was required because of the difference between the flightline separation (600 ft) and the sampling interval along flightlines at 9 ft. The gridded data have been used to produce color maps discussed here.

The total-field airborne magnetic data have been processed and reduced to the pole as described by McCafferty and others (this volume). Reduction to the pole produces magnetic maps where the causative source for magnetic anomalies is directly beneath the high or low. Magnetic highs are caused by a greater abundance of magnetic minerals (primarily magnetite) in comparison to surrounding lithology. Conversely, relative magnetic lows are caused by an absence of magnetic minerals relative to surrounding lithology. McCafferty and others (this volume) give additional details about geologic features and processes that can be associated with magnetic anomalies. In addition, they give a statistical estimation of the magnetic properties of the geologic map units and their distribution in the Boulder River watershed.

Electromagnetic data were reduced to apparent resistivities (Fraser, 1978) and converted to apparent conductivities at three frequencies (900 Hz, 7,200 Hz, and 56,000 Hz). The apparent conductivity was computed based on a homogeneous half space (an electrically conductive and homogeneous Earth). The use of the term "apparent" reflects the fact that the Earth is not homogeneous and the calculated conductivities are an estimate of the true electrical conductivity. The depth of investigation varies inversely as a function of frequency and conductivity of the subsurface (Spies, 1989). For rocks that have an intermediate conductivity (5 millisiemens per meter), the lowest frequency provides information from a depth of at least 200 ft. The highest frequency provides information from a depth of 10–30 ft. In this study, the apparent conductivity map at 7,200 Hz was used because it provides information from an intermediate depth (30–100 ft), which is the zone that typically would immediately underlie a mine-waste repository.

Electrical conductivity of subsurface materials is determined by a variety of physical and electrochemical properties of the underlying rock and pore fluids (Olhoeft, 1985). Pore fluids affect subsurface conductivity primarily because of the charged ions that are dissolved in the water. Conductivity of the pore fluid increases as the dissolved-solids concentration increases. Therefore, the presence of ground water creates higher conductivity in rocks below the water table than in similar but unsaturated rocks above the water table. If ground water has high concentrations of dissolved solids, subsurface

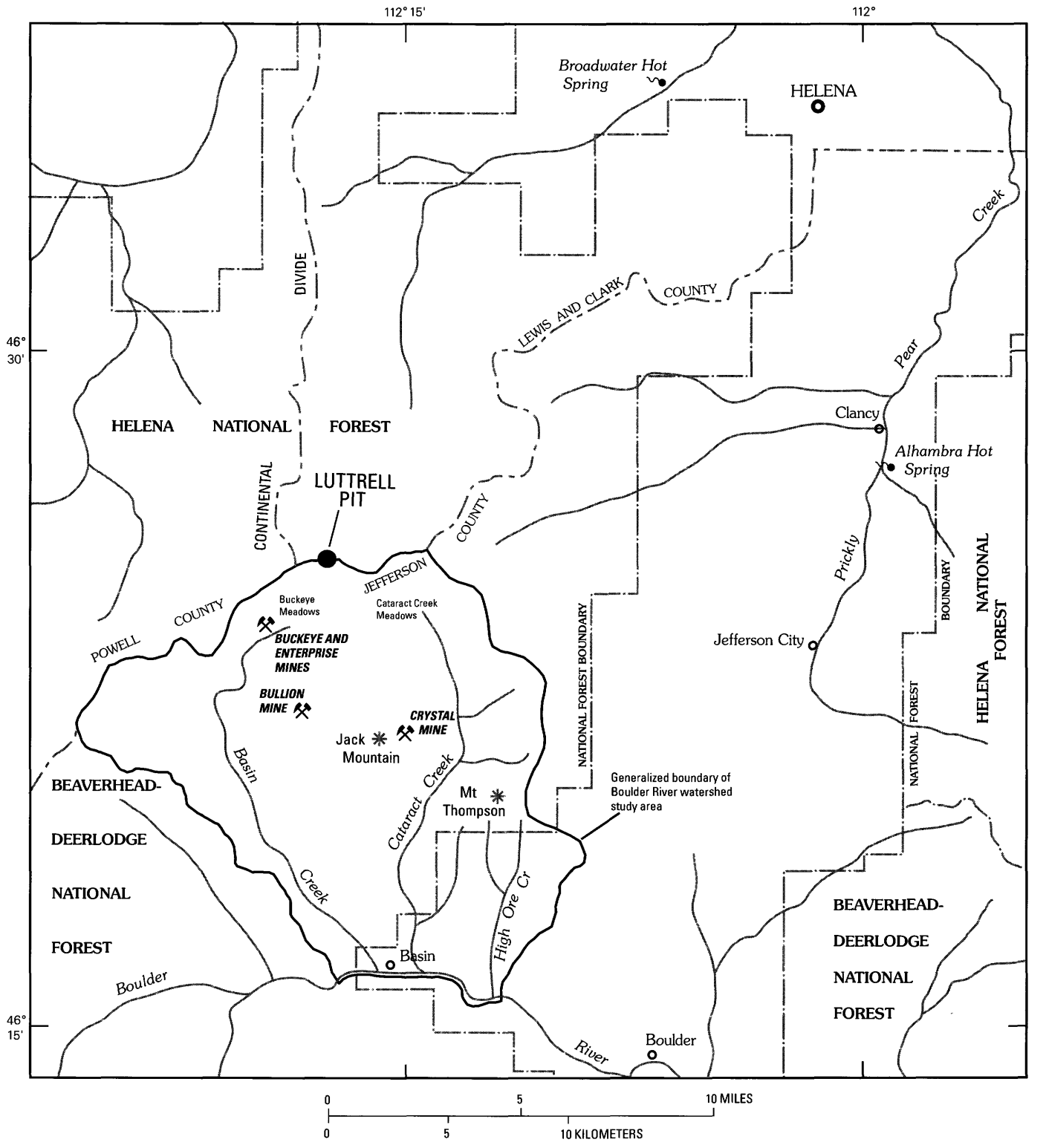

Figure 1. Location of the Luttrell mine-waste repository, in the Boulder River watershed. Base modified from U.S. Geological Survey 1:250,000 Butte, 1947, and White Sulphur Springs, 1958.

conductivity can be much higher than in rocks with fresh (potable) water. The amount of pore space (porosity) in rocks also can affect subsurface conductivity because conductivity increases as more pore space within rocks is filled with fluids. Mineralogy of rocks is important in determining subsurface conductivity. For instance, the presence of clay tends to increase conductivity. In addition, some clay minerals such as montmorillonite that have large cation exchange capacity can have higher electrical conductivity than clay minerals such as kaolinite that have small cation exchange capacity. Glacial moraines, some types of soil, and weathered volcanic rocks can contain significant amounts of clay minerals. Massive or interconnected metallic mineral deposits are another cause of high conductivity. Power lines, some fences, and pipelines also can cause high conductivity anomalies. McCafferty and others (this volume) estimated the apparent electrical properties associated with each of the mapped geologic units.

Seismicity interpretations were based on published peak ground acceleration, epicenter, and isoseismal maps (Neumann, 1937). These data were compared with Quaternary fault maps to determine location of active faults near the Luttrell pit and to predict earthquake activity of faults mapped in and near the study area. These data also were used to predict geologic controls of active faults and possible local surface disturbances during earthquakes.

Fracture studies were based on published data (Ruppel, 1963; Becraft and others, 1963) as well as mapping and interpretation of linear features from remote sensing imagery. Two data sets were used to generate base images for lineament mapping. Landsat Thematic Mapper (TM) (≈100 ft spatial resolution) and India Remote Sensing (IRS) 1-C panchromatic (17 ft spatial resolution) data were processed and filtered to enhance linear features (McDougal and others, this volume, Chapter D9). Linear features considered to represent faults, fractures, or other linear geologic features were mapped as a vector coverage from each base image. The azimuth and line length were calculated from the endpoints of each mapped vector. A digital map showing wet soil types (wetland areas; McDougal and others, this volume) was draped over a digital elevation model (DEM) and combined with the map of linear features to identify areas where there is an overlap of a high occurrence of fractures and saturated soils. These are areas of possible ground-water recharge or discharge.

Geological Characterization

Setting

Geologic information provides the basic framework for assessing many important geotechnical and hydrologic characteristics of a potential repository site. The Basin Creek mine (fig. 1) is in the northern part of the Late Cretaceous Boulder batholith–Elkhorn Mountains Volcanics complex, which is an important geologic feature of west-central Montana (O'Neill and others, this volume). The Basin Creek mine site is underlain at depth by the Butte pluton of the Boulder batholith (Lund and others, 2002). The Late Cretaceous volcano-plutonic complex was intruded and overlain by Eocene dikes and volcanic rocks of the Lowland Creek Volcanics episodes and by Eocene-Oligocene volcanic necks and volcanic rocks of the Helena volcanic field (O'Neill and others, this volume, pl. 1).

At the Basin Creek mine, a series of Eocene-Oligocene purplish-gray and purple pyroclastic rhyolite tuffs and flows (O'Neill and others, this volume, pl. 1) of the Helena volcanic field overlie the Butte pluton and are the primary host of the gold deposits. These rhyolitic rocks are commonly porphyritic and contain phenocrysts of sanidine and biotite. They are characterized by spherulitic and fiamme textures of welded tuffs. The rocks are dated about 34 Ma (Chadwick, 1978; O'Neill and others, this volume) and originated as deposits from local vents near the Basin Creek mine. Recognized vents are in an east-northeast-trending zone and include, from west to east, the peak west of the Josephine mine, Pauper Peak, Luttrell Peak, and Red Mountain (O'Neill and others, this volume). The Eocene-Oligocene rhyolites were deposited nonconformably on the Late Cretaceous Butte pluton. Prior to deposition of the rhyolites, the plutonic rocks were exposed to erosion and weathering from about Late Cretaceous to late Eocene (for as long as 38 m.y.), and a thin carbonaceous clay was locally deposited on them (O'Neill and others, this volume). This clay was probably developed in a basin which was later in-filled by the Helena volcanic rocks, which metamorphosed the clay to shale (Dan Adams, Basin Creek Mine, Inc., written commun., 1999). This young sediment is age equivalent to the Oligocene siltstone and sandstone described by O'Neill and others (this volume). After deposition of the volcanic materials, a north-trending set of minor down-to-the-west normal faults dropped the depositional contact zone to the west (fig. 2). Hydrothermal mineralization and alteration followed the faulting. The Paupers and Columbia pits are located entirely in the Eocene-Oligocene pyroclastic rhyolites. The Luttrell pit, the westernmost pit, is in the faulted contact zone between the rhyolitic rocks and the underlying plutonic rocks (O'Neill and others, this volume).

Disseminated gold deposits exploited at the Luttrell pit were localized primarily along the contact between plutonic and Helena volcanic rocks: hydrothermal fluids moved along the weathered upper surface of the plutonic rocks, up the minor down-to-the-west normal faults, and into the base of the rhyolites (fig. 2). The hydrothermal solutions resulted in argillic alteration that changed feldspars to clays throughout the mineralized areas, including most of the Luttrell pit area. Mineralization at the Basin Creek mine produced disseminated pyrite and cassiterite in the host rocks. Gold occurs as inclusions in pyrite (and possibly arsenopyrite) grains as well as free gold in zones where the pyrite had oxidized. The Eocene-Oligocene deposits at the Basin Creek mine are notably different in mineralogy from Late Cretaceous quartz-vein and Eocene breccia-pipe mineral deposits found elsewhere in the Boulder River watershed (O'Neill and others, this volume; Lund and others, 2002).

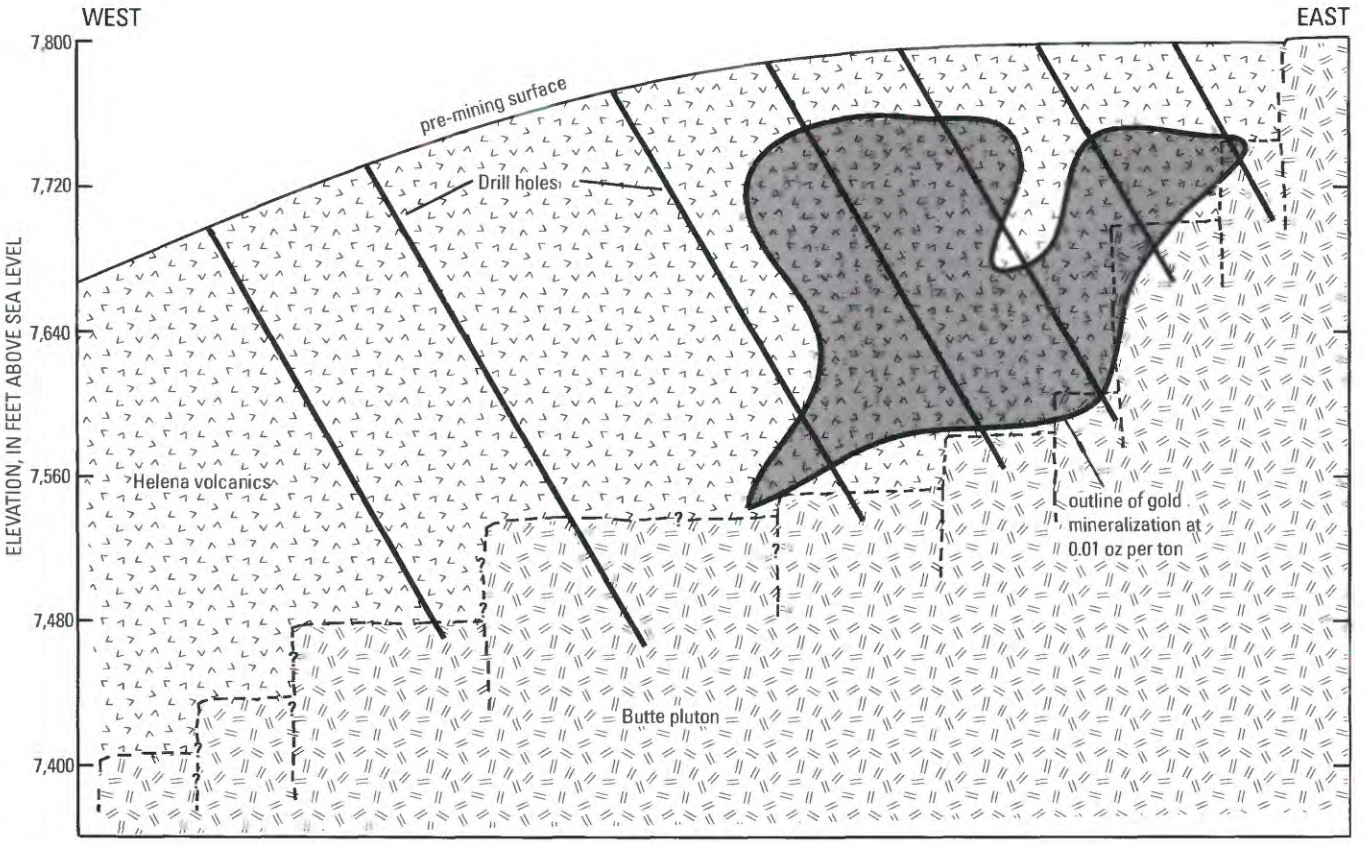

Figure 2. North-south cross section near north end of Luttrell pit, showing geologic interpretation and gold values exceeding 0.01 oz/ton from drill hole data (provided by Pegasus Gold Corporation). Dashed lines are interpreted surfaces and faults, queried where uncertain. No horizontal scale.

Faults

The presence of faults, particularly possible active faults, near a mine-waste repository is important in characterizing the area because they present important engineering constraints. Faults also can be conduits for or barriers to ground-water flow and therefore can significantly influence the hydrology of a repository site. The northeast-trending Butte-Helena fault zone is an important structural feature in the regional tectonic setting of the Luttrell pit (O'Neill and others this volume, fig. 1). McDougal and others (this volume, fig. 6) suggest that the pit is located near the north edge of this structural zone. On a more local scale, Ruppel (1963) described four types of faults that can occur in the area of the Luttrell pit: (1) east-trending fault zones, (2) north-trending faults, (3) north 20° east-trending faults, and (4) northeast- and northwest-trending faults. The latter faults have been the most recently active since they offset glacial deposits. They also control some post-glacial drainages and are marked by prominent fault scarps 50–300 ft high.

The largest mapped fault near the Luttrell pit is an east-northeast-trending normal fault that traverses the south side of the Basin Creek mine and cuts the upper Basin and Banner Creek basins (O'Neill and others, this volume, pl. 1). This fault is shown on the Basin quadrangle mapped by Ruppel (1963) and continues a short distance to the east-northeast in the geologic map of the Jefferson City quadrangle (Becraft and others, 1963). It is grouped with the northeast-trending faults described by Ruppel (1963). In general more faults are shown on the Basin quadrangle (Ruppel, 1963) than on the Jefferson City quadrangle map (Becraft and others, 1963), reflecting the presence of more geologic units to show offset. Our geologic interpretation is that a fault zone controls the northeast trend of Eocene-Oligocene vents. Consequently we have extended the fault shown by Ruppel (1963) and Becraft and others (1963) east-northeast to the general area of Chessman Reservoir. The fault zone that contains this structure is likely composed of several other structures that may have different traces associated with the different ages and possibly styles of faulting. The entire northeast-trending fault zone is covered, so the east-northeast fault shown by O'Neill and others (this volume, pl. 1) is approximately located.

Interpretation of the geologic map suggests that four periods of movement have taken place along this fault from middle Tertiary through Holocene time and that the direction of movement may have reversed through time. Characteristics of the fault which suggest this are:

1. The fault parallels the Eocene-Oligocene vents located along the east-northeast trend from the peak west of the Josephine mine to Red Mountain, suggesting that

the fault was active before the Eocene-Oligocene eruption and may have served as a conduit for the magmas and hydrothermal mineralizing fluids.

2. The Eocene-Oligocene rhyolites are preferentially preserved north of the fault, indicating post-Oligocene (but pre-Pleistocene) down-to-the-north offset after deposition of the rhyolite.

3. The fault also appears to bound the Basin Creek basin along its north edge and may have controlled preservation of glacial deposits on the south side. This would indicate a possible episode of Pleistocene movement.

4. As mapped by O'Neill and others (this volume, pl. 1), the fault cuts the glacial deposits in upper Basin Creek with down-to-the-south movement. Thus, it may have had a fourth episode of movement that included Holocene postglacial activity.

In summary, the long east-northeast-trending fault is part of a larger fault zone that trends northeast. The normal faulting has been active, at least intermittently, for more than 34 m.y. as well as within the last 10,000 years. Therefore, future movement within the fault zone is possible.

A second set of faults in the Luttrell pit area consists of a north-trending zone of minor, down-to-the-west faults (fig. 2) that cut the contact between the Butte pluton and overlying rhyolitic rocks. Movement along these faults preceded mineralization, which took place about 34 Ma. That the faults do not offset mineralized rocks indicates that no movement has occurred on these particular faults since mineralization. Therefore, movement along these faults is highly unlikely to occur in the future. Other short northwest- and northeast-trending faults also cut the contact between the Eocene-Oligocene rhyolites and the Late Cretaceous plutonic rocks (O'Neill and others, this volume, pl. 1). These do not appear to be part of larger fault systems or zones, have only minor offsets, and, from our data, likely have not been active since 35 Ma.

Joints

Joints or fractures occur in almost all rocks. The orientation, intensity, and permeability of joints are important factors in controlling movement of ground water as well as leachate that may be lost from a repository. Orientation and intensity of joints are characteristics that are relatively easy to define. Estimating the permeability of fractured rock requires a more detailed investigation that was beyond the scope of this study.

The Eocene-Oligocene rhyolites that host the Basin Creek mine are relatively free of joints in comparison to either the Late Cretaceous Elkhorn Mountains Volcanics (O'Neill and others, this volume, pl. 1) or the Butte pluton. Many of the joints in the Eocene-Oligocene volcanic rocks are primary features that include cooling joints, some of which are columnar joints. The other common types of joints are platy joints that formed secondarily along the flow and compaction layering in the pyroclastic rocks (Ruppel, 1963).

The underlying plutonic rocks of the Butte pluton have a complex joint pattern (O'Neill and others, this volume, fig. 11) and are more extensively weathered along these surfaces. Several major and minor joint sets have been reported (Ruppel, 1963). Joints of a steeply dipping north-trending set are generally spaced about 1–5 ft apart and those of a steeply dipping east-trending set are spaced about 5–10 ft apart. Joints of the gently dipping east-trending set are spaced about 1–15 ft apart. Several other orientations of joints are present but are not as common. Many joints are probably related to shrinkage during cooling of the magma, and some have been intruded by late-stage aplite dikes (Becraft and others, 1963; Ruppel, 1963). The preferred orientation of the joint sets indicates that they formed in response to regional stress patterns either during or after cooling (O'Neill and others, this volume). Although jointing is pervasive in the Butte pluton, most joints are thought to be tight at depths greater than about 50 ft. Therefore, we hypothesize that little ground water moves through the pluton relative to the amount that flows in the overlying shallow unconsolidated deposits and weathered plutonic rocks (McDougal and others, this volume).

Airborne Magnetic and Electromagnetic Data

Airborne magnetic and electromagnetic data for the Basin Creek mine area (Smith, Labson, and Hill, 2000; McCafferty and others, this volume) provide additional information about the subsurface lithology, structure, and ground water of the area. Reduced-to-the-pole magnetic field data are shown as a color-shaded relief map (fig. 3). The sun angle used to produce the shading is from the northwest in order to enhance northeast-trending features. McCafferty and others (this volume) give a detailed discussion of the interpretation of the magnetic field data, some of which also appears herein. Figure 4 is a color-shaded relief map (northwest illumination) of the 7,200 Hz apparent conductivity for the Luttrell repository study area.

A number of linear features are defined by anomalous conductivity and magnetization (figs. 3, 4) that we interpret primarily as faults or lithologic contacts. Many more linear features are imaged in the geophysical data than are shown as mapped structures on the geologic map (O'Neill and others, this volume, pl. 1). The main reason for this greater density of possible structural features in the geophysical maps is that much of the bedrock in the watershed is covered by glacial or other surficial deposits and is thus not mappable by surface inspection.

None of the linear features shown by geophysical maps in figures 3 and 4 trend through the Luttrell pit. Thus, although numerous small faults have been mapped in the area by mine geologists (fig. 2), none appear either to have a geophysical

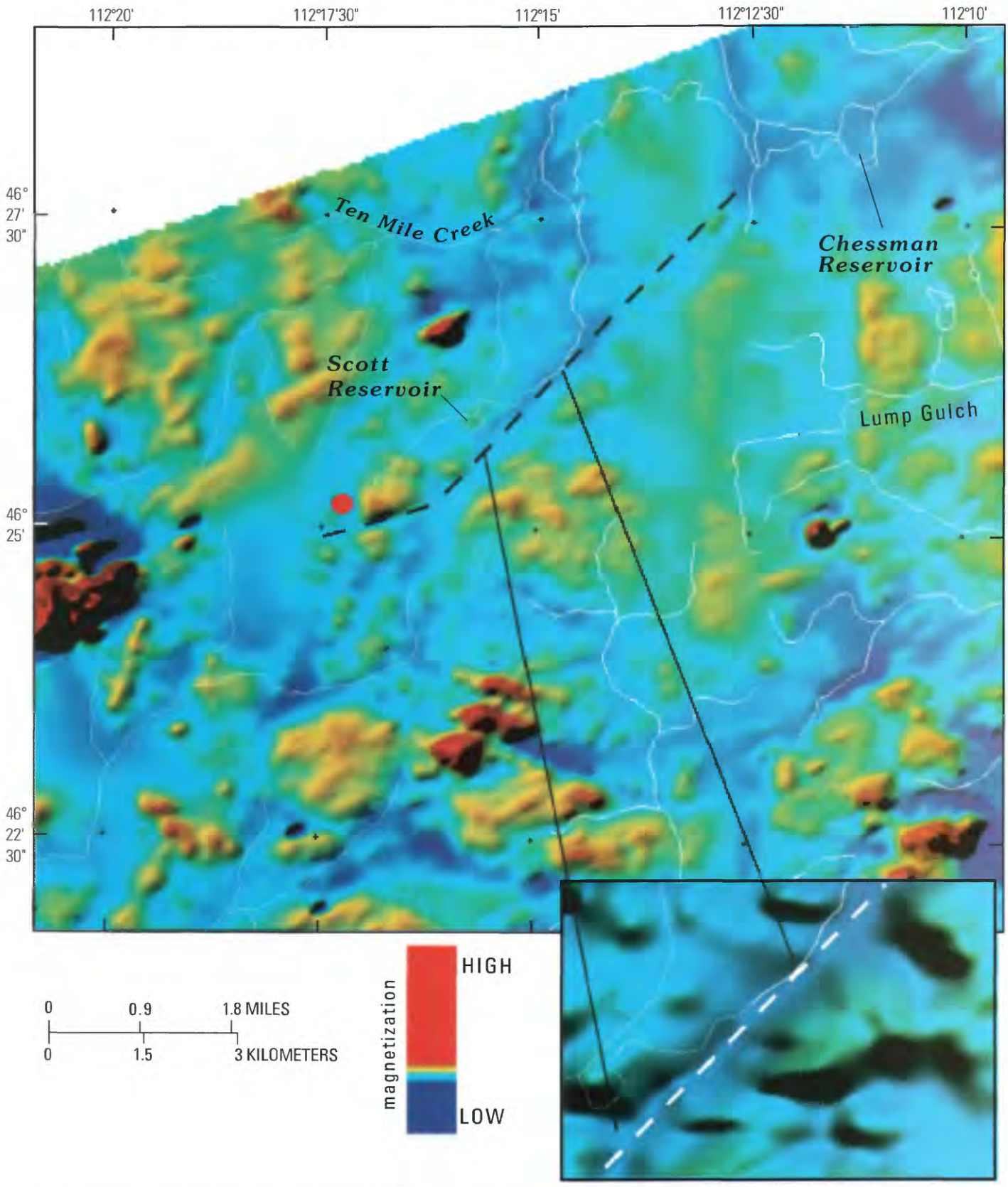

Figure 3. Color-shaded relief map of reduced-to-pole magnetic anomalies for Luttrell pit study area. Red filled circle is the location of the mine-waste repository. Dashed line shows linear feature discussed in text. A part of the linear feature is shown in the enlargement to give greater detail (no scale).

signature or to be part of a regional structure defined by a geophysical signature.

A linear geophysical feature observed about 1,600 ft south of the Luttrell pit is defined by remarkably intense and narrow (less than 150 ft) magnetic low and conductivity high anomalies (dashed line, figs. 3, 4). The northeast-trending feature is obvious on 1:24,000-scale geophysical maps, portions of which are shown at a smaller scale in figures 3 and 4. An enlargement of a portion of the geophysical map is shown in each figure in order to better display its character. Though many other linear and curvilinear features are seen on the airborne geophysical maps, these anomalies are important not only for their relatively unique geophysical signature but also for their correlation with geologic features, as discussed herein. The narrow magnetic low is probably caused by alteration that has destroyed magnetic minerals along a possible structural zone. The relative high conductivity might be associated with alteration that produced clays, or water with high concentrations of dissolved solids in ground water along a structure, or both. No unusually high concentrations of dissolved solids have been measured in springs around the area. Therefore, the anomalously high specific conductance of shallow ground water is not a likely cause of the electrical conductivity high. If the high conductivity is caused by moist clays, then the linear feature might be a subsurface barrier to ground-water flow.

The long fault south of Luttrell pit that trends east-northeast toward Chessman Reservoir (O'Neill and others, this volume, pl. 1) probably controlled the spatial location of intrusive rocks. Small, closed magnetic high and apparent conductivity low anomalies probably caused by the young, shallow intrusive igneous rocks define the east-northeast trend of the structure shown on the geologic map. This trend may indicate discrete structures that could control local ground-water flow in the crystalline rocks. The west end of this east-northeast geologic feature merges with the more northeast-trending narrow magnetic and apparent conductivity anomaly west of Scott Reservoir.

McCafferty and others (this volume) give an extensive discussion of the acid-neutralizing potential (ANP) of different lithologies in the Boulder River watershed. In summary, high ANP is associated with bedrock that has both high magnetic signature and low electrical conductivity. Conversely, low ANP is associated with rocks having low magnetization and high electrical conductivity. Desborough, Briggs, and Mazza (1998) and Desborough, Briggs, and others (1998) presented results of geochemical tests for ANP of soils and bedrock in the Boulder River watershed that were used by McCafferty and others (this volume) to develop an environmental geologic map of the study area.

Figures 3 and 4 show that the Luttrell repository (red dot in figures) is located in an area of moderate magnetic field and low apparent conductivity. Consequently, the area has low ANP based on the geophysical signature. This interpretation is supported by the observed high hydrothermal alteration of the Helena volcanics and the underlying Butte pluton. This style of alteration would remove minerals that produce ANP (Desborough, Briggs, and Mazza, 1998).

Seismicity

Earthquakes have the potential both to compromise the integrity of mine-waste repositories and to cause release of the stored waste or leachate. Therefore, the seismicity of the area near the Luttrell pit is an important geotechnical parameter in site selection and repository design. The seismic characteristics of the area are particularly important because large earthquakes took place about 50 mi northwest of the Luttrell pit in 1925 (magnitude 6.6) and 1935 (magnitudes 6.25 and 6.0; Stickney and others, 2000). The repository is located in a highly active tectonic belt. Information on regional seismicity was obtained from reports of damage from nearby earthquakes, earthquake data, and maps of Quaternary faults. Unfortunately, little information about modern seismic activity within the Boulder batholith or the study area is available.

Helena Earthquakes of 1935

Devastating earthquakes occurred in 1935 within 12 mi of Helena, Mont. A sequence of four earthquakes with magnitudes greater than 5.5 took place between October 12 and November 28. The main shock of magnitude 6.25 occurred October 18 (Neumann, 1937; Stickney and others, 2000). The Mercalli intensities in the Helena area ranged from VI to VIII; observed damage from VIII intensity earthquakes is described by Neumann (1937, p. 36) as:

> "***slight in specially designed structures; considerable in ordinary substantial buildings, with partial collapse; great in poorly built structures. Panel walls thrown out of frame structures. Fall of chimneys, factory stacks, columns, monuments, walls. Heavy furniture overturned. Sand and mud ejected in small amounts. Changes in well water. Persons driving motorcars disturbed."

Most of the damage from the 1935 Helena earthquakes was from ground shaking and not ground breakage. Newspaper accounts of the earthquake damage (O'Brian and Nava, 1998) indicate no reported damage in underground mines and little damage in areas underlain by the Boulder batholith during the Helena earthquakes. There were some reports of boulders falling in the mountainous areas (Schmidt, 1986).

The Luttrell pit is located approximately on the margin of the area of highest intensity activity on the isoseismal map constructed from data on the 1935 Helena earthquake (fig. 5). Because the isoseismal lines have been generalized, and based just on damage reports described, it is doubtful that the intensity of disturbance was as high as shown on the map in areas underlain by rocks of the Boulder batholith.

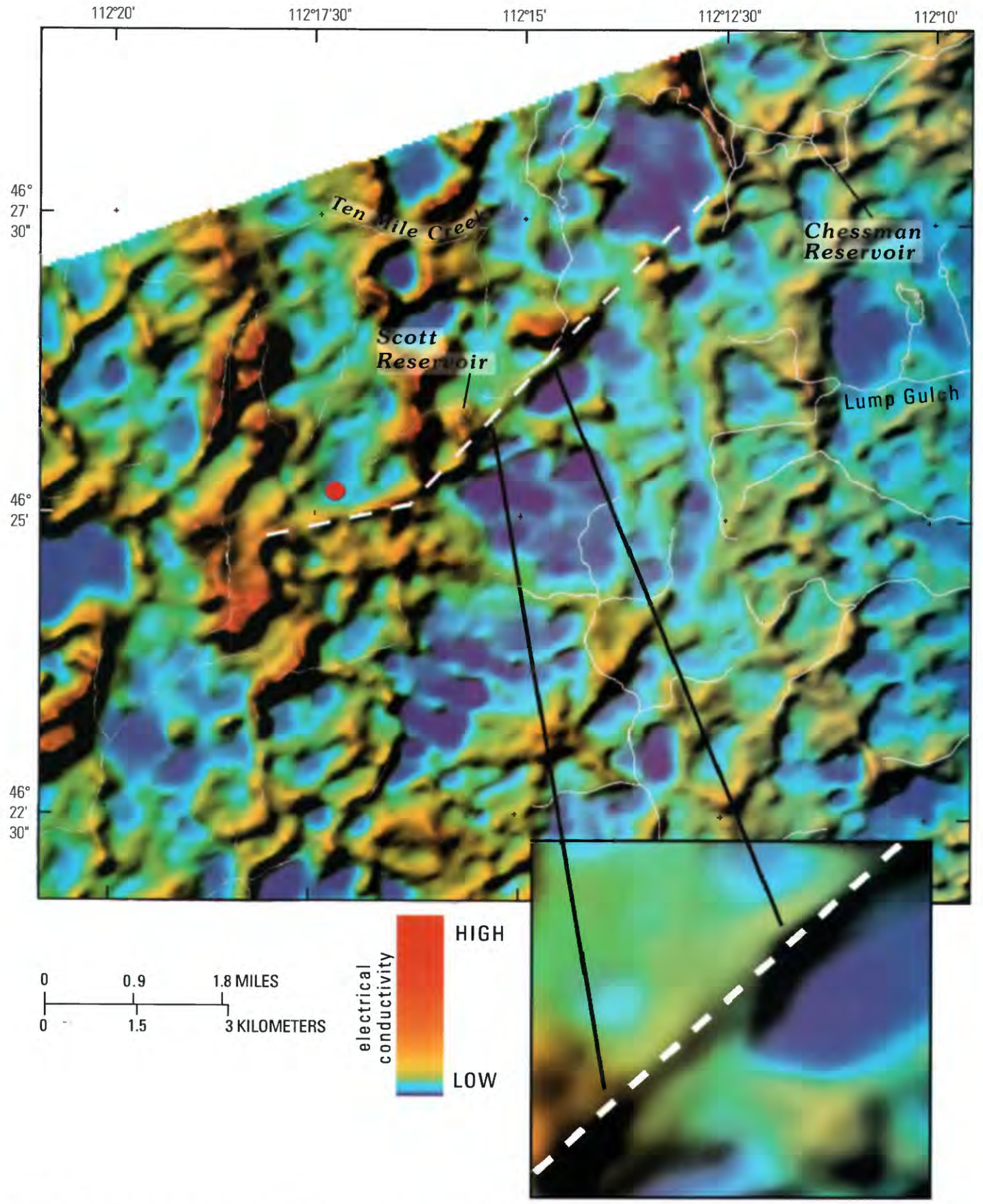

Figure 4. Color-shaded relief map of 7,200 Hz apparent conductivity for Luttrell pit study area. Red filled circle is the location of the mine-waste repository. Dashed line shows linear feature discussed in text. A part of the linear feature is shown in the enlargement to give greater detail (no scale).

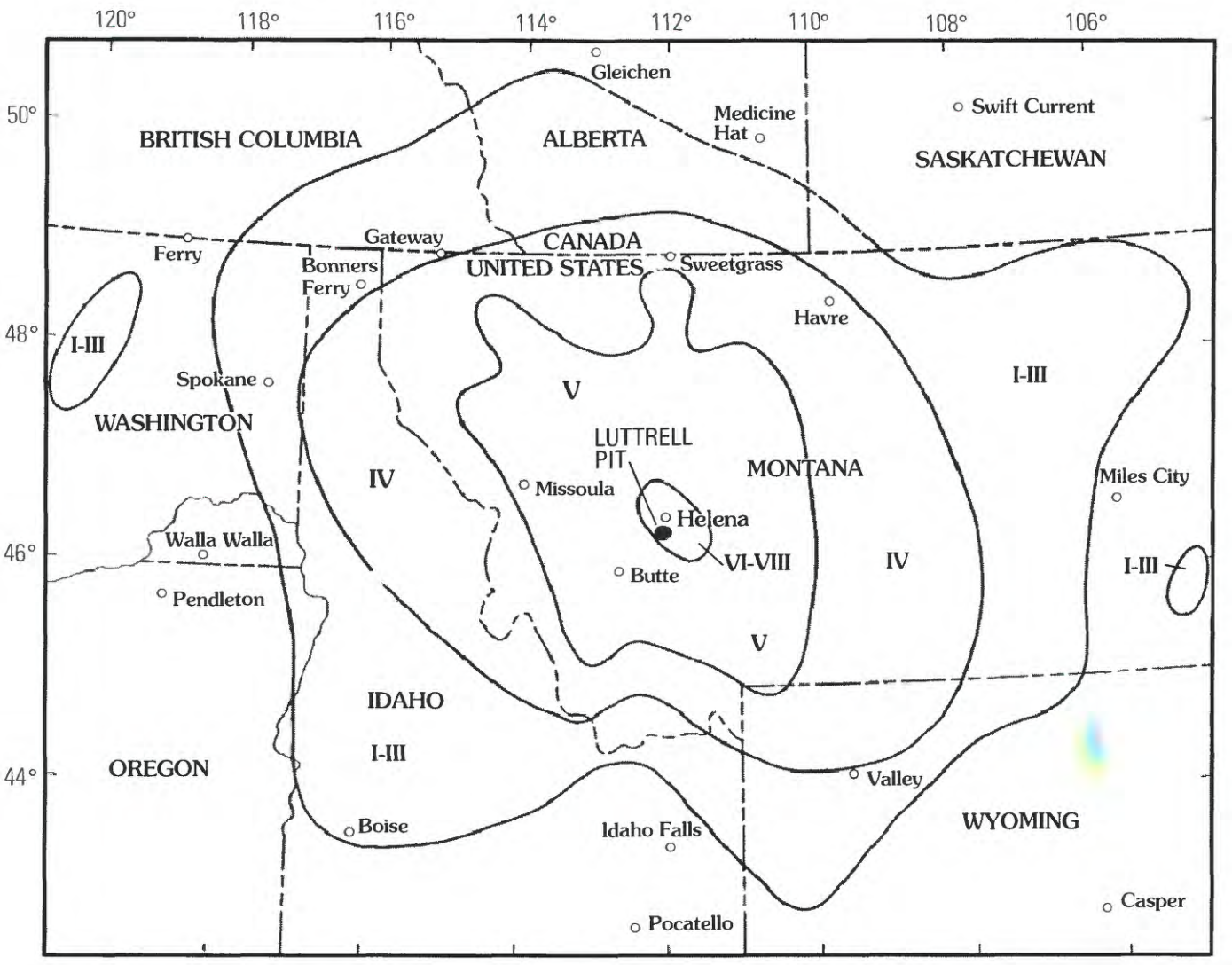

Figure 5. Isoseismal map from main shock of Helena earthquake of October 18, 1935 (Neumann, 1937). Luttrell pit (solid circle) is located just on margin of highest magnitude disturbance.

Earthquake Data

A map depicting peak ground acceleration with a 10 percent probability of being exceeded over a 50-year period for Montana is in figure 6. Peak ground acceleration is shown in various levels of percent gravity (% g), ranging from less than 2 to more than 30 percent. This map can be viewed as a generalized seismic hazard map, where the highest peak acceleration is associated with the highest earthquake hazard. For the entire United States, the highest peak ground acceleration, greater than 100 percent gravity, occurs along the San Andreas fault system in California. In the Rocky Mountain region, the arcuate north-south Intermountain seismic belt has a high seismic hazard; in local areas in the Yellowstone Park region, peak ground acceleration could exceed 30 percent gravity. In the area of the Luttrell repository, peak acceleration is expected to be between 10 and 15 percent gravity.

In a regional context, the Luttrell pit is located within the Intermountain seismic belt and north of its intersection with the Centennial tectonic belt. These two tectonic features are defined by local faulting and earthquake epicenter distribution (fig. 7). Stickney and Bingler (1981) suggested that the Centennial tectonic belt poses the greatest seismic hazard in the area. This is also an area of high acceleration probability, as shown in figure 6. The tectonic feature is far enough to the south of the Luttrell pit that it is not a consideration in the seismic risk assessment of the mine-waste repository site.

A more detailed local map of earthquake epicenters is shown in figure 8. The sedimentary and younger volcanic rocks surrounding the Boulder batholith are sites of most of the recent earthquake epicenters (Stickney, 1998; Stickney and others, 2000). In general, the regional stress patterns in southwest Montana produce northeasterly expansion (Freidline and others, 1976). Recent fault plane solutions (Stickney, 1998; fig. 8) are consistent with northeast expansion, but this

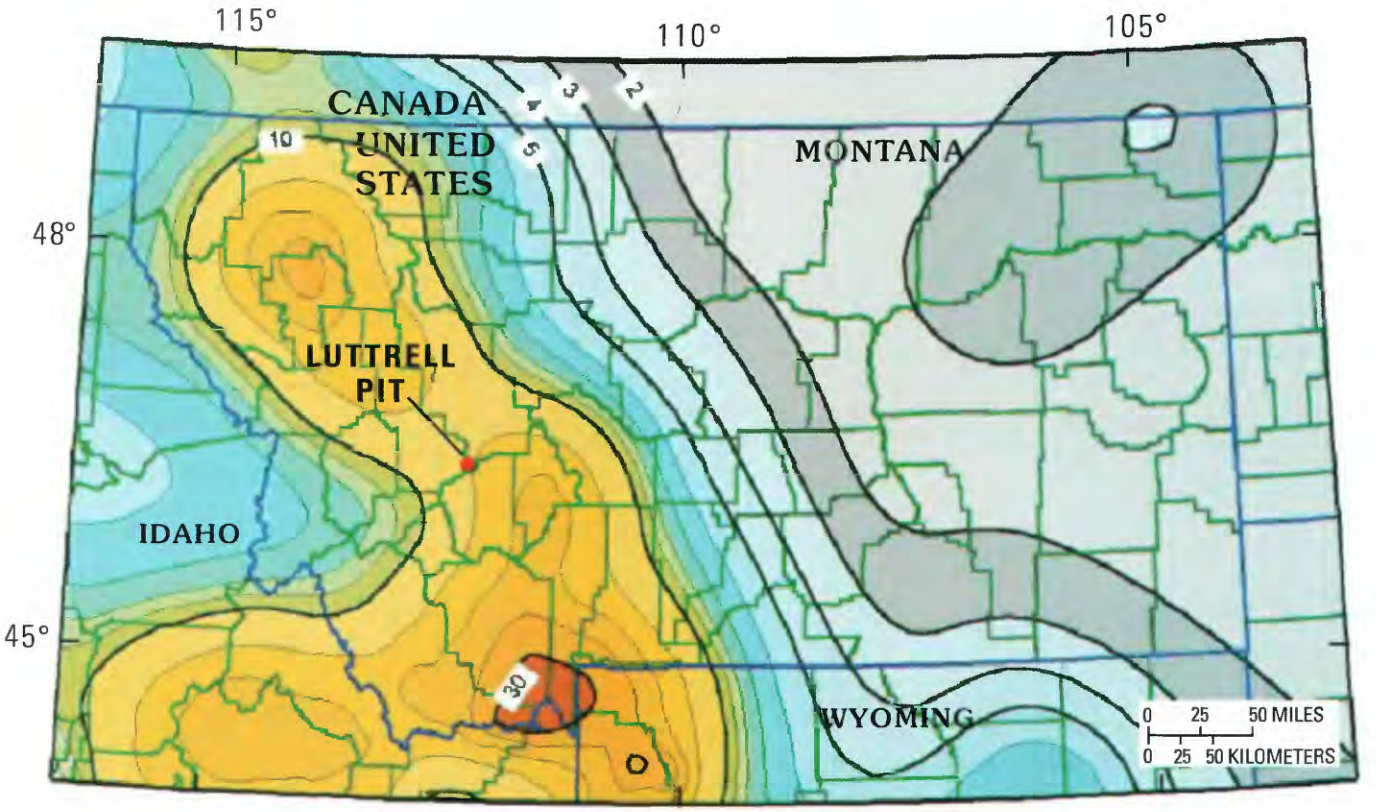

Figure 6. Peak acceleration in percent of gravity (% g) that has a 10 percent probability of being exceeded in 50 years. Modified from Montana Bureau of Mines and Geology (2001a) at URL http://mbmgquake.mtech.edu/seismicity_in_montana.html.

direction of expansion is difficult to extrapolate to the faulting in the Luttrell pit area, for the following reasons: The younger faults in the batholith are normal faults rather than strike-slip faults defined by the fault plane solutions in figure 8. In addition, the fault plane solutions may not represent earthquakes within the batholith. However, the northeast regional expansion may indicate that northwest-trending faults may be preferentially open and more likely to be ground-water flow paths in the bedrock. A few faults that have a northwest trend are located 3 mi northwest of the Luttrell pit (O'Neill and others, this volume, pl. 1).

No regional-scale Quaternary faults have been mapped near the Luttrell pit (O'Neill and others, this volume, pl. 1; Stickney and others, 2000). The northwest-to-southeast-trending Bald Butte fault zone (fig. 8) is about 15 mi northeast of the mine-waste respository area, as shown by a recent geologic compilation (Thamke, 2000). This fault zone is suspected to be the source of the 1935 earthquakes (Schmidt, 1986). The youngest interpreted ground breakage along the faults is Pleistocene (Stickney and Bingler, 1981). No record exists of seismically active faults near the Basin Creek mine. In addition, no ground breakage features that would indicate recent activity on faults were noted in our fieldwork in the immediate area of the pit.

Epicenter locations (fig. 8) for earthquakes in the Helena area from 1982 through 1996 (Stickney, 1998) show few epicenters that come within 2 mi of the Luttrell pit. Earthquakes in the area southeast of Helena (fig. 8) are as large as magnitude 5 (Stickney, 1998) and may be associated with exposed local Quaternary faults (Stickney and others, 2000). The earthquakes may also be associated with the Butte-Helena fault zone (O'Neill and others, this volume), a regional tectonic feature. Earthquake hypocenters are poorly known, in part because the distribution of seismic stations was not ideal, and epicenter localities are uncertain. Schmidt (1986) stated that the Helena earthquakes occurred at a depth of about 10.5 mi, which is as deep as the Boulder batholith (O'Neill and others, this volume).

Interpreted Fracture Mapping from Remote Sensing Data

The statistical analysis of the orientation of interpreted linear features and their orientation presented here provides a general view of possible directions of preferential local ground-water flow in the bedrock aquifer by identifying

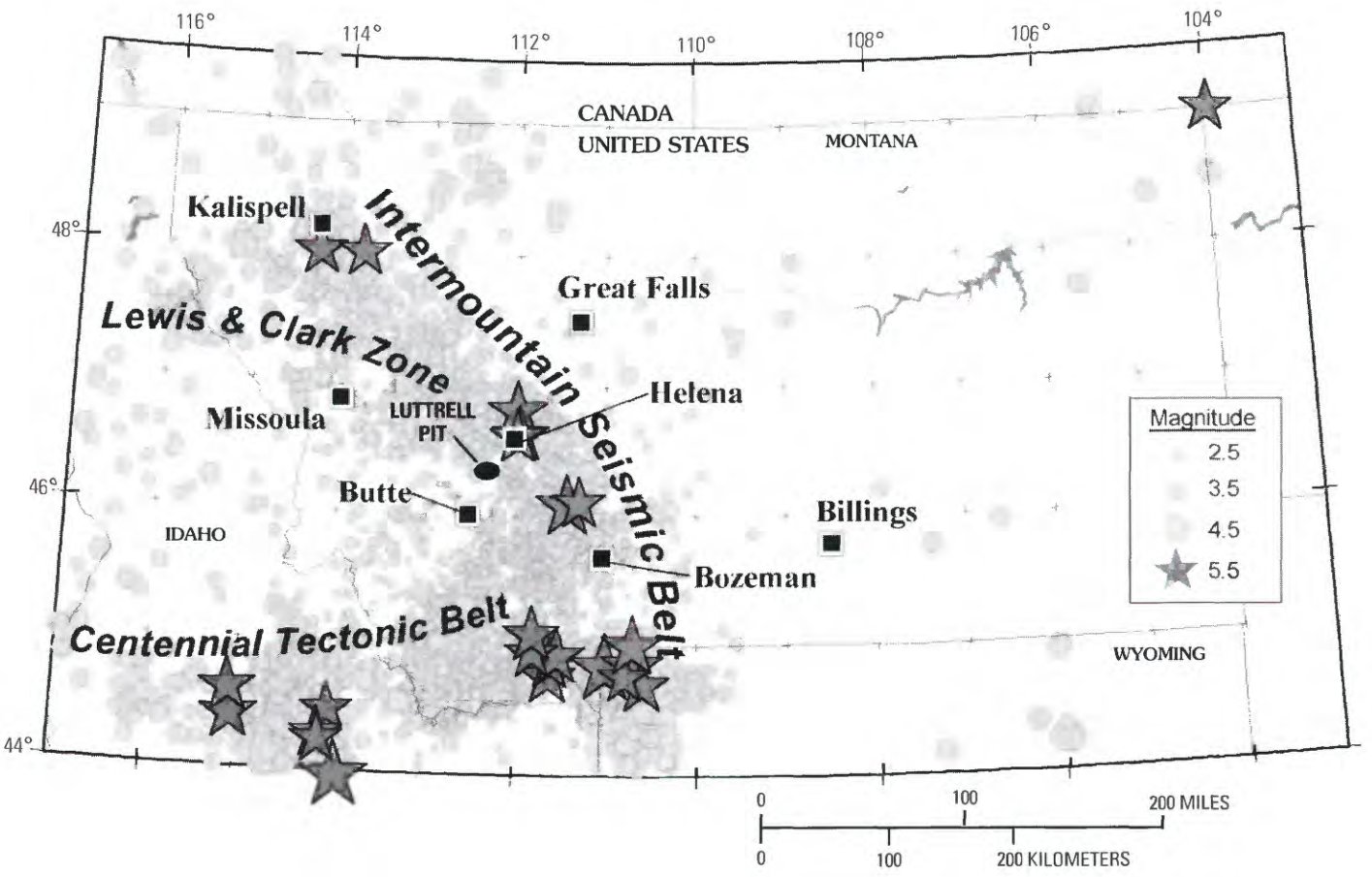

Figure 7. Epicenters from earthquakes in Rocky Mountain region defining the Intermountain seismic belt and the Centennial tectonic belt. Modified from Montana Bureau of Mines and Geology (2001b) at URL http://mbmgquake.mtech.edu/interm_s_b.html.

principal azimuths and locations of possible fractures. McDougal and others (this volume) give a detailed analysis of linear features and their hydrologic interpretation for the Boulder River watershed. The discussion of fracture orientation here is similar, but focuses on a smaller area near the Luttrell pit.

To identify and map all fractures and faults from remotely sensed data is not possible because of ground resolution limitations, vegetation cover, and glacial or other surficial cover. In most cases, to determine if a linear feature marks the surface expression of a fault, fracture, joint, mineralized vein, or lithologic contact is also impossible. Mapped linear features used in this study provide a representation of the spatial distribution and orientation of bedrock fractures near the Luttrell pit mine-waste repository. The interpretation is a statistical sample of naturally occurring linear features that could be related to surface expression of structures.

Linear Feature Analysis

The lineament azimuths, calculated from the geographic coordinates of the endpoints of each mapped vector, were used to generate rose diagrams for the Luttrell pit study area. Rose diagrams are polar histograms, which represent distribution of the two-dimensional (horizontal plane) orientations of mapped linear features. The statistical parameters of total number of data points (N), maximum percentage, mean percentage, standard deviation, vector mean (direction), R magnitude, standard error of the mean, and the Rayleigh probability distribution were calculated for each diagram (McDougal and others, this volume). The R magnitude is a measure of the strength of the vector mean. Data sets with a large dispersion about the mean have small values for R, and data sets that are tightly grouped around the mean have a large value for R. The Rayleigh test was used to calculate uniformity within the data set. In this case, the chosen significance level was 0.1 (90 percent confidence interval). If the calculated value is less than 0.1, then the conclusion can be made that the data are non-uniform and show a preferred orientation (McEachran, 1990).

The diagram representing the primary lineament orientation (fig. 9*A*) for the Luttrell pit study area shows a vector mean of 81.2°. The small confidence angle of 7.51°, R magnitude of 0.564, and Rayleigh value of 0.00 indicate that the data have a moderate vector mean strength, and a strong preferred orientation. However, note in figure 9*A* that the distribution is strongly bimodal with peaks in the rose diagram at 85° and 105°.

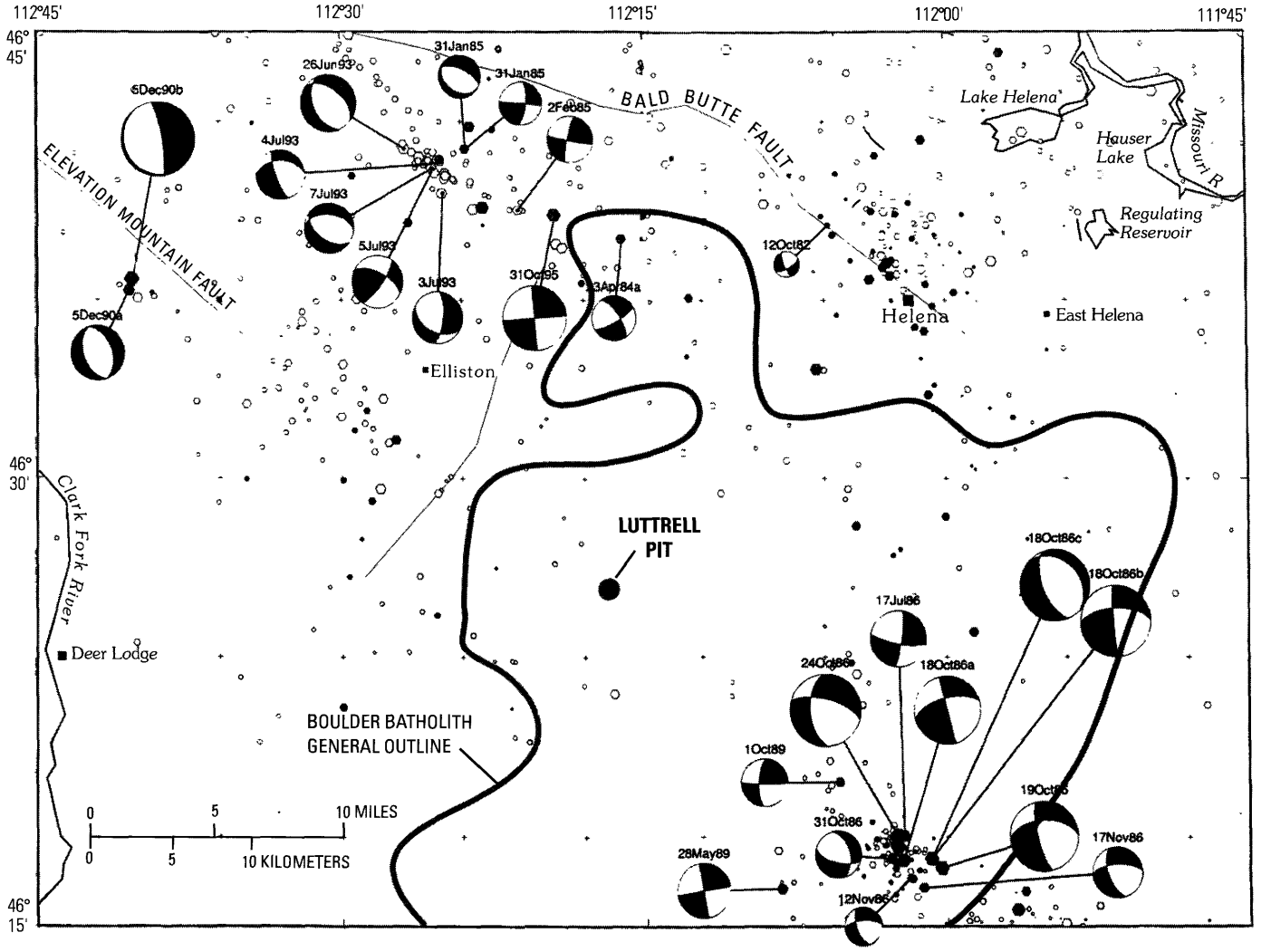

Figure 8. Earthquake epicenters and fault plane (nodal) solutions for the Helena area (Stickney, 1998). Fault plane solutions for selected earthquakes are shown as circles whose solid areas denote direction of compression. Larger and darker symbols for epicenters show greater magnitudes for earthquakes.

Secondary lineament orientation was plotted by filtering out the azimuths within the vector mean of the primary bimodal orientation described preceding. The resulting diagram (fig. 9*B*) shows a possible secondary orientation with a vector mean of 39.6°. The larger confidence angle (31.32°) and Rayleigh value, and smaller *R* magnitude, indicate that the filtered data set is less preferentially oriented than the primary trend. A possible tertiary trend lies between approximately 110° and 140°. The 39.6° trend correlates with the general trend of the apparent conductivity and magnetic geophysical anomalies (dashed line in figs. 3 and 4). The interpreted geologic structure in the area of Scott and Chessman Reservoirs (O'Neill and others, this volume, pl. 1) trends northeast 55°, which corresponds to the main secondary orientation in figure 9. These linear features, together are collinear with the northeast-trending fault zone described in the geologic section.

Hydrological Implications

Ground-water flow near the Luttrell pit likely is consistent with the regional ground-water flow model developed for the Boulder River watershed (McDougal and others, this volume). Hydrologic characteristics of the bedrock north of the Luttrell pit have been described by Thamke (2000). The highest hydraulic conductivity occurs in the upper unconsolidated deposits and shallow weathered bedrock, which together form an unconfined aquifer. Oligocene sediments deposited locally on the Butte pluton (O'Neill and others, this volume) constitute a relatively unknown (not mapped) aquifer. Hydraulic conductivity generally decreases dramatically with depth within the rhyolitic rocks of the Helena volcanic field because fractures are filled with clays produced during weathering of the volcanic rocks. In the Basin Creek mine area, the Helena volcanic rocks are the host to mineralization which has

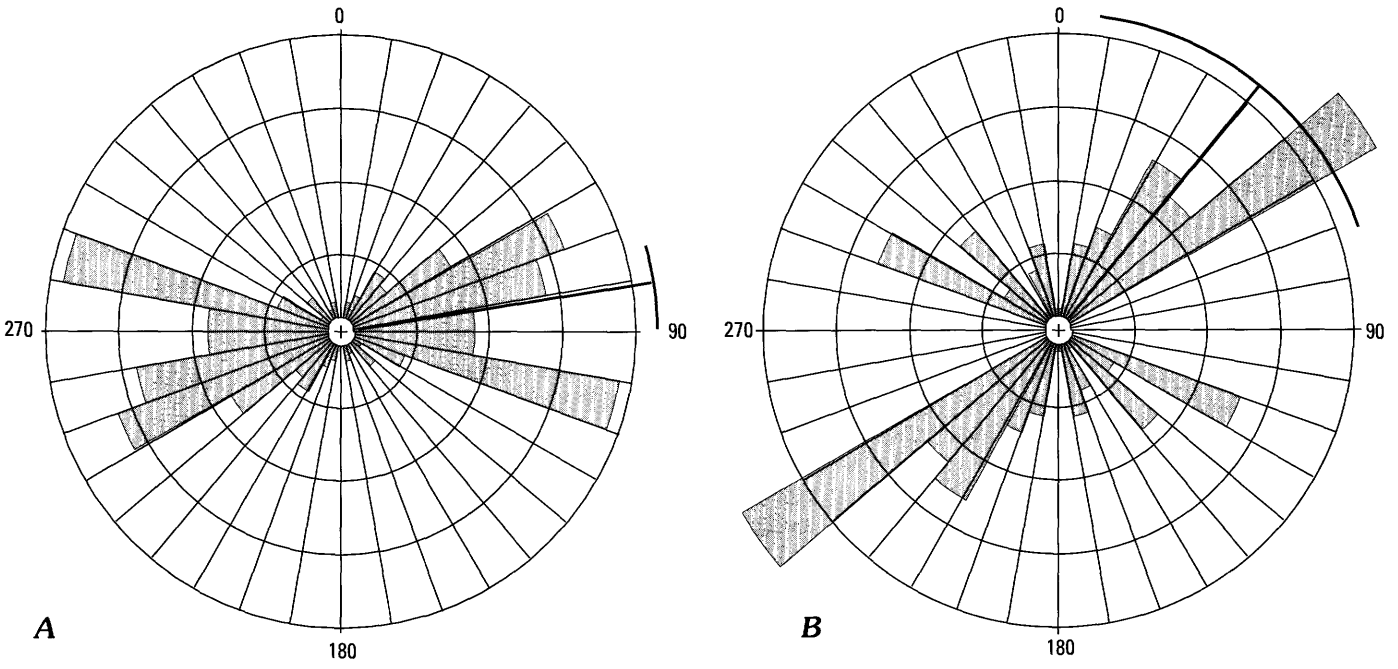

Boulder Basin - primary lineament orientation	Statistics
N = 205	Vector mean = 81.2
Class interval = 10 degrees	Conf. angle = 7.51
Maximum percentage = 18.5	*R* magnitude = 0.564
Mean percentage = 5.56 Standard deviation = 5.46	Rayleigh = 0.0000

Boulder Basin - secondary lineament orientation	Statistics
N = 71	Vector mean = 39.6
Class interval = 10 degrees	Conf. angle = 31.32
Maximum percentage = 23.9	*R* magnitude = 0.247
Mean percentage = 7.69 Standard deviation = 6.19	Rayleigh = 0.0132

Figure 9. Rose diagrams and statistical analysis of lineament orientations in the Luttrell pit study area. *A*, primary lineament orientations; *B*, secondary lineament orientations.

accompanied intense alteration to clays; this clay alteration significantly reduced hydraulic conductivity. The clay has been used to construct a cap designed to reduce infiltration into the back-filled Paupers and Columbia pits (Dan Adams, Basin Creek Mine, Inc., oral commun., 1999).

In the underlying fractured granodioritic bedrock aquifer, hydraulic conductivity decreases because joints and fractures become increasingly tight with increasing depth. In areas of greater fracture density near fault zones, permeability may be somewhat higher. The direction of shallow ground-water flow is controlled by the hydraulic gradient, which likely mimics the topographic slope. Locally, topography slopes away from the Luttrell pit generally in all directions, and therefore, shallow ground water likely flows in all directions away from the pit. The direction of deeper ground-water flow also is a function of the hydraulic gradient, which may be controlled to some extent by fracture orientation. The regional and subregional fracture geometry observed in outcrops is generally heterogeneous and anisotropic, and the local ground-water flow regime near the Basin Creek mine is assumed to be associated with the orientation of these fractures. Recharge to the local ground-water system comes primarily from approximately 30 in. mean annual precipitation (mainly as snowfall). Intense rainstorms in spring and summer can contribute sudden influxes of recharge.

The results of the lineament orientation analysis indicate that ground-water flow, assuming some control by fracture permeability, could have a preferred flow direction to the east-northeast or west-southwest, depending on the hydraulic gradient. Secondary and tertiary preferred flow directions to the northeast (southwest) and east-southeast (west-northwest), respectively, also are indicated by the rose diagrams.

The wet soils map (fig. 10) shows an area of inferred shallow ground water to the southwest of the Basin Creek mine site. Note that detailed soil mapping is not available north of the Boulder River watershed. This zone of wet soils coincides with a relatively high density of mapped linear features that indicate possible fractures, which may function as conduits for ground-water flow. This area of possible shallow ground water lies along the northeast fracture zone discussed in the previous geologic and geophysical sections. Observed springs in the area could also be associated with a lithologic contact between the Helena volcanics and the underlying Butte pluton. Potentiometric surface maps based on monitoring well

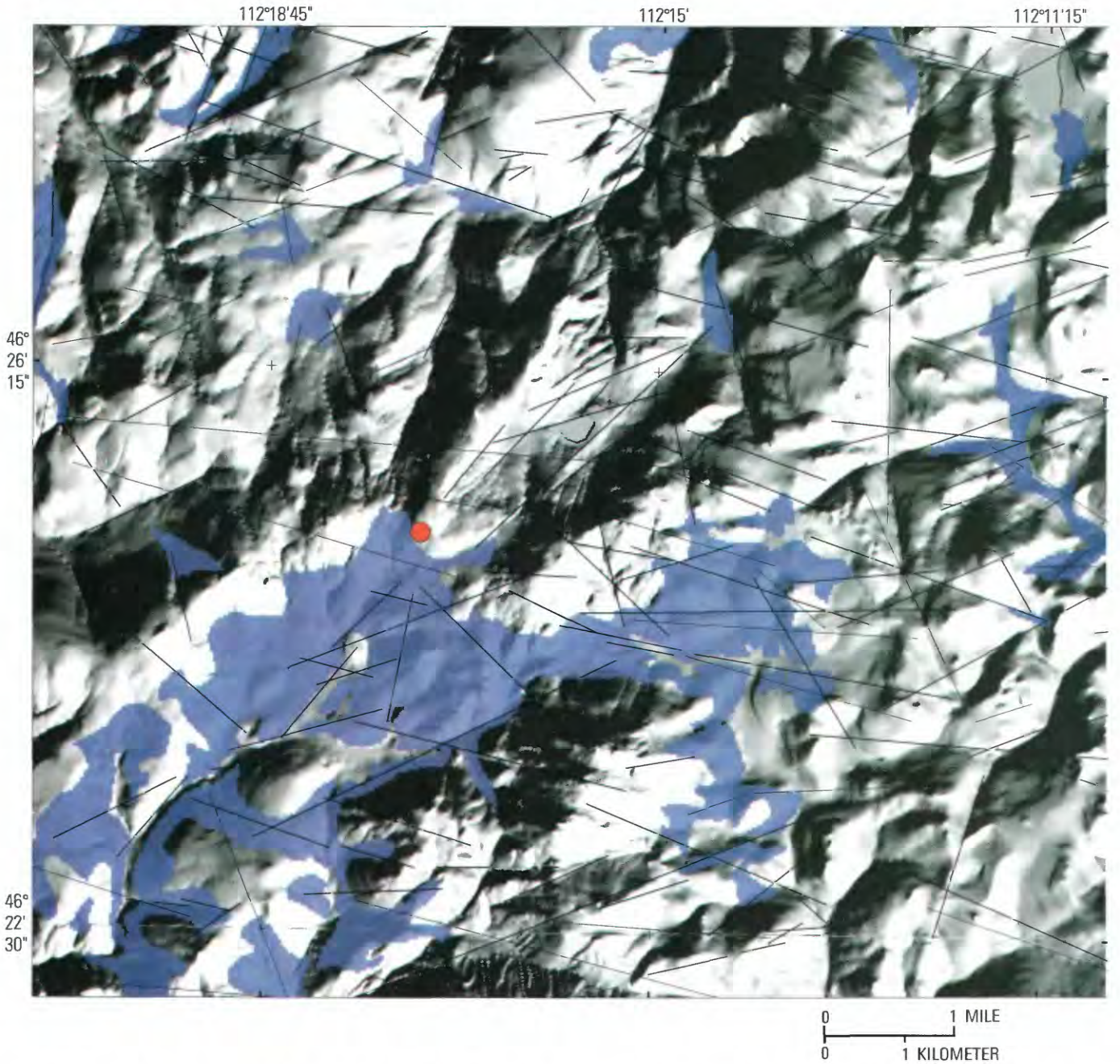

Figure 10. Digital map showing wet soils (blue) in the study area (McDougal and others, this volume) draped over a digital elevation model (DEM) and combined with mapped lineaments (black lines; McDougal and others, this volume) for Luttrell pit study area. Red dot, Luttrell pit.

data in and around the Basin Creek mine indicate ground-water flow directions to the north-northwest, northeast, and southwest (Olympus Environmental Science and Engineering, Inc., 1996). The combination of the wet soils map and linear feature orientation suggests that some ground water could flow from the Luttrell pit area to the southwest, and suggests a possible location where subsurface ground water could be monitored.

A high density of linear features also occurs at the Continental Divide south of the Luttrell pit (McDougal and others, this volume). This part of the northeast-trending structural zone could serve to recharge possible fracture-controlled ground water in the area of the mine-waste repository, as it is an area of high topography.

Figure 11 shows interpreted linear features and mapped structures superimposed on 7,200 Hz apparent electrical conductivity. The intersections of areas of high electrical conductivity and interpreted linear features mark possible areas of ground-water discharge or recharge. High electrical conductivity may be caused by wet soils and rocks, and linear features may indicate fractures that control ground-water storage or flow. Increased fracturing may indicate increased

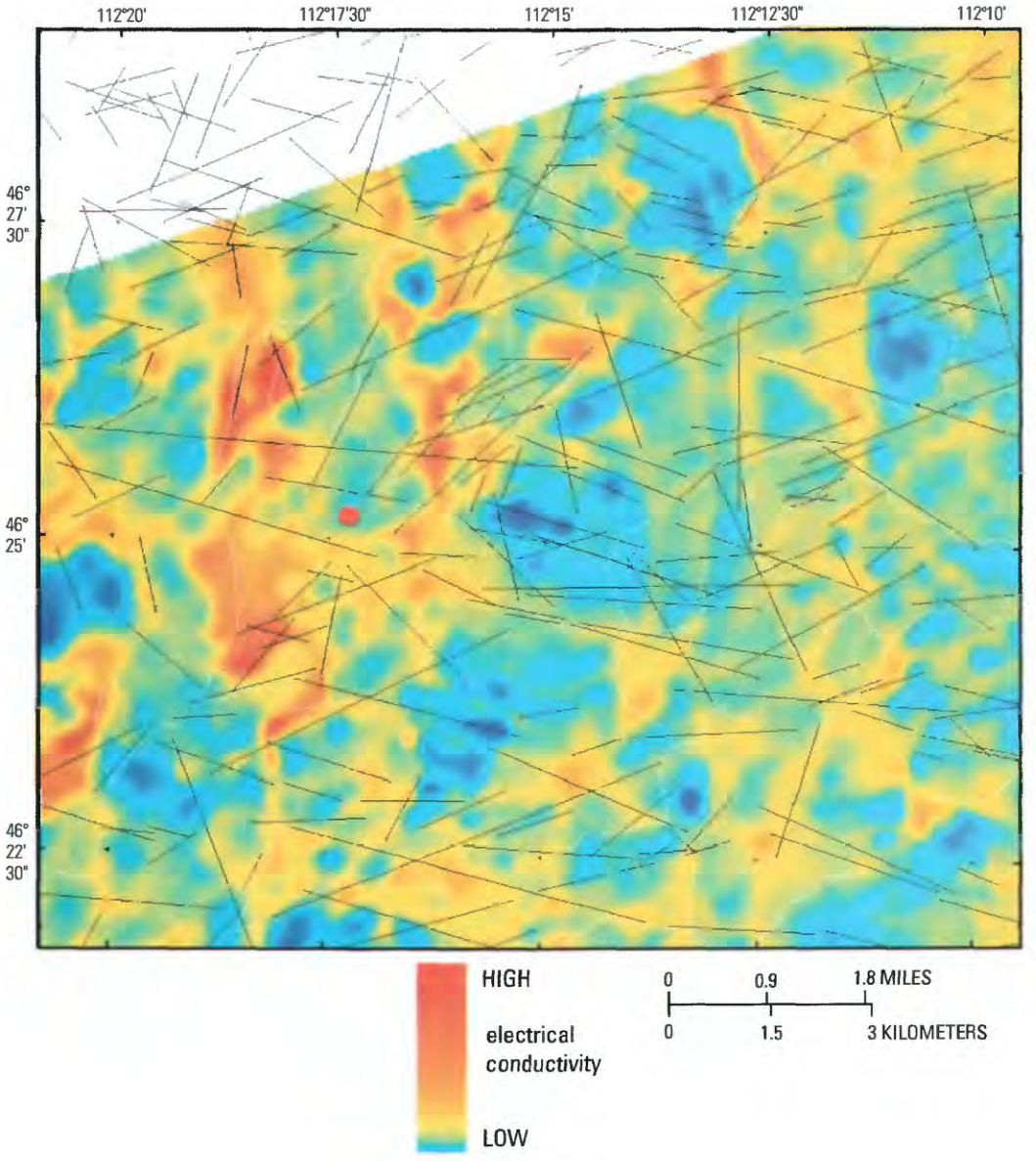

Figure 11. Color map of 7,200 Hz apparent conductivity superimposed with the linear features described in this study. Red dot, Luttrell pit.

interconnectedness and therefore increased permeability in the bedrock. The area of the Luttrell pit mine-waste repository does not show any of the features that would indicate local ground-water discharge or recharge.

Conclusions

Geologic studies indicate that faulting has occurred at least intermittently near the Luttrell pit from before the Oligocene through the Holocene. There is no evidence of recent rejuvenation of faults beneath the mine-waste repository, as drill information from premining development indicates that mineralized rocks are not offset by structures. An east-northeast-trending normal fault on the south of the Basin Creek mine has had a complex movement history from at least middle Tertiary through Holocene and may have localized bedrock fracturing. This structure is grouped with northeast-trending structures described in detail by Ruppel (1963). The northeast trend probably is a fault zone with a collinear trend with the Butte-Helena fault zone described by O'Neill and others (this volume) that controls the location of young intrusive rocks.

The airborne magnetic and electromagnetic survey provides information about variations in subsurface lithologies and structures. Many previously unknown structural trends are suggested from the geophysical data, but none actually intersect the pit area. A major northeast-trending linear feature defined by a narrow low magnetic and high conductivity signature starts about 0.25 mi southwest of the pit and trends northeast just south of Scott Reservoir. Another geophysical trend is associated with the east-northeast structure inferred from geologic mapping. Potential sites for fracture-controlled springs are indicated by the intersection of lineaments and high subsurface conductivity. None of these areas occur at the Luttrell pit. The airborne geophysical data interpretation in terms of environmental geology suggests that the mine-waste repository site is located in an area of low acid-neutralizing potential (McCafferty and others, this volume).

A high seismic hazard characterizes the region surrounding the Luttrell pit owing to (1) its location in the Intermountain seismic belt, (2) large historical earthquakes in the nearby Helena area, and (3) continuing earthquake activity in the Helena area and an area southeast of the mine-waste repository. Fault plane solutions for deep earthquakes suggest that northwest-southeast extension might cause northeast-trending fractures to be preferentially open. However, current stress patterns within shallow plutonic rocks and the younger volcanic rocks are a matter of speculation. Newspaper accounts (O'Brian and Nava, 1998) describing damage from the 1935 Helena earthquakes did not indicate any impact on the mines that were actively operating in the Boulder batholith. Therefore, seismic hazard at the pit is considered low.

No major lineaments that trend through the Luttrell pit were identified from remote sensing images or airborne geophysical data. Analysis of linear feature orientations suggests that preferential paths of ground-water flow have a primary azimuth to the east-northeast or west-southwest. Possible secondary and tertiary preferential flow azimuths may be to the northeast (southwest) and east-southeast (west-northwest) respectively. Wet soils and lineament maps suggest a possible preferential ground-water flow southwest of the Luttrell pit that could be considered in design of monitoring activities around the repository. Coincidence of linear features and subsurface high electrical conductivity might indicate areas of ground-water recharge or discharge. No such areas occur at the Luttrell pit mine-waste repository.

References Cited

Becraft, G.E., Pinckney, D.M., and Rosenblum, Sam, 1963, Geology and mineral deposits of the Jefferson City quadrangle, Jefferson and Lewis and Clark Counties, Montana: U.S. Geological Survey Professional Paper 428, 101 p.

Chadwick, R.A., 1978, Geochronology of post-Eocene rhyolitic and basaltic volcanism in southwestern Montana: Isochron/West, v. 5, p. 25–28.

Desborough, G.A., and Driscoll, Rhonda, 1998, Mineralogical characteristics and acid-neutralizing potential of drill core samples from eight sites considered for metal-mine related waste repositories in northern Jefferson, Powell, and Lewis and Clark counties, Montana: U.S. Geological Survey Open-File Report 98–790, 6 p.

Desborough, G.A., Briggs, P.H., and Mazza, Nilah, 1998, Chemical and mineralogical characteristics and acid-neutralizing potential of fresh and altered rocks and soils of the Boulder River headwaters in Basin and Cataract Creeks of northern Jefferson Co., Montana: U.S. Geological Survey Open-File Report 98–40, 21 p.

Desborough, G.A., Briggs, P.H., Mazza, Nilah, and Driscoll, Rhonda, 1998, Acid-neutralizing potential of minerals in intrusive rocks of the Boulder batholith in northern Jefferson Co., Montana: U.S. Geological Survey Open-File Report 98–364, 21 p.

Fraser, D.C., 1978, Resistivity mapping with an airborne multicoil electromagnetic system: Geophysics, v. 43, p. 114–172.

Freidline, R.A., Smith, R.B., and Blackwell, D.D., 1976, Seismicity and contemporary tectonics of the Helena, Montana area: Bulletin of the Seismological Society of America, v. 66, p. 81–95.

Lund, Karen, Aleinikoff, J.N., Kunk, M.J., Unruh, D.M., Zeihen, G.D., Hodges, W.C., du Bray, E.A., and O'Neill, J.M., 2002, SHRIMP U-Pb and $^{40}Ar/^{39}Ar$ age constraints for relating plutonism and mineralization in the Boulder batholith region, Montana: Economic Geology, v. 97, p. 241–267.

McEachran, D.B., 1990, Rosy 2-D orientation analysis for the Macintosh, users manual: Rockware Earth Science Software, 19 p.

Montana Bureau of Mines and Geology, 2001a, Seismicity in Montana. Accessed December 3, 2001, at URL http://mbmgquake.mtech.edu/seismicity_in_montana.html.

Montana Bureau of Mines and Geology, 2001b, Intermountain Seismicity Belt. Accessed December 3, 2001, at URL http://mbmgquake.mtech.edu/interm_s_b.html.

Neumann, Frank, 1937, United States earthquakes, 1935: U.S. Department of Commerce, Coast and Geodetic Survey, 90 p.

O'Brian, E.H., and Nava, S.J., 1998, Personalizing the earthquake threat in the Intermountain Region, Technical Report to the U.S. Geological Survey for grant 1434-95-G-266, 78 p.

Olhoeft, G.R., 1985, Low-frequency electrical properties: Geophysics, v. 50, no. 12, p. 2492–2503.

Olympus Environmental Science and Engineering Inc., 1996, Basin repository evaluation report for the Basin Creek mine, Jefferson and Lewis & Clark Counties, Montana: Report prepared for Abandoned Mine Reclamation Bureau, Montana Department of Environmental Quality, 33 p.

Ruppel, E.T., 1963, Geology of the Basin quadrangle, Jefferson, Lewis and Clark, and Powell Counties, Montana: U.S. Geological Survey Bulletin 1151, 121 p.

Schmidt, R.G., 1986, Geology, earthquake hazards, and land use in the Helena area, Montana—A review: U.S. Geological Survey Professional Paper 1316, 64 p.

Smith, B.D., Labson, V., and Hill, P., 2000, Airborne geophysical survey in the Boulder watershed, Jefferson and Lewis and Clark counties, Montana: U.S. Geological Survey Open-File Report 00–240.

Smith, B.D., McCafferty, A.E., and McDougal, R.R., 2000, Utilization of airborne magnetic, electromagnetic, and radiometric data in abandoned mine land investigations, *in* ICARD 2000; Proceedings of the Fifth International Conference on Acid Rock Drainage, Volume 2: Society for Mining, Metallurgy, and Exploration, Inc., p. 1525–1530.

Spies, B.R., 1989, Depth of investigation in electromagnetic sounding methods: Geophysics, v. 54, p. 872–888.

Stickney, M.C., 1998, Seismic source zones in Southwest Montana: U.S. Geological Survey grant number 1434–95–G–2628, unpublished report, U.S. Geological Survey library, Denver, Colo., 32 p.

Stickney, M.C., and Bartholomew, M.J., 1987a, Seismicity and late Quaternary faulting of the northern Basin and Range Province, Montana and Idaho: Bulletin of the Seismological Society of America, v. 77, p. 1602–1625.

Stickney, M.C., and Bartholomew, M.J., 1987b, Preliminary map of late Quaternary faults in Western Montana: Montana Bureau of Mines and Geology Open-File Report 186, scale 1:500,000.

Stickney, M.C., and Bingler, E.C., 1981, Earthquake hazard evaluation of the Helena Valley area, Montana: Montana Bureau of Mines and Geology Report MBMG-83, 52 p.

Stickney, M.C., Haller, M.K., and Machette, M.N., 2000, Quaternary faults and seismicity in western Montana: Montana Bureau of Mines and Geology Special Publication 114, scale 1:500,000.

Thamke, J.N., 2000, Hydrology of the Helena area bedrock, west-central Montana, 1993–1998, *with a section on* Geologic setting and a generalized bedrock geologic map, by M.W. Reynolds: U.S. Geological Survey Water-Resources Investigations Report 00–4212, 119 p.

Evaluating the Success of Remediation in the Boulder River Watershed

By Susan E. Finger, Stanley E. Church, and David A. Nimick

Chapter F of

Integrated Investigations of Environmental Effects of Historical Mining in the Basin and Boulder Mining Districts, Boulder River Watershed, Jefferson County, Montana

Edited by David A. Nimick, Stanley E. Church, and Susan E. Finger

Professional Paper 1652–F

U.S. Department of the Interior
U.S. Geological Survey

Contents

Tables

Chapter F
Evaluating the Success of Remediation in the Boulder River Watershed

By Susan E. Finger, Stanley E. Church, and David A. Nimick

Abstract

Historical mining has resulted in contamination of land, water, and biological resources in many areas of the Boulder River watershed. Other chapters in this volume have characterized the extent and severity of this contamination and have presented an ecological risk-based synthesis concluding that areas downstream from the Comet, Crystal, and Bullion mines were among the most contaminated in the watershed. Federal and State land managers have targeted these sites, among others in the watershed, for remediation. Monitoring can provide a means to determine the success of remedial activities and the rate or extent of recovery of the ecosystem. Monitoring tools should include measures of physical, chemical, and biological conditions similar to measurements used in the pre-remediation watershed assessment. Factors including the geology, water quality, and presence of a biological community for recolonization will determine the rate of success of ecological restoration. In addition to the reduction of trace-element concentrations in water and streambed sediment, restoration of a healthy riparian corridor is essential to ecological recovery of the aquatic environment. The importance of monitoring in documenting the success of remediation is often overlooked because of funding limitations. However, a well-designed and carefully implemented monitoring program is an extremely valuable means not only to evaluate the success of an ongoing project, but also to document ways to improve success in future restoration activities.

Introduction

Historical mining has resulted in contamination of land, water, and biological resources in many areas of the Boulder River watershed. Other chapters in this volume have characterized the extent and severity of this contamination (Nimick and Cleasby, this volume, Chapter D5; Church, Unruh, and others, this volume, Chapter D8) and have presented an ecological risk-based synthesis concluding that areas downstream from the Comet, Crystal, and Bullion mines were among the most contaminated in the watershed (Finger, Farag, and others, this volume, Chapter C). Pre-remediation assessment studies demonstrated that fish were absent from many of these stream reaches, and where fish populations did exist, their health had been compromised (Farag and others, this volume, Chapter D10). The potential for biological recovery in this aquatic environment is dependent on successful remediation of historical mine wastes and mine drainage in affected areas in the Boulder River watershed.

Mine and mill site remediation has been initiated at several locations throughout the Boulder River watershed (this volume, Chapter A). In 1997, remediation efforts began at the Comet mine in High Ore Creek. The Montana Department of Environmental Quality removed about 500,000 yd^3 of mill tailings from a breached tailings repository in the High Ore Creek valley (Gelinas and Tupling, this volume, Chapter E2). In 1999, the Bureau of Land Management began removal and in-place treatment of tailings deposits on the High Ore Creek flood plain. The USDA Forest Service also initiated remediation efforts at the Buckeye and Enterprise mine site in 2000 and at the Bullion mine in 2002. The USEPA began remediation activities in the Basin Creek and Cataract Creek basins after these areas were added to the National Priority List (Superfund) in 1999. Mining wastes were removed from the town of Basin, and in 2002, remediation was started at the Crystal mine. However, as of 2003, no work has been initiated to reduce or eliminate acidic drainage coming from mine adits such as those at the Crystal, Bullion, or Enterprise mines.

The terms remediation and restoration are closely linked, but they refer to distinct phases in the process of ecological recovery. Remediation is the cleanup of a contaminated area. Remedial actions remove or isolate contaminants from the environment. These actions are critical to promoting the recovery of both the terrestrial and aquatic ecosystems. Remediation at mine sites can involve the in-place treatment or physical removal of mine waste and mill tailings from a stream, its associated flood plain, and the terrestrial landscape.

Remediation at these sites can also involve actions that reduce or eliminate metal and acid loading from draining mines. Actual cleanup activities may cause adverse effects on the environment that must be addressed early in the planning phases of a project, because some remedial options may preclude achievement of restoration goals. Successful remedial actions result from risk-management decisions that are based on cost-benefit analyses that evaluate the potential outcomes of various alternatives ranging from a simple "no action" alternative to more costly and complicated alternatives such as complete removal of contaminated material. Performance measures for successful remediation might include (1) major sources of contamination in the watershed have been reduced or eliminated, (2) trace-element concentrations in water no longer exceed acute or chronic criteria for aquatic life, (3) trace-element concentrations in streambed sediment no longer exceed sediment-quality guidelines, (4) stream banks have been stabilized and erosion has been minimized, and (or) (5) flood-plain revegetation has reduced or eliminated the transport of contaminated sediment, mine waste, or mill tailings downstream.

Completion of this remediation or cleanup process marks the beginning of the restoration phase of ecosystem recovery. Restoration is the process of returning an ecosystem to a close approximation of its historical condition prior to a physical or chemical disturbance (National Research Council, 1992). Although an injured ecosystem may never return to conditions identical to those that existed prior to mining, it may be restored to conditions that are functionally equivalent to those of the previous environment. The underlying goal of restoration is ecological recovery. This goal must be ecologically realistic and based on the geologic, hydrologic, and biologic characteristics of the watershed. Achievement of this goal is contingent on restoration of the ecosystem's structure and function both locally and within a broader landscape or watershed context. Therefore, in an area affected by historical mining, an understanding of premining conditions in the watershed is required (Church, Unruh, and others, this volume). Although successful remediation actions, such as physical removal of mine waste and mill tailings or reduction in acidic mine drainage, may be part of the restoration process, these remedial steps do not necessarily ensure that ecological recovery will occur. Restoration may require such things as creation of viable fisheries habitat, restocking a stream with fish, reintroduction of terrestrial species, or revegetation of the flood plain to compensate for ecological losses. Performance measures for successful restoration might include (1) self-sustaining populations of fish throughout the watershed, (2) successfully reproducing colonies of nesting birds, and (or) (3) a healthy riparian corridor.

Monitoring is an important but often undervalued and underutilized tool for determining the success of remedial efforts and assessing ecological recovery. Adequate and appropriate monitoring procedures are the most direct measure of the success of remedial strategies and the resulting rates of recovery for populations, communities, or ecosystems. However, monitoring rarely receives the attention necessary to develop and implement a successful plan. Following remediation of a site, funding limitations often reduce the frequency of monitoring or eliminate it completely. Kondolf and Micheli (1995) indicated that despite increased commitment to stream restoration, postrestoration monitoring has generally been neglected as well. Monitoring plans need not be exhaustive or complex. Rather, they need to be designed to address specific questions and applied in a consistent manner.

Purpose and Scope

The purpose and scope of this chapter are to identify factors that influence ecological recovery and discuss the appropriate procedures and tools for monitoring the success of remediation and restoration in the Boulder River watershed. We describe different types of monitoring, the questions each type is intended to address, and the endpoints that should be considered as a part of their design. Information from this chapter should have broad applicability to other watersheds impaired by historical mining.

Monitoring Strategies

Monitoring is an important tool for evaluating the success of remediation and restoration efforts and assessing the overall status of ecological recovery. Without collecting and analyzing comprehensive monitoring data, land managers cannot objectively evaluate the success of a remedial or restoration action or determine whether remediation and restoration goals have been met. As a tool, monitoring provides information for four basic purposes:

- Performance evaluation—This strategy is used to evaluate project implementation and ecological effectiveness.
- Trend assessment—This strategy includes an extended sampling plan to identify changes across spatial and temporal scales.
- Risk assessment—This strategy is used to identify hazard sources, causal relationships, and resource injury within an ecosystem.
- Baseline characterization—This strategy is used to quantify ecological conditions prior to an actual disturbance. It may also be used to collect information at a reference site to determine premining baseline conditions for a comparable disturbed habitat.

The type and extent of necessary monitoring will depend on specific management objectives (Kondolf, 1995). In the case of a historical mining area, the strategy most appropriate for evaluating the success of remediation and restoration would be performance evaluation. The three components of

performance evaluation include (1) implementation monitoring, (2) effectiveness monitoring, and (3) validation monitoring. Implementation monitoring addresses the question: "Were the remediation and restoration measures properly executed?" Exploring this question may yield valuable information that will help with potential refinement of remediation or restoration practices. Effectiveness monitoring addresses the question: "Did remediation and restoration measures achieve the desired results?" Monitoring variables should focus on indicators that document achievement of desired conditions. Variables should be sensitive enough to detect change, should be both detectable and measurable, and should have statistical validity. This level of monitoring is more time consuming than implementation monitoring. However, if effectiveness-monitoring data indicate that restoration goals are not being met, problems can be evaluated in a timely manner, and ecologically beneficial adjustments can be made to the remediation and restoration designs. The most costly level of monitoring is validation monitoring. This addresses the question: "Are the underlying assumptions used in the remediation and restoration designs and the cause-effect relationships correct?" This level of monitoring is usually performed when the desired results of the remediation or restoration actions are not occurring and when further corrective action has not achieved the desired results. This level of monitoring requires scientific expertise to design and implement.

Monitoring Tools

Monitoring involves measurement of chemical, physical, and biological parameters to evaluate the magnitude of change that occurs following remedial and restoration activities and to estimate the rate of recovery of an ecosystem. A comprehensive list of all potential variables available for use in a monitoring program would be overwhelming. Therefore, we present a refined list of the types of monitoring variables applicable to an ecosystem affected by historical mining activities. An ideal monitoring program would include a combination of these chemical, physical, and biological variables.

Biological communities provide an integrated response to the chemical and physical attributes of their environment. Understanding the response of the biological community to remediation and restoration activities is the most important outcome of monitoring. Important physical and chemical variables that may significantly affect the quality of aquatic habitat include temperature, turbidity, dissolved oxygen, pH, alkalinity/acidity, hardness, nutrients, flow, channel characteristics, spawning gravel/interstitial space, pool/riffle ratio, shade, in-stream cover, bed material load, dissolved constituents, and suspended solids. For a remediated historical mining area, chemical variables would include measures of trace-element concentrations in water, in streambed sediment, and in biota deemed problematic during the assessment phase of the project. For the chemical analysis of water, measurement of the fraction (total recoverable or dissolved) that relates specifically to national or State water-quality criteria or that may be linked to bioavailability is most valuable in determining potential habitat improvement.

Ultimately, the goal of mine and mill site remediation is to restore a healthy self-sustaining ecosystem. This success can be documented through measurement of biological endpoints (table 1). Selection of biological measurements is generally determined by the species at risk. For example, in the Boulder River watershed, land managers are interested in establishing a healthy ecosystem that would support a successful trout fishery. In this case, measures of successful ecological restoration could include assessment of fish population densities, survival and health of individual fish (Karr, 1981; Farag and others, this volume), trace-element concentrations in biofilm and invertebrates, and indices of health of the aquatic invertebrate community (Klemm and others, 1990; Pflakin and others, 1989). If the species of interest were fish-eating birds such as kingfishers or eagles, focus should be on the trace-element concentrations in the tissues of fish and on the reproductive health of the birds of interest.

Factors Influencing Restoration Success

Successful ecological restoration of a stream or river that has been adversely affected by mining is dependent on the suitability of both the physical and chemical conditions in the aquatic environment. The basic geologic character of a mining area strongly influences the water quality and the biological community that can exist in an ecosystem. Therefore, knowledge of the geology of a region is critical to defining achievable restoration goals. Not only do the streambed sediment, mine waste, and mill tailings represent sources and sinks for contamination in the watershed (Church, Unruh, and others, this volume) prior to remediation, but also the nature of the mineral content, buffering capacity, acidity, and organic richness of rocks in the watershed all influence the ability of an ecosystem to recover following remediation. In addition to toxicological issues associated with sediment contamination, excessive sedimentation in the streambed can physically limit suitable habitat for survival and reproduction of benthic invertebrates and fish. If remediation addresses removal of contaminated sediment from the stream and flood plain, repair of the stream channel, and stabilization of the stream banks and flood plain, then underlying geologic characteristics of the region, such as the acid-neutralization capacity of the rocks in the Boulder River watershed (McCafferty and others, this volume, Chapter D2; McDougal and others, this volume, Chapter D9), or the particle size distribution of sediment in the streambed, will determine the potential for recovery of habitat that will support a healthy aquatic community and lead to the reestablishment of a healthy riparian corridor.

In an aquatic system, both the quality and the quantity of water also influence the ability of a system to recover. The

Table 1. Examples of biological components and corresponding parameters that may be measured to evaluate progress of ecological recovery.

Biological component	Parameter
Primary productivity	Periphyton or biofilm density
	Aquatic macrophytes species and density
	Concentration of trace elements
Aquatic invertebrate community	Species composition
	Numbers of individuals
	Diversity
	Biomass
	Concentration of trace elements
Fish community	Species composition
	Age class distribution
	Fish health assessment
	Population density
	Concentration of trace elements
	In-stream exposure experiments
Riparian wildlife/terrestrial community	Amphibian/reptile species composition
	Amphibian/reptile population density
	Mammal species composition
	Mammal population density
	Mammal health assessment
	Passerine bird species composition
	Passerine bird population density
	Passerine bird reproductive health
	Fish-eating bird species composition
	Fish-eating bird health and population density
Riparian vegetation	Species composition
	Condition
	Successional changes
	Soil toxicity assessment

water serves as a primary pathway of contaminant exposure for the biological community as well as a means to transport contamination downstream through the watershed. Remediation of targeted mine sites should result in reduction of potential contaminant load in watershed streams. During the initial assessment of the Boulder River watershed, many aspects of water and sediment chemistry, geology, hydrology, biology, and ecology were characterized. Although it was important to determine the status of the biological community in the watershed during this assessment phase, chemical variables such as trace-element concentrations in water and sediment were used to calculate hazard quotients for identifying areas of concern (Finger, Farag, and others, this volume). These quotients were useful in focusing attention on general stream reaches to target for remediation. For aquatic environments impacted by historical mining, significant scientific literature linking biological exposure and effects exists, thus making the ecological risk assessment approach useful for anticipating adverse effects on the biological community. Actual measures of fish health, population status, and toxicological assessment of larval fish survival (Farag and others, this volume) provided confirmation of effects predicted from physical measures. Overall, the measurement of physical variables during the assessment phase was extremely important for determining sources and extent of contamination in the watershed and for assessing the severity of contamination at specific sites.

If the remedial activities in any watershed are adequate, the effects of sources of contamination will be eliminated or greatly reduced. The potential for successful ecological restoration will then be greatest where healthy biological communities (1) exist in the watershed outside the zone of contamination and (2) are capable of recolonizing previously impaired stream reaches. This is the case in the Boulder River watershed where fish and invertebrates inhabit many stream reaches within the watershed (Finger, Farag, and others, this volume, fig. 1). Potentially, reestablishment of the native trout species is even possible because a reproductively viable population of westslope cutthroat currently exists in High Ore

Creek upstream from the Comet mine. Successful remediation and restoration of stream reaches affected by the Comet mine could lead to successful ecological recovery of this species by providing habitat where these native trout can survive and reproduce. However, some type of physical barrier would be necessary in High Ore Creek to prevent the migration and resultant competition of more aggressive brook and rainbow trout from the Boulder River.

Monitoring in the Boulder River Watershed

In the Boulder River watershed, the primary focus of the watershed approach has been on the identification of factors affecting the health and potential for recovery of the aquatic community and its supporting habitat. Ongoing monitoring of High Ore Creek has shown that remediation has substantially reduced dissolved zinc concentrations, but that dissolved arsenic concentrations have increased slightly (Gelinas and Tupling, this volume). Continued improvements in water quality and reduced sediment loading should result in improved survival, growth, and reproduction in the aquatic community.

The selection of appropriate monitoring endpoints for use in the Boulder River watershed can be determined based on the watershed assessment. The same variables used to document impairment to the watershed can provide a measure of ecological recovery following remediation. These variables would include, at a minimum, concentrations of arsenic, cadmium, copper, lead, and zinc in water samples collected over a range of flow conditions, trace-element concentrations in streambed sediment and biofilm collected at low flow, in-stream exposures with larval fish, fish population assessment, and measures of fish health. Monitoring sites should correspond to those used in the watershed study with the possible addition of sites in areas of anticipated recovery. This approach would support the establishment of monitoring sites downstream of the Bullion mine on Bullion Mine tributary and on Jack Creek, downstream of the Crystal mine on Uncle Sam Gulch, on Cataract Creek upstream and downstream of the confluence with Uncle Sam Gulch, downstream of Comet mine on High Ore Creek, and at several locations on the Boulder River.

Future monitoring that incorporates biological and chemical measurements will be able to demonstrate the degree of success of remediation projects in the watershed. However, the success of any ecological recovery will be determined not only by the degree of improvement achieved in the aquatic environment, but also by the recovery of associated flood-plain and riparian habitat within the watershed. Although not specifically addressed in this volume, the issues of revegetation of the riparian area and stabilization of the flood plain are important to land managers in the overall environmental restoration of an area (Kondolf, 1995). Monitoring the improvement of flood-plain and riparian soils after the physical removal of tailings can be accomplished through use of both geochemical characterization and soil toxicity assessments. Such monitoring can determine the potential for successful revegetation of an area. In addition, monitoring the health and recovery of wildlife communities dependent on this terrestrial habitat can provide valuable information on ecological recovery. Only through a well-designed and rigorously implemented monitoring program can the success of a remedial effort be validated.

Summary

Monitoring includes measures of chemical, physical, and biological parameters to evaluate the magnitude of change that occurs following remedial activities and to estimate the rate of recovery of an ecosystem. Historical mining activities have resulted in the degradation of fisheries and their supporting habitat in the Boulder River watershed. As a result of remediation in the watershed, improvements in water quality and reduced trace-element concentrations in streambed sediment should result in ecological recovery, improved physical habitat, and greater survival, growth, and reproduction rates in the aquatic community. The presence of trout in some stream reaches in the Boulder River watershed provides a local source of fish to repopulate areas where no fish were present prior to remediation.

The selection of appropriate monitoring endpoints to evaluate recovery in the Boulder River watershed can be determined based on the physical, chemical, and biological measurements used during the pre-remediation watershed assessment. This would include, at a minimum, measures of cadmium, copper, lead, zinc, and arsenic in water samples collected at high and low flows, measures of bed sediment concentrations at low flow, and chemical analysis of biofilm at low flow, in-stream exposures with larval fish, fish population assessment, and measures of fish health. Monitoring sites should correspond to those used in the watershed study with the possible addition of sites in areas of anticipated recovery.

References Cited

Karr, J.R., 1981, Assessment of biotic integrity using fish communities: Fisheries, v. 6, p. 21–27.

Klemm, D.J., Lewis, P.A., Fulk, F., and Lazorchak, J.M., 1990, Macroinvertebrate field and laboratory methods for evaluating the biological integrity of surface waters, EPA/600/4–90–030: U.S. Environmental Monitoring Systems Laboratory, Cincinnati, Ohio.

Kondolf, G.M., 1995, Five elements for effective evaluation of stream restoration: Restoration Ecology, v. 3, p. 133–136.

Kondolf, G.M., and Micheli, E.R., 1995, Evaluating stream restoration projects: Environmental Management, v. 19, p. 1–15.

National Research Council, 1992, Restoration of aquatic ecosystems—Science, technology, and public policy: Washington, D.C., National Academy Press, 552 p.

Plafkin, J.L., Barbour, M.T., Porter, K.D., Gross, S.K., and Hughes, R.M., 1989, Rapid bioassessment protocols for use in streams and rivers, EPA444/4–89–001: U.S. Environmental Protection Agency, Washington, D.C.

Digital Databases and CD-ROM for the Boulder River Watershed

By Carl L. Rich, David W. Litke, Matthew Granitto, Richard T. Pelltier, and Tracy C. Sole

Chapter G of

Integrated Investigations of Environmental Effects of Historical Mining in the Basin and Boulder Mining Districts, Boulder River Watershed, Jefferson County, Montana

Edited by David A. Nimick, Stanley E. Church, and Susan E. Finger

Professional Paper 1652–G

U.S. Department of the Interior
U.S. Geological Survey

Contents

Figures

Tables

Chapter G
Digital Databases and CD-ROM for the Boulder River Watershed

By Carl L. Rich, David W. Litke, Matthew Granitto, Richard T. Pelltier, and Tracy C. Sole

Abstract

A large amount of digital data was produced as part of the Boulder River watershed study. Included are biologic, hydrologic, geochemical, geologic, and base cartographic data. Most were collected in the Basin Creek, Cataract Creek, and High Ore Creek subbasins of the Boulder River watershed, and in the portion of the Boulder River into which these creeks flow. A lesser amount was collected throughout the remainder of the Boulder River watershed. The data were converted to a common projection. Hydrography and road features, sample-site locations, and inactive mine and mine-related site locations were revised using digital orthophoto quadrangle (DOQ) imagery. The data are available, in formats compatible with widely used commercial software, on a CD-ROM that accompanies this volume. The data and the CD-ROM are described in this chapter.

Introduction

Digital datasets were an integral component of work conducted by U.S. Geological Survey scientists to understand issues related to inactive mines in the Boulder River watershed in southwest Montana. A large amount of information was produced as part of this multidisciplinary study. Analyses of the digital data layers have produced many results that are described and illustrated in the numerous maps and images that are provided in other chapters of this volume.

Data were obtained as part of various topical studies of the Boulder River watershed. During these studies, samples of many media, including rocks, soils, water, and aquatic life, were collected and analyzed. Other data sources used in this investigation included previous USGS regional studies, and the work of other Federal and State agencies. The different types of information were gathered from several different platforms including helicopters, fixed-wing aircraft, satellites, and ground fieldwork.

To make this information useful to others, the various datasets have been converted to a common map projection, and to formats compatible with widely used commercial software. The localities of the sample-site data were revised using digital orthophoto quadrangle (DOQ) image files. The data are organized in descriptive tables presented in this chapter, and in a digital relational database and a geographic information system (GIS) database on a CD-ROM that accompanies this volume. In addition, the CD-ROM provides data viewing software for elementary spatial comparisons and analysis of the various layers.

Purpose and Scope

The purpose of this chapter is to provide a comprehensive review of the digital data that were generated as part of the Boulder River watershed study, and which are placed on the CD-ROM that accompanies this volume. Included are a relational database, a GIS database, map, image, and graphic products created during the study, and two data viewers that allow visual spatial comparisons and analysis of the data. The relational database contains biologic, hydrologic, geochemical, and geologic sample-site data collected and produced for the Boulder River watershed study, and an inventory and description of mine-related sites located and compiled for the study. The GIS database contains the same sample-site data and mine-related site information stored as data layers and associated tables, as well as base cartographic, geologic, hydrologic, geochemical, and geophysical data in vector and raster formats.

The base cartographic data cover the Basin, Bison Mountain, Chessman Reservoir, Jefferson City, Mount Thompson, Three Brothers, Thunderbolt Creek, and Wickes 7.5-minute quadrangles at a level of detail similar to U.S. Geological Survey 1:24,000-scale topographic maps. Geologic, geochemical, and geophysical data (collectively referred to in this chapter as "Geoscientific Data") also exist within these same eight quadrangles. The sample sites and mine-related

sites are located primarily within the Basin Creek, Cataract Creek, and High Ore Creek watersheds, and along the approximately 9-mile reach of the Boulder River that extends from just upstream to just downstream of these tributaries. There are also less detailed base data, and some sample-site data, throughout the remainder of the entire Boulder River watershed.

The Boulder River watershed GIS database contains data for various layers and scales over areas of varying extent, including the Boulder River watershed study area as previously defined in Church, Nimick, and others (this volume, Chapter B), an eight-quadrangle area which includes the "Boulder River watershed study area," and the Boulder River watershed in its entirety. Figure 1 shows the area of the

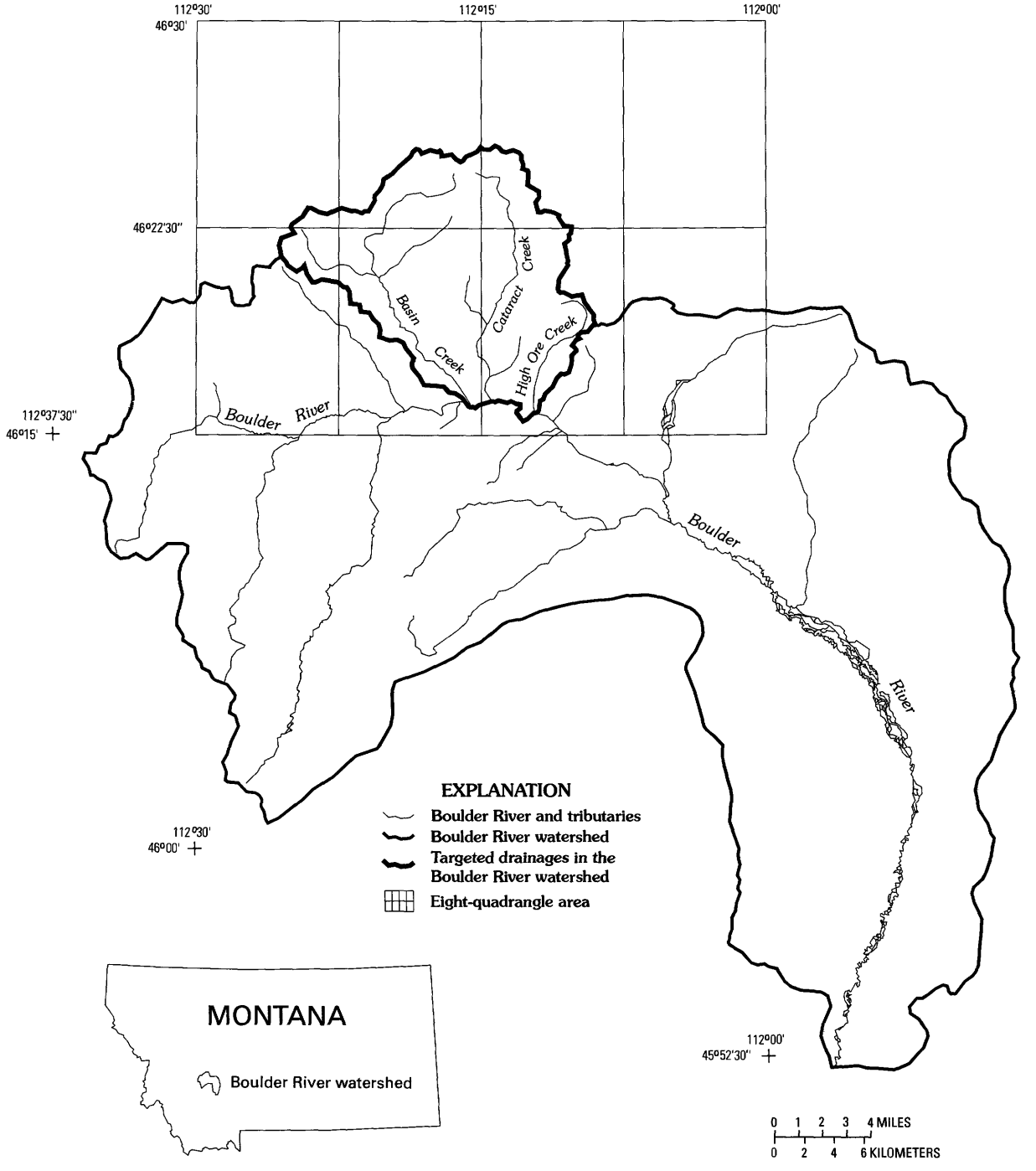

Figure 1. Geographic extent of database for Boulder River watershed study.

targeted drainages of the northern part of the Boulder River watershed.

The data are available on the CD-ROM in formats from the software used to create them, and in several other formats including ASCII textfiles, ESRI shapefiles, .dbf files, and TIFF image files. The *x*,*y* coordinates of the ArcInfo coverages, ESRI shapefiles, and TIFF image files are in UTM (Universal Transverse Mercator) meters, zone 12, and are cast on the North American Datum of 1927 (NAD27). The FieldSites table in the relational (Access) database also contains the longitude and latitude values of the field site locations in decimal degrees, also in NAD27.

The main body of this chapter begins with a synopsis of the various data layers organized under three broad themes, including (1) base cartographic data, (2) sample-site data and mine-related site data, and (3) data layers pertaining to geologic, geochemical, biologic, geophysical, and remote sensing information. (This third group of data layers is collectively referred to in this chapter as "Geoscientific Data.") A brief description of the utility of the data is given followed by a descriptive table that includes relevant information about individual data files. This synopsis of the data is followed by an explanation of the relational database. The report concludes with a description of the data viewer software that is provided on the CD-ROM and an explanation of the content and format of the CD-ROM itself.

Acknowledgments

The authors acknowledge the assistance of Paul Martin, Rick Poss, Stewart Wright, John Erickson, Steve Howard, Earl Wilson, and Eric Wong in the creation of the base cartographic data for the Boulder River watershed GIS database.

Base Cartographic Data

In general, the base cartographic data were initially collected from the eight 7.5-minute U.S. Geological Survey topographic maps mentioned previously, and then revised where possible using 1993 and 1998 digital orthophoto quadrangles (DOQ's). DOQ's were not available for the Wickes and Jefferson City quadrangles; however, the Boulder River watershed study area is entirely contained within the remaining six quadrangles. When available, U.S. Geological Survey Digital Line Graph (DLG) files were used as the initial source, but where necessary, data were scanned or digitized from stable-base separates of the appropriate 7.5-minute topographic map. These topographic maps were all 1985 Provisional Editions. During the 5-year period of this study, newly revised (1996) versions of the Thunderbolt Creek, Basin, Mount Thompson, and Wickes quadrangles were released to the public. A visual inspection of these maps was performed, and information in the GIS database was updated where appropriate.

Base cartographic layers created as just described include hydrography, roads and trails, miscellaneous transportation, hypsography (vector topographic contours), administrative and political boundaries, Public Land Survey System (PLSS), and cultural features. The hydrography and roads and trails layers were revised using DOQ files as just described. The remaining layers were not, and thus their content reflects the content of the 7.5-minute topographic maps. The location and description of inactive mines and mine-related features were of utmost importance to this study, and are described separately later in this chapter and in detail in the Mine Inventory chapter (Martin, this volume, Chapter D3). The Boulder River watershed study area boundary layer was created from the hypsography and hydrography layers. Figure 2 shows selected base cartographic data and the outline of the target drainages in the Boulder River watershed.

The base cartographic data vector layers exist on the Boulder River watershed CD-ROM as export files of ArcInfo coverages in the /bldr_cd/gis_db/basecart/e00 directory, and as ESRI shapefiles in the /bldr_cd/gis_db/basecart/shape directory. A complete list of base cartographic data coverages and the data themes they contain is in table 1. Due to shapefile naming restrictions, the names of some of the shapefiles are abbreviated versions of their corresponding ArcInfo coverage names. For a complete listing of the shapefile names, see the /bldr_cd/gis_db/basecart/README.txt file on the CD-ROM which accompanies this volume.

The first 16 coverages listed in table 1 contain data that lie entirely within the eight-quadrangle area. The Administrative Boundaries theme contains USDA Forest Service boundaries but does not include inholding boundaries. The Political Boundaries theme contains county boundaries, those being the only political boundaries that exist in the eight-quadrangle area.

In addition to the naturally occurring features contained in the Hydrography theme, there are lines labeled as "network flow lines," which connect streams where they flow into and out of lakes and marshes. These lines and all lines representing streams have been created from beginning to end in the downstream direction. Thus, by using all the linear features that represent streams, along with the "network flow lines," one can perform network flow modeling. The Springs theme contains all springs shown on the 7.5-minute topographic maps for the eight-quadrangle area, plus 13 others located as part of this study.

A typical USGS DLG Miscellaneous Culture Features file would contain the contents of the Miscellaneous Culture Features theme, the Miscellaneous Culture Point Features theme, and the Mine-related Point Features from Topographic Maps theme. Because of the importance of mine-related sites to this study, they were separated from the other cultural point features and stored in a separate coverage called MINE_TOPO_PTS. This coverage contains all mine-related point features exactly as they are shown on the 7.5-minute topographic maps. A separate coverage, MINE_SITES, which was created using the digital orthophoto quadrangle files and

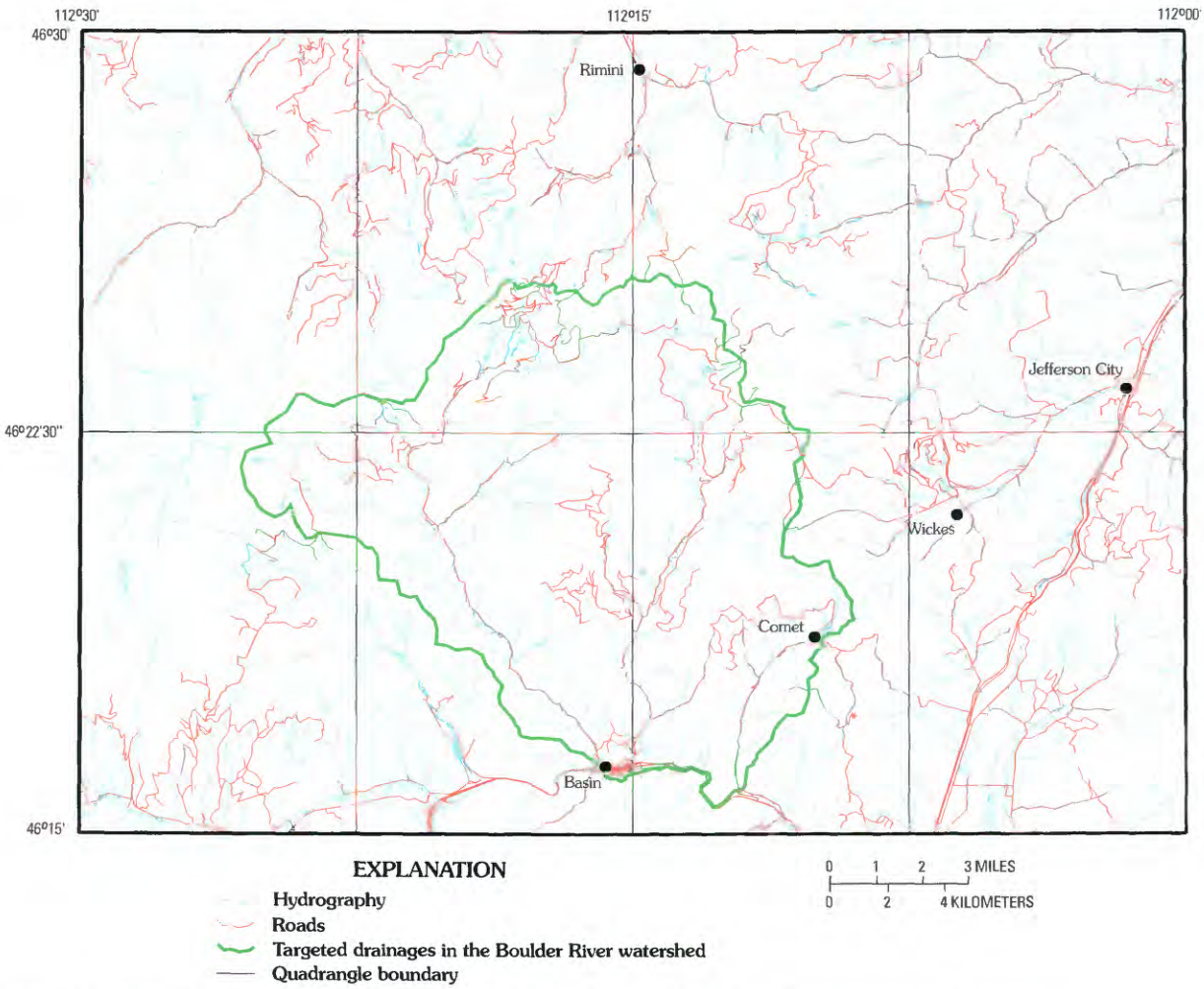

Figure 2. Selected data within the eight-quadrangle area from the Boulder River watershed GIS database.

a wide variety of other sources, is described briefly in this chapter under the "Site Data" section, and in greater detail in Martin (this volume, Chapter D3).

As previously mentioned, most of the data gathered for the Boulder River watershed study was collected within the eight-quadrangle area. However, a few samples were collected within the portion of the Boulder River watershed that lies outside the eight-quadrangle area. The last seven coverages listed in table 1 contain less-detailed data that cover the entire Boulder River watershed. These coverages were created to serve as visual reference for the data collected outside the eight-quadrangle area. The vast majority of the Boulder River watershed lies within Jefferson County, except for one very small portion of Broadwater County at the southeast edge of the watershed. The Basin-wide County Boundaries theme delineates this small section of county boundary. The Basin-wide Hydrography theme contains the Boulder River and selected tributaries, and the Basin-wide Highways theme contains major highways within and near the Boulder watershed. The Jefferson River theme contains a section of the Jefferson River that lies just upstream and just downstream from the mouth of the Boulder River. The Subbasins theme contains selected subbasin boundaries within the watershed, as selected by project scientists for the purpose of meaningfully interpreting the data collected for the study.

Other related base cartographic data in the GIS database include an elevation grid created directly from USGS 10-meter Digital Elevation Model (DEM) files, and individual Digital Raster Graphic (DRG) files of the topographic maps. Slope grids in percent and degrees, and aspect and shaded-relief grids were also derived from the elevation grid. All of the elevation-related grids are listed in table 2. The elevation and elevation-derived grids exist on the CD-ROM in the /bldr_cd/gis_db/basecart/elev directory as a compressed tar file (elevation.tar.gz), which when uncompressed produces an entire ArcInfo workspace containing all of the elevation-related grids. The elevation and elevation-derived data also exist as TIFF files on the Boulder River watershed CD-ROM in the /bldr_cd/gis_db/basecart/elev directory. Additionally, the raw elevation data values also exist in that directory in a flat, ASCII file called elevation.ascii.

For more detailed information describing the sources, creation and content of the base cartographic data in the Boulder River watershed GIS database, see the metadata located

Table 1. Base cartographic data coverages in the Boulder River watershed GIS database.

Coverage name	Theme	File name	Data format
ADMINBND	Administrative Boundaries	adminbnd.e00	ArcInfo vector coverage
HYDRO	Hydrography	hydro.e00	ArcInfo vector coverage
HYPSO	Hypsography	hypso.e00	ArcInfo vector coverage
MINE_TOPO_PTS	Mine-related Point Features from Topographic Maps	mine_topo_pts.e00	ArcInfo vector coverage
MISC_CUL	Miscellaneous Culture Features	misc_cul.e00	ArcInfo vector coverage
MISC_CUL_PTS	Miscellaneous Culture Point Features	misc_cul_pts.e00	ArcInfo vector coverage
MISCTR	Miscellaneous Transportation Features	misctr.e00	ArcInfo vector coverage
PLACE_NAMES	Place Names	place_names.e00	ArcInfo vector coverage
PLSS	Public Land Survey System	plss.e00	ArcInfo vector coverage
POLBND	Political Boundaries	polbnd.e00	ArcInfo vector coverage
QUADS	Quadrangle Boundaries	quads.e00	ArcInfo vector coverage
Q8OUTLINE	Outline of Eight-Quadrangle Area	q8outline.e00	ArcInfo vector coverage
ROADS	Roads	roads.e00	ArcInfo vector coverage
SPRINGS	Springs	springs.e00	ArcInfo vector coverage
STUDY_AREA_BD	Study Area Boundary	study_area_bd.e00	ArcInfo vector coverage
USFS_CFF_OWN	USDA Forest Service Cartographic Feature File (CFF) Ownership Lines	usfs_cff_own.e00	ArcInfo vector coverage
ALL_BLDR_COBD	Basin-wide County Boundaries	all_bldr_cobd.e00	ArcInfo vector coverage
ALL_BLDR_HY	Basin-wide Hydrography	all_bldr_hy.e00	ArcInfo vector coverage
ALL_BLDR_RD	Basin-wide Highways	all_bldr_rd.e00	ArcInfo vector coverage
ALL_BLDR_USFS	Basin-wide USDA Forest Service Boundaries	all_bldr_usfs.e00	ArcInfo vector coverage
ALL_BLDR_WSHD	Boulder River Watershed	all_bldr_wshd.e00	ArcInfo vector coverage
JEFFRIVER	Jefferson River	jeffriver.e00	ArcInfo vector coverage
SUBBASINS	Subbasins	subbasins.e00	ArcInfo vector coverage

Table 2. Elevation and elevation-derived grids in the Boulder River watershed GIS database.

Grid name	Theme	File name	Data format
ELEVATION	Elevation	elevation.tar.gz	ArcInfo grid
HILSHD	Shaded Relief	elevation.tar.gz	ArcInfo grid
SLOPE_DEGREE	Slope in Degrees	elevation.tar.gz	ArcInfo grid
SLOPE_PERCENT	Percent Slope	elevation.tar.gz	ArcInfo grid
ASPECT	Slope Aspect	elevation.tar.gz	ArcInfo grid

on the CD-ROM accompanying this volume, in the /bldr_cd/gis_db/basecart/meta directory. Because the ESRI shapefile versions of the base cartographic data were created from the ArcInfo coverages, and due to shapefile naming limitations, the shapefiles in some cases have abbreviated versions of the coverage names listed in table 1. These differences are fully described in the README.txt file in the /bldr_cd/gis_db/basecart directory on the CD-ROM. The CD-ROM is described at the end of this chapter in the Boulder River watershed CD-ROM section.

Site Data

As part of the watershed approach, many kinds of scientific data were collected in the Boulder River watershed study area for site characterization, analysis, and monitoring purposes. A wide range of rock, sediment, water, and biological samples was collected, measured, and analyzed, and an inventory of mine-related sites and descriptions was compiled. In order to have a single, integrated and standardized collection of project information, all data were integrated spatially using a GIS, and conceptually using a relational database. Field sampling sites that should be considered co-located for analysis purposes were grouped together resulting in 425 Analysis Sites. Inactive mines and other mine-related features are represented as 143 Mine Sites. Associations between Field Sites and Mine Sites were defined and represented as relationships in the databases. The sample-site and mine-site data are available on the Boulder River watershed CD-ROM in a relational (Access) database, in a GIS (ArcInfo) database, and in several other formats.

Sample-Site Data

Figure 3 shows the distribution of the sample sites for the Boulder River watershed study. The majority of sites are in the area of targeted drainages in the Boulder River watershed; some are elsewhere in the Boulder River watershed; a few are outside the Boulder River watershed, but within the eight-quadrangle area. (See figure 1 for the spatial relationship of these three areas.) For detailed localities of specific sample sites, see the appropriate chapter of this volume, as listed in table 5 in the "Relational Database" section, or extract the FIELD_SITES data from the accompanying CD-ROM.

As previously mentioned, the sample-site data and mine-related site data exist in a number of different formats on the CD-ROM accompanying this volume. The file names of the data as they exist in the various formats are shown in table 3. Owing to differences in the allowed lengths of file names and attribute names, some of the ArcInfo, ESRI shapefile, and .dbf file names and attribute names are abbreviated versions of those that exist in the analogous relational (Access) database tables. These differences are delineated in the README.txt file on the Boulder River watershed CD-ROM in the /bldr_cd/gis_db/sitedata directory.

The coverage, file, and attribute names used in the remainder of this section are from the ArcInfo GIS database. Access relational database table and attribute names are used in the "Relational Database" section later in this chapter.

The sample data exist in the GIS database as two point feature data layers (FIELD_SITES and ANALYSIS_SITE) and 10 associated tables. The FIELD_SITES data layer contains one point feature for each sample site. Attributes for each site include a unique identifier called SITENUMBER, various information provided by the person who collected the sample(s) at the site, and locational information generated by the GIS. A table called LOC_MASTER contains the attributes ELEVATION, TOWNSHIP, RANGE, SECTION, LITHOLOGY, STRAT_UNIT (stratigraphic unit), GEOL_AGE (geologic age), and SUBBASIN for each sample site. Values for these attributes were assigned by using the GIS to perform spatial overlays with the FIELD_SITES coverage and the appropriate base cartographic and geologic coverages.

Sample sites that are considered co-located for purposes of spatial analysis are assigned the same value for an identifier called AMLI_ANALYSIS_ID. Because the location chosen to represent the "analysis site" is not always exactly the same as that of the sample sites that are logically considered to be co-located there, a second point feature data layer, ANALYSIS_SITE, is used to contain the locations of the analysis sites. The same attributes that were added to the FIELD_SITES data layer using spatial overlay were also added to the ANALYSIS_SITE data layer.

Because the AMLI_ANALYSIS_ID exists in the attribute tables for both the FIELD_SITES and ANALYSIS_SITE data layers, the two can be related to each other and to other data tables containing actual sample data and results. The relationship between the two point feature data layers is one-to-many, since more than one field site can have the same AMLI_ANALYSIS_ID. In order to aid GIS users not familiar

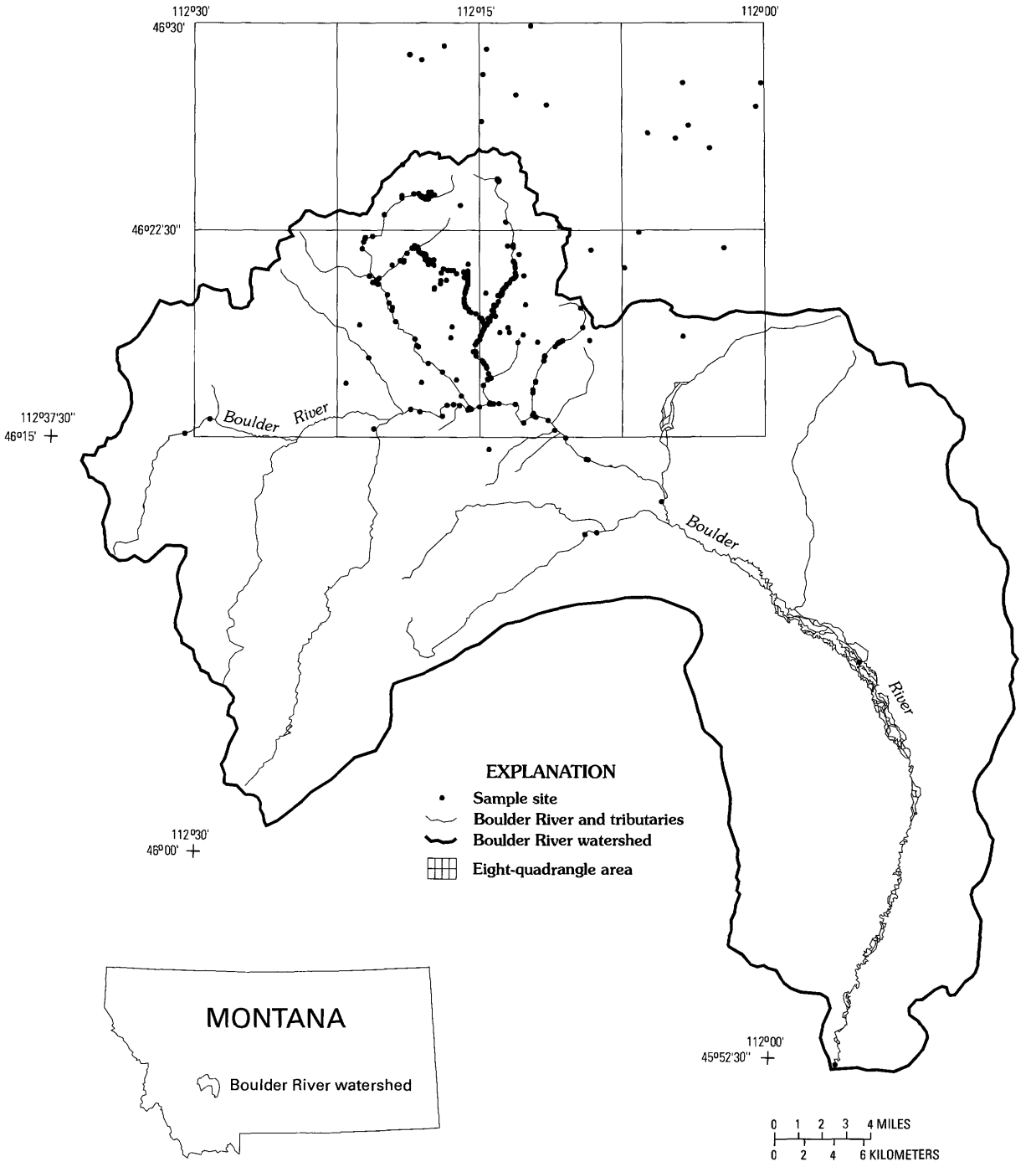

Figure 3. Distribution of Boulder River watershed study sample sites.

with techniques for dealing with one-to-many relationships, the attribute table for the ANALYSIS_SITE data layer also contains the SITENUMBERs of the field sites associated with each analysis site.

A table called FS_MS_ASSOCS contains a list of field sites that are associated with specific mine-related sites. There are 18 such relationships in the table, with the identifiers SITENUMBER and mine-related site AMLI_MINE_ID listed for each relationship. For a complete description of the inventory of mining-related sites created for this study, see Martin (this volume).

There are eight other tables that contain the actual sample data and results, as well as various characteristics of the samples and results. These tables were initially created using the Access relational database and then converted to INFO files and .dbf files for inclusion in the GIS database. These

Table 3. File names for site data in various formats.

Export files for ArcInfo coverages or Info files	Shapefiles or dBASE files	Access tables	ASCII tables
analysis_site.e00 (coverage)	anlysite.shp	SpatialAnalysisSites	SpatialAnalysisSites.tab
Analytic_meth.e00 (Info file)	an_meth.dbf	AnalyticMethod	AnalyticMethod.tab
field_sites.e00 (coverage)	fldsite.shp	FieldSites	FieldSites.tab
fs_ms_assocs.e00 (Info file)	fmsassoc.dbf	FieldSiteMineSiteAssocs	FieldSiteMineSiteAssocs.tab
lab_name.e00 (Info file)	labname.dbf	LabName	LabName.tab
loc_master.e00 (Info file)	locmastr.dbf	LocationMaster	LocationMaster.tab
mine_sites.e00 (coverage)	minesite.shp	MineSites	MineSites.tab
mine_sites.e00 (mine_sites.aditflow is part of mine_sites coverage)	msadflow.dbf	MineSitesAditFlow	MineSitesAditFlow.tab
parameter.e00 (Info file)	parametr.dbf	Parameter	Parameter.tab
project.e00 (Info file)	project.dbf	Project	Project.tab
qual_result.e00 (Info file)	qualres.dbf	QualitativeResult	QualitativeResult.tab
result.e00 (Info file)	result.dbf	Result	Result.tab
sample.e00 (Info file)	sample.dbf	Sample	Sample.tab
Sample_media.e00 (Info file)	sampmed.dbf	SampleMedia	SampleMedia.tab

tables are described in the "Relational Database" section of this chapter. Effective use of the data in many of these tables requires dealing with one-to-many relationships. The relationships between the primary sample and results tables are shown in figure 4, and explained in the "Relational Database" section of this chapter. A bitmap file (relationship_diagram.bmp) containing a complete diagram of the relationships of all the files in the Boulder River watershed relational database exists on the accompanying CD-ROM in both the /bldr_cd/rel_db and /bldr_cd/gis_db/sitedata directories. Because effective use of the sample-site data requires an understanding of these relationships, this diagram is important for users of the GIS database, as well as for users of the relational database.

The FIELD_SITES and ANALYSIS_SITE coverages exist on the Boulder River watershed CD-ROM as export files in the /bldr_cd/gis_db/sitedata/e00 directory. Ten other tables containing information about, and data collected at, the field sites also exist in that directory as INFO files. These coverages and tables also exist as ESRI shapefiles and .dbf files, respectively, in the /bldr_cd/gis_db/sitedata/shape and /bldr_cd/gis_db/sitedata/dbf directories.

Mine-Related Site Data

An inventory of inactive mines and mine-related sites in the Boulder River watershed study area was compiled from existing State and Federal sources. In some cases, multiple shafts, adits, prospects, and disturbed areas were located at a given site, but in each case a single point location was chosen to best represent the site. The location of each mine-related site was verified where possible with digital orthophoto quadrangle (DOQ) images, and by persons with local knowledge of the area.

A number of descriptive attributes were gathered from a variety of sources and assigned to the mine-related sites wherever available. One hundred forty-three mine-related sites are stored in an ArcInfo coverage called MINE_SITES, which exists on the Boulder River watershed CD-ROM as an export

file in the /bldr_cd/gis_db/sitedata/e00 directory. There is also an ArcInfo lookup table called MINE_SITES.ADITFLOW, which contains information about flowing adits that exist at some of the mine-related sites. The MINE_SITES.ADITFLOW lookup table is part of the MINE_SITES coverage, and is therefore contained in the mine_sites.e00 file. A detailed description of the mine inventory data is in Martin (this volume).

In addition, the MINE_SITES coverage and related tables are also available on the Boulder River watershed CD-ROM as an ESRI shapefile and .dbf files, respectively, in the /bldr_cd/gis_db/sitedata/shape and /bldr_cd/gis_db/sitedata/dbf directories. The mine-related site data are also part of the Boulder River watershed relational database, which is described later in this chapter.

Geoscientific Data

Geologic Data

Two geologic maps were generated from the original geologic map products of Ruppel (1963) and Becraft and others (1963). The first map is a reinterpretation of bedrock geology and is described in O'Neill and others (this volume, Chapter D1). Four data files are provided to create this map. All data are provided in both ArcInfo Export format and ESRI shapefile format. The first data file is the geology polygon and line file (geology.e00, geologyp.shp, and geologyl.shp). This data file updates previously published maps by providing a geologic framework in the context of current geologic nomenclature and modern knowledge for geologic units in the Boulder River watershed. The second data file depicts the geologic structure (faults.e00 and faults.shp). This line file contains the faults that have been mapped in the geologic map area. The third data file is an alteration coverage (alter.e00 and alter.shp). This is a polygon file that shows areas of probable Late Cretaceous alteration. The fourth data file shows the veins that have been mapped for the geologic area (veins.e00 and veins.shp). All of these data files are provided in ArcInfo export format in the /bldr_cd/gis_db/geosci/geology/e00 directory, as well as in ESRI shapefile format in the /bldr_cd/gis_db/geosci/geology/shape directory. O'Neill and others (this volume) provide a comprehensive discussion of geologic features. A PDF format map file also is provided (geol_pl1.pdf). It is located in the /bldr_cd/gis_db/geosci/geology/pdf directory. Throughout this volume, this geologic map is listed and described as plate 1. O'Neill and others (this volume) also contains a second oversize image, which is listed and described as plate 2. The illustration is a fence diagram correlating Quaternary deposits in the area of the inactive Buckeye mine. It is provided on the CD-ROM as a PDF in the /bldr_cd/gis_db/geosci/geology/pdf directory and is named geol_pl2.pdf. The topographic base was simplified for inclusion under the geology in plate 1. A PDF of the complete topographic base is provided in the /bldr_cd/gis_db/geosci/geology/pdf directory and is named topobase.pdf.

The second geologic map provides a reinterpretation of study area geology in a geoenvironmental context, as described by McCafferty and others (this volume, Chapter D2). This map depicts geologic units in terms of their relative acid-neutralizing potential based on mineralogical data and acid-leachate studies. Geologic units with higher acid-neutralizing potential are shown in lighter shades of green, and units with relatively low acid-neutralizing potential are shown in darker greens. This map (e_geo.tif) is provided in GeoTIFF format. It is located in the /bldr_cd/gis_db/geosci/geophys/geotiff directory.

Geochemical Data for Streambed Sediment and Water

Eleven files provided in the geochemistry section depict geochemical data for streambed sediment and water. The original geochemical data consisted of concentration data for trace elements in either sediment or water. These data were reinterpreted as hazard quotients to indicate the relative hazard of the trace elements to aquatic biota. These hazard quotients are presented in "ribbon" maps that illustrate the distribution of hazard quotients of selected trace elements as a band of color that runs along the streams and resembles a ribbon. The relative magnitude of the hazard quotient is depicted with different colors. Development of the hazard-quotient ribbon maps is described in more detail by Finger, Farag, and others (this volume, Chapter C).

The geochemistry section contains five streambed-sediment ribbon maps. The elements shown and their corresponding file names are: cadmium (sed_cd.e00 and sed_cd.shp), copper (sed_cu.e00 and sed_cu.shp), lead (sed_pb.e00 and sed_pb.shp), zinc (sed_zn.e00 and sed_zn.shp) and a combination of cadmium, copper, and zinc data (sed_all.e00 and sed_all.shp). A map is provided that shows the localities of all the streambed-sediment sample sites (sed.e00 and sed.shp). All these files are provided in ArcInfo export format in the /bldr_cd/gis_db/geosci/geochem/e00 directory, as well as in ESRI shapefile format in the /bldr_cd/gis_db/geosci/geochem/shape directory.

This section also contains four water geochemical data maps. The elements shown and their corresponding file names are: cadmium (wat_cd.e00 and wat_cd.shp), copper (wat_cu.e00 and wat_cu.shp), zinc (wat_zn.e00 and wat_zn.shp) and a combination of cadmium, copper, and zinc data (wat_all.e00 and wat_all.shp). A map is provided that shows the localities of all the water sample sites (water.e00 and water.shp). All these files are provided in ArcInfo export format in the /bldr_cd/gis_db/geosci/geochem/e00 directory and in ESRI shapefile format in the /bldr_cd/gis_db/geosci/geochem/shape directory. Chapter D5 (Nimick and Cleasby) in this volume contains a detailed description of the water geochemical data.

Biological Data

The one map provided in this section shows the estimated distribution of trout prior to 1997. This file illustrates the distribution of trout by type in the watershed (fish.e00 and fish.shp). The map is based on two types of biological sample sites. The first type of sample site is the fish abundance and health assessment; the second type is the 96-hour survival experiment. This file is provided in ArcInfo export format in the /bldr_cd/gis_db/geosci/biologic/e00 directory and in ESRI shapefile format in the /bldr_cd/gis_db/geosci/biologic/shape directory. Chapter D10 (Farag and others) in this volume contains a detailed description of the biological data.

Geophysical Data

Images of magnetic anomaly and apparent resistivity data and related interpretive products are part of the work described in McCafferty and others (this volume, Chapter D2) and are provided in the /bldr_cd/gis_db/geosci/geophys/geotiff directory on the accompanying CD-ROM. Vector files that define the extent of the airborne geophysical survey are available in ArcInfo export format (gp_poly.e00) in the /bldr_cd/gis_db/geosci/geophys/e00 directory, and in ESRI shapefile format (gp_poly.shp) in the /bldr_cd/gis_db/geosci/geophys/shape directory.

The images provided on the CD-ROM were derived from grids of data collected along closely spaced (200 m) flightlines as part of a high-resolution airborne geophysical survey over the Boulder River watershed area. The images provide a depiction of the magnetic anomaly and apparent resistivity fields but do not allow for detailed data manipulations or interpretation at specific sites. The reader is referred to Smith and others (2000) for the basic magnetic anomaly and apparent resistivity flightline data and grids that would permit these types of analyses. The following text discusses the various geophysical image files that can be found in the /bldr_cd/gis_db/geosci/geophys/geotiff directory.

Images relating to the magnetic anomaly data include a reduced-to-pole magnetic anomaly map, a high-pass magnetic anomaly map, and an image of a model that illustrates estimates of magnetic susceptibility and volume percent magnetite. Except at the north magnetic pole, magnetic anomalies are distorted in shape and positioned off their causative sources. In order to correct for the distortion and dislocation of magnetic anomalies in the study area, a reduction-to-pole operation was applied to the magnetic anomaly field to produce the reduced-to-pole magnetic anomaly image (rtp_mag.tif). To emphasize magnetic anomalies caused by lateral variations in magnetic properties of rocks from surface elevations to approximate depths of 200 m, a filter was applied to the reduced-to-pole data to create the high-pass magnetic anomaly image (rtp_mag_hipass.tif). From these data, models of magnetic susceptibilities and corresponding values for percent magnetite were calculated (mag_magnetite.tif).

Images that portray apparent resistivity of rocks as measured from the airborne geophysical survey are provided on the CD-ROM. The images represent electrical resistivity of rocks at three frequencies resulting in different depths of penetration. The image produced using the highest frequency (56,000 Hz) shows resistivities of rocks at depths from the topographic surface to a few meters to 10 m. The mid-frequency (7,200 Hz) image (res7200.tif) maps electrical resistivities of rocks from the surface to depths of approximately 30 m. The lowest frequency (900 Hz) image (res900.tif) maps resistivities of rocks at depths to approximately 60 m.

For nearly all the Cretaceous- and Tertiary-age volcanic and plutonic rocks exposed in the Boulder River watershed, increased amounts of acid-consuming calcic and mafic minerals are associated with increased levels of the mineral magnetite. Magnetite is the main source for magnetic anomalies and, in part, resistivity anomalies. McCafferty and others (this volume) have converted the magnetic and apparent resistivity anomaly data to maps of volume percent magnetite to infer places in the watershed with low acid-neutralizing potential. Estimates for volume percent magnetite calculated from the 900-Hz apparent resistivity data are shown in the image file em_magnetite.tif. Volume percent magnetite estimates modeled from the magnetic anomaly data are given in the mag_magnetite.tif file. Low values in both geophysical magnetite models have been combined to produce an integrated product that represents locations of rocks with little to no acid-neutralizing potential (gp_low_ANP.tif).

Remote Sensing Data

The remote sensing section includes three vector files and five raster files. The first vector file represents linear features (lin_f.e00 and lin_f.shp) that were mapped from remote sensing base images. They are assumed to represent the spatial distribution, spatial frequency, and orientation of faults, joints, and fractures associated with structurally controlled ground-water flow. The second vector file is a wet soil coverage (wetsoil.e00 and wetsoil.shp). This coverage shows areas of saturated soils that are associated with shallow ground water. The third file illustrates wetlands (wetland.e00 and wetland.shp) that are defined as areas that have soils with perennial or seasonal high water tables. The vector files are provided in ArcInfo export format in the /bldr_cd/gis_db/geosci/remosens/e00 directory, and in ESRI shapefile format in the /bldr_cd/gis_db/geosci/remosens/shape directory. See Chapter D9 in this volume (McDougal and others) for a detailed description of these files.

The five raster files included in the remote sensing section show the linear features in terms of spatial frequency (frequency.tif), number of intersections (intersect.tif), and total length within a grid cell (length.tif). The contour maps represent zones of least occurrence of linear features, shortest linear features, and least number of intersections with cooler colors, and zones of higher occurrence, greater length, and

greater occurrence of intersections with warm colors. Two derivative maps have been produced from these images. The first is a combination of the spatial frequency and the length of the mapped linear features (frequency_length.tif). The second is a combination of the spatial frequency of the linear features and the number of the linear feature intersections (frequency_intersect.tif). These five files are provided in the GeoTIFF format. See Chapter D9 (McDougal and others) in this volume for a detailed description of the files. The files can be found in the /bldr_cd/gis_db/geosci/remosens/geotiff directory.

The geologic maps and the geochemical, biological, geophysical, and remote sensing data are listed in table 4, and are available on the CD-ROM in the /bldr_cd/gis_db/geosci directory.

Relational Database

The Boulder River watershed relational database was constructed to be used as a tool for data synthesis and analysis, and as an archive of data collected during the Boulder River watershed study. It includes data collected by U.S. Geological Survey biologists, geologists, and hydrologists within or adjacent to the Boulder River watershed during the period 1995 to 2000[1]. It is a tabular relational database containing field measurements made at point locations, and laboratory analyses of samples collected at point locations. Quality-assurance data are not included; information on field and laboratory quality-assurance practices is located in individual chapters in this report or in previously published reports. A Geographic Information System (GIS) representation of the database is discussed elsewhere in this chapter.

Contents of Database

The Boulder River watershed relational database contains data contributed by eight U.S. Geological Survey scientists or teams (table 5). These data sets comprise all of the available data collected as part of the project. Data were collected at 479 sites (fig. 3). Twenty-four media types were sampled, including 1,038 water samples, 1,094 earth material samples, and 79 biological material samples. Water media sampled included surface water (streams), ground water (well water), and springs. Earth media sampled included soils, bedrock, and various types of sediment. Biological media sampled included biofilm, fish tissue, invertebrate tissue, and tree tissue. The database contains 67,366 results, which are quantitative, qualitative, or descriptive measurements; the database contains 776 defined measurement types (parameters).

[1]Forty-eight analyses of bedrock samples collected during 1952–54 also are included in the database.

Database Structure

Because of the scope and complexity of data collected as part of the Boulder River watershed study, a relational database structure was designed for data storage. Data are grouped into logical units (tables), and relationships are defined to link the tables. This structure provides efficient storage of information (that is, the information need not be repeated), and also provides for built-in data-verification checks; for example, a result cannot exist without corresponding site, sample, and parameter information. The relational database structure also is powerful and efficient for retrieving subsets of data to meet user requirements.

The primary tables in the Boulder River watershed relational database (directory rel_db on the accompanying CD-ROM) are the FieldSites, Sample, Result, and Parameter tables (fig. 4). The FieldSites table contains information about each of the 479 sites in the database. A SiteNumber uniquely identifies each site. Sites that are considered co-located for purposes of spatial analysis are assigned the same AMLIAnalysisID. A ProjectCode for each site indicates what project and scientist established the site. The attribute PPSiteLabel contains the label which is used for a field site on figures or diagrams elsewhere in this Professional Paper. These labels are not always exactly the same as the field sites' SiteNumber. Additional characteristics in the FieldSites table include locational coordinates, SiteComment, and a Stream designation which indicates if a site is located on a stream, and if so, which one.

The Sample table contains information about material collected at each site, such as the date and time of collection, and the type of material (sample media) collected at the site. Media type should be carefully noted when data are analyzed, so that data of different types are not mistakenly equated; for example, the database contains analyses for arsenic in fish livers and in fish gills, organs which might have different characteristics relative to the bioaccumulation of metals. Optional characteristics in the Sample table include SamplePreparation, SampleComment, and CollectionMethod.

The Result table contains measurements made at sites. The characteristic measured is identified using a ParameterCode, a succinct 20-character-length field that can be used as a column name in a data report or spreadsheet. Measurements consist of a numeric value and an optional ValueRemarkCode, which is used to qualify results such as nondetections or estimates. Optional characteristics in the Result table include AnalyticMethodShortName and LabShortName.

The Parameter table is a lookup table that contains a complete description of each characteristic measured. Although the Result table contains a short description of the characteristic measured (ParameterCode), a lengthier description is needed owing to the highly specific nature of laboratory measurements. For example, the ParameterCode "Ag_ss" is shorthand for "Silver, sediment, suspended, ground finer than 0.15 millimeters, laboratory, micrograms per gram." The Parameter table also includes a ConstituentName field to

Table 4. Geologic maps and geochemical, biological, geophysical, and remote sensing data in the Boulder River watershed GIS database.

Subject	Description	File name	File format(s)	Chapter
Geology				
	Geology	geology.e00, geologyp.shp (polys), geologyl.shp (lines)	ArcInfo vector coverage	O'Neill and others (D1)
	Structure	faults.e00, faults.shp	ArcInfo vector coverage	O'Neill and others (D1)
	Alteration areas—possible Late Cretaceous alteration	alter.e00, alter.shp	ArcInfo vector coverage	O'Neill and others (D1)
	Veins	veins.e00, veins.shp	ArcInfo vector coverage	O'Neill and others (D1)
	Geologic Map Plate	geol_pl1.pdf	PDF map	O'Neill and others (D1)
	Correlation Diagram	geol_pl2.pdf	PDF map	O'Neill and others (D1)
	GeoEnvironmental Map	e_geo.tif	GeoTIFF	McCafferty and others (D2)
Geochemistry				
	Location map that shows the localities of all the streambed-sediment samples	sed.e00, sed.shp	ArcInfo vector coverage	Church and others (D8)
Sediment Ribbon Maps				
	Ribbon map that shows the concentration of cadmium in the streambed sediment recast as hazard quotient values	sed_cd.e00, sed_cd.shp	ArcInfo vector coverage	Church and others (D8)
	Ribbon map that shows the concentration of copper in the streambed sediment recast as hazard quotient values	sed_cu.e00, sed_cu.shp	ArcInfo vector coverage	Church and others (D8)
	Ribbon map that shows the concentration of lead in the streambed sediment recast as hazard quotient values	sed_pb.e00, sed_pb.shp	ArcInfo vector coverage	Church and others (D8)
	Ribbon map that shows the concentration of zinc in the streambed sediment recast as hazard quotient values	sed_zn.e00, sed_zn.shp	ArcInfo vector coverage	Church and others (D8)
	Ribbon map that shows the concentration of cadmium + copper + zinc in the streambed sediment recast as hazard quotient values	sed_all.e00, sed_all.shp	ArcInfo vector coverage	Church and others (D8)
	Location map that shows the localities of all the water samples	water.e00, water.shp	ArcInfo vector coverage	Nimick and Cleasby (D5)
Water Ribbon Maps				
	Ribbon map that shows the concentration of cadmium in the water recast as hazard quotient values in terms of the EPA water quality standards	wat_cd.e00, wat_cd.shp	ArcInfo vector coverage	Nimick and Cleasby (D5)
	Ribbon map that shows the concentration of copper in the water recast as hazard quotient values in terms of the EPA water quality standards	wat_cu.e00, wat_cu.shp	ArcInfo vector coverage	Nimick and Cleasby (D5)

Table 4. Geologic maps and geochemical, biological, geophysical, and remote sensing data in the Boulder River watershed GIS database.—Continued

Subject	Description	File name	File format(s)	Chapter
Water Ribbon Maps—Continued				
	Ribbon map that shows the concentration of zinc in the water recast as hazard quotient values in terms of the EPA water quality standards	wat_zn.e00, wat_zn.shp	ArcInfo vector coverage	Nimick and Cleasby (D5)
	Ribbon map that shows the concentration of cadmium + copper + zinc in the water recast as hazard quotient values in terms of the EPA water quality standards	wat_all.e00, wat_all.shp	ArcInfo vector coverage	Nimick and Cleasby (D5)
Biological data				
	Estimated distribution of trout population prior to 1997	fish.e00, fish.shp	ArcInfo vector coverage	Farag and others (D10)
Geophysics				
	56K Hz. resistivity	res56K.tif	GeoTiff	McCafferty and others (D2)
	7200 Hz. resistivity	res7200.tif	GeoTiff	McCafferty and others (D2)
	900 Hz. resistivity	res900.tif	GeoTiff	McCafferty and others (D2)
	Reduced-to-the-pole magnetic anomaly	rtp_mag.tif	GeoTiff	McCafferty and others (D2)
	Reduced-to-the-pole high pass magnetic anomaly	rtp_mag_hipass.tif	GeoTiff	McCafferty and others (D2)
	Volume percent magnetite estimated from 900-Hz resistivity	em_magnetite.tif	GeoTiff	McCafferty and others (D2)
	Volume percent magnetite estimated from the high pass magnetic anomaly data	mag_magnetite.tif	GeoTiff	McCafferty and others (D2)
	Geophysically-inferred bedrock with low acid-neutralizing potential	gp_low_ANP.tif	GeoTiff	McCafferty and others (D2)
	Outline of the geophysical study area boundary	gp_poly.e00, gp_poly.shp	ArcInfo vector coverage	McCafferty and others (D2)
Remote sensing				
	The spatial frequency of mapped linear features	frequency.tif	GeoTiff	McDougal and others (D9)
	The combined spatial frequency and intersections of mapped linear features	frequency_intersect.tif	GeoTiff	McDougal and others (D9)
	The combined spatial frequency and length of mapped linear features	frequency_length.tif	GeoTiff	McDougal and others (D9)
	The number of intersections of mapped linear features	intersect.tif	GeoTiff	McDougal and others (D9)
	The length of mapped linear features	length.tif	GeoTiff	McDougal and others (D9)
	Areas that have soils with perennial or seasonal high water tables	wetland.e00, wetland.shp	ArcInfo vector coverage	McDougal and others (D9)
	Areas of saturated soils that are associated with linear features	wetsoil.e00, wetsoil.shp	ArcInfo vector coverage	McDougal and others (D9)
	Linear features that have been delineated from fracture analysis	lin_f.e00, lin_f.shp	ArcInfo vector coverage	McDougal and others (D9)

Table 5. Data sources for sample-site data in the Boulder River watershed relational database.

[Not all data have been published elsewhere in the documents listed in the Reference column. See appropriate chapter in this volume or the accompanying CD-ROM for access to all of the data]

AMLI Project Component	Contact scientist	Media sampled	Number of sites	Number of samples	Number of results	Reference	Chapter in which data are primarily used
Characterization of water-quality conditions	D.A. Nimick	Surface water, ground water	111	858	14,682	Nimick and Cleasby (2000)	D5
Uncle Sam Gulch, Bullion Mine tributary, and Cataract Creek metal-loading study	B.A. Kimball	Surface water	168	172	7,186	Kimball and others (this volume)	D6
Rare earth geochemistry of acidic waters	P.L. Verplanck	Surface water	8	8	429	Verplanck and others (1999)	Data not used
Characterization of ecosystem health	A.M. Farag	Biota	15	67	331	Farag and others (this volume)	D10
Characterization of stream sediment and mine wastes	D.L. Fey	Biota, rock, sediment, soil, mine wastes	95	607	28,226	Fey and Church (1998); Fey and others (1999); Fey, Church, and Finney (2000); Fey and Church (1999); Fey, Desborough, and Finney (2000)	D4, D8, E1
Characterization of tailings core	S.E. Church	Sediment, soil, mine wastes	1	232	8,768	Church, Unruh, and others (this volume)	E1
Chemical and lead isotope compositions of mine wastes and premining sediment	D.M. Unruh	Biota, sediment	21	186	5,691	Unruh and others (2000)	D8
Chemical compositions of mine wastes	D.L. Fey	Rock, soil	21	33	941	Desborough and others (1998)	D1, D2, D4
Rock geochemistry	B.S. Van Gosen	Rock	39	48	1,112	Ruppel (1963); Becraft and others (1963)	D1
TOTAL			**479**	**2,211**	**67,366**		

group results according to the element or compound type (for example, zinc), and a Ppcode field which lists the corresponding measurement code (where available) in the U.S. Geological Survey's National Water Information System and the U.S. Environmental Protection Agency's STORET database.

Relationships between these tables are depicted as lines in figure 4. The FieldSites table is linked to the Sample table by including a common field (Site Number) in both tables; therefore a sample cannot exist without a corresponding site in the FieldSites table. The symbols "1" and "∞" on the relationship line indicate a one-to-many relationship, that is, a site may have many samples. Similarly a sample may have many results, and a parameter may have many results.

The Boulder River watershed relational database contains 10 tables in addition to the 4 principal tables. The Qualitative Result table includes measurements that are text values (as opposed to number values in the Result table). The SpatialAnalysisSites table provides site groupings so that data may be extracted from sites that are logically co-located for analysis purposes. The AnalyticMethod table provides additional information on laboratory techniques used. The LabName table provides additional information about analytical laboratories that produced chemical results. The Project table

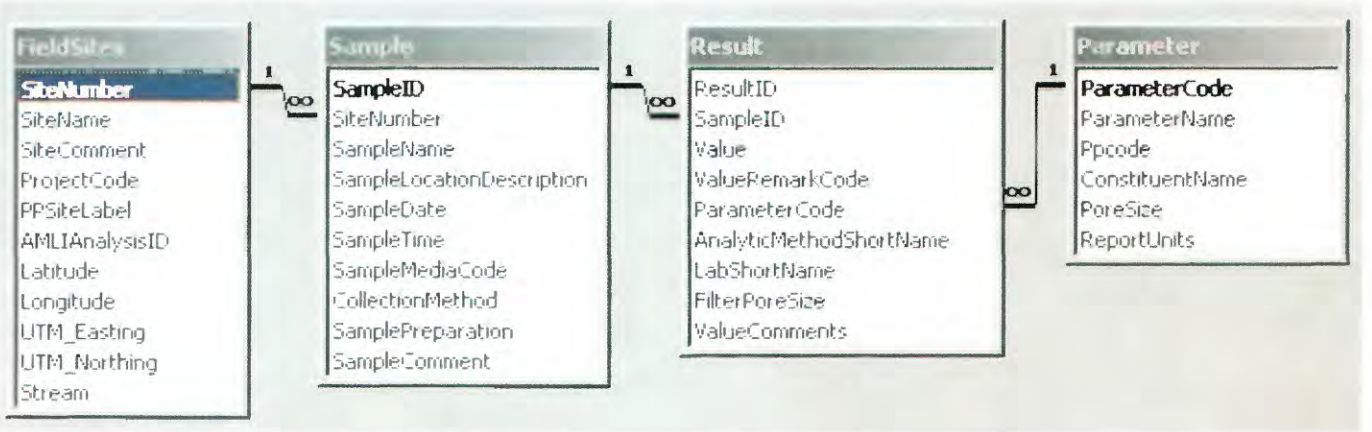

Figure 4. Primary tables in the relational database and the relationships between tables.

provides additional information about projects that provided data to the Boulder River watershed relational database. The SampleMedia table provides additional information about the media types sampled. The LocationMaster table contains characteristics for each field site derived by map overlay using a GIS system. The MineSites table contains information about the mine-related sites located in the study area, and the MineSitesAditFlow table contains data about flowing adits that exist at certain mine-related sites. The FieldSiteMineSiteAssocs table lists certain field sites that are associated with mine-related sites.

A bitmap file (relationship_diagram.bmp), containing a complete diagram of the relationships of all the files in the Boulder River watershed relational database, exists on the accompanying CD-ROM in the /bldr_cd/rel_db directory.

Relational databases can be implemented using a variety of proprietary or nonproprietary software packages. The Boulder River watershed relational database is provided on the CD-ROM attached to this report in a format compatible with proprietary software (Microsoft Access 2000) in the /bldr_cd/rel_db/mdb directory, and in a nonproprietary format in the /bldr_cd/rel_db/ascii directory. A README.txt file on the CD-ROM in /bldr_cd/rel_db provides technical details about how to use the database in these two formats. A more complete discussion of the creation and content of the database is included on the CD-ROM in a Federal Geographic Data Committee-compliant metadata file in /bldr_cd/rel_db/meta.

Data may be extracted from the Boulder River watershed relational database to meet specific user needs. Within relational database software packages, queries may be constructed and saved to retrieve data using user-defined criteria; the Microsoft Access version of the Boulder River watershed relational database on the CD-ROM contains several example queries. Suppose a scientist wishes to examine downstream patterns of zinc concentrations in water along the mainstem of Cataract Creek during August 1997. To extract the necessary data from the database, a series of linked queries is constructed. The initial query is used to select the database fields of interest and to place conditions on retrieving the data. For the Zinc Synoptic data, the user would like a table that includes the site name, the instantaneous water discharge, the zinc concentration and the distance of the sampling point from the starting point on the stream. The query qselZnSynopticData (fig. 5) selects the fields of interest.

The query combines data from three tables, the FieldSites table (which contains the SiteName and Stream), the Sample

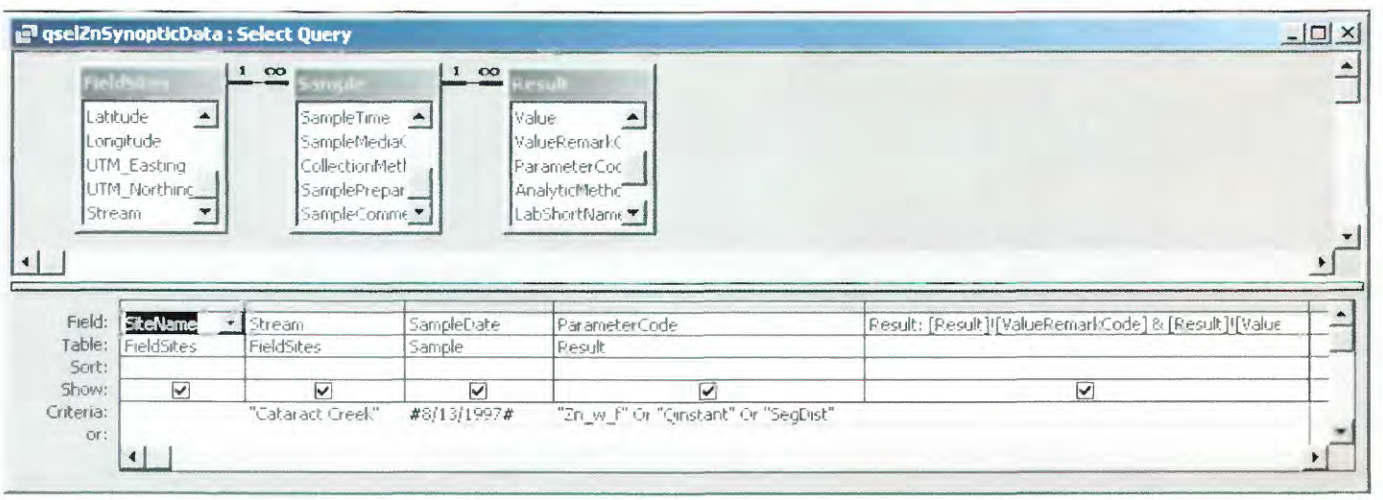

Figure 5. Graphical view of the qselZnSynopticData query.

table (which contains the SampleDate), and the Result table (which contains result information). Conditions are placed on this query so that only data with a Stream of "Cataract Creek" are selected, only samples taken on 8/13/97 are selected, and only results for water discharge, zinc concentration, and downstream distance are selected. This query also constructs the Result value as a concatenation of the numerical result along with any remark code. The graphical view of the query shown in figure 5 is translated into a Structured Query Language (SQL) statement as follows:

SELECT FieldSites.SiteName, FieldSites.Stream, Sample.SampleDate, Result.ParameterCode, [Result]![ValueRemarkCode] & [Result]![Value] AS Result FROM (FieldSites INNER JOIN Sample ON FieldSites.SiteNumber = Sample.SiteNumber) INNER JOIN Result ON Sample.SampleID = Result.SampleID WHERE (((FieldSites.Stream)="Cataract Creek") AND ((Sample.SampleDate)=#8/13/1997#) AND ((Result.ParameterCode)="Zn_w_f" Or (Result.ParameterCode)="Qinstant" Or (Result.ParameterCode)="SegDist"));

The second query in this example (qselZnSynopticData_Crosstab) is a crosstab query which pivots the results of interest so that they appear as columns rather than rows. The third query (qmakZnSynopticResults) makes a new table containing the results sorted by downstream distance. A portion of this table is shown in figure 6.

Data Viewer Software

Two freeware GIS data viewer software packages are provided on the accompanying CD-ROM. These products are GIS data explorers. The purpose of the data viewer software is to give the user the capabilities to perform elementary GIS analysis on the digital data. The vector coverages and raster images provided on the CD-ROM are useful for illustrating the processes and dynamics, in terms of mine drainage, that occur in the watershed.

ZnSynopticResults : Table

SiteName	Discharge	Zinc Concentration	Distance
CC-150	4.13	<10	150
CC-850	4.27	<10	850
CC-1370	4.38	<10	1370
CC-1610	4.45	<10	1610
CC-1690	4.59	<10	1690
CC-2490	4.55	<10	2490
CC-3450	6	<10	3450
CC-3850	6.14	<10	3850
CC-4660	6.43	33	4660
Cataract Creek below Hoodoo Creek	6.53	53	4940
CC-5940	6.6	47	5940
CC-6800	6.67	36	6800
CC-7900	6.74	35	7900
CC-8700	6.81	45	8700
CC-9220	6.99	45	9220
CC-10380	7.24	47	10380
CC-11055	7.59	42	11055
CC-12115	7.91	56	12115
CC-13255	8.16	57	13255
CC-14055	8.33	52	14055
CC-14855	8.44	60	14855
CC-15655	8.55	56	15655
CC-16845	8.83	58	16845
CC-17645	9.22	53	17645
CC-18545	9.53	30	18545
CC-19245	9.75	30	19245
Cataract Creek above Uncle Sam Gulch	9.57	31	19700
Cataract Creek below Uncle Sam Gulch	11.51	470	20050
CC-20730	11.69	460	20730
CC-21130	11.86	457	21130
CC-21715	11.93	422	21715

Record: 2 of 46

Figure 6. The reformatted results of the qselZnSynopticData query.

The two data viewer software packages are ArcExplorer 2.0 and MapSheets Express 1.3. ArcExplorer 2.0 was written by Environmental Systems Research Institute, Inc. MapSheets Express was written by ERDAS, Inc.

Using these two products, the spatial data can be displayed, queried, and overlaid to produce map output. MapSheets Express enables the user to generate maps that can be imported into PowerPoint presentations. In addition, Word and WordPerfect documents can be output from MapSheets Express.

The two software packages have some important differences. ArcExplorer is better at handling vector files than raster files. Raster images can be displayed in ArcExplorer, but one cannot query the images. The raster images can only be displayed one at a time as a background for vector files. Basically, this image is a static backdrop with no inherent analysis properties.

In contrast, MapSheets Express has more functionality for raster images than ArcExplorer provides. The user is able to query pixels of the raster images. The attributes of these pixels are accessible in the data tables for user output. In addition, MapSheets Express allows the user to control the transparency of the images, which allows several raster images to be displayed on top of one another. In summary, for vector data work, ArcExplorer is a more effective tool, and for raster data work, MapSheets Express is better.

The two packages have similar platform requirements. ArcExplorer 2.0 requires a PC with Windows 98/2000/NT/XP operating systems. It requires Internet Explorer 4.0 for the internet capabilities of the software. MapSheets Express 1.3 requires Windows 95 or Windows NT version 4.0 operating system or later. Both ArcExplorer 2.0 and MapSheets Express 1.3 need 16 MB RAM and an IBM/PC or compatible system with 486-class processor or better.

Boulder River Watershed CD-ROM

The directory structure for the data and information contained on the Boulder River watershed CD-ROM is shown in figure 7.

The rel_db directory contains the relational database version of the sample-site data collected for the study, and the mine-related site inventory compiled for the study. The directory itself contains a README.txt file which describes the contents of the directory, and a bitmap file (relationship_diagram.bmp) which is a diagram of all the tables in the relational database, and the relationships between them. The mdb subdirectory contains the Microsoft Access version of the relational database (BoulderAMLI.mdb), the ascii subdirectory contains relational database tables in the form of flat, ASCII files, and the meta subdirectory contains metadata for the relational database.

The gis_db directory contains three subdirectories (basecart, sitedata, and geosci), each of which contains different types of data in formats suitable for use in Geographic Information Systems. The basecart subdirectory contains base cartographic data used as reference for the other data. The basecart subdirectory itself contains a README.txt file describing the base cartographic data. Below this subdirectory, the e00 subdirectory contains ArcInfo export files of base cartographic data stored as ArcInfo coverages. The shape subdirectory contains ESRI shapefiles and .dbf files of the data contained in the ArcInfo coverages. The elev subdirectory contains a compressed tar file, which when uncompressed creates an ArcInfo workspace containing an elevation grid, and slope, aspect and shaded relief grids derived from the elevation grid. The elev subdirectory also includes TIFF image file representations of the elevation data, and TIFF

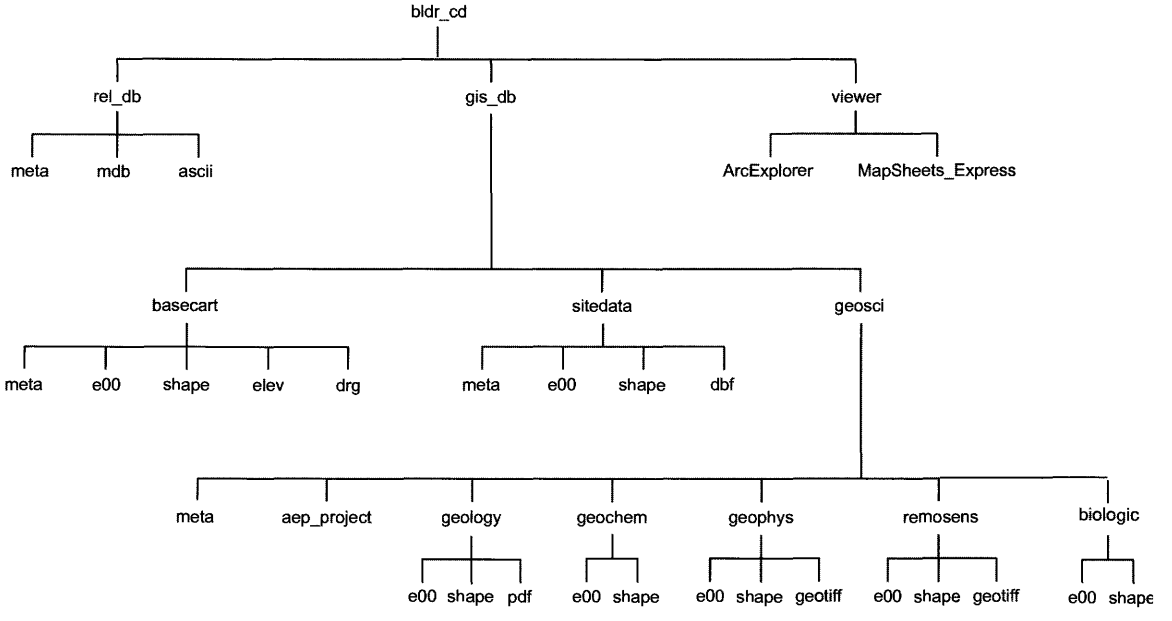

Figure 7. Directory tree structure for the Boulder River watershed CD-ROM.

images of legends for the elevation data image files. The meta subdirectory contains metadata for the data in the e00, shape, and elev subdirectories. The drg subdirectory contains U.S. Geological Survey Digital Raster Graphic (DRG) image files for the eight 7.5-minute quadrangles which contain the majority of the data in the Boulder River watershed study.

The second subdirectory under the gis_db directory, the sitedata subdirectory, contains the sample-site and mine-related site data from the relational database, but in formats directly compatible with Geographic Information Systems. A README.txt file at the sitedata level provides descriptive information about the data stored beneath it. The e00 subdirectory contains the site data as ArcInfo export files of coverages and ArcInfo export files of INFO files. The shape subdirectory contains three site data layers (field sites, analysis sites, and mine-related sites) as ESRI shapefiles. The dbf subdirectory contains 11 tables which contain information about the sites, and data collected at the sites. These tables are in the form of .dbf files. The meta subdirectory contains metadata about the data in the e00, shape, and dbf subdirectories.

The third subdirectory under the gis_db directory, the geosci subdirectory, contains geoscientific and hydrologic data sets, as well as a sample ArcExplorer project file. A README.txt file in the geosci subdirectory lists the contents of the directory. There are seven subdirectories: geology, geochem (geochemistry), geophys (geophysics), remosens (remote sensing), biologic, meta (metadata), and aep_project (ArcExplorer project file). The meta subdirectory contains metadata about all of the interpretive geoscientific data. In each of the data subdirectories, an e00 subdirectory contains data as ArcInfo export files of coverages, a shape subdirectory contains data as shape files, and a geotiff subdirectory (if one exists) contains data in the GeoTIFF format. The pdf subdirectory under the geology directory contains the geology map of Chapter D1 in a PDF format. It also contains a PDF of a fence diagram showing correlation of Quaternary deposits in Buckeye meadow, in the Basin Creek drainage, which is a second plate discussed in Chapter D1. A PDF of the complete topographic base also is included in this directory.

The viewer directory contains two data viewer software packages. The directory itself contains a README.txt file which summarizes the directory's contents. There are two subdirectories: ArcExplorer and MapSheets_Express. The ArcExplorer subdirectory contains a file (ae2setup.exe) which is an executable file that allows one to install the ArcExplorer 2.0 data viewer software. The ArcExplorer.pdf file, created when the ae2setup.exe file is run, is a User Guide for ArcExplorer which includes a tutorial. Similarly, the MapSheets_Express subdirectory contains an executable file (mxsetup.exe) that allows one to install the MapSheets Express 1.3 data viewer software. The Readme.txt file, created when the mxsetup.exe file is run, provides various types of information about the MapSheets Express program.

An ArcExplorer project file (boulder_aml.aep, located in the /bldr_cd/gis_db/geosci/aep_project directory on the CD-ROM) is available as an example of how to use the ArcExplorer software to display and use the data on the CD-ROM. The data files have been organized, and their attributes have been displayed, in the legend defined in the project file.

References Cited

Becraft, G.E., Pinckney, D.M., and Rosenblum, Sam, 1963, Geology and mineral deposits of the Jefferson City quadrangle, Jefferson, and Lewis and Clark Counties, Montana: U.S. Geological Survey Professional Paper 428, 101 p.

Desborough, G.A., Briggs, P.H., and Mazza, N., 1998, Chemical and mineralogical characteristics and acid-neutralizing potential of fresh and altered rocks and soils of the Boulder River headwaters in Basin and Cataract Creeks of northern Jefferson Co., Montana: U.S. Geological Survey Open-File Report 98–0040, 21 p.

Fey, D.L., and Church, S.E., 1998, Analytical results for 42 fluvial tailings cores and 7 stream sediment samples from High Ore Creek, northern Jefferson County, Montana: U.S. Geological Survey Open-File Report 98–0215, 49 p.

Fey, D.L., and Church, S.E., 1999, Analytical results for 35 mine-waste tailings cores and six bed sediment samples, and an estimate of the volume of contaminated materials at Buckeye meadow on upper Basin Creek, northern Jefferson County, Montana: U.S. Geological Survey Open-File Report 99–0537, 59 p.

Fey, D.L., Church, S.E., and Finney, C.J., 2000, Analytical results for the Bullion Mine and Crystal Mine waste samples and bed sediments from a small tributary to Jack Creek and from Uncle Sam Gulch, Boulder River watershed, Montana: U.S. Geological Survey Open-File Report 00–0031, 71 p.

Fey, D.L., Desborough, G.A., and Finney, C.J., 2000, Analytical results for total-digestions, EPA–1312 leach, and net acid production for twenty-three abandoned metal-mining related wastes in the Boulder River watershed, northern Jefferson County, Montana: U.S. Geological Survey Open-File Report 00–0114, 17 p.

Fey, D.L., Unruh, D.M., and Church, S.E., 1999, Chemical data and lead isotopic compositions in stream-sediment samples from the Boulder River watershed, Jefferson County, Montana: U.S. Geological Survey Open-File Report 99–0575, 147 p.

Nimick, D.A., and Cleasby, T.E., 2000, Water-quality data for streams in the Boulder River Abandoned Mine Lands Initiative study area: U.S. Geological Survey Open-File Report 00–0099, 70 p.

Ruppel, E.T., 1963, Geology of the Basin quadrangle, Jefferson, Lewis and Clark, and Powell Counties, Montana: U.S. Geological Survey Bulletin 1151, 121 p.

Smith, B.D., Labson, V.F., and Hill, Pat, 2000, Airborne geophysical survey in the Boulder River watershed, Jefferson and Lewis and Clark counties, Montana: U.S. Geological Survey Open-File Report 00–240, one CD-ROM.

Unruh, D.M., Fey, D.L., and Church, S.E., 2000, Chemical data and lead isotopic compositions of geochemical baseline samples from streambed sediments and smelter slag, lead isotopic compositions in fluvial tailings, and dendrochronology results from the Boulder River watershed, Jefferson County, Montana: U.S. Geological Survey Open-File Report 00–0038, 14 p.

Verplanck, P.L., Nordstrom, D.K., and Taylor, H.E., 1999, Overview of rare earth element investigations in acid waters of U.S. Geological Survey abandoned mine land watersheds: U.S. Geological Survey Water-Resources Investigations Report 99–4018, p. 83–92.

GPO U.S. GOVERNMENT PRINTING OFFICE 2005—774-303